



**Michigan  
Technological  
University**

Michigan Technological University  
**Digital Commons @ Michigan Tech**

---

Dissertations, Master's Theses and Master's Reports

---

2023

# MULTISCALE MOLECULAR MODELING STUDIES OF THE DYNAMICS AND CATALYTIC MECHANISMS OF IRON(II)- AND ZINC(II)-DEPENDENT METALLOENZYMES

Sodiq O. Waheed  
*Michigan Technological University, [sowaheed@mtu.edu](mailto:sowaheed@mtu.edu)*


Copyright 2023 Sodiq O. Waheed

---

## Recommended Citation

Waheed, Sodiq O., "MULTISCALE MOLECULAR MODELING STUDIES OF THE DYNAMICS AND CATALYTIC MECHANISMS OF IRON(II)- AND ZINC(II)-DEPENDENT METALLOENZYMES", Open Access Dissertation, Michigan Technological University, 2023.  
<https://doi.org/10.37099/mtu.dc.etr/1584>

Follow this and additional works at: <https://digitalcommons.mtu.edu/etr>

 Part of the [Bioinformatics Commons](#), [Biophysics Commons](#), [Computational Chemistry Commons](#), [Inorganic Chemistry Commons](#), and the [Structural Biology Commons](#)

MULTISCALE MOLECULAR MODELING STUDIES OF THE DYNAMICS AND  
CATALYTIC MECHANISMS OF IRON(II)- AND ZINC(II)-DEPENDENT  
METALLOENZYMES

By

Sodiq O. Waheed

A DISSERTATION

Submitted in partial fulfillment of the requirements for the degree of

DOCTOR OF PHILOSOPHY

In Chemistry

MICHIGAN TECHNOLOGICAL UNIVERSITY

2023

© 2023 Sodiq O. Waheed

This dissertation has been approved in partial fulfillment of the requirements for the Degree of DOCTOR OF PHILOSOPHY in Chemistry.

Department of Chemistry

Dissertation Co-Advisor: *Christo Z. Christov, Ph.D.*

Dissertation Co-Advisor: *Tatyana G. Karabancheva-Christova, Ph.D.*

Committee Member: *Tarun K. Dam, Ph.D.*

Committee Member: *Haiying Liu, Ph.D.*

Committee Member: *Stephen Techtmann, Ph.D.*

Department Chair: *Sarah A. Green, Ph.D.*

# Table of Contents

Author Contribution Statement.....	ix
Acknowledgements.....	xi
List of Abbreviations .....	xiii
Abstract.....	xvi
<b>1 Introduction.....</b>	<b>1</b>
1.1 Molecular Mechanics .....	3
1.1.1 Bond Stretching .....	4
1.1.2 Angle Bending .....	4
1.1.3 Torsional Terms .....	5
1.1.4 Electrostatic Interactions.....	6
1.1.5 Van der Waals Interactions.....	7
1.2 Molecular Dynamics Simulations .....	8
1.3 Classical Metadynamics Simulations.....	9
1.4 Quantum Mechanics.....	11
1.4.1 Density Functional Theory .....	13
1.5 Quantum Mechanics and Molecular Mechanics (QM/MM) Methods.....	15
1.5.1 Additive and Subtractive QM/MM Schemes.....	16
1.5.2 Handling of the Electrostatic QM/MM Interactions.....	17
1.5.3 Mechanical Embedding .....	18
1.5.4 Electrostatic Embedding.....	18
1.5.5 Polarized Embedding.....	18
1.5.6 Treatment of the QM and MM Boundary.....	19
1.6 QM/MM Metadynamics.....	20
1.7 Reaction Path Modeling .....	21
1.8 References .....	22
<b>2 Conformational Flexibility Influences Structure-Function Relationships in Nucleic Acid N-Methyl Demethylases.....</b>	<b>29</b>
2.1 Introduction .....	30
2.2 Computational Methods .....	34
2.2.1 System Preparation .....	34
2.2.2 MD Simulations.....	35
2.2.3 QM/MM calculations.....	36
2.2.4 Molecular Mechanics/Generalized Born Surface Area (MM/GBSA).....	37
2.3 Results and Discussion.....	37
2.4 Conclusions .....	50
2.5 References .....	51

3	Role of Structural Dynamics in Selectivity and Mechanism of Non-Heme Fe(II) and 2-Oxoglutarate-Dependent Oxygenases Involved in DNA Repair.....	55
3.1	Introduction .....	57
3.2	Results and Discussion.....	64
3.2.1	The Nature of the Substrate Influences the Conformational Dynamics of the Enzyme-Substrate Complexes for O <sub>2</sub> Activation in AlkB-ssDNA, AlkB-dsDNA, and AlkBH2-dsDNA systems.....	64
3.2.2	Flexibility of the 2OG Binding Sites .....	66
3.2.3	Interactions of the Iron-Coordinating Residues.....	66
3.2.4	Dynamics of the Substrate Binding Sites.....	67
3.2.5	Long-Range Correlated Motions .....	67
3.2.6	Dynamics of AlkB-ssDNA, AlkB-dsDNA, and AlkBH2-dsDNA with undamaged DNA.....	70
3.2.7	Reaction Mechanism of the Dioxygen Activation.....	71
3.2.8	Formation of the “in-line” Fe(IV)=O intermediate via a potential ‘ferryl flip’ in AlkBH2 .....	77
3.2.9	Rotation of the C1 carboxylate of 2OG from the ‘off-line’ to an ‘in-line’ binding mode in AlkBH2 .....	80
3.2.10	O <sub>2</sub> Activation for “in-line” Fe(III)-superoxo Complex .....	82
3.2.11	Conformational Flexibility Modulates the Structure of the Reactive Complex (Fe(IV)=O) for the Substrate Hydroxylation in AlkB-ssDNA, AlkB-dsDNA, and AlkBH2-dsDNA systems. ....	83
3.2.12	Mechanism of DNA Substrate Hydroxylation in AlkB-ssDNA, AlkB-dsDNA, and AlkBH2-dsDNA complexes.....	87
3.2.13	Hydrogen Atom Abstraction (HAT).....	89
3.2.14	Effects of the Conformational Flexibility on HAT .....	89
3.2.15	Molecular orbital interactions driving $\sigma$ - and $\pi$ -pathways.....	91
3.2.16	Effects of residues from the second sphere and beyond on HAT.....	92
3.2.17	Mechanism of Rebound Hydroxylation.....	97
3.3	Computational Methods .....	99
3.3.1	Model Preparation.....	99
3.3.2	Molecular Dynamic Simulations .....	101
3.3.3	QM/MM Calculations.....	102
3.4	Conclusions .....	103
3.5	References .....	107
4	Catalytic Mechanism of Human Ten-Eleven Translocation -2 (TET2) Enzyme: Effects of Conformational Changes, Electric Field and Mutations .....	116
4.1	Introduction .....	117
4.2	Computational Methods .....	122
4.2.1	System Preparation .....	122
4.2.2	Molecular Dynamic Simulations .....	124
4.2.3	QM/MM Calculations.....	125
4.3	Results and Discussion.....	126

4.3.1	Conformational Dynamics Facilitates the Formation of a Reactive Complex between TET2 Fe(IV)=O and the 5mC (dsDNA) substrate (TET2·Fe(IV)=O/dsDNA).....	126
4.3.2	Single/Double Mutations in the Second Sphere and Beyond Influence the Substrate Binding in TET2·Fe(IV)=O/dsDNA Complex.....	129
4.3.3	Effects of the Mutations on the Structure of the Substrate Binding Site and the Iron Center.....	130
4.3.4	Effects of Mutations on the Substrate Binding Affinity and Long-Range Correlated Motions.....	132
4.3.5	Mechanism of the Hydrogen Atom Abstraction (HAT) in the WT TET2-dsDNA .....	136
4.3.6	Energy Decomposition Analysis and Long-Range Correlated Motions of the HAT-Transition State-Stabilizing Residues .....	138
4.3.7	Influence of Electric Field and Kinetic Isotope Effects on the HAT	140
4.3.8	Mechanism of the Rebound Hydroxylation in the WT TET2-dsDNA	142
4.3.9	Effect of Mutations on Hydrogen Atom Abstraction Reaction of TET2·Fe(IV)=O/dsDNA Complex.....	144
4.3.10	Stabilization of the HAT Transition State in the Mutant Forms: Local Interactions, Energy Decomposition and Long-Range Correlated Motions	146
4.3.11	How the Mutations Alter the HAT Electric Field and KIE? .....	148
4.4	Conclusions .....	150
4.5	References .....	152
5	How Human TET2 Enzyme Catalyzes the Oxidation of Unnatural Cytosine Modifications in Double-Stranded DNA .....	159
5.1	Introduction .....	160
5.2	Computational Methods .....	165
5.2.1	System Setup.....	165
5.2.2	MD Simulations.....	166
5.2.3	QM/MM Calculations.....	167
5.3	Results and Discussion.....	169
5.3.1	Structure and Dynamics of the ES Complex for Substrate Oxidation (Fe(IV)=O of Human TET2 with dsDNA Containing Different Alkylated Substituted Bases: 5eC,5vC, and 5eyC).....	169
5.3.2	Dynamics of Fe(IV)=O species of TET2 bound to N4 methylated 4mC and 4dmC dsDNA substrates.....	172
5.3.3	Reactions Mechanisms of TET2 with dsDNA containing 5eC, 5vC, and 5eyC.....	174
5.3.4	Mechanism of 5eC Substrate Oxidation .....	176
5.3.5	Hydroxylation and Desaturation of 5eC Radical Substrate Intermediates .....	184

5.3.6	Energetic Effects of Individual Residues on the Stabilization of the Transition States and Products .....	187
5.3.7	Oxidation of Unsaturated Substrates by TET2 .....	189
5.3.8	Hydrogen Atom Abstraction in 5vC and 5eyC Substrates .....	190
5.3.9	Rebound Hydroxylation and Desaturation Reactions in 5vC and 5eyC Radical substrates Intermediates .....	193
5.3.10	Mechanism of 4mC and 4dmC dsDNA substrates Oxidation by TET2	196
5.3.11	Post Hydroxylation Reactions for hydroxylated intermediates of IM2 <sub>OH<sub>eyβ</sub></sub> , IM2 <sub>OH<sub>vβ</sub></sub> , and IM2 <sub>OH<sub>4m</sub></sub> of 5eyC, 5vC, and 4mC Substrates .....	197
5.3.12	Rearrangement Reactions of IM2 <sub>OH<sub>eyβ</sub></sub> and IM2 <sub>OH<sub>vβ</sub></sub> in Enzyme and Water	198
5.3.13	Decomposition of hemiaminal intermediate of 4mC.....	203
5.4	Conclusions .....	205
5.5	References .....	208
6	What is The Catalytic Mechanism of Enzymatic Histone N-Methyl Arginine Demethylation and Can it be Influenced by an External Electric Field?.....	214
6.1	Introduction .....	216
6.2	Methods .....	220
6.2.1	System Setup and MD Simulation.....	220
6.2.2	QM/MM Calculations.....	222
6.3	Results and Discussion.....	224
6.3.1	Dynamics and Substrate Binding in the Histone H4 Tail with N-Methylated Arginine by KDM4E.....	224
6.3.2	Reaction Mechanism of Demethylation of Methylated Arginine in H4 by KDM4E .....	227
6.3.3	Effect of an oriented External Electric field (EEF) on the C-H and N-H Hydrogen Abstraction Reactions During N-methyl Arginine Demethylation .....	234
6.4	Conclusions .....	240
6.5	References .....	241
7	Mechanism of the Early Catalytic Events in the Collagenolysis by Matrix Metalloproteinase-1 .....	244
7.1	Introduction .....	246
7.2	Methods.....	252
7.2.1	System Preparation and Setup .....	252
7.2.2	MD Simulations.....	253
7.2.3	MetD Simulations .....	254
7.2.4	QM/MM MD and MetD Simulations .....	255
7.3	Results and Discussion.....	256
7.3.1	Conformational Dynamics of the Open and Closed Forms of MMP-1•THP Complex with 5C and 4C States of the Catalytic zinc(II).....	256

7.3.2	Classical MetD for the Conformational Transformation from Open to Closed MMP-1•THP Complex .....	263
7.3.3	QM/MM MetD of the Transition of Open-5C to Open-4C form of MMP-1•THP Complex .....	267
7.3.4	QM/MM MetD of the Coordination of the Scissile Bond Glycine Carbonyl Oxygen to the Catalytic zinc(II) in the Closed-4C Form .....	269
7.4	Conclusions .....	272
7.5	References .....	274
A	Appendix A: Supporting Information for Chapter 2.....	279
A.1	Methods.....	279
A.1.1	System Preparation .....	279
A.1.2	MCPB .....	280
A.1.3	MD Simulations .....	281
A.1.4	QM cluster calculations .....	282
A.1.5	QM/MM calculations.....	283
A.1.6	Molecular Mechanics/Generalized Born Surface Area (MM/GBSA).....	284
B	Appendix B: Supporting Information for Chapter 3.....	307
C	Appendix C: Supporting Information for Chapter 4.....	473
C.1	QM/MM Calculations of the Dioxygen Activation in the WT TET2.....	473
C.2	Comparison between the Dynamics of Fe(IV)=O Complexes of TET2-dsDNA and AlkBH2-dsDNA .....	476
C.3	How the Mutations Alter the HAT Electric Field? .....	489
D	Appendix D: Supporting Information for Chapter 5.....	530
D.1	Dynamics of Fe(IV)=O species of TET2 bound to N4 methylated 4mC and 4dmC dsDNA substrates.....	530
D.2	HAT in 4mC and 4dmC .....	531
D.2.1	Hydrogen Atom Abstraction.....	531
D.2.2	Mechanism of Rebound Hydroxylation.....	537
E	Appendix E: Supporting Information for Chapter 6.....	687
F	Appendix F: Supporting Information for Chapter 7 .....	718
G	Copyright documentation.....	733
G.1	Copyright Permission for Chapter 2.....	733
G.2	Copyright Permission for Chapter 3.....	734
G.3	Copyright Permission for Chapter 4.....	735
G.4	Copyright Permission for Chapter 5.....	736
G.5	Copyright Permission for Chapter 6.....	737
G.6	Copyright Permission for Chapter 7.....	743
G.7	Copyright Permission for Chapter 3 Cover Image.....	746



G.8	Copyright Permission for Chapter 6 Cover Image .....	747
G.9	Copyright Permission for Chapter 7 Cover Image .....	753

## Author Contribution Statement

All the projects described in this dissertation were carried out under the direction of Dr. Christo Z. Christov and Dr. Tatyana G. Karabancheva-Christova in the Department of Chemistry, Michigan Technological University. The dissertation contains seven chapters, of which chapter 1 (introduction) was freshly prepared for the dissertation and the other six chapters are based on the already published peer-reviewed research papers.

In Chapter 2, the preliminary results were first obtained by Dr. Warispreet Singh and were included in his doctoral dissertation submitted to Northumbria University Newcastle, United Kingdom. The author of this dissertation re-performed some of the calculations, analyzed the results and wrote the manuscript published in “*Organic and Biomolecular Chemistry* **2019**, 17, 2223-2231”. The contents of the manuscript are reused in its entirety in this dissertation with the permission from Royal Society of Chemistry (RSC) Publishing.

The work in Chapter 3 is published in “*ACS Central Science* **2020**, 6(5), 795-814”. The work was selected as the supplementary front cover ([here](#)) of the May 2020 issue of the journal. The cover picture was designed by the author of this dissertation. Chapter 4 is published in “*ACS Catalysis* **2021**, 11(7), 3877-3890”, and Chapter 5 is also published in “*ACS Catalysis* **2022**, 12(9), 5327-5344”. These are peer-reviewed research papers by the author of this dissertation and are reproduced with the permission from American Chemical Society (ACS) Publishing.

Chapter 6 of the dissertation is published in “*Chemistry – A European Journal* **2021**, 27(46), 11827-11836”, reproduced with permission from Wiley-VCH publishing. The author of this dissertation was responsible for the external electric fields (EEFs)

calculations part of the work, analyzed the results and wrote this section of the manuscript, while Dr. Rajeev Ramanan, the former postdoctoral researcher in the lab, performed the baseline study, analyzed it, and wrote the section of the manuscript. The work was specified as a “Hot Paper” and selected as the Front Cover ([here](#)) and Cover Profile ([here](#)) of the August 2021 issue of the Chemistry – A European Journal. The author of this dissertation designed the cover picture.

The chapter 7 of this dissertation is published in “*ChemPhysChem* **2023**, 24(3), e202200649” as a peer-reviewed paper by the author of this dissertation and reproduced with permission from Wiley-VCH publishing. The work was specified as a “Very Important Paper” and selected as the Front Cover ([here](#)) and Cover Profile ([here](#)) of the February 2023 issue of the ChemPhysChem Journal. The cover picture was designed by Sarah Atkinson and the author of this dissertation.

## Acknowledgements

*“No one who achieves success does so without the help of others. The wise and confident acknowledge this help with gratitude.”*

*Alfred North Whitehead*

To begin with, all praises, honor, and adoration are unto God Almighty, who in His infinite mercies has bestowed me with the gift of life and guided me through my years in this citadel of learning, giving me the strength, courage, and wisdom to complete this PhD program. I am incredibly grateful to my Co-Advisors, Dr. Christo Z. Christov and Dr. Tatyana G. Karabancheva-Christova, for their guidance and support during the program. I also want to express my sincere appreciation to my committee members, Dr. Tarun K. Dam, Dr. Haiying Liu, and Dr. Stephen Techtmann, who despite their busy schedules, contributed immensely to this journey.

Furthermore, I am thankful to my former and current lab members, Dr. Rajeev Ramanan, Dr. Shobhit Chaturvedi, Ann Varghese, and others, for all their support. I would like to thank Dr. Sarah Green and Dr. John Jaszczak, the current and former department chair, respectively, for providing all the necessary support during the program. I also want to express my sincere gratitude to my graduate teaching assistant (GTA) supervisor, Kelley Smith, and both the current and former department office staff, including Charlene Page, Megan Jarvi, Kimberly McMullan, Annie Ruohonen, and Denise Laux, for all their help and for providing necessary information pertinent for the successful completion of the program.

I appreciate the Department of Chemistry for all the financial support. I would also appreciate the support from other funding sources such as Doctoral Finishing Fellowship from Graduate School, NIH, NSF, Outstanding Graduate Students Summer Fellowship from the department, and Graduate Student Government (GSG) for the travel support for conferences. Also, I am thankful for the financial support from ACS Upper Peninsula Local Section (UPLS) for the ACS Fall 2022 National Meeting and Exposition, the Advancing Science Conference Grant (ASCG) from the National Organization for the professional Advancement of Black Chemists and Chemical Engineers (NOBCCChE) for the 2019, and 2022 NOBCCChE National Conferences and for always providing the free yearly ACS membership renewal.

Finally, I would like to express heartfelt gratitude to my friends and families, including the family of Ogunsanya, for all their countless support and encouragement all these years. You have all been the shoulders I have cried on during these years and have shown me numerous times that you all have my back. I will never take this for granted. To everyone that influenced my life positively on my way to greatness, I say a big thank you!

## List of Abbreviations

2OG	2-Oxoglutarate
Ala/A	Alanine
AMBER	Assisted Model Building with Energy Refinement
Arg/R	Arginine
Asn/N	Asparagine
Asp/D	Aspartate
CAT	Catalytic domain
CHARMM	Chemistry at HARvard Macromolecular Mechanics
Cys/C	Cysteine
DFT	Density Functional Theory
DNA	Deoxyribonucleic Acid
DSBH	Double Stranded $\beta$ Helix
dsDNA	Double Stranded DNA
EDA	Energy Decomposition Analysis
EEF	External Electric Fields
FF	Forcefield
FTO	Fat Mass and Obesity-Associated
GGA	Generalized Gradient Approximation
Gln/Q	Glutamine
Glu/E	Glutamate
Gly/G	Glycine
GROMOS	GRoningen MOlecular Simulation
His/H	Histidine

HPX	Hemopexin domain
Ile/I	Isoleucine
IM	Intermediate
LAMMPS	Large-scale Atomic/Molecular Massively Parallel Simulator
LDA	Local Density Approximation
Leu/L	Leucine
LSCF	Localized Self Consistent Field
Lys/K	Lysine
MCPB	Metal Center Parameter Builder
MD	Molecular Dynamics
Met/M	Methionine
MetD	Metadynamics
MM	Molecular Mechanics
MMGBSA	Molecular Mechanics Generalized Born Surface Area
MMP	Matrix Metalloproteinases
MMPBSA	Molecular Mechanics Poisson-Boltzmann Surface Area
NPT	Isobaric-isothermal ensemble
NVT	Canonical ensemble
ONIOM	Our own N-layered Integrated Molecular Orbital and Molecular Mechanics
OPLS	Optimized Potential Liquid Simulation
PC	Product Complex
PD	Product
PDB	Protein Data Bank
PES	Potential Energy Surface

Phe/F	Phenylalanine
PME	Particle Mesh Ewald
Pro/P	Proline
QM	Quantum Mechanics
QM/MM	Quantum Mechanics/Molecular Mechanics
RC	Reactant Complex
RNA	Ribonucleic Acid
Ser/S	Serine
SNO	Spin Natural Orbital
ssDNA	Single Stranded DNA
TET	Ten-Eleven Translocation
THP	Triple Helical Peptide
Thr/T	Threonine
TIP3P	Transferable Intermolecular Potential 3-Point
Trp/W	Tryptophan
TS	Transition State
Tyr/Y	Tyrosine
Val/V	Valine
WT	Wildtype
ZAFF	Zinc Amber Force Field
ZCT	Zero-Curvature Tunneling
ZPE	Zero Point Energy



## Abstract

Enzymes are biological systems that aid in specific biochemical reactions. They lower the reaction barrier, thus speeding up the reaction rate. A detailed knowledge of enzymes will not be achievable without computational modeling as it offers insight into atomistic details and catalytic species, which are crucial to designing enzyme-specific inhibitors and impossible to gain experimentally. This dissertation employs advanced multiscale computational approaches to study the dynamics and reaction mechanisms of non-heme Fe(II) and 2-oxoglutarate (2OG) dependent oxygenases, including AlkB, AlkBH2, TET2, and KDM4E, involved in DNA and histone demethylation. It also focuses on Zn(II) dependent matrix metalloproteinase-1 (MMP-1), which helps collagen degradation. Chapter 2 investigates the substrate selectivity and dynamics on the enzyme-substrate complexes of DNA repair enzymes, AlkB and FTO. Chapter 3 unravels the mechanisms and effects of dynamics on the demethylation of 3-methylcytosine substrate by AlkB and AlkBH2 enzymes. The results imply that the nature of DNA and conformational dynamics influence the electronic structure of the iron center during demethylation. Chapter 4 delineates how second-coordination and long-range residue mutations affect the oxidation of 5-methylcytosine substrate to 5-hydroxymethylcytosine by TET2 enzyme. The results reveal that mutations affect DNA binding/interactions and the energetic contributions of residues stabilizing key catalytic species. Chapter 5 describes the reparation of unnatural alkylated substrates by TET2, their effects on second-coordination interactions and long-range correlated motions in TET2. The study reveals that post-hydroxylation reactions occur in aqueous solution outside the enzyme environment. Chapter 6 establishes how applying external electric fields (EEFs) enhances specificity of KDM4E for C—H over

N—H activation during dimethylated arginine substrate demethylation. The results reveal that applying positive EEFs parallel to Fe=O bond enhances C—H activation rate, while inhibiting the N—H one. Chapter 7 addresses the formation of catalytically competent MMP-1•THP complex of MMP-1. The studies reveal the role of MMP-1's catalytic domain  $\alpha$ -helices, the linker, and changes in coordination states of catalytic Zn(II) during the transition. Overall, the presented results contribute to the in-depth understanding of the fundamental mechanisms of the studied enzymes and provide a background for developing enzyme-specific inhibitors against the associated disorders and diseases.

# 1 Introduction

Metalloenzymes are a class of enzymes that utilize metal ion as a cofactor in the active site of the enzymes for their enzymatic activities.<sup>1,2</sup> The catalytic activities of these enzymes depend on the presence of the metal ion cofactor, enhancing various forms of reactions, such as oxidation, reductions, and hydrolytic processes.<sup>1,2</sup> Enzymes are complex biomolecules found in nature, containing long chains of amino acid residues bound together via peptide bonds. They act as catalysts, making chemical reactions occur faster with excellent specificity. Enzymes have been greatly studied experimentally using X-ray crystallography and NMR spectroscopy.<sup>3-5</sup> These techniques have revealed the structure of enzymes and provided suggestions on how reactions occur.<sup>3</sup> Understanding the catalytic mechanisms of enzymes and their mode of action at the atomic level could contribute to the prediction of drug metabolism, inhibitors design, and design of catalysts for specific transformations.<sup>3,4</sup> Comprehensive knowledge of enzymes will not be completed without computational modeling as they offer an unparalleled opportunity to explore important conformational changes and enzymatic reaction mechanisms in detail, giving insight into processes that are of great biological importance. Hence, computational enzymology has the possibility to positively impact the development of predictive models of drug metabolism and structure-based design.<sup>6,7</sup>

Several computational methods, such as combined QM/MM methods,<sup>8-10</sup> molecular mechanics,<sup>11</sup> molecular dynamics simulations,<sup>12,13</sup> and quantum mechanics,<sup>8</sup> among others, have been employed to properly understand enzymes. Molecular dynamics simulations can

offer insight into conformational dynamics and flexibilities of biological systems using Newton's law of motion. The simulations can be carried out using molecular mechanics or its combination with quantum mechanics. Molecular mechanics are empirical methods that reproduce experimental data from some set of parameters.<sup>6</sup> These parameters and potential function of MM methods are described as a forcefield, which has been developed for proteins. MM calculations can be employed for large biomolecular systems because they are faster than QM methods. However, a typical MM method cannot model chemical reactions as it cannot provide the involved electronic details.<sup>7,9</sup> Hence, quantum mechanics has become a method of choice, but it is limited to only a few hundred atoms or even less if a more accurate and expensive QM level of theory is to be used. Enzymes are too large to be fully described using only QM methods, and due to the limitation of MM, as it cannot model processes involving bond cleavage and formation, a combined QM/MM becomes a valuable method. Combined QM/MM methods take the merit of both QM and MM methods in the study of enzymes.<sup>10,14-16</sup> Here, a small portion of the system where bond broken and formation occur (mostly the active site) is treated with quantum mechanics using ab initio or DFT methods, while the remaining larger part is treated with the low computational cost MM method.<sup>7,10,16</sup> QM/MM methods have been successfully applied to many enzymatic reactions and have provided beneficial insight into the catalytic processes, tremendously contributing to the increased knowledge of enzyme catalysis.<sup>17-22</sup>

## 1.1 Molecular Mechanics

Molecular mechanics (MM) method employs classical-type models for the prediction of molecular energy of systems based on their conformations. This permits the prediction of the relative energies between different molecules or between different conformers and equilibrium geometries. MM is the fastest and simplest way to evaluate biochemical systems containing thousands of atoms, as it neglects the systems' quantum mechanical and electronic aspects, including bond cleavage/formation.<sup>7,16</sup> Although MM is fast, it has limited precision significantly lower than quantum mechanics calculations and requires parameterization.

MM utilizes forcefields to calculate the potential energies between atoms. The system's energy is split into the summation of contributions from different processes, such as the bonds stretching, angles bending, and rotations around simple bonds (torsional angles),<sup>11,15</sup> etc. These all require parameters derived from experimental data or quantum mechanical calculations. The dependability of the forcefield is dependent on the exactness of the parameterization process.

Forcefield energy is the summation of all contributions from both the non-bonded and bonded interactions. The bonded interactions encompass bond stretching, angle, and torsional rotation, whereas the non-bonded interactions are electrostatic and van der Waals interactions, and a typical forcefield consists of all these terms.<sup>11,15</sup> The MM energy can be expressed as:

$$E_{MM} = E_{Bonds} + E_{Angles} + E_{Torsions} + E_{vdW} + E_{Electrostatic}$$

### 1.1.1 Bond Stretching

Bond stretching portrays the possible bonds [Figure 1.1a] like single, double, and triple bonds in the molecules. It accounts for the change in energy due to the shortening and elongation of chemical bonds in the molecules. The interaction is generally approximated by a harmonic potential using Hooke's law form.<sup>23,24</sup>

$$E_{Bonds} = \sum_{bonds} \frac{K_l}{2} (r - r_0)^2$$

In the above equation,  $K_l$  is the bond stretching force constant, whereas  $r_0$  and  $r$  are, respectively, equilibrium bond length and bond length. The force constant is determined from quantum calculations or via vibrational spectroscopy.

### 1.1.2 Angle Bending

The term accounts for the energy changes due to decrease or increase in bond angles [Figure 1.1b] from the reference values. The harmonic potential approximation is also employed similarly to the bond stretching mode.

$$E_{Angles} = \sum_{angles} \frac{K_\theta}{2} (\theta - \theta_0)^2$$

$K_\theta$  is the bending mode force constant, whereas  $\theta_0$  and  $\theta$  are, respectively, the equilibrium angle and the angle. As in bond stretching, the bending force constants are also determined by quantum calculation or experimentally via vibrational spectroscopy.

### 1.1.3 Torsional Terms

Torsions depict the rotation around bonds and are very important in determining the structure of molecules. They are often calculated via Fourier expansion of various cosine functions. The torsional energy originates from the steric and electrostatic nonbonded interactions between two atoms, D and G, which are connected via an intermediate bond E—F [Figure 1.1c]. The torsional energy can be expressed in terms of cosine functions:

$$E_{Torsions} = \sum_{n=1}^N \frac{V_n}{2} [1 + \cos(n\omega - \gamma)]$$

$V_n$  is the torsional force constant, and each torsion may be associated with several  $V_n$ ,  $n$  is the multiplicity, which accounts for the number of minima as the torsion is rotated through  $360^\circ$ .  $\omega$  is the torsional angle, while  $\gamma$  is the phase factor where the cosine function has its minimum.

Torsions are useful for conformational state sampling to find local and global minima.<sup>15</sup>



**Figure 1.1.** View of bonded interactions: a) bond stretching, b) angle bending, and c) torsional angle.

### 1.1.4 Electrostatic Interactions

Electrostatic term depicts the non-bonded interactions due to the existence of atomic charges and is represented by considering a Coulomb expansion. The electrostatic interactions term can be expressed as:

$$E_{Electrostatic} = \sum_{k < l}^N \frac{q_k q_l}{\epsilon r_{kl}}$$

$q_k$  and  $q_l$  are the atomic charges,  $r_{kl}$  denotes the distance between  $k$  and  $l$  atoms while  $\epsilon$  represents dielectric constant.

In all the available force fields, the difference in the electrostatic energy term depends on how the atomic charges are computed. Several available atomic charges include Mulliken charges,<sup>25</sup> Restrained Electrostatic Potential (RESP) charges,<sup>26</sup> Merz-Kollman charges,<sup>27</sup> Pullman charges,<sup>28</sup> Natural Bond Orbital (NBO) charges,<sup>29</sup> and Gasteiger charges,<sup>30</sup> etc.



### 1.1.5 Van der Waals Interactions

These interactions, expressed in terms of Lennard-Jones functions, describe the non-electrostatic attractive and repulsive interatomic forces. At small distances, the interactions are attractive, but when more than a few atoms separate the interacting atoms, the attraction rapidly falls to zero.

The van der Waals energy term is expressed as:

$$E_{vdw} = \sum_{i < j}^N \frac{A_{ij}}{r_{ij}^{12}} - \frac{B_{ij}}{r_{ij}^6}$$

$A_{ij}$  and  $B_{ij}$  are the Lennard-Jones parameters while,  $r_{ij}$  depicts the distance between  $i$  and  $j$  atoms.

Numerous force fields are available for biochemical systems, and in most biological simulations, CHARMM,<sup>31</sup> GROMOS,<sup>32</sup> OPLS,<sup>33</sup> and AMBER<sup>34,35</sup> are the commonly used molecular force fields. Several MM forcefields for biomolecular systems explicitly denote all atoms in proteins, while the others explicitly treat only polar hydrogen and non-hydrogen atoms.<sup>7</sup>

The development of forcefield parameters for organic molecules (non-standard amino acids or nucleic acids), whose information is not available in the library of the commercial software, can be done using webserver such as LigParGen,<sup>36</sup> SwissParam,<sup>37</sup> Charmm-GUI,<sup>38</sup> or using the Antechamber module<sup>39</sup> that is available in AMBER.

## 1.2 Molecular Dynamics Simulations

Molecular dynamics (MD) simulations estimate the atomic motions in molecules by employing the classical method to determine the acceleration and the force experienced by the atoms.

Simulations can capture various biochemical processes, such as protein folding, conformational changes, and ligand binding, and are commonly useful in the determination of X-ray structure and drug design.<sup>40,41</sup> An MD simulation generates a series of configurations of the system called trajectory as a function of time by integrating Newton's law of motion.<sup>42</sup>

$$\frac{d^2 x_i}{dt^2} = -\frac{F_{xi}}{m_i}$$

This expression gives the trajectory of the molecules where  $m_i$  is the particle mass and  $F_{xi}$  is the force acting along  $x_i$  coordinate. This integration, which gives the trajectory, describes the velocities, acceleration, and positions of the atoms making up the system as a function of time. The forces involved in the simulation are estimated using molecular mechanics force field (MMFF), which is fit to specific experimental data or the results from quantum mechanical calculations.

An appropriate time step ( $\Delta\tau$ ) needs to be selected during simulations and should be short compared to the period of the highest frequency motion in the system. For the fastest motion with period  $\tau$ , a good rule for selecting  $\Delta\tau$  can be:

$$\frac{\tau}{\Delta\tau} \approx 20$$

Simulations are often performed between nanoseconds (ns) to microsecond ( $\mu$ s) timescale, and the timesteps are in order of 1 femtosecond (fs).<sup>40,41,43</sup> These timesteps are often extended using the SHAKE algorithm<sup>44</sup> by fixing the motions of bonds involving hydrogen atoms as implemented in the available MD simulation packages. Simulation quality is determined by thermodynamic parameters such as cell dimension, kinetic energy, volume, potential energy, and temperature.<sup>13</sup> The temperature always fluctuates at about constant values during the entire simulation time. Also, root mean square deviation (RMSD), which measures the stability of the conformations generated during the simulation, can be used to determine the convergence of the simulation aside from the thermodynamic parameters.<sup>13</sup> MD simulations are applicable in protein-membrane interactions, structural determination and refinement, molecular recognition, ion transport in biological systems and can be performed with several software packages such as AMBER,<sup>35,45</sup> NAMD,<sup>46</sup> LAMMPS,<sup>47,48</sup> GROMACS,<sup>32,49</sup> CHARMM,<sup>31</sup> OpenMM,<sup>50,51</sup> and Desmond,<sup>52</sup> etc.

### **1.3 Classical Metadynamics Simulations**

Metadynamics belongs to the enhanced sampling methods, which allow the exploration of the free energy of complex biochemical systems.<sup>53-57</sup> It uses parameters termed collective variables (CVs), describing the reaction coordinate of the process under investigation. The main idea of metadynamics involves biasing the system's dynamics along the specified CVs using history-dependent bias repulsion potential.<sup>53,54,56</sup> The Gaussian potential is

added to the bias in the CVs space, thereby preventing the system from reexamining the already sampled configurations. The efficiency of metadynamics depends strongly on the choice of the CVs because if proper CVs are not considered, both the free energy and the transition states arising from such calculations will be wrong.<sup>43,54</sup> Collective variables that are functions of the atomic coordinates of the system, which must be carefully selected for metadynamics simulations, should fulfill the following guidelines: i) the CVs should be able to discriminate between the initial and final states as well as all the associated intermediates and transition states. Each state should correspond to different values of the CVs; otherwise, any bias added to one state will disfavor other states that possess the same CVs value.<sup>53,54</sup> ii) the number of CVs to be used should be limited. This is necessary because the central focus of metadynamics is to disfavor the already explored conformation. Using too large CVs number will make the filling of the multidimensional space difficult and more computationally expensive. It can make the system to never return to the same value of all the CVs.<sup>53,54</sup> iii) the CVs should portray all the slow events that are vital for the process under study.

Different CVs have been employed, and their selection is greatly dependent on the nature of the specific processes to be studied. Examples of commonly used CVs include geometry-related CVs such as bond lengths, angles, and dihedrals. These are the simplest forms of CVs used for biochemical systems' free energy surface calculations. Others are coordination numbers, dipole moment, radius of gyration (RoG), potential energy, number of hydrogen bonds, and the center of mass between atoms or groups of atoms pertinent to the process of interest.

A set of parameters determines the accuracy of the reconstruction of free energy during metadynamics simulations: i) Gaussian height, ii) Gaussian width, and iii) the deposition time.<sup>43,56</sup> The Gaussian height and deposition time govern the height and the rate at which the Gaussians are assigned. The error on the reconstructed profile is not determined by the deposition time and Gaussian height separately but by the ratio between the Gaussian height and the Gaussian deposition time.<sup>56,58</sup> Hence to achieve free energy profiles that are accurately reasonable, the Gaussian height must be amply small compared to the principal free energy barrier and must also not be added too often in time.<sup>43</sup> The method is applicable in the study of protein folding,<sup>59</sup> chemical reactions,<sup>55</sup> phase transitions,<sup>60,61</sup> for example, in the study of the conformational transition of a protein from an open conformational state to the closed one and vice versa.

## 1.4 Quantum Mechanics

Quantum mechanics methods are the most accurate approaches for the elucidation of the electronic structure of molecules and can model chemical reactions involving bond cleavage and formation, unlike molecular mechanics methods.<sup>14,15</sup> The quantum mechanics methods rely strongly on the Schrödinger equation to fully describe a molecule's electronic structure. The time-independent Schrödinger equation is expressed as:

$$\left[\frac{\hbar^2}{2m}\nabla^2 + V\right]\psi_n = E_n\psi_n$$

where the expression in the square bracket [] portrays the total energy operator consisting of both kinetic and potential energy, this operator is often called Hamiltonian with  $\hat{H}$  symbol in quantum mechanics. Schrödinger equation can be simplified to:

$$\hat{H}_n \psi_n = E_n \psi_n$$

The  $\hat{H}$ , which acts on wavefunction, is the summation of both the potential energy and the kinetic energy of the system, resulting in the total energy as an eigenvalue. The  $\hat{H}$  can be expressed mathematically as:

$$\hat{H} = \sum_a \frac{\hbar^2}{2m_e} \nabla_a^2 - \sum_b \frac{\hbar^2}{2m_b} \nabla_b^2 - \sum_a \sum_b \frac{Z_b e^2}{r_{ab}} + \sum_{a < c} \frac{e^2}{r_{ac}} + \sum_{b < d} \frac{Z_b Z_d e^2}{r_{bd}}$$

where  $a$  and  $c$  run over electrons,  $b$  and  $d$  run over nuclei,  $Z$  is the atomic number,  $e$  is the charge on the electron,  $m_b$  and  $m_e$  are the masses of nucleus and electron, respectively, and  $\nabla^2$  is the Laplacian operator. The Laplacian has the form:

$$\nabla_i^2 = \frac{\partial^2}{\partial x_i^2} + \frac{\partial^2}{\partial y_i^2} + \frac{\partial^2}{\partial z_i^2}$$

Schrödinger equation can be solved exactly for a single electron system such as hydrogen atom.<sup>15</sup> But the equation is difficult to be accurately solved for systems comprising more than one electron because of mathematical limitations. Therefore, for multi-electron systems, approximations are needed, and one of such approximations is the Born Oppenheimer approximation.<sup>62,63</sup> The approximation assumes the molecular systems nuclear and electronic motions can be separated, and the electronic wavefunction is not

dependent on their velocities but on their nuclear positions. The electron motion is much faster than the nuclear motion and the latter can thus be considered fixed.<sup>62,63</sup>

### 1.4.1 Density Functional Theory

In 1964, Hohenberg and Kohn introduced DFT, which predicts the properties of molecules based on the electron density of the molecules.<sup>64</sup> The electron density, a square of the wavefunction, is independent on the number of electrons; rather, it depends on the three spatial coordinates. DFT calculates the overall electronic energy by only considering the distribution of the total electron density. Hohenberg and Kohn suggested that in an inhomogeneous gas model, the electron density  $\rho(r)$  can be used to define the system's ground state energy. The energy functional is expressed as:

$$E[\rho(r)] = \int V_{e/ext}(r)\rho(r)dr + F[\rho(r)]$$

$F[\rho(r)]$  is the kinetic energy and the interelectronic interactions contributions while  $\int V_{e/ext}(r)\rho(r)dr$  is the electrons interaction with an external potential.

Kohn and Sham considered  $F[\rho(r)]$  to be the summation of three terms, namely, the kinetic energy of the system ( $E_{KE}[\rho(r)]$ ), Coulomb energy of electrons ( $E_H[\rho(r)]$ ) and the exchange and correlation energies ( $E_{XC}[\rho(r)]$ ).<sup>65</sup> Hence  $F[\rho(r)]$  is defined as:

$$F[\rho(r)] = E_{KE}[\rho(r)] + E_H[\rho(r)] + E_{XC}[\rho(r)]$$

The exchange-correlation energy describes the change in the kinetic energy between the real and the non-interacting systems, as well as the one involving quantum mechanics and classical mechanics electron-electron repulsion.<sup>15</sup> The main merit of DFT is the inclusion of the correlation energy function; however, finding an appropriate functional to describe the exchange-correlational energy is the challenge of DFT.<sup>66-68</sup> To address the challenge, various approximations have been put forward, leading to various functionals. The first approximation is local density approximation (LDA), the simplest approximation that includes interaction between electrons and the other electrons charge density, thereby simplifying electron-electron interactions. Local-spin density approximation (LSDA) is a generalized LDA with the inclusion of electron spin. This approximation is insufficient for molecules with nonuniform electron density but works perfectly for the solid-state electronic band structures calculations.<sup>15</sup> Generalized gradient approximation (GGA) method is an advancement to the LDA, with the inclusion of gradient correction factor. The gradient relates to non-uniformity that depicts the electron density and is referred to as gradient-corrected functionals. The gradient corrections are classified into separate correlational and exchange functionals like the Lee-Yang-Parr correlation function and the Becke exchange functional.<sup>69,70</sup> GGA methods give better energy barriers, structural energy difference, and total energies and are reliable for metallic, covalent, and ionic bonds; however, GGA fails for van der Waals interactions.<sup>71,72</sup> GGA methods were later improved to give meta-GGA where the functionals rely on the gradient, density, and their second-order derivatives.<sup>73</sup> The hybrid methods density functionals include a certain



percentage of Hartree-Fock, or exact exchange and are now the methods of choice for computational chemistry calculations.<sup>68,73</sup>

## 1.5 Quantum Mechanics and Molecular Mechanics

### (QM/MM) Methods

Warshel and Levitt first presented QM/MM as suitable methods to explore enzymatic reaction mechanisms in 1976.<sup>74</sup> The methods concomitantly use the merits of both the QM and MM methods and thus become a valuable tool for modeling biochemical systems. The system to be studied is separated into two parts [Figure 1.2]: the QM part, which is always the active site where the reaction occurs and the MM part, containing the rest of the enzyme.

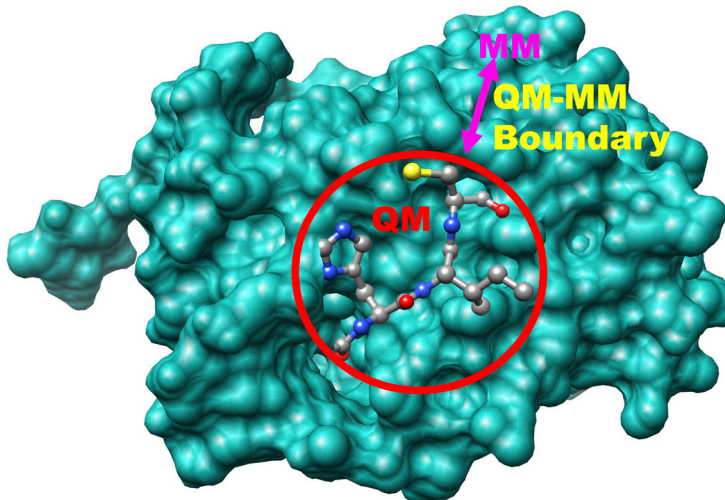


**Figure 1.2.** Representation of combined QM/MM methods.

The QM part captures the active site of the enzyme with the other surrounding catalytically important residues and is therefore used to model the bond cleavage/formation processes in the reaction mechanisms. However, the MM part, which always contains an enormous number of atoms, is always treated with an MM force field to annotate the effects of the protein environments. The QM/MM energy contains three different types of interaction, namely: i) the interactions between the QM region atoms, ii) interactions between atoms that are present in the MM regions, and (iii) interaction between the QM and MM regions atoms.<sup>9,14,16</sup> The first two interactions are relatively straightforward to be studied at both the QM and MM level, respectively, whereas the third interactions are more complex to be described, and numerous methods have been proposed.<sup>9,14</sup> These methods are categorized into additive and subtractive QM/MM schemes.<sup>9,10,14,16</sup>

### 1.5.1 Additive and Subtractive QM/MM Schemes

Additive methods calculate the final energy of the whole system as the summation of the QM and MM regions individual energies as well as the coupling term between them.<sup>9,14</sup>

The final energy of an additive QM/MM scheme is:

$$E_{QM/MM}^{full\ system} = E_{QM}^{QM\ region} + E_{MM}^{MM\ region} + E_{QM/MM}^{coupling}$$

The main drawback with this method is that it is difficult to accurately calculate the coupling energy between the two regions, particularly when link atoms are present.<sup>9,14</sup>

In the subtractive schemes, the energy of the various parts of the systems is calculated at different levels of theory. Various energies that are obtained are then combined to estimate

the final energy of the full system. In practice, the energy of the whole system is achieved in three steps: the total energy of the complete system is first computed at MM level, followed by the calculation of the energy of the QM part at the QM level of theory, and finally computing the QM region energy at MM level.<sup>10,14</sup> The complete energy of the system is then expressed as:

$$E_{QM/MM}^{full\ system} = E_{MM}^{full\ system} + E_{QM}^{QM\ region} - E_{MM}^{QM\ region}$$

The commonly used subtractive method is ONIOM method developed by Morokuma and coworkers.<sup>75-77</sup> Subtractive schemes have numerous merits over the other schemes, and the principal one is that no communication is required between the QM and the MM protocols,<sup>9,14</sup> making it relatively simple to implement. However, the schemes require a whole set of MM parameters for the QM regions, which is always hard to accomplish.<sup>78</sup> The coupling term between QM and MM region is wholly handled at MM level, which is difficult for electrostatic interaction.<sup>79</sup>

## 1.5.2 Handling of the Electrostatic QM/MM Interactions

The utmost challenge with QM/MM approaches is dealing with the non-bonded interactions between QM and MM regions.<sup>9</sup> The interactions, which include van der Waals forces and electrostatic interactions, are essential to be added in biochemical systems.<sup>9,10</sup> Three alternatives that can be used to handle the interactions are mechanical embedding, electrostatic embedding and polarized embedding.<sup>9,10,14,16</sup>

### **1.5.3 Mechanical Embedding**

Mechanical embedding method is the easiest and least computationally difficult method for the treatment of electrostatic interactions between the two partitioned regions.<sup>80</sup> This method neglects the electrostatics effects of the MM in the QM part, and the QM computation is carried out in gas phase. Electrostatic interaction between the two regions is either neglected or implemented by MM methods using the classical point charge approach for the distribution of QM charge.<sup>9,10</sup> One weakness of this method is that the QM region needs accurate MM parameters, and a single set of MM charges is not sufficient for the QM region.<sup>9,14</sup>

### **1.5.4 Electrostatic Embedding**

In electrostatic embedding, the QM layer is polarized by the MM part charge distribution.<sup>10,14</sup> This is achieved by incorporating certain one-electron terms obtained from the parameterized MM point charges into the QM protocol.<sup>10</sup> The results are better than the mechanical embedding scheme but neglect the polarization of MM part by the QM subsystem.<sup>9,14</sup>

### **1.5.5 Polarized Embedding**

Here, the polarization of MM part by the QM layer charge distribution is encompassed in the calculation.<sup>9,14</sup> The method is most appropriately used when the force field is based on explicit polarizability, and back-coupling of polarized charge density to QM calculation can sometimes be omitted. The merits of the method include more accurate treatment of

the solvation effect, and it allows coupling to systems where the force fields are based on polarization. However, the major drawbacks are the requirement for the polarized forcefields and are difficult to apply reliably when using link atoms due to the danger of electrostatic instabilities close to the boundaries.

### **1.5.6 Treatment of the QM and MM Boundary**

QM/MM method is a more straightforward procedure in a situation where the two regions are not covalently linked. However, the procedure becomes more complex where a covalent bond exists between the two regions, especially in enzymatic systems. To address this, two strategies are commonly applied: i) the link atom method and ii) the frozen orbital method [Figure 1.3].<sup>9,10,14,16</sup> In the first method, QM and MM boundary atoms are capped by adding a group of atoms or atoms generally referred to as “link atoms”. Hydrogen atoms are commonly used as link atoms; however, alternatives like pseudohalogens, methyl groups, or hydrogen-like atoms can also be employed.<sup>14</sup> The link atoms are invisible to the MM region and are treated as real atoms. The link atoms added extra degrees of freedom to the system under study; however, they are located at a fixed position, which enhances the removal of these additional degrees of freedom.<sup>9,81</sup> Numerous studies have reported that QM/MM results are dependent on how the link atoms are placed, and as such, it was suggested that link atoms should not cut across unsaturated or polar bonds.<sup>81</sup>

The frozen orbital approach involves using frozen and localized orbitals to saturate the dangling bonds between the two regions. The most common approaches are generalized hybrid orbital and localized self-consistent field.<sup>10,14</sup> In localized self-consistent field,

orbitals are introduced at the QM atoms, while in generalized hybrid orbital additional orbitals are positioned on the MM atoms [Figure 1.3]. The frozen orbital method offers a better description of the QM charge distribution around the QM/MM boundary than when link atoms are used.<sup>10</sup> The frozen orbital approach is advantageous over the link atoms because the delocalized representation in the orbital reduces/prevents the over-polarization effects typical of the link atom approach.<sup>9</sup>

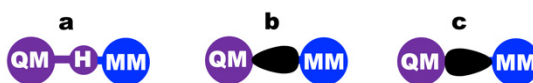


**Figure 1.3.** Various methods to saturate dangling bonds between QM and the MM regions: a) hydrogen link atom method, (b) and (c) are localized self-consistent field and generalized hybrid orbitals frozen orbitals approaches, respectively.

## 1.6 QM/MM Metadynamics

In QM/MM metadynamics, the active site of the enzymes is studied at any level of quantum mechanics during the metadynamics simulations compared to classical metadynamics, where the complete system is treated at molecular mechanics level. The method also uses collective variables (CVs) as in the classical metadynamics for the evaluation of the free energy surface. However, this is different from QM/MM methods described in the previous section, as QM/MM metadynamics takes into account the conformation of the enzymes and the effects of dynamics during the studied process. In the static QM/MM,

the MM layer is only reduced to point charges, and is employed in the QM/MM region wavefunction.<sup>8,82</sup>

## 1.7 Reaction Path Modeling

Reaction pathway studies investigate the complete reaction path of an enzymatic process. It enables the determination of energetic and structural information of the key catalytic species, such as the reactants, transition states, and all the associated intermediates during an enzymatic reaction.

Transition state structures connote the saddle points and energy maxima on the potential energy surface (PES).<sup>83</sup> These are theoretical entities that computational chemistry methods can only determine due to their unstable nature as they exist for a short time.<sup>83</sup> In transition state structures, the old bonds are partially cleaved, possessing slightly higher bond distances between the two atoms when compared to the starting complex, while the new ones are partly formed. The forces within the transition state internal degree of freedom are zero and possess one imaginary vibrational frequency.<sup>84</sup>

Different methods for reaction path modeling studies include adiabatic mapping and Nudged Elastic Band (NEB) methods. In adiabatic mapping, a reaction coordinate such as the distance between two different atoms, angles, dihedral angles, or combination of bond distances is defined in the starting structure. The system energy is then optimized at a fixed value of the reaction coordinate using force constant to uphold the needed reaction coordinate value.<sup>85</sup> The coordinate is subjected to scan by gradually increasing the reaction

coordinate in a stepwise manner, and each structure is energetically optimized at each step, giving the potential energy profile. It is the simplest method for the calculation of PES in many QM/MM calculations. In the NEB method, the starting and end structures must be known, and the transition states structures are interpolated between these two known reactants and products complexes.<sup>86</sup> The method works via optimizing a series of intermediate images along the reaction. NEB differs from the plain elastic band method because additional repulsive terms are incorporated between the images in NEB to enhance sampling near transition states.<sup>87</sup>

## 1.8 References

- (1) Hoppert, M. Metalloenzymes. In *Encyclopedia of Geobiology*; Reitner, J., Thiel, V., Eds.; Encyclopedia of Earth Sciences Series; Springer Netherlands: Dordrecht, 2011; pp 558–563.
- (2) Plaunt, A. J.; de Lourdes Betancourt-Mendiola, M.; Smith, B. D. Biomolecule Recognition Using Transition Metal Ions and Hydrogen Bonding. In *Comprehensive Supramolecular Chemistry II*; Elsevier, 2017; pp 575–591.
- (3) van der Kamp, M. W.; Mulholland, A. J. Computational Enzymology: Insight into Biological Catalysts from Modelling. *Nat. Prod. Rep.* **2008**, *25* (6), 1001.
- (4) Maveyraud, L.; Mourey, L. Protein X-Ray Crystallography and Drug Discovery. *Molecules* **2020**, *25* (5), 1030.
- (5) Sikic, K.; Tomic, S.; Carugo, O. Systematic Comparison of Crystal and NMR Protein Structures Deposited in the Protein Data Bank. *Open Biochem. J.* **2010**, *4*, 83–95.
- (6) Mulholland, A. J. Modelling Enzyme Reaction Mechanisms, Specificity and Catalysis. *Drug Discov. Today* **2005**, *10* (20), 1393–1402.
- (7) Lonsdale, R.; Harvey, J. N.; Mulholland, A. J. A Practical Guide to Modelling Enzyme-Catalysed Reactions. *Chem. Soc. Rev.* **2012**, *41* (8), 3025.
- (8) Ahmadi, S.; Barrios Herrera, L.; Chehelamirani, M.; Hostaš, J.; Jalife, S.; Salahub, D. R. Multiscale Modeling of Enzymes: QM-Cluster, QM/MM, and QM/MM/MD: A Tutorial Review. *Int. J. Quantum Chem.* **2018**, *118* (9), e25558.
- (9) Senn, H. M.; Thiel, W. QM/MM Methods for Biomolecular Systems. *Angew. Chem. Int. Ed Engl.* **2009**, *48* (7), 1198–1229.



- (10) Sousa, S. F.; Ribeiro, A. J. M.; Neves, R. P. P.; Brás, N. F.; Cerqueira, N. M. F. S. A.; Fernandes, P. A.; Ramos, M. J. Application of Quantum Mechanics/Molecular Mechanics Methods in the Study of Enzymatic Reaction Mechanisms. *WIREs Comput. Mol. Sci.* **2017**, *7* (2).
- (11) Vanommeslaeghe, K.; Guvench, O.; MacKerell, A. D. Molecular Mechanics. *Curr. Pharm. Des.* **2014**, *20* (20), 3281–3292.
- (12) Adcock, S. A.; McCammon, J. A. Molecular Dynamics: Survey of Methods for Simulating the Activity of Proteins. *Chem. Rev.* **2006**, *106* (5), 1589–1615.
- (13) Yu, H.; Dalby, P. A. A Beginner's Guide to Molecular Dynamics Simulations and the Identification of Cross-Correlation Networks for Enzyme Engineering. *Methods Enzymol.* **2020**, *643*, 15–49.
- (14) Cerqueira, N. M. F. S. A.; Fernandes, P. A.; Ramos, M. J. Protocol for Computational Enzymatic Reactivity Based on Geometry Optimisation. *ChemPhysChem* **2018**, *19* (6), 669–689.
- (15) Tzeliou, C. E.; Mermigki, M. A.; Tzeli, D. Review on the QM/MM Methodologies and Their Application to Metalloproteins. *Molecules* **2022**, *27* (9), 2660.
- (16) Groenhof, G. Introduction to QM/MM Simulations. In *Biomolecular Simulations*; Monticelli, L., Salonen, E., Eds.; Methods in Molecular Biology; Humana Press: Totowa, NJ, 2013; Vol. 924, pp 43–66.
- (17) Waheed, S. O.; Ramanan, R.; Chaturvedi, S. S.; Lehnert, N.; Schofield, C. J.; Christov, C. Z.; Karabancheva-Christova, T. G. Role of Structural Dynamics in Selectivity and Mechanism of Non-Heme Fe(II) and 2-Oxoglutarate-Dependent Oxygenases Involved in DNA Repair. *ACS Cent. Sci.* **2020**, *6* (5), 795–814.
- (18) Waheed, S. O.; Varghese, A.; Chaturvedi, S. S.; Karabancheva-Christova, T. G.; Christov, C. Z. How Human TET2 Enzyme Catalyzes the Oxidation of Unnatural Cytosine Modifications in Double-Stranded DNA. *ACS Catal.* **2022**, *12* (9), 5327–5344.
- (19) Waheed, S. O.; Chaturvedi, S. S.; Karabancheva-Christova, T. G.; Christov, C. Z. Catalytic Mechanism of Human Ten-Eleven Translocation-2 (TET2) Enzyme: Effects of Conformational Changes, Electric Field, and Mutations. *ACS Catal.* **2021**, *11* (7), 3877–3890.
- (20) Ramanan, R.; Waheed, S. O.; Schofield, C. J.; Christov, C. Z. What Is the Catalytic Mechanism of Enzymatic Histone N-Methyl Arginine Demethylation and Can It Be Influenced by an External Electric Field? *Chem. Weinh. Bergstr. Ger.* **2021**, *27* (46), 11827–11836.
- (21) Vasilevskaya, T.; Khrenova, M. G.; Nemukhin, A. V.; Thiel, W. Mechanism of Proteolysis in Matrix Metalloproteinase-2 Revealed by QM/MM Modeling. *J. Comput. Chem.* **2015**, *36* (21), 1621–1630.
- (22) Chen, B.; Kang, Z.; Zheng, E.; Liu, Y.; Gault, J. W.; Wang, Q. Hydrolysis Mechanism of the Linkers by Matrix Metalloproteinase-9 Using QM/MM Calculations. *J. Chem. Inf. Model.* **2021**, *61* (10), 5203–5211.
- (23) Mulholland, A. J. Computational Enzymology: Modelling the Mechanisms of Biological Catalysts. *Biochem. Soc. Trans.* **2008**, *36* (1), 22–26.
- (24) Waheed, S. O. Establishing the Mechanism of Glutaredoxin, University of Porto, 2018.

- (25) Mulliken, R. S. Criteria for the Construction of Good Self-Consistent-Field Molecular Orbital Wave Functions, and the Significance of LCAO-MO Population Analysis. *J. Chem. Phys.* **1962**, *36* (12), 3428–3439.
- (26) Bayly, C. I.; Cieplak, P.; Cornell, W.; Kollman, P. A. A Well-Behaved Electrostatic Potential Based Method Using Charge Restraints for Deriving Atomic Charges: The RESP Model. *J. Phys. Chem.* **1993**, *97* (40), 10269–10280.
- (27) Besler, B. H.; Merz, K. M.; Kollman, P. A. Atomic Charges Derived from Semiempirical Methods. *J. Comput. Chem.* **1990**, *11* (4), 431–439.
- (28) Berthod, H.; Pullman, A. Sur Le Calcul Des Caractéristiques Du Squelette  $\sigma$  Des Molécules Conjuguées. *J. Chim. Phys.* **1965**, *62*, 942–946.
- (29) Reed, A. E.; Curtiss, L. A.; Weinhold, F. Intermolecular Interactions from a Natural Bond Orbital, Donor-Acceptor Viewpoint. *Chem. Rev.* **1988**, *88* (6), 899–926.
- (30) Gasteiger, J.; Marsili, M. Iterative Partial Equalization of Orbital Electronegativity—a Rapid Access to Atomic Charges. *Tetrahedron* **1980**, *36* (22), 3219–3228.
- (31) Brooks, B. R.; Brucoleri, R. E.; Olafson, B. D.; States, D. J.; Swaminathan, S.; Karplus, M. CHARMM: A Program for Macromolecular Energy, Minimization, and Dynamics Calculations. *J. Comput. Chem.* **1983**, *4* (2), 187–217.
- (32) van Gunsteren, W. F.; Berendsen, H. J. C. Computer Simulation of Molecular Dynamics: Methodology, Applications, and Perspectives in Chemistry. *Angew. Chem. Int. Ed. Engl.* **1990**, *29* (9), 992–1023.
- (33) Jorgensen, W. L.; Tirado-Rives, J. The OPLS [Optimized Potentials for Liquid Simulations] Potential Functions for Proteins, Energy Minimizations for Crystals of Cyclic Peptides and Crambin. *J. Am. Chem. Soc.* **1988**, *110* (6), 1657–1666.
- (34) Weiner, S. J.; Kollman, P. A.; Case, D. A.; Singh, U. C.; Ghio, C.; Alagona, G.; Profeta, S.; Weiner, P. A New Force Field for Molecular Mechanical Simulation of Nucleic Acids and Proteins. *J. Am. Chem. Soc.* **1984**, *106* (3), 765–784.
- (35) Weiner, P. K.; Kollman, P. A. AMBER: Assisted Model Building with Energy Refinement. A General Program for Modeling Molecules and Their Interactions. *J. Comput. Chem.* **1981**, *2* (3), 287–303.
- (36) Dodda, L. S.; Cabeza de Vaca, I.; Tirado-Rives, J.; Jorgensen, W. L. LigParGen Web Server: An Automatic OPLS-AA Parameter Generator for Organic Ligands. *Nucleic Acids Res.* **2017**, *45* (W1), W331–W336.
- (37) Zoete, V.; Cuendet, M. A.; Grosdidier, A.; Michielin, O. SwissParam: A Fast Force Field Generation Tool for Small Organic Molecules. *J. Comput. Chem.* **2011**, *32* (11), 2359–2368.
- (38) Jo, S.; Kim, T.; Iyer, V. G.; Im, W. CHARMM-GUI: A Web-Based Graphical User Interface for CHARMM. *J. Comput. Chem.* **2008**, *29* (11), 1859–1865.
- (39) Wang, J.; Wang, W.; Kollman, P. A.; Case, D. A. Automatic Atom Type and Bond Type Perception in Molecular Mechanical Calculations. *J. Mol. Graph. Model.* **2006**, *25* (2), 247–260.
- (40) Durrant, J. D.; McCammon, J. A. Molecular Dynamics Simulations and Drug Discovery. *BMC Biol.* **2011**, *9* (1), 71.

- (41) Adcock, S. A.; McCammon, J. A. Molecular Dynamics: Survey of Methods for Simulating the Activity of Proteins. *Chem. Rev.* **2006**, *106* (5), 1589–1615.
- (42) Lodola, A.; Mulholland, A. J. Computational Enzymology. In *Biomolecular Simulations*; Monticelli, L., Salonen, E., Eds.; Methods in Molecular Biology; Humana Press: Totowa, NJ, 2013; Vol. 924, pp 67–89.
- (43) De Vivo, M.; Masetti, M.; Bottegoni, G.; Cavalli, A. Role of Molecular Dynamics and Related Methods in Drug Discovery. *J. Med. Chem.* **2016**, *59* (9), 4035–4061.
- (44) Ryckaert, J.-P.; Ciccotti, G.; Berendsen, H. J. C. Numerical Integration of the Cartesian Equations of Motion of a System with Constraints: Molecular Dynamics of n-Alkanes. *J. Comput. Phys.* **1977**, *23* (3), 327–341.
- (45) Pearlman, D. A.; Case, D. A.; Caldwell, J. W.; Ross, W. S.; Cheatham, T. E.; DeBolt, S.; Ferguson, D.; Seibel, G.; Kollman, P. AMBER, a Package of Computer Programs for Applying Molecular Mechanics, Normal Mode Analysis, Molecular Dynamics and Free Energy Calculations to Simulate the Structural and Energetic Properties of Molecules. *Comput. Phys. Commun.* **1995**, *91* (1–3), 1–41.
- (46) Nelson, M. T.; Humphrey, W.; Gursoy, A.; Dalke, A.; Kalé, L. V.; Skeel, R. D.; Schulten, K. NAMD: A Parallel, Object-Oriented Molecular Dynamics Program. *Int. J. Supercomput. Appl. High Perform. Comput.* **1996**, *10* (4), 251–268.
- (47) FrantzDale, B.; Plimpton, S. J.; Shephard, M. S. Software Components for Parallel Multiscale Simulation: An Example with LAMMPS. *Eng. Comput.* **2010**, *26* (2), 205–211.
- (48) Freitas, R.; Asta, M.; de Koning, M. Nonequilibrium Free-Energy Calculation of Solids Using LAMMPS. *Comput. Mater. Sci.* **2016**, *112*, 333–341.
- (49) Christen, M.; Hünenberger, P. H.; Bakowies, D.; Baron, R.; Bürgi, R.; Geerke, D. P.; Heinz, T. N.; Kastenholz, M. A.; Kräutler, V.; Oostenbrink, C.; Peter, C.; Trzesniak, D.; van Gunsteren, W. F. The GROMOS Software for Biomolecular Simulation: GROMOS05. *J. Comput. Chem.* **2005**, *26* (16), 1719–1751.
- (50) Eastman, P.; Pande, V. OpenMM: A Hardware-Independent Framework for Molecular Simulations. *Comput. Sci. Eng.* **2010**, *12* (4), 34–39.
- (51) Eastman, P.; Swails, J.; Chodera, J. D.; McGibbon, R. T.; Zhao, Y.; Beauchamp, K. A.; Wang, L.-P.; Simmonett, A. C.; Harrigan, M. P.; Stern, C. D.; Wiewiora, R. P.; Brooks, B. R.; Pande, V. S. OpenMM 7: Rapid Development of High Performance Algorithms for Molecular Dynamics. *PLOS Comput. Biol.* **2017**, *13* (7), e1005659.
- (52) *Schrödinger Release 2017-3: Desmond Molecular Dynamics System*; D. E. Shaw Research: New York, NY, **2017**; Maestro-Desmond Interoperability Tools, Schrödinger, New York, NY, **2017**.
- (53) Bussi, G.; Laio, A. Using Metadynamics to Explore Complex Free-Energy Landscapes. *Nat. Rev. Phys.* **2020**, *2* (4), 200–212.
- (54) Barducci, A.; Bonomi, M.; Parrinello, M. Metadynamics. *WIREs Comput. Mol. Sci.* **2011**, *1* (5), 826–843.
- (55) Ensing, B.; De Vivo, M.; Liu, Z.; Moore, P.; Klein, M. L. Metadynamics as a Tool for Exploring Free Energy Landscapes of Chemical Reactions. *Acc. Chem. Res.* **2006**, *39* (2), 73–81.

- (56) Laio, A.; Gervasio, F. L. Metadynamics: A Method to Simulate Rare Events and Reconstruct the Free Energy in Biophysics, Chemistry and Material Science. *Rep. Prog. Phys.* **2008**, *71* (12), 126601.
- (57) Sutto, L.; Marsili, S.; Gervasio, F. L. New Advances in Metadynamics: New Advances in Metadynamics. *Wiley Interdiscip. Rev. Comput. Mol. Sci.* **2012**, *2* (5), 771–779.
- (58) Laio, A.; Rodriguez-Fortea, A.; Gervasio, F. L.; Ceccarelli, M.; Parrinello, M. Assessing the Accuracy of Metadynamics. *J. Phys. Chem. B* **2005**, *109* (14), 6714–6721.
- (59) Gil-Ley, A.; Bussi, G. Enhanced Conformational Sampling Using Replica Exchange with Collective-Variable Tempering. *J. Chem. Theory Comput.* **2015**, *11* (3), 1077–1085.
- (60) Martoňák, R.; Laio, A.; Bernasconi, M.; Ceriani, C.; Raiteri, P.; Zipoli, F.; Parrinello, M. Simulation of Structural Phase Transitions by Metadynamics. *Z. Für Krist. - Cryst. Mater.* **2005**, *220* (5–6), 489–498.
- (61) Waheed, S. O.; Varghese, A.; DiCatri, I.; Kaski, B.; LaRouche, C.; Fields, G. B.; Karabancheva-Christova, T. G. Mechanism of the Early Catalytic Events in the Collagenolysis by Matrix Metalloproteinase-1. *ChemPhysChem* **2023**, *24*(3), e202200649. <https://doi.org/10.1002/cphc.202200649>.
- (62) Combes, J. M.; Duclos, P.; Seiler, R. The Born-Oppenheimer Approximation. In *Rigorous Atomic and Molecular Physics*; Velo, G., Wightman, A. S., Eds.; Springer US: Boston, MA, 1981; pp 185–213.
- (63) Woolley, R. G.; Sutcliffe, B. T. Molecular Structure and the Born—Oppenheimer Approximation. *Chem. Phys. Lett.* **1977**, *45* (2), 393–398.
- (64) Hohenberg, P.; Kohn, W. Inhomogeneous Electron Gas. *Phys. Rev.* **1964**, *136* (3B), B864–B871.
- (65) Kohn, W.; Sham, L. J. Self-Consistent Equations Including Exchange and Correlation Effects. *Phys. Rev.* **1965**, *140* (4A), A1133–A1138.
- (66) Kristyan, S. Theory of Variational Calculation with a Scaling Correct Moment Functional to Solve the Electronic Schrödinger Equation Directly for Ground State One-Electron Density and Electronic Energy. *Int. J. Quantum Chem.* **2013**, *113* (10), 1479–1492.
- (67) Kristyán, S.; Csonka, G. I. New Development in RECEP (Rapid Estimation of Correlation Energy from Partial Charges) Method. *Chem. Phys. Lett.* **1999**, *307* (5–6), 469–478.
- (68) Sousa, S. F.; Fernandes, P. A.; Ramos, M. J. General Performance of Density Functionals. *J. Phys. Chem. A* **2007**, *111* (42), 10439–10452.
- (69) Lee, C.; Yang, W.; Parr, R. G. Development of the Colle-Salvetti Correlation-Energy Formula into a Functional of the Electron Density. *Phys. Rev. B Condens. Matter* **1988**, *37* (2), 785–789.
- (70) Becke, A. D. Density-Functional Exchange-Energy Approximation with Correct Asymptotic Behavior. *Phys. Rev. Gen. Phys.* **1988**, *38* (6), 3098–3100.
- (71) Tao, J.; Perdew, J. P. Test of a Nonempirical Density Functional: Short-Range Part of the van Der Waals Interaction in Rare-Gas Dimers. *J. Chem. Phys.* **2005**, *122* (11), 114102.

- (72) Patton, D. C.; Pederson, M. R. Application of the Generalized-Gradient Approximation to Rare-Gas Dimers. *Phys. Rev. A* **1997**, *56* (4), R2495–R2498.
- (73) Zhao, Y.; Truhlar, D. G. The M06 Suite of Density Functionals for Main Group Thermochemistry, Thermochemical Kinetics, Noncovalent Interactions, Excited States, and Transition Elements: Two New Functionals and Systematic Testing of Four M06-Class Functionals and 12 Other Functionals. *Theor. Chem. Acc.* **2008**, *120* (1–3), 215–241.
- (74) Warshel, A.; Levitt, M. Theoretical Studies of Enzymic Reactions: Dielectric, Electrostatic and Steric Stabilization of the Carbonium Ion in the Reaction of Lysozyme. *J. Mol. Biol.* **1976**, *103* (2), 227–249.
- (75) Chung, L. W.; Sameera, W. M. C.; Ramozzi, R.; Page, A. J.; Hatanaka, M.; Petrova, G. P.; Harris, T. V.; Li, X.; Ke, Z.; Liu, F.; Li, H.-B.; Ding, L.; Morokuma, K. The ONIOM Method and Its Applications. *Chem. Rev.* **2015**, *115* (12), 5678–5796.
- (76) Chung, L. W.; Hirao, H.; Li, X.; Morokuma, K. The ONIOM Method: Its Foundation and Applications to Metalloenzymes and Photobiology: ONIOM Method. *Wiley Interdiscip. Rev. Comput. Mol. Sci.* **2012**, *2* (2), 327–350.
- (77) Dapprich, S.; Komáromi, I.; Byun, K. S.; Morokuma, K.; Frisch, M. J. A New ONIOM Implementation in Gaussian98. Part I. The Calculation of Energies, Gradients, Vibrational Frequencies and Electric Field Derivatives. *J. Mol. Struct. THEOCHEM* **1999**, *461–462*, 1–21.
- (78) Cao, L.; Ryde, U. On the Difference Between Additive and Subtractive QM/MM Calculations. *Front. Chem.* **2018**, *6*, 89.
- (79) Kumbhar, S.; Fischer, F. D.; Waller, M. P. Assessment of Weak Intermolecular Interactions Across QM/MM Noncovalent Boundaries. *J. Chem. Inf. Model.* **2012**, *52* (1), 93–98.
- (80) Zhang, Y.; Lin, H.; Truhlar, D. G. Self-Consistent Polarization of the Boundary in the Redistributed Charge and Dipole Scheme for Combined Quantum-Mechanical and Molecular-Mechanical Calculations. *J. Chem. Theory Comput.* **2007**, *3* (4), 1378–1398.
- (81) Sousa, S. F.; Fernandes, P. A.; Ramos, M. J. Computational Enzymatic Catalysis – Clarifying Enzymatic Mechanisms with the Help of Computers. *Phys. Chem. Chem. Phys.* **2012**, *14* (36), 12431.
- (82) Brunk, E.; Rothlisberger, U. Mixed Quantum Mechanical/Molecular Mechanical Molecular Dynamics Simulations of Biological Systems in Ground and Electronically Excited States. *Chem. Rev.* **2015**, *115* (12), 6217–6263.
- (83) Wolfenden, R. Analog Approaches to the Structure of the Transition State in Enzyme Reactions. *Acc. Chem. Res.* **1972**, *5* (1), 10–18.
- (84) Tuñón, I.; Williams, I. H. The Transition State and Cognate Concepts. In *Advances in Physical Organic Chemistry*; Elsevier, 2019; Vol. 53, pp 29–68.
- (85) Ranaghan, K. E.; Mulholland, A. J. Investigations of Enzyme-Catalysed Reactions with Combined Quantum Mechanics/Molecular Mechanics (QM/MM) Methods. *Int. Rev. Phys. Chem.* **2010**, *29* (1), 65–133.
- (86) Ayala, P. Y.; Schlegel, H. B. A Combined Method for Determining Reaction Paths, Minima, and Transition State Geometries. *J. Chem. Phys.* **1997**, *107* (2), 375–384.

(87) Czerminski, R.; Elber, R. Self-Avoiding Walk between Two Fixed Points as a Tool to Calculate Reaction Paths in Large Molecular Systems. *Int. J. Quantum Chem.* **1990**, *38* (S24), 167–185.

## 2 Conformational Flexibility Influences Structure-Function Relationships in Nucleic Acid N-Methyl Demethylases

**Sodiq O. Waheed**,<sup>a,&</sup> Rajeev Ramanan,<sup>a,&</sup> Shobhit S. Chaturvedi,<sup>a</sup> Jon Ainsley,<sup>b</sup> Martin Evison,<sup>b</sup> Jennifer M. Ames,<sup>c</sup> Christopher J. Schofield,<sup>d, \*</sup> Christo Z. Christov,<sup>a,b, \*</sup> and Tatyana G. Karabancheva-Christova<sup>a,b,\*</sup>

<sup>a</sup> Department of Chemistry, Michigan Technological University, Houghton, Michigan 49931, United States.

<sup>b</sup> Faculty of Health and Life Sciences, Northumbria University, Newcastle upon Tyne, NE1 8ST, United Kingdom.

<sup>c</sup> Centre for Research in Biosciences, Faculty of Health and Applied Sciences, University of the West of England, Bristol, BS16 1QY, United Kingdom. Present address: Jenny Ames Consulting Ltd, Reading, RG6 5PY, United Kingdom.

<sup>d</sup> The Chemistry Research Laboratory, The Department of Chemistry, Mansfield Road, University of Oxford, Oxford, OX1 3TA, United Kingdom.

<sup>&</sup>S.O.W., and R.R. made equal contributions to this article.

\*Corresponding authors: C.J.S. (christopher.schofield@chem.ox.ac.uk), C.Z.C. (christov@mtu.edu), and T.G.K.C. (tatyanak@mtu.edu)

---

The content of this chapter was previously published in the *Org. Biomol. Chem.*, **2019**, 17, 2223-2231. DOI: 10.1039/C9OB00162J, reproduced with permission from the Royal Society of Chemistry.

## 2.1 Introduction

N-Methylation of DNA/RNA bases can be toxic causing mutagenesis or can be regulatory.<sup>1-4</sup> 2-Oxoglutarate (2OG) and Fe(II) dependent oxygenases play key roles in N-methyl demethylation of nucleic acids in organisms ranging from bacteria to humans (Figure 2.1).<sup>4-7</sup> 2OG oxygenases typically employ an active site containing a single Fe(II) ion ligated by one Asp and two His residues; ligation of water and 2OG (in a bidentate manner) completes a six coordinate (6C) octahedral geometry<sup>8,9</sup> (Figure A1). AlkB is a bacterial repair enzyme with broad substrate specificity towards alkylated bases/exocyclic bridge-containing lesions.<sup>10,11</sup> AlkB type enzymes are the likely precursors of eukaryotic 2OG dependent nucleic acid oxygenases, some of which are linked to important biological processes and diseases. The Fat Mass and Obesity-Associated Protein (FTO) is an eukaryotic AlkB homolog which likely mainly demethylates N-methylated bases in RNA; mutations to the FTO gene in humans are linked to changes in body mass.<sup>11-13</sup>

Crystal structures of AlkB<sup>10</sup> and FTO<sup>5</sup> reveal a distorted double stranded beta helix (DSBH, or 'jelly roll') catalytic core fold which is conserved in 2OG oxygenases. The nucleic acid oxygenase subfamily of 2OG oxygenases manifests characteristic elements, including an Arg-containing motif involved in 2OG C5 carboxylate binding. In addition to its core DSBH fold (aa. 91-214), AlkB contains an N-terminal extension (aa.13-44), a nucleotide recognition lid (aa. 45-90) and active site bordering loop (aa. 132-143). FTO has an N-terminal AlkB-like domain (aa. 32-326), a C-terminal domain (residues 327-498), and a loop involved in the recognition of single stranded substrates. AlkB and FTO recognize



specific differently alkylated DNA/RNA bases<sup>1,2,11,14</sup>. Clinically observed mutations in FTO, e.g. R316Q, S319F, and R322Q correlate with pathological changes including growth retardation, developmental delay, and facial dysmorphism<sup>15-17</sup>. Other substitutions in AlkB (T51A, W69A, Y76A, D135A, R161A) and FTO (F114D, C392D) are reported to affect catalysis.<sup>5,18</sup> Substitutions of the active site residues in AlkB and FTO have also been reported to result in changing of substrate selectivity.<sup>10</sup>

Studies on the modification of methyl groups on DNA and RNA are of interest from basic research and applied perspectives because of the importance of methylation in regulation and its ability to define particular types of tissues/cells. Methylation of DNA bases are part of normal gene expression and epigenetic processes, but abnormal DNA methylation patterns are characteristic of certain cancers and genetic disorders. Tissue and age-related methylation patterns are useful in forensic investigations of trace amounts of biological samples.<sup>19</sup>

Studies on nucleic acid oxygenases, including AlkB/FTO catalysis,<sup>20-24</sup> indicate that they operate via the overall consensus mechanism for 2OG oxygenases (Scheme 2.1). The limited solution NMR studies on 2OG oxygenases, including on AlkB and a prolyl hydroxylase, imply major conformational changes, especially for AlkB, during Fe(II), co-substrate and substrate binding/catalysis.<sup>25,26</sup> However, there is not yet an understanding of how long-range conformational dynamics and correlated motions influence structure-function relationships. There is also incomplete knowledge regarding flexibility in the 2OG binding site; this is important with respect to understanding how 2OG co-substrate binding

selectivity is achieved and in their inhibition, since most reported 2OG oxygenase inhibitors chelate Fe(II) and compete with 2OG.<sup>27</sup> How conformational flexibility influences substrate selectivity, e.g. the experimental finding that 1-methyladenine (1MA) is a better substrate than 6-methyladenine (6MA) for AlkB is also unclear.

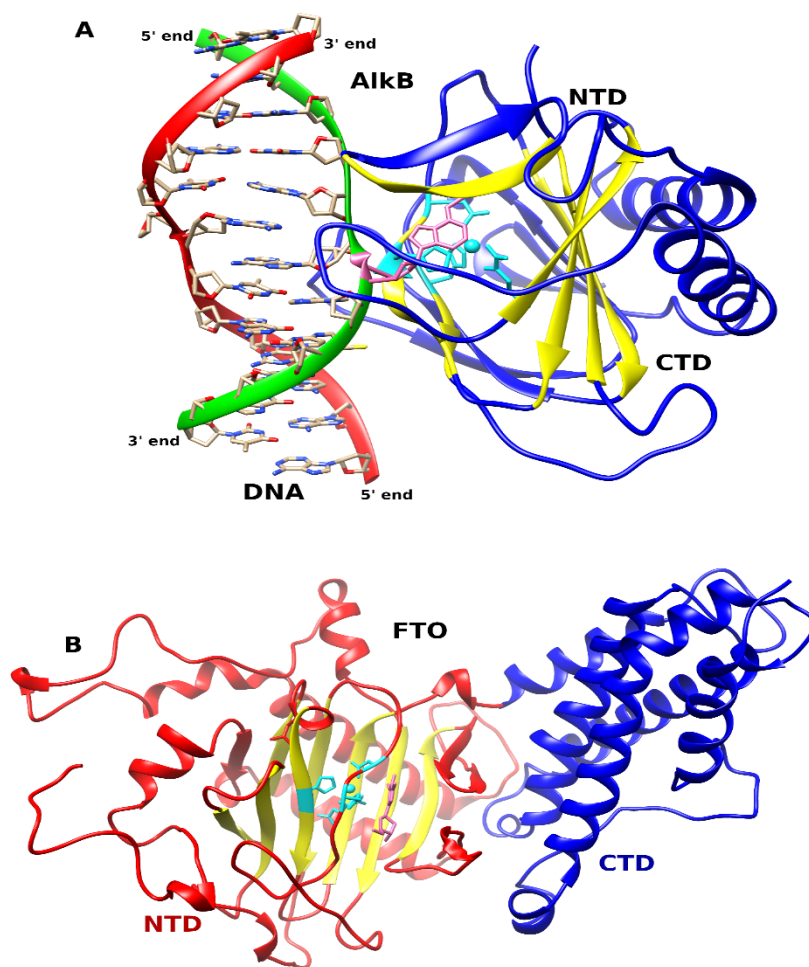
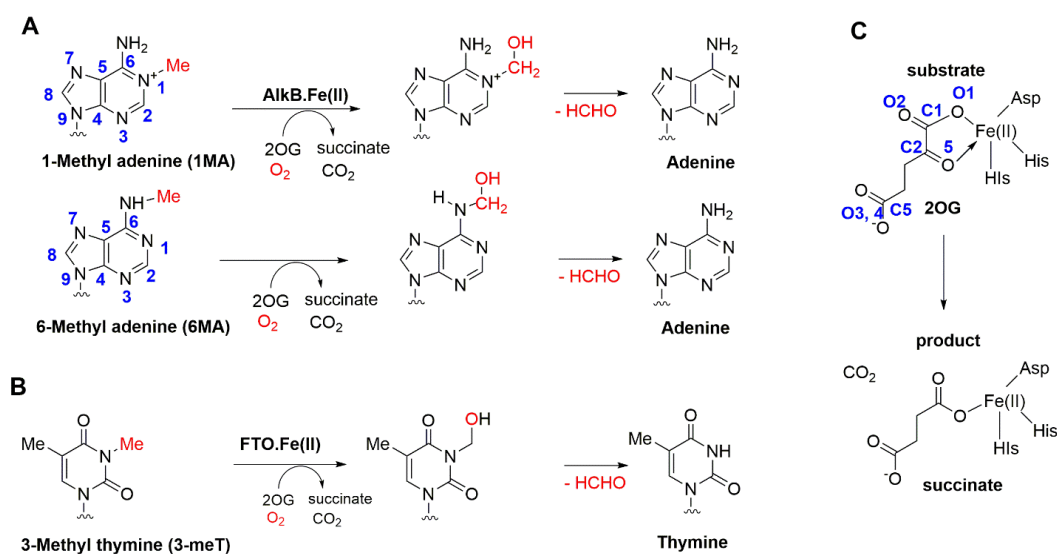


**Figure 2.1.** Average structures of AlkB and FTO derived from MD simulations. Coloring: double stranded beta helix (DSBH) core fold (yellow), active site (cyan), and substrate (pink).

We report investigations on this missing knowledge using long-range Molecular Dynamics (MD) simulations, free energy calculations, and Combined Quantum Mechanics and Molecular Mechanics (QM/MM) studies on enzyme-substrate complexes of representative nucleic acid oxygenases, i.e. AlkB and its larger and apparently more complex human homologue FTO. Related computational strategies have been successfully implemented for investigating structure-function relationships of various other enzymes.<sup>28-33</sup> The results show conformational dynamics exercise distinct effects in AlkB and FTO and are important in determining substrate selectivity. Specific residues in AlkB/FTO play important roles in correlated motions/flexibility and are important in maintaining the productive geometry of reactant complexes.



**Scheme 2.1.** Reactions catalysed by AlkB (A) and FTO (B). Demethylation proceeds via hydroxylation, which is mediated via an Fe=O (IV) intermediate, to form a hemiaminal which fragments to give formaldehyde and the product. (C) Both the AlkB and FTO reactions are coupled to the conversion of 2-oxoglutarate and O<sub>2</sub> to succinate and CO<sub>2</sub>.

## 2.2 Computational Methods

### 2.2.1 System Preparation

An X-ray crystal structure of FTO (PDB ID code: 4IDZ<sup>3</sup>) was used for building the FTO model used in the computational studies. Missing residues from loop regions were added using Modeller.<sup>34</sup> A crystal structure of the AlkB (PDB: 4NID<sup>10</sup> in complex with Mn(II), 2-oxoglutarate (2OG) and double stranded DNA containing N6-methyladenine (6MA)) was used in computational studies. The Mn(II) was replaced with Fe(II). AlkB was also modelled with the nucleoside only (6MA (nsd)) instead of double stranded DNA to compare with the FTO single base simulations and to investigate how the DNA affects the conformational dynamics of AlkB. A wildtype structure of AlkB (PDB: 3BIE<sup>35</sup>) with substrate N1-Methyladenine (m1A) was also used in simulation studies. The parameters for the substrate were developed using Antechamber. The likely protonation states of ionisable sidechains of the proteins were assessed using the H++ server.<sup>36</sup> Histidine residues coordinating with the metal centre were assigned protonation states based on visual inspection of their local environment. The Amber parameters for the active site containing Fe(II) high spin S=2, M=5, ground state <sup>8,9,14,22</sup> and the coordinating ligands (2OG, with bidentate ligation), histidine, and aspartic acid (both via monodentate ligation) were prepared using the Metal Centre Parameter Builder (MCPB) using MCPB.py v1.0 Beta2<sup>37</sup> for a 5-coordinate (5C) distorted square pyramidal active site.

## 2.2.2 MD Simulations

Molecular dynamics simulations were performed using the GPU version<sup>38</sup> of PMEMD engine integrated with Amber 14.<sup>39</sup> The FF14SB<sup>40</sup> force field was used in all the simulations and the Leap module was used to add missing hydrogen atoms and counter ions for neutralisation of the protein system. All the systems were immersed into a truncated octahedral box with TIP3P water molecules,<sup>41</sup> such that no protein atom was within 10 Å of any box edge. Periodic boundary conditions were employed in all the simulations. Long-range electrostatic interactions were calculated using the Particle Mesh Ewald (PME) method<sup>42</sup> with a direct space and vdW cut-off of 8 Å. The various systems were subjected to energy minimization using first steepest descent (5000 steps) followed by conjugate gradient (5000 steps) to eliminate clashes. Solute molecules were restrained using a restrained potential of 100 kcal mol<sup>-1</sup> Å<sup>2</sup>; only solvent and ions were allowed to minimize. This was followed by full minimization of the entire system with both steepest descent (5000 steps) and conjugate gradient (5000 steps) treatments to relax the system prior to productive simulation. The systems were then subjected to controlled heating from 0 to 300K at constant volume using the Langevin thermostat<sup>43</sup> with a collision frequency of 1 ps<sup>-1</sup> using a canonical ensemble (NVT) MD simulation for 400 ps. The solute molecules were restrained using a harmonic potential of 10 kcal mol<sup>-1</sup> Å<sup>2</sup> during the heating process. The SHAKE algorithm<sup>44</sup> was used to constrain bonds involving hydrogen. This was followed by equilibration at 300K in an isothermal-isobaric ensemble (NPT) for 1 ns without restraints on solute molecules. The pressure was maintained at 1 bar using the Berendsen barostat.<sup>45</sup> A productive MD run with explicit solvent for continuous 1μs was

performed in an NPT ensemble with a target pressure set at 1 bar and constant pressure coupling of 2ps. The frames from the productive run were saved every 10 ps. Trajectories were analysed using CPPTRAJ,<sup>46</sup> VMD,<sup>47</sup> UCSF Chimera,<sup>48</sup> and R (Bio3D<sup>49</sup>).

### **2.2.3 QM/MM calculations**

Snapshots for the QM/MM calculations were obtained from the MD simulations on all the systems. These snapshots were first subjected to energy minimization for 10,000 steps by using both steepest descend (5000) and conjugate gradient (5000) algorithms in Amber14. Active site residues were restrained with a restrained potential of  $100 \text{ kcal mol}^{-1} \text{ \AA}^2$  in the energy minimization, to maintain the geometry of the active site. The energy minimized snapshots of all the enzymes were prepared using the Schlegel's toolkit TAO<sup>50</sup> for ONIOM<sup>51-55</sup> calculation in Gaussian09.<sup>56</sup> Residues within 20 Å of Fe(II), including water molecules, were allowed to move freely during geometry optimization; the rest of the system was frozen during geometry optimization in ONIOM. Hydrogen atoms were used as the link atoms to saturate the dangling bond in the QM/MM calculation.<sup>57</sup> The electrostatic embedding scheme was used in the geometry optimization however, we also used the mechanical embedding scheme for some snapshots.

## **2.2.4 Molecular Mechanics/Generalized Born Surface Area (MM/GBSA)**

The binding free energy calculations with AlkB were performed using the Molecular Mechanics/Generalized Born Surface Area (MM/GBSA) approach.<sup>58-60</sup> More details of computational methods are provided in the Supporting Information.

## **2.3 Results and Discussion**

MD simulations of the complex of AlkB with Fe(II), 2OG and DNA substrate containing 6-methyl adenine (AlkB-6MA(DNA)) imply the Fe(II) centre and its ligands (His131, His187, and Asp133) are conformationally stable, as are second sphere interactions of (i) the two ligating histidines with C129 and F185, and (ii) the interaction of D133 with W178 (Figure A2). However, interactions between the non-coordinating carboxyl oxygen of the monodentate ligating D133 with R210 are strengthened compared to the crystal structure, in agreement with NMR studies showing the presence of a hydrogen bond stabilising monodentate coordination of the Fe(II) ligating carboxylate in some 2OG oxygenases<sup>25</sup> (Figure A2).

To explore the effects of the flexibility of the DNA substrate on the enzyme-substrate complex, we performed simulations with AlkB complexed with Fe(II), 2OG and 6MA nucleoside (AlkB-6MA (nsd)). The results reveal that the average distance between the substrate methyl group and Fe(II) is not substantially different in AlkB-6MA (DNA) and

AlkB-6MA (nsd) (Figure 2.2) indicating that this interaction is not influenced by the bulk DNA, at least once a substrate is bound.

1-Methyl adenine (1MA) is reported to be a better AlkB substrate than 6MA.<sup>10,11,14</sup> To investigate the atomistic reasons for this, we simulated the AlkB, Fe(II), 2OG with the 1MA nucleoside (AlkB-1MA (nsd)). The simulations show that the distance between the methyl group of 1MA and Fe(II) is stable during the simulation and is lower compared to the analogous distances in AlkB-6MA(nsd) and AlkB-6MA(DNA) (Figure 2.2). An apparently key hydrogen bond between the N6 of 1MA and D135, as observed in the crystal structure, is stable with 1MA in contrast to 6MA in AlkB-6MA (nsd) and AlkB-6MA (DNA), consistent with 1MA being a better substrate for AlkB than 6MA (Figure 2.3).



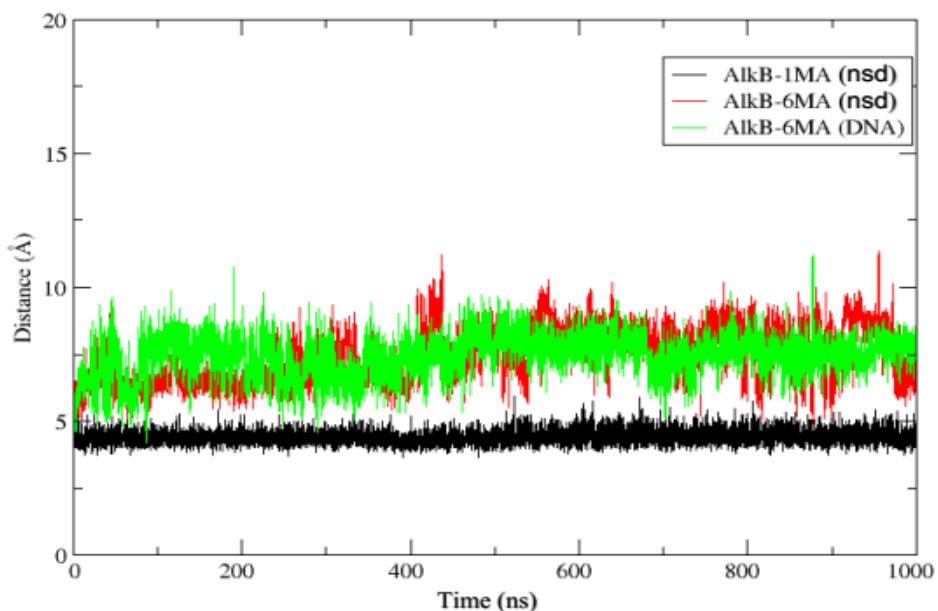


**Figure 2.2.** The distance between Fe(II) and the carbon atom of the substrate methyl group in AlkB-1MA (nsd), AlkB-6MA (nsd), and AlkB-6MA (DNA) during the MD simulations. The results show the overall binding mode of 6MA at the active site is not strongly affected depending on if it is in a nucleic acid sequence or not. 1MA is apparently better positioned for demethylation than 6MA during the entire simulations.

The adenine ring in AlkB-1MA (nsd) is bound/orientated by stable interactions with the H131, W69, and Y78 side chains. With 6MA, stacking interactions of the adenine ring of AlkB-6MA (DNA) and AlkB-6MA (nsd) with W69 and H131 manifest more flexibility than with 1MA. The stability of the interactions in 1MA likely reflects its stronger binding in the active site of the AlkB compared with 6MA. To calculate the binding affinities of 1MA and 6MA, we performed free energy calculations; the MMGBSA method gave

relative free energies of binding of -4.8 for AlkB-1MA) and -2.0 kcal/mol for AlkB-6MA) (Table A1), again consistent with the experimental observations<sup>10</sup>.

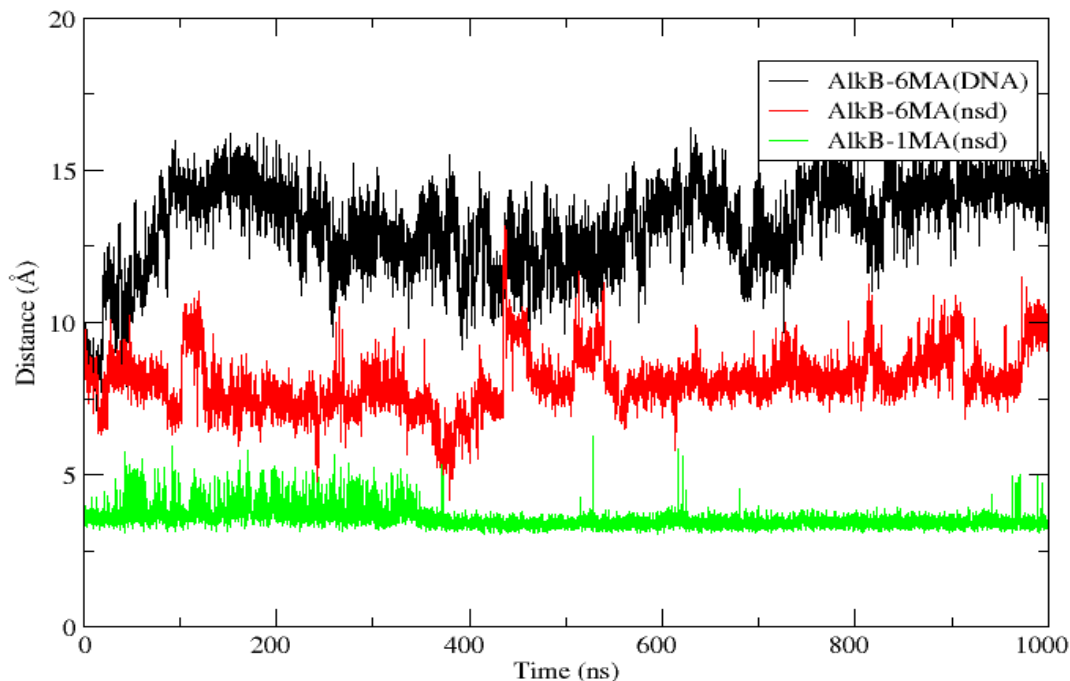


**Figure 2.3.** The hydrogen bond interactions of the N6 of the substrates (1MA(nsd), 6MA(nsd) and 6MA(DNA)) with D135 in AlkB. Distances were measured between the centres of masses of the substrates and the carboxyl group of the ligating aspartate (D135).

In FTO, Fe(II), 2OG and the N-methyl group of the 3-methyl thymidine (3-meT) substrate make stable interactions (Figure A3). The Y108 and H132 side chains are positioned to stabilize the 3-meT substrate ring via  $\pi$ - $\pi$  stacking interactions (Figure A3); the deoxyribose ring of 3-meT is stabilized by the L109 side chain, as proposed from crystallographic analyses<sup>12</sup> (Figure A3). A hydrogen bond between E234 and O4 of 3-meT

and a hydrophobic cluster formed by L203, Y106, and Y108 involved in binding the 3-meT methyl group are also stable (Figure A3). R96 is involved in binding both the non-ligating C1 carboxylate oxygen (O1) of 2OG and 3-meT, the latter via hydrogen bonds with O2 of 3-meT. The key role of R96 is confirmed by inhibition<sup>61,62</sup> and mutagenesis studies, including by showing the R96H variant manifests reduced activity.<sup>7</sup>

In AlkB, R204 makes a stable electrostatic interaction with the non-coordinating 2OG C5 carboxylate with an average distance of 4.0 Å (Figure A4). The C5 carboxylate of 2OG is further stabilised by hydrogen bonds with the side chains of Y122, N120, and N206, as observed crystallographically.<sup>10</sup> The R210 side chain is positioned to hydrogen bond with the D133 carboxylate in AlkB-1MA (nsd), in contrast to AlkB-6MA (DNA) and AlkB-6MA (nsd) where limited interactions are observed (Figure A5). The hydrogen bond analysis supports the presence of hydrogen bonds interaction between the non-coordinating 2OG carboxylate oxygen atoms (O3, O4) and R204 (94%), Y122 (93%), while potential hydrogen bonds between 2OG and N206 (1%) and N120 (1%) are unstable indicating some flexibility in the 2OG binding site (Figure A6).

In FTO, the 2OG C5 carboxylate is bound by interactions with R316, Y295 and S318; R204, Y122, N120 and N206 serve the same purpose in AlkB (Figure A6). Hydrogen bonds between the non-coordinating oxygen (O1) of C1 of 2OG in FTO with the side chains of R96 and N205 which are observed in the crystal structure show limited stability (30% and 36%, respectively) during the MD trajectories. In FTO, hydrogen bonds stabilising the non-coordinating C5 carboxylate of 2OG (O3 and O4) group are found to

be more stable - R316 (98%) S318 (97%) and Y295 (77%). Overall, the MD simulations indicate some flexibility in the 2OG binding sites in both AlkB (in agreement with NMR data<sup>25</sup>) and FTO which might be important for the design of enzyme-specific 2OG analogues.

In the AlkB-6MA(DNA) complex, the DNA has an average RMSD value of 4.0 Å (Figure A7), by contrast to 1.4 Å for the protein alone. This result indicates that DNA contributes to the relatively high flexibility of the complex in agreement with other simulations of AlkB with dsDNA.<sup>33</sup> NMR studies also reveal the importance of the DNA conformation in dynamics of the overall complex.<sup>25</sup> The distance between the centre of mass of protein and DNA was 28.2 Å, larger than the same distance observed in the crystal structure (24.0 Å) of the AlkB-6MA(DNA) complex (Figure A8). This observation indicates a more open structure of the AlkB-6MA(DNA) than the crystallographic study indicates, likely reflecting crystal packing effects. AlkB-6MA (nsd) and AlkB-1MA (nsd) showed equilibration with an average RMSD value of 1.4 Å (Figure A9), further supporting the crystallographic observations that AlkB-6MA (nsd) and AlkB-1MA (nsd) manifest near identical structures apart from the active site loop.<sup>10</sup> The active site loop of AlkB-6MA (nsd) and AlkB-6MA (DNA) manifests a conformational change around 200-250ns and greater structural fluctuations in contrast to the AlkB-1MA (nsd) which could contribute to the weaker binding of 6MA (Figure A10). The DSBH core shows low structural fluctuations which probably helps to maintain a stable environment for the Fe(II) centre and co-substrates/intermediates, possibly to help prevent self-oxidation.<sup>63</sup>

Principal Component Analysis (PCA) suggests that the AlkB-6MA(DNA) complex mainly manifests motion in its the active site loop region and N- and C-terminal regions; the methylated DNA base showed limited flexibility (Figures 2.4A and A11). However, AlkB-1MA (nsd) showed more limited motion of the active site loop (Figures A12 and A13) which would contribute to the stronger binding of 1MA in AlkB-1MA (nsd) than the 6MA in AlkB-6MA (nsd).

Dynamic Cross Correlation Analysis (DCCA) was performed to investigate collective, correlated motions in AlkB and FTO. In AlkB-6MA (DNA) residues of the active site loop (133-139;  $\beta$ 6- $\beta$ 7) show correlation with residues 187-195 in the DSBH (loop linking  $\beta$ 11 and  $\beta$ 12) (Figure 2.5). Residues 152-160 in the loop near the DNA show correlation towards residues 187-195 of the DSBH. However, there is reduction in correlated motion in the AlkB-6MA (nsd) and AlkB-1MA (nsd) systems compared to AlkB-6MA (DNA) complex (Figure 2.5). These results thus support the proposal of important contributions by DNA dynamics to collective motions of the enzyme-substrate complex.

Experimental studies show that the T51A, W69A, Y76A, D135A, and R161A substitutions adversely affect AlkB catalysis<sup>18</sup> (Figure A14). From the DCCA (Figure 2.5), D135 and R161 show positive correlations with the coordinating aspartic acid (D133) and histidines (H131 and H187) respectively. Thus, the D135A and R161A substitutions will likely affect the functioning of the catalytic domain. T51, W69 and Y76 also show positive correlations with the nucleotide recognition lid residues, which is involved in substrate binding<sup>10</sup>, thus the T51A, W69A and Y76A substitutions likely affect substrate binding.

The FTO NTD manifests larger structural deviations compared to the CTD, due to the larger number of loop regions in NTD. The linker connecting NTD to the CTD shows lower RMSDs indicating a stable connection between the two domains. The PCA shows that the main motion involves residues from the L1 loop in the NTD region (Figures 2.4B and A15) and a movement of the CTD towards the NTD domain. DCCA (Figure 2.5) shows that residues 90-115 of NTD have a positive correlation with CTD residues 380 to 390 from  $\alpha 8$  helix. These motions might contribute to substrate binding by FTO and may be used for modulation of enzyme activity.

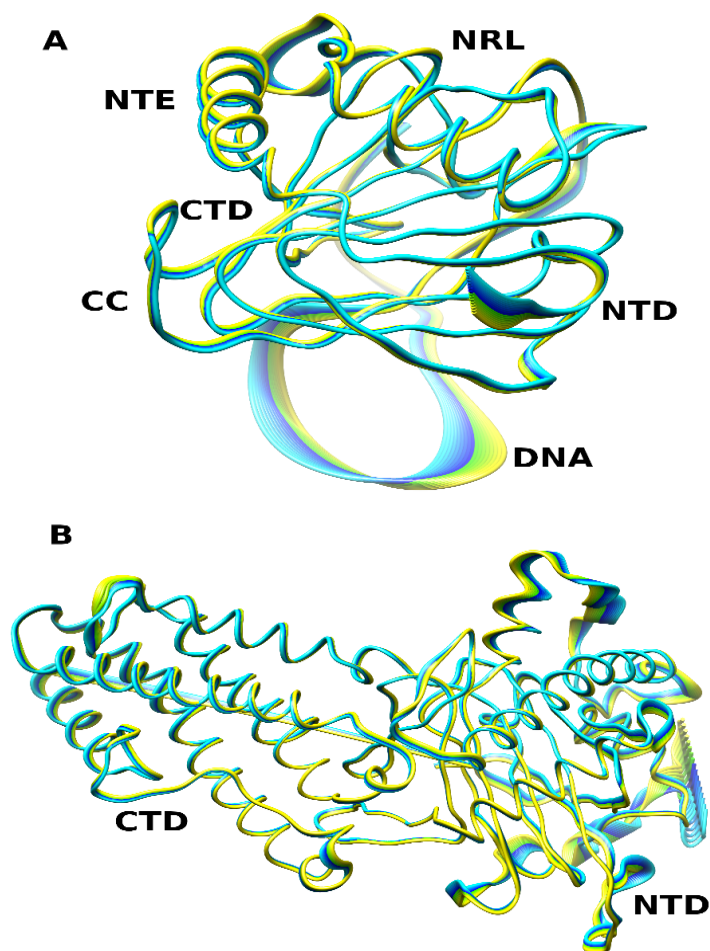


**Figure 2.4.** Principal Component Analysis for AlkB-6MA (DNA) (A) and FTO (B). NTE: N-terminal extension; NRL: nucleotide-recognition lid; CC is the catalytic core while NTD and CTD are the N-terminal domain and C-terminal domain, respectively. Yellow to blue represents the main direction of motion of proteins residues.

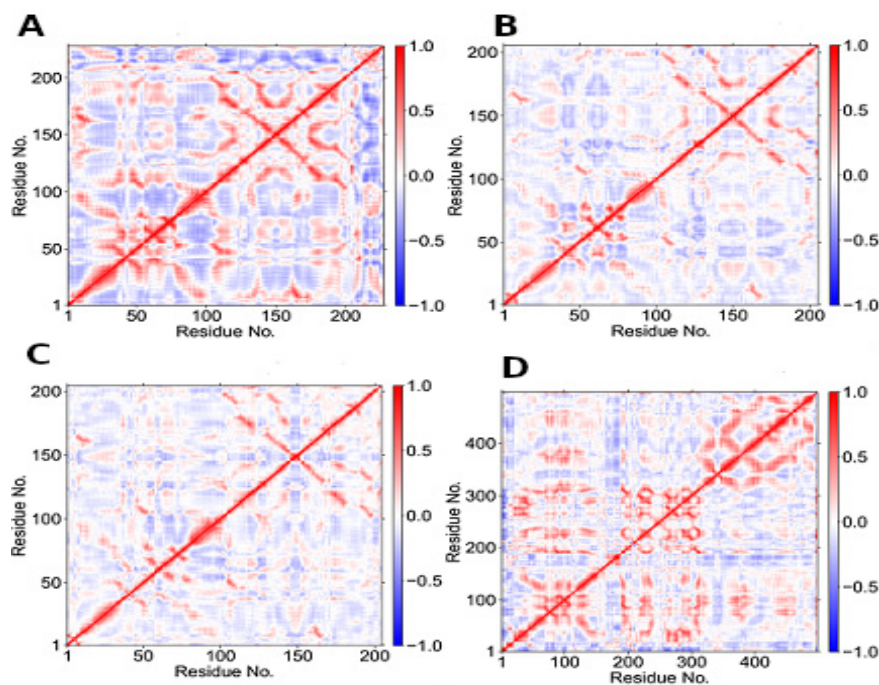


**Figure 2.5.** Dynamic Cross Correlation for AlkB-6MA (DNA) (A), AlkB-6MA (nsd) (B), AlkB-1MA (nsd) (C) and FTO (D). Residue numbers in (A): 1-203 (protein), 204 (2OG), 205 (Fe), 206-229 (DNA), and 211 (substrate). (B) 1-203 (protein), 204 (2OG), 205 (Fe) and 206 (substrate). (C) 1-202 (protein), 203 (2OG), 204 (Fe) and 205 (substrate). (D) 1-495 (protein), 496 (2OG), 497 (Fe), and 498 (substrate).

Mutations of F114 or C392 (F114D, C392D) (Figure A16), which are involved in this correlated motion, might be involved in the disruption of inter-domain interactions and thus to lead to reduction in FTO activity, as observed experimentally<sup>5</sup>. Notably, the clinically observed mutations S319F and R322Q<sup>15-17</sup> (Figure A16) have positive correlations with the Fe(II) coordinating residues (H231, D233, H307), Fe, 2OG and the substrate (m3T), while R316Q has positive correlation with all the aforementioned, except



the coordinating D233. These mutations are thus predicted to alter the correlated dynamics within the active site, including with respect to the binding of the substrate, in a manner possibly related to the reported pathologies.<sup>15-17</sup>

To further investigate the effects of the protein environment and flexibility on the geometric and electronic structure of the reactant complexes, QM/MM geometry optimizations of the enzyme-substrate complexes of AlkB and FTO were performed. The Fe(II) coordination geometry of AlkB was maintained during QM/MM optimizations (Figure 2.6 and Table A2). The second sphere interactions of the AlkB enzyme analysed from QM/MM snapshots are presented in Table A3. For example, the MD simulations and QM/MM optimizations of various snapshots manifest a consistent distance of  $\sim 3.9$  Å between the side chain of R204 and the 2OG C5 carboxylate. These QM/MM results are consistent with the MD and crystallographic studies with AlkB.

Superposition of the structures of AlkB-1MA (nsd) and AlkB-6MA (nsd) optimized using QM/MM imply that the complex with 1MA is more productive compared to that of AlkB-6MA (nsd), based on the closer positioning of the methyl group of 1MA to the non-heme Fe (II) (Figure 2.6), consistent with the experimental observations<sup>10</sup> and the MD simulations. Superposition of the QM/MM optimized structures of the AlkB-6MA (nsd) and AlkB-6MA (DNA) complexes (using snapshots from the MD) shows overall consistency with the trends observed in MD; however, small differences are apparent (Figures A17 and A18) indicating the importance of performing QM/MM minimizations.

With FTO, the Fe(II) coordination geometry and active site interactions also remained stable during QM/MM optimizations of MD snapshots (Figure 2.7). Thus, the QM/MM optimizations manifested a consistent distance of  $\sim 4.0$  Å between the R316 side chain and the 2OG C5 carboxylate 2OG, validating the role of this electrostatic interaction.

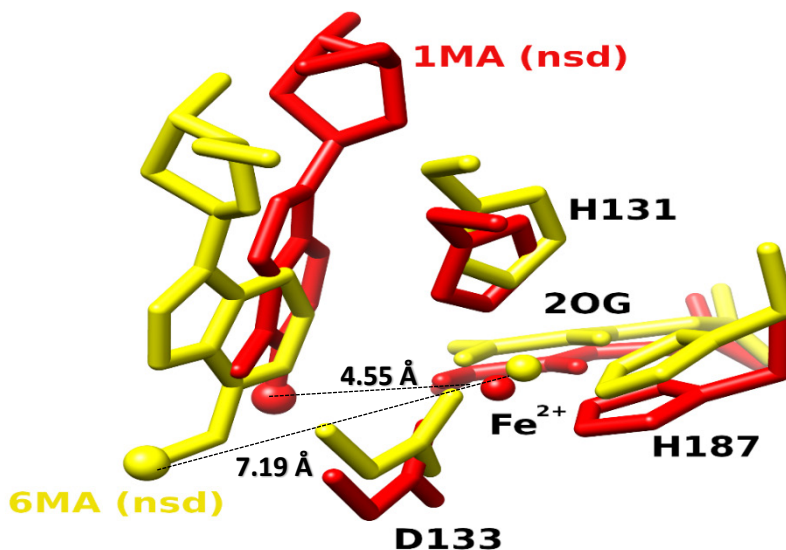


**Figure 2.6.** Overlaid QM/MM optimized structures of the AlkB-1MA and AlkB-6MA complexes (with Fe(II) and 2OG) showing the active site. The methyl groups are shown as larger spheres.

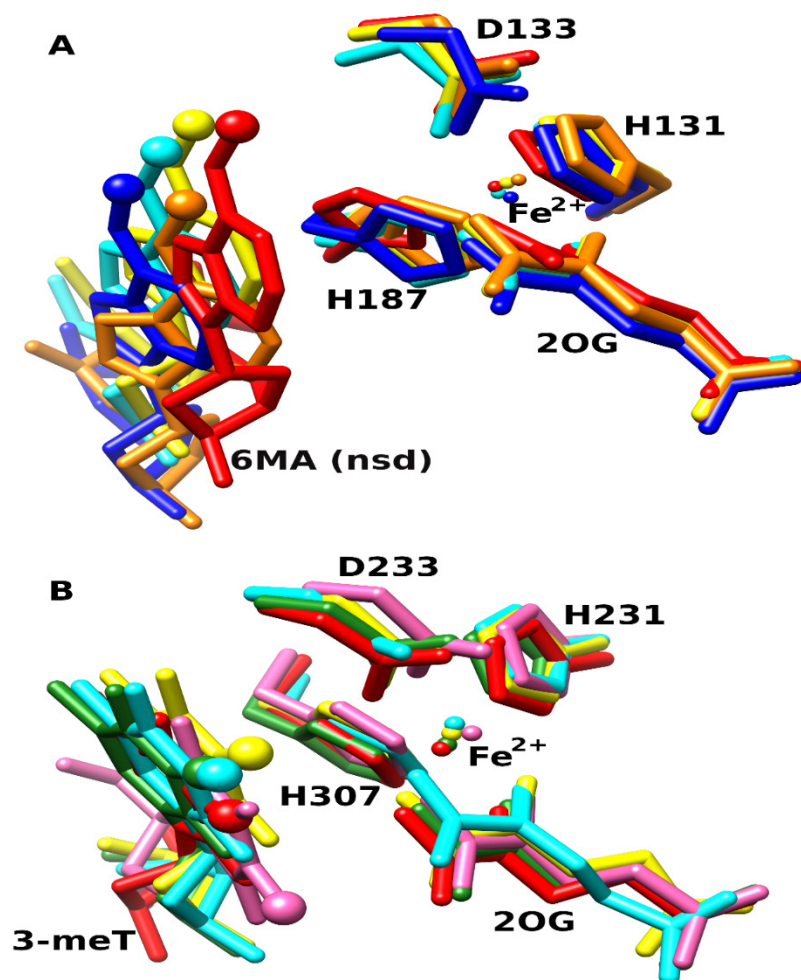


**Figure 2.7.** Overlaid multiple QM/MM optimized snapshots of AlkB-6MA at: (A) at 200ns (orange), 300ns (yellow), 400ns (cyan), 500ns (blue), and FTO (B) at 200ns (red), 300ns (green), 700ns (cyan), 800ns (pink). The red and yellow structures in A and B represent views from QM/MM minimized structures of AlkB and FTO, respectively. The overlay was done using Chimera. The methyl group is shown as the larger sphere.

Comparison of the structures of the QM/MM optimized MD snapshots of AlkB-6MA (DNA) (Figure 2.7A, Table A2) and FTO-3MT (nsd) (Figure 2.7B and Table A4) also indicate that in both enzymes there are fine structural differences in the reactant complexes due to conformational fluctuations (in respect to QM/MM minimized initial crystal structures), thus supporting the importance of accounting for the protein conformational dynamics in reaction mechanism calculations.

## 2.4 Conclusions

The results of our experimentally-based multilevel computational studies on two homologous N-methyl nucleic acid demethylases, bacterial AlkB and human FTO, complement reported biophysical (crystallographic and NMR) and kinetic studies of these enzymes,<sup>10,13,25</sup> and provide new insights into the effects of the conformational dynamics, collective motions, and electronic structural features, which are difficult to define experimentally. The results show that the flexibility of the dsDNA substrate has a substantial effect on the dynamics and correlated motions in AlkB-substrate complexes, including motions between the core jelly-roll motif and an active site loop involved in substrate binding. The results inform on how key residues in AlkB-and FTO influence activity via modulating correlated motions. The computations also inform on the underlying reasons why 1MA is a better substrate for AlkB than 6MA; future analogous studies on the selectivities of other nucleic acid oxygenases acting on both DNA and various forms of RNA are thus of interest. Most reported 2OG oxygenase inhibitors, including compounds in clinical applications, bind at the active site and ligate Fe(II), with

consequent issues with respect to achieving selectivity.<sup>64</sup> Our computational studies with FTO reveal its CTD and NTD domains move in respect to one another in a manner which likely important for substrate binding, an observation that suggests new opportunities for selective inhibition of some 2OG oxygenases via binding away from the active site.

## 2.5 References

1. C. Loenarz, W. Ge, M.L. Coleman, N.R. Rose, C.D. Cooper, R.J. Klose, P.J. Ratcliffe and C.J. Schofield, *Hum. Mol. Genet.* 2010, **19**, 217-222.
2. C.J. Schofield and Z. Zhang, *Curr. Opin. Struct. Biol.* 1999, **9**, 722-731.
3. W. Aik, M. Demetriades, M.K.K. Hamdan, E.A.L. Bagg, K.K. Yeoh, C. Lejeune, Z. Zhang, M.A. McDonough and C.J. Schofield, *J. Med. Chem.* 2013, **56**, 3680-3688.
4. I.J. Clifton, M.A. McDonough, D. Ehrismann, N.J. Kershaw, N. Gravatino and C.J. Schofield, *J. Inorg. Biochem.*, 2006, **100**, 644-669.
5. Z. Han, T. Niu, J. Chang, X. Lei, M. Zhao, Q. Wang, W. Cheng, J. Wang, Y. Feng, and J. Chai, *Nature* 2010, **464**, 1205-1209.
6. Y. Fu, G. Jia, X. Pang, R.N. Wang, X. Wang, C.J. Li, S. Smemo, Q. Dai, K.A. Bailey, M.A. Nobrega, K.L. Han, Q. Cui and C. He, *Nat. commun.* 2013, **4**, 1798.
7. D. Meyre, K. Proulx, H. Kawagoe-Takaki, V. Vatin, R. Gutierrez-Aguilar, D. Lyon, M. Ma, H. Choquet, F. Horber, W. Van Hul, L. Van Gaal, B. Balkau, S. Visvikis-Siest, F. Pattou, I.S. Farooqi, V. Saudek, S. O'Rahilly, P. Froguel, B. Sedgwick and G.S. Yeo, *Diabetes* 2010, **59**, 311-318.
8. E.I. Solomon, T.C. Brunold, M.I. Davis, J.N. Kemsley, S. Lee, N. Lehnert, F. Neese, A.J. Skulan, Y. Yang and J. Zhou, *Chem. Rev.* 2000, **100**, 235-350.
9. R.H. Holm and E.I. Solomon, *Chem. Rev.* 2014, **114**, 4039-4040.
10. C. Zhu and C. Yi, *Angew. Chem. Int. Ed.* 2014, **53**, 3659-3662.
11. B.I. Fedeles, V. Singh, J.C. Delaney, D. Li and J.M. Essigmann, *J. Biol. Chem.* 2015, **290**, 20734-20742.
12. G. Zheng and C. He, in 2-Oxoglutarate-Dependent Oxygenases, ed. C.J. Schofield and R.P. Hausinger, Royal Society of Chemistry, Cambridge, 2015, series No. 3, ch. 9, pp. 263-274.
13. T. Gerken, C.A. Girard, Y.L. Tung, C.J. Webby, V. Saudek, K.S. Hewitson, G.S.H. Yeo, M.A. McDonough, S. Cunliffe, L.A. McNeil, J. Galvanovskis, P. Rorsman, P. Robins, X. Prieur, A.P. Coll, M. Ma, Z. Jovanovic, I.S. Farooqi, B. Sedgwick, I. Barroso, T. Lindahl, C.P. Ponting, F.M. Ashcroft, S.O. Rahilly and C.J. Schofield, *Science*, 2007, **318**, 1469-1472.
14. R.P. Hausinger, *Crit. Rev. Biochem. Mol. Biol.*, 2004, **39**, 21-68.
15. G. Jia, Y. Fu, X. Zhao, Q. Dai, G. Zheng, Y. Yang, C. Yi, T. Lindahl, T. Pan, Y.G. Yang and C. He, *Nat. Chem. Biol.*, 2011, **7**, 885-887.

16. L. Rohena, M. Lawson, E. Guzman, M. Ganapathi, M.T. Cho, E. Haverfield and K. Anyane Yeboa, *Am. J. Med. Genet A.*, 2016, **170**, 1023-1028.
17. H. Daoud, D. Zhang, F. McMurray, A. Yu, S.M. Luco, J. Vanstone, O. Jarinova, N. Caron, J. Wickens, S. Shishodia, H. Choi, M.A. McDonough, C.J Schofield, M.E. Harper, D.A. Dymont and C.M. Armour, *J. Med. Genet.*, 2016, **53**, 200-207.
18. P.J. Holland, T. Hollis, *PLoS One*. 2010, **5**, e8680.
19. A. Vidaki and M. Kayser, *Genome Biol.* 2017, **18**, 238.
20. D. Fang, R.L. Lord and G.A. Cisneros, *J. Phys. Chem. B*. 2013, **117**, 6410-6420.
21. M.G. Quesne, R. Latifi, L.E. Gonzalez-Ovalle, D. Kumar and S.P. de Visser, *Chem. Eur. J.* 2014, **20**, 435-446.
22. B. Wang, Z. Cao, D.A. Sharon, and S. Shaik, *ACS Catal.* 2015, **5**, 7077-7090.
23. H. Torabifard and G.A. Cisneros, *Chem. Sci.*, 2017, **8**, 6230-6238.
24. H. Liu, J. Llano, and J.W. Gauld, *J. Phys. Chem. B* 2009, **113**, 4887-4898.
25. B. Bleijlevens, T. Shivarattan, E. Flashman, Y. Yang, P.J. Slimpson, P. Koivisto, B. Sedgwick, C.J. Schofield and S.J. Mathews, *EMBO Rep.* 2008, **9**, 872-877.
26. R. Chowdhury, I.K.H. Leung, Y. Tian, M.I. Abboud, W. Ge, C. Domene, F. Cantrelle, I. Landrieu, A.P. Hardy, C.W. Pugh, P.J. Ratcliffe, T.D.W. Claridge and C.J. Schofield, *Nat. Commun.* 2016, **7**, 12673.
27. N.R. Rose, M.A. McDonough, O.N.F. King, A. Kawamura and C.J. Schofield, *Chem. Soc. Rev.* 2011, **40**, 4364-4397.
28. C.Z. Christov, A. Lodola, T.G. Karabancheva-Christova, S. Wan, P.V. Coveney, and A.J. Mulholland, *Biophys J.*, 2013, **104**, L5-L7.
29. T.G. Karabancheva-Christova, J. Torras, A.J. Mulholland, A. Lodola and C.Z. Christov, *Scientific Reports*, 2017, **7**, 17395.
30. W. Singh, G.B. Fields, C.Z. Christov and T.G. Karabancheva-Christova, *RSC Adv.*, 2016, **6**, 23223.
31. J. Ainsley, A.J. Mulholland, G.W. Black, O. Sparagano, C.Z. Christov, and T.G. Karabancheva-Christova, *ACS Omega*, 2018, **3**, 4847-4859.
32. T.G. Karabancheva-Christova, C.Z. Christov and G.B. Fields, *J. Phys. Chem. B*, 2018, **122**, 5316-5326.
33. X. Pang, K. Han and Q. Cui, *J. Comput. Chem.* 2013, **34**, 1620-1635.
34. A. Fiser and A. Sali, *Method Enzymol.* 2003, **374**, 461-491.
35. C.G. Yang, C. Yi, E.M. Duguid, C.T. Sullivan, P.A. Rice and C. He, *Nature*, 2008, **452**, 961-965.
36. J.C. Gordon, J.B. Myers, T. Folta, V. Shoja, L.S. Heath, and A. Onufriev, *Nuclei Acids Res.*, 2005, **33**, W368-371.
37. P. Li and K.M. Merz, *J. Chem. Info. Model.* 2016, **56**, 599-604.
38. R. Salomon-Ferrer, A.W. Götz, D. Poole, S. Le Grand, and R.C. Walker, *J. Chem. Theory Comput.* 2013, **9**, 3878-3888.
39. D. Case, V. Babin, J. Berryman, R. Betz, Q. Cai, D. Cerutti, T. Cheatham III, T. Darden, R. Duke and H. Gohlke, *Amber*, 2014, **14**, 29-31.
40. J.A. Maier, C. Martinez, K. Kasavajhala, L. Wickstrom, K.E. Hauser, and C. Simmerling, *J. Chem. Theory Comput* 2015, **11**, 3696-3713.

41. W.L. Jorgensen, J. Chandrasekhar, J.D. Madura, R.W. Impey, and M.L. Klein, *J. Chem. Phys.* 1983, **79**, 926-935.
42. T. Darden, D. York, and L. Pedersen, *J. Chem. Phys.* 1993, **98**, 10089-10092.
43. R. Davidchack, R. Handel and M.V. Tretyakov, *J. Chem. Phys.* 2009, **130**, 234101.
44. J.P. Ryckaert, G. Ciccotti, and H.J. Berendsen, *J. Comput. Phys.* 1977, **23**, 327-341.
45. H.J. Berendsen, J.V. Postma, W.F. van Gunsteren, A. DiNola, and J. Haak, *J. Chem. Phys.* 1984, **81**, 3684-3690.
46. D.R. Roe and T.E. Cheatham III, *J. Chem. Theory Comput.* 2013 **9**, 3084-3095.
47. W. Humphrey, A. Dalke and K. Schulten, *J. Mol. Graph.* 1996, **14**, 27-38.
48. E.F. Pettersen, T.D. Goddard, C.C. Huang, G.S. Couch, D.M. Greenblatt, E.C. Meng, and T.E. Ferrin, *J. Comput. Chem.* 2004, **25**, 1605-1612.
49. B.J. Grant, A.P. Rodrigues, K.M. ElSawy, J.A. McCammon, and L.S. Caves, *Bioinformatics (Oxford, England)* 2003, **22**, 2695-2696.
50. P. Tao and H.B. Schlegel, *J. Comput. Chem.* 2010, **31**, 2363-2369.
51. F. Maseras and K. Morokuma, *J. Comput. Chem.* 1995, **16**, 1170-1179.
52. M. Svensson, S. Humbel, and K. Morokuma, *J. Chem. Phys.* 1996, **105**, 3654-3661.
53. S. Dapprich, I. Komáromi, K.S. Byun, K. Morokuma and M.J. Frisch, *J. Mol. Struct: THEOCHEM* 1999, **461**, 1-21.
54. T. Vreven, K. Morokuma, O. Farkas, H.B. Schlegel, and M.J. Frisch, *J. Comput. Chem.* 2003, **24**, 760-769.
55. T. Vreven and K. Morokuma, *J. Comput. Chem.* 2000, **21**, 1419-1432.
56. M.J.T. Frisch, G. W. Schlegel, H. B. Scuseria, G. E. Robb, M. A. Cheeseman, J. R. Scalmani, G. Barone, V. Mennucci, B. Petersson, G. A. Nakatsuji, H. Caricato, M. Li, X. Hratchian, H. P. Izmaylov, A. F. Bloino, J. Zheng, G. Sonnenberg, J. L. Hada, M. Ehara, M. Toyota, K. Fukuda, R. Hasegawa, J. Ishida, M. Nakajima, T. Honda, Y. Kitao, O. Nakai, H. Vreven, T. Montgomery, J. A., Jr. Peralta, J. E. Ogliaro, F. Bearpark, M. Heyd, J. J. Brothers, E. Kudin, K. N. Staroverov, V. N. Kobayashi, R. Normand, J. Raghavachari, K. Rendell, A. Burant, J. C. Iyengar, S. S. Tomasi, J. Cossi, M. Rega, N. Millam, N. J. Klene, M. Knox, J. E. Cross, J. B. Bakken, V. Adamo, C. Jaramillo, J. Gomperts, R. Stratmann, R. E. Yazyev, O. Austin, A. J. Cammi, R. Pomelli, C. Ochterski, J. W. Martin, R. L. Morokuma, K. Zakrzewski, V. G. Voth, G. A. Salvador, P. Dannenberg, J. J. Dapprich, S. Daniels, A. D. Farkas, Ö. Foresman, J. B. Ortiz, J. V. Cioslowski, J. Fox, Gaussian 09. *Gaussian, Inc* Revision D.01(Wallingford CT) 2009.
57. H.M. Senn and W. Thiel, *Angew. Chem. Int. Ed.* 2009, **48**, 1198-1229.
58. P.A. Kollman, I. Massova, C. Reyes, B. Kuhn, S. Huo, L. Chong, M. Lee, T. Lee, Y. Duan, W. Wang, O. Donini, P. Cieplak, J. Srinivasan, D.A. Case, and T.E. 3rd Cheatham, *Acc. Chem. Res.* 2000, **33**, 889-897.
59. I. Massova and P.A. Kollman, *Perspectives in Drug Discovery and Design* 2000, **18**, 113-135.
60. V. Tsui and D.A. Case, *Biopolymers* 2000, **56**, 275-291.
61. M. Padariya and U. Kalathiya, *Comp. Biol. Chem.* 2016, **64**, 414-425.
62. T.A. Muller and R.P. Hausinger in 2-Oxoglutarate-Dependent Oxygenases, ed. C.J. Schofield and R.P. Hausinger, Royal Society of Chemistry, Cambridge, 2015, series No. 3, ch. 8, pp. 246-262.

63. M. Mantri, Z. Zhang, M.A. McDonough, O.N.F. King, A. Kawamura and C.J. Schofield, *FEBS Journal*, 2012, **279**, 1563-1575.
64. T.L. Yeh, T.M. Leissing, M.I. Abboud, C.C. Thinner, O. Atasoylu, J.P. Holt-Martyn, D. Zhang, A. Tumber, K. Lippi, C.T. Lohans, I.K.H. Leung, H. Morcrette, I.J. Clifton, T.D.W. Claridge, A. Kawamura, E. Flashman, X. Lu, P.J. Ratcliffe, R. Chowdhury, C.W. Pugh and C.J. Schofield, *Chem. Sci.* 2017, **8**, 7651-7668.



### **3 Role of Structural Dynamics in Selectivity and Mechanism of Non-Heme Fe(II) and 2-Oxoglutarate-Dependent Oxygenases Involved in DNA Repair**

**Sodiq O. Waheed,<sup>a</sup> Rajeev Ramanan,<sup>a</sup> Shobhit S. Chaturvedi,<sup>a</sup> Nicolai Lehnert,<sup>b</sup> Christopher J. Schofield,<sup>c</sup> Christo Z. Christov,<sup>a\*</sup> and Tatyana G. Karabancheva-Christova<sup>a\*</sup>**

<sup>a</sup> Department of Chemistry, Michigan Technological University, Houghton, Michigan 49931, USA.

<sup>b</sup> Department of Chemistry, University of Michigan, Ann Arbor, Michigan 48109, USA.

<sup>c</sup> The Chemistry Research Laboratory, The Department of Chemistry, Mansfield Road, University of Oxford, Oxford, OX1 3TA, United Kingdom.

\*Corresponding authors: C.Z.C. ([christov@mtu.edu](mailto:christov@mtu.edu)), and T.G.K.C. ([tatyanak@mtu.edu](mailto:tatyanak@mtu.edu))

---

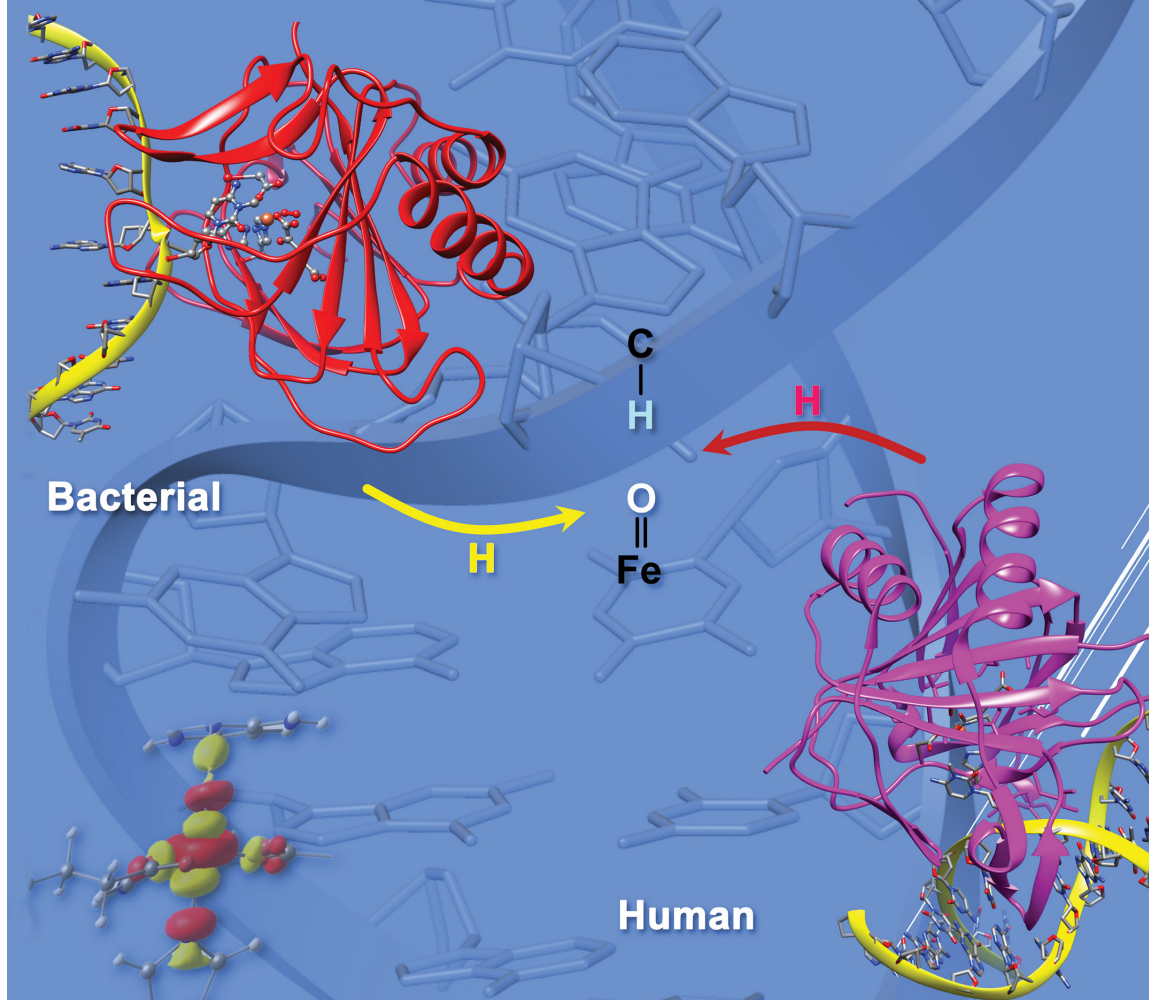
The content of this chapter was previously published in the *ACS Cent. Sci.*, **2020**, *6*, 795-814. DOI: 10.1021/acscentsci.0c00312, reproduced with permission from the American Chemical Society. The work was selected as the Supplementary Front Cover of the May 2020 Issue of the Journal.

# ACS central science

MAY 2020

VOLUME 6 | NUMBER 5

PUBS.ACS.ORG/CENTRALSCIENCE



### 3.1 Introduction

Alkylation of DNA by endogenous and exogenous sources can cause cytotoxicity and/or cancer-linked mutations.<sup>1-4</sup> Direct repair of damaged DNA bases occurs via processes involving DNA glycosylases, O<sup>6</sup>-methylguanine DNA methyltransferases, and AlkB type oxygenases.<sup>5,6</sup> AlkB family oxygenases utilize 2-oxoglutarate (2OG) and Fe(II) to catalyze demethylation of alkylated DNA bases. AlkB homologs exist in most bacteria and many eukaryotes. In humans, nine AlkB homologs have been identified (AlkBH1 to AlkBH8 and FTO), most of which are reported to act on DNA and/or RNA.<sup>6-9</sup> The AlkB oxygenases that are involved in repair have distinct substrate selectivities for different types of alkylated DNA. For example, AlkB and AlkBH3 prefer to repair methylation damage in single-stranded nucleic acids (ssDNA) rather than double-stranded DNA (dsDNA), whereas AlkBH2 more efficiently acts on duplex dsDNA compared to ssDNA.<sup>6,10-12a</sup> The effectiveness of the AlkB-related enzymes also depends on the identity of the nucleobase and the nature and position of the alkylated group. AlkB-related enzymes are reported to act on multiple monoalkylated DNA nucleobases, i.e. 1-methyladenine (m<sub>1</sub>A), 3-methylcytosine (m<sub>3</sub>C), 1-methylguanine (m<sub>1</sub>G), 3-methylthymine (m<sub>3</sub>T), 6-methyladenine (m<sub>6</sub>A), 4-methylcytosine (m<sub>4</sub>C) and exocyclic bridge-containing lesions, e.g. ethenoadenine (εA) and ethenocytosine (εC).<sup>6,13a,14</sup> In the cases of AlkB, AlkBH2, and AlkBH3, alkylated adenines and cytosines are more efficiently repaired than their guanine and thymine analogs, and alkyl groups on the endo nitrogen nucleobase atoms are more efficiently repaired than alkyl groups on exocyclic amines.<sup>6,10-12a</sup> AlkB and AlkBH2 are

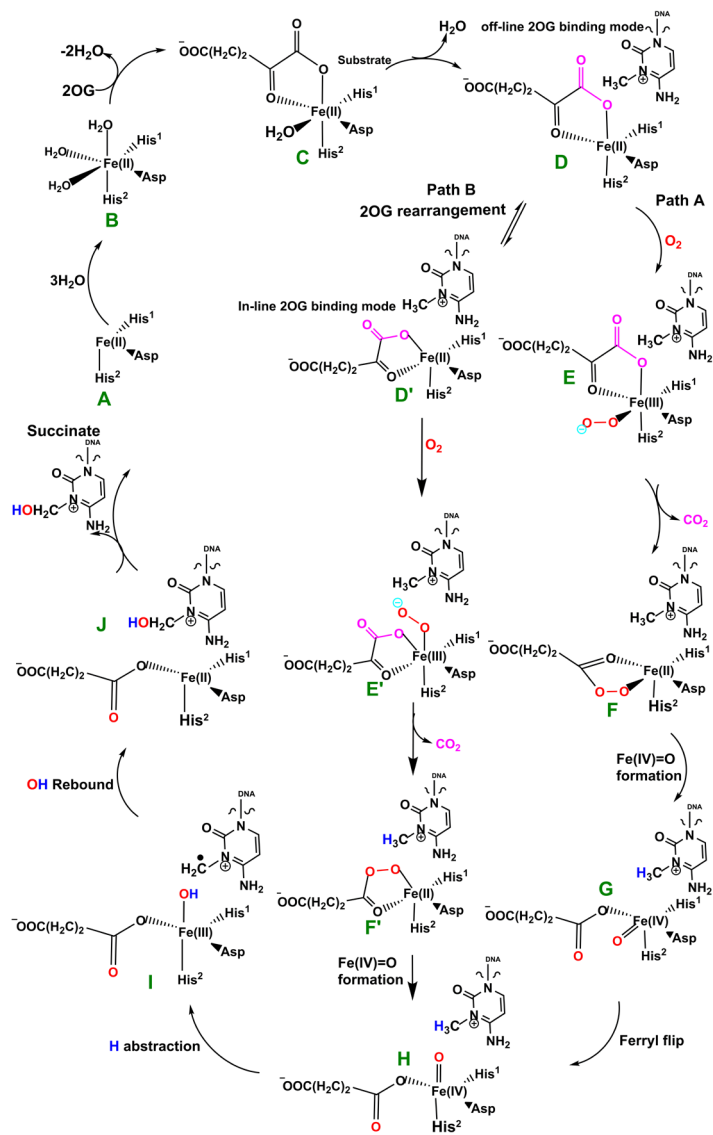
proposed to efficiently repair  $m_1A$  and  $m_3C$  owing to their cationic nature which is believed to enhance the rate of dealkylation.<sup>6,10-12a</sup>

Crystal structures of AlkB (*Escherichia coli*) and its homologs reveal that they have a modified double-stranded  $\beta$ -helix (DSBH) core fold,<sup>1,10,11</sup> which is made up of eight  $\beta$ -strands that support the active site, and which is conserved in 2OG oxygenases.<sup>6,10,11</sup> AlkB interacts almost exclusively with the DNA strand that contains the damaged base and uses a base-flipping mechanism to access the damaged base, resulting in significant distortions in the DNA; AlkB compresses the two bases that flank the flipped-out bases to maintain base stacking.<sup>10-12a</sup> By contrast, AlkBH2 interacts extensively with both strands of its dsDNA substrate. AlkBH2 contains a catalytically important hydrophobic hairpin motif, located between  $\beta_3$  and  $\beta_4$ , which bears an aromatic ‘finger’ Phe102 that intercalates into the duplex stack, filling the gap resulting from the flipping of the damaged base and so helping maintain the normal length and stacking of dsDNA in the enzyme-substrate complex.<sup>10,11</sup> Compared to AlkB, AlkBH2 has extra DNA-binding motifs that grasp the complementary strand of the dsDNA; AlkBH2 uses a positively charged RKK loop (Arg241, Lys242 and Lys243) and an additional long, flexible loop containing DNA-binding residues Arg198, Gly204 and Lys205 to bind the complementary DNA strand.<sup>10-12a</sup>

The available evidence implies that the AlkB homologs have three Fe coordinating residues (His<sup>1</sup>, Asp and His<sup>2</sup>) and employ a typical 2OG-oxygenase catalytic cycle (Scheme 3.1), which has two main stages: dioxygen activation and substrate oxidation. The first stage

involves oxidative decarboxylation of 2OG, to give succinate and CO<sub>2</sub>, leading to formation of a Fe(IV)=O intermediate, which for some 2OG oxygenases has been shown to have a high-spin quintet ground state (S=2, M=5).<sup>15-17</sup> Crystallographic analyses show that the 2OG ligates the metal in an “off-line” mode where the C2 carbonyl oxygen is positioned trans to a carboxylate oxygen of the Fe-coordinating aspartate.<sup>10,11</sup> One of the C1 carboxylate oxygens of 2OG occupies an axial position (trans to His<sup>2</sup>); the sixth coordination site of the octahedral geometry is occupied by a water. Subsequent formation of the reactive Fe(IV)=O intermediate via such a binding mode (“off-line” geometry) of O<sub>2</sub> would require rearrangement to position the ferryl adjacent to the oxidized substrate C-H bond (“in-line” geometry). This could occur via a 2OG C1 carboxylate rearrangement at the five-coordination state or a “ferryl flip” to position the activated oxygen near the substrate.<sup>18a</sup> Studies on PHF8, another 2OG dependent demethylase acting on N-methyl lysine-residues in histones, imply the former is more likely.<sup>18b</sup>

In the second stage of the catalytic cycle, the methyl group of the substrate is hydroxylated by the Fe(IV)=O species. The hydroxylated hemiaminal product can then undergo a spontaneous, non-enzymatic reaction to give the final demethylated product with the release of formaldehyde, the rate of which is dependent on the product.<sup>19</sup>



**Scheme 3.1.** The proposed catalytic cycle for demethylation of a monoalkyl substrate (exemplified with m<sub>3</sub>C) by AlkB family members.

Biochemical and structural studies have led to a consensus mechanism for 2OG oxygenases<sup>4,6,12a,b,13a</sup> (Scheme 3.1). Prior to O<sub>2</sub> binding, the resting state (C) contains an Fe(II) complex which is then ligated by 2OG (in a bidentate manner), two histidine- (His<sup>1</sup> and His<sup>2</sup>), and one aspartate-residue (Scheme 3.1). The sixth coordination site is normally occupied by a water molecule.<sup>10,11,20a</sup> Binding of the substrate (e.g. 3-methylcytosine (m<sub>3</sub>C) DNA) induces the loss of the ligating water, leading to the opening of the site to give a five-coordinate complex (D) with (at least in some cases, as observed by crystallography) an “off-line” 2OG binding mode. From the five-coordinate complex (D), (at least) two reactions paths are possible from the “off-line” mode, i.e. paths A and B (Scheme 3.1). In path A, dioxygen binds to the five-coordinate complex (D) in an ‘end on’ manner to give an Fe(III)-superoxo complex (E) (Figures 3.1, B1). Oxidative decarboxylation of 2OG, which in some cases proceeds via an Fe(II)-peroxysuccinate intermediate (F),<sup>20b</sup> would result in the formation of a Fe(IV)-oxo complex (G), which is incorrectly oriented to react with substrate. The ferryl intermediate (G) could then reorient (“ferryl flip”) towards the methyl group of the substrate to orientate the reactive Fe(IV)=O species (H) in a catalytically productive manner. In path B, the “off-line” 2OG binding mode of the five-coordinate complex (D) first rearranges to an “in-line” 2OG binding mode of the five-coordinate complex (D’) with an open site adjacent to the substrate C-H bond (trans to His<sup>2</sup>). Dioxygen binds to the open site to give the “in-line” Fe(III)-superoxo complex (E’) which undergoes decarboxylation of 2OG to give the reactive Fe(IV)=O species (H). The active Fe(IV)=O complex enables hydrogen atom abstraction followed by rebound hydroxylation to give the hydroxylated product (J).

Owing to their pathological and biological roles, 2OG oxygenases have been the subject of computational analyses.<sup>21-33</sup> Studies have been reported on the mechanism of bacterial AlkB in the repair of 1-methyl adenine (m<sub>1</sub>A) and exocyclic bridge-containing ethenoadenine ( $\epsilon$ A) single stranded DNA (ssDNA) substrates using DFT and QM/MM methods.<sup>22,24,27-29</sup> Several dynamics studies have shown the importance of conformational dynamics for catalysis in AlkB and its human homologs.<sup>34a-c,35a-d</sup> For example, dynamics studies on human AlkB homolog 5 (AlkBH5) imply that its 2OG binding pocket undergoes conformational changes that expand the active site to permit catalytically productive substrate binding.<sup>34a</sup> Dynamics studies with the homology modeled AlkB human homolog 1 (AlkBH1) show the importance of two predicted disulfide bridges and a zinc finger domain for DNA recognition and binding.<sup>34b</sup> Recent molecular dynamics studies on the enzyme-substrate complex of bacterial AlkB using m<sub>1</sub>A and m<sub>6</sub>A ssDNA and dsDNA substrates have shown how conformational flexibility can influence the structure-function relationships and substrate selectivity.<sup>34c</sup> Bleijlevens and co-workers have reported that AlkB is a dynamic protein that exhibits different folding states in its apo- and-holo forms, and that a fully folded and catalytically competent complex can occur only when both 2OG and Fe<sup>2+</sup> are bound to the enzyme.<sup>35a</sup> It has also been shown that AlkB exhibits significantly different dynamics properties when bound with 2OG or succinate; this is substantially because 2OG makes interactions with both active site ion and the larger  $\beta$ -sheet of the DSBH, helping to maintain a well folded conformation.<sup>35b</sup> Dynamics studies on AlkB by Pang et al. reveal that the DNA undergoes substantial structural relaxation upon binding to AlkB which changes the protein-DNA interaction, highlighting that crystal



packing may have an important role for the structural features of protein-DNA complexes.<sup>35c</sup> Similarly, studies on AlkB dynamics by Ergel et al. show that an important conformational transition during the catalysis by AlkB involves the movement of the nucleotide recognition lid away from the active site into a more open position where it participates in fewer constraining interactions with the Fe(II)/2OG core.<sup>35d</sup> However, the studies on nucleic acid oxygenases to date<sup>24,27-29</sup> have not investigated the 2OG rearrangement or “ferryl flip” processes that may be required to produce a catalytically productive Fe(IV)=O species. They also did not consider the effect of the nature of the substrate (ss/dsDNA) and conformational dynamics of the entire complex on determining substrate selectivity and mechanism. Although some studies have explored the substrate oxidation step by modelling the ferryl complex,<sup>24,27,29,32</sup> none have analysed the dynamics and collective motions of the reactive oxidising intermediates.

To investigate the roles of structural dynamics in bacterial and eukaryotic AlkB homolog selectivity and mechanism, we performed molecular dynamic simulations to explore variations in the conformational behaviour of Fe(III)-superoxo and ferryl complexes in AlkB-ssDNA, AlkB-dsDNA, and AlkBH2-dsDNA. The human homolog of AlkB 2 (AlkBH2) was chosen to explore the generality of the results for AlkB and because of its role in human DNA repair.<sup>10,11</sup> The m<sub>3</sub>C mono-alkylated substrates were studied because of their biological importance and lack of previous computational work on them. Combined QM/MM methods were used to explore the mechanisms of the three enzyme-substrate complexes during demethylation of 3-methylcytosine (m<sub>3</sub>C) substrates, including dioxygen activation, ‘ferryl flip’ / 2OG rearrangement and substrate hydroxylation steps.

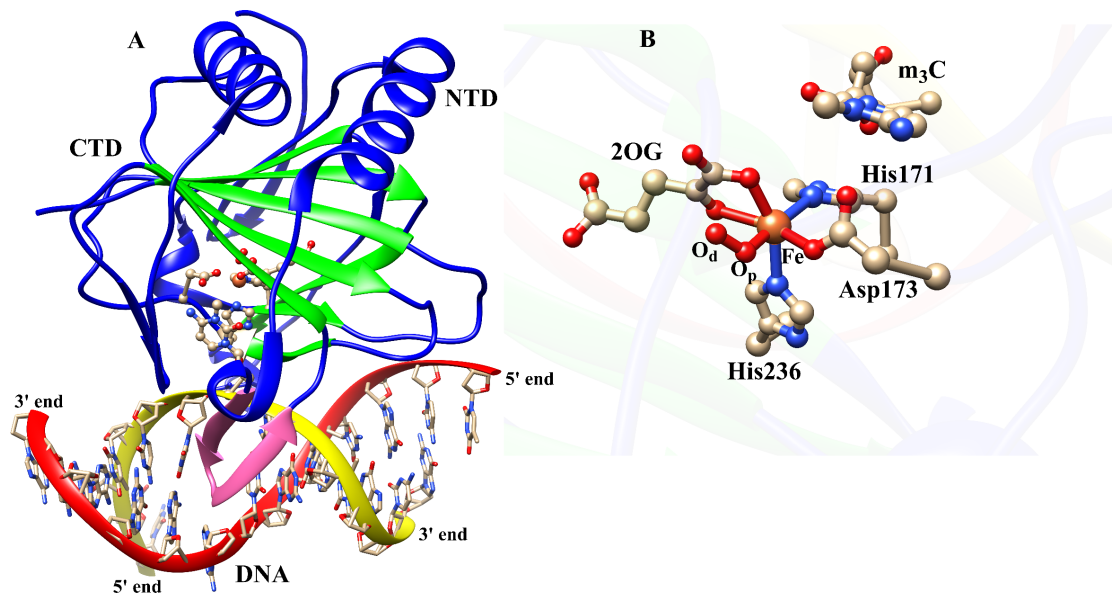


**Figure 3.1.** Average structure of AlkBH2-dsDNA (A) and the view of the active site (B) derived from the Fe(III)-superoxo intermediate MD simulations. Coloring: double stranded beta helix (DSBH) core fold (green) and the hydrophobic  $\beta$ -hairpin (pink).

## 3.2 Results and Discussion

### 3.2.1 The Nature of the Substrate Influences the Conformational Dynamics of the Enzyme-Substrate Complexes for O<sub>2</sub> Activation in AlkB-ssDNA, AlkB-dsDNA, and AlkBH2-dsDNA systems

#### Overall Dynamics of the enzyme-substrate complexes

To obtain insight into the structural dynamics of the three enzyme-substrate complexes of interest (AlkB-ssDNA, AlkB-dsDNA, and AlkBH2-dsDNA), we first carried out the MD simulations on their Fe(III)-superoxo complexes with coordinated 2OG. The results reveal that the active sites, proteins, and the protein-DNA complexes of the three enzymes are stable with average RMSDs of 0.38 Å, 1.03 Å, and 1.13 Å, respectively, for AlkB-ssDNA; 0.51 Å, 1.52 Å, and 3.05 Å, respectively, for AlkBH2-dsDNA; and 0.42 Å, 1.59 Å, and 2.95 Å, respectively, for AlkB-dsDNA (Figure B2). The dsDNA in both AlkBH2-dsDNA and AlkB-dsDNA exhibited large fluctuations during the simulations, which affects the overall RMSD of the protein-DNA complexes. Hence, the DNA contributes substantially to the overall flexibility of the complexes, in agreement with conclusions from previous studies on the dynamics of the resting state of AlkB.<sup>34c,35c</sup> By contrast, AlkB-ssDNA shows a more compact structure than both AlkB-dsDNA and AlkBH2-dsDNA, due to the smaller number of nucleotides. This observation is supported by analyses on the distance between the centre of mass of the protein and the DNA (Figures B3-B6). Centre of mass analyses reveal average values of 15.8 Å, 19.7 Å and 25.2 Å between the protein and DNA for AlkB-ssDNA, AlkBH2-dsDNA, and AlkB-dsDNA, respectively. This trend implies that the AlkBH2-dsDNA complex structure is more compact than that of AlkB-dsDNA, in agreement with crystallographic observations, i.e. AlkBH2-dsDNA forms a stabilizing interaction with both DNA chains, whereas AlkB-dsDNA only forms direct interactions with one of the DNA chains.<sup>10,11</sup>

### 3.2.2 Flexibility of the 2OG Binding Sites

In the 2OG binding site of AlkBH2-dsDNA, the hydrogen bonding interactions between the C5 carboxylate oxygens of 2OG and Tyr161 (98% of the MD snapshots) and Arg248 (93%) are stable. O4 of the 2OG C5 carboxylate makes an electrostatic interaction with Arg248 (93%). Similarly, with AlkB-ssDNA, the 2OG makes analogous strong hydrogen bonding interactions with Tyr122 (>99%), Arg204 (99%) and an electrostatic interaction with Arg204 (99%). In AlkB-dsDNA, 2OG (O3, O4) make interactions with Ser145 (61%, 54%) and Trp178 (41%, 30%). These interactions are less stable along the MD time course when compared with AlkBH2-dsDNA and AlkB-ssDNA, implying that 2OG is more effectively stabilized in both these enzyme-substrate complexes compared to AlkB-dsDNA.

### 3.2.3 Interactions of the Iron-Coordinating Residues

Hydrogen bonding interactions involving the Fe-coordinating histidines (His<sup>1</sup> and His<sup>2</sup>) (100% of the MD snapshots in all AlkBH2-dsDNA, AlkB-ssDNA, and AlkB-dsDNA) may enhance active site stability. The non-coordinating oxygen of the Fe-coordinating aspartate is also apparently stabilized via hydrogen bonding interactions, with Arg254 (>99%), Arg210 (99%) and Arg210 (47%) in AlkBH2-dsDNA, AlkB-ssDNA, and AlkB-dsDNA, respectively (Figures B7-B9). The Fe-coordinating axial histidine (His<sup>2</sup>) residues are stabilized via  $\pi$ - $\pi$  stacking with nearby Phe- and Trp-residues in AlkBH2-dsDNA (Phe195 and Phe197) and AlkB-ssDNA (Phe154 and Trp178); these stacking interactions are apparently weaker in AlkB-dsDNA (Phe154 and Trp178) (Figures B10-B12), possibly

reflecting weaker binding of the DNA to AlkB in this complex, as the protein only interacts with one of the duplex DNA chains.<sup>10,11</sup>

### 3.2.4 Dynamics of the Substrate Binding Sites

In the three enzyme-substrate complexes, the heteroaromatic ring of the substrate base ( $m_3C$ ) is stabilized via  $\pi$ -stacking interactions with aromatic residues, which are important in substrate recognition.<sup>10,11</sup> Phe124 and Tyr122 (AlkBH2-dsDNA), Trp69 and Tyr76 (AlkB-ssDNA), and Trp69 and Tyr76 (AlkB-dsDNA), as well as the imidazole groups of the coordinating equatorial histidine ( $His^1$ ) residues, participate in  $\pi$ -stacking interactions, which likely help promote a catalytically productive orientation of the substrate. The exocyclic amine (N4) of the substrate is stabilized by interactions with Glu175 (AlkBH2-dsDNA), Asp135 (AlkB-ssDNA), and Asp135 (AlkB-dsDNA), but the interaction is weaker in the latter case. The intercalating residue, Phe102, that helps in flipping of the damaged base into the active site in AlkBH2-dsDNA,<sup>10,11</sup> forms a stable and continuous  $\pi$ -stacking interaction with the nearby bases; this enhances the stability of the duplex DNA in AlkBH2-dsDNA.

### 3.2.5 Long-Range Correlated Motions

Collective dynamics provides insight into correlated motions between remote regions of the enzyme-substrate complex. In the AlkBH2-dsDNA and AlkB-dsDNA complexes, Dynamic Cross Correlation Analysis (DCCA) (Figures 3.2A, B13-B16) shows that the  $\beta$ -sheets of the DSBH core have positive correlations with one another. These are more

intense in AlkBH2-dsDNA and AlkB-dsDNA than in AlkB-ssDNA, implying that the nature of DNA substrate is capable of influencing the overall correlation motion of the Fe center region via a long-range interaction.

In AlkBH2-dsDNA, residues Tyr161 and Arg248, that bind to 2OG, have a positive correlation with  $\beta 6$  and  $\beta 7$  that form the substrate recognition lid, as well as one of the  $\beta$ -strands ( $\beta 9$ ) of the DSBH, indicating that binding of 2OG might influence the substrate binding site and the orientation of the Fe center. The DNA binding residues (198-214) manifest a positive correlation with Fe, the metal ion coordinating His236 and nearby residues (230-238), implying that such correlated motions might also be of importance for productive substrate orientation. With AlkB-ssDNA, the 2OG binding residues (Tyr122 and Arg204) manifest a positive correlation with Fe, the metal coordinating aspartate, and the loop bearing the metal coordinating HXD motif. The 2OG binding residues (Ser145 and Trp178) in AlkB-dsDNA only show positive correlation with residues on  $\beta 7$  (147-150). These observations imply that the correlated motions of the 2OG binding residues in AlkB-ssDNA likely influence substrate binding more than in AlkB-dsDNA. Further, the DNA binding residues (155-166) in AlkB-ssDNA show positive correlation with the Fe coordinating 2OG, His131, Asp133 and His187, and the nearby residues (126-135 and 183-192). The DNA binding residues (155-166) in AlkB-dsDNA only show positive correlation with the two-metal ion coordinating histidines (His131 and His187), implying that there are stronger correlated motions in AlkB-ssDNA compared to AlkB-dsDNA. Differences in correlation motions could reflect the stronger binding of AlkB to ssDNA compared to dsDNA (where the protein only interacts with the strand that contains the damaged base).

Overall, the analyses imply that complex correlated motions of the molecules are important during catalysis.

Biophysical analyses reveal that AlkBH2-dsDNA contains a hydrophobic  $\beta$ -hairpin ( $\beta$ 3- $\beta$ 4) (aa 89-108) that is close to the active site and which is important in enabling the preference of AlkBH2 for dsDNA substrates.<sup>10,11</sup> DCCA reveals that this hydrophobic  $\beta$ -hairpin has a strong positive correlation with residues 123-128 and the substrate. Residues 123-128 belong to  $\beta$ 6 and  $\beta$ 7 and are proposed to form a substrate recognition lid.<sup>10,11</sup> Such correlated motions might contribute to the binding of the substrate as proposed on the basis of experimental studies.<sup>10,11</sup>

Studies on AlkBH2 have revealed that the D173A, H236A and R203H substitutions cause loss of activity.<sup>36</sup> DCCA shows that D173 and H236 have a strong positive correlation with the Fe center, 2OG, and the coordinating histidines and aspartate. R203 which is located in  $\alpha$ 4, shows a strong correlation with the DNA-binding flexible long loop (residues 200-206). Such correlated motions might potentially contribute to the loss of activity with the D173A and H236A variants, while the R203H substitution might affect DNA binding. Additional studies are needed to validate these proposals.

PCA shows that AlkB-ssDNA (Figure B17) has limited motion for the loop connecting  $\beta$ 6 to  $\beta$ 7 and its N- and C-terminal regions. AlkBH2-dsDNA (Figure 3.2B) has limited motions at its N- and C-terminal regions, whereas AlkB-dsDNA (Figure B18) shows major motion in its complexed DNA and limited motions at its N- and C-terminal regions. These

observations support the preferences of AlkB and AlkBH2 for ssDNA and dsDNA, respectively.

### **3.2.6 Dynamics of AlkB-ssDNA, AlkB-dsDNA, and AlkBH2-dsDNA with undamaged DNA**

MD simulations with the non-methylated DNA substrate reveals that it can bind to the enzymes (Figures B19-B21). The studies show that the protein-DNA complexes in both AlkBH2-dsDNA and AlkB-ssDNA are more rigid than the AlkB-dsDNA complex (Figures B22-B24). The measured distance between the Fe center and N3 of the substrate in comparison with the N-methylated DNA substrates in all the three systems implies that the undamaged DNA systems are not catalytically productive (Figures B25-B26), even though the complexes are stable. Binding free energy calculations using the Molecular Mechanics/Generalized Born Surface Area (MM/GBSA)<sup>13b</sup> method reveals weaker binding of undamaged DNA to the respective enzyme compared with the results obtained for the damaged DNA substrates. In the undamaged DNA complexes, the relative free energies of binding of DNA to protein in AlkBH2-dsDNA, AlkB-ssDNA and AlkB-dsDNA are -125.26, -26.55 and -32.87 kcal/mol, respectively. Values of -143.03, -37.10 and -45.99 kcal/mol for the damaged DNA complexes of AlkBH2-dsDNA, AlkB-ssDNA and AlkB-dsDNA complexes, respectively, are consistent with the catalytically productive nature of the latter complexes.



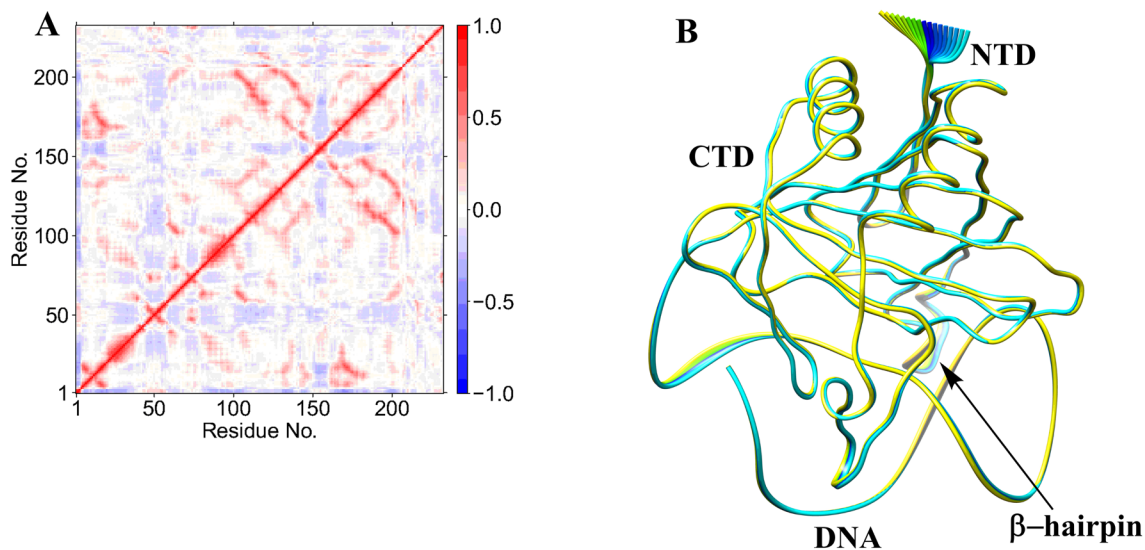


**Figure 3.2.** Dynamic Cross Correlation (A) and Principal Component Analysis (B) for the AlkBH2-dsDNA Fe(III)-superoxo complex. In A, residue numbers are as follows: 1-206 (protein), 207 (Fe), 208 (O<sub>2</sub>), 209 (2OG), 210-235 (DNA) and 216 (m<sup>3</sup>C substrate). NTD and CTD are the N-terminal and C-terminal domains, respectively. Yellow to blue represents the direction of motion of residues in B.

### 3.2.7 Reaction Mechanism of the Dioxygen Activation

#### O<sub>2</sub> Activation for the “off-line” Fe(III)-superoxo Complex

QM/MM calculations were carried out using a snapshot from the productive MD trajectories of the “off-line” Fe(III)-superoxo complex, taking the distance between the distal oxygen (O<sub>d</sub>) of the superoxide and the C2 of the 2OG as a reaction coordinate (Figures B2D, B28 and B29). The QM region (Figure 3.3) contains the iron-dioxygen (Fe-O<sub>2</sub>) unit, 2OG, the methylimidazole groups of His171 (His<sup>1</sup>) (His131 for AlkB) and His236

(His<sup>2</sup>) (His187 for AlkB), the acetate group of Asp173 (Asp133 for AlkB), the methylguanidium group of Arg254 (Arg210 for AlkB) and the 3-methylcytosine part of the DNA substrate.

The potential energy profile and the optimized geometries of the stationary points obtained for the dioxygen activation process (Scheme 3.2) are presented in Figures 3.4 and 3.5, respectively. In the optimized QM/MM model of the reactant (RC1), the Fe-O<sub>p</sub> and O<sub>p</sub>-O<sub>d</sub> distances are 2.11 Å and 1.27 Å, respectively. The Fe center oxidation state was determined via a spin density analysis. The spin densities of Fe and dioxygen are 4.19 and -0.68, respectively, supporting the Fe(III) oxidation state of this complex; the values compare favorably with previous studies on 2OG oxygenases.<sup>23-26</sup> The relatively long O<sub>p</sub>-O<sub>d</sub> bond and the spin density value of O<sub>2</sub> supports the superoxide character of RC1.<sup>23,24</sup> In the first transition state (TS1) the O<sub>p</sub>-O<sub>d</sub> bond distance increases to 1.37 Å, while the Fe-O<sub>p</sub> and O<sub>d</sub>-C2 bond lengths shorten to 2.00 Å and 1.42 Å, respectively, in agreement with the results of previous studies.<sup>24,25a</sup> The C1-C2 distance increases from 1.55 Å to 1.83 Å, pointing to the partial cleavage of the bond in readiness to eliminate CO<sub>2</sub>.

Decarboxylation proceeds via a Fe(II)-peroxysuccinate intermediate<sup>20b</sup> (IM1), involving the cleavage of C1-C2 of 2OG and formation of a bond between O<sub>d</sub> and C2 of 2OG, with an activation barrier of 11.8 kcal/mol, including the zero-point energy contribution, calculated at the UB3LYP/def2-TZVP level. Formation of this intermediate (IM1) is highly exergonic with an energy of -34.3 kcal/mol. The highly exergonic nature of this step is likely due to release of CO<sub>2</sub> and formation of succinate. At this stage, the C1-C2 bond is

completely cleaved with a distance of 3.48 Å while the peroxy bridge O<sub>p</sub>-O<sub>d</sub> bond is elongated to 1.45 Å. In AlkBH2-dsDNA, hydrophobic interactions of Met226 with Phe197 and Ile184 including  $\pi$ -stacking interaction of Phe195 and Phe197 enhances stabilization of TS1. TS1 is further stabilized by networks of hydrogen bonding interactions of Arg254 with Thr252 and the non-coordinating oxygen of the iron ligating Asp173. TS1 derived from AlkB-ssDNA is stabilized by hydrophobic interaction of Ile143 with Trp178, hydrogen bonding interaction of Arg210 with the non-coordinating oxygen of the iron ligating Asp133 and hydrogen bonding interaction of Thr208 with the non-coordinating oxygen of C1-carboxylate of the 2OG. In addition to the hydrophobic interaction of Ile143 with Trp178, TS1 in AlkB-dsDNA is stabilized by hydrogen bonding networks of Arg183 and Arg210 with Glu136 and the non-coordinating oxygen of the iron ligating Asp133, as well as by a salt bridge interaction of Arg210 with the 2OG C1-carboxylate. The DCCA shows that the residues involved in the stabilization of TS1 in AlkBH2-dsDNA have positive correlation with the Fe-center and DSBH core residues. In AlkB-dsDNA, the TS1 stabilizing residues manifest positive correlation with nucleotide recognition lid residues, while in AlkB-ssDNA the residues have positive correlation with residues that make up the DSBH core. This indicates that long-range interactions with DSBH residues might be more important for O<sub>2</sub> activation in AlkBH2-dsDNA and AlkB-ssDNA than in AlkB-dsDNA. The results suggest that modification of residues in the DSBH, might selectively influence dioxygen activation process in AlkBH2-dsDNA and AlkB-ssDNA, whereas with AlkB-dsDNA targeting residues in the nucleotide recognition lid may be more productive in this regard.

The next step, i.e., reaction of IM1 to IM2, involves homolytic cleavage of the O<sub>p</sub>-O<sub>d</sub> bond of IM1; this is faster than the decarboxylation step with a barrier of 6.7 kcal/mol and a barrierless process with ZPE contribution. This result implies that the decarboxylation step is rate-limiting in the oxygen activation phase of catalysis. IM2 has a partial bond of length 2.10 Å between the two oxygen atoms and the Fe-O<sub>p</sub> bond length is 1.77 Å. The partial O<sub>p</sub>-O<sub>d</sub> bond then breaks and IM2 rearranges to form IM3 with a new Fe-O<sub>p</sub> bond length of 1.62 Å. The spin density of 3.16 for Fe reveals the formation of the ferryl (Fe(IV)=O) species. IM3 is thermodynamically stable with an overall reaction energy of -43.8 kcal/mol at the BS2+ZPE theory level, inferring dioxygen activation is exergonic. The Fe(IV)-oxo group in IM3 is incorrectly positioned (“off-line” geometry) to react with the substrate and thus, if an intermediate, it must undergo rearrangement, i.e. the Fe(IV)-oxo migrates towards the methyl group of the nucleobase substrate (“in-line” geometry).

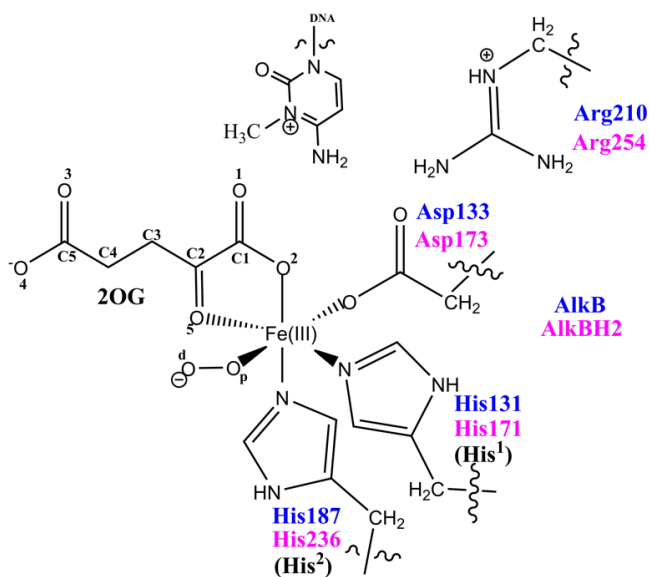
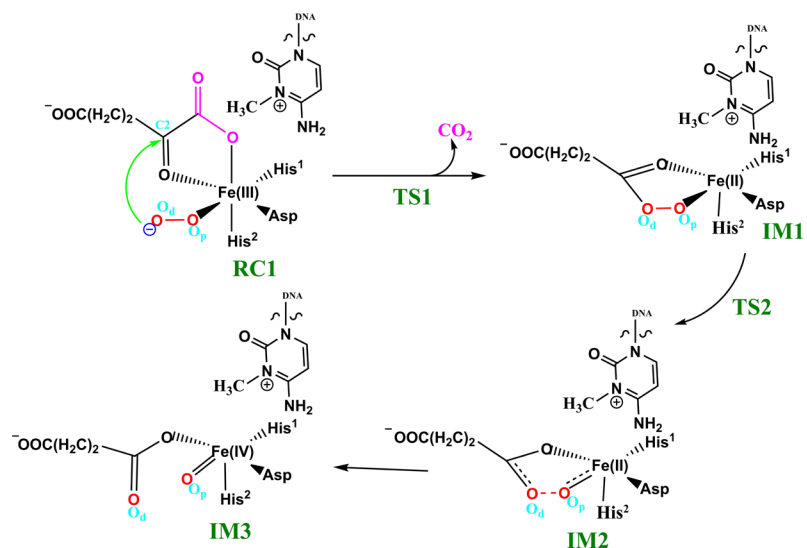


**Figure 3.3.** The QM region of AlkB / AlkBH2 used in the QM/MM calculations.



**Scheme 3.2.** Mechanism of dioxygen activation.

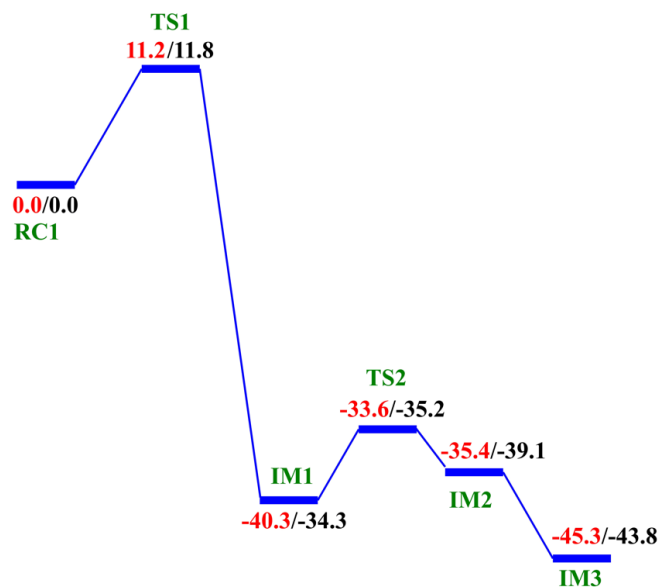


**Figure 3.4.** QM/MM Reaction Profile for the dioxygen activation step by AlkBH2-dsDNA. Relative energies are in kcal/mol at UB3LYP/def2-TZVP (BS2) (in red) and BS2 with ZPE (in black).

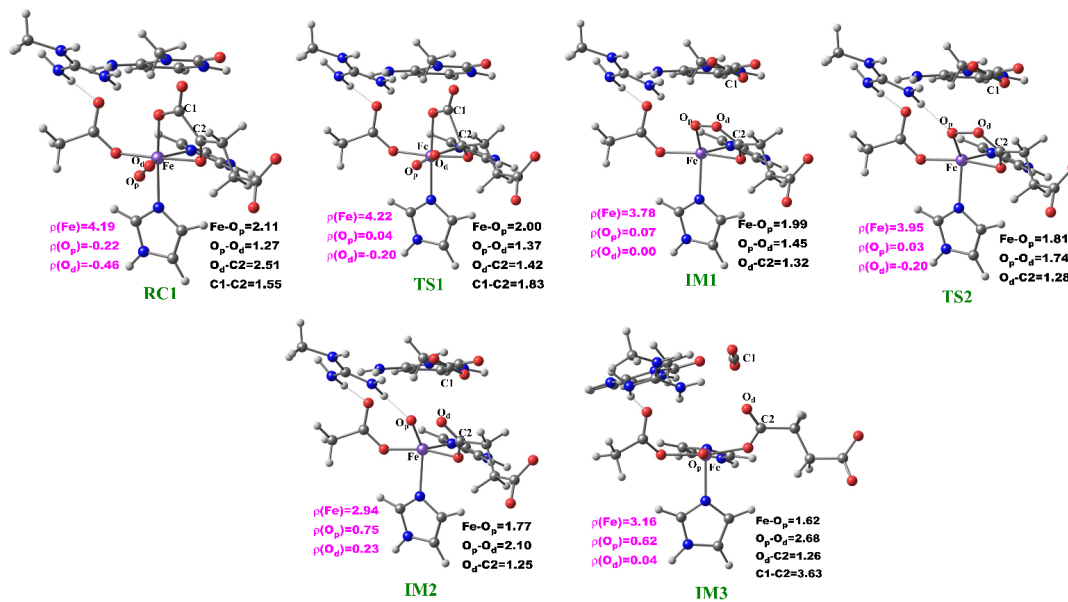


**Figure 3.5.** The reaction state geometries of the dioxygen activation step (stationary points) in AlkBH2-dsDNA. Distances (Å) and the spin densities are in black and pink, respectively.

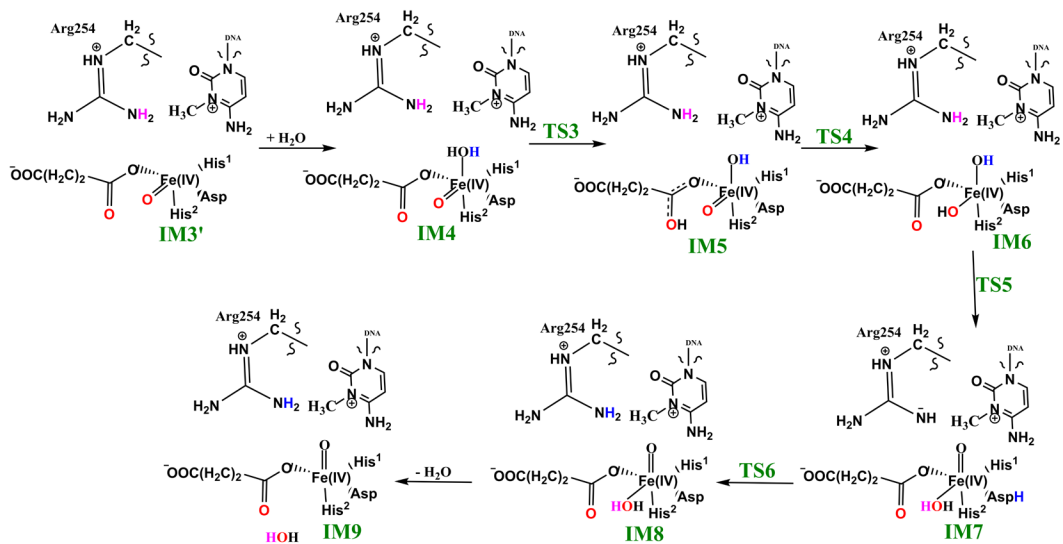
The dioxygen activation step in AlkB-ssDNA and AlkB-dsDNA with the same substrate (m<sub>3</sub>C) manifests similar behavior as observed in AlkBH2-dsDNA with the rate-determining step having barriers of 11.3 kcal/mol and 13.2 kcal/mol with ZPE correction, respectively. The detailed geometries of the stationary points are presented in the SI (Figures B30 and B31).

### 3.2.8 Formation of the “in-line” Fe(IV)=O intermediate via a potential ‘ferryl flip’ in AlkBH2

We then investigated the two proposed mechanistic possibilities for obtaining a productive ferryl intermediate using QM/MM calculations. In one mechanism, formation of the “in-line” Fe(IV)=O intermediate from IM3 (wherein the oxo group is not productively oriented to react with the substrate) has been proposed to occur via oxygen atom exchange with the use of a water molecule.<sup>13a,18a,23</sup> Such a process has been termed a “ferryl flip”, i.e. the oxo group in IM3 flips toward the target methyl group of the m<sub>3</sub>C substrate to give a productive Fe(IV)=O intermediate (Scheme 3.3). IM3' comprises IM3 with two water molecules added to the QM region. The ferryl flip process begins with the binding of one water molecule to the open coordination site of the iron center, leading to the formation of a six-coordinate ferryl complex (IM4) with bond lengths of 2.12 Å and 1.62 Å for Fe-O<sub>1</sub> and Fe-O<sub>p</sub>, respectively. One of the protons (H<sub>1</sub>) from the coordinated water molecule is then transferred to the non-coordinating carboxylate oxygen of the succinate to give IM5. This step passes through TS3 with a barrier 6.6 kcal/mol at the BS2+ZPE level of theory. The so transferred proton (H<sub>1</sub>) to succinate is then transferred to the oxo (O<sub>p</sub>) group of the “off-line” Fe(IV)=O to give a ‘dihydroxylated’ Fe(IV) complex, IM6, with Fe-O<sub>1</sub> and Fe-O<sub>p</sub> bond lengths of 1.82 Å and 1.74 Å, respectively. The formation of this ‘dihydroxylated’ complex is slightly endergonic with an energy of 5.2 kcal/mol at BS2+ZPE level of theory. The equatorial hydroxyl group is then converted to H<sub>2</sub>O using the proton (H<sub>a</sub>) from the Arg254 guanidino group, concomitant with the spontaneous transfer of a proton (H<sub>2</sub>) from

the axial hydroxyl group to the non-coordinating carboxylate oxygen (O<sub>2</sub>) of the coordinating aspartate, to give IM7. This passes through TS5 with a barrier of 18.3 kcal/mol; the so formed IM7 is slightly endergonic with an energy of 6.7 kcal/mol at the BS2+ZPE level of theory. Subsequently, the proton (H<sub>2</sub>) from the non-coordinating carboxylate of the coordinating aspartate in IM7 is transferred to the deprotonated NH (N<sub>a</sub>H) group of Arg254, resulting in the “flipped” Fe(IV)=O complex, IM8. IM8 can then release the bound water molecule to give the “in-line” 5-coordinate complex, IM9. The optimized “ferryl flip” reaction states geometries and energy profile are presented in (Figures 3.6 and B32) and Figure 3.7, respectively. The overall “ferryl flip” process proceeds with a very high barrier of 21.7 kcal/mol, at the BS2+ZPE level of theory, which is higher than the previously reported barrier of 10.9 kcal/mol and 18.1 kcal/mol for oxygen atom exchange for Asqj<sup>23</sup> and PHF8,<sup>18b</sup> respectively. We also explored the possibility of direct transfer of the proton (H<sub>2</sub>) from the axial hydroxyl (O<sub>1</sub>H<sub>2</sub>) group to the equatorial hydroxyl group (O<sub>p</sub>H<sub>1</sub>) of the ‘dihydroxylated’ Fe(IV) complex, IM6 (Figure B33). This transfer results in a barrier of 24.3 kcal/mol at the BS2+ZPE level of theory, which is 2.6 kcal/mol higher than the one observed via proton transfer through Arg254; thus, this process is not energetically viable in agreement with the studies on the histone demethylase, PHF8.<sup>18b</sup> These high barriers could in part be due to the compact nature of the active site and steric effects arising from the nucleobase ring (cytosine) of the substrate, as well as the second sphere residue Arg254.





**Scheme 3.3.** The proposed ferryl flip mechanism by AlkBH2-dsDNA.

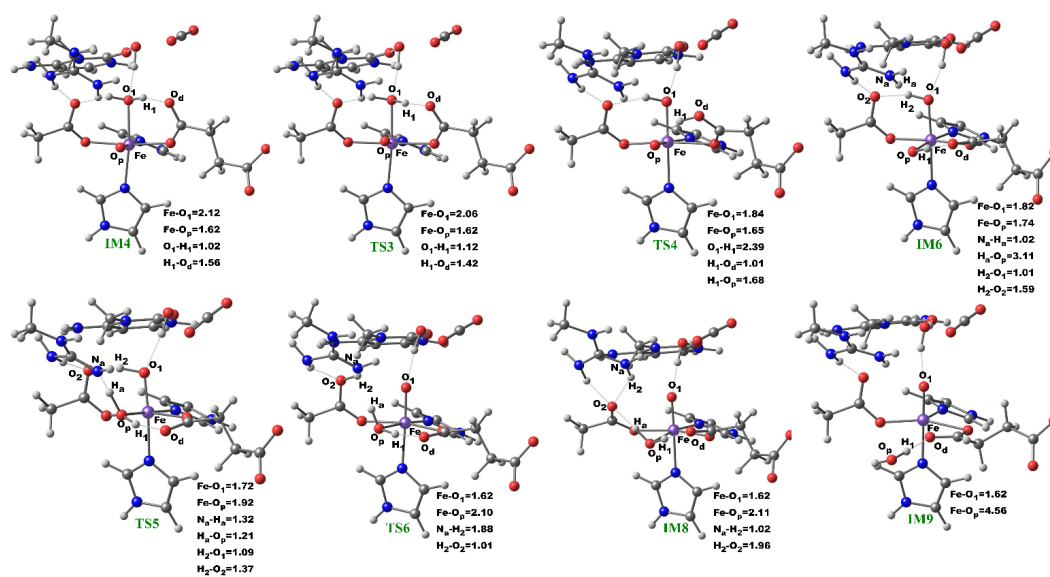


**Figure 3.6.** The reaction state geometries of the proposed ferryl flip mechanism stationary points in AlkBH2-dsDNA. Distances are in Å.

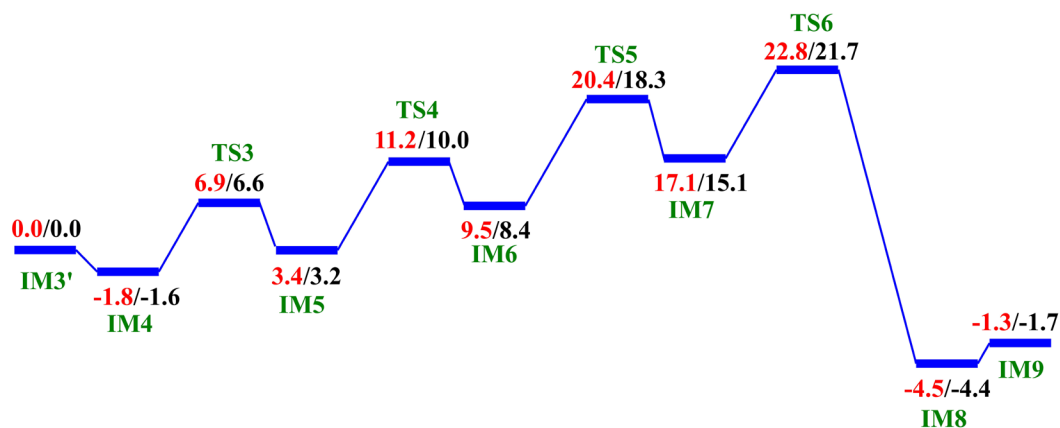


**Figure 3.7.** QM/MM Reaction Profile for the proposed ferryl flip mechanism by AlkBH2-dsDNA. Relative energies are in kcal/mol at UB3LYP/def2-TZVP (BS2) (in red) and BS2 with ZPE (in black).

### 3.2.9 Rotation of the C1 carboxylate of 2OG from the ‘off-line’ to an ‘in-line’ binding mode in AlkBH2

The change in the 2OG binding mode from the “off-line” to the “in-line” geometry to enable a productive ferryl orientation was then explored by performing a potential energy scan via the changing of the dihedral angle  $N^{\epsilon}$  (His<sup>1</sup>)-Fe-O5 (2OG)-O2 (2OG) of the five-coordinate enzyme-substrate (ES1) complex of AlkBH2-dsDNA. The five-coordinate ES1 complex contains a Fe(II) center (high spin state S=2, M=5) ligated by two histidiny residues (His<sup>1</sup> and His<sup>2</sup>), one aspartyl residue and the 2OG co-substrate which is bound in an ‘off-line’ bidentate manner. First, we performed a 1  $\mu$ s MD of the five-coordinate enzyme-substrate complex (Figures B34 and B35). We then used an MD snapshot to

perform QM/MM calculations for the proposed 2OG reorientation. QM/MM optimizations were first carried out on the ES1 snapshots of the system. The potential energy scans were then performed on the optimized ES1 complex with 2° increment of the N<sup>ε</sup> (His<sup>1</sup>)-Fe-O5-O2 dihedral angle.

The optimized stationary point geometries of the 2OG rotation are presented in Figure 3.8. In the optimized QM/MM model of the MD simulated ES1 complex snapshot, the bond lengths of Fe-O2 and Fe-O5 are 2.05 Å and 2.34 Å, respectively. The bonds are marginally elongated compared to the Fe(III)-superoxo complexes (RC1), where the Fe-O2 and Fe-O5 bond lengths are 2.03 Å and 2.18 Å, respectively. The shorter bond lengths observed in the Fe(III)-superoxo complex are likely due to the oxidation of Fe(II) to Fe(III), which strengthens metal-ligand bonds. The dihedral angle potential energy scan resulted in the rotation of the 2OG C1 carboxylate from the ‘off-line’ binding mode (ES1) to the ‘in-line’ mode (ES2). The transition state has dihedral angle of 151.6° with Fe-O2 and Fe-O5 bond lengths are 2.07 Å and 2.36 Å, respectively. The rotation proceeds rapidly with barriers of 2.94 kcal/mol at the BS2+ZPE level. This value is about 1.5 kcal/mol higher than the value obtained for another 2OG oxygenase, PHF8,<sup>18b</sup> possibly due to increased steric effects in the active site as well as the strong hydrogen bonding interaction of the second-sphere arginine residue (Arg254) with the C1 carboxylate of 2OG in the enzyme, which is absent in PHF8.

Formation of the ‘in-line’ five-coordinate AlkBH2-dsDNA enzyme substrate complex (ES2) is slightly exergonic with relative energies of -1.98 kcal/mol at the BS2+ZPE level.

The dihedral angle of the formed ‘in-line’ complex (ES2) is 153.6° while the Fe-O2 and Fe-O5 bond lengths are 2.04 Å and 2.35 Å, respectively. Overall, these calculations imply 2OG rotation is energetically favourable in agreement with the results for PHF8.<sup>18b</sup>

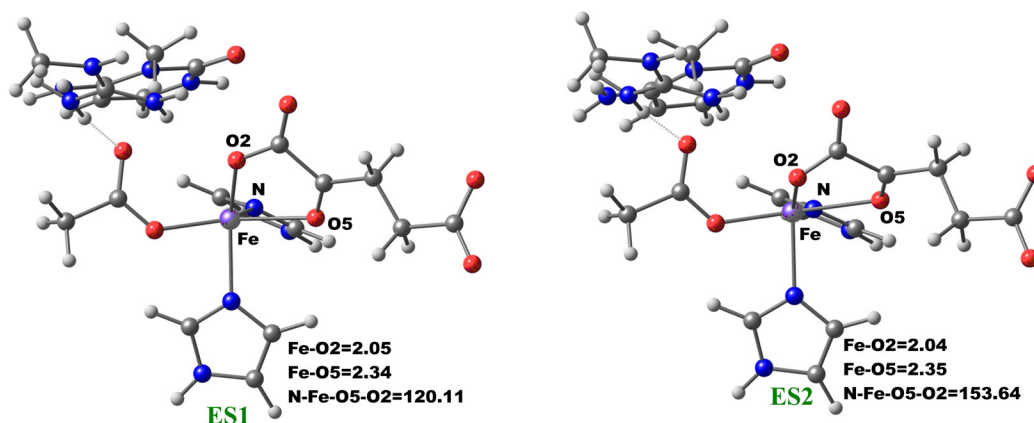


**Figure 3.8.** The reaction state geometries of the 2OG rotation stationary points in AlkBH2-dsDNA. The distances and angle are in Å and degrees, respectively.

### 3.2.10 O<sub>2</sub> Activation for “in-line” Fe(III)-superoxo Complex

After the formation of the ‘in-line’ five-coordinate enzyme substrate complex (ES2), dioxygen binds to the vacant Fe coordination site to give the ‘in-line’ Fe(III)-superoxo complex, which was then subjected to 1 μs MD simulations (Figures B36 and B37). An MD snapshot was then used for the QM/MM study. The obtained results are similar to those obtained for the ‘off-line’ Fe(III)-superoxo complex. The rate determining decarboxylation step has a barrier of 9.6 kcal/mol, at the BS2+ZPE level of theory, in comparison to 11.8 kcal/mol obtained for the ‘off-line’ Fe(III)-superoxo complex.

Therefore, for the ‘in-line’ Fe(III)-superoxo complex, the rate-determining decarboxylation barrier is 2.2 kcal/mol lower than for the ‘off-line’ Fe(III)-superoxo complex, implying that the dioxygen activation is faster in ‘in-line than ‘off-line’ geometry. Formation of the ‘in-line’ Fe(IV)=O complex (IM3) is also thermodynamically favourable with a reaction energy of -63.4 kcal/mol at the BS2+ZPE level of theory, in comparison to -43.8 kcal/mol obtained for the ‘off-line’ Fe(IV)=O via ‘off-line’ Fe(III)-superoxo complex, indicating the exergonic nature of the dioxygen activation reaction. The geometries of the stationary points are presented in Figure B38.

### **3.2.11 Conformational Flexibility Modulates the Structure of the Reactive Complex (Fe(IV)=O) for the Substrate Hydroxylation in AlkB-ssDNA, AlkB-dsDNA, and AlkBH2-dsDNA systems.**

RMSD analyses of the active site, protein, protein-DNA complex, and DNA for all the three Fe(IV)=O complexes of the three systems show stable structures with average RMSD values of 2.05 Å, 1.67 Å and 1.75 Å for the protein-DNA complex in AlkBH2-dsDNA, AlkB-ssDNA and AlkB-dsDNA, respectively (Figure B39). These analyses reveal the stability of the active site, protein, protein-DNA complex and the DNA in both AlkB-ssDNA and AlkBH2-dsDNA while they show some flexibility in AlkB-dsDNA. DNA contributes significantly to the overall RMSD of the protein-DNA complexes in both AlkB-substrate complexes, while minimal contribution is observed in AlkBH2-dsDNA. Center of mass analyses shows a similar trend to that observed for the Fe(III)-superoxo

complexes with average values of 17.5 Å, 26.7 Å and 19.3 Å for AlkB-ssDNA, AlkB-dsDNA, and AlkBH2-dsDNA, respectively (Figure B40). This observation indicates that AlkBH2-dsDNA is more structurally compact than AlkB-dsDNA in the ferryl complex as observed for the superoxo complex, a difference arising from the observed stronger interactions between the protein and dsDNA in AlkBH2-dsDNA.<sup>10,11</sup> Hydrogen bonding analysis shows that the non-metal-coordinating C4 carboxylate oxygens (O3, O4) of the succinate interact with Arg 248 (76%, 84%) and Tyr 161 (84%, 18%) in AlkBH2-dsDNA. Similar hydrogen bonding interactions are observed in the AlkBs where the succinate C4 carboxylate oxygens (O3, O4) interact with Ser 145 and Trp 178 with (55%, 61%) and (18%, 17%), respectively, in AlkB-ssDNA and (38%, 37%), (37%, 39%), respectively, in AlkB-dsDNA. These results imply more flexibility in the binding of succinate compared with that of 2OG, likely reflecting stronger binding of the 2OG co-substrate compared to the succinate co-product. These observations could be of relevance to inhibitor design in terms of optimizing the chain length of bonding in the 2OG/succinate pocket. In AlkBH2-dsDNA, the residues involved in the stabilization of the succinate have positive correlation with residues 159-166 ( $\beta$ 8), 188-192 ( $\beta$ 10) and 238-250 ( $\beta$ 14, which contains coordinating His236 and  $\beta$ 15). In the AlkBs, the residues that stabilize the succinate manifest positive correlation with 174-178 (loop connecting  $\beta$ 9 and  $\beta$ 10) and 206-209 ( $\beta$ 12). All these residues are in the vicinity of the non-coordinating C4-carboxylate of the succinate, indicating that the correlated motions likely aid in the overall binding of the succinate. The results reveal stable hydrogen bonding interactions between the iron coordinating His<sup>1</sup> and His<sup>2</sup> residues (>99% of the structures in the MD simulations) in the AlkBH2-dsDNA,

AlkB-ssDNA, and AlkB-dsDNA complexes. Analysis of the distances between the oxo group of the Fe(IV)=O intermediate and the methyl carbon of the substrate ( $m_3C$ ) reveals that the substrate is closer to the metal centre in the ferryl complex than in the superoxo complex (Figures B39D, B41 and B42). This observation is supported by Molecular Mechanics/Generalized Born Surface Area (MM/GBSA)<sup>13b</sup> calculations, which predict how strongly the substrates bind to the proteins. In the Fe(III)-superoxo complex, the relative free energies of binding of  $m_3C$  DNA substrates to AlkBH2-dsDNA, AlkB-ssDNA and AlkB-dsDNA are -143.03, -37.10 and -45.99 kcal/mol, respectively, while values of -168.89, -56.01 and -67.91 kcal/mol are obtained for the ferryl complex of AlkBH2-dsDNA, AlkB-ssDNA and AlkB-dsDNA, respectively. These results show that the  $m_3C$  substrate binds better to the proteins in the ferryl complex than in the superoxo complex in all three enzymes, reflecting formation of more productive complexes necessary for hydroxylation. The calculations also show that the substrate in AlkBH2-dsDNA binds better than in ds-AlkB complexes, possibly due to stronger interactions between the two strands of the dsDNA and the protein in AlkBH2-dsDNA. The MMGBSA method provides binding free energies of a set of ligands with similar size and structure.<sup>13c,d</sup> We compared the relative free energies of the AlkBH2-dsDNA and AlkB-dsDNA complexes, and the Fe(III)-superoxo and Fe(IV)-oxo intermediates in the same system. The effect of the size of the substrate is reduced by calculating the relative free energies for AlkB and the methylated nucleotide only (excluding the rest of the DNA fragments) in both AlkB-ssDNA and AlkB-dsDNA. The results show stronger binding between AlkB and methylated ssDNA (-11.26 and -18.19 kcal/mol for the Fe(III)-superoxo and Fe(IV)-oxo complexes, respectively)

compared to dsDNA (-6.46 and -9.11 kcal/mol for the Fe(III)-superoxo and Fe(IV)-oxo complexes, respectively), in accord with experimental observations.<sup>10,11</sup>

DCCA (Figures 3.9A, B15, B16, B43 and B44) for the ferryl proteins reveals correlated motions that are similar but differ in details to that observed in the Fe(III)-superoxo systems, indicating that complex correlated motions are involved in the binding of DNA and the succinate co-product and contribute to the proper positioning of the substrate in respect to Fe(IV)=O for the hydrogen abstraction step.

PCA provides insight into the essential dynamics and the direction of motion in flexible regions of proteins<sup>37a,b</sup> PCA of AlkBH2-dsDNA (Figure 3.9B) has limited motions in the N- and C-terminal regions of the protein and major motions at the hydrophobic  $\beta$ -hairpin region. The observed motion of the hydrophobic  $\beta$ -hairpin, which is not observed in the Fe(III)-superoxo complex, is towards the Fe center, resulting in compaction of the complex, and hence likely a complex that favors catalysis. AlkB-ssDNA (Figure B45) has motions in its N- and C-terminal regions, while AlkB-dsDNA (Figure B46) shows major motions at the loops connecting  $\beta 6$  to  $\beta 7$  and  $\beta 4$  to  $\alpha 2$ , in the DNA substrate (reduced motion when compared with the superoxo complex) and limited motions in the N- and C-terminal regions. The PCA results also support experimental observations that the protein in the AlkBH2-dsDNA complex makes strong interactions with both DNA chains while AlkB-dsDNA protein makes interactions with one of the DNA chains only<sup>10,11</sup> PCA indicates that the duplex DNA in AlkBH2 is more rigid than in AlkB, arising from the above stated variation in the proteins' interaction with dsDNA.



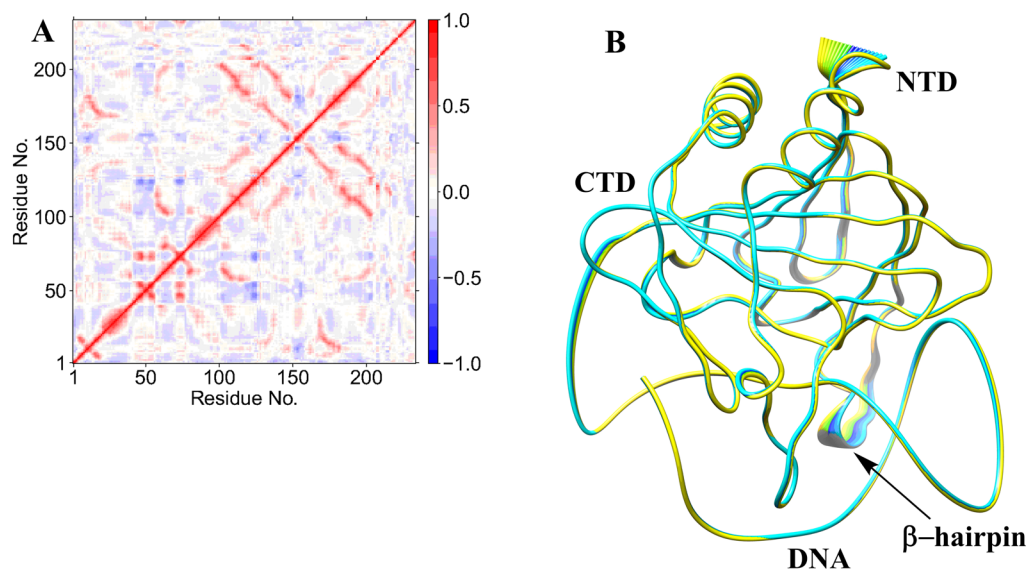


**Figure 3.9.** Dynamic Cross Correlation (A) and Principal Component Analysis (B) for AlkBH2-dsDNA at the ferryl complex stage. In A, residue numbers are as follows: 1-206 (protein), 207 (Fe), 208 (O), 209 (succinate), 210-235 (DNA) and 216 ( $m_3C$  substrate). NTD and CTD are the N-terminal domain and C-terminal domain, respectively. Yellow to blue represents the direction of motion of protein residues in B.

### 3.2.12 Mechanism of DNA Substrate Hydroxylation in AlkB-ssDNA, AlkB-dsDNA, and AlkBH2-dsDNA complexes

Steps involved in the hydroxylation of the  $m_3C$  DNA substrate (Scheme 3.4) comprise: (i) hydrogen atom abstraction (HAT) followed by (ii) rebound hydroxylation. HAT involves the cleavage of the C-H bond in substrate, which subsequently attacks the Fe(IV)-oxo group from the equatorial or axial position.<sup>25b,38</sup> An electron is transferred from the substrate into the d-orbitals of the Fe(IV) center. HAT has been reported to occur via two

possible channels for 2OG oxygenases: i) a  $\sigma$ -channel and ii) a  $\pi$ -channel<sup>25b,c,38</sup> (Figure 3.10). In the  $\sigma$ -channel, an  $\alpha$ -spin electron shifts from  $\sigma_{\text{CH}}$  of the substrate to  $\sigma_{z^2}^*$  of the metal; this results in a TS that assumes a trajectory with linear Fe-O-H arrangement (approximately  $180^\circ$ ). In the  $\pi$ -channel, the hydrogen atom approaches the Fe(IV)-oxo metal centre in a sideways manner, leading to the transfer of a  $\beta$ -spin electron into the antibonding  $\pi^*$  orbitals of the Fe(IV) center. This overlap results in a TS with an optimal Fe-O-H angle of roughly  $120^\circ$ . As the substrate approaches the Fe(IV)=O group, the Fe-O bond gradually elongates and polarizes to form the electron acceptor, a ferric-oxyl species.<sup>25b,c,38</sup>

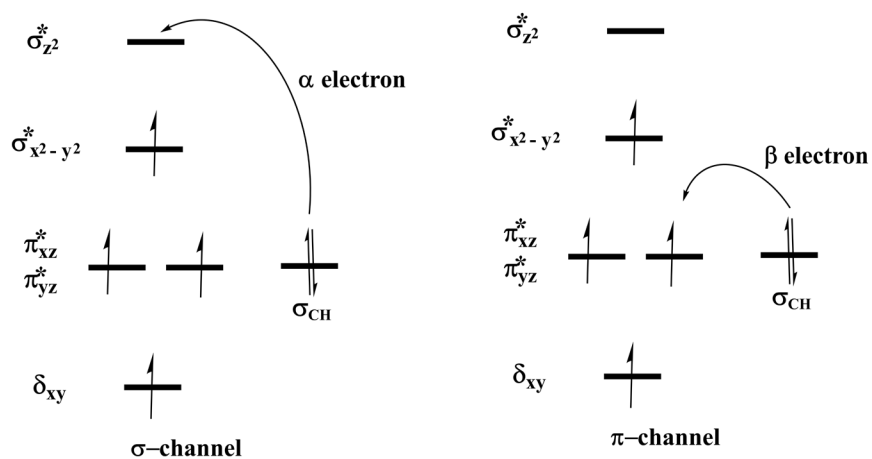
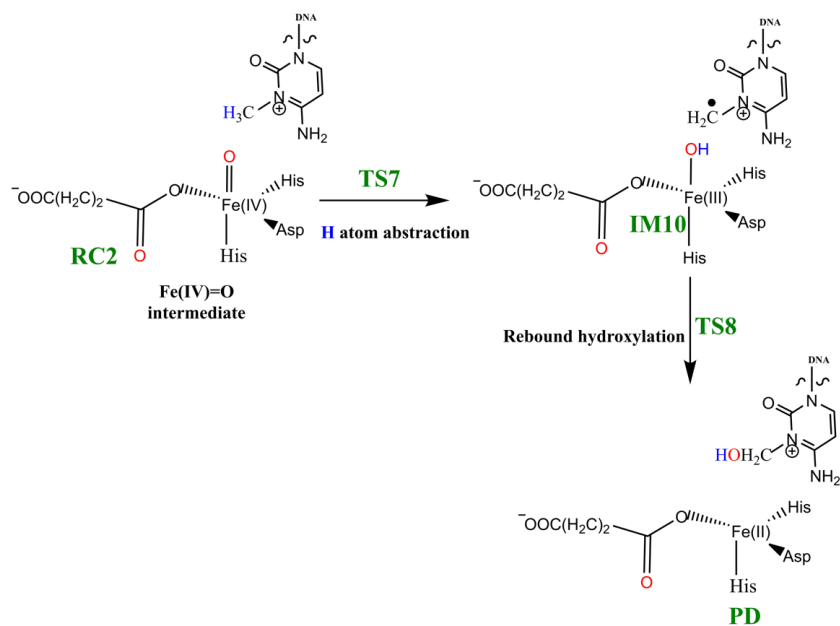


**Figure 3.10.** Reaction channels for HAT by the Fe(IV)=O complexes.



**Scheme 3.4.** Mechanism of hydrogen atom abstraction and rebound hydroxylation steps.

### 3.2.13 Hydrogen Atom Abstraction (HAT)

The reactive Fe(IV)=O species (RC2) generated from the dioxygen activation phase abstracts a hydrogen atom from the methyl group of lesioned DNA substrate (m<sub>3</sub>C), leading to formation of the ferric-hydroxo (Fe(III)-OH) group and a methylene (R-<sup>•</sup>CH<sub>2</sub>) radical (IM10). The formation of IM10 passes through TS7.

### 3.2.14 Effects of the Conformational Flexibility on HAT

To explore the effects of conformational flexibility, QM/MM calculations were performed using five (5) well-equilibrated snapshots from the ferryl complex production MD trajectories. The snapshots were used to explore the effect of conformational variations on

the potential energy barrier of the rate-determining hydrogen atom abstraction step. Calculations were carried out with the quintet spin state of the Fe(IV)-oxo intermediate because previous studies have shown the preference of non-heme iron enzymes for this spin state.<sup>15,23-26</sup> Our calculations reveal the HAT to be the rate-determining step in substrate hydroxylation in agreement with other studies on non-heme iron enzymes.<sup>24,27-30</sup> The calculated barriers at the B3LYP/def2-TZVP level (BS2) for the five snapshots vary between 24.9 and 27.5 kcal/mol without zero-point energy (ZPE) correction and with ZPE, they vary between 21.6 and 24.7 kcal/mol (Table 3.1). The average barriers calculated using the Boltzmann weighted average<sup>39</sup> were found to be 22.2 kcal/mol and 25.3 kcal/mol with and without ZPE, respectively. The Boltzmann weighted average has been employed in various QM/MM studies of enzyme reactions, where multiple snapshots have been used in the mechanistic studies<sup>31,39-43</sup> in order to eliminate the contributions of unreasonably high barriers and stronger weights the lower and more representative barriers.<sup>43</sup> The calculated barrier is consistent with the experimentally-derived value of 20.1 kcal/mol, calculated from the  $k_{\text{cat}}$  value of 2.6 min<sup>-1</sup> at 37 °C.<sup>44</sup> In AlkB-ssDNA, the Boltzmann weighted average barriers are 25.6 and 21.9 kcal/mol, without and with ZPE, respectively, while 25.1 and 22.3 kcal/mol were obtained for AlkB-dsDNA without and with ZPE, respectively (Tables B1 and B3). Our calculated energy barriers match with previously reported HAT values for other similar non-heme iron enzyme models using QM/MM or DFT methods.<sup>24,27-30</sup> Comparison of key distances and angles in both RC2 and TS7 for all the five snapshots used for AlkBH2-dsDNA are presented in Table 3.1 and are included in the SI for both AlkB complexes (Tables B2 and B4). Subsequent calculations and

molecular orbital analysis were performed using the snapshots giving the lowest barrier for the HAT.

### 3.2.15 Molecular orbital interactions driving $\sigma$ - and $\pi$ - pathways

During hydrogen atom abstraction, the substrate C-H bond cleaves and reacts with the Fe(IV)-oxo group, leading to the elongation of the Fe-O<sub>p</sub> bond and its polarisation to form an Fe(III)-oxyl radical (Fe(III)-O<sup>•</sup>) at TS7. The obtained spin density of 4.00 for Fe at the TS7 confirms the 3+ oxidation state for the Fe center. Figure 3.11 shows the electron shift with orbital occupations in RC2 and TS7 in HAT. In RC2, the  $\sigma_{x^2-y^2}^*$  orbital is half filled, and  $\sigma_z^*$  is a virtual orbital. An alpha electron is transferred from the substrate ( $\sigma_{CH}$ ) into the antibonding  $\sigma_z^*$  orbital located along the Fe-O axis to give the radical carbon IM10 intermediate. HAT proceeds via a  $\sigma$ -channel and the calculated spin density for the carbon atom of the substrate at TS7 varies between -0.392 and -0.337 in all the snapshots. These observations support transfer of an  $\alpha$ -electron to the 3d orbital of the Fe metal (Table 3.1). The Fe-O<sub>p</sub>-H angle in all the snapshots varies between 141.89 and 151.36° at the transition state (TS7) (Table 3.1), i.e. it deviates from 180°, likely because of constraints in geometry as the m<sub>3</sub>C DNA substrate cannot move freely in the protein environment. Previous studies on other non-heme iron enzymes have also reported an analogous Fe-O<sub>p</sub>-H angle that deviates from 180°, but which still proceeds via the  $\sigma$ -channel for hydrogen atom transfer.<sup>28,29,32</sup>

With both AlkB-ssDNA and AlkB-dsDNA, the HAT transition state (TS7) Fe-O<sub>P</sub>-H angle in all the snapshots varies between 118.37 and 145.55° (AlkB-ssDNA) and 129.88 and 139.31° (AlkB-dsDNA) (Tables B2 and B4). These results and the calculated spin densities (Table B4) at the carbon of the m<sub>3</sub>C substrate, which vary between -0.342 and -0.314, imply that AlkB-dsDNA hydrogen atom transfer can also proceed via a  $\sigma$ -channel, with the transfer of an  $\alpha$ -electron from the substrate to the 3d orbitals of the Fe center. However, with AlkB-ssDNA, the calculated spin density for the carbon varies between -0.366 and 0.469 (Table B2). This implies that there is a competition between  $\sigma$  and  $\pi$  channels, as proposed in previous studies on AlkB.<sup>28</sup> The observed  $\sigma$  and  $\pi$  competition in the hydrogen atom transfer channel in AlkB-ssDNA could be due to reduced steric constraints experienced by m<sub>3</sub>C substrate in AlkB-ssDNA when compared to the substrate in duplex DNA, so that it can relatively more easily adopt a conformation which can undergo hydrogen abstraction via both  $\sigma$  and  $\pi$  channels. With AlkBH2-dsDNA and AlkB-dsDNA, m<sub>3</sub>C is more restrained due to the duplex nature of the dsDNA as the second strand of the DNA enhances the stability of the strand that contains the substrate, making the HAT to proceed only through the  $\sigma$ -channel.

### **3.2.16 Effects of residues from the second sphere and beyond on HAT**

In AlkBH2-dsDNA, the transition state is stabilized by second sphere residues. Thr252, Arg110 and Tyr122 stabilize the non-coordinating oxygen of succinate, O2 of the cytosine ring of the m<sub>3</sub>C substrate (hydrogen bonding interaction), and the exocyclic amine (N4) of

the substrate (hydrogen bonding interaction), respectively. Further, a strong  $\pi$ -stacking interaction of Phe124 with the cytosine ring of the substrate enhances the stability and proper orientation of the substrate. Networks of hydrogen bonding interactions of second sphere residues, Glu175, Arg254 and Tyr122 enhance the stability of the TS. These residues are in the vicinity of the Fe center and the substrate. However, in both AlkB-ssDNA and AlkB-dsDNA the transition states are stabilized by T-shaped  $\pi$ -stacking interactions between Trp69 and Tyr76 and the cytosine ring of the substrate; the Fe center is stabilized via the hydrogen bonding interactions of Arg210 with the non-coordinating oxygen of the coordinating aspartate. The residues that stabilize the TS for HAT in the AlkBH2-dsDNA show positive correlated motions with the Fe, metal coordinating residues (His171, Asp173 and His236), substrate recognition lid residues and the double-stranded  $\beta$ -helix (DSBH) core residues, while in bacterial AlkB (both with ss- and dsDNA), the residues show positive correlation with Fe, metal ligating residues and DSBH residues, indicating that more second sphere residues and stronger correlation motions participate in the overall stabilization of TS7 in human homolog than in bacterial AlkB and thus confirm their importance in catalysis. The finding suggests that while the three systems follow the same overall mechanism, modification of the orientation of second sphere residues in the substrate binding lid could influence HAT in AlkBH2, whereas such modifications are less likely to affect AlkB. Thus, although the details are complex, targeting second sphere residues could be a way to obtain selective inhibitors for specific 2OG-oxygenases.

At the IM10 stage, the Fe(IV)=O species is completely reduced to the Fe(III)-OH intermediate with the generation of a substrate carbon radical. The formation of IM10 is

slightly endergonic with the energy of 6.5 kcal/mol, including ZPE. The Fe-O<sub>p</sub> and O<sub>p</sub>-H distances are 1.85 Å and 0.95 Å, respectively, confirming the formation of the Fe(III)-OH complex. The calculated spin density of 4.24 for the Fe center supports the 3+ oxidation state assignment for iron at this stage. The optimized reaction state geometries for the HAT and the spin natural orbitals (SNO) of the HAT transition states for the snapshots with the lowest barrier in AlkBH2-dsDNA and AlkBs are presented in Figures 3.12 and 3.13, and Figures B47 and B48, respectively.



**Table 3.1.** Selected distances, angles and barriers for the different snapshots of RC2 and TS7 for the HAT step in AlkBH2-dsDNA, calculated at the B3LYP/def2-TZVP level.

	D(Fe-O <sub>p</sub> ) (Å)	d(O <sub>p</sub> -H) (Å)	d(C-H) (Å)	<(Fe-O <sub>p</sub> -H) (deg)	<(C-H <sub>p</sub> -O) (deg)	C <sub>substrate</sub> spin density in TS7	Barrier without ZPE (kcal/mol)	Barrier with ZPE (kcal/mol)	
<b>Snapshot1</b>									
RC2	1.610	2.689	1.102	125.46	158.54				
TS7	1.744	1.233	1.313	145.15	169.88	-0.379	24.9	21.6	
<b>Snapshot2</b>									
RC2	1.610	3.203	1.099	114.00	146.87				
TS7	1.778	1.285	1.281	141.89	166.29	-0.337	27.5	24.7	
<b>Snapshot3</b>									
RC2	1.617	3.337	1.101	130.74	154.64				
TS7	1.750	1.239	1.321	151.36	173.07	-0.392	25.2	22.6	
<b>Snapshot4</b>									
RC2	1.613	2.737	1.102	130.18	172.29				
TS7	1.743	1.242	1.307	148.76	176.37	-0.377	26.3	23.3	
<b>Snapshot5</b>									
RC2	1.615	2.522	1.102	127.94	155.59				
TS7	1.739	1.260	1.305	148.99	170.17	-0.369	24.9	22.0	
<b>Energy barrier Boltzmann weighted average</b>								25.3	22.2

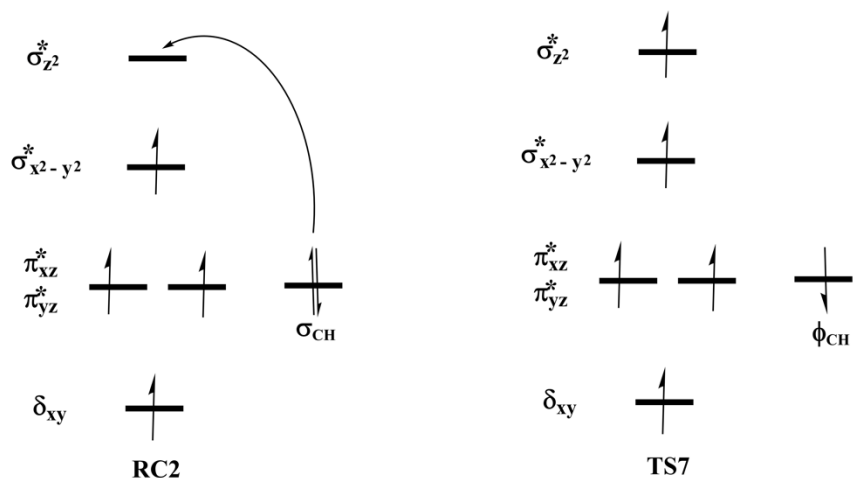


**Figure 3.11.** Orbital occupancy diagram during hydrogen atom abstraction.

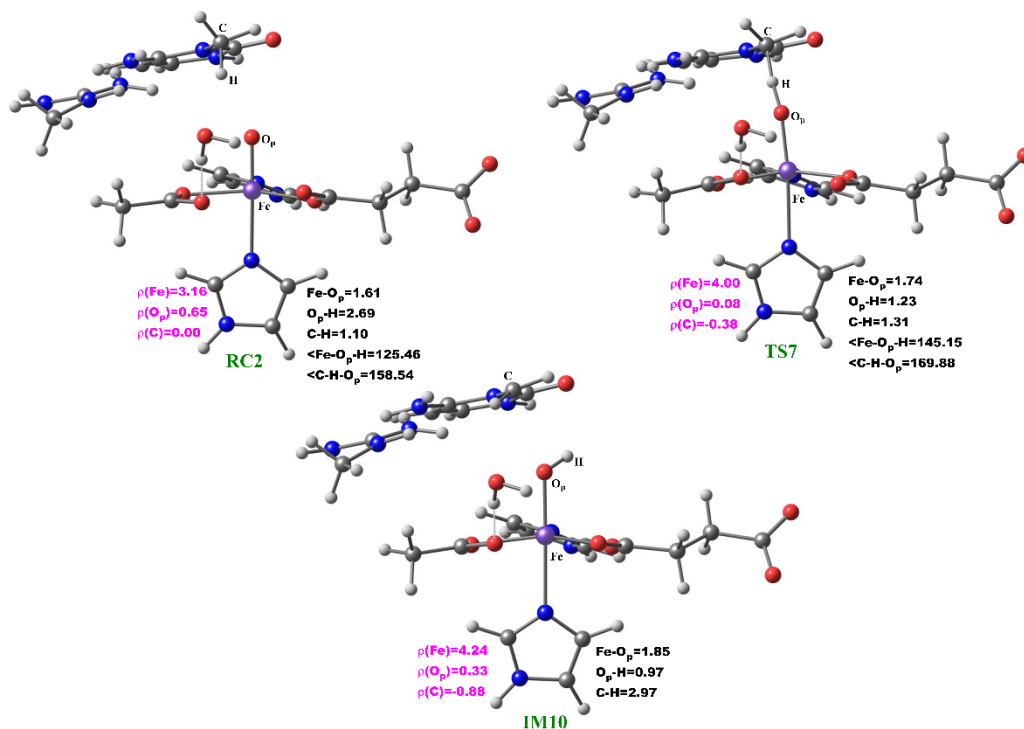


**Figure 3.12.** The reaction state geometries of the hydrogen atom abstraction step stationary points in AlkBH2-dsDNA. Distances ( $\text{\AA}$ ) and spin densities are in black and pink, respectively.

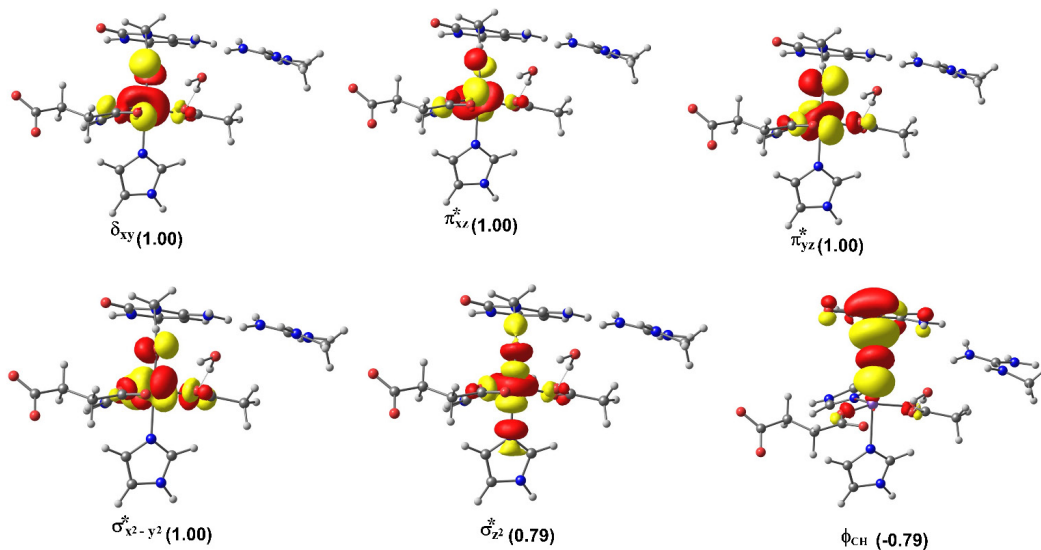


**Figure 3.13.** The spin natural orbitals (SNO) with their respective populations (in parentheses) for the hydrogen atom abstraction transition state in the AlkBH2-dsDNA complex.

### 3.2.17 Mechanism of Rebound Hydroxylation

The radical (IM10) formed by HAT undergoes a radical rebound process via TS8, in which a hydroxyl (OH) group is transferred from the Fe(III)-OH complex to the radical, leading to reduction of Fe(III) to Fe(II) and formation of the hydroxylated product (PD). The rebound reaction occurs rapidly in AlkBH2-dsDNA with a barrier of 12.6 kcal/mol and the overall reaction is highly exothermic (-31.6 kcal/mol), indicating formation of the product (PD) is both thermodynamically and kinetically favored. The rebound barriers in AlkB-ssDNA and AlkB-dsDNA are 17.4 and 15.8 kcal/mol, respectively. These barriers imply that the rebound process in both AlkB enzymes occurs at a slower rate than with AlkBH2-

dsDNA. The slightly higher rebound barrier found in AlkB-ssDNA compared to AlkB-dsDNA could be due to the fact that the Fe(III)-linked OH group in IM10 makes a hydrogen bonding interaction with the iron-coordinating Asp133 in agreement with previous studies.<sup>28,29</sup> The hydroxylated products (PD) in both AlkB complexes are stable with energies of -23.1 and -33.9 kcal/mol in AlkB-ssDNA and AlkB-dsDNA, respectively. In the PD, the hydroxyl group of the hydroxylated product forms a hydrogen bonding interaction with the iron-ligating aspartate in AlkBH2-dsDNA and AlkB-ssDNA. With AlkBH2-dsDNA, PD is further stabilized via a strong  $\pi$ -stacking interaction of the substrate base with Phe124. The exocyclic amine (N4) of the substrate forms a strong hydrogen bonding interaction with Glu175 and Tyr122, and the O2 of the nucleobase ring (cytosine) forms a stable interaction with Arg110; in both AlkB-ssDNA and AlkB-dsDNA, the stability of the product is enhanced by interaction with Tyr76. The obtained distances and spin densities are in good agreement with reported values.<sup>24,28,29,31-33</sup> The reaction state geometries for TS8 and PD as well as the substrate hydroxylation step energy profile for AlkBH2-dsDNA are presented in Figures B49 and 3.14, respectively.

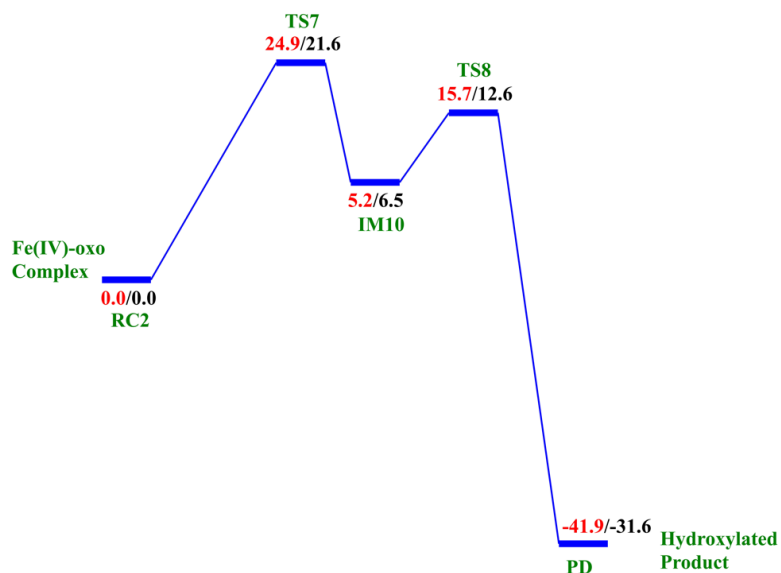


**Figure 3.14.** QM/MM reaction profile for the substrate hydroxylation step by AlkBH2-dsDNA as calculated using UB3LYP/def2-TZVP (BS2) (in red) and BS2 with ZPE (in black). Relative energies are in kcal/mol.

## 3.3 Computational Methods

### 3.3.1 Model Preparation

X-ray crystal structures of AlkBH2-dsDNA, AlkB-dsDNA and AlkB-ssDNA (PDB codes, 3RZJ,<sup>10</sup> 3O1M,<sup>45</sup> and 3I49,<sup>46</sup> respectively, in complex with 3-methylcytosine (m<sub>3</sub>C) substrates) were used. Crystallographically unobserved residues from the loop region (residues 204 to 206) of AlkBH2-dsDNA were added using Modeller.<sup>47</sup> This process was followed by replacement of the Mn(II) used for crystallization with Fe(II) in the AlkBH2-dsDNA and AlkB-dsDNA structures using GaussView 6.0. The protonation states of the

ionizable side chains were assessed with the H++ server<sup>48a</sup> and with the PROPKA software (Table B5);<sup>48b</sup> the histidine residues that are coordinated to the Fe(II) center were assigned protonation states based on visual inspection of their local environments.

The Fe(II) center is in the high spin state ( $S=2$   $M=5$ )<sup>15-17</sup>; the octahedrally coordinated Fe binds 2OG (in a bidentate fashion), two histidine (His<sup>1</sup>, His<sup>2</sup>) and one aspartate residue. The sixth coordination site in AlkB enzymes is occupied by a water in the crystal structures;<sup>10,11</sup> this was substituted with a dioxygen (O<sub>2</sub>), bound in an end on manner, to give a Fe(III)-superoxo complex. The parameters for the active site were prepared using the Metal Center Parameter Builder (MCPB.py)<sup>49</sup> as implemented in Amber. The metal center parameters were derived based on the bonded and electrostatic model approach in which the coordinating ligands are connected to the metal through covalent bonds. The bond and the angle force constants were derived using the Seminario method;<sup>50</sup> point charge parameters for the electrostatic potential were obtained using the ChgModB method. MCPB tools have been successfully used for description of the mononuclear non-heme iron center and iron-sulfur Rieske cluster.<sup>34c,51,52</sup> Molecular dynamics simulations using parameters generated via the MCPB tool have successfully reproduced the crystallographically observed geometry of metal-ligand complexes for other 2OG oxygenases.<sup>34c,51,52</sup> The parameters for 2OG and the substrate (m<sub>3</sub>C) were generated using the Antechamber module of Amber 16.<sup>53</sup> The Leap module in Amber was used to add missing hydrogen atoms and the protein systems were neutralized using counter ions: Na<sup>+</sup> for AlkBH2-dsDNA and AlkB-dsDNA and Cl<sup>-</sup> for AlkB-ssDNA, to compensate for the negative charge of the AlkBH2-dsDNA and AlkB-dsDNA systems, and the positive charge

of the AlkB-ssDNA system. The systems were surrounded by a rectangular box solvated with Transferable Intermolecular Potential 3-Point (TIP3P) water molecules<sup>54</sup> within a distance of at least 10 Å from the surface of the proteins.

A two-stage minimization of the geometries using MM was performed to eliminate clashes and bad contacts, prior to the MD simulations. In the first stage of minimization, only water molecules and ions were minimized, while the solute molecules were restrained with a 500 kcal.mol<sup>-1</sup>Å<sup>-2</sup> harmonic potential. In the final stage of minimization, all atoms were optimized with no restraints. The systems were subjected to 5000 steps of steepest descent, followed by 5000 steps of conjugate gradient energy minimization. The minimization steps were done with the CPU version of SANDER in Amber16.

Similar procedures were used to prepare the parameters for the ferryl complex of the three enzyme-DNA complexes, where the 2OG co-substrate was substituted with succinate, which was modelled with monodentate carboxylate binding.

### **3.3.2 Molecular Dynamic Simulations**

Molecular dynamics simulations were performed using the GPU version<sup>55</sup> of the PMEMD engine integrated with Amber16.<sup>56</sup> The FF14SB<sup>57</sup> force field was used in all the simulations and periodic boundary conditions were employed in all simulations. Long-range electrostatic interactions were calculated using the Particle Mesh Ewald (PME) method<sup>58</sup> with a direct space and vdW cut-off of 10 Å. The minimized systems were first heated for 50 ps by linearly increasing the temperature from 0 to 300 K in a canonical

ensemble (NVT) using Langevin thermostat.<sup>59</sup> The heated systems were further subjected to constant temperature heating (at 300 K) for 1 ns in an NPT ensemble. The solute molecules were restrained with the harmonic potential of  $10 \text{ kcal mol}^{-1} \text{ \AA}^2$  during the heating processes. Thereafter, systems were equilibrated within an NPT ensemble at a fixed temperature and pressure of 300 K and 1 bar, respectively for 3 ns without any restraints on solute molecules. The MD productive runs were performed for 1  $\mu\text{s}$  in an NPT ensemble with a target pressure set at 1 bar and constant pressure coupling of 2 ps. The pressure was held constant using Berendsen barostat<sup>60</sup> and the SHAKE algorithm<sup>61</sup> was used to constrain the bond lengths of those bonds involving hydrogen atoms.

Trajectories were analysed using CPPTRAJ,<sup>62</sup> VMD,<sup>63</sup> UCSF Chimera,<sup>64</sup> and R (Bio3D).<sup>65</sup> The analyses of the Root Mean Square Deviation (RMSD) of the enzymes with respect to the minimized crystal structure, Root mean square fluctuations (RMSF), electrostatic interactions, and hydrogen bonding were performed. The Bio3D package in R was used to produce Principal Component Analysis (PCA) and dynamic cross correlation analysis (DCCA) as used in the previous studies.<sup>34c,51</sup>

### **3.3.3 QM/MM Calculations**

All QM/MM calculations were performed using the ChemShell package,<sup>66</sup> that combines Turbomole<sup>67</sup> and DL\_POLY.<sup>68</sup> The former was used for the QM region while the MM region was treated with the latter. The electronic embedding scheme, which includes the polarisation of the QM region by the MM charge distribution in the QM calculation, was used to describe the interaction between the QM and MM regions. Hydrogen atoms were



used as the linked atoms to complete valences of bonds spanning between the two regions. The MM region was described with the Amber force field and the QM part was accounted for with Density Functional Theory (DFT) using the unrestricted B3LYP (UB3LYP) functional. The QM region used for the Fe(III)-superoxo complex involves the non-heme iron center, its coordinating residues (two His (His<sup>1</sup> and His<sup>2</sup>), Asp, 2OG, and O<sub>2</sub>), the methylguanidinium group of Arg (Arg254 in AlkBH2-dsDNA and Arg210 in AlkBs), and the 3-methyl-cytosine part of the substrate (Figure 3.3). In the ferryl complex, 2OG, and O<sub>2</sub> were replaced with succinate and an oxygen atom, respectively. All geometry optimizations were performed with the def2-SVP basis set (labelled as BS1) for all the atoms. After the full geometry optimizations, linear transit scans along the reaction coordinate were performed with 0.1 Å increments to locate the transition states (the geometry that corresponds to the highest energy in the PES) using DL-find optimizer.<sup>69</sup> Transition states were reoptimized using the partitioned rational function optimization (P-RFO) algorithm implemented in the HDLC code.<sup>70</sup> The fully optimized geometries of the minima and the transition states were characterized via frequency calculations. The energies of the optimized stationary points were recalculated via single-point energy calculation using a larger basis set, def2-TZVP (labelled as BS2) for all the atoms.

### 3.4 Conclusions

Our MD and QM/MM computations inform on the roles of dynamics in influencing the selectivity and mechanisms of methylated DNA repair by AlkB and its human homolog AlkBH2. Based on the general mechanism of 2OG oxygenases, reaction path calculations

of dioxygen activation and substrate oxidation steps were performed. Dioxygen activation involves oxidative decarboxylation of the 2OG co-substrate to succinate, leading to formation of the Fe(IV)=O intermediate. Following dioxygen activation, decarboxylation is the rate-limiting step, with barriers of 11.3, 11.8 and 13.2 kcal/mol for AlkB-ssDNA, AlkBH2-dsDNA and AlkB-dsDNA, respectively. The DCCA implies that the correlated motions of the residues that stabilize the decarboxylation process transition state are more important for catalysis in AlkBH2-dsDNA and AlkB-ssDNA than in AlkB-dsDNA. We also explored the 2OG rearrangement and ‘ferryl flip’ mechanistic paths in the formation of the reactive Fe(IV)=O intermediate from the “off-line” binding mode of the 2OG co-substrate in the enzymes. The calculations reveal that 2OG rearrangement is more energetically viable than the ‘ferryl flip’.

Prior to the QM/MM calculations, we performed a series of 1  $\mu$ s MD simulations on both the Fe(III)-superoxo and the ferryl complexes. The dynamics studies reveal the importance of conformational flexibility of the DNA component in the overall motion of the protein-DNA complexes. They also reveal flexibility in the binding of succinate compared to 2OG, likely reflecting preferred binding of the 2OG co-substrate compared to the succinate co-product. Residues Tyr161 and Arg248 (AlkBH2-dsDNA), Tyr122 and Arg204 (AlkB-ssDNA), and Ser145 and Trp178 (AlkB-dsDNA) are involved in binding 2OG and the succinate product, while His171, Tyr122 and Phe124 (AlkBH2-dsDNA), and Trp69, Tyr76 and His131 (AlkBs) enhance DNA substrate binding. MD studies also reveal the importance of the hydrophobic  $\beta$ -hairpin in AlkBH2-dsDNA as these residues have a strong positive correlation with the substrate recognition lid residues and such correlated

motion might contribute significantly to the binding of the substrate. The dynamics studies reveal that this hydrophobic  $\beta$ -hairpin is more flexible in the ferryl-complex than in the Fe(III)-superoxo complex. In the ferryl complex, it moves towards the Fe center, leading to the compaction of the complex, and hence, a mode that favors catalysis. The results also reveal that AlkB-ssDNA is more structurally compact than AlkB-dsDNA with the protein in the latter only interacting with one of the duplex DNA strands. The  $m_3C$  DNA substrate binds better to the active site of the protein in the ferryl compared to the Fe(III)-superoxo complex, resulting in a more productive complex for the substrate oxidation step.

After dioxygen activation, the reactive Fe(IV)=O species enables hydrogen atom abstraction (HAT) of the substrate methyl group to give a methylene radical intermediate which subsequently undergoes rebound hydroxylation to give the hydroxylated product. The QM/MM calculations imply HAT is rate-limiting for substrate oxidation in agreement with studies on some 2OG oxygenases.<sup>27-30</sup> However, if one considers the entire catalytic cycle in 2OG-oxygenases, including substrate binding and the product release, the rate-determining step can vary and, at least in some cases, is dissociation of the enzyme product complex.<sup>19</sup>

To explore the effect of conformational variations of the protein on the energy barrier, we used multiple snapshots (5 snapshots for each of the systems studied) to investigate the HAT for the three systems. The results reveal that the hydrogen abstraction occurs via the  $\sigma$ -channel in both AlkBH2-dsDNA and AlkB-dsDNA. With AlkB-ssDNA, the  $\sigma$ - and  $\pi$ -channels compete, due to the reduced steric constraints experienced by the  $m_3C$  DNA

substrate in AlkB-ssDNA when compared to AlkBH2-dsDNA and AlkB-dsDNA. The rebound hydroxylation occurs at a faster rate than HAT, resulting in hydroxylated products that are both thermodynamically and kinetically stable.

The studies reported here provide in-depth insight into the relationship between dynamic behaviors and the catalytic mechanisms of AlkB-ssDNA, AlkB-dsDNA, and AlkBH2-dsDNA. Various 2OG oxygenases are current targets for medicinal chemistry, with the vast majority of inhibitors reported being active site Fe chelators / 2OG competitors, resulting in blockage of catalysis.<sup>71</sup> Our results on the roles of dynamics in catalysis, suggest that analogous studies aimed at understanding the modes of action of active site binding inhibitors, including those in clinical / agrochemical use and trials may be productive.<sup>71</sup> In addition, inhibitors that bind to other regions of the protein (for example, substrate binding lid region), might provide better selectivity for a desired AlkB target over the other analogous enzymes. Our studies have suggested potential targets in this regard.

At least in some cases there is a desire to identify allosteric inhibitors or even compounds enhancing 2OG oxygenase activity. Indeed, in some cases structure-activity relationships for 2OG oxygenase inhibitors are difficult to rationalise on the basis of active site interactions alone, especially those observed by 'static' crystallography.<sup>72</sup> The dynamic and selective roles of the different regions of the overall enzyme-substrate complexes in substrate recognition and catalysis by the 2OG oxygenase-substrate complexes implies that there is scope for identifying modulators that act on specific steps during catalysis.

### 3.5 References

1. Clifton, I. J.; McDonough, M.A.; Ehrismann, D.; Kershaw, N. J.; Granatino, N.; Schofield, C. J. Structural studies on 2-oxoglutarate oxygenases and related double-stranded  $\beta$ -helix fold proteins. *J. Inorg. Biochem.* 2006, 100(4), 644-669.
2. Aik, W.; Demetriades, M.; Hamdan, M. K. K. et al. Structural Basis for Inhibition of the Fat Mass and Obesity Associated Protein (FTO). *J Med Chem.* 2013, 56(9), 3680-3688.
3. Loenarz, C.; Ge, W.; Coleman, M. L.; Rose, N.R.; Cooper, C. D.; Klose, R. J.; Ratcliffe, P. J.; Schofield, C.J. PHF8, a gene associated with cleft lip/palate and mental retardation, encodes for an N 1-dimethyl lysine demethylase. *Hum. Mol. Genet.* 2010, 19(2), 217-222.
4. Schofield, C. J.; Zhang, Z. Structural and mechanistic studies on 2-oxoglutarate-dependent oxygenases and related enzymes. *Curr. Opin. Struct. Biol.* 1999, 9(6), 722-731.
5. Samson, L.; Cairns, J. A new pathway for DNA repair in *Escherichia coli*. *Nature.* 1977, 267(5608), 281-283.
6. Fedeles, B. I.; Singh, V.; Delaney, J. C.; Li, D.; Essigmann, J. M. The AlkB Family of Fe(II)/ $\alpha$ -Ketoglutarate-dependent Dioxygenases: Repairing Nucleic Acid Alkylation Damage and Beyond. *J. Biol. Chem.* 2015, 290(34), 20734-20742.
7. Yi, C.; He, C. DNA Repair by Reversal of DNA Damage. *Cold Spring Harb. Perspect. Biol.* 2013, 5(1), a012575-a012575.
8. Aravind, L.; Koonin, E. V. The DNA-repair protein AlkB, EGL-9, and leprecan define new families of 2-oxoglutarate- and iron-dependent dioxygenases. *Genome Biol.* 2001, 2(3), research0007.1.
9. Sedgwick, B.; Bates, P.; Paik, J.; Jacobs, S.; Lindahl, T. Repair of alkylated DNA: Recent advances. *DNA Repair (Amst).* 2007, 6(4), 429-442.
10. Yi, C.; Chen, B.; Qi, B. Zhang, W.; Jia, G.; Zhang, L.; Li, C. J.; Dinner, A. R.; Yang, C. G.; He, C. Duplex interrogation by a direct DNA repair protein in search of base damage. *Nat. Struct. Mol. Biol.* 2012, 19(7), 671-676.

11. Yang, C-G.; Yi, C.; Duguid, E. M.; Sullivan, C. T.; Jian, X.; Rice, P. A.; He, C. Crystal structures of DNA/RNA repair enzymes AlkB and ABH2 bound to dsDNA. *Nature*. 2008, 452(7190), 961-965.
12. (a) Zheng, G.; Fu, Y.; He, C. Nucleic Acid Oxidation in DNA Damage Repair and Epigenetics. *Chem Rev*. 2014, 114(8), 4602-4620. (b) Chaturvedi, S. S.; Ramanan, R.; Waheed, S. O.; Karabancheva-Christova, T. G.; Christov, C. Z. Structure-function relationships in KDM7 histone demethylases. *Adv. Protein Chem. Struct. Biol.* 2019, 117, 113-125.
13. (a) Hausinger, R. P. Fe(II)/ $\alpha$ -Ketoglutarate-Dependent Hydroxylases and Related Enzymes. *Crit. Rev. Biochem. Mol. Biol.* 2004, 39(1), 21-68. (b) Miller III, B. R.; McGee Jr., T. D.; Swails, J. M.; Homeyer, N.; Gohlke, H.; Roitberg, A. E. MMPBSA.py: An efficient program for end-state energy calculations. *J. Chem. Theory. Comput.* 2012, 8(9), 3314-3321. (c) Genheden, S.; Ryde, U. The MM/PBSA and MM/GBSA methods to estimate ligand-binding affinities. *Expert Opin Drug Discov.* 2015, 10(5), 449-461. (d) Hou, T.; Wang, J.; Li, Y.; Wang, W. Assessing the performance of the MM/PBSA and MM/GBSA methods. 1. The accuracy of binding free energy calculations based on molecular dynamics simulations. *J. Chem. Inf. Model.* 2011, 51(1), 69-82.
14. Zhu, C.; Yi, C. Switching demethylation activities between AlkB family RNA/DNA demethylases through exchange of active-site residues. *Angew. Chem. Int. Ed. Engl.* 2014, 53(14), 3659-3662.
15. Krebs, C.; Fujimori, D. G.; Walsh, C. T.; Bollinger, J. M. Non-heme Fe(IV)-oxo intermediates. *Acc. Chem. Res.* 2007, 40(7), 484-492.
16. Solomon, E. I. Geometric and Electronic Structure Contributions to Function in Bioinorganic Chemistry: Active Sites in Non-Heme Iron Enzymes. *Inorg. Chem.* 2001, 40(15), 3656-3669.
17. Solomon, E. I.; Light, K. M.; Liu, L. V.; Srnec, M.; Wong, S. D. Geometric and Electronic Structure Contributions to Function in Non-heme Iron Enzymes. *Acc. Chem. Res.* 2013, 46(11), 2725-2739.

18. (a) Zhang, Z.; Ren, J.; Harlos, K.; McKinnon, C. H.; Clifton, I. J.; Schofield, C. J. Crystal structure of a clavamate synthase-Fe(II)-2-oxoglutarate-substrate-NO complex: evidence for metal centred rearrangements. *FEBS Lett.* 2002, 517, 7-12. (b) Chaturvedi, S. S.; Ramanan, R.; Lehnert, N.; Schofield, C. J.; Karabencheva-Christova, T. G.; Christov, C. Z. Catalysis by the Non-heme Fe(II) Histone Demethylase PHF8 Involves Iron Center Rearrangement and Conformational Modulation of Substrate Orientation. *ACS Catal.* 2020, 10(2), 1195-1209.
19. Shishodia, S.; Zhang, D.; El-Sagheer, A. H.; Brown, T.; Claridge, T. D. W.; Schofield, C. J.; Hopkinson, R. J. NMR analyses on N-hydroxymethylated nucleobases - implications for formaldehyde toxicity and nucleic acid demethylases. *Org. Biomol. Chem.* 2018, 16, 4021-4032.
20. (a) Solomon, E. I.; Brunold, T. C.; Davis, M. I.; Kemsley, J. N.; Lee, S. K.; Lehnert, N.; Neese, F.; Skulan, A.J.; Yang, Y. S.; Zhou, J. Geometric and Electronic Structure/Function Correlations in Non-Heme Iron Enzymes. *Chem. Rev.* 2000, 100(1), 235-350. (b) Mitchell, A. J.; Dunham, N. P.; Martinie, R. J.; Bergman, J. A.; Pollock, C. J.; Hu, K.; Allen, B. D.; Chang, W.; Silakov, A.; Bollinger, J. M.; Krebs, C.; Boal, A. K. Visualizing the reaction cycle in an Iron(II)- and 2-(oxo)-glutarate dependent hydroxylase. *J. Am. Chem. Soc.*, 2017, 139, 13830-13836.
21. Wang, B.; Cao, Z.; Sharon, D. A.; Shaik, S. Computations reveal a rich mechanistic variation of demethylation of N-methylated DNA/RNA nucleotides by FTO. *ACS Catal.* 2015, 5, 7077-7090.
22. (a) Wang, B.; Usharani, D.; Li, C.; Shaik, S. Theory uncovers an unusual mechanism of DNA repair of a lesioned adenine by AlkB enzymes. *J. Am. Chem. Soc.* 2014, 136(39), 13895-13901. (b) Torabifard, H.; Cisneros, G. A. Computational investigation of O<sub>2</sub> diffusion through an intra-molecular tunnel in AlkB; Influence of polarization on O<sub>2</sub> transport. *Chem. Sci.* 2017, 8(9), 6230-6238.
23. Song, X.; Lu, J.; Lai, W. Mechanistic insights into dioxygen activation, oxygen atom exchange and substrate epoxidation by AsqJ dioxygenase from quantum

mechanical/molecular mechanical calculations. *Phys. Chem. Chem. Phys.* 2017, 19(30), 20188-20197.

24. Liu, H.; Llano, J.; Gault, J. W. A DFT study of nucleobase dealkylation by the DNA repair enzyme AlkB. *J. Phys. Chem. B.* 2009, 113(14), 4887-4898.

25. (a) Wójcik, A.; Radoń, M.; Borowski, T. Mechanism of O<sub>2</sub> Activation by  $\alpha$ -Ketoglutarate Dependent Oxygenases Revisited. A Quantum Chemical Study. *J. Phys. Chem. A.* 2016, 120(8), 1261-1274. (b) Geng, C.; Ye, S.; Neese, F. Analysis of reaction channels for alkane hydroxylation by Nonheme Iron(IV)-oxo complexes. *Angew. Chem. Int. Ed.* 2010, 49, 5717-5720. (c) Neidig, M. L.; Decker, A.; Choroba, O. W.; Huang, F.; Kavana, M.; Moran, G. R.; Spencer, J. B.; Solomon, E. I. Spectroscopic and electronic structure studies of aromatic electrophilic attack and hydrogen atom abstraction by non-heme iron enzymes. *Proc. Natl. Acad. Sci.* 2006, 103(35), 12966-12973.

26. Cortopassi, W. A.; Simion, R.; Honsby, C. E.; França, T. C. C.; Paton, R. S. Dioxygen Binding in the Active Site of Histone Demethylase JMJD2A and the Role of the Protein Environment. *Chem. Eur. J.* 2015, 21(52), 18983-18992.

27. Cisneros, G. A. DFT study of a model system for the dealkylation step catalyzed by AlkB. *Interdiscip. Sci. Comput. Life Sci.* 2010, 2(1), 70-77.

28. Quesne, M. G.; Latifi, R.; Gonzalez-Ovalle, L. E.; Kumar, D.; De Visser, S. P. Quantum mechanics/molecular mechanics study on the oxygen binding and substrate hydroxylation step in AlkB repair enzymes. *Chem. Eur. J.* 2014, 20(2), 435-446.

29. Fang, D.; Lord, R. L.; Cisneros, G. A. Ab initio QM/MM calculations show an intersystem crossing in the hydrogen abstraction step in dealkylation catalyzed by AlkB. *J. Phys. Chem. B.* 2013, 117(21), 6410-6420.

30. Torabifard, H.; Cisneros, G. A. Insight into wild-type and T1372E TET2-mediated 5hmC oxidation using ab initio QM/MM calculations. *Chem Sci.* 2018, 9(44), 8433-8445.

31. Álvarez-Barcia, S.; Kästner, J. Atom Tunneling in the Hydroxylation Process of Taurine/ $\alpha$ -Ketoglutarate Dioxygenase Identified by Quantum Mechanics/Molecular Mechanics Simulations. *J. Phys. Chem. B.* 2017, 121(21), 5347-5354.



32. Fang, D.; Cisneros, G. A. Alternative pathway for the reaction catalyzed by DNA dealkylase AlkB from Ab initio QM/MM calculations. *J. Chem. Theory Comput.* 2014, 10(11), 5136-5148.
33. Godfrey, E.; Porro, C. S.; de Visser, S. P. Comparative Quantum Mechanics/Molecular Mechanics (QM/MM) and density functional theory calculations on the oxo-iron species of taurine/ $\alpha$ -ketoglutarate dioxygenase. *J. Phys. Chem. A.* 2008, 112(11), 2464-2468.
34. (a) Purslow, J. A.; Nguyen, T. T.; Egner, T. K.; Dotas, R. R.; Khatiwada, B.; Venditti, V. Active site breathing of human Alkbh5 revealed by solution NMR and accelerated molecular dynamics. *Biophys. J.* 2018, 115(10), 1895-1905. (b) Silvestrov, P.; Muller, T. A.; Clark, K. N.; Hausinger, R. P.; Cisneros, G. A. Homology modeling molecular dynamics, and site-directed mutagenesis study of AlkB human homolog 1 (ALKBH1). *J. Mol. Graph. Model.* 2014, 54, 123-130. (c) Waheed, S. O.; Ramanan, R.; Chaturvedi, S. S.; Ainsley, J.; Evison, M.; Ames, J. M.; Schofield, C. J.; Christov, C. Z.; Karabancheva-Christova, T. G. Conformational flexibility influences structure-function relationships in nucleic acid N-methyl demethylases. *Org. Biomol. Chem.* 2019, 17(8), 2223-2231.
35. (a) Bleijlevens, B.; Shivarattan, T.; van de Boom, K. S.; de Haan, A.; van der Zwan, G.; Simpson, P. J.; Mathews, S. J. Changes in protein dynamics of the DNA repair dioxygenase AlkB upon binding of Fe(2+) and 2-oxoglutarate. *Biochemistry* 2012, 51, 3334-3341. (b) Bleijlevens, B.; Shivarattan, T.; Flashman, E.; Yang, Y.; Simpson, P. J.; Koivisto, P.; Sedgwick, B.; Schofield, C. J.; Mathews S. J. Dynamic states of the DNA repair enzyme AlkB regulate product release. *Embo. Rep.* 2008, 9, 872-877. (c) Pang, X.; Han, K.; Cui, Q. A simple but effective modeling strategy for structural properties of non-heme Fe(II) sites in proteins: Test of force field models and application to proteins in the AlkB family. *J. Comput. Chem.* 2013, 34(19), 1620-1635. (d) Ergel, B.; Gill, M.L.; Brown, L.; Yu, B.; Palmer, A.G., 3rd; Hunt, J.F. Protein dynamics control the progression and efficiency of the catalytic reaction cycle of the Escherichia coli DNA-repair enzyme AlkB. *J. Biol. Chem.* 2014, 289, 29584-29601.

36. Lee, D. H.; Jin, S. G.; Cai, S.; Chen, Y.; Pfeifer, G. P.; O'Connor, T. R. Repair of methylation damage in DNA and RNA by mammalian AlkB homologues. *J. Biol. Chem.* 2005, 280(47), 39448-39459.
37. (a) Hünenberger, P. H.; Mark, A. E.; van Gunsteren, W. F. Fluctuation and Cross-Correlation Analysis of Protein Motions Observed in Nanosecond Molecular Dynamics Simulations. *J. Mol. Biol.* 1995, 252, 492–503. (b) Balsera, M. A.; Wriggers, W.; Oono, Y.; Schulten, K. Principal Component Analysis and Long Time Protein Dynamics. *J. Phys. Chem.* 1996, 100, 2567–2572.
38. Shaik, S.; Chen, H.; Janardanan, D. Exchange-enhanced reactivity in bond activation by metal-oxo enzymes and synthetic reagents. *Nature Chemistry.* 2011, 3, 19-26.
39. Logunov, I.; Schulten, K. Quantum chemistry: Molecular dynamics study of the dark-adaptation process in bacteriorhodopsin. *J. Am. Chem. Soc.* 1996, 118(40), 9727-9735.
40. Christov, C. Z.; Lodola, A.; Karabancheva-Christova, T. G.; Wan, S.; Coveney, P. V.; Mulholland, A. J. Conformational effects on the pro-s hydrogen abstraction reaction in Cyclooxygenase-1: An integrated QM/MM and MD study. *Biophys. J.* 2013, 104(5), L5-L7.
41. Lonsdale, R.; Hoyle, S.; Grey, D. T.; Ridder, L.; Mulholland, A. J. Determinants of reactivity and selectivity in soluble epoxide hydrolase from quantum mechanics/molecular mechanics modeling. *Biochemistry.* 2012, 51(8), 1774-1786.
42. Lonsdale, R.; Houghton, K. T.; Zurek, J.; Bathelt, C. M.; Foloppe, N.; de Groot, M. J.; Harvey, J. N.; Mulholland, A. J. Quantum mechanics/molecular mechanics modeling of regioselectivity of drug metabolism in cytochrome P450 2C9. *J. Am. Chem. Soc.* 2013, 135(21), 8001-8015.
43. Lonsdale, R.; Harvey, J. N.; Mulholland, A. J. Compound I reactivity defines alkene oxidation selectivity in cytochrome p450cam. *J. Phys. Chem. B* 2010, 114(2), 1156-1162.

44. Chen, F.; Bian, K.; Tang, Q.; Fedeles, B. I.; Singh, V.; Humulock, Z. T.; Essigmann, J. M.; Li, D. Oncometabolites d- and l-2-Hydroxyglutarate Inhibit the AlkB Family DNA Repair Enzymes under Physiological Conditions. *Chem Res Toxicol.* 2017, 30(4), 1102-1110.
45. Yi, C.; Jia, G.; Hou, G.; Dai, Q.; Zhang, W.; Zheng, G.; Jian, X.; Yang, C. G.; Cui, Q.; He, C. Iron-catalysed oxidation intermediates captured in a DNA repair dioxygenase. *Nature.* 2010, 468(7321), 330-333.
46. Yu, B.; Hunt, J. F.; Enzymological and structural studies of the mechanism of promiscuous substrate recognition by the oxidative DNA repair enzyme AlkB. *Proc. Natl. Acad. Sci.* 2009, 106(34), 14315-14320.
47. Fiser, A.; Šali, A. Modeller: Generation and Refinement of Homology-Based Protein Structure Models. *Methods Enzymol.* 2003, 374, 461-491.
48. (a) Gordon, J. C.; Myers, J. B.; Folta, T.; Shoja, V.; Heath, L. S.; Onufriev, A. H<sup>++</sup>: A server for estimating pK<sub>a</sub>s and adding missing hydrogens to macromolecules. *Nucleic Acids Res.* 2005, 33, W368-371. (b) Olsson, M. H.; Sondergaard, C. R.; Rostkowski, M.; Jensen, J. H. PROPKA3: Consistent treatment of internal and surface residues in empirical pK<sub>a</sub> predictions. *J. Chem. Theory. Comput.* 2011, 7(2), 525-537.
49. Li, P.; Merz, K. M. MCPB.py: A Python Based Metal Center Parameter Builder. *J. Chem. Inf. Model.* 2016, 56(4), 599-604.
50. Seminario, J. M. Calculation of intramolecular force fields from second-derivative tensors. *Int. J. Quantum Chem.* 1996, 60(7), 1271-1277.
51. Chaturvedi, S. S.; Ramanan, R.; Waheed, S. O.; Ainsley, J.; Evison, M.; Ames, J. M.; Schofield, C. J.; Karabencheva-Christova, T. G.; Christov, C. Z. Conformational Dynamics Underlies Different Functions of Human KDM7 Histone Demethylases. *Chem. Eur. J.* 2019, 25(21), 5422-5426.
52. Pabis, A.; Geronimo, I.; York, D. M.; Paneth, P. Molecular dynamics simulation of nitrobenzene dioxygenase using AMBER force field. *J. Chem. Theory Comput.* 2014, 10(6), 2246-2254.

53. Wang, J.; Wang, W.; Kollman, P. A.; Case, D. A. Automatic atom type and bond type perception in molecular mechanical calculations. *J. Mol. Graph. Model.* 2006, 25(2), 247-260.
54. Jorgensen, W. L.; Chandrasekhar, J.; Madura, J. D.; Impey, R. W.; Klein, M. L. Comparison of Simple Potential Functions for Simulating Liquid Water. *J. Chem. Phys.* 1983, 79, 926-935.
55. Götz, A. W.; Williamson, M. J.; Xu, D.; Poole, D.; LeGrand, S.; Walker, R. C. Routine microsecond molecular dynamics simulations with AMBER on GPUs. 1. generalized born. *J. Chem. Theory Comput.* 2012, 8(5), 1542-1555.
56. Case, D. A.; Betz, R. M.; Cerutti, D. S.; Cheatham, T. E.; Daeden, T. A.; Duke, R. E.; Giese, T. J.; Gohlke, H.; Goetz, A. W.; Homeyer, N.; et al. AMBER 2016. University of California: San Francisco 2016.
57. Maier, J. A.; Martinez, C.; Kasavajhala, K.; Wickstrom, L.; Hauser, K. E.; Simmerling, C. ff14SB: Improving the Accuracy of Protein Side Chain and Backbone Parameters from ff99SB. *J. Chem. Theory Comput.* 2015, 11(8), 3696-3713.
58. Deserno, M.; Holm, C. How to mesh up Ewald sums. I. A theoretical and numerical comparison of various particle mesh routines. *J. Chem. Phys.* 1998, 109(18), 7678-7693.
59. Davidchack, R. L.; Ouldridge, T. E.; Tretyakov, M. V. New Langevin and gradient thermostats for rigid body dynamics. *J. Chem. Phys.* 2015, 142, 144114.
60. Bresme, F. Equilibrium and nonequilibrium molecular-dynamics simulations of the central force model of water. *J. Chem. Phys.* 2001, 115(16), 7564-7574.
61. Ryckaert, J-P.; Ciccotti, G.; Berendsen, H. J. Numerical integration of the cartesian equations of motion of a system with constraints: molecular dynamics of n-alkanes. *J. Comput. Phys.* 1977, 23(3), 327-341.
62. Roe, D. R.; Cheatham, T. E. PTRAJ and CPPTRAJ: Software for Processing and Analysis of Molecular Dynamics Trajectory Data. *J. Chem. Theory Comput.* 2013, 9(7), 3084-3095.
63. Humphrey, W.; Dalke, A.; Schulten, K. VMD: Visual Molecular Dynamics. *J. Mol. Graphics.* 1996, 14, 27-38.

64. Pettersen, E. F.; Goddard, T. D.; Huang, C. C.; Couch, G. S.; Greenblatt, D. M.; Meng, E. C.; Ferrin, T. E. UCSF Chimera--a visualization system for exploratory research and analysis. *J. Comput. Chem.* 2004, 25(13), 1605-1612.
65. Grant, B. J.; Rodrigues, A. P. C.; ElSawy, K. M.; McCammon, J. A.; Caves, L. S. D. Bio3d: An R package for the comparative analysis of protein structures. *Bioinformatics.* 2006, 22(21), 2695-2696.
66. Sherwood, P.; De Vries, A. H.; Guest, M. F.; et al. QUASI: A general purpose implementation of the QM/MM approach and its application to problems in catalysis. *J. Mol. Struct. Theochem.* 2003, 632, 1-28.
67. Ahlrichs, R.; Bär, M.; Häser, M.; Horn, H.; Kölmel, C. Electronic structure calculations on workstation computers: The program system turbomole. *Chem. Phys. Lett.* 1989, 162(3), 165-169.
68. Smith, W.; Forester, T. R. DL-POLY-2.0: A general-purpose parallel molecular dynamics simulation package. *J. Mol. Graph.* 1996, 14(3), 136-141.
69. Kästner, J.; Carr, J. M.; Keal, T. W.; Thiel, W.; Wander, A.; Sherwood, P. DL-FIND: An open-source geometry optimizer for atomistic simulations. *J. Phys. Chem. A.* 2009, 113(43), 11856-11865.
70. Billeter, S. R.; Turner, A. J.; Thiel, W. Linear scaling geometry optimisation and transition state search in hybrid delocalised internal coordinates. *Phys. Chem. Chem. Phys.* 2000, 2(10), 2177-2186.
71. Rose, N. R.; McDonough, M. A.; King, O. N. F.; Kawamura, A.; Schofield, C. J. Inhibition of 2-oxoglutarate dependent oxygenase. *Chem. Soc. Rev.*, 2011, 40, 4364-4397.
72. Yeh, T-L.; Leissing, T. M.; Abboud, M. I.; Thinnies, C. C.; Atasoylu, O.; Holt-Martyn, J. P.; Zhang, D.; Tumber, A.; Lippl, K.; Lohans, C. T.; Leung, I. K. H.; Morcrette, H.; Clifton, I. J.; Claridge, T. D. W.; Kawamura, A.; Flashman, E.; Lu, X.; Ratcliffe, P. J.; Chowdhury, R.; Pugh, C. W.; Schofield, C. J. Inhibition of 2-oxoglutarate dependent oxygenase. *Chem. Sci.*, 2017, 8, 7651-7668.

## 4 Catalytic Mechanism of Human Ten-Eleven Translocation -2 (TET2) Enzyme: Effects of Conformational Changes, Electric Field and Mutations

Sodiq O. Waheed,<sup>a</sup> Shobhit S. Chaturvedi,<sup>a</sup> Tatyana G. Karabancheva-Christova,<sup>a</sup> and Christo Z. Christov<sup>a#</sup>

<sup>a</sup> Department of Chemistry, Michigan Technological University, Houghton, Michigan 49931, United States.

<sup>#</sup>Corresponding author: christov@mtu.edu

---

The content of this chapter was previously published in the *ACS Catal.*, **2021**, 11, 3877-3890. DOI: 10.1021/acscatal.0c05034, reproduced with permission from the American Chemical Society.

## 4.1 Introduction

Methylation at cytosine DNA bases in the genome is strongly linked to various normal and pathological processes in the cell, including the regulation of gene expression, genomic imprinting, embryonic development, active DNA demethylation, oncogenesis, and other epigenetic inheritance processes.<sup>1-7</sup> The methylation of DNA is catalyzed by DNA methyltransferases (DNMTs), acting on cytosine and adenine bases, respectively.<sup>3,5</sup> TET enzymes oxidize C-methylation of cytosine bases<sup>8,9a</sup> and recent study show that the enzymes are also proficient as direct N-demethylases of cytosine bases at the exocyclic amine N4 position<sup>9b</sup> in a similar manner as other non-heme Fe(II)- and 2OG - dependent enzymes such as bacterial AlkBs and human AlkBs (AlkBH1-AlkBH8 and FTO).<sup>8,9a</sup> The TET enzymes possess enzymatic activity toward 5-methylcytosine (5mC), and they include TET1-3 and the AID/APOBEC subfamily of enzymes.<sup>10a,11,12</sup> TET proteins contain a conserved double stranded beta helix (DSBH) domain, a cysteine rich domain, and binding sites for Fe(II) and 2OG co-substrate that together form the core catalytic region in the C-terminus.<sup>10a,13,14</sup> [Figure 4.1] The overall structure of TET2 [Figure 4.1] is stabilized by three zinc cations (zinc fingers) coordinated by residues from both the cysteine rich and the DSBH domains, thus bringing flexible regions from the two domains together to facilitate the stability of the overall structure.<sup>13</sup> TET enzymes belong to the Fe(II)- and 2OG - dependent oxygenase family of enzymes, and catalyze the successive oxidation of 5mC to 5-hydroxymethylcytosine (5hmC), 5-formylcytosine (5fC), and finally 5-carboxylcytosine (5caC).<sup>10a,b,13,15</sup> TET2 has been referred to as a de novo 5mC

dioxygenase whose the iterative oxidation of the 5mC to the various oxidized forms is not controlled by the opposite strand cytosine-guanine dinucleotides (CpG).<sup>10b</sup> Crystallographic studies revealed that substrate binding by TET enzymes involves flipping of the methylated base from the DNA strand into the iron center for demethylation,<sup>9a,13</sup> similarly to the nucleic acids N-methyl demethylases (AlkB and its human homologs).<sup>8,9a,16,17</sup>

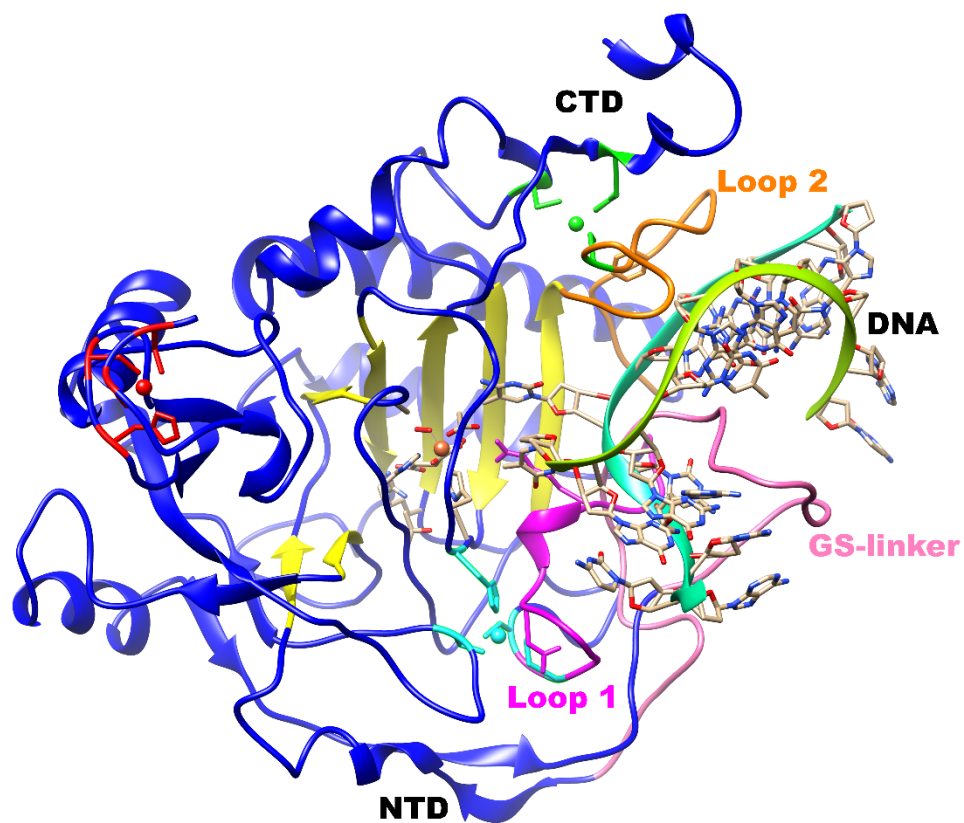
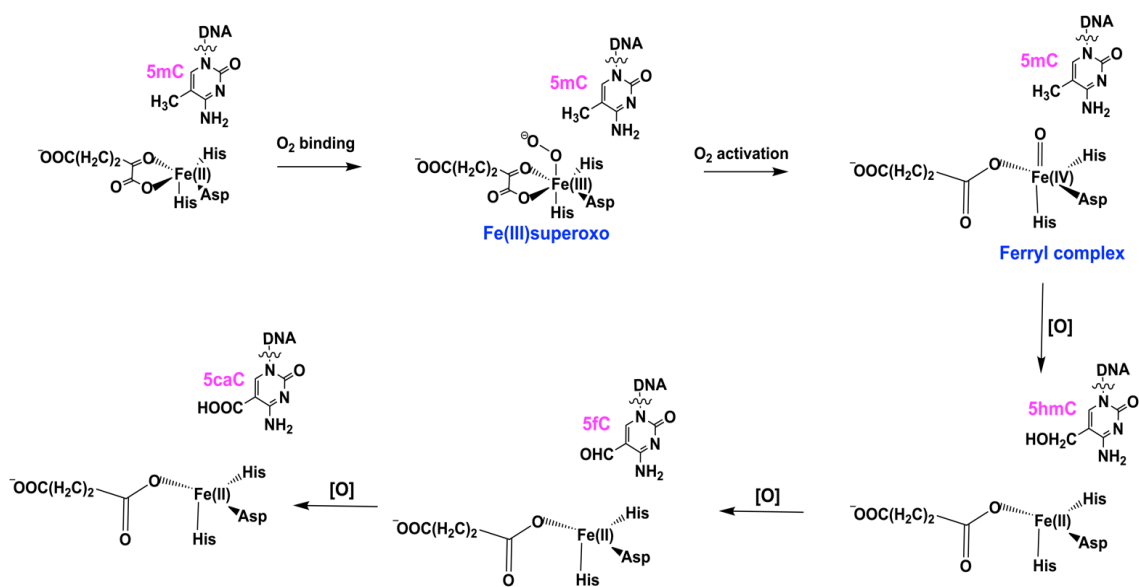


**Figure 4.1.** Average MD structure of Human TET2 bound to dsDNA derived from the Fe(III)-O<sub>2</sub> intermediate simulations. Coloring: Double Stranded Beta Helix (DSBH) fold (yellow), and the three zinc finger regions (Zn1 (cyan), Zn2 (red) and Zn3 (green))



The catalysis commences with dioxygen ( $O_2$ ) binding to the five-coordinate Fe (II) center, and formation of the Fe(III)-superoxo complex. The first step of the reaction mechanism is a dioxygen activation and involves the formation of an active Fe(IV)-oxo (ferryl) intermediate coupled with decarboxylation of 2OG to succinate and  $CO_2$ . The formed ferryl intermediate performs hydrogen atom abstraction (HAT) from the methyl group at the C5 position of 5mC, followed by rebound hydroxylation, producing 5hmC [Scheme 4.1]. Oxidation of 5mC to 5hmC is the first reaction step catalyzed by TET enzymes. Some studies have shown that the oxidation reaction rate is significantly reduced for the 5hmC as it is stable in mammalian genome DNA.<sup>15,18,19</sup> In particular, studies reported that the hydrogen atom abstraction (HAT) process is more efficient in 5mC than 5hmC and 5fC.<sup>15,18,19</sup>



**Scheme 4.1.** The overall proposed reaction mechanism for successive oxidation of 5mC to 5hmC, 5fC and 5caC by TET enzymes

The catalytic mechanism of TET enzymes and nucleic acids N-methyl demethylases (NADMs) has been extensively studied both experimentally and computationally which provided an understanding of the three-dimensional structures, substrate binding, and their kinetics.<sup>7,12,13,15,17,18,20-28</sup> However, the effects of the conformational dynamics on the catalytic process in the flexible TET2-dsDNA complex are still poorly understood. It is particularly important to reveal how long-range correlated motions in the TET2 enzyme influence its catalysis. The current study aims to provide this missing knowledge by exploring the mechanism of the first oxidation step of 5mC dsDNA substrate to 5hmC intermediate.

Several experimental studies have shown that the TET2-dsDNA enzyme is frequently mutated in myeloid malignancies, such as myelodysplastic syndrome (MDS), chronic myelomonocytic leukemia (CMML), acute myeloid leukemia (AML), and myeloproliferative neoplasms (MPN).<sup>2,11,29,30</sup> Most of the leukemia-associated mutations inhibit or abolish the TET2 catalytic activity.<sup>31</sup> The mutations may alter active site interactions, the catalytic core domain and/or influence long-range interactions, thus affecting the TET2 activity.<sup>11,13,32</sup> Such clinically important mutations include the single substitution W1291A and the double substitution K1299E-S1303N [Figure 4.2A], causing myelodysplastic syndrome and refractory anemia, respectively.<sup>13,32</sup> Also, several experimental mutations performed in vitro such as Y1902A, N1387A, H1904R, S1290A-Y1295A, and M1293A-Y1294A [Figure 4.2A] demonstrated to influence substrate binding, catalysis, and enzyme turnover.<sup>13</sup> Recent studies elegantly demonstrated the power of the computational and experimental methods to provide a unique insight into the

effect of a single mutation of TET2 (T1372E) on the oxidation of 5hmC to 5fC/caC.<sup>21a,33</sup> The QM/MM calculations by Torabifard et al on the effect of T1372E mutation in halting the iterative oxidation of 5hmC by TET2 revealed the orientation of the water molecule in the active site is essential for iterative oxidation in the wild-type (WT). The electron localization function (ELF) and non-covalent interaction (NCI) revealed that the process involves a hydrogen atom transfer from the hydroxyl moiety, followed by a proton transfer with the participation of the water molecule. The study found that unfavorable orientation of the substrate in T1372E mutant due to the formation of a hydrogen bond between the substrate and the mutant site which is absent in the WT resulted in the much larger energy barrier observed in the mutant.<sup>21a</sup> The calculations corroborate the experimental study by Liu et al that first reported T1372E as a “5hmC-stalling” mutant.<sup>33</sup> Nevertheless, the effects of the above clinical and experimental mutants on the TET2-dsDNA structure, and reaction mechanism are unknown, which is an important barrier to understanding their role and molecular pathology. Therefore, it is important to complete the knowledge gap about how mutations linked to diseases influence the long-range interactions in TET2 and thus in turn influence its reaction mechanism during the first oxidation of 5mC to 5hmC.

The present study tests the hypothesis that the conformational changes in the wild type (WT) TET2 influence the mechanism by affecting the active site interactions, the local electric field, and long-range correlation motions in TET2-dsDNA complex. Furthermore, we hypothesize that mutations linked to diseases influence the long-range interactions observed in WT TET2 and affect the reaction mechanism by altering key structural determinants and the internal electric field.

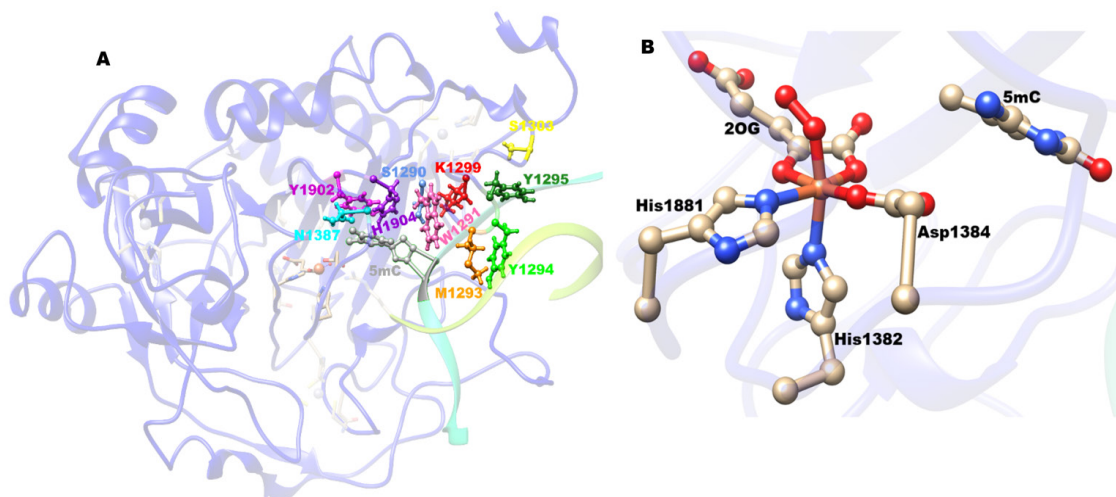


**Figure 4.2.** The structure of TET2 showing the locations of the individual substituted residues (A) and QM region used for the QM/MM calculations (B).

## 4.2 Computational Methods

### 4.2.1 System Preparation

X-ray crystal structure of human TET2-dsDNA (PDB code, 4NM6<sup>13</sup>) was used as the initial structure, and the missing residues were added using Modeller.<sup>34</sup> The N-oxalylglycine (NOG) used for crystallization was converted to 2OG by replacing the NH in NOG with methylene (CH<sub>2</sub>) group using GaussView 6.0. The protonation states of the ionizable side chains were evaluated with the Propka software,<sup>35</sup> and the histidine residues

that are coordinated to the Fe(II) center were assigned protonation states based on visual inspection of their local environments.

The active site Fe(II) is octahedrally coordinated to the co-substrate 2OG in a bidentate manner, to two histidines (His1382 and His1881), an aspartate (Asp1384) residue, and a water molecule. To generate parameters for the Fe(III)-superoxo complex, the water molecule was substituted with O<sub>2</sub>, bound in an end on manner. The active site parameters were prepared using the Metal Center Parameter Builder (MCPB.py),<sup>36</sup> in Amber 18. Bond and angle force constants were derived using the Seminario method;<sup>37</sup> point charge parameters for the electrostatic potential were obtained using the ChgModB method. The zinc ion and its coordinating residues in the Zn finger regions were described using the Zinc Amber force field (ZAFF) method.<sup>38</sup> The parameters for 2OG and the substrate (5mC) were generated using the Antechamber module of Amber 18.<sup>39</sup> The Leap module in Amber was used to add hydrogen atoms to the protein systems and then neutralized using Na<sup>+</sup> counter ions. The systems were surrounded by a rectangular box solvated with TIP3P water molecules<sup>40</sup> within a distance of at least 10 Å from the protein's surface. Previous molecular dynamics simulations using these parameter generation procedures have successfully reproduced the geometry of non-heme iron systems.<sup>41-43</sup> Similar procedures were used to prepare the parameters for the ferryl complex, where the 2OG co-substrate was substituted with succinate, which was modeled with monodentate binding of the coordinating carboxylate. The parameters for all the mutants were developed by making use of the wild-type parameter after manually substituting the various mutants' residues.

## 4.2.2 Molecular Dynamic Simulations

A two-stage minimization of the geometries using MM was first performed before the MD simulations. Only water molecules and Na<sup>+</sup> were minimized in the first stage of the minimization, while the solute molecules were restrained with 500 kcal.mol<sup>-1</sup>Å<sup>-2</sup> harmonic potential and all atoms were optimized without restraints during the final minimization stage. The systems were subjected to 5000 steps of steepest descent, followed by 5000 steps of conjugate gradient energy minimization.

The minimized systems were first heated for 50 ps by linearly increasing the temperature from 0 to 300 K in a canonical ensemble (NVT) using Langevin thermostat.<sup>44</sup> The heated systems were further subjected to constant temperature heating (at 300 K) for 1 ns in an NPT ensemble. The solute molecules were restrained with the harmonic potential of 10 kcal mol<sup>-1</sup> Å<sup>2</sup> during the heating processes. After that, the systems were equilibrated within an NPT ensemble at a fixed temperature and pressure of 300 K and 1 bar, respectively, for 3 ns without any restraints on solute molecules. The MD productive runs were performed for 1 μs in an NPT ensemble with a target pressure set at 1 bar and constant pressure coupling of 2 ps. The pressure was held constant using Berendsen barostat,<sup>45</sup> and the SHAKE algorithm<sup>46</sup> was used to constrain the bond lengths of those bonds involving hydrogen atoms. The simulations were performed using the GPU version<sup>47</sup> of the PMEMD engine integrated with Amber18.<sup>48</sup> The FF14SB<sup>49</sup> force field was used in all the simulations, and periodic boundary conditions were employed in all simulations. Long-

range electrostatic interactions were calculated using the Particle Mesh Ewald (PME) method<sup>50</sup> with a direct space and vdW cut-off of 10 Å.

The hydrogen bonding analysis was done using CPPTRAJ,<sup>51</sup> and the dynamic cross correlation analysis was done with Bio3D.<sup>52</sup> The binding free energy values were calculated using molecular mechanics/ generalized Born surface area (MM/GBSA)<sup>53</sup> method as implemented in Amber18.

### **4.2.3 QM/MM Calculations**

QM/MM calculations were performed using the ChemShell package,<sup>54</sup> that combines Turbomole<sup>55</sup> (for QM region) and DL\_POLY<sup>56</sup> (for MM region). The electronic embedding method was used to describe the interaction between the QM and MM regions. Hydrogen linked atoms were used to complete valences of bonds spanning between the two regions. The MM region was described with the Amber force field, and the QM part was represented with the unrestricted B3LYP (UB3LYP) functional. The non-heme iron center, the primary coordinating sphere residues, and the substrate-bound in the active site were included in the QM region [Figure 4.2B]. The QM/MM geometry optimizations were performed with the def2-SVP basis set (labeled as B1) for all the atoms. After that, linear transit scans along the reaction coordinate were performed with 0.1 Å increments to locate the transition states using DL-find optimizer.<sup>57</sup> Transition states were reoptimized using the partitioned rational function optimization (P-RFO) algorithm implemented in the HDLC code.<sup>58</sup> The fully optimized geometries of the minima and the transition states were characterized via frequency calculations. The energies of the optimized stationary points

were recalculated via single-point energy calculation using a larger basis set, def2-TZVP (labeled as B2) for all the atoms. Electric field calculations were done using TITAN code<sup>59</sup> as in other studies.<sup>60,61</sup> Energy decomposition analysis (EDA)<sup>21a,b</sup> calculations were then carried out on the optimized reactants, and transition states geometries to determine the non-bonded interactions of all the residues.

The primary kinetic isotope effects (KIEs) were computed and compared with the experiment. The tunneling correction was considered during the calculations using the zero-curvature tunneling (ZCT) method as implemented in ChemShell. Hessian calculations were carried out in DL-FIND using ChemShell. The rate constant and KIEs were calculated on both deuterated and non-deuterated systems using transition state theory (TST).

## **4.3 Results and Discussion**

### **4.3.1 Conformational Dynamics Facilitates the Formation of a Reactive Complex between TET2 Fe(IV)=O and the 5mC (dsDNA) substrate (TET2·Fe(IV)=O/dsDNA)**

The active oxidizing species necessary for the oxidation of the methylated substrates in non-heme Fe(II) and 2OG-dependent enzymes is the ferryl intermediate. We performed MD simulations to explore the role of the structural dynamics of this reactive complex. TET2-Fe(IV)=O forms a stable complex with dsDNA (an average RMSD of 2.57 Å) [Figure 4.3A]. The plots of the time-dependent fluctuations of the distance between the



oxygen (O) from the oxo group of Fe(IV)=O and the methyl carbon (C) of the substrate [Figure 4.3B], and the Fe-O-C angle [Figure 4.3C], which determine the efficiency of the substrate oxidation showed average values of 3.66 Å and 143.32°, respectively. The proper orientation of the substrates' 5-methylcytosine ring with respect to the iron-oxygen bond of Fe(IV)=O is stabilized by a stacking interaction with the phenyl ring of Tyr1902. The dsDNA substrate in the TET2·Fe(IV)=O/dsDNA complex exhibits similar shape and orientation as in the crystal structure [Figure C3] supported by a hydrogen bonding network with Ser1828 (72.4%), His1904 (60.2%), and Arg1262 (64.6%). The substrate and the Fe(IV) center coordinated ligands are stabilized by a series of second sphere residues via hydrogen bonding interactions. For example, the non-coordinating (C4) succinate carboxylate group is stabilized by hydrogen bonding interactions with Arg1896 (89.6%), and Ser1898 (54.9%). In contrast, in the human AlkBH2-dsDNA (a human non-heme Fe(II)- and 2OG-dependent enzyme that demethylates N-methylated bases in dsDNA), the C4 succinate carboxylate is stabilized by hydrogen bonds with Arg248 (84%) and Tyr161 (84%).<sup>22</sup> The lower stability of the hydrogen bond with Ser1898 in TET2 compared to the one with Tyr161 in AlkBH2 might lead to more flexible succinate binding in TET2-dsDNA when compared to AlkBH2-dsDNA. The backbones of the Fe-coordinating histidines (His1382 and His1881) are stabilized additionally via hydrogen bonding interactions (87.8%) with each other. In contrast to AlkBH2-dsDNA, in TET2-dsDNA the non-coordinating oxygen of the aspartate ligand (Asp1384) is stabilized by Asn1387 -23% of the trajectory and by a stable solvent-mediated hydrogen bonding interaction (74.7%).

Comparing the MD simulations and the crystal structures of TET2-dsDNA with AlkBH2-dsDNA reveals key differences in the DNA interactions and binding in both enzymes<sup>13,17,22</sup> (The detailed comparison is presented in the SI).

The principal component analysis (PCA) [Figure 4.4], which shows the main direction of motions in a protein<sup>62,63a</sup> reveals that the cysteine-rich N-terminal (Cys-N) region, the GS linker region, loop 2 (L2), and the DNA are flexible regions in TET2·Fe(IV)=O/dsDNA. The Cys-N region moves toward the DSBH core for more significant interaction and better stability. The L2 and GS linker residues move towards DNA and the L2 forms scissors around DNA. These motions collectively enhance the binding of the DNA to the protein. The dynamic cross-correlation provides insights into the collective, correlated motions of the different domains of the proteins. Long-range correlated motions have been implicated in substrate binding, allosteric regulation, product release and protein folding.<sup>63b,c</sup> The DCCA map illustrates the covariance matrix of  $\alpha$  carbon atoms and ranges from +1 to -1, denoting correlated and anti-correlated motions, respectively. The dynamic cross-correlation analysis (DCCA) [Figure 4.5], of the flexible regions observed in the PCA reveals that the residues that contribute to the motion in the Cys-N region have a positive correlation with the Zn2 finger and its four coordinating residues (Cys1193, Cys1271, Cys1273, and His1380), and two  $\beta$ - sheets from the DSBH core ( $\beta$ 8 and  $\beta$ 17), which are directly opposite to the Fe center and its first coordinating sphere residues.

Furthermore, the residues from the L2 and GS linker regions of the protein, which participate in the essential motion with the DNA substrate show a positive correlation with

each other, the Zn3 finger, and its coordinating residues as well as DNA. The GS linker also shows a positive correlation with the loop 1 (L1) region, and the iron coordinating HxD loop. Even though the function of the GS linker remains elusive, its correlated motions with L1, L2, DNA, Zn3 finger, and the iron-coordinating HxD loop suggests about its importance in DNA binding. Overall, the long-range correlated motions observed in the WT ferryl complex might aid catalysis as well as DNA interactions and binding, resulting in stabilizing the overall structure of the WT TET2-dsDNA complex. In comparison, the studies on the AlkBH2-dsDNA complex show main direction of motions at the hydrophobic  $\beta$ -hairpin region which moves toward the Fe center, resulting in a complex that likely favor catalysis.<sup>22</sup>

#### **4.3.2 Single/Double Mutations in the Second Sphere and Beyond Influence the Substrate Binding in TET2·Fe(IV)=O/dsDNA Complex**

TET2 mutations influence substrate binding, catalysis, and DNA interactions,<sup>13</sup> and can also result in various diseases such as myelodysplastic syndrome and refractory anemia.<sup>13,32</sup> The TET2 mutations subject of this study have either been performed experimentally in vitro or clinically related to diseases. They include second sphere substitutions (W1291A, N1387A, Y1902A, and H1904R), substitutions in remote to the active site regions (M1293A-Y1294A, and K1299E-S1303N), or a combination of both (S1290A-Y1295A) [Figure 4.2A]. Mutant forms W1291A and K1299E-S1303N are mutations clinically linked to myelodysplastic syndrome and refractory anemia,

respectively,<sup>13,32</sup> while the rest of the studied mutant forms are experimentally-performed in vitro mutations found to influence the substrate binding and the TET2 enzymatic activity.<sup>13</sup> The distance between the oxo group (O) of the Fe(IV)=O intermediate and the alpha carbon (CA) of the respective substituted residue varies between 9.2 and 25.9 Å in the mutant forms of TET2· Fe(IV)=O/dsDNA (Table C1). To understand how these mutant forms affect the binding of dsDNA substrate to TET2, we performed a series of 1 μs MD simulations of all the seven single and double mutants: H1904R, K1299E-S1303N, M1293A-Y1294A, N1387A, S1290A-Y1295A, W1291A, and Y1902A. The mutation sites are located close to the 5mC dsDNA substrate binding region and loop2 (L2), as depicted in Figure 4.2A. The simulations show stable systems with average RMSDs [Figure 4.3A] between 2.61 and 3.35 Å (Table C2) compared to 2.57 Å in the WT TET2, suggesting some structural perturbations upon the mutation with the most profound effect in M1293A-Y1294A and W1291A mutant forms.

### **4.3.3 Effects of the Mutations on the Structure of the Substrate Binding Site and the Iron Center**

The average O - C distances [Figure 4.3B] varies between 3.78 and 11.27 Å (Table C2) while the average Fe-O-C angles [Figure 4.3C] ranges between 111.56 and 140.06° (Table C2) in comparison with 3.66 Å and 143.32°, respectively, for the WT TET2·Fe(IV)=O/dsDNA. The changes in the key HAT geometric parameters (distance and angle) in the mutant forms can lead to changes in the rate and mechanism of the HAT reaction. Furthermore, in all mutant forms, the substrate participates in a smaller number

of hydrogen bonds when compared to the WT, suggesting that the residue substitutions might influence its stability. For example, while in the WT TET2·Fe(IV)=O/dsDNA complex, the substrate is stabilized by interactions with Ser1828 (72.4%), His1902 (60.2%), and Arg1262 (64.6%), in K1299E-S1303N, N1387A, and S1290A-Y1295A mutants, the substrate is supported by hydrogen bonds with Ser1828 (25.1%, 43.4%, and 32.6%, respectively). In contrast in S1290A-Y1295A and Y1902A mutants, the hydrogen bonds between the substrate and Arg1262 are found to be 21.6% and 38.4%, respectively. The N1387A mutant form shows a hydrogen bonding interaction between the substrate and His1904 in 42.4% of the MD trajectories. Interestingly, the substitute Arg in the H1904R mutant stabilized the substrate (89.9%) more than His1904 in the WT, however other hydrogen bonding interactions observed in the WT are lost in this mutant. All these results indicate weaker stabilization of the substrate in the mutant forms when compared to the WT. The mutations also influence the overall stability of the iron center where the non-coordinating (C4) succinate carboxylate group is stabilized by a hydrogen bond with Arg1896 with a presence between 15.3% and 42.3% (Table C2) and Ser1898 (between 11.8% and 35.8%) (Table C2) in comparison to WT values of 89.6% and 54.9%, respectively. Also, the hydrogen bonding interaction between the two coordinating histidines (His1382 and His1881) backbones varies between 14.3% and 61.6% in comparison to 87.8% in the WT (Table C2). The above interactions are weaker when compared to the observed in the WT. This indicates that in both mutant forms the substrates are less stabilized in the active sites.

#### **4.3.4 Effects of Mutations on the Substrate Binding Affinity and Long-Range Correlated Motions**

The effects of the mutations on the stability of the TET2·Fe(IV)=O/dsDNA complex were further confirmed by calculating the binding free energies between the substrate and the protein using MM/GBSA.<sup>53</sup> The binding free energies of the mutant forms suggest a weaker substrate binding (see the SI) and vary between -108.43 kcal/mol and -63.98 kcal/mol (Table C2) in reference to -122.09 kcal/mol in the WT. The most profound effect is observed in the mutant form W1291A. Even though there are variations in the stability of the active site of the protein-DNA complexes, in the mutant forms and the WT, the radius of gyration (ROG) [Figure 4.3D] shows a similar volume of TET2 enzyme for all WT and mutation forms. This indicates that the mutations only influence the delicate interactions in the tertiary structure of TET2 and dsDNA, however, does not lead to a more dramatic disruption of the overall structure.

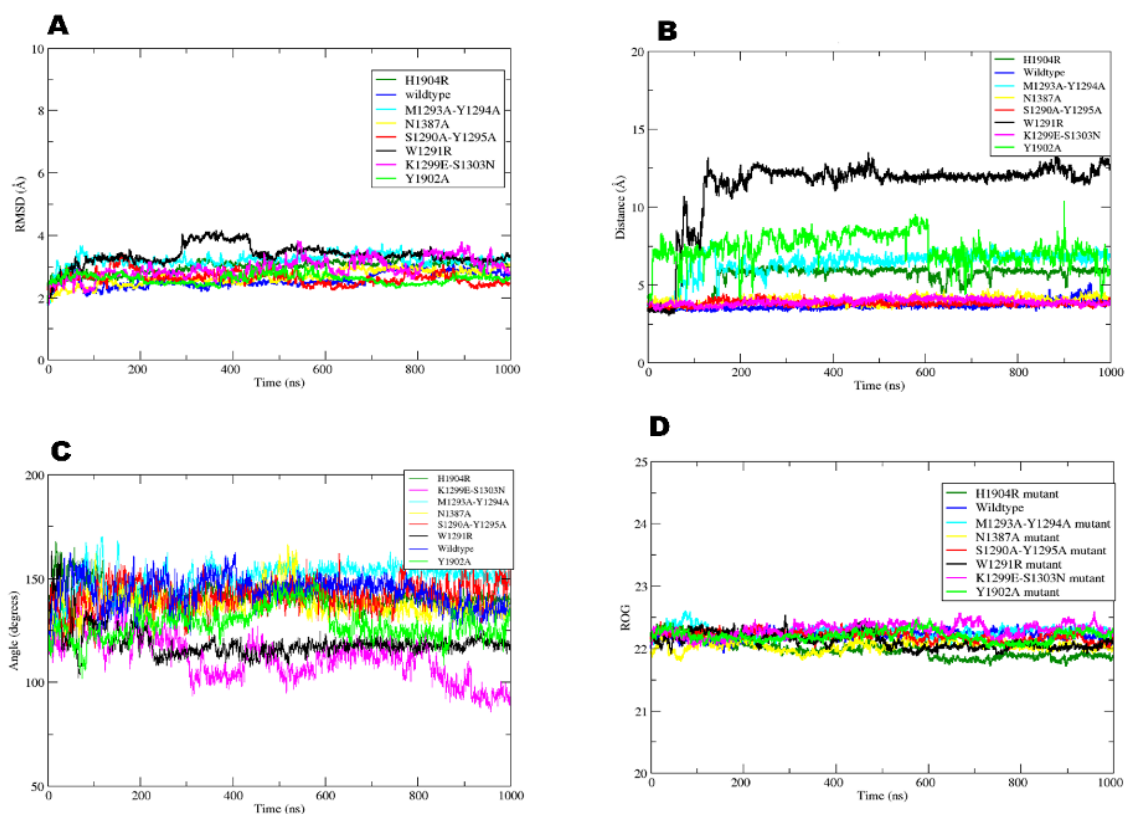


**Figure 4.3.** Plots of RMSD (A), distance between oxo group (O) of the ferryl and the substrate methyl carbon (B), angle between Fe, O and the substrate methyl carbon (C), and the radius of gyration (D) of both the WT TET2·Fe(IV)=O/dsDNA and the mutants.

The PCA of the double mutant forms [Figure 4.4] K1299E-S1303N, M1293A-Y1294A, and S1290A-Y1295A show a motion in the GS linker region, which moves it away from the DNA in K1299E-S1303N and S1290A-Y1295A forms, thus weakening the DNA-linker interactions. Interestingly, in the M1293A-Y1294A mutant form, the GS linker moves towards DNA as in the WT complex, thus enhancing the interactions of DNA with the protein. DCCA [Figure C7-C9] of the GS linker in these mutant forms reveals a positive

correlation with the Cys-N region in M1293A-Y1294A mutant, while in K1299E-S1303N and S1290A-Y1295A mutants, the GS linker has a positive correlation with  $\beta$ 12 in the GS linker vicinity. The Cys-N region harbors the Zn1 finger region, which stabilizes the overall protein structure while the  $\beta$ 12 only provides support for the GS linker region. Thus, the long-range correlated motion observed in the M1293A-Y1294A mutant form helps for the stabilization of this complex more than the K1299E-S1303N and S1290A-Y1295A. Besides, the PCA shows that the Cys-N region moves toward the protein (in M1293A-Y1294A) and away from it (in S1290A-Y1295A) supporting the DCCA results.

In the single mutant forms [Figure 4.4, C10-C13], Y1902A, and H1904R, the GS linker becomes more rigid. In contrast, in N1387A and W1291A, the linker remains flexible with the direction of motion towards the DNA and positively correlated with the DNA interacting loop 1 (L1). These correlated motions might enhance DNA stabilization. Also, in N1387A and Y1902A mutant forms, there is reduced flexibility around the Cys-N region, and this region becomes completely rigid in W1291A. However, in H1904R, the Cys-N region moves away from the DSBH, resulting in weakening the interactions within the DSBH region. The substitutions N1387A and H1904R show additional motions at  $\beta$ 13 and  $\alpha$ 6, respectively, which all have a positive correlation with  $\beta$ 12 that supports the GS linker.

Overall, DCCA and PCA analyses of the WT TET2·Fe(IV)=O/dsDNA and the mutant forms reveal that the correlated motions with the participation of the GS linker and Cys-N



regions contribute less to the DNA binding to the enzyme in the mutant forms than in the WT.

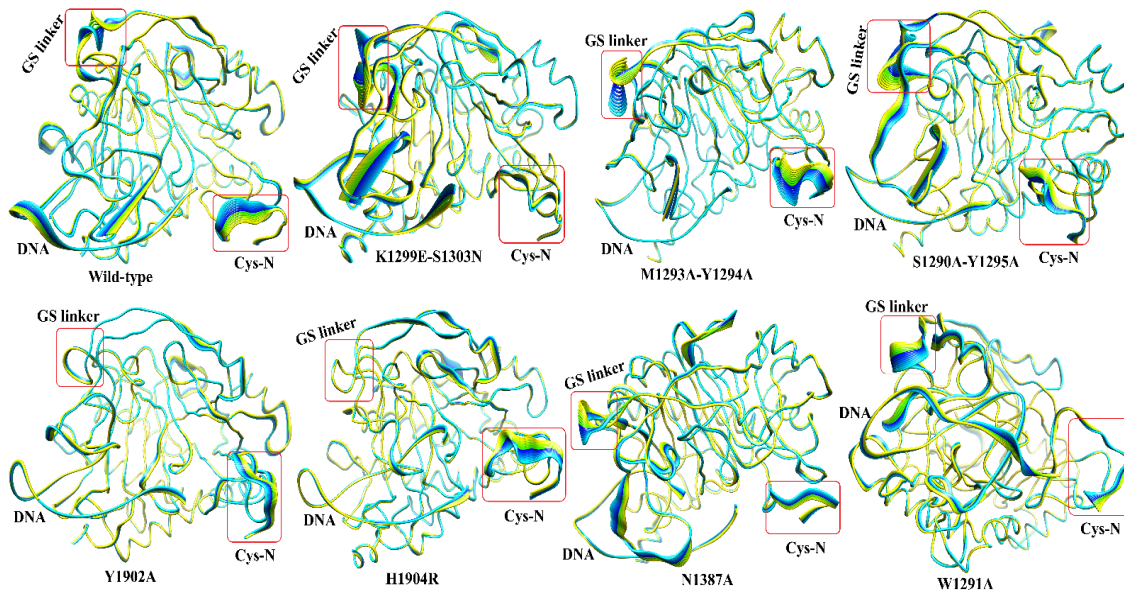


**Figure 4.4.** Principal component analysis for the WT TET2·Fe(IV)=O/dsDNA and its various mutants. Residues numbers are as follows: 1-445 (protein), 446-448 (Zn), 449 (Fe), 450 (O), 451 (succinate), 452-475 (DNA). Yellow to blue represents the direction of motion of residues.

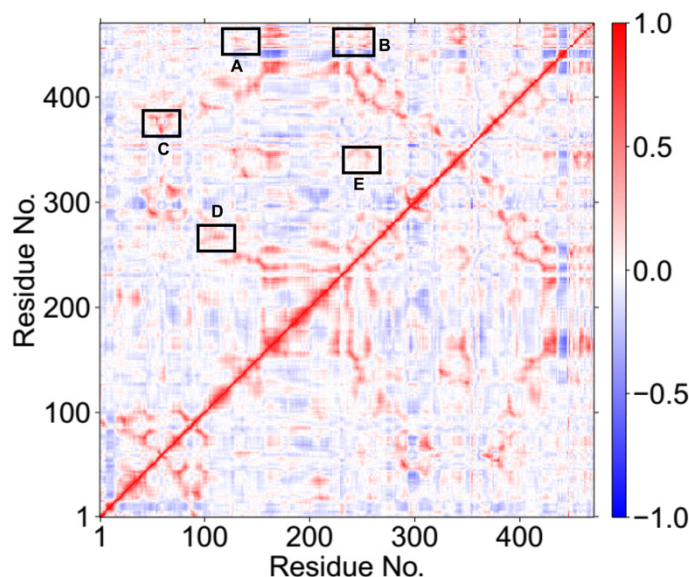


**Figure 4.5.** Dynamics cross correlation for the WT TET2·Fe(IV)=O/dsDNA MD simulations. Residue numbers 1-445 (protein), 446-448 (Zn), 449 (Fe), 450 (O), 451 (succinate), 452-475 (DNA). Boxes in the figure denote: (A) L2 residues show correlation with the DNA. (B) GS linker residues have correlation with the DNA. (C) Correlation of Zn3 coordinating site with L1. (D) L1 residues have correlation with GS linker residues. (E) Iron coordinating HxD loop residues show correlation with GS linker residues.

### 4.3.5 Mechanism of the Hydrogen Atom Abstraction (HAT) in the WT TET2-dsDNA

HAT involves the abstraction of a hydrogen atom from the methyl group of the substrate by the electrophilic Fe(IV)=O intermediate, resulting in Fe(III)-OH center and a reactive radical formation at the methylene carbon of the substrate.<sup>8,9,64</sup> This step has been reported

as the rate-limiting one during the substrate oxidation by Fe(II)/2OG dependent enzymes.<sup>21a-27,65,66a</sup> Studies have shown that the relative structure of ferryl to the substrates determine the reaction and the electron transfer mechanism.<sup>66b-e</sup> We used five snapshots from MD to explore this mechanistic step. The calculations were done at the quintet state of the Fe(IV)=O intermediate as it was previously demonstrated that non-heme Fe (II)- and 2OG-dependent enzymes favor this spin state.<sup>27,67-70</sup> The results revealed that the reaction barrier varies from 16.3 to 19.1 kcal/mol [Table C3] at the B2+ZPE level of theory, with Boltzmann weighted averaged<sup>22,71</sup> value of 17.1 kcal/mol, which is within the range of previously reported barriers for HAT for 2OG dependent oxygenases.<sup>24-28,65,72</sup> The TS<sub>HAT</sub> Fe-O-H angle varies from 149.4 to 160.1°, suggesting that in all reaction paths, an  $\alpha$ -electron is transferred from the substrate to the vacant 3d-orbital of the Fe. This is further confirmed by the TS<sub>HAT</sub> spin density values of the methyl carbon of the substrate, which vary between -0.322 and -0.253, showing that a  $\beta$ -electron is left on the substrate and the reaction proceeds via  $\sigma$ -pathway [Figure 4.6]. Recent computational studies on other DNA repair enzymes, AlkB and AlkBH2, bound to duplex DNA, have shown that the HAT proceeds via the same pathway.<sup>22</sup> The TS<sub>HAT</sub> geometry is stabilized by several key interactions and in particular Arg1261 stabilizes the non-coordinating oxygen of the succinate. A network of hydrophobic interactions including residues Val1900, Val1395, Leu1872, and Thr1393 surrounding the Fe center and the methyl group of the substrate enhance the stabilization of the TS<sub>HAT</sub>. Besides, the cytosine ring of the substrate is stabilized by stacking interaction with Tyr1902. This substrate stabilization and proper orientation are further enhanced by stacking interaction of the imidazole group of His1904

and the phenyl ring of Tyr1902 and a hydrogen bonding interaction between N3 of the substrate and NH group of His1904. Further, the exocyclic nitrogen (N4) of the substrate is stabilized via a hydrogen bonding interaction with Asn1387, enhancing its stability in the WT.

HAT results in the formation of the Fe(III)-OH complex, and methylene substrate radical with an O-H distance of 0.97 Å, and the Fe-O is elongated from 1.62 to 1.85 Å. This elongation indicates the formation of the ferric-hydroxo complex and the spin density of 4.23 indicates about +3 oxidation of the Fe at this reaction state. The formed intermediate is almost thermoneutral with energy of -0.4 kcal/mol at the B2+ZPE level of theory, unlike in AlkBH2-dsDNA, where the formed Fe(III)-OH intermediate is slightly endothermic with energy of 6.5 kcal/mol at the B2+ZPE level of theory.<sup>22</sup> This implies that the ferric-hydroxo intermediate is more energetically favorable and stable in TET2 than in AlkBH2.

#### **4.3.6 Energy Decomposition Analysis and Long-Range Correlated Motions of the HAT-Transition State-Stabilizing Residues**

To gain insights into the role of the individual residues in the reaction steps during catalysis, we performed energy decomposition analysis (EDA) as developed by Cisneros<sup>21a,b</sup> on the QM/MM optimized RC and TS<sub>HAT</sub> geometries. This was achieved by calculating the differences in the nonbonded interaction energies (i.e., Coulomb and van der Waals interaction energies) between the individual residues of MM environment and the QM for

the RC and the TS structures.<sup>21a-d</sup> This analysis is only obtained in an approximate manner and thus provides a qualitative assessment of individual residues in the reaction steps.<sup>21c,d</sup> A negative energy difference between the TS and the RC structures refers to a stabilizing contribution to the TS and vice versa. EDA has been employed in various QM/MM and MD simulations to study numerous protein systems.<sup>21a-f</sup> The results as presented in Table 4.1 show that residues Thr1393, Val1395, Leu1872, and Arg1261, which take part in the stabilization of the TS<sub>HAT</sub> when compared to the RC in the WT TET2·Fe(IV)=O/dsDNA, contribute with energies of -1.36, -0.82, -0.60, and -4.46 kcal/mol, respectively.

The DCCA of the residues that stabilize the TS<sub>HAT</sub> shows that residues that are involved in hydrophobic interactions have a positive correlation with the DNA-interacting loops residues (L1), the succinate-stabilizing residues, the Fe center, and the loop (iron-chelating motif 1) from the DSBH core [Figure 4.4]. Also, Arg1261 that stabilizes the succinate non-coordinating oxygen has a positive correlation with both the DNA-interacting loops (L1 and L2), a loop that harbors the coordinating His1881 and GS linker residues. Asn1387 involved in stabilizing the exocyclic nitrogen of the substrate has a positive correlation with the Fe center and its oxo group, implying that this residue might be important in catalysis. Tyr1902 also has a positive correlation with GS linker residues, the loop containing iron HxD motif, the third zinc finger (Zn3), and its coordinating residues (Cys1289, Cys1298, Cys1358, and His1912). The DNA-interacting loops are crucial for DNA binding and the Zn finger is important for the overall structural stabilization.<sup>13</sup> These results show that complex correlation motions between the residues that stabilize the TS<sub>HAT</sub> with loop 1, loop 2, Zn3 finger, and GS linker regions, ensure the overall stabilization of

the transition state and the metal center. In comparison, in AlkBH2, the HAT transition state is stabilized by residues Thr252, Arg110, Tyr122, Arg254, and Glu175, which all have a correlation with the iron center and its coordinating residues and with the substrate recognition lid, suggesting that modification of the second sphere residues in the substrate binding lid could influence HAT in AlkBH2<sup>22</sup> but not in the TET2.

### **4.3.7 Influence of Electric Field and Kinetic Isotope Effects on the HAT**

Recent studies have shown that the internal electric fields along the reaction coordinate in small molecules and enzymes can be an important factor that defines the reaction mechanism and specificity.<sup>59-61,73</sup> To evaluate how the conformational changes involved in HAT can influence the electric field, we performed calculations of the local electric field along the direction of Fe=O bond in the ferryl complex reactant geometries using TITAN.<sup>59</sup> The results, as shown in Table C4, reveal that in all the five snapshots used for the WT calculations, the value of the electric field intensity exhibits slight variations as a function of the conformational changes in the RCs. Importantly in RCs with similar HAT distance and angle, it is the change in the electric field that contributes to the differences in the activation energies of the reaction paths. For example, snapshots 1 and 4 with almost the same distance between the oxo group oxygen (O) and the hydrogen atom (H) show an electric field intensity of -0.0479 au for snapshot 4, which is -0.0034 au lower than in snapshot 1 with the lowest barrier. The higher barrier observed in snapshot 4, although its favorable electric field value could be due to the constraint in Fe-O-H angle (127.8°) in

snapshot 4 compared to the corresponding value of  $149.7^\circ$  in snapshot 1. The calculated electric field values of the transition states (Table C4) follow the similar trend as the various reactant complexes but becomes less negative at this reaction state in all cases.

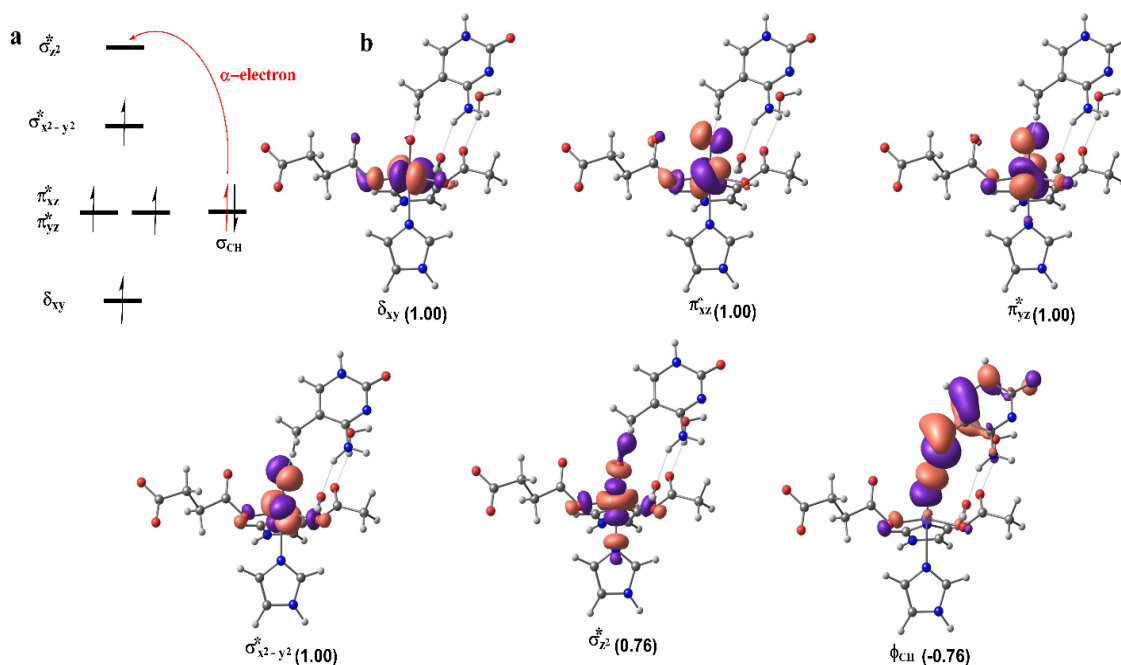


**Figure 4.6.** Electron shift diagram (a) and the spin natural orbitals (SNOs) (b) with their respective populations (in parentheses) during HAT in the WT TET2·Fe(IV)=O/dsDNA, calculated from the transition state structure.

The hydrogen atom abstraction barriers in enzymes can exhibit a kinetic isotope effect (KIE) when the transferred hydrogen atom is substituted with a heavier isotope active site dynamic.<sup>72</sup> To estimate the KIE contributions and to evaluate the tunneling effect on the system, we performed primary KIE calculations by replacing the transferred hydrogen atom with deuterium as tunneling is very sensitive to the mass of the tunneling particle.

The calculated KIE value of 8.55 at 303 K for the WT is in very good agreement with the experimental value<sup>74</sup> of 9 for KIE in TET2 and also with other observed experimental KIE for Fe/2OG enzyme substrates<sup>15</sup>. The calculated KIE indicates a low tunneling contribution in the HAT reaction in the WT TET2.

#### **4.3.8 Mechanism of the Rebound Hydroxylation in the WT TET2-dsDNA**

After the formation of Fe(III)-OH intermediate and substrate radical, the intermediate undergoes a rebound reaction, where the hydroxyl group (OH) of the ferric-hydroxo intermediate is transferred to the methylene radical, leading to the formation of the hydroxylated product. The process passes through a  $TS_{\text{Reb}}$  with a barrier of 10.1 kcal/mol, including ZPE correction. The rebound TS barrier in TET2 is 2.5 kcal/mol lower than the barrier obtained for another human DNA repair enzyme, AlkBH2,<sup>22</sup> indicating that the process of rebounding of the hydroxyl group from the Fe(III)-OH to the substrate radical is faster in TET2 than in AlkBH2. The observed lower TS barrier in TET2 could be due to a better orientation of the Fe-OH to methylene carbon radical ( $O_p$ -C distance) compared to AlkBH2. The rebound process occurs faster than the HAT, confirming the rate-limiting nature of the HAT in substrate oxidation. The rebound hydroxylation results in a highly stable product (PD) with energy of -24.9 kcal/mol. The optimized geometries of the stationary points and the potential energy profile are presented in Figures 4.7 and 4.8, respectively.



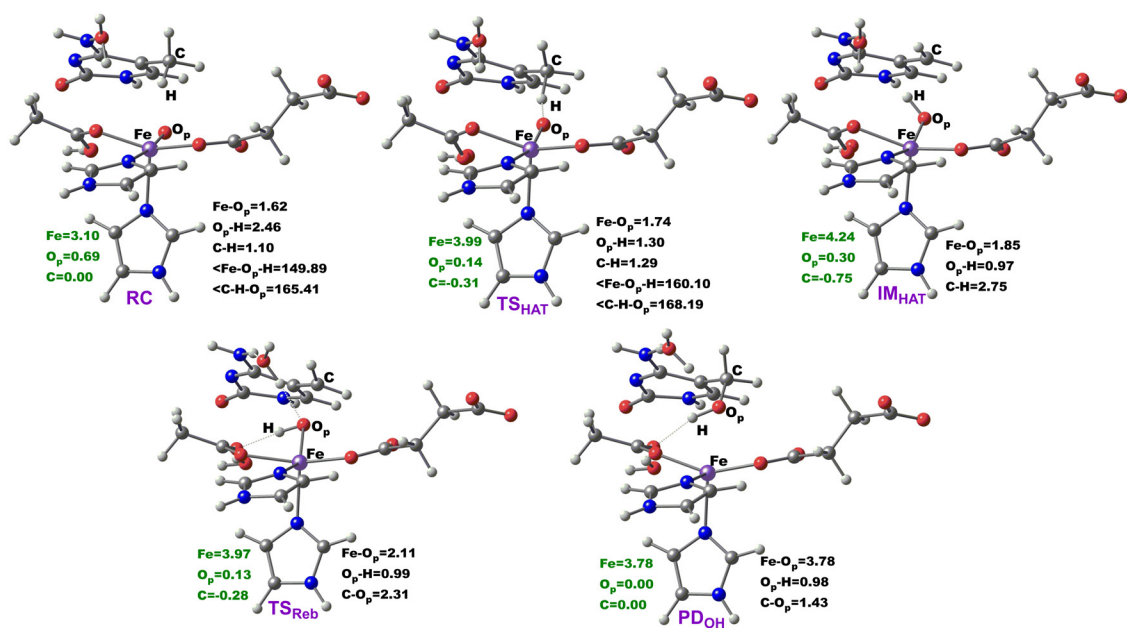


**Figure 4.7.** Stationary points geometries along the HAT and Rebound hydroxylation steps in the WT TET2·Fe(IV)=O/dsDNA. Distances (Å) and spin densities are in black and green, respectively.

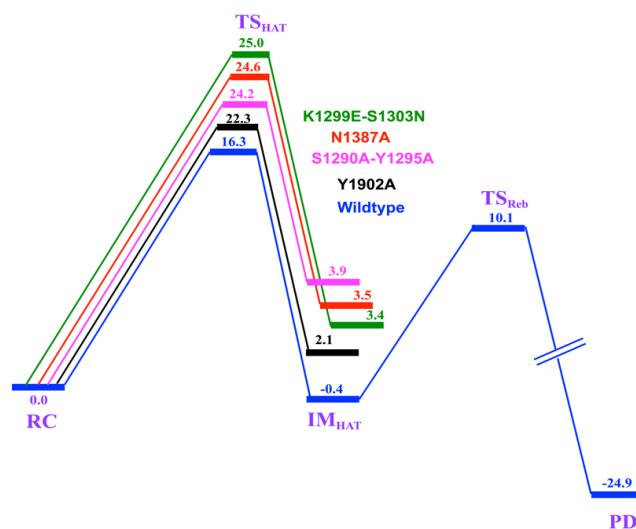


**Figure 4.8.** The energetic reaction profile for the hydroxylation of 5-methylcytosine substrate by TET2 as calculated at UB3LYP/def2-TZVP+ZPE level. The relative energies are in kcal/mol.

#### 4.3.9 Effect of Mutations on Hydrogen Atom Abstraction Reaction of TET2·Fe(IV)=O/dsDNA Complex

To quantify the effect of the mutations on the rate-limiting HAT step of the reaction mechanism of the oxidation of 5mC to 5hmC by human TET2 enzyme, we performed QM/MM calculations on K1299E-S1303N, S1290A-Y1295A, Y1902A, and N1387A. In these mutant forms, the distance between the oxo-group of Fe(IV)=O intermediate and the substrate's methyl carbon is favorable for substrate oxidation.<sup>75</sup> The calculations revealed barriers of 25.0 kcal/mol, 24.2 kcal/mol, 22.3 kcal/mol, and 24.6 kcal/mol at the B2+ZPE level of theory for K1299E-S1303N, S1290A-Y1295A, Y1902A, N1387A mutants, respectively, in comparison to 16.3 kcal/mol obtained for the WT. The activation barriers

for the mutant forms are higher than the one obtained for the WT, implying that the mutations decrease the rate of the rate-limiting HAT step in comparison to the WT complex. In the optimized  $\text{TS}_{\text{HAT}}$  structures, the Fe-O-H angles are 113.7, 145.3, 149.5, and 146.1° for K1299E-S1303N, S1290A-Y1295A, Y1902A, N1387A, respectively, in comparison to 160.10° for the WT. Lower Fe-O-H angle value in the K1299E-S1303N suggests for HAT proceeding via a  $\pi$ -pathway, where a  $\beta$ -electron is transferred into the 3d-orbital of Fe, leaving an  $\alpha$ -electron on the substrate (Figure 4.9). In the remaining three mutants, HAT proceeds via a  $\sigma$ -pathway with an  $\alpha$ -electron transfer to the 3d-orbital of Fe, similar to the WT, where the Fe-O-H angle and spin density at  $\text{TS}_{\text{HAT}}$  are 160.10° and -0.312, respectively. These observations are validated by the methyl carbon spin density values of 0.365, -0.260, -0.294, and -0.291 for K1299E-S1303N, S1290A-Y1295A, Y1902A, N1387A, respectively. The results demonstrate that residue substitution has a strong influence on the HAT transfer mechanism, switching the nature of the overlapping MOs.

The HAT leads to the formation of the Fe(III)-OH complex intermediate with reaction energies of 3.4, 3.9, 2.1, and 3.5 kcal/mol at B2+ZPE level of theory for K1299E-S1303N, S1290A-Y1295A, Y1902A, N1387A mutants, respectively, in respect to -0.4 kcal/mol obtained for the WT complex. This clearly shows that the formation of the ferric-hydroxo intermediate is slightly endothermic in the mutants and the formed products are less stable than in the WT. Figure 4.8 and (Figures 4.10 and C14) show the potential energy profile and the optimized geometries of the stationary points, respectively.

#### **4.3.10 Stabilization of the HAT Transition State in the Mutant Forms: Local Interactions, Energy Decomposition and Long-Range Correlated Motions**

In all the mutant forms, the  $TS_{\text{HAT}}$  is stabilized by hydrophobic interactions between Val1900, Val1395, and Thr1393 around the Fe center and the substrate's methyl group unlike in the WT where Leu1872 is inclusive. In K1299E-S1303N and N1387A, the stacking interactions between the substrate's cytosine ring and Tyr1902 are preserved as in the WT complex. However, the extra stacking interactions between His1904 and Tyr1902, which enhance the substrate stabilization are lost in these mutant forms, and the His1904 imidazole group is re-oriented to form hydrogen bonding interaction with the O2 of the substrate in the N1387A mutant. In the Y1902A mutant form, the substrate is very unstable due to the substitution Tyr1902Ala, which causes the loss of extra stacking interaction between the Tyr and the imidazole group of His1904 and thus affect the orientation of the substrate (Figure C15). The substituted Tyr1902 residue helps in the stabilization of the substrate's cytosine ring in the WT complex, and its substitution to Ala weakens the substrate stability, with Ala forming stable hydrophobic interaction with a nearby Thr1393 residue.

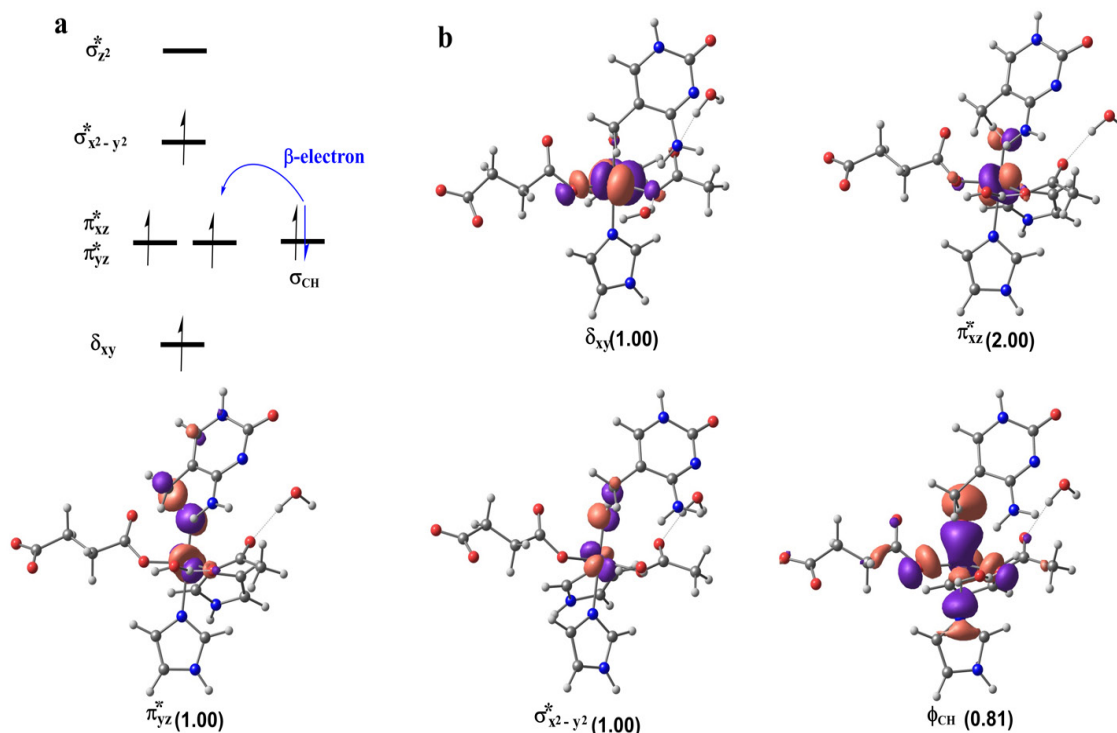


**Figure 4.9.** Electron shift diagram (a) and the spin natural orbitals (SNOs) (b) with their respective populations (in parentheses) during HAT in the K1299E-S1303N TET2-Fe(IV)=O/dsDNA mutant, calculated from the transition state structure.

The residues involved in hydrophobic interactions in all transition states of mutant forms have positive correlated motions with iron, the loop containing iron ligating HxD motif, and the residues that stabilize the succinate. The result implies that the residues enhance the stabilization of the metal center mainly via long-range interactions in contrast to the WT where they also involve a correlated motion with the DNA substrate. This difference contributes to the weaker binding of the DNA in all the mutants which further explains the observed differences in the free energies of binding. Tyr1902, a residue involved in the

cytosine ring stabilization in K1299E-S1303N and N1387A mutant forms shows correlated motion with the DNA-interacting loop2, the Zn3 finger region (in N1387A), and the iron-ligand HxD motif loop (in K1299E-S1303N). This correlated motion involving Tyr1902 probably enhances the interaction of DNA to the protein in N1387A.

EDA of the mutant forms shows that residues Arg1261, His1904, and Val1900 contribute with higher energies than in the WT (Table 4.1), which leads to the increased reaction barrier observed in the mutants. For example, in K1299E-S1303N, residues Thr1393, Val1900, Tyr1902, Asn1387, His1904, and Arg1261 have energies 0.65, 1.11, 0.73, 0.50, 1.11, and 2.67 kcal/mol, respectively. Also, in N1387A and Y1902, the substitutions led to destabilization of the systems by 1.32 and 1.85 kcal/mol, respectively. This contributes to the higher barriers observed in the mutants with respect to the WT (where N1387 and Y1902 contribute energies -0.05 and 0.04 kcal/mol, respectively). A change in sign of the individual residues interaction energy (from positive to negative) from the reactant complex to the transition state results in the lowering of the reaction barrier and vice versa.<sup>21a</sup> Our results indicate that residues involved in transition state stabilization, contribute with more energy to the stabilization of the TS<sub>HAT</sub> in the WT than in the mutants (Table 4.1).

#### **4.3.11 How the Mutations Alter the HAT Electric Field and KIE?**

The mutation of residues in the second sphere with respect to the active site and beyond influenced the electric field along the reaction coordinate (Table C5), with similar trend

observed at both the reactants and transition states complexes. The differences in electric field likely result in a higher activation energy barrier in K1299E-S1303N and Y1902A mutant forms than WT snapshots with similar O-H distances and Fe-O-H angles. The complete analysis is presented in the SI. There are only small differences in the KIE values obtained for the mutant forms when compared to the WT, indicating that KIE would not reflect sensitively the effect of the various substitutions in the system at 303 K. The temperature dependence plot of KIE, however, show that the double mutant forms are more strongly dependent on temperature than the single ones (Figure C16).

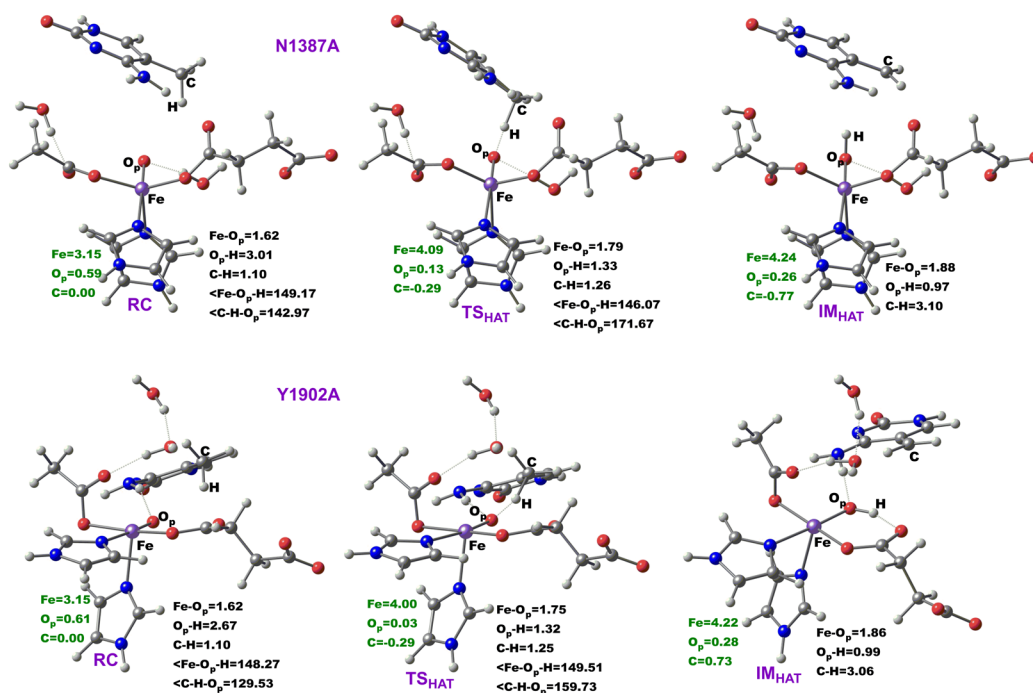


**Figure 4.10.** Stationary points geometries along the HAT step in the N1387A and Y1902A mutants. Distances (Å) and spin densities are in black and green, respectively.

**Table 4.1.** Energy Decomposition Analysis (EDA) (in kcal/mol) of the residues that stabilize the TS<sub>HAT</sub> in the wild-type and the mutants

Residues	WT	N1387A	Y1902A	K1299E- S1303N	S1290A- Y1295A
<b>Thr1393</b>	-1.36	0.52	0.08	0.65	-0.14
<b>Val1395</b>	-0.82	-0.28	-0.01	-0.02	0.06
<b>Val1900</b>	0.08	0.51	0.27	1.11	0.69
<b>Leu1872</b>	-0.60	0.05	0.02	0.01	-0.02
<b>Arg1261</b>	-4.46	3.37	-1.63	2.67	2.53
<b>Tyr1902</b>	0.04	0.81	1.85	0.73	0.68
<b>His1904</b>	0.01	0.41	0.47	1.11	0.90
<b>Asn1387</b>	-0.05	1.32	-0.01	0.50	0.29

## 4.4 Conclusions

In this study, we have investigated how conformational dynamics of the WT TET2·Fe(IV)=O/dsDNA complex and single and double mutations (generated in vitro and with clinical implications in human patients) influence key structural determinants and the catalytic mechanism of the oxidation of 5mC dsDNA substrate to 5hmC using MD and hybrid QM/MM computational approaches.

The studies reveal that the substitutions affect the substrate's binding and the DNA interactions to the TET2 enzyme, thereby affecting the overall structural stability of the protein-DNA complexes. We identified hydrogen bonding interactions that are not present



in the binding sites of the substrate and the succinate binding in the WT. The GS linker and the Cys-rich N-terminal (Cys-N) subdomain correlated motions contribute stronger to the DNA interactions to TET2 in the WT than in the mutant forms, thus enhancing the overall structural formation in the WT. The calculated energy barriers show that the mutations decrease the rate of the 5mC oxidation to 5hmC in comparison to the WT. The calculated rate-determining HAT barrier for the WT is in good agreement with other reported Fe(II) and 2OG dependent enzymes. Remarkably, the results enabled us to identify key residues that are crucial for the HAT during the oxidation and to delineate their energy contributions and crucial long-range correlated interactions. The calculations reveal that the K1299E-S1303N variant uses  $\pi$ -pathway for the HAT. In contrast, the WT and other mutants use  $\sigma$ -pathway for the HAT, implying that residue substitutions can influence the molecular orbital interactions. The electric field calculations reveal the importance of conformational changes and mutations to alter the electric field along the direction of Fe=O bond, thus contributing to efficient catalysis. For example, the K1299E-S1303N and Y1902A mutants with similar O-H distances and Fe-O-H angles as WT show a higher HAT barrier, as the intensity of the local electric field along the direction of the Fe=O bond are reduced in mutant forms. The synergistic effects between the substrate orientation, internal electric field and long-range interactions contribute to the overall stability of the transition states in comparison to the reactant complexes. Kinetic isotope effect (KIE) calculations for the rate-determining step are in good agreement with the energy barrier, suggesting low tunneling contributions. The KIEs for the single mutant forms are weakly dependent on temperature, while in the double mutant forms, the KIEs strongly depend on temperature,

especially at lower temperatures. Our calculations provide a molecular basis to understand the molecular pathology involved in the human TET2 enzyme and emphasize the crucial effects of protein sites in the second sphere and beyond on the catalytic events.

## 4.5 References

- (1) Bird, A. DNA Methylation Patterns and Epigenetic Memory. *Genes and Development*. 2002, 16, 6–21.
- (2) Cimmino, L.; Abdel-Wahab, O.; Levine, R. L.; Aifantis, I. TET Family Proteins and Their Role in Stem Cell Differentiation and Transformation. *Cell Stem Cell*. 2011, 9, 93–204.
- (3) Branco, M. R.; Ficz, G.; Reik, W. Uncovering the Role of 5-Hydroxymethylcytosine in the Epigenome. *Nat. Rev. Genet.* 2012, 13 (1), 7–13.
- (4) Williams, K.; Christensen, J.; Helin, K. DNA Methylation: TET Proteins-Guardians of CpG Islands? *EMBO Reports*. 2012, 13, 28–35.
- (5) Pastor, W. A.; Aravind, L.; Rao, A. TETonic Shift: Biological Roles of TET Proteins in DNA Demethylation and Transcription. *Nature Reviews Molecular Cell Biology*. 2013, 14, 341–356.
- (6) Wu, H.; Zhang, Y. Mechanisms and Functions of Tet Protein-mediated 5-Methylcytosine Oxidation. *Genes and Development*. 2011, 25, 2436–2452.
- (7) Tan, L.; Shi, Y. G. Tet Family Proteins and 5-Hydroxymethylcytosine in Development and Disease. *Development*. 2012, 139 (11), 1895–1902.
- (8) Fedeles, B. I.; Singh, V.; Delaney, J. C.; Li, D.; Essigmann, J. M. The AlkB Family of Fe(II)/ $\alpha$ -Ketoglutarate-Dependent Dioxygenases: Repairing Nucleic Acid Alkylation Damage and Beyond. *J. Biol. Chem.* 2015, 290 (34), 20734–20742.
- (9) (a) Zheng, G.; Fu, Y.; He, C. Nucleic Acid Oxidation in DNA Damage Repair and Epigenetics. *Chem. Rev.* 2014, 114 (8), 4602–4620. (b) Ghanty, U.; Wang, T.; Kohli, R. M. Nucleobase Modifiers Identify TET enzymes as Biofunctional DNA Dioxygenases Capable of Direct N-Demethylation. *Angew. Chem. Int. Ed.* 2020, 59, 11312–11315.
- (10) (a) Rasmussen, K. D.; Helin, K. Role of TET Enzymes in DNA Methylation, Development, and Cancer. *Genes and Development*. 2016, 30, 733–750. (b) Crawford, D. J.; Liu, M. Y.; Nabel, C. S.; Cao, X.; Garcia, B. A.; Kohli, R. M. TET2 Catalyzes Stepwise 5-methylcytosine Oxidation by an Iterative and de novo Mechanism. *J. Am. Chem. Soc.* 2016, 138, 730–733.
- (11) An, J.; Rao, A.; Ko, M. TET Family Dioxygenases and DNA Demethylation in Stem Cells and Cancers. *Experimental and Molecular Medicine*. 2017, 49, 1–12.
- (12) Kavooosi, S.; Sudhamalla, B.; Dey, D.; Shriver, K.; Arora, S.; Sappa, S.; Islam, K. Site- And Degree-Specific C-H Oxidation on 5-Methylcytosine Homologues for Probing Active DNA Demethylation. *Chem. Sci.* 2019, 10 (45), 10550–10555.

- (13) Hu, L.; Li, Z.; Cheng, J.; Rao, Q.; Gong, W.; Liu, M.; Shi, Y. G.; Zhu, J.; Wang, P.; Xu, Y. Crystal Structure of TET2-DNA Complex: Insight into TET-Mediated 5mC Oxidation. *Cell*. 2013, 155 (7), 1545–1555.
- (14) Xue, J. H.; Chen, G. D.; Hao, F.; Chen, H.; Fang, Z.; Chen, F. F.; Pang, B.; Yang, Q. L.; Wei, X.; Fan, Q. Q.; Xin, C.; Zhao, J.; Deng, X.; Wang, B. A.; Zhang, X. J.; Chu, Y.; Tang, H.; Yin, H.; Ma, W.; Chen, L.; Ding, J.; Weinhold, E.; Kohli, R. M.; Liu, W.; Zhu, Z. J.; Huang, K.; Tang, H.; Xu, G. L. A Vitamin-C-Derived DNA Modification Catalysed by an Algal TET Homologue. *Nature* 2019, 569 (7757), 581–585.
- (15) Hu, L.; Lu, J.; Cheng, J.; Rao, Q.; Li, Z.; Hou, H.; Lou, Z.; Zhang, L.; Li, W.; Gong, W.; Liu, M.; Sun, C.; Yin, X.; Li, J.; Tan, X.; Wang, P.; Wang, Y.; Fang, D.; Cui, Q.; Yang, P.; He, C.; Jiang, H.; Luo, C.; Xu, Y. Structural Insight into Substrate Preference for TET-Mediated Oxidation. *Nature*. 2015, 527 (7576), 118–122.
- (16) Lee, D. H.; Jin, S. G.; Cai, S.; Chen, Y.; Pfeifer, G. P.; O'Connor, T. R. Repair of Methylation Damage in DNA and RNA by Mammalian AlkB Homologues. *J. Biol. Chem.* 2005, 280 (47), 39448–39459.
- (17) Yi, C.; Chen, B.; Qi, B.; Zhang, W.; Jia, G.; Zhang, L.; Li, C. J.; Dinner, A. R.; Yang, C. G.; He, C. Duplex interrogation by a direct DNA repair protein in search of base damage. *Nat. Struct. Mol. Biol.* 2012, 19 (7), 671–676.
- (18) Ito, S.; Shen, L.; Dai, Q.; Wu, S. C.; Collins, L. B.; Swenberg, J. A.; He, C.; Zhang, Y. Tet Proteins Can Convert 5-Methylcytosine to 5-Formylcytosine and 5-Carboxylcytosine. *Science*. 2011, 333 (6047), 1300–1303.
- (19) Bachman, M.; Uribe-Lewis, S.; Yang, X.; Williams, M.; Murrell, A.; Balasubramanian, S. 5-Hydroxymethylcytosine Is a Predominantly Stable DNA Modification. *Nat. Chem.* 2014, 6 (12), 1049–1055.
- (20) Waheed, S. O.; Ramanan, R.; Chaturvedi, S. S.; Ainsley, J.; Evison, M.; Ames, J. M.; Schofield, C. J.; Christov, C. Z.; Karabencheva-Christova, T. G. Conformational Flexibility Influences Structure-Function Relationships in Nucleic Acid N-Methyl Demethylases. *Org. Biomol. Chem.* 2019, 17 (8), 2223–2231.
- (21) (a) Torabifard, H.; Cisneros, G. A. Insight into Wild-Type and T1372E TET2-Mediated 5hmC Oxidation Using Ab Initio QM/MM Calculations. *Chem. Sci.* 2018, 9 (44), 8433–8445. (b) Leddin, E. M.; Cisneros, G. A. Comparison of DNA and RNA substrate on TET2 structure. *Adv. Protein Chem. Strut. Biol.* 2019, 117, 91-112. (c) Liu, H.; Zhang, Y.; Yang, W. How is the Active Site of Enolase Organized To Catalyze Two Different Reaction Steps?. *J. Am. Chem. Soc.* 2000, 122(28), 6560-6570. (d) Cisneros, G. A.; Perera, L.; Schaaper, R. M.; Pedersen, L. C.; London, R. E.; Pedersen, L. G.; Darden, T. A. Reaction Mechanism of the  $\epsilon$  Subunit of *E. coli* DNA Polymerase III: Insights into Active Site Metal Coordination and Catalytically Significant Residues. *J. Am. Chem. Soc.* 2009, 131(4), 1550-1556. (e) Cui, Q.; Karplus, M. Catalysis and Specificity in Enzymes: A Study of Triosephosphate Isomerase and Comparison with Methyl Glyoxal Synthase. *Adv. Protein Chem.*, 2003, 66, 315-372. (f) Martí, S.; Andrés, J.; Moliner, V.; Silla, E.; Tuñón, I.; Bertrán, J. Preorganization and reorganization as related factors in enzyme catalysis: the chorismite mutase case. *Chem. -Eur. J.*, 2003, 9, 984-991.
- (22) Waheed, S. O.; Ramanan, R.; Chaturvedi, S. S.; Lehnert, N.; Schofield, C. J.; Christov, C. Z.; Karabencheva-Christova, T. G. Role of Structural Dynamics in Selectivity

and Mechanism of Non-Heme Fe(II) and 2-Oxoglutarate-Dependent Oxygenases Involved in DNA Repair. *ACS Cent. Sci.* 2020, 6 (5), 795–814.

(23) Wang, B.; Usharani, D.; Li, C.; Shaik, S. Theory Uncovers an Unusual Mechanism of DNA Repair of a Lesioned Adenine by AlkB Enzymes. *J Am Chem Soc.* 2014, 136(39), 13895-13901.

(24) Liu, H.; Llano, J.; Gault, J. W. A DFT Study of Nucleobase Dealkylation by the DNA Repair Enzyme AlkB. *J. Phys. Chem. B.* 2009, 113 (14), 4887–4898.

(25) Quesne, M. G.; Latifi, R.; Gonzalez-Ovalle, L. E.; Kumar, D.; De Visser, S. P. Quantum Mechanics/Molecular Mechanics Study on the Oxygen Binding and Substrate Hydroxylation Step in AlkB Repair Enzymes. *Chem. - A Eur. J.* 2014, 20 (2), 435–446.

(26) Fang, D.; Lord, R. L.; Cisneros, G. A. Ab Initio QM/MM Calculations Show an Intersystem Crossing in the Hydrogen Abstraction Step in Dealkylation Catalyzed by AlkB. *J. Phys. Chem. B* 2013, 117 (21), 6410–6420.

(27) Wang, B.; Cao, Z.; Sharon, D. A.; Shaik, S. Computations Reveal a Rich Mechanistic Variation of Demethylation of N-Methylated DNA/RNA Nucleotides by FTO. *ACS Catal.* 2015, 5 (12), 7077–7090.

(28) Lu, J.; Hu, L.; Cheng, J.; Fang, D.; Wang, C.; Yu, K.; Jiang, H.; Cui, Q.; Xu, Y.; Luo, C. A Computational Investigation on the Substrate Preference of Ten-Eleven-Translocation 2 (TET2). *Phys. Chem. Chem. Phys.* 2016, 18 (6), 4728–4738.

(29) Ko, M.; An, J.; Pastor, W. A.; Koralov, S. B.; Rajewsky, K.; Rao, A. TET Proteins and 5-Methylcytosine Oxidation in Hematological Cancers. *Immunol. Rev.* 2015, 263 (1), 6–21.

(30) Huang, Y.; Rao, A. Connections between TET Proteins and Aberrant DNA Modification in Cancer. *Trends Genet.* 2014, 30 (10), 464–474.

(31) Ko, M.; Huang, Y.; Jankowska, A. M.; Pape, U. J.; Tahiliani, M.; Bandukwala, H. S.; An, J.; Lamperti, E. D.; Koh, K. P.; Ganetzky, R.; Liu, X. S.; Aravind, L.; Agarwal, S.; Maclejewski, J. P.; Rao, A. Impaired Hydroxylation of 5-Methylcytosine in Myeloid Cancers with Mutant TET2. *Nature* 2010, 468 (7325), 839–843.

(32) Langemeijer, S. M. C.; Kuiper, R. P.; Berends, M.; Knops, R.; Aslanyan, M. G.; Massop, M.; Stevens-Linders, E.; Van Hoogen, P.; Van Kessel, A. G.; Raymakers, R. A. P.; Kamping, E. J.; Verhoef, G. E.; Verburch, E.; Hagemeyer, A.; Vandenberghe, P.; De Witte, T.; Van Der Reijden, B. A.; Jansen, J. H. Acquired Mutations in TET2 Are Common in Myelodysplastic Syndromes. *Nat. Genet.* 2009, 41 (7), 838–842.

(33) Liu, M. Y.; Torabifard, H.; Crawford, D. J.; DeNizio, J. E.; Cao, X-J.; Garcia, B. A.; Cisneros, G. A.; Kohli, R. M. Mutations along a TET2 active site scaffold stall oxidation at 5-hydroxymethylcytosine. *Nat. Chem. Biol.* 2017, 13(2), 181-187.

(34) Fiser, A.; Šali, A. Modeller: Generation and Refinement of Homology-Based Protein Structure Models. *Methods Enzymol.* 2003, 374, 461–491.

(35) Olsson, M. H.; Sondergaard, C. R.; Rostkowski, M.; Jensen, J. H. PROPKA3: Consistent treatment of internal and surface residues in empirical pKa predictions. *J. Chem. Theory. Comput.* 2011, 7(2), 525-537.

(36) Li, P.; Merz, K. M. MCPB.Py: A Python Based Metal Center Parameter Builder. *J. Chem. Inf. Model.* 2016, 56 (4), 599–604.

- (37) Seminario, J. M. Calculation of Intramolecular Force Fields from Second-Derivative Tensors. *Int. J. Quantum Chem.* 1996, 60(7), 1271-1277.
- (38) Peters, M. B.; Yang, Y.; Wang, B.; Füsti-Molnár, L.; Weaver, M. N.; Merz, K. M. Structural Survey of Zinc-Containing Proteins and Development of the Zinc AMBER Force Field (ZAFF). *J. Chem. Theory Comput.* 2010, 6 (9), 2935–2947.
- (39) Wang, J.; Wang, W.; Kollman, P. A.; Case, D. A. Automatic Atom Type and Bond Type Perception in Molecular Mechanical Calculations. *J. Mol. Graph. Model.* 2006, 25 (2), 247–260.
- (40) Jorgensen, W. L.; Chandrasekhar, J.; Madura, J. D.; Impey, R. W.; Klein, M. L. Comparison of Simple Potential Functions for Simulating Liquid Water. *J. Chem. Phys.* 1983, 79 (2), 926–935.
- (41) Chaturvedi, S. S.; Ramanan, R.; Waheed, S. O.; Ainsley, J.; Evison, M.; Ames, J. M.; Schofield, C. J.; Karabencheva-Christova, T. G.; Christov, C. Z. Conformational Dynamics Underlies Different Functions of Human KDM7 Histone Demethylases. *Chem. - A Eur. J.* 2019, 25 (21), 5422–5426.
- (42) Bian, K.; Lenz, S. A. P.; Tang, Q.; Chen, F.; Qi, R.; Jost, M.; Drennan, C. L.; Essigmann, J. M.; Wetmore, S. D.; Li, D. DNA repair enzymes ALKBH2, ALKBH3, and AlkB oxidize 5-methylcytosine to 5-hydroxymethylcytosine, 5-formylcytosine and 5-carboxylcytosine in vitro. *Nucleic Acids Research* 2019, 47(11), 5522-5529.
- (43) Pabis, A.; Geronimo, I.; York, D. M.; Paneth, P. Molecular Dynamics Simulation of Nitrobenzene Dioxygenase Using AMBER Force Field. *J. Chem. Theory Comput.* 2014, 10 (6), 2246–2254.
- (44) Davidchack, R. L.; Ouldridge, T. E.; Tretyakov, M. V. New Langevin and Gradient Thermostats for Rigid Body Dynamics. *J. Chem. Phys.* 2015, 142 (14), 144114.
- (45) Bresme, F. Equilibrium and Nonequilibrium Molecular-Dynamics Simulations of the Central Force Model of Water. *J. Chem. Phys.* 2001, 115 (16), 7564–7574.
- (46) Ryckaert, J.-P.; Ciccotti, G.; Berendsen, H. J. Numerical Integration of the Cartesian Equations of Motion of a System with Constraints: Molecular Dynamics of n-Alkanes. *J. Comput. Phys.* 1977, 23 (3), 327–341.
- (47) Götz, A. W.; Williamson, M. J.; Xu, D.; Poole, D.; Le Grand, S.; Walker, R. C. Routine Microsecond Molecular Dynamics Simulations with AMBER on GPUs. 1. Generalized Born. *J. Chem. Theory Comput.* 2012, 8 (5), 1542–1555.
- (48) Case, D.A.; Betz, R.M.; Curetti, D.S.; Cheatham, T.E.; Daeden, T.A.; Duke, R.E.; Giese, T.J.; Gohlke, H.; Goetz, A.W.; Homeyer, N.; Izadi, S.; Janowski, P.; Kaus, J.; Kovalenko, A.; Lee, T.S.; LeGrand, S.; Li, P.; Lin, C.; Luchko, T.; Luo, R.; Madej, B., P. A. AMBER 2018. University of California: San Francisco; 2018.
- (49) Maier, J. A.; Martinez, C.; Kasavajhala, K.; Wickstrom, L.; Hauser, K. E.; Simmerling, C. Ff14SB: Improving the Accuracy of Protein Side Chain and Backbone Parameters from Ff99SB. *J. Chem. Theory Comput.* 2015, 11 (8), 3696–3713.
- (50) Deserno, M.; Holm, C. How to Mesh up Ewald Sums. I. a Theoretical and Numerical Comparison of Various Particle Mesh Routines. *Journal of Chemical Physics.* 1998, 109(18), 7678–7693.

- (51) Roe, D. R.; Cheatham, T. E. PTRAJ and CPPTRAJ: Software for Processing and Analysis of Molecular Dynamics Trajectory Data. *J. Chem. Theory Comput.* 2013, 9 (7), 3084–3095.
- (52) Grant, B. J.; Rodrigues, A. P. C.; ElSawy, K. M.; McCammon, J. A.; Caves, L. S. D. Bio3d: An R Package for the Comparative Analysis of Protein Structures. *Bioinformatics* 2006, 22 (21), 2695–2696.
- (53) Miller, B. R.; McGee, T. D.; Swails, J. M.; Homeyer, N.; Gohlke, H.; Roitberg, A. E. MMPBSA.Py: An Efficient Program for End-State Free Energy Calculations. *J. Chem. Theory Comput.* 2012, 8 (9), 3314–3321.
- (54) Sherwood, P.; De Vries, A. H.; Guest, M. F.; Schreckenbach, G.; Catlow, C. R. A.; French, S. A.; Sokol, A. A.; Bromley, S. T.; Thiel, W.; Turner, A. J.; Billeter, S.; Terstegen, F.; Thiel, S.; Kendrick, J.; Rogers, S. C.; Casci, J.; Watson, M.; King, F.; Karlsen, E.; Sjøvoll, M.; Fahmi, A.; Schäfer, A.; Lennartz, C. QUASI: A General Purpose Implementation of the QM/MM Approach and Its Application to Problems in Catalysis. *J. Mol. Struct. THEOCHEM* 2003, 632, 1–28.
- (55) Ahlrichs, R.; Bär, M.; Häser, M.; Horn, H.; Kölmel, C. Electronic Structure Calculations on Workstation Computers: The Program System Turbomole. *Chem. Phys. Lett.* 1989, 162 (3), 165–169.
- (56) Smith, W.; Forester, T. R. DL\_POLY\_2.0: A General-Purpose Parallel Molecular Dynamics Simulation Package. *J. Mol. Graphics.* 1996, 14(3), 136-141.
- (57) Kästner, J.; Carr, J. M.; Keal, T. W.; Thiel, W.; Wander, A.; Sherwood, P. DL-FIND: An Open-Source Geometry Optimizer for Atomistic Simulations. *J. Phys. Chem. A* 2009, 113 (43), 11856–11865.
- (58) Billeter, S. R.; Turner, A. J.; Thiel, W. Linear Scaling Geometry Optimisation and Transition State Search in Hybrid Delocalised Internal Coordinates. *Phys. Chem. Chem. Phys.* 2000, 2 (10), 2177–2186.
- (59) Stuyver, T.; Huang, J.; Mallick, D.; Danovich, D.; Shaik, S. TITAN: A Code for Modeling and Generating Electric Fields-Features and Applications to Enzymatic Reactivity. *J. Comput. Chem.* 2020, 41, 74-82.
- (60) Laconsay, C. J.; Tsui, K. Y.; Tantillo, D. J. Tipping the balance: theoretical interrogation of divergent extended heterolytic environment. *Chem. Sci.* 2020, 11, 2231-2242.
- (61) Dubey, K. D.; Stuyver, T.; Kalita, S.; Shaik, S. Solvent Organization and Rate Regulation of a Menshutkin Reaction by Oriented External Electric Fields are Revealed by Combined MD and QM/MM Calculations. *J. Am. Chem. Soc.* 2020, 142(22), 9955-9965.
- (62) Balsera, M. A.; Wriggers, W.; Oono, Y.; Schulten, K. Principal Component Analysis and Long Time Protein Dynamics. *J. Phys. Chem.* 1996, 100, 2567-2572.
- (63) (a) Hünenberger, P. H.; Mark, A. E.; Van Gunsteren, W. F. Fluctuation and Cross-Correlation Analysis of Protein Motions Observed in Nanosecond Molecular Dynamics Simulations. *J. Mol. Biol.* 1995, 252, 492-503. (b) Arnold, A. E.; Ornstein, R. L. Molecular Dynamics Study of Time-Correlated Protein Domain Motions and Molecular Flexibility: Cytochrome P450BM-3. *Biophys J.* 1997, 73, 1147-1159. (c) Tang, Q.; Kaneko, K. Long-range correlation in protein dynamics: Confirmation by structural data and normal mode analysis. *PLoS Comput. Biol.* 2020, 16(2), e1007670.

- (64) Chaturvedi, S. S.; Ramanan, R.; Waheed, S. O.; Karabencheva-Christova, T. G.; Christov, C. Z. Structure-function relationships in KDM7 histone demethylases. *Adv. Protein Chem. Strut. Biol.* 2019, 117, 113-125.
- (65) Chaturvedi, S. S.; Ramanan, R.; Lehnert, N.; Schofield, C. J.; Karabencheva-Christova, T. G.; Christov, C. Z. Catalysis by the Non-Heme Iron(II) Histone Demethylase PHF8 Involves Iron Center Rearrangement and Conformational Modulation of Substrate Orientation. *ACS Catal.* 2020, 10 (2), 1195–1209.
- (66) (a) Ghafoor, S.; Mansha, A.; de Visser, S. P. Selective Hydrogen Atom Abstraction from Dihydroflavonol by a Non-heme Iron Center is the Key Step in the Enzymatic Flavonol Synthesis and Avoids Byproducts. *J. Am. Chem. Soc.* 2019, 141, 20278-20292. (b) Yan, L.; Liu, Y. Insights into the Mechanism and Enantioselectivity in the Biosynthesis of Ergot Alkaloid Cycloclavine Catalyzed by Aj\_EasH from *Aspergillus japonicus*. *Inorg. Chem.* 2019, 58, 13771-13781. (c) Bai, J.; Yan, L.; Liu, Y. Catalytic mechanism of the PrhA (V150L/A232S) double mutant involved in the fungal meroterpenoid biosynthetic pathway: a QM/MM Study. *Phys. Chem. Chem. Phys.* 2019, 21, 25658-25668. (d) Su, H.; Sheng, X.; Zhu, W.; Ma, G.; Liu, Y. Mechanistic Insights into the Decoupling Desaturation and Epoxidation Catalyzed by Dioxygenase AsqJ involved in the Biosynthesis of Quinolone Alkaloids. *ACS Catal.* 2017, 7, 5534-5543. (e) Ma, G.; Zhu, W.; Su, H.; Cheng, N.; Liu, Y. Uncoupling Epimerization and Desaturation by Carbapenem Synthase: Mechanistic Insights from QM/MM Studies. *ACS Catal.* 2015, 5, 5556-5566.
- (67) Song, X.; Lu, J.; Lai, W. Mechanistic Insights into Dioxygen Activation, Oxygen Atom Exchange and Substrate Epoxidation by AsqJ Dioxygenase from Quantum Mechanical/Molecular Mechanical Calculations. *Phys. Chem. Chem. Phys.* 2017, 19 (30), 20188–20197.
- (68) Krebs, C.; Fujimori, D. G.; Walsh, C. T.; Bollinger, J. M. Non-Heme Fe(IV)-Oxo Intermediates. *Acc. Chem. Res.* 2007, 40, 484–492.
- (69) Solomon, E. I. Geometric and Electronic Structure Contributions to Function in Bioinorganic Chemistry: Active Sites in Non-Heme Iron Enzymes. *Inorg. Chem.* 2001, 40(15), 3656-3669.
- (70) Solomon, E. I.; Light, K. M.; Liu, L. V.; Srnec, M.; Wong, S. D. Geometric and Electronic Structure Contributions to Function in Non-Heme Iron Enzymes. *Acc. Chem. Res.* 2013, 46 (11), 2725–2739.
- (71) Logunov, I.; Schulten, K. Quantum chemistry: Molecular dynamics study of the dark-adaptation process in bacteriorhodopsin. *J. Am. Chem. Soc.* 1996, 118(40), 9727-9735.
- (72) Álvarez-Barcia, S.; Kästner, J. Atom Tunneling in the Hydroxylation Process of Taurine/ $\alpha$ -Ketoglutarate Dioxygenase Identified by Quantum Mechanics/Molecular Mechanics Simulations. *J. Phys. Chem. B* 2017, 121 (21), 5347–5354.
- (73) Meir, R.; Chen, H.; Lai, W.; Shaik, S. Oriented Electric Fields Accelerate Diels-Alder Reactions and Control the endo/exo Selectivity. *ChemPhysChem*, 2010, 11, 301-310.
- (74) Jonasson, N. S. W.; Daumann, L. J. 5-Methylcytosine Is Oxidized to the Natural Metabolites of TET Enzymes by a Biomimetic Iron(IV)-Oxo Complex. *Chem. - A Eur. J.* 2019, 25 (52), 12091–12097.

(75) Koski, M. K.; Hieta, R.; Bollner, C.; Kivirikko, K. I.; Myllyharju, J.; Wierenga, R. K. The Active Site of an Algal Prolyl 4-Hydroxylase Has a Large Structural Plasticity. *J. Biol. Chem.* 2007, 282, 37112-37123.



## 5 How Human TET2 Enzyme Catalyzes the Oxidation of Unnatural Cytosine Modifications in Double-Stranded DNA

Sodiq O. Waheed,<sup>&</sup> Ann Varghese,<sup>&</sup> Shobhit S. Chaturvedi,<sup>&</sup> Tatyana G. Karabancheva-Christova,<sup>&#</sup> and Christo Z. Christov<sup>&#</sup>

<sup>&</sup>Department of Chemistry, Michigan Technological University, Houghton, Michigan 49931, United States.

<sup>#</sup>Corresponding co-authors: christov@mtu.edu, tatyanak@mtu.edu

---

The content of this chapter was previously published in the *ACS Catal.*, **2022**, 12, 5327-5344. DOI: 10.1021/acscatal.2c00024, reproduced with permission from the American Chemical Society.

## 5.1 Introduction

Ten-eleven translocation (TET) enzymes are important epigenetic modulators with important roles in various physiological and pathological processes, especially in embryogenesis, cell differentiation, carcinogenesis, and neural development.<sup>1-6</sup> Three mammalian family members of TET proteins have been identified, namely, TET1, TET2, and TET3.<sup>2,6,7</sup> All three TET proteins contain a similar catalytic C-terminal domain which harbors the conserved double-stranded  $\beta$ -helix (DSBH) fold and a cysteine-rich (Cys) region.<sup>1,3,4</sup> TET enzymes belong to non-heme Fe(II) and 2-oxoglutarate (2OG) dependent oxygenases that convert 5-methyl-cytosine (5mC) to 5-hydroxymethylcytosine (5hmC) and subsequently convert 5hmC into 5-formylcytosine (5fC) and 5-carboxylcytosine (5caC).<sup>3,5,7,8</sup> These oxidized 5mC bases act as intermediates in active DNA demethylation pathways, involving their conversion to unmodified cytosine via either active excision or passive replication-dependent processes.<sup>7,9,10</sup> In addition, the different oxidized intermediates exercise their own epigenetic rules.<sup>3,6,8</sup> Studies have revealed that the catalytic domains in TET enzyme preferentially bind to cytosines on CpG islands without interacting with adjacent bases.<sup>1,7</sup> TET loss-of-function is firmly associated with cancer; TET2 loss-of-function mutations are frequently observed in myelodysplastic syndromes, myeloid malignancies, and peripheral T-cell lymphomas (PTCLs), which are a heterogeneous and poorly understood group of aggressive non-Hodgkin lymphomas that are resistant to conventional therapies.<sup>1,6</sup>

The crystal structure of the human TET2-double-stranded (ds) DNA complex [Figure 5.1] reported by Hu et al. revealed that the structure contains loop 1, loop 2, GS linker, and three Zn finger regions of which two of the Zn(II) regions (Zn2 and Zn3 finger regions) bring the DSBH and the Cys-rich domains together to facilitate a compact catalytic domain formation,<sup>7</sup> unlike other Fe(II)/2OG DNA modifying enzymes, AlkB and its human homologues (AlkBH1-8, AlkBH9/FTO), which lack Zn(II) finger regions.<sup>8,11a,b</sup> Recent computational studies on TET2 and its various mutants have shown the importance of these structural elements' correlated motions on the interaction of DNA with the TET2 enzyme and the overall structural formation.<sup>12</sup>

The demethylation process in 2OG-dependent oxygenases involves the activation of dioxygen followed by substrate oxidation.<sup>8,11a,13-15a</sup> The dioxygen activation mechanism, which passes through the Fe(II)peroxysuccinate intermediate<sup>16-18</sup> starts with the binding of molecular oxygen to the Fe(II) center, leading to the formation of highly reactive Fe(IV)=O species.<sup>17,19-21</sup> Various experimental and computational studies have addressed the mechanisms of dioxygen activation by non-heme Fe(II) enzymes.<sup>18,20,21</sup> After the formation of the Fe(IV)=O intermediate, it abstracts a hydrogen atom from the substrate to generate an Fe(III)-hydroxyl intermediate which undergoes a hydroxyl rebound reaction with the substrate radical carbon to complete the hydroxylation.<sup>17,19-21</sup>

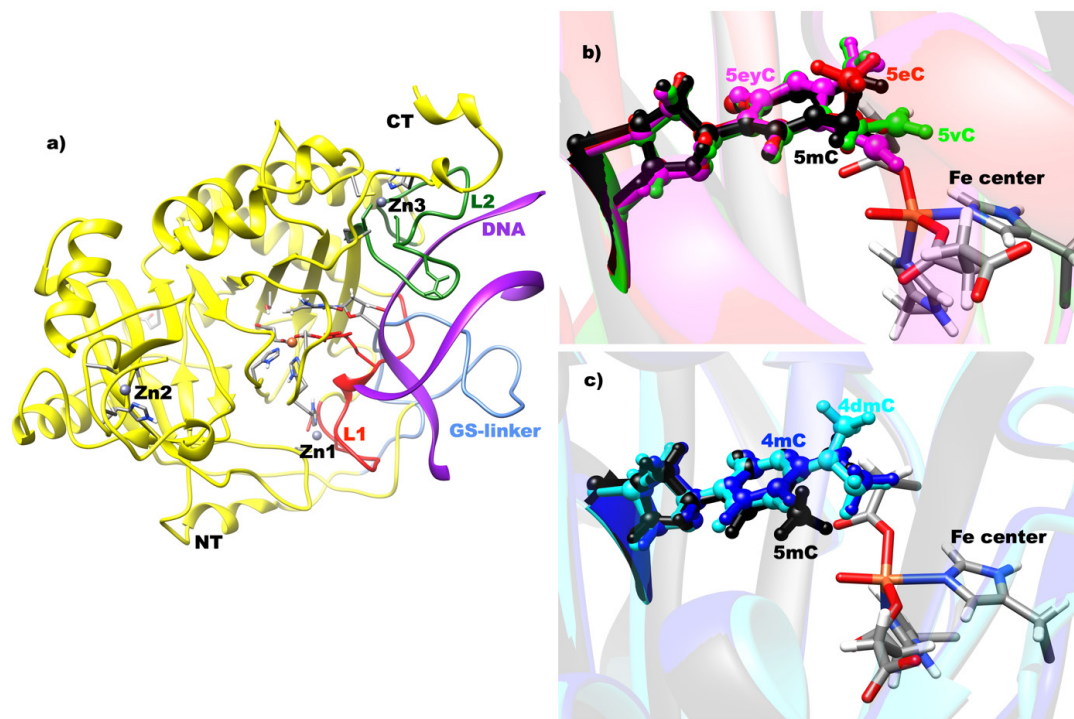


**Figure 5.1.** (a) Protein structure for the human TET2-dsDNA complex derived from the average molecular dynamics (MD) structure of ferryl intermediate simulations with the 5eC substrate. (b) Overlaid structure of the C5-alkylated 5eC, 5vC, and 5eyC unnatural substrates with the natural 5mC substrate. (c) Overlaid structure of the N4-methylated 4mC, 4dmC substrates with the natural C5-methylated 5mC substrate. In both (b) and (c), the Fe center depicts the one of 5mC dsDNA-bound TET2.

A recent work by Islam and co-workers has reported that TET2 can oxidize 5-ethylcytosine (5eC) to 5-hydroxyethylcytosine (5heC) in a site- and degree-specific manner to offer the mono-hydroxylated product via benzylic C—H activation.<sup>22</sup> The study revealed that C—H hydroxylation in both the natural 5mC substrate and the unnatural 5eC showed comparable activity, and further oxidation of 5heC was nearly undetectable, implying that 5heC cannot undergo successive oxidations as in 5hmC generated after the first oxidation of the 5mC natural substrate of TET2.<sup>22</sup> The hydroxylated product of 5eC acts as a docking site for the protein implicated in transcription and has the potential to control chromatin-dependent processes.<sup>22</sup>

Another study by Kohli and co-workers has demonstrated that TET enzymes can also hydroxylate unnatural nucleobases at the 5-position on the cytosine base, 5-vinylcytosine (5vC), and 5-ethynylcytosine (5eyC) aside from 5mC in DNA in a similar manner as another Fe(II) and 2OG dependent dioxygenase,<sup>9</sup> thymine hydroxylase, which acts on the free thymine nucleobase.<sup>23,24</sup> TET catalyzes the oxidation of 5vC to produce 5-formylmethylcytosine (5fmC) as the major product of the reaction. In contrast to 5vC, the 5eyC DNA substrate serves as an alternative probe, functioning as an activity-based cross-linker of TET enzymes.<sup>9,25</sup> Oxidation of the 5eyC substrate by TET produces a high-energy ketene intermediate, which reacts and forms a covalent cross-link with the TET enzyme. These unnatural substrates have been reported to be used to detect and quantify the TET activity either in vitro or in cell extracts.<sup>9,25</sup>

TET enzymes are different from other DNA repair enzymes because the alkyl group to be oxidized is not linked to a heteroatom,<sup>7,8,10</sup> but the C5-position carbon of the cytosine base. However, the latest studies by Kohli and co-workers show that TET enzymes are also proficient as direct N-demethylases of the cytosine bases in a similar manner as the AlkB-type of other DNA demethylases. They reported that N-demethylase activity can be observed on substrates that lack a 5-methyl group, and as such, TET enzymes can be similarly proficient in either oxidation of 5mC or demethylation of 4-methylcytosine (4mC) and 4,4-dimethylcytosine (4dmC) substrates, which have potential biological and mechanistic implications.<sup>10</sup>

Although the experimental studies discovered the catalytic promiscuity of TET2 with unnatural substrates, knowledge about the respective catalytic mechanisms and the potential differences from the natural 5mC substrates is still missing. To complete the missing information, we performed molecular dynamics (MD) simulations and combined quantum mechanics and molecular mechanics (QM/MM) studies on the catalytic mechanisms of TET2 with these new substrates. Also, the accommodation of these substrates with unnatural alkylations in the active site of TET2 bound to dsDNA would involve conformational changes; it is important to explore how these changes influence the active site and second sphere residues interactions, long-range correlated motions in the TET2 enzyme. Hence, this current study aims at completing this missing knowledge in comparison to our previously reported study on the 5mC natural substrate of the TET2 enzyme.<sup>12</sup> Furthermore, the study aims to explore the mechanisms of the post-hydroxylation reactions for 5vC and 5eyC that are currently missing as well if these

reactions take place within the enzyme environment or in the water solvent. In addition, this work aims to reveal that the role of the second coordination sphere (SCS) and long-range correlated motions in the catalysis of TET2 with unnatural substrates might be important; however, it is completely unexplored. The study also delineates the role of the SCS residues in stabilizing the TSs with respect to the RCs in the catalyzed reactions.

## 5.2 Computational Methods

### 5.2.1 System Setup

The initial structure was obtained from the X-ray crystal structure of human TET2-DNA (PDB code, 4NM6, in complex with the 5-methylcytosine (5mC) substrate)<sup>7</sup> and the missing residues were added using Modeller.<sup>26</sup> The N-oxalylglycine (NOG) used for crystallization was converted to 2OG, and the methyl group of the 5mC substrate was modified to ethyl, vinyl, and ethynyl groups to give the unnatural 5eC, 5vC, and 5eyC substrates, respectively, using GaussView 6.0. However, in 4mC and 4dmC substrates, the methyl group at position 5 of the cytosine in 5mC was removed, and the hydrogen atoms at the exocyclic N4 position were replaced with one and two methyl groups to give the 4mC and 4dmC substrates, respectively. The protonation state of the ionizable side chain was estimated using Propka,<sup>27</sup> while the Fe-ligating histidine residues were assigned the protonation state based on visual inspection of their local environment. The Fe(IV) ion is coordinated by a monodentate succinate, two histidine residues (His1382 and His1881), and one aspartate residue (Asp1384). The missing hydrogen atoms in the crystal structure were added to the protein followed by neutralization with Na<sup>+</sup> counterions using the Leap

module in Amber18.<sup>28</sup> The parameters for the non-standard residues/ligands, succinate, 5eC, 5vC, 5eyC, 4mC, and 4dmC substrates were generated using Antechamber<sup>29</sup> as implemented in Amber package. To generate the Fe(IV)=O intermediate metal center parameter, we used the Metal Center Parameter Builder (MCPB.py)<sup>30</sup> module in Amber as used in various studies.<sup>11b,15b,31,32</sup> The high spin quintet state of Fe was assigned to the ground state as various studies have shown the preference of non-heme Fe(II) and 2OG oxygenases for this spin state.<sup>11b,33-35</sup> The 4-coordinated zinc metal centers and the coordinating residues in the Zn finger regions were described using Amber's Zinc Amber force field (ZAFF) method.<sup>36</sup> The systems were surrounded by a rectangular box solvated with TIP3P water molecules<sup>37</sup> within 10 Å from the protein's surface.

## 5.2.2 MD Simulations

After the initial setup, the systems were minimized in two steps to remove the bad contacts. In the first step, only the solvent molecules and Na<sup>+</sup> counterions were minimized with the solute molecules restrained with harmonic potential of 500 kcal/mol/Å<sup>2</sup> while in the second stage of minimization, all of the systems were geometrically minimized without any constraints. The minimizations were performed using 5000 steps of steepest descent followed by 5000 steps of conjugate gradient minimizer. The CPU version of the Amber18 code (SANDER) was used for the energy minimization. The systems were gently annealed by gradually increasing the temperature from 0 to 300 K in an NVT ensemble for 50 ps using a Langevin thermostat.<sup>38</sup> Subsequently, density equilibration was done at a constant temperature of 300 K for 1 ns in an NPT ensemble. The solute molecules were restrained



with a weak restraint of 10 kcal/mol/ Å<sup>2</sup>. Thereafter, all of the restraints were removed, and the systems were further equilibrated for 3 ns in an NPT ensemble at a fixed temperature and pressure of 300 K and 1 bar, respectively. Production MD runs were performed for 1000 ns in an NPT ensemble with the target pressure set at 1 bar and a constant pressure coupling of 2 ps. The pressure was held constant using the Berendsen barostat,<sup>39</sup> and the covalent bonds that contain hydrogens were constrained using the SHAKE algorithm.<sup>40</sup> Long-range electrostatic interactions were treated using the Particle Mesh Ewald (PME) method<sup>41</sup> with a vdW cutoff of 10 Å. The GPU version of the PMEMD engine integrated with Amber18<sup>42</sup> was used for the productive MD simulations. The FF14SB<sup>43</sup> force field was used in all of the simulations, and the periodic boundary conditions were also used in all of the simulations. The obtained trajectories were analyzed using the cpptraj module<sup>44</sup> in Ambertools utilities, and the dynamic cross-correlation analysis was done with Bio3D.<sup>45</sup>

### 5.2.3 QM/MM Calculations

The reaction mechanism was performed using combined QM/MM methods. The QM region included the Fe, oxygen atom of the ferryl, the side chain of Asp1384, the imidazole groups of the Fe-ligating His1382 and His1881 residues, succinate, and the alkylated bases of the substrates (5-ethylcytosine, 5-vinylcytosine, 5-ethynylcytosine, 4-methylcytosine, and 4,4-dimethylcytosine parts of 5eC, 5vC, 5eyC, 4mC, and 4dmC substrates, respectively). The ChemShell suite<sup>46</sup> of programs was used for the QM/MM calculations. The QM calculations were performed with Turbomole<sup>47</sup> and the MM calculations with DL\_POLY<sup>48</sup> software. The MM region was described using the Amber ff14SB force

field,<sup>43</sup> and the electronic embedding scheme<sup>49</sup> was used to describe the interaction between the QM and MM regions. The QM/MM boundary was treated using hydrogen link atoms. The B3LYP functional with def2-SVP basis set was used for all geometry optimizations as in previous studies.<sup>14,17</sup> Afterward, a relaxed potential energy scan was performed along the reaction coordinate with 0.1 Å increment to locate the transition states. The DL-find optimizer<sup>50</sup> implemented in ChemShell was used for reactant optimization and scanning while the transition states were reoptimized using the partitioned rational function optimization (P-RFO) algorithm in the HDLC code.<sup>51</sup> The local minimum and the first-order saddle points were verified with frequency calculations. The energies of optimized stationary points were recalculated via single point calculation using def2-TZVP basis set (labeled BS) for all of the atoms. Grimme's D3 dispersion correction<sup>52</sup> was applied in single-point calculations. Energy decomposition analysis (EDA) calculations were then performed on the optimized stationary point geometries using the method developed by Cisneros and co-workers<sup>53-55</sup> to determine the energetic contributions of the individual residues.

## 5.3 Results and Discussion

### 5.3.1 Structure and Dynamics of the ES Complex for Substrate Oxidation (Fe(IV)=O of Human TET2 with dsDNA Containing Different Alkylated Substituted Bases: 5eC, 5vC, and 5eyC)

The Fe(IV)=O intermediate is the reactive oxidizing complex that performs the oxidation of alkylated substrates in 2OG oxygenases;<sup>8,11a,15a,b,56</sup> hence we performed MD simulation of 1  $\mu$ s on the ferryl complexes of TET2 bound to 5eC, 5vC and 5eyC alkylated dsDNA substrates, enabling us to gain insight into the conformational dynamics of the complexes. Figure D1 shows the root mean square deviations (RMSDs) of the protein-DNA complexes of the systems. The RMSD profiles show the stability of the complexes during simulations. Furthermore, the O-C distance and Fe-O-C angle, which are crucial for efficient substrate oxidation<sup>57a,58</sup> show average values between 3.43 to 4.67 Å and 115.89 to 140.48°, respectively [Figures D2 and D3]. Analyses of the primary coordination sphere show that the Fe(IV) center is stabilized by several interactions. For example, the backbones of the Fe-coordinating histidines (His1382 and His1881) are stabilized via hydrogen bonding interactions with each other [Figure D4] similarly as TET2 bound to the natural 5mC substrate. In 5mC substrate complex, we observed that the non-coordinating oxygen of the aspartate ligand is stabilized by a solvent-mediated hydrogen bonding interaction with Asn1387 (in 74.7% of the trajectories).<sup>12</sup> However, in 5eC substrate complex, the interaction weakens and reduces to 10.2%, likely due to steric effects arising from the variations in the size of the alkyl substituents. The stabilization of the non-coordinating

oxygen of Fe-coordinating Asp or Glu residues is a common feature in 2OG enzymes.<sup>8,57b</sup> For example, in AlkB and AlkBH2, an Arg residue forms direct hydrogen bonding interactions with the non-coordinating oxygen of the Fe-coordinating carboxylate residue while in histone JmjC demethylases, KDM4A/E and KDM7B, Asn is employed.<sup>15b,17,18</sup> The networks of hydrogen bonding interactions [Figure D4] of iron coordinating His1382, Asp1384, and His1881 residues with the backbones of His1380, Ala1876, and Glu1879, respectively, in 5eC substrate are preserved as in the natural substrate, enhancing the stability of the Fe center (Table D1). The non-coordinating carboxylate part of the succinate is also stabilized via hydrogen bonding interactions with Arg1896 (70.8%) and Ser1898 (84.4%) like in 5mC substrate.<sup>12</sup> The heteroaromatic cytosine ring of the substrates are stabilized by  $\pi$ -stacking interactions with Tyr1902, which is conserved during the simulations in both 5mC and 5eC substrates [Figure D5] and thereby aid the orientation of the substrate in the active site. The substrates' exocyclic amine (N4) in both complexes are stabilized by hydrogen bonding interactions with Asn1387. These interactions are very stable in both complexes, especially during the last 500 ns of the simulation [Figure D6]. The stable hydrophobic interactions [Figure D7] between the methylene group of the ethyl substituent in the 5eC substrate and methylene C2 of the Fe-coordinated succinate and Val1900 likely help in the proper orientation of the reactant complex.

The principal component analysis (PCA) [Figure 5.2a], which shows the flexible parts of the protein, and the direction of motions<sup>59,60a</sup> reveal major motions in the GS-linker and loop 2 (L2) regions in TET2-dsDNA-5eC, unlike in 5mC<sup>12</sup> where in addition to those two

motions, the cysteine-rich N-terminal (Cys-N) region and the DNA also experienced some motions. The GS-linker and L2 in TET2-dsDNA-5eC complex move towards the solvents; in contrast to TET2-dsDNA-5mC complex, the same regions move towards the binding surface to aid better binding of the protein to DNA. Also, the observed motions in the DNA and Cys-N regions, which move toward the protein, help in the compaction of the protein-DNA complex in TET2-dsDNA with 5mC dsDNA substrate. These observed differences might be related to the pressure on the enzyme exercised by the unnatural 5eC substrate.

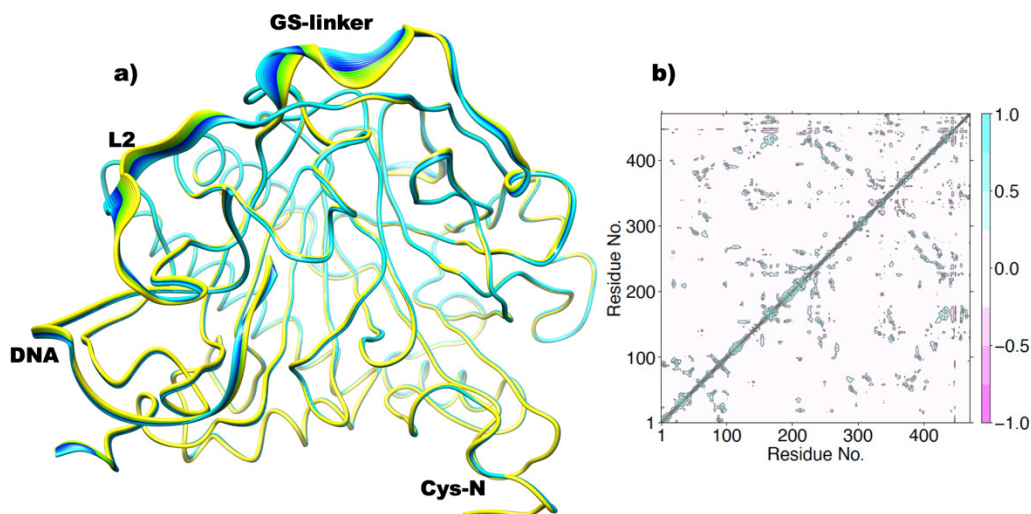


**Figure 5.2.** Principal component analysis (a) and dynamic cross correlation (b) of the ferryl complex of TET2 bound to 5eC dsDNA substrate. Residues numbers are as follows: 1-445 (TET protein), 446-448 (Zn), 449 (Fe), 450 (O), 451 (succinate), and 452-475 (DNA). In part (b), residues numbers range 6-17, 157-181, 332-363, and 452-472 on both axes denote the Cys-N, L2, GS-linker, and DNA, respectively. Yellow to blue represents the direction of motion of residues in part (a).

In addition, the distance between the center of mass of the protein and that of the DNA [Figure D8] reveals average values of 22.3 and 27.1 Å for TET2-dsDNA-5mC and TET2-dsDNA-5eC complexes, respectively, indicating that the former complex is more structurally compact than the latter. The observed motions in TET2-dsDNA-5eC complex likely explain the observed expansion of the protein-DNA complex.

The dynamic cross-correlation analysis (DCCA) [Figure 5.2b] demonstrates that several correlated motions are similar to the TET2 complexed with the natural 5mC substrate. For example, the positively correlated motion of GS linker and L2 with L1, DNA, DSBH core antiparallel  $\beta 7$  and  $\beta 17$ , and Zn3 site are also preserved in TET2 bound to 5eC substrate. However, the characteristic correlated motions between L2 and the Fe-coordinating HxD motif loop observed in TET2 with the natural substrate disappear.<sup>12</sup> The long-range correlated motions observed in TET2-dsDNA-5eC complex might assist in the interaction and binding of DNA to the TET2 protein, thereby enhancing the overall structural formation and stability via long-range interactions.

### **5.3.2 Dynamics of Fe(IV)=O species of TET2 bound to N4 methylated 4mC and 4dmC dsDNA substrates**

The dynamics of the TET2 bound to 4mC and 4dmC substrates reveal similar interactions in the active center as well as in the second sphere region with the details presented in the SI (section 1). In TET2-dsDNA-4dmC complex, the PCA [Figure 5.3b] show motions in the GS-linker, cys-rich N-terminal (Cys-N), and GS-linker supporting  $\beta 12$  and  $\beta 13$ , while

in TET2-dsDNA-4mC [Figure 5.3a], the cys-rich N-terminal (Cys-N),  $\beta$ 12 and  $\beta$ 13 regions become rigid with new motions in the DNA and loop 2 (L2) regions. These observed motions differ from TET2 bound to natural 5mC substrate, which reveals motion in three different regions (i.e., GS-linker, DNA, and Cys-N). In TET2-dsDNA-4dmC, the Cys-N moves towards the loop containing the binding residues from the Zn1 finger region.  $\beta$ 12 and  $\beta$ 13 sheets, which support the GS-linker, move towards Zn2 finger binding residues. These motions aid in stabilizing the first two Zn finger regions via long-range interactions, which in turn assist in the overall structural stability of the protein-DNA complex. However, in TET2-dsDNA-4mC, the GS-linker region moves toward  $\beta$ 12 to enhance its stability while L2 and DNA move in parallel and potentially weaken the interactions between the L2 and the DNA. The DCCA of TET2-dsDNA-4dmC [Figure D9] confirms that the Cys-N region has a positive correlation with the Zn1 finger region and its coordinating residues while the GS-linker has a positive correlation with L1, L2, DNA,  $\beta$ 6 and  $\beta$ 7 elements of DSBH core, supporting the experimental data on the importance of the linker in DNA binding. The antiparallel  $\beta$ 12 and  $\beta$ 13 regions that support the GS-linker positively correlate with each other, thus increasing the linker stability.

However, in TET2-dsDNA-4mC complex [Figure D10], the L2 positively correlates with the Zn3 finger region and its coordinating residues, DNA, and the iron-coordinating HxD loop, while the GS-linker shows a positive correlation with DNA, L1 and  $\beta$ 12. DNA shows a positive correlation with L1, L2, GS linker,  $\beta$ 16 and  $\beta$ 17 of DSBH core, Fe-coordinating His1382, Asp1384, and loop containing the HxD residues. Overall, the long-range

correlated motions in both complexes might aid in DNA recognition and binding to TET2 and specifically in the overall structural stability of the ES complex.

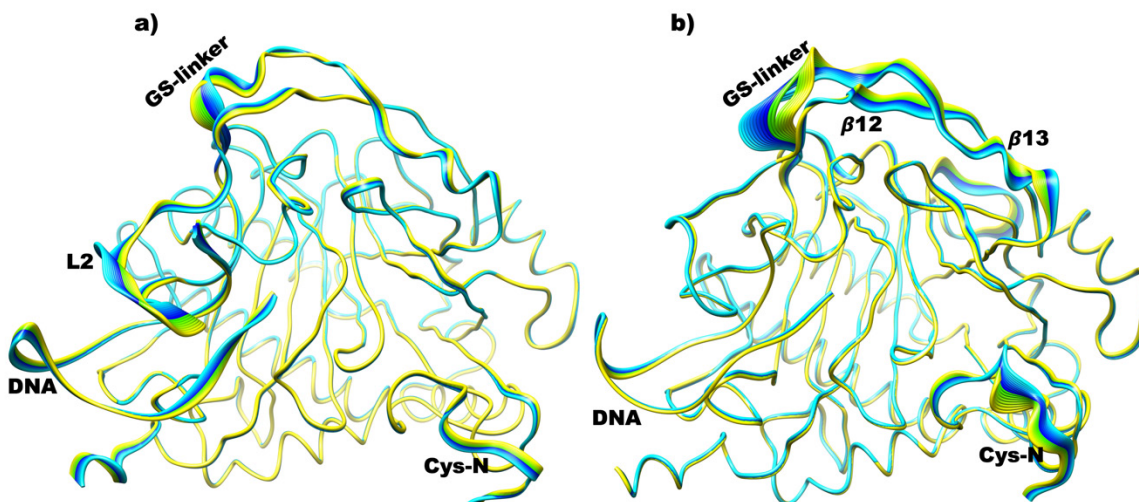


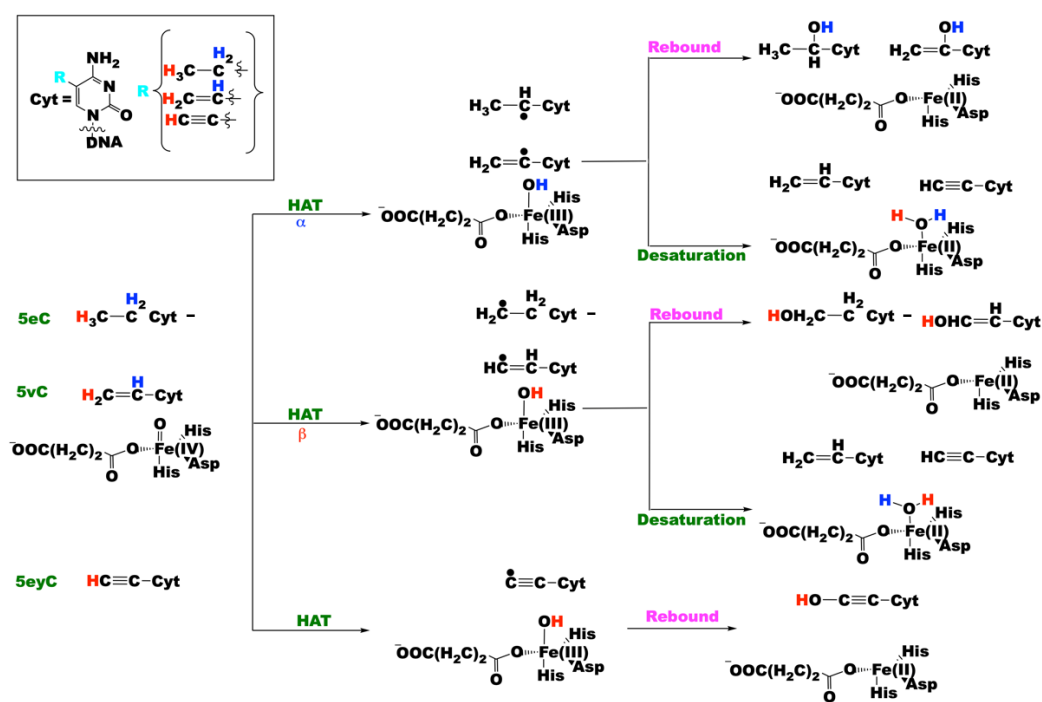
**Figure 5.3.** Principal component analysis of the ferryl complex of TET2 bound to 4mC dsDNA (a) and 4dmC (b) substrates. Residues numbers are as follows: 1-445 (TET protein), 446-448 (Zn), 449 (Fe), 450 (O), 451 (succinate), and 452-475 (DNA). Yellow to blue represents the direction of motion of residues.

### 5.3.3 Reactions Mechanisms of TET2 with dsDNA containing 5eC, 5vC, and 5eyC

To understand the mechanisms of 5eC, 5vC, and 5eyC dsDNA substrates oxidation by the highly electrophilic Fe(IV)=O intermediate of human TET2, we performed computational studies using combined QM/MM methods as depicted in scheme 5.1. The substrates oxidation has been proposed to occur via two stages:<sup>8,11a,19,35,61</sup> i) hydrogen atom



abstraction (HAT) and ii) rebound hydroxylation or desaturation. Due to the chemical nature of the alkyl substituents in 5eC and 5vC substrates, different alternative pathways for HAT can occur to generate the radical substrates intermediates, which either undergo rebound hydroxylation or desaturation via the second HAT to give the alcohol or desaturated products, respectively (Scheme 5.1). Previous experimental and computational studies have reported a high spin quintet state as the ground state for the ferryl species,<sup>17,18,33,34,62</sup> hence, this study was conducted at this spin state.



**Scheme 5.1.** Possible reaction mechanisms pathways explored for the oxidation of the unnatural 5eC, 5vC, and 5eyC dsDNA substrates by TET2.

### 5.3.4 Mechanism of 5eC Substrate Oxidation

#### Hydrogen Atom Abstraction

To explore the oxidation of 5eC, we first performed the HAT from the alkyl group of the lesioned DNA substrate by the highly reactive Fe(IV)=O species, leading to the Fe(III)—OH intermediate and a radical substrate. Various studies have reported HAT to be the rate-determining step in 2OG oxygenases.<sup>12,17,19,15b,35,61,62</sup> The HAT was carried out on both the CH<sub>2</sub> (C<sub>α</sub>) and CH<sub>3</sub> (C<sub>β</sub>) carbons of the lesioned substrate to determine the regioselectivity of oxidation on the ethyl group of the 5eC substrate, resulting in the formation of the Fe(III)—OH center, and a secondary radical (R—•CH—CH<sub>3</sub>) (**IM1<sub>eα</sub>**) and a primary radical substrate (R—CH<sub>2</sub>—•CH<sub>2</sub>) (**IM1<sub>eβ</sub>**), respectively. To evaluate the effect of conformational flexibility on the rate-determining HAT step, we used five (5) well-equilibrated structures from the last 500ns production MD trajectories by taking the average O—C distance and Fe—O—C angle into account, as these have been shown to determine the substrate oxidation efficiency.<sup>35,60b</sup> The calculated energy barriers at the B3LYP/def2-TZVP (BS) + ZPE level for the five (5) snapshots vary between 15.8 and 23.3 kcal/mol, and 17.4 and 25.7 kcal/mol for HAT from CH<sub>2</sub> (C<sub>α</sub>) and CH<sub>3</sub> (C<sub>β</sub>) carbons, respectively. The Boltzmann weighted average was found to be 16.7 and 18.4 kcal/mol for HAT from CH<sub>2</sub> (C<sub>α</sub>) and CH<sub>3</sub> (C<sub>β</sub>), respectively, which is in agreement with the previously reported HAT barriers for Fe(II)/2OG dependent enzymes.<sup>12,17,19,37,61</sup> The slightly higher barrier obtained in the latter likely reflects the preference for HAT from the methylene (CH<sub>2</sub>) carbon of the ethyl substituent of 5eC substrate, which is also partly confirmed from

the O—C $\alpha$  and O—C $\beta$  distances plots from the productive simulation [Figure D11]. Subsequent calculations were done using the structure that gives the lowest energy barrier for the HAT. Figures 5.4, 5.5, and D12 summarize the calculated energy profile and the stationary point geometries for the hydroxylation and desaturation reactions of 5eC dsDNA to give the alcohol and desaturated products, respectively.

Both transition states, **TS<sub>H1e $\alpha$</sub>**  and **TS<sub>H1e $\beta$</sub>**  for HAT from C $\alpha$  and C $\beta$ , respectively, have the Fe—O bond elongated from 1.62 Å to a nearly similar distance of 1.76 and 1.78 Å, respectively [Figure 5.5]. The Fe—O bond polarizes at the TS to form an efficient electron acceptor, ferric-oxyl species.<sup>34</sup> In addition, the C—H and O—H distances are 1.24 Å and 1.44 Å, respectively, in **TS<sub>H1e $\alpha$</sub>**  but are 1.24 and 1.34 Å, respectively, in **TS<sub>H1e $\beta$</sub>** . The obtained electron spin density of 4.00 and 4.05 for the Fe at **TS<sub>H1e $\alpha$</sub>**  and **TS<sub>H1e $\beta$</sub>** , respectively, confirm the ferric nature of the Fe center in both pathways at the transition states. The two transition states show a difference in the orientation of the substrate ethyl group with respect to the iron-oxo species. The Fe—O—H $\alpha$  angle in **TS<sub>H1e $\alpha$</sub>**  is 152.56° while the corresponding Fe—O—H $\beta$  angle is 143.06° in **TS<sub>H1e $\beta$</sub>** . The variation in the angles is likely due to the type of carbon where the hydrogen is to be abstracted from (i.e., CH<sub>2</sub> (C $\alpha$ ) vs CH<sub>3</sub> (C $\beta$ )), as the substrate ethyl group has to undergo changes to favor the respective HAT.

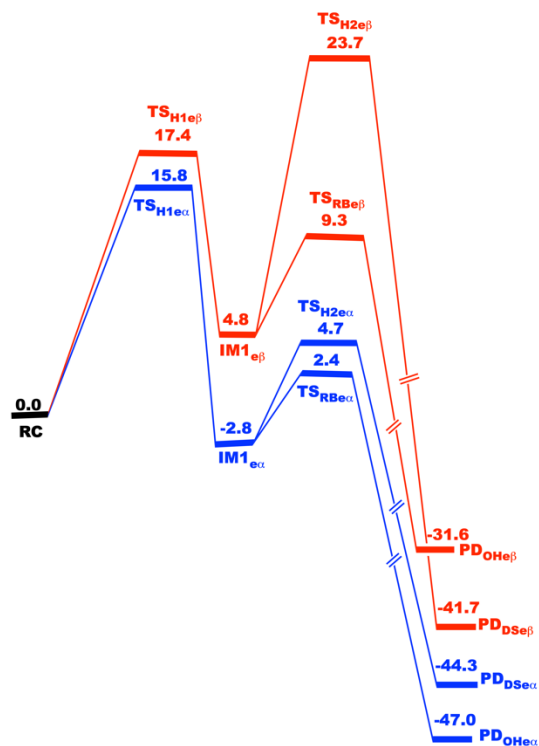


**Figure 5.4.** QM/MM potential energy profile for the hydroxylation and desaturation reactions of 5eC dsDNA substrate by TET2, calculated using UB3LYP/def2-TZVP with ZPE. The relative energies are in kcal/mol.

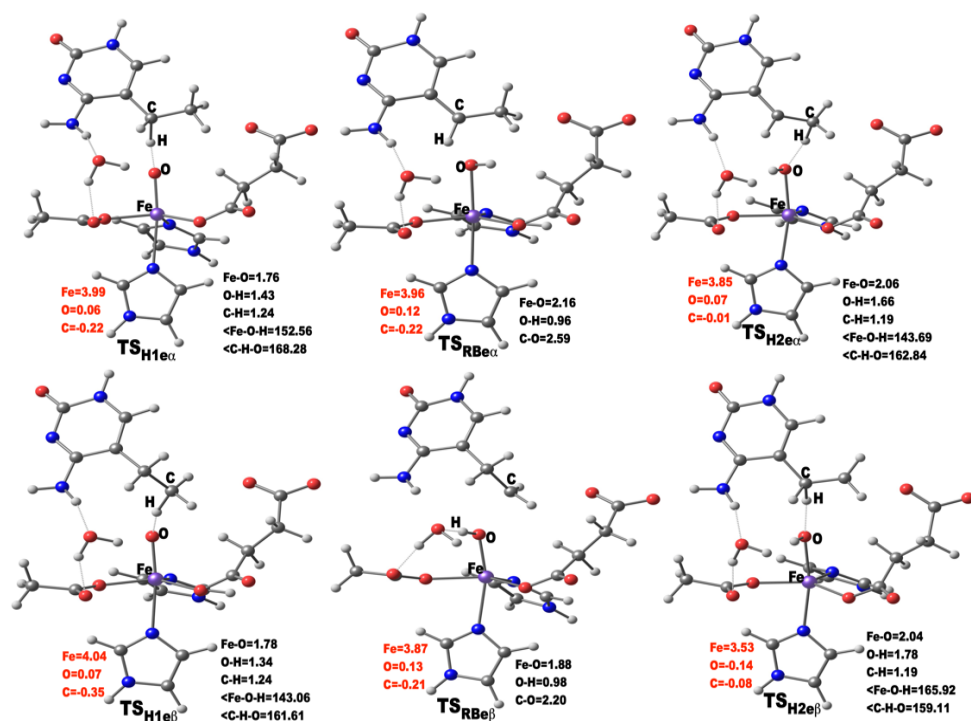


**Figure 5.5.** The transition states structures obtained during hydroxylation and desaturation processes of 5eC dsDNA by TET2. Distances (Å), the spin densities are in black and red, respectively, while the Fe—O—H and C—H—O angles are in degrees.

During the hydrogen atom abstraction, one electron from the substrate is transferred to the Fe(IV)=O species to give the Fe(III)—OH intermediate. Two possible pathways have been proposed in the literature for the electron transfer<sup>17,63,64</sup> [Figure 5.6]: i)  $\sigma$ -pathway, where an  $\alpha$ -spin electron is being transferred from the substrate to the unoccupied antibonding  $\sigma^*_z$  orbital of the Fe, resulting in a fully exchange-enhanced Fe 3d orbitals with five unpaired electrons and leaves a  $\beta$ -electron on the substrate. ii)  $\pi$ -pathway, where a  $\beta$ -spin

electron is transferred into one of the singly occupied antibonding  $\pi^*$  orbitals of the Fe(IV)=O, resulting in an  $\alpha$ -electron remaining on the substrate.

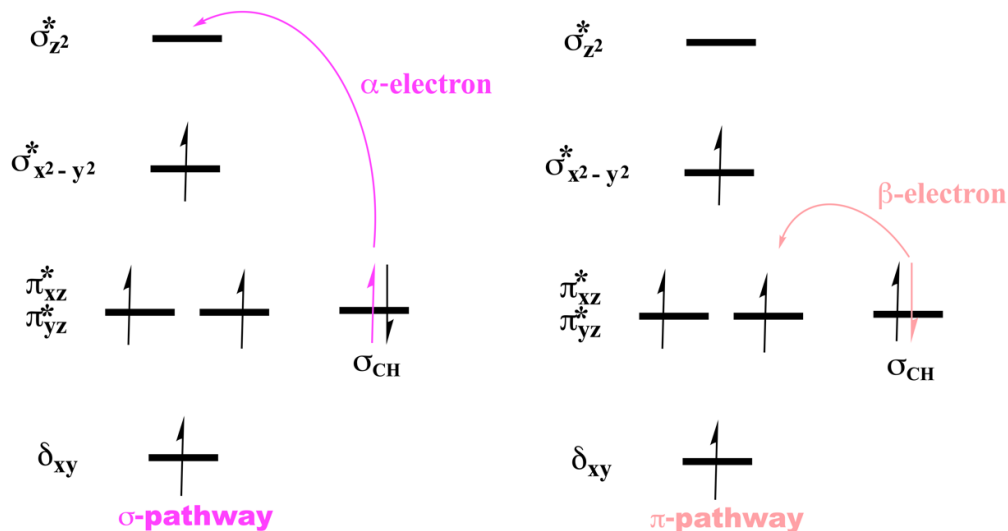


**Figure 5.6.** Possible reaction pathways for the HAT by the ferryl complex.

During the HAT via both  $C_\alpha$  and  $C_\beta$ , the electron transfer proceeds via  $\sigma$ -pathway as an  $\alpha$ -electron is transferred from the substrate to the  $\sigma_{z^2}^*$  orbital Fe(IV)=O, leaving a  $\beta$ -electron on the radical substrate, thereby strengthening stabilizing exchange interactions with other unpaired electrons of the Fe 3d-orbitals. The calculated spin densities for the  $C_\alpha$  and  $C_\beta$  at the transition states are -0.224 and -0.354, respectively, supporting the transfer of an  $\alpha$ -electron to the Fe(IV)=O  $\sigma_{z^2}^*$  orbital. The spin natural orbital (SNO) of the two HAT transition states presented in Figures D13 and D14 also supports the electron transfer

mechanism. Also, the values of Fe—O—H<sub>α</sub> and Fe—O—H<sub>β</sub> angles - 152.56° and 143.06°, respectively, additionally support the σ-transfer mechanism. Even though in an ideal case, a Fe—O—H angle of 180° is preferred for an effective σ-transfer<sup>63,64</sup> but numerous cases in the literature are reported for σ-transfer at angles quite lower than the ideal 180°. <sup>17,19,35</sup> Geometric constraints (described in the MD analysis) facilitate the stability of the 5eC and its proper orientation in the protein environment. Studies on other 2OG oxygenase enzymes have also reported similar Fe—O—H angle values for HATs that proceed via σ-pathway. <sup>17,19,35</sup> The σ-pathway is conserved in all the snapshots [Table D2] for the HAT via both the C<sub>α</sub> and C<sub>β</sub>, implying that the change in conformational flexibility does not alter the MO mechanism of the HAT. Thus the σ-transfer HAT is conserved across 5eC and 5mC substrates.

Similar to the natural 5mC substrate, **TS<sub>H1eα</sub>** and **TS<sub>H1eβ</sub>** are stabilized by second coordination sphere residues. For example, the cytosine base of the substrate is stabilized via stacking interactions with Tyr1902 and His1904 while the Asn1387 sidechain and NH group of His1904 form hydrogen bonding interactions with exocyclic N4 amine and N3 of the substrate, respectively, aiding in the proper orientation of the substrate in the active site. A series of hydrophobic interactions of residues Thr1393, Val1395, and Val1900 in the vicinity of the Fe center and the substrate also enhance the stability of the two transition states [Figures D15 and D16].

Importantly, in the 5eC HAT transition states, the non-coordinating oxygen of the Fe-ligating Asp1384 is stabilized by hydrogen bonding interaction with the hydroxyl group of

Thr1393, which was not observed in 5mC.<sup>12</sup> Furthermore, the stabilization of the methylene (CH<sub>2</sub>) and methyl (CH<sub>3</sub>) groups of the ethyl substituent of 5eC substrate by the isopropyl sidechain of Val1900 varies in both **TS<sub>H1eα</sub>** and **TS<sub>H1eβ</sub>**. In the **TS<sub>H1eα</sub>**, the methyl part of the ethyl group is better stabilized by hydrophobic interaction with the Val1900. In contrast, in **TS<sub>H1eβ</sub>**, the methylene moiety of the ethyl group is more favorably stabilized one via the same interaction.

The dynamic correlation analysis of these TSs stabilizing residues using the dynamic correlation plot from the simulation performed for the ferryl species of the enzyme complex shows that residues Thr1393, Val1395, and Val1900, which are involved in hydrophobic interactions, have a positive correlation with anti-parallel DSBH core β7 and β17, the loop containing Fe-chelating HxD motif, and Cys-rich β6 while Asn1387 shows a positive correlation with DNA interacting loop (L2) residues, Fe center, and the ferryl oxo group, suggesting their importance in catalysis and DNA binding. Tyr1902 and His1904 that stabilize the cytosine ring of the substrate have a positive correlation with Zn3 site, GS-linker, the loop containing HxD Fe-chelating residues, and DNA. These correlated motions are similar to what was observed in the HAT transition state for TET2 bound to the natural 5mC dsDNA substrate, implying that TET2 uses a universal network of correlated motions of catalytically important interactions for both the 5mC and the unnatural 5eC substrate.

After the formation of the transition states, the reaction leads to Fe(III)—OH and radical substrate intermediates, **IM1<sub>eα</sub>** and **IM1<sub>eβ</sub>** for respective HAT from C<sub>α</sub> and C<sub>β</sub>. In both intermediates, the O—H distance reduces to 0.97 and 0.98 Å in both complexes,



respectively, and the Fe—O bond elongates to 1.88 and 1.87 Å, respectively, when compared with the starting distance of 1.62 Å in the **RC**. These values signify the formation of the ferric-hydroxo intermediate with spin densities of 4.24 for Fe, pointing to the intermediates' Fe(III) character. The **IM1<sub>eα</sub>** is 2.8 kcal/mol lower in energy than the **RC** while **IM1<sub>eβ</sub>** is 4.8 kcal/mol above the **RC**, implying that the formed radical intermediate is exothermic and better stabilized via HAT from C<sub>α</sub> than from C<sub>β</sub>. The difference in the stabilities of the intermediates is likely due to the formation of a benzylic radical substrate intermediate in **IM1<sub>eα</sub>** in comparison to the formation of primary radical substrate intermediate in **IM1<sub>eβ</sub>**. The benzylic radical is more stable than the primary radical due to the resonance stabilization effect of the benzylic radical. Overall, the HAT from C<sub>α</sub> is both kinetically and thermodynamically favorable when compared to C<sub>β</sub> as the former occurs via a lower barrier than the latter with a more stable relative energy of the formed radical substrate intermediate.

The QM/MM calculations of the HAT step were also performed in solution, without the protein environment. The rate-determining barrier (18.8 kcal/mol) is consistent with those reported within the protein environment (15.8 kcal/mol). The Fe(III)—OH - radical substrate intermediate, however, is endothermic, unlike in the protein, likely illustrating the importance of the protein environment in the stabilization of the Fe(III)—OH - substrate radical intermediate [Table D3]. We performed additional QM/MM calculations with two different QM region sizes of atoms 56 and 83 in the QM region (for more details, see Table D3 in the SI). The QM/MM calculations for 5eC substrate show slight changes

in the HAT energy barrier (values of 14.3 and 16.7 kcal/mol in models with 56 and 83 QM region atoms, respectively) and the stability of Fe(III)—OH intermediate [Table D3]. The results were also compared with the one of QM-only model where the rate-determining HAT barrier is higher by ~8kcal/mol and the Fe(III)-OH radical intermediate is destabilized by ~9kcal/mol [Table D3] when compared to the QM/MM model, highlighting the vital importance of the MM environment in the catalysis.

### 5.3.5 Hydroxylation and Desaturation of 5eC Radical Substrate Intermediates

After the formation of the Fe(III)—OH species and radical substrate intermediates, the hydroxyl group from the ferric-hydroxo species can either undergo rebound to the radical to produce alcohol products or abstract second hydrogen atom from the adjacent C—H bond to form the desaturated products with Fe(II)—OH<sub>2</sub> center. From the **IM1<sub>eα</sub>**, the process of OH rebound passes through **TSRB<sub>eα</sub>** with a barrier of 5.2 kcal/mol from the intermediate. However, the abstraction of the second hydrogen atom that initiates the competitive desaturation reaction passes through **TSH<sub>2eα</sub>** that is 2.3 kcal/mol higher than the rebound transition state **TSRB<sub>eα</sub>**, suggesting that the rebounding of OH to the radical substrate might be more preferable than the abstraction of the second hydrogen from the C—H bond of the substrate radical to form the desaturated product. Due to the small difference in the activation barriers, however, both types of reaction could still occur with close probability. Analysis of the **TSRB<sub>eα</sub>** and **TSH<sub>2eα</sub>** geometries reveal that in **TSRB<sub>eα</sub>**, the Fe—O bond elongates to 2.16 Å while the C<sub>α</sub>—O bond shorten to 2.59 Å when compared

to 3.51 Å in **IM1<sub>eα</sub>**, pointing to the readiness to form the hydroxylated product. In the desaturation pathway involving the second HAT from C<sub>β</sub>, in the **TS<sub>H2eα</sub>**, the Fe—O bond lengthens to 2.06 Å with O—H and C<sub>β</sub>—H distance of 1.66 and 1.19 Å, respectively, depicting a more reactant-type transition state structure. In the TS for the second HAT, Fe—O—H angle is 143.69, which deviates from the first HAT from C<sub>α</sub> (152.56°), implying that the process of abstracting second hydrogen to form Fe(II)—OH<sub>2</sub> involves a slight change in the orientation of the substrate to favor the desaturation.

Furthermore, we explored the possibilities of both rebound and desaturation from **IM1<sub>eβ</sub>**. The desaturation barrier, **TS<sub>H2eβ</sub>**, via second HAT, is 14.4 kcal/mol higher than the rebound one, **TS<sub>RBeβ</sub>**, indicating that the rebound occurs through a lower energy path than the desaturation. The rebound and desaturation reactions from **IM1<sub>eβ</sub>** being less favored than **IM1<sub>eα</sub>** could be due to the structural differences in the radical intermediate formed after HAT and, in particular, the orientation of the alkyl substituent in the substrate. In addition, long-range interactions could contribute towards the preference of **IM1<sub>eα</sub>** vs. **IM1<sub>eβ</sub>**. Analyses of the key distances for both transition states are similar to the observed results from **IM1<sub>eα</sub>** (Figure 5.5). The hydroxylation and the desaturation from **IM1<sub>eα</sub>** result in highly exothermic **PD<sub>OH<sub>eα</sub></sub>** and **PD<sub>DSeα</sub>** products, with the energy of -47.0 and -44.3 kcal/mol, respectively, indicating that the hydroxylated substrate is both kinetically and thermodynamically preferred. The distance of 1.42 Å for C<sub>α</sub>—O confirms the formation of hydroxylated product (**PD<sub>OH<sub>eα</sub></sub>**), while in the case of desaturation (**PD<sub>DSeα</sub>**), C<sub>α</sub>—C<sub>β</sub> and

Fe—O distance of 1.34 and 2.13 Å, depict the formation of  $C_{\alpha}=C_{\beta}$  unsaturated and Fe(II)—OH<sub>2</sub> bonds, respectively.

Similarly, the formed **PD<sub>OH $\epsilon$  $\beta$</sub>**  and **PD<sub>DS $\epsilon$  $\beta$</sub>**  from **IM1 $\epsilon$  $\beta$**  are also highly exothermic by -31.6 and -41.7 kcal/mol, respectively, but the desaturated product is ~10 kcal/mol stable than the alcohol product even though the alcohol product occurs via a lower rebound barrier than the one for desaturation [Figure 5.4]. The result indicates that in the C <sub>$\beta$</sub> -centered reaction, rebound hydroxylation is kinetically preferred while desaturation is thermodynamically preferred. This observed reactivity pattern from **IM1 $\epsilon$  $\beta$**  implies that the rebound is favored over the desaturation, but the relative energies of the corresponding product give a more stable **PD<sub>DS $\epsilon$  $\beta$</sub>**  than **PD<sub>OH $\epsilon$  $\beta$</sub>** .

Overall, the substrate oxidation either via CH<sub>2</sub> (C <sub>$\alpha$</sub> ) or CH<sub>3</sub> (C <sub>$\beta$</sub> ) results in more stable products than the **RC**. The C—H activation from C <sub>$\alpha$</sub>  gives both stable **PD<sub>OH $\epsilon$  $\alpha$</sub>**  and **PD<sub>DS $\epsilon$  $\alpha$</sub>**  products than the ones from C <sub>$\beta$</sub> . The C <sub>$\alpha$</sub>  hydroxylation product is more stable than the desaturation product, while in C <sub>$\beta$</sub> , the reverse is the case. In both cases, the rebound hydroxylation proceeds with lower activation energy than the desaturation reaction. The stability of products formed via CH<sub>2</sub> (C <sub>$\alpha$</sub> ) and the lower barriers involved when compared to CH<sub>3</sub> (C <sub>$\beta$</sub> ) likely show the preference for substrate oxidation at the CH<sub>2</sub> position over the terminal CH<sub>3</sub> position of the ethyl group.

The DFT-D3 dispersion corrected energies at BS + ZPE level show the same trends as the calculations without D3 correction with slight differences in both reaction barriers and reaction energies (for more details, see Tables D4-D7 in the SI).

### 5.3.6 Energetic Effects of Individual Residues on the Stabilization of the Transition States and Products

To obtain further insight into the energetic contributions towards the stabilization of the TSs of HAT, rebound and desaturation reactions, we performed energy decomposition analysis (EDA)<sup>54,55</sup> on the QM/MM optimized **RC**, **TS<sub>H1e $\alpha$</sub>** , **TS<sub>H1e $\beta$</sub>** , **TS<sub>RBe $\alpha$</sub>** , **TS<sub>H2e $\alpha$</sub>** , **TS<sub>H2e $\beta$</sub>** , **TS<sub>RBe $\beta$</sub>** , **PDO<sub>He $\alpha$</sub>** , **PDO<sub>Se $\alpha$</sub>** , **PDO<sub>He $\beta$</sub>** , and **PDO<sub>Se $\beta$</sub>** . We calculated the differences in the non-bonded intermolecular interaction energies (i.e., the Coulomb and van der Waals) between the individual residues of the MM environment and the QM region when the system goes from the reactants to the transition states and the products.<sup>54,55</sup> A negative contribution refers to a stabilizing contribution to the transition states and products, while the opposite applies to a positive one.<sup>54,55</sup>

The EDA [Figure 5.7 and Table D8] based on the optimized structure of HAT transition states, **TS<sub>H1e $\alpha$</sub>**  and **TS<sub>H1e $\beta$</sub>** , and the **RC** reveal that C1263, R1269, H1380, and E1874 contribute sensitively to the stabilization of **TS<sub>H1e $\alpha$</sub>** . In contrast, the transition state **TS<sub>H1e $\beta$</sub>**  is stabilized by T1372 and T1393. The variations in the magnitude of energetic contributions and the residues likely account for the observed lower barrier for **TS<sub>H1e $\alpha$</sub>**  than **TS<sub>H1e $\beta$</sub>** . For the rebound reaction, the **TS<sub>RBe $\alpha$</sub>**  is stabilized by H1380, C1263, and charged

residues K1299, E1874, and E1879 while in **TS<sub>RBεβ</sub>**, charged residues R1261 and E1874 destabilize the rebound transition state. The desaturation **TS<sub>H2εα</sub>** and **TS<sub>H2εβ</sub>** are stabilized by similar residues, C1263, K1299, H1380, T1393, E1874, and E1879 but with different magnitude of energetic contributions, and this likely contribute to the lower barrier observed for **TS<sub>H2εα</sub>** when compared to **TS<sub>H2εβ</sub>**.

The alcohol product of the rebound to C<sub>β</sub>, **PDO<sub>Hεβ</sub>**, is stabilized by both positively and negatively charged residues, R1261, R1269, K1299, D1376, K1826, E1874, and E1879 while in **PDO<sub>Hεα</sub>**, K1310 and K1905 further stabilized the product in addition to the one observed for **PDO<sub>Hεβ</sub>**. The energetic contributions of these stabilizing residues are significantly greater in **PDO<sub>Hεα</sub>**, than **PDO<sub>Hεβ</sub>**, and this might likely be one of the reasons for a more thermodynamically stable **PDO<sub>Hεα</sub>** over **PDO<sub>Hεβ</sub>** product. Notably, the desaturated products, **PD<sub>DSeα</sub>** and **PD<sub>DSeβ</sub>**, are stabilized by different residues, R1359, V1371, and T1393, while R1261 significantly destabilizes the two products.

Experimental mutagenesis studies have shown that mutation of some of these transition states/products stabilizing residues either results in reduction/loss of enzymatic activity and might lead to refractory anemia and chronic myelomonocytic leukemia.<sup>7,65,66</sup> For example, mutant K1299E/S1303N has been reported to significantly reduce TET2 activity and also result in refractory anemia.<sup>7</sup> T1372E mutant has been demonstrated both experimentally and computationally to halt the successive oxidation of 5hmC to 5fC/5caC<sup>54,67</sup> while variant T1393A reduces the oxidation of 5mC to 5hmC by 75% in TET2.<sup>66</sup> The identified residues are part of the network of electrostatic and Van der Waals interactions that most

strongly contribute towards the energetic stabilization of the TS and PD in respect to RC.

These residues may be important as potential targets for mutagenesis studies.

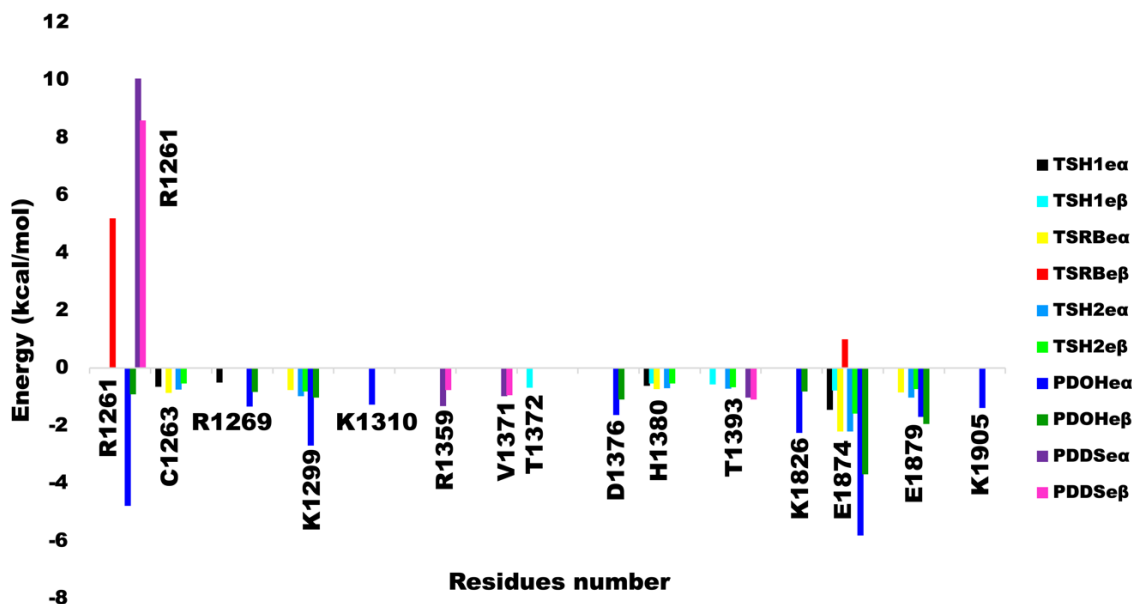


**Figure 5.7.** Energy decomposition analysis (EDA) of the residues stabilizing the transition states and the products.

### 5.3.7 Oxidation of Unsaturated Substrates by TET2

In a recent study, TET2 enzyme has been reported to be catalytically active towards unsaturated 5-vinylcytosine (5vC) and 5-ethynylcytosine (5eyC) substrate similar to saturated 5-ethylcytosine (5eC) and 5-methylcytosine (5mC) substrates.<sup>9</sup> We explored the oxidation of the 5vC and 5eyC substrates. The Fe(IV)=O intermediate can abstract a hydrogen atom from either carbon (i.e., C<sub>α</sub> or C<sub>β</sub>) of the 5vC vinyl group in a similar

manner as the ethyl group in 5eC while in 5eyC substrate, the intermediate can only abstract the terminal hydrogen atom [Scheme 5.1]. After the HAT, the radical substrate intermediate undergoes rebound to give the hydroxylated product in 5eyC while in 5vC, both alcohol and desaturated products are possible.

### 5.3.8 Hydrogen Atom Abstraction in 5vC and 5eyC Substrates

The HAT step was studied using 5 well-equilibrated snapshots from the MD to understand the effect of conformational dynamics on this rate-determining step. The Boltzmann weighted average barrier of 22.7 kcal/mol is found for 5eyC while 19.4 kcal/mol and 23.3 kcal/mol are obtained for HAT from  $C_\alpha$  and  $C_\beta$ , respectively, for the 5vC. These barriers are slightly higher than the reported HAT barriers for 5mC and 5eC substrate, likely due to the unsaturated nature of the vinyl and ethynyl groups of 5vC and 5eyC, respectively, making the C—H bonds to be slightly stronger in both than in 5mC and 5eC substrates. Despite the variations in the barriers, they are all in good agreement with the previously reported values for the HAT for non-heme Fe(II) and 2OG dependent oxygenases.<sup>12,18,54,61</sup> Subsequent calculations were then performed using RCs that showed the lowest barriers.

In the 5vC substrate, HAT from  $C_\beta$  is 3.6 kcal/mol higher than the one from  $C_\alpha$ , implying that the rate-determining HAT from  $C_\alpha$  is faster than  $C_\beta$ , and thus likely shows the preference of HAT from  $C_\alpha$  over  $C_\beta$ . This can be due to the combined effects of the closer proximity of the  $C_\alpha$ -H bond to the Fe(IV)=O species than  $C_\beta$ -H and the restriction in the conformational freedom of the vinyl group inside the TET2 pocket, which may be partly due to the rigid C=C bond of the vinyl substituent.



Figure D17 shows the transition state geometries,  $\text{TS}_{\text{H1}\nu\alpha}$  and  $\text{TS}_{\text{H1}\nu\beta}$ , for HAT from  $\text{C}_\alpha$  and  $\text{C}_\beta$ , respectively, for 5vC substrate.  $\text{TS}_{\text{H1}\nu\alpha}$  has a symmetric HAT transition state with nearly equal O—H and C—H distances of 1.28 and 1.27 Å, respectively, whereas in  $\text{TS}_{\text{H1}\nu\beta}$ , the transition state is product-like, i.e., late TS with the transferring hydrogen atom closer to the acceptor atom than the donor atom. The values obtained for O—H and C—H distances are 1.14 and 1.39 Å, respectively. In both TSs, the Fe—O bond elongated to similar distances of 1.79 Å for  $\text{TS}_{\text{H1}\nu\alpha}$  and 1.75 Å for  $\text{TS}_{\text{H1}\nu\beta}$ . The Fe—O—H angle varies from 135.22 to 150.88° in the  $\text{TS}_{\text{H1}\nu\alpha}$  from the five scans, whereas in  $\text{TS}_{\text{H1}\nu\beta}$ , the values between 114.52 and 120.65° are obtained, indicating that an  $\alpha$ -electron might be shifted from the substrate to the Fe(IV)=O orbital in  $\text{TS}_{\text{H1}\nu\alpha}$ , while a  $\beta$ -electron might be transferred in the case of  $\text{TS}_{\text{H1}\nu\beta}$ . These observations are further confirmed by calculating the spin densities values of both  $\text{C}_\alpha$  and  $\text{C}_\beta$  of the vinyl group at the respective transition state. In  $\text{TS}_{\text{H1}\nu\alpha}$ , the  $\text{C}_\alpha$  spin density varies between -0.373 and -0.247, while values from 0.557 to 0.646 are obtained for  $\text{C}_\beta$  in  $\text{TS}_{\text{H1}\nu\beta}$  for all the snapshots. These results reveal that a  $\beta$ -electron is left on the vinyl group of the 5vC substrate in  $\text{TS}_{\text{H1}\nu\alpha}$  while in  $\text{TS}_{\text{H1}\nu\beta}$ , an  $\alpha$ -electron remains in the substrates, suggesting that HAT from  $\text{C}_\alpha$  and  $\text{C}_\beta$  proceed via  $\sigma$ - and  $\pi$ -pathway, respectively [Table D9]. By modifying the structural determinants for the  $\sigma$ - and  $\pi$ -pathways, one could switch between the two mechanisms, which is an example of how the protein environment might influence the orbital mechanism of HAT. The analysis of the Spin Natural Orbitals<sup>63</sup> [Figures D18 and D19] confirms the spin density results.

Similarly, in 5eyC, the abstraction of the only terminal hydrogen by the active Fe(IV)=O complex passes through **TS<sub>H1eyβ</sub>**, which possess C—H and O—H distances of 1.44 and 1.09 Å, respectively, in a similar manner as HAT from the terminal C<sub>β</sub> in 5vC substrate. The results indicate that the HAT from the terminal carbon (C<sub>β</sub>) in both unsaturated 5vC and 5eyC dsDNA substrates possess late transition states with product-like properties. The observed Fe—O—H angle in **TS<sub>H1eyβ</sub>** varies between 127.16 to 138.79° and the calculated spin densities of the terminal carbon at the transition state range between -0.214 to -0.117, pointing to a σ-electron transfer mechanism for the HAT in 5eyC substrate [Table D10].

The HAT results in the reduction of Fe(IV)=O species to Fe(III)—OH complex with the generation of radical substrates intermediates, **IM1<sub>eyβ</sub>** for 5eyC, **IM1<sub>vα</sub>** and **IM1<sub>vβ</sub>**, for HAT from C<sub>α</sub> and C<sub>β</sub> of the vinyl group of 5vC, respectively. The formed **IM1<sub>eyβ</sub>** is endergonic with an energy of 7.9 kcal/mol at the BS + ZPE level of theory, while in **IM1<sub>vα</sub>** and **IM1<sub>vβ</sub>** of 5vC substrate, the intermediates are also endergonic with the energy of 3.4 and 9.3 kcal/mol, respectively. In all the intermediates, the elongation of the Fe—O bond by ~0.25 Å when compared to **RC** and the O—H distances of ~0.98 Å confirms the formation of the ferric-hydroxo intermediate. The calculated spin densities between 4.23 and 4.24 in all the intermediates support the +3-oxidation state assigned for Fe at the reaction state.

### 5.3.9 Rebound Hydroxylation and Desaturation Reactions in 5vC and 5eyC Radical substrates Intermediates

Similarly to 5eC, the formed of the Fe(III)—OH complex and the substrates radical intermediates, **IM1<sub>vα</sub>** and **IM1<sub>vβ</sub>** of 5vC substrate can undergo radical rebound processes via **TS<sub>RBvα</sub>** and **TS<sub>RBvβ</sub>**, respectively, in which the hydroxyl (OH) group is transferred from the ferric-hydroxo complex to the radical carbons, resulting in the formation of hydroxylated intermediates, **IM2<sub>OHvα</sub>** and **IM2<sub>OHvβ</sub>**, and reduction of Fe(III) to Fe(II). Alternatively, **IM1<sub>vα</sub>** and **IM1<sub>vβ</sub>** can undergo desaturation by abstracting another hydrogen atom from the adjacent carbon via **TS<sub>H2vα</sub>** and **TS<sub>H2vβ</sub>** to form the desaturated products, **IM2<sub>DSvα</sub>** and **IM2<sub>DSvβ</sub>** and Fe(II)—OH<sub>2</sub> center, similarly to 5eC. The imaginary frequency values for all the obtained transition states are presented in Table D11.

The rebound reaction occurs more rapidly in **TS<sub>RBvα</sub>** with a barrier of 11.8 kcal/mol and the overall reaction is highly exothermic with energy of -35.5 kcal/mol, implying that the formed **IM2<sub>OHvα</sub>** is very stable. However, the rebound barrier leading to the formation of **IM2<sub>OHvβ</sub>** is 17.7 kcal/mol, and thus slower than the one of **IM2<sub>OHvα</sub>** with overall reaction energy of -29.2 kcal/mol. The calculated desaturation pathways where a second hydrogen atom is abstracted from the adjacent carbon pass through **TS<sub>H2vα</sub>** and **TS<sub>H2vβ</sub>** and result in higher barriers of 20.9 and 25.1 kcal/mol, respectively. The resultant desaturated products, **IM2<sub>DSvα</sub>** and **IM2<sub>DSvβ</sub>** are ~22.0 kcal/mol more stable than the **RC** but less stable than the hydroxylated intermediates. Overall, the results imply that the rebound hydroxylation of

5vC is both kinetically and thermodynamically preferred over the competitive desaturated reaction, possibly due to the change in the orientation of C $\beta$  methine radical group in the RC for the rebound reaction. In addition, the study reveals that the rebound hydroxylation on C $\alpha$ -based radical is preferred (again both kinetically and thermodynamically) over a rebound hydroxylation of C $\beta$ -based radical.

The rebound hydroxylation in 5eyC passes through **TS<sub>RBey $\beta$</sub>**  possesses a barrier of 17.4 kcal/mol and the formed terminal hydroxylated intermediate, **IM<sub>2OHey $\beta$</sub>**  is 32.9 kcal/mol below the **RC**, suggesting the formation of a stable product. The optimized geometries of the stationary points and QM/MM energy profile are presented in Figures D17, D20, D21, and 5.8, respectively. In summary, the rebound hydroxylation proceeds with lowest activation barrier (5.2 kcal/mol) in C $\alpha$  atom of 5eC followed by 5mC (10.1 kcal/mol),<sup>12</sup> followed by C $\alpha$  atom of 5vC (11.8 kcal/mol) and 17.4 kcal/mol in 5eyC.

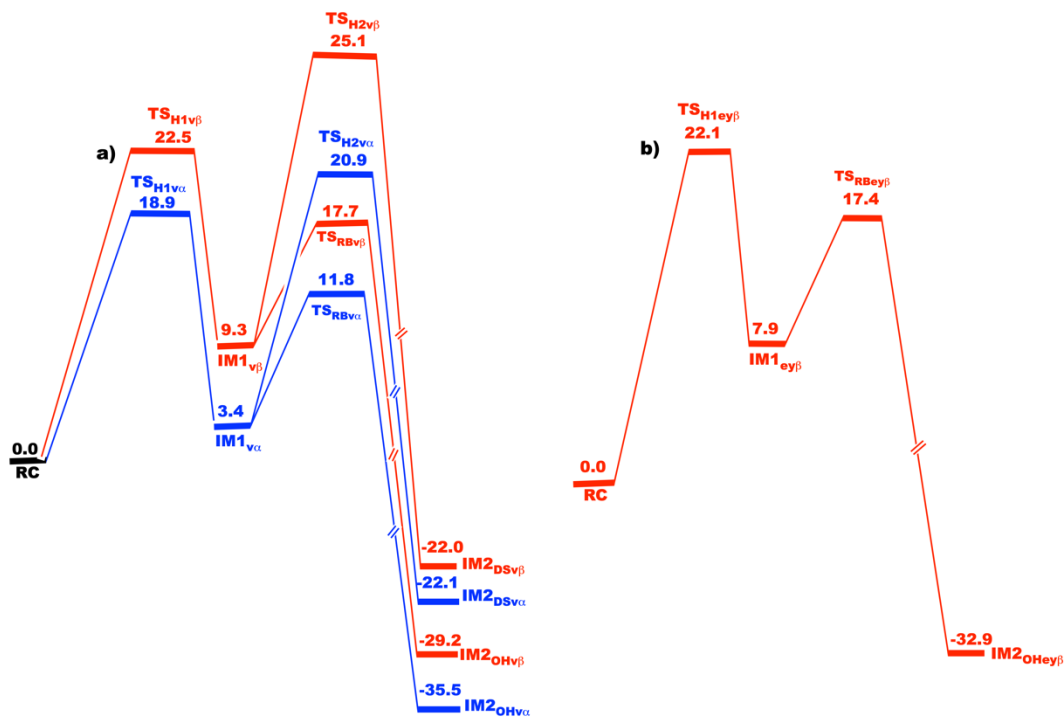


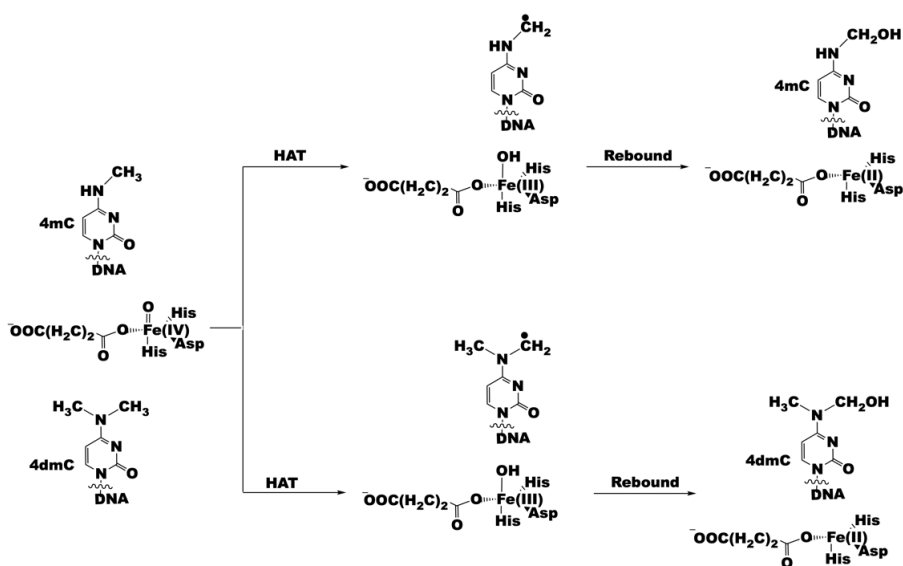
**Figure 5.8.** QM/MM potential energy profile for the hydroxylation and desaturation reactions of 5vC (a) and for the hydroxylation of 5eyC (b) dsDNA substrates by TET2, calculated using UB3LYP/def2-TZVP with ZPE. The relative energies are in kcal/mol.

Even though various studies have shown that non-heme Fe(II) and 2OG dependent enzymes prefer high spin quintet spin state as the ground state,<sup>17,18,33,34</sup> we also performed calculations at septet higher spin state for 5eC, 5vC, 5eyC, and 4mC substrates, and the result indeed revealed that the quintet Fe(IV)=O species is more potent oxidants for C—H activation and thus the oxidation of the substrate is faster at quintet than septet spin state in all cases [Tables D4-D7]. Comparison of the Fe(IV)=O complex energies at both spin states revealed that the quintet ground state is more stable than the septet by 16.4, 16.9, 14.3, and 15.2 kcal/mol in 5eC, 5vC, 5eyC, and 4mC substrates, respectively, thus

supporting the previous experimental and computational studies on the favorable ground state for non-heme 2OG enzymes.<sup>20,21,34</sup>

### 5.3.10 Mechanism of 4mC and 4dmC dsDNA substrates Oxidation by TET2

The discovery that TET2 oxidizes 4mC and 4dmC (lacking C5 alkylations) demonstrate the potential of TET2 to act as indirect (on C5 alkylations) and direct demethylase (on 4mC and 4dmC). Aiming to provide insight into how TET2's catalytic mechanism and interactions of direct demethylation might differ from indirect demethylation, we performed QM/MM studies of TET2 with dsDNA containing 4mC and 4dmC (Scheme 5.2).



**Scheme 5.2.** Reaction mechanisms for the hydroxylation of the unnatural 4mC and 4dmC dsDNA substrates by TET2.

The oxidation of the substrates using 5 well-equilibrated snapshots gave Boltzmann weighted average of 10.8 and 14.0 kcal/mol for the rate-determining HAT step of 4mC and 4dmC substrates, respectively. During the HAT, the electron transfer occurred via  $\sigma$ -channel, where an  $\alpha$ -electron was transferred into the unoccupied antibonding orbital of the Fe. The HAT results in exothermic Fe(III)—OH intermediates with energies of -5.7 and -7.7 kcal/mol for 4mC and 4dmC, respectively, at BS + ZPE level of theory. The rebound hydroxylation of the radical intermediates led to the formation of highly exothermic hydroxylated intermediates, **IM2<sub>OH4m</sub>** and **IM2<sub>OH4dm</sub>** for 4mC and 4dmC with overall energies of -37.6 and -42.8 kcal/mol, respectively. **IM2<sub>OH4dm</sub>** is more stable than **IM2<sub>OH4m</sub>** by 5.2 kcal/mol as the OH group of the **IM2<sub>OH4dm</sub>** is locked in a strong hydrogen bonding interaction with the negatively charged oxygen atom of the C4 carboxylate of the succinate, unlike in **IM2<sub>OH4m</sub>** where the OH group forms weaker hydrogen bonding interaction with the non-coordinating carbonyl oxygen of the Fe-ligating Asp1382. Detailed analyses are provided in the SI (section 2).

### **5.3.11 Post Hydroxylation Reactions for hydroxylated intermediates of IM2<sub>OH $\gamma$ $\beta$</sub> , IM2<sub>OH $\nu$ $\beta$</sub> , and IM2<sub>OH4m</sub> of 5eyC, 5vC, and 4mC Substrates**

The decomposition of the hydroxylated hemiaminal intermediate of the DNA base has been a subject of discussion about whether the hydrolysis to the unmodified base would proceed in the enzyme or an aqueous solution. A recent study on FTO has reported that the decomposition of the hemiaminal intermediate to formaldehyde and unmodified DNA base

proceed faster in an aqueous solution.<sup>61</sup> Another study demonstrated that the stabilities and reactivities of the hemiaminal intermediate vary depending on the position of the N-methyl group on the substrate. The fragmentation of the hemiaminal intermediate where the hydroxymethyl is linked to the endocyclic nitrogen was found to be faster than the exocyclic counterparts, which are very slow due to their stability.<sup>68</sup>

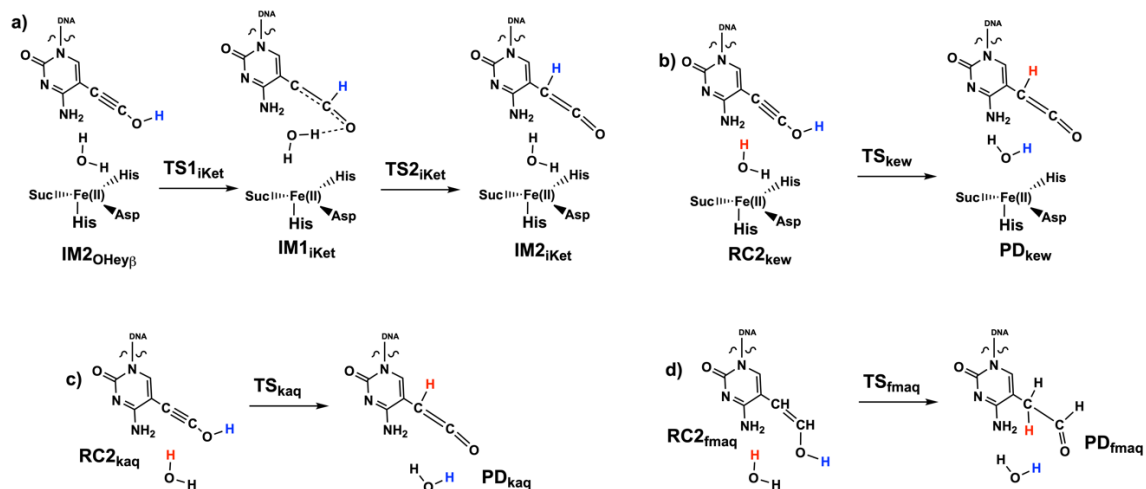
### 5.3.12 Rearrangement Reactions of $\text{IM2}_{\text{OHey}\beta}$ and $\text{IM2}_{\text{OHV}\beta}$ in Enzyme and Water

Studies on the ability of TET enzymes to act on unnatural modifications of cytosine base at C5 position by Kohli and co-workers<sup>9</sup> have suggested that the  $\text{IM2}_{\text{OHey}\beta}$ , formed during the oxidation of 5eyC can undergo rearrangement to give a ketene intermediate. To achieve this, we explored using QM/MM methods two possible pathways: i) rearrangement in the enzyme where the proton from the hydroxyl (OH) group is transferred to the  $C_\alpha$  of the substituent with or without mediation via water molecule; ii) rearrangement in aqueous solution outside of the enzyme.

The rearrangement in (i) involving the transfer of the OH proton to the  $C_\alpha$  generated an intermediate,  $\text{IM1}_{\text{iKet}}$  where the proton is first temporarily transferred to the  $C_\beta$  [Scheme 5.3a]. This passes through  $\text{TS1}_{\text{iKet}}$  with a 53.4 kcal/mol barrier, which is too high to favor such a pathway. After the formation of  $\text{IM1}_{\text{iKet}}$ , the proton is transferred to the  $C_\alpha$  to generate the ketene product. This transfer proceeds via  $\text{TS2}_{\text{iKet}}$  with a barrier of 24.7 kcal/mol, resulting in a highly exothermic ketene product,  $\text{IM2}_{\text{iKet}}$ . This calculated pathway



has a remarkably high energy barrier, with the  $\text{TS1}_{\text{Ket}}$  being the rate-determining step, even though the formed product is very stable. Next, we explored the possibility of mediating the rearrangement via water molecules in the enzyme [Scheme 5.3b]. The assistance with water resulted in a barrier of 28.4 kcal/mol, which is 25.0 kcal/mol lower than the rate-determining step barrier observed for the rearrangement without water molecules but still too high to be feasible.<sup>61</sup> Various studies have reported the role of water molecules in the reduction of activation barriers.<sup>61,69,70</sup> For example, a study by Shaik and co-workers on FTO reported a 25.6 kcal/mol barrier for the water-assisted decomposition of hydroxylated intermediate of 6-methyladenine substrate in contrast to 59.0 kcal/mol obtained without the assistance of water molecules.<sup>61</sup> Also, a study on the catalytic mechanism of HIV-1 protease revealed that the rate of degradation of the substrate was lowered by almost 10 kcal/mol in the water-assisted pathway.<sup>69</sup> Our study, in agreement with previous works, demonstrates the role of water in enhancing the reaction rate.



**Scheme 5.3.** Reaction scheme for a) formation of ketene inside the enzyme without the assistance of water molecule; b) formation of ketene with the assistance of water inside the enzyme; c) formation of ketene with the assistance of water outside the enzyme in the water solvent; d) formation of 5-formylmethylcytosine (5fmC) outside the enzyme in the water solvent.

The rearrangement results in a highly stable product with energy of -26.5 kcal/mol. We, therefore, performed a QM/MM study of the rearrangement in an aqueous solution outside of the enzyme [Scheme 5.3c], where the hydroxylated 5eyC substrate was embedded in a water box containing 896 water molecules. The hydroxylated cytosine part was included in the QM part with one water molecule, and the remaining water molecules remained in the MM. We are conscious that QM/MM calculations using a single structure might not provide the most accurate value of the activation and reaction energies in highly disordered media and protein environment.<sup>12,17,71,72</sup> The formation of the ketene proceeded faster with

a barrier of 10.4 kcal/mol, suggesting that the rearrangement of **IM2**<sub>OHeyβ</sub> to ketene takes place in aqueous solution outside of the enzyme. Figures 5.9 and D22 present the potential energy profile for the rearrangement of **IM2**<sub>OHeyβ</sub> as well as the optimized stationary point geometries involved in these reactions.

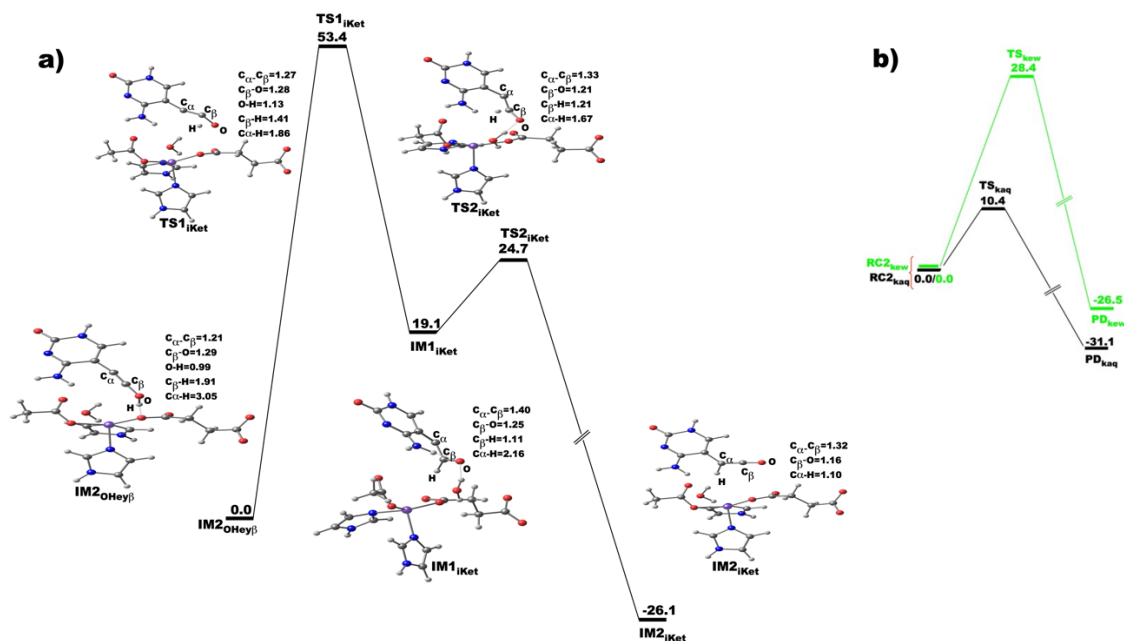


**Figure 5.9.** QM/MM potential energy profiles for the formation of ketene inside the enzyme without the assistance of water molecule (a) and the ketene formation with the assistance of water (b) inside (green) and outside (black) of the enzyme. The relative energies and the distances are in kcal/mol and Å, respectively.

Similarly, we carried out the tautomerization of **IM2<sub>OH $\beta$</sub>**  to generate 5-formylmethylcytosine (5fmC) product which has been reported by Ghanty et al., to be the predominant product of the oxidation of 5vC by TET2.<sup>9</sup> We performed the calculations via direct transfer of the OH proton to the C $\alpha$  of the substituent with and without the assistance of water molecule in a similar manner as above ketene intermediate formation. The QM/MM potential energy scan shows an increase in energy without leading to the formation of the desired product. Furthermore, we explored the possibility of mediating the proton transfer via the noncoordinating oxygen of the iron coordinating succinate (Suc) as the hydroxyl group is locked in hydrogen bonding interaction with it. The proton transfer to the succinate resulted in protonated succinate (SucH) product, and it passes through a transition state with an energy barrier of 1.62 kcal/mol, indicating a very rapid process [Figure D23]. On an attempt to transfer the proton from the SucH to the C $\alpha$  of the substrate substituent, it falls back to the hydroxylated **IM2<sub>OH $\beta$</sub>**  intermediate. We then explored the tautomerization mechanism in an aqueous solution outside the enzyme [Scheme 5.3d]. The calculations showed the formation of a very stable and exothermic 5-formylmethylcytosine (5fmC), with a reaction barrier and overall reaction energy of 17.8 and -12.1 kcal/mol, respectively [Figure D23], implying that as the ketene formation reaction, the formation of 5-formylmethylcytosine proceeds in water and not in the enzyme.

### 5.3.13 Decomposition of hemiaminal intermediate of 4mC

The hemiaminal intermediate **RC3** formed after the oxidation of 4mC undergoes decomposition to form the demethylated cytosine base and formaldehyde.<sup>10</sup> The demethylation is first studied in the enzyme with the aid of a water molecule, as presented in Figures 5.10 and D24. The decomposition starts from **RC3**, where the proton from the hydroxyl group is first transferred to the N3 of the base. This transfer is mediated via a water molecule with an energy barrier of 17.6 kcal/mol, resulting in the generation of an endothermic **IM1** with an energy of 6.0 kcal/mol. Thereafter, the C4—N4 bond cleaves to give **IM2** intermediate, which passes through **TS2** of energy barrier 14.6 kcal/mol. This bond cleavage leads to the elimination of the formaldehyde from the hemiaminal intermediate. Subsequently, a water-assisted proton shift from N3 to N4 via **TS3** led to the demethylated cytosine product (**PD<sub>dm</sub>**). The calculated overall barrier of 50.9 kcal/mol for the rate-determining step is too high to be feasible even though the formed product is stable by the energy of -3.3 kcal/mol. Hence, we explored the possibility of decomposing the hemiaminal intermediate in an aqueous solution outside of the enzyme environment using QM/MM.

As presented in Figure D25, the results reveal that the demethylation in aqueous solution proceeds with a barrier of 20.4 kcal/mol. This result is in good agreement with the previously reported experimental<sup>56</sup> and computational studies by Shaik and co-workers on the decomposition of N<sup>6</sup>-hydroxymethyladenosine (hm<sup>6</sup>A) by other human N-alkylated nucleic acid demethylase (FTO), where the hydrolysis of the hm<sup>6</sup>A proceeded in aqueous

solution outside of the enzyme after the in-enzyme hydroxylation of the methyl group of the adenine base.<sup>61</sup> The product formed here is endothermic with an energy of 4.1 kcal/mol in contrast to -3.3 kcal/mol obtained inside the enzyme, indicating the role of the protein environment in the stabilization of the product in the latter.

The studies demonstrate the post-hydroxylation steps, e.g., ketene formation after the 5eyC hydroxylation, the formation of 5-formylmethylcytosine after hydroxylation of 5vC, and the formaldehyde separation from hemiaminal of 4mC proceeds in the water solvent and not in the enzyme environment, nevertheless of the diversity of the chemical transformations of the respective hydroxylated intermediates. The finding implies that TET2 as a Fe(II)/2OG enzyme is specialized in providing the suitable catalytic environment only for the reactions of the dioxygen activation and the substrate oxidation (HAT and rebound hydroxylation) of several different alkylated forms of cytosine in dsDNA, while the post-hydroxylation reactions proceed non-enzymatically in the water solvent.

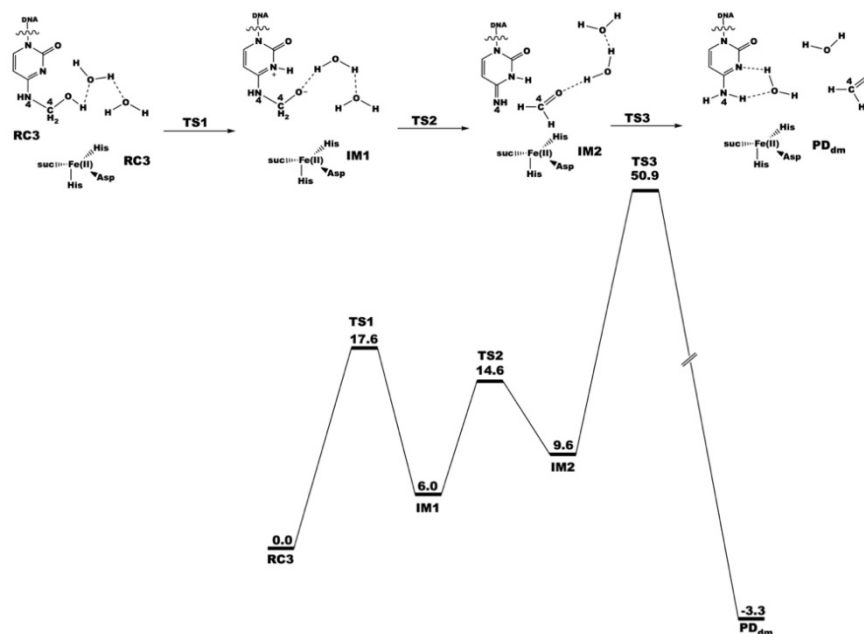


**Figure 5.10.** Reaction scheme and the QM/MM potential energy profile for the decomposition of hemiaminal intermediate of 4mC hydroxylation inside the enzyme, calculated using UB3LYP/def2-TZVP with ZPE. The relative energies are in kcal/mol.

## 5.4 Conclusions

We report the MD and QM/MM studies on the dynamics and the reaction mechanisms involved in the oxidation of unnatural C5-position modifications of cytosine (5eC, 5vC, and 5eyC) as well as demethylation of exocyclic N4 mono- and di-methylated (4mC and 4dmC) lesions of cytosine by TET2 enzyme. We studied the possible hydroxylation and desaturation pathways in the oxidation of 5eC and 5vC dsDNA substrates, while in the case of 5eyC, 4mC, and 4dmC, we explored the hydroxylation pathway. Due to the nature of the ethyl and vinyl substituents of 5eC and 5vC, respectively, we explored oxidation at

both C $\alpha$  and C $\beta$  carbons of the two substituents. We then carried out QM/MM modeling of the rearrangement reactions of the hydroxylated intermediates of 5eyC and 5vC substrates to produce ketene intermediate and 5-formylmethyl-cytosine (5fmC), respectively. The hydroxylated intermediate of 4mC (hemiaminal) was demethylated to unmodified cytosine and formaldehyde. These post-hydroxylated reactions were studied both inside and outside of the enzyme with the participation of water molecules, showing that in all cases, the post-hydroxylation reactions proceed in the water solvent outside the enzyme environment.

The dynamics studies reveal that the variations in the alkylation status on the cytosine base influence the overall collective motions of the key structural motifs of the enzyme and the second coordination sphere interactions. The QM/MM calculations reveal that HAT from the N-methylated substrates is faster than the counterparts from C5-position modifications. HAT from C $\alpha$  has lower barriers than C $\beta$  in 5eC and 5vC, resulting in more stable Fe(III)—OH intermediates than the one from C $\beta$ . Furthermore, we explored the effects of conformational flexibilities on the HAT by using multiple snapshots. The results show variations in the HAT reaction barriers, implying that the conformational changes affect the HAT rate. The calculations reveal that  $\sigma$ -pathway is used for the HAT electron transfer mechanism except for HAT from C $\beta$  in 5vC substrate, where a  $\pi$ -pathway is favored. The electron transfer pathways are preserved in all the snapshots for all the systems, suggesting that the change in conformations does not affect the electron transfer pathways used during the HAT, nevertheless, the conformational changes can influence the energetic changes



along the reaction path. The calculations also identified the key residues crucial for the HAT and their contributions to catalysis, DNA interaction, and structural stability via long-range interactions.

Furthermore, the hydroxylation pathway in 5eC and 5vC is energetically favored than the desaturation one, showing the preference for the former pathway. The rearrangement of the hydroxylated intermediates of 5eyC to ketene intermediate proceeds with a barrier of 28.4 and 10.4 kcal/mol with the assistance of water molecules in and outside of the enzyme, respectively, indicating that the rearrangement is faster outside of the enzyme as in 5vC. Our calculated barrier for the decomposition of the hemiaminal intermediate of 4mC in an aqueous solution outside of the enzyme is 20.4 kcal/mol, which is lower than the calculated one inside the enzyme, but the demethylated product is more stable inside the enzyme, possibly due to the extra stabilization from the protein environment.

The results delineate the fine and delicate changes in interactions in the active site and beyond that are involved in the TET2-catalyzed oxidation of unnatural cytosine alkylations in dsDNA. The study provides an insight into the nature of the delicate but important differences between the key catalytic interactions involved in the catalysis of the unnatural substrates in comparison to the natural substrates. Overall, the study explains the atomistic and electronic structural mechanism of the substrate promiscuity of TET2 and its catalytic strategy as an indirect and direct demethylase.

## 5.5 References

- (1) Tsiouplis, N. J.; Bailey, D. W.; Chiou, L. F.; Wissink, F. J.; Tsagaratou, A. TET-Mediated Epigenetic Regulation in Immune Cell Development and Disease. *Front. Cell Dev. Biol.* **2021**, *8*, 623948.
- (2) Mahfoudhi, E.; Talhaoui, I.; Cabagnols, X.; Della Valle, V.; Secardin, L.; Rameau, P.; Bernard, O. A.; Ishchenko, A. A.; Abbes, S.; Vainchenker, W.; Sapparbaev, M.; Plo, I. TET2-Mediated 5-Hydroxymethylcytosine Induces Genetic Instability and Mutagenesis. *DNA Repair* **2016**, *43*, 78–88.
- (3) Bird, A. DNA Methylation Patterns and Epigenetic Memory. *Genes Dev.* **2002**, *16* (1), 6–21.
- (4) Cimmino, L.; Abdel-Wahab, O.; Levine, R. L.; Aifantis, I. TET Family Proteins and Their Role in Stem Cell Differentiation and Transformation. *Cell Stem Cell* **2011**, *9* (3), 193–204.
- (5) Branco, M. R.; Ficz, G.; Reik, W. Uncovering the Role of 5-Hydroxymethylcytosine in the Epigenome. *Nat. Rev. Genet.* **2012**, *13* (1), 7–13.
- (6) Pastor, W. A.; Aravind, L.; Rao, A. TETonic Shift: Biological Roles of TET Proteins in DNA Demethylation and Transcription. *Nat. Rev. Mol. Cell Biol.* **2013**, *14* (6), 341–356.
- (7) Hu, L.; Li, Z.; Cheng, J.; Rao, Q.; Gong, W.; Liu, M.; Shi, Y. G.; Zhu, J.; Wang, P.; Xu, Y. Crystal Structure of TET2-DNA Complex: Insight into TET-Mediated 5mC Oxidation. *Cell* **2013**, *155* (7), 1545–1555.
- (8) Zheng, G.; Fu, Y.; He, C. Nucleic Acid Oxidation in DNA Damage Repair and Epigenetics. *Chem. Rev.* **2014**, *114* (8), 4602–4620.
- (9) Ghanty, U.; DeNizio, J. E.; Liu, M. Y.; Kohli, R. M. Exploiting Substrate Promiscuity To Develop Activity-Based Probes for Ten-Eleven Translocation Family Enzymes. *J. Am. Chem. Soc.* **2018**, *140* (50), 17329–17332.
- (10) Ghanty, U.; Wang, T.; Kohli, R. M. Nucleobase Modifiers Identify TET Enzymes as Bifunctional DNA Dioxygenases Capable of Direct N-Demethylation. *Angew. Chem. Int. Ed.* **2020**, *59* (28), 11312–11315.
- (11) (a) Fedeles, B. I.; Singh, V.; Delaney, J. C.; Li, D.; Essigmann, J. M. The AlkB Family of Fe(II)/ $\alpha$ -Ketoglutarate-Dependent Dioxygenases: Repairing Nucleic Acid Alkylation Damage and Beyond. *J. Biol. Chem.* **2015**, *290* (34), 20734–20742. (b) Waheed, S. O.; Ramanan, R.; Chaturvedi, S. S.; Ainsley, J.; Evison, M.; Ames, J. M.; Schofield, C. J.; Christov, C. Z.; Karabencheva-Christova, T. G. Conformational Flexibility Influences Structure–Function Relationships in Nucleic Acid N -Methyl Demethylases. *Org. Biomol. Chem.* **2019**, *17* (8), 2223–2231.
- (12) Waheed, S. O.; Chaturvedi, S. S.; Karabencheva-Christova, T. G.; Christov, C. Z. Catalytic Mechanism of Human Ten-Eleven Translocation-2 (TET2) Enzyme: Effects of Conformational Changes, Electric Field, and Mutations. *ACS Catal.* **2021**, *11* (7), 3877–3890.
- (13) Hausinger, R. P. Fe(II)/ $\alpha$ -Ketoglutarate-Dependent Hydroxylases and Related Enzymes. *Crit. Rev. Biochem. Mol. Biol.* **2004**, *39* (1), 21–68.

- (14) Schofield, C. J.; Zhang, Z. Structural and Mechanistic Studies on 2-Oxoglutarate-Dependent Oxygenases and Related Enzymes. *Curr. Opin. Struct. Biol.* **1999**, *9* (6), 722–731.
- (15) (a) Chaturvedi, S. S.; Ramanan, R.; Waheed, S. O.; Karabancheva-Christova, T. G.; Christov, C. Z. Structure-Function Relationships in KDM7 Histone Demethylases. In *Advances in Protein Chemistry and Structural Biology*; Elsevier, 2019; Vol. 117, pp 113–125. (b) Ramanan, R.; Waheed, S. O.; Schofield, C. J.; Christov, C. Z. What Is the Catalytic Mechanism of Enzymatic Histone N-Methyl Arginine Demethylation and Can It Be Influenced by an External Electric Field? *Chem. – Eur. J.* **2021**, *27* (46), 11827–11836.
- (16) Mitchell, A. J.; Dunham, N. P.; Martinie, R. J.; Bergman, J. A.; Pollock, C. J.; Hu, K.; Allen, B. D.; Chang, W.; Silakov, A.; Bollinger, J. M.; Krebs, C.; Boal, A. K. Visualizing the Reaction Cycle in an Iron(II)- and 2-(Oxo)-Glutarate-Dependent Hydroxylase. *J. Am. Chem. Soc.* **2017**, *139* (39), 13830–13836.
- (17) Waheed, S. O.; Ramanan, R.; Chaturvedi, S. S.; Lehnert, N.; Schofield, C. J.; Christov, C. Z.; Karabancheva-Christova, T. G. Role of Structural Dynamics in Selectivity and Mechanism of Non-Heme Fe(II) and 2-Oxoglutarate-Dependent Oxygenases Involved in DNA Repair. *ACS Cent. Sci.* **2020**, *6* (5), 795–814.
- (18) Chaturvedi, S. S.; Ramanan, R.; Lehnert, N.; Schofield, C. J.; Karabancheva-Christova, T. G.; Christov, C. Z. Catalysis by the Non-Heme Iron(II) Histone Demethylase PHF8 Involves Iron Center Rearrangement and Conformational Modulation of Substrate Orientation. *ACS Catal.* **2020**, *10* (2), 1195–1209.
- (19) Quesne, M. G.; Latifi, R.; Gonzalez-Ovalle, L. E.; Kumar, D.; de Visser, S. P. Quantum Mechanics/Molecular Mechanics Study on the Oxygen Binding and Substrate Hydroxylation Step in AlkB Repair Enzymes. *Chem. – Eur. J.* **2014**, *20* (2), 435–446.
- (20) Wójcik, A.; Radoń, M.; Borowski, T. Mechanism of O<sub>2</sub> Activation by  $\alpha$ -Ketoglutarate Dependent Oxygenases Revisited. A Quantum Chemical Study. *J. Phys. Chem. A* **2016**, *120* (8), 1261–1274.
- (21) Song, X.; Lu, J.; Lai, W. Mechanistic Insights into Dioxygen Activation, Oxygen Atom Exchange and Substrate Epoxidation by AsqJ Dioxygenase from Quantum Mechanical/Molecular Mechanical Calculations. *Phys. Chem. Chem. Phys.* **2017**, *19* (30), 20188–20197.
- (22) Kavooosi, S.; Sudhamalla, B.; Dey, D.; Shriver, K.; Arora, S.; Sappa, S.; Islam, K. Site- and Degree-Specific C–H Oxidation on 5-Methylcytosine Homologues for Probing Active DNA Demethylation. *Chem. Sci.* **2019**, *10* (45), 10550–10555.
- (23) Thornburg, L. D.; Stubbe, J. Mechanism-Based Inactivation of Thymine Hydroxylase, an  $\alpha$ -Ketoglutarate-Dependent Dioxygenase, by 5-Ethynyluracil. *Biochemistry* **1993**, *32* (50), 14034–14042.
- (24) Thornburg, L. D.; Lai, M. T.; Wishnok, J. S.; Stubbe, J. A Non-Heme Iron Protein with Heme Tendencies: An Investigation of the Substrate Specificity of Thymine Hydroxylase. *Biochemistry* **1993**, *32* (50), 14023–14033.
- (25) Ghanty, U.; Serrano, J. C.; Kohli, R. M. Harnessing Alternative Substrates to Probe TET Family Enzymes. In *TET Proteins and DNA Demethylation*; Bogdanovic, O., Vermeulen, M., Eds.; Methods in Molecular Biology; Springer US: New York, NY, 2021; Vol. 2272, pp 265–280.

- (26) Fiser, A.; Šali, A. Modeller: Generation and Refinement of Homology-Based Protein Structure Models. In *Methods in Enzymology*; Elsevier, 2003; Vol. 374, pp 461–491.
- (27) Olsson, M. H. M.; Søndergaard, C. R.; Rostkowski, M.; Jensen, J. H. PROPKA3: Consistent Treatment of Internal and Surface Residues in Empirical p  $K_a$  Predictions. *J. Chem. Theory Comput.* **2011**, 7 (2), 525–537.
- (28) Case, D.A.; Betz, R.M.; Curetti, D.S.; Cheatham, T.E.; Daeden, T.A.; Duke, R.E.; Giese, T.J.; Gohlke, H.; Goetz, A.W.; Homeyer, N.; Izadi, S.; Janowski, P.; Kaus, J.; Kovalenko, A.; Lee, T.S.; LeGrand, S.; Li, P.; Lin, C.; Luchko, T.; Luo, R.; Madej, B. P. A. AMBER 2018. University of California: San Francisco; **2018**.
- (29) Wang, J.; Wang, W.; Kollman, P. A.; Case, D. A. Automatic Atom Type and Bond Type Perception in Molecular Mechanical Calculations. *J. Mol. Graph. Model.* **2006**, 25 (2), 247–260.
- (30) Li, P.; Merz, K. M. MCPB.Py: A Python Based Metal Center Parameter Builder. *J. Chem. Inf. Model.* **2016**, 56 (4), 599–604.
- (31) Chaturvedi, S. S.; Ramanan, R.; Waheed, S. O.; Ainsley, J.; Evison, M.; Ames, J. M.; Schofield, C. J.; Karabencheva-Christova, T. G.; Christov, C. Z. Conformational Dynamics Underlies Different Functions of Human KDM7 Histone Demethylases. *Chem. – Eur. J.* **2019**, 25 (21), 5422–5426.
- (32) Bian, K.; Lenz, S. A. P.; Tang, Q.; Chen, F.; Qi, R.; Jost, M.; Drennan, C. L.; Essigmann, J. M.; Wetmore, S. D.; Li, D. DNA Repair Enzymes ALKBH2, ALKBH3, and AlkB Oxidize 5-Methylcytosine to 5-Hydroxymethylcytosine, 5-Formylcytosine and 5-Carboxylcytosine in Vitro. *Nucleic Acids Res.* **2019**, 47 (11), 5522–5529.
- (33) Solomon, E. I. Geometric and Electronic Structure Contributions to Function in Bioinorganic Chemistry: Active Sites in Non-Heme Iron Enzymes. *Inorg. Chem.* **2001**, 40 (15), 3656–3669.
- (34) Solomon, E. I.; Light, K. M.; Liu, L. V.; Srnec, M.; Wong, S. D. Geometric and Electronic Structure Contributions to Function in Non-Heme Iron Enzymes. *Acc. Chem. Res.* **2013**, 46 (11), 2725–2739.
- (35) Fang, D.; Lord, R. L.; Cisneros, G. A. *Ab Initio* QM/MM Calculations Show an Intersystem Crossing in the Hydrogen Abstraction Step in Dealkylation Catalyzed by AlkB. *J. Phys. Chem. B* **2013**, 117 (21), 6410–6420.
- (36) Peters, M. B.; Yang, Y.; Wang, B.; Füsti-Molnár, L.; Weaver, M. N.; Merz, K. M. Structural Survey of Zinc-Containing Proteins and Development of the Zinc AMBER Force Field (ZAFF). *J. Chem. Theory Comput.* **2010**, 6 (9), 2935–2947.
- (37) Jorgensen, W. L.; Chandrasekhar, J.; Madura, J. D.; Impey, R. W.; Klein, M. L. Comparison of Simple Potential Functions for Simulating Liquid Water. *J. Chem. Phys.* **1983**, 79 (2), 926–935.
- (38) Davidchack, R. L.; Ouldridge, T. E.; Tretyakov, M. V. New Langevin and Gradient Thermostats for Rigid Body Dynamics. *J. Chem. Phys.* **2015**, 142 (14), 144114.
- (39) Bresme, F. Equilibrium and Nonequilibrium Molecular-Dynamics Simulations of the Central Force Model of Water. *J. Chem. Phys.* **2001**, 115 (16), 7564–7574.

- (40) Ryckaert, J.-P.; Ciccotti, G.; Berendsen, H. J. C. Numerical Integration of the Cartesian Equations of Motion of a System with Constraints: Molecular Dynamics of n-Alkanes. *J. Comput. Phys.* **1977**, *23* (3), 327–341.
- (41) Deserno, M.; Holm, C. How to Mesh up Ewald Sums. I. A Theoretical and Numerical Comparison of Various Particle Mesh Routines. *J. Chem. Phys.* **1998**, *109* (18), 7678–7693.
- (42) Götz, A. W.; Williamson, M. J.; Xu, D.; Poole, D.; Le Grand, S.; Walker, R. C. Routine Microsecond Molecular Dynamics Simulations with AMBER on GPUs. 1. Generalized Born. *J. Chem. Theory Comput.* **2012**, *8* (5), 1542–1555.
- (43) Maier, J. A.; Martinez, C.; Kasavajhala, K.; Wickstrom, L.; Hauser, K. E.; Simmerling, C. Ff14SB: Improving the Accuracy of Protein Side Chain and Backbone Parameters from Ff99SB. *J. Chem. Theory Comput.* **2015**, *11* (8), 3696–3713.
- (44) Roe, D. R.; Cheatham, T. E. PTRAJ and CPPTRAJ: Software for Processing and Analysis of Molecular Dynamics Trajectory Data. *J. Chem. Theory Comput.* **2013**, *9* (7), 3084–3095.
- (45) Grant, B. J.; Rodrigues, A. P. C.; ElSawy, K. M.; McCammon, J. A.; Caves, L. S. D. Bio3d: An R Package for the Comparative Analysis of Protein Structures. *Bioinformatics* **2006**, *22* (21), 2695–2696.
- (46) Sherwood, P.; de Vries, A. H.; Guest, M. F.; Schreckenbach, G.; Catlow, C. R. A.; French, S. A.; Sokol, A. A.; Bromley, S. T.; Thiel, W.; Turner, A. J.; Billeter, S.; Terstegen, F.; Thiel, S.; Kendrick, J.; Rogers, S. C.; Casci, J.; Watson, M.; King, F.; Karlsen, E.; Sjøvoll, M.; Fahmi, A.; Schäfer, A.; Lennartz, C. QUASI: A General Purpose Implementation of the QM/MM Approach and Its Application to Problems in Catalysis. *J. Mol. Struct. THEOCHEM* **2003**, *632* (1–3), 1–28.
- (47) Ahlrichs, R.; Bär, M.; Häser, M.; Horn, H.; Kölmel, C. Electronic Structure Calculations on Workstation Computers: The Program System Turbomole. *Chem. Phys. Lett.* **1989**, *162* (3), 165–169.
- (48) Smith, W.; Forester, T. R. DL\_POLY\_2.0: A General-Purpose Parallel Molecular Dynamics Simulation Package. *J. Mol. Graph.* **1996**, *14* (3), 136–141.
- (49) Sousa, S. F.; Ribeiro, A. J. M.; Neves, R. P. P.; Brás, N. F.; Cerqueira, N. M. F. S. A.; Fernandes, P. A.; Ramos, M. J. Application of Quantum Mechanics/Molecular Mechanics Methods in the Study of Enzymatic Reaction Mechanisms. *WIREs Comput. Mol. Sci.* **2017**, *7*, e1281.
- (50) Kästner, J.; Carr, J. M.; Keal, T. W.; Thiel, W.; Wander, A.; Sherwood, P. DL-FIND: An Open-Source Geometry Optimizer for Atomistic Simulations. *J. Phys. Chem. A* **2009**, *113* (43), 11856–11865.
- (51) Grimme, S.; Antony, J.; Ehrlich, S.; Krieg, H. A. A consistent and accurate ab initio parametrization of density functional dispersion correlation (DFT-D) for the 94 elements H-Pu. *Phys. Chem. Chem. Phys.* **2000**, *2* (10), 2177–2186.
- (52) Billeter, S. R.; Turner, A. J.; Thiel, W. Linear Scaling Geometry Optimisation and Transition State Search in Hybrid Delocalised Internal Coordinates. *J. Chem. Phys.* **2010**, *132*, 154104.
- (53) Cisneros, G. A.; Perera, L.; Schaaper, R. M.; Pedersen, L. C.; London, R. E.; Pedersen, L. G.; Darden, T. A. Reaction Mechanism of the  $\epsilon$  Subunit of *E. Coli* DNA

Polymerase III: Insights into Active Site Metal Coordination and Catalytically Significant Residues. *J. Am. Chem. Soc.* **2009**, *131* (4), 1550–1556.

(54) Torabifard, H.; Cisneros, G. A. Insight into Wild-Type and T1372E TET2-Mediated 5hmC Oxidation Using *Ab Initio* QM/MM Calculations. *Chem. Sci.* **2018**, *9* (44), 8433–8445.

(55) Leddin, E. M.; Cisneros, G. A. Comparison of DNA and RNA Substrate Effects on TET2 Structure. In *Advances in Protein Chemistry and Structural Biology*; Elsevier, 2019; Vol. 117, pp 91–112.

(56) Fu, Y.; Jia, G.; Pang, X.; Wang, R. N.; Wang, X.; Li, C. J.; Smemo, S.; Dai, Q.; Bailey, K. A.; Nobrega, M. A.; Han, K.-L.; Cui, Q.; He, C. FTO-Mediated Formation of N6-Hydroxymethyladenosine and N6-Formyladenosine in Mammalian RNA. *Nat. Commun.* **2013**, *4*, 1798.

(57) (a) Ma, G.; Zhu, W.; Su, H.; Cheng, N.; Liu, Y. Uncoupled Epimerization and Desaturation by Carbapenem Synthase: Mechanistic Insights from QM/MM Studies. *ACS Catal.* **2015**, *5* (9), 5556–5566. (b) Light, K. M.; Hangasky, J. A.; Knapp, M. J.; Solomon, E. I. Spectroscopic Studies of the Mononuclear Non-heme Fe<sup>II</sup> Enzyme FIH: Second-Sphere Contributions to Reactivity. *J. Am. Chem. Soc.* **2013**, *135*, 9665–9674.

(58) Su, H.; Sheng, X.; Zhu, W.; Ma, G.; Liu, Y. Mechanistic Insights into the Decoupled Desaturation and Epoxidation Catalyzed by Dioxygenase AsqJ Involved in the Biosynthesis of Quinolone Alkaloids. *ACS Catal.* **2017**, *7* (8), 5534–5543.

(59) Balsera, M. A.; Wriggers, W.; Oono, Y.; Schulten, K. Principal Component Analysis and Long Time Protein Dynamics. *J. Phys. Chem.* **1996**, *100* (7), 2567–2572.

(60) (a) Hünenberger, P. H.; Mark, A. E.; van Gunsteren, W. F. Fluctuation and Cross-Correlation Analysis of Protein Motions Observed in Nanosecond Molecular Dynamics Simulations. *J. Mol. Biol.* **1995**, *252* (4), 492–503. (b) Su, H.; Sheng, X.; Zhu, W.; Ma, G.; Liu, Y. Mechanistic Insights into the Decoupled Desaturation and Epoxidation Catalyzed by Dioxygenase AsqJ Involved in the Biosynthesis of Quinolone Alkaloids. *ACS Catal.* **2017**, *7* (8), 5534–5543.

(61) Wang, B.; Cao, Z.; Sharon, D. A.; Shaik, S. Computations Reveal a Rich Mechanistic Variation of Demethylation of *N*-Methylated DNA/RNA Nucleotides by FTO. *ACS Catal.* **2015**, *5* (12), 7077–7090.

(62) Wang, B.; Usharani, D.; Li, C.; Shaik, S. Theory Uncovers an Unusual Mechanism of DNA Repair of a Lesioned Adenine by AlkB Enzymes. *J. Am. Chem. Soc.* **2014**, *136* (39), 13895–13901.

(63) Shaik, S.; Chen, H.; Janardanan, D. Exchange-Enhanced Reactivity in Bond Activation by Metal–Oxo Enzymes and Synthetic Reagents. *Nat. Chem.* **2011**, *3* (1), 19–27.

(64) Neidig, M. L.; Decker, A.; Choroba, O. W.; Huang, F.; Kavana, M.; Moran, G. R.; Spencer, J. B.; Solomon, E. I. Spectroscopic and Electronic Structure Studies of Aromatic Electrophilic Attack and Hydrogen-Atom Abstraction by Non-Heme Iron Enzymes. *Proc. Natl. Acad. Sci.* **2006**, *103* (35), 12966–12973.

(65) Sappa, S.; Dey, D.; Sudhamalla, B.; Islam, K. Catalytic Space Engineering as a Strategy to Activate C–H Oxidation on 5-Methylcytosine in Mammalian Genome. *J. Am. Chem. Soc.* **2021**, *143* (31), 11891–11896.

- (66) Sudhamalla, B.; Wang, S.; Snyder, V.; Kavooosi, S.; Arora, S.; Islam, K. Complementary Steric Engineering at the Protein–Ligand Interface for Analogue-Sensitive TET Oxygenases. *J. Am. Chem. Soc.* **2018**, *140* (32), 10263–10269.
- (67) Liu, M. Y.; Torabifard, H.; Crawford, D. J.; DeNizio, J. E.; Cao, X.-J.; Garcia, B. A.; Cisneros, G. A.; Kohli, R. M. Mutations along a TET2 Active Site Scaffold Stall Oxidation at 5-Hydroxymethylcytosine. *Nat. Chem. Biol.* **2017**, *13* (2), 181–187.
- (68) Shishodia, S.; Zhang, D.; El-Sagheer, A. H.; Brown, T.; Claridge, T. D. W.; Schofield, C. J.; Hopkinson, R. J. NMR analyses on N-hydroxymethylated nucleobases - implications for formaldehyde toxicity and nuclei acid demethylases. *Org. Biomol. Chem.* **2018**, *16*(21), 4021-4032.
- (69) Lawal, M. M.; Sanusi, Z. K.; Govender, T.; Tolufashe, G. F.; Maguire, G. E. M.; Honarparvar, B.; Kruger, H. G. Unraveling the concerted mechanism of the human immunodeficiency virus type 1 (HIV-1) protease: a hybrid QM/MM study. *Struct. Chem.* **2019**, *30*, 409-417.
- (70) Wallin, G.; Aqvist, J. The transition state for peptide bond formation reveals the ribosome as a water trap. *Proc. Natl. Acad. Sci USA* **2010**, *107*(5), 1888-1893.
- (71) Christov, C. Z.; Lodola, A.; Karabencheva-Christova, T. G.; Wan, S.; Coveney, P. V.; Mulholland, A. J. Conformational effects on the pro-S hydrogen abstraction reaction in cyclooxygenase-1: an integrated QM/MM and MD study. *Biophys. J.* **2013**, *104*(5), L5-7.
- (72) Claeysens, F.; Ranaghan, K. E.; Manby, F. R.; Harvey, J. N.; Mulholland, A. J. Multiple high-level QM/MM reaction paths demonstrate transition-state stabilization in chorismate mutase: correlation of barrier height with transition-state stabilization. *Chem. Commun.* **2005**, 5068-5070.

## 6 What is The Catalytic Mechanism of Enzymatic Histone N-Methyl Arginine Demethylation and Can it be Influenced by an External Electric Field?

Rajeev Ramanan,<sup>a,b,&</sup> **Sodiq O. Waheed**,<sup>a,&</sup> Christopher J. Schofield,<sup>c</sup> and Christo Z. Christov<sup>a,\*</sup>

[a] Dr. R. Ramanan, S. O. Waheed, Dr. C. Z. Christov

Department of Chemistry, Michigan Technological University, Houghton, Michigan 49931, United States.

[b] Present address: Dr. R. Ramanan

Department of Chemistry, National Institute of Technology, Rourkela, Odisha 769001, India.

[c] Prof. Dr. C. J. Schofield

The Department of Chemistry and the Ineos Oxford Institute for Antimicrobial Research, The Chemistry Research Laboratory, Mansfield Road, University of Oxford, OX1 5JJ,

United Kingdom.

&R.R. and S.O.W. made equal contributions to this article.

\*Corresponding author: christov@mtu.edu

---

The content of this chapter was previously published in the *Chem. Eur. J.* **2021**, 27, 11827-11836. DOI: 10.1002/chem.202101174, reproduced with permission from Wiley-VCH. The work was selected as the Front Cover and Cover Profile of the August 2021 Issue of the Journal.



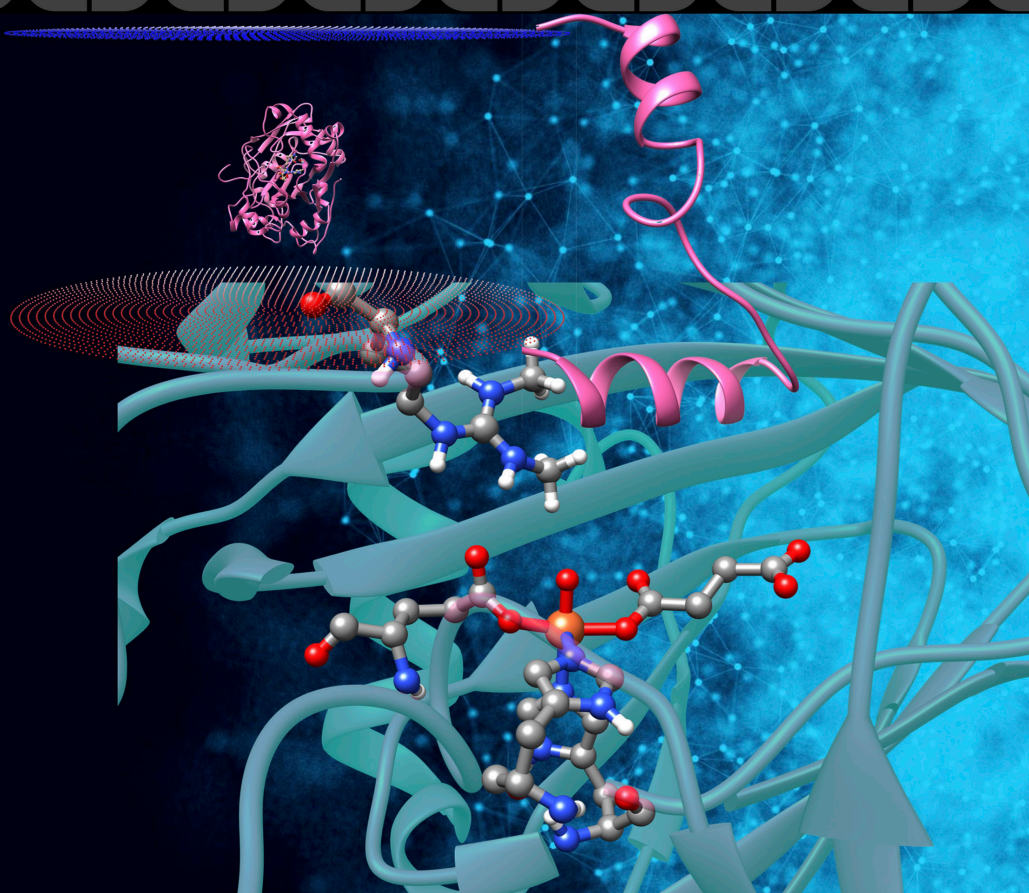
# Chemistry A European Journal

 **Chemistry  
Europe**  
European Chemical  
Societies Publishing

**Front Cover:**

*C. Z. Christov et al.*

What Is the Catalytic Mechanism of Enzymatic Histone N-Methyl Arginine Demethylation and Can It Be Influenced by an External Electric Field?



© Library of [1501/2021]. See the Terms and Conditions (<https://onlinelibrary.wiley.com/terms-and-conditions>) on Wiley Online Library for rules of use; OA articles are governed by the applicable Creative Commons License.

46/2021

WILEY-VCH

## 6.1 Introduction

Epigenetic processes regulate normal eukaryotic development and dysregulation of them correlate with human diseases, including brain disorders and cancer.<sup>[1,2]</sup> Methylation and demethylation of N-methylated lysine- and arginine-residues histone tails in nucleosomes are dynamic events that regulate transcription.<sup>[1,2]</sup> The non-heme Fe(II) and 2-oxoglutarate (2OG)-dependent Jumonji-C (JmjC) oxygenases are the largest family of N<sup>ε</sup>-methyl lysine histone demethylases (KDMs).<sup>[3-5]</sup> In humans, there are 60-70 2OG-oxygenases, which have roles in processes including fatty acid metabolism, the hypoxic response, collagen biosynthesis, and translational regulation.<sup>[6,7]</sup>

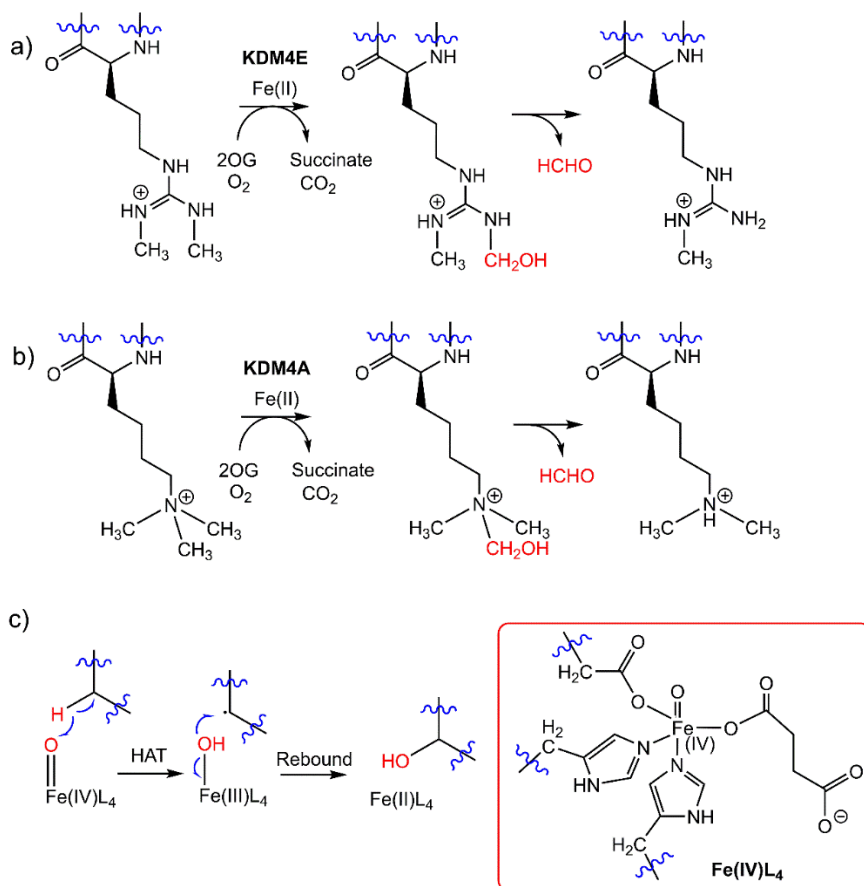
In addition to the histone lysine demethylase (KDM) activities of some JmjC 2OG-oxygenases, recent in vitro studies have identified arginine demethylase (RDM) activities for some, but not all, JmjC KDMs, including for KDM3A, KDM4A, KDM4E, KDM5C, and KDM6B.<sup>[8]</sup> Arginine methylation can modulate binding of histones with ‘reader’ domain containing proteins,<sup>[9]</sup> so regulating transcription.<sup>[10,11]</sup> Arginine methylation can also inhibit lysine methylation; it is, e.g., reported that the H3R2me2a mark hinders mixed-lineage leukemia 1 (MLL1) cells from methylating H3K4me3.<sup>[10]</sup>

The mechanisms of dioxygen activation by non-heme Fe (II) enzymes have been explored using experimental and computational methods;<sup>[2,12-14]</sup> however, there are no such studies reported on the recently reported JmjC KDM catalyzed histone arginine demethylation (RDM) reaction.<sup>[15-17]</sup> The 2OG oxygenases have evolved to activate O<sub>2</sub> to enable production of a ferryl intermediate that effects C-H bond cleavage, typically generating an

alcohol product.<sup>[7,12-14]</sup> Details of the mechanism leading to the ferryl intermediate and studies on model systems have been reported.<sup>[15-26a]</sup> Following substrate binding, the consensus 2OG oxygenase mechanism<sup>[7,12-26a-c]</sup> involves initial generation of a Fe(III)-superoxo complex; oxidative decarboxylation of 2OG generates a Fe(II)-peroxysuccinate intermediate which reacts to give a high-spin (S=2) state ferryl intermediate, which abstracts a hydrogen atom from the substrate. Hydrogen atom transfer (HAT) through a high spin surface is favored by spin exchange enhanced reactivity at the transition state,<sup>[27,28a]</sup> generating an Fe(III)-hydroxyl intermediate that undergoes a low barrier hydroxyl rebound reaction with the substrate radical carbon to complete hydroxylation [Scheme 6.1]. Despite the apparent observance of the consensus mechanism by many of its members, the 2OG oxygenase family accepts both small and large molecule substrates, catalyzing a large range of two-electron oxidations with differences in regio- and stereo-selectivities.<sup>[6,12]</sup>

KDM4E [Figure 6.1] is a JmjC 2OG oxygenase that in addition to KDM activity, at least in isolated form, also has RDM activity, including as shown by its demethylation of a histone H4 fragment with a symmetrically demethylated arginine at residue R3 (H4R3me2s).<sup>[8]</sup> The mechanisms of histone lysine demethylation (KDM) by 2OG-demethylases have been recently explored,<sup>[15,16,18]</sup> providing insights into their reaction mechanisms, alternative mechanistic strategies, residues that stabilize the transition states, and long-range correlated motions involved in their catalysis. KDM4E is a relatively efficient arginine demethylase (RDM), while KDM4A is a relatively more efficient lysine demethylase (KDM).<sup>[8]</sup> The mechanism of histone lysine demethylation catalyzed by

KDM4A<sup>[18]</sup> has been explored, but the previous study did not include the new RDM activity. Elucidating mechanistic differences between the RDM and KDM reactions may in the long term enable strategies for selective modulation of either the RDM or KDM activities. Here we report investigations on the differences in active site interactions in KDM4E and KDM4A that might in part account for the differences in their KDM and RDM selectivity.



**Scheme 6.1.** Outline mechanisms for arginine- and lysine-demethylation by the JmjC 2OG oxygenases. a) KDM4E catalyzed demethylation of a symmetrically N-dimethylated arginine residue. b) KDM4A catalyzed demethylation of an N-trimethylated lysine residue.

c) Hydrogen atom transfer (HAT) and rebound steps in the C-H bond cleavage step by the ferryl intermediate, coordination of which is shown in the inset.

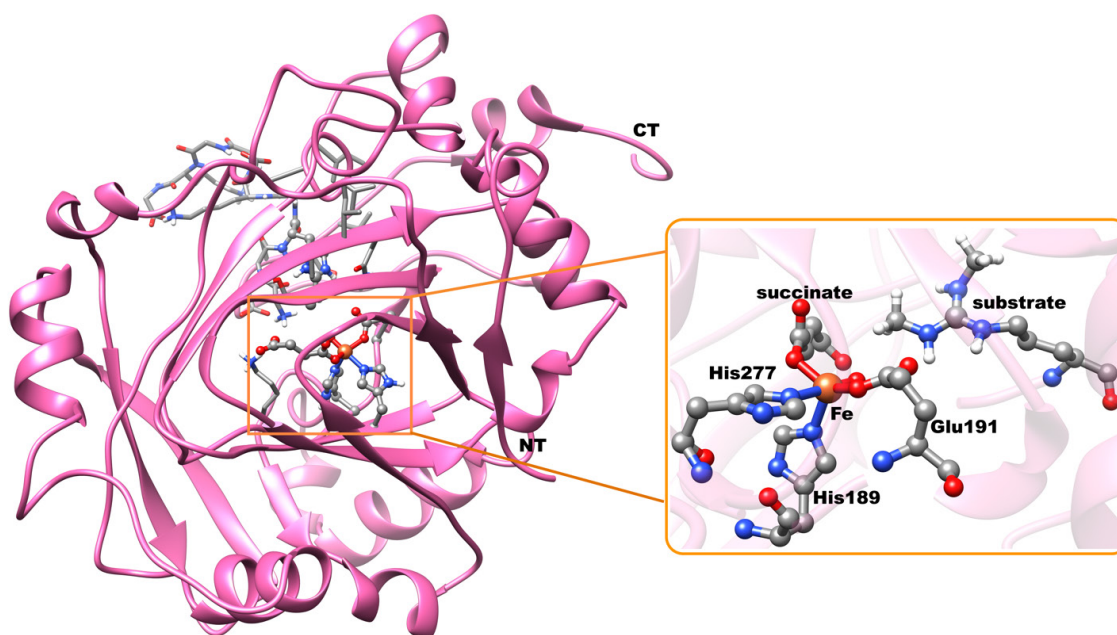


**Figure 6.1.** Model of KDM4E at the Fe(IV)=O intermediate state. The active site is shown in the inset. The QM region contains the imidazole groups of His189 and His277, the Fe and oxo atoms of Fe(IV)=O, the Glu191 sidechain, succinate, and the dimethyl guanidinium group of the substrate. NT and CT are the N- and C-termini, respectively.

We performed computational molecular dynamics (MD) and quantum mechanical and molecular mechanical (QM/MM) studies on substrate binding and mechanism of the KDM4E RDM activity. We investigated alternative mechanistic proposals, i.e., C-H or N-H hydrogen abstraction, and explored the effects of long-range interactions. We also explored the effects of applying an external electric field (EEF) on the reaction mechanism and product selectivity.<sup>[28b-g]</sup> Comparison of the results for the RDM activity of KDM4E

with the KDM activity of KDM4A imply both proceed via ferryl mediated C-H abstraction, but that there are differences in the interactions leading to the formation of intermediates.

## 6.2 Methods

### 6.2.1 System Setup and MD Simulation

KDM4E is a human KDM4 family JmjC KDM that catalyzes histone H3 K9me3/2 N<sup>ε</sup>-methyl lysine demethylation.<sup>[29,30]</sup> The available crystal structure of KDM4E does not contain the histone substrate. However, KDM4A has been crystallized with a fragment of the H4 histone tail (H4(1-9)R3me2s ) that contains an N-methylated arginine substrate (PDB ID: 5FWE).<sup>[29]</sup> KDM4E and KDM4A are related (66% amino acid identity) with some key differences in the binding sites. Aiming to understand the catalytic mechanism and interactions in the more effective RDM enzyme, we chose to work with KDM4E and complemented the lack of an experimental enzyme-substrate structure of KDM4E by modeling.

The substrate H4(1-9)R3me2s coordinates from the KDM4A structure were superimposed on a KDM4E structure modeled at the ferryl oxidation state (based on a KDM4E crystal structure (PDB ID: 2w2i).<sup>[31]</sup> The overlaid structures gave an RMSD of 0.651 Å [Figure E1]. The Ni in the KDM4E crystal structure was replaced with an Fe and the 2OG analogue pyridine-2,4-dicarboxylic acid (PD2) was manually modified to succinate [Figure E2]. Missing hydrogen atoms were added to the protein followed by neutralization with an appropriate number of counter ions were performed using the Leap module of Amber16.<sup>[32]</sup>

Antechamber as implemented in Amber was used to generate parameters for non-standard ligands /residues such as succinate and substrate. The Metal Center Parameter Builder (MCPB.py) program was used to generate parameters for the metal (Fe(IV)-oxo) intermediate.<sup>[33a]</sup> The high spin state of Fe (S=2, M=5) was assigned to the ground state, based on previous studies with KDM4A, KDM7B(PHF8), AlkB, AlkBH2 and other 2OG oxygenases.<sup>[16-18,33b-e]</sup> The active site Fe is ligated by a monodentate chelating succinate, two histidine residues (His189 and His277) and one glutamic acid, Glu191 (monodentate) [Figure E3], as revealed by crystallographic studies of KDM4E.<sup>[29,31]</sup>

Note that in addition to the iron binding, active site, the KDM4 KDMs contain a zinc binding site (Zn binding residues are Cys234, His240, Cys306, and Cys308 in KDM4A) as observed crystallographically.<sup>[29]</sup> In the case of the KDM4E crystal structure (PDB 2W2I) on which our modeling studies were based, the zinc binding site was not apparent, hence was not included in our studies, which focused on the catalytic importance of the interactions in the active site.

MD simulations were performed with the FF14SB force field.<sup>[34]</sup> The protein was fully immersed in a rectangular box made of TIP3P water molecules.<sup>[35]</sup> The edge of the box was kept 10 Å away from the protein surface. Periodic boundary conditions were used for MD simulations. Long-range electrostatic interactions were calculated using the Particle Mesh Ewald (PME) method with a direct space and vdW cut-off of 10 Å.<sup>[36]</sup> Initial energy minimizations were performed in two steps, i.e., first the steepest descent for 5000 steps, followed by the conjugate gradient method for another 5000 steps. Solute molecules were

restrained using a potential of 500 kcal/mol  $\text{\AA}^2$  in the first minimization where only the solvent and counterions were allowed to minimize. A full minimization of the entire protein and solvents with steepest descent (5000 steps) and conjugate gradient (5000 steps) was carried out. The CPU version of the Amber16 code (SANDER) was used for energy minimization. The temperature of the system was gradually increased from 0 to 300 K in an NVT ensemble for 100 ps. The system was subsequently run for 1ns in an NPT ensemble. The temperature was kept constant at 300 K and pressure at 1.0 atm, using Langevin-thermostat<sup>[37]</sup> and Barendsen barostat<sup>[38]</sup> with a pressure relaxation time of 1 ps. Before moving to the final productive simulations, equilibration for  $\sim 3$  ns was performed. The SHAKE algorithm was used to constrain all bonds with hydrogen.<sup>[39]</sup> Production MD runs were performed for 1000 ns in an NPT ensemble with a target pressure set at 1 bar and a constant pressure coupling of 2ps. Two other replicas simulations were performed at different initial velocities and the production runs were done for 300 ns [Figure E4]. The GPU version of the Amber16 code (PMEMD) was used for the final productive molecular dynamics simulations.<sup>[32]</sup>

## 6.2.2 QM/MM Calculations

The quantum mechanical (QM) region in the hybrid quantum mechanical/molecular mechanics (QM/MM) calculations included the Fe, the ferryl O, the imidazole sidechains of both coordinating histidines, the glutamate sidechain from the gamma carbon, succinate, and the substrate residue (methylated arginine H4(1-9)R3me2s). The QM region contains a total of 60 atoms; 4 linked hydrogen atoms were used to complete the valences of bonds



spanning between the QM and the MM regions. The ChemShell suite of programs was used for QM/MM calculations.<sup>[40,41]</sup> The QM calculations were performed with Turbomole,<sup>[42]</sup> and MM calculations with DL\_POLY software.<sup>[43]</sup> The Amber force fields generated for the MD simulation were used in DL\_POLY. The electronic embedding scheme was employed to calculate the polarizing effect of the enzyme on the QM region.<sup>[44]</sup> The B3LYP<sup>[45]</sup> functional with the def2-SVP basis set (B1) was used for all geometry optimizations, which can yield accurate barriers and proper electronic structure for Fe metal containing systems.<sup>[16-18,46]</sup> As in previous studies, transition states were defined by two step calculations. At first, a relaxed potential energy surface (adiabatic mapping) scan was performed by gradually changing the reaction coordinate.<sup>[16-18]</sup> The highest energy point on the scanned surface was used as an initial guess for the final TS optimization. The DL-find optimizer implemented in Chemshell was used for reactant optimization and scanning,<sup>[47]</sup> while the HDLC optimizer was used for the final TS optimization.<sup>[48]</sup> The local minimum and the first-order saddle points were verified with frequency calculations. The B3LYP/def2-TZVP level of theory (B2) single point calculations were used to refine the final energies.<sup>[16-18]</sup> The Grimme's D3 dispersion correction<sup>[49a]</sup> is applied in single-point calculations and the energy profile is presented in the supporting information. The external electric fields (EEFs) were applied for the QM/MM calculations using TITAN code<sup>[49b]</sup> as in other studies.<sup>[50,51]</sup> The TITAN code was used to generate uniform electric fields on the entire model of the enzyme used for the QM/MM calculations [Figures E5-E6]. To achieve this, two circular parallel charge plates were generated, consisting of 7082 point charges in total with 3541 positive charges and 3541 negative charges. The distance between the

center of the plate and the Fe atom is 46.8 Å and the radius of the plate is 92.4 Å. The solvated enzyme-substrate complex with the added point charges were subjected to QM/MM reaction path calculations using ChemShell, accounting for the polarization effect of the added new point charges on the QM Hamiltonian in addition to the already incorporated effect of the point charges of the MM part (protein and water atoms).

## 6.3 Results and Discussion

### 6.3.1 Dynamics and Substrate Binding in the Histone H4 Tail with N-Methylated Arginine by KDM4E

To investigate KDM4E substrate interactions, we performed a 1 μs MD simulation and two other replicas simulations for 300 ns each at different initial velocities of the KDM4E.H4(1-9)R3me2s complex at the ferryl intermediate stage [Figure E4], the primary coordination sphere of which is given in Scheme 6.1. The replicas showed very similar RMSD profiles to the initial simulation. As with the KDM activity of KDM4A, with KDM4E, the Fe(IV)-oxo is coordinated by two histidines (His189 and His277), a glutamate (Glu191), and a succinate oxygen, in each case in a monodentate manner. Also, similarly to KDM4A, the non-coordinating 'C-1' oxygen of succinate is stabilized by interactions with Tyr133/Lys207; Phe186 makes CH-π interactions with the succinate methylenes. The non-coordinating oxygen of Glu191 is stabilized by a hydrogen bond with Asn291, which in turn is hydrogen bonded with Ser197. Stabilization of succinate and the non-coordinating oxygens of Fe-ligating Glu- or Asp residues is a common feature in 2OG oxygenases. For example, as for KDM4E, with the JmjC KDMs PHF8<sup>[30]</sup> and KDM4A,<sup>[52]</sup>

the non-coordinating oxygen of the Fe-ligating Asp (in PHF8)/Glu (in KDM4A) is stabilized by hydrogen bonding with an Asn residue, while in AlkB and AlkBH2 an Arg residue is employed to do this [Figures E7-E9].<sup>[53-56]</sup> The non-coordinating succinate carboxylate is positioned to interact with Lys207, Tyr133, again similarly to the analogous intermediate in KDM catalysis by KDM4A. Overall, the coordinating environment of the iron center employed in the RDM reaction of KDM4E appears to be very similar to that of the KDM reaction of KDM4A.

The symmetrically dimethylated arginine (R3me2s) of the H4 histone tail binds deeply within the KDM4E active site, as observed in structures of KDM4A complexed with substrates including H4(1-9)R3me2s.<sup>[29]</sup> The MD simulations [Figure 6.2b] with KDM4E imply the crystallographically observed binding mode is stable. After the first 100ns of simulation, the symmetrically substituted N-methyl arginine groups occupy distinct regions, with one close to the ferryl oxygen and one directed away from it [Figure 6.2a and b].

Note that although irrelevant in the case of the symmetrically substituted N-methyl arginine substrate studied here, previous reports show KDM4E, like some other JmjC KDMs, can oxidize ‘asymmetrically substituted’ substrate analogues, e.g., Lys derivatized with N $\epsilon$  Me and isopropyl groups, raising issues of chemo- and regio-selectivity (KDM4E selective hydroxylation of the isopropyl occurs).<sup>[57]</sup> In such cases, the preferred binding mode of the different alkyl groups likely contributes to the observed regioselectivity (along with relative C-H bond strengths).<sup>[57]</sup>

The KDM4E residues preceding Asn291, i.e., Ile290, Ala289, appear to form a rim around the dimethylguanidium group of dimethylated arginine substrate [Figure 6.3] and likely contribute to the rigidity of the active site restricting substrate arginine side chain movement [Figure 6.2b]. Lys242, Tyr178, and Asn291 are second sphere residues that help orient the symmetrically substituted N-methyl arginine substrate sidechain in the active site [Figure 6.3].

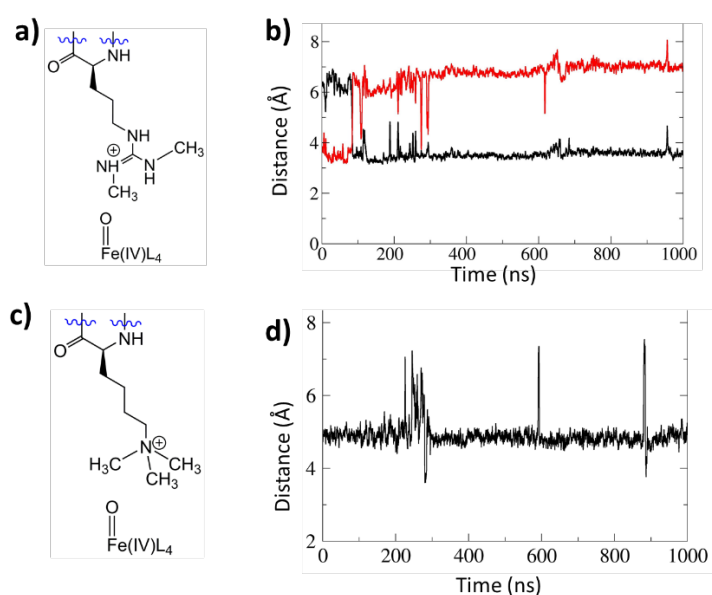


**Figure 6.2.** Mechanism of JmjC catalyzed N-methyl arginine demethylation. a) The symmetrically dimethylated arginine is positioned with one methyl group adjacent to the ferryl oxygen. b) Dynamics of the arginine N-methyl groups at the active site of KDM4E. Distances of the two N-methyl carbon (red and black) to the Fe(IV)-oxygen. c) The N<sup>+</sup>-trimethylated lysine and the ferryl-oxygen. d) Distance of the substrate N<sup>+</sup>-trimethylated N to the ferryl-oxygen in KDM4A during a 1  $\mu$ s simulation.<sup>[18]</sup>

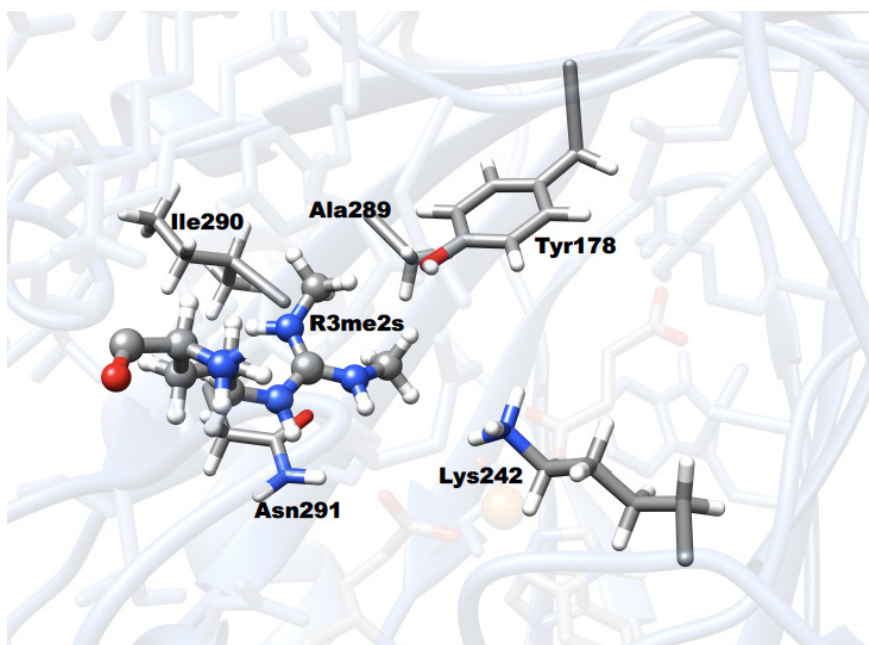


**Figure 6.3.** Residues that stabilize the symmetrical dimethylated Arginine (R3me2s) of the H4R3me2s substrate in the KDM4E active site.

### 6.3.2 Reaction Mechanism of Demethylation of Methylated Arginine in H4 by KDM4E

We then modeled reaction pathways for the KDM4E catalyzed RDM reaction, considering both initial reaction of a methyl group C-H bond or reaction of the N-H bond of the N(H)-methyl group. The distance plots in Figure 6.2b imply that the active site ensures that one of the methyl groups is always close to the ferryl group. The N-H bond is only rarely close to the ferryl group implying a conformational preference for cleavage of the methyl C-H bond. The C-H activation possibility was modeled from a snapshot where a methyl hydrogen is close to the ferryl oxygen, i.e., at 864ns where there is an O-CH hydrogen distance of 2.55Å. The N-H activation possibility was modeled from an enzyme-substrate

complex at 916ns with an initial O-NH hydrogen distance of 2.09 Å. The results were tested using another snapshot (945ns) where the substrate N-H and C-H hydrogens are positioned near equidistantly to the ferryl oxygen, i.e., 3.03 and 2.65 Å, respectively. These structures were chosen in order to investigate factors governing a preference towards C-H or N-H HAT and in particular whether appropriate positioning of either C-H/ or N-H with respect to Fe(IV)=O bond or the difference in the bond strength between C-H and N-H is most important. The analysis of the MD trajectories for the selected snapshot at 864ns used for C-H activation reveals that the HAT distance and angle geometric parameters are present in 45.3% and 6.4% of all MD snapshots, respectively. In the snapshot used for N-H activation (916ns), the geometric parameters are present in 22.2% and 32.5% from the trajectories, respectively. In the snapshot selected at 945ns, where both C-H and N-H possibilities were tested, the HAT distance and angle geometric parameters occurred in 45.3% and 22% from the MD trajectories, respectively, in the C-H pathway while in the N-H pathway, the geometric parameters are present in 22.4% and 18.1% from all MD snapshots, respectively.

The potential energy profile for CH activation [Figure 6.4b] in KDM4E shows that the reaction proceeds by the generally accepted mechanism of HAT, followed by a rebound step, as occurs for the KDM activity of vs. KDM4A [Figure 6.4d] [Scheme 6.1c]. The barrier for the HAT during the RDM activity of KDM4E is 16.3 kcal/mol at the QM(B2+ZPE)/MM level of theory and 17.5 kcal/mol at the QM(B1)/MM level of theory. The energy barrier for the HAT of arginine demethylation in KDM4E is lower than the barrier for lysine demethylation in KDM4A<sup>[18]</sup> by 5.3 kcal/mol, which suggests that the

more effective catalytic KDM performance of KDM4A is due to events prior to C-H bond cleavage.

The transition state geometry for CH activation in KDM4E is given in Figure 6.5a. The Fe-O distance is 1.74 Å, which is elongated from the 1.62 Å of the starting IM1(CH) ferryl complex and the Fe-O-H angle is 157.2°. The Mulliken spin density at the carbon radical center of the substrate is -0.9, which implies a  $\sigma$  electron transfer process. The spin natural orbital (SNO) of the KDM4E HAT transition state [Figure 6.6] shows electron transfer to the  $\sigma^*z^2$  orbital of the Fe metal, supporting this proposal.

The optimized reactant geometry showed similar interactions as in the MD simulation, with the stabilization of succinate and non-coordinating oxygen of glutamate intact. Glu191, Asn291, and Ser197 bring rigidity to the active site by making a network of hydrogen bonds. The evolution of the hydrogen bonds involving Glu191, Asn291, Ser197, Tyr178 and Ser1 H4 substrate during MD simulation is shown in Figure 6.4a. Long MD (i.e. 1000 ns) studies reveal that the Ser1 H4 substrate residue makes strong hydrogen bonding stabilization with Tyr178. Overall, the active site interactions involving Glu191, Asn291, and out of the active site hydrogen-bonded stabilization from Ser1(substrate) with Tyr178 help to productively orientate the N-methylated arginine side chain in the KDM4E active site. Generation of the hydrogen bonding network Glu191, Asn291, and H4Ser1 distinguishes KDM4E RDM catalysis from the KDM activities of KDM4A or PHF8 [Figure E7].<sup>[31]</sup> In KDM4A and PHF8, steric repulsions from the active site residues contribute to the productive orientation of the substrate. For example, in KDM4A, Lys241

(KDM4A), Tyr177 (KDM4A), and Asn290 (KDM4A), and or in PHF8, Ile191 (PHF8), Arg460 (PHF8) and Phe250 (PHF8) provide the steric repulsion to generate a tailor-made active site for efficient catalysis.

Figures 6.5a and b show the interactions that stabilize the transition states during the CH hydrogen abstractions in KDM4E (RDM catalysis) and KDM4A (KDM catalysis), respectively. With KDM4E, the non-coordinating oxygen of the coordinating Glu191 is stabilized by hydrogen bonding with Asn291. Networks of hydrogen bonding interactions of second sphere residues, Tyr178, Asp136, H4Ser1 (substrate), and Glu311 enhance the stability of the TS. In KDM4A, the non-coordinating oxygens of both the Fe ligating Glu190 and the succinate are stabilized via hydrogen bonding interactions with Asn290 and Asn198, respectively.<sup>[18]</sup> Binding of the non-polar part of the H3K9me3 substrate in KDM4A is stabilized by the phenyl ring of Tyr175. Overall, the H4R3me2s substrate in KDM4E appears to be more precisely stabilized than the H3K9me3 substrate in KDM4A.<sup>[18]</sup>



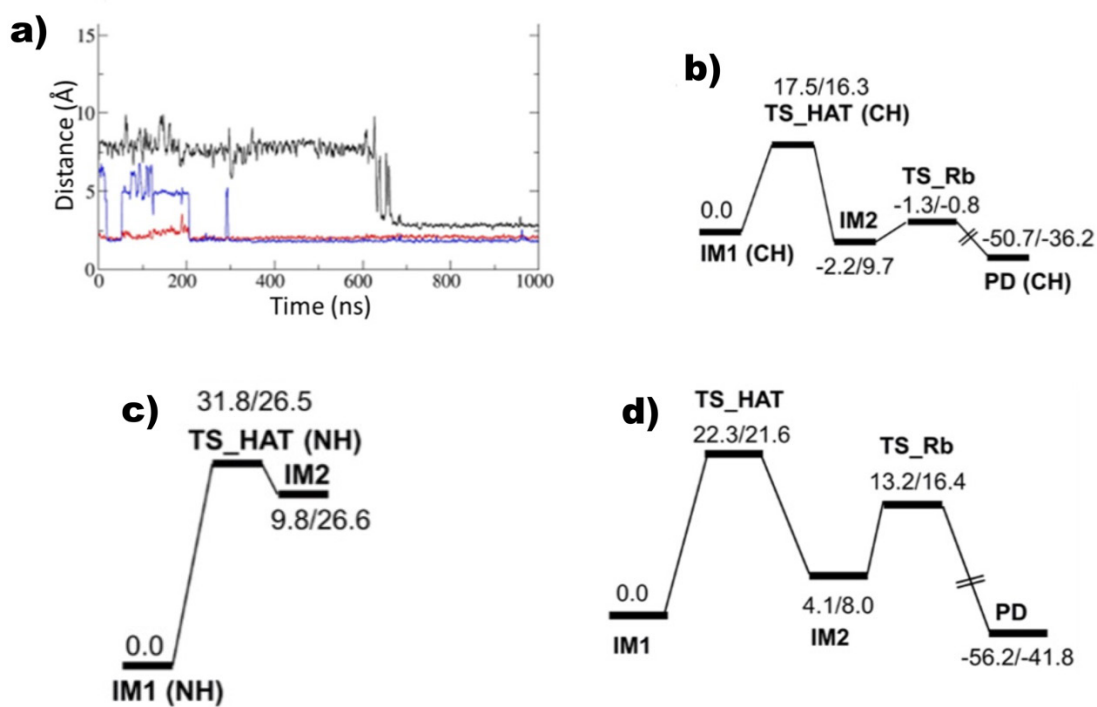


**Figure 6.4.** Distance plots for Glu191-Asn291 in red; Ser197-Asn291 in blue; and Tyr178-Ser1 in black for the RDM reaction of KDM4E (a). Potential energy profile for C-H activation (b) and N-H activation for the RDM activity of KDM4E (c). Potential energy profile for HAT and the rebound steps during KDM4A KDM catalysis (d).<sup>[18]</sup> Energies are given in kcal/mol at the QM(B1)/MM followed by QM(B2+ZPE)/MM level of theory.

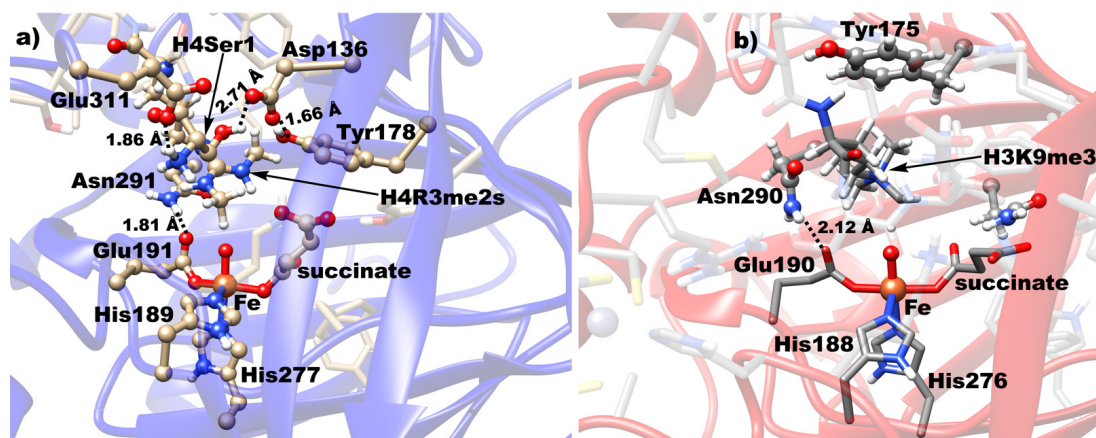


**Figure 6.5.** The optimized transition state geometry for C-H hydrogen abstractions in (a) KDM4E and (b) KDM4A with their respective stabilizing residues.

We explored the possibility for HAT of the NH hydrogen as this has been proposed in model studies of KDMs.<sup>[25b]</sup> The barrier for NH hydrogen abstraction is higher than for CH abstraction, being 26.5 kcal/mol at the QM(B2+ZPE)/MM level of theory and 31.8 kcal/mol at the QM(B2)/MM level of theory [Figure 6.4c]. The DFT-D3 dispersion corrected energies at QM(B2+ZPE)/MM level of theory show the same trend and also support the preference of HAT via C-H over N-H [Figure E10]. The potential NH activation mechanism proceeds via a transition state where the Fe-O bond is elongated to 1.69 Å, with the O—H and N---H distances being 1.19 and 1.34 Å, respectively. The Fe-O-H angle is 142.5°, suggesting a possible  $\sigma$  trajectory where the electron is shifted to the  $\sigma^*z^2$  orbital. The electronic structure shows an electron density of -0.03 at the N, suggesting the alpha electron of the N-H  $\sigma$  bond shifts to the Fe  $\sigma^*z^2$  orbital. Thus, both the -CH activation and -NH activation transition states have a similar electronic structure. The

higher barrier for N-H bond activation over C-H bond activation is explained on the basis of the higher bond dissociation energy (BDE) for the N-H bond, making it less reactive as it was demonstrated in the case of the KDM activity of KDM7B (PHF8).<sup>[16]</sup> The presence of an alpha amino group significantly reduces the C-H bond dissociation energy. The C-H BDEs alpha to an amino group has a value around 91 kcal/mol while the N-H has ~100 kcal/mol.<sup>[58]</sup>

The rebound steps in both the KDM4A KDM and KDM4E RDM reactions are lower in energy compared to the HAT step [Figures 6.4b and 6.4d]. The rebound reaction in the KDM4E RDM reaction has a lower barrier compared to the KDM4A KDM reaction. One of the oxygens of the non-coordinating carboxylate of the succinate in KDM4E makes a stabilizing interaction with the C-H hydrogen of the methylene radical at the rebound TS [Figure E11]. Such a stabilizing interaction is absent in the rebound TS in KDM4A KDM catalysis [Figure E12]. The optimized stationary point geometries along the reaction mechanism in KDM4E are presented in Figure E13.

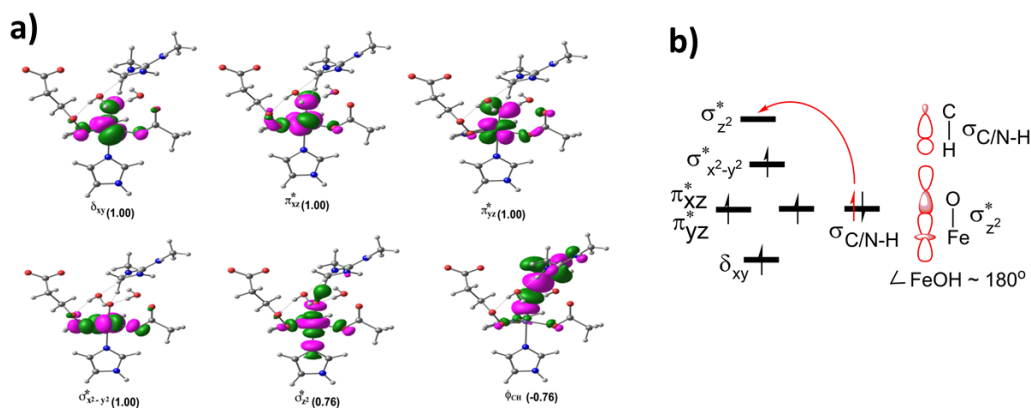


**Figure 6.6.** Electronic structure details of the HAT in KDM4E. a) Spin natural orbitals (SNO) with their respective orbital occupancies (in parentheses) for the CH hydrogen atom abstraction transition state mechanism. b) The electron shift diagram for a  $\sigma$ -trajectory of HAT.

### 6.3.3 Effect of an oriented External Electric field (EEF) on the C-H and N-H Hydrogen Abstraction Reactions During N-methyl Arginine Demethylation

To further investigate the possibility of hydrogen atom abstraction via C-H or N-H abstraction pathways for the RDM reaction we applied external electric fields (EEFs) to the KDM4E Fe(IV)=O complex. EEFs have the ability to control catalysis/inhibition of reactions and their selectivity.<sup>[28b-d]</sup> We oriented EEFs both parallel and orthogonal to the Fe=O bond (i.e., reaction axis) in the Fe(IV)=O complex and then performed the HAT on the optimized ferryl complex geometries. The orthogonal direction is defined along the

Fe-N<sup>ε</sup> (His189) bond, which is perpendicular to Fe=O bond [Figure E6]. In the orthogonal direction, electric field strengths of  $\pm 0.0025$  au were applied [Table 6.1], resulting in barriers of 20.1 and 36.9 kcal/mol for HAT via C-H and N-H pathways, respectively at an electric field strength of -0.0025 au. When the electric field strength was changed to +0.0025 au, the obtained barriers are 17.4 and 40.8 kcal/mol for HAT via C-H and N-H, respectively. These barriers are higher than the 16.3 and 26.5 kcal/mol values calculated at B2+ZPE level of theory, obtained for HAT via C-H and N-H pathways, respectively, without an external electric field. Pronounced EEFs effects were observed for N-H activation as the barriers increased by 10.4 and 14.3 kcal/mol with an electric field strength of -0.0025 or +0.0025 au, respectively, compared with the values without EEFs. These results suggest that an applied external electric field with either a positive or negative field strengths in an orthogonal direction to the reaction axis inhibit (to a different extents) the rate of hydrogen atom abstraction in both C-H and N-H HAT pathways, thereby slowing the rate of demethylation. The EEF in an orthogonal direction to Fe=O bond, however, exercises a much stronger effect on the barrier of the N-H HAT pathway.

We then applied EEFs of strength  $\pm 0.0025$  au in the parallel direction to the Fe=O bond. The results [Figure 6.7, Table 6.2] show that at -0.0025 au field strength, the barriers increase for both the C-H and N-H HAT pathways, compared to the absence of an EEF. However, with a +0.0025 au field strength, a slightly lower barrier was observed than the one obtained without EEFs for HAT via C-H abstraction, while the barrier for N-H

abstraction increases with almost similar magnitude as observed when EEFs were oriented orthogonal to the Fe=O bond.

Due to variations in the results, we doubled ( $\pm 0.0050$  au) and tripled ( $\pm 0.0075$  au) the magnitude of the EEF applied parallel to the Fe=O bond. The results [Figure 6.7, Table 6.2, at B2+ZPE level] reveal that for C-H activation with  $-0.0050$  and  $-0.0075$  au field strengths, the barrier increases by 5.5 and 5.6 kcal/mol, respectively; for N-H activation, the barrier increase by 11.1 and 7.6 kcal/mol, respectively, compared with the values without EEFs. However, with analogous positive field strengths, the barriers for C-H activation decrease by 2.5 and 4.2 kcal/mol for the  $+0.0050$  and  $+0.0075$  au field strengths, respectively; for the N-H activation, the barriers increase by 12.2 kcal/mol and 13.9 kcal/mol for the  $+0.0050$  and  $+0.0075$  au field strengths, respectively. The EEF results show that negative fields parallel to the reaction axis increase the barriers for both C-H and N-H HAT. However, the positive parallel fields have a significant barrier-lowering effect on C-H HAT, while for N-H HAT, they slow reaction. Overall, the results indicate that applying positive EEFs parallel to the reaction axis enhances the rate of C-H activation in a field strength dependent manner. By contrast, application of either positive or negative EEFs parallel to the reaction axis inhibits the rate of N-H activation, likely reflecting the preference for C-H activation over N-H activation.

To investigate the results, we analyzed the spin densities of the optimized Fe(IV)=O complexes. The results [Tables 6.1 and 6.2] reveal that in the C-H activation pathway where positive EEFs were applied parallel to the reaction axis, the oxo group of the

Fe(IV)=O is more polar than in the Fe(IV)=O complex without an EEF; increasing the magnitude of the applied EEFs increases such polarity, thereby increasing the rate of the HAT. However, in the other tested systems, the oxo group becomes less polar compared to the respective ferryl complex without an EEF, thus slowing HAT. The effects of the EEF are different for the C-H (decrease of the barrier for a positive EEF) and N-H (increase of the barrier in all cases) HAT processes with the effect being more profound for the former [Figure 6.4]. The observations indicate that after applying the EEF and optimizing the RCs structures, there are changes in the local interactions that are responsible for the observed differences.

With the EEFs, the HAT proceeds (for both C-H and N-H HAT) via an  $\sigma$  trajectory where an  $\alpha$  electron is transferred from the substrate to the vacant d-orbital of the Fe in the HAT transition state in a similar manner as without EEFs, indicating that the electron transfer mechanism is preserved with or without EEFs.

**Table 6.1.** Energy barriers and spin densities for the C-H and N-H activations with EEFs oriented orthogonal to the Fe(IV)=O bond reaction axis, calculated at the B1 and B2+ZPE levels of theory.

Electric field strength (au)	Barrier for C-H (kcal/mol)	Barrier for N-H (kcal/mol)	Difference (kcal/mol)	Spin density of Fe of Fe(IV)=O in C-H	Spin density of O of Fe(IV)=O in C-H	Spin density of Fe of Fe(IV)=O in N-H	Spin density of O of Fe(IV)=O in N-H
-0.0025	21.7/20.1	40.3/36.9	18.6/16.8	3.145	0.551	3.149	0.603
0.0000	17.5/16.3	31.8/26.5	14.3/10.2	3.136	0.582	3.145	0.619
0.0025	19.9/17.4	46.1/40.8	26.2/23.4	3.139	0.575	3.153	0.592

**Table 6.2.** Energy barriers and spin densities for the C-H and N-H activations with EEFs oriented parallel to the Fe(IV)=O bond reaction axis, calculated at the B1 and B2+ZPE levels of theory.

<b>Electric field strength (au)</b>	<b>Barrier for C-H (kcal/mol)</b>	<b>Barrier for N-H (kcal/mol)</b>	<b>Difference (kcal/mol)</b>	<b>Spin density of Fe of Fe(IV)=O in C-H</b>	<b>Spin density of O of Fe(IV)=O in C-H</b>	<b>Spin density of Fe of Fe(IV)=O in N-H</b>	<b>Spin density of O of Fe(IV)=O in N-H</b>
<b>-0.0075</b>	24.2/21.9	42.2/34.1	18.0/12.2	3.181	0.543	3.149	0.605
<b>-0.0050</b>	23.1/21.8	44.1/37.6	21.0/15.8	3.164	0.557	3.156	0.597
<b>-0.0025</b>	18.6/18.8	44.8/39.1	26.2/20.3	3.152	0.567	3.169	0.580
<b>0.0000</b>	17.5/16.3	31.8/26.5	14.3/10.2	3.136	0.582	3.145	0.619
<b>0.0025</b>	16.8/16.0	43.9/36.4	27.1/20.4	3.126	0.590	3.152	0.601
<b>0.0050</b>	14.5/13.8	42.6/38.7	28.1/25.2	3.114	0.601	3.164	0.587
<b>0.0075</b>	12.4/12.1	45.6/40.4	33.2/28.3	3.100	0.615	3.173	0.572



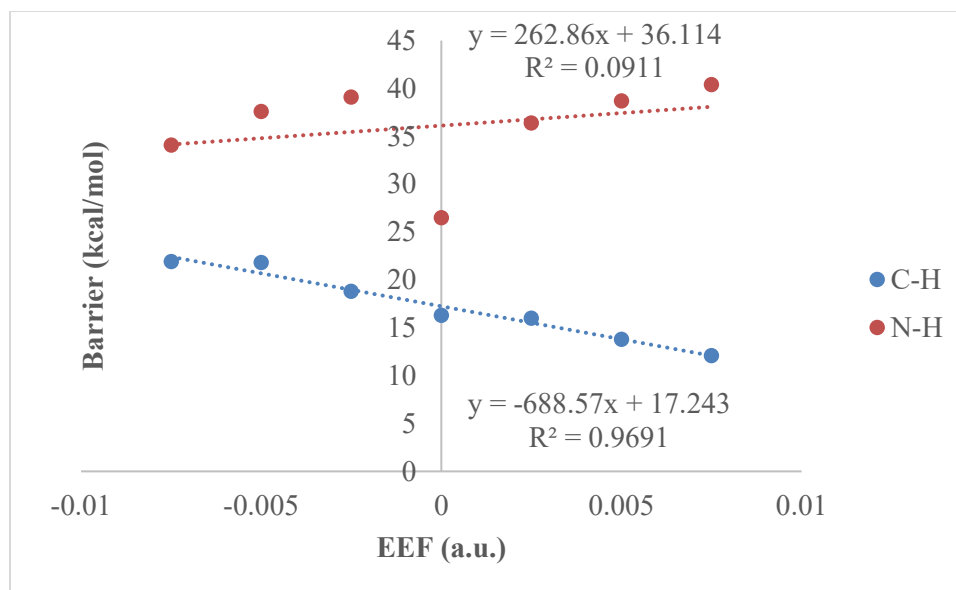


**Figure 6.7.** The relationship between the C-H and N-H pathways H-abstraction barriers and the EEF strength applied parallel to the Fe=O bond during KDM4E N-methyl arginine demethylation.

The presence of an EEF has been demonstrated to influence the spin densities and ultimately the rate of HAT reactions,<sup>[28b,d-e,49]</sup> accelerate the rates of photochemical process in polar solvents,<sup>[28f]</sup> and to change the reactivity of heme-containing enzymes.<sup>[28b,e,49]</sup> There are no previous reports of studies of EEF effects on non-heme Fe(II) enzymes. We calculated the internal field from the protein scaffold without any applied EEF and used it as a background for the reaction path calculations with different values of the EEF. Our results provide evidence that altering the EEF increases the rate of hydrogen atom abstraction via C-H pathway, while inhibiting the rate of the N-H HAT pathway.

## 6.4 Conclusions

Our studies with MD and QM/MM calculations reveal the crucial role of a hydrogen-bonded scaffold at the active site of KDM4E for efficient RDM activity. Both interactions within and out of the active site are important in defining substrate selectivity and efficiency. Active site interactions of KDM4E by Glu191, Asn291 and Ser197 and an out of active site hydrogen-bond between Ser1(substrate) and Tyr178 collectively work to productively orientate the N-methylated arginine side chain in the active site. Despite the similarity of the different methylated substrates (histone tails with positively charged N-methylated arginine or N-methylated lysine-residues), there are differences in the interactions that bind the substrates, which stabilize the transition state, hence which might contribute to specificity and reaction rates. Importantly, such differences include not only the first sphere and the active site interactions, but also second sphere and more distant interactions.

We also show that an applied EEF can enhance the specificity of a non-heme oxygenase towards a particular reaction pathway. Thus, negative fields parallel to the reaction axis increase the barriers for both C-H and N-H activation processes during the KDM4E RDM reaction, implying that applying these fields in the stated direction inhibits both pathways. However, the positive fields have a significant barrier-lowering effect on C-H activation, while in N-H activation, they slow the reaction. The results suggest that further studies on the effects of EEFs on catalysis by non-heme Fe oxygenases are of interest.

## 6.5 References

- [1] A. T. Hauser, D. Robaa, M. Jung, *Curr. Opin. Chem. Biol.* 2018, 45, 73–85.
- [2] J. R. Horton, M. Gale, Q. Yan, X. Cheng, *Cancer Drug Discov. Dev.* 2017, 151–219.
- [3] Y. I. Tsukada, J. Fang, H. Erdjument-Bromage, M. E. Warren, C. H. Borchers, P. Tempst, Y. Zhang, *Nature* 2006, 439, 811–816.
- [4] K. Yamane, C. Toumazou, Y.-I. Tsukada, H. Erdjument-Bromage, P. Tempst, J. Wong, Y. Zhang, *Cell* 2006, 125, 483–495.
- [5] J. R. Whetstone, A. Nottke, F. Lan, M. Huarte, S. Smolikov, Z. Chen, E. Spooner, E. Li, G. Zhang, M. Colaiacovo, Y. Shi, *Cell* 2006, 125, 467–481.
- [6] R. P. Hausinger in *2-oxoglutarate-Dependent Oxygenases* (Eds.: C. J. Schofield, R. P. Hausinger), Royal Society of Chemistry, Cambridge, 2015, pp. 1–58.
- [7] S. Martinez, R. P. Hausinger, *J. Biol. Chem.* 2015, 290, 20702–20711.
- [8] L. J. Walport, R. J. Hopkinson, R. Chowdhury, R. Schiller, W. Ge, A. Kawamura, C. J. Schofield, *Nat. Commun.* 2016, 7, 11974.
- [9] A. N. Iberg, A. Espejo, D. Cheng, D. Kim, J. Michaud-Levesque, S. Richard, M. T. Bedford, *J. Biol. Chem.* 2008, 283, 3006–3010.
- [10] A. Di Lorenzo, M. T. Bedford, *FEBS Lett.* 2011, 585, 2024–2031.
- [11] D. Hyllus, C. Stein, K. Schnabel, E. Schiltz, A. Imhof, Y. Dou, J. Hsieh, U. M. Bauer, *Genes Dev.* 2007, 21, 3369–3380.
- [12] E. I. Solomon, S. Goudarzi, K. D. Sutherlin, *Biochem.* 2016, 55, 6363–6374.
- [13] M. Costas, M. P. Mehn, M. P. Jensen, L. Que, *Chem. Rev.* 2004, 104, 939–986.
- [14] M. R. A. Blomberg, T. Borowski, F. Himoto, R. Z. Liao, P. E. M. Siegbahn, *Chem. Rev.* 2014, 114, 3601–3658.
- [15] S. S. Chaturvedi, R. Ramanan, S. O. Waheed, J. Ainsley, M. P. Evison, J. M. Ames, C. J. Schofield, T. G. Karabencheva-Christova, C. Z. Christov, *Chem. Eur. J.* 2019, 20, 5422–5426.
- [16] S. S. Chaturvedi, R. Ramanan, N. Lehnert, C. J. Schofield, T. G. Karabencheva-Christova, C. Z. Christov, *ACS Catal.* 2020, 10, 1195–1209.
- [17] S. O. Waheed, R. Ramanan, S. S. Chaturvedi, N. Lehnert, C. J. Schofield, C. Z. Christov, T. G. Karabencheva-Christova, *ACS Cent. Sci.* 2020, 6, 795–814.
- [18] R. Ramanan, S. S. Chaturvedi, N. Lehnert, C. J. Schofield, T. G. Karabencheva-Christova, C. Z. Christov, *Chem. Sci.* 2020, 11, 9950–9961.
- [19] H. Torabifard, G. A. Cisneros, *Chem. Sci.* 2018, 9, 8433–8445.
- [20] B. Wang, D. Usharani, C. Li, S. Shaik, *J. Am. Chem. Soc.* 2014, 136, 13895–13901.
- [21] M. G. Quesne, R. Latifi, L. E. Gonzalez-Ovalle, D. Kumar, S. P. De Visser, *Chem. Eur. J.* 2014, 20 (2), 435–446.
- [22] D. Fang, R. L. Lord, G. A. Cisneros, *J. Phys. Chem. B* 2013, 117, 6410–6420.
- [23] J. Lu, L. Hu, J. Cheng, D. Fang, C. Wang, K. Yu, H. Jiang, Q. Cui, Y. Xu, C. A. Luo, *Phys. Chem. Chem. Phys.* 2016, 18, 4728–4738.
- [24] S. Ye, C. Riplinger, A. Hansen, C. Krebs, J. M. Bollinger, F. Neese, *Chem. Eur. J.* 2012, 18, 6555–6567.

- [25] (a) T. Borowski, A. Bassan, P. E. M. Siegbahn, *Chem. Eur. J.* 2004, 10, 1031–1041; (b) N. Alberro, M. Torrent-Sucarrat, I. Arrastia, A. Arrieta, F. P. Cossio, *Chem. Eur. J.* 2017, 23, 137–148.
- [26] (a) A. Wójcik, M. Radoń, T. Borowski, *J. Phys. Chem. A* 2016, 120, 1261–1274; (b) S. O. Waheed, R. Ramanan, S. S. Chaturvedi, J. Ainsley, M. Evison, J. M. Ames, C. J. Schofield, C. Z. Christov, T. G. Karabancheva-Christova, *Org. Biomol. Chem.* 2019, 17, 2223–2231; (c) S. S. Chaturvedi, R. Ramanan, S. O. Waheed, T. G. Karabancheva-Christova, C. Z. Christov, *Adv. Protein Chem. Struct. Biol.* 2019, 117, 113–125.
- [27] D. Usharani, D. Janardanan, C. Li, S. Shaik, *Acc. Chem. Res.* 2013, 46, 471–482.
- [28] (a) S. Shaik, H. Chen, D. Janardanan, *Nat. Chem.* 2011, 3, 19–27; (b) S. Shaik, D. Mandal, R. Ramanan, *Nat. Chem.* 2016, 8, 1091–1098; (c) R. Meir, H. Chen, W. Lai, S. Shaik, *ChemPhysChem* 2010, 11, 301–310; (d) S. Shaik, R. Ramanan, D. Danovich, D. Mandal, *Chem. Soc. Rev.* 2018, 47, 5125–5145; (e) T. Stuyver, R. Ramanan, D. Mallick, S. Shaik, *Angew. Chem. Int. Ed.* 2020, 59, 7915–7920; *Angew. Chem.* 2020, 132, 7989–7994; (f) N. S. Hill, M. L. Coote, *J. Am. Chem. Soc.* 2018, 140, 17800–17804; (g) S. Shaik, D. David, J. Joy, Z. Wang, T. Stuyver, *J. Am. Chem. Soc.* 2020, 142, 12551–12562.
- [29] L. Hillringhaus, W. W. Yue, N. R. Rose, S. S. Ng, C. Gileadi, C. Loenarz, S. H. Bello, J. E. Bray, C. J. Schofield, U. Oppermann, *J. Biol. Chem.* 2011, 286, 41616–41625.
- [30] S. S. Ng, K. L. Kavanagh, M. A. McDonough, D. Butler, E. S. Pilka, B. M. R. Lienard, J. E. Bray, P. Savitsky, O. Gileadi, F. Von Delft, N. R. Rose, J. Offer, J. C. Scheinost, T. Borowski, M. Sundstrom, C. J. Schofield, U. Oppermann, *Nature* 2007, 448, 87–91.
- [31] L. J. Walport, R. J. Hopkinson, R. Chowdhury, R. Schiller, W. Ge, A. Kawamura, C. J. Schofield, *Nat. Commun.* 2016, 7, 11974.
- [32] R. Salomon-Ferrer, A. W. Götz, D. Poole, S. Le Grand, R. C. Walker, *J. Chem. Theory Comput.* 2013, 9, 3878–3888.
- [33] (a) P. Li, K. M. Merz, *J. Chem. Inf. Model.* 2016, 56, 599–604; (b) C. Krebs, D. G. Fujimori, C. T. Walsh, J. M. Bollinger, *Acc. Chem. Res.* 2007, 40, 484–492; (c) E. I. Solomon, K. M. Light, L. V. Liu, M. Srnc, S. D. Wong, *Acc. Chem. Res.* 2013, 46, 2725–2739; (d) X. Song, J. Lu, W. Lai, *Phys. Chem. Chem. Phys.* 2017, 19, 20188–20197; (e) S. O. Waheed, S. S. Chaturvedi, T. G. Karabancheva-Christova, C. Z. Christov, *ACS Catal.* 2021, 11, 3877–3890.
- [34] J. A. Maier, C. Martinez, K. Kasavajhala, L. Wickstrom, K. E. Hauser, C. Simmerling, *J. Chem. Theory Comput.* 2015, 11, 3696–3713.
- [35] W. L. Jorgensen, J. Chandrasekhar, J. D. Madura, R. W. Impey, M. L. Klein, *J. Chem. Phys.* 1983, 79, 926–935.
- [36] T. Darden, D. York, L. J. Pedersen, *Chem. Phys.* 1993, 98, 10089–10092.
- [37] J. A. Lzaguirre, D. P. Catarello, J. M. Wozniak, R. D. Skeel, *J. Chem. Phys.* 2001, 114, 2090–2098.
- [38] H. J. C. Berendsen, J. P. M. Postma, W. F. Van Gunsteren, A. Dinola, J. R. Haak, *J. Chem. Phys.* 1984, 81, 3684–3690.
- [39] J. P. Ryckaert, G. Ciccotti, H. J. C. Berendsen, *J. Comput. Phys.* 1977, 23, 327–341.
- [40] P. Sherwood, A. H. De Vries, M. F. Guest, G. Schreckenbach, C. R. A. Catlow, S. A. French, A. A. Sokol, S. T. Bromley, W. Thiel, A. J. Turner, S. Billeter, F. Terstegen, S.

- Thiel, J. Kendrick, S. C. Rogers, J. Casci, M. Watson, F. King, E. Karlsen, M. Sjøvoll, A. Fahmi, A. Schäfer, C. Lennartz, *J. Mol. Struct. THEOCHEM* 2003, 632, 1–28.
- [41] S. Metz, J. Kästner, A. A. Sokol, T. W. Keal, P. Sherwood, *Wiley Interdiscip. Rev. Comput. Mol. Sci.* 2014, 4, 101–110.
- [42] R. Ahlrichs, M. Bär, M. Häser, H. Horn, C. Kölmel, *Chem. Phys. Lett.* 1989, 162, 165–169.
- [43] W. Smith, T. R. Forester, *J. Mol. Graph.* 1996, 14, 136–141.
- [44] D. Bakowies, W. Thiel, *J. Phys. Chem.* 1996, 100, 10580–10594.
- [45] A. D. Becke, *J. Chem. Phys.* 1993, 98, 5648–5652.
- [46] A. Schäfer, H. Horn, R. Ahlrichs, *J. Chem. Phys.* 1992, 97, 2571–2577.
- [47] J. Kästner, J. M. Carr, T. W. Keal, W. Thiel, A. Wander, P. Sherwood, *J. Phys. Chem. A* 2009, 113, 11856–11865.
- [48] S. R. Billeter, A. J. Turner, W. Thiel, *Phys. Chem. Chem. Phys.* 2000, 2, 2177–2186.
- [49] (a) S. Grimme, J. Antony, S. Ehrlich, H. A. Krieg, *J. Chem. Phys.* 2010, 132, 154104; (b) T. Stuyver, J. Huang, D. Mallick, D. Danovich, S. Shaik, *J. Comput. Chem.* 2020, 41, 74–82.
- [50] C. J. Laconsay, K. Y. Tsui, D. J. Tantillo, *Chem. Sci.* 2020, 11, 2231–2242.
- [51] K. D. Dubey, T. Stuyver, S. Kalita, S. Shaik, *J. Am. Chem. Soc.* 2020, 142, 9955–9965.
- [52] J. R. Horton, A. K. Upadhyay, H. H. Qi, X. Zhang, Y. Shi, X. Cheng, *Nat. Struct. Mol. Biol.* 2010, 17, 38–44.
- [53] C. Yi, G. Jia, G. Hou, Q. Dai, W. Zhang, G. Zheng, X. Jian, C. G. Yang, Q. Cui, C. He, *Nature* 2010, 468, 330–333.
- [54] B. Yu, J. F. Hunt, *Proc. Natl. Acad. Sci.* 2009, 106, 14315–14320.
- [55] C. Yi, B. Chen, B. Qi, W. Zhang, G. Jia, L. Zhang, C. J. Li, A. R. Dinner, C. G. Yang, C. He, *Nat. Struct. Mol. Biol.* 2012, 19, 671–676.
- [56] C-G. Yang, C. Yi, E. M. Duguid, C. T. Sullivan, X. Jian, P. A. Rice, C. He, *Nature* 2008, 452, 961–965.
- [57] R. J. Hopkinson, L. J. Walport, M. Münzel, N. R. Rose, T. J. Smart, A. Kawamura, T. D. W. Claridge, C. J. Schofield, *Angew. Chem. Int. Ed.* 2013, 52, 7709–7713; *Angew. Chem.* 2013, 125, 7863–7867.
- [58] J. Lalevée, X. Allonas, J. Fouassier, *J. Am. Chem. Soc.* 2002, 124, 9613–9621.

## 7 Mechanism of the Early Catalytic Events in the Collagenolysis by Matrix Metalloproteinase-1

**Sodiq O. Waheed**,<sup>a</sup> Ann Varghese,<sup>a</sup> Isabella DiCastri,<sup>a</sup> Brenden Kaski,<sup>b</sup> Ciara LaRouche,<sup>c</sup> Gregg B. Fields<sup>d</sup> and Tatyana G. Karabencheva-Christova<sup>a#</sup>

[a] S. O. Waheed, A. Varghese, I. DiCastri, Prof. Dr. T. G. Karabencheva-Christova

Department of Chemistry, Michigan Technological University, Houghton, Michigan 49931, United States.

E-mail: [tatyanak@mtu.edu](mailto:tatyanak@mtu.edu), <http://chem.sites.mtu.edu/karabencheva-christova/>

[b] B. Kaski

Department of Kinesiology and Integrative Physiology, Michigan Technological University, Houghton, Michigan 49931, United States.

[c] C. LaRouche

Department of Chemical Engineering, Michigan Technological University, Houghton, Michigan 49931, United States.

[d] Prof. Dr. G. B. Fields

Department of Chemistry & Biochemistry and I-HEALTH, Florida Atlantic University, Jupiter, Florida 33458, United States.

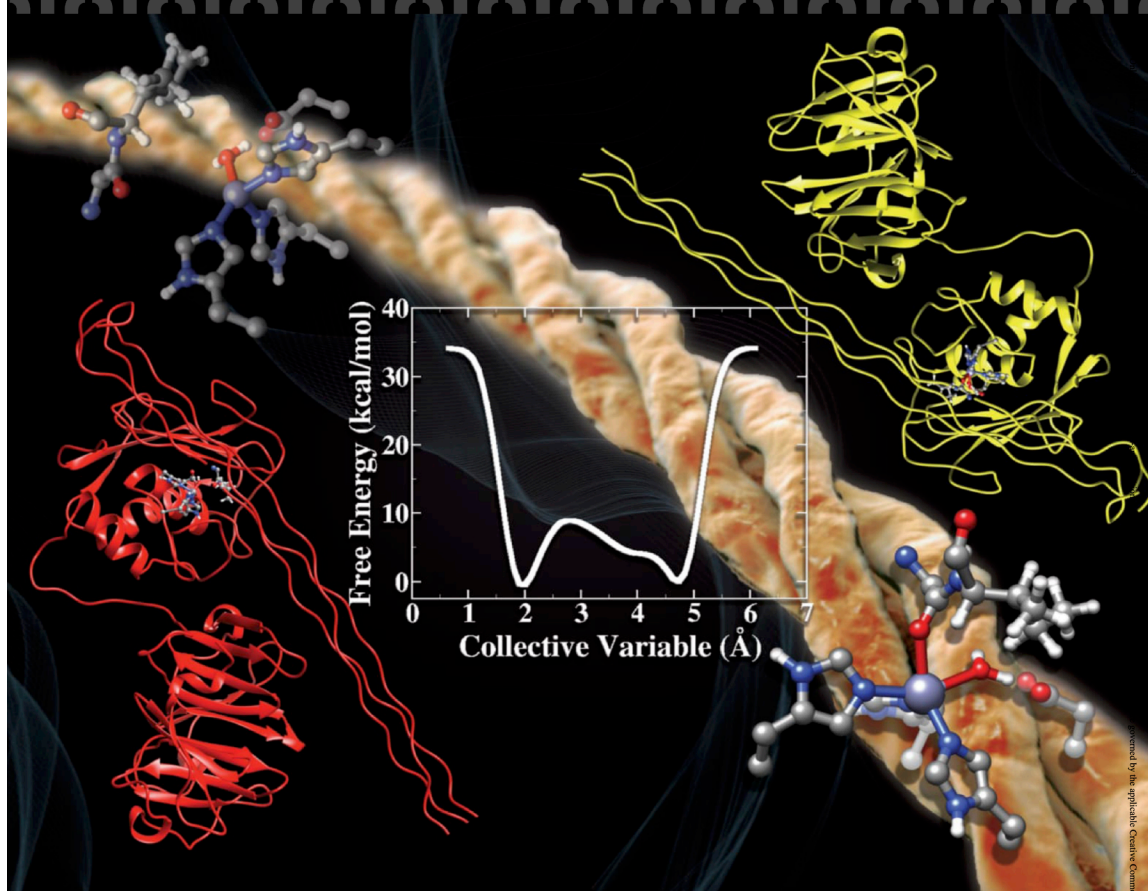
---

The content of this chapter was previously published in the *ChemPhysChem.*, **2022**, e202200649. DOI: 10.1002/cphc.202200649, reproduced with permission from Wiley-VCH. The work was selected as the Front Cover and Cover Profile of the February 2023 Issue of the Journal.

**Front Cover:**

*Tatyana G. Karabancheva-Christova and co-workers*

Mechanism of the Early Catalytic Events in the Collagenolysis by Matrix Metalloproteinase-1



## 7.1 Introduction

Matrix metalloproteinases (MMPs) are a family of zinc(II) dependent proteases involved in the hydrolysis of a variety of proteins in the extracellular environment of various tissues.<sup>1-4</sup> MMPs are involved in biological processes such as embryogenesis, cell mobility, cell proliferation, wound healing, and apoptosis.<sup>5-9</sup> Deregulation of MMP activity contributes to the progression of numerous pathologies such as cancer, arthritis, ulcer, and neurodegenerative and cardiovascular diseases.<sup>3,7,10-12</sup>

Human interstitial collagenase, MMP-1, the subject of the present study, is a highly conformationally flexible and structurally complex multidomain metalloproteinase comprised of a catalytic domain (CAT) where substrate hydrolysis takes place, a hemopexin-like (HPX) domain that participates and cooperates in substrate binding, and a linker region that connects the two domains and modulates allosteric communications between them [Figures 7.1, 7.2a].<sup>12-18</sup> Although the enzyme's active site is in the CAT domain, MMP-1 still requires both the CAT and HPX domains for collagen hydrolysis, emphasizing the critical interplay between these key structural elements for its function.<sup>12,15,17,19,20</sup> Enzyme activity may depend upon equilibrium changes in protein conformations preceding the chemical transformation. Furthermore, complex enzyme-catalyzed reaction mechanisms may also include transitioning from an inactive initially formed enzyme-substrate complex to a catalytically active Michaelis complex that is competent for catalysis.<sup>15,21,22</sup> The available X-ray crystallographic structure of MMP-1 with a collagen-model triple-helical peptide (THP) substrate revealed specific interactions



of the individual THP strands with the CAT and HPX domain.<sup>23</sup> However, MMP-1 was captured in a closed conformation in the crystallographic structure with substrate bound in a non-productive manner as the collagen cleavage site was not correctly positioned for hydrolysis. NMR and small angle x-ray scattering (SAXS) studies of MMP-1 and MMP-1•THP complex in solution indicated that MMP-1 exists as an equilibrium between an open and closed conformations.<sup>12</sup> In the closed conformation, the leading (L) chain of the THP is well-separated from the other two chains to facilitate the coordination of the scissile bond's Gly carbonyl oxygen to the catalytic zinc(II) that results in the reduction in the distance between scissile bond and the zinc(II) when compared to the open form. Also, the interdomain distance between the CAT and HPX domains is larger in the open conformation than in the closed form and is also accompanied by a larger catalytic pocket opening.<sup>12,15</sup> The study proposed a mechanism of collagen binding that involves initial substrate binding to the open conformation of the enzyme, which then converts to closed conformation, the catalytically productive form of the MMP-1•THP.<sup>12</sup> Experimental studies by Bertini et al. and Cerofolini et al., specifically using NMR spectroscopy and small angle x-ray scattering (SAXS) methods, revealed that the conformational transition from open to closed form involves a twist in the linker region and re-orientation of the CAT domain by evaluating the differences in the almost perpendicular *hA* and *hC* helices.<sup>12,15</sup> The movement of the domain drove the leading strand of the THP substrate into the active site, enabling the polypeptide to establish a number of hydrogen bonding interactions and the carbonyl oxygen of the scissile bond to coordinate to the zinc(II) ion during the transition to the closed conformation.<sup>12,15</sup> The closed conformation is the catalytically

active one, and the ability of this conformation to perform collagenolysis is believed to be initiated by the coordination of the carbonyl group of the scissile peptide bond of the THP substrate to the catalytic zinc(II) in the CAT domain.<sup>12,15</sup>

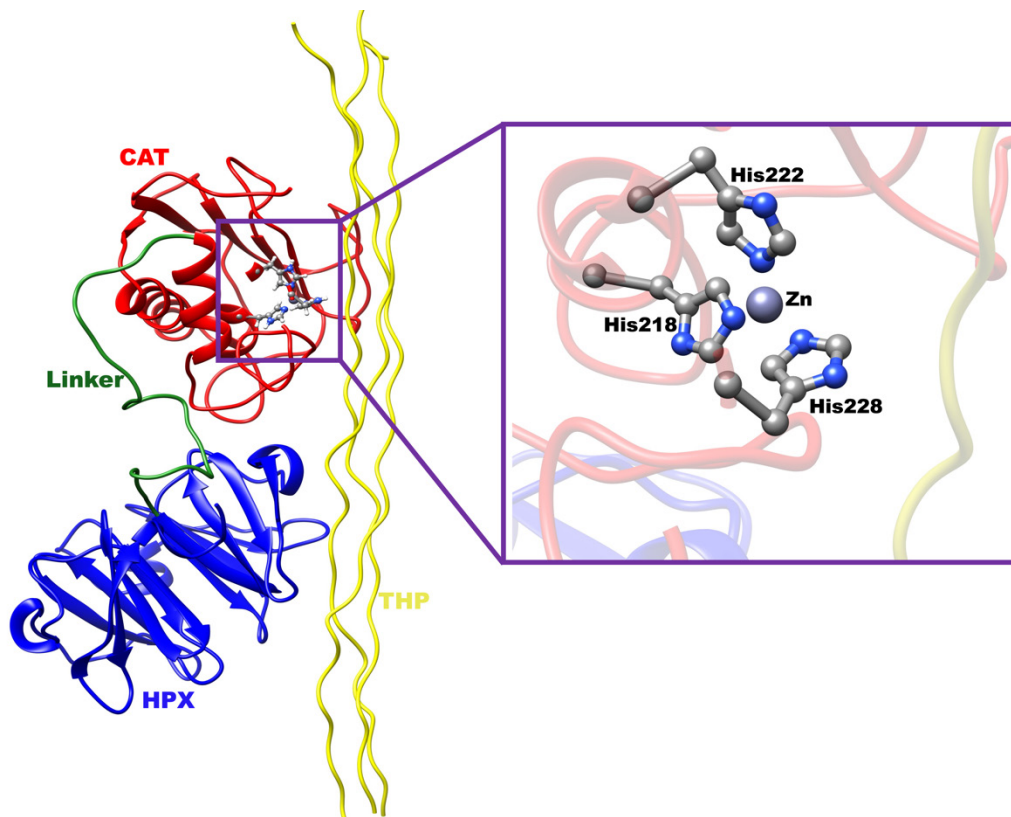


**Figure 7.1.** NMR-derived MMP-1•THP structure. Pictured are the CAT domain (in red), HPX domain (in blue), linker region (in green), and THP substrate (in yellow). The catalytic zinc(II) site with coordinating histidine residues is shown in the zoomed-in view in the inset.

The formation of the catalytically productive ES complex also involves unwinding of the THP substrate because the MMP-1 catalytic cleft is too narrow to accommodate native

triple-helical collagen.<sup>23,24</sup> Two strands of the THP substrate bind simultaneously, enabling one strand of THP to gain access to the active site in the CAT domain.<sup>12,15,23,25</sup> Although the experimental studies detected the open-closed conformational transition and provided some structural insights into the process, the complete atomistic mechanism and dynamics of the binding process and its free energy costs are still missing.

The coordination state of the catalytic zinc(II) in MMP-1 has been extensively studied and discussed.<sup>16,23,26</sup> The zinc(II) ion can exhibit different coordination states that also can change during substrate binding and catalysis.<sup>27</sup> For instance, X-ray crystallographic studies revealed that the catalytic zinc(II) ion in MMPs could have a coordination number of four, five, or six, binding one, two, or three water molecules, respectively, in addition to the three conserved histidine residues.<sup>27</sup>

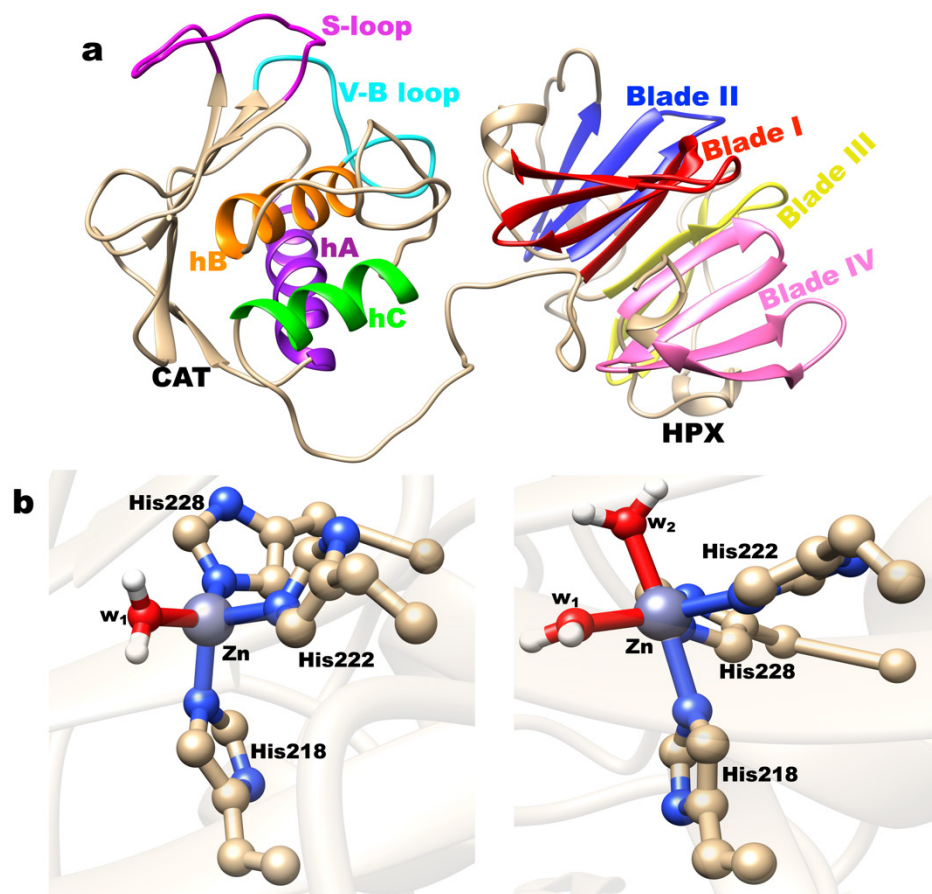


**Figure 7.2.** MMP-1 structure showing (a) the different structural elements of the CAT and HPX domains, (b, left) the catalytic zinc(II) site of open-4C, and (b, right) the catalytic zinc(II) site of open-5C.

The crystal structure of substrate-free human MMP-1<sup>13</sup> revealed the catalytic zinc(II) coordinated to three histidine residues and a water molecule occupying the fourth coordination state, while two other available MMP-1 crystal structures indicate the three coordination (3C) state. A study by Tierney and co-workers using fluorescence, circular dichroism (CD), and X-ray absorption spectroscopic methods reported five coordination

(5C) state for catalytic zinc(II) and four coordination (4C) for the structural zinc(II) site in substrate-free MMP-1.<sup>26</sup>

The study further demonstrated that the five-coordinated (5C) Co(II)-substituted catalytic site changes to a six-coordinated (6C) one upon the removal of the structural zinc(II) ion in MMP-1.<sup>26</sup> The different coordination states and geometries of the zinc(II) exhibit similar electronic stabilities, which allows for change in the catalytic zinc(II) coordination number through the catalytic cycle.<sup>28</sup> Furthermore, the proteolysis reaction required an open coordination sphere of the catalytic zinc(II) with at least one water molecule [Figure 7.2b].<sup>28</sup> The coordinated water molecule(s) serves as a nucleophile and is essential for substrate hydrolysis in MMPs [Scheme F1].<sup>29-31</sup>

Although the coordination state of the catalytic zinc(II) in MMPs and in particular in MMP-1 has been intensively studied, there is still lack of information as to how the coordination state is influenced by the complex conformational changes involved in the THP binding and the formation of the catalytically productive MMP-1•THP. In addition to the experimental studies, some aspects of the structure-function relationships and catalysis in MMPs have been studied computationally.<sup>16,17,30-33</sup> Such studies have been performed often with small substrate models, which certainly provided valuable mechanistic insights; however, they ignored the effects of the flexibility of the large THP substrate and its interactions with the MMP-1 enzyme. Nevertheless, the atomistic nature of the conformational transitions, their free energy cost, and the associated changes in the

coordination state of the catalytic zinc(II) that lead to formation of the catalytically productive MMP-1 ES complex remain unknown.

In the present study, we captured and characterized the significant conformational changes in the MMP-1•THP complex at the atomic scale of accuracy, revealing the transition from its open to catalytically productive closed conformation, including the changes in the coordination state of the catalytic zinc(II) center. To provide this vitally important information, we implemented classical molecular dynamics (MD),<sup>34-36</sup> well-tempered (WT) classical metadynamics (MetD),<sup>36-38</sup> combined quantum mechanics/molecular mechanics (QM/MM) MD,<sup>39,40</sup> and QM/MM MetD simulations.<sup>39,41</sup> Classical MD and MetD have been broadly applied in exploring structural and dynamical properties of zinc(II)-containing enzymes<sup>42-49</sup> and QM/MM MD and MetD have been extensively applied to explore events related to changes in the electronic structure and catalytic mechanisms of zinc(II)-dependent enzymes.<sup>45,46,48,50-54</sup>

## 7.2 Methods

### 7.2.1 System Preparation and Setup

The initial coordinates of the NMR-derived open and closed forms of MMP-1•THP structures were obtained from Bertini et al.<sup>12</sup> The protonation states of the three histidine residues coordinated to the catalytic zinc(II) were assigned based on a visual inspection of their local environment. We generated force field parameters for both four- and five-coordination states of the catalytic zinc(II), with one or two water molecules coordinated

to the catalytic zinc(II) site, respectively. The catalytically active form of MMP-1 was prepared by modifying Ala219 to Glu219 manually. The leap module in AMBER 20<sup>55</sup> was used to add the hydrogen atoms to the protein systems. The catalytic zinc(II) force field parameters were obtained using the AMBER metal center parameter builder (MCPB.py)<sup>56</sup> as implemented in AMBER 20. The bond and angle force constants were derived using the Seminario method.<sup>57</sup> The point charge parameters for the electrostatic potential were obtained using the ChgModB method. The structural zinc(II) and its coordinated three histidines and aspartate were described using the Zinc Amber Force Field (ZAFF)<sup>58</sup> in AMBER 20. The systems were then immersed in a rectangular box containing TIP3P water molecules<sup>59</sup> within a radius of 10 Å from the surface of the protein and then neutralized using Cl<sup>-</sup> counterions to compensate for the positive charge of the MMP-1•THP complex.

A two-stage minimization of the geometries using MM was performed to eliminate bad contacts before the MD simulations. In the first stage of the minimization, only the solvent molecules and Cl<sup>-</sup> counterions were minimized with the protein restrained with a harmonic force constant of 500 kcal/mol/Å<sup>2</sup>, while in the second minimization, the entire systems were minimized without any restraints. The systems were subjected to 5000 steps of steepest descent followed by 5000 steps of conjugate gradient minimization. The CPU version of AMBER 20 code (SANDER)<sup>55</sup> was used for the energy minimization.

### **7.2.2 MD Simulations**

All the standard MM MD simulations used the GPU-accelerated PMEMD code<sup>60</sup> in AMBER 20.<sup>55</sup> The minimized systems were heated by gradually increasing the temperature

from 0 to 300 K in a canonical ensemble (NVT) for 50 ps using a Langevin thermostat.<sup>61</sup> The heated systems were then subjected to density equilibration at a constant temperature of 300 K for 1 ns in an isothermal-isobaric ensemble (NPT) by applying a weak restraint of force constant 10 kcal/mol/Å<sup>2</sup> on the solute molecules. After that, all the restraints were removed, and the systems were further equilibrated for 3 ns in an NPT ensemble at a temperature of 300 K and pressure of 1 bar, respectively. The production MD runs were performed for 1 μs in an NPT ensemble with a target pressure set at 1 bar and constant pressure coupling of 2 ps. The pressure was held constant using Berendsen barostat,<sup>62</sup> and the SHAKE algorithm<sup>63</sup> was used to constrain the covalent bonds to hydrogens. Long-range electrostatic interactions were treated using the particle mesh Ewald (PME) method<sup>64</sup> with a van der Waals cutoff of 10 Å. The AMBER ff14SB force field<sup>65</sup> was used for all protein residues, and periodic boundary conditions were employed in all simulations. The obtained trajectories were analyzed using the cpptraj module<sup>66</sup> in AMBER 20, and the dynamic cross-correlation analysis (DCCA) and principal component analysis (PCA) were done with Bio3D.<sup>67</sup>

### 7.2.3 MetD Simulations

The MM MetD simulations<sup>37,68–70</sup> were performed with the AMBER20<sup>55</sup> code patched with Plumed 2.4.1.<sup>71,72</sup> For the MM MetD simulations, we used equilibrated snapshots taken from the production phase of the classical MD simulations. In all the simulations, the Gaussian-shaped potential was deposited every 500,000 steps, with an initial height of 1.0 kcal/mol and a decay corresponding to a bias factor of 10. The Gaussian width ( $\sigma$ ) was set



to 1.0 Å for the two applied collective variables (CVs) - CV1 and CV2. The CV1 is the distance between the catalytic zinc(II) and the scissile bond glycine carbonyl oxygen atom. The CV2 represents the distance between the center of masses of residues that make up  $\alpha$ -helix *hB* (Glu219-Gly221) and residues of the  $\alpha$ -helix *hC* and the linker (Ala249-Gln268) [Figure F1]. The upper wall limits for CV1 and CV2 were set at 10 Å and 15 Å, respectively, based on their values from the classical MD simulation, using a harmonic force constant of 500 kcal/mol/Å<sup>2</sup>. The free energy surface (FES) plots were reconstructed from the Gaussians deposited during the run using `sum_hills`<sup>71,72</sup> tool provided in the directory utilities.

#### 7.2.4 QM/MM MD and MetD Simulations

The calculations were performed using well-equilibrated snapshots from the classical MD simulation. All QM/MM MD simulations were carried out with the CP2K 6.1 software package<sup>73</sup> that combines QUICKSTEPS<sup>74</sup> and FIST for the QM and MM part, respectively. A real-space multigrid method was used to compute the electrostatic coupling between the QM and the MM region.<sup>75,76</sup> The QM region contained the catalytic zinc(II), imidazole groups of His218, His222, and His228, and Zn-coordinating water molecule(s) altogether 28 and 31 atoms in 4C and 5C coordination states, respectively. The QM region was treated at the DFT (B3LYP) level,<sup>77,78</sup> employing both dual basis set (DZVP-MOLOPT-SR) of Gaussian and plane-waves (GPW) formalism.<sup>74</sup> At the same time, the remaining part of the system was accounted for at the MM level using the same force field and parameters as in the classical MD. The wave function was presented with Gaussian double zeta valence

polarized (DZVP) basis set,<sup>79</sup> and the auxiliary plane-wave basis set was expanded up to a density cut-off of 360 rydberg (Ry) with Goedecker—Teter—Hutter (GTH) potential used to converge the electron density.<sup>80</sup> Hydrogen link atoms were used to complete the valences of bonds spanning between the QM and the MM region.<sup>81,82</sup> The QM/MM MD simulations were performed in an NVT ensemble using a 0.5 fs integration step. The well-tempered QM/MM MetD method was used to explore the FES.<sup>38,69,83–85</sup> The conversion from open-5C to open-4C was modeled by applying as a CV the distance between the catalytic zinc(II) and the oxygen atom of the coordinated water molecule. The process of coordination of the scissile bond Gly775 carbonyl to the catalytic zinc(II) was simulated applying as a CV the distance between the Gly775 carbonyl oxygen atom and the catalytic zinc(II). The Gaussian height was set at 0.6 kcal/mol, while the time deposition between two consecutive Gaussians was set to 10 fs.

## **7.3 Results and Discussion**

### **7.3.1 Conformational Dynamics of the Open and Closed Forms of MMP-1•THP Complex with 5C and 4C States of the Catalytic zinc(II)**

Our initial studies aimed to characterize the dynamics of the open and closed conformations of the MMP-1•THP complex in different coordination states of the catalytic zinc(II). Therefore, we performed a series of classical MD simulations of open and closed forms of MMP-1•THP complexes with 5C or 4C coordination number of the catalytic zinc(II). The

following systems were simulated: open-4C, open-5C, closed-4C, and closed-5C. Both open and closed 4C conformations contain three histidine residues and a water molecule coordinated to the catalytic zinc(II). In contrast, the open and closed 5C conformations have three histidine residues and two water molecules coordinated to the catalytic zinc(II).

A network of stabilizing hydrogen bonding interactions between zinc(II) coordinated histidine residues and residues from the second coordination sphere (SCS) were observed in the catalytic site for all of the modeled forms. Namely, zinc(II) ligand His218 participates in hydrogen bonding interactions with Leu235 (84%, 81%, 89%, and 74%) and Arg214 (26%, 20%, 38%, and 14%) in the open-4C, open-5C, closed-4C and closed-5C complexes, respectively [Figures F2-F3]. His222 zinc(II) coordinated ligand is hydrogen bonded to Glu219 (31%, 23%, 44% and 22%) and Gly225 (58%, 59%, 55% and 40%) in the open-4C, open-5C, closed-4C and closed-5C complexes, respectively [Figures F4-F5]. In addition to these common hydrogen bonding interactions, the third zinc(II)-coordinated ligand (His228) of the closed-4C form specifically forms hydrogen bonds with Gln774 (34%) and Ser227(26%) [Figure 7.3a]. All these interactions may help enhance the stability of the active site. The observed variations in hydrogen bond stability are a result of the different combinations between conformations and coordination states in the MMP-1•THP complex.

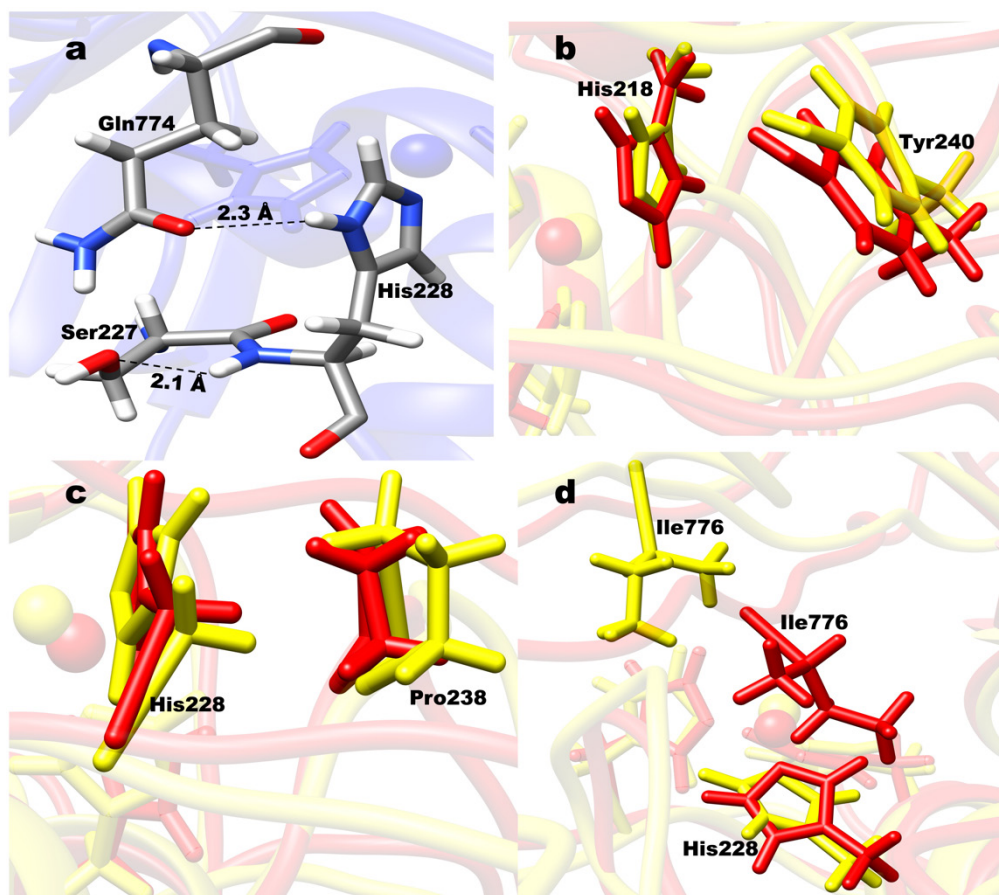


**Figure 7.3.** (a) Hydrogen bonding interactions of catalytic zinc(II)-coordinated His228 with Ser227 and Gln774. (b) Stacking interactions between catalytic zinc(II)-coordinated His218 and Tyr240 in open-4C (in red) and open-5C (in yellow). (c) Hydrophobic interactions between catalytic zinc(II) coordinated His228 and Pro238 in open-4C (in red) and open-5C (in yellow). (d) Hydrophobic interactions between catalytic zinc(II) coordinated His228 and Ile776 in open-4C (in red) and open-5C (in yellow). The interactions in panels b-d were evaluated considering the distances between the center of masses of the side chains atoms of the involved residues. The graphics of the respective distances as a function of time are presented in Figures F8-F10 of the SI.

Our further analysis focused on the distance between oxygen from the carbonyl group of the Gly775 scissile bond and catalytic zinc(II) in the different conformations since it is

essential for forming the catalytically productive reactant complex (RC) of MMP-1•THP. In the 4C and 5C open conformations, the distance between the catalytic zinc(II) and the scissile bond Gly775 carbonyl oxygen is around 10 Å [Figure F6], which demonstrates the catalytically unproductive nature of the open (extended) conformation at both coordination states and that the open conformation can exist at both 4C and 5C coordination states. Therefore, a conformational transition from the open to the closed form should take place in order to generate the catalytically productive conformation.

In the closed-4C conformation, the distance between the catalytic zinc(II) and the scissile bond Gly775 carbonyl oxygen equilibrates at around 5 Å [Figure F6], indicating that a 4C state might exist in the closed conformation. In the closed-5C conformation, the distance increased from about 5 Å to approximately 7.5 Å and remained stable for the last 600 ns [Figure F6]. This indicates the formation of a partly open MMP-1•THP form, thus suggesting the closed-5C conformation with two coordinating water molecules as unstable one. The linker region radius of gyration (ROG) [Figure F7] showed average values of 13.8, 13.9, 13.2, and 10.4 Å in the open-4C, open-5C, closed-5C, and closed-4C systems, respectively, which indicates that only the closed-4C exhibits conformational changes in the linker region as proposed by the experiments.<sup>12,15</sup> Hence, our study suggests that the closed-4C form of MMP-1•THP, where the catalytic zinc(II) is coordinated by three histidine residues and a water molecule, represents a key intermediate conformational state. This state will further transform into the catalytically productive RC after coordinating the scissile bond's Gly775 carbonyl oxygen to the catalytic zinc(II).

Analysis of second sphere interactions in the open 5C and 4C conformations reveals a strong and stable stacking interaction between the imidazole group of zinc(II)-coordinated His218 and the phenyl ring of Tyr240 during the last 550 ns of the open-4C MD. In contrast, the same interaction is unstable in the open-5C form [Figures 7.3b, F8]. Furthermore, the imidazole group of the third zinc(II) coordinating His228 residue participates in hydrophobic interactions with the side chains of Pro238 and the THP's scissile bond Ile776 [Figures 7.3c, 7.3d, F9-F10]. The hydrophobic interaction between His228 and Pro238 is stable for both the 5C and 4C states [Figure F9]. However, the interaction between His228 and Ile776 appears stable in the open-4C and unstable in the open-5C [Figure F10]. This suggests that the coordination state of the catalytic zinc(II) might influence the local interactions between the catalytic zinc(II) and SCS in the open conformation of the MMP-1•THP complex.

PCA [Figure F11] shows that the open-5C form exhibits more limited overall motions than the open-4C form [Figure F11], especially for the HPX domain. To explore how long-range correlated motions are influenced by the conformational and coordination states of MMP-1•THP complex we performed DCCA. In open-4C, the linker region and the CAT domain  $\alpha$ -helices *hA* and *hC* exhibit some correlated motions with the catalytic zinc(II), moving towards the S-loop and the substrate. The study by Teixeira and co-workers<sup>15</sup> experimentally demonstrated the importance of the two helices for re-orientation of the CAT domain during the transition from the open to closed conformation in the MMP-1•THP complex. CAT domain structural elements such as the S-loop, V-B loop, and the

loop connecting  $\alpha$ -helix *hA* and  $\beta$ 1 move towards the substrate [Figures 7.2a, 7.4, and F12]. DCCA of the open-5C and open-4C forms show a similar extent of anti-correlated motions, slightly more intensive in the open-4C [Figures 7.4 and F12]. For example, anti-correlated motions between HPX domain blade II residues and CAT domain V-B-loop residues, as well as the one between HPX domain blade IV residues and residues from  $\alpha$ -helix *hA* and  $\beta$ 1- $\beta$ 3 in the CAT domain, are more pronounced in the open-4C form. Furthermore, in the open-4C form, the linker region, and HPX domain blade I show a positive correlation with CAT domain residues from the  $\alpha$ -helix *hA* and  $\beta$ 1- $\beta$ 2. Experimental studies show the role of the linker region and  $\alpha$ -helix *hA* residues of the CAT domain in achieving a transition from open to closed conformation.<sup>15</sup> The observed correlation motions are in agreement with the experimental data indicating the synergy between these two components. CAT domain S-loop residues in the open-4C form correlate with blade IV HPX domain residues. The S-loop assists the structural zinc(II) site stabilization and binding of peptidic substrates.<sup>16,23</sup> At the same time, the HPX domain also promotes substrate binding to MMP-1;<sup>23</sup> therefore, the observed correlated motion might enhance the overall stability of MMP-1•THP complex in the open-4C state. The significantly correlated motions between the CAT domain's structural elements, the HPX domain blade residues, and the connecting linker region indicate the synergistic cooperation between the HPX and the CAT domain in the MMP-1•THP as suggested by experimental studies.<sup>12,15</sup>

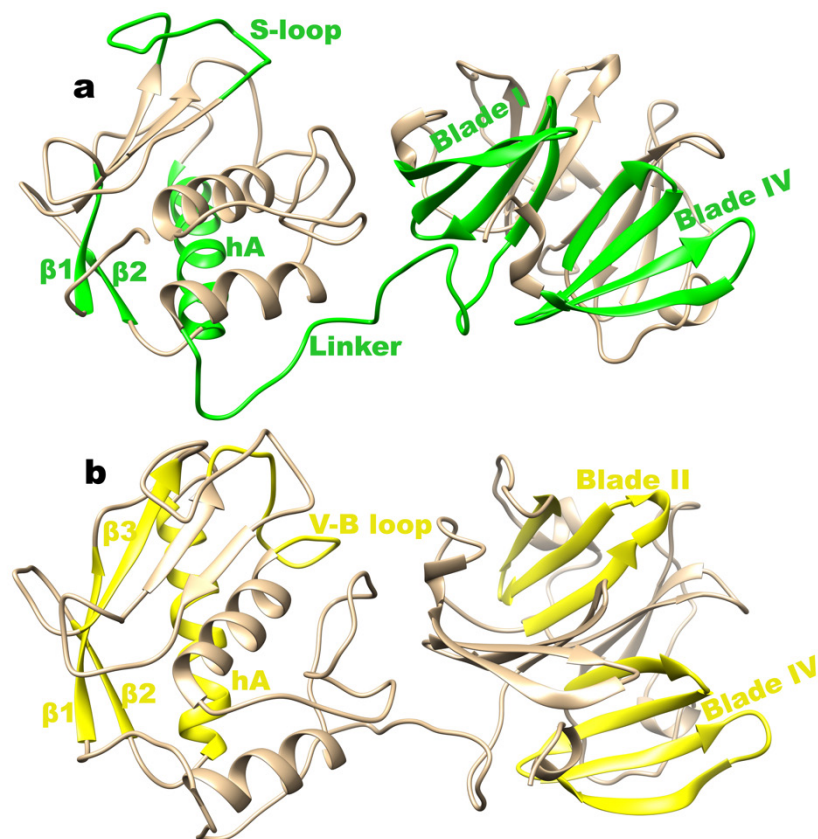


**Figure 7.4.** Correlated and anti-correlated motions of key structural elements of the open forms of MMP-1•THP complex. Panel (a) represents a correlated motion between S-loop and blade IV of HPX; a correlated motion between blade I of the HPX and residues from  $\alpha$ -helix *hA* and  $\beta$ 1- $\beta$ 2; a correlated motion between the linker residues and the residues that constitute  $\alpha$ -helix *hA* and  $\beta$ 1- $\beta$ 2. Panel (b) shows an anti-correlated motion between V-B loop residues and blade II of HPX; and an anti-correlated motion between blade IV of the HPX and residues from  $\alpha$ -helix *hA* and  $\beta$ 1- $\beta$ 3. The DCCA graphs are presented in Figure F12 of the SI.



### 7.3.2 Classical MetD for the Conformational Transformation from Open to Closed MMP-1•THP Complex

A critical step of early catalytic events in the MMP-1 catalytic cycle involves the transformation of the open conformation of the MMP-1•THP complex to its closed catalytically competent form. This transition did not occur spontaneously during our standard MD simulations since it involves complex and large-scale motions, as suggested by experimental data.<sup>12,15</sup> We therefore performed experimentally guided MetD simulations<sup>68–70,86–88</sup> to elucidate the conformational and energetic changes associated with the transition. MetD has been proven to be an effective and reliable tool for exploring large scale molecular motions that cannot be observed with standard MD.<sup>89–91</sup>

The transition from open to closed form of MMP-1•THP was modeled for the two different possible coordination states (5C and 4C) of catalytic zinc(II). We performed two sets of MetD simulations for 600 ns, with one collective variable (CV1) and with two collective variables (the same CV1 and an additional CV2) for each coordination state. The CVs were chosen based on experimental NMR and SAXS studies.<sup>12,15</sup> The CV1 includes the distance between the catalytic zinc(II) and scissile bond Gly carbonyl oxygen. The MetD simulations with one CV for both coordination states showed only one minimum on FES that corresponded to the open conformation [Figures F13-F14]. In the direction from open to the closed form, the free energy kept increasing without forming a stable closed conformation [Figures F13-F14]. The time dependence of CV1 shows that in most snapshots, the CV1 corresponds to the open or partly open conformation for both

coordination states [Figure F15]. This implies that CV1 alone is not sufficient to represent the conformational transition from open to closed conformation for any of the coordination states. We therefore performed another MetD simulation implementing two CVs, CV1 (the same as above) and CV2. The new CV2 includes the distance between the center of masses of the  $\alpha$ -helix *hB* (Glu219-Gly221) and the center of masses of the  $\alpha$ -helix *hC*, including the linker region (Ala249-Gln268).<sup>12,15</sup> The 600 ns MetD [Figures 7.5a, F16] for the 4C reveal two stable minima on the FES [Figure 7.5b], corresponding to the open-4C and a newly formed closed-4C. This transition is favorable with a low free energy barrier of 1.8 kcal/mol, resulting in an exergonic closed-4C form of MMP-1•THP stabilized by -3.7 kcal/mol [Figure 7.5b]. This indicates that forming a closed-4C form from the open-4C one is both kinetically and thermodynamically favored. In contrast, the FES of the MetD simulation for the open-5C to closed-5C transition shows only one free energy minima [Figure 7.5c] that is representative of the open-5C form.

The analysis of the MetD of the 4C state showed that nearly 50% of generated structures are representative of the closed-4C form (distance  $\leq 5$  Å), with the rest of the structures representing an open or partly open conformation [Figure 7.5a]. In contrast, for 5C, less than 10% of the snapshots are characterized by a distance corresponding to the closed form, while the vast majority are in open or partly open form. [Figure 7.5a]. Overall the results reveal that the conformational transition from open to closed conformation occurs at the 4C coordination state of the catalytic zinc(II) and conform with the experimentally-

suggested role of the mutual orientation between  $\alpha$ -helices hA, hB and hC and the linker region to facilitate the conformational change.<sup>12,15</sup>

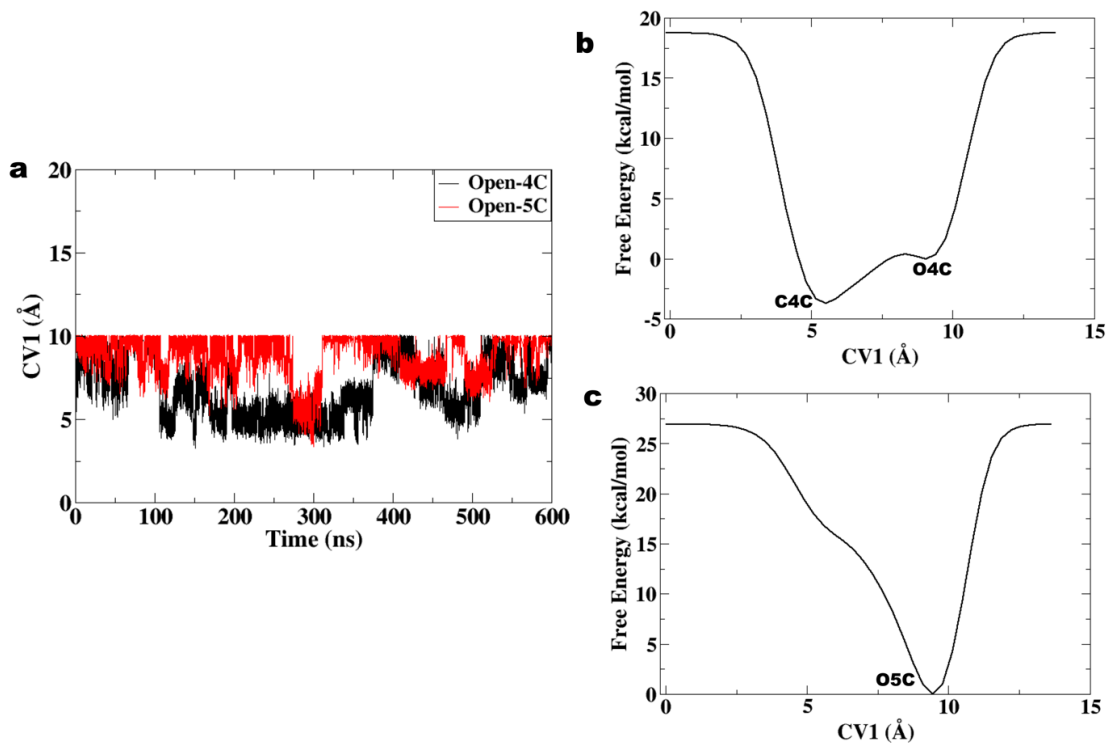


**Figure 7.5.** (a) Distance between catalytic zinc(II) and carbonyl oxygen of scissile bond Gly (CV1). (b) FES as a function of CV1 for transition from open-4C (O4C) to closed-4C (C4C) form of MMP-1•THP ES complex. (c) FES as a function of CV1 for open-5C (O5C) transition.

Although the key structural difference between the open and the closed forms is the distance between the scissile bond and the catalytic zinc(II) (changed from 10 to 5 Å), other interesting differences are shown in Figure 7.6. Figure 7.6a reveals that the major differences between the closed and open forms of substrate-bound MMP-1 lie in the

orientation of the three helices ( $hA$ ,  $hB$ , and  $hC$ ) of the CAT domain. Transition to the closed form involves a change in the orientation between these helices, as depicted in Figure 7.6b. In the closed-4C MMP-1•THP, both  $\alpha$ -helices  $hA$  and  $hC$  move closer to the central  $\alpha$ -helix  $hB$ , with average distances of 8.9 and 14.3 Å, respectively, in comparison to 10.2 and 15.8 Å in the open form. Importantly, in the MetD, the distance between the center of mass of the L-chain to the center of mass of the M+T chains of THP increases from 3.1 to 3.9 Å revealing an un-splitting of the L chain of THP as proposed experimentally.<sup>12,15</sup> All the above structural features of the MetD-generated closed-4C conformation agree with the experimental data, thus demonstrating that the MetD successfully represented the complex conformational transition of the transformation of the open conformation of the MMP-1•THP complex to the closed one.

Furthermore, hydrogen bonding analysis showed that the zinc(II) coordinating His218 formed hydrogen bonding interactions with Leu235 and Arg214 (93% and 67%, respectively, in the closed-4C and 84% and 53%, respectively, in the open-4C MMP-1•THP) while zinc(II)-coordinating His222 exhibited hydrogen bonding interactions with Glu219, Gly225, and Leu226 (56%, 50%, and 40%, respectively, in closed-4C and 31%, 41%, and 13%, respectively, in open-4C MMP-1•THP). These hydrogen bonding interactions are more intensive in the closed form than in the open one, thus facilitating the formation of a more compact and stable closed conformation. In addition, in the closed-4C form, the interdomain distance (measured between CAT domain Ser142 and HPX domain Ser366) and the distance representing the opening of the catalytic pocket (measured

between Asn171 and Thr230) showed average values of 43.6 and 26.0 Å, respectively compared to 45.9 and 27.8 Å in the open-4C form. These changes indicate a more compressed nature of the two domains as well as a tighter catalytic pocket necessary for the catalytic activities in the closed form of the MMP-1•THP complex.

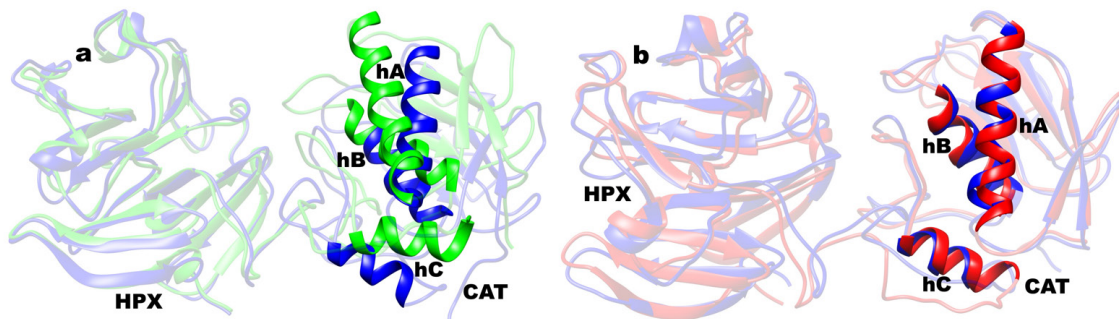


**Figure 7.6.** (a) Superposition of the averaged open-4C MMP-1•THP (green) from the standard MD and the averaged closed-4C structure (blue) from MetD simulations. (b) Superposition of the averaged closed-4C form the standard MD (red) and averaged closed-4C form (blue) from MetD.

### 7.3.3 QM/MM MetD of the Transition of Open-5C to Open-4C form of MMP-1•THP Complex

The MM MetD simulations revealed that the transition from open to the closed form of the MMP-1•THP complex is feasible only at the 4C state of the catalytic zinc(II). In the 4C state, a water molecule occupies one coordination site in addition to the three protein histidine residues forming the catalytic zinc(II) first coordination sphere; in contrast, in the

5C state, there is a second water molecule coordinated. The question, however, of how the 5C state transforms into a 4C state remains unknown. The catalytic zinc(II) center is characterized by internal dynamics that might contribute to its function.<sup>16</sup> We, therefore, carried out a QM/MM MD simulation,<sup>39-41,83,84,92</sup> which allowed account for both the conformational flexibility and changes in the electronic structure of the zinc(II) center. We first explored whether in the open conformation, a conversion from the 5C into 4C state happens spontaneously. The results indicated that both water molecules remain coordinated to catalytic zinc(II) [Figure F17], suggesting that the water removal process proceeds with an energy barrier. Therefore, we performed QM/MM MetD simulation using the distance between catalytic zinc(II) and the coordinated water oxygen as a CV. The process of water molecule dissociation occurred early in the simulation (Figure 7.7a). It passed through a transition state (TS1) with the water oxygen at 4.38 Å from catalytic zinc(II) (Figure 7.7b). The free energy of activation of the process is 17.4 kcal/mol. The reaction leads to an exergonic 4C state of the open conformation (PC1) stabilized by -21.1 kcal/mol. The geometries of RC1, TS1, and PC1 are presented in Figure 7.7c and the overlaid structures of RC1 and PC1 are presented in Figure F18. Overall, the calculations imply that the formed open-4C form is thermodynamically more stable than the open-5C form of the MMP-1•THP complex.

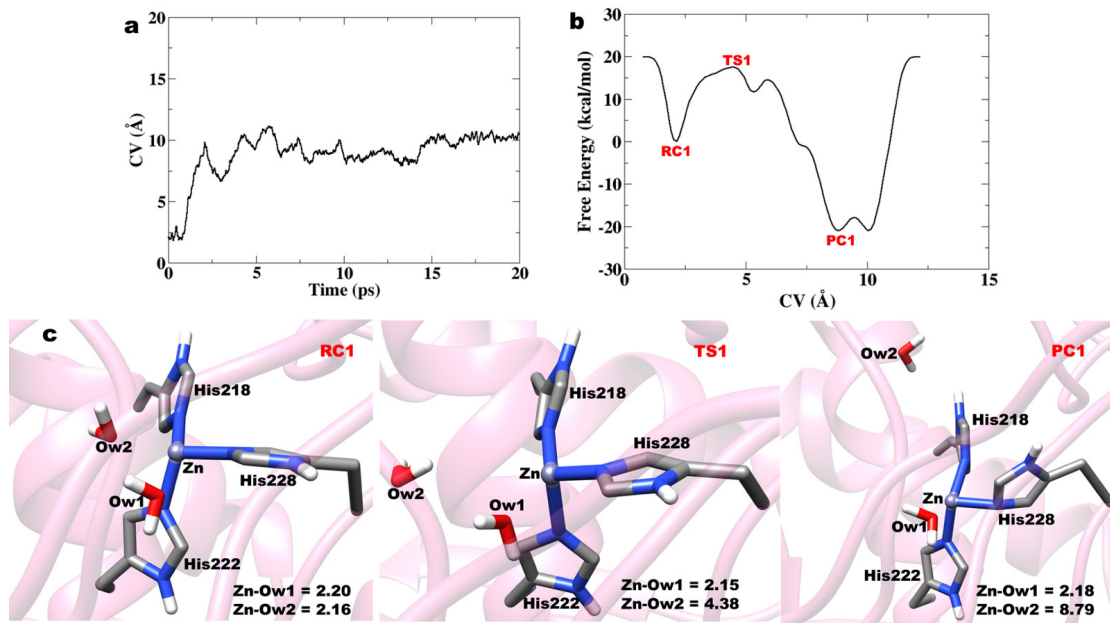


**Figure 7.7.** QM/MM MetD of the water dissociation from the catalytic zinc(II). (a) Dependence of the CV (distance between catalytic zinc(II) and the oxygen atom of the zinc(II) coordinating water molecule) as a function of time. (b) FES of the water dissociation as a function of the CV. (c) Geometries of RC1, TS1, and PC1, with the distances in Å.

### 7.3.4 QM/MM MetD of the Coordination of the Scissile Bond Glycine Carbonyl Oxygen to the Catalytic zinc(II) in the Closed-4C Form

After a transition from open to closed conformation, the next and final step of early catalytic events involves the coordination of the carbonyl oxygen of the scissile bond glycine to the catalytic zinc(II) in the closed-4C MMP-1•THP complex. This leads to the

formation of a new closed-5C MMP-1•THP form which is the catalytically competent RC for catalysis.

We used the closed-4C form generated in our previous MM MetD simulations as an RC (RC2) for this reaction and performed QM/MM MetD simulations [Figure 7.8]. The distance between the catalytic zinc(II) and the carbonyl oxygen of the scissile bond glycine was applied as a CV [Figures 7.8b, E1]. The system reached the 5C state, where the carbonyl oxygen is coordinated to the zinc(II) [Figure 7.8]. In the reactant (**RC2**) complex, the Zn—O1, Zn—Ow, and Zn—N3 distances are 4.76, 2.08, and 1.95 Å, respectively [Figure 7.8c]. The coordination of the glycine carbonyl oxygen passes through a transition state (**TS2**) with a free energy barrier of 8.9 kcal/mol [Figure 7.8a]. At the **TS2**, the Zn—O1 bond reduces to 2.74 Å approaching the product complex (**PC2**). The formation of the five-coordinate closed form of the MMP-1•THP complex (**PC2**) is almost thermoneutral with a free energy of -0.57 kcal/mol [Figure 7.8a]. The key bond lengths of the formed **PC2** are 2.03 and 2.30 Å for Zn—O1 and Zn—Ow, respectively, implying that the carbonyl oxygen of the scissile bond Gly is coordinated to the catalytic zinc(II). The overlaid structures of RC2 and PC2 are presented in Figure F19.

Furthermore, we observed that as the substrate approaches the catalytic zinc(II), the distance between zinc(II) and the N3 atom from the third Zn-coordinating His228 residue weakens from 1.95 Å in the **RC2** to 2.09 and 2.16 Å in **TS2** and **PC2**, respectively, possibly due to steric effects in the active site. The Zn-coordinating His218 in the **PC2** orients in such a way that the ethyl moiety of the *sec*-butyl side chain of the scissile bond Ile776



forms a hydrophobic interaction with His218 imidazole side chain, enhancing the stability of the **PC2** complex, which is the catalytically competent RC for collagenolysis.

Overall the QM/MM MetD simulations imply that coordination of the scissile bond Gly carbonyl oxygen to the catalytic zinc(II) center is kinetically feasible with the formation of thermoneutral product.

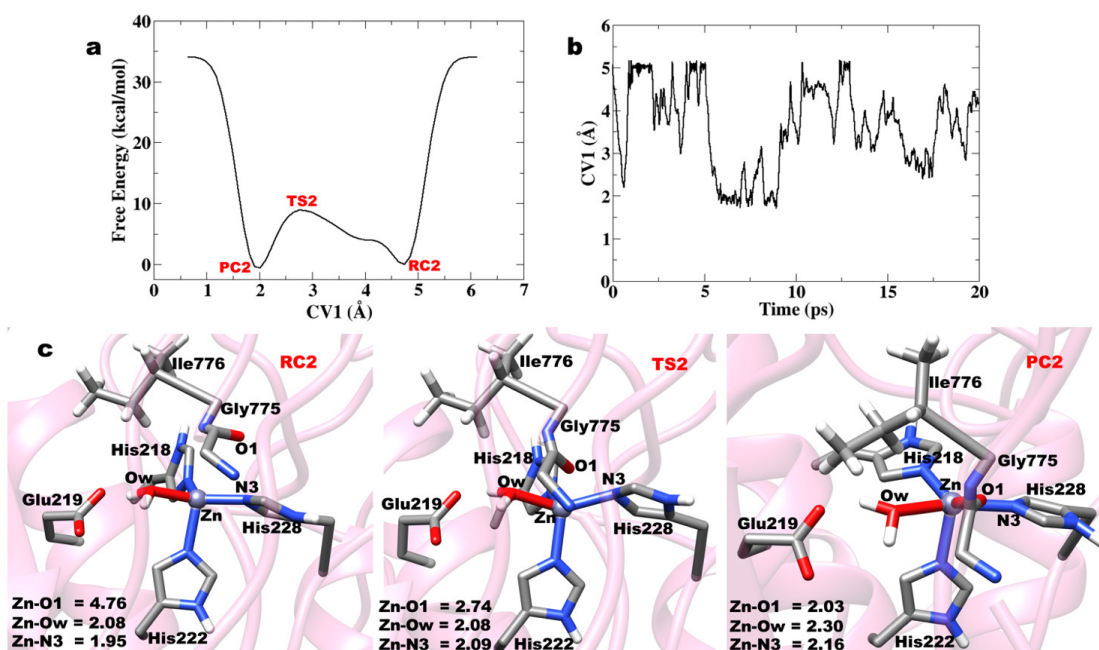
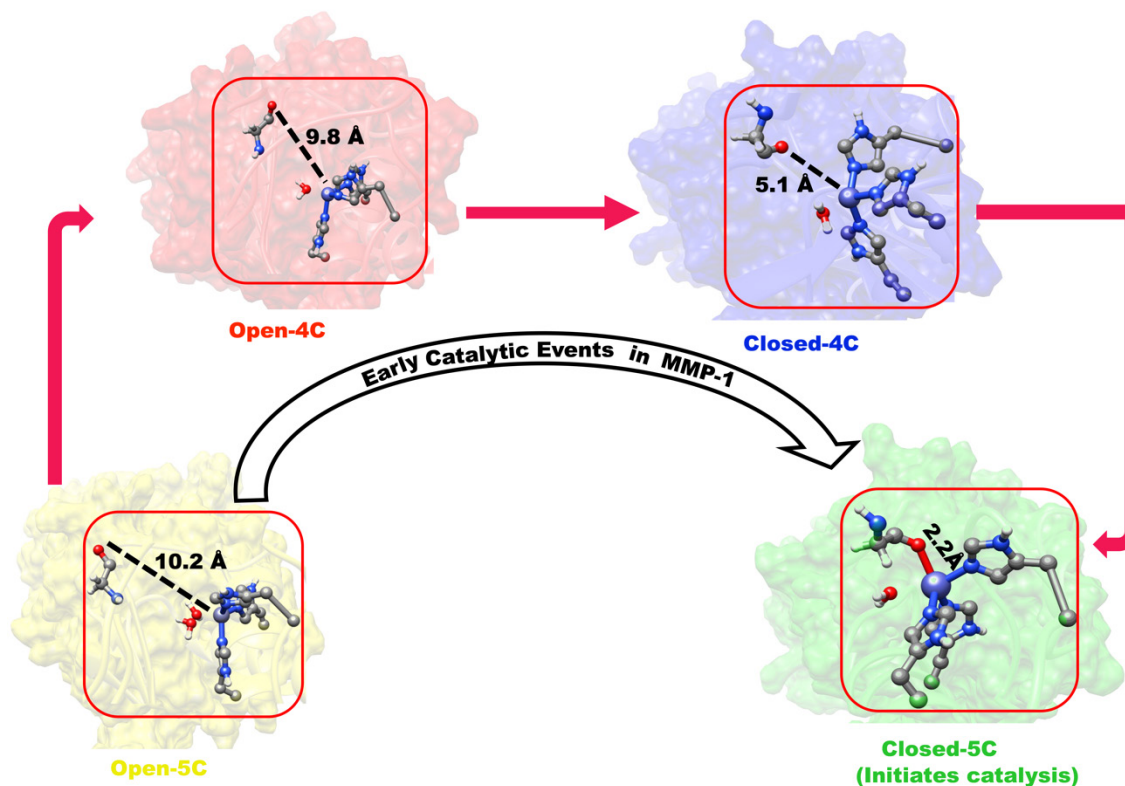


**Figure 7.8.** (a) Free energy profile for the coordination of scissile bond Gly carbonyl oxygen to the catalytic zinc(II). (b) The collective variable (CV) as a function of time. (c) Geometries of the RC2, TS2, and the PC2 for the formation of the catalytically competent five-coordinated closed form of MMP-1•THP complex. Distances in (c) are in Å.

## 7.4 Conclusions

Our simulations provided insights at the atomic level of accuracy into the complex process of formation of catalytically productive RC of MMP-1•THP for collagenolysis. The studies provided unique insights into the atomistic mechanism of the time-dependent evolution of MMP-1•THP complex from the catalytically inactive to a catalytically active form. This process is initiated by a change of the coordination state of the catalytic zinc(II) from 5C to 4C via dissociation of a water molecule in the open conformation, followed by a significant conformational rearrangement to closed 4C conformation and subsequent coordination of the scissile bond carbonyl oxygen to the catalytic zinc(II) [Scheme 7.1]. The results revealed the crucial participation of the CAT domain  $\alpha$ -helices *hA*, *hB*, and *hC* and the linker region in the conformational transition from open to the closed form of MMP-1•THP in agreement with experimental studies. The results demonstrate that such a transition occurs in the open-4C form instead of the open-5C one. The QM/MM MetD simulations showed that the dissociation of the water molecule from the open-5C catalytic zinc(II) proceeds with a feasible free energy barrier leading to the formation of a stable exergonic open-4C state. The last step of the early catalytic events is the coordination of the scissile bond glycine carbonyl to the catalytic zinc(II) center of the closed-4C form. The process is energetically feasible, leading to a thermoneutral catalytically productive ES complex. The study suggests that the elucidated interactions between the *hA*, *hB*, and *hC* and the linker region can be used as molecular tools for modulating the reactivity of MMP-1 and as a target for MMP-1 inhibitor design efforts. NMR and X-ray

crystallographic structural studies have indicated that MMP-1 domain orientation upon binding of the collagen triple-helix is different than that for MT1-MMP.<sup>12,15,23,93,94</sup> In turn, the differing domain orientations result in subtle differences between the two MMPs in the secondary binding sites (exosites) that interact with the triple-helix. This knowledge drives the development of exosite-based inhibitors.<sup>95</sup> The present study has revealed long-range correlated motions that occur during MMP-1 catalyzed collagenolysis. A comparable study with other MMPs may reveal unique motions that in combination with exosite binding information, lay the groundwork for the design of truly selective MMP inhibitors. Overall, a fundamental understanding of the early catalytic events of collagenolysis is essential for revealing the molecular pathology of MMP-1-related diseases and providing new horizons for inhibitor design.



**Scheme 7.1.** Evolution of the Early Catalytic Events in the MMP-1•THP Complex.

## 7.5 References

- (1) C. Streuli, *Curr. Opin. Cell Biol.* **1999**, *11* (5), 634–640.
- (2) V. M. Weaver, C. D. Roskelley, *Trends Cell Biol.* **1997**, *7* (1), 40–42.
- (3) G. A. Rosenberg, *Lancet Neurol.* **2009**, *8* (2), 205–216.
- (4) S. P. Gupta, V. M. Patil, *Exp. Suppl.* **2012**, *103*, 35–56.
- (5) H. Laronha, J. Caldeira, *Cells* **2020**, *9* (5), E1076.
- (6) K. A. McCall, C. Huang, C. A. J. Fierke, *Nutr.* **2000**, *130* (5S Suppl), 1437S–46S.
- (7) T. Klein, R. Bischoff, *Amino Acids* **2011**, *41* (2), 271–290.
- (8) A. G. Marneros, B. R. Olsen, *Matrix Biol.* **2001**, *20* (5–6), 337–345.
- (9) A. F. Parisi, B. L. Vallee, *Am. J. Clin. Nutr.* **1969**, *22* (9), 1222–1239.
- (10) P.S. Burrage, K. S. Mix, C. E. Brinckerhoff, *Front. Biosci. J. Virtual Libr.* **2006**, *11*, 529–543.
- (11) S. Löffek, O. Schilling, C.-W. Franzke, *Eur. Respir. J.* **2011**, *38* (1), 191–208.
- (12) I. Bertini, M. Fragai, C. Luchinat, M. Melikian, M. Toccafondi, J. L. Lauer, G. B. Fields, *J. Am. Chem. Soc.* **2012**, *134* (4), 2100–2110.
- (13) S. Iyer, R. Visse, H. Nagase, K. R. Acharya, *J. Mol. Biol.* **2006**, *362* (1), 78–88.

- (14) T. G. Karabancheva-Christova, C. Z. Christov, G. B. Fields, *J. Phys. Chem. B* **2018**, *122* (21), 5316–5326.
- (15) L. Cerofolini, G. B. Fields, M. Fragai, C. F. G. C. Geraldés, C. Luchinat, G. Parigi, E. Ravera, D. I. Svergun, J. M. C. Teixeira, *J. Biol. Chem.* **2013**, *288* (42), 30659–30671.
- (16) A. Varghese, S. S. Chaturvedi, G. B. Fields, T. G. Karabancheva-Christova, *J. Biol. Inorg. Chem.* **2021**, *26* (5), 583–597.
- (17) L. Kumar, A. Nash, C. Harms, J. Planas-Iglesias, D. Wright, J. Klein-Seetharaman, S. K. Sarkar, *Biophys. J.* **2020**, *119* (2), 360–374.
- (18) A. Pardo, M. Selman, *Int. J. Biochem. Cell Biol.* **2005**, *37* (2), 283–288.
- (19) I. M. Clark, T. E. Cawston, *Biochem. J.* **1989**, *263* (1), 201–206.
- (20) M. H. M. Olsson, W. W. Parson, A. Warshel, *Chem. Rev.* **2006**, *106* (5), 1737–1756.
- (21) R. Vianello, C. Domene, J. Mavri, *Front. Neurosci.* **2016**, *10*, 327.
- (22) K. A. Henzler-Wildman, M. Lei, V. Thai, S. J. Kerns, M. Karplus, D. Kern, *Nature* **2007**, *450* (7171), 913–916.
- (23) S. W. Manka, F. Carafoli, R. Visse, D. Bihan, N. Raynal, R. W. Farndale, G. Murphy, J. J. Enghild, E. Hohenester, H. Nagase, *Proc. Natl. Acad. Sci. U. S. A.* **2012**, *109* (31), 12461–12466.
- (24) L. Chung, D. Dinakarpanian, N. Yoshida, J. L. Lauer-Fields, G. B. Fields, R. Visse, H. Nagase, *EMBO J.* **2004**, *23* (15), 3020–3030.
- (25) I. Bertini, V. Calderone, M. Fragai, C. Luchinat, M. Maletta, K. J. Yeo, *Angew. Chem. Int. Ed Engl.* **2006**, *45* (47), 7952–7955.
- (26) H. Yang, K. Makaroff, N. Paz, M. Aitha, M. W. Crowder, D. L. Tierney, *Biochemistry* **2015**, *54* (23), 3631–3639.
- (27) B. L. Vallee, D. S. Auld, *Biochemistry* **1990**, *29* (24), 5647–5659.
- (28) M. L. Zastrow, V. L. Pecoraro, *Biochemistry* **2014**, *53* (6), 957–978.
- (29) V. Pelmeshnikov, P. E. M. Siegbahn, *Inorg. Chem.* **2002**, *41* (22), 5659–5666.
- (30) T. Vasilevskaya, M. G. Khrenova, A. V. Nemukhin, W. J. Thiel, *Comput. Chem.* **2015**, *36* (21), 1621–1630.
- (31) E. Decaneto, T. Vasilevskaya, Y. Kutin, H. Ogata, M. Grossman, I. Sagi, M. Havenith, W. Lubitz, W. Thiel, N. Cox, *Phys. Chem. Chem. Phys.* **2017**, *19* (45), 30316–30331.
- (32) A. Varghese, S. S. Chaturvedi, S. S.; DiCatri, B.; Mehler, E.; Fields, G. B.; Karabancheva-Christova, T. G. *ChemPhysChem* **2022**, *23* (4). e202100680
- (33) B. Chen, Z. Kang, E. Zheng, Y. Liu, J. W. Gauld, Q. J. Wang, *Chem. Inf. Model.* **2021**, *61* (10), 5203–5211.
- (34) M. Karplus, J. A. McCammon, *Nat. Struct. Biol.* **2002**, *9* (9), 646–652.
- (35) S. A. Adcock, J. A. McCammon, *Chem. Rev.* **2006**, *106* (5), 1589–1615.
- (36) M. De Vivo, M. Masetti, G. Bottegoni, A. J. Cavalli, *Med. Chem.* **2016**, *59* (9), 4035–4061.
- (37) L. Sutto, S. Marsili, F. L. Gervasio, *Wiley Interdiscip. Rev. Comput. Mol. Sci.* **2012**, *2* (5), 771–779.
- (38) A. Barducci, G. Bussi, M. Parrinello, *Phys. Rev. Lett.* **2008**, *100* (2), 020603.
- (39) E. Brunk, U. Rothlisberger, *Chem. Rev.* **2015**, *115* (12), 6217–6263.

- (40) S. Ahmadi, L. Barrios Herrera, M. Chehelamirani, J. Hostaš, S. Jalife, D. R. Salahub, *Int. J. Quantum Chem.* **2018**, *118* (9), e25558.
- (41) L. Raich, A. Nin-Hill, A. Ardèvol, C. Rovira, *Methods Enzymol.* **2016**, *577*, 159–183.
- (42) G. Sharma, K. M. Merz, *J. Chem. Theory Comput.* **2022**, *18* (4), 2556–2568.
- (43) M. D. Peris-Díaz, R. Guran, C. Domene, V. de los Rios, O. Zitka, V. Adam, A. Krężel, *J. Am. Chem. Soc.* **2021**, *143* (40), 16486–16501.
- (44) P. Horx, A. Geyer, *Chem. Sci.* **2021**, *12* (34), 11455–11463.
- (45) Z. Yang, R. M. Twidale, S. Gervasoni, R. Suardíaz, C. K. Colenso, E. J. M. Lang, J. Spencer, A. J. Mulholland, *J. Chem. Inf. Model.* **2021**, *61* (11), 5658–5672.
- (46) F. Fan, Y. Zheng, Y. Fu, Y. Zhang, H. Zheng, C. Lyu, L. Chen, J. Huang, Z. Cao, *Phys. Chem. Chem. Phys.* **2022**, *24* (18), 10933–10943.
- (47) A. Pietropaolo, A. Magri, V. Greco, V. Losasso, D. La Mendola, S. Sciuto, P. Carloni, E. Rizzarelli, *ACS Chem. Neurosci.* **2018**, *9* (5), 1095–1103.
- (48) E. Bellomo, A. Abro, C. Hogstrand, W. Maret, C. Domene, *J. Am. Chem. Soc.* **2018**, *140* (12), 4446–4454.
- (49) R. C. Dash, A. M. Zaino, M. K. A. Hadden, *Biochim. Biophys. Acta Gene Regul. Mech.* **2018**, *1861* (6), 594–602.
- (50) R. Tripathi, N. N. Nair, *ACS Catal.* **2015**, *5* (4), 2577–2586.
- (51) W. A. Zalloum, N. J. Zalloum, *Phys. Chem. B* **2021**, *125* (20), 5321–5337.
- (52) D. K. Chakravorty, K. M. Merz, *Acc. Chem. Res.* **2015**, *48* (2), 439–448.
- (53) C. E. Valdez, M. Sparta, A. N. J. Alexandrova, *Chem. Theory Comput.* **2013**, *9* (1), 730–737.
- (54) S. Nedd, R. L. Redler, E. A. Proctor, N. V. Dokholyan, A. N. J. Alexandrova, *Mol. Biol.* **2014**, *426* (24), 4112–4124
- (55) D. A. Case, R. M. Betz, D. S. Cerutti, T. E. Cheatham III, T. A. Darden, R. E. Duke, T. J. Giese, H. Gohlke, A. W. Goetz, N. Homeyer, S. Izadi, P. Janowski, J. Kaus, A. Kovalenko, T. S. Lee, S. LeGrand, P. Li, C. Lin, T. Luchko, R. Luo, B. Madej, D. Mermelstein, K. M. Merz, G. Monard, H. Nguyen, H. T. Nguyen, I. Omelyan, A. Onufriev, D. R. Roe, A. Roitberg, C. Sagui, C. L. Simmerling, W. M. Botello-Smith, J. Swails, R. C. Walker, J. Wang, R. M. Wolf, X. Wu, L. Xiao, P. A. Kollman, AMBER 2020, University of California, San Francisco **2020**.
- (56) P. Li, K. M. Merz, *J. Chem. Inf. Model.* **2016**, *56* (4), 599–604.
- (57) J. M. Seminario, *Int. J. Quantum Chem.* **1996**, *60* (7), 1271–1277.
- (58) M. B. Peters, Y. Yang, B. Wang, L. Füsti-Molnár, M. N. Weaver, K. M. Merz, *J. Chem. Theory Comput.* **2010**, *6* (9), 2935–2947.
- (59) W. L. Jorgensen, J. Chandrasekhar, J. D. Madura, R. W. Impey, M. L. Klein, *J. Chem. Phys.* **1983**, *79* (2), 926–935.
- (60) A. W. Götz, M. J. Williamson, D. Xu, D. Poole, S. Le Grand, R. C. Walker, *J. Chem. Theory Comput.* **2012**, *8* (5), 1542–1555.
- (61) R. L. Davidchack, T. E. Ouldridge, M. V. Tretyakov, *J. Chem. Phys.* **2015**, *142* (14), 144114.
- (62) F. Bresme, *J. Chem. Phys.* **2001**, *115* (16), 7564–7574.

- (63) J.-P. Ryckaert, G. Ciccotti, H. J. C. Berendsen, *J. Comput. Phys.* **1977**, *23* (3), 327–341.
- (64) M. Deserno, C. Holm, How to Mesh up Ewald Sums. I. *J. Chem. Phys.* **1998**, *109* (18), 7678–7693.
- (65) J. A. Maier, C. Martinez, K. Kasavajhala, L. Wickstrom, K. E. Hauser, C. J. Simmerling, *Chem. Theory Comput.* **2015**, *11* (8), 3696–3713.
- (66) D. R. Roe, T. E. Cheatham, *J. Chem. Theory Comput.* **2013**, *9* (7), 3084–3095.
- (67) B. J. Grant, A. P. C. Rodrigues, K. M. ElSawy, J. A. McCammon, L. S. D. Caves, *Bioinforma. Oxf. Engl.* **2006**, *22* (21), 2695–2696.
- (68) A. Barducci, M. Bonomi, M. Parrinello, *WIREs Comput. Mol. Sci.* **2011**, *1* (5), 826–843.
- (69) G. Bussi, A. Laio, *Nat. Rev. Phys.* **2020**, *2* (4), 200–212.
- (70) O. Valsson, P. Tiwary, M. Parrinello, *Annu. Rev. Phys. Chem.* **2016**, *67*, 159–184.
- (71) The PLUMED consortium. *Nat. Methods* **2019**, *16* (8), 670–673.
- (72) M. Bonomi, D. Branduardi, G. Bussi, C. Camilloni, D. Provasi, P. Raiteri, D. Donadio, F. Marinelli, F. Pietrucci, R. A. Broglia, M. Parrinello, *Comput. Phys. Commun.* **2009**, *180* (10), 1961–1972.
- (73) *CP2K Version 6.1*, the CP2K Developers Group. CP2K: Open Source Molecular Dynamics, **2018**. CP2K is freely available from [https://www.cp2k.org/version\\_history](https://www.cp2k.org/version_history).
- (74) J. VandeVondele, M. Krack, F. Mohamed, M. Parrinello, T. Chassaing, J. Hutter, *Comput. Phys. Commun.* **2005**, *167* (2), 103–128.
- (75) T. Laino, F. Mohamed, A. Laio, M. Parrinello, *J. Chem. Theory Comput.* **2005**, *1* (6), 1176–1184.
- (76) A. Laio, J. VandeVondele, U. Rothlisberger, *J. Chem. Phys.* **2002**, *116* (16), 6941–6947.
- (77) A. D. Becke, *Phys. Rev. Gen. Phys.* **1988**, *38* (6), 3098–3100.
- (78) C. Lee, W. Yang, R. G. Parr, *Phys. Rev. B Condens. Matter* **1988**, *37* (2), 785–789.
- (79) J. VandeVondele, J. Hutter, *J. Chem. Phys.* **2007**, *127* (11), 114105.
- (80) S. Goedecker, M. Teter, J. Hutter, *Phys. Rev. B Condens. Matter* **1996**, *54* (3), 1703–1710.
- (81) H. M. Senn, W. Thiel, *Angew. Chem. Int. Ed Engl.* **2009**, *48* (7), 1198–1229.
- (82) S. F. Sousa, A. J. M. Ribeiro, R. P. P. Neves, N. F. Brás, N. M. F. S. A. Cerqueira, P. A. Fernandes, M. J. Ramos, *WIREs Comput. Mol. Sci.* **2017**, *7* (2).
- (83) R. Sun, O. Sode, J. F. Dama, G. A. Voth, *J. Chem. Theory Comput.* **2017**, *13* (5), 2332–2341.
- (84) R. David, H. Jamet, V. Nivière, Y. Moreau, A. Milet, *J. Chem. Theory Comput.* **2017**, *13* (6), 2987–3004.
- (85) A. Laio, M. Parrinello, *Proc. Natl. Acad. Sci. U. S. A.* **2002**, *99* (20), 12562–12566.
- (86) D. Branduardi, G. Bussi, M. J. Parrinello, *Chem. Theory Comput.* **2012**, *8* (7), 2247–2254.
- (87) P. Tiwary, M. A. Parrinello, *J. Phys. Chem. B* **2015**, *119* (3), 736–742.
- (88) G. Bussi, D. Branduardi, Free-Energy Calculations with Metadynamics: Theory and Practice. In *Reviews in Computational Chemistry*; A. L. Parrill, K. B. Lipkowitz, Eds.; John Wiley & Sons, Inc: Hoboken, NJ, USA, 2015; pp 1–49.

- (89) C. G. Don, M. Smieško, *J. Chem. Inf. Model.* **2020**, *60* (12), 6642–6653.
- (90) D. Callegari, A. Lodola, D. Pala, S. Rivara, M. Mor, A. Rizzi, A. M. Capelli, *J. Chem. Inf. Model.* **2017**, *57* (2), 159–169.
- (91) R. Chowdhury, V. Sai Sreyas Adury, A. Vijay, R. K. Singh, A. Mukherjee, *Chem. Asian J.* **2021**, *16* (12), 1634–1642.
- (92) L. Scalvini, A. Ghidini, A. Lodola, D. Callegari, S. Rivara, D. Piomelli, M. Mor, *ACS Catal.* **2020**, *10* (20), 11797–11813.
- (93) T. C. Marcink, J. A. Simoncic, B. An, A. M. Knapinska, Y. G. Fulcher, N. Akkaladevi, G. B. Fields, S. R. Van Doren, *Structure.* **2019**, *27*(2), 281-292.
- (94) Y. Zhao, T. C. Marcink, R. R. S. Gari, B. P. Marsh, G. M. King, R. Stawikowska, G. B. Fields, S. R. Van Doren, *Structure.* **2015**, *23*(2), 257-269.
- (95) J. L. Lauer-Fields, J. K. Whitehead, S. Li, R. P. Hammer, K. Brew, G. B. Fields, *J. Biol. Chem.* **2008**, *283*(29), 20087-20095.



## **A      Appendix A: Supporting Information for Chapter 2**

### **A.1      Methods**

#### **A.1.1      System Preparation**

An X-ray crystal structure of FTO (PDB ID code: 4IDZ<sup>1</sup>) was used for building the FTO model used in the computational studies. Missing (i.e. not observed by crystallography) residues from loop regions were added using Modeller.<sup>2</sup> The substrate 3-methylthymidine (3-meT) was modelled into the 4IDZ<sup>1</sup> based structure using another structure (3LFM<sup>3</sup>) by aligning the two structures using Maestro (Schrodinger LLC, New York). This was followed by replacement of Ni(II) with Fe(II) and N-oxalylglycine with 2-oxoglutarate (2OG) using GaussView 5.0.<sup>4</sup> A crystal structure of the AlkB (PDB: 4NID<sup>5</sup> in complex with Mn(II), 2OG and double stranded DNA containing N6-methyladenine (6MA) was used in computational studies. The Mn(II) was replaced with Fe(II) using GaussView 5.0.<sup>4</sup> AlkB was also modelled with the nucleoside only (6MA (nsd)) instead of double stranded DNA to compare with the FTO single base simulations and to investigate how the DNA effect the conformational dynamics of AlkB. The Amber parameters for N6-methyladenine were developed using the appropriate CIF file and the AM1-BCC charge model available in Antechamber and prepgen from AmberTools15. A wildtype structure of AlkB (PDB: 3BIE<sup>6</sup>) with substrate N1-methyladenine (m1A) was also used in the simulation studies. The parameters for the substrate were developed using Antechamber.

The likely protonation states of ionisable residue sidechains were assessed using the H++ server.<sup>7</sup> Histidine residues coordinating with the metal centre were assigned protonation states based on visual inspection of their local environment. The cofactor analogue N-oxalylglycine was modelled to 2OG by replacing its NH with a methylene using GaussView 5.0.<sup>4</sup> Hydrogen atoms were added to 2OG and 3-methylthymidine using the reduce program in Amber.<sup>8</sup> The amber parameters for 2OG and 3-methylthymidine were developed using the General Amber force field (GAFF)<sup>9</sup> using Antechamber. The atomic charges of the cofactors were calculated based on the electrostatic potential from single point HF/6-31G\* calculations using Gaussian09.<sup>10</sup> The restrained electrostatic potential (RESP)<sup>11</sup> method was used for the charge fitting procedure.

### **A.1.2 MCPB**

The Amber parameters for the active site containing Iron (Fe(II) high spin S=2, M=5 , ground state<sup>12-19</sup> and the coordinating ligands (2OG (bidentate ligation), histidine and aspartic acid (both monodentate ligation) were prepared using the Metal Centre Parameter Builder (MCPB) and MCPB.py v1.0 Beta2<sup>21</sup> for a 5-coordinate (5C) distorted square pyramidal active site. The binding of the substrate in the vicinity of the Fe(II) in the presence of 2OG results in the dissociation of coordinated water giving a 5C distorted square pyramidal geometry.<sup>12,15</sup> The metal centre parameters were derived based on the bonded and electrostatic model approach in which the coordinating ligands are connected to metal through covalent bonds. The bond and the angle force constants were derived using the Seminario method; point charge parameters for the electrostatic potential were obtained using the ChgModB method. Pabis *et al.* have applied the MCPB tools for

description of the mononuclear non-heme iron centre and iron-sulfur Rieske cluster.<sup>22</sup> Molecular dynamics simulations run using these parameters have successfully reproduced the crystallographically observed geometry of metal-ligand complexes.<sup>22</sup>

### **A.1.3 MD Simulations**

Molecular dynamics simulations were performed using the GPU version<sup>23</sup> of the PMEMD engine integrated with Amber 14.<sup>24</sup> The FF14SB<sup>25</sup> force field was used in all the simulations and the Leap module was used to add missing hydrogen atoms and counter ions for neutralisation of the protein system. All the systems were immersed into a truncated octahedral box with TIP3P water molecules<sup>26</sup>, such that no protein atom was within 10 Å of any box edge. Periodic boundary conditions were employed in all the simulations. Long-range electrostatic interactions were calculated using the Particle Mesh Ewald (PME) method<sup>27</sup> with a direct space and vdW cut-off of 8 Å. The various systems were subjected to energy minimization using first steepest descent (5000 steps) followed by conjugate gradient (5000 steps) to eliminate clashes. Solute molecules were restrained using a restrained potential of 100 kcal mol<sup>-1</sup> Å<sup>2</sup>; only solvent and ions were allowed to minimize. This was followed by full minimization of the entire system with both steepest descent (5000 steps) and conjugate gradient (5000 steps) treatments to relax the system prior to productive simulation. All the energy minimization, heating and equilibration steps were performed with the CPU version of PMEMED. The systems were then subjected to controlled heating from 0 to 300K at constant volume using Langevin thermostat<sup>28</sup> with a collision frequency of 1 ps<sup>-1</sup> using a canonical ensemble (NVT) MD simulation for 400 ps. The solute molecules were restrained using harmonic potential of 10 kcal mol<sup>-1</sup> Å<sup>2</sup> during

the heating process. The SHAKE algorithm<sup>29</sup> was used to constrain bonds involving hydrogen. This was followed by equilibration at 300K in an NPT ensemble for 1 ns without restraints on solute molecules; pressure was maintained at 1 bar using Berendsen barostat.<sup>30</sup> A productive MD run with explicit solvent for continuous 1 $\mu$ s was performed in a NPT ensemble with a target pressure set at 1 bar and constant pressure coupling of 2ps. The frames from the productive run were saved every 10 ps.

Trajectories were analysed using CPPTRAJ,<sup>31</sup> VMD,<sup>32</sup> UCSF Chimera,<sup>33</sup> and R (Bio3D<sup>34</sup>). The Root Mean Square Deviation (RMSD) of C $\alpha$  atoms of the protein with respect to minimized crystal structure, Root mean square fluctuations (RMSF), electrostatic interactions, hydrogen bonding, solvent accessible surface area (SASA), and cluster analysis were performed. The Bio3D package<sup>34</sup> in R was used to produce PCA and domain cross correlations as described by Singh *et al.*<sup>35</sup>

#### **A.1.4 QM cluster calculations**

Snapshots of structures were obtained from the equilibrated MD trajectory of the systems described above. GaussView 5.0<sup>4</sup> was used to set up QM calculations and Gaussian09 code<sup>10</sup> was used to run all QM calculations. In all the calculations, the Fe(II) (high spin S=2, M=5, ground state<sup>12-19</sup>) and the coordinating ligands (2OG (bidentate ligation), histidine and aspartic acid(both with monodentate ligation) were used. The histidine and aspartic acid residues were truncated and restrained at their C $\beta$  positions; hydrogen atoms were added to saturate bonds. The geometry optimization, frequency calculations and single point calculations were performed with Density Functional Theory (DFT) using

unrestricted UB97X functional with 10 % exact HF (Hartree Fork) exchange with 6-311G\* basis set of the Fe and its coordinating atoms (oxygen and nitrogen) from the ligands; for the rest of the atoms, we employed 6-31G\*<sup>36</sup>. A conductor-like polarizable continuum model (CPCM) with  $\epsilon=4.3$  (diethyl ether as solvent)<sup>37</sup> was used in the QM calculations to mimic the hydrophobic active site.<sup>38-40</sup>

### **A.1.5 QM/MM calculations**

Snapshots for the QM/MM calculations were obtained from the MD simulations on all the systems. In particular, snapshots were taken from the minimized crystal structure, 800ns, 700ns, 300ns, 200ns for FTO and minimized crystal structure, 200ns, 300ns, 400ns, 500ns for AlkB. The residues of all the enzymes including the water molecules which are within 35 Å of Fe(II) (except for AlkB where whole protein and DNA were used and water up to 35 Å) were involved in QM/MM optimization. These snapshots were first subjected to energy minimization for 10,000 steps by using both steepest descend (5000) and conjugate gradient (5000) algorithms in Amber14. Active site residues were restrained with a restrained potential of  $100 \text{ kcal mol}^{-1} \text{ \AA}^2$  in the energy minimization, in order to maintain the geometry of the active site. The energy minimized snapshots of all the enzymes were prepared using the Schlegel's toolkit TAO<sup>41</sup> for ONIOM<sup>42-46</sup> calculation in Gaussian09.<sup>10</sup> Residues within 20 Å of Fe(II), including water molecules, were allowed to move freely during geometry optimization; the rest of the system was frozen during geometry optimization in ONIOM. The QM/MM system was prepared using GaussView 5.0; all calculations were run using Gaussian09. Residues were assigned with the standard bonded and non-bonded terms available from the ff99SB force field available in Gaussian09. The

electrostatic embedding scheme was used in the geometry optimization; however, we also used the mechanical embedding scheme for some snapshots. The non-bonded van der Waals parameters for the Fe(II) were obtained using the method of Li *et al.*<sup>47</sup> The QM region in the QM/MM calculation is consistent with the QM calculation performed above and link atoms were used to saturate the dangling bond in the QM/MM calculation.<sup>48</sup>

### A.1.6 Molecular Mechanics/Generalized Born Surface Area (MM/GBSA)

The binding free energy calculations with AlkB were performed using the Molecular Mechanics/Generalized Born Surface Area (MM/GBSA) approach.<sup>49-51</sup> The binding free energy was calculated taking into account 2000 snapshots of equilibrated trajectory from a 1 $\mu$ s molecular dynamic production run. The following set of equations describes the calculation of the binding free energy:

$$\Delta G = G_{\text{complex}} - G_{\text{receptor}} - G_{\text{ligand}} \quad (1)$$

$$\Delta G_{\text{bind}} = E_{\text{gas}} + G_{\text{sol}} - T\Delta S \quad (2)$$

$$E_{\text{gas}} = E_{\text{int}} + E_{\text{vdw}} + E_{\text{ele}} \quad (3)$$

$$G_{\text{sol}} = G_{\text{GB}} + G_{\text{SA}} \quad (4)$$

$$G_{\text{SA}} = \gamma \text{SASA} \quad (5)$$

$E_{\text{gas}}$  signifies the gas-phase energy;  $E_{\text{int}}$  signifies internal energy; and  $E_{\text{ele}}$  and  $E_{\text{vdw}}$  signify the electrostatic and van der Waals contributions, respectively.  $E_{\text{gas}}$  is evaluated directly from the FF14SB force field terms. The solvation free energy, denoted by  $G_{\text{sol}}$ , can be

decomposed into polar and nonpolar contribution states. The polar solvation contribution, GGB, is determined by solving the GB equation, whereas, GSA, the nonpolar solvation contribution is estimated from the solvent accessible surface area (SASA) determined using a water probe radius of 1.4 Å. T and S correspond to temperature and total solute entropy, respectively.

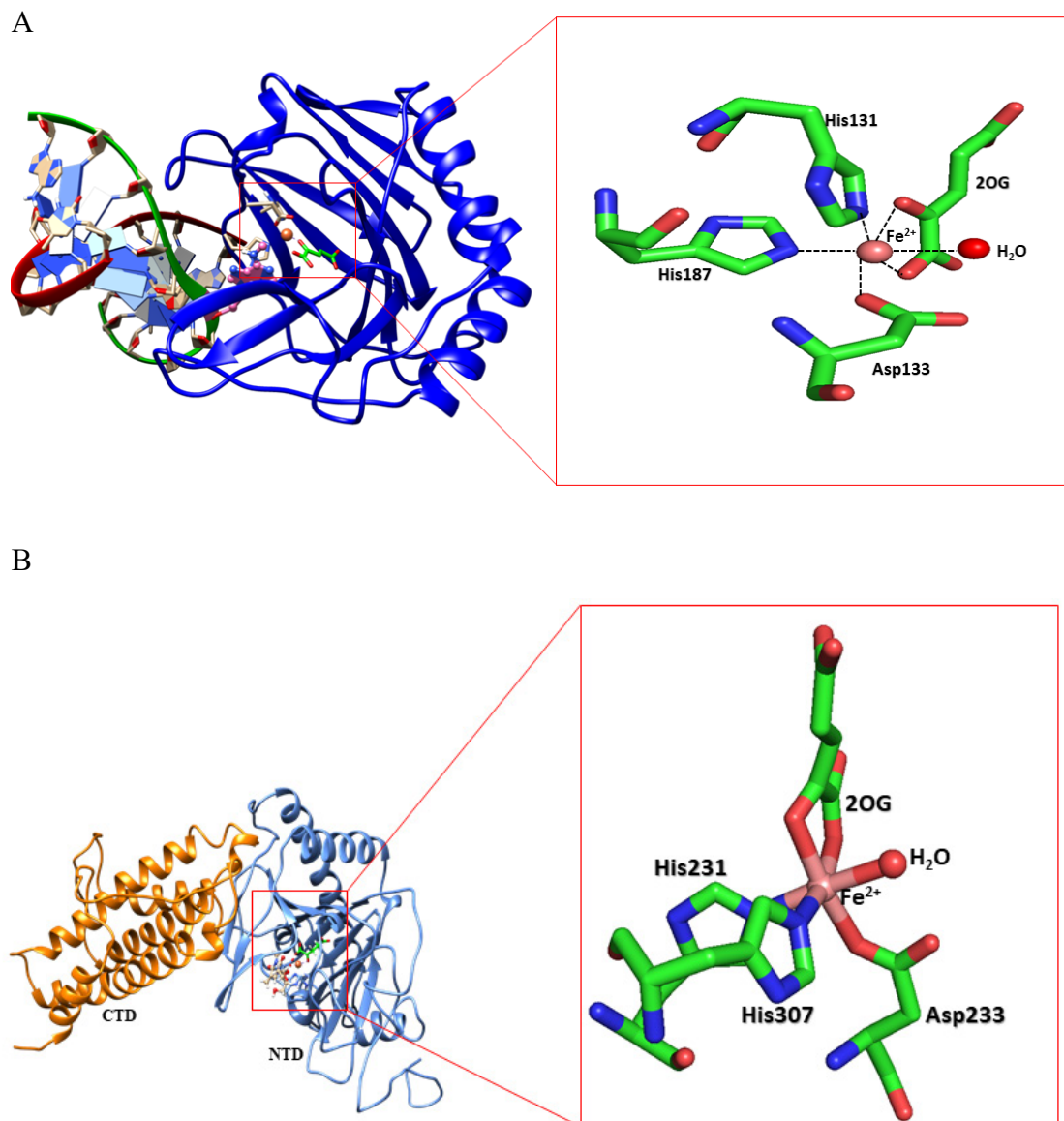


**Figure A1.** Views from the active sites of AlkB (A) and FTO (B). Note the conserved triad of metal binding residues (HDH), bidentate binding of the co-substrate 2OG, and that octahedral coordination of Fe(II) is completed by a water molecule.



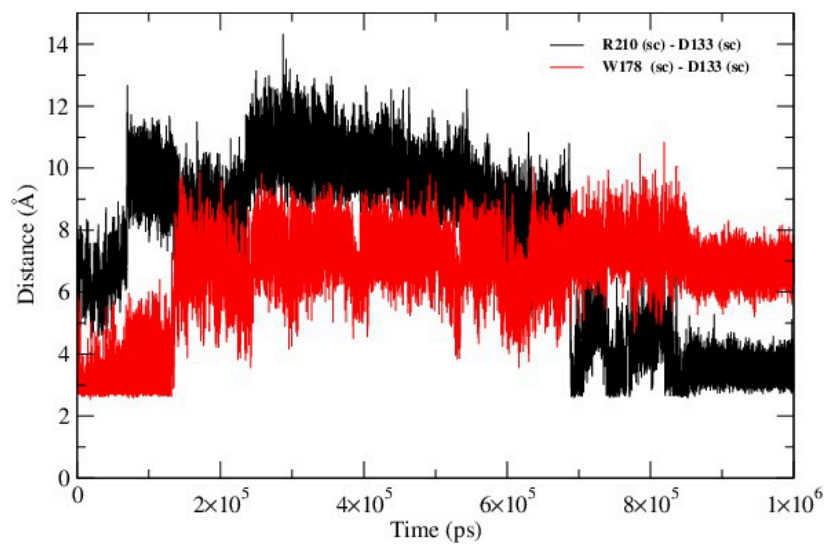


**Figure A2.** Interactions of the AlkB R210 and W178 sidechains with the sidechain of D133 in AlkB-DNA complex MD simulation. Distances were measured between the centres of masses of the atoms forming the guanidino group of arginine (R210), the indole group of tryptophan (W178) and carboxyl group of aspartate (D133). Note W178 interacts more strongly with D133 during the last 200 ns of the simulation than in the crystal structure.

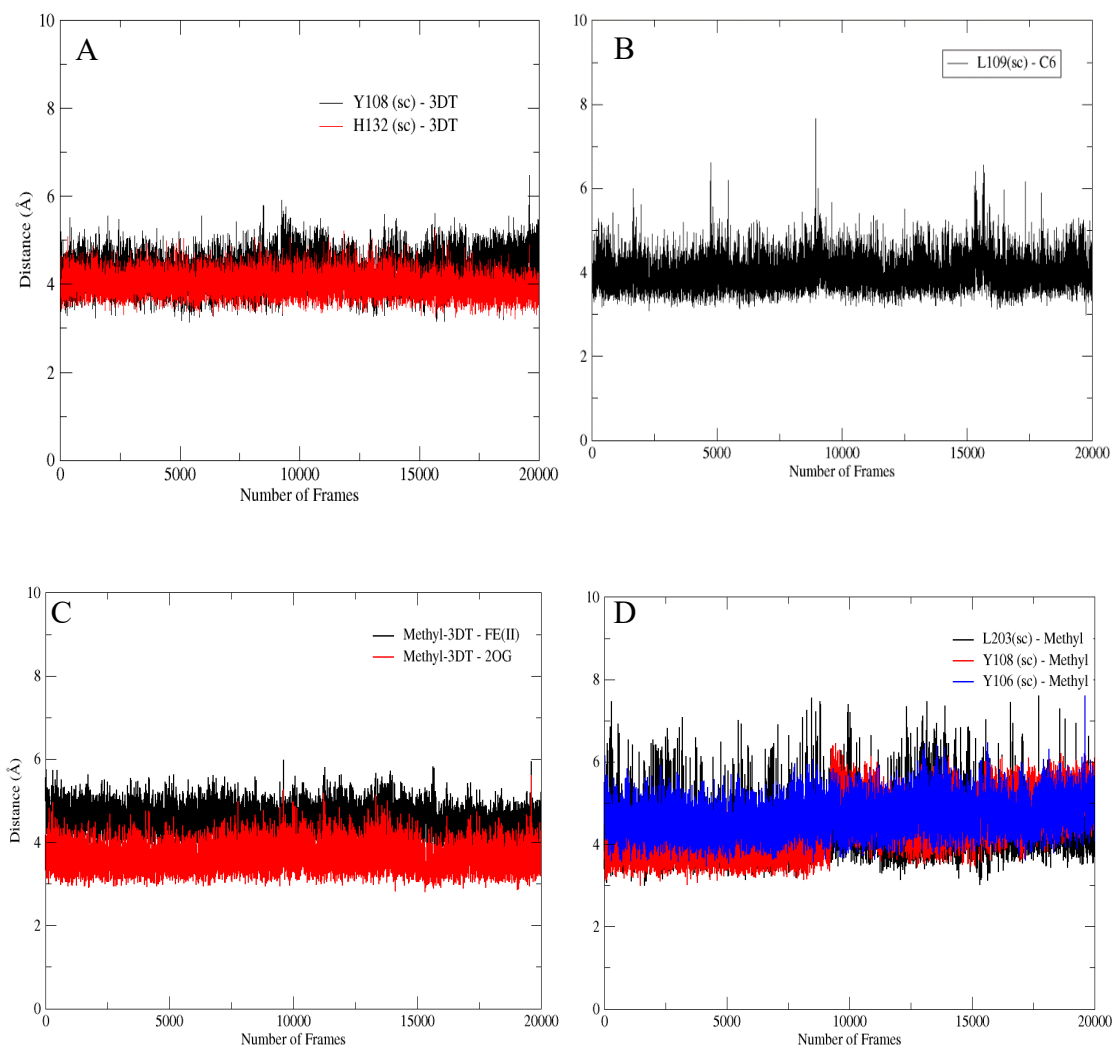


**Figure A3.** The interaction of 3-meT in FTO during the 1  $\mu$ s trajectory. (A) Hydrophobic interactions of the side chains of Y108 and H231 with the thymidine ring of 3-meT; (B) Hydrophobic interactions between the side chain of L109 and the sugar ring of 3-meT; (C) Interaction of the substrate methyl group (to be de-methylated) of 3-meT; (D) van der Waals interactions of the neighboring residues with the methyl group of 3-meT.

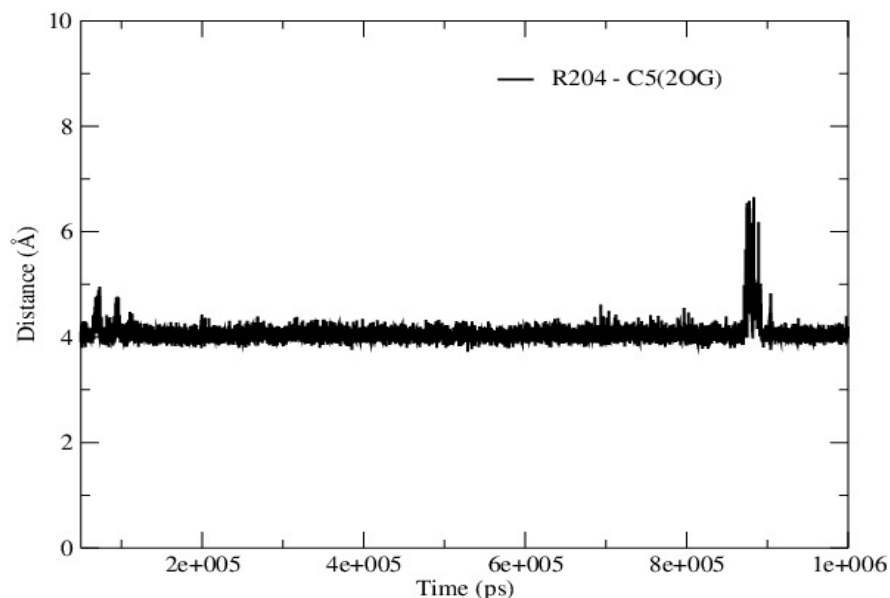


**Figure A4.** Electrostatic interactions of the side chain of R204 of with the non-metal coordinating C5 carboxylate of 2OG. Distances were measured between the centres of masses of the atoms of the guanidino group of arginine (R204) and the C5 carboxylate of 2OG.

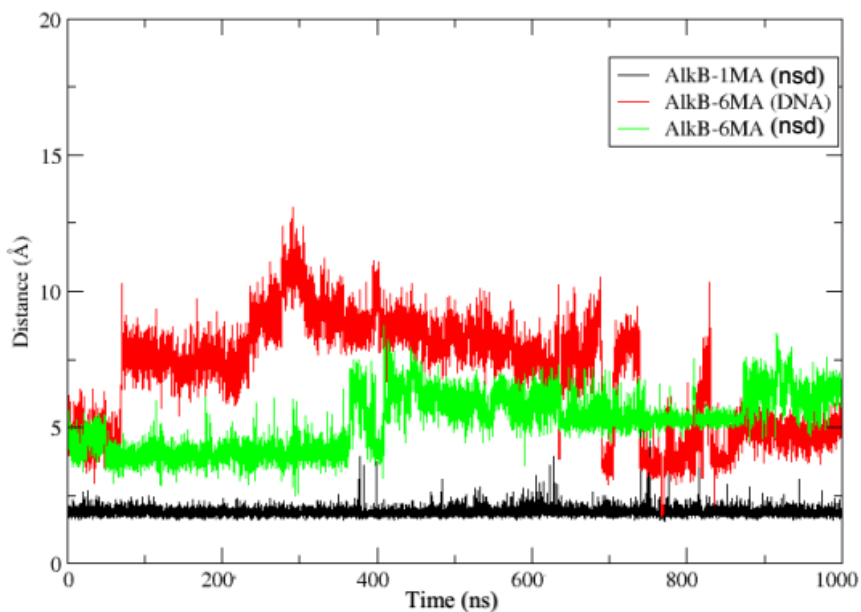


**Figure A5.** Hydrogen bond interactions of the side chain of R210 with the non-metal coordinating carboxylate oxygen of D133. Distances were measured between the centres of masses of the atoms of the guanidino group of R210 and the carboxylate of D133.

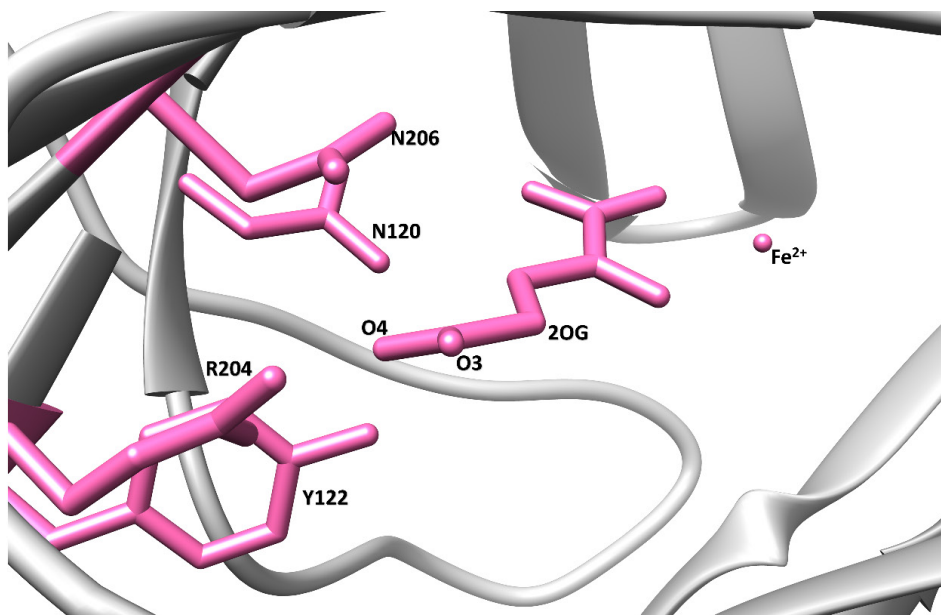


**Figure A6.** The 2OG co-substrate in AlkB and residues that are involved in its binding.

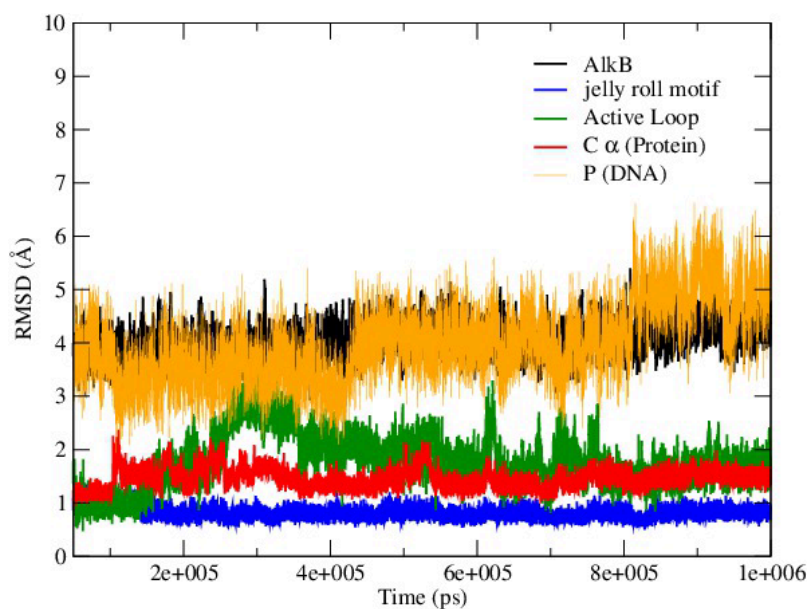


**Figure A7.** The RMSD profile of the full AlkB complex (AlkB-6MA(DNA)) along with the active site bordering loop (residues 133-139), DSBH core motif (residues 187-195), and DNA. The overall RMSD of the full AlkB complex was performed using the C $\alpha$  and P atoms of protein and DNA, respectively. Note that different parts of the complex are characterized by different flexibilities.

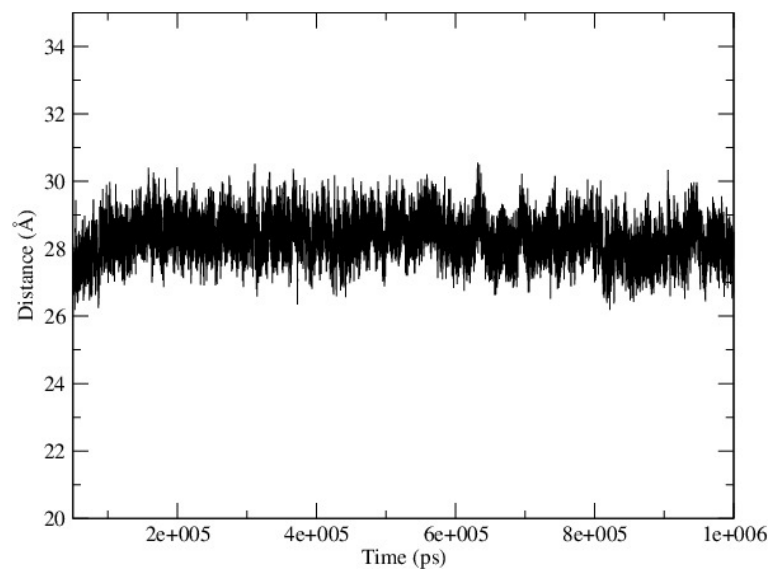


**Figure A8.** The distance between centre of mass of the protein and DNA in the AlkB-6MA(DNA) complex during the MD simulation.

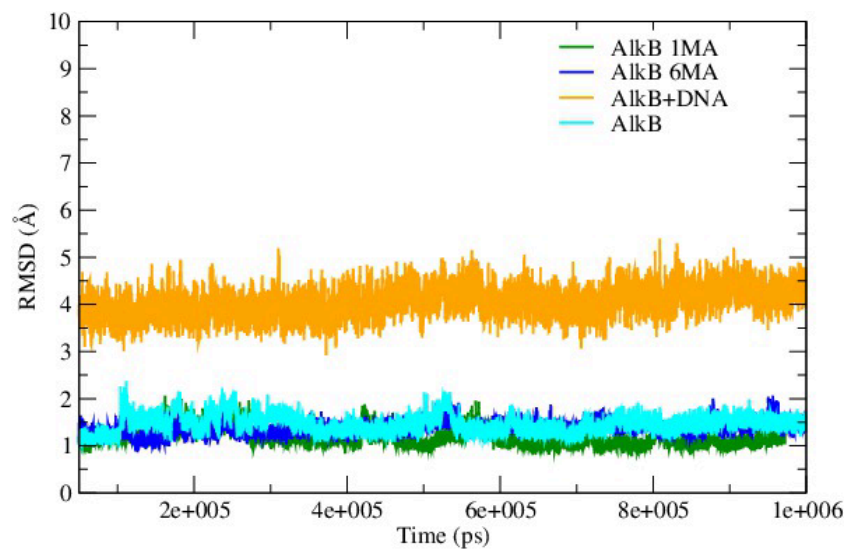


**Figure A9.** RMSD analysis of the AlkB-1MA in comparison to AlkB-6MA and AlkB-6MA(DNA) complexes. Note, that the bulk DNA is the most flexible component of the system.

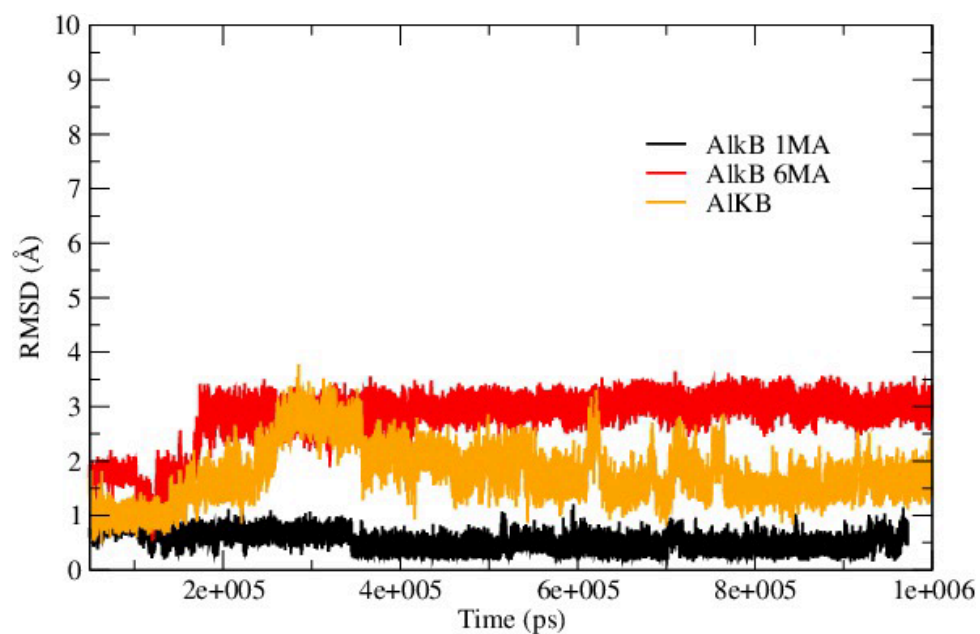


**Figure A10.** The RMSD of the active site region (residues 132-187) of wildtype AlkB and its variants, during the MD simulation.

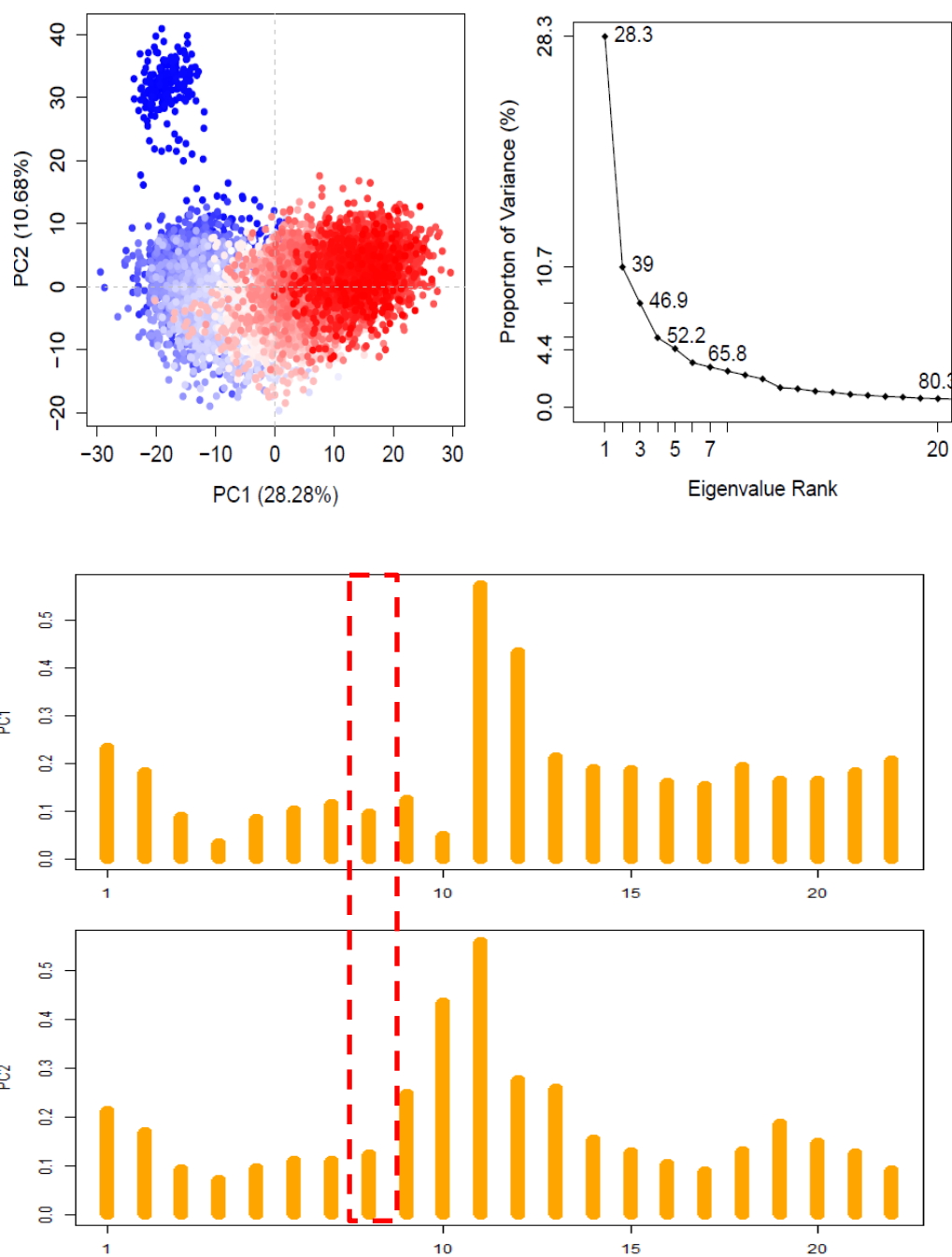


**Figure A11.** The contribution of individual DNA bases from the PC1 and PC2 in the AlkB-6MA(DNA). The region marked by the red dotted line is the methylated base 6MA. PC1 and PC2 are shown as a function of residue numbers.

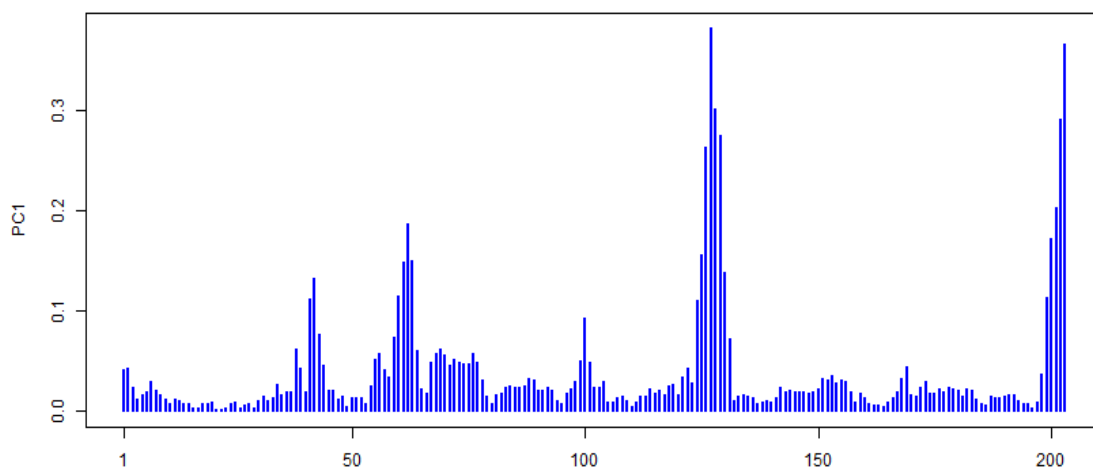
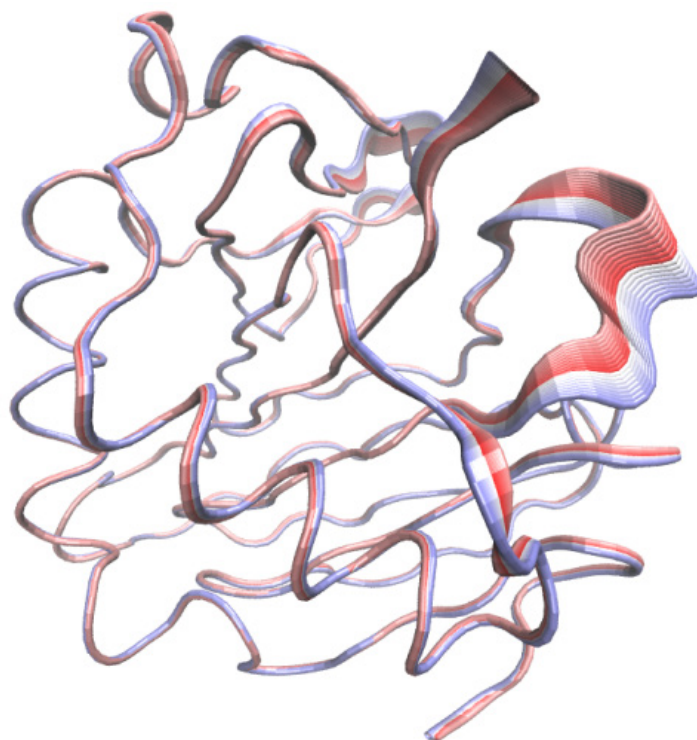


**Figure A12.** PCA analysis of the AlkB-6MA(nsd) complex, showing projection of the PC1 on the enzyme residues indicating the major motions in the protein by removing the noise from translational and rotational data from the MD trajectory. The PC1 is shown as a function of residue numbers.



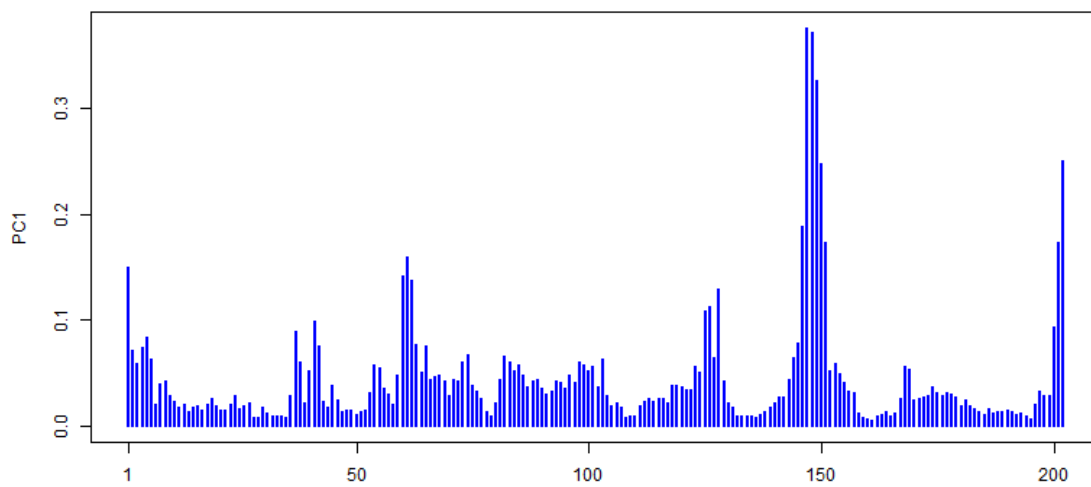
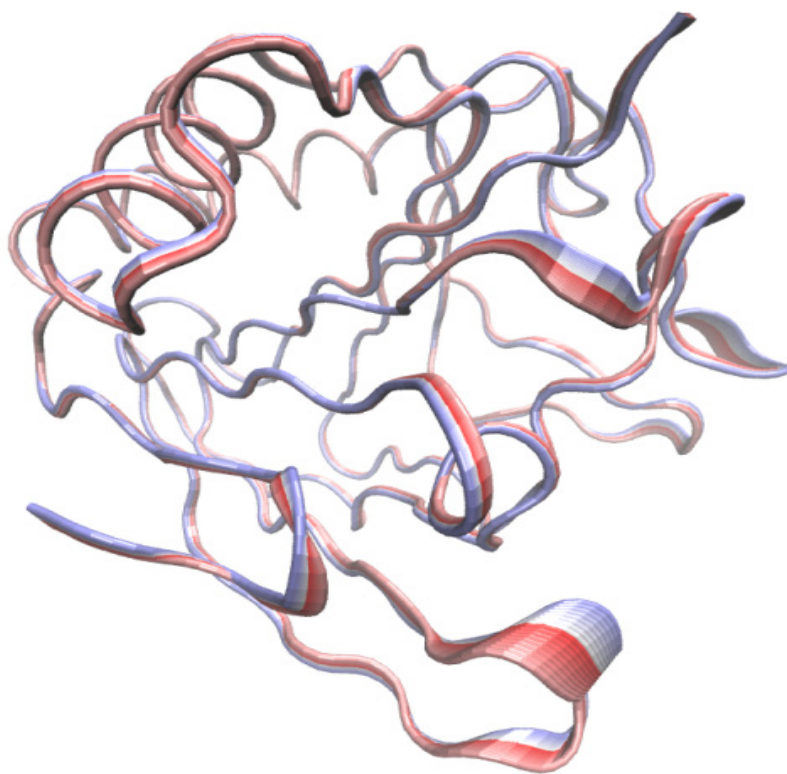


**Figure A13.** PC1 of the AlkB-IMA system. The PC1 is shown as a function of residue numbers.

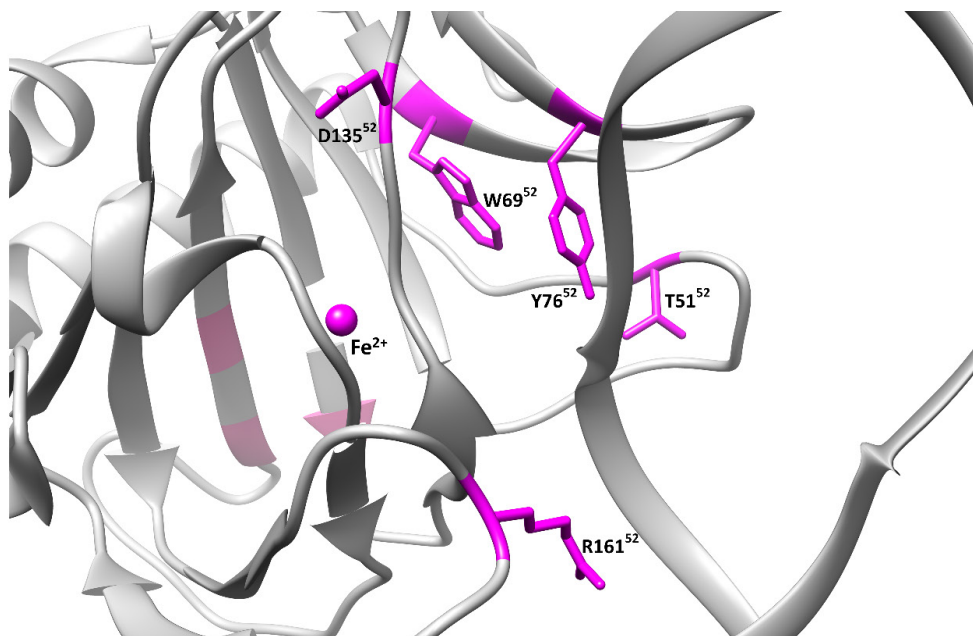


**Figure A14.** The positions of AlkB residues whose substitution is reported to influence the activity of the enzyme.<sup>52</sup>

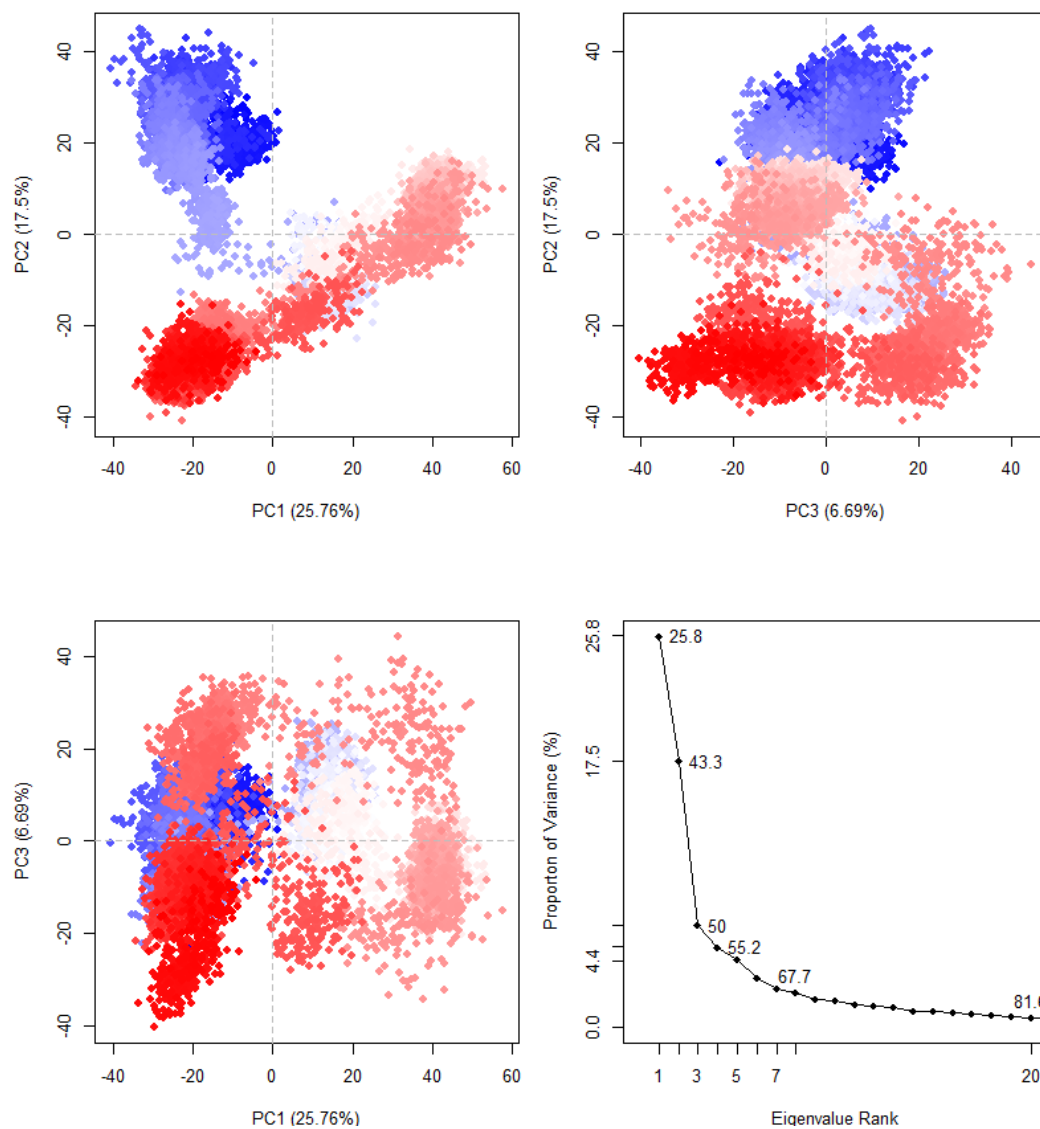


**Figure A15.** The projection of the first three principal components for the last 900 ns FTO equilibrated trajectories. The first three eigenvectors represent half of the overall variance in the data set.

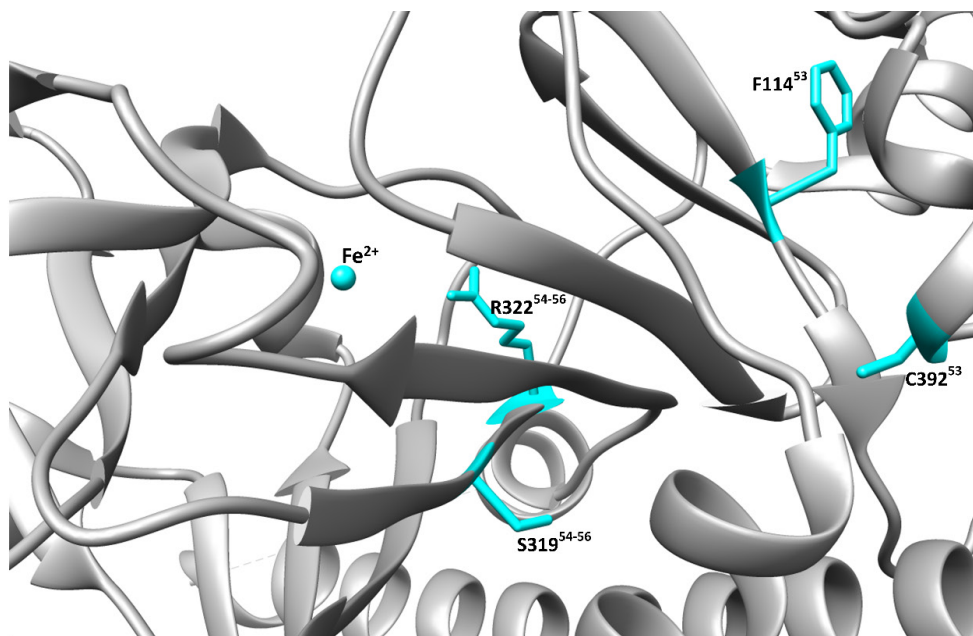


**Figure A16.** The positions of FTO residues whose substitutions influence the enzyme activity<sup>53</sup> (F114 and C392) as well as those correlated with pathological changes (R322 and S319).<sup>54-56</sup>

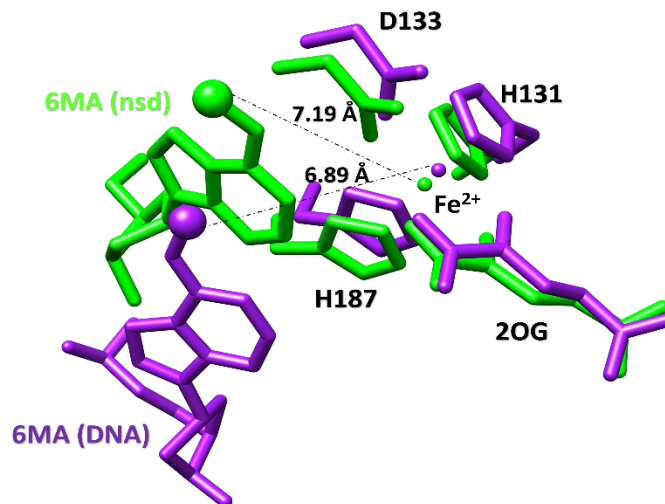


**Figure A17.** Overlaid QM/MM optimized structures of AlkB-6MA (nsd) (green) and AlkB-6MA (DNA) (purple). The methyl group is shown as the larger sphere.

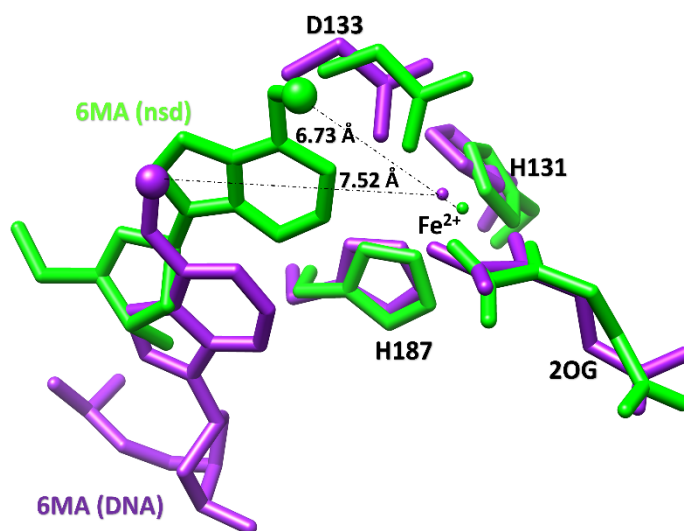


**Figure A18.** The overlaid MD structures of AlkB-6MA (nsd) (green) and AlkB-6MA (DNA) (purple). The methyl group is shown as the larger sphere.

**Table A1.** The relative free energy (in kcal/mol) of binding of 6MA and 1MA to AlkB enzymes calculated using MMGBSA.

<b>Energy Component</b>	<b>AlkB 6MA</b>	<b>AlkB 1MA</b>
$\Delta E_{\text{vdW}}$	-34.2588	-34.9231
$\Delta E_{\text{ele}}$	-14.5910	39.4729
$\Delta E_{\text{ele, sol}}(\text{GB})$	29.1608	-27.2597
<b>ESURF</b>	-3.6987	-3.9800
$\Delta G_{\text{gas}}$	-48.8498	4.5497
$\Delta G_{\text{solv}}$	25.4621	-31.2397
<b>T<math>\Delta</math>S</b>	-21.3820	-21.8505
<b><math>\Delta H(\text{GB})</math></b>	-23.3877	-26.6900
<b><math>\Delta G_{\text{pred}}(\text{GB})</math></b>	-2.0057	-4.8395

**Table A2.** QM/MM analysis of distances (in Å) to the non-heme Fe (II) of the ligands in ALKB complexed with DNA. Distances of the metal coordinating nitrogen of His and oxygen of Asp from the Fe (II) are given.

Name	Equatorial	Axial	ASP	2OG	2OG	Base
	His 131	His 187	133	(O1)	(O5)	(methyl)
QM Cluster minimized	2.13	2.14	2.07	2.08	2.13	7.31
QM/MM Minimized crystal structure (3BIE 1MA, base only)	2.12	2.11	2.05	2.01	2.36	4.88
QM/MM 200ns (6MA, base only )	2.10	2.13	2.06	2.09	2.27	7.21
QM/MM Minimized crystal structure Minimized	2.16	2.18	2.34	2.04	2.29	5.66
QM/MM 200ns	2.18	2.15	2.15	2.06	2.27	7.25
QM/MM 400ns	2.19	2.17	2.11	2.04	2.27	6.69
QM/MM 500ns	2.18	2.18	2.13	2.02	2.27	8.50
QM/MM (Average)	2.18	2.17	2.18	2.04	2.27	7.025
MD (Average)	2.30	2.13	2.10	2.00	2.19	7.44

**Table A3.** QM/MM analysis of second sphere interactions within the active site of AlkB (PDB: 4NID, 3BIE). Distances are in Angstrom (Å) and were measured between the centres of masses of the guanidino groups of arginine (R204 and R210), the phenol ring of a tyrosine (Y122), the amido groups of asparagines (N206, N120), the indole group of a tryptophan (W178), the carboxyl group of an aspartate (D133) and the C5 carboxyl group of 2OG.

<b>Name</b>	<b>R204 (sc) – C5 (2OG)</b>	<b>Y122 (sc) – C5-(O3) 2OG</b>	<b>N206 (sc)- C5- (O4) 2OG</b>	<b>N120 (sc) O1 2OG</b>	<b>T208 (sc) – O1 2OG</b>	<b>W178 (sc) –D133 (OD2)</b>	<b>R210(sc) – D133 (OD2)</b>
<b>Minimized (3BIE, 1MA base only)</b>	4.05	2.62	3.06	5.16	3.44	5.49	2.85
<b>200ns – (6MA- base only)</b>	4.01	2.59	3.25	3.10	4.00	6.78	5.53
<b>QM/MM Minimized</b>	3.96	2.65	2.89	2.87	2.90	2.90	5.67
<b>QM/MM 200ns</b>	3.99	2.69	3.52	2.90	4.08	5.19	2.87
<b>QM/MM 400ns</b>	3.96	2.74	3.58	2.86	3.95	3.97	3.87
<b>QM/MM 500ns</b>	3.99	2.71	3.52	2.82	3.50	5.45	7.17
<b>QM/MM (Average)</b>	3.97	2.70	3.37	2.86	3.60	4.37	4.89
<b>MD (Average)</b>	4.06	3.02	3.47	2.98	4.18	6.54	7.48



**Table A4.** QM/MM analysis of distances to the Fe(II) of FTO. Distances (in Å) of the coordinating nitrogen of His and oxygen of Asp from the Fe(II) are given.

Name	Equatorial His 231	Axial His 307	ASP 233	2OG (O1)	2OG (O5)	Base (methyl)
QM Cluster minimized	2.15	2.13	2.08	2.08	2.15	5.51
QM/MM Minimized	2.17	2.13	2.11	2.11	2.23	4.67
* QM/MM Minimized (EE)	2.18	2.12	2.13	2.09	2.16	4.71
QM/MM Minimized (Lan12dz-ECP)	2.25	2.20	2.15	2.08	2.32	4.66
* QM/MM Minimized (EE) (Lan12dz-ECP)	2.20	2.16	2.20	2.07	2.40	4.36
QM/MM 200ns	2.12	2.13	2.13	2.15	2.13	4.65
QM/MM 300ns	2.12	2.16	2.21	2.05	2.19	5.01
QM/MM 700ns	2.09	2.17	2.15	2.13	2.15	5.34
QM/MM 800ns	2.14	2.12	2.14	2.14	2.16	5.82
QM/MM (Average)	2.13	2.14	2.15	2.12	2.17	5.1
MD (Average)	2.18	2.14	1.98	2.15	2.33	4.50

## References

1. W. Aik, M. Demetriades, M.K.K. Hamdan, E.A.L. Bagg, K.K. Yeoh, C. Lejeune, Z. Zhang, M.A. McDonoug and C.J. Schofield, *J. Med. Chem.* 2013, **56**, 3680-3688.
2. A. Fiser and A. Sali, *Method enzymology.* 2003, **374**, 461-491.
3. Z. Han, T. Niu, J. Chang, X. Lei, M. Zhao, Q. Wang, W. Cheng, J. Wang, Y. Feng, and J. Chai, *Nature*, 2010, **464**, 1205-1209.
4. R.K. Dennington, and T. Millam, *J. Semichem Inc*, 2009.
5. C. Zhu and C. Yi, *Ang. Chemie Intnal Ed.* 2014, **53**, 3659-3662.
6. C.G. Yang et al., *Nature*, 2008, **452**, 961-965.
7. J.C. Gordon et al., *Nuclei Acids Research*, 2005, **33**, W368-371.
8. J.M Word, S.C. Lovell, J.S. Richardson and D.C. Richardson, *J. Mol. Biol.* 1999, **285**, 1735-1747.
9. J. Wang, R.M. Wolf, J.W. Caldwell, P.A. Kollman, and D.A. Case, *J. Comput. Chem.*, 2004, **25**, 1157-1174.
10. M.J.T. Frisch, G. W. Schlegel, H. B. Scuseria, G. E. Robb, M. A. Cheeseman, J. R. Scalmani, G. Barone, V. Mennucci, B. Petersson, G. A. Nakatsuji, H. Caricato, M. Li, X. Hratchian, H. P. Izmaylov, A. F. Bloino, J. Zheng, G. Sonnenberg, J. L. Hada, M. Ehara, M. Toyota, K. Fukuda, R. Hasegawa, J. Ishida, M. Nakajima, T. Honda, Y. Kitao, O. Nakai, H. Vreven, T. Montgomery, J. A., Jr. Peralta, J. E. Ogliaro, F. Bearpark, M. Heyd, J. J. Brothers, E. Kudin, K. N. Staroverov, V. N. Kobayashi, R. Normand, J. Raghavachari, K. Rendell, A. Burant, J. C. Iyengar, S. S. Tomasi, J. Cossi, M. Rega, N. Millam, N. J. Klene, M. Knox, J. E. Cross, J. B. Bakken, V. Adamo, C. Jaramillo, J. Gomperts, R. Stratmann, R. E. Yazyev, O. Austin, A. J. Cammi, R. Pomelli, C. Ochterski, J. W. Martin, R. L. Morokuma, K. Zakrzewski, V. G. Voth, G. A. Salvador, P. Dannenberg, J. J. Dapprich, S. Daniels, A. D. Farkas, Ö. Foresman, J. B. Ortiz, J. V. Cioslowski, J. Fox, Gaussian 09. *Gaussian, Inc* Revision D.01(Wallingford CT) 2009.
11. W.D. Cornell, P. Cieplak, C.I. Bayly, and P.A. Kollmann, *J. Am. Chem. Soc.* 1993, **115**, 9620-9631.
12. E. I. Solomon, A. Decker and N. Lehnert, *Proc. Natl. Acad. Sci. U.S.A.*, 2003, **100**, 3589-3594.
13. E.I. Solomon, S. Goudarzi and K.D. Sutherlin, *Biochem.* 2016, **55**, 6363-6374.
14. R.P. Hausinger, *Crit. Rev. Biochem. Mol. Biol.*, 2004, **39**, 21-68.
15. E.I. Solomon, T.C. Brunold, M.I. Davis, J.N. Kemsley, S. Lee, N. Lehnert, F. Neese, A.J Skulan, Y. Yang and J. Zhou, *Chem. Rev.* 2000, **100**, 235-350.
16. R.H. Holm and E.I. Solomon, *Chem. Rev.* 2014, **114**, 4039-4040.
17. B. Wang, Z. Cao, D.A. Sharon, and S. Shaik, *ACS Catalysis* 2015, **5**, 7077-7090.
18. E.G. Pavel et al. *J. Am. Chem. Soc.* 1998, **120**, 743-753.
19. J. Zhou et al., *J. Am. Chem. Soc.* 2001, **123**, 7388-7398.

20. J. Zhou, M. Gunsior, B.O. Bachmann, C.A. Townsend, and E.I. Solomon, *J. Am. Chem. Soc.* 1998, **120**, 13539-13540.
21. P. Li and K.M. Merz, *J. Chem. Info and Model* 2016, **56**, 599-604.
22. A. Pabis, I. Geronimo, D.M. York, and P. Paneth, *J. Chem. Theo. Comput* 2014, **10**, 2246-2254.
23. R. Salomon-Ferrer, A.W. Götz, D. Poole, S. Le Grand, and R.C. Walker, *J. chem. Theo comput* 2013, **9**, 3878-3888.
24. D. Case, V. Babin, J. Berryman, R. Betz, Q. Cai, D. Cerutti, T. Cheatham III, T. Darden, R. Duke and H. Gohlke, Amber, 2014, **14**, 29-31.
25. J.A. Maier, *et al. J. chem. Theo. comput* 2015, **11**, 3696-3713.
26. W.L. Jorgensen, J. Chandrasekhar, J.D. Madura, R.W. Impey, and M.L. Klein, *J. chem. Phys.* 1983, **79**, 926-935.
27. T. Darden, D. York, and L. Pedersen, *J. chem. Phys.* 1993, **98**, 10089-10092.
28. R. Davidchack, R. Handel and M.V. Tretyakov, *J. Chem. Phys.* 2009, **130**, 234101.
29. J.P. Ryckaert, G. Ciccotti, and H.J. Berendsen, *J. Comput. Phys.* 1977, **23**, 327-341.
30. H.J. Berendsen, J.V. Postma, W.F. van Gunsteren, A. DiNola, and J. Haak, *J. chem. Phys.* 1984, **81**, 3684-3690.
31. D.R. Roe and T.E. Cheatham III, *J. chem. theo comput.* 2013 **9**, 3084-3095.
32. W. Humphrey, A. Dalke and K. Schulten, *J. Mol. Graph.* 1996, **14**, 27-38.
33. E.F. Pettersen, *et al.*, *J Comput Chem* 2004, **25**, 1605-1612.
34. B.J. Grant, A.P. Rodrigues, K.M. ElSawy, J.A. McCammon, and L.S. Caves, *Bioinformatics (Oxford, England)* 2003, **22**, 2695-2696.
35. W. Singh, G. Fields, C. Christov and T.G. Karabancheva-Christova, *RSC Advances* 2016.
36. G. Schenk, M.Y. Pau, and E.I. Solomon, *J Am Chem Soc* 2004, 126, 505-515.
37. V. Barone and M. Cossi, *J. Phys. Chem A* 1998, **102**, 1995-2001.
38. P. Walter, J. Metzger, C. Thiel, and V. Helms, *PloS one* 2013, **8**, e58583.
39. P.E. Siegbahn and T. Borowski, *Acct. chem. Resear.* 2006, **39**, 729-738.
40. P.E. Siegbahn and F. Himo *Wiley Interdisciplinary Reviews: Computational Molecular Science* 2011, **1**, 323-336.
41. P. Tao and H.B. Schlegel, *J. Comput. Chem.* 2010, **31**, 2363-2369.
42. F. Maseras and K. Morokuma, *J. Comput. Chem.* 1995, **16**, 1170-1179.
43. M. Svensson, S. Humbel, and K. Morokuma, *J. chem. phys.* 1996, **105**, 3654-3661.
44. S. Dapprich, I. Komáromi, K.S. Byun, K. Morokuma and M.J. Frisch, *J. Mol. Struc: THEOCHEM* 1999, **461**, 1-21.
45. T. Vreven, K. Morokuma, O. Farkas, H.B. Schlegel, and M.J. Frisch, *J Comput Chem* 2003, **24**, 760-769.
46. T. Vreven and K. Morokuma, *J. Comput. Chem.* 2000, **21**, 1419-1432.
47. P. Li, B.P. Roberts, D.K. Chakravorty, and K.M. Merz Jr., *J Chem Theory Comput* 2013, **9**, 2733-2748.

48. H.M. Senn and W. Thiel, *Angewandte Chemie International Edition* 2009, **48**, 1198-1229.
49. P.A. Kollman, I. Massova, C. Reyes, B. Kuhn, S. Huo, L. Chong, M. Lee, T. Lee, Y. Duan, W. Wang, O. Donini, P. Cieplak, J. Srinivasan, D.A. Case, and T.E. 3rd Cheatham, *Acc. Chem. Res* 2000, **33**, 889-897.
50. I. Massova and P.A. Kollman, *Perspectives in drug discovery and design* 2000, **18**, 113-135.
51. V. Tsui and D.A. Case, *Biopolymers* 2000, **56**, 275-291.
52. P.J. Holland, T. Hollis, *PLoS One*. 2010, **5**, e8680.
53. Z. Han, T. Niu, J. Chang, X. Lei, M. Zhao, Q. Wang, W. Cheng, J. Wang, Y. Feng, and J. Chai, *Nature* 2010, **464**, 1205-1209.
54. G. Jia, Y. Fu, X. Zhao, Q. Dai, G. Zheng, Y. Yang, C. Yi, T. Lindahl, T. Pan, Y.G. Yang and C. He, *Nat. Chem. Biol.*, 2011, **7**, 885-887.
55. L. Rohena, M. Lawson, E. Guzman, M. Ganapathi, M.T. Cho, E. Haverfield and K. Anyane-Yeboah, *Am. J. Med. Genet A.*, 2016, **170**, 1023-1028.
56. H. Daoud, D. Zhang, F. McMurray, A. Yu, S.M. Luco, J. Vanstone, O. Jarinova, N. Caron, J. Wickens, S. Shishodia, H. Choi, M.A. McDonough, C.J Schofield, M.E. Harper, D.A. Dymant and C.M. Armour, *J. Med. Genet.*, 2016, **53**, 200-207.

## B Appendix B: Supporting Information for Chapter 3

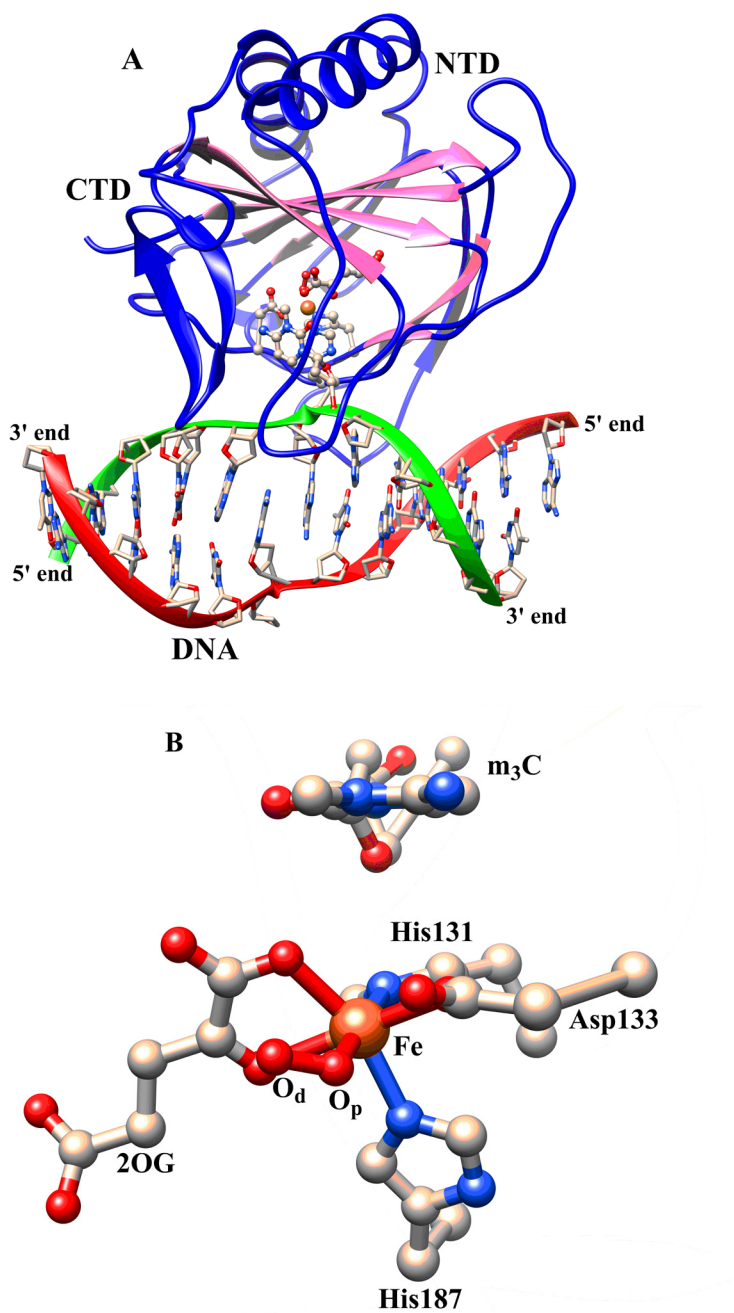


**Figure B1** Average structure of AlkB-dsDNA (A) and a view of the AlkB-dsDNA active site (B) derived from the Fe(III)-superoxo MD simulations. Coloring in (A): double stranded beta helix (DSBH) core fold (pink).  $m_3C$ : 3-methylcytosine.

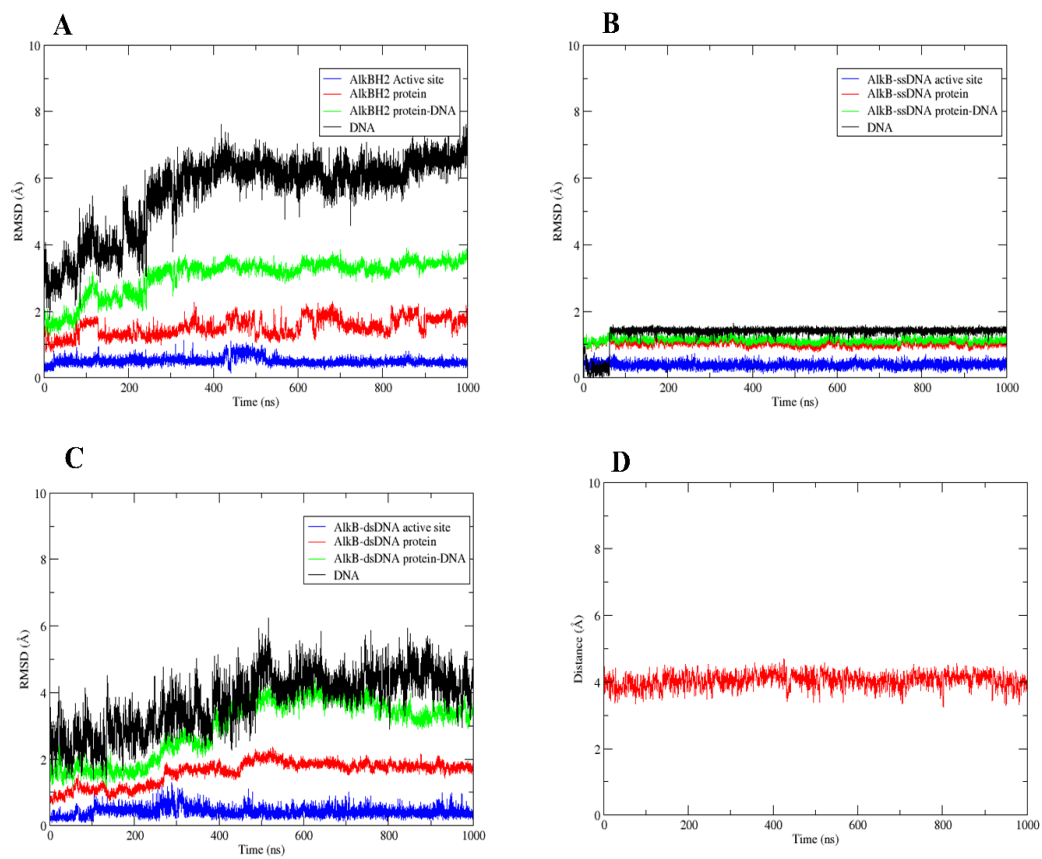


**Figure B2** RMSD Plots for AlkBH2-dsDNA (A), AlkB-ssDNA (B), AlkB-dsDNA (C) and plot of the distance between the distal oxygen ( $O_d$ ) of the superoxide and C2 of 2OG (D) in the AlkBH2-dsDNA Fe(III)-superoxo complex.

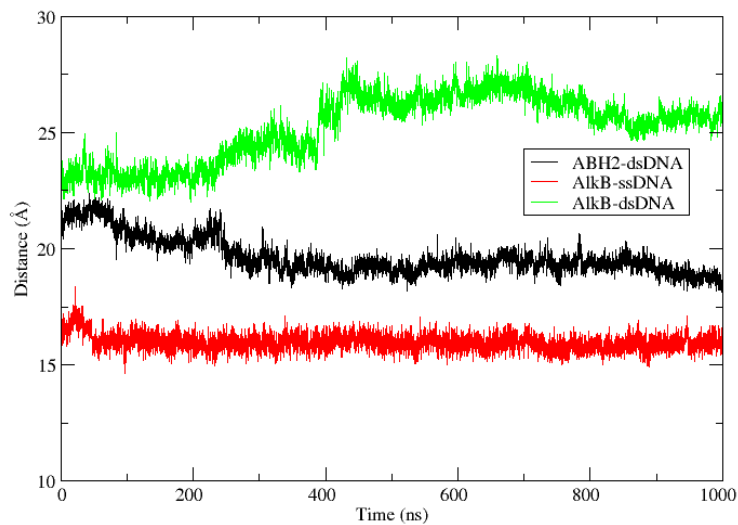


**Figure B3** Measured distances between the center of mass of the protein and the DNA molecule in the AlkBH2-dsDNA, AlkB-ssDNA and AlkB-dsDNA complexes, during MD simulations of the Fe(III)-superoxo intermediates.

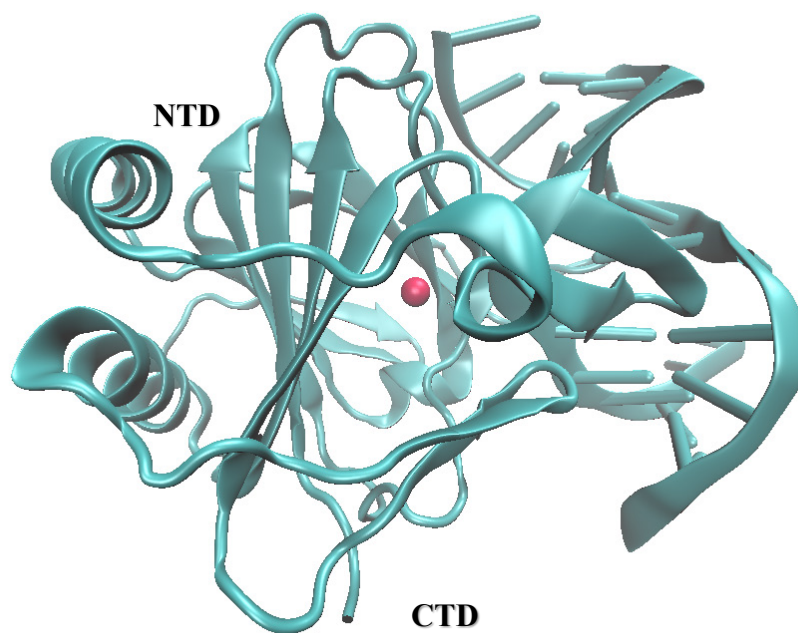


**Figure B4** View of the structure of AlkBH2-dsDNA showing the location of the center of mass (in red sphere) of the protein-DNA complex. NTD and CTD are N-terminal Domain and C-terminal Domain, respectively.

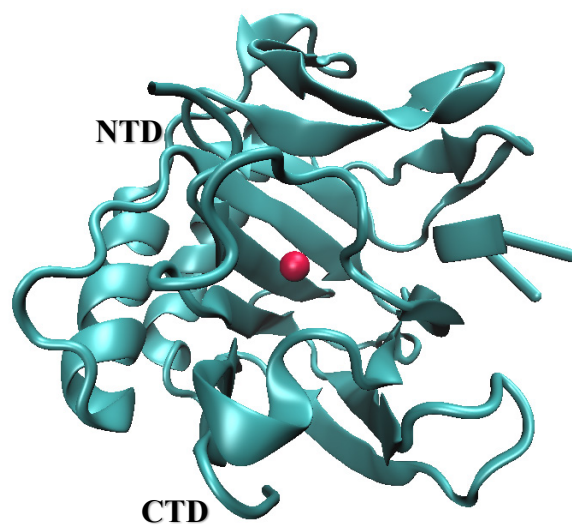


**Figure B5** View of the structure of AlkB-ssDNA showing the location of the center of mass (in red sphere) of the protein-DNA complex. NTD and CTD are N-terminal Domain and C-terminal Domain, respectively.

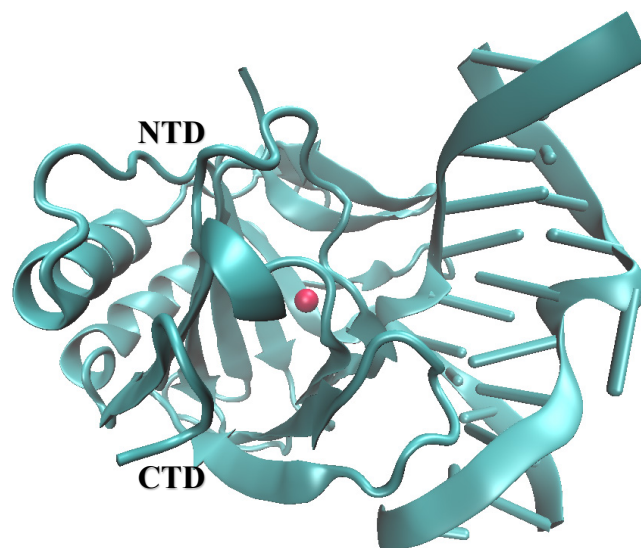


**Figure B6** View of the structure of AlkB-dsDNA showing the location of the center of mass (in red sphere) of the protein-DNA complex. NTD and CTD are N-terminal Domain and C-terminal Domain, respectively.



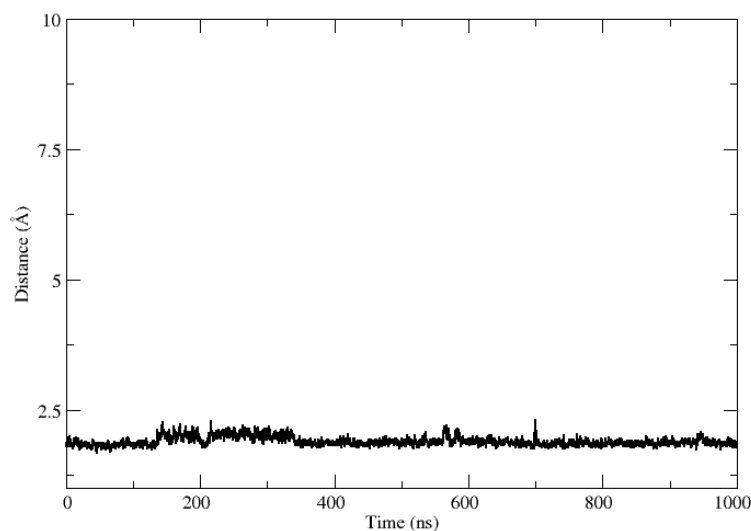


**Figure B7** Hydrogen bonding interaction of Arg254 side chain with the non metal ion coordinating carboxylate oxygen of Asp173 in the AlkBH2-dsDNA complex during the Fe(III)-superoxo MD simulations. The distance was measured between the center of mass of the atoms forming the guanidino group of Arg254 and the carboxylate of Asp173.

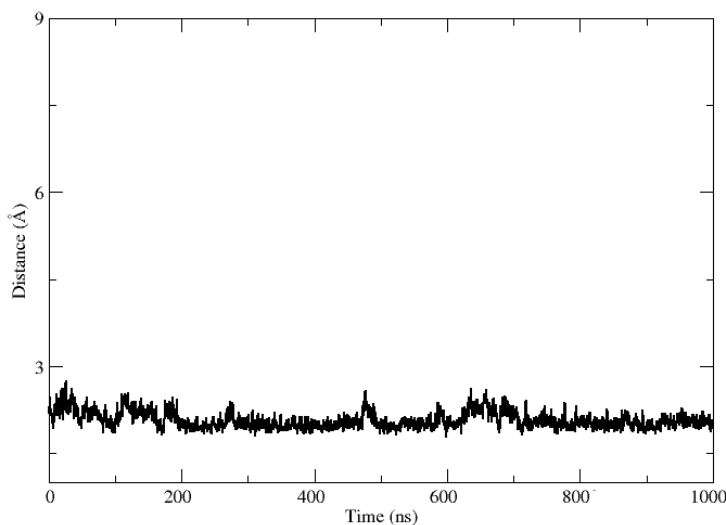


**Figure B8** Hydrogen bonding interaction of Arg210 side chain with the non metal ion coordinating carboxylate oxygen of Asp133 in the AlkB-ssDNA complex during the Fe(III)-superoxo MD simulations. The distance was measured between the center of mass of the atoms forming the guanidino group of Arg210 and the carboxylate of Asp133.

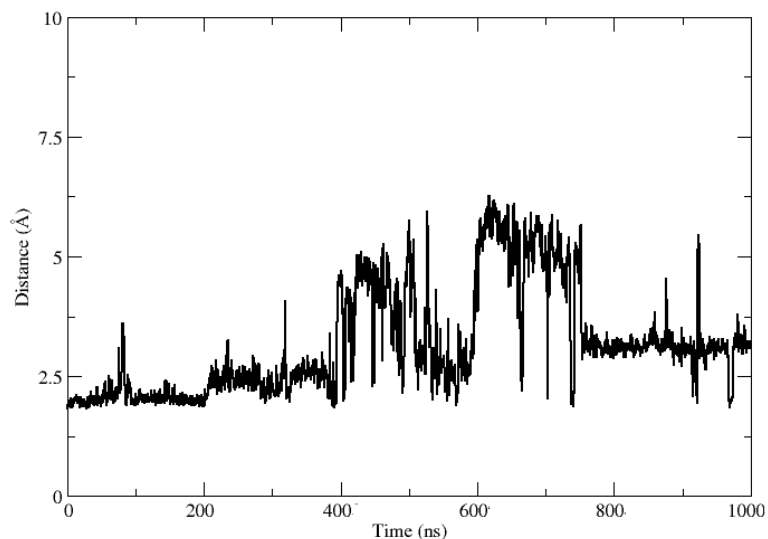


**Figure B9** Hydrogen bonding interaction of Arg210 side chain with the non meta ion coordinating carboxylate oxygen of Asp133 in the AlkB-dsDNA complex during the Fe(III)-superoxo MD simulations. The distance was measured between the center of mass of the atoms forming the guanidino group of Arg210 and the carboxylate of Asp133.

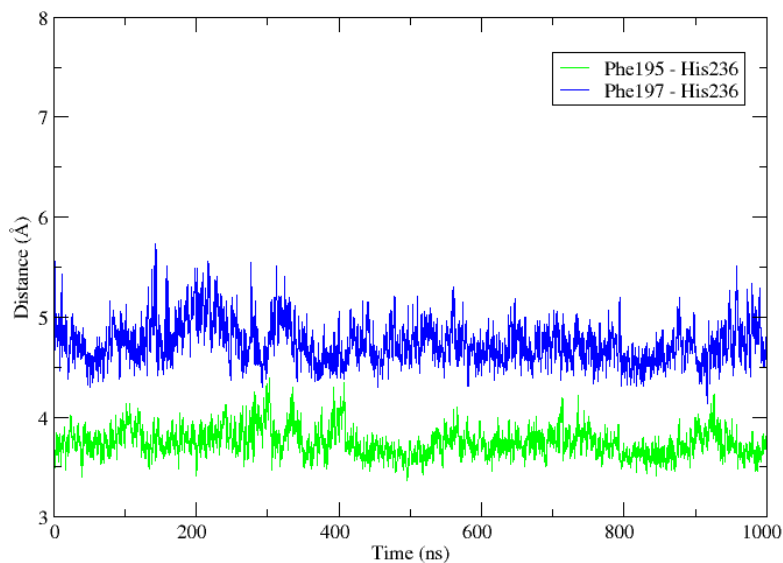


**Figure B10** Stacking interaction of the iron coordinating residue His236 (His<sup>2</sup>) with Phe195 and Phe197 at the Fe(III)-superoxo intermediate stage of the AlkBH2-dsDNA complex. Distances were measured between the center of mass of the atoms forming the imidazole ring of His236 and the phenyl groups of Phe195 and Phe197.

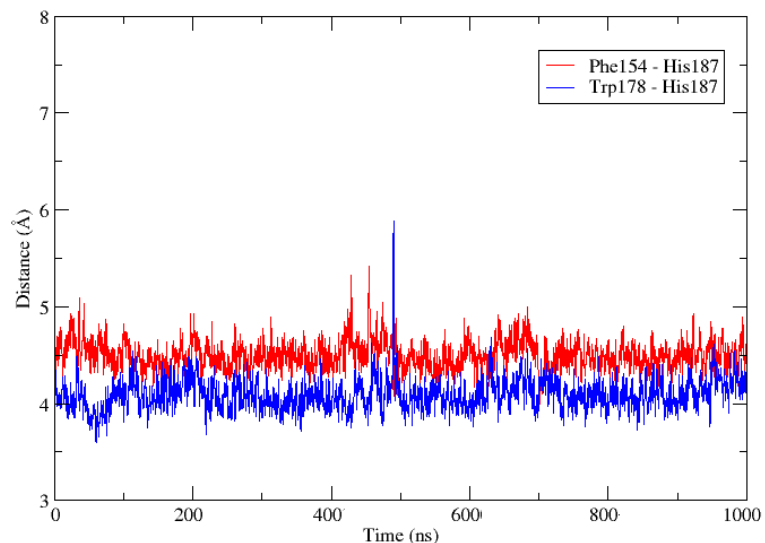


**Figure B11** Stacking interactions of the iron coordinating residue His187 (His<sup>2</sup>) with Phe154 and Trp178 at the Fe(III)-superoxo intermediate stage of the AlkB-ssDNA complex. Distances were measured between the center of mass of the atoms forming the imidazole ring of His187, the phenyl group of Phe154, and the indole group of Trp178.

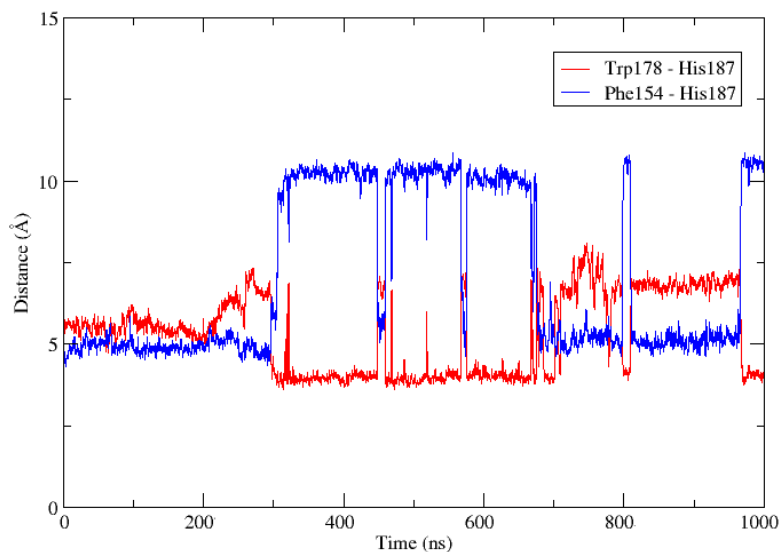


**Figure B12** Stacking interactions of the iron coordinating residue His187 (His<sup>2</sup>) with Phe154 and Trp178 at the Fe(III)-superoxo intermediate stage of the AlkB-dsDNA complex. Distances were measured between the center of mass of the atoms forming the imidazole group of His187, phenyl group of Phe154, and indole group of Trp178.

With AlkBH2-dsDNA, DCCA shows that residues 57-87, belonging to ( $\beta$ 1-  $\beta$ 2) and ( $\alpha$ 1), manifest a positive correlation with residues 210-237 ( $\beta$ 11-  $\beta$ 13), and residues 152-197 ( $\beta$ 8-  $\beta$ 10) manifest a positive correlation with residues 210-250 ( $\beta$ 11-  $\beta$ 14) and ( $\alpha$ 5) (Figure 3.2A). Similarly, in AlkB-ssDNA (Figure B13), residues 17-27 ( $\beta$ 1) show a positive correlation with 174-178 (the loop connecting  $\beta$ 9 to  $\beta$ 10), and residues 114-159 ( $\beta$ 5-  $\beta$ 8) have a positive correlation with residues 164-210 ( $\beta$ 9-  $\beta$ 12) and ( $\alpha$ 3). With AlkB-dsDNA (Figure B14), residues 43-60 ( $\alpha$ 1) have a positive correlation with residues 65-93 ( $\beta$ 3-  $\beta$ 4); residues 15-26 ( $\beta$ 1) show a positive correlation with residues 98-113 ( $\alpha$ 2); residues 58-63 ( $\beta$ 2) have a positive correlation with 113-128 ( $\beta$ 5); residues 93-133 ( $\alpha$ 3) and ( $\beta$ 5-  $\beta$ 6) have positive correlations with residues 128-178 ( $\beta$ 6- $\beta$ 10); residues 113-184 ( $\beta$ 5-  $\beta$ 8) have a positive correlation with residues 158-191 ( $\beta$ 9-  $\beta$ 11); and residues 123-193 ( $\beta$ 6-  $\beta$ 11) and ( $\alpha$ 3) show a negative correlation with the DNA. Figures B15 and B16 contain the annotated secondary structures of AlkBH2-dsDNA and AlkBs, respectively.

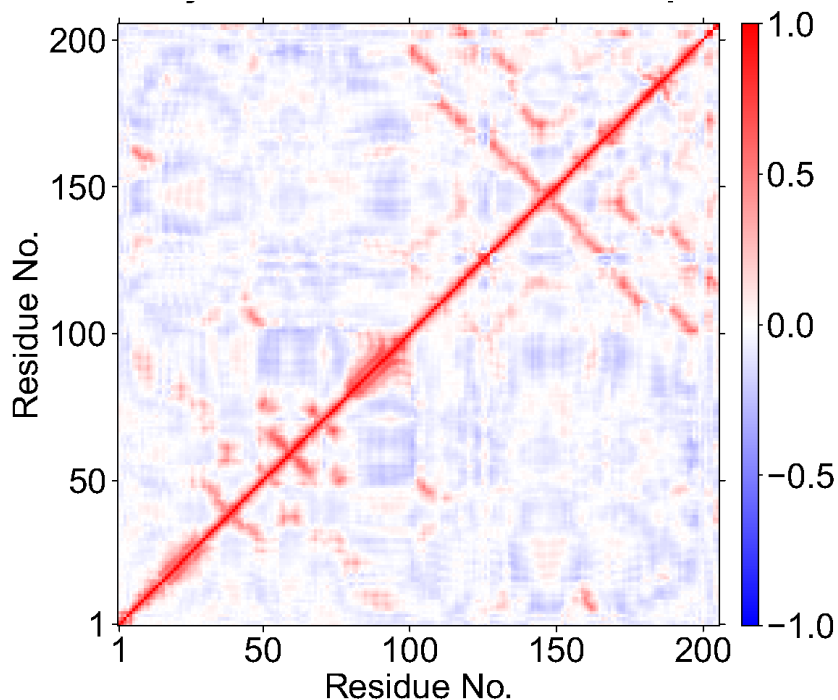


**Figure B13** Dynamic cross correlation for the Fe(III)-superoxo intermediate stage of the AlkB-ssDNA complex. Residue numbers 1-200 (protein), 201 (Fe), 202 (O<sub>2</sub>), 203 (2OG), 204-206 (DNA) and 205 (m<sub>3</sub>C substrate).

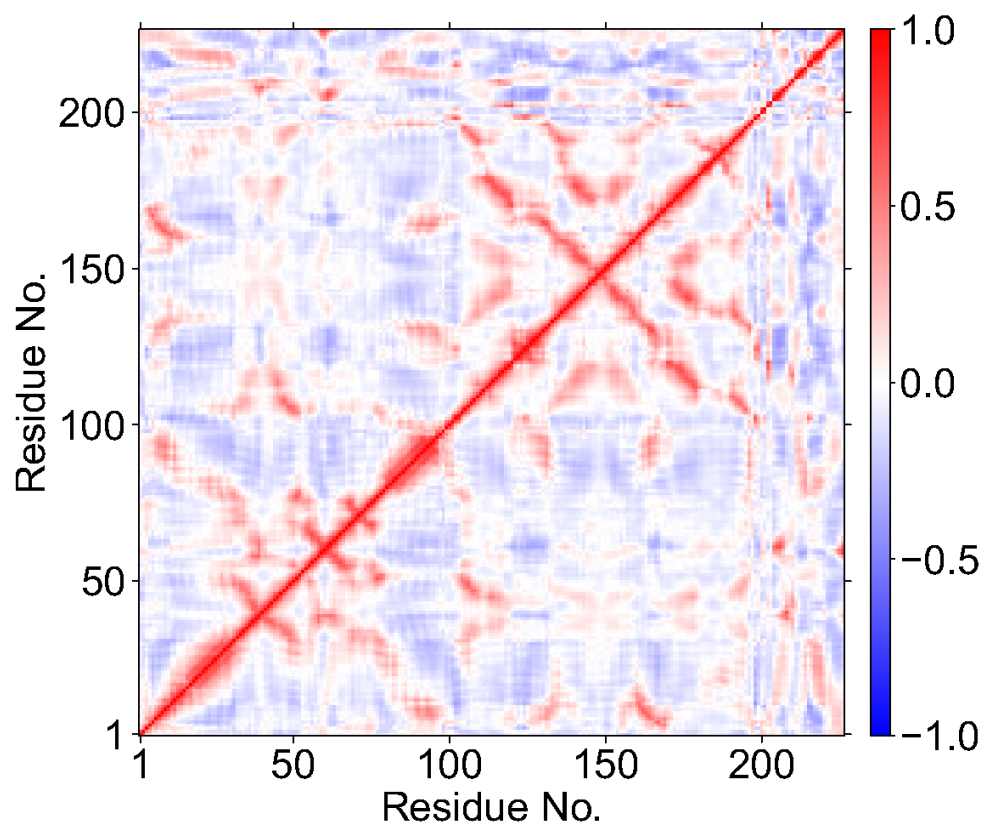


**Figure B14** Dynamic cross correlation for the Fe(III)-superoxo intermediate stage of the complex AlkB-dsDNA. Residue numbers 1-201 (protein), 202 (Fe), 203 (O<sub>2</sub>), 204 (2OG), 205-229 (DNA) and 211 (m<sub>3</sub>C substrate).

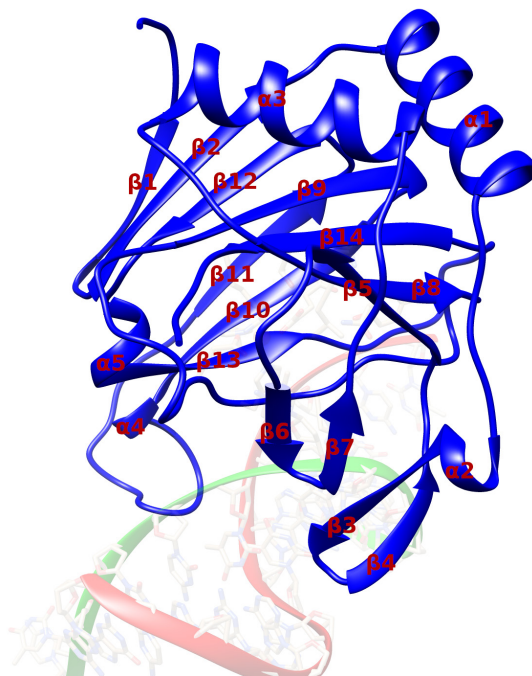


**Figure B15** Annotation of the secondary structure of AlkBH2-dsDNA (PDB code, 3RZJ<sup>1</sup>).

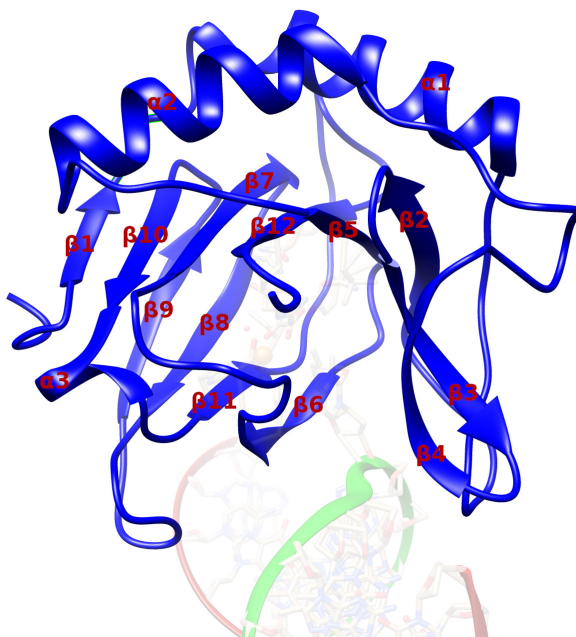


**Figure B16** Annotation of the secondary structure of AlkBs (PDB code, 3O1M<sup>2</sup>). The structure of AlkB-dsDNA was used for this purpose.

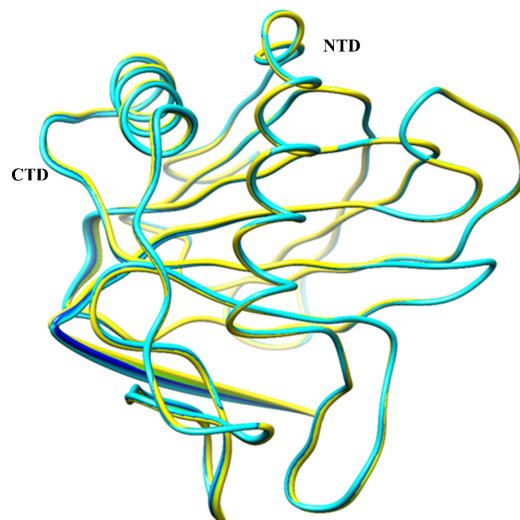


**Figure B17** PCA for the AlkB-ssDNA Fe(III)-superoxo MD simulation. Yellow to blue coloring represents the main direction of motion of protein residues. NTD and CTD are N-terminal Domain and C-terminal Domain, respectively.

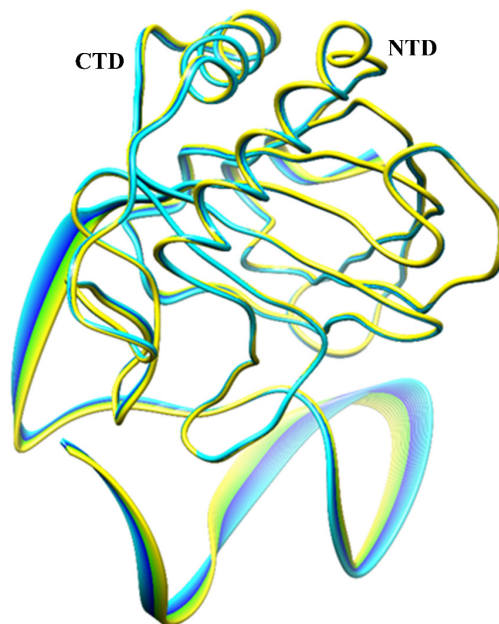


**Figure B18** PCA for the AlkB-dsDNA Fe(III)-superoxo MD simulation. Yellow to blue coloring represents the main direction of motion of protein residues. NTD and CTD are N-terminal Domain and C-terminal Domain, respectively.

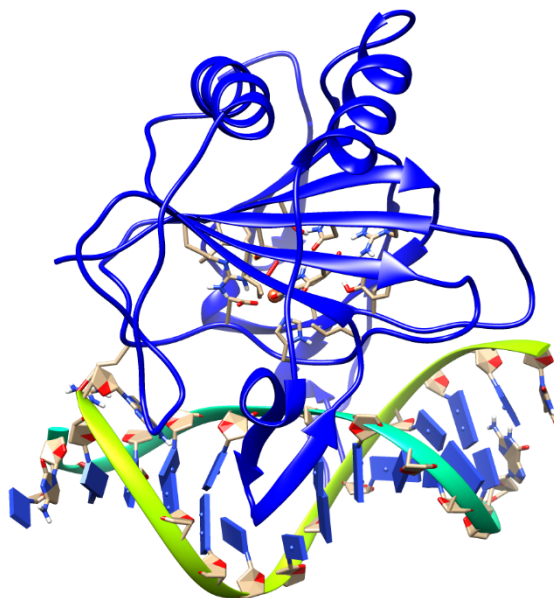


**Figure B19** View of an MD structure of AlkBH2-dsDNA with undamaged DNA.

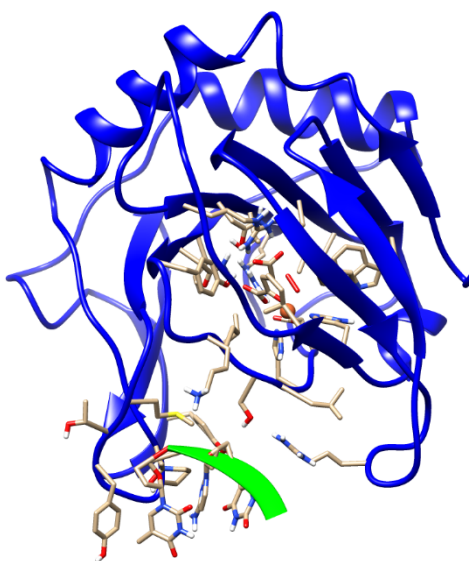


**Figure B20** View of an MD structure of AlkB-ssDNA with undamaged DNA.



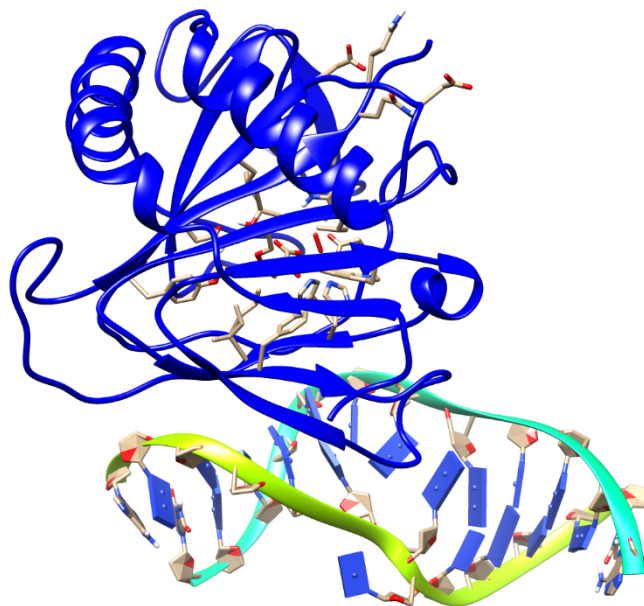


**Figure B21** View of an MD structure of AlkB-dsDNA with undamaged DNA.

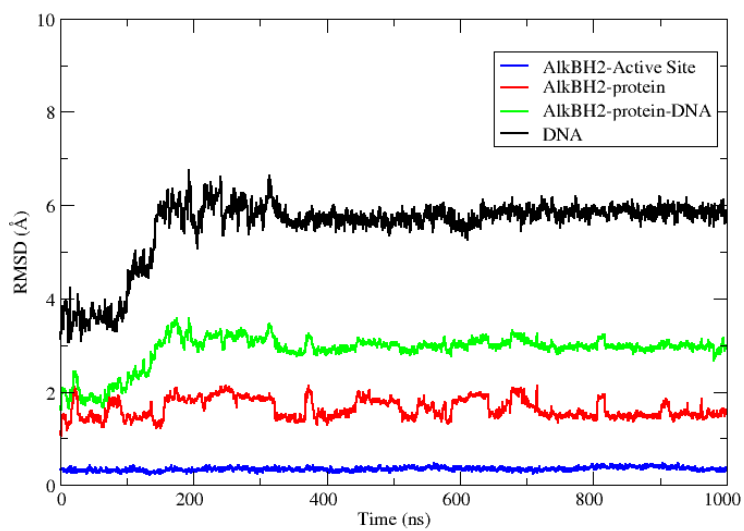


**Figure B22** RMSD Plot for AlkBH2-dsDNA with undamaged DNA.

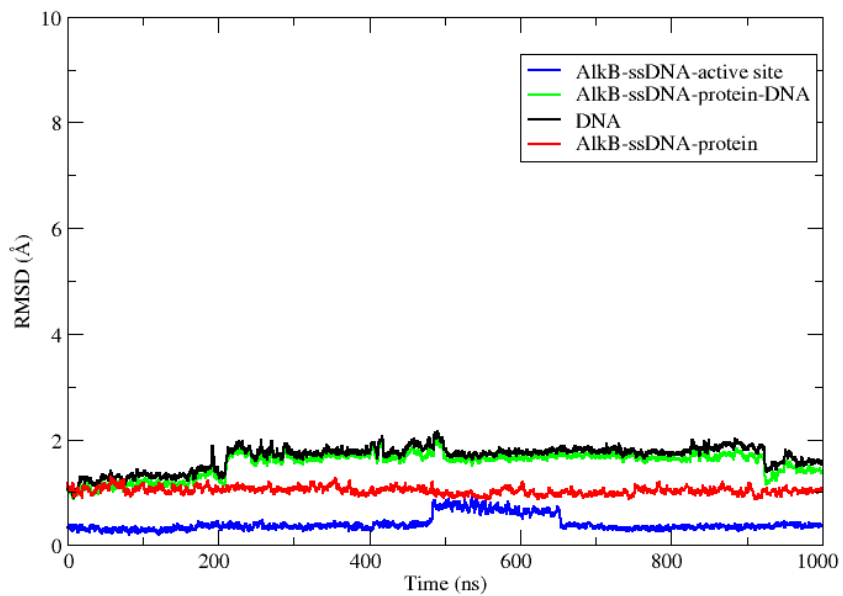


**Figure B23** RMSD Plot for AlkB-ssDNA with undamaged DNA.

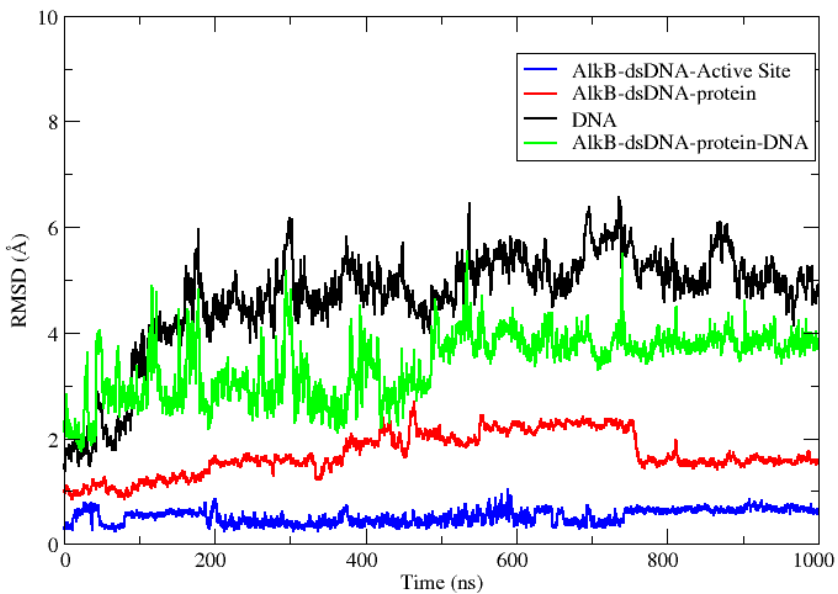


**Figure B24** RMSD Plot for AlkB-dsDNA with undamaged DNA.

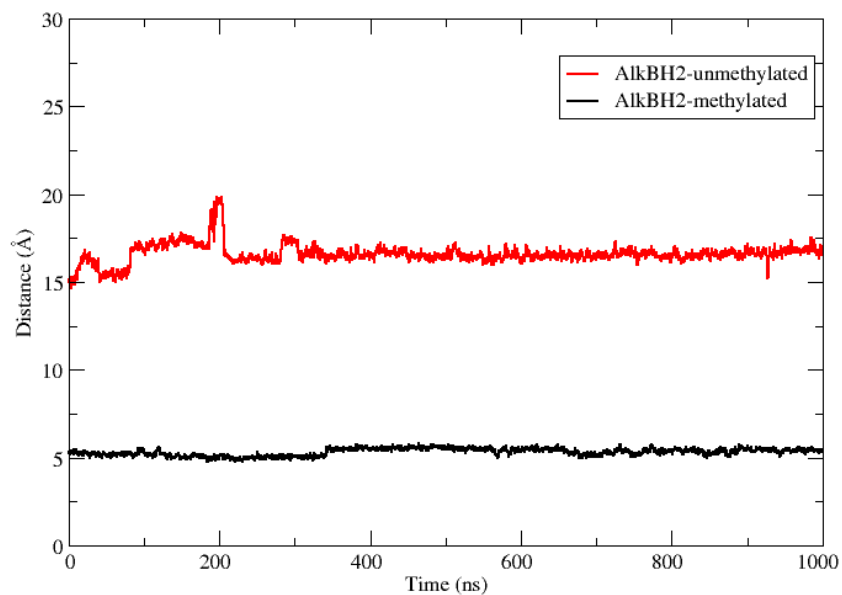


**Figure B25** The distance between Fe center (Fe) and N3 of the substrate in the AlkBH2-dsDNA Fe(III)-superoxo complex MD simulations.

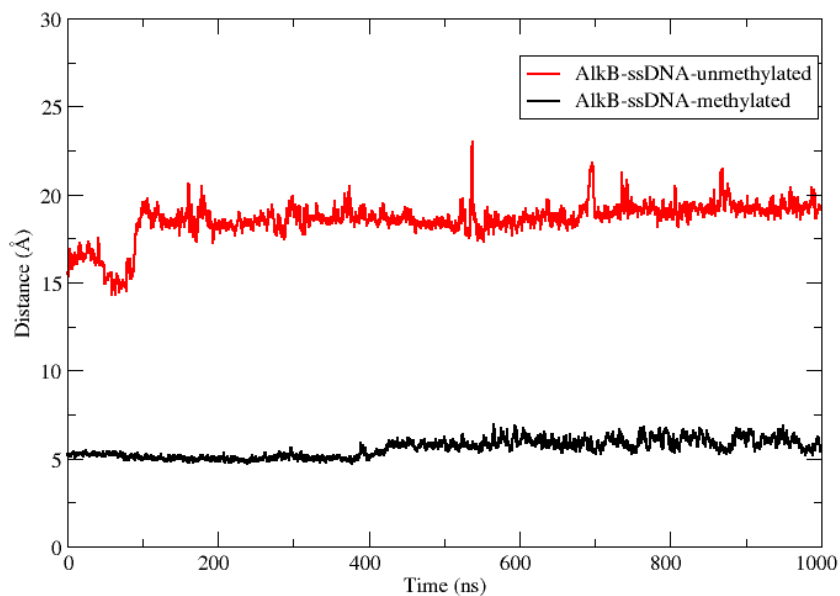


**Figure B26** The distance between Fe center (Fe) and N3 of the substrate in the AlkB-ssDNA Fe(III)-superoxo complex MD simulations.

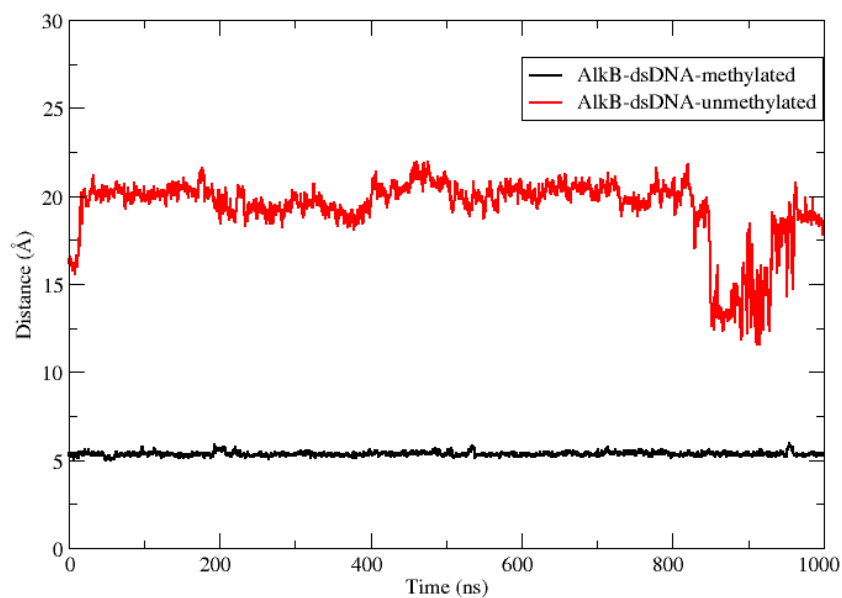


**Figure B27** The distance between Fe center (Fe) and N3 of the substrate in the AlkB-dsDNA Fe(III)-superoxo complex MD simulations.

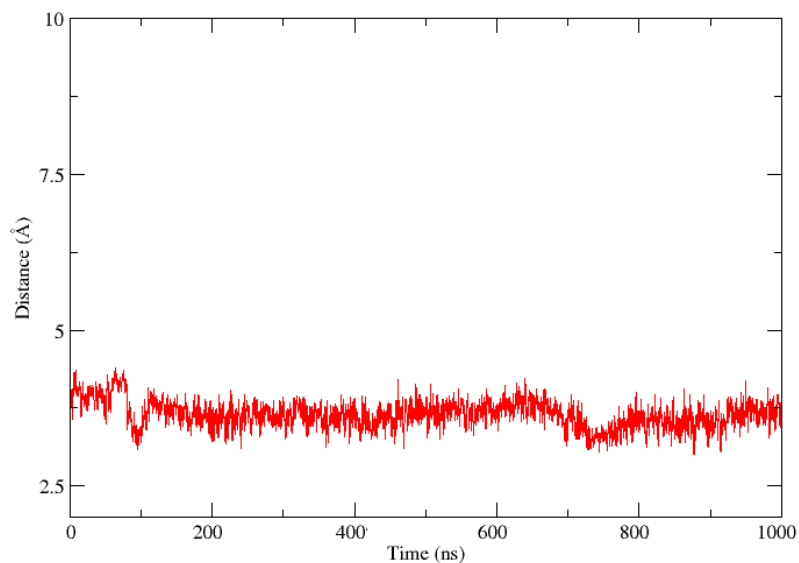


**Figure B28** The distance between distal oxygen (O<sub>d</sub>) of the superoxide and C2 of 2OG in the AlkB-ssDNA Fe(III)-superoxo complex MD simulations.

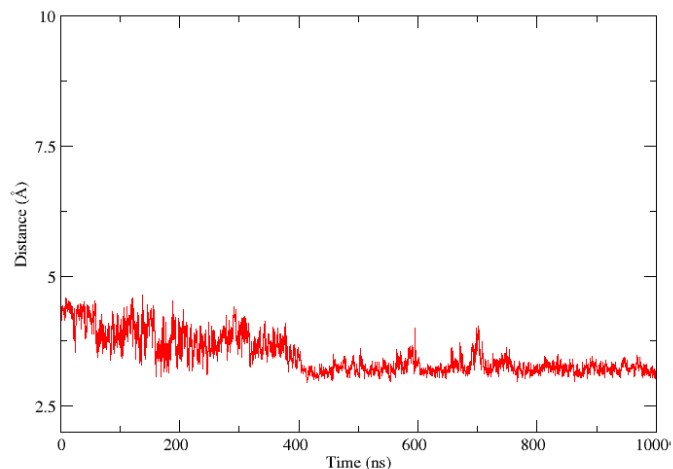


**Figure B29** The distance between distal oxygen ( $O_d$ ) of the superoxide and C2 of 2OG in AlkB-dsDNA Fe(III)-superoxo complex MD simulations.

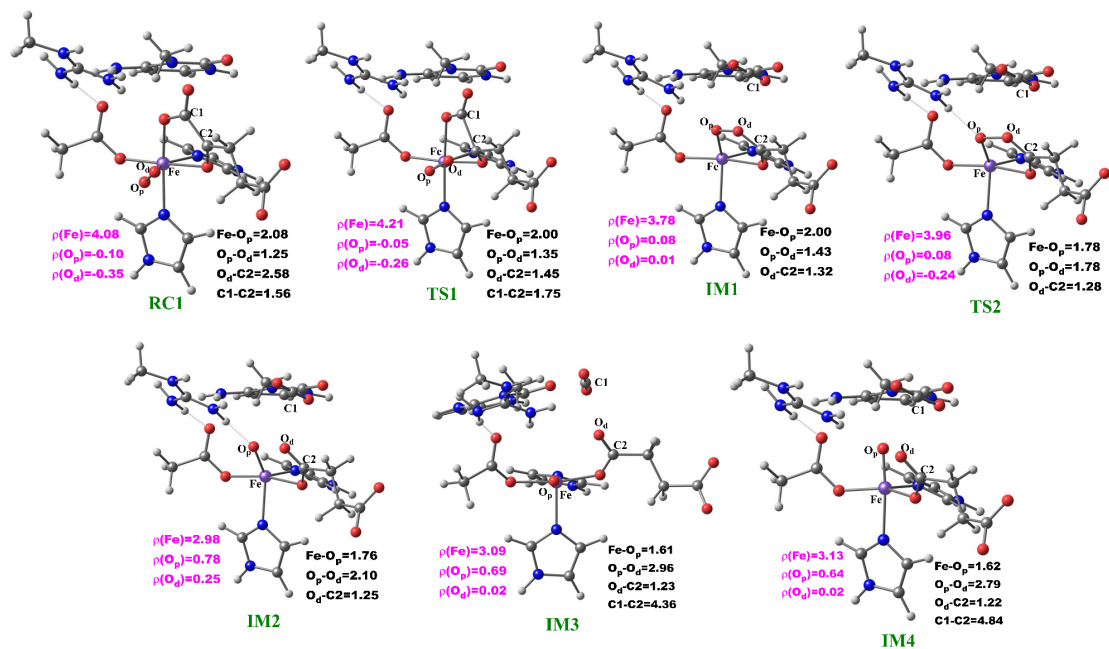


**Figure B30** The reaction state geometries of the dioxygen activation step stationary points in AlkB-ssDNA. Distances ( $\text{\AA}$ ) and spin densities are in black and pink, respectively.

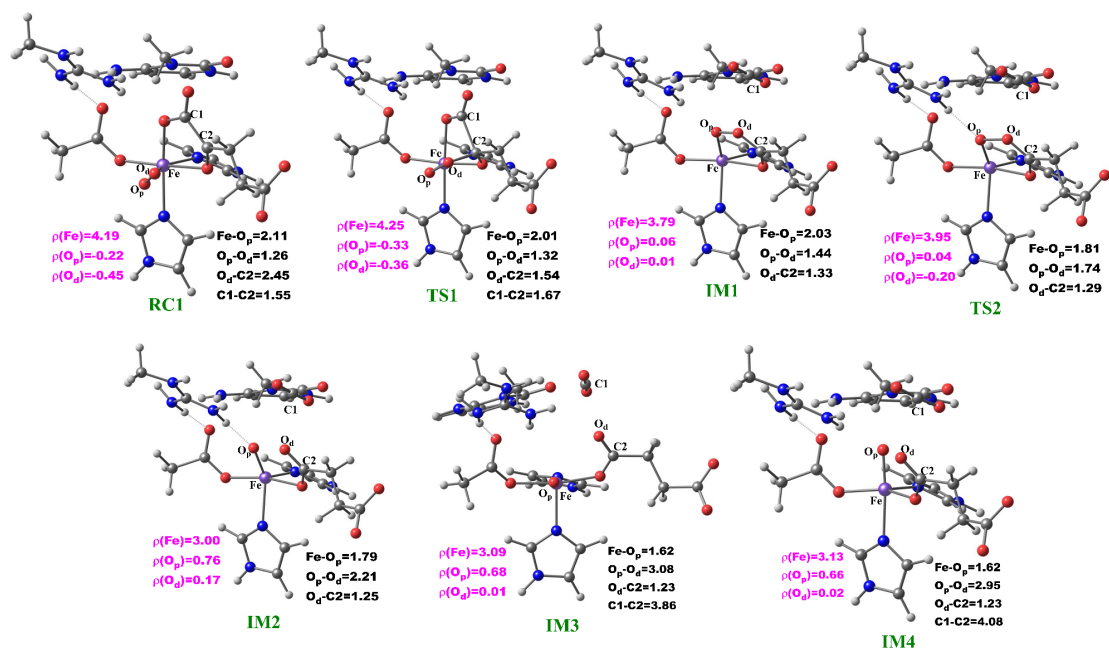


**Figure B31** The reaction state geometries of the dioxygen activation step stationary points in AlkB-dsDNA. Distances (Å) and spin densities are in black and pink, respectively.

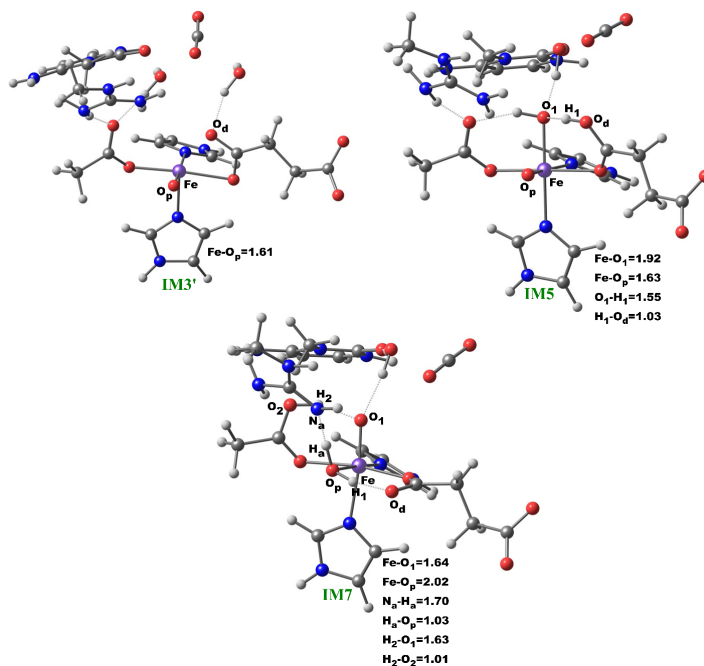


**Figure B32** The reaction state geometries (IM3', IM5 and IM7) for the proposed ferryl flip mechanism stationary points in AlkBH2-dsDNA. Distances are in Å.

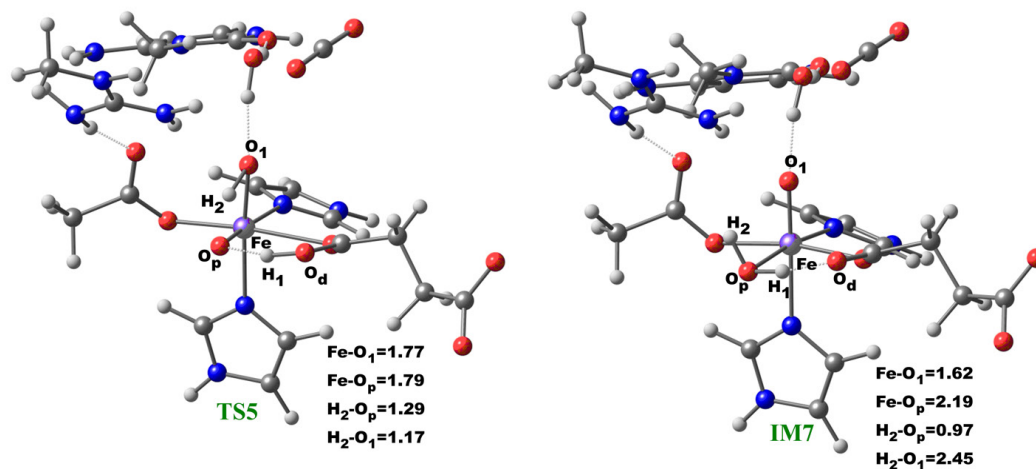


**Figure B33** The reaction state geometries for the proposed ferryl flip mechanism stationary points via the direct proton transfer from IM6 in the AlkBH2-dsDNA complex. Distances are in Å.

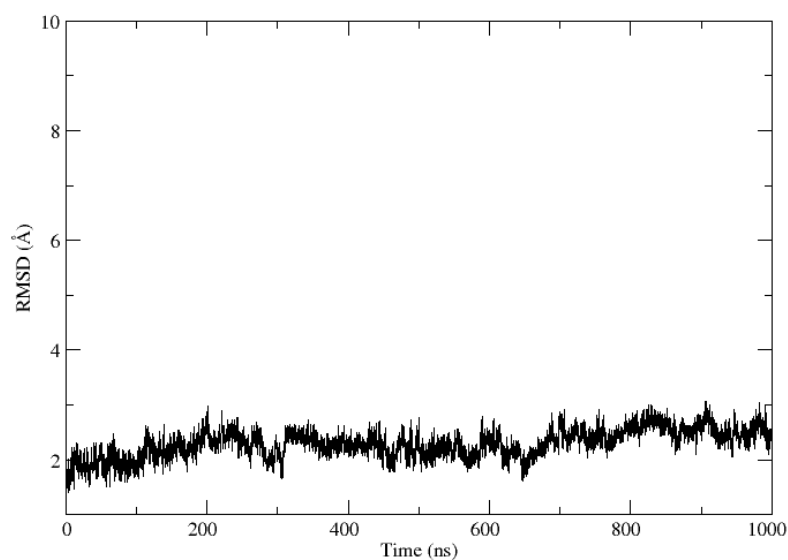


**Figure B34** RMSD plot for the Protein-DNA complex of AlkBH2-dsDNA Fe(II) five-coordinate enzyme-substrate complex MD Simulations.

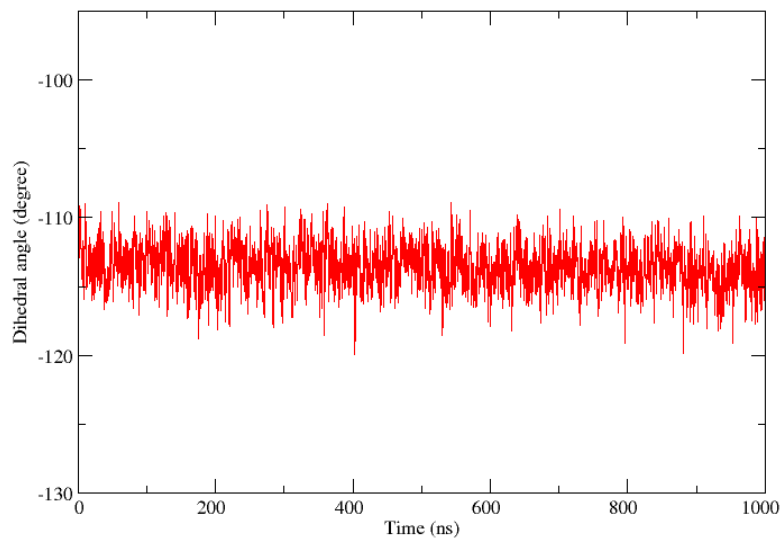


**Figure B35** The  $N^\epsilon$  (His<sup>1</sup>)-Fe-O5-O2 dihedral angle in AlkBH2-dsDNA Fe(II) five-coordinate enzyme-substrate complex MD Simulations.

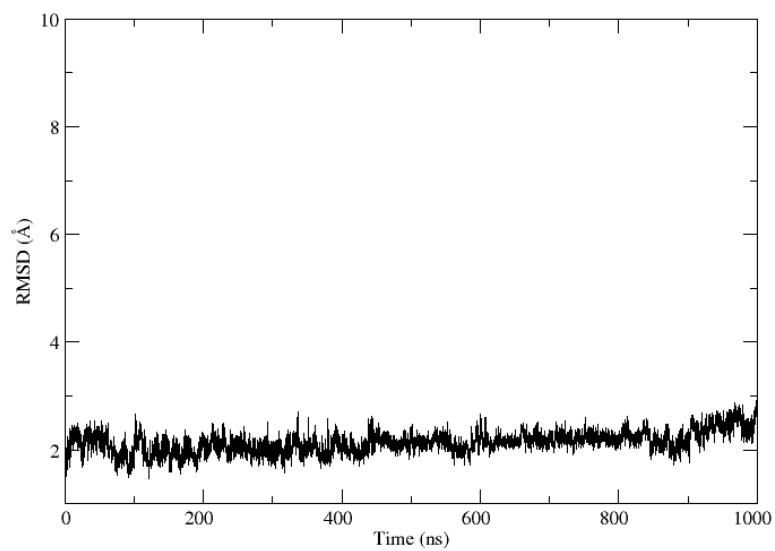


**Figure B36** RMSD plot for the Protein-DNA complex of AlkBH2-dsDNA “in-line” Fe(III)-superoxo complex MD simulations.



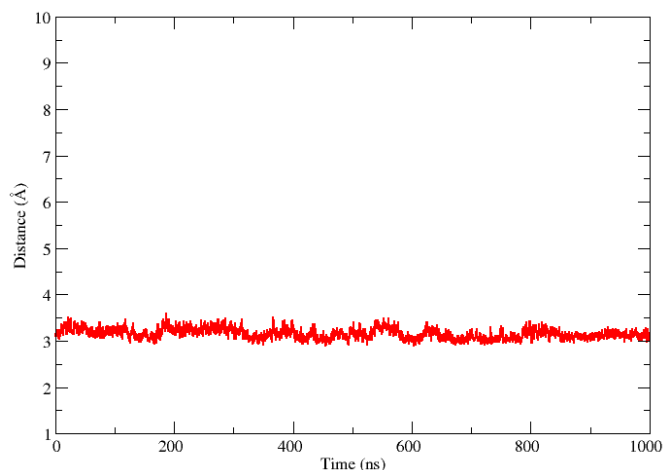


**Figure B37** The distance between distal oxygen ( $O_d$ ) of the superoxide and C2 of 2OG in AlkBH2-dsDNA “in-line” Fe(III)-superoxo complex MD simulations.

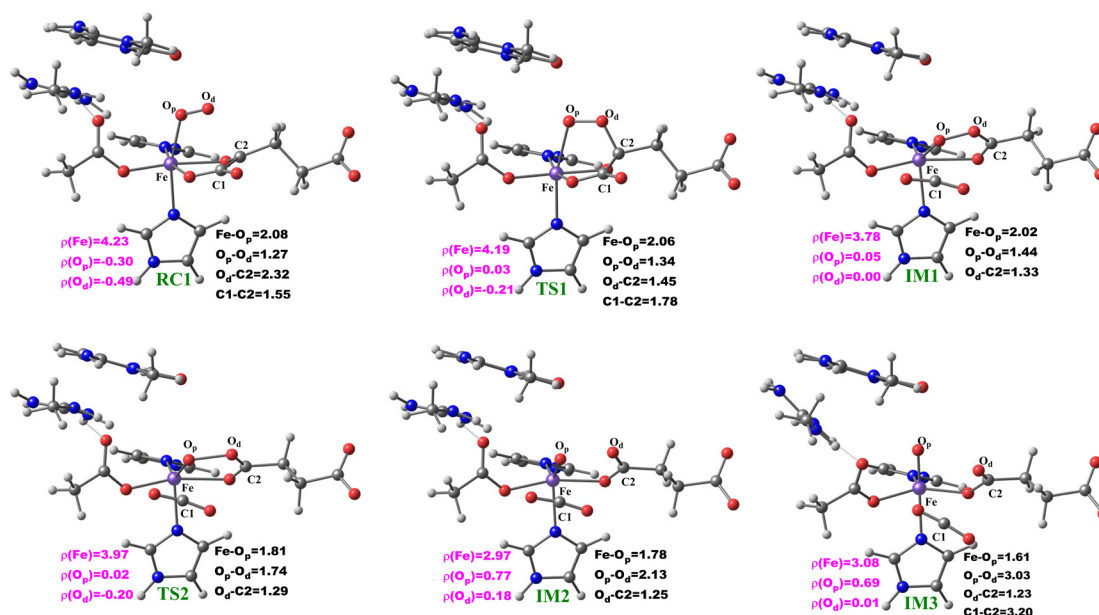


**Figure B38** The reaction state geometries of the dioxygen activation step stationary points of AlkBH2-dsDNA via “in-line” Fe(III)-superoxo complex. Distances (Å) and spin densities are in black and pink, respectively.

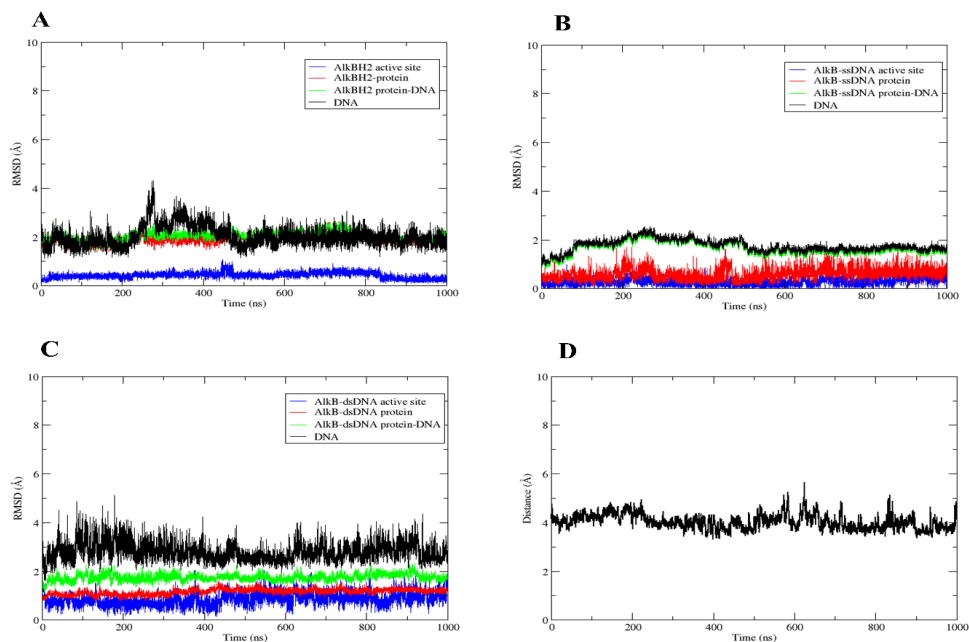


**Figure B39** RMSD Plots for AlkBH2-dsDNA (A), AlkB-ssDNA (B), AlkB-dsDNA (C) and plot of the distance between the proximal oxygen ( $O_p$ ) and the carbon of the methyl-group of  $m_3C$  (D) at the ferryl intermediate stage of the AlkBH2-dsDNA complex reaction.

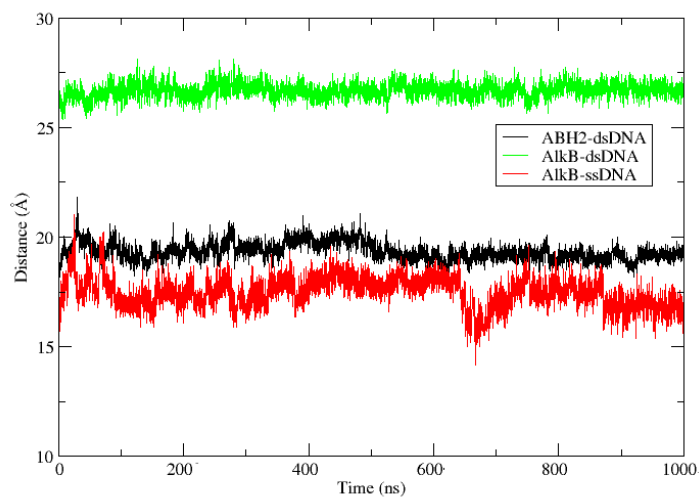


**Figure B40** The distance between the center of masses of the protein and the DNA in the AlkBH2-dsDNA, AlkB-ssDNA and AlkB-dsDNA complexes during the MD simulations of the ferryl complex.

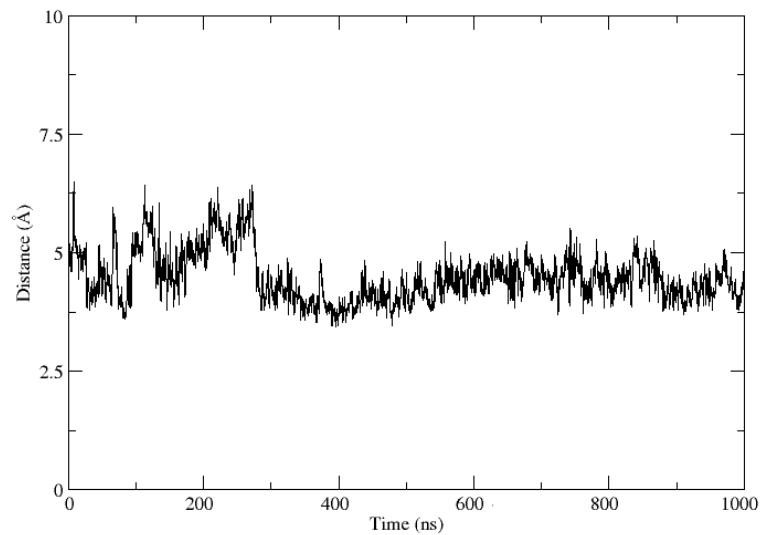


**Figure B41** Distance between proximal oxygen ( $O_p$ ) and the methyl carbon of  $m_3C$  DNA substrate in the AlkB-ssDNA ferryl complex MD simulations.

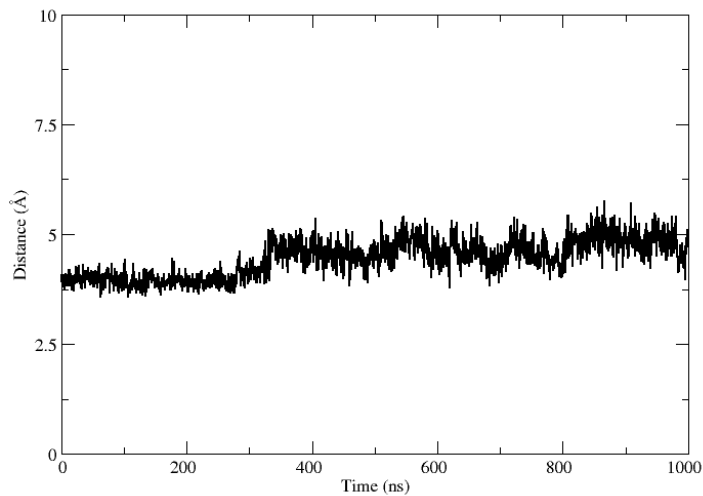


**Figure B42** Distance between the proximal oxygen ( $O_p$ ) and the methyl carbon of  $m_3C$  DNA substrate in the AlkB-dsDNA ferryl complex MD simulations.

Dynamic cross correlation analysis (DCCA) of AlkBH2-dsDNA (Figure 3.9A) shows that residues 95-101 ( $\beta$ 3) and 103-108 ( $\beta$ 4), belonging to a crystallographically observed  $\beta$ -hairpin,<sup>10,11</sup> have a strong positive correlation with residues 123-128; this aids in substrate recognition. Residues 166-175, located on the first strand of the double-stranded  $\beta$ -helix (DSBH) core fold, which includes the coordinating HXD motif, have a strong positive correlation with the Fe center, the oxo group of the Fe(IV)=O species, succinate, and DNA. This observation implies that these residues are important for the proper orientation of the reactive groups. Residues 151-173 (belonging to  $\beta$ 8) and 178-190 (belonging to  $\beta$ 8 and the loop connecting  $\beta$ 8- $\beta$ 9) have a positive correlation with residues 234-255 ( $\beta$ 13- $\beta$ 14) and 168-179 ( $\beta$ 12 and  $\alpha$ 5), respectively. Moreover, residues belonging to  $\beta$ 9 (aa 182-188) and  $\beta$ 10 (aa 193-202) have a positive correlation with residues belonging to  $\beta$ 14 (aa 242-255) and  $\beta$ 13 (aa 231-238), respectively.

DCCA calculations with AlkB-ssDNA (Figure B35) reveals that residues 122-136 located on the first strand of the DSBH, which include the coordinating HXD motif, have a strong positive correlation with the Fe center, the oxo group of the Fe(IV)=O species, succinate, and residues belonging to  $\alpha$ 3 and  $\beta$ 11 (aa 183-192). Residues 117-123 (in  $\beta$ 5) and 143-150 (in  $\beta$ 7) have a positive correlation with residues 203-209, which belong to  $\beta$ 12 and the loop connecting  $\beta$ 11 and  $\beta$ 12. Residues 142-157, belonging to  $\beta$ 7- $\beta$ 8 have a positive correlation with residues 165-178 (in  $\beta$ 9) and 185-192 (in  $\alpha$ 3 and  $\beta$ 9).

With AlkB-dsDNA (Figure B36), DCCA shows that residues 50-57 and 79-89, which belong to the nucleotide recognition lid, have a positive correlation with the DNA substrate. Residues 114-124 (in  $\beta$ 5) and 121-136 (in  $\beta$ 5 and  $\beta$ 6) have a positive correlation with residues 203-211 (in  $\beta$ 12) and 180-192 (in  $\beta$ 10 and  $\beta$ 11), respectively. Residues 129-136 located on the first strand of the DSBH, which includes the coordinating HXD motif, have a positive correlation with residues that belong to  $\beta$ 8 (aa 158-162). Figures S15 and S16 contain the annotated secondary structures of AlkBH2-dsDNA and AlkBs, respectively.

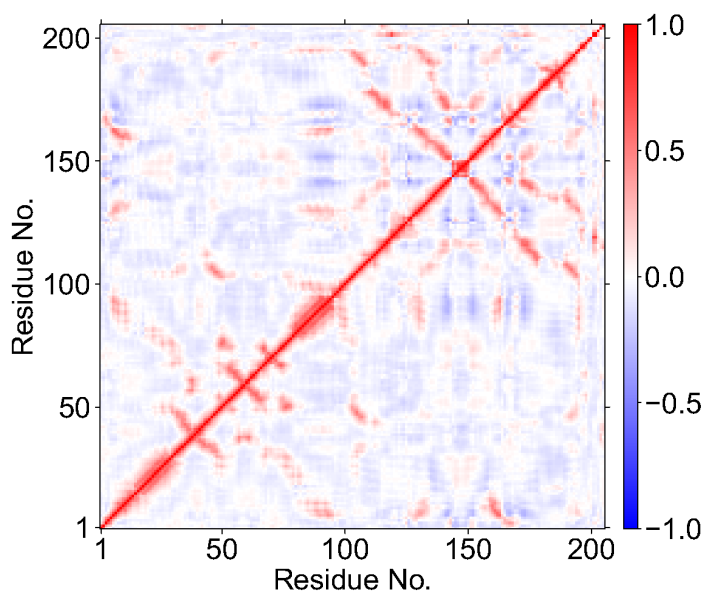


**Figure B43** Dynamic cross correlation for the ferryl complex of AlkB-ssDNA. Residue numbers 1-200 (protein), 201 (Fe), 202 (O), 203 (succinate), 204-206 (DNA), and 205 ( $m_3C$  substrate).

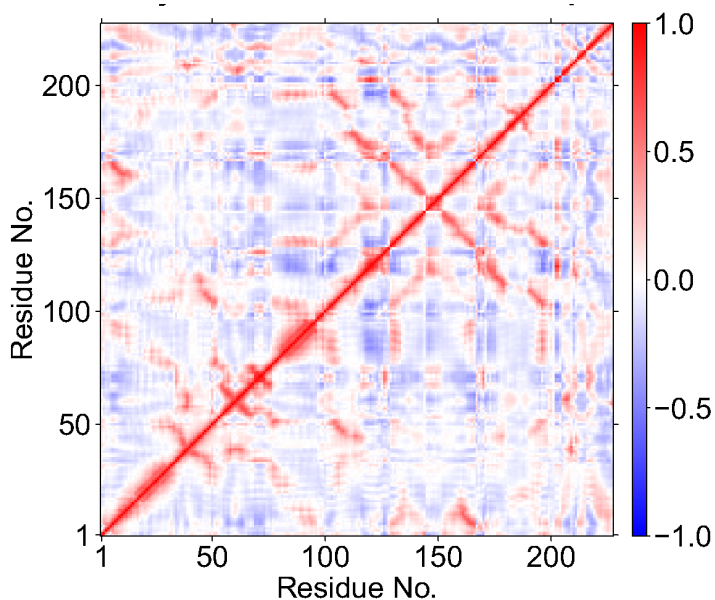


**Figure B44** Dynamic cross correlation for the ferryl complex of AlkB-dsDNA. Residue numbers 1-201 (protein), 202 (Fe), 203 (O), 204 (succinate), 205-229 (DNA), and 211 ( $m_3C$  substrate).

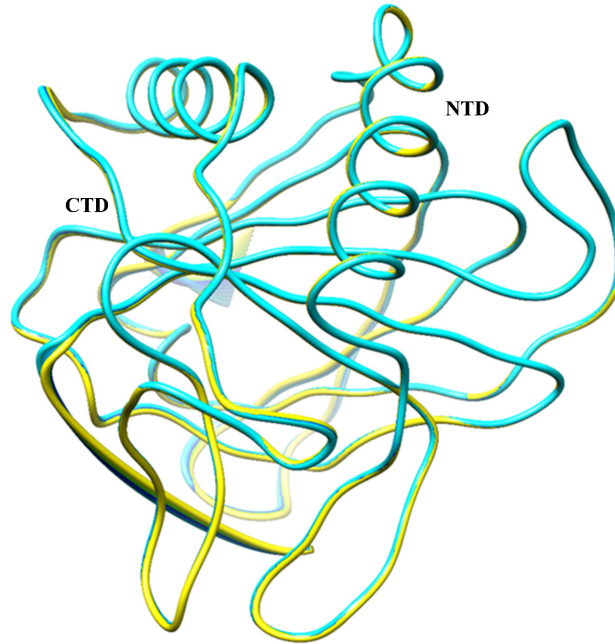


**Figure B45** PCA for the AlkB-ssDNA ferryl MD simulation. Yellow to blue coloring represents the main direction of motion of protein residues. NTD and CTD are N-terminal Domain and C-terminal Domain, respectively.

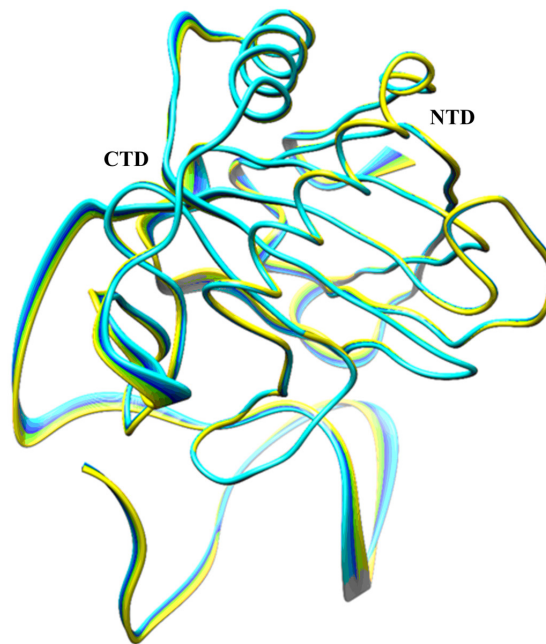


**Figure B46** PCA for the AlkB-dsDNA ferryl MD simulation. Yellow to blue coloring represents the main direction of motion of protein residues. NTD and CTD are N-terminal Domain and C-terminal Domain, respectively.

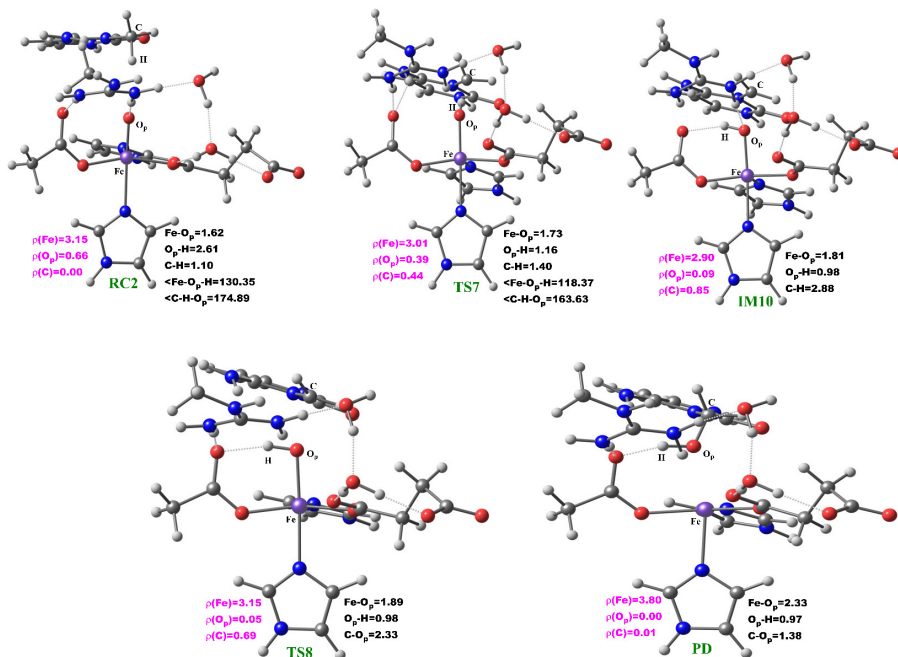


**Figure B47** The reaction state geometries of the hydrogen atom abstraction and rebound hydroxylation steps stationary points in AlkB-ssDNA. Distances (Å) and spin densities are in black and pink, respectively.

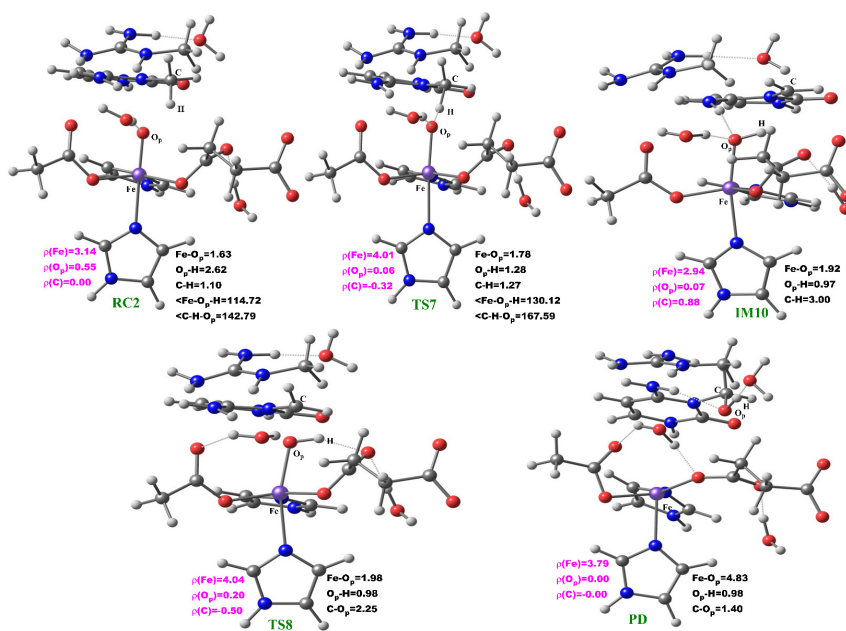


**Figure B48** The reaction state geometries of the hydrogen atom abstraction and rebound hydroxylation steps stationary points in AlkB-dsDNA. Distances (Å) and spin densities are in black and pink, respectively.

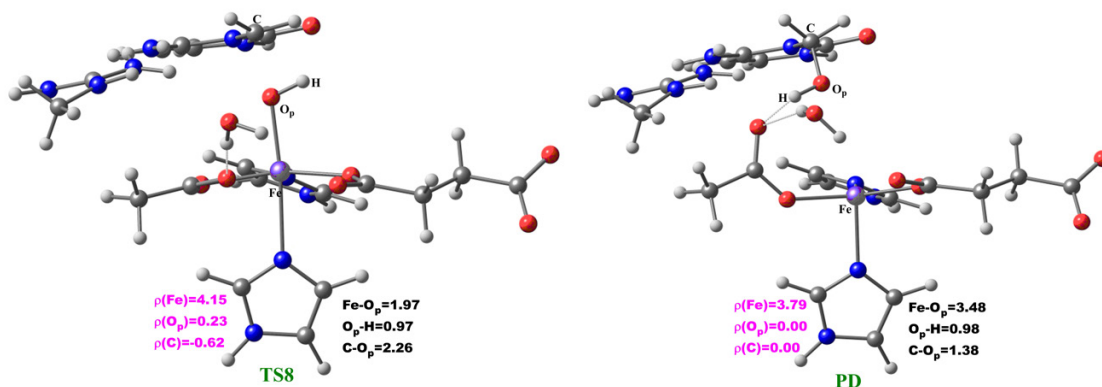


**Figure B49** Optimized geometries of the rebound hydroxylation stationary points in AlkBH2-dsDNA. Distances and angles are in Å and degrees, respectively.

**Table B1.** Calculated activation barriers (in kcal/mol) at B3LYP/def2-TZVP (BS2) for all the multiple snapshots with and without ZPE in the AlkB-ssDNA complex.

Snapshot	Barrier (BS2)	Barrier (BS2+ZPE)
1.	26.6	23.6
2.	27.2	24.1
3.	31.3	26.7
4.	25.6	22.1
5.	24.8	21.0
<b>Boltzmann weighted average</b>	<b>25.6</b>	<b>21.9</b>



**Table B2.** Selected distances and angles for the different snapshots RC2 and TS7 for HAT step in the AlkB-ssDNA complex, calculated at B3LYP/def2-TZVP.

	<b>d(Fe–O<sub>p</sub>)</b> (Å)	<b>d(O<sub>p</sub>–H)</b> (Å)	<b>d(C–H)</b> (Å)	<b>&lt;(Fe–O<sub>p</sub>–H)</b> (deg)	<b>&lt;(C–H<sub>p</sub>–O)</b> (deg)	<b>Barrier with ZPE</b> (kcal/mol)	<b>C<sub>substrate</sub> spin density in TS7</b>
<b>Snapshot 1</b>							
<b>RC2</b>	1.623	2.472	1.099	137.46	175.36		
<b>TS7</b>	1.775	1.254	1.293	140.45	169.59	23.6	-0.356
<b>Snapshot 2</b>							
<b>RC2</b>	1.622	2.468	1.101	123.22	142.43		
<b>TS7</b>	1.735	1.191	1.377	121.88	165.21	24.1	0.418
<b>Snapshot 3</b>							
<b>RC2</b>	1.626	3.344	1.101	125.10	144.26		
<b>TS7</b>	1.726	1.161	1.404	120.04	173.05	26.7	0.465
<b>Snapshot 4</b>							
<b>RC2</b>	1.627	2.605	1.103	130.35	174.89		
<b>TS7</b>	1.729	1.163	1.400	118.37	163.63	22.1	0.439
<b>Snapshot 5</b>							
<b>RC2</b>	1.621	2.831	1.103	128.44	172.09		
<b>TS7</b>	1.749	1.232	1.295	145.55	168.20	21.0	-0.366

**Table B3.** Calculated activation barriers (in kcal/mol) at B3LYP/def2-TZVP (BS2) for all the multiple snapshots with and without ZPE in the AlkB-dsDNA complex.

Snapshot	Barrier (BS2)	Barrier (BS2+ZPE)
1.	26.2	23.6
2.	24.1	21.5
3.	25.6	22.1
4.	27.4	24.9
5.	29.0	25.3
<b>Boltzmann weighted average</b>	<b>25.1</b>	<b>22.3</b>

**Table B4.** Selected distances and angles for the different snapshots RC2 and TS7 for HAT step in the AlkB-dsDNA complex, calculated at B3LYP/def2-TZVP.

	d(Fe–Op) (Å)	d(Op–H) (Å)	d(C–H) (Å)	<(Fe–Op–H) (deg)	<(C–Hp–O) (deg)	Barrier with ZPE (kcal/mol)	Csubstrate spin density in TS7
<b>Snapshot1</b>							
<b>RC2</b>	1.611	3.258	1.103	126.24	153.66	23.6	-0.342
<b>TS7</b>	1.748	1.269	1.279	139.91	175.39		
<b>Snapshot 2</b>							
<b>RC2</b>	1.622	2.603	1.103	127.49	175.45	21.5	-0.324
<b>TS7</b>	1.772	1.296	1.263	129.88	168.70		
<b>Snapshot 3</b>							
<b>RC2</b>	1.633	2.620	1.101	114.72	142.79	22.1	-0.330
<b>TS7</b>	1.781	1.279	1.269	130.12	167.59		
<b>Snapshot 4</b>							
<b>RC2</b>	1.615	3.292	1.099	118.94	144.01	24.9	-0.314
<b>TS7</b>	1.783	1.306	1.273	138.81	165.12		
<b>Snapshot 5</b>							
<b>RC2</b>	1.627	2.874	1.099	115.41	154.39	25.3	-0.323
<b>TS7</b>	1.772	1.309	1.275	133.70	168.83		

**Table B5.** Calculated pKa values of the ionisable side chains of AlkBH2-dsDNA, AlkB-ssDNA and AlkB-dsDNA, done using Propka software. The yellow highlighted ones are the iron-coordinating residues.

AlkBH2-dsDNA			AlkB-ssDNA			AlkB-dsDNA		
Residues	pKa	pK model	Residues	pKa	pK model	Residues	pKa	pK model
ASP 66	3.28	3.80	ASP 36	3.05	3.80	ASP 36	3.03	3.80
ASP 79	1.92	3.80	ASP 39	4.20	3.80	ASP 39	4.21	3.80
ASP 117	3.43	3.80	ASP 82	1.70	3.80	ASP 82	1.78	3.80
ASP 143	3.72	3.80	ASP 111	3.94	3.80	ASP 111	3.98	3.80
ASP 163	2.97	3.80	ASP 115	4.16	3.80	ASP 115	4.11	3.80
ASP 166	4.37	3.80	ASP 133	-2.93	3.80	ASP 133	-2.79	3.80
ASP 173	-2.44	3.80	ASP 135	5.28	3.80	ASP 135	6.83	3.80
ASP 174	4.97	3.80	ASP 138	1.31	3.80	ASP 138	1.66	3.80
ASP 194	3.31	3.80	ASP 163	3.35	3.80	ASP 163	3.18	3.80
ASP 201	3.40	3.80	ASP 174	4.03	3.80	ASP 174	3.98	3.80
GLU 63	4.26	4.50	ASP 202	2.87	3.80	ASP 202	3.75	3.80
GLU 77	3.70	4.50	GLU 31	4.51	4.50	GLU 31	4.54	4.50
GLU 80	4.61	4.50	GLU 136	3.89	4.50	GLU 136	3.87	4.50
GLU 84	4.89	4.50	GLU 171	3.81	4.50	GLU 171	4.65	4.50
GLU 86	3.61	4.50	GLU 181	4.67	4.50	GLU 181	4.63	4.50
GLU 88	3.88	4.50	HIS 66	6.35	6.50	HIS 66	6.42	6.50
GLU 90	4.55	4.50	HIS 72	6.11	6.50	HIS 72	5.52	6.50
GLU 139	4.77	4.50	HIS 97	6.49	6.50	HIS 97	5.91	6.50
GLU 170	5.39	4.50	HIS 131	-1.92	6.50	HIS 131	-1.92	6.50
GLU 175	8.44	4.50	HIS 172	4.58	6.50	HIS 172	4.34	6.50
GLU 177	4.48	4.50	HIS 187	0.85	6.50	HIS 187	0.72	6.50
HIS 55	6.05	6.50	HIS 197	5.38	6.50	HIS 197	5.30	6.50
HIS 59	5.96	6.50	CYS 64	9.22	9.00	CYS 64	9.25	9.00
HIS 106	4.51	6.50	CYS 100	13.18	9.00	CYS 100	13.07	9.00
HIS 144	5.65	6.50	CYS 117	18.79	9.00	CYS 117	18.84	9.00
HIS 167	3.68	6.50	CYS 203	11.44	9.00	CYS 203	10.66	9.00
HIS 171	-2.32	6.50	TYR 55	10.20	10.00	TYR 55	10.34	10.00
HIS 199	5.61	6.50	TYR 76	12.92	10.00	TYR 76	15.62	10.00
HIS 220	6.36	6.50	TYR 78	15.22	10.00	TYR 78	16.21	10.00
HIS 228	6.13	6.50	TYR 109	11.36	10.00	TYR 109	11.40	10.00
HIS 233	5.75	6.50	TYR 122	12.54	10.00	TYR 122	12.52	10.00
HIS 236	0.57	6.50	TYR 186	10.12	10.00	TYR 186	11.44	10.00
CYS 169	13.72	9.00	TYR 205	11.44	10.00	TYR 205	12.44	10.00
TYR 69	9.89	10.00	LYS 87	10.37	10.50	LYS 87	10.38	10.50
TYR 91	13.29	10.00	LYS 127	10.17	10.50	LYS 127	9.54	10.50
TYR 115	11.08	10.00	LYS 134	10.33	10.50	LYS 134	9.21	10.50
TYR 122	16.56	10.00	LYS 160	10.61	10.50	LYS 160	10.67	10.50
TYR 161	11.60	10.00	LYS 166	10.25	10.50	LYS 166	10.14	10.50
TYR 235	11.21	10.00	LYS 193	10.27	10.50	LYS 193	10.33	10.50
LYS 75	11.50	10.50	LYS 214	10.53	10.50	LYS 214	10.56	10.50
LYS 87	11.32	10.50	ARG 23	12.35	12.50	ARG 23	12.47	12.50
LYS 104	10.18	10.50	ARG 24	13.82	12.50	ARG 24	12.65	12.50
LYS 111	10.13	10.50	ARG 35	12.41	12.50	ARG 35	12.40	12.50
LYS 132	9.92	10.50	ARG 47	12.73	12.50	ARG 47	12.66	12.50
LYS 162	11.33	10.50	ARG 73	12.41	12.50	ARG 73	12.41	12.50

LYS 200	10.08	10.50	ARG 102	12.22	12.50	ARG 102	12.04	12.50
LYS 242	10.02	10.50	ARG 121	12.28	12.50	ARG 121	12.15	12.50
LYS 243	10.18	10.50	ARG 140	14.01	12.50	ARG 140	14.08	12.50
LYS 255	10.28	10.50	ARG 161	12.56	12.50	ARG 161	9.67	12.50
ARG 58	12.20	12.50	ARG 167	12.23	12.50	ARG 167	11.43	12.50
ARG 61	12.49	12.50	ARG 183	12.17	12.50	ARG 183	12.37	12.50
ARG 98	12.20	12.50	ARG 204	10.43	12.50	ARG 204	10.37	12.50
ARG 110	9.61	12.50	ARG 210	13.09	12.50	ARG 210	12.86	12.50
ARG 140	13.36	12.50						
ARG 142	12.53	12.50						
ARG 160	13.99	12.50						
ARG 172	12.90	12.50						
ARG 176	12.40	12.50						
ARG 193	10.55	12.50						
ARG 198	11.52	12.50						
ARG 203	13.06	12.50						
ARG 209	12.67	12.50						
ARG 210	12.42	12.50						
ARG 215	11.95	12.50						
ARG 241	12.34	12.50						
ARG 248	9.14	12.50						
ARG 254	11.60	12.50						

**Dioxygen activation step reaction states cartesian coordinates for AlkBH2-dsDNA via ‘off-line’ Fe(III)-superoxo complex**

RC1

QM/MM (BS1) = -3428.050920 a.u.

QM/MM (BS2+ZPE) = -3430.055821 a.u.

6	35.034000670	35.287516737	30.406645110
7	35.821561871	34.925606648	31.473095110
1	36.553334286	34.199392415	31.464118374
6	35.447607248	35.644997988	32.538496132
1	35.903135576	35.554584948	33.520444235
7	34.442880118	36.461713919	32.221215069
6	34.172002941	36.244116631	30.886910178
1	33.369134589	36.764262364	30.374786454
6	29.304433005	38.355113365	31.673558766
1	28.870761713	37.641242709	32.388046341
1	28.831623859	39.337546432	31.820975424
6	30.804472962	38.505349246	31.895490216
8	31.373756464	39.568148262	31.588446675
8	31.416967846	37.509569492	32.440548858
6	32.325054224	33.056485971	34.489161986
7	31.265987623	33.375302029	33.671461474
1	30.520675118	32.760388445	33.318334759
6	31.347204954	34.676592620	33.356268015

1	30.637743361	35.204117318	32.724816161
7	32.408441446	35.226024430	33.934444564
6	33.033355914	34.224737788	34.643448942
1	33.954028784	34.405889892	35.191208996
6	29.317154511	44.311490844	33.742325652
1	29.581742892	45.258307123	33.239546839
1	28.631002752	43.756162952	33.088128553
7	30.501276544	43.511944836	34.020546761
1	31.121765497	43.809816889	34.775431421
6	30.867811848	42.376611357	33.379247384
7	30.173291109	41.907976870	32.338179265
1	29.725999309	42.559805774	31.699605203
1	30.552343165	41.055768248	31.875291854
7	31.916709017	41.695980061	33.842421720
1	32.430218233	42.029592655	34.658211871
1	32.279191268	40.861619598	33.368301082
26	33.003121451	37.241978544	33.567939439
6	34.423500864	39.507940019	34.636705557
8	34.842948104	40.643046835	34.858740695
8	33.588754372	39.182148252	33.716743435
6	34.896635263	38.293566230	35.476329905
8	34.648565922	37.177527639	35.004553062
6	35.701484214	38.496105832	36.721215911
6	35.740506099	37.258464055	37.608060163
6	36.539382798	37.379264050	38.915135863
8	36.092277421	36.720979062	39.889491046
8	37.588481510	38.075768267	38.916505951
1	36.189095458	36.423032998	37.041562006
1	34.713751399	36.953582420	37.856543384
1	35.292286735	39.370973294	37.250396039
1	36.722558090	38.800370495	36.420840696
8	32.031130537	37.584369268	35.419284846
8	32.534582623	38.313925584	36.322990478
8	36.795645506	38.982803203	29.772603356
6	35.912511158	38.759292576	28.964223338
7	34.640022689	39.333122040	29.109937654
6	34.447267177	40.243994854	30.245143071
6	33.591872046	39.086001641	28.254181624
7	32.407566007	39.581178511	28.542662950
6	33.851540888	38.318165775	27.078945990
6	35.078119521	37.757642849	26.912848586
7	36.068076103	37.925796165	27.858907761
1	33.992064489	41.174739364	29.879567441
1	35.425631147	40.460556209	30.678704527
1	31.559792600	39.419431076	27.961262453
1	35.307809144	37.148058223	26.034767605
1	33.053906666	38.149983053	26.359554730
1	33.800936795	39.786772524	31.008804633
1	32.203305198	39.971276940	29.459187748
1	35.048324503	34.752780105	29.456951006
1	29.055490876	38.010764769	30.669806215
1	32.532002789	32.036640860	34.813438973

1	28.774296358	44.539172583	34.659676935
1	36.918719064	37.401704156	27.817596566

**TS1**

**QM/MM (BS1) = -3428.034641 a.u.**

**QM/MM (BS2+ZPE) = -3430.036944 a.u.**

6	35.013937301	35.291708826	30.389086490
7	35.821311354	34.961074065	31.451486395
1	36.566986610	34.249125197	31.443496178
6	35.439930897	35.683142888	32.513098323
1	35.907217083	35.630015858	33.492150948
7	34.408436389	36.465822303	32.196538047
6	34.130865702	36.229446403	30.868301088
1	33.312027273	36.725903776	30.359374146
6	29.286856536	38.299409357	31.745986700
1	28.864795452	37.554311503	32.435252539
1	28.793705579	39.266075742	31.927256674
6	30.783884823	38.474516649	31.981346119
8	31.322851158	39.564971410	31.709691988
8	31.420603256	37.479176700	32.492244501
6	32.313355391	33.010437284	34.497713909
7	31.239760302	33.331526222	33.699250487
1	30.483435947	32.720246165	33.364188899
6	31.322143362	34.630829890	33.376528524
1	30.604441326	35.160755359	32.756570971
7	32.397888175	35.174652056	33.932182897
6	33.031959251	34.173903270	34.632238529
1	33.966583890	34.353394694	35.155888082
6	29.279641882	44.341950387	33.723367401
1	29.552272757	45.291608295	33.230910534
1	28.579382221	43.804877871	33.069165671
7	30.455281876	43.524230945	33.978660112
1	31.094326074	43.812747615	34.721415706
6	30.780952530	42.377264161	33.340532220
7	30.058896233	41.907197344	32.320268552
1	29.594725578	42.553118376	31.688964867
1	30.425255464	41.043094257	31.869591752
7	31.827960325	41.678315341	33.784752089
1	32.354035156	41.998860099	34.596489388
1	32.138947311	40.837548341	33.287376551
26	33.015240033	37.171407852	33.624981957
6	34.388602460	39.598071521	34.540070356
8	34.916162157	40.640253722	34.865915703
8	33.705230216	39.229342777	33.571321135
6	34.482086273	38.177501456	35.690982729
8	34.614586086	37.157945276	34.912616326
6	35.482152235	38.446004838	36.805814150
6	35.639762520	37.194574364	37.672614781
6	36.474596162	37.336328111	38.955706168
8	36.047995059	36.690328518	39.948982290
8	37.522775301	38.032489464	38.927265505

1	36.119311145	36.407229321	37.064550423
1	34.647086305	36.819394357	37.958971948
1	35.118966988	39.299304549	37.396917329
1	36.442613070	38.742150742	36.360825657
8	32.228306272	37.778830244	35.356762776
8	33.157925143	38.368328423	36.178579182
8	36.789627893	38.999192706	29.767995387
6	35.905812684	38.765420375	28.963844478
7	34.630656146	39.336279783	29.107770017
6	34.435042378	40.252023918	30.237988103
6	33.580793477	39.076277813	28.258850152
7	32.396189839	39.574347568	28.544204031
6	33.837390202	38.293602928	27.093360455
6	35.067042794	37.739682648	26.926277131
7	36.061290765	37.923778407	27.864469827
1	34.002058345	41.190889034	29.865558769
1	35.410611398	40.451591142	30.686408231
1	31.541958009	39.396946864	27.977158064
1	35.295333304	37.123645044	26.052249748
1	33.037772570	38.114549197	26.379001570
1	33.771995176	39.803641329	30.992709035
1	32.203975909	40.000942802	29.445617987
1	35.031337802	34.750672736	29.443018578
1	29.046381116	37.985285387	30.730326805
1	32.528769584	31.990936784	34.817530704
1	28.750875687	44.561366171	34.650907346
1	36.913661151	37.402374591	27.824780094

#### IM1

QM/MM (BS1) = -3428.111730 a.u.

QM/MM (BS2+ZPE) = -3430.110558 a.u.

6	35.074123884	35.248243911	30.278106189
7	35.861421904	34.895308880	31.347486703
1	36.581490559	34.159776222	31.355168002
6	35.494730900	35.637813830	32.402361845
1	35.949049339	35.561167834	33.386342058
7	34.501776376	36.460033934	32.075352298
6	34.225973956	36.222758328	30.747876264
1	33.416920512	36.731942133	30.233352298
6	29.266980348	38.378906343	31.650593388
1	28.782893853	37.695479461	32.363727307
1	28.828295213	39.380743711	31.768201000
6	30.769137183	38.443238580	31.923396415
8	31.379257093	39.526598561	31.710818009
8	31.325385377	37.403192001	32.386056307
6	32.324683599	33.084907763	34.528435024
7	31.247535218	33.409216094	33.736735874
1	30.509663098	32.790673714	33.376402712
6	31.304977064	34.722768225	33.458522898
1	30.589948982	35.256462293	32.838192984
7	32.363994007	35.278208980	34.036022465



6	33.016154732	34.262252359	34.700961005
1	33.950377800	34.443949924	35.224920392
6	29.316842465	44.308844190	33.717429360
1	29.594050152	45.254447267	33.219276360
1	28.631088860	43.762296888	33.055310176
7	30.489286081	43.495438591	34.001925278
1	31.092770357	43.778379019	34.774902439
6	30.799696692	42.299142438	33.437738779
7	30.147186325	41.829097852	32.374199789
1	29.794955232	42.481927340	31.675807748
1	30.534468409	40.939083379	31.968312546
7	31.755533105	41.571094743	34.013089362
1	32.252177516	41.943199744	34.821361545
1	32.094526321	40.678665539	33.633252453
26	33.098314188	37.208230783	33.439869681
6	35.383597217	41.013078276	33.823025161
8	34.811322402	41.886446669	34.346064981
8	35.976193369	40.161844489	33.307557905
6	34.828310098	38.111683564	35.655628264
8	34.723985396	37.056969748	35.034159254
6	35.757558153	38.326483791	36.827796972
6	35.755343271	37.107009489	37.747488547
6	36.542970673	37.260313551	39.054453056
8	36.065790915	36.665448477	40.054904249
8	37.606871033	37.933422048	39.034308723
1	36.192003133	36.253194968	37.200556776
1	34.723574680	36.825011346	38.002584842
1	35.455951437	39.239221468	37.361884658
1	36.774400955	38.504803971	36.437843013
8	33.206890348	39.023009826	34.244508125
8	34.113367562	39.176240956	35.386024918
8	36.763502645	38.948994751	29.769611409
6	35.880169564	38.719837189	28.961985791
7	34.601527208	39.273496760	29.120126649
6	34.392410981	40.147728040	30.278880380
6	33.560347243	39.049498777	28.250075314
7	32.377708975	39.546564545	28.540202387
6	33.829630013	38.304869048	27.061633803
6	35.057273663	37.746129836	26.895057584
7	36.044616845	37.903607271	27.846397366
1	34.042825848	41.129639291	29.928262627
1	35.347810224	40.252120032	30.796668073
1	31.533975767	39.397869993	27.948808843
1	35.291626354	37.148626084	26.010069114
1	33.036730212	38.147899180	26.334371385
1	33.647027339	39.714400105	30.963498245
1	32.164212985	39.899742177	29.470401273
1	35.062330470	34.690153819	29.341909793
1	29.026462890	38.020079019	30.649862843
1	32.534990608	32.061377446	34.838634923
1	28.776862058	44.539895418	34.635636201
1	36.895730519	37.380278383	27.805107178

**TS2****QM/MM (BS1) = -3428.102605 a.u.****QM/MM (BS2+ZPE) = -3430.111891 a.u.**

6	35.059649214	35.270838441	30.297040389
7	35.845856489	34.931374050	31.372697782
1	36.569532206	34.197851361	31.385115085
6	35.475845729	35.682552559	32.418483188
1	35.922248591	35.618830458	33.406979674
7	34.478657744	36.497278588	32.077149860
6	34.204111760	36.245076987	30.751319504
1	33.392375208	36.745414679	30.232904440
6	29.308713133	38.333098273	31.627712865
1	28.851025752	37.629613044	32.338530236
1	28.866964327	39.328801392	31.778663189
6	30.818607312	38.412507617	31.848997666
8	31.408104296	39.495026904	31.607371847
8	31.399986997	37.372927142	32.298483859
6	32.319605995	33.152177754	34.524319750
7	31.258742858	33.466339322	33.705740200
1	30.537870262	32.838124509	33.326765045
6	31.301583440	34.780450741	33.436236217
1	30.600364217	35.304955307	32.793858726
7	32.335321792	35.349784775	34.047787351
6	32.985479115	34.339592503	34.726182524
1	33.898471682	34.539396910	35.279342769
6	29.321522271	44.261162923	33.724928532
1	29.602320235	45.199171142	33.214144167
1	28.636073874	43.706970756	33.068562833
7	30.491066339	43.447717567	34.025043323
1	31.088414424	43.735418711	34.801253911
6	30.818401447	42.253353255	33.463479267
7	30.180898424	41.785161556	32.388745892
1	29.825263732	42.441837396	31.695088781
1	30.575634340	40.909151706	31.967699600
7	31.770830873	41.532886580	34.051891681
1	32.255138580	41.921265410	34.860603404
1	32.121168205	40.623935594	33.708339238
26	33.112423525	37.264876869	33.455136751
6	35.373338804	41.008497432	33.811017579
8	34.818227975	41.889085126	34.340323635
8	35.951335252	40.157609383	33.278346760
6	34.803018479	38.144079796	35.653992255
8	34.636803249	37.067170809	35.046614356
6	35.801387486	38.283580248	36.793310951
6	35.779915125	37.062957129	37.710967410
6	36.560019737	37.216046525	39.023907659
8	36.074879492	36.624337691	40.023009255
8	37.624237921	37.888936271	39.011676235
1	36.208207626	36.199882032	37.171536834
1	34.743098733	36.795292074	37.962256710
1	35.570768654	39.204864334	37.347080993

1	36.805601474	38.419961571	36.356297180
8	33.058457601	38.965817555	34.075505761
8	34.150992758	39.222331691	35.406155191
8	36.782594000	38.952908281	29.761261559
6	35.898264299	38.726473591	28.953953452
7	34.621604791	39.283426798	29.111718441
6	34.418394711	40.170023691	30.262715931
6	33.576949999	39.053689189	28.246693797
7	32.393251847	39.542597711	28.544470540
6	33.844783141	38.311404964	27.056143837
6	35.072078804	37.752840465	26.887621855
7	36.059787044	37.908380264	27.839163946
1	34.052998794	41.142405846	29.902678998
1	35.378783577	40.291891713	30.766799383
1	31.549911008	39.399800114	27.950994133
1	35.305981652	37.155758271	26.002246419
1	33.050098664	38.153158720	26.331073669
1	33.686873650	39.738600857	30.962552652
1	32.178287375	39.882387021	29.480181591
1	35.060429406	34.711335213	29.361613824
1	29.047531183	37.994795777	30.625015140
1	32.528679211	32.129151754	34.837007306
1	28.779197142	44.507337957	34.637807839
1	36.910053876	37.383694767	27.797643557

**IM2**

**QM/MM (BS1) = -3428.108480 a.u.**

**QM/MM (BS2+ZPE) = -3430.118173 a.u.**

6	35.050210126	35.287806377	30.322082924
7	35.835804936	34.957775354	31.402031400
1	36.563620254	34.227519196	31.417041406
6	35.462043669	35.712256236	32.443128507
1	35.906202381	35.660818440	33.433394514
7	34.459323560	36.519323869	32.093086737
6	34.187447382	36.258916417	30.767089611
1	33.377912534	36.755040180	30.242042934
6	29.325314382	38.297840844	31.605171195
1	28.883859533	37.586027678	32.317578686
1	28.882788103	39.290851980	31.772220456
6	30.838578732	38.391899947	31.787831518
8	31.416451130	39.456769331	31.490080239
8	31.437384816	37.362142505	32.268060903
6	32.332957360	33.197704085	34.527208830
7	31.278768698	33.504658359	33.697134180
1	30.565754633	32.871229562	33.311040188
6	31.317175589	34.815329644	33.420873498
1	30.619136007	35.331051631	32.769075937
7	32.343310490	35.393161651	34.040551635
6	32.991725841	34.388894233	34.732480400
1	33.895926212	34.599412838	35.295207852
6	29.312098153	44.231420304	33.732243439
1	29.589503631	45.164193331	33.209822725

1	28.625741053	43.668736991	33.083934506
7	30.483624964	43.424411431	34.040939987
1	31.076605219	43.719869319	34.817531726
6	30.831290982	42.234061564	33.481127958
7	30.198917317	41.762312344	32.400209872
1	29.847478222	42.421124710	31.705513303
1	30.602765051	40.904343099	31.966776033
7	31.788600513	41.526902733	34.069138351
1	32.259105060	41.923772218	34.882523391
1	32.157669677	40.606190481	33.742916283
26	33.107051228	37.326596716	33.453007850
6	35.369850197	41.015625550	33.795874352
8	34.824273052	41.904675206	34.321024769
8	35.946771993	40.168201744	33.255953577
6	34.784257134	38.218331333	35.663452033
8	34.510619134	37.147974603	35.023040356
6	35.850444350	38.213514815	36.757318357
6	35.795948121	36.995033795	37.674321865
6	36.569434922	37.149910354	38.993259798
8	36.074399628	36.573281602	39.997064515
8	37.637710171	37.816189740	38.983796363
1	36.209357914	36.115275808	37.149798714
1	34.753637552	36.752368285	37.926940870
1	35.717642668	39.138898400	37.335653431
1	36.838843446	38.291210581	36.272633670
8	32.970574775	39.056983264	33.801118303
8	34.230083298	39.323474239	35.470004617
8	36.793116563	38.953220575	29.756011517
6	35.910507978	38.730016755	28.945951472
7	34.634559569	39.288592557	29.100827761
6	34.433091778	40.180947449	30.248810412
6	33.590685937	39.056172406	28.234989809
7	32.405512212	39.540281306	28.532544515
6	33.860613759	38.314869578	27.044065181
6	35.087991953	37.756608853	26.877223448
7	36.073561380	37.911802205	27.831129819
1	34.040141501	41.141173419	29.886028049
1	35.399300806	40.328923114	30.734301010
1	31.563853162	39.400692899	27.935989191
1	35.323581823	37.159077313	25.992631554
1	33.066396884	38.155552575	26.318707495
1	33.726196822	39.741182221	30.967617937
1	32.185941389	39.871295714	29.470893646
1	35.060760084	34.729899830	29.385762304
1	29.054713785	37.970896963	30.601203894
1	32.534405587	32.174040426	34.842801363
1	28.772992708	44.487962243	34.644174836
1	36.923783592	37.386964685	27.790629587

### IM3

QM/MM (BS1) = -3428.112549 a.u.

QM/MM (BS2+ZPE) = -3430.125638 a.u.

6	35.016539773	35.289167431	30.603818373
7	35.774435605	34.892424091	31.679722823
1	36.514053549	34.175014198	31.658772479
6	35.342076800	35.551267023	32.764652862
1	35.752563424	35.420350746	33.760868441
7	34.330919579	36.360904076	32.449485815
6	34.116187119	36.204549079	31.096580713
1	33.311223130	36.724917310	30.589214489
6	29.473444762	38.308792908	31.697549789
1	29.058816136	37.546217948	32.374052519
1	28.981047359	39.266089326	31.920921723
6	30.973883713	38.472663814	31.957541678
8	31.466408267	39.626875977	31.894499983
8	31.660093633	37.442599899	32.266271766
6	32.233690762	33.001335097	34.503824620
7	31.198097378	33.318779024	33.655405061
1	30.479612324	32.700449702	33.257780848
6	31.257919035	34.634366811	33.384881772
1	30.566993421	35.161980960	32.733626163
7	32.279342433	35.184726760	34.022905103
6	32.904300759	34.180626959	34.722622929
1	33.794297393	34.379582819	35.309786950
6	29.341735656	44.399789185	33.713971944
1	29.633824681	45.362644583	33.260711738
1	28.660481878	43.888472594	33.021196833
7	30.506937148	43.569097699	33.975295449
1	31.136321374	43.840983053	34.731752713
6	30.787237992	42.385539546	33.382369783
7	30.058185448	41.912145432	32.365511984
1	29.667976838	42.559299923	31.684666767
1	30.437624628	41.033523224	31.953539812
7	31.791548612	41.649571978	33.857252954
1	32.356021719	41.972329602	34.642474028
1	32.029506842	40.776166632	33.373679576
26	32.950872410	37.168676779	33.807342554
6	35.597482300	41.118134560	33.806080890
8	34.870261857	41.740567329	34.478656987
8	36.329962108	40.536932536	33.124692050
6	34.812448978	37.885503238	35.369058580
8	34.383887036	36.691900010	35.315853549
6	35.759894492	38.282150876	36.495820662
6	35.786365287	37.215272238	37.589222659
6	36.575082196	37.456970443	38.882193865
8	36.134214327	36.832544327	39.885290431
8	37.605667102	38.179949917	38.870281583
1	36.196252268	36.284572104	37.158772041
1	34.755418800	36.972024697	37.880075351
1	35.417791153	39.254867895	36.884853530
1	36.765772948	38.462220406	36.078390598
8	31.892409685	37.811356907	34.844651583
8	34.398662908	38.712689878	34.507225875
8	36.820796200	38.975234709	29.731106001

6	35.938920987	38.719759712	28.932074555
7	34.658797252	39.280776339	29.071001046
6	34.446988179	40.173388766	30.214968977
6	33.627091946	39.050463039	28.193334511
7	32.455414267	39.597084287	28.438190301
6	33.887835351	38.247993861	27.042921465
6	35.111149416	37.674682589	26.899943419
7	36.097952445	37.862828776	27.845873163
1	34.161563978	41.171598465	29.851609731
1	35.385469716	40.236548013	30.770279179
1	31.603877515	39.428436969	27.864417423
1	35.341954984	37.043430398	26.037535493
1	33.097532763	38.076766142	26.316926719
1	33.658942140	39.774061522	30.872386707
1	32.269988357	40.075933462	29.312625828
1	35.079698380	34.801521944	29.631049030
1	29.201787658	38.019668134	30.682327348
1	32.467897743	31.983312293	34.815022277
1	28.786965454	44.593449584	34.632009516
1	36.952888335	37.345171531	27.812886751

**Ferryl flip mechanism reaction states coordinate AlkBH2-dsDNA  
IM3'**

**QM/MM (BS1) = -3580.810509 a.u.**

**QM/MM (BS2+ZPE) = -3582.962240 a.u.**

6	35.039985247	35.175720984	30.678143212
7	35.773272511	34.730309810	31.750960056
1	36.511646835	34.012721452	31.714822483
6	35.321051054	35.344521224	32.853741588
1	35.710936172	35.169537918	33.851748622
7	34.322702107	36.173499864	32.551455762
6	34.134991343	36.076058747	31.189571693
1	33.343908990	36.623591753	30.687663138
6	29.537182394	38.250299222	31.749361845
1	29.076941584	37.499445961	32.409344736
1	29.082857823	39.224801690	31.975845723
6	31.039112069	38.332391277	32.041515773
8	31.594182379	39.458774780	32.016864358
8	31.664072268	37.259459803	32.332532372
6	32.197092217	32.815714408	34.506143173
7	31.145030875	33.147117491	33.683303132
1	30.413110000	32.542307769	33.290828374
6	31.201793920	34.467886600	33.434224074
1	30.497065690	35.008370758	32.808754409
7	32.237977055	35.003360566	34.060425913
6	32.873767687	33.987101801	34.729164560
1	33.772469768	34.174713721	35.303007358
6	29.284807795	44.248030204	33.712370479
1	29.522638476	45.170557423	33.155054880
1	28.593848191	43.650655893	33.102673693
7	30.490180549	43.481404916	33.997393023

1	31.133905469	43.836965597	34.705338740
6	30.833655166	42.295346586	33.444991667
7	30.092025555	41.715307873	32.492971929
1	29.666838848	42.316038120	31.784460373
1	30.533510736	40.861756015	32.094660679
7	31.913475459	41.661387458	33.899067567
1	32.502868030	42.077763374	34.619736663
1	32.217248923	40.803467268	33.434358585
26	32.930468277	36.963911097	33.908454812
6	35.817930535	41.869189924	33.151483791
8	34.986484040	42.034603863	33.954728986
8	36.618140550	41.865168801	32.306544117
6	34.754883029	37.532057631	35.572583161
8	34.332377028	36.346993096	35.523030045
6	35.674142901	37.990161983	36.689156073
6	35.883701161	36.892016917	37.727740176
6	36.586184282	37.265080110	39.037218288
8	36.068715079	36.782430903	40.081724011
8	37.630268118	37.966261809	38.998743974
1	36.471595944	36.072600516	37.274962812
1	34.908752549	36.465757029	37.990870017
1	35.203996633	38.883393039	37.136487382
1	36.610594477	38.361619329	36.242854358
8	31.846932134	37.583158939	34.931887601
8	34.353340411	38.344997729	34.672540837
8	35.752264005	38.851368692	29.225891290
6	35.224917725	38.444464493	28.197385982
7	33.912700364	38.814845815	27.852487360
6	33.211567497	39.759268356	28.737269524
6	33.236059810	38.312982955	26.759350919
7	31.984572502	38.644525535	26.536163387
6	33.955430458	37.456551668	25.876480175
6	35.238641757	37.142571740	26.154389313
7	35.861903387	37.589016958	27.301331850
1	32.750547965	40.547501766	28.131676397
1	33.928206966	40.204631920	29.428448863
1	31.483589711	38.283889779	25.717145884
1	35.803273781	36.516595875	25.468390757
1	33.475978053	37.043538340	24.996437317
1	32.420157870	39.241680296	29.296461860
1	31.397181903	39.219567889	27.168347268
8	36.635429961	39.829297557	34.269291538
1	37.089331863	39.403757539	33.528585781
1	33.570942578	39.571619495	31.798870256
8	34.508032468	39.843419715	31.798865520
1	35.739658775	39.430923700	34.233097296
1	34.909517972	39.375865580	31.048106876
1	35.122270092	34.722361251	29.690336816
1	29.269618259	37.984145815	30.726796875
1	32.459455752	31.799692354	34.800985295
1	28.766739733	44.513030206	34.634025407
1	36.749251325	37.195796234	27.542088152

**IM4****QM/MM (BS1) = -3580.818612 a.u.****QM/MM (BS2+ZPE) = -3582.964722 a.u.**

6	35.004749736	35.239871729	30.548858204
7	35.774438193	34.859127132	31.621226528
1	36.523593742	34.152206061	31.600465703
6	35.338743603	35.518817382	32.705136112
1	35.773431608	35.425375512	33.696186677
7	34.313054185	36.302897941	32.388442700
6	34.090165722	36.142208613	31.041095415
1	33.278694848	36.657594878	30.536008325
6	29.293842538	38.188134061	31.748126672
1	28.855163214	37.394267104	32.372716849
1	28.781327070	39.131099634	31.983900283
6	30.775188933	38.344735304	32.076766376
8	31.217694653	39.526162407	32.181610026
8	31.488032381	37.317333342	32.276424142
6	32.346082167	33.088437333	34.577820290
7	31.303585079	33.418899265	33.744473085
1	30.588131649	32.803145157	33.336460133
6	31.356784305	34.737205381	33.495186007
1	30.674817148	35.272109551	32.841967637
7	32.380820156	35.286836718	34.134110585
6	33.014612905	34.269414651	34.811483341
1	33.914903852	34.450205196	35.391324702
6	29.489875800	44.530378996	33.809017083
1	29.919715796	45.527413207	33.625938614
1	28.935269367	44.240607900	32.907803230
7	30.566417586	43.590884471	34.085487885
1	31.200809353	43.821075415	34.853274871
6	30.653609285	42.316973309	33.638603255
7	29.881449385	41.846521034	32.656850122
1	29.583118753	42.492605185	31.923581585
1	30.207386809	40.929965703	32.283774674
7	31.518732605	41.494819018	34.237460484
1	32.147994343	41.845956974	34.957927488
1	31.643314360	40.550385687	33.870339884
26	33.051720867	37.270655119	33.732996204
6	36.877131400	41.459820415	32.854971295
8	35.997017261	41.841666283	33.510159226
8	37.829960583	41.115250491	32.277976574
6	35.033298050	38.489423080	35.527482956
8	34.629121045	37.384663918	34.997859166
6	35.919659221	38.409597565	36.762784536
6	35.773574168	37.164450685	37.625874000
6	36.567046084	37.214835137	38.941963552
8	36.067822193	36.605490012	39.925479745
8	37.661036029	37.838741591	38.949644332
1	36.120907641	36.278520925	37.063557105
1	34.715422430	36.984402571	37.869605479
1	35.702888899	39.312208357	37.351602463
1	36.967221027	38.522424050	36.433659719



8	32.071445361	38.030331871	34.777142367
8	34.766087558	39.623607519	35.079783794
8	35.834728124	38.957944742	28.865848573
6	35.238868954	38.439265687	27.930090838
7	33.896170972	38.743158671	27.657840367
6	33.197965721	39.686563821	28.549558468
6	33.182865240	38.180985188	26.618428462
7	31.923346175	38.502353881	26.426406581
6	33.869832530	37.263557969	25.770044167
6	35.163009871	36.962194917	26.020876025
7	35.838787374	37.504977112	27.092865246
1	32.728448105	40.475096237	27.951096502
1	33.909166253	40.134434647	29.244339578
1	31.398930072	38.118948665	25.633146018
1	35.693633584	36.269985630	25.374303555
1	33.349427648	36.773125289	24.954770573
1	32.410652846	39.156850944	29.103724753
1	31.352841014	39.097566407	27.056764906
8	33.721201590	39.065716954	32.835876146
1	32.854969676	39.463179430	32.549599334
1	34.821767250	39.909247561	31.604780979
8	35.290608005	40.579206347	31.069652656
1	34.084766802	39.496916649	33.686552572
1	35.557863619	40.082130440	30.277585235
1	35.074715435	34.750579178	29.577382566
1	29.080678898	37.933632735	30.709927429
1	32.553583489	32.058931848	34.869588987
1	28.792407354	44.597570970	34.643936436
1	36.726192839	37.127596590	27.357568834

### TS3

**QM/MM (BS1) = -3580.806149 a.u.**

**QM/MM (BS2+ZPE) = -3582.951774 a.u.**

6	35.014830483	35.227739001	30.497666851
7	35.776543334	34.845958937	31.575616640
1	36.524686853	34.138045531	31.562784462
6	35.335436229	35.504458274	32.656432156
1	35.763414711	35.412564358	33.650345365
7	34.312129453	36.288771808	32.331173990
6	34.098094967	36.130830556	30.982842573
1	33.291110325	36.648343505	30.472982701
6	29.288144982	38.181379081	31.739214512
1	28.856835578	37.385627846	32.366071917
1	28.776102895	39.123794400	31.978756526
6	30.773168391	38.339735490	32.044920489
8	31.223330100	39.518389328	32.117591813
8	31.482527737	37.309907143	32.253996923
6	32.353845801	33.127122974	34.579032243
7	31.310498283	33.453602470	33.744861279
1	30.600807572	32.833710927	33.332844011
6	31.355222089	34.772789630	33.500389836
1	30.672410413	35.302749379	32.844154594
7	32.373296398	35.330833525	34.143548890

6	33.012213303	34.313285551	34.819016708
1	33.909743088	34.500096238	35.401497203
6	29.488716913	44.512114586	33.806475249
1	29.921896255	45.506990786	33.618687452
1	28.932772349	44.220189819	32.906718755
7	30.561424624	43.569422031	34.087636482
1	31.194406870	43.799296353	34.856663436
6	30.654147141	42.296532367	33.636954571
7	29.892269086	41.828265266	32.646535875
1	29.591701971	42.478671604	31.918133234
1	30.226835322	40.917724997	32.263810695
7	31.513888886	41.474108031	34.242732545
1	32.138811429	41.825719278	34.966508493
1	31.649027018	40.529227075	33.880319971
26	33.091392063	37.297106187	33.650557374
6	36.859998508	41.438651542	32.881413409
8	35.980007504	41.780984490	33.559814171
8	37.818292277	41.135839815	32.290589328
6	34.990078350	38.427115809	35.530641832
8	34.674706807	37.321480350	34.958575830
6	35.915014367	38.384008162	36.737076518
6	35.776959834	37.153270916	37.626127486
6	36.569837832	37.223814397	38.941942660
8	36.073699072	36.614551680	39.927028768
8	37.656757128	37.859168796	38.947906757
1	36.124484906	36.257922600	37.079218190
1	34.720298788	36.975030900	37.877722931
1	35.721960929	39.298647803	37.313993672
1	36.954051250	38.472150819	36.374646258
8	32.254083702	38.255964710	34.653758013
8	34.587565480	39.548572519	35.138338908
8	35.830176507	38.944202622	28.891150791
6	35.238878304	38.435498072	27.947315711
7	33.897421217	38.743346359	27.671463078
6	33.200040196	39.686552497	28.564436451
6	33.186148007	38.186121907	26.628071162
7	31.927096449	38.508230225	26.434086218
6	33.874665527	37.272954754	25.776136998
6	35.168204211	36.972616486	26.025894694
7	35.841848728	37.509381386	27.102370280
1	32.730164867	40.474684024	27.965674547
1	33.912591305	40.134511595	29.258252373
1	31.404378623	38.126187630	25.639083742
1	35.700721680	36.285492931	25.375063485
1	33.355553986	36.786472356	24.957682476
1	32.413030297	39.157885930	29.120028386
1	31.354609482	39.100021001	27.065895447
8	33.728877999	39.083385859	32.847812283
1	32.855934927	39.429913342	32.516926841
1	34.820990841	39.961005557	31.686488825
8	35.290412220	40.592295732	31.103027886
1	33.889540424	39.383211794	33.912739470

1	35.544457295	40.050159498	30.336926706
1	35.081988802	34.729270035	29.530668524
1	29.072528235	37.926884619	30.701520284
1	32.557988402	32.096931760	34.870749875
1	28.791573862	44.586554230	34.641051568
1	36.729431177	37.130523470	27.364356104

**IM5**

**QM/MM (BS1) = -3580.810798 a.u.**

**QM/MM (BS2+ZPE) = -3582.957150 a.u.**

6	35.013101238	35.240445516	30.454990744
7	35.774571461	34.852198455	31.530269515
1	36.519114801	34.140567701	31.516962306
6	35.338705581	35.513457187	32.612582884
1	35.768722703	35.408073670	33.604177010
7	34.322404371	36.307648646	32.292160873
6	34.105683834	36.152473381	30.944238442
1	33.299987623	36.676533365	30.437585305
6	29.214366175	38.202131646	31.711214828
1	28.765821388	37.420055356	32.343505048
1	28.701787464	39.150813407	31.923263740
6	30.693111769	38.349201677	32.053064633
8	31.145671852	39.521579526	32.171624758
8	31.388935358	37.308018113	32.245574966
6	32.377869352	33.140589820	34.560678858
7	31.338358946	33.464329253	33.720871404
1	30.620199701	32.845558872	33.323651524
6	31.399468033	34.777014788	33.449095325
1	30.723344665	35.308771257	32.786653560
7	32.426947854	35.332981857	34.078812013
6	33.053223212	34.322307801	34.775664624
1	33.954788106	34.508216659	35.351922122
6	29.472208281	44.516619028	33.804899502
1	29.899658782	45.512873602	33.611056192
1	28.907736518	44.220899017	32.911928299
7	30.550085387	43.577655130	34.074288711
1	31.192052507	43.808202528	34.834885802
6	30.634293358	42.303955586	33.621292401
7	29.856475553	41.838116424	32.643744375
1	29.562484100	42.485733987	31.910079839
1	30.176814350	40.914317233	32.272805099
7	31.502237197	41.479572824	34.213108102
1	32.128192133	41.833046366	34.934000992
1	31.648889570	40.545715656	33.820759346
26	33.052837389	37.314187928	33.608213711
6	36.809234307	41.441700587	32.884758555
8	35.938033165	41.757657167	33.589360581
8	37.771243133	41.186094233	32.279028694
6	35.103434832	38.339571720	35.592817338
8	34.780011831	37.278021235	35.035153313
6	35.960640591	38.376710956	36.831729505
6	35.828992605	37.140350445	37.708280476
6	36.596926268	37.229451257	39.032989500

8	36.089483836	36.626946064	40.014191850
8	37.678371706	37.874399883	39.042212493
1	36.207100841	36.257284355	37.162449765
1	34.771018141	36.941364141	37.935611540
1	35.696178773	39.287289628	37.387544764
1	37.009988545	38.516034118	36.517964592
8	32.201763789	38.093726210	34.753136141
8	34.735790843	39.512808958	35.163612265
8	35.845180952	38.935650398	28.909336687
6	35.249356120	38.434474050	27.964726934
7	33.906066730	38.742272585	27.698843127
6	33.208582630	39.668575150	28.610391473
6	33.195079032	38.201629922	26.646689120
7	31.937752899	38.530356226	26.453754164
6	33.881781616	37.297013036	25.783614156
6	35.175277353	36.991927069	26.027698564
7	35.850242104	37.517127752	27.108833190
1	32.758852582	40.482402498	28.030588874
1	33.917421858	40.080228767	29.330447179
1	31.413821442	38.153109856	25.657205787
1	35.707729363	36.312476372	25.368325265
1	33.361314445	36.822792156	24.959008938
1	32.406452549	39.133337292	29.137193224
1	31.367266629	39.121832132	27.087960429
8	33.705142452	38.969085558	32.876142872
1	32.873474866	39.393022888	32.558821619
1	34.787168488	39.769018326	31.774568076
8	35.283004887	40.417335800	31.222257437
1	34.218171016	39.408571751	34.276055635
1	35.545206070	39.905144564	30.439066043
1	35.071795086	34.733194202	29.492016984
1	29.016439606	37.928179494	30.674951051
1	32.570191240	32.110785504	34.861648423
1	28.782296094	44.590366936	34.645524116
1	36.737704752	37.135536530	27.367233420

#### TS4

**QM/MM (BS1) = -3580.795662 a.u.**

**QM/MM (BS2+ZPE) = -3582.946226 a.u.**

6	35.023800038	35.223205281	30.415980315
7	35.781826201	34.826401832	31.491120247
1	36.527724801	34.116784121	31.477231101
6	35.345355387	35.479988689	32.576787080
1	35.773798534	35.372849860	33.568254902
7	34.332757782	36.278284817	32.256437038
6	34.118750374	36.135451517	30.907648280
1	33.316940086	36.667232212	30.402949035
6	29.183161000	38.199057729	31.701073776
1	28.726499687	37.421593806	32.333555949
1	28.674363637	39.151462771	31.905944007
6	30.662030136	38.339100122	32.043252782
8	31.117106546	39.510389935	32.171559267

8	31.350631741	37.292024524	32.223049536
6	32.386494164	33.166107181	34.549234002
7	31.339190464	33.485096359	33.717408018
1	30.616919791	32.863146639	33.331067541
6	31.398963389	34.795918502	33.436950569
1	30.716374813	35.324009737	32.778609007
7	32.433885627	35.355919574	34.051881955
6	33.064444521	34.348775337	34.750527895
1	33.970142882	34.537734843	35.319684120
6	29.466511286	44.514537530	33.804326657
1	29.896186654	45.509092921	33.606292459
1	28.897708419	44.218838220	32.914028513
7	30.541740310	43.572010073	34.071373786
1	31.183148867	43.799249600	34.833370408
6	30.622634768	42.298587495	33.616971256
7	29.841887904	41.835134055	32.640304125
1	29.551707045	42.483903336	31.906303689
1	30.155800378	40.907846559	32.271332208
7	31.490425945	41.472172195	34.206155755
1	32.114614837	41.825765734	34.928735192
1	31.636362151	40.540015559	33.806630298
26	33.072695130	37.332239323	33.529297921
6	36.725724803	41.345700896	32.979124596
8	35.843271146	41.562476520	33.708508728
8	37.700374409	41.186964841	32.360439280
6	35.117985058	38.200871606	35.678190138
8	34.861293996	37.207770759	34.986967306
6	36.210644079	38.218041100	36.714165614
6	35.957708906	37.085502710	37.716275307
6	36.681520394	37.223790272	39.058986608
8	36.157468688	36.614075526	40.026361598
8	37.734780868	37.909808561	39.094997051
1	36.260753429	36.121503685	37.271629800
1	34.882236091	37.001550655	37.936741117
1	36.195982811	39.188252661	37.224441117
1	37.194672288	38.110575303	36.232272014
8	32.241971158	38.155656532	34.699040097
8	34.405296679	39.298465729	35.635990999
8	35.855314844	38.942478214	28.933647878
6	35.258066621	38.443945746	27.988415664
7	33.912917474	38.748027858	27.725658162
6	33.209064726	39.661202821	28.645586951
6	33.204962772	38.216669409	26.666686877
7	31.947535693	38.545345950	26.473760896
6	33.894360906	37.321787236	25.795694495
6	35.187611999	37.015948774	26.039358461
7	35.859837235	37.532270445	27.126333161
1	32.755707740	40.478460672	28.073696018
1	33.913275346	40.070149756	29.371135892
1	31.425216930	38.171366508	25.674632065
1	35.722522978	36.344320941	25.373706654
1	33.376924364	36.856755726	24.964200638

1	32.410106471	39.115719478	29.166493604
1	31.375141803	39.132601391	27.110208400
8	33.694256995	38.867091284	32.729613877
1	32.866291275	39.352195942	32.506358970
1	34.776616571	39.771219364	31.764625212
8	35.260765467	40.443875653	31.228796766
1	33.577084854	39.100226073	35.101372829
1	35.545121142	39.947272444	30.442966492
1	35.074354637	34.713207204	29.453996159
1	28.992842545	37.920389423	30.664642308
1	32.578833414	32.138079694	34.856206999
1	28.780106734	44.591388873	34.647540736
1	36.747301752	37.148352038	27.381256453

**IM6**

**QM/MM (BS1) = -3580.796277 a.u.**

**QM/MM (BS2+ZPE) = -3582.948764 a.u.**

6	34.977870178	35.238519877	30.446338188
7	35.760876655	34.892564583	31.522028987
1	36.520622491	34.195773668	31.512478481
6	35.324258243	35.566861850	32.595174693
1	35.760875618	35.507222717	33.587528432
7	34.284757654	36.327953113	32.263666002
6	34.052988925	36.137944762	30.922459697
1	33.226202126	36.625537283	30.414656213
6	29.203055000	38.152491295	31.608152664
1	28.748390046	37.395862732	32.264947865
1	28.737633730	39.126860025	31.812143217
6	30.696135265	38.247908118	31.868422345
8	31.223918318	39.395099755	31.826629757
8	31.349326785	37.195240678	32.136100137
6	32.345507301	33.077569816	34.486278679
7	31.277678112	33.382060045	33.674383913
1	30.538789358	32.757900973	33.325284941
6	31.337965027	34.683593985	33.354431733
1	30.635678606	35.204131664	32.711344498
7	32.395420331	35.244826182	33.925478978
6	33.039030604	34.256927703	34.635050571
1	33.959534974	34.461672223	35.172368392
6	29.359368869	44.308569579	33.746357724
1	29.663980672	45.269763848	33.299120725
1	28.709770288	43.795509307	33.025698200
7	30.528996441	43.493465432	34.046074081
1	31.170913829	43.830070010	34.765457996
6	30.821198296	42.272959870	33.532682602
7	30.087936618	41.721953244	32.567205437
1	29.686423449	42.337865587	31.857647931
1	30.443808847	40.819640385	32.172553221
7	31.851421155	41.605038955	34.062237086
1	32.397734920	42.031107187	34.809140551
1	32.189191215	40.724673225	33.671385928
26	32.980161604	37.245715742	33.581824049

6	36.456386421	41.258050099	33.393591934
8	35.477421655	41.452535951	33.996221070
8	37.492797849	41.107540500	32.886303060
6	34.527021645	37.914394480	36.005462761
8	34.520589368	37.143852492	34.973713162
6	35.809147400	38.025929687	36.806485205
6	35.903969919	36.804317319	37.736126264
6	36.652164043	37.033470065	39.053573389
8	36.164436666	36.456688740	40.060351425
8	37.685628525	37.750520505	39.039378305
1	36.397742655	35.966288478	37.212454628
1	34.893162606	36.467058185	38.005268946
1	35.747133885	38.944169078	37.406259768
1	36.683559981	38.097397599	36.143659347
8	31.831136690	37.833722784	34.747707126
8	33.519284183	38.516297992	36.432249546
8	35.827574161	38.879952540	29.075258986
6	35.246123826	38.432663798	28.094086159
7	33.908822346	38.758273180	27.816104778
6	33.197352261	39.649633186	28.751144715
6	33.215084631	38.267120364	26.727782861
7	31.962263209	38.606253579	26.526330168
6	33.914879854	37.405042925	25.832814591
6	35.204946972	37.091141649	26.080070850
7	35.859002347	37.561158882	27.198851802
1	32.765126190	40.491063859	28.197730397
1	33.894099127	40.027218849	29.500720859
1	31.446755931	38.247840870	25.715260987
1	35.753173295	36.452379025	25.392284638
1	33.410991806	36.980463910	24.972435562
1	32.381220415	39.101117621	29.241556222
1	31.385232393	39.183823167	27.167202542
8	33.472042901	38.890436018	32.975628296
1	32.685881230	39.190922545	32.424289056
1	34.681258868	39.679139268	31.987767854
8	35.212523875	40.291223934	31.430961123
1	32.423883087	38.212926830	35.525603344
1	35.466164769	39.754428999	30.660508624
1	35.043163014	34.726934088	29.486086060
1	28.981626136	37.869948692	30.578975195
1	32.557458214	32.057636804	34.807029028
1	28.771563401	44.506356725	34.642701569
1	36.749336676	37.173504817	27.437601892

**TS5**

**QM/MM (BS1) = -3580.776832 a.u.**

**QM/MM (BS2+ZPE) = -3582.933015 a.u.**

6	35.053840208	35.243862678	30.364342956
7	35.769485956	34.883502936	31.481294182
1	36.501300594	34.156552125	31.516964539
6	35.321180845	35.599128533	32.520809383
1	35.715438512	35.542493809	33.529931579

7	34.337740996	36.403659698	32.123348568
6	34.157197774	36.199926748	30.776182791
1	33.382272187	36.715034132	30.217256563
6	29.309216185	38.287356203	31.333403101
1	28.854557322	37.617364803	32.077861117
1	28.878173783	39.291927088	31.438065111
6	30.800618530	38.354709190	31.555703044
8	31.373610020	39.473961458	31.413694413
8	31.425028829	37.317505970	31.930990628
6	32.389782572	33.425359445	34.458020112
7	31.339137588	33.700204493	33.613399754
1	30.638520659	33.046005684	33.238128221
6	31.365250993	35.000432623	33.297443709
1	30.673710533	35.484889823	32.617500814
7	32.382880201	35.606819034	33.904102466
6	33.034099159	34.631115075	34.637505488
1	33.919710084	34.866389428	35.219640838
6	29.356543713	44.098781143	33.912732178
1	29.783335066	45.027172698	33.492906364
1	28.693454616	43.659720662	33.155658936
7	30.399095000	43.151737693	34.283056730
1	31.053282552	43.429803499	35.016457079
6	30.626756239	41.913962643	33.738871458
7	29.942917678	41.567491618	32.622360211
1	29.720291629	42.318157846	31.966508015
1	30.372368019	40.785035908	32.112981139
7	31.463443007	41.066010961	34.308402923
1	31.922154177	41.455729123	35.131506791
1	31.669114402	39.762635580	34.192924848
26	33.073017664	37.541239518	33.275358401
6	36.818873599	40.993880133	33.384818085
8	35.816450654	40.996679904	33.976550822
8	37.858400060	40.997339216	32.862441203
6	34.325081923	38.013654744	35.951577107
8	34.451914025	37.496927977	34.769972899
6	35.585001390	38.167886919	36.787703281
6	35.752444491	36.924087604	37.676329971
6	36.563583608	37.113716874	38.968832781
8	36.116817117	36.505107797	39.976627419
8	37.602343398	37.821169239	38.935237979
1	36.242017702	36.118433335	37.098478337
1	34.760829981	36.557586517	37.976115359
1	35.444657969	39.054393164	37.422640990
1	36.463586185	38.326779781	36.147199839
8	31.840881881	38.572264551	34.333197592
8	33.231824979	38.332816698	36.450299507
8	35.878374103	38.967414654	28.896073256
6	35.280856835	38.472364549	27.947678515
7	33.945378366	38.801062717	27.667597512
6	33.262620957	39.753194814	28.561799402
6	33.225666938	38.250671196	26.625399362
7	31.973928593	38.593095237	26.424929245



6	33.899126962	37.320995449	25.779121812
6	35.189652596	37.008348979	26.025950560
7	35.870208744	37.540535447	27.100674272
1	32.785434219	40.538997539	27.966734706
1	33.990621333	40.205757670	29.236654623
1	31.442842173	38.200679589	25.640752603
1	35.714378321	36.316644558	25.373423671
1	33.373682609	36.840140317	24.961988222
1	32.479953914	39.236567861	29.133505891
1	31.411580160	39.206735959	27.045338435
8	33.545623626	38.944263875	32.400307521
1	32.644012747	39.307957979	31.910922755
1	34.864435113	40.052194857	31.724932351
8	35.473298349	40.566808751	31.163828061
1	32.209823799	38.453480684	35.274791987
1	35.598710213	39.989827296	30.388996017
1	35.121142722	34.703884582	29.419905900
1	29.055032519	37.902378452	30.345855577
1	32.569528372	32.409366252	34.809469414
1	28.740448154	44.360383276	34.772998359
1	36.757237928	37.156514275	27.356954311

#### IM7

**QM/MM (BS1) = -3580.784869 a.u.**

**QM/MM (BS2+ZPE) = -3582.938244 a.u.**

6	35.072401888	35.222755946	30.343779414
7	35.786889982	34.854280969	31.457672572
1	36.515633424	34.125063480	31.491288837
6	35.342490548	35.567618584	32.500742124
1	35.737766543	35.499051035	33.509511470
7	34.363692801	36.379983921	32.110256332
6	34.182636361	36.182579280	30.762317707
1	33.412741504	36.703486812	30.201659577
6	29.310048433	38.319246815	31.266916451
1	28.824310498	37.698747538	32.034081325
1	28.911125968	39.340776652	31.319045665
6	30.787031830	38.325797659	31.529479776
8	31.365581067	39.490306267	31.380017811
8	31.405248660	37.330039475	31.920615764
6	32.400426559	33.378114643	34.466389410
7	31.341625578	33.664237855	33.637000705
1	30.629354213	33.018133887	33.270149519
6	31.378217614	34.966340411	33.323880150
1	30.671068880	35.452461142	32.661955835
7	32.411007903	35.561657630	33.914855316
6	33.059595522	34.576843201	34.636563902
1	33.955608696	34.801935258	35.207134363
6	29.372082395	44.232621298	33.920707175
1	29.780927246	45.191702250	33.555050199
1	28.723860643	43.823656081	33.135137691
7	30.436336034	43.295477881	34.231773078

1	31.103604975	43.552982950	34.960219105
6	30.579741094	42.018618255	33.736289819
7	29.794233492	41.690772888	32.655490131
1	29.699679159	42.421880725	31.946026231
1	30.154267822	40.858980967	32.196515938
7	31.386643020	41.135655137	34.256759769
1	31.878522751	41.524545635	35.064864843
1	31.623403727	39.452599012	34.245901343
26	33.135400147	37.492138563	33.322407804
6	36.806870113	40.997555983	33.361962571
8	35.818733149	40.997560677	33.976243878
8	37.832922181	41.003878043	32.812304771
6	34.307998325	38.024983010	36.006364860
8	34.459920054	37.482337142	34.841075451
6	35.550122233	38.195923206	36.863312788
6	35.756853411	36.926026065	37.704296337
6	36.566923632	37.106811000	38.996497352
8	36.114439444	36.505263666	40.005850042
8	37.610119726	37.808159893	38.961074349
1	36.265763997	36.155335706	37.096761839
1	34.776934369	36.524009918	37.996586433
1	35.367771764	39.051265774	37.529246006
1	36.429675528	38.412362813	36.240822719
8	31.735269289	38.444330966	34.422720036
8	33.204670830	38.352539785	36.479220600
8	35.868826094	38.941129563	28.900799799
6	35.286610897	38.454428594	27.938860348
7	33.953622741	38.782641803	27.644645020
6	33.259986194	39.727289159	28.535880750
6	33.244145648	38.234384634	26.594099258
7	31.991179931	38.570789226	26.388786153
6	33.929730118	37.315185109	25.747429635
6	35.219862362	37.009242484	26.003208416
7	35.887599663	37.533844006	27.089432637
1	32.802750761	40.527555843	27.944292453
1	33.974545272	40.161271078	29.237261415
1	31.467076491	38.181123579	25.598812575
1	35.755811307	36.329827618	25.347423536
1	33.415545890	36.838393625	24.920910849
1	32.457612988	39.205078957	29.073415697
1	31.424512638	39.184223955	27.004827424
8	33.587230219	38.883354430	32.581543659
1	32.307120968	39.432132357	31.738450502
1	34.826184091	40.010433866	31.758622807
8	35.408455202	40.528021048	31.173478079
1	32.160472019	38.390285474	35.351959238
1	35.562193390	39.932662363	30.418479069
1	35.131711815	34.681989022	29.399257954
1	29.053111357	37.896916422	30.295480554
1	32.580526855	32.360325306	34.812418418
1	28.741440308	44.437940954	34.785693718
1	36.773706421	37.150183002	27.349416366

**TS6****QM/MM (BS1) = -3580.776499 a.u.****QM/MM (BS2+ZPE) = -3582.927398 a.u.**

6	35.030665112	35.279114847	30.414406119
7	35.751180731	34.916209026	31.526179102
1	36.477430986	34.184150110	31.555956684
6	35.313452052	35.639958966	32.567102449
1	35.709757144	35.571998579	33.575974762
7	34.334259804	36.453954931	32.179561761
6	34.144833013	36.244146217	30.833998078
1	33.377920122	36.770468433	30.273593085
6	29.160648778	38.206605448	31.441647021
1	28.765265318	37.443173379	32.128733005
1	28.604325726	39.140403967	31.596120025
6	30.609839664	38.443572110	31.775745316
8	30.929372228	39.709498712	31.752122822
8	31.368925886	37.524821921	32.099276507
6	32.353126326	33.364049836	34.440752031
7	31.330483233	33.646143380	33.565754159
1	30.638478562	32.994774050	33.171325768
6	31.362549586	34.954391562	33.273100100
1	30.679127191	35.444021824	32.587975369
7	32.354787006	35.554605332	33.922535091
6	32.984919542	34.569610967	34.657730410
1	33.851214740	34.803064385	35.269097363
6	29.660892975	44.550354157	33.991534100
1	30.201834142	45.496782306	34.147123504
1	29.250288525	44.585462188	32.970106977
7	30.622264243	43.472881675	34.144106939
1	31.387419773	43.626613715	34.803641050
6	30.557071183	42.210725302	33.608044009
7	29.457923179	41.932515650	32.835138420
1	29.072895548	42.717309773	32.317756346
1	29.628945486	41.154577515	32.201261970
7	31.464056884	41.284854006	33.831529013
1	32.235122731	41.648117360	34.396105278
1	31.523057327	39.363522436	34.448895540
26	33.068660540	37.511571523	33.455060280
6	36.523115403	41.169378085	33.345389782
8	35.559896269	41.306379540	33.984843500
8	37.536875488	41.052367253	32.785155448
6	34.279808333	37.989000434	36.132409742
8	34.368938821	37.386668431	34.993680422
6	35.551461956	38.143225349	36.944825722
6	35.791516489	36.858741146	37.756071844
6	36.583062924	37.054662175	39.055393801
8	36.111576357	36.481280025	40.071978730
8	37.629959915	37.751307989	39.018239727
1	36.329007171	36.117706547	37.137635707
1	34.823699339	36.420330543	38.034776626
1	35.395913833	38.989043388	37.628903836

1	36.406612623	38.368298641	36.291683051
8	31.616334416	38.404514977	34.678333164
8	33.207057801	38.388880392	36.623605569
8	35.800343668	38.930482279	29.005094073
6	35.238823905	38.464087719	28.021284038
7	33.902492487	38.777067804	27.718825802
6	33.179213436	39.692958394	28.618778334
6	33.217438745	38.247251071	26.642763562
7	31.959117531	38.560350019	26.432754173
6	33.933638277	37.375721860	25.771229800
6	35.226121360	37.086250823	26.033160547
7	35.868187658	37.582437051	27.148036980
1	32.710181298	40.489406079	28.030718342
1	33.874124057	40.136691393	29.332717920
1	31.454338253	38.187404701	25.622221392
1	35.786233109	36.445002469	25.358308940
1	33.441724727	36.923024609	24.918380276
1	32.387016541	39.144682497	29.147308109
1	31.369564846	39.141189864	27.058860554
8	33.576027728	38.953082502	32.929886204
1	31.609272758	40.065951094	32.409731686
1	34.549787077	40.014972820	31.789132871
8	35.152894018	40.552390449	31.242785032
1	32.127121274	38.393356676	35.571720322
1	35.411168632	39.951099057	30.522380032
1	35.104697909	34.744778612	29.467267666
1	28.976123100	37.855571544	30.426367361
1	32.536729924	32.347354193	34.788152397
1	28.833560066	44.539515823	34.701090373
1	36.755005202	37.196776694	27.402582106

#### IM8

**QM/MM (BS1) = -3580.809733 a.u.**

**QM/MM (BS2+ZPE) = -3582.969357 a.u.**

6	34.989439548	35.268346148	30.413311463
7	35.753019447	34.922049656	31.501966613
1	36.497616706	34.209145342	31.509926852
6	35.323076194	35.628946756	32.558551415
1	35.741636400	35.565055159	33.558661395
7	34.309398379	36.414087220	32.205317362
6	34.085472830	36.202024803	30.866127742
1	33.281357027	36.705248104	30.336525791
6	29.034929403	38.122967364	31.747740848
1	28.530309233	37.332057968	32.330740038
1	28.467894110	39.046804349	31.923063558
6	30.417381037	38.304420962	32.358646401
8	30.575392554	39.359614976	33.030101389
8	31.274256690	37.367322250	32.297842486
6	32.336408193	33.136721191	34.445418285
7	31.295645542	33.423071642	33.592819554
1	30.575605770	32.784860448	33.230988826

6	31.348682041	34.725218088	33.274234138
1	30.655147752	35.230675041	32.610040134
7	32.372188841	35.307697033	33.884566068
6	33.003338308	34.328257817	34.618471517
1	33.894516701	34.556517281	35.193926539
6	29.589739369	44.714697491	33.756461934
1	30.011874855	45.729370471	33.714979645
1	29.084939590	44.542116539	32.796581692
7	30.699635498	43.791074733	33.937450724
1	31.432149888	44.061519804	34.595275339
6	30.720493384	42.489037133	33.568992840
7	29.723036329	41.950770884	32.854895866
1	29.331168871	42.502341088	32.092564026
1	29.845589149	40.938659365	32.673035929
7	31.733873203	41.721626382	33.967063399
1	32.459097086	42.097262704	34.575396700
1	31.166565595	38.621891947	34.599390205
26	32.958879497	37.292780708	33.560459846
6	36.243663036	41.314233541	33.335292138
8	35.323709762	41.548551782	34.012520851
8	37.233456033	41.128500624	32.752334108
6	34.428261834	37.863986585	36.077858273
8	34.362271299	37.090529348	35.049401226
6	35.755101046	37.965395281	36.810883583
6	35.893048426	36.755630726	37.754254856
6	36.629248303	37.023757017	39.071721496
8	36.128211345	36.484891655	40.093861278
8	37.668735600	37.732598197	39.047057725
1	36.419908249	35.931492238	37.241140359
1	34.895342218	36.383394140	38.024135972
1	35.731798874	38.892675554	37.399779639
1	36.594339676	38.024512604	36.103030975
8	31.559430812	37.840807430	35.043511768
8	33.452728550	38.472496753	36.559461672
8	35.709621981	38.917617583	29.136172415
6	35.170440366	38.476644990	28.128179155
7	33.832970900	38.777307706	27.815834157
6	33.079398716	39.658635809	28.724951309
6	33.171439573	38.274444024	26.712634856
7	31.908146496	38.567319532	26.501377910
6	33.918627540	37.459473388	25.812970206
6	35.212138015	37.181841587	26.083110058
7	35.828000207	37.640161949	27.229019626
1	32.635905979	40.479012488	28.148423957
1	33.745124386	40.069044347	29.484585859
1	31.417988464	38.211697996	25.673603381
1	35.794811909	36.580590587	25.389866880
1	33.449571902	37.038100763	24.931886948
1	32.268583794	39.090646542	29.202202332
1	31.294887019	39.096100031	27.150459813
8	33.386910241	38.826392468	33.251973175
1	31.815384592	40.763458129	33.606100246

1	34.274010191	39.790304888	31.985322473
8	34.835236896	40.389143273	31.452731829
1	32.224891518	38.174009510	35.751847632
1	35.202621259	39.819961521	30.753948843
1	35.055539174	34.740407391	29.462007712
1	28.931411856	37.848800796	30.697891271
1	32.541700808	32.120384959	34.781547620
1	28.851073817	44.687459002	34.557522850
1	36.715979089	37.253274827	27.477584207

**IM9**

**QM/MM (BS1) = -3580.809487 a.u.**

**QM/MM (BS2+ZPE) = -3582.964970 a.u.**

6	35.056123634	35.265828735	30.419145070
7	35.809354446	34.865776794	31.495686655
1	36.544826344	34.144713451	31.481522453
6	35.392960490	35.536502427	32.578478410
1	35.814377544	35.428049741	33.573172933
7	34.394999906	36.352794535	32.254469689
6	34.170604829	36.199682585	30.907055802
1	33.386707402	36.745921943	30.390758050
6	29.276528658	38.226136306	31.827512382
1	28.814154681	37.455004603	32.460267933
1	28.779640005	39.187022160	32.030585469
6	30.760666256	38.388088627	32.155888170
8	31.318948153	39.466595814	31.915791831
8	31.334662976	37.374985689	32.716262645
6	32.366377930	33.063706557	34.483507712
7	31.287828848	33.403788068	33.701131590
1	30.534350159	32.797603020	33.351496080
6	31.363059469	34.713206685	33.417047562
1	30.640293799	35.259084927	32.819845546
7	32.439474511	35.249212226	33.980498712
6	33.082970033	34.225838392	34.643415551
1	34.020536114	34.393334638	35.164217041
6	29.369034969	44.333961541	33.717888226
1	29.690952561	45.300972685	33.295641146
1	28.715049932	43.847340594	32.983277770
7	30.524305200	43.492940985	34.001594733
1	31.179859877	43.804688865	34.719017380
6	30.809996784	42.299420119	33.428590463
7	30.035128952	41.777925814	32.470574676
1	29.649280736	42.414291752	31.771702799
1	30.415210966	40.904842939	32.046572432
7	31.859624376	41.606919228	33.873192572
1	32.440299859	41.973604147	34.626319946
1	32.153437290	40.754874683	33.383736283
26	33.088860072	37.222360276	33.635875404
6	36.211455271	41.262510470	33.415914223
8	35.297106651	41.486594429	34.104341888
8	37.198610515	41.085556429	32.825466171
6	33.890773529	37.351819008	36.035948726

8	34.617537873	36.819824112	35.151987030
6	34.406666127	37.557504019	37.443194081
6	35.905756829	37.839478285	37.506313999
6	36.590630731	37.640363105	38.868563873
8	36.050068413	36.902557678	39.734083880
8	37.701662543	38.220038623	38.993478274
1	36.134877349	38.858956126	37.160368405
1	36.421965442	37.166512142	36.801478013
1	34.196333342	36.629574027	37.996827722
1	33.810373782	38.342121666	37.932254858
8	30.395125376	38.382750959	37.132872038
8	32.707989509	37.696113082	35.712108559
8	35.713226387	38.982051634	29.193396436
6	35.183726298	38.552501532	28.174775058
7	33.849372500	38.855566862	27.852916517
6	33.095662053	39.750647398	28.750120609
6	33.195597335	38.346771626	26.747984399
7	31.927122802	38.616136636	26.537754464
6	33.956245550	37.558473799	25.837449495
6	35.250854109	37.291968786	26.109812649
7	35.852976765	37.730501015	27.270703992
1	32.622711188	40.539351590	28.153309110
1	33.769333134	40.201718862	29.478218788
1	31.445267059	38.258880296	25.706195307
1	35.847026812	36.723154494	25.402488752
1	33.498462953	37.152847648	24.943134669
1	32.309944256	39.192386567	29.276472242
1	31.308125457	39.139497068	27.185163759
8	33.585642132	38.740668701	33.372848022
1	31.258714114	38.196778176	36.713534750
1	34.239794346	39.800932349	32.000554750
8	34.786220228	40.440513695	31.502602859
1	29.769682584	38.084649539	36.458189667
1	35.175668325	39.908546597	30.786428515
1	35.104611674	34.758426051	29.455683214
1	29.082846244	37.962271654	30.787834602
1	32.566963608	32.038476989	34.794533502
1	28.775037756	44.520515825	34.612556950
1	36.738036826	37.338553873	27.521739080

**Cartesian coordinates for direct hydrogen transfer from IM6**

**TS5**

**QM/MM (BS1) = -3580.768659 a.u.**

**QM/MM (BS2+ZPE) = -3582.923454 a.u.**

6	34.986517860	35.264723205	30.439962813
7	35.771527088	34.921154791	31.516033557
1	36.521556303	34.213705606	31.509512268
6	35.353642128	35.616567654	32.582122923
1	35.793225959	35.554467111	33.572821559
7	34.322314908	36.393413090	32.250423653

6	34.079069351	36.184054949	30.910820311
1	33.257638557	36.679095890	30.401358449
6	29.250841203	38.158504310	31.655163771
1	28.835058961	37.368766534	32.299748095
1	28.729630448	39.099861878	31.880073764
6	30.739650998	38.349422603	31.936184555
8	31.190666354	39.508952166	31.939532972
8	31.433681909	37.297828598	32.183241701
6	32.326418475	33.105603960	34.467852812
7	31.271554467	33.415491003	33.639365524
1	30.545867099	32.789033132	33.266837150
6	31.325886932	34.722844241	33.345010007
1	30.636029853	35.249573024	32.692868015
7	32.364069330	35.286733322	33.951027217
6	33.003212491	34.288484527	34.653155730
1	33.913096622	34.494392766	35.206788938
6	29.376579454	44.426978270	33.689963722
1	29.706920416	45.415265292	33.328824110
1	28.723704425	43.997308950	32.920312403
7	30.532309186	43.572992761	33.913695757
1	31.234952436	43.885305405	34.584804779
6	30.756959523	42.358353425	33.357599213
7	29.891806421	41.796982424	32.505296911
1	29.443715986	42.404036048	31.820208561
1	30.240199206	40.899739606	32.093899156
7	31.850123877	41.682043575	33.713230699
1	32.502171395	42.059894705	34.397605924
1	32.091900374	40.827807315	33.196232586
26	32.968821912	37.256054330	33.567423903
6	36.192155621	41.328927221	33.366318223
8	35.274480990	41.612000012	34.028347585
8	37.189002450	41.097471564	32.811551635
6	34.726850102	37.648332970	36.146821742
8	34.684493422	36.926803654	35.137030353
6	35.975757788	37.826615574	36.965767567
6	36.056419154	36.640083974	37.944548735
6	36.697470845	36.983301972	39.287642695
8	36.139809852	36.497201619	40.304639371
8	37.721937795	37.713296187	39.274651467
1	36.627187941	35.811046088	37.490879211
1	35.047302022	36.264448838	38.159478504
1	35.890235759	38.767457003	37.526114547
1	36.859116222	37.886398098	36.316224947
8	32.014831550	38.048534451	34.851704384
8	33.685006771	38.241934109	36.649514622
8	35.697708979	38.924215995	29.168957639
6	35.165306664	38.490983433	28.154055726
7	33.831801074	38.797055448	27.831278417
6	33.072012253	39.677675379	28.738114138
6	33.180196869	38.299617689	26.720436055
7	31.920650314	38.596331352	26.495838467
6	33.931894691	37.486613497	25.822642756



6	35.222546815	37.206740467	26.100639531
7	35.829323531	37.658066254	27.254102532
1	32.633646101	40.499666260	28.160059004
1	33.731586360	40.085476772	29.503520858
1	31.436421957	38.237563015	25.666476163
1	35.810179174	36.611095909	25.406913373
1	33.469501230	37.075022026	24.933479904
1	32.259271999	39.114555468	29.216308673
1	31.306579169	39.134870546	27.135788114
8	33.547319031	38.929233881	33.444303270
1	32.712473874	38.966321840	34.265278956
1	34.271306058	39.810872573	32.050149591
8	34.790384144	40.432095977	31.495371932
1	32.872616234	38.104600866	35.993565840
1	35.160419914	39.877138953	30.787606987
1	35.050723518	34.743839867	29.484648466
1	29.036876035	37.882897051	30.622532727
1	32.536508309	32.085419969	34.789029096
1	28.779608641	44.566130285	34.591257169
1	36.716366526	37.269315777	27.503101087

#### IM7

**QM/MM (BS1) = -3580.806871 a.u.**

**QM/MM (BS2+ZPE) = -3582.968370 a.u.**

6	35.015169416	35.276934208	30.486930898
7	35.768757041	34.908157457	31.575098978
1	36.501953689	34.184075221	31.578808764
6	35.348866552	35.615869225	32.635532576
1	35.763611883	35.532966449	33.635859090
7	34.351998444	36.423760136	32.287308424
6	34.128046426	36.223466764	30.945838907
1	33.335377425	36.744804961	30.417332839
6	29.279800074	38.213702598	31.679717759
1	28.843298869	37.445826764	32.335016129
1	28.784618055	39.174132402	31.885337353
6	30.772278453	38.374801859	31.956938739
8	31.286466634	39.497436698	31.818104738
8	31.404587596	37.333139607	32.368559119
6	32.333054442	33.124359081	34.472934988
7	31.291994489	33.426115517	33.624717480
1	30.574352302	32.796704260	33.242886159
6	31.342520729	34.734294086	33.332839507
1	30.648591378	35.252658953	32.679707324
7	32.363741669	35.307941957	33.956553309
6	32.996420220	34.313902043	34.669913774
1	33.888441196	34.531438343	35.247078107
6	29.302166645	44.272483363	33.709112636
1	29.575680357	45.201456024	33.179905494
1	28.598277627	43.715208062	33.076868921
7	30.479432250	43.457549849	33.979508854
1	31.147644455	43.785005541	34.679059930

6	30.774282098	42.274865956	33.392282093
7	30.003191252	41.754926982	32.435247036
1	29.597268756	42.391766279	31.748812506
1	30.384836186	40.879255986	32.003277806
7	31.830270549	41.580040739	33.836801492
1	32.437463066	41.980034021	34.551100474
1	32.178571987	40.782659886	33.290851769
26	32.964360096	37.294316909	33.645538355
6	36.203138340	41.349636843	33.313412892
8	35.293037204	41.570230216	34.009195322
8	37.187587875	41.191124983	32.713799558
6	34.359183407	37.757403751	36.216531822
8	34.314441624	37.042943614	35.146143500
6	35.697206843	37.906057213	36.915155373
6	35.914373343	36.680037211	37.823804537
6	36.636840520	36.977066994	39.140275832
8	36.116030077	36.481490447	40.174506341
8	37.682298302	37.676298977	39.103937050
1	36.487419608	35.903236178	37.287694267
1	34.941922950	36.246890255	38.091080366
1	35.644225574	38.816736359	37.528151509
1	36.511294985	38.021638970	36.185817697
8	31.487443089	37.924513730	35.127680813
8	33.358711967	38.266929278	36.759820360
8	35.728120965	38.918691003	29.155654594
6	35.191290035	38.485399470	28.142494225
7	33.860965651	38.803032208	27.819759403
6	33.115992116	39.704161912	28.718277733
6	33.200454774	38.298358798	26.717421264
7	31.941360380	38.601045951	26.497181122
6	33.942180479	37.471807441	25.824242676
6	35.232605580	37.186813249	26.098904719
7	35.846494814	37.643094486	27.246584738
1	32.683826509	40.523168302	28.131311820
1	33.785745513	40.112427753	29.474730192
1	31.450917360	38.240069760	25.672404091
1	35.813628155	36.582192470	25.407710197
1	33.472940496	37.054490647	24.941141210
1	32.299294643	39.158415139	29.209184566
1	31.336931311	39.153617052	27.134169313
8	33.387593213	38.852507344	33.453953315
1	31.356513086	38.835642693	34.822377645
1	34.228846098	39.697269156	32.030614600
8	34.807216532	40.300613967	31.523565940
1	32.154807701	38.044660339	35.906232205
1	35.173045300	39.752397884	30.807584630
1	35.080215857	34.762064356	29.528418865
1	29.058820751	37.933451407	30.649817413
1	32.539693538	32.104049093	34.795944485
1	28.780323755	44.529225194	34.630975398
1	36.733096708	37.253382911	27.495651917

## 2OG rearrangement reaction states coordinate for AlkBH2-dsDNA

### ES1

QM/MM (BS1) = -3275.477127 a.u.

QM/MM (BS2+ZPE) = -3277.299466 a.u.

6	40.282292761	37.751724933	43.589363266
7	39.163005387	36.975104270	43.775674071
1	39.034422972	36.278106088	44.520428839
6	38.288583132	37.250948135	42.797769544
1	37.317404389	36.772601631	42.700839951
7	38.779626021	38.173898505	41.975769360
6	40.028939760	38.494947045	42.459444409
1	40.669199452	39.209155104	41.951024720
6	41.400547203	39.782137053	37.309684846
1	41.255565919	38.871285437	36.712854810
1	41.336485989	40.665567937	36.656453231
6	40.358406632	39.891123473	38.410097035
8	40.106312067	41.007737343	38.911264455
8	39.780339824	38.808911892	38.744434771
6	38.782531252	34.187572378	39.668170403
7	39.930430542	34.700397421	39.102669099
1	40.781853960	34.193792693	38.879589937
6	39.780893195	36.031989019	38.976931727
1	40.534430554	36.699475294	38.569109734
7	38.591292727	36.408872739	39.431971381
6	37.960114495	35.267451468	39.871612205
1	36.968879627	35.300457449	40.317404650
6	38.994893188	44.666414464	34.930489515
1	39.292663714	45.703960115	35.161711995
1	39.910149120	44.074640574	34.784711565
7	38.193658745	44.065668876	35.988429154
1	37.184597960	44.183793637	35.954201292
6	38.662635124	43.196089911	36.916402194
7	39.963407624	43.000256170	37.096504289
1	40.687284053	43.718336753	36.930531761
1	40.213146286	42.304187678	37.829445444
7	37.774928313	42.475606170	37.614283991
1	36.772676060	42.591927881	37.462036500
1	38.069485928	41.851688789	38.370770508
26	38.224643878	38.465417155	39.969836429
6	35.913334785	40.253157098	39.832081770
8	35.246710180	41.281702713	39.783504357
8	37.137441473	40.107446920	39.495385406
6	35.254082741	38.916423606	40.298987917
8	36.002081530	37.975395969	40.545460052
6	33.757074341	38.822944079	40.383049575
6	33.211458010	37.414357027	40.166354010
6	31.688009331	37.253944649	40.322705916
8	31.062467699	38.169820787	40.936005044
8	31.189347866	36.216972997	39.839800767
1	33.689532205	36.715716548	40.875041787

1	33.470906170	37.050372288	39.159312089
1	33.325186726	39.549253263	39.677648042
1	33.458348069	39.200822250	41.379623275
8	39.281637951	41.845072898	43.986596878
6	40.467664377	41.739037891	43.765971257
7	41.021162078	42.184824478	42.537327240
6	40.081116520	42.800364872	41.587148542
6	42.343179516	42.049414471	42.200793867
7	42.800942644	42.428226195	41.026782792
6	43.227719783	41.484053669	43.163765992
6	42.720293915	41.042832595	44.333258465
7	41.385954510	41.180291349	44.662790563
1	39.177590432	43.075622065	42.138397160
1	39.838707461	42.092988561	40.780341804
1	43.811672782	42.355653769	40.846885441
1	43.385671206	40.519314717	45.010180229
1	44.279080261	41.339672467	42.924470405
1	40.534978406	43.706692287	41.162822981
1	42.235097195	42.694369759	40.225410070
1	41.199885566	37.603295827	44.158625565
1	42.402551833	39.743273037	37.736936101
1	38.685261182	33.143525251	39.965779958
1	38.424407458	44.649306005	34.001877292
1	41.028694678	40.793622772	45.512981908

**TS for 2OG rearrangement**

**QM/MM (BS1) = -3275.469836 a.u.**

**QM/MM (BS2+ZPE) = -3277.294776 a.u.**

6	40.326673354	37.695317544	43.660963213
7	39.208358777	36.919617205	43.852890917
1	39.073882688	36.233695347	44.606106673
6	38.339884739	37.169373250	42.864611922
1	37.365561873	36.697761839	42.773577841
7	38.840569423	38.070149172	42.024907749
6	40.083685909	38.409762669	42.511813578
1	40.724577725	39.114835255	41.993606999
6	41.351067934	39.821771746	37.416453728
1	41.182739583	38.900115416	36.841814761
1	41.283818443	40.689559044	36.743709712
6	40.322340948	39.960390616	38.529506907
8	39.998531129	41.101815877	38.931475021
8	39.821858595	38.884637812	38.974648089
6	38.729312494	34.257486927	39.702731043
7	39.869867698	34.794800832	39.146197728
1	40.727359138	34.302802952	38.914063322
6	39.701234795	36.126098071	39.038959186
1	40.450658165	36.809309355	38.649926413
7	38.506446442	36.483444752	39.495963061
6	37.891244690	35.325459878	39.916150143
1	36.897506354	35.333588300	40.358899905
6	38.965147633	44.706294008	34.910747457

1	39.251451516	45.748189755	35.136838638
1	39.886535427	44.122515166	34.771307024
7	38.165666486	44.102443033	35.966676534
1	37.154148683	44.191460516	35.918039854
6	38.644417271	43.228402823	36.884208240
7	39.948504570	43.045663123	37.063803125
1	40.667281333	43.770793549	36.910584673
1	40.190626344	42.361908019	37.809668508
7	37.771587458	42.491341853	37.579516310
1	36.765752897	42.553523757	37.419354588
1	38.106143227	41.837668566	38.290246468
26	38.177305962	38.561608731	40.111255678
6	35.854844321	40.130863548	39.565378003
8	35.302009404	41.225499348	39.503362192
8	36.954537495	39.765962004	39.013981337
6	35.224537453	39.000084269	40.415120219
8	36.003792106	38.215574658	40.949230898
6	33.729748458	38.889283544	40.533091677
6	33.218325265	37.481086659	40.204620733
6	31.695525220	37.286327529	40.350997166
8	31.052845251	38.187272433	40.967346815
8	31.218243532	36.246987423	39.853446248
1	33.712965851	36.744093286	40.861002308
1	33.480242740	37.200639868	39.171311945
1	33.259898922	39.642935580	39.887651170
1	33.449368327	39.147050592	41.568918936
8	39.328670886	41.841674845	43.959125769
6	40.519362740	41.733753828	43.763461115
7	41.100246559	42.196312297	42.553482873
6	40.181548917	42.836291002	41.598681044
6	42.425552717	42.046067568	42.235017882
7	42.913117394	42.435526280	41.077168938
6	43.283258660	41.448227607	43.202502650
6	42.751340379	41.001407965	44.357697373
7	41.414975167	41.157625783	44.671134059
1	39.286226114	43.144786341	42.146024234
1	39.918810646	42.136185215	40.791977994
1	43.925396995	42.342278232	40.914829730
1	43.398294496	40.455979344	45.034441990
1	44.335347985	41.288917548	42.978935814
1	40.663427653	43.724388043	41.168375437
1	42.378496340	42.745570367	40.268597627
1	41.246178145	37.556610445	44.229591922
1	42.363374179	39.772413072	37.817536141
1	38.651302195	33.205119054	39.975684484
1	38.397693665	44.677002454	33.980583322
1	41.044377518	40.772773188	45.516425937

**ES2**

**QM/MM (BS1) = -3275.479068 a.u.**

**QM/MM (BS2+ZPE) = -3277.302619 a.u.**

6	40.319343381	37.637908109	43.663323312
7	39.195953788	36.869798728	43.852338043
1	39.057527550	36.183861863	44.604791414
6	38.330866632	37.128818196	42.863153330
1	37.351834333	36.668045134	42.770634562
7	38.840497127	38.027801932	42.027683188
6	40.083353803	38.358035915	42.516239161
1	40.725501710	39.065315811	42.002703767
6	41.356727876	39.813460393	37.454826878
1	41.213009463	38.901491383	36.858006971
1	41.292671949	40.691985528	36.795954467
6	40.294832246	39.913982723	38.541785412
8	39.912133556	41.041365266	38.928859784
8	39.829170337	38.819647803	38.981023230
6	38.710393799	34.203224399	39.725214499
7	39.849147191	34.739284244	39.163621719
1	40.710443998	34.248555251	38.943927037
6	39.674291068	36.068372421	39.041194144
1	40.421135165	36.752725940	38.649164091
7	38.477438496	36.425154724	39.493391704
6	37.866688987	35.269055462	39.925483285
1	36.870316332	35.275554526	40.362721448
6	38.973776915	44.686320118	34.922736470
1	39.266055020	45.726817466	35.148837430
1	39.891339827	44.096575056	34.781111176
7	38.174028905	44.086367872	35.981381026
1	37.162484966	44.174589895	35.931247551
6	38.649637948	43.218871791	36.907538766
7	39.953940977	43.041440342	37.102732843
1	40.673410788	43.771470864	36.985558728
1	40.179867509	42.349162769	37.844619512
7	37.777454843	42.477221309	37.597689691
1	36.773020533	42.520771416	37.424352508
1	38.122357932	41.830601589	38.311832090
26	38.169527712	38.504501155	40.107002760
6	35.836865148	40.050765263	39.562928907
8	35.286531943	41.144734930	39.469453815
8	36.913578895	39.653467171	38.990893593
6	35.236654262	38.971074180	40.498513061
8	36.031263692	38.200081581	41.028832370
6	33.751715410	38.874253317	40.696378377
6	33.217920502	37.519407183	40.204155438
6	31.697223847	37.313483725	40.355533554
8	31.051112497	38.201673653	40.984879426
8	31.226373996	36.279755279	39.840234926
1	33.720311170	36.703575259	40.751306626
1	33.456153803	37.367091947	39.137810797
1	33.256515384	39.702939132	40.176627145
1	33.538500795	38.982738659	41.772152390
8	39.609560165	41.900749690	43.785672748
6	40.802739406	41.712762795	43.699825244
7	41.525610228	42.127610564	42.545090556

6	40.731044170	42.796112314	41.502112970
6	42.844868494	41.823873761	42.313363489
7	43.484515081	42.141601841	41.211922009
6	43.541766233	41.106362599	43.331287830
6	42.888301362	40.753987084	44.450687522
7	41.566805994	41.077574637	44.686763690
1	39.879705891	43.288799394	41.981405341
1	40.371423080	42.067625667	40.760457037
1	44.446108286	41.769953516	41.129430203
1	43.421546307	40.134478019	45.157532100
1	44.578968559	40.813645526	43.192844319
1	41.347946598	43.547350382	40.994344645
1	43.123357102	42.603565229	40.367845535
1	41.235687476	37.496418157	44.236351601
1	42.361715986	39.765213483	37.874038582
1	38.637879069	33.153074715	40.008047620
1	38.405136178	44.663881473	33.993106682
1	41.114086386	40.724686222	45.505596531

**Dioxygen Activation step reaction states cartesian coordinates for AlkBH2-dsDNA via ‘In-line’ Fe(III)-superoxo Complex**

**RC1**

**QM/MM (BS1) = -3419.786229 a.u.**

**QM/MM (BS2+ZPE) = -3421.791578 a.u.**

6	24.763326076	30.785773224	41.867313615
7	25.935481433	30.226951132	41.405918013
1	26.137727347	29.221911565	41.310700166
6	26.795100616	31.218067882	41.131308343
1	27.806566988	31.074998410	40.767272036
7	26.244946701	32.399107966	41.393799409
6	24.967788735	32.146680438	41.855162922
1	24.286630960	32.946873121	42.130072392
6	24.760952510	36.673214524	43.929300794
1	25.606130192	36.730086462	44.628103175
1	24.542277838	37.685845202	43.560509909
6	25.104440547	35.799184373	42.730590159
8	24.441684111	35.817233953	41.700004739
8	26.187657422	35.075084240	42.874987718
6	29.291152868	31.708420762	44.707088266
7	28.358287786	32.418506392	45.423075863
1	28.145636934	32.346693997	46.427104882
6	27.770435003	33.290559018	44.591581594
1	26.986504080	33.983932733	44.885135936
7	28.279504025	33.181029911	43.369481854
6	29.226513348	32.187307825	43.421994335
1	29.759782402	31.866918841	42.533342382
6	24.315341461	42.184938532	41.133067381
1	24.000384534	42.695840470	40.206135259

1	23.488129066	42.255472022	41.849684562
7	24.645254715	40.791041138	40.899989986
1	25.560083087	40.582167739	40.515543784
6	23.867963786	39.720770770	41.186855814
7	22.616602115	39.846908951	41.588123614
1	22.055723820	40.692515828	41.505811236
1	22.075030630	39.010286732	41.883248576
7	24.412223629	38.502343281	41.034391689
1	25.431784735	38.385245633	41.107700751
1	23.891820578	37.654739640	41.292383410
26	27.387107058	34.172622306	41.681483033
8	26.920203753	34.877353679	39.782708628
8	27.843479673	35.229795374	38.981560965
6	29.733449426	35.532693330	40.696963160
8	30.614459498	36.342005283	40.408407214
8	28.813113197	35.660652442	41.587082738
6	29.668253418	34.175637754	39.956092410
8	28.986123211	33.282813794	40.487717946
6	30.543227171	33.938822426	38.760538085
6	32.002366637	33.630007813	39.155933510
6	32.969821454	33.608486343	37.957814907
8	34.094504933	34.164197852	38.125373941
8	32.583439643	33.049529311	36.904259137
1	32.046790548	32.628020471	39.616494006
1	32.373626563	34.356364300	39.891532379
1	30.517407221	34.853211142	38.151872068
1	30.127859004	33.116162395	38.161753300
8	24.871652072	33.225768863	38.048252749
6	23.787473068	33.589007107	38.475718469
7	23.459416174	34.952622422	38.513181149
6	24.478171867	35.902677198	38.053991348
6	22.253465182	35.423826843	38.958292221
7	22.029487117	36.728842721	38.923177595
6	21.283484422	34.493608239	39.411814004
6	21.582872161	33.166559897	39.379171456
7	22.800873550	32.722704468	38.928452492
1	24.725752888	36.596053771	38.870052899
1	24.107103091	36.444624319	37.169878472
1	22.775217450	37.368156419	38.684703450
1	20.860225153	32.429764786	39.728343767
1	20.319822827	34.838354395	39.783008481
1	25.381660484	35.345661807	37.797197558
1	21.241541950	37.141146486	39.459448952
1	23.944326158	30.185820878	42.264004466
1	23.887798936	36.328254300	44.483081075
1	29.842684596	30.874625307	45.141444355
1	25.182478824	42.699468266	41.547071324
1	23.015268866	31.747654137	38.871146359

**TS1**

**QM/MM (BS1) = -3419.772852 a.u.**

**QM/MM (BS2+ZPE) = -3421.775893 a.u.**



6	24.787971565	30.781619553	41.862134128
7	25.955283579	30.220051762	41.388026461
1	26.157264105	29.214152498	41.296970678
6	26.814534073	31.207903297	41.105745737
1	27.824836748	31.069153060	40.735298263
7	26.267681394	32.390981073	41.376845412
6	24.994789539	32.141618360	41.852252892
1	24.321226378	32.943608839	42.138150785
6	24.834532940	36.644675677	43.893292277
1	25.674990757	36.667910808	44.599896694
1	24.650246973	37.669904637	43.539793551
6	25.172138684	35.780463903	42.681288916
8	24.488274152	35.803072339	41.663688818
8	26.263879509	35.069577807	42.800020664
6	29.321222333	31.717790025	44.699920116
7	28.370620230	32.417397988	45.405524043
1	28.139091583	32.334567492	46.404818773
6	27.798537231	33.297658296	44.575269250
1	27.005286607	33.986035599	44.855465661
7	28.336772312	33.203642993	43.363876279
6	29.285210842	32.211115981	43.419749771
1	29.837553117	31.917659647	42.532875383
6	24.290330179	42.191898207	41.137915613
1	23.978731739	42.702954517	40.209723928
1	23.463532199	42.270551208	41.854330050
7	24.609341836	40.794968850	40.908095172
1	25.526495895	40.577044383	40.533597899
6	23.823209826	39.730551558	41.194297676
7	22.574906054	39.862411633	41.596459278
1	22.015338309	40.710023440	41.517771499
1	22.031948638	39.023341069	41.881858290
7	24.358804757	38.508904090	41.040295730
1	25.378684105	38.393033317	41.103274025
1	23.839197012	37.663445129	41.302405270
26	27.495954082	34.099859053	41.659150838
8	27.036495592	34.818197843	39.673133784
8	28.173023799	34.922156069	38.967827206
6	29.701025291	35.708486827	40.567998045
8	30.648596172	36.406902914	40.252949883
8	28.835740636	35.798877260	41.483235296
6	29.318002258	34.260823432	39.605270204
8	28.949443533	33.374096330	40.495528147
6	30.397648922	33.939660198	38.572659089
6	31.790021640	33.586376297	39.107693743
6	32.843847359	33.545450840	37.983087936
8	33.965660783	34.094175372	38.203039058
8	32.514665391	32.990863272	36.906597788
1	31.761643753	32.582233595	39.563164809
1	32.125460912	34.300103656	39.872498063
1	30.476342056	34.814250409	37.910120130
1	30.036447174	33.112143971	37.938311741

8	24.845994786	33.248117701	38.084765916
6	23.750393068	33.598781222	38.496072235
7	23.407023863	34.957738386	38.526894063
6	24.424661686	35.916725314	38.083289892
6	22.188728722	35.416001237	38.952073023
7	21.949190846	36.717171219	38.902003631
6	21.226732311	34.475679127	39.401746481
6	21.543046085	33.151910297	39.377209108
7	22.770263403	32.721049636	38.938064754
1	24.646008591	36.617767215	38.899853119
1	24.069838138	36.445700084	37.184892140
1	22.690818012	37.361920801	38.664246754
1	20.828157044	32.406941895	39.724752945
1	20.255193738	34.809070028	39.761260878
1	25.339212303	35.365782592	37.857191197
1	21.158771421	37.129992229	39.434581241
1	23.965852163	30.185790551	42.258586913
1	23.946982644	36.315549103	44.433660196
1	29.863399165	30.880089697	45.138519889
1	25.160899325	42.702056868	41.550122877
1	22.995687175	31.748490412	38.880748365

**IM1**

**QM/MM (BS1) = -3419.850338 a.u.**

**QM/MM (BS2+ZPE) = -3421.846925 a.u.**

6	24.597938474	30.621611704	41.853563754
7	25.783604223	30.071150370	41.423292172
1	26.012618738	29.071203631	41.358047041
6	26.624350781	31.070636571	41.120387553
1	27.646293180	30.930654282	40.785696019
7	26.047432283	32.248279374	41.326847618
6	24.775443177	31.985289791	41.792225559
1	24.080806855	32.779576793	42.050515001
6	24.766397125	36.705348854	43.918862111
1	25.587561881	36.764425430	44.646952765
1	24.548149393	37.719703735	43.551974047
6	25.163759237	35.819028377	42.737545574
8	24.602647358	35.970781304	41.638944194
8	26.105490631	34.979364130	42.963143186
6	29.295675084	31.674657973	44.669859170
7	28.376467702	32.407953180	45.380488525
1	28.156100007	32.344809035	46.382978135
6	27.794964512	33.273547244	44.534243038
1	27.006567004	33.970148655	44.808786174
7	28.291037755	33.138758872	43.309489971
6	29.223854545	32.132270365	43.375907812
1	29.743193383	31.790242402	42.486502633
6	24.104877980	42.226288500	41.217362115
1	23.769573807	42.738708992	40.297948348
1	23.300124699	42.316725850	41.960871909
7	24.436791010	40.835891741	40.975273028

1	25.426954961	40.598542965	40.876579767
6	23.648421358	39.758176225	41.176348534
7	22.385794785	39.836396247	41.536724787
1	21.847449529	40.696874258	41.619599453
1	21.853066428	38.973509347	41.761308876
7	24.219851691	38.556860048	40.944501995
1	25.239487401	38.569970721	40.897304936
1	23.861450598	37.667603505	41.332168972
26	27.231848179	33.955424849	41.620323579
8	27.999873161	35.402078954	40.428073309
8	28.913965750	35.014117126	39.391636496
6	29.187786321	36.779198101	41.763783669
8	30.273753198	36.482855724	41.432100412
8	28.262690392	37.259678332	42.292457379
6	29.379125162	33.774663007	39.504446502
8	29.000350956	33.011788480	40.384082418
6	30.427465245	33.476315261	38.462345657
6	31.848064314	33.789494036	38.961005132
6	32.923382531	33.678331618	37.864313426
8	34.066774146	34.145584302	38.132411225
8	32.589081365	33.140979750	36.781927851
1	32.138627260	33.104311539	39.774374509
1	31.900961041	34.797194147	39.402323332
1	30.214943709	34.067417149	37.560961679
1	30.348742393	32.417898124	38.179197183
8	24.980292050	33.172601175	38.184364842
6	23.883728489	33.552614762	38.570953975
7	23.608277126	34.922642340	38.675135544
6	24.712530574	35.845949693	38.388491950
6	22.389574767	35.418769501	39.057788857
7	22.224214867	36.729928645	39.125856165
6	21.340575149	34.503201006	39.334604122
6	21.599938524	33.170020531	39.265690824
7	22.841560221	32.703974970	38.910293653
1	25.042263432	36.312026291	39.327456895
1	24.384553003	36.592596926	37.650464358
1	23.026031574	37.349895094	39.126335329
1	20.830258867	32.442047858	39.517436449
1	20.361188449	34.866694991	39.641896885
1	25.543435404	35.268366505	37.976676621
1	21.368007713	37.114787659	39.570582096
1	23.797191340	30.020831138	42.284764470
1	23.884822579	36.350430446	44.452647240
1	29.842881154	30.844957127	45.117329108
1	24.998923159	42.721745379	41.595876341
1	23.029440730	31.723783148	38.847864449

**TS2**

**QM/MM (BS1) = -3419.840647 a.u.**

**QM/MM (BS2+ZPE) = -3421.852688 a.u.**

6	24.564900806	30.637996376	41.854176313
---	--------------	--------------	--------------

7	25.744958292	30.089242511	41.403834473
1	25.973763988	29.089053102	41.337804328
6	26.578543838	31.087324964	41.084767865
1	27.595065885	30.955236502	40.732448077
7	26.002435240	32.265371720	41.303335135
6	24.737996944	32.001382817	41.791220673
1	24.047837451	32.794688285	42.061863239
6	24.788451603	36.669273010	43.946032992
1	25.611561979	36.689143288	44.674023874
1	24.606179505	37.695569728	43.593707722
6	25.148220285	35.794516601	42.744446744
8	24.600858019	36.004832151	41.651834851
8	26.043714595	34.895119943	42.949000787
6	29.268519634	31.718721102	44.680193541
7	28.331087498	32.421148743	45.399598692
1	28.113063640	32.342610796	46.401665046
6	27.729992013	33.283952208	44.566715174
1	26.925296941	33.957484057	44.849654708
7	28.233640434	33.178073821	43.341467591
6	29.191214839	32.191777981	43.393501108
1	29.717708466	31.877857930	42.497807542
6	24.018882168	42.276393341	41.178252472
1	23.667484038	42.823661858	40.286096180
1	23.226039915	42.335439510	41.936534555
7	24.342778756	40.895401009	40.870293120
1	25.330283030	40.690335723	40.696320051
6	23.627029924	39.795023254	41.189355267
7	22.403022637	39.839411912	41.671304092
1	21.812050027	40.669966288	41.684387528
1	21.909620982	38.961313696	41.922924947
7	24.231589710	38.609920963	40.961438662
1	25.244353815	38.653555024	40.850356219
1	23.910238200	37.710598246	41.359224413
26	27.219691818	33.941937999	41.602756662
8	27.775100288	35.303642016	40.549031734
8	29.058262019	34.880728835	39.452812265
6	28.979571547	36.934036470	41.918758036
8	30.065717370	36.571186737	41.693879957
8	27.987165113	37.424903641	42.284121673
6	29.418917195	33.660471441	39.643555924
8	28.889409682	32.910191809	40.490379199
6	30.563535697	33.189358817	38.761528059
6	31.861441841	33.976965199	38.976524806
6	32.934647878	33.749157447	37.893917273
8	34.095770873	34.185289868	38.144332880
8	32.582821860	33.191541736	36.826690076
1	32.315803518	33.768924604	39.959391455
1	31.629300254	35.054990131	38.987523898
1	30.254933401	33.303001525	37.711021863
1	30.713477954	32.115485778	38.945222664
8	24.992534397	33.139608651	38.165870754
6	23.906312134	33.531265862	38.568400112

7	23.651360144	34.903828956	38.694271996
6	24.766680367	35.817056732	38.415863241
6	22.438556953	35.411045477	39.080941537
7	22.285531905	36.723179540	39.155465495
6	21.379463538	34.506117503	39.356714063
6	21.621908550	33.170626355	39.276413971
7	22.855987070	32.693026843	38.910115723
1	25.062983076	36.313035120	39.350131580
1	24.467570753	36.538761031	37.641031927
1	23.091600467	37.337106229	39.148670970
1	20.844632358	32.449672228	39.525557817
1	20.405846241	34.880340170	39.669535887
1	25.613728674	35.225476832	38.060708486
1	21.433198196	37.111460468	39.605034900
1	23.771439585	30.032241993	42.291838549
1	23.895929898	36.335329495	44.475139839
1	29.828959521	30.889430549	45.111762348
1	24.921516249	42.753105603	41.560436267
1	23.032429946	31.711303698	38.838981590

## IM2

**QM/MM (BS1) = -3419.849387 a.u.**

**QM/MM (BS2+ZPE) = -3421.854806 a.u.**

6	24.599400903	30.651292426	41.839371569
7	25.774969596	30.107069217	41.368999047
1	26.007463493	29.107207342	41.302185656
6	26.599368662	31.107425619	41.035350807
1	27.611183513	30.989497532	40.665013142
7	26.019918452	32.282253675	41.267781743
6	24.764568987	32.014518976	41.777143817
1	24.075170027	32.805526603	42.055589303
6	24.780396112	36.619820814	43.933332489
1	25.616883454	36.617751419	44.645839037
1	24.618524750	37.650443773	43.584628495
6	25.084008648	35.740379551	42.720474808
8	24.498338436	35.943130777	41.653102559
8	25.984817416	34.827252706	42.896657002
6	29.246436644	31.759082392	44.633640914
7	28.289175125	32.439612553	45.348375382
1	28.065967119	32.347903357	46.348364101
6	27.682672803	33.299763294	44.520024479
1	26.863100808	33.954403436	44.802115567
7	28.203709465	33.215732704	43.298894916
6	29.180012601	32.245972622	43.351003524
1	29.724608721	31.959667007	42.456863707
6	24.009092050	42.264730957	41.177959800
1	23.660491182	42.806288435	40.281205185
1	23.216391517	42.332981868	41.935598584
7	24.326358471	40.879625553	40.881679782
1	25.312180421	40.665886178	40.705447512
6	23.600117022	39.788421832	41.204891598

7	22.374102640	39.846179528	41.680431923
1	21.786903042	40.679337012	41.680469717
1	21.875729905	38.971643331	41.933174444
7	24.192113691	38.594421377	40.992578267
1	25.205857123	38.615766477	40.885462187
1	23.832471799	37.704453143	41.370488072
26	27.202810762	33.976116812	41.542940011
8	27.481617406	35.430095916	40.562338283
8	29.038125570	34.868939639	39.218112387
6	28.893662415	36.936694199	41.907481893
8	29.944012265	36.521446457	41.622465307
8	27.940443672	37.459915325	42.331509205
6	29.382413602	33.723915983	39.581033352
8	28.807947713	33.053772546	40.507484002
6	30.585680982	33.107398278	38.867793661
6	31.849156319	33.970335275	38.984470249
6	32.974581149	33.590733928	38.004881239
8	34.160997208	33.732416295	38.411060931
8	32.633934397	33.216937519	36.851893471
1	32.255784557	33.971948461	40.007844374
1	31.572294508	35.014542542	38.758839987
1	30.331873063	33.020295290	37.799650056
1	30.753697362	32.090237890	39.254051105
8	24.986484155	33.184917072	38.201778499
6	23.890245328	33.567851389	38.583372373
7	23.617945358	34.938193187	38.694024749
6	24.723593385	35.863248169	38.416751703
6	22.394621525	35.433761675	39.060095858
7	22.223520174	36.745385865	39.111921563
6	21.344965256	34.519392380	39.339709555
6	21.603211776	33.186080934	39.271400673
7	22.845088151	32.719927235	38.918374010
1	24.957361371	36.427123978	39.328552716
1	24.450161372	36.525701534	37.581320450
1	23.023364256	37.366462115	39.088945988
1	20.832544558	32.457812329	39.519065257
1	20.364131775	34.884903472	39.639778922
1	25.607470746	35.276588232	38.155785683
1	21.373664851	37.129885462	39.569636837
1	23.804215718	30.046835453	42.275696695
1	23.887677649	36.303850862	44.473039868
1	29.811157618	30.937340918	45.073979982
1	24.912967512	42.742180273	41.556270023
1	23.030836821	31.739836221	38.848434579

### IM3

QM/MM (BS1) = -3419.876731 a.u.

QM/MM (BS2+ZPE) = -3421.892680 a.u.

6	24.623812045	30.602038782	41.857291781
7	25.806238410	30.051937531	41.420096090
1	26.025383361	29.051496631	41.329635382

6	26.668420144	31.048154460	41.169227417
1	27.689827708	30.909484366	40.831164289
7	26.101392661	32.218710034	41.422140153
6	24.819545566	31.964449320	41.852142405
1	24.134639961	32.758184358	42.133759879
6	25.032758154	36.780239701	44.100208815
1	25.777987779	36.676958447	44.904288745
1	24.891586761	37.851425816	43.904214003
6	25.585883055	36.161595021	42.814203895
8	25.538009040	36.822558503	41.771732482
8	26.167607854	35.013325223	42.921934127
6	29.197852601	31.747192314	44.617764898
7	28.233390630	32.406951743	45.340977950
1	28.036925417	32.322593910	46.346825370
6	27.591719384	33.243980852	44.514299998
1	26.770685441	33.890737206	44.808026493
7	28.095000535	33.162983236	43.287666939
6	29.099348722	32.223886382	43.332424444
1	29.657666703	31.961497675	42.438909384
6	24.352215886	42.151597216	41.107164673
1	24.409865985	42.423509051	40.036581302
1	23.410447862	42.561984428	41.501111682
7	24.407234096	40.720194936	41.326972827
1	25.322019996	40.281527999	41.491587973
6	23.353111703	39.894118568	41.202391807
7	22.149446916	40.351543161	40.858775868
1	21.865674669	41.309923900	41.024942261
1	21.365092550	39.675688588	40.878144819
7	23.490317601	38.572950391	41.357406260
1	24.393359280	38.122193289	41.573745450
1	22.643804350	38.092823433	41.719354598
26	27.171634713	33.994148733	41.558242483
8	26.506168128	34.673643743	40.263684867
8	29.354987742	35.440406130	39.569728343
6	29.641592971	36.531278417	41.994913188
8	30.787215751	36.304736123	41.991197755
8	28.517638767	36.792879074	42.103090829
6	29.505964853	34.234996312	39.768997058
8	28.875096019	33.567609094	40.697598527
6	30.543463369	33.453984171	38.959315454
6	31.921575448	34.120998753	39.053890837
6	32.990470786	33.654107614	38.049921573
8	34.191768585	33.784868333	38.420827066
8	32.614265630	33.241176382	36.921880829
1	32.344837182	34.039499906	40.067732866
1	31.777896141	35.201148046	38.877999643
1	30.224761466	33.460667061	37.903458503
1	30.572793754	32.403248270	39.285080709
8	24.829274378	33.299620241	38.176328005
6	23.731894826	33.637156220	38.582963880
7	23.404395752	34.996614181	38.719371138
6	24.463258493	35.973627569	38.426996331

6	22.157093300	35.436791130	39.077197962
7	21.946002812	36.744599746	39.139730023
6	21.148490634	34.477161723	39.345724179
6	21.470879649	33.154984669	39.288785813
7	22.728503666	32.742798932	38.937839779
1	24.680723392	36.564824053	39.328435111
1	24.151413605	36.612381704	37.586340580
1	22.732504564	37.384082241	39.144434541
1	20.736533004	32.394479771	39.547594499
1	20.148909927	34.790993947	39.641268767
1	25.371056317	35.423553920	38.170652950
1	21.101528122	37.137176170	39.590218340
1	23.815072117	30.006177024	42.280323482
1	24.098740095	36.395645456	44.509799896
1	29.782771719	30.940212630	45.059036630
1	25.171998003	42.642639132	41.631476074
1	22.962992038	31.772429153	38.879786405

**Substrate hydroxylation step reaction states cartesian coordinates for AlkBH2-dsDNA**

**Snapshot 1**

**RC2**

**QM/MM (BS1) = -3309.777979 a.u.**

**QM/MM (BS2+ZPE) = -3311.663829 a.u.**

6	24.526979716	36.782905040	44.666764018
7	25.711314055	36.185705437	45.033308847
1	25.888946115	35.670164403	45.907803361
6	26.621915804	36.448315960	44.077811118
1	27.649418977	36.095040176	44.113177785
7	26.089352609	37.187368679	43.112339235
6	24.777153409	37.410224036	43.465585829
1	24.126735503	38.040545060	42.862806232
6	25.126171798	41.663270377	40.230351723
1	25.728389165	42.539451050	40.521688214
1	25.086340198	41.683323014	39.131028523
6	25.908338392	40.417255677	40.637403885
8	25.503237809	39.618236105	41.540792625
8	27.014103356	40.204566561	40.080211516
6	28.855036481	39.935627750	45.058633519
7	27.844882146	40.830825578	44.805324529
1	27.551675441	41.629162109	45.382825388
6	27.272108439	40.497737530	43.640311092
1	26.415329789	41.015156646	43.223026578
7	27.865310785	39.434805930	43.113279191
6	28.862568531	39.067435139	43.991108379
1	29.494880002	38.207173091	43.789164011
6	24.424833235	43.058298664	34.911541255
1	23.489165386	43.231533330	34.353179520
1	24.436385915	43.765564066	35.758545804
7	24.542434903	41.690551163	35.385608344
1	25.275806354	41.084205244	35.002789769



6	23.765899533	41.183423560	36.356058759
7	22.716251144	41.869790963	36.808736129
1	22.349185858	42.717846158	36.362323239
1	22.219017457	41.499769699	37.627534478
7	24.052968068	39.985013709	36.885472238
1	24.988427108	39.586455186	36.791415724
1	23.321594028	39.473471324	37.399209699
26	27.092567525	38.257238191	41.512603829
8	26.463283795	37.363101363	40.329923889
8	29.538342314	38.359424244	39.558478855
6	29.711168105	37.576131709	40.488837013
8	28.874811406	37.431122145	41.478940425
6	31.014801508	36.771658209	40.566734401
6	30.989247830	35.369723020	41.176512606
6	32.365986021	34.665110225	41.207090658
8	32.361168317	33.407287687	41.192437713
8	33.404630561	35.378815624	41.267620222
1	30.287853671	34.710613833	40.643342021
1	30.617075391	35.416441455	42.216251796
1	31.723699760	37.393192657	41.141702278
1	31.413770959	36.739019567	39.542573697
8	23.451389915	33.311773734	42.187055389
6	22.608664800	34.162492271	42.365850633
7	22.441531119	35.233260342	41.452873276
6	23.366750686	35.270305628	40.307788510
6	21.488273446	36.200182123	41.602191961
7	21.405773331	37.194171644	40.726002709
6	20.579644120	36.110094507	42.697988591
6	20.727478209	35.101960962	43.598765159
7	21.742735099	34.187784203	43.465454217
1	23.896998503	34.313506917	40.278025428
1	24.097885733	36.086449232	40.428454105
1	20.736098882	37.953170647	40.888844048
1	20.046421364	34.999985003	44.449793800
1	19.771483594	36.832597234	42.800226397
1	22.800907904	35.392571878	39.373729043
1	21.999731665	37.286353363	39.906646972
8	27.112043037	39.689189551	37.270211256
1	28.036895672	39.376753783	37.195006967
1	27.053739187	39.939291821	38.216799312
1	23.667809963	36.855312866	45.333586154
1	24.121789146	41.803954440	40.629714712
1	29.396231933	39.959311554	46.004473826
1	25.265334090	43.308305688	34.264144840
1	21.887207241	33.495073176	44.172031694

**TS7**

**QM/MM (BS1) = -3309.739955 a.u.**

**QM/MM (BS2+ZPE) = -3311.629373 a.u.**

6	24.375061929	36.710689454	44.851814148
7	25.567182460	36.131664550	45.220133245

1	25.770178885	35.645108035	46.104034170
6	26.462038863	36.361045355	44.243758982
1	27.489875661	36.009090779	44.278165531
7	25.910805908	37.059051679	43.261143189
6	24.604742429	37.292998078	43.626257266
1	23.947541301	37.909231165	43.016937626
6	25.004673850	41.450203661	40.253148388
1	25.694561621	42.248741909	40.573578103
1	24.974925151	41.493266132	39.155169055
6	25.613602397	40.112452185	40.662620906
8	25.212595931	39.456240852	41.662995834
8	26.607027259	39.666364522	40.013368423
6	28.766898814	39.806310901	44.959635176
7	27.752192343	40.695875431	44.709819128
1	27.468767157	41.501304519	45.282314736
6	27.154939594	40.333236750	43.563255275
1	26.283830084	40.839138619	43.161995661
7	27.731129173	39.259068478	43.042181439
6	28.747115941	38.914953414	43.907153223
1	29.377864852	38.048754679	43.719254585
6	24.417850979	43.091246415	34.894524422
1	23.480415377	43.265744555	34.339522424
1	24.430858494	43.793177598	35.745712039
7	24.540036360	41.720787890	35.357960399
1	25.267311673	41.113144509	34.965565822
6	23.763134381	41.205047108	36.322809532
7	22.716665723	41.888306875	36.786625775
1	22.350709291	42.742684097	36.351683400
1	22.221261587	41.511598610	37.603320476
7	24.047734240	39.998763898	36.834436400
1	24.978191222	39.594300752	36.721954982
1	23.313638573	39.481346058	37.338004196
26	26.733713986	37.924275034	41.450277778
8	25.696499187	36.884526170	40.508925264
8	29.394156399	38.331334631	39.561424430
6	29.484870376	37.442333686	40.407515154
8	28.530210071	37.119794422	41.232606654
6	30.823673290	36.693497586	40.542852315
6	30.855259023	35.294570606	41.159709101
6	32.252726982	34.626223402	41.179722341
8	32.278001419	33.368240571	41.154404041
8	33.276935381	35.360146410	41.244087440
1	30.167653842	34.610579658	40.640796652
1	30.492771089	35.333053662	42.203551632
1	31.485555985	37.359425539	41.125740160
1	31.259543752	36.676659505	39.532316030
8	23.672748822	33.354607203	42.218060725
6	22.840395381	34.218417401	42.359382711
7	22.745050542	35.297885018	41.424088018
6	23.715756163	35.307113366	40.361721398
6	21.765913465	36.260797964	41.510986627
7	21.716323799	37.244768213	40.625411078

6	20.800956672	36.171013958	42.555317150
6	20.897555481	35.172352601	43.474268257
7	21.916429075	34.255510958	43.407596295
1	24.240318960	34.347990890	40.328881388
1	24.694872856	36.165523099	40.531343884
1	21.002121874	37.972570994	40.735132625
1	20.170957245	35.082417483	44.288612643
1	19.993232939	36.900538296	42.614032604
1	23.271211523	35.582115696	39.395898723
1	22.377557728	37.369627362	39.864899322
8	27.048507169	39.637045753	37.239292302
1	27.995705652	39.397655126	37.183968525
1	26.889187785	39.693083597	38.207439775
1	23.529220283	36.822653104	45.530108603
1	24.021304260	41.682056254	40.662166666
1	29.335049539	39.870787487	45.887597913
1	25.255587862	43.346065528	34.245423924
1	22.014304175	33.567170375	44.126331433

**IM10**

**QM/MM (BS1) = -3309.767645 a.u.**

**QM/MM (BS2+ZPE) = -3311.653160 a.u.**

6	24.548571841	36.763564511	44.680134977
7	25.744888113	36.194936887	45.056242225
1	25.934376384	35.702075580	45.941019298
6	26.645473383	36.445378270	44.088321589
1	27.679623086	36.112236939	44.128350366
7	26.096321968	37.146544782	43.102986783
6	24.782452188	37.359211604	43.460809851
1	24.120426155	37.968140346	42.849141272
6	25.069308168	41.583851381	40.228555536
1	25.705020333	42.434394237	40.526718573
1	25.045166842	41.596783351	39.129124575
6	25.765021122	40.305053341	40.675626088
8	25.379086920	39.608440050	41.650132218
8	26.826129172	39.948614115	40.067637683
6	28.874690341	39.933009053	45.055919707
7	27.872517602	40.836049118	44.800154780
1	27.573625248	41.628399654	45.382176076
6	27.313249821	40.514120429	43.622903399
1	26.460984483	41.041388312	43.207196273
7	27.903496067	39.453804822	43.090090385
6	28.887119741	39.075711747	43.977690058
1	29.516447118	38.212004733	43.778138439
6	24.411537079	42.999332920	34.906026958
1	23.486199866	43.213400627	34.344850419
1	24.436519754	43.686456385	35.769065737
7	24.484164249	41.618966943	35.352439361
1	25.209175657	41.001849971	34.970912338
6	23.707489674	41.129179907	36.331468935
7	22.679776681	41.839982843	36.795186530

1	22.328082582	42.696278623	36.352098450
1	22.181416757	41.482352428	37.618712104
7	23.972364805	39.922795006	36.854867357
1	24.897289165	39.506213071	36.747317013
1	23.249617170	39.433661076	37.400213098
26	27.038423533	38.187985785	41.400858962
8	26.200480752	37.074713839	40.188185255
8	29.523501723	38.360119080	39.617579492
6	29.699708328	37.516773230	40.500756884
8	28.844830044	37.290339105	41.452721772
6	31.013751043	36.730999975	40.539572347
6	31.005812189	35.329441228	41.147683865
6	32.385176068	34.635611324	41.180030190
8	32.387731433	33.377499220	41.154069331
8	33.419048556	35.354831729	41.253512811
1	30.308736825	34.663914359	40.616531584
1	30.632704810	35.376404534	42.186926899
1	31.727901734	37.357160317	41.103043933
1	31.396418475	36.707348954	39.508689853
8	23.414892221	33.305354845	42.135888600
6	22.587978706	34.162607442	42.340318895
7	22.458983914	35.270303654	41.425729689
6	23.372518268	35.292024480	40.383305681
6	21.488836469	36.244157123	41.578876147
7	21.384652502	37.223448661	40.687476880
6	20.608545035	36.157763127	42.691364218
6	20.740828817	35.142379864	43.588421146
7	21.732123942	34.201311667	43.436182741
1	23.967341341	34.392876498	40.246975482
1	26.223383035	36.133522068	40.415079949
1	20.718722887	37.982978000	40.863184767
1	20.063659054	35.048044156	44.443060030
1	19.806702695	36.886141679	42.801854369
1	23.583157013	36.227026211	39.870658474
1	21.877152248	37.261508952	39.797333002
8	27.065763327	39.652539163	37.243142924
1	28.010883541	39.403080029	37.185704967
1	26.938033237	39.788575949	38.205888407
1	23.688750973	36.838227278	45.345868305
1	24.069525251	41.763880794	40.623638874
1	29.410947431	39.952274735	46.004668616
1	25.266241883	43.237947900	34.273089433
1	21.876499667	33.508524941	44.142705707

**TS8**

**QM/MM (BS1) = -3309.753653 a.u.**

**QM/MM (BS2+ZPE) = -3311.643711 a.u.**

6	24.353001672	36.700556752	44.869996779
7	25.551282515	36.130900788	45.234322106
1	25.765771723	35.656392931	46.122035706
6	26.434192371	36.348846285	44.245674328

1	27.465310317	36.006243636	44.276500797
7	25.870398066	37.029227149	43.256850059
6	24.567707430	37.266060898	43.634710222
1	23.901058674	37.870943874	43.024142808
6	24.976190869	41.424645940	40.233062772
1	25.674707404	42.216751578	40.550745882
1	24.932662463	41.479453600	39.135928609
6	25.587292736	40.080255348	40.615442738
8	25.183067645	39.402139210	41.607186907
8	26.576893509	39.653815459	39.957421339
6	28.761138027	39.812602972	44.953538917
7	27.744044151	40.697328208	44.696892349
1	27.449730973	41.497221054	45.271604781
6	27.165427634	40.337610575	43.538047514
1	26.297148264	40.841860437	43.126922312
7	27.754178594	39.271194860	43.016902075
6	28.758824871	38.927955240	43.894786372
1	29.397224040	38.065862334	43.712899351
6	24.421679486	43.062384823	34.895618872
1	23.489572985	43.263649743	34.340742865
1	24.444939441	43.750036725	35.758121600
7	24.517649299	41.682841262	35.337447383
1	25.240812328	41.072055610	34.942539516
6	23.742639987	41.171362949	36.306139951
7	22.707671763	41.864639116	36.780541481
1	22.345531604	42.721873318	36.347933370
1	22.213728490	41.491202510	37.599805569
7	24.018228169	39.959488511	36.808578852
1	24.946462437	39.550873503	36.695096770
1	23.287467154	39.451153284	37.325965297
26	26.671858050	37.884039693	41.463025933
8	25.503003060	36.739572171	40.353628251
8	29.331248797	38.251929622	39.564106432
6	29.418610902	37.355040782	40.402708060
8	28.445111897	36.999484630	41.194756637
6	30.772674775	36.639021169	40.557770768
6	30.828102594	35.235691414	41.161164968
6	32.236061015	34.590577118	41.175245401
8	32.278033757	33.333127665	41.134935424
8	33.249652669	35.337408219	41.248327742
1	30.154622175	34.543859303	40.633685341
1	30.463099094	35.257221403	42.204573463
1	31.407766951	37.315794367	41.158213895
1	31.230360823	36.642881232	39.556547236
8	23.699415815	33.401134372	42.213997004
6	22.860028576	34.255853833	42.372468000
7	22.764955412	35.353555734	41.434319575
6	23.707167653	35.366961588	40.414702556
6	21.759755376	36.303900081	41.527382522
7	21.695060013	37.292125904	40.643994174
6	20.799066615	36.185493354	42.567046522
6	20.902097748	35.183123882	43.482086369

7	21.935265118	34.277484440	43.411117001
1	24.329388968	34.476528986	40.384510713
1	26.050273583	36.020414246	40.000891001
1	20.971571915	38.008243626	40.762317170
1	20.174529959	35.077713383	44.292723271
1	19.980896690	36.902863257	42.629422132
1	23.437631269	35.869977647	39.492205733
1	22.361684829	37.445914152	39.894268161
8	27.024291865	39.588546568	37.205807543
1	27.977042687	39.370775028	37.161936971
1	26.858288041	39.672779129	38.171830978
1	23.512112983	36.815359724	45.553951314
1	23.999275241	41.659747199	40.655473214
1	29.326859542	39.878067929	45.882915499
1	25.267483481	43.309876953	34.254190333
1	22.033734294	33.584139920	44.124944491

**PD**

**QM/MM (BS1) = -3309.851902 a.u.**

**QM/MM (BS2+ZPE) = -3311.714112 a.u.**

6	24.435134797	36.690708076	44.876468447
7	25.612850134	36.107028290	45.279963459
1	25.785563306	35.609704971	46.164062910
6	26.539700239	36.343346694	44.338826288
1	27.566387325	35.993595823	44.413903866
7	26.027347937	37.049391088	43.337303411
6	24.708741591	37.277847744	43.661427476
1	24.050233232	37.857707912	43.020016104
6	24.795746703	41.269155958	40.113610501
1	25.594276849	41.948404948	40.439169161
1	24.647579232	41.370024470	39.029898719
6	25.144585388	39.810908605	40.416853894
8	26.050992894	39.617676659	41.297809419
8	24.555253741	38.901245850	39.795527365
6	29.004003433	39.916463395	45.317919602
7	28.092889827	40.859459624	44.912219736
1	27.792037797	41.708196006	45.409733252
6	27.597146166	40.470841658	43.723510196
1	26.840135796	41.017228661	43.166033786
7	28.137041762	39.321155474	43.342194210
6	29.020622980	38.958624428	44.330892688
1	29.596681798	38.037148631	44.275680573
6	24.484649303	42.864162931	34.943529940
1	23.576546123	43.171626396	34.398950034
1	24.569559090	43.520334740	35.828091728
7	24.438909027	41.466138924	35.340462535
1	25.226624965	40.846107434	35.117851112
6	23.610916281	41.030063733	36.308545257
7	22.611899756	41.797203604	36.743074387
1	22.319051966	42.674240217	36.298580151
1	22.068612895	41.457746384	37.545326327

7	23.801756647	39.817253530	36.838451564
1	24.697189604	39.350647612	36.716056274
1	23.141004524	39.427828543	37.521911049
26	27.166719498	38.071258529	41.889620240
8	24.506035229	36.288675048	40.532608935
8	29.165699331	38.170198704	39.458182340
6	29.479530936	37.335633233	40.324198747
8	28.721090654	37.031320812	41.323780814
6	30.844393718	36.641429815	40.276792789
6	30.933031547	35.278612086	40.967913839
6	32.332627121	34.630091635	41.017400289
8	32.366264379	33.371892561	41.002419752
8	33.348053877	35.373564148	41.106367838
1	30.244760127	34.554626128	40.508068616
1	30.587730549	35.385846389	42.011736405
1	31.564084481	37.330421234	40.754894511
1	31.152328129	36.582405676	39.222722187
8	23.493505274	33.467766873	42.083359853
6	22.642406263	34.304406571	42.279003169
7	22.445587438	35.382507821	41.375416242
6	23.431037620	35.474555055	40.243169682
6	21.465436521	36.320991956	41.538648616
7	21.313113988	37.318309594	40.677100095
6	20.581166817	36.204670256	42.653656814
6	20.760829674	35.195387819	43.546091861
7	21.787734094	34.298024185	43.392586103
1	23.778177271	34.445760213	40.096614508
1	24.379765642	37.227224468	40.255020225
1	20.606493330	38.028239996	40.883564124
1	20.093236141	35.081390011	44.406419167
1	19.758961143	36.907772868	42.773732387
1	22.860499851	35.785221269	39.352487688
1	21.823679141	37.466770245	39.804213804
8	26.662025672	38.557812080	37.840678645
1	27.482330366	38.509846586	38.367889979
1	25.949800805	38.382537780	38.479739666
1	23.576602237	36.797254803	45.539519698
1	23.876236927	41.570003437	40.615666162
1	29.483068343	39.950949284	46.296374945
1	25.353767789	43.057002651	34.314631519
1	21.943990785	33.598142854	44.089524023

## Snapshot 2

### RC2

QM/MM (BS1) = -3461.229779 a.u.

QM/MM (BS2+ZPE) = -3463.249318 a.u.

6	23.741634603	37.364676179	43.845800212
7	24.922306855	36.902004778	44.375894064
1	25.042991384	36.504612831	45.318949730
6	25.893464347	37.100639952	43.468525626
1	26.931665706	36.821629549	43.629020725
7	25.402713579	37.677782388	42.377508001

6	24.054697340	37.853046491	42.597069245
1	23.421450384	38.362634810	41.875400200
6	24.366742305	41.597055147	38.852054998
1	24.851759220	42.569579969	39.027759901
1	24.499936938	41.376119037	37.783605719
6	25.163661847	40.549334545	39.617859834
8	24.625623668	39.698575520	40.390132041
8	26.419238049	40.505224859	39.467629853
6	27.791454702	40.845904325	44.250957068
7	26.796081610	41.671052516	43.779885809
1	26.417333741	42.526537152	44.206567510
6	26.339624803	41.157718156	42.628077788
1	25.551471839	41.622341760	42.046537699
7	26.991690588	40.045798527	42.320991918
6	27.908944920	39.835326542	43.327907387
1	28.575987607	38.978418975	43.304550763
6	25.120607388	42.422664140	33.295314691
1	24.252132270	42.398281060	32.614386367
1	24.993895525	43.311159493	33.939302559
7	25.237956872	41.216491460	34.084267507
1	26.089264130	40.645458714	34.040954482
6	24.299371886	40.794523416	34.959357658
7	23.136327962	41.431562736	35.096931566
1	22.877804307	42.264897489	34.560990120
1	22.410373888	40.985373127	35.679944705
7	24.556518797	39.711134177	35.687325283
1	25.511231888	39.352157180	35.776537762
1	23.939576766	39.394266248	36.447663617
26	26.494307128	38.648460301	40.805871849
8	26.145687877	37.583227192	39.649995996
8	28.987625540	38.353787633	38.884726259
6	29.193165868	37.909901024	40.016707505
8	28.356370867	38.043344514	41.006708760
6	30.533450129	37.235773279	40.348954505
6	30.491205306	35.930454103	41.152210384
6	31.873554454	35.314606881	41.487184472
8	31.905823667	34.070856849	41.655734924
8	32.872337188	36.077846731	41.602456957
1	29.908652054	35.158620594	40.626841327
1	29.968349900	36.099689406	42.111544029
1	31.135454699	37.970743819	40.913251115
1	31.048684298	37.079866776	39.390419796
8	22.827921688	34.038616645	41.831908413
6	21.860267245	34.758884466	41.903814002
7	21.544942693	35.676385856	40.864373680
6	22.442838648	35.672159518	39.697575888
6	20.486358580	36.538170654	40.920139633
7	20.263069599	37.418651766	39.955611981
6	19.609742467	36.461221678	42.043040208
6	19.864978725	35.577996813	43.036902001
7	20.973066386	34.770890530	42.989773354
1	21.852055303	35.688232563	38.774094066



1	23.033515368	34.752512289	39.730572365
1	20.796339066	37.510435501	39.080657580
1	19.196928284	35.507732156	43.899939690
1	18.742609947	37.105491571	42.107321655
1	23.117697340	36.539353460	39.710248948
1	19.494722273	38.072885310	40.083207824
8	27.517154743	42.905874799	40.330885981
1	28.215744723	42.689733357	40.963606220
1	27.286767236	42.048913028	39.915970493
8	23.655390120	38.343719930	37.944770482
1	22.678545932	38.205380122	37.743364621
1	23.687820129	38.690887145	38.851533224
8	26.729836180	38.347158291	36.909265910
1	25.993499167	37.918548230	37.378734413
1	27.364902733	38.538348337	37.625991429
1	22.832404926	37.476485828	44.436450119
1	23.304025126	41.703872432	39.069516679
1	28.257776706	41.005122901	45.223202177
1	26.019628251	42.586727926	32.701250818
1	21.162317607	34.151649869	43.751808442

**TS7**

**QM/MM (BS1) = -3461.191003 a.u.**

**QM/MM (BS2+ZPE) = -3463.210017 a.u.**

6	23.494496111	37.292507208	44.081041010
7	24.688298146	36.862756591	44.608640046
1	24.839894738	36.495369655	45.557132182
6	25.644956366	37.034304139	43.684489888
1	26.686987910	36.768935422	43.841977541
7	25.131298419	37.561254986	42.582574345
6	23.786318869	37.735235765	42.811322054
1	23.148154370	38.225675715	42.080092702
6	24.160877215	41.380044272	38.904935353
1	24.722040890	42.301670752	39.131001816
1	24.300540114	41.188903132	37.833095730
6	24.840658484	40.251395287	39.661707688
8	24.318995044	39.641532938	40.630623135
8	26.034224452	39.928951359	39.334173853
6	27.705890582	40.681415657	44.152611593
7	26.668755150	41.472594669	43.716641978
1	26.297830908	42.330841632	44.143731183
6	26.165510804	40.920925048	42.601846313
1	25.321698283	41.336472516	42.064124281
7	26.826115752	39.819844387	42.277231187
6	27.797506388	39.653653928	43.240674714
1	28.479755121	38.807252656	43.212220345
6	25.071042176	42.626466650	33.139411385
1	24.218690512	42.567172646	32.440406424
1	24.931464675	43.546155727	33.734284772
7	25.169027773	41.462951170	33.990586947
1	25.977462577	40.833027088	33.922914977

6	24.169995346	41.071763054	34.804152431
7	23.010115902	41.723134331	34.862200911
1	22.771184505	42.542219230	34.298484231
1	22.292449670	41.310458337	35.473575198
7	24.334213721	39.994665955	35.567389942
1	25.256280598	39.588200174	35.774268978
1	23.560910370	39.716599017	36.170348110
26	26.060731211	38.287190337	40.798478820
8	25.134204693	37.086225164	39.870188120
8	28.754188617	38.348008874	38.860686604
6	28.873204523	37.735218366	39.922643048
8	27.906190463	37.589488460	40.786715151
6	30.247017115	37.150689758	40.313578397
6	30.281610427	35.815782960	41.066065895
6	31.688787603	35.264021230	41.416127181
8	31.767893479	34.021544175	41.584737594
8	32.657864729	36.062248417	41.543933985
1	29.761808389	35.028760572	40.499472766
1	29.723123304	35.906688160	42.015440773
1	30.756773004	37.916785737	40.928002048
1	30.828639259	37.083340407	39.382006571
8	23.102151510	33.858727708	41.826427190
6	22.203689463	34.662893819	41.812953559
7	22.090807240	35.607396012	40.735845342
6	23.122227177	35.529396995	39.735435271
6	21.088820581	36.549578895	40.685731728
7	21.023868063	37.452863102	39.720924210
6	20.096035684	36.541052971	41.707272391
6	20.175189636	35.648607982	42.726252281
7	21.216864573	34.759675877	42.800834274
1	22.763363747	35.801281175	38.736358330
1	23.595648612	34.543165774	39.755669184
1	21.587565211	37.494438717	38.866443905
1	19.414965721	35.634094386	43.513752706
1	19.271702792	37.246791405	41.658429929
1	24.111858352	36.311926176	39.955038718
1	20.329297883	38.191056527	39.819024343
8	27.223523734	42.430248859	40.154986368
1	27.906987224	42.238971519	40.811556239
1	27.021448088	41.556852207	39.764072085
8	24.134529009	38.063242631	37.545463135
1	23.157074959	37.969050192	37.369047204
1	24.350281908	37.728479965	38.441839621
8	26.579245183	38.489529281	36.500048439
1	25.746989952	38.076164764	36.820767170
1	27.035933383	38.767916377	37.314185891
1	22.601039674	37.444818248	44.686519549
1	23.107621350	41.559214815	39.120845803
1	28.207695265	40.888226503	45.097856882
1	25.980963593	42.756386592	32.553552056
1	21.309140856	34.167073782	43.601009468

**Snapshot 3****RC2****QM/MM (BS1) = -3386.916214 a.u.****QM/MM (BS2+ZPE) = -3388.864703 a.u.**

6	24.688519083	37.096837813	44.602907723
7	25.646947538	36.145147377	44.849313314
1	25.596961233	35.404359518	45.567329650
6	26.669102883	36.356236738	44.006985459
1	27.564577788	35.741049342	43.982546598
7	26.413333590	37.401764974	43.226139040
6	25.174378951	37.880262754	43.582289828
1	24.741179167	38.754607452	43.097562230
6	26.426071516	42.572645942	41.517916621
1	27.399754183	42.918844340	41.887995264
1	26.321221341	42.876594231	40.466329368
6	26.321520993	41.045966605	41.582495608
8	27.376961709	40.448286980	42.032005090
8	25.292698168	40.455553187	41.243560242
6	29.729591094	38.696331189	45.789220555
7	29.052711632	39.889271739	45.772147027
1	28.998188119	40.587623811	46.526379407
6	28.452534068	40.010634000	44.581934449
1	27.857189883	40.866689799	44.283420584
7	28.708811197	38.953146379	43.821516416
6	29.509288012	38.115395843	44.563036874
1	29.862476555	37.168636598	44.163595995
6	27.481414027	45.448599114	37.372061583
1	26.865190687	46.331529512	37.141416678
1	27.789592680	45.542850932	38.428596124
7	26.775770612	44.198440549	37.135229125
1	27.283683836	43.428438221	36.690310145
6	25.718675805	43.792376747	37.878214478
7	25.046842725	44.643062174	38.646452095
1	25.171490225	45.660334610	38.633102207
1	24.241742748	44.292201518	39.187963582
7	25.373309443	42.503149862	37.822517472
1	26.034641687	41.861419570	37.388488626
1	24.600207020	42.086744751	38.377167334
26	27.696809737	38.510767063	42.026770500
8	26.874574191	38.177682170	40.674875450
8	29.465762093	37.924055320	39.380344611
6	29.787306430	37.311276035	40.403148171
8	29.276661709	37.529965851	41.577977275
6	30.857698160	36.239684792	40.372817536
6	30.385332597	34.884878468	40.898161203
6	31.504271175	33.832607720	40.872043840
8	31.154222255	32.646482963	40.660019153
8	32.681944273	34.224000771	41.068124622
1	29.535104807	34.499979078	40.314310832
1	30.028205450	34.988087363	41.938491051
1	31.715717841	36.570719950	40.980762554

1	31.211993732	36.137490648	39.338988096
8	22.274330175	34.637095370	41.720542743
6	21.774314413	35.675190931	42.081856449
7	21.951932545	36.865147847	41.330519457
6	22.788572343	36.766089973	40.123487674
6	21.371113777	38.052558590	41.665551649
7	21.537464683	39.120869325	40.897380026
6	20.589698134	38.118060293	42.853020030
6	20.419273769	37.000110965	43.604731897
7	21.000411218	35.814189496	43.243583850
1	22.194057759	37.014723242	39.234782777
1	23.140582351	35.734718979	40.036010526
1	21.047416261	39.983914597	41.130762100
1	19.822912098	37.032304865	44.519393705
1	20.158989377	39.061913572	43.160568677
1	23.652342541	37.443679987	40.210769725
1	22.106526905	39.135665550	40.053684194
8	27.579071418	39.865052952	38.450603066
1	26.806809932	39.526168932	38.930085502
1	28.278591088	39.268759809	38.793763447
8	23.543729688	40.973276178	39.326332288
1	22.790947503	41.496931383	39.730205693
1	24.147804426	40.791734815	40.092456598
1	23.845628325	37.268998604	45.272208223
1	25.636787949	43.053020317	42.096137366
1	30.202636734	38.340294512	46.704388860
1	28.380067737	45.488980709	36.756547034
1	20.905571209	35.003981344	43.821978705

**TS7**

**QM/MM (BS1) = -3386.878586 a.u.**

**QM/MM (BS2+ZPE) = -3388.828717 a.u.**

6	24.546414623	36.916959486	44.875006563
7	25.576636482	36.051224438	45.137907435
1	25.606308487	35.344441852	45.889400428
6	26.559234632	36.294787511	44.259481192
1	27.493631153	35.741734923	44.238989269
7	26.207674874	37.277310841	43.437895677
6	24.950293871	37.682002941	43.811962872
1	24.442311620	38.508988091	43.321486715
6	26.765476861	42.769009147	41.739921622
1	27.596051896	42.924481465	42.444446647
1	26.918357962	43.404849277	40.856878731
6	26.700213250	41.321827652	41.252905305
8	27.063898374	40.411252696	42.071349021
8	26.330196563	41.122855615	40.082403834
6	29.604250134	38.594380768	45.711558624
7	28.943798144	39.795423852	45.696346318
1	28.912290205	40.492634590	46.452773566
6	28.319295699	39.912027059	44.514728986
1	27.718341059	40.768379445	44.229479975

7	28.538274589	38.848880570	43.751282895
6	29.346693973	38.011469268	44.489174625
1	29.687297190	37.054152990	44.100861354
6	27.459813499	45.395774741	37.312269994
1	26.843360618	46.288813711	37.125958220
1	27.733160483	45.407797775	38.382044719
7	26.787388461	44.161555889	36.945172656
1	27.315843060	43.466457231	36.407126195
6	25.709020257	43.656630368	37.577279706
7	25.005964307	44.390375312	38.440234790
1	25.111144794	45.407245632	38.531872070
1	24.199795535	43.976058393	38.928392330
7	25.352211220	42.398558793	37.290733729
1	26.065365459	41.786821686	36.894971997
1	24.656184490	41.919031864	37.880581557
26	27.157940003	38.407674202	41.955535284
8	25.745996083	38.132442754	40.958409879
8	28.863369218	37.702240209	38.929370673
6	29.184052700	37.207652556	40.015009254
8	28.608601235	37.482997026	41.147152201
6	30.350302952	36.235124692	40.110451123
6	30.053757986	34.923903100	40.837140261
6	31.254184071	33.955880476	40.813163605
8	30.979332133	32.733469627	40.716568870
8	32.408125046	34.442644211	40.897030769
1	29.188521221	34.407244740	40.394085588
1	29.790322036	35.128284186	41.890805137
1	31.185018318	36.739912971	40.626541019
1	30.692444244	36.018727366	39.090294210
8	22.634546293	34.848017622	41.722477553
6	22.104717156	35.897353870	41.987822917
7	22.463201859	37.089908486	41.274565964
6	23.550160144	36.977194822	40.342382700
6	21.768611840	38.271617572	41.428014253
7	22.119374741	39.343283650	40.743790960
6	20.682446231	38.304059010	42.346663391
6	20.411934224	37.219574052	43.121004380
7	21.133855655	36.061882401	42.986245065
1	23.335436215	37.468871449	39.385955445
1	23.848915368	35.931275746	40.227776381
1	21.605599445	40.231199433	40.829131729
1	19.612204189	37.249437228	43.865600183
1	20.092882762	39.211289080	42.427185277
1	24.664693967	37.568384966	40.735216611
1	22.917922097	39.409932699	40.112043205
8	27.435687646	40.023727788	37.799236880
1	27.052206441	40.349151682	38.637055442
1	27.833756792	39.172978213	38.066232552
8	23.834516481	41.028322910	39.221744934
1	23.413556742	41.847774084	39.611426748
1	24.730273480	40.966546805	39.633374131
1	23.713016665	37.096628910	45.554148718

1	25.853981014	43.093847681	42.241641229
1	30.117157770	38.266463740	46.615695504
1	28.375127719	45.482932848	36.726889215
1	20.991233644	35.288584601	43.604016835

**Snapshot 4**

**RC2**

**QM/MM (BS1) = -3387.759704 a.u.**

**QM/MM (BS2+ZPE) = -3389.705321 a.u.**

6	25.791583624	38.862391534	45.691503203
7	27.157436618	38.756990131	45.775370177
1	27.720823816	38.859531924	46.634749626
6	27.628247595	38.527310975	44.538094406
1	28.683756316	38.399391826	44.313103289
7	26.631867580	38.480121155	43.660169511
6	25.471177505	38.693744115	44.364790359
1	24.503356788	38.763803489	43.871644297
6	23.623288598	40.661675446	39.596286299
1	23.995247848	41.611577914	39.183451642
1	23.275245742	40.077820635	38.729665339
6	24.811382239	39.931117387	40.191620573
8	24.778530556	39.451604032	41.375072853
8	25.848628624	39.805548484	39.492405730
6	28.631810197	42.253580314	42.849030356
7	27.374260656	42.725753606	42.575539447
1	27.040743112	43.687405301	42.721894078
6	26.647101143	41.717958639	42.075049642
1	25.607619810	41.823973035	41.787904848
7	27.374540633	40.611335921	41.994773057
6	28.623614395	40.928128574	42.481521583
1	29.409304246	40.180105359	42.534102190
6	22.079003904	39.003877967	34.855261503
1	21.012854588	38.818619796	34.671497607
1	22.168269036	40.031602834	35.248753339
7	22.652907352	38.037051972	35.774146230
1	23.498720708	37.525337175	35.500034442
6	22.284867676	37.905446902	37.061736470
7	21.197631086	38.522949766	37.532527186
1	20.561278775	39.073170786	36.945643174
1	20.903815336	38.360110158	38.505226461
7	23.026674964	37.136849037	37.869029892
1	24.014922774	36.974724697	37.643178096
1	22.850750104	37.145789614	38.884556647
26	26.682960919	38.641440305	41.540920972
8	26.073106169	37.172518447	41.273124030
8	28.193365251	36.759134509	39.322613230
6	28.904323500	37.405415704	40.086352084
8	28.471688671	38.277458455	40.966413558
6	30.421521256	37.270804120	40.027939192
6	31.067532375	36.521585493	41.200094506
6	32.582841191	36.339220562	40.984225733

8	33.101736251	35.256022827	41.362314728
8	33.204699692	37.283406037	40.436661755
1	30.613631727	35.530565048	41.349638420
1	30.915568968	37.085801822	42.138294981
1	30.874901670	38.272314255	39.964832958
1	30.654023430	36.741062424	39.096555806
8	25.574112618	34.584525071	46.271218747
6	24.527801888	35.171777772	46.136458945
7	23.910758646	35.276695126	44.865655948
6	24.610183276	34.632915002	43.740431713
6	22.738295165	35.943262135	44.650874026
7	22.244107068	36.011094027	43.425774221
6	22.080749163	36.544555760	45.765589515
6	22.642859117	36.448543681	47.001936104
7	23.838076786	35.804416513	47.187555767
1	23.948571795	33.898408863	43.262353888
1	25.485778547	34.113526463	44.136965419
1	21.371970050	36.506121457	43.190668437
1	22.149865146	36.886762150	47.873676732
1	21.130649010	37.049739059	45.614931620
1	24.931407127	35.391425394	43.008980879
1	22.693633775	35.556848901	42.632795737
8	22.736527496	37.219015230	40.667835440
1	21.813617852	37.600829728	40.679110149
1	23.322499609	37.853126925	41.118258737
8	25.915461377	37.354982308	37.884765840
1	25.877243011	38.276988673	38.199134460
1	26.603680843	36.973827228	38.478097232
1	25.169051284	39.201486050	46.519474046
1	22.769232005	40.886278718	40.235197891
1	29.364835625	42.904442014	43.325601534
1	22.597495657	38.971119334	33.897054587
1	24.300685024	35.801107276	48.074096890

**TS7**

**QM/MM (BS1) = -3387.728665 a.u.**

**QM/MM (BS2+ZPE) = -3389.668228 a.u.**

6	25.790958543	38.887644745	45.921499728
7	27.159027886	38.854086923	46.001658566
1	27.727997957	39.006075058	46.848871622
6	27.637237311	38.601210874	44.773955516
1	28.696054453	38.512113232	44.548474635
7	26.639725306	38.466745591	43.910218255
6	25.473070393	38.649483635	44.608231368
1	24.499421456	38.640197336	44.121157138
6	23.632613448	40.599152525	39.565714343
1	23.988113819	41.566246130	39.180533801
1	23.222338045	40.072471553	38.688002860
6	24.871714960	39.816679897	39.988254613
8	24.848525878	39.118996265	41.078621387
8	25.848548591	39.852001774	39.226296023

6	28.569439202	42.075444827	42.841962591
7	27.295642713	42.513361305	42.590410248
1	26.944636793	43.468252321	42.742821228
6	26.586605637	41.478402209	42.112498479
1	25.540797185	41.555665416	41.838509423
7	27.333287176	40.387166690	42.029476596
6	28.583192726	40.744225139	42.485117083
1	29.392489507	40.019700320	42.531896807
6	22.075455533	39.036642691	34.828648919
1	21.005879106	38.877277565	34.642442082
1	22.188867393	40.055976585	35.236958238
7	22.627571229	38.041539046	35.729169857
1	23.465015567	37.520673483	35.446848249
6	22.241617274	37.879700043	37.006944506
7	21.158180181	38.498796259	37.482290103
1	20.535970492	39.076391814	36.906934821
1	20.865908073	38.325508501	38.453259303
7	22.963590580	37.074586270	37.797665610
1	23.962074790	36.946100896	37.588984778
1	22.780393549	37.067119780	38.810652975
26	26.533375846	38.254646471	41.820052244
8	25.726410455	36.729962449	42.068908477
8	27.930659995	36.520373873	39.326218118
6	28.677802087	37.030243434	40.160974908
8	28.273275625	37.779480359	41.149078507
6	30.187186372	36.855939232	40.035348208
6	30.957756730	36.391146598	41.274930784
6	32.465541931	36.250489586	40.977703057
8	33.040910887	35.198281128	41.364846577
8	33.024229426	37.190741994	40.359510310
1	30.581187690	35.427813331	41.649529866
1	30.830434524	37.129328116	42.087012334
1	30.613847468	37.822099512	39.713754345
1	30.346327815	36.149332492	39.212296147
8	25.690354762	34.745553819	46.158062109
6	24.629348737	35.302386072	46.029512414
7	24.042531925	35.452790254	44.732874407
6	24.798124735	34.938113229	43.623723137
6	22.810585948	36.037198791	44.536556738
7	22.335007681	36.154889107	43.313129213
6	22.091215124	36.503014472	45.676149199
6	22.645379599	36.396573697	46.915314578
7	23.886443867	35.843589351	47.091579244
1	24.184901867	34.332868592	42.946689923
1	25.688098266	34.410029239	43.975080219
1	21.411691623	36.564181653	43.103476452
1	22.109862765	36.756110219	47.797990310
1	21.105449367	36.941501637	45.540668335
1	25.279108981	35.881631078	42.857985046
1	22.865504455	35.911577160	42.477821999
8	22.754699697	37.165982256	40.615041961
1	21.840658656	37.568758915	40.608879258



1	23.391672765	37.836834145	40.937483158
8	25.824992293	37.323765480	37.800725879
1	25.879377452	38.259695462	38.073774301
1	26.483558739	36.896767495	38.397418847
1	25.147250023	39.239954913	46.727467598
1	22.809132615	40.803244257	40.250033867
1	29.301033031	42.759152453	43.272522315
1	22.592862811	39.002629416	33.869899672
1	24.331681322	35.836112759	47.986945202

**Snapshot 5**

**RC2**

**QM/MM (BS1) = -3307.735939 a.u.**

**QM/MM (BS2+ZPE) = -3309.615721 a.u.**

6	24.041723945	41.695961846	41.500221569
7	25.181630939	41.650996126	42.262388432
1	25.338855231	42.107413356	43.176498134
6	26.101890622	40.944694970	41.594926685
1	27.102950570	40.755052645	41.972180908
7	25.605594283	40.522756692	40.435914541
6	24.314940667	40.987522687	40.355252736
1	23.690569866	40.812043294	39.481602773
6	24.974164088	40.560362112	34.962892107
1	25.570974074	41.426409105	34.630149141
1	24.816004682	39.926756411	34.080420516
6	25.806534860	39.755498831	35.963017946
8	25.812746644	40.187090075	37.176923525
8	26.470150187	38.805785258	35.535059567
6	28.547063218	43.487502530	39.294856756
7	27.648716764	43.706981271	38.282185680
1	27.417429835	44.606970772	37.841908130
6	27.086767806	42.531757708	37.965436695
1	26.325247211	42.402553981	37.206633943
7	27.577417194	41.555207382	38.717044366
6	28.497552701	42.137030136	39.560201480
1	29.046171721	41.552182779	40.294426520
6	25.813986760	36.977140846	32.165911670
1	25.108974781	37.259099047	31.368702001
1	26.319905156	37.897997886	32.508817438
7	25.149391233	36.324447785	33.278413214
1	25.667677369	35.596432957	33.780153083
6	24.123799940	36.896986675	33.946994124
7	23.353755574	37.804343530	33.342845286
1	23.418840296	38.045876997	32.353111959
1	22.587014852	38.222657886	33.890226418
7	23.875623552	36.533413536	35.209018917
1	24.657888044	36.199305213	35.789227448
1	23.068364061	36.934008577	35.706648598
26	26.587135190	39.617034841	38.877778966
8	25.684050467	38.283552265	39.001118287
8	28.544341955	36.916391377	38.532650204

6	28.975382897	37.876556656	39.176627663
8	28.308590607	38.969503391	39.417821219
6	30.398946227	37.879006402	39.722934184
6	30.503609956	37.881582559	41.250905132
6	31.944253074	37.647723093	41.747582135
8	32.897791117	38.101533278	41.066619404
8	32.067008035	37.009811546	42.822492086
1	29.867215655	37.100901080	41.694297663
1	30.144180571	38.843747958	41.658849836
1	30.930170979	38.757371557	39.321325213
1	30.907923103	36.987856558	39.340137787
8	22.751702808	38.269821137	43.064554217
6	21.871381941	38.780926988	42.414616735
7	21.735840010	38.503247719	41.025045942
6	22.719337422	37.561297272	40.448677005
6	20.763717850	39.067972058	40.248493866
7	20.708013832	38.841306339	38.944352464
6	19.785589983	39.906720057	40.870296147
6	19.890034527	40.184908039	42.196173409
7	20.923693974	39.678223876	42.940155658
1	23.554821492	38.079987779	39.905134700
1	22.201596614	36.863580731	39.778370147
1	21.308398854	38.205354272	38.405624958
1	19.143563315	40.812196052	42.691931369
1	18.956250957	40.306373940	40.288071885
1	23.153216141	36.989231625	41.274705588
1	20.019279985	39.379113030	38.405379970
8	26.510792820	36.250833382	36.490252379
1	26.608572097	37.170826524	36.155314444
1	26.863619433	36.334104254	37.396118859
1	23.208836993	42.362226674	41.724849749
1	24.012870757	40.941925611	35.306973124
1	29.068758308	44.327594083	39.753275493
1	26.576543734	36.343428764	31.713160978
1	21.059730263	39.985203769	43.882084509

**TS7**

**QM/MM (BS1) = -3307.696418 a.u.**

**QM/MM (BS2+ZPE) = - 3309.580645 a.u.**

6	23.999011690	41.794394752	41.633831373
7	25.160901653	41.772031441	42.362207904
1	25.350617269	42.259354643	43.252664351
6	26.055135876	41.032981103	41.695125635
1	27.065156229	40.849850209	42.049992586
7	25.520392179	40.566178427	40.573799457
6	24.232590538	41.037565625	40.513913812
1	23.581355281	40.828530139	39.667872127
6	24.960759631	40.528485655	35.052084609
1	25.598216891	41.386521270	34.778302186
1	24.804588836	39.950781931	34.131009405
6	25.739073280	39.628516665	36.017401169

8	25.675136424	39.920221490	37.266785447
8	26.417825442	38.717644109	35.526278871
6	28.484729842	43.357153971	39.307702952
7	27.578215284	43.549770992	38.298001037
1	27.338099329	44.444500053	37.852995965
6	27.031249747	42.355639883	38.006391971
1	26.267108020	42.208794848	37.252503234
7	27.534214105	41.395969586	38.766573997
6	28.450591538	42.007699539	39.591281536
1	29.015121706	41.447895728	40.334210674
6	25.845833076	36.982669140	32.152977891
1	25.146191356	37.280310201	31.356554637
1	26.350697631	37.895402626	32.518094746
7	25.173985460	36.307100296	33.246879399
1	25.687515446	35.565393674	33.732737373
6	24.149835889	36.868489395	33.925753732
7	23.387242339	37.794435485	33.341620653
1	23.455825140	38.056161541	32.357153719
1	22.623619254	38.209597151	33.895467606
7	23.894178295	36.470871871	35.176264623
1	24.675256218	36.122472444	35.749977726
1	23.094089648	36.873282191	35.683164738
26	26.275563558	39.374736792	39.051150980
8	24.991148788	38.240366501	39.349976033
8	28.422832265	36.680589762	38.527019176
6	28.752166096	37.637924599	39.240751388
8	27.955105078	38.601817634	39.580040160
6	30.186229488	37.756628972	39.750775554
6	30.350497409	37.797829707	41.273509282
6	31.811306429	37.585099395	41.726192631
8	32.741865701	38.038795658	41.015219380
8	31.969481219	36.959434776	42.804755191
1	29.737995487	37.024750230	41.761065777
1	29.998295077	38.766724691	41.671352792
1	30.634867663	38.664018382	39.312008989
1	30.751061652	36.902078281	39.362876433
8	22.873566020	38.251269399	43.058894052
6	22.007681601	38.764689142	42.398072083
7	21.884811655	38.453019771	40.997160868
6	22.823404584	37.489949224	40.477338346
6	20.913880012	39.025204625	40.204566434
7	20.861633453	38.799179782	38.903635349
6	19.937452312	39.867605687	40.817955643
6	20.031782427	40.166785681	42.139700920
7	21.062741969	39.676637943	42.897044900
1	23.890922580	37.975761313	39.904966400
1	22.376514164	36.856186098	39.703378984
1	21.455731770	38.164115864	38.355215850
1	19.279164757	40.800743963	42.618476423
1	19.109380867	40.260535903	40.230029316
1	23.264463248	36.912129675	41.295436001
1	20.166085671	39.335527552	38.370000417

8	26.518143955	36.153842082	36.432388963
1	26.600425450	37.083977801	36.117156160
1	26.936772203	36.198689960	37.315470971
1	23.177288646	42.477651948	41.848303213
1	24.004182026	40.925020377	35.392359228
1	29.027293704	44.205748254	39.724331709
1	26.608245330	36.353552184	31.693623198
1	21.178139149	39.991699906	43.839059732

**Dioxygen activation step reaction states cartesian coordinates for AlkB-ssDNA**

**RC1**

**QM/MM (BS1) = -3425.036952 a.u.**

**QM/MM (BS2+ZPE) = -3427.041479 a.u.**

6	28.069778968	29.955598654	39.667639263
7	28.221667068	29.211622708	38.518265786
1	27.465895238	28.738993149	38.008269947
6	29.529971338	29.214927208	38.193582999
1	29.947750500	28.697137647	37.333843217
7	30.230842093	29.920593674	39.070005845
6	29.333325273	30.386520351	40.001698297
1	29.669866742	30.970153971	40.854425111
6	33.352042106	31.589649717	43.259226271
1	33.797124830	30.671727711	43.682790065
1	34.040604283	32.412361739	43.502273905
6	33.332116328	31.437585708	41.736042170
8	32.319768442	30.850048326	41.181242270
8	34.316098875	31.830456094	41.102167018
6	31.677318972	25.932796409	40.764529988
7	31.616207805	26.657885960	41.934066970
1	31.385569140	26.305922150	42.871044781
6	31.901091769	27.938299144	41.632724848
1	31.928870400	28.755935770	42.344560113
7	32.141701801	28.076123200	40.337850953
6	32.008867923	26.830503822	39.777347798
1	32.152297575	26.672398996	38.710366012
6	36.661289752	34.960907454	41.774312925
1	36.736723969	36.005629901	41.456260206
1	36.349563738	34.939446200	42.829188109
7	35.698898532	34.264448947	40.933777541
1	35.503741725	33.272111237	41.114994343
6	34.864483924	34.846724291	40.068226742
7	34.849799467	36.185498481	39.907269210
1	35.088245974	36.755123769	40.722276693
1	34.119186168	36.588561542	39.328371753
7	34.046919923	34.086721487	39.327468204
1	34.071549589	33.067642382	39.384822419
1	33.491031781	34.492035916	38.584735470
6	33.411105055	31.235069072	36.985201650
8	33.935105374	32.023000205	36.216542374
8	32.880790223	31.511685048	38.134527553

6	33.318763493	29.716475198	36.636369626
8	32.616258702	29.027696598	37.390472099
6	34.001407378	29.187470884	35.424763397
6	34.261603582	27.683811450	35.435456979
6	34.826631082	27.161419063	34.095959631
8	34.239233784	27.559529347	33.057248325
8	35.791802753	26.362759946	34.149930757
1	33.313420247	27.146869991	35.623218264
1	34.956070377	27.422523579	36.248691061
1	34.929543902	29.755614766	35.267788549
1	33.378083178	29.457113828	34.550011888
26	32.390235352	30.016586411	39.357625073
8	34.397042827	29.458623994	39.372077174
8	35.182903491	29.633932379	38.420253364
8	28.862979400	33.338453776	37.895392508
6	28.114155958	33.602889580	38.802265685
7	28.603141258	34.004091915	40.071873927
6	30.069960049	34.016933137	40.251046993
6	27.798391305	34.338563613	41.125670637
7	28.302514604	34.787089725	42.250272559
6	26.384144480	34.165778695	40.970794580
6	25.886570104	33.795556528	39.768214690
7	26.703839834	33.545044659	38.694884127
1	30.435228413	35.044747207	40.375073292
1	30.524890311	33.565399499	39.364889941
1	29.274086499	35.120004943	42.428197265
1	24.809803788	33.709744823	39.648681122
1	25.709518715	34.396215342	41.793067782
1	30.323024780	33.430496433	41.145665387
1	27.675638704	34.997809915	43.017953302
1	27.130320972	30.009063628	40.217755150
1	32.405198891	31.755428693	43.773106196
1	31.338816367	24.899215296	40.692464751
1	37.675245120	34.572949208	41.677100599
1	26.323798831	33.212022621	37.831960227

**TS1**

**QM/MM (BS1) = -3425.020416 a.u.**

**QM/MM (BS2+ZPE) = -3427.023464 a.u.**

6	28.085685962	29.957627176	39.685034636
7	28.248312455	29.233723526	38.523235480
1	27.496189122	28.769313947	38.000060709
6	29.559494158	29.240015094	38.211097972
1	29.997612973	28.748019426	37.346108185
7	30.250846649	29.925180789	39.112427334
6	29.346192726	30.377642720	40.042320795
1	29.673329270	30.948609451	40.906616614
6	33.401343000	31.491073356	43.237318296
1	33.801547476	30.547878565	43.649376803
1	34.113258239	32.284427990	43.506654566
6	33.392766905	31.383790342	41.709095422

8	32.429738026	30.722066088	41.143510482
8	34.329150396	31.883054344	41.084320869
6	31.677782447	25.856983708	40.772374469
7	31.634263672	26.577107535	41.945990646
1	31.410428167	26.224706994	42.884557671
6	31.919621297	27.856785263	41.647282868
1	31.965706666	28.669808320	42.362607819
7	32.141934581	27.997552735	40.349543183
6	31.998428055	26.756483377	39.784074117
1	32.125915258	26.606658994	38.714080889
6	36.696724292	35.007264688	41.779421153
1	36.771266575	36.050678173	41.456343932
1	36.390017281	34.989507944	42.835803915
7	35.731740653	34.304928626	40.948552847
1	35.541108767	33.314634037	41.138197728
6	34.893529982	34.875170802	40.079932523
7	34.872686627	36.211709128	39.905140156
1	35.104698925	36.787721299	40.717644640
1	34.142462674	36.606520092	39.320121456
7	34.086286414	34.098755290	39.345538395
1	34.089931810	33.084061910	39.466817211
1	33.466841549	34.495809437	38.651027441
6	33.396570482	31.315584496	37.051709646
8	33.842184442	32.005811126	36.168867494
8	32.808327601	31.564875744	38.142388984
6	33.614495453	29.578637309	36.954100495
8	32.546163566	29.060863237	37.508446695
6	34.075744536	29.123473759	35.581480160
6	34.329980665	27.614668156	35.524546800
6	34.853349537	27.131649631	34.152607214
8	34.239775555	27.542522834	33.136010855
8	35.830788061	26.343235591	34.168849548
1	33.384690040	27.077952317	35.728510704
1	35.055068190	27.320244624	36.298602414
1	34.991493396	29.672023436	35.324561383
1	33.315790491	29.412564089	34.842252527
26	32.414498589	29.883983504	39.333449246
8	34.374697878	29.519585954	39.140561720
8	34.757110056	29.572929688	37.849635753
8	28.855903046	33.332660286	37.913313842
6	28.101679069	33.599635595	38.814746679
7	28.584568422	33.997992613	40.087892794
6	30.049994080	34.001480785	40.275191276
6	27.775294248	34.342410922	41.134964947
7	28.275292430	34.789889565	42.262252762
6	26.361250494	34.178931470	40.970472485
6	25.869553102	33.806874979	39.765828339
7	26.692000192	33.547610153	38.698700172
1	30.426025322	35.028723185	40.369317293
1	30.504911219	33.516514549	39.406631639
1	29.249838873	35.111487169	42.447004224
1	24.793012026	33.727269358	39.640584822

1	25.682033254	34.415856994	41.787189030
1	30.289866053	33.443140065	41.191096958
1	27.642753497	35.009869314	43.022576607
1	27.142243373	30.007182524	40.228659197
1	32.453034610	31.683229268	43.739169498
1	31.324734717	24.828526095	40.696879032
1	37.708083394	34.613833860	41.677282694
1	26.317123970	33.215144645	37.833306041

**IM1**

**QM/MM (BS1) = -3425.120278 a.u.**

**QM/MM (BS2+ZPE) = -3427.118763 a.u.**

6	28.017477767	29.968887739	39.673237153
7	28.174057965	29.196111994	38.543741140
1	27.423593041	28.704850771	38.045007342
6	29.482275730	29.205932761	38.217188982
1	29.906010666	28.661892945	37.376693884
7	30.176721390	29.947468708	39.066204469
6	29.277337881	30.424743390	39.989417427
1	29.612008327	31.028344022	40.829505487
6	33.381126497	31.562096807	43.261874480
1	33.857799012	30.680996340	43.726917929
1	34.057973610	32.407626042	43.461111858
6	33.359619877	31.322764003	41.745476819
8	32.274298839	30.915579472	41.191084443
8	34.428800532	31.490044038	41.134958481
6	31.735064683	25.989375003	40.732212286
7	31.663169265	26.717057756	41.899884739
1	31.406893914	26.369393511	42.831376173
6	31.993667154	27.989051794	41.604133136
1	32.005724685	28.808663113	42.314312061
7	32.280362809	28.122039577	40.317126446
6	32.121064295	26.877847125	39.755377004
1	32.281485278	26.718379646	38.691352927
6	36.635798835	34.781198897	41.874251652
1	36.643789554	35.834747534	41.579253699
1	36.349071683	34.720954639	42.934779434
7	35.697741211	34.051696600	41.033910746
1	35.559353148	33.042432732	41.180433952
6	34.820280394	34.616460368	40.195869718
7	34.689128745	35.953842737	40.116198866
1	34.913195780	36.524736114	40.933657804
1	33.984841368	36.345560761	39.499578664
7	34.089152453	33.840645658	39.391108600
1	34.191700585	32.822514065	39.372221412
1	33.338817760	34.228421375	38.831083318
6	31.769979671	33.339938087	36.584507012
8	31.833002839	32.746581522	35.589454057
8	31.698985388	33.983783675	37.553925632
6	33.489443011	29.561239157	36.674551553
8	32.704356147	28.952744954	37.406940693

6	34.103185641	29.039585523	35.408840988
6	34.409649808	27.544043573	35.428771158
6	34.960291539	27.057774672	34.069793097
8	34.324147142	27.437968363	33.052998529
8	35.970695667	26.315659419	34.090409318
1	33.478891767	26.984135614	35.632663173
1	35.131406130	27.296771850	36.221775270
1	35.006306184	29.621001732	35.179949417
1	33.398505345	29.251389029	34.587179186
26	32.315151667	30.069795512	39.313255159
8	33.246185225	31.362430812	38.103860906
8	33.876757968	30.798019751	36.949456785
8	28.810135871	33.272240865	38.025732733
6	28.042755024	33.569855748	38.907848219
7	28.503050006	33.992313864	40.179841230
6	29.963431282	33.995641277	40.404105490
6	27.677116162	34.370373124	41.201650927
7	28.161861715	34.847259713	42.324436417
6	26.265502179	34.210360439	41.013176190
6	25.794981878	33.819785099	39.805610334
7	26.636119884	33.532978867	38.759811567
1	30.329508620	35.023934174	40.519567023
1	30.442377761	33.536614040	39.537469459
1	29.138817957	35.155889410	42.519806044
1	24.720542678	33.747085908	39.661168600
1	25.570930803	34.463899901	41.811830693
1	30.184978491	33.422119128	41.315115584
1	27.516140570	35.101000971	43.062758687
1	27.082432262	30.013674561	40.231584150
1	32.436649705	31.734176326	43.778032932
1	31.390772587	24.957585187	40.661926864
1	37.667512872	34.454640860	41.743893224
1	26.279507564	33.200773408	37.886633646

**TS2**

**QM/MM (BS1) = -3425.105649 a.u.**

**QM/MM (BS2+ZPE) = -3427.116983 a.u.**

6	28.028933925	29.971653924	39.671382445
7	28.190129475	29.216515751	38.530236712
1	27.441238155	28.726152679	38.026688919
6	29.495659205	29.237984361	38.201276003
1	29.924697163	28.711214884	37.352657706
7	30.184640538	29.970224790	39.065841464
6	29.284527659	30.428161409	39.999058264
1	29.617078761	31.021265985	40.847208175
6	33.357212676	31.567515571	43.259222979
1	33.841239887	30.696830266	43.736518421
1	34.024549728	32.422526112	43.448975257
6	33.353817824	31.304806838	41.745721293
8	32.294497154	30.818865667	41.197033644
8	34.417303759	31.510275072	41.144371581



6	31.772013828	25.996919991	40.703267455
7	31.693563375	26.720732881	41.873909042
1	31.431753476	26.370480917	42.802943685
6	32.030200313	27.992044185	41.586875798
1	32.038471326	28.809881374	42.298648123
7	32.327707085	28.130096459	40.302151534
6	32.169716630	26.888090505	39.733498774
1	32.342947813	26.734755549	38.670426592
6	36.634746333	34.780160112	41.869343068
1	36.641039991	35.840761475	41.602511070
1	36.344745035	34.693350986	42.927256502
7	35.699879458	34.069558607	41.009370834
1	35.541851520	33.063121483	41.153421634
6	34.849757371	34.651058850	40.153491431
7	34.748017176	35.993130126	40.075482413
1	34.949402701	36.552820143	40.906442229
1	34.057966895	36.394196670	39.448831371
7	34.119222850	33.896350570	39.331471499
1	34.169686918	32.871762708	39.305405889
1	33.379254776	34.306526185	38.772835857
6	31.166333191	33.793831278	36.744236164
8	30.728549129	33.304246076	35.788495189
8	31.609586586	34.305338696	37.692968446
6	33.504336053	29.670799814	36.673550641
8	32.793648473	28.999425150	37.471348284
6	34.049578642	29.084894356	35.387369060
6	34.370291758	27.593807782	35.437190548
6	34.915717707	27.082620004	34.084390266
8	34.294552269	27.462592690	33.058070899
8	35.912379297	26.321419174	34.116624151
1	33.449394389	27.028565802	35.669383555
1	35.103673713	27.372554552	36.227235580
1	34.934273190	29.662130837	35.088270893
1	33.300318845	29.274916742	34.601665085
26	32.314535477	30.085293118	39.260689041
8	33.120153392	31.425990471	38.413717443
8	33.818759659	30.895303532	36.863257002
8	28.806169127	33.289533022	38.142042791
6	28.018283047	33.587830418	39.007169471
7	28.453918465	34.007634789	40.285966484
6	29.910700605	34.002830219	40.542278676
6	27.606907454	34.410984748	41.281292892
7	28.068836430	34.909607424	42.404174555
6	26.199764346	34.249703709	41.063070683
6	25.754119107	33.847041474	39.849927495
7	26.617124908	33.548287071	38.824795464
1	30.306061146	35.026553622	40.543203905
1	30.400199975	33.429099368	39.753147337
1	29.047154213	35.208734606	42.613438550
1	24.682926605	33.774675152	39.684108089
1	25.487478185	34.510336146	41.843734900
1	30.091694248	33.538581558	41.520794890

1	27.404885636	35.186634328	43.117412097
1	27.090566082	30.010466768	40.224579224
1	32.411673735	31.734895171	43.774982130
1	31.426092883	24.965827107	40.630786465
1	37.668072594	34.460198962	41.735443761
1	26.280953937	33.221363314	37.941572711

**IM2**

**QM/MM (BS1) = -3425.110527 a.u.**

**QM/MM (BS2+ZPE) = -3427.123113 a.u.**

6	28.042722675	29.955511864	39.676054530
7	28.199973241	29.204414827	38.532449239
1	27.447327403	28.726927622	38.022070620
6	29.506868931	29.208919888	38.210028680
1	29.930569576	28.686669833	37.356060760
7	30.198730829	29.925211735	39.084787830
6	29.301511587	30.393204881	40.013996668
1	29.634371977	30.983184083	40.863980919
6	33.404204864	31.523283598	43.238113305
1	33.871644978	30.642950936	43.714174245
1	34.079255437	32.369090699	43.438477433
6	33.411205668	31.274548076	41.724354603
8	32.367826066	30.740154198	41.180733757
8	34.449849165	31.529499139	41.104881485
6	31.767323143	25.967597428	40.672308665
7	31.689537516	26.689115007	41.843575972
1	31.438880006	26.336809670	42.774752413
6	32.006740335	27.964342333	41.553593010
1	32.017729547	28.777407317	42.269660804
7	32.290460188	28.108771912	40.266637327
6	32.146104989	26.865224973	39.699502051
1	32.321512579	26.711366682	38.636710593
6	36.635259968	34.827604747	41.835924535
1	36.658586652	35.885322570	41.557549774
1	36.341360105	34.755882301	42.894125466
7	35.691589245	34.123154679	40.980817260
1	35.545809687	33.115231382	41.115072973
6	34.823582471	34.710847983	40.146755402
7	34.742425609	36.053859767	40.059952415
1	34.970055283	36.610791616	40.885893366
1	34.026162200	36.457686747	39.464320786
7	34.054259617	33.963405535	39.355179110
1	34.070450536	32.940381196	39.350905565
1	33.312199658	34.380456152	38.802930781
6	31.163793961	33.884937206	36.805513440
8	30.768126899	33.329860007	35.867368380
8	31.557210770	34.475493015	37.730512154
6	33.629340425	29.781322615	36.730178417
8	33.006050040	29.106284156	37.631238566
6	34.108940010	29.096225729	35.461114148
6	34.368688817	27.595746391	35.528501347

6	34.879150125	27.055422278	34.170527897
8	34.250020575	27.435567470	33.149381216
8	35.863716898	26.277102448	34.192994260
1	33.431776094	27.063940894	35.778113657
1	35.105176407	27.352948958	36.309634558
1	35.009018217	29.623026581	35.116665602
1	33.349669937	29.303961926	34.688523085
26	32.307273662	30.140061286	39.241793185
8	32.715033377	31.656511326	38.457953311
8	33.856032455	31.010487157	36.810027306
8	28.804724610	33.258911218	38.165530731
6	28.016350011	33.576760892	39.022391413
7	28.450716524	34.005181851	40.299162434
6	29.907575533	33.996147308	40.556975166
6	27.602516886	34.422815902	41.287173501
7	28.062324115	34.926824904	42.408732268
6	26.195136739	34.269516206	41.065380811
6	25.750497508	33.863042349	39.853186163
7	26.615083369	33.551796077	38.833540489
1	30.311642855	35.016058868	40.524206966
1	30.394047061	33.392500125	39.787741262
1	29.042501094	35.219208865	42.619160612
1	24.679214226	33.796007128	39.685206577
1	25.482489414	34.539004768	41.842663449
1	30.082000329	33.564329465	41.551286771
1	27.395631527	35.219082466	43.113216822
1	27.106115595	30.000154929	40.231789619
1	32.455958875	31.698107885	43.746378327
1	31.420671705	24.936327348	40.606111041
1	37.664211701	34.491097590	41.709083728
1	26.281385323	33.227477322	37.948421593

**IM3**

**QM/MM (BS1) = -3425.123364 a.u.**

**QM/MM (BS2+ZPE) = -3427.140790 a.u.**

6	28.275017068	29.882160145	39.668316371
7	28.435021492	29.170442881	38.498961352
1	27.679077753	28.723743277	37.967429052
6	29.751003262	29.159773064	38.200186660
1	30.184585318	28.683564664	37.324483008
7	30.447545124	29.817617036	39.118501638
6	29.540252040	30.272363774	40.045369761
1	29.873994659	30.831184586	40.915043640
6	33.388825296	31.416719079	43.112141941
1	33.763347483	30.443214301	43.474527803
1	34.131754746	32.173439757	43.400452291
6	33.350225118	31.386690874	41.577866360
8	32.378204422	30.742021124	40.997015969
8	34.264797056	31.936271314	40.970133632
6	31.722825538	25.771306536	40.741430676
7	31.667513005	26.518992543	41.895148926

1	31.417010106	26.193431492	42.836615869
6	31.992269951	27.784875129	41.573355642
1	32.031318665	28.615927561	42.268858206
7	32.252418635	27.886177588	40.280227922
6	32.093374519	26.637702394	39.740440812
1	32.245360951	26.447174904	38.679745858
6	36.721373691	35.014519872	41.722714656
1	36.781176012	36.061104288	41.405883257
1	36.392743491	34.983783903	42.772473733
7	35.793302372	34.298809125	40.862245636
1	35.610686082	33.307387076	41.042298380
6	34.975989175	34.856459486	39.963600472
7	34.871841822	36.194780742	39.860944716
1	35.022814255	36.751500482	40.705169366
1	34.205134189	36.585684421	39.203518662
7	34.294305615	34.069847475	39.124236946
1	34.337739763	33.056597505	39.241907683
1	33.525366536	34.432955991	38.572170204
6	31.093919338	33.787135265	36.700336011
8	30.529729569	33.471387049	35.738771826
8	31.665165517	34.111007977	37.663928744
6	33.500725683	30.151705874	36.660875856
8	32.612426438	29.521699123	37.417658495
6	33.913143036	29.438050477	35.385222093
6	34.330026418	27.973721656	35.543337376
6	34.772734183	27.315453987	34.212523668
8	34.142503236	27.647380089	33.176302241
8	35.705450800	26.475541080	34.271662078
1	33.478874198	27.385849236	35.936607360
1	35.149576738	27.872227105	36.272266098
1	34.731020929	30.017860395	34.941026953
1	33.079092994	29.492792059	34.668957222
26	32.597728106	29.746739326	39.302842851
8	34.200610666	29.648999547	39.430065174
8	33.939679201	31.257915691	36.955965771
8	28.774403368	33.277302519	38.200800035
6	27.980939020	33.598203784	39.053133336
7	28.410824752	34.012808867	40.335290561
6	29.865729620	33.987098144	40.598169244
6	27.561216189	34.438311471	41.318761022
7	28.020092013	34.928086690	42.447276026
6	26.154159073	34.307816007	41.083944773
6	25.713684589	33.913134008	39.866302927
7	26.581945501	33.593886460	38.852309252
1	30.284302357	35.001051210	40.557189107
1	30.341992398	33.366675175	39.836006429
1	29.004467955	35.202379690	42.663995117
1	24.642794808	33.863042566	39.690795032
1	25.438583763	34.582725228	41.856681724
1	30.031557227	33.562853278	41.596879847
1	27.350079156	35.236839289	43.141492588
1	27.318244842	29.963976191	40.184029827

1	32.456874478	31.620067592	43.639573810
1	31.347468600	24.750322863	40.672388428
1	37.739325972	34.634857750	41.634981275
1	26.254820694	33.277070284	37.962034371

**IM4**

**QM/MM (BS1) = -3425.131228 a.u.**

**QM/MM (BS2+ZPE) = -3427.147412 a.u.**

6	27.926273337	29.928082622	39.667485124
7	28.088178911	29.147615471	38.545616243
1	27.335142371	28.677172896	38.030146066
6	29.401366704	29.116080994	38.247737861
1	29.826835584	28.576328048	37.405738280
7	30.089098533	29.834539489	39.120272752
6	29.188199085	30.349618065	40.016128829
1	29.515457250	30.962357381	40.851670187
6	33.401950971	31.490220148	43.190193400
1	33.869869863	30.612688792	43.670655073
1	34.085821029	32.333655455	43.370504055
6	33.389206780	31.224438896	41.679801466
8	32.319077009	30.702793569	41.169807692
8	34.416419350	31.444548818	41.035091785
6	31.713376411	26.014727980	40.608758420
7	31.644623063	26.714642596	41.793709367
1	31.423942037	26.340962410	42.724615176
6	31.920426720	28.000864813	41.521756172
1	31.931200092	28.800779742	42.250636300
7	32.169095248	28.173110484	40.229841093
6	32.045583760	26.936495972	39.641307392
1	32.205489472	26.805232032	38.573092634
6	36.668288974	34.815111047	41.714956574
1	36.676690964	35.853773182	41.367375917
1	36.347304199	34.801336092	42.767958047
7	35.768084023	34.037773015	40.873160621
1	35.683480895	33.028528156	41.023893310
6	34.855268107	34.556945475	40.038432438
7	34.628836586	35.881270994	39.999946403
1	34.840547655	36.458204537	40.816156647
1	33.935343398	36.254887351	39.360523631
7	34.193099825	33.750645663	39.204405521
1	34.341098409	32.741992746	39.215941649
1	33.363703601	34.072210675	38.714460140
6	31.101084303	33.952784164	36.806595020
8	30.618892273	33.464108533	35.872295714
8	31.597053997	34.463284393	37.730436207
6	33.784766715	29.916332803	36.920628304
8	32.945854820	29.310421439	37.756007046
6	34.015628508	29.229244157	35.581916604
6	34.372099644	27.741466100	35.636562844
6	34.805534404	27.170607707	34.261869235
8	34.156753487	27.549588070	33.254398754
8	35.759766791	26.352898749	34.268611313

1	33.497811779	27.158043600	35.983137154
1	35.187207903	27.555630628	36.353950872
1	34.817017884	29.787341689	35.080150292
1	33.114903313	29.359891760	34.960439804
26	32.186629537	30.119323386	39.289955866
8	32.101634696	31.626173668	38.712417071
8	34.349871364	30.962254223	37.200100927
8	28.760492986	33.298961844	38.161006742
6	27.971108118	33.591715954	39.025536531
7	28.407436498	34.005208410	40.305862734
6	29.866363944	33.985966044	40.555185875
6	27.561187450	34.426422917	41.293467276
7	28.023513038	34.936698071	42.411726898
6	26.153468534	34.269400178	41.074530847
6	25.706708329	33.858681770	39.864029232
7	26.569426861	33.550797932	38.842239554
1	30.291580624	34.992130489	40.447627747
1	30.337484940	33.314017948	39.832008368
1	29.005912858	35.227638151	42.612964592
1	24.635283105	33.788256142	39.698115782
1	25.441301919	34.538767808	41.852336634
1	30.037472048	33.624347003	41.576998065
1	27.358804108	35.232307320	43.116463721
1	26.991869170	29.974703038	40.226754926
1	32.461305137	31.679260746	43.707413265
1	31.392332930	24.975171932	40.543019307
1	37.705161262	34.488895535	41.634045367
1	26.236014163	33.225170808	37.957493575

## 2OG rearrangement reaction state coordinates for AlkB-ssDNA

### ES1

QM/MM (BS1) = -3274.903190 a.u.

QM/MM (BS2+ZPE) = -3276.725383 a.u.

6	27.983339902	29.969201568	39.678452190
7	28.130917065	29.212825708	38.536962528
1	27.375018650	28.736202417	38.031870792
6	29.438112714	29.212719608	38.209079748
1	29.849197149	28.678474190	37.356149403
7	30.141654454	29.931236159	39.070470908
6	29.247704918	30.406418225	40.000799257
1	29.590367751	30.991441957	40.850637265
6	33.323595061	31.624227259	43.269676188
1	33.830113279	30.760131427	43.734927227
1	33.983647919	32.488780961	43.442463704
6	33.267152630	31.357447560	41.760802078
8	32.179316275	30.911652379	41.245577666
8	34.312589048	31.535702499	41.108905148
6	31.727974734	25.988192493	40.762277973
7	31.647299260	26.710046586	41.933057803

1	31.388743452	26.357573035	42.862378424
6	31.970135832	27.984842792	41.646596843
1	31.972415998	28.800553138	42.361577347
7	32.260989360	28.125578201	40.360474059
6	32.113280172	26.882625787	39.791317828
1	32.284524205	26.728147480	38.728244085
6	36.621504196	34.732669618	41.899836552
1	36.630772937	35.802219422	41.679010177
1	36.334876101	34.605489291	42.953914028
7	35.675302222	34.058638897	41.021455358
1	35.484888510	33.056574026	41.160426512
6	34.867018900	34.664076277	40.144174319
7	34.853555128	36.004684124	40.007689595
1	35.098246953	36.576772536	40.819006537
1	34.144302301	36.419052469	39.411191533
7	34.071576752	33.919979080	39.365275034
1	34.091584552	32.898658311	39.386825222
1	33.531833601	34.342730588	38.620352761
6	33.522005081	31.157007908	36.987349300
8	34.024224495	31.928388779	36.184258884
8	33.022119793	31.449463271	38.136912841
6	33.458551468	29.625827288	36.672518767
8	32.854687931	28.922125816	37.484336310
6	34.117952253	29.098415978	35.447525385
6	34.321146638	27.587496470	35.412351788
6	34.906316010	27.108581355	34.066305157
8	34.301192428	27.504207665	33.036848145
8	35.908135555	26.354628915	34.104323928
1	33.348875245	27.080608209	35.552569397
1	34.984605265	27.267821330	36.230713656
1	35.069054398	29.634368241	35.304350161
1	33.514795088	29.428468887	34.578699735
26	32.261095571	30.067525230	39.371812686
8	28.875921784	33.315765619	37.872583466
6	28.131724695	33.578583606	38.784061739
7	28.626845054	33.980329586	40.050917211
6	30.094445509	33.988412266	40.225137004
6	27.827742322	34.313614102	41.109513284
7	28.339118536	34.759046791	42.232043874
6	26.412005942	34.144667571	40.960218755
6	25.908826664	33.772743221	39.760260331
7	26.721111233	33.519462013	38.683507811
1	30.455417017	35.011085866	40.394961540
1	30.545011827	33.581561096	39.315860214
1	29.311533468	35.090273474	42.405940144
1	24.831469210	33.686786960	39.644504946
1	25.741414488	34.378363124	41.784976963
1	30.357011062	33.358085892	41.086916463
1	27.720211897	34.965486763	43.007557572
1	27.051524321	30.011506696	40.242364697
1	32.385050981	31.778723631	43.801966709
1	31.384587421	24.956632181	40.684587578

1	37.655313966	34.421217273	41.750497647
1	26.336326732	33.184835838	37.823310910

**TS for 2OG rearrangement**

**QM/MM (BS1) = -3274.893943 a.u.**

**QM/MM (BS2+ZPE) = -3276.718908 a.u.**

6	27.926032218	29.906776549	39.703487306
7	28.092383081	29.149112873	38.566114172
1	27.343258918	28.680929837	38.043448529
6	29.407627511	29.130839568	38.269259727
1	29.837712928	28.616943735	37.413196351
7	30.097669770	29.829596788	39.158225371
6	29.186712356	30.322930783	40.061140640
1	29.513411276	30.915052877	40.911876493
6	33.236120543	31.655748183	43.288164683
1	33.736029798	30.776771861	43.731992945
1	33.893732836	32.511720869	43.508816456
6	33.250813689	31.462093975	41.767530762
8	32.160281971	31.132360006	41.152219105
8	34.346708000	31.592991328	41.213161406
6	31.719705112	26.124113045	40.714216767
7	31.656901710	26.841179730	41.888513604
1	31.419114114	26.478884480	42.819463625
6	31.964139164	28.122517710	41.595225549
1	31.981158044	28.929535092	42.319770540
7	32.224619880	28.273973758	40.305786294
6	32.074795328	27.029930577	39.739350220
1	32.218310056	26.873512010	38.671804770
6	36.666037705	34.707826858	41.902660771
1	36.663897025	35.782566022	41.709261801
1	36.369144006	34.551705969	42.950003789
7	35.739604481	34.040908168	40.998728847
1	35.526778949	33.044454110	41.147655787
6	34.966848934	34.650040808	40.094285393
7	34.942866262	35.993819956	39.983592165
1	35.139072506	36.555276605	40.815479327
1	34.273373664	36.414197342	39.347603880
7	34.214347916	33.912832356	39.266083558
1	34.284585988	32.888487636	39.208980253
1	33.713521497	34.367912492	38.512569769
6	33.855055112	31.079989292	37.116146184
8	34.270916430	31.939253947	36.352147441
8	33.729399212	31.158193043	38.397290157
6	33.367017304	29.719715398	36.577385773
8	32.431708057	29.202257186	37.194040393
6	34.040355125	29.138933519	35.379236966
6	34.228203274	27.620651018	35.402151753
6	34.826112229	27.107475184	34.070649284
8	34.254963223	27.516601097	33.027390345
8	35.801816490	26.324166647	34.134923100
1	33.250178555	27.127027924	35.547998856



1	34.888451717	27.321868716	36.231567139
1	35.002042762	29.648633351	35.228589829
1	33.436627676	29.413640483	34.493631333
26	32.167143299	30.301109810	39.298965103
8	28.875590800	33.263407325	37.916438173
6	28.125125580	33.553877342	38.815828609
7	28.613131839	33.986298663	40.074886205
6	30.080016285	34.023167797	40.248275094
6	27.808959149	34.315313454	41.131614186
7	28.312217434	34.767774136	42.254753018
6	26.394842602	34.137600499	40.976832640
6	25.897968116	33.761837507	39.775697664
7	26.716096178	33.502482843	38.704217618
1	30.405057425	35.035136316	40.518099573
1	30.535988338	33.735308196	39.298311432
1	29.282437250	35.101631126	42.436426135
1	24.821323157	33.674789527	39.654845175
1	25.719620423	34.369424426	41.798295027
1	30.376647576	33.314065706	41.035029162
1	27.685622347	34.975526335	43.023666109
1	26.987155915	29.962481155	40.254373507
1	32.288659197	31.794616740	43.808837170
1	31.408293821	25.081622461	40.648614103
1	37.703364245	34.407390560	41.755151438
1	26.334680589	33.169716408	37.841801744

## ES2

**QM/MM (BS1) = -3274.906024 a.u.**

**QM/MM (BS2+ZPE) = -3276.727311 a.u.**

6	27.923549387	29.907144941	39.708879321
7	28.097440809	29.156442941	38.568408595
1	27.352671568	28.684236655	38.043188242
6	29.414087479	29.149371159	38.273933749
1	29.849424039	28.646878959	37.413741615
7	30.097871773	29.846649303	39.169251716
6	29.180913833	30.329188277	40.071879975
1	29.500217056	30.920352174	40.926112885
6	33.213997103	31.676072209	43.301050954
1	33.717823539	30.800483383	43.747090059
1	33.864389016	32.536525153	43.527174319
6	33.242788039	31.484807485	41.781293927
8	32.153656476	31.171322634	41.151106626
8	34.345900761	31.602620925	41.240952340
6	31.718438108	26.144532392	40.711673875
7	31.658956114	26.859849437	41.886938979
1	31.422368269	26.496103040	42.817618718
6	31.966138951	28.141788128	41.593913305
1	31.985665321	28.946901387	42.320663960
7	32.222382736	28.295138397	40.304004792
6	32.070323712	27.051989822	39.737034726
1	32.210284347	26.895475967	38.668993649

6	36.693352210	34.712742089	41.910224132
1	36.689369723	35.784998232	41.702868932
1	36.395453127	34.568887286	42.958879605
7	35.771045722	34.031491983	41.013347162
1	35.559088649	33.037736612	41.175504539
6	35.011768627	34.622289202	40.085759061
7	34.979891846	35.964358897	39.957658040
1	35.156343735	36.537649870	40.785945495
1	34.323752836	36.371685258	39.300025987
7	34.282650279	33.866260922	39.254194067
1	34.359024632	32.841345939	39.223577179
1	33.794575286	34.301634513	38.481122035
6	33.902369003	31.056066041	37.153125392
8	34.330278168	31.931971145	36.413373021
8	33.807904922	31.082123856	38.438378336
6	33.343770335	29.746208926	36.567686393
8	32.381218642	29.261121985	37.168125450
6	33.987056858	29.170593379	35.350097651
6	34.223583218	27.658002692	35.404563997
6	34.808445345	27.126377718	34.073977396
8	34.233275661	27.525717799	33.029434721
8	35.777593571	26.335780230	34.143192807
1	33.263864698	27.139787562	35.584772267
1	34.909453814	27.397616391	36.225939440
1	34.926590627	29.704531736	35.155740463
1	33.338974550	29.398710515	34.484915651
26	32.169267940	30.337988511	39.309138509
8	28.862577654	33.270275537	37.918139806
6	28.112659423	33.560246768	38.818387906
7	28.601767366	33.995955386	40.075822012
6	30.068942494	34.039703528	40.243898904
6	27.798774900	34.320203830	41.134957115
7	28.302366197	34.772899112	42.257906730
6	26.384900907	34.138070265	40.982498049
6	25.886811530	33.762650662	39.781744980
7	26.703790462	33.506039877	38.708762102
1	30.387067129	35.047354199	40.535907821
1	30.522073157	33.779739733	39.284536017
1	29.271615808	35.109839311	42.438713948
1	24.810174678	33.673902282	39.662208618
1	25.710452919	34.366981426	41.805412990
1	30.376135951	33.313943514	41.011357021
1	27.675934832	34.977302461	43.027836031
1	26.982134002	29.959600964	40.255736482
1	32.262538145	31.808404151	43.816105737
1	31.410983253	25.100891164	40.645705523
1	37.730552081	34.410367944	41.765816286
1	26.322259799	33.172821721	37.846571573

## Substrate hydroxylation step reaction states cartesian coordinates for AlkB-ssDNA

### Snapshot 1

#### RC2

QM/MM (BS1) = -3371.376168 a.u.

QM/MM (BS2+ZPE) = -3373.322789 a.u.

6	24.428634865	27.784285884	25.352006656
7	25.464882364	26.935186433	25.669233319
1	25.770322112	26.126901375	25.114739416
6	25.986888664	27.335373828	26.843976580
1	26.824167068	26.847491227	27.335946810
7	25.332726321	28.394620090	27.299268218
6	24.367710466	28.700352838	26.374735539
1	23.685920774	29.534780946	26.517340087
6	21.983414961	31.225851746	31.109367927
1	21.685973611	30.391751729	31.763637021
1	22.003428762	32.161623530	31.680702986
6	23.391224478	31.013519856	30.570833115
8	23.611468234	29.844084783	30.022857575
8	24.235475649	31.880423074	30.709885333
6	24.293225011	25.212480623	30.263139088
7	23.100310497	25.871276479	30.463884477
1	22.270311047	25.471407845	30.906568515
6	23.306237669	27.179963439	30.245556300
1	22.558400116	27.956289562	30.363085657
7	24.565429735	27.398130905	29.887250364
6	25.199093344	26.175387458	29.896010004
1	26.257540908	26.074824196	29.674748608
6	26.168050532	36.182217498	32.207509913
1	26.090388484	36.915545948	31.390194482
1	25.252914305	35.579613085	32.224095519
7	27.323672915	35.318430563	32.070327495
1	28.240201374	35.688565071	32.347902304
6	27.320386549	34.109252749	31.488918743
7	26.245060326	33.644328328	30.857194563
1	25.415994695	34.202323342	30.646865503
1	26.167466405	32.655404674	30.626662156
7	28.423790891	33.353246064	31.538299399
1	29.123720297	33.480872128	32.267899562
1	28.406081477	32.433668871	31.090907266
26	25.243618407	29.283930572	29.200582187
8	25.579203785	30.722488583	28.527218981
8	27.919262480	30.867269441	30.271358253
6	27.998521934	29.675394554	29.969719971
8	26.967940420	28.880495622	29.902968939
6	29.324256969	29.063228305	29.550372497
6	29.507147871	27.559642453	29.807298471
6	30.233750060	27.263985346	31.130147559
8	29.636940767	26.616386759	32.020827176
8	31.420558445	27.701658069	31.208066247
1	30.150370627	27.145694000	29.015323291

1	28.540126281	27.039132572	29.786897603
1	30.137006648	29.637672683	30.016969107
1	29.378155847	29.293460843	28.470193232
8	26.659341018	30.116740059	23.287640349
6	25.706039571	30.869396353	23.301329889
7	25.557565278	31.860688234	24.296200660
6	26.608281425	31.940996089	25.333755332
6	24.524930403	32.767061867	24.314849268
7	24.440662233	33.672052935	25.270825204
6	23.548862739	32.703838505	23.274072615
6	23.636563444	31.722107709	22.347057682
7	24.679666000	30.827688433	22.349364757
1	26.234190999	31.585074180	26.304985125
1	26.937766744	32.983169146	25.436204836
1	24.795489671	33.550472541	26.245470026
1	22.872173347	31.612372270	21.580512813
1	22.709129376	33.396941917	23.273287120
1	27.449831083	31.316325799	25.026619127
1	23.659572674	34.333718567	25.195525572
8	28.912719310	32.124673528	27.712237529
1	29.851208562	31.808534668	27.713598647
1	28.562248948	31.789740922	28.554635061
8	24.335775349	33.199059657	27.926272216
1	24.709127811	32.402165356	28.350215001
1	24.185025425	33.856088595	28.672729849
1	23.670310045	27.565675365	24.600195357
1	21.227724132	31.311752909	30.328586476
1	24.347242504	24.124188674	30.290889201
1	26.217132468	36.751731785	33.135578744
1	24.684213220	30.106503347	21.656657107

**TS7**

**QM/MM (BS1) = -3371.336675 a.u.**

**QM/MM (BS2+ZPE) = -3373.285174 a.u.**

6	24.350133050	27.715431373	25.226912557
7	25.423423507	26.901576465	25.505308093
1	25.708489185	26.068969384	24.978094160
6	26.027996888	27.372287132	26.611247035
1	26.904630363	26.916850124	27.064783624
7	25.391810744	28.442527115	27.059789186
6	24.344219272	28.677286436	26.206285535
1	23.647624989	29.495863975	26.371009120
6	22.139818017	31.309110939	30.820524633
1	21.917608299	30.495679717	31.530245147
1	22.207401948	32.254706237	31.369888348
6	23.504419386	31.059008906	30.204230457
8	23.633580736	30.049721141	29.400390245
8	24.458753517	31.761281838	30.526323625
6	24.355693417	25.399517258	30.172588319
7	23.170352524	26.083075852	30.326561055
1	22.325145611	25.703388488	30.754769099

6	23.402529931	27.382484436	30.057897237
1	22.654467621	28.166077321	30.116979220
7	24.668040950	27.571569188	29.711055100
6	25.278418114	26.341104071	29.783299865
1	26.338143483	26.211590717	29.580453551
6	26.175961123	36.408122260	32.228553710
1	26.160215512	37.185212102	31.449707148
1	25.241594548	35.842025484	32.175415456
7	27.303029784	35.511401524	32.081161595
1	28.237717745	35.851976239	32.334685996
6	27.224843999	34.251569969	31.628789455
7	26.096899475	33.787591008	31.090742846
1	25.350934305	34.389747531	30.740496295
1	25.962269957	32.794070259	30.906650579
7	28.276261311	33.437171908	31.728656738
1	29.042755051	33.604003313	32.376963025
1	28.241313245	32.521546913	31.272530487
26	25.441009094	29.566010569	28.856010316
8	25.873009249	30.993011079	27.888009970
8	28.151101160	31.031160435	30.266474227
6	28.149595074	29.854466791	29.909505151
8	27.059543658	29.155429741	29.752961964
6	29.436826332	29.154530383	29.516245994
6	29.536485166	27.647221817	29.801065372
6	30.264611566	27.326478538	31.119263737
8	29.664920543	26.670328727	32.001727126
8	31.457711795	27.745702301	31.199228759
1	30.151596265	27.186649837	29.011814158
1	28.542669914	27.178175540	29.793237247
1	30.275795367	29.691598295	29.978614367
1	29.503138464	29.356423437	28.431276801
8	26.542104884	29.970368155	23.582715319
6	25.630579297	30.767159261	23.523131025
7	25.477586645	31.787326556	24.509001908
6	26.462009457	31.827011378	25.566009137
6	24.502289792	32.767980657	24.424418868
7	24.433120081	33.728308895	25.320839455
6	23.577875025	32.709547629	23.338410805
6	23.667967356	31.708436954	22.433442068
7	24.673142155	30.772485964	22.503205865
1	26.093009324	31.324011194	26.699009542
1	26.726493172	32.853063521	25.843698047
1	24.734828929	33.643368655	26.328992309
1	22.936263073	31.615635812	21.631949006
1	22.770632727	33.438051136	23.278612193
1	27.331037728	31.213609379	25.320187111
1	23.692086282	34.423662644	25.170248336
8	28.989604054	32.233884874	27.649258372
1	29.918406929	31.891470956	27.643967012
1	28.646995695	31.929218614	28.506472793
8	24.444209917	33.363496343	27.932408200
1	24.952856528	32.601221734	28.280960289

1	24.253333159	33.990279172	28.694094534
1	23.567795003	27.475247128	24.506963930
1	21.306780027	31.360437565	30.119467856
1	24.393145709	24.313582465	30.258671271
1	26.198197299	36.918226199	33.191552590
1	24.691571874	30.058373575	21.803437090

**Snapshot 2**

**RC2**

**QM/MM (B1) = -3369.665144 a.u.**

**QM/MM (B2+ZPE) = -3371.606048 a.u.**

6	43.336524795	30.520830215	31.354033780
7	42.488813868	29.446448970	31.496181404
1	42.752933345	28.485431219	31.735625489
6	41.242414197	29.860319809	31.202048390
1	40.369234085	29.214547090	31.220731686
7	41.247352373	31.140714181	30.867911032
6	42.547170154	31.574498351	30.954269626
1	42.828588520	32.590139815	30.681007173
6	40.781551461	35.173614218	27.353355980
1	40.572674278	34.823956641	26.329780006
1	40.183519478	36.087719655	27.494766259
6	40.262557969	34.114044671	28.303560528
8	41.039759298	33.435263521	29.047566960
8	39.028638250	33.858825929	28.311152301
6	40.606763956	29.085236464	26.973786987
7	41.313360700	30.153236895	26.458405807
1	41.917708418	30.159997356	25.640565221
6	41.048351480	31.232381407	27.215006298
1	41.501048038	32.200046508	27.036391503
7	40.200070608	30.926712261	28.187541639
6	39.911210507	29.586398583	28.047768793
1	39.217514009	29.091547151	28.721957563
6	35.737281256	38.390099183	29.756346952
1	36.005856024	38.893451159	30.696059736
1	36.502552898	38.631288611	29.017194398
7	35.653493415	36.952688306	29.957335715
1	34.912744757	36.620899151	30.587301116
6	36.455190412	36.033806468	29.409921505
7	37.400301148	36.340833706	28.514974878
1	37.693115865	37.294638961	28.274679452
1	37.983942727	35.570040824	28.191793933
7	36.281658158	34.736139873	29.728041832
1	35.850144936	34.472180440	30.628275522
1	36.996308408	34.098021104	29.390486555
26	39.658013878	32.180923730	29.856339983
8	39.272013614	33.229943288	31.031414572
8	37.830460512	31.309191696	32.370788257
6	37.582199350	30.751782275	31.309092989
8	38.306626563	30.894984931	30.212369817
6	36.451935649	29.743346623	31.203707430

6	35.743153774	29.590423664	29.867601452
6	34.843159706	28.339551244	29.805060808
8	34.290300992	28.135146419	28.693619502
8	34.743563510	27.628696576	30.832551154
1	36.466990382	29.511961103	29.040242163
1	35.121689267	30.470144057	29.626492660
1	35.743271230	29.950915076	32.017243122
1	36.878306766	28.759859069	31.462249675
8	41.815923540	31.355717611	35.117960366
6	42.257515498	32.407286469	34.706895183
7	41.398180150	33.431788763	34.254101272
6	39.951634738	33.153903851	34.369201753
6	41.841989642	34.603648029	33.697565623
7	40.998606570	35.502118056	33.230106237
6	43.259678209	34.826737997	33.637523389
6	44.101566128	33.878368085	34.112780043
7	43.626171227	32.703194825	34.645558640
1	39.811885392	32.432179491	35.179498008
1	39.553411781	32.734340277	33.432199378
1	41.394725512	36.407456116	32.933513169
1	45.184686953	34.009414136	34.064363595
1	43.639533693	35.745019012	33.192036358
1	39.424121942	34.084559867	34.609629753
1	39.970928281	35.387929025	33.139679783
8	38.285026320	35.427691790	32.430095649
1	37.384341157	35.220312756	32.742045045
1	38.472849286	34.705161302	31.795071218
8	35.457096365	34.086915087	32.343923378
1	35.623691147	33.292472925	32.919206026
1	34.503782143	34.246338486	32.492769984
1	44.422465245	30.448199664	31.413409441
1	41.843508862	35.409878789	27.420384740
1	40.726153318	28.070269352	26.594768159
1	34.805686024	38.825714968	29.395186967
1	44.275857646	32.006479657	34.949644181

**TS7**

**QM/MM (BS1) = -3369.626225 a.u.**

**QM/MM (BS2+ZPE) = -3371.567654 a.u.**

6	43.440532080	30.457823943	31.398793629
7	42.596520044	29.382737458	31.548569026
1	42.860172861	28.415371543	31.759342319
6	41.343035468	29.801479209	31.296547223
1	40.471786271	29.153551945	31.328760380
7	41.338430536	31.085768707	30.980393789
6	42.641214550	31.516481067	31.035009284
1	42.918247418	32.534598392	30.764579215
6	40.782574953	35.152604569	27.444010943
1	40.565916225	34.789938334	26.425689646
1	40.193296631	36.073681630	27.572777225
6	40.248725381	34.112907882	28.413395807

8	41.035292020	33.387766883	29.109932605
8	39.009988181	33.925311160	28.471394544
6	40.593458122	29.080625298	27.057557264
7	41.286667253	30.157060021	26.542961198
1	41.870852583	30.176559742	25.711157043
6	41.039220082	31.224374431	27.320868376
1	41.487114293	32.195413710	27.151387127
7	40.214773967	30.902005896	28.309266171
6	39.922438134	29.563417187	28.156102653
1	39.243699329	29.057781346	28.837747102
6	35.721953631	38.398747701	29.761175800
1	35.987475174	38.898369597	30.703606888
1	36.491042933	38.641956565	29.026516464
7	35.633571342	36.960870746	29.954458224
1	34.884773649	36.625632170	30.572874601
6	36.439801773	36.045346564	29.407498831
7	37.389890432	36.357782448	28.520546574
1	37.680644924	37.313218745	28.285822814
1	38.000622743	35.592593845	28.232887012
7	36.266866537	34.745784525	29.718051458
1	35.833634976	34.473768649	30.614747725
1	36.975332848	34.108371706	29.365479676
26	39.744433603	32.119207661	29.987458628
8	39.451216679	33.269213658	31.252420011
8	37.776817148	31.314157580	32.491802130
6	37.570978930	30.757013314	31.419677408
8	38.337575425	30.901165509	30.354512647
6	36.440292527	29.752340810	31.272418047
6	35.774639995	29.594188209	29.914141622
6	34.869858624	28.346502913	29.828335680
8	34.320356428	28.158895449	28.712119983
8	34.765105379	27.619188430	30.843904774
1	36.525613410	29.506440736	29.111739507
1	35.166902647	30.475454478	29.645703826
1	35.705287427	29.966293871	32.060644028
1	36.851795552	28.767320473	31.547507358
8	41.757619045	31.293440482	34.710647118
6	42.218562221	32.378412066	34.432544228
7	41.387522997	33.420705331	33.927847761
6	40.000664391	33.106590806	33.733940860
6	41.866101556	34.663707451	33.566704651
7	41.050138617	35.592460328	33.113371297
6	43.272832365	34.903329985	33.687609307
6	44.074774842	33.930854985	34.183347708
7	43.569867726	32.713027700	34.577246868
1	39.749478334	32.118075762	34.116482654
1	39.704768767	33.029747311	32.391708179
1	41.456401962	36.522596841	32.923470348
1	45.152327462	34.079686637	34.270361360
1	43.681060994	35.860189165	33.366937620
1	39.327536044	33.912838595	34.047344530
1	40.030675276	35.484815436	32.956077599



8	38.309285789	35.542389275	32.302556830
1	37.423854737	35.315484469	32.642208750
1	38.511075696	34.805980855	31.683721085
8	35.430537562	34.093802302	32.325616015
1	35.583846905	33.312946290	32.920409560
1	34.475128238	34.256019111	32.458797969
1	44.527820826	30.387242228	31.428605205
1	41.846645259	35.383428949	27.494427342
1	40.708328120	28.075204422	26.652586817
1	34.792479067	38.835679730	29.396162426
1	44.205932662	32.010880707	34.897221073

**Snapshot 3**

**RC2**

**QM/MM (BS1) = -3446.808270 a.u.**

**QM/MM (BS2+ZPE) = -3448.819020 a.u.**

6	38.731158862	39.615048522	35.771533460
7	39.157576076	38.353465221	35.425596676
1	40.052357160	37.911441110	35.660772428
6	38.217381380	37.777040275	34.662437716
1	38.303622365	36.780397640	34.236708920
7	37.196252692	38.605411028	34.491996699
6	37.496275417	39.759452420	35.179349806
1	36.817911999	40.607758169	35.199093325
6	33.967330723	42.121818180	32.359880231
1	34.347072445	42.070511720	31.330734460
1	32.878908681	42.284222217	32.351758667
6	34.245499676	40.813103977	33.081175190
8	35.249725358	40.151810553	32.580473557
8	33.548735093	40.451787985	34.020135103
6	39.197837881	38.813010671	30.361061951
7	38.770348925	40.123749225	30.434410792
1	39.219885490	40.944570233	30.025034520
6	37.631891719	40.138653084	31.154058634
1	37.059299657	41.029391086	31.387501150
7	37.311814547	38.912887484	31.544516581
6	38.280774740	38.072043812	31.054416452
1	38.241468830	37.003102007	31.236642258
6	28.445085068	38.731952025	32.265216930
1	27.972223655	38.943657104	33.238917102
1	28.786648164	39.684890684	31.837388623
7	29.552598111	37.793623198	32.380644871
1	29.347508917	36.809424949	32.200495769
6	30.788635205	38.113635530	32.798864928
7	31.069384506	39.357023055	33.205259471
1	30.403224657	40.139896900	33.170554974
1	32.024022586	39.610658218	33.484543882
7	31.759152371	37.195864271	32.781027950
1	31.544044766	36.206964657	32.641391489
1	32.676580829	37.400848958	33.190558398
26	35.797773036	38.357119841	32.928428892

8	34.490579091	37.911059277	33.786107613
8	34.354839967	35.454753972	32.495014775
6	35.546610205	35.530445756	32.218232282
8	36.265333230	36.619732638	32.322435199
6	36.332184827	34.359123753	31.659133166
6	35.636373764	33.020814101	31.808762711
6	36.087802921	31.962639422	30.792306801
8	36.615867347	32.354503171	29.731737855
8	35.822492229	30.757708208	31.089553472
1	34.553065891	33.167436617	31.659598371
1	35.744959443	32.625688038	32.828755076
1	37.338703980	34.363331294	32.107481421
1	36.506436916	34.543243526	30.585099294
8	36.751541901	36.523673245	39.170070459
6	36.201204134	37.585002026	38.961758686
7	34.977099643	37.647452879	38.263704668
6	34.427503216	36.367948563	37.785005568
6	34.313523882	38.818819698	37.978688616
7	33.193711479	38.789436729	37.296455780
6	34.890513428	40.045265958	38.450573030
6	36.065995743	40.009310904	39.124885659
7	36.713495411	38.821004613	39.368575719
1	33.351752434	36.319324174	37.992728456
1	34.950918768	35.559411235	38.302028266
1	32.677879874	39.653273624	37.083311821
1	36.541390967	40.929080569	39.475926547
1	34.395196607	40.994713889	38.253773344
1	34.569736954	36.267398985	36.697834199
1	32.762034847	37.941710938	36.856304592
8	31.191282279	40.319638445	36.129406751
1	30.248210352	40.649848779	36.121048910
1	31.164643698	39.599827680	35.478311530
8	31.852308458	36.819341275	35.967747441
1	30.874181793	36.775839656	35.829930683
1	32.227728728	35.993448665	35.588052271
8	33.073533606	34.628354711	34.770702037
1	33.447923764	33.748216813	35.044519274
1	33.666840613	34.941132904	34.055082292
1	39.380008419	40.340446404	36.262307834
1	34.457446267	42.959690082	32.855687399
1	40.161084823	38.494874542	29.962298800
1	27.683422277	38.327107738	31.598855004
1	37.594642969	38.834924896	39.841183068

**TS7**

**QM/MM (BS1) = -3446.767386 a.u.**

**QM/MM (BS2+ZPE) = -3448.776399 a.u.**

6	38.891593482	39.688946865	35.933965977
7	39.314240778	38.420426828	35.614860740
1	40.224376735	37.990321805	35.802207510
6	38.339950283	37.799672139	34.936067773

1	38.413212915	36.785186498	34.552503201
7	37.298640579	38.607051462	34.790219078
6	37.623925987	39.794070889	35.407510329
1	36.939772116	40.637833476	35.425056302
6	33.957480517	41.972645346	32.503161644
1	34.341196730	41.868897268	31.478068445
1	32.871808281	42.153533434	32.475065465
6	34.199299433	40.688984940	33.293213990
8	35.215458687	40.001358952	32.870469335
8	33.450510218	40.376708481	34.213085432
6	39.122062170	38.721901695	30.548868904
7	38.636161730	40.012147193	30.593286429
1	39.031882181	40.831327376	30.133529133
6	37.534551352	40.007915993	31.369944801
1	36.930993378	40.880157741	31.593658372
7	37.294327498	38.786642996	31.828633963
6	38.279745941	37.970842854	31.324602327
1	38.305823674	36.911131244	31.557892652
6	28.439416241	38.733844913	32.244081633
1	27.967588756	38.935473045	33.220658127
1	28.762021070	39.693995137	31.816705805
7	29.564943213	37.815989838	32.354109056
1	29.385183146	36.832627122	32.145485413
6	30.762630557	38.149046225	32.864782098
7	30.973870500	39.373795857	33.354434929
1	30.296009361	40.143510254	33.281173101
1	31.905786810	39.648899435	33.692887665
7	31.764283331	37.261606426	32.857812633
1	31.586427763	36.278607901	32.644716765
1	32.619873327	37.450679177	33.386323103
26	35.870114651	38.243183603	33.285650306
8	34.573904013	37.773525004	34.326984130
8	34.390124580	35.572257764	32.401323266
6	35.618512275	35.524882303	32.357253734
8	36.402535741	36.475409147	32.792096354
6	36.354215921	34.352127839	31.738093275
6	35.559610396	33.059697473	31.776105897
6	36.049765094	31.992382322	30.788974868
8	36.608237569	32.380115376	29.743169682
8	35.783097231	30.787631568	31.087858200
1	34.512901195	33.287382965	31.510285846
1	35.531411435	32.646065495	32.793599773
1	37.343473994	34.249835061	32.208887525
1	36.558907528	34.602946239	30.682304922
8	37.211822002	36.880272892	38.109335277
6	36.482486697	37.837037582	38.265977516
7	35.229235779	37.911048270	37.597890641
6	34.909976562	36.849357320	36.691571868
6	34.359956836	38.982483336	37.724223475
7	33.181554034	38.926800226	37.155259924
6	34.816653805	40.120888371	38.461973333
6	35.998477563	40.056041753	39.125465452

7	36.779356081	38.924217455	39.091531575
1	33.899694780	36.445677498	36.819584617
1	35.704624114	36.103606672	36.666368923
1	32.540894697	39.729312373	37.161585253
1	36.370479268	40.915807655	39.686658200
1	34.211119935	41.024738459	38.501881632
1	34.801556568	37.349536450	35.383116512
1	32.799026692	38.103935325	36.636805271
8	30.882236955	40.182452932	36.315388948
1	29.981278721	40.603647832	36.192853225
1	30.842501306	39.435764280	35.695673123
8	31.845651816	36.860795084	35.909501325
1	30.862190398	36.823180313	35.811821327
1	32.197983511	36.040225541	35.497615747
8	33.079099577	34.695229492	34.680631534
1	33.445212132	33.812332421	34.956514457
1	33.666205410	35.014141405	33.962179564
1	39.556486867	40.438978366	36.362261267
1	34.454897606	42.829260220	32.957974260
1	40.069069578	38.440246808	30.088526841
1	27.680140717	38.318312849	31.581585516
1	37.629002660	38.898771173	39.618243715

#### Snapshot 4

##### RC2

QM/MM (BS1) = -3370.511712 a.u.

QM/MM (BS2+ZPE) = -3372.448429 a.u.

6	36.513129844	33.978991689	42.373119936
7	37.239677146	33.769299028	41.224526323
1	38.256358709	33.689311040	41.127223179
6	36.397099752	33.749850531	40.182499690
1	36.696984610	33.610757482	39.147278398
7	35.154462209	33.945158990	40.600066848
6	35.202465517	34.087953290	41.965959954
1	34.306739724	34.266235180	42.554515473
6	30.573235193	36.355770982	41.476410058
1	30.811665576	37.245542076	40.877557766
1	29.512529677	36.102092543	41.329856134
6	31.416469128	35.172234055	41.018672283
8	32.501387694	35.536571808	40.384233858
8	31.063578511	34.016204020	41.211948923
6	36.160160983	38.005167651	38.632506158
7	35.286401141	38.488297467	39.586732363
1	35.307615095	39.405222032	40.036535671
6	34.367578539	37.531144636	39.823309255
1	33.546199525	37.628576333	40.526391648
7	34.609531628	36.456805297	39.080029135
6	35.728927124	36.740541507	38.332212642
1	36.152110487	36.012329444	37.647716018
6	26.681996493	33.053241172	37.553514837
1	26.348737828	32.157218479	38.106895373

1	26.517331874	33.926845356	38.198473533
7	28.077724110	32.948319887	37.156510608
1	28.271917830	32.466524015	36.277546371
6	29.118880786	33.042538430	38.010928195
7	28.946402563	33.550022243	39.238139941
1	28.083750290	34.013918197	39.543361583
1	29.730926584	33.580921770	39.892049919
7	30.324373156	32.621887053	37.636981673
1	30.521790418	32.145152264	36.733345384
1	31.140272815	32.860358049	38.206282126
26	33.650149606	34.548125170	39.245968505
8	32.778363157	33.175398073	39.196957325
8	32.992071997	34.374558853	36.424116949
6	34.190601659	34.121205286	36.565034834
8	34.769685249	34.099736782	37.727309102
6	35.109902648	33.882639984	35.380162936
6	34.685138097	32.694782446	34.483921978
6	34.895481402	33.106681952	33.020336386
8	33.955329110	33.747696367	32.480344267
8	36.015451627	32.870490180	32.502948534
1	33.627255102	32.461949188	34.657995771
1	35.293932222	31.811909316	34.724666495
1	36.147188266	33.771843471	35.723037799
1	35.059048910	34.814294314	34.792563063
8	35.796981620	29.351046350	41.914331934
6	35.008271633	29.869508300	42.670878639
7	33.690713376	30.182290668	42.257583339
6	33.357049192	29.908896201	40.848565716
6	32.741660724	30.718982446	43.085361403
7	31.540391517	30.987434360	42.606010605
6	33.098246951	30.983275673	44.443061834
6	34.373787106	30.743800139	44.846131070
7	35.311338788	30.219980317	43.992162558
1	33.218404260	30.857156494	40.301654346
1	32.444908791	29.297514192	40.794358423
1	31.343558859	30.944316982	41.612618356
1	34.693810714	30.985321922	45.860098223
1	32.368778960	31.423018490	45.121369111
1	34.185169691	29.347179033	40.408542943
1	30.753059243	31.286840318	43.198100197
8	30.986702730	31.359339316	35.254144274
1	31.715125665	30.686216182	35.196624496
1	31.244481712	32.095391462	34.649016458
8	31.628173043	33.716466692	33.986498174
1	32.010602011	34.083352496	34.810428833
1	32.385418410	33.747380544	33.344369147
1	36.982302261	34.162062580	43.339778928
1	30.745688974	36.610652861	42.522049692
1	37.071540860	38.509308339	38.311108879
1	26.028381050	33.172577918	36.689447179
1	36.267805356	30.168758426	44.279426407

TS7

QM/MM (BS1) = -3370.472795 a.u.

QM/MM (BS2+ZPE) = -3372.413181 a.u.

6	36.578788246	34.000734053	42.444048669
7	37.301280956	33.729012738	41.307971310
1	38.315684839	33.636280865	41.207635980
6	36.457569715	33.669620244	40.268456877
1	36.757095219	33.473944409	39.242627279
7	35.217310246	33.904050395	40.672350624
6	35.271318701	34.112225354	42.029484740
1	34.381060129	34.335011527	42.609990611
6	30.596970963	36.302632855	41.474206771
1	30.837053717	37.180748444	40.858774794
1	29.535530007	36.049096029	41.332861188
6	31.437786499	35.108287022	41.039200005
8	32.522765470	35.436012790	40.408168735
8	31.059172830	33.957622390	41.261712889
6	36.149799713	37.949029300	38.639654242
7	35.255432942	38.429822296	39.573727293
1	35.253403855	39.354342370	40.006456617
6	34.356434013	37.456431227	39.822290340
1	33.526114840	37.551756460	40.514583015
7	34.632813675	36.372754651	39.104646381
6	35.754147712	36.667032569	38.363136792
1	36.205840616	35.934252305	37.702575781
6	26.705090693	33.054916383	37.549215505
1	26.366795637	32.162135530	38.104898755
1	26.537453749	33.931878938	38.188249268
7	28.105350845	32.943869374	37.165334067
1	28.303912781	32.447685898	36.295166889
6	29.131450857	33.019915669	38.040977276
7	28.938239391	33.534549487	39.261856411
1	28.074455191	34.008869015	39.546069595
1	29.706314767	33.560125840	39.932740956
7	30.338463405	32.579229641	37.694382159
1	30.545489091	32.106913614	36.790034820
1	31.144683486	32.767252662	38.296100121
26	33.726604627	34.477107662	39.278812404
8	32.879664838	32.969378368	39.282791494
8	33.070662740	34.347703652	36.563723401
6	34.271022186	34.069212399	36.651272909
8	34.879425360	34.000693311	37.796186559
6	35.146246044	33.858239150	35.429828089
6	34.707042601	32.679776916	34.529237019
6	34.904391186	33.102885894	33.065432633
8	33.957595518	33.743028013	32.535337727
8	36.020891167	32.873193058	32.537707277
1	33.650603799	32.447407529	34.712964438
1	35.317368530	31.794537765	34.758159245
1	36.196374328	33.750559052	35.732717716
1	35.064314319	34.798128992	34.859246694

8	35.944780159	30.534576171	41.591047710
6	35.096396721	30.636263056	42.447688509
7	33.743882629	30.927971395	42.100045631
6	33.423954257	30.936902426	40.702568814
6	32.755199655	31.145058747	43.039213479
7	31.564730829	31.541373829	42.630158381
6	33.074374808	30.934365656	44.412677545
6	34.350163041	30.622574183	44.761118634
7	35.333645996	30.455101992	43.816508965
1	33.201639930	32.156599225	40.050119254
1	32.455084923	30.458752458	40.509482048
1	31.448981688	32.089116643	41.769953039
1	34.635909574	30.549937408	45.811773285
1	32.316059259	31.121279575	45.171061385
1	34.252766687	30.544712524	40.112151988
1	30.753621944	31.555015632	43.265450263
8	30.996628005	31.349879627	35.295559056
1	31.722330831	30.674232254	35.226389504
1	31.259602205	32.096075630	34.705717552
8	31.657380420	33.725443400	34.074716107
1	32.040320388	34.083186631	34.900968558
1	32.412946046	33.755346069	33.429060431
1	37.046630672	34.213950483	43.405157158
1	30.768682217	36.577532181	42.514885844
1	37.045692255	38.475384971	38.310422425
1	26.053008482	33.171557924	36.683622720
1	36.281398184	30.337877177	44.113151221

#### IM10

QM/MM (BS1) = -3370.497094 a.u.

QM/MM (BS+ZPE) = -3372.433476 a.u.

6	36.523982041	34.030838168	42.293123306
7	37.254117912	33.771476572	41.158490538
1	38.263221762	33.617273713	41.080391760
6	36.431157499	33.816444149	40.101364117
1	36.735981047	33.648550342	39.072161116
7	35.199219629	34.107033453	40.493392186
6	35.234934912	34.240812494	41.859934445
1	34.345195829	34.481176109	42.433699242
6	30.584517337	36.259747558	41.524416738
1	30.726876992	37.159521070	40.910478766
1	29.545379345	35.918468424	41.413669624
6	31.517266223	35.169190889	41.028183450
8	32.536227427	35.603132548	40.371140282
8	31.253047737	33.967481396	41.212941485
6	36.191204203	38.097061624	38.552211003
7	35.315064530	38.581002595	39.504277727
1	35.350524792	39.488672120	39.972372136
6	34.371348784	37.642685574	39.709304599
1	33.547790470	37.740350999	40.409941738
7	34.598149967	36.580647363	38.942187029

6	35.734010528	36.851977647	38.214162554
1	36.152682316	36.123404061	37.527352711
6	26.702596607	33.055917200	37.493118097
1	26.409148941	32.132143997	38.023100245
1	26.517460448	33.904713682	38.164355296
7	28.090838286	33.013107412	37.062457834
1	28.282280840	32.567054521	36.164737503
6	29.156403152	33.145462056	37.880719164
7	29.003354931	33.681171754	39.103311399
1	28.134420763	34.115009588	39.433213625
1	29.773380495	33.655503853	39.766275536
7	30.355326067	32.748340026	37.475703064
1	30.519027197	32.201244640	36.605337932
1	31.204271776	33.006194732	38.001306096
26	33.710163333	34.726921012	39.107014640
8	32.694073254	33.235216153	39.043052202
8	33.098984571	34.482284365	36.345887274
6	34.281932598	34.163563453	36.502594909
8	34.845235430	34.127431532	37.669004507
6	35.197281147	33.863969627	35.329367233
6	34.732172678	32.679246533	34.448623136
6	34.922115444	33.086742204	32.981841059
8	33.972871214	33.720021366	32.449130038
8	36.040221308	32.861637743	32.454001110
1	33.674624165	32.462529939	34.645271831
1	35.334372869	31.789533998	34.682007543
1	36.226592667	33.715317975	35.681981873
1	35.188153516	34.787331173	34.725928355
8	35.900884864	30.442978928	41.789318016
6	35.080794899	30.530964605	42.672641720
7	33.705255061	30.809141617	42.349176195
6	33.396839072	30.831709678	41.001724863
6	32.739762645	31.050472759	43.316877555
7	31.543234744	31.470367905	42.932785944
6	33.095684670	30.839675975	44.675143180
6	34.378225649	30.520478090	44.997064360
7	35.342821125	30.359580340	44.030259828
1	32.228192377	33.219519396	39.904092247
1	32.353272215	30.787412499	40.707580223
1	31.412382482	32.009956674	42.075638188
1	34.682188961	30.445122572	46.040126720
1	32.359224364	31.035360282	45.452693041
1	34.217355564	30.754785906	40.297622317
1	30.727681474	31.448050638	43.561406901
8	30.987281153	31.349744592	35.178783407
1	31.718499964	30.677638520	35.154095674
1	31.269294171	32.089156172	34.589162987
8	31.661727643	33.725590602	33.965934600
1	32.054758391	34.109464404	34.777364892
1	32.415460321	33.742857184	33.318930888
1	36.984057526	34.179338216	43.270029446
1	30.765624737	36.547285679	42.560075591



1	37.121961011	38.583131597	38.259815617
1	26.031958568	33.179335924	36.642777127
1	36.301071322	30.250650685	44.294576656

**TS8**

**QM/MM (BS1) = -3370.487244 a.u.**

**QM/MM (BS2+ZPE) = -3372.420750 a.u.**

6	36.653754237	34.040814525	42.473578267
7	37.381586154	33.802450644	41.332653243
1	38.392729030	33.682545853	41.235591610
6	36.548664101	33.823309658	40.282453895
1	36.850592324	33.657033218	39.251838218
7	35.315170259	34.080636208	40.686105067
6	35.356116000	34.212052864	42.050214248
1	34.465185082	34.431684696	42.630285939
6	30.588356306	36.316894827	41.515039426
1	30.789165631	37.210417693	40.907180817
1	29.532897768	36.033730505	41.392415336
6	31.460679797	35.175593600	41.025089594
8	32.562404223	35.527985695	40.475627796
8	31.071120451	33.994010665	41.128333420
6	36.191701307	38.014588525	38.593209000
7	35.308600481	38.499852576	39.537794422
1	35.326170410	39.417969182	39.984471160
6	34.390141752	37.542388891	39.771279997
1	33.567492157	37.635912709	40.473410496
7	34.640948024	36.466162812	39.032905366
6	35.766090210	36.747448593	38.293252539
1	36.196988862	36.012559832	37.620101401
6	26.716383473	33.034353143	37.498757591
1	26.397074180	32.123091367	38.035061424
1	26.531983612	33.893792247	38.156334540
7	28.117192260	32.958186693	37.109275738
1	28.325392175	32.479440829	36.231805364
6	29.143985532	33.060758955	37.980124433
7	28.944022732	33.592800329	39.191384755
1	28.073625245	34.061008558	39.466058117
1	29.700951365	33.632885923	39.874976968
7	30.354068006	32.624610977	37.633071704
1	30.555173755	32.123337260	36.740713987
1	31.168195488	32.838865394	38.209444309
26	33.793352362	34.548801035	39.306156664
8	32.962560507	32.872101778	39.576219543
8	33.041190065	34.246575240	36.568003704
6	34.251185839	34.003591705	36.659495196
8	34.877673344	33.995576924	37.793005087
6	35.124162636	33.795131308	35.432339151
6	34.682300501	32.634028384	34.512860877
6	34.887075760	33.078263324	33.056985070
8	33.943401852	33.726774514	32.530752692
8	36.006697437	32.858001163	32.531264634

1	33.624368043	32.405013267	34.690870166
1	35.288325828	31.742530416	34.730167430
1	36.173391335	33.680814237	35.735182999
1	35.049463436	34.743918069	34.874474087
8	35.925106270	30.611125835	41.555674486
6	35.084254739	30.657342276	42.421806005
7	33.695672613	30.868214420	42.071173107
6	33.399461727	30.891271461	40.715167482
6	32.702982551	31.017102090	43.031649843
7	31.466999639	31.291123103	42.636672923
6	33.059308803	30.868183727	44.397253113
6	34.350960183	30.614833542	44.740300060
7	35.330255171	30.479217229	43.782692782
1	32.247182024	33.125316971	40.204250526
1	32.394039183	30.604042538	40.421346503
1	31.286663039	31.741175918	41.743510475
1	34.653011789	30.564086132	45.787120351
1	32.300401999	31.025674222	45.161793596
1	34.240929553	30.760759878	40.046856580
1	30.669996185	31.290236911	43.290578271
8	30.973018450	31.333990297	35.272868359
1	31.696498695	30.654332078	35.216617167
1	31.244843489	32.076194378	34.680703872
8	31.644372333	33.705158396	34.068646793
1	32.035697395	34.035742430	34.903551848
1	32.399676906	33.739157325	33.422508100
1	37.113682848	34.241441823	43.441194764
1	30.775981995	36.590325348	42.553355214
1	37.102879774	38.525666784	38.282371205
1	26.060519302	33.158114075	36.637019382
1	36.279682215	30.367546595	44.076104527

**PD**

**QM/MM (BS1) = -3370.577826 a.u.**

**QM/MM (BS2+ZPE) = -3372.485246 a.u.**

6	36.890681544	33.969772802	42.641096544
7	37.632200494	33.736128521	41.509184762
1	38.647174813	33.697476721	41.401087704
6	36.799788774	33.668936393	40.457985434
1	37.122240586	33.494292248	39.434138394
7	35.553298915	33.856919959	40.852921009
6	35.586471016	34.041244725	42.211742677
1	34.683999223	34.236859450	42.783377780
6	30.623016755	36.180831837	41.574976518
1	30.823862275	37.052008002	40.932952744
1	29.565749218	35.902717627	41.469415340
6	31.499481771	35.034175986	41.107662412
8	32.676015271	35.319471433	40.750006649
8	31.004153477	33.871055416	41.028177936
6	36.255938106	38.023907982	38.672778234
7	35.386487641	38.516784947	39.624116815

1	35.391793659	39.448258642	40.041263880
6	34.498283145	37.537247039	39.907518792
1	33.690176425	37.639906214	40.626611294
7	34.756187086	36.447094116	39.200677007
6	35.852477597	36.735991170	38.425592265
1	36.283250638	35.994970922	37.756408147
6	26.657029228	32.968631906	37.473096088
1	26.349690485	32.039957325	37.984050087
1	26.487804064	33.804737357	38.161653851
7	28.045238082	32.903187841	37.046988062
1	28.237803514	32.387889054	36.186336894
6	29.116860181	33.202392304	37.802524515
7	28.993471149	33.914723228	38.928962609
1	28.097622111	34.277424104	39.273783606
1	29.734779957	33.863029924	39.630790555
7	30.325188893	32.780876754	37.419584335
1	30.480386542	32.151768377	36.602822403
1	31.161802820	33.284477755	37.711587268
26	34.028024295	34.401750165	39.548470425
8	33.005141061	32.448361070	40.316049607
8	32.950138859	33.967206261	36.688534226
6	34.183208111	33.820564535	36.759425536
8	34.826469238	33.761733990	37.873402013
6	35.028195617	33.758778239	35.496667266
6	34.682366018	32.586758314	34.551389505
6	34.908228446	33.046021612	33.103153334
8	33.970236091	33.700856444	32.572290709
8	36.029715404	32.824191224	32.582955721
1	33.630035626	32.307544569	34.689743358
1	35.321906537	31.722476027	34.783140390
1	36.094075904	33.741951074	35.762556364
1	34.834830821	34.707851665	34.970707272
8	35.782382191	30.611768780	41.584150615
6	34.973680554	30.721011676	42.476043471
7	33.615244064	31.040556549	42.204193059
6	33.228564437	31.156858468	40.754676729
6	32.654975501	31.149797799	43.179704499
7	31.410872152	31.460212396	42.858609110
6	33.037726489	30.925640227	44.535316241
6	34.336669836	30.648316232	44.820312983
7	35.280612657	30.524134228	43.833255763
1	32.126524166	32.869960786	40.584339795
1	32.337324929	30.518007970	40.632746279
1	31.147180504	31.915102472	41.988580344
1	34.668428077	30.555535437	45.855687414
1	32.304823630	31.062651112	45.328324941
1	34.068586234	30.730353496	40.198850674
1	30.634195031	31.372834606	43.530583543
8	30.932821368	31.256738372	35.206406581
1	31.662921483	30.582506559	35.192330164
1	31.227416978	31.995295612	34.621905126
8	31.661209430	33.656151714	34.089322928

1	32.044823613	33.917485756	34.952209087
1	32.427874316	33.706466744	33.457166352
1	37.329187071	34.244027399	43.600557138
1	30.820938142	36.502685843	42.597377830
1	37.153979246	38.540521795	38.334104948
1	25.990470887	33.121327266	36.624301988
1	36.240039045	30.409632496	44.090865651

**Snapshot 5**

**RC2**

**QM/MM (BS1) = -3369.803340 a.u.**

**QM/MM (BS2+ZPE) = -3371.752763 a.u.**

6	27.876122977	22.152655995	36.130907149
7	29.183237979	22.358925482	36.508160822
1	29.799117650	21.655490652	36.934042270
6	29.504247164	23.634600630	36.227433540
1	30.479623384	24.072597628	36.423391029
7	28.470194332	24.267193385	35.684773977
6	27.439538141	23.352999042	35.615300068
1	26.474859653	23.633963030	35.196291141
6	24.099329271	26.985660418	35.126197645
1	24.133967435	27.667703363	35.987031771
1	23.849179448	27.584387406	34.236890163
6	25.459584390	26.336041305	34.884707708
8	26.437929696	26.899175525	35.567146209
8	25.620843002	25.389351631	34.129760695
6	28.744303739	26.173446499	39.707386787
7	27.401683060	26.480281169	39.614320067
1	26.757370405	26.635021021	40.386249780
6	27.103406615	26.668943315	38.314817438
1	26.117168578	26.946849944	37.955948653
7	28.182662032	26.483498466	37.566197104
6	29.217300939	26.181294949	38.422268651
1	30.222889490	26.002656860	38.054411928
6	26.289576574	31.862606052	30.619661464
1	26.341992448	31.468355883	29.593720258
1	25.368802048	31.498689016	31.096929880
7	27.477494988	31.516594146	31.407110258
1	28.219075306	32.215652549	31.455893881
6	27.748558922	30.395415344	32.094167396
7	26.917613859	29.351437820	32.135466114
1	26.044766155	29.298064754	31.600133168
1	27.211253854	28.515222289	32.633307269
7	28.899805173	30.352578896	32.776706662
1	29.499006108	31.174946779	32.757147763
1	29.201177305	29.568028877	33.361629681
26	28.317247709	26.407441334	35.449018347
8	28.370287906	26.541500113	33.834497698
8	30.500407169	28.848917758	34.587366695
6	30.891616506	27.886472657	35.249226868
8	30.106947062	26.991273173	35.783328836
6	32.363935708	27.618628000	35.539356201

6	33.399286389	28.604400128	34.981805658
6	34.651678686	27.886156151	34.413367569
8	34.420325647	26.844381787	33.730771654
8	35.784833023	28.363897673	34.638029511
1	33.703883058	29.351209474	35.729971307
1	32.950280219	29.167744029	34.145565823
1	32.551154507	26.636887181	35.085627552
1	32.465963913	27.476151550	36.627949723
8	29.543475883	21.201387705	31.443638014
6	28.373856466	21.347103894	31.706397722
7	27.728400348	22.595948507	31.520986487
6	28.579329208	23.726536049	31.105120179
6	26.391067722	22.795099306	31.731536452
7	25.870902695	23.995379539	31.556563084
6	25.591710307	21.681349888	32.135872972
6	26.202370126	20.495436499	32.392570039
7	27.555675688	20.336340127	32.230538791
1	28.619892290	24.484969884	31.904674865
1	28.186008719	24.172255727	30.179336716
1	26.458140478	24.815581832	31.453053040
1	25.631401728	19.636947179	32.749900866
1	24.517699772	21.802761119	32.269636989
1	29.587387689	23.343819234	30.922126474
1	24.884787781	24.188818562	31.785866826
8	26.647010712	29.483422008	36.635842306
1	27.462083981	29.944892329	36.303736708
1	26.565727573	28.659565041	36.125337167
8	31.852331874	26.697729716	32.614957265
1	31.564276202	27.611352749	32.751517677
1	32.775474510	26.690509161	32.964278518
1	27.354783589	21.214048615	36.318760156
1	23.321336800	26.242348568	35.300216414
1	29.235788905	25.871784087	40.632324323
1	26.252043122	32.951283761	30.581722011
1	27.992827119	19.489404957	32.533147357

#### TS7

**QM/MM (BS1) = -3369.767004 a.u.**

**QM/MM (BS2+ZPE) = -3371.719255 a.u.**

6	27.809743914	21.829926174	36.205695775
7	29.118068324	22.042902639	36.569311804
1	29.741807738	21.360936519	37.015874313
6	29.443345044	23.305898731	36.248146739
1	30.421606025	23.740999505	36.432272724
7	28.409192663	23.923845866	35.692708180
6	27.372606125	23.014361845	35.661491770
1	26.395456691	23.298680272	35.277717877
6	24.128941035	26.907890598	35.172860167
1	24.198316484	27.590743179	36.033443114
1	23.892991890	27.538122381	34.300636024
6	25.474242891	26.236473806	34.916770150

8	26.528299607	26.993780537	35.130385654
8	25.582262234	25.080737592	34.518730046
6	28.678978120	26.058289761	39.515302468
7	27.343823497	26.392269092	39.424803506
1	26.717561448	26.606572177	40.196974079
6	27.033672156	26.512963823	38.115842485
1	26.045251876	26.804687947	37.772551699
7	28.090243253	26.255841990	37.360198143
6	29.127179794	25.980886592	38.221601130
1	30.124551927	25.757371542	37.853994337
6	26.272428760	31.885694267	30.563108561
1	26.275974453	31.503340368	29.531826295
1	25.370016976	31.523947525	31.074468328
7	27.485222653	31.510074773	31.292552771
1	28.270873403	32.157491952	31.244672824
6	27.699684016	30.455432882	32.093875258
7	26.813719527	29.464985054	32.225824007
1	25.976817791	29.368477073	31.641338962
1	26.984861275	28.733471026	32.906984402
7	28.840715521	30.429485829	32.790912748
1	29.445289469	31.247877871	32.743107733
1	29.167739600	29.631744231	33.347784526
26	28.270743120	25.988809201	35.117437751
8	28.282137581	25.613541827	33.408781761
8	30.393372212	28.770225836	34.448480782
6	30.776783953	27.761685857	35.045763195
8	29.996055493	26.782265093	35.400350206
6	32.227448809	27.564424776	35.481377187
6	33.287775889	28.527835890	34.919025440
6	34.556449059	27.800149862	34.395378982
8	34.348700850	26.736580417	33.737442325
8	35.682334559	28.293938504	34.623332719
1	33.583264930	29.290190337	35.654945821
1	32.865888439	29.079556746	34.061385057
1	32.485310649	26.544041455	35.177427490
1	32.224316122	27.564786353	36.585772079
8	29.669255389	21.439353025	31.686567831
6	28.484072001	21.524620213	31.889860479
7	27.812006417	22.780994197	31.797537285
6	28.619942413	23.948438850	31.555221228
6	26.445544413	22.913426614	31.905150146
7	25.923377112	24.124097385	31.864275527
6	25.660136212	21.732329146	32.058332640
6	26.291773405	20.545091995	32.260547819
7	27.660309371	20.443383805	32.230895467
1	28.561937702	24.769786521	32.555899676
1	28.243875082	24.546842833	30.713363567
1	26.499647680	24.927909816	32.121449240
1	25.725110907	19.637924643	32.477905628
1	24.574071908	21.805131288	32.102678392
1	29.676305141	23.682582179	31.470929965
1	24.907453744	24.260062907	31.971390829

8	26.682418369	29.392115500	36.595580094
1	27.497766917	29.879320574	36.303756087
1	26.628314118	28.610053313	36.015929628
8	31.829454431	26.581084678	32.566225279
1	31.598352000	27.519697530	32.622290090
1	32.738846491	26.550161004	32.952819661
1	27.266107500	20.915713648	36.443902040
1	23.326717268	26.191969820	35.351638785
1	29.182748485	25.821010588	40.452309055
1	26.247677880	32.975167123	30.540667440
1	28.094795272	19.591406455	32.523006902

**Dioxygen activation step reaction states cartesian coordinates for AlkB-dsDNA**

**RC1**

**QM/MM (BS1) = -3412.915331 a.u.**

**QM/MM (BS2+ZPE) = -3414.926892 a.u.**

6	44.351819855	30.348043233	23.773765187
7	44.848874081	31.121427882	24.804058722
1	45.801263582	31.507500225	24.871066448
6	43.869955417	31.282940584	25.716041460
1	43.991825758	31.830645466	26.647504646
7	42.760615755	30.655116255	25.328300790
6	43.050390983	30.066504828	24.111726364
1	42.309251115	29.479193405	23.574289214
6	38.799762279	27.301256167	23.895628902
1	38.525344584	26.344675885	24.369584637
1	37.863991083	27.722202651	23.495658671
6	39.192737115	28.236747487	25.049625229
8	40.374618437	28.780152196	25.105501754
8	38.332156714	28.432115817	25.909685428
6	44.121528266	27.420440304	28.292152647
7	43.569308094	26.579396692	27.347673410
1	43.847022436	25.617777018	27.120093416
6	42.572583505	27.244276610	26.735013640
1	41.971055433	26.835615235	25.928593186
7	42.444427983	28.460734765	27.243682529
6	43.404275295	28.588555868	28.220066111
1	43.508174088	29.506127585	28.793541978
6	33.383600999	32.044620588	25.929921161
1	33.357730084	33.141262711	25.872465302
1	32.723641535	31.681948204	25.128348764
7	34.700359659	31.505984275	25.669825855
1	34.744457909	30.621333257	25.147507822
6	35.903213593	31.942306485	26.083578274
7	36.066906616	33.084130465	26.766013504
1	35.342371060	33.807223855	26.810718996
1	37.017334467	33.332392173	27.052663703
7	36.949893615	31.157719334	25.819801683
1	36.786167815	30.308514709	25.270980893
1	37.916748610	31.434085713	26.000808105

26	41.095966171	29.967759242	26.517693794
6	39.798328115	32.330492066	27.576931579
8	38.946615205	33.179821492	27.815446640
8	39.839629325	31.554557603	26.542425496
6	40.992412724	32.105112417	28.541867396
8	41.892536266	31.362418514	28.135550197
6	41.048021739	32.862309184	29.840968363
6	42.082413165	32.355451123	30.852514921
6	42.010613009	33.097943838	32.213062665
8	41.533337841	32.456391615	33.183836323
8	42.442443124	34.278504641	32.248606109
1	43.092929553	32.488826735	30.433171718
1	41.920777816	31.280719828	31.019393893
1	40.028214734	32.852938730	30.259891209
1	41.233353968	33.925318537	29.591677798
8	40.084527131	29.368527763	28.270174635
8	39.563639534	30.184155446	29.083592892
8	44.872894760	35.313321097	23.973951458
6	44.094829628	34.718441608	23.251651279
7	42.741775145	34.593958751	23.622222946
6	42.347944741	35.315456274	24.832415225
6	41.831139153	33.834378114	22.933172016
7	40.593831123	33.725941229	23.387132652
6	42.258092079	33.170910465	21.751900497
6	43.542536414	33.331068044	21.339357284
7	44.422695765	34.116071748	22.044479052
1	43.001744926	36.185468567	24.936704006
1	42.439944195	34.669959188	25.720714598
1	40.298386713	34.114339597	24.272419042
1	43.908868048	32.805998904	20.454441487
1	41.568742979	32.550690233	21.182959859
1	41.317580984	35.670153582	24.728846088
1	39.901954382	33.157552205	22.875261965
1	44.966096224	29.969105406	22.956980034
1	39.459235318	27.065677087	23.060365388
1	45.023089339	27.191367326	28.860290412
1	32.935712530	31.714165901	26.867078003
1	45.363887229	34.205086362	21.718584101

#### TS1

**QM/MM (BS1) = -3412.895796 a.u.**

**QM/MM (BS2+ZPE) = -3414.905834 a.u.**

6	44.364245735	30.329393640	23.759372661
7	44.846202514	31.122683524	24.783071203
1	45.794526129	31.519036157	24.848011010
6	43.863657769	31.279775469	25.690958776
1	43.960334473	31.840426746	26.617985356
7	42.767769591	30.626690949	25.304468489
6	43.067808017	30.027742441	24.096917942
1	42.336843232	29.423470866	23.565275420
6	38.826579929	27.354731349	23.935751804



1	38.542236531	26.397547571	24.403399455
1	37.895057729	27.782736813	23.532224698
6	39.215930340	28.281184946	25.103012636
8	40.407297884	28.795209141	25.199419322
8	38.338787754	28.489319761	25.942831895
6	44.170759213	27.396924122	28.306512538
7	43.614882162	26.553426742	27.365408002
1	43.882291428	25.587644691	27.144706148
6	42.631485325	27.225438953	26.738908554
1	42.024395187	26.825503066	25.933430035
7	42.518694279	28.445898297	27.235375155
6	43.468272737	28.572908309	28.220164517
1	43.574479585	29.496802387	28.783722740
6	33.327509115	32.045771655	25.906301335
1	33.286637274	33.142167594	25.851753834
1	32.656202091	31.677372281	25.117010020
7	34.644615333	31.523855697	25.618061667
1	34.690881750	30.636590717	25.100458874
6	35.848719258	31.973904865	26.012252500
7	36.008799017	33.119356324	26.689252481
1	35.276148242	33.833828066	26.750869097
1	36.956663920	33.380706600	26.968295270
7	36.898190823	31.196861839	25.735789535
1	36.727906680	30.348798438	25.186972877
1	37.869005688	31.478726233	25.879960082
26	41.176522803	29.995391169	26.581367285
6	39.665951605	32.269524036	27.536665006
8	38.894100803	33.174876479	27.802518840
8	39.755821058	31.561437923	26.469273436
6	40.795767220	31.709803147	28.627546383
8	41.859057116	31.316236294	27.977305662
6	40.918849694	32.586359225	29.873170296
6	42.071354705	32.225740434	30.824088297
6	42.015027067	33.017483612	32.161579836
8	41.485141049	32.423805007	33.138018977
8	42.491639071	34.180160701	32.179006172
1	43.028496936	32.435919202	30.321666107
1	42.028451945	31.149559426	31.046809794
1	39.951763365	32.540889352	30.399531089
1	41.022148776	33.626797670	29.525533224
8	40.287975125	29.421252560	28.295940545
8	39.998245538	30.467679345	29.049142078
8	44.897381034	35.309794617	23.986222095
6	44.115188744	34.718287300	23.265765008
7	42.764824328	34.589139984	23.644167334
6	42.376066252	35.299433237	24.863481639
6	41.849960538	33.837255177	22.952797925
7	40.616497918	33.721998414	23.415749319
6	42.268083898	33.189108696	21.759719128
6	43.551362582	33.348473001	21.343605705
7	44.436997002	34.123473599	22.052732836
1	43.035594801	36.164022103	24.975493487

1	42.463738693	34.643296835	25.744543148
1	40.333649646	34.086626780	24.315375238
1	43.912299059	32.829628817	20.452777066
1	41.574491209	32.576469664	21.187882948
1	41.347820675	35.661786448	24.763095381
1	39.920715715	33.159948352	22.902585058
1	44.985827154	29.952211094	22.947315284
1	39.484865748	27.114759341	23.100802378
1	45.072967464	27.168286990	28.873797873
1	32.902129460	31.708941297	26.851639786
1	45.377902129	34.209704503	21.725266392

**IM1**

**QM/MM (BS1) = -3412.989066 a.u.**

**QM/MM (BS2+ZPE) = -3414.994183 a.u.**

6	44.403438222	30.402143188	23.709171192
7	44.904872459	31.169541873	24.741349382
1	45.864401047	31.531520215	24.822957843
6	43.910514726	31.365776805	25.633447443
1	44.033171832	31.921771847	26.560725610
7	42.791584689	30.772039265	25.230655147
6	43.087215243	30.165926904	24.025236079
1	42.338947701	29.589682228	23.484598819
6	38.777161172	27.278493920	23.840535973
1	38.488878615	26.337601441	24.336101973
1	37.846025790	27.720654924	23.451185927
6	39.258450843	28.230269739	24.950526566
8	40.402074529	28.800382605	24.868890651
8	38.473935755	28.402976339	25.904336394
6	43.967767894	27.479422056	28.235891109
7	43.439868963	26.650815200	27.267239669
1	43.756579149	25.711412291	27.004763378
6	42.401616930	27.295473985	26.696241378
1	41.822655580	26.897511881	25.867675121
7	42.214864103	28.483504035	27.255122468
6	43.191673811	28.612985585	28.218463546
1	43.267671199	29.513864453	28.820901913
6	33.358158585	31.888372544	25.944919494
1	33.333439578	32.982371167	25.835969895
1	32.706043365	31.489941071	25.154816242
7	34.676436148	31.333431634	25.722476959
1	34.738908004	30.461433508	25.179485940
6	35.856463365	31.753060985	26.205097321
7	35.949630688	32.908015890	26.893562150
1	35.233888814	33.640629464	26.842235386
1	36.852253348	33.195018219	27.248965607
7	36.921179436	30.977089580	26.031993642
1	36.813246074	30.125409744	25.473797398
1	37.886582448	31.240963926	26.298539476
26	41.075496675	30.095369860	26.320679554
6	38.786072385	35.058234003	26.710541584

8	38.084899173	34.993403700	27.636880630
8	39.497906824	35.122210485	25.796721024
6	40.728587713	31.833741380	28.760557122
8	41.699817998	31.257117226	28.285479309
6	40.617589933	32.347548618	30.179406345
6	41.839431636	33.121985768	30.678298875
6	41.831125130	33.410347681	32.199998205
8	41.301322695	32.561858609	32.960578680
8	42.394166289	34.473838977	32.561222803
1	41.950028485	34.081680026	30.151213258
1	42.750359448	32.536717049	30.460833231
1	40.486366067	31.464955983	30.828330637
1	39.699400058	32.946802085	30.268691930
8	39.636265571	31.469194640	26.743808550
8	39.613085168	32.030941394	28.068989446
8	45.020920813	35.299577824	23.849431522
6	44.237755667	34.696136501	23.138029701
7	42.884816730	34.594090252	23.503455818
6	42.483084164	35.356143919	24.683353455
6	41.966987854	33.830014074	22.828955367
7	40.725543304	33.761210173	23.275633756
6	42.392783390	33.127262729	21.670882931
6	43.676880574	33.272861214	21.255304739
7	44.561452358	34.067578860	21.944622914
1	43.205143668	36.163345921	24.824506041
1	42.457827751	34.710203583	25.575653932
1	40.424882476	34.200906142	24.136716331
1	44.037826036	32.731666064	20.379326729
1	41.700101013	32.496276831	21.118626124
1	41.496256586	35.791033176	24.510909285
1	40.026860311	33.184198582	22.783348025
1	45.017326361	29.996414598	22.905061131
1	39.423512906	27.024083189	23.000552679
1	44.865123114	27.253750396	28.811992865
1	32.899289593	31.606015079	26.892432468
1	45.502863309	34.152520662	21.618275230

## TS2

**QM/MM (BS1) = -3412.976382 a.u.**

**QM/MM (BS2+ZPE) = -3414.994860 a.u.**

6	44.388843439	30.385732597	23.715280443
7	44.880767070	31.157011173	24.749903474
1	45.837592648	31.527723834	24.832617508
6	43.886492143	31.343164183	25.641019726
1	43.999936558	31.898538473	26.569568818
7	42.774288102	30.734685923	25.234330537
6	43.076301677	30.130673714	24.028503039
1	42.334006646	29.547520285	23.487633873
6	38.808986056	27.298401182	23.833422243
1	38.500004720	26.356315043	24.313920583
1	37.887892087	27.762797224	23.445710165

6	39.291286011	28.217622302	24.971650888
8	40.451911606	28.767110623	24.932847505
8	38.493042462	28.374831941	25.911726767
6	43.950358820	27.472008410	28.259174892
7	43.431804894	26.650280207	27.278931216
1	43.758062640	25.717128739	27.005427569
6	42.382663357	27.285262584	26.720112575
1	41.809909642	26.892071627	25.885649505
7	42.178817406	28.461968447	27.298300834
6	43.155687551	28.592609869	28.262568977
1	43.212922976	29.485506495	28.878857247
6	33.361671746	31.914914948	25.941458045
1	33.348795958	33.010356823	25.848849116
1	32.700255891	31.536953236	25.148885414
7	34.671553980	31.348343791	25.699996102
1	34.717023323	30.482862784	25.146128331
6	35.860000831	31.721852143	26.203173497
7	35.984625190	32.857704998	26.917724055
1	35.291956592	33.612781368	26.877041734
1	36.891620236	33.099521083	27.296630941
7	36.898588288	30.915697558	26.015905865
1	36.754843496	30.090361525	25.426231512
1	37.878774639	31.135232799	26.272578585
26	41.085800502	30.110035520	26.366911235
6	38.780023709	35.022617543	26.752551410
8	38.066755088	34.997026992	27.670537732
8	39.499960476	35.053394810	25.842337262
6	40.691354458	31.873958460	28.728519419
8	41.637977763	31.183020933	28.305224722
6	40.635326161	32.397419345	30.161535706
6	41.898703631	33.088810509	30.674822922
6	41.876332372	33.391960041	32.194846474
8	41.329463246	32.556222474	32.957725605
8	42.441284427	34.455742787	32.554990280
1	42.079581866	34.036696240	30.146357903
1	42.772006708	32.442198282	30.477297226
1	40.439763401	31.519479544	30.801266534
1	39.760347529	33.057529323	30.254663441
8	39.644126086	31.181931230	26.588518602
8	39.645344708	32.159470567	28.030222625
8	45.005185251	35.303043887	23.853542086
6	44.221681029	34.702322615	23.140459894
7	42.868090771	34.602394276	23.504666199
6	42.466155387	35.367155145	24.683274402
6	41.949640842	33.839329282	22.829421006
7	40.708423139	33.769242824	23.275804469
6	42.376180020	33.136756010	21.670912988
6	43.660987989	33.280298482	21.256635366
7	44.546314423	34.073167797	21.947298609
1	43.180452067	36.182742098	24.816244145
1	42.451375022	34.726939269	25.579753457
1	40.406904679	34.202442598	24.140307900

1	44.022279829	32.738145066	20.381218453
1	41.682825381	32.507991106	21.116920628
1	41.473629544	35.790312976	24.514580823
1	40.010267561	33.194009724	22.780386464
1	45.008399389	29.986843962	22.912095781
1	39.452227905	27.038553398	22.992716369
1	44.853863747	27.250623509	28.827272514
1	32.904623705	31.623066932	26.886973327
1	45.488170872	34.156588066	21.621845097

**IM2**

**QM/MM (BS1) = -3412.986491 a.u.**

**QM/MM (BS2+ZPE) = -3414.995616 a.u.**

6	44.400980310	30.385265503	23.704762098
7	44.885473652	31.161639161	24.738407887
1	45.841088996	31.536668184	24.823504325
6	43.888188902	31.350778895	25.623909187
1	43.995139402	31.916259587	26.547075160
7	42.780849360	30.735544497	25.212366046
6	43.088208847	30.126535966	24.010761959
1	42.351067950	29.543645099	23.463156181
6	38.808465382	27.318969058	23.863555459
1	38.491882844	26.379265238	24.343321438
1	37.892016437	27.790197578	23.471709707
6	39.290132902	28.237639400	24.997229024
8	40.439728533	28.821593987	24.927721238
8	38.525923679	28.387964495	25.960951586
6	43.918311402	27.519890034	28.211569493
7	43.409919997	26.687902508	27.234297692
1	43.729199074	25.745461180	26.985602319
6	42.388910045	27.332434121	26.635538858
1	41.826086680	26.927751477	25.800756631
7	42.192738991	28.523674255	27.184458652
6	43.142346839	28.653442535	28.174561895
1	43.187170290	29.550348769	28.785837205
6	33.368101651	31.945583309	25.937752080
1	33.344483534	33.041313475	25.852160284
1	32.708364812	31.565702970	25.144554093
7	34.683906077	31.395907417	25.688384974
1	34.735066563	30.527820488	25.139839404
6	35.876441151	31.809246427	26.149113188
7	35.994629926	32.942799489	26.862588315
1	35.284297297	33.682207952	26.853413980
1	36.902835105	33.191933899	27.235795978
7	36.932797057	31.030737686	25.924563178
1	36.779436865	30.208667286	25.332058129
1	37.916809994	31.325576627	26.051005065
26	41.032119497	30.208313626	26.276412612
6	38.813187390	35.057623883	26.832810035
8	38.025997988	35.072184105	27.688003693
8	39.597141338	35.065537819	25.976400709

6	40.464990243	31.835646635	28.658750791
8	41.276903393	30.956098891	28.194114603
6	40.552398286	32.154465217	30.157348078
6	41.746822421	33.026172729	30.573519706
6	41.829487909	33.341626003	32.093963049
8	41.327374345	32.520218001	32.901432385
8	42.430808051	34.402100629	32.404151480
1	41.742759838	33.987635386	30.036571769
1	42.690174177	32.522988868	30.293537871
1	40.611243664	31.197829202	30.696439818
1	39.614558858	32.650610381	30.447802643
8	39.759151530	31.437049598	26.011910847
8	39.597723089	32.422495140	27.978918086
8	44.999865686	35.292559764	23.891003951
6	44.210267660	34.692279096	23.183903632
7	42.867178305	34.565322679	23.575145370
6	42.470791472	35.326152539	24.758798060
6	41.948771081	33.786032888	22.917563002
7	40.733431712	33.654364677	23.416133644
6	42.353315573	33.134653150	21.719971545
6	43.626583149	33.305438201	21.280712004
7	44.519720461	34.088790163	21.973036520
1	43.170938127	36.156572589	24.874744595
1	42.482601089	34.691475492	25.659094188
1	40.465630124	34.006220832	24.329040066
1	43.975444034	32.786597726	20.386214368
1	41.657380597	32.508403367	21.166104547
1	41.465728197	35.725143649	24.605216175
1	40.032964666	33.078571083	22.924776974
1	45.022874017	29.986191248	22.903478579
1	39.453249995	27.059695680	23.023854661
1	44.806860011	27.293291965	28.800807990
1	32.915526185	31.643002436	26.882044189
1	45.459568704	34.173343956	21.642115940

**IM3**

**QM/MM (BS1) = -3413.001422 a.u.**

**QM/MM (BS2+ZPE) = -3415.021109 a.u.**

6	44.263701153	30.249137449	23.755945757
7	44.719185792	31.032952796	24.798491661
1	45.654498706	31.454000902	24.876537786
6	43.726867477	31.137128909	25.705508557
1	43.798722789	31.692787754	26.636500008
7	42.654265204	30.454638962	25.306535767
6	42.976070002	29.897301954	24.086163002
1	42.262084240	29.288850889	23.537105003
6	38.787634256	27.318088830	23.890803086
1	38.595952017	26.369163202	24.419866472
1	37.818653827	27.642765102	23.484679180
6	39.108747303	28.356137516	24.981139983
8	40.299517549	28.871005458	25.072768944

8	38.169883357	28.627560407	25.737521796
6	44.117195119	27.396625052	28.330335267
7	43.574172641	26.552075329	27.385882045
1	43.870756639	25.599452425	27.144550056
6	42.551214581	27.195507037	26.792855512
1	41.953439387	26.778380054	25.987604069
7	42.399921150	28.400812670	27.317029369
6	43.368992661	28.547962057	28.278552554
1	43.464488675	29.463814477	28.856532666
6	33.797652001	31.930035500	26.077982833
1	33.748908183	33.016330414	25.913566123
1	33.310060760	31.462128758	25.211572793
7	35.161354144	31.421212773	26.100112867
1	35.326780419	30.611667898	25.479218713
6	36.233795489	31.957122305	26.696090494
7	36.155368007	33.153111736	27.317420363
1	35.408126789	33.830673059	27.130329011
1	36.967485891	33.498654161	27.814374617
7	37.389253917	31.291122563	26.719167120
1	37.497960021	30.347451449	26.329064727
1	38.220487990	31.698745825	27.162575564
26	41.065550709	29.866127270	26.587475154
6	38.962295780	35.099117873	26.918021543
8	38.382818858	35.328798346	27.898613756
8	39.538610762	34.880049985	25.933718500
6	40.800569726	32.084191971	28.483269001
8	41.529299626	31.435707282	27.609793386
6	41.473169255	32.280503294	29.844410460
6	41.138664949	33.573661130	30.591485019
6	41.598032723	33.586706165	32.071661604
8	41.281388964	32.606237519	32.793236186
8	42.232801307	34.602259611	32.460731509
1	40.043314204	33.703657670	30.586316757
1	41.575831271	34.446950591	30.082219472
1	42.560993407	32.160367904	29.719682546
1	41.138540688	31.426106800	30.462449629
8	39.881262445	29.486163035	27.622565253
8	39.659594879	32.492117186	28.259071756
8	44.979344224	35.291298820	23.862795380
6	44.192341061	34.690798278	23.153805628
7	42.839826863	34.594763222	23.522081269
6	42.444726444	35.358253415	24.704311182
6	41.917915052	33.833570119	22.850173766
7	40.676216173	33.772855396	23.296751897
6	42.340938228	33.120414350	21.696529908
6	43.625235642	33.259627819	21.278441352
7	44.511814733	34.057224507	21.961214150
1	43.161451011	36.171980728	24.835504567
1	42.431092457	34.715137923	25.598410067
1	40.373725488	34.222099670	24.152556379
1	43.984122895	32.711911078	20.405462471
1	41.644966284	32.490906545	21.146349969

1	41.452632944	35.784610578	24.540111000
1	39.976086590	33.201209900	22.800480181
1	44.906061309	29.905159114	22.945316581
1	39.453309358	27.085429903	23.059650994
1	45.029109767	27.177567801	28.885756655
1	33.190914233	31.669082699	26.945070046
1	45.452516142	34.139529339	21.632156004

**IM4**

**QM/MM (BS1) = -3413.006828 a.u.**

**QM/MM (BS2+ZPE) = -3415.027170 a.u.**

6	44.433352135	30.356812060	23.684492641
7	44.926587676	31.121621079	24.720577529
1	45.876241579	31.512774148	24.793694347
6	43.945153473	31.273008197	25.633090190
1	44.063505362	31.826713674	26.561966149
7	42.844812613	30.643417532	25.234512796
6	43.131755266	30.068332162	24.014903782
1	42.392837271	29.486863533	23.468152456
6	38.788849523	27.292539099	23.894143920
1	38.513319497	26.347493584	24.389895217
1	37.852005488	27.728674817	23.513564902
6	39.253552276	28.242810319	25.006949524
8	40.455785385	28.701945117	24.997368008
8	38.441330494	28.512448268	25.908546613
6	43.953634883	27.509564479	28.172570083
7	43.442077341	26.659125860	27.212981650
1	43.748121960	25.704670616	26.992314382
6	42.443262719	27.303020698	26.580306718
1	41.876384861	26.889014210	25.753750874
7	42.266797939	28.513528229	27.091743406
6	43.203413465	28.657215489	28.090806514
1	43.261664926	29.570273435	28.676279142
6	33.663549760	31.939604289	26.037076749
1	33.609503581	33.028953191	25.895833621
1	33.132121529	31.491631416	25.185858414
7	35.023593378	31.430613099	25.986566273
1	35.169624872	30.608067153	25.380002847
6	36.122254540	31.929636749	26.566517862
7	36.092045912	33.105542776	27.225877429
1	35.357199554	33.806372139	27.079806871
1	36.924274213	33.408499826	27.718357025
7	37.257567862	31.232559851	26.534253470
1	37.329417787	30.333035608	26.057037797
1	38.133924911	31.625170163	26.895685706
26	41.083984927	30.089515651	26.267987655
6	38.957587065	35.035715130	26.992872109
8	38.341077642	35.208879246	27.963520605
8	39.571509781	34.876853686	26.020543485
6	40.396514130	31.643621859	28.746997680
8	41.078755782	30.742835517	28.085697520



6	40.875540029	31.825808214	30.195025440
6	41.229606965	33.260458601	30.604563095
6	41.601654359	33.443428048	32.101691323
8	41.239870262	32.557928341	32.918313648
8	42.226606763	34.495842061	32.393465730
1	40.370329207	33.924091756	30.400465177
1	42.066052767	33.655164074	30.005599575
1	41.722024689	31.149422861	30.380802284
1	40.052380862	31.482519725	30.844587089
8	40.158375732	31.253517074	25.644967722
8	39.428040118	32.267950956	28.313281726
8	44.974918313	35.298236735	23.887851399
6	44.190554750	34.695043951	23.176978945
7	42.842715367	34.576619026	23.554928254
6	42.442305231	35.341671128	24.734415112
6	41.926777754	33.799847410	22.889666857
7	40.700884252	33.688749139	23.364128946
6	42.344869057	33.129778120	21.707068521
6	43.623215645	33.292006635	21.280487702
7	44.510767714	34.080871856	21.974747895
1	43.129509930	36.184572215	24.838954718
1	42.471392363	34.715163228	25.639902580
1	40.420398519	34.055762734	24.266043023
1	43.980718984	32.764757295	20.394265191
1	41.652053676	32.500520198	21.152671653
1	41.430179308	35.725059124	24.584534118
1	40.004940815	33.109019211	22.870506979
1	45.050123496	29.962621767	22.876857561
1	39.431427265	27.043428772	23.049688348
1	44.833277122	27.284296370	28.775522096
1	33.100786721	31.661725838	26.928226927
1	45.451449093	34.167068337	21.646630230

## 2OG Rearrangement Coordinates for AlkB-dsDNA

### ES1

QM/MM (BS1) = -3269.997721 a.u.

QM/MM (BS2+ZPE) = -3271.827539 a.u.

6	31.621630967	27.064892502	30.383328851
7	31.290609156	28.283254955	30.937978508
1	30.455212897	28.506277606	31.492304826
6	32.242764866	29.172789475	30.605992482
1	32.209514944	30.218875533	30.900156606
7	33.185627254	28.596320020	29.867525478
6	32.807341411	27.275346458	29.719890402
1	33.407468094	26.583483338	29.136043475
6	36.059488890	26.076296070	26.055058722
1	35.926350111	26.212964154	24.970603831
1	37.092688836	25.735600200	26.199046099
6	35.963643174	27.452846404	26.725924396
8	34.978828936	27.678311917	27.515598634

8	36.848151193	28.283939488	26.461746773
6	31.135259935	30.671443003	26.365917382
7	31.442302021	29.475351658	25.755019539
1	30.862070016	28.947175257	25.091511826
6	32.641230783	29.071596397	26.212502474
1	33.116329636	28.136198910	25.929676491
7	33.137275059	29.950262960	27.077962122
6	32.201396180	30.955704750	27.185220958
1	32.357511131	31.798837225	27.852794547
6	42.559020644	28.450845263	29.156063981
1	42.716478970	28.607381386	30.228772439
1	42.949226364	27.443958047	28.942641685
7	41.160705224	28.471248951	28.794057910
1	40.901073032	27.863304229	28.005773779
6	40.109645672	28.973376363	29.465771221
7	40.252895933	29.829089249	30.493192515
1	41.146156157	29.969660391	30.971966874
1	39.404996851	30.125913770	30.978888957
7	38.895976530	28.642439469	29.026931577
1	38.821152481	27.797918173	28.448147903
1	38.040510293	28.970608142	29.486364852
26	34.629653768	29.375192639	28.534618207
6	36.483869284	31.011270827	30.208305159
8	37.389588219	31.327876352	30.986370084
8	36.312646937	29.894915703	29.622080761
6	35.404945481	32.073748579	29.826822011
8	34.419353686	31.685959304	29.215607968
6	35.632782968	33.497685814	30.234483214
6	34.817011433	34.552394043	29.492816327
6	35.050913836	35.984172251	30.009846138
8	35.273999989	36.137062983	31.238518731
8	34.989024170	36.921996195	29.164935352
1	33.740379751	34.334444757	29.607161916
1	35.017608124	34.525964190	28.411113973
1	36.716789741	33.692351920	30.188557264
1	35.402222171	33.541618480	31.314738548
8	33.153910968	28.118377443	35.391288723
6	33.445972946	27.159572536	34.705137611
7	34.641517355	27.157427744	33.943602468
6	35.506816541	28.334237304	34.076400965
6	34.996582504	26.149427228	33.075441851
7	36.047032121	26.282825600	32.291085437
6	34.196018995	24.975235524	33.064442907
6	33.065127525	24.949836402	33.805682483
7	32.674244850	26.010807428	34.584553615
1	35.083528009	28.979228958	34.851128263
1	35.563534055	28.881199481	33.122422662
1	36.652253823	27.110601166	32.260053652
1	32.421361224	24.079850505	33.794397741
1	34.482691202	24.121940776	32.459041576
1	36.516981963	28.018646645	34.373711090
1	36.285566899	25.578814353	31.579813217

1	30.969532273	26.192002242	30.413282390
1	35.370647445	25.291660790	26.367968076
1	30.186981755	31.192316334	26.233528570
1	43.171432294	29.151480047	28.588498833
1	31.775401880	25.960891561	35.019941050

**TS for 2OG rearrangement**

**QM/MM (BS1) = -3269.991780 a.u.**

**QM/MM (BS2+ZPE) = -3271.820336 a.u.**

6	31.586386090	27.132211019	30.369041013
7	31.251395084	28.366857271	30.883251838
1	30.416884012	28.598178660	31.437217284
6	32.196090707	29.250820952	30.511399731
1	32.168695661	30.306614650	30.768748243
7	33.133894553	28.653826712	29.782679934
6	32.764237405	27.327169649	29.686828942
1	33.361365807	26.621806989	29.116311260
6	36.096829727	26.043363777	26.065189222
1	35.922290734	26.199775205	24.988897563
1	37.124949270	25.671786060	26.160088451
6	36.073288864	27.411826743	26.756591117
8	35.100667769	27.688190286	27.546207045
8	37.006108570	28.190291467	26.497757348
6	31.177435557	30.649315948	26.379680282
7	31.488303495	29.463462336	25.751813387
1	30.909323448	28.943899132	25.080537341
6	32.689153001	29.055811388	26.207476539
1	33.166586938	28.126990787	25.905148601
7	33.181448675	29.921115406	27.086685016
6	32.242771851	30.922451415	27.205196362
1	32.390102777	31.755336892	27.888465830
6	42.608503898	28.404804582	29.043989675
1	42.744752318	28.513321813	30.125779729
1	43.002177602	27.408441188	28.796071811
7	41.221330759	28.440005194	28.649641830
1	40.955123085	27.817357251	27.876321365
6	40.191244677	29.069191191	29.235660225
7	40.366897196	29.895663901	30.281460834
1	41.214058187	29.854205150	30.855378395
1	39.528423354	30.227790090	30.759873141
7	38.982714973	28.897054441	28.704738543
1	38.844193859	28.228330024	27.949730580
1	38.143450572	29.406769466	29.001019683
26	34.704917235	29.367303125	28.558092886
6	36.617992348	31.281649275	29.699149765
8	37.600770619	31.562969558	30.389822624
8	36.494111145	30.322352921	28.868865391
6	35.347146149	32.157376666	29.795554461
8	34.277613814	31.631401013	29.517192099
6	35.514373150	33.580028218	30.240487142

6	34.663537384	34.626655275	29.519472022
6	34.972976241	36.054750012	30.008414698
8	35.258342893	36.206825256	31.224409733
8	34.921899772	36.983700601	29.153154586
1	33.591830627	34.430292737	29.698709474
1	34.811836757	34.585973154	28.429557568
1	36.584354196	33.827043300	30.187429551
1	35.264356612	33.600517484	31.315999821
8	32.945365776	28.112147344	35.361265794
6	33.198053601	27.103254630	34.736938438
7	34.289887889	27.071719408	33.832257315
6	35.111146706	28.283599682	33.742257822
6	34.531024897	26.022315535	32.980426303
7	35.378180003	26.126032138	31.977103953
6	33.843701736	24.803663633	33.217329242
6	32.842286578	24.796106326	34.119949739
7	32.480396635	25.916296588	34.823066062
1	34.859290663	28.924905182	34.591769714
1	34.915150307	28.817632630	32.799488611
1	35.860921329	26.990820679	31.714620523
1	32.286260288	23.887978883	34.297685332
1	34.103128448	23.904346843	32.669842741
1	36.174300689	28.007480100	33.785070071
1	35.346252607	25.383069048	31.264650286
1	30.940940985	26.255645792	30.424730737
1	35.398602636	25.273875233	26.394481846
1	30.235182040	31.180079713	26.243608751
1	43.227952716	29.131498790	28.518379546
1	31.576144764	25.900170520	35.249728682

**ES2**

**QM/MM (BS1) = -3269.999004 a.u.**

**QM/MM (BS2+ZPE) = -3271.830009 a.u.**

6	31.653611334	27.117420980	30.345688939
7	31.321170396	28.344856558	30.879582989
1	30.477979193	28.572994252	31.421989245
6	32.280738482	29.226887530	30.538111720
1	32.255249728	30.278807682	30.811252982
7	33.226431837	28.635415297	29.814895133
6	32.843367073	27.315236464	29.685026125
1	33.437859966	26.615379766	29.104469395
6	36.127778267	26.029331410	26.043909983
1	35.965839614	26.183108254	24.965439500
1	37.152687328	25.654388087	26.153381246
6	36.099483000	27.398879278	26.729883769
8	35.117766963	27.684699256	27.503019392
8	37.038417169	28.173724446	26.481082957
6	31.214984070	30.649302613	26.377394946
7	31.525414251	29.466529220	25.743935980
1	30.943290532	28.947391622	25.075111919
6	32.724271732	29.054886709	26.201045712

1	33.200513180	28.125639194	25.899367700
7	33.216352825	29.915503058	27.085022971
6	32.278891892	30.917310649	27.206349614
1	32.425565352	31.746169171	27.894545203
6	42.607166408	28.407886855	29.074248368
1	42.742556936	28.547399912	30.152730186
1	43.023652282	27.414353506	28.854494466
7	41.219618823	28.387276602	28.681193293
1	40.964687536	27.722490603	27.940135987
6	40.187457663	29.098144425	29.159219809
7	40.339166239	30.000642364	30.144851827
1	41.141064890	29.967967553	30.779819726
1	39.494174177	30.474358700	30.467937340
7	39.001219497	28.922713478	28.582030329
1	38.884848001	28.221387478	27.853423506
1	38.159678687	29.464167777	28.809828916
26	34.761631383	29.361127187	28.533666889
6	36.688914075	31.353910984	29.556494406
8	37.711800891	31.675494120	30.175167889
8	36.548877349	30.395996688	28.735059733
6	35.390648477	32.172311175	29.760025654
8	34.329296714	31.615431867	29.514104361
6	35.524289085	33.582609983	30.252439113
6	34.681757131	34.632078283	29.523709203
6	34.986358059	36.056458551	30.024853647
8	35.273107547	36.198930265	31.240927678
8	34.931892168	36.990540916	29.174541189
1	33.607696218	34.433819201	29.685777700
1	34.846442695	34.597927369	28.436039285
1	36.590072295	33.848480042	30.231241267
1	35.236235207	33.577918446	31.318276749
8	32.878833448	28.107698307	35.307865491
6	33.133225927	27.091310174	34.696287063
7	34.203844436	27.060141734	33.767815999
6	35.005660625	28.280756413	33.633963090
6	34.451061780	25.994918907	32.939254493
7	35.277518351	26.094946938	31.916580374
6	33.800350583	24.767866687	33.222468172
6	32.811345875	24.764384679	34.140127828
7	32.437446847	25.893803692	34.821063391
1	34.786496353	28.923203555	34.491697195
1	34.760699158	28.808833428	32.698941526
1	35.649693674	26.986008950	31.577092727
1	32.273628546	23.850992055	34.343924179
1	34.064494402	23.863522755	32.685155702
1	36.071662882	28.013997849	33.629409885
1	35.233525078	25.339821667	31.216573496
1	31.003672180	26.243050162	30.379186462
1	35.424259800	25.262499123	26.368097174
1	30.273735280	31.181886002	26.241479627
1	43.212770197	29.131972144	28.529260420
1	31.536542144	25.877689298	35.254749383

## Substrate hydroxylation step reaction states cartesian coordinates for AlkB-dsDNA

### Snapshot 1

#### RC2

QM/MM (BS1) = -3375.982529 a.u.

QM/MM (BS2+ZPE) = -3377.931323 a.u.

6	27.513498642	22.629163518	37.006586909
7	27.067532430	23.585801841	37.891787747
1	26.274960111	23.489520226	38.536976848
6	27.893289656	24.641015571	37.845554246
1	27.754109097	25.543113378	38.434624120
7	28.866604148	24.412289781	36.972199008
6	28.660234260	23.153007899	36.454852215
1	29.361204744	22.709916326	35.757497679
6	31.459532509	24.418974189	32.197653092
1	30.988141812	25.296891850	31.737316088
1	32.508067451	24.349266120	31.873235720
6	31.498535661	24.510642474	33.712235284
8	30.704245896	25.443262415	34.214181802
8	32.270499707	23.830301452	34.363428218
6	26.399296206	27.450541292	34.872800151
7	26.664435656	26.626605526	33.799122336
1	26.045748970	26.424118640	33.006263060
6	27.890105300	26.094460979	33.983858336
1	28.372308633	25.413398593	33.288954552
7	28.425092661	26.534698254	35.114663084
6	27.507270315	27.383523147	35.682001977
1	27.715320203	27.885073089	36.624344613
6	35.714964168	27.862752652	35.916142526
1	34.657037023	28.166793817	35.999336111
1	36.012711198	27.502203253	36.913939344
7	35.880640315	26.854135053	34.875885662
1	36.406904782	27.079165831	34.022698935
6	35.109657289	25.751696264	34.795354563
7	34.206266819	25.456190633	35.727279171
1	33.885209240	26.140022823	36.411493659
1	33.573424784	24.663778792	35.563031062
7	35.211816608	24.987286096	33.688303645
1	36.094298418	25.030201376	33.163205999
1	34.773835105	24.058668164	33.661741683
26	30.183773317	25.714738827	36.050047632
8	31.436353741	25.027006490	36.794326437
8	32.578597597	27.629576852	37.280597100
6	31.426872213	28.065347040	37.330509829
8	30.380026891	27.487034615	36.828978074
6	31.125008306	29.442254140	37.914703795
6	31.961812308	29.889972118	39.118212369
6	31.711888317	31.382772459	39.357705614
8	30.884369392	31.707227578	40.249859540
8	32.311007675	32.191381580	38.591952887
1	33.026447690	29.707227688	38.917674507

1	31.672424871	29.315045930	40.012228978
1	30.050284424	29.488113894	38.145564233
1	31.310163552	30.146215422	37.083234391
8	29.117790850	21.875809588	41.428275000
6	29.567584707	21.217007123	40.506056170
7	30.758324641	21.605413429	39.862559607
6	31.469557544	22.757280071	40.417076921
6	31.245512813	21.011718577	38.716864420
7	32.328833386	21.478355235	38.139916097
6	30.532872686	19.890540278	38.195135647
6	29.451972490	19.429673726	38.867818850
7	28.983983499	20.062814392	39.999976635
1	31.395331248	23.619205049	39.732831682
1	32.527006599	22.498066094	40.568200254
1	32.782500513	22.311469549	38.494550040
1	28.917501103	18.549974495	38.513560633
1	30.890409182	19.388533090	37.299046680
1	31.018701412	23.005588177	41.381253765
1	32.623907044	21.152844800	37.155177732
8	34.786376219	28.164111248	38.930001050
1	34.554419585	27.952840364	39.857753100
1	33.985446445	27.925572082	38.426915917
8	32.742523633	21.039239292	35.655893001
1	33.385513842	20.652654457	35.021367944
1	31.838857672	20.799279683	35.293645774
1	26.900753372	21.777642737	36.710744187
1	30.928542928	23.543028264	31.825045897
1	25.443338849	27.950291492	35.029205361
1	36.277928549	28.767427949	35.686575481
1	28.144514491	19.731491156	40.430661197

**TS7**

**QM/MM (BS1) = -3375.952287 a.u.**

**QM/MM (BS2+ZPE) = -3377.893800 a.u.**

6	27.399831014	22.422807490	36.932698112
7	26.992417768	23.324799826	37.889399814
1	26.204323452	23.214975798	38.535258932
6	27.857786271	24.346160045	37.923822164
1	27.758844593	25.199474325	38.588952182
7	28.818475398	24.151869883	37.031633402
6	28.563036237	22.946033421	36.416855680
1	29.247148197	22.530268254	35.685191910
6	31.426533968	24.247394774	32.421369627
1	31.007101397	25.175894351	32.012221854
1	32.472730661	24.147782020	32.092342184
6	31.474578521	24.266708421	33.942112416
8	30.898750000	25.326525882	34.483418381
8	32.085926132	23.423529119	34.580248933
6	26.445927416	27.376078809	34.944827594
7	26.740438918	26.559404937	33.874237544
1	26.138906454	26.358435335	33.070646362

6	27.953750496	26.008536643	34.105465215
1	28.443656924	25.323373886	33.419404041
7	28.454056644	26.425763948	35.257904153
6	27.524025729	27.280197913	35.794774517
1	27.695363252	27.764352714	36.754421831
6	35.721150187	27.751503301	35.896838118
1	34.663595524	28.047352812	36.002560229
1	36.043462810	27.393861662	36.888063963
7	35.865084351	26.738717235	34.854533265
1	36.395360150	26.960121096	34.001310681
6	35.099114428	25.635328975	34.785752261
7	34.204709143	25.340684363	35.729182272
1	33.895473956	26.011681957	36.433239266
1	33.604546963	24.521728023	35.605507802
7	35.181669058	24.862731959	33.676379224
1	36.062156409	24.920601402	33.147592804
1	34.809001018	23.902077387	33.704325767
26	30.300965170	25.467282554	36.335188802
8	31.508946149	24.612446662	37.264647550
8	32.661998413	27.519123150	37.297521273
6	31.502047223	27.916170439	37.449424037
8	30.443782526	27.260114583	37.103778793
6	31.207328870	29.316553418	37.980920003
6	32.083526843	29.830254000	39.129988642
6	31.786677986	31.319381406	39.342622602
8	30.936715631	31.627691793	40.219150268
8	32.369738163	32.138295556	38.575637326
1	33.143380410	29.674547209	38.887963871
1	31.853352208	29.273215537	40.052167149
1	30.143305169	29.359333837	38.256755703
1	31.352083650	29.985193892	37.112152780
8	29.561006520	22.207467857	40.485555897
6	29.885819929	21.383502447	39.657829417
7	30.981686612	21.642381465	38.774730095
6	31.764810789	22.807120339	39.042046014
6	31.297403522	20.835482958	37.684619649
7	32.221893781	21.217700678	36.834533171
6	30.590729926	19.605251155	37.561596331
6	29.630660127	19.289248923	38.466296632
7	29.278412645	20.142540331	39.491890661
1	31.590256831	23.725032196	38.168725718
1	32.841890531	22.603112778	38.961116969
1	32.532827585	22.184717273	36.806014026
1	29.097372689	18.346228231	38.384366537
1	30.811688113	18.933876930	36.734977647
1	31.467210786	23.261616454	39.990677350
1	32.505652598	20.638511734	35.978170756
8	34.877187147	28.102502104	38.918323087
1	34.640147680	27.893463586	39.844787395
1	34.083414272	27.845828548	38.413113599
8	32.855582897	20.104090905	34.488730262
1	32.904338875	19.108891595	34.409875581



1	31.878336613	20.213125332	34.291837781
1	26.755324531	21.614295335	36.587753451
1	30.861025282	23.424017385	31.985116353
1	25.493290716	27.893748400	35.056938408
1	36.272299844	28.660275081	35.655104310
1	28.489542265	19.917606255	40.063782849

**Snapshot 2**

**RC2**

**QM/MM (BS1) = -3528.063820 a.u.**

**QM/MM (BS2+ZPE) = -3530.159254 a.u.**

6	27.871007140	21.612468272	41.928123500
7	27.900134029	22.615105189	42.873033905
1	27.596506486	22.535973156	43.851587029
6	28.398035458	23.724078830	42.295826418
1	28.515861472	24.672075656	42.814111961
7	28.691520198	23.488139989	41.023065163
6	28.373652579	22.168375676	40.776960843
1	28.499560564	21.723543047	39.794174269
6	28.916651647	22.926306439	35.728216460
1	28.225006627	23.391707077	35.009958825
1	29.914530065	22.975595696	35.262996388
6	28.974914062	23.787229398	36.974894790
8	28.728027083	23.281822326	38.124685873
8	29.289691720	24.999181440	36.903898032
6	24.970855058	25.764235325	40.069949642
7	24.806850450	24.746505516	39.152053926
1	23.924953842	24.334653599	38.823136721
6	26.030607965	24.344843389	38.759650411
1	26.207850752	23.538743516	38.055748608
7	26.972172880	25.063914899	39.357901256
6	26.323685011	25.954938725	40.182848259
1	26.871837831	26.680600809	40.774597431
6	34.557709834	27.283698061	36.418512645
1	33.681079831	27.846317576	36.782073946
1	35.207613798	27.114480369	37.293372900
7	34.148424401	26.039611471	35.793446981
1	34.508716853	25.815229628	34.865918878
6	33.301187643	25.161812092	36.362785983
7	32.923921662	25.322416398	37.631987267
1	33.367365423	25.979888580	38.294059413
1	32.147841405	24.776801231	38.008751393
7	32.798643446	24.155928746	35.637261776
1	33.106741580	24.062658208	34.659819633
1	32.566558830	23.261280771	36.111594031
26	29.084190095	24.788734898	39.378270506
8	30.689559164	24.557981581	39.409698941
8	28.663610421	28.704027408	39.059470778
6	29.440695041	27.768828834	39.286950494
8	29.045996452	26.664593525	39.841832570
6	30.906729056	27.903070254	38.934734398

6	31.312726457	29.314610465	38.531545171
6	31.162698373	30.402003961	39.613826620
8	31.153877798	30.059099612	40.825990136
8	31.097238946	31.592627418	39.194169450
1	30.743526178	29.648852574	37.651250515
1	32.374542050	29.309941714	38.226093241
1	31.108328163	27.191961544	38.116819409
1	31.496147923	27.529913630	39.783151565
8	31.652253380	21.730879296	44.099143121
6	31.545515286	20.861791074	43.257241221
7	32.007218065	21.068674374	41.931542059
6	32.649310986	22.356236383	41.652452523
6	31.854868004	20.157172659	40.913927356
7	32.291795773	20.444164521	39.697817442
6	31.227479167	18.919519653	41.208135947
6	30.829595990	18.681882762	42.482991659
7	30.980974397	19.610947579	43.483188693
1	32.764273474	22.881634444	42.604884468
1	32.030586813	22.963449242	40.970463796
1	32.677502714	21.339949836	39.423313396
1	30.369820337	17.736584130	42.743996700
1	31.083068395	18.162876188	40.437831385
1	33.640959813	22.184003556	41.207841873
1	32.149111939	19.780579198	38.926020563
8	32.780654621	21.581776917	36.674533577
1	33.318427571	21.405634047	35.862041126
1	32.217445512	20.769352010	36.786609138
8	28.300252827	29.894343609	41.847029468
1	29.119404407	29.613180592	41.401182273
1	27.608878041	29.664799150	41.202834327
8	26.093335980	29.127539243	39.662668695
1	26.125553048	30.073198344	39.433111901
1	26.977820535	28.807029595	39.354588422
8	34.136887792	26.830958963	39.643562195
1	34.539609591	26.066163554	40.132080872
1	33.801310500	27.438968482	40.345098332
1	27.357377092	20.661201283	42.067201229
1	28.626680268	21.884103516	35.861621806
1	24.166690127	26.224234751	40.644220148
1	35.093028413	27.917982638	35.711982805
1	30.619090752	19.391316509	44.389154982

**TS7**

**QM/MM (BS1) = -3528.029559 a.u.**

**QM/MM (BS2+ZPE) = -3530.125014 a.u.**

6	27.799647387	21.462995257	41.977020298
7	27.848875481	22.460587687	42.926188178
1	27.542133714	22.389649958	43.903336521
6	28.386493420	23.555674240	42.360724737
1	28.538286003	24.493019215	42.889732543
7	28.683333778	23.318187815	41.090005582

6	28.326834030	22.010806911	40.834434445
1	28.440198015	21.569602327	39.848644801
6	28.931794176	22.842701186	35.752125799
1	28.227380024	23.365845650	35.086972228
1	29.914930605	22.891562497	35.257981106
6	29.048316487	23.597087567	37.060353693
8	28.723682565	23.050722027	38.159632426
8	29.493613305	24.783666676	37.101174310
6	25.065399993	25.730832514	40.090944728
7	24.877494126	24.728069288	39.161869201
1	23.987462481	24.327641361	38.843066039
6	26.095395003	24.306458946	38.763670952
1	26.248726074	23.500108787	38.053746678
7	27.056433657	24.993937521	39.365151900
6	26.426705476	25.887644005	40.200104353
1	26.992272948	26.590743205	40.805317854
6	34.521594175	27.254171727	36.437195750
1	33.661431056	27.837681515	36.809768861
1	35.173089899	27.066013332	37.306857749
7	34.084592560	26.020695464	35.809729161
1	34.370983440	25.832534143	34.849352630
6	33.283188849	25.113614829	36.403780429
7	32.964581721	25.232473040	37.692779737
1	33.395966400	25.920611880	38.329371961
1	32.267910940	24.616083406	38.123714462
7	32.770472404	24.119139349	35.668857865
1	33.089984653	24.024231092	34.695351552
1	32.503695028	23.228527900	36.127618836
26	29.288597058	24.539982257	39.429061600
8	30.976635731	23.940287588	39.593544764
8	28.661514731	28.385707015	39.209995347
6	29.579979858	27.570911405	39.352194582
8	29.437106854	26.410236178	39.909176439
6	30.977548160	27.903400244	38.863737184
6	31.183240775	29.354526749	38.459331956
6	31.120506510	30.408347251	39.583617626
8	31.153777397	30.036572552	40.783859938
8	31.066809963	31.611465906	39.193178952
1	30.442529667	29.649290134	37.700509249
1	32.169445659	29.466482319	37.973904303
1	31.169228256	27.233319704	38.008127371
1	31.690417083	27.581632118	39.633288081
8	31.282132027	21.980933681	43.794571827
6	31.267643107	21.049374285	43.018289451
7	31.696157926	21.228436108	41.663726591
6	32.219175340	22.519415856	41.302580756
6	31.641754371	20.224204054	40.713137420
7	32.030383789	20.484566654	39.477925324
6	31.182559829	18.944256927	41.112704905
6	30.827542444	18.745749016	42.408754695
7	30.873428102	19.754319492	43.342893433
1	32.275029358	23.157969364	42.187641987

1	31.498457215	23.162124813	40.488645318
1	32.208199346	21.418283299	39.118354294
1	30.479242334	17.771290564	42.737698533
1	31.106218926	18.128033221	40.395172629
1	33.178242591	22.430427176	40.772841187
1	31.964034773	19.759254948	38.752864131
8	32.630282534	21.518492049	36.606642237
1	33.233853511	21.368780688	35.835585756
1	32.081492278	20.689650805	36.659274503
8	28.245047045	29.891569440	41.820154958
1	29.022278035	29.536356058	41.355214747
1	27.511572421	29.649772839	41.227958440
8	26.118179793	29.085176212	39.682545503
1	26.237027553	30.005439679	39.389692363
1	26.972252183	28.658521567	39.432477460
8	34.154162207	26.799781903	39.679118578
1	34.519628753	26.025468278	40.182656004
1	33.829892723	27.427252413	40.368366393
1	27.249437633	20.529603511	42.095832751
1	28.614141186	21.804024239	35.843307500
1	24.258132590	26.201847611	40.651775757
1	35.067763613	27.879819121	35.731269691
1	30.548017230	19.556315251	44.267487713

### Snapshot 3

#### RC2

**QM/MM (BS1) = -3453.536340 a.u.**

**QM/MM (BS2+ZPE) = -3455.550390 a.u.**

6	29.743526712	21.863207163	45.728228760
7	30.202554378	22.989525843	46.378482468
1	30.619257765	23.020710480	47.318835382
6	30.027438350	24.050857450	45.572083519
1	30.265929106	25.080985220	45.837575317
7	29.486359074	23.653045325	44.424099704
6	29.302573555	22.290506314	44.500758384
1	28.860408546	21.714677529	43.690637415
6	25.935071453	22.473129124	40.389531642
1	25.144928205	23.167540381	40.698542278
1	26.019133603	22.511340150	39.297841057
6	27.291575981	22.836629591	40.988835492
8	27.214863028	23.715028348	41.984959629
8	28.327453760	22.374405382	40.560416993
6	26.103374626	25.814580344	46.107095593
7	25.371799668	24.789316485	45.543616318
1	24.511276032	24.357383334	45.904150863
6	26.012678837	24.385616655	44.433568458
1	25.668573737	23.597489546	43.770199965
7	27.113310855	25.104186679	44.251837693
6	27.194621400	25.999942493	45.293318289
1	28.053280751	26.665789106	45.392294284
6	31.306993933	26.555017327	37.088426620
1	31.278556816	26.818351225	38.160682250

1	32.333220218	26.228448680	36.856345492
7	30.342412237	25.527220741	36.756007728
1	29.434497735	25.837899243	36.389993674
6	30.420575325	24.233021108	37.107659059
7	31.474584103	23.760469164	37.777763978
1	32.110618733	24.372188861	38.306642612
1	31.463466301	22.777174336	38.031640769
7	29.394139069	23.435072898	36.786660146
1	28.699491962	23.804212278	36.122217339
1	29.514308411	22.416309854	36.659221728
26	28.604369335	24.667177549	42.862470226
8	29.839802972	24.304128005	41.856606502
8	30.904368524	27.202632991	42.671106233
6	29.820887277	27.148651487	42.080488177
8	28.758047721	26.594263551	42.584172841
6	29.636365250	27.809698590	40.714876969
6	29.214584471	29.280245387	40.826475635
6	30.268012170	30.183838490	41.488452815
8	29.839513332	31.021518588	42.336412582
8	31.464050703	30.044120409	41.141112209
1	28.275141710	29.392458566	41.382918160
1	29.034837083	29.671703135	39.807796498
1	28.898832593	27.231026430	40.148003286
1	30.583090765	27.769305908	40.163114287
8	34.282201468	22.268058477	45.174578926
6	33.593980473	21.446253174	44.601921998
7	32.885124682	21.782541257	43.423458446
6	33.034004833	23.160520983	42.935534369
6	32.079584557	20.902476930	42.735747128
7	31.361051236	21.337833698	41.715476766
6	32.045567683	19.546372957	43.169909147
6	32.683240493	19.210209220	44.320765749
7	33.427687719	20.127841825	45.029473725
1	33.305860347	23.157765821	41.869208514
1	33.828283956	23.633820628	43.519296769
1	30.820256774	20.686865761	41.119927963
1	32.585080722	18.203475476	44.728387724
1	31.449404400	18.809603199	42.634689170
1	32.095582834	23.723658774	43.056978372
1	31.184504307	22.326114789	41.547187007
8	28.771433514	24.945555242	39.376055502
1	28.627456349	24.103842978	38.914865925
1	29.232996997	24.665415961	40.194042665
8	33.243572793	25.313062110	39.492962329
1	33.172596513	26.139519877	40.028319871
1	34.192669805	25.144732928	39.406271200
8	30.302348074	27.452958669	45.429579616
1	29.901690849	28.329089335	45.252349090
1	30.622837390	27.211218532	44.533523642
1	29.560204266	20.906940365	46.218141015
1	25.620151706	21.476004339	40.697159734
1	25.848800448	26.274854630	47.061771922

1	31.081685707	27.454643622	36.515734676
1	33.734182540	19.892586289	45.951801348

**TS7**

**QM/MM (BS1) = -3453.499251 a.u.**

**QM/MM (BS2+ZPE) = -3455.515109 a.u.**

6	29.673496258	21.777341079	45.862805282
7	30.165934138	22.887367228	46.514824552
1	30.604268851	22.905673083	47.444379154
6	29.992461109	23.959150011	45.722726238
1	30.260690156	24.980518427	45.990511839
7	29.416070492	23.587175680	44.586227834
6	29.210397954	22.229987339	44.653959944
1	28.732771755	21.671600527	43.853149018
6	25.973720342	22.437495069	40.389857350
1	25.200351087	23.152296965	40.695962073
1	26.052794245	22.454034488	39.297310101
6	27.338783645	22.786399737	40.974901508
8	27.300572634	23.634177992	41.986578848
8	28.364658058	22.333355362	40.495342146
6	26.075589561	25.816510708	46.158075778
7	25.348056607	24.792784606	45.588491755
1	24.489058848	24.356251567	45.946000941
6	25.992234634	24.403430544	44.471975857
1	25.649938612	23.614030579	43.808268776
7	27.088705002	25.126634886	44.292100519
6	27.164093149	26.011896062	45.341550351
1	28.021538361	26.678789621	45.448776690
6	31.293307854	26.566721325	37.092061280
1	31.271375764	26.835641885	38.162883628
1	32.319063276	26.241946261	36.855338531
7	30.329651725	25.535960764	36.768283074
1	29.418692422	25.840024387	36.406372996
6	30.426458427	24.235554999	37.096095674
7	31.501413395	23.768312513	37.738660039
1	32.126886917	24.380082932	38.278027284
1	31.516756149	22.779070860	37.963673280
7	29.411458347	23.431171581	36.771879251
1	28.698718125	23.797309748	36.126062536
1	29.527031404	22.411195531	36.650386119
26	28.685897330	24.600607401	42.898963204
8	30.163981109	24.103208611	42.037911941
8	30.896731956	27.247198769	42.672637767
6	29.848292039	27.146151733	42.025942184
8	28.805186360	26.497389559	42.438912469
6	29.678601231	27.857129620	40.682120320
6	29.233444882	29.315482744	40.836065449
6	30.277959554	30.219202713	41.510794604
8	29.840442668	31.050656415	42.360265167
8	31.475920202	30.088267931	41.167223651
1	28.294580168	29.398162906	41.399791347

1	29.039958593	29.731248059	39.829405885
1	28.959787795	27.287690735	40.085491647
1	30.633840821	27.849739199	40.143423363
8	33.585993564	22.468007736	45.027795064
6	33.047377423	21.531402725	44.479081247
7	32.320585460	21.726559072	43.260321430
6	32.375751447	23.036286479	42.663538109
6	31.626630057	20.710703502	42.619071546
7	30.854740482	21.004098531	41.594957695
6	31.786478856	19.385319412	43.114032750
6	32.487400449	19.178908640	44.257982028
7	33.099830990	20.212085043	44.936209913
1	32.753808898	23.007292598	41.630539346
1	32.933806783	23.718923606	43.309768577
1	30.391676622	20.257209104	41.047699354
1	32.546975790	18.178564045	44.684937869
1	31.288542242	18.552695831	42.621598637
1	31.241637860	23.578483526	42.485317213
1	30.526250990	21.949601567	41.383685218
8	29.045163813	24.918378879	39.550652799
1	28.827420123	24.028077655	39.227041168
1	29.606048707	24.702230171	40.325639522
8	33.217201901	25.347979411	39.502495130
1	33.154662040	26.169366378	40.045893297
1	34.162316315	25.142853952	39.463570486
8	30.233457181	27.459319104	45.419269867
1	29.852327026	28.344103824	45.240328633
1	30.574125592	27.219504146	44.530470993
1	29.467118104	20.820066977	46.341450945
1	25.640673491	21.450802839	40.711704451
1	25.821531590	26.271519755	47.115409905
1	31.063163858	27.463364532	36.516620556
1	33.487047139	20.035666387	45.841147814

**IM10**

**QM/MM (BS1) = -3453.533512 a.u.**

**QM/MM (BS2+ZPE) = -3455.541810 a.u.**

6	29.738510387	21.792012921	45.732711304
7	30.209556928	22.922351845	46.367862362
1	30.619147972	22.963821582	47.310792724
6	30.051462944	23.971683870	45.542785425
1	30.304102280	25.001967251	45.793993041
7	29.507672449	23.566164184	44.398279056
6	29.305490793	22.207571840	44.499175774
1	28.851849099	21.623616142	43.701708570
6	25.889005790	22.459069615	40.331446692
1	25.125487852	23.157084003	40.696276129
1	25.904069191	22.494353963	39.236732763
6	27.282015452	22.822824606	40.823680839
8	27.314473343	23.575136310	41.918121669
8	28.279573659	22.486510783	40.216583891

6	26.109590463	25.804234198	46.079705723
7	25.384821932	24.774460606	45.517033009
1	24.527527435	24.337657368	45.878916427
6	26.028986868	24.380998583	44.402505081
1	25.687968824	23.587232212	43.743545244
7	27.123389359	25.106901210	44.215746270
6	27.195844477	25.999050395	45.259909451
1	28.048781104	26.671777551	45.359338829
6	31.281568459	26.513863609	37.073481988
1	31.239547472	26.762498011	38.149095607
1	32.311737352	26.196644841	36.843119193
7	30.326351342	25.487622053	36.715127092
1	29.421299821	25.801238764	36.346203341
6	30.389735145	24.193729385	37.078921692
7	31.437489043	23.720405514	37.764872083
1	32.027972609	24.338092167	38.333132718
1	31.397124577	22.747254750	38.053922534
7	29.376899384	23.399653223	36.735516736
1	28.677500885	23.765925045	36.076371644
1	29.473693936	22.375027795	36.656383126
26	28.687616685	24.581732617	42.761938026
8	30.284303161	24.266057565	41.739123056
8	30.910849347	27.119044078	42.512815565
6	29.813197205	27.147612395	41.928818405
8	28.766479955	26.534955048	42.366311975
6	29.632469897	27.935303551	40.632797646
6	29.192066058	29.383457700	40.859371389
6	30.256588741	30.269147816	41.525842542
8	29.834545284	31.108082100	42.375858608
8	31.450975554	30.118867531	41.178252509
1	28.274906020	29.442508362	41.460338749
1	28.958478097	29.835869952	39.877471837
1	28.905475677	27.393830049	40.019269215
1	30.583206300	27.950411059	40.085992455
8	34.373293712	22.273623321	45.159893496
6	33.666424537	21.471345219	44.587162556
7	33.000970536	21.844872479	43.367373844
6	33.289245367	23.114517154	42.887614771
6	32.123827686	20.996393255	42.689815480
7	31.400635679	21.483755087	41.697068822
6	32.058016493	19.643350112	43.121529207
6	32.671515973	19.276484644	44.278974177
7	33.431783058	20.169394960	45.007398472
1	33.039622902	23.357597936	41.857240530
1	33.974139731	23.702505417	43.489918870
1	30.850452104	20.844966253	41.094861096
1	32.535724746	18.272079470	44.684095970
1	31.434811919	18.929189791	42.585130752
1	31.010049380	24.855239873	42.004138378
1	31.163534701	22.485122381	41.612403155
8	28.983533883	25.040993322	39.441219082
1	28.733401572	24.148419631	39.144945398



1	29.567589035	24.812909238	40.202852789
8	33.129797536	25.254047814	39.657993229
1	33.115067998	26.141759662	40.090588306
1	34.068946159	25.041464014	39.553291118
8	30.313049250	27.427591219	45.294251546
1	29.918649514	28.310920151	45.138223703
1	30.632031347	27.192299831	44.397976917
1	29.539760567	20.844063821	46.232669640
1	25.584351283	21.464588144	40.657421475
1	25.851638934	26.266165306	47.032673709
1	31.058252934	27.420427217	36.511040943
1	33.727133767	19.918072598	45.929123764

**TS8**

**QM/MM (BS1) = -3453.514459 a.u.**

**QM/MM (BS2+ZPE) = -3455.525257 a.u.**

6	29.681312153	21.665218559	45.884433068
7	30.197430545	22.766727319	46.531857122
1	30.629420355	22.785758899	47.463536112
6	30.047969612	23.837025596	45.732525362
1	30.339613402	24.852852527	45.994738203
7	29.463566187	23.476035117	44.597930970
6	29.227247809	22.124648697	44.674212367
1	28.730173955	21.576506709	43.878371886
6	26.072706561	22.389111895	40.354567604
1	25.314944002	23.122106466	40.661022045
1	26.143030433	22.393478677	39.261964474
6	27.441509596	22.741310301	40.928288957
8	27.429104263	23.462717324	42.016005733
8	28.472819840	22.404353894	40.348640602
6	26.114436208	25.821386590	46.119539889
7	25.402738614	24.788383884	45.547923863
1	24.547069623	24.343838206	45.903030378
6	26.057119549	24.411402896	44.430385388
1	25.730700241	23.614072103	43.767385383
7	27.143025365	25.149776247	44.249702552
6	27.199900092	26.032999687	45.300817752
1	28.046790006	26.711448916	45.407992253
6	31.272235159	26.512655265	37.072299954
1	31.246646576	26.765783122	38.146940448
1	32.297111544	26.187043195	36.831279371
7	30.304855167	25.491573472	36.730880815
1	29.400693686	25.804883621	36.361263308
6	30.387394425	24.186605035	37.050866662
7	31.458855522	23.704631206	37.691686933
1	32.071707399	24.308780753	38.252069208
1	31.453055538	22.716293071	37.922080790
7	29.375222998	23.393036661	36.709146569
1	28.661416871	23.765461359	36.069644410
1	29.475411275	22.369052109	36.612822932
26	28.793165352	24.511041797	42.917000565
8	30.580435211	24.199993627	42.111794144

8	31.057150722	26.978511392	42.366983284
6	29.911058631	27.085382769	41.863872100
8	28.885969410	26.489912851	42.327365964
6	29.696496063	27.940362147	40.612985916
6	29.219008557	29.364426745	40.898036873
6	30.282338570	30.273401486	41.533455895
8	29.858340120	31.126111698	42.369833846
8	31.474198058	30.128160799	41.177153053
1	28.329610681	29.379191050	41.542553119
1	28.921179123	29.835018633	39.942211641
1	28.970404937	27.407883674	39.989920029
1	30.635719231	28.004156555	40.050517201
8	33.525449035	22.543502491	45.102002372
6	33.025946083	21.607202196	44.522677223
7	32.367471792	21.822210727	43.251177877
6	32.451481040	23.091341884	42.700057504
6	31.684842740	20.809936683	42.567086105
7	30.963840352	21.144795341	41.520122745
6	31.805878992	19.485654292	43.065792857
6	32.464999286	19.261374321	44.234267828
7	33.066197231	20.282258572	44.946082037
1	32.591546374	23.160379195	41.623149528
1	32.865305158	23.848635819	43.360044173
1	30.505127547	20.426329179	40.930286284
1	32.493873017	18.258226679	44.661604762
1	31.312317996	18.661336015	42.554110504
1	31.088262073	25.026635981	42.232525928
1	30.675886309	22.110295753	41.337382574
8	29.181415964	24.929053230	39.588026461
1	28.923654625	24.000613610	39.421600497
1	29.787123694	24.794616512	40.342477169
8	33.188752088	25.201717952	39.525883134
1	33.176050194	26.090708541	39.955450741
1	34.127117540	24.989964029	39.412037862
8	30.406870291	27.381976394	45.192840309
1	30.003632835	28.259019119	45.025784687
1	30.738159707	27.133690085	44.306372308
1	29.446843551	20.717741909	46.369592623
1	25.712504968	21.416886726	40.690871563
1	25.848278594	26.275034868	47.074228681
1	31.048725887	27.419241945	36.509973074
1	33.449987777	20.085867115	45.848361209

**PD**

**QM/MM (BS1) = -3453.609297 a.u.**

**QM/MM (BS2+ZPE) = -3455.604508 a.u.**

6	29.782674594	21.702401093	45.631315212
7	30.220690415	22.849663343	46.260875920
1	30.590031893	22.916538991	47.218408954
6	30.116568960	23.871731829	45.391619710
1	30.355444020	24.904858273	45.642250565

7	29.643395010	23.442415502	44.223545607
6	29.436841434	22.083744576	44.357955384
1	29.050599718	21.473513835	43.543529807
6	26.278122522	22.211502294	40.139318377
1	25.422670800	22.883352402	39.973682532
1	26.764686667	22.002773080	39.177420932
6	27.237213110	22.920949424	41.075200378
8	26.735550395	23.623478790	42.025445281
8	28.479019723	22.909663412	40.915518132
6	26.052816735	25.943401772	46.179259849
7	25.262657755	24.957886241	45.627909412
1	24.362365347	24.599932319	45.967403086
6	25.890562571	24.493240681	44.533182244
1	25.488885955	23.730982439	43.870245179
7	27.041366234	25.129863280	44.348557726
6	27.165601786	26.035755119	45.377038512
1	28.057170262	26.659597478	45.480651226
6	31.349914235	26.549620799	37.048837140
1	31.353238151	26.803570865	38.125385688
1	32.358756396	26.194576954	36.776177393
7	30.341299986	25.567513048	36.721722937
1	29.468493177	25.906239490	36.299797973
6	30.348266006	24.276544842	37.090893348
7	31.378218344	23.767198346	37.794958831
1	31.933888201	24.370561260	38.398180254
1	31.295278505	22.796817544	38.088114825
7	29.337981916	23.505710600	36.720938480
1	28.645089742	23.868947426	36.054518487
1	29.406354983	22.473522525	36.742388976
26	28.416150508	24.423871444	42.854268529
8	33.178849187	23.772602188	42.359226149
8	30.495400189	27.561698217	42.741531337
6	29.765450859	27.134418418	41.834221309
8	29.142586604	26.015209590	41.846432371
6	29.571739669	27.979345630	40.563422577
6	29.148759525	29.416469354	40.861251180
6	30.220319144	30.287728790	41.533185766
8	29.807886043	31.127696314	42.384320094
8	31.411973026	30.151641828	41.163402769
1	28.241420736	29.451240818	41.482540365
1	28.893853702	29.913213049	39.905639355
1	28.846412670	27.483216865	39.906728518
1	30.526668024	28.013408319	40.015260735
8	34.854171276	22.115466630	45.192050359
6	34.137547121	21.355030229	44.570718088
7	33.685826646	21.665866500	43.265271899
6	34.227013356	22.887173104	42.638685787
6	32.807525665	20.874196724	42.549663097
7	32.347672340	21.320845500	41.394744785
6	32.448955367	19.608514983	43.082722623
6	32.902905186	19.270010383	44.315182405
7	33.703784588	20.119361929	45.047013199

1	34.754101413	22.569854443	41.720501536
1	34.954806950	23.295210203	43.352772611
1	31.680207005	20.765911348	40.832201857
1	32.613896169	18.320140951	44.766231825
1	31.789317252	18.940767644	42.531778959
1	33.389300598	24.340505802	41.584572285
1	32.393104905	22.324707775	41.229470998
8	28.851234020	25.078332703	39.318110551
1	28.783914249	24.114301944	39.449870844
1	29.056397320	25.376841436	40.227288924
8	33.312348600	25.397595884	40.081368308
1	33.133478826	26.299643859	40.465583996
1	34.178223774	25.479987104	39.653954723
8	30.102558786	27.621271928	45.488786496
1	29.722051731	28.512040341	45.341957706
1	30.346549985	27.387673564	44.567326289
1	29.574081411	20.766418331	46.149477817
1	25.870559301	21.280487252	40.533235296
1	25.837885622	26.406020276	47.142512702
1	31.139302119	27.461368396	36.489886183
1	33.919598544	19.865012503	45.989723756

#### Snapshot 4

##### RC2

**QM/MM (BS1) = -3387.649551 a.u.**

**QM/MM (BS2+ZPE) = -3389.601928 a.u.**

6	28.147647136	43.730064062	43.113309518
7	29.412446532	43.278708386	43.408698698
1	30.052598939	43.655280431	44.123849237
6	29.691071329	42.259639563	42.579589182
1	30.631143705	41.713879185	42.594106689
7	28.670312531	42.030694016	41.765234270
6	27.693176056	42.942850276	42.081938848
1	26.764334986	42.999031749	41.519358840
6	25.885963190	42.097265350	37.195442225
1	26.395165549	42.499997447	36.307275158
1	25.267421954	41.251756747	36.860492612
6	26.935677240	41.543949443	38.143210490
8	27.005108354	41.983973343	39.346881463
8	27.746154917	40.687080061	37.747134553
6	31.468356518	43.859757897	38.754516656
7	30.294490062	44.402947209	38.287671402
1	30.161278288	45.323400185	37.851606234
6	29.304782870	43.541164146	38.565178047
1	28.262211576	43.733031921	38.348039090
7	29.772589492	42.458171616	39.164817612
6	31.127981975	42.641053908	39.299541780
1	31.744889208	41.892615897	39.790121882
6	22.610906892	38.892616784	34.069814105
1	21.526553800	38.968449545	33.869426074
1	23.062084955	39.849250222	33.757533524

7	22.904868569	38.613091105	35.456701048
1	23.334612349	37.721475040	35.725800030
6	22.764562556	39.523282477	36.438398840
7	22.237524865	40.733488556	36.205120305
1	21.633674103	40.938154885	35.403168165
1	22.087002307	41.290333330	37.055197792
7	23.188521248	39.245276039	37.660453584
1	23.599371438	38.355537357	37.966402454
1	23.039171363	39.970090747	38.372323410
26	28.558360750	40.869029106	39.989604539
8	27.568350240	39.762843705	40.625857624
8	29.377001722	37.744913126	39.591015259
6	30.289436255	38.555548376	39.659146476
8	30.159267642	39.840435902	39.865622590
6	31.739229630	38.109719258	39.526760886
6	32.239880786	37.493421019	40.832363917
6	33.578202127	36.756572180	40.736558673
8	34.210249529	36.781154839	39.648496784
8	33.947164990	36.139919561	41.767887428
1	31.500656323	36.770285777	41.212742673
1	32.326915325	38.259197083	41.622215303
1	32.366575921	38.959920615	39.225849276
1	31.792426666	37.359513208	38.725045309
8	26.467207845	41.248784835	45.453745834
6	25.603062387	42.077191535	45.287985881
7	24.599877337	41.897484841	44.299452665
6	24.646285309	40.626301503	43.562382767
6	23.631613213	42.825251047	44.030250022
7	22.804979886	42.654059222	43.010379320
6	23.520714637	43.960346020	44.892449997
6	24.454782270	44.146015700	45.860568243
7	25.499668942	43.269147985	46.015606059
1	25.107477876	40.759181408	42.573099527
1	23.629246700	40.230270923	43.449490125
1	22.098223569	43.365231719	42.836105551
1	24.402935584	45.005375115	46.534057774
1	22.687523752	44.649925656	44.774784806
1	25.248551578	39.922552029	44.144741139
1	22.857831908	41.883044356	42.331376482
8	24.239346708	37.166931886	39.227323992
1	23.513389242	37.026848322	39.858225296
1	24.647337583	38.002921838	39.589011218
8	24.831880978	39.642420421	39.992912140
1	24.104532903	40.161445870	40.424494653
1	25.698100520	39.921583899	40.346809040
1	27.750721505	44.676124332	43.481395555
1	25.242409581	42.872970346	37.610397444
1	32.378278592	44.459094502	38.784596202
1	23.025895756	38.107529967	33.437761692
1	26.218220430	43.458748991	46.684715707

**TS7****QM/MM (BS1) = -3387.608678 a.u.****QM/MM (BS2+ZPE) = -3389.562261 a.u.**

6	28.084061499	43.949678208	43.297184139
7	29.345598920	43.483807550	43.583351453
1	30.015170275	43.871134964	44.262760027
6	29.583560981	42.421508930	42.801741532
1	30.513223969	41.859073743	42.813389591
7	28.535881978	42.175979852	42.030709172
6	27.586997742	43.125553711	42.319192715
1	26.651235160	43.179749410	41.768155334
6	25.880942314	42.034255823	37.461851421
1	26.534943470	42.368587818	36.641522252
1	25.275560917	41.200418400	37.079084372
6	26.741009297	41.501137823	38.597637102
8	26.792037621	42.106657389	39.713781915
8	27.452980773	40.476677228	38.435004037
6	31.367509395	43.750222656	38.873898255
7	30.186104205	44.290052873	38.426459497
1	30.054937718	45.204757926	37.978335676
6	29.199156705	43.440059292	38.761737550
1	28.152306684	43.644606312	38.580449542
7	29.667348970	42.369637129	39.380114625
6	31.027350470	42.548790960	39.465529807
1	31.661545717	41.817580045	39.962721790
6	22.681893258	38.885030377	33.965344567
1	21.597777464	38.977139948	33.769379659
1	23.146327745	39.838245600	33.664015368
7	22.976244319	38.583629876	35.347393968
1	23.373546714	37.672785758	35.603278103
6	22.857651798	39.484305275	36.337326139
7	22.362822401	40.709517017	36.109804968
1	21.745447360	40.920882142	35.319446800
1	22.221461981	41.263027905	36.963430467
7	23.276566775	39.181026592	37.556510483
1	23.634621644	38.263630821	37.848415073
1	23.124205681	39.888376207	38.283940480
26	28.202000376	40.775971435	40.506818493
8	26.952278504	39.962160327	41.495802404
8	29.044409169	37.617359601	39.873499082
6	29.940141821	38.441242883	40.028437920
8	29.767658782	39.657574608	40.463198650
6	31.397972637	38.077238639	39.756703561
6	32.064715253	37.530529468	41.022335116
6	33.385781976	36.779177405	40.823721770
8	33.967253902	36.825306489	39.708297443
8	33.799770822	36.129681114	41.818238119
1	31.386403790	36.834890551	41.539726878
1	32.243008414	38.344266596	41.745159699
1	31.939757650	38.959332303	39.383010114
1	31.419780698	37.314477928	38.966950963

8	26.810320029	40.969369066	45.590165506
6	25.937203339	41.729659668	45.253906475
7	25.088673774	41.408783936	44.141536373
6	25.366858867	40.153762534	43.493342112
6	24.075120290	42.245661669	43.724361595
7	23.348940300	41.968876895	42.660073300
6	23.803523872	43.424870566	44.483651370
6	24.601072436	43.744248695	45.534790684
7	25.671110120	42.956604064	45.873440845
1	26.200651872	40.216037340	42.532886845
1	24.468260980	39.705208328	43.055846108
1	22.707260407	42.689239010	42.300907795
1	24.405344176	44.637064183	46.134933745
1	22.941031590	44.042475255	44.231379361
1	25.876426051	39.477997721	44.187810405
1	23.432556830	41.151191337	42.050566103
8	24.151741203	36.914203885	39.026360798
1	23.404390968	36.782790045	39.630984895
1	24.616006480	37.702662878	39.441553622
8	24.892523389	39.226792486	39.921873127
1	24.076726136	39.685577260	40.258534989
1	25.650953754	39.470781997	40.508761499
1	27.715572610	44.926003099	43.611942725
1	25.238113138	42.862693999	37.759388235
1	32.278765609	44.347375163	38.840908679
1	23.085086337	38.096316696	33.330180508
1	26.311203079	43.254975977	46.581415212

### Snapshot 5

#### RC2

**QM/MM (BS1) = -3454.993953 a.u.**

**QM/MM (BS2+ZPE) = -3457.012097 a.u.**

6	30.556341623	22.656880214	48.650120925
7	31.469747296	23.627821023	48.995964055
1	32.202435574	23.543577365	49.713515694
6	31.253901807	24.702055204	48.216952802
1	31.830220261	25.620774738	48.284393585
7	30.244817950	24.477971113	47.382675743
6	29.797310414	23.196950830	47.635419052
1	28.983609905	22.754182585	47.061798905
6	25.489304614	24.019734720	45.195384191
1	24.921444450	24.898513427	45.524752932
1	25.311598623	23.867061004	44.120344586
6	26.992506209	24.219456755	45.385449376
8	27.320269670	25.298291524	46.073103358
8	27.811193166	23.435846741	44.931969187
6	28.130104746	27.238075658	50.324107598
7	27.124923333	26.336502165	50.040853172
1	26.386274884	26.020826113	50.675770529
6	27.296824541	25.907753921	48.779178652
1	26.658510400	25.198075138	48.268672523

7	28.349876688	26.489938998	48.228231051
6	28.888522987	27.322002429	49.180889717
1	29.778866391	27.906701018	48.970707049
6	29.868800525	27.324628000	37.888739861
1	29.572792446	27.932971081	38.759108470
1	30.959839196	27.164388769	37.960880442
7	29.145929300	26.065657173	37.873987347
1	28.795941660	25.721655189	36.979276320
6	28.957584857	25.264685604	38.940413629
7	29.512340010	25.574831966	40.138510778
1	30.344792428	26.174472770	40.182185105
1	29.459348676	24.852719862	40.863755236
7	28.219473465	24.171820325	38.826563609
1	27.565888015	24.035094836	38.043958978
1	27.997139606	23.609741724	39.658737771
26	29.115549155	25.957557337	46.315840640
8	29.624153167	25.618133445	44.808557379
8	31.714996651	27.639001573	45.045321615
6	30.922241893	28.244607161	45.756408714
8	29.932871449	27.695027192	46.427953026
6	31.030557977	29.758157140	45.931010583
6	32.442835073	30.255385038	46.244205328
6	32.748149961	31.716325865	45.810167423
8	31.996341510	32.225996276	44.937369758
8	33.742139519	32.261526887	46.336751227
1	33.162135108	29.614683313	45.707173279
1	32.691968081	30.154976136	47.313592336
1	30.293124440	30.108979468	46.667799222
1	30.749974976	30.208281997	44.965175562
8	34.067300640	22.045261261	46.280494489
6	33.306547801	21.193337638	45.860974006
7	32.358476885	21.501621370	44.857637209
6	32.353136529	22.877233668	44.350756547
6	31.448806583	20.602096227	44.350015233
7	30.594866811	20.963923293	43.418006582
6	31.468629351	19.274767019	44.878343359
6	32.366946308	18.955234699	45.840722398
7	33.284674895	19.869537889	46.310820208
1	32.519285056	22.879420504	43.264413356
1	33.161736648	23.420215093	44.844112915
1	29.942923584	20.257412435	43.037340721
1	32.356696801	17.958933070	46.277221485
1	30.747826987	18.541543304	44.520942522
1	31.396155733	23.366524547	44.582843073
1	30.381705055	21.924129975	43.099608103
8	29.277530660	23.370967038	42.459366678
1	28.809430171	23.532171362	43.305909817
1	28.530283049	22.995805129	41.885558964
8	28.421972447	27.145117372	42.699053994
1	28.518917169	26.752177250	41.812397563
1	28.941775438	26.564507481	43.288608319
8	31.875955178	25.751465908	43.001536065



1	31.130238874	25.133409397	43.033280873
1	31.736885730	26.323415977	43.788319772
1	30.427151035	21.740243675	49.225581239
1	25.100149083	23.149409097	45.723738808
1	28.287639786	27.641411197	51.324392799
1	29.690993652	27.910839645	36.987181238
1	33.861309140	19.648763437	47.097410369

**TS7**

**QM/MM (BS1) = -3454.951357 a.u.**

**QM/MM (BS2+ZPE) = -3456.971787 a.u.**

6	30.615522303	22.506379447	48.834224712
7	31.555510000	23.449714698	49.176680557
1	32.285088086	23.356638807	49.894128900
6	31.385186508	24.520469634	48.387150927
1	31.996562827	25.415655497	48.450708358
7	30.374848532	24.322209150	47.551376439
6	29.880983413	23.060736765	47.810577129
1	29.053256627	22.642195572	47.238338452
6	25.639088192	24.000174414	45.247697633
1	25.128063712	24.907823433	45.589827319
1	25.423596675	23.873376877	44.174535252
6	27.159853900	24.117325530	45.383426268
8	27.601514265	25.287292771	45.797967913
8	27.900177189	23.186484445	45.089302944
6	28.224692999	27.189549623	50.248301084
7	27.203225558	26.327742816	49.909613933
1	26.430001546	26.028572538	50.510315007
6	27.429757363	25.901650475	48.648580189
1	26.780952369	25.221556913	48.108369086
7	28.532557638	26.438660802	48.155084012
6	29.043571979	27.244908358	49.142450647
1	29.968041924	27.799152463	48.997325644
6	29.874800601	27.309336317	37.885038811
1	29.570314801	27.909493937	38.758494931
1	30.966465638	27.155983640	37.960984483
7	29.161949057	26.044520358	37.855561781
1	28.784855809	25.725674190	36.962828030
6	28.994460679	25.217194936	38.904516287
7	29.575647452	25.494928112	40.097407094
1	30.392762166	26.115552259	40.151756820
1	29.549762012	24.751838876	40.800247896
7	28.250425687	24.128839994	38.779048102
1	27.579992705	24.017093475	38.006763401
1	28.024633831	23.555981930	39.602281470
26	29.481454511	25.699001545	46.184249625
8	30.305238101	24.896191778	44.835395376
8	32.154832424	27.819611763	45.080715413
6	31.171822961	28.246756568	45.685576217
8	30.136477047	27.535700585	46.051050769
6	31.088975478	29.734455080	46.038716230

6	32.426381941	30.363250597	46.438850770
6	32.718799706	31.780524930	45.871396432
8	31.961602695	32.216032032	44.963905319
8	33.717210847	32.368971210	46.343122717
1	33.239310683	29.720956906	46.066688132
1	32.558778750	30.403959461	47.532433508
1	30.294881129	29.898452141	46.782038938
1	30.772539152	30.270032076	45.125967609
8	33.558251653	22.354823649	46.457652681
6	32.912981203	21.444719798	45.981737308
7	31.981165669	21.704039479	44.923452830
6	31.973115433	23.033089883	44.385093155
6	31.178634795	20.716749628	44.361910471
7	30.366963204	20.999649886	43.375895291
6	31.289925654	19.395298049	44.893441315
6	32.191368403	19.129932143	45.868404273
7	33.023866152	20.107820970	46.374209827
1	31.870594940	23.028738327	43.294415177
1	32.846531807	23.590708711	44.728280206
1	29.798986700	20.236318218	42.969316356
1	32.249470028	18.128550079	46.292830129
1	30.637245098	18.611904976	44.511610481
1	31.016200901	23.801434886	44.732227313
1	30.077644343	21.943765313	43.035249508
8	29.125014416	23.291469502	42.434055664
1	28.685673181	23.395763384	43.303531678
1	28.374795904	22.939896499	41.839341676
8	28.513707202	26.729724889	42.713848700
1	28.516977173	26.463169217	41.775605901
1	28.968807156	25.992194697	43.154488938
8	32.232710630	25.970994523	43.080864751
1	31.438845382	25.514601144	43.417060937
1	32.334585839	26.649133924	43.784742576
1	30.444318360	21.610041523	49.430324415
1	25.212335279	23.146288099	45.773841564
1	28.337296070	27.607471028	51.248665804
1	29.697176384	27.900989122	36.987005445
1	33.651224947	19.892976038	47.122698369

## References

1. Yi, C.; Chen, B.; Qi, B. Zhang, W.; Jia, G.; Zhang, L.; Li, C. J.; Dinner, A. R.; Yang, C. G.; He, C. Duplex interrogation by a direct DNA repair protein in search of base damage. *Nat. Struct. Mol. Biol.* 2012, 19(7), 671-676.
2. Yi, C.; Jia, G.; Hou, G.; Dai, Q.; Zhang, W.; Zheng, G.; Jian, X.; Yang, C. G.; Cui, Q.; He, C. Iron-catalysed oxidation intermediates captured in a DNA repair dioxygenase. *Nature*. 2010, 468(7321), 330-333.

## C Appendix C: Supporting Information for Chapter 4

### C.1 QM/MM Calculations of the Dioxygen Activation in the WT TET2

The dioxygen activation step commences from the Fe(III)superoxo intermediate, where dioxygen ( $O_2$ ) binds to Fe(II) center in an end on manner. One of the MD trajectories of the Fe(III)-superoxo complex was used in this calculation, taking into account the distance between the distal oxygen ( $O_d$ ) of the superoxide and the C2 of the 2OG cosubstrate. We performed the QM/MM optimization of the reactant complex geometry (**RC'**). The optimized geometry results in Fe- $O_p$ ,  $O_p$ - $O_d$ , and  $O_d$ -C2 distances of 2.08, 1.28, and 2.57 Å, respectively, which are in good agreement with the previously reported results.<sup>1,2</sup> The reaction starts with the nucleophilic attack of C2 by the distal oxygen ( $O_d$ ), passes through a **TS1** and then results in an Fe(II) peroxysuccinate intermediate, **IM1**. This step is termed decarboxylation, involving the cleavage of C1-C2 bond of 2OG and the formation of new bond between the superoxide  $O_d$  and the C2 of 2OG. At the first TS (**TS1**), the  $O_p$ - $O_d$  and C1-C2 distances elongate to 1.36 and 1.73 Å, respectively, in readiness for the decarboxylation while the  $O_d$ -C2 distance shortens to 1.46 Å, to favor the formation of the new bond. The decarboxylation proceeds with a barrier of 9.1 kcal/mol at B2+ZPE level of theory and the formed **IM1** is highly exothermic with energy of -38.2 kcal/mol at B2+ZPE level. The high exothermic nature of the **IM1** could be due to the elimination of  $CO_2$ . At **IM1**, the  $O_d$ -C2 distance reduces to 1.32 Å.

The next step (**IM1** to **IM2**) involves the cleavage of the **IM1** O<sub>p</sub>-O<sub>d</sub> bond. This step occurs rapidly with reaction barrier of 5.8 kcal/mol at B2 level and a barrierless system with ZPE when compared to the decarboxylation step, indicating that the decarboxylation step is the rate determining step of the dioxygen activation, in agreement with previous studies.<sup>1-3</sup> At the **IM2**, there is a partial bond of 2.20 Å between the O<sub>p</sub> and O<sub>d</sub> superoxide oxygen atoms and the Fe-O<sub>p</sub> distance is 1.79 Å. The partial bond between the superoxide oxygen atoms break to form the **IM3** with the new Fe-O<sub>p</sub> bond of 1.62 Å, that is characteristic of Fe(IV)=O intermediate. The **IM3** results in energy of -62.9 kcal/mol at B2+ZPE level of theory. The calculations reveal overall reaction energy to be -62.9 kcal/mol at B2+ZPE level of theory, inferring that the dioxygen activation step is exothermic in nature. The detailed geometries of the stationary points and the potential energy profile of the dioxygen activation are shown in Figures C1 and C2, respectively.

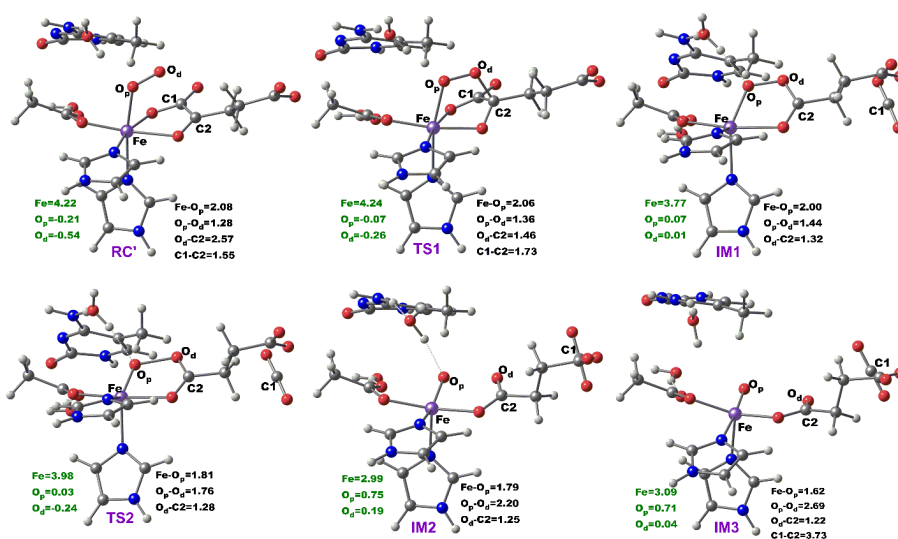


**Figure C1.** Stationary points geometries involved during the dioxygen activation step in the WT TET2-dsDNA. Distances (Å) and spin densities are in black and green, respectively.

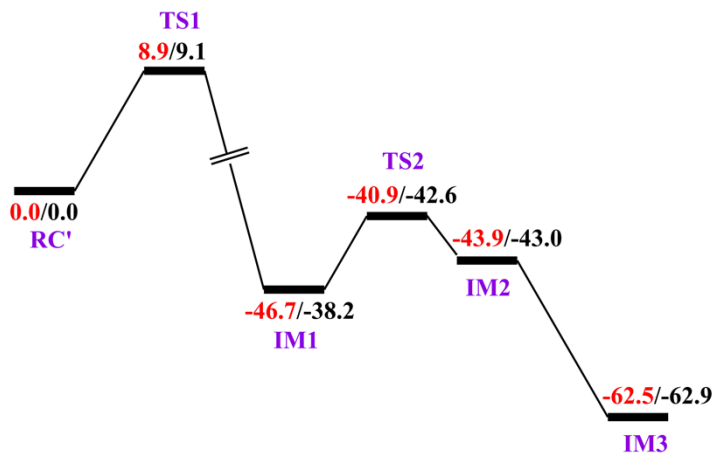


**Figure C2.** QM/MM potential energy profile for the dioxygen activation by WT TET2-dsDNA. The relative energies are in kcal/mol at UB3LYP/def2-TZVP (B2) and at B2+ZPE in red and black, respectively.

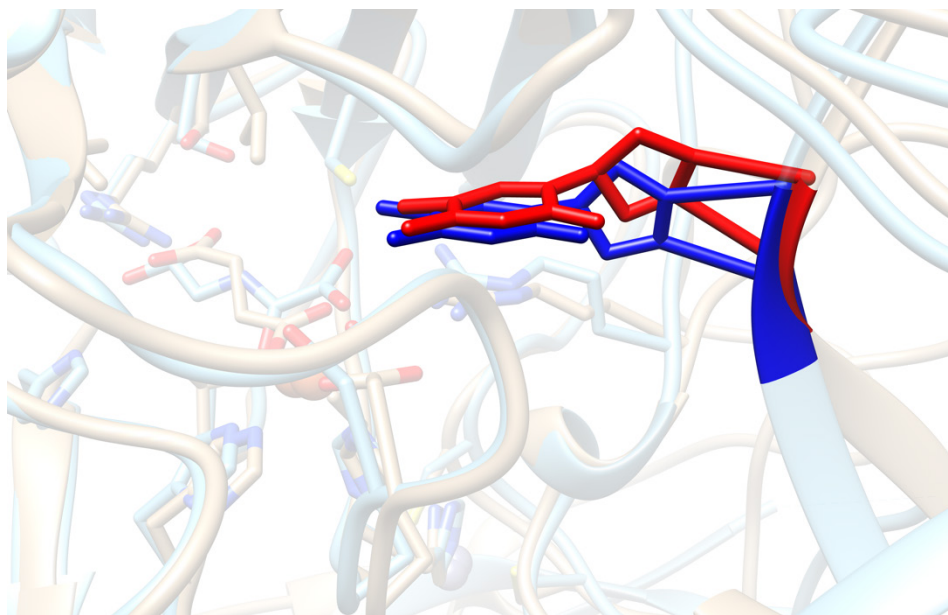


**Figure C3.** Overlaid crystal structure of TET2 and the average structure from the Fe(IV)=O complex MD simulation. The blue and red structures show the orientations of the 5-methyl cytosine (5mC) dsDNA substrate in the crystal structure and average MD structure, respectively.

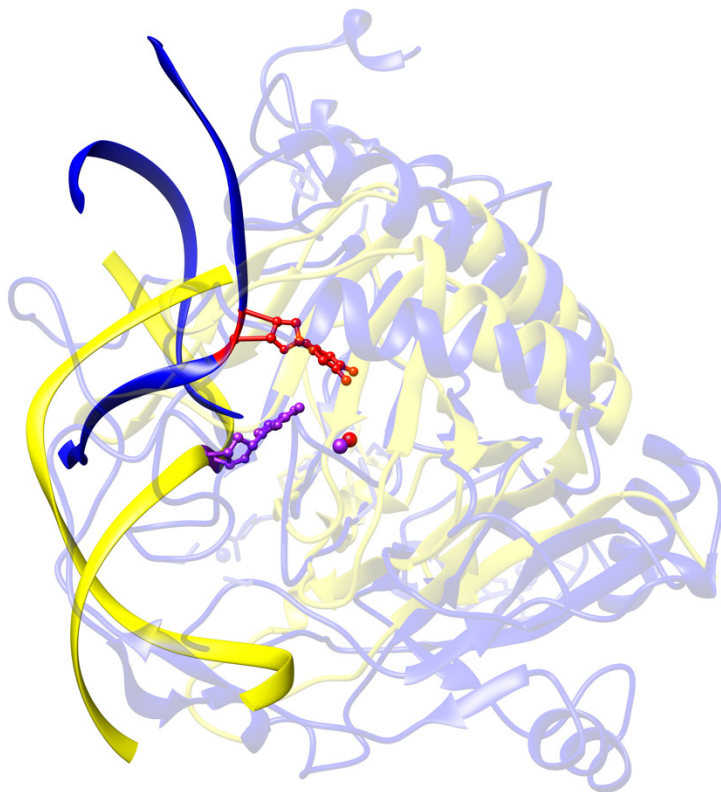


**Figure C4.** Overlaid crystal structures of TET2 (PDB code, 4NM6<sup>4</sup>) and AlkBH2 (PDB code, 3RZJ<sup>5</sup>) bound to 5-methyl cytosine (5mC) and 3-methyl cytosine (3mC) dsDNA substrates, respectively. Coloring: TET2 (blue), AlkBH2 (yellow), 5mC (red), 3mC (purple), TET2 Fe center (red), and AlkBH2 Fe center (purple).

## C.2 Comparison between the Dynamics of Fe(IV)=O Complexes of TET2-dsDNA and AlkBH2-dsDNA

The overlaid structures of TET2 and AlkBH2 [Figure C4] show differences in the binding position of the duplex DNA.<sup>4</sup> The angle between the first coordination sphere histidine (His1382 in TET2 and His171 in AlkBH2), the iron center, and the substrate's methyl carbon has value of 107.8° and 56.8° in TET2 and AlkBH2, respectively. In TET2-dsDNA complex, TET2 loops L1 (aa 1256-1273) and L2 (aa 1288-1312) interact with dsDNA, while in AlkBH2-dsDNA, the hydrophobic  $\beta$ -hairpin (aa 89-108) and substrate's

recognition lid (aa 119-131) interact with the dsDNA. The  $\beta$ -hairpin determines the preference of the AlkBH2 for duplex DNA, and it contains an intercalating Phe102 residue that aids the flipping of the damaged base to the active site.<sup>5,6</sup> Our recent study on AlkBH2-dsDNA showed that this intercalating residue forms a stable  $\pi$ -stacking interaction with the nearby bases of the dsDNA, enhancing the stability of the protein-DNA complex.<sup>1</sup> In TET2-dsDNA, the loops L1 and L2 have a positive correlation with each other, the GS linker, the Zn fingers coordination sites (which are absent in AlkBH2-dsDNA), and the DNA [Figure 4.5]. This implies that such correlated motion might enhance the binding of the DNA to the protein and the overall stability of the TET2-dsDNA. By contrast, in AlkBH2-dsDNA, the hydrophobic  $\beta$ -hairpin exhibited some motion towards the Fe center, favoring catalysis.<sup>1</sup> The dynamics cross-correlation analysis showed that the  $\beta$ -hairpin has strong positive correlations with the substrate's recognition lid residues and contributes to the substrate binding. On the other hand, the substrate recognition lid in AlkBH2-dsDNA has a positive correlation with the residues that stabilize the succinate, implying that the succinate binding influences the substrate binding site and the Fe center orientation via long-range interactions.<sup>1</sup>

In TET2-dsDNA, the 5mC ring is stabilized by Tyr1902, an interaction conserved during the MD [Figure C5]. The 3-methylcytosine (3mC) base in AlkBH2-dsDNA is stabilized by a couple of  $\pi$ -stacking interactions with aromatic residues such as Phe124 and the imidazole ring of the iron-coordinating equatorial His171 [Figure C5]. 5mC base in TET2 is more flexible than the 3mC base in AlkBH2. Furthermore, the exocyclic amine (N4) of the substrates in both complexes is stabilized by interactions with different residues,

namely-Asn1387 and Glu175 in TET2 and AlkBH2, respectively. The interaction of Asn1387 with the amine group in TET2-dsDNA is very stable [Figure C6], however, the corresponding interaction with Glu175 in AlkBH2-dsDNA is less stable during the last 500 ns of the simulation [Figure S6]. The observed differences in their interactions might be due to the shorter carbon length of the sidechain in Asn1387, making it slightly more rigid in TET2 than Glu175 in AlkBH2. The stronger stabilization of the exocyclic amine might compensate for the weaker stacking interaction in TET2.



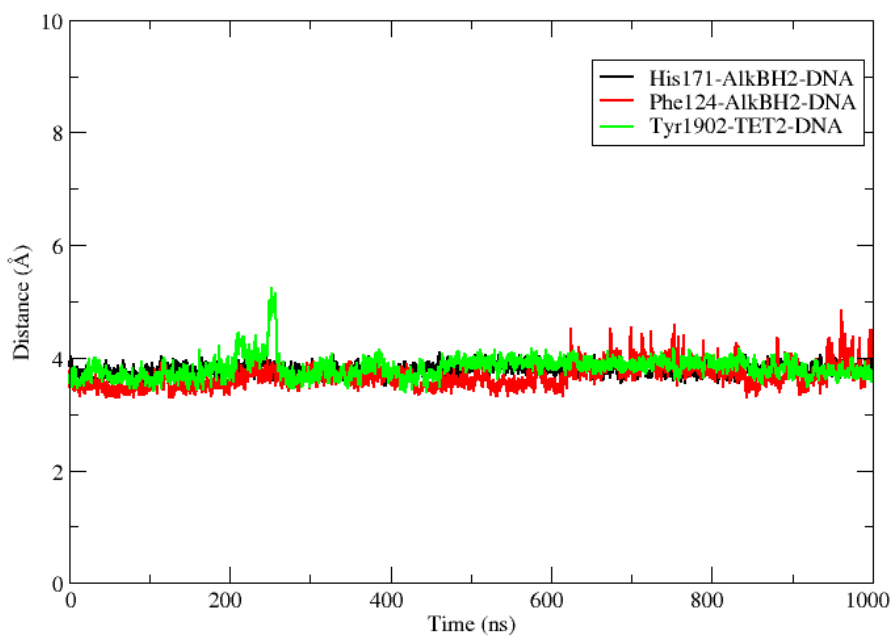
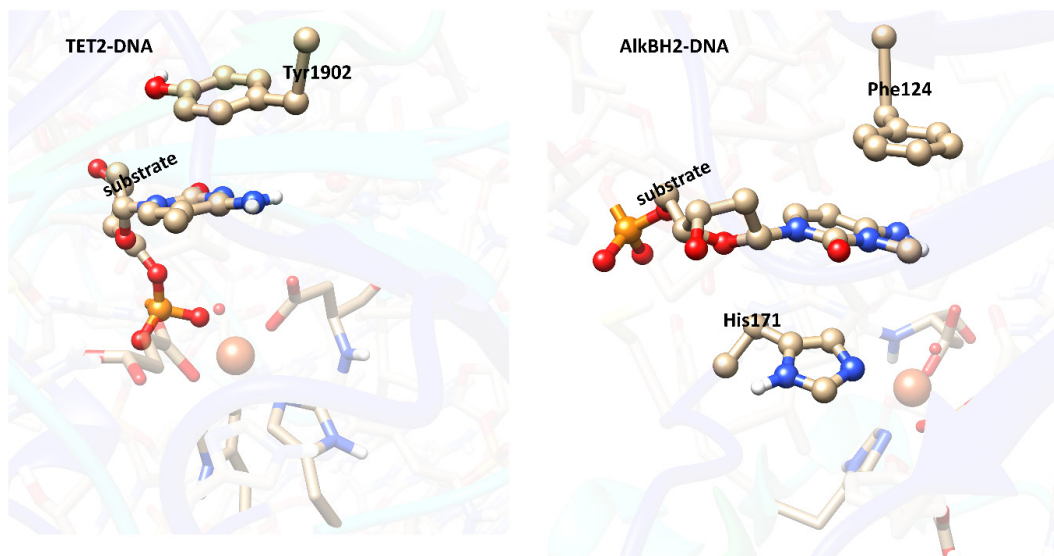


**Figure C5.** Stacking Interaction of the residues that stabilize the cytosine rings of the substrates in the AlkBH2-dsDNA and TET2-dsDNA ferryl complexes MD simulations. Distances were measured between the center of mass of the atoms forming imidazole ring of His171 and phenyl rings of Phe124 and Tyr1902.

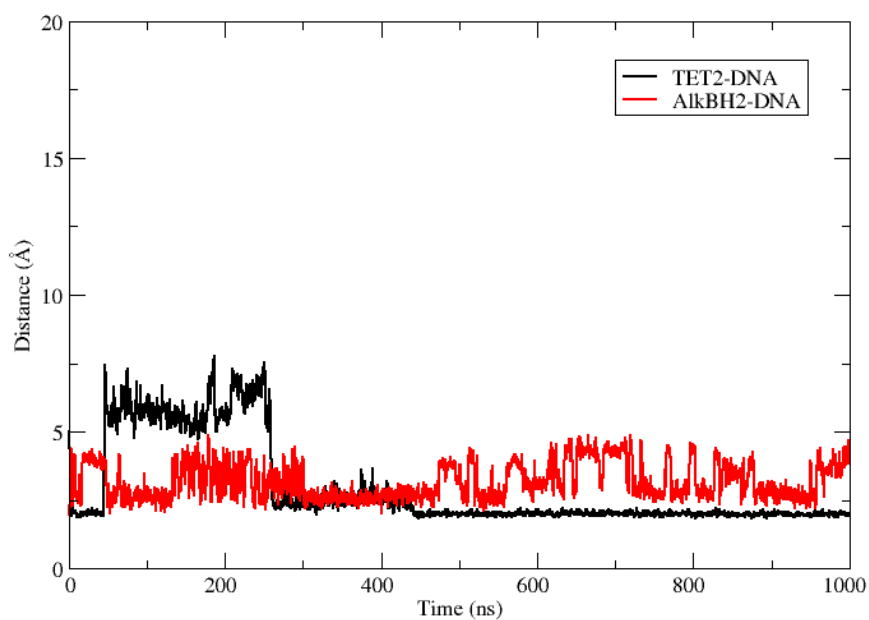
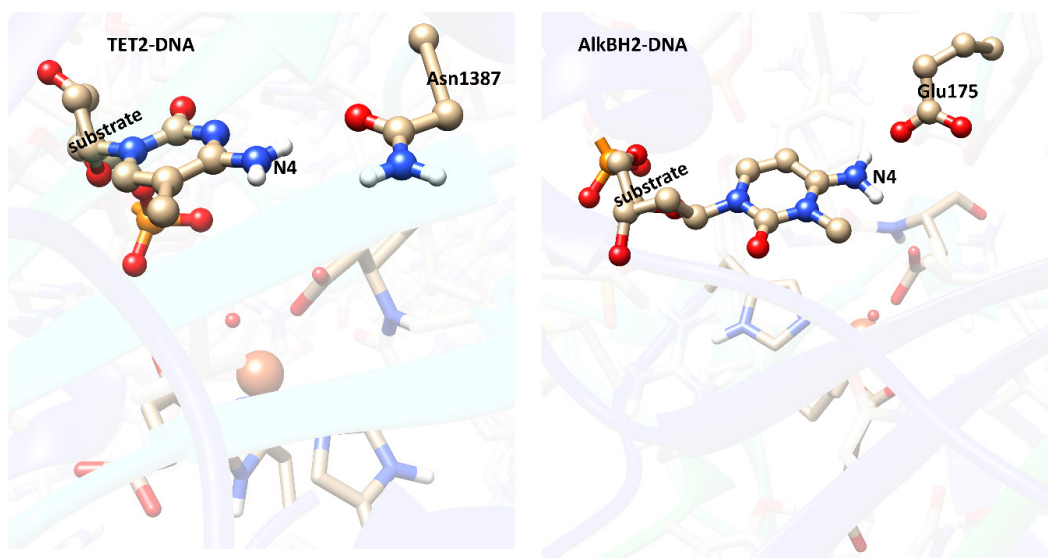


**Figure C6.** Hydrogen bonding interaction of Glu175 and Asn1387 side chains with the exocyclic amine (N4) of the substrates in the ferryl complexes MD simulations of AlkBH2-dsDNA and TET2-dsDNA, respectively. The distances were measured between the center of mass of the atom forming the carboxylate of the two residues and the bases of the substrates.

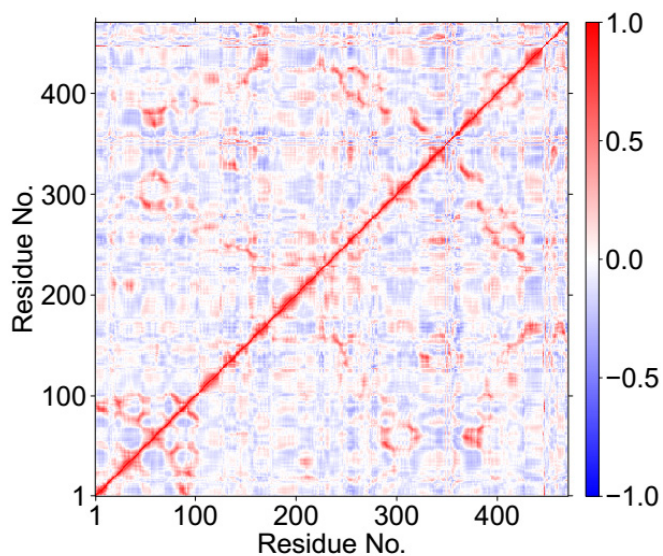


**Figure C7.** Dynamics cross correlation for the TET2-dsDNA K1299E-S1303N mutant ferryl complex MD simulations. Residue numbers 1-445 (protein), 446-448 (Zn), 449 (Fe), 450 (O), 451 (succinate), 452-475 (DNA).

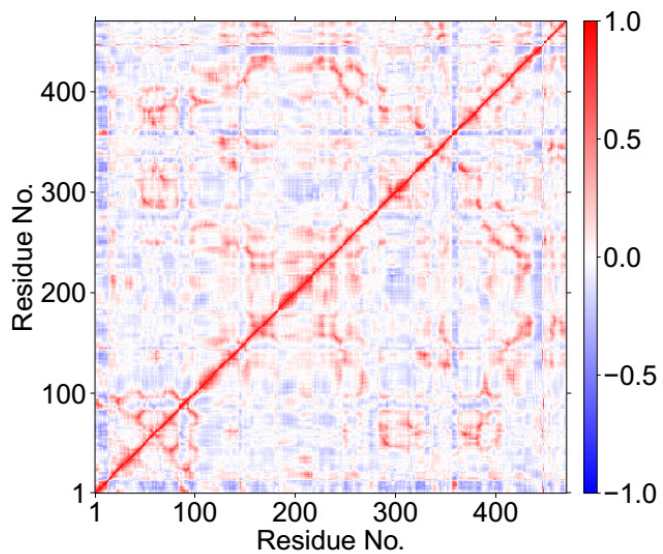


**Figure C8.** Dynamics cross correlation for the TET2-dsDNA M1293A-Y1294A mutant ferryl complex MD simulations. Residue numbers 1-445 (protein), 446-448 (Zn), 449 (Fe), 450 (O), 451 (succinate), 452-475 (DNA).

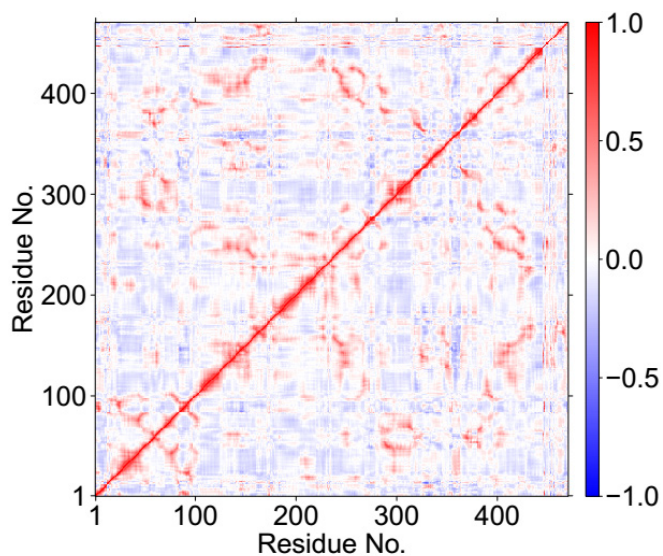


**Figure C9.** Dynamics cross correlation for the TET2-dsDNA S1290A-Y1295A mutant ferryl complex MD simulations. Residue numbers 1-445 (protein), 446-448 (Zn), 449 (Fe), 450 (O), 451 (succinate), 452-475 (DNA).

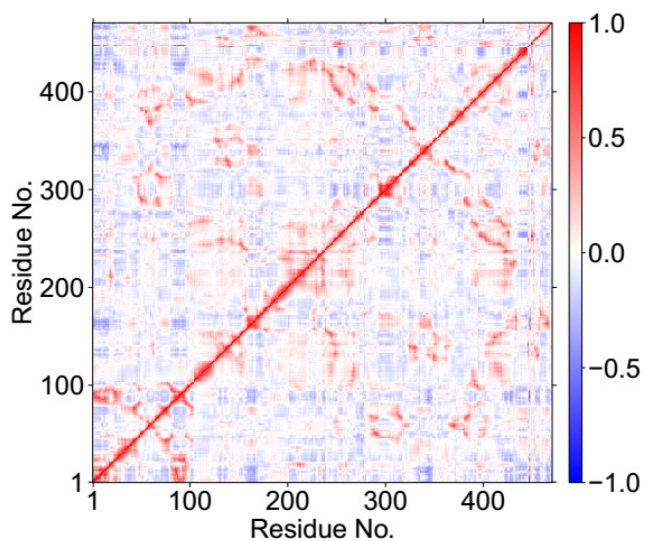


**Figure C10.** Dynamics cross correlation for the TET2-dsDNA Y1902A mutant ferryl complex MD simulations. Residue numbers 1-445 (protein), 446-448 (Zn), 449 (Fe), 450 (O), 451 (succinate), 452-475 (DNA).

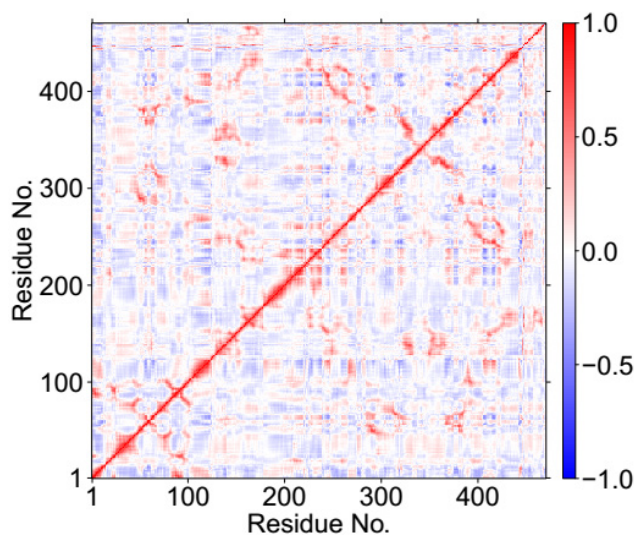


**Figure C11.** Dynamics cross correlation for the TET2-dsDNA H1904R mutant ferryl complex MD simulations. Residue numbers 1-445 (protein), 446-448 (Zn), 449 (Fe), 450 (O), 451 (succinate), 452-475 (DNA).

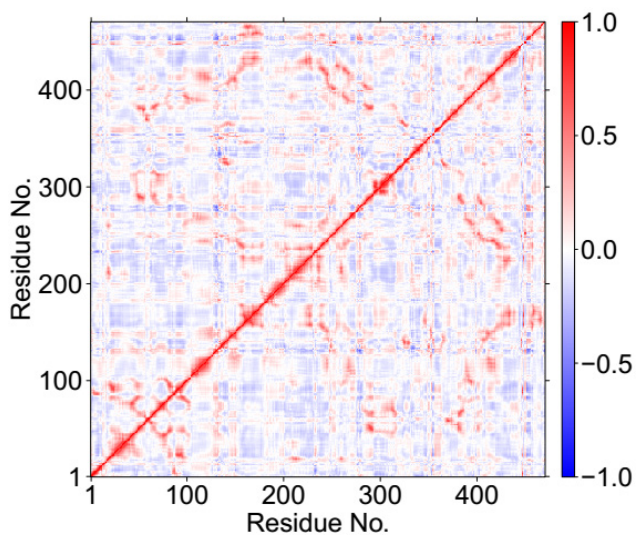


**Figure C12.** Dynamics cross correlation for the TET2-dsDNA N1387A mutant ferryl complex MD simulations. Residue numbers 1-445 (protein), 446-448 (Zn), 449 (Fe), 450 (O), 451 (succinate), 452-475 (DNA).

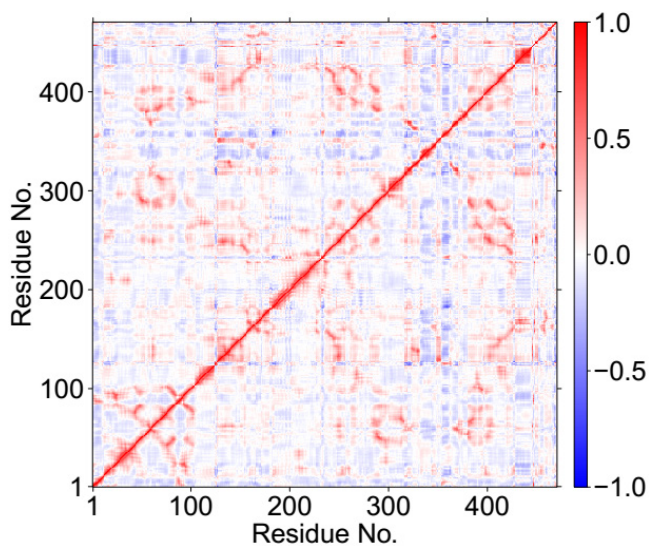


**Figure C13.** Dynamics cross correlation for the TET2-dsDNA W1291A mutant ferryl complex MD simulations. Residue numbers 1-445 (proteins), 446-448 (Zn), 449 (Fe), 450 (O), 451 (succinate), 452-475 (DNA).

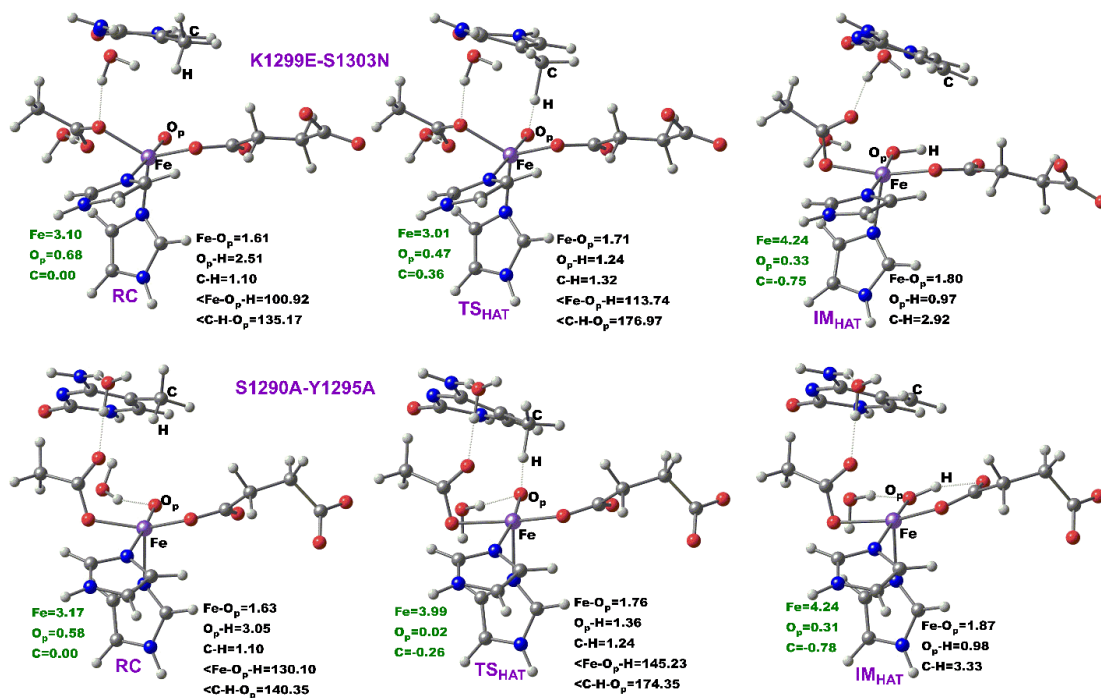


**Figure C14.** Stationary points geometries involved during the HAT in the K1299E-S1303N and S1290A-Y1295A TET2-dsDNA double mutants. Distances (Å) and spin densities are in black and green, respectively.

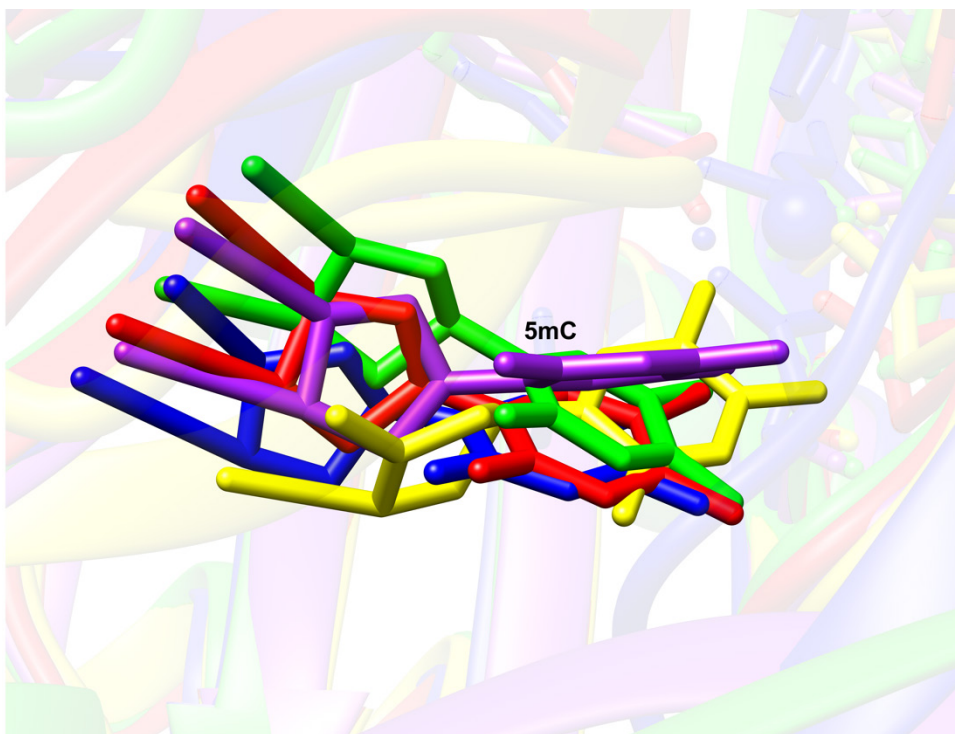


**Figure C15.** Overlaid Structures showing the orientations of 5mC substrate in both the WT TET2 and the mutants. Coloring: WT (red), K1299E-S1303N (blue), N1387A (yellow), S1290A-Y1295A (green) and Y1902A (purple).

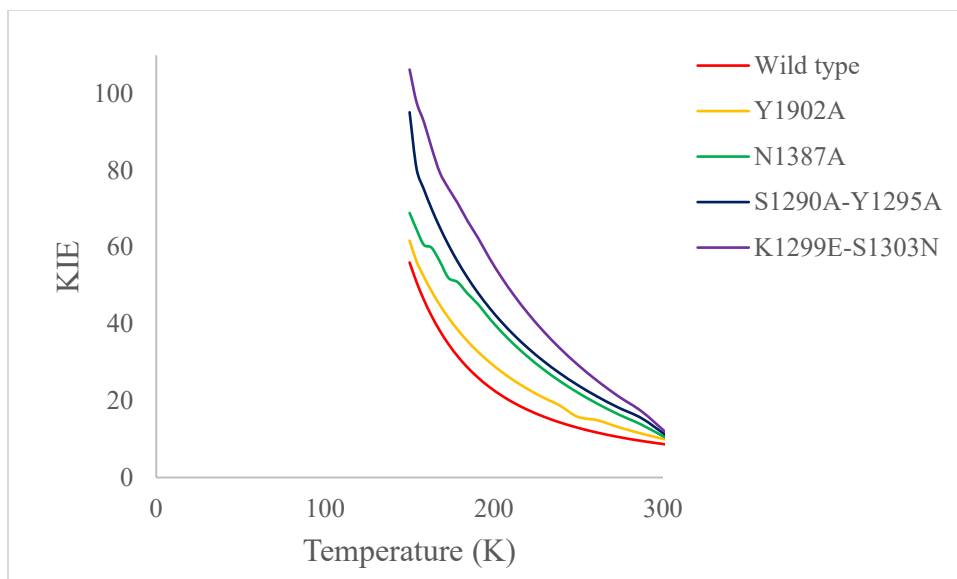


**Figure C16.** Temperature dependence of KIEs for the WT TET2-dsDNA and the studied mutants.

**Table C1.** Distance between the oxo group (O) of the Fe(IV)=O and the alpha carbon (CA) of the residues to be mutated.

Residues	Distance (Å)
Y1902A	9.2
N1387A	9.5
H1904R	11.9
S1290A-Y1295A	13.1 (22.0)
<b>*W1291A</b>	<b>14.3</b>
<b>*K1299E-S1303N</b>	<b>18.4 (25.9)</b>
M1293A-Y1294A	18.5 (21.4)

\*the bolded ones are the clinical mutations.

**Table C2.** Average RMSD, O-C distances, and Fe-O-C angles, and hydrogen bonding interactions percentages between Arg1896, Ser1898 and C4 carboxylate of the succinate and the interactions between the coordinating histidines (His1382 and His1881), and the MMGBSA binding energies for the WT and the various mutants.

	Average RMSD (Å)	Average O-C distance (Å)	Average Fe-O-C Angle (deg)	Arg1896 – C4 succinate (%)	Ser1898 – C4 succinate (%)	His1382-His1881 (%)	MMGBSA (kcal/mol)
<b>WT</b>	2.57	3.66	143.32	89.6	54.9	87.8	-122.09
<b>K1299E-S1303N</b>	2.92	3.89	111.56	27.9	24.1	14.3	-76.65
<b>S1290A-Y1295A</b>	2.61	3.78	140.06	15.3	14.9	43.8	-95.52
<b>Y1902A</b>	2.66	7.31	128.24	23.5	26.7	46.9	-102.94
<b>H1904R</b>	2.97	5.48	138.99	21.9	11.8	49.1	-90.18
<b>M1293A-Y1294A</b>	3.19	6.33	136.47	36.8	28.7	58.5	-80.11
<b>N1387A</b>	2.65	3.94	137.37	42.3	35.8	61.6	-108.43
<b>W1291A</b>	3.35	11.27	118.89	17.7	20.7	44.7	-63.98



**Table C3.** Selected distances and angles for the different snapshots RC2 and TS7 for HAT step in the WT TET2-dsDNA complex, calculated at B3LYP/def2-TZVP.

	<b>d(Fe–O<sub>p</sub>)</b> (Å)	<b>d(O<sub>p</sub>–H)</b> (Å)	<b>d(C–H)</b> (Å)	<b>&lt;(Fe–O<sub>p</sub>–H)</b> (deg)	<b>Barrier with ZPE</b> (kcal/mol)	<b>C<sub>substrate</sub> spin density</b> in TS <sub>HAT</sub>
<b>Snapshot 1</b>						
<b>RC</b>	1.624	2.458	1.103	149.89	16.3	-0.313
<b>TS<sub>HAT</sub></b>	1.738	1.301	1.294	160.11		
<b>Snapshot 2</b>						
<b>RC</b>	1.618	2.537	1.104	143.24	17.8	-0.322
<b>TS<sub>HAT</sub></b>	1.745	1.315	1.257	150.57		
<b>Snapshot 3</b>						-0.299
<b>RC</b>	1.617	2.671	1.102	147.64	17.4	
<b>TS<sub>HAT</sub></b>	1.744	1.320	1.267	156.05		
<b>Snapshot 4</b>						
<b>RC</b>	1.619	2.473	1.102	127.88	18.2	-0.253
<b>TS<sub>HAT</sub></b>	1.732	1.365	1.233	149.43		
<b>Snapshot 5</b>						
<b>RC</b>	1.622	2.562	1.103	138.22	19.1	-0.264
<b>TS<sub>HAT</sub></b>	1.747	1.344	1.277	150.04		

**Table C4.** Selected distances, angles and the calculated activation barriers and electric field (EF) values for the different RC WT snapshots.

Ferryl complexes	d(O <sub>p</sub> -H) (Å)	< (Fe-O <sub>p</sub> -H) (deg)	Barrier (kcal/mol)	RC EF (a.u.)	TS EF (a.u.)	TS-RC (a.u.)
WT snapshot 1	2.44	149.66	16.3	-0.0445	-0.0435	0.0010
WT snapshot 2	2.54	143.24	17.8	-0.0442	-0.0428	0.0014
WT snapshot 3	2.67	147.64	17.4	-0.0437	-0.0424	0.0013
WT snapshot 4	2.47	127.88	18.2	-0.0479	-0.0463	0.0016
WT snapshot 5	2.56	138.22	19.1	-0.0447	-0.0438	0.0009

**Table C5.** Selected distances, angles and the calculated activation barriers and electric field (EF) values for the different RC WT snapshot 1 and the various mutants.

Ferryl complexes	d(O <sub>p</sub> -H) (Å)	< (Fe-O <sub>p</sub> -H) (deg)	Barrier (kcal/mol)	RC EF (a.u.)	TS EF (a.u.)	TS-RC (a.u.)
WT snapshot 1	2.44	149.66	16.3	-0.0445	-0.0435	0.0010
K1299E-S1303N	2.51	127.92	25.0	-0.0404	-0.0400	0.0004
S1290A-Y1295A	3.05	130.09	24.2	-0.0457	-0.0434	0.0023
Y1902A	2.62	148.27	22.3	-0.0425	-0.0405	0.0020
N1387A	3.01	149.17	24.6	-0.0463	-0.0447	0.0016

### C.3 How the Mutations Alter the HAT Electric Field?

The electric field is weaker in Y1902A and K1299E-S1303N mutant forms, suggesting that residue substitution could influence the local electric field of the enzyme along the direction of the Fe=O bond. We further compared the electric field of the WT snapshot 4 with the K1299E-S1303N mutant form and the WT snapshot 3 with the Y1902A mutant form, that have similar O-H distances, and Fe-O-H angles in the reactant complexes. The O-H distance and Fe-O-H angle direct the HAT reaction in enzymes.<sup>7,8</sup> The results show that the double mutant form K1299E-S1303N has 0.0075 a.u. weaker electric field than WT snapshot 4, while the single mutant form Y1902A has 0.0012 a.u. that is weaker than WT snapshot 3. The results show that even though the two sets of compared profiles (snapshot 4 vs. K1299E-S1303N, and snapshot 3 vs. Y1902A) have similar geometries, residue substitutions and changes in the protein environment play a crucial role to modulate the electric field. The differences in electric field likely result in a higher activation energy barrier in K1299E-S1303N and Y1902A mutant forms than in the WT.

#### Dioxygen activation step stationary points cartesian coordinates for WT TET2-dsDNA

RC'

QM/MM (B1) = -3373.927802 a.u.

QM/MM (B2+ZPE) = -3375.941225 a.u.

6	52.488853114	37.432066653	43.777337111
7	51.310435347	38.112276163	43.980709665
1	50.936428393	38.399670375	44.892789459
6	50.750411202	38.362448851	42.786147705
1	49.793794539	38.861541485	42.653451975
7	51.506594982	37.877262234	41.809221230
6	52.594761797	37.286250343	42.414083510
1	53.370872433	36.800014542	41.830315373
6	54.386546616	35.416541390	38.306280973
1	53.668675407	34.707499773	37.874505946
1	55.051728425	35.785088547	37.514888798
6	53.678028806	36.617637350	38.928950813

8	52.427833415	36.431127923	39.251333526
8	54.268958759	37.678535058	39.115068590
6	48.265118499	34.780791214	41.560515432
7	49.412924723	34.033737536	41.419165008
1	49.562148140	33.072324521	41.758121599
6	50.306060701	34.779031906	40.745619823
1	51.306986672	34.450648620	40.485437604
7	49.792336185	35.966159481	40.442414415
6	48.512658276	35.984692697	40.948924351
1	47.875791060	36.859638197	40.844590986
26	50.963449983	37.626115675	39.733560613
8	50.114723358	37.458107941	37.846107051
8	49.457437070	38.422087080	37.316592636
6	50.609563661	40.320507074	38.862739812
6	49.204759675	39.926343981	39.386489115
6	46.699244919	40.320670103	38.913674360
6	45.577043455	41.345703135	38.600573994
8	51.528464904	39.456520258	39.161184826
8	50.775856627	41.380497364	38.278261281
8	49.146790086	38.888129355	40.059949817
8	44.512772803	40.831206019	38.204010204
6	48.085810985	40.902385080	39.186847526
8	45.778696516	42.584584742	38.763406442
1	46.347255872	39.711255353	39.763185919
1	46.742192743	39.632216804	38.054384072
1	48.060313045	41.516322644	40.110224587
1	48.389998536	41.602883860	38.399458646
7	57.207123849	41.185318364	36.245851205
6	57.779496811	39.894823411	36.119131034
7	56.927879100	38.893355478	35.776243740
6	55.601335392	39.042138885	35.764998766
6	54.975903119	40.301813554	36.110246947
6	53.487496558	40.425282836	36.266056393
6	55.835065643	41.337825686	36.298927318
8	58.984298265	39.705940673	36.291420939
7	54.853761512	37.987195061	35.423843740
1	55.313797160	37.122697843	35.135419067
1	53.833661682	37.969424781	35.446312145
1	52.942920929	40.118182582	35.359189641
1	53.187197180	41.451911083	36.516281967
1	53.122816766	39.775202069	37.077915239
1	55.440523453	42.332407367	36.525666365
8	52.180366268	36.871409274	35.683183296
1	51.591233057	37.031615643	36.442478744
1	51.613771065	36.374706616	35.051834271
8	56.575703999	39.183239452	38.938524932
1	55.932173955	38.448258107	38.933223311
1	57.467183701	38.774049684	38.850694277
1	53.079485045	37.024920006	44.597978844
1	54.989550616	34.887523137	39.044246545
1	47.405526776	34.437714321	42.136247689
1	57.766797790	42.004790192	36.369153669

**TS1**

**QM/MM (B1) = -3373.913976 a.u.**

**QM/MM (B2+ZPE) = -3375.926678 a.u.**

6	52.489474760	37.431391031	43.753816754
7	51.324463820	38.141396692	43.941851523
1	50.950222425	38.444079861	44.849385034
6	50.776929333	38.388202326	42.740301990
1	49.837185375	38.911203320	42.580724659
7	51.528250836	37.869525186	41.776075165
6	52.599710742	37.263063563	42.393839390
1	53.370689968	36.755685978	41.821411018
6	54.331960385	35.416841592	38.301879996
1	53.617265568	34.701980063	37.874684792
1	54.991243063	35.787742582	37.506293218
6	53.616957481	36.617947072	38.920618161
8	52.357749879	36.442376459	39.206385385
8	54.218665632	37.667944639	39.137682191
6	48.246465504	34.740179633	41.593173944
7	49.391842984	33.988081425	41.456824081
1	49.538632794	33.027280985	41.797843660
6	50.290429229	34.727932418	40.785995798
1	51.289867090	34.394187069	40.528377682
7	49.781156543	35.914915295	40.479013827
6	48.500560496	35.941964005	40.981340273
1	47.870658877	36.821654060	40.872891021
26	50.878002108	37.596036970	39.757105440
8	49.974644414	37.645438042	37.904456081
8	49.281134753	38.807542783	37.727180745
6	50.738001678	40.296825984	38.761737486
6	49.182585857	39.566372586	38.967087596
6	46.659670361	40.144056810	38.820030890
6	45.569895922	41.219600138	38.545089098
8	51.625034047	39.474965419	39.120762495
8	50.786939144	41.421148157	38.316574322
8	49.280464524	38.814555773	40.027539642
8	44.464988743	40.748508945	38.206214693
6	48.103575851	40.643192190	38.849984963
8	45.826456440	42.449169522	38.687775033
1	46.393235771	39.659569632	39.775373713
1	46.531590401	39.369850084	38.047253509
1	48.254673509	41.333505890	39.693770353
1	48.325788629	41.223599877	37.947512011
7	57.211745440	41.193361498	36.238201112
6	57.773453739	39.897805071	36.109499580
7	56.913150203	38.903329554	35.768091818
6	55.587737167	39.061382802	35.763076424
6	54.974319361	40.327363803	36.106258697
6	53.487840777	40.463098249	36.266671006
6	55.841319650	41.356972398	36.292045098
8	58.976626677	39.699433946	36.280803569
7	54.830261285	38.011062209	35.429184524

1	55.285412362	37.144143328	35.139597450
1	53.809768196	38.000006352	35.459945667
1	52.936684876	40.146135661	35.367281851
1	53.199215589	41.496831098	36.502293998
1	53.130167155	39.823718473	37.090149399
1	55.454477090	42.354845488	36.517957395
8	52.105458085	36.974219264	35.742421715
1	51.493585185	37.232662643	36.457934757
1	51.547119365	36.441467740	35.135469968
8	56.543119910	39.157050507	38.929310627
1	55.895764999	38.425024479	38.945942790
1	57.432934836	38.745611550	38.841269630
1	53.074515065	37.026278081	44.579455090
1	54.943869597	34.893969776	39.036889859
1	47.384915951	34.404149873	42.170134682
1	57.776905647	42.008807906	36.363155466

**IM1**

**QM/MM (B1) = -3373.998671 a.u.**

**QM/MM (B2+ZPE) = -3376.002137 a.u.**

6	52.689904347	37.364036901	43.869505516
7	51.546531539	38.112692473	44.033166482
1	51.153105802	38.419873277	44.929987291
6	51.038852121	38.378493934	42.815733989
1	50.114837205	38.922310708	42.638526113
7	51.793834049	37.840920008	41.867342471
6	52.823363553	37.193799490	42.511517620
1	53.570056798	36.635713484	41.953687068
6	54.593188316	35.367197813	38.309173000
1	53.920642170	34.643014038	37.829004767
1	55.283502657	35.772250437	37.559768024
6	53.775096794	36.501944084	38.925517067
8	52.640130602	36.155596437	39.410841641
8	54.226733002	37.661825206	38.946824971
6	48.283768674	34.734696880	41.601660699
7	49.410792837	33.957921115	41.457265568
1	49.544346051	32.997239429	41.801103148
6	50.318426483	34.678759178	40.772450178
1	51.312029065	34.329238134	40.508949251
7	49.838027682	35.877308800	40.468707237
6	48.565684255	35.930711696	40.987533747
1	47.952193089	36.824195000	40.894667823
26	51.148310382	37.450361559	39.870033071
8	51.033896270	38.364940313	38.095988030
8	50.068743787	39.426248631	37.985649128
6	49.157124505	43.941819296	38.817311607
6	49.332964622	39.598959840	39.071483012
6	46.929539577	40.271468139	38.579733893
6	45.921646511	41.433416947	38.366329716
8	48.688201806	44.044192292	39.877077997
8	49.673908645	43.832348283	37.781874447
8	49.466569013	38.897917251	40.076583715

8	44.731246705	41.070353379	38.253764703
6	48.351105669	40.728798024	38.931547687
8	46.359625035	42.612292389	38.314058629
1	46.517726153	39.609491615	39.358472487
1	46.942068986	39.681631048	37.646820714
1	48.337096427	41.274607288	39.887170212
1	48.708439481	41.410548801	38.152275005
7	57.219814864	41.187842047	36.261992317
6	57.801221304	39.900492424	36.122032873
7	56.954115301	38.897495327	35.779968100
6	55.624521214	39.032775993	35.780999070
6	54.993983958	40.285882625	36.150017041
6	53.504019409	40.401295951	36.313254189
6	55.846863571	41.328173445	36.331797268
8	59.008724150	39.722784718	36.283001538
7	54.884192447	37.984800672	35.421082180
1	55.356123206	37.124096125	35.138964089
1	53.862473584	37.937284259	35.493457118
1	52.960114898	40.085941918	35.409042694
1	53.212583294	41.437400170	36.542081115
1	53.133027527	39.740394075	37.116132807
1	55.448092471	42.320228728	36.563312781
8	52.194619853	37.117564877	35.814478040
1	51.692957577	37.544228337	36.547658389
1	51.544434600	36.622459514	35.282482996
8	56.719232845	38.911958583	38.957896010
1	56.007645606	38.247425323	38.849484885
1	57.579814485	38.479532895	38.776633371
1	53.238802503	36.931119830	44.705783542
1	55.165674257	34.823577808	39.060707735
1	47.414686865	34.411186226	42.174465188
1	57.774714059	42.011335823	36.379964257

**TS2**

**QM/MM (B1) = -3373.987085 a.u.**

**QM/MM (B2+ZPE) = -3376.009183 a.u.**

6	52.686302512	37.387040458	43.833253927
7	51.542847973	38.138814249	43.992246094
1	51.141184751	38.439189935	44.888292135
6	51.047226467	38.415928525	42.773720152
1	50.125797408	38.961071020	42.588606352
7	51.811367379	37.883081898	41.827588586
6	52.834173861	37.227361663	42.476298535
1	53.583447956	36.671259753	41.921019846
6	54.547815447	35.301224592	38.328926097
1	53.855221188	34.577574016	37.877916879
1	55.215732932	35.697909638	37.555025627
6	53.777267066	36.451889214	38.972387190
8	52.635798222	36.142188446	39.483512023
8	54.267821996	37.590508655	39.006071068
6	48.331030108	34.771772404	41.532796275
7	49.459677929	33.991613281	41.409685808

1	49.587204783	33.034763176	41.768017674
6	50.373678155	34.696517890	40.721172681
1	51.371928712	34.348262569	40.477859791
7	49.894210954	35.889643403	40.387125494
6	48.615340724	35.954923984	40.895841036
1	48.008266531	36.850000561	40.782873552
26	51.176467813	37.508743182	39.830558200
8	51.387863054	38.447993836	38.303248602
8	50.180538884	39.721484005	38.145633809
6	49.143507059	43.986044550	38.792080848
6	49.392767673	39.683671047	39.157113575
6	46.964784184	40.263784411	38.588534783
6	45.925170371	41.400873287	38.379232676
8	48.685673810	44.095031112	39.856227027
8	49.645629132	43.874548448	37.749915258
8	49.492540927	38.857028307	40.096663489
8	44.742637595	41.014040177	38.260173595
6	48.312383230	40.748302106	39.136134745
8	46.335448837	42.590065616	38.322658252
1	46.507595287	39.501932164	39.239307729
1	47.111762768	39.787965448	37.602032427
1	48.191854041	41.129004602	40.162479131
1	48.655672730	41.568232259	38.496444966
7	57.231641240	41.187354437	36.261702630
6	57.809984008	39.898519762	36.130339797
7	56.961881501	38.896432252	35.788179164
6	55.632904461	39.036484218	35.781008262
6	55.002966138	40.294450942	36.134269816
6	53.512073735	40.423626738	36.276620809
6	55.858827522	41.333797689	36.317668617
8	59.016182846	39.717235395	36.299363884
7	54.891841413	37.987058544	35.425079834
1	55.361533049	37.122551816	35.151495419
1	53.871781102	37.938928116	35.511231827
1	52.978737100	40.101410288	35.368655119
1	53.226364689	41.465023709	36.486657413
1	53.118669292	39.782314327	37.084091717
1	55.461606896	42.328805839	36.538535294
8	52.241260451	37.092486976	35.933130729
1	51.812582269	37.558846441	36.688281041
1	51.532517481	36.681667934	35.408709196
8	56.707042014	38.925808691	38.956907142
1	56.019657553	38.234069853	38.870972259
1	57.580166134	38.508831534	38.793464530
1	53.232442872	36.953452861	44.670988863
1	55.141863667	34.767129524	39.070489646
1	47.458548299	34.454270462	42.103791307
1	57.787642685	42.009998883	36.380408184

**IM2**

**QM/MM (B1) = -3373.998434 a.u.**

**QM/MM (B2+ZPE) = -3376.009700 a.u.**



6	52.778742089	37.340297835	43.953472166
7	51.642004185	38.098143554	44.123809576
1	51.242294611	38.394888851	45.021853393
6	51.139907322	38.393421950	42.917490673
1	50.220275386	38.943796807	42.743626435
7	51.898052074	37.862366085	41.964678546
6	52.920631745	37.189522563	42.595819964
1	53.670709586	36.642324320	42.032792495
6	54.444486662	35.251539484	38.349037092
1	53.716413757	34.536402084	37.943960745
1	55.093419236	35.613597610	37.542280325
6	53.758712620	36.448715235	38.999051691
8	52.567938453	36.233089736	39.472955540
8	54.342720114	37.529531243	39.085223687
6	48.389572130	34.840416827	41.529578925
7	49.510163868	34.052022404	41.381100542
1	49.622389943	33.080543834	41.705015286
6	50.438953598	34.777513437	40.735032637
1	51.429673290	34.422116081	40.475296314
7	49.979001268	35.993863211	40.456166260
6	48.694178186	36.048658632	40.952805368
1	48.103383014	36.956782175	40.870852635
26	51.285302169	37.678006431	39.984719630
8	51.902050431	38.902698536	38.822407891
8	50.381042302	40.486285574	39.015976764
6	49.272724936	43.968484422	38.567638330
6	49.462744141	39.935395293	39.661680616
6	47.206267665	40.375622387	38.556985822
6	46.073080339	41.426388806	38.380343472
8	48.953384178	43.979831495	39.688304999
8	49.634911075	43.973707475	37.464993125
8	49.573523302	38.783426445	40.224851497
8	44.913897545	40.978144164	38.242201079
6	48.118817416	40.646312637	39.771231890
8	46.409592264	42.641391311	38.362884941
1	46.757596691	39.372943368	38.615868454
1	47.818873491	40.417549783	37.640558234
1	47.627747337	40.315048552	40.699214069
1	48.299184735	41.726245671	39.839193775
7	57.294164633	41.221725071	36.231868088
6	57.827204680	39.913479508	36.114778953
7	56.943370452	38.935947605	35.789456053
6	55.619959473	39.118679241	35.805517762
6	55.036250990	40.408172397	36.122719464
6	53.555165670	40.622618704	36.252339410
6	55.929075781	41.418239212	36.282868244
8	59.026330968	39.689500829	36.285360769
7	54.837682059	38.079321941	35.501147317
1	55.278732568	37.194758825	35.246969848
1	53.826800745	38.069858141	35.679056238
1	53.006049568	40.261188061	35.369286560
1	53.328209846	41.689067207	36.390014084

1	53.139456025	40.078924684	37.113891344
1	55.564586694	42.430368051	36.480519407
8	52.166322253	37.591572402	36.358309012
1	51.997253863	38.124924950	37.173347657
1	51.345233259	37.637779567	35.850860161
8	56.614934745	39.085729379	38.927234321
1	55.980764761	38.343244046	38.880840574
1	57.511214809	38.690280613	38.831991566
1	53.310661529	36.884483074	44.788554156
1	55.057760611	34.732792128	39.085829849
1	47.509938670	34.510869710	42.082490308
1	57.870303092	42.029675704	36.355370051

**IM3**

**QM/MM (B1) = -3374.016223 a.u.**

**QM/MM (B2+ZPE) = -3376.041409 a.u.**

6	52.697848202	37.391827412	43.840358036
7	51.540321945	38.112726139	44.022550424
1	51.143798616	38.398348680	44.925736923
6	51.027437720	38.403474963	42.816010823
1	50.093189045	38.934485494	42.660358754
7	51.796118988	37.908421376	41.855599112
6	52.841119349	37.264904391	42.477699944
1	53.619378694	36.768009526	41.905599287
6	54.335463269	35.319884705	38.298235701
1	53.630469985	34.607538530	37.851560354
1	54.987344064	35.721126273	37.509584061
6	53.626631868	36.500193905	38.971033888
8	52.326231368	36.390690796	39.062220600
8	54.273976830	37.450569140	39.402019891
6	48.430420618	34.888949175	41.522459655
7	49.568332259	34.124838188	41.379184185
1	49.692424509	33.152933446	41.697804902
6	50.487472722	34.877151914	40.747641597
1	51.482490889	34.535268380	40.486833484
7	50.003551918	36.084822420	40.474065098
6	48.714262203	36.107920922	40.957932450
1	48.102124170	37.000426037	40.865066643
26	51.137083346	37.769740794	39.833290675
8	51.943548495	38.972997151	39.098079386
8	50.158394250	40.869571084	39.759219254
6	49.337191589	43.631890358	38.910051206
6	49.278436606	40.029467498	39.856124282
6	47.206726689	40.497895696	38.436055782
6	45.960708883	41.419917688	38.352432150
8	48.831120331	43.824897398	39.940395505
8	49.868677057	43.465238541	37.890452162
8	49.489856691	38.722715929	39.967768992
8	44.848063858	40.866628007	38.207969979
6	47.805640800	40.434191852	39.860160021
8	46.165654226	42.661946503	38.437749684
1	46.941123521	39.488313544	38.087738236

1	47.967963958	40.913901776	37.759402380
1	47.221892935	39.737294610	40.481256691
1	47.757568963	41.438041125	40.307054367
7	57.218333522	41.178663335	36.266601647
6	57.786043125	39.886039148	36.137844588
7	56.927995847	38.887529808	35.802983681
6	55.602589648	39.040366665	35.808071482
6	54.982208256	40.302567695	36.154653168
6	53.493908673	40.444903199	36.307891131
6	55.847224861	41.336737973	36.328681399
8	58.990681466	39.692493813	36.304247629
7	54.850952348	37.983732056	35.476511052
1	55.306700972	37.122153521	35.173499852
1	53.833040681	37.972500312	35.506176544
1	52.950513479	40.116899581	35.407191193
1	53.215183004	41.488483311	36.512639598
1	53.113201166	39.831440883	37.141824410
1	55.457858443	42.334972559	36.548684432
8	52.226835635	36.792520911	35.815991159
1	51.942251545	36.712837898	36.740874762
1	51.559716890	36.305497704	35.286082719
8	56.554993521	39.032608021	38.977525739
1	55.944050989	38.279265913	39.090328892
1	57.455698242	38.649554174	38.873251886
1	53.246501587	36.949871538	44.672056177
1	54.957709815	34.795715923	39.023579517
1	47.549936892	34.541652676	42.063015728
1	57.780367863	41.997760088	36.381364037

**Substrate hydroxylation steps cartesian coordinates for the WT TET2-DSDNA**

**Snapshot 1**

**RC**

**QM/MM (B1) = -3185.642667 a.u.**

**QM/MM (B2+ZPE) = -3187.461526 a.u.**

6	52.636297019	37.405390452	43.820032047
7	51.468629197	38.109941624	44.002167697
1	51.070059307	38.389895688	44.906284002
6	50.953036489	38.395754527	42.795173670
1	50.012027707	38.915455312	42.639375437
7	51.729843867	37.913045401	41.834923977
6	52.782952742	37.283157254	42.457365869
1	53.568357096	36.798742035	41.884580986
6	54.314919094	35.329676442	38.293168553
1	53.616174939	34.613374847	37.842975369
1	54.966295451	35.736923632	37.507111099
6	53.594450900	36.503552794	38.965374935
8	52.294910367	36.386638214	39.046335218
8	54.233280105	37.457004506	39.403473482
6	48.409031406	34.863247279	41.523922613
7	49.550997275	34.105041990	41.383119491

1	49.680994328	33.135232922	41.705338899
6	50.464273565	34.859011872	40.744982270
1	51.461100074	34.521992201	40.484620338
7	49.972120101	36.061254368	40.464156154
6	48.683722686	36.079827479	40.950348817
1	48.066015956	36.968024096	40.852827334
26	51.083907981	37.755381029	39.808645589
8	51.878506610	38.968255559	39.076904470
8	50.023935788	40.829440340	39.749317512
6	49.168930280	39.963417536	39.752200893
6	47.354112200	41.272310817	38.521277206
6	45.892222245	41.773731709	38.495876757
8	49.413114877	38.659526202	39.876185138
8	44.984556578	40.943249846	38.273726137
6	47.676448763	40.307243733	39.673109310
8	45.719468252	43.016302401	38.680229944
1	47.537859220	40.746954694	37.568296165
1	48.024069367	42.140424385	38.579229381
1	47.068365174	39.394828160	39.599866209
1	47.431155496	40.800501579	40.630906631
7	57.216924424	41.177328475	36.258400506
6	57.783828079	39.883759273	36.133556427
7	56.925578729	38.885654319	35.798031920
6	55.600470219	39.039419406	35.800883217
6	54.980921196	40.302268583	36.145991775
6	53.492767979	40.445391179	36.298558069
6	55.846025153	41.336253696	36.319377013
8	58.987454448	39.689216121	36.304352623
7	54.848448429	37.983638789	35.468037459
1	55.304163303	37.121345583	35.166763124
1	53.830436510	37.972425475	35.497044987
1	52.949443911	40.113664170	35.399103428
1	53.216970168	41.490858455	36.497780872
1	53.111306219	39.836916603	37.135893306
1	55.457454792	42.334937834	36.538725084
8	52.222522681	36.803549636	35.806412522
1	51.936562710	36.728166364	36.731319016
1	51.559099758	36.309679882	35.278021233
8	56.503832590	39.048867114	38.970075723
1	55.894489968	38.294908975	39.088808566
1	57.406939110	38.667281427	38.882483352
1	53.193650824	36.971562677	44.650223302
1	54.939035541	34.807553856	39.018381615
1	47.531278044	34.515290706	42.068479843
1	57.779398616	41.996243217	36.372303623

**T<sub>SHAT</sub>**

**QM/MM (B1) = -3185.610546 a.u.**

**QM/MM (B2+ZPE) = -3187.435561 a.u.**

6	52.678486565	37.460587909	43.701193601
7	51.524500842	38.198929393	43.850153917
1	51.087924759	38.458738949	44.743878229

6	51.082228161	38.539668788	42.627480406
1	50.164533066	39.087181664	42.436044826
7	51.894229657	38.064850325	41.688541956
6	52.890325885	37.375523439	42.345433282
1	53.679119509	36.875577481	41.791762169
6	54.466900742	35.260334262	38.246578571
1	53.775521464	34.556225090	37.766938885
1	55.146367971	35.665183491	37.484117961
6	53.731427500	36.429843298	38.902851130
8	52.438309717	36.401190768	38.820269332
8	54.360908815	37.323673689	39.480071424
6	48.522585784	34.980010589	41.403352667
7	49.654255039	34.203826619	41.279880809
1	49.768472656	33.238207290	41.616770434
6	50.581411341	34.942186396	40.635471795
1	51.573494824	34.580752239	40.387941612
7	50.112927674	36.145960437	40.330487044
6	48.822638662	36.184950841	40.811119091
1	48.215153202	37.078852248	40.696744340
26	51.350528350	37.957087500	39.631264079
8	52.191200818	39.103014361	38.630158838
8	50.133664226	41.031459206	39.640067466
6	49.317300473	40.123456045	39.646544485
6	47.415332758	41.352884758	38.466891099
6	45.941261498	41.818169495	38.476398583
8	49.629761477	38.841273054	39.736348235
8	45.045651097	40.970530425	38.269879970
6	47.808532383	40.407858981	39.612694704
8	45.745823438	43.057492235	38.664853440
1	47.584218142	40.823216644	37.513521208
1	48.061958193	42.239937146	38.498470725
1	47.237499939	39.470407472	39.557052018
1	47.567492427	40.893479392	40.575855020
7	57.024728310	41.118322646	36.416497696
6	57.646920664	39.849316914	36.202654233
7	56.823127056	38.834203871	35.846619578
6	55.494642273	38.911810535	35.928918796
6	54.824127443	40.119782772	36.402958178
6	53.371236475	40.189332236	36.607367982
6	55.662725112	41.198656911	36.581195691
8	58.861104182	39.711973770	36.320235285
7	54.787723038	37.846411031	35.555104145
1	55.283886263	37.034237949	35.182853298
1	53.771400327	37.759286077	35.625666487
1	52.776025351	39.646351642	35.859266248
1	52.991668028	41.208809082	36.761388524
1	52.895909832	39.584027283	37.647358009
1	55.239816895	42.168034160	36.861878749
8	52.220590036	36.731939090	35.883579693
1	52.036905570	36.573459961	36.829574092
1	51.542029547	36.248888063	35.367036244
8	56.542129619	38.974730450	39.030578330

1	55.934414126	38.221120256	39.178968087
1	57.443873475	38.593085538	38.931083186
1	53.214003897	37.016139214	44.540093997
1	55.064348752	34.726742542	38.985769389
1	47.632582096	34.639052416	41.932227206
1	57.566086495	41.955732820	36.491650899

**IM<sub>HAT</sub>**

**QM/MM (B1) = -3185.645154 a.u.**

**QM/MM (B2+ZPE) = -3187.462102 a.u.**

6	52.668343570	37.415338815	43.804251754
7	51.502118311	38.125214246	43.990498571
1	51.098855905	38.394919855	44.896144077
6	50.995633882	38.435455378	42.789392477
1	50.056880665	38.956202124	42.628058304
7	51.779415345	37.965063752	41.823442101
6	52.825867032	37.314510128	42.442811786
1	53.609004026	36.836925496	41.861952801
6	54.398492840	35.295461312	38.300908712
1	53.725577414	34.577232580	37.815486320
1	55.066279444	35.728771705	37.542353356
6	53.633573678	36.436836635	38.979220911
8	52.339793620	36.358537595	38.944974131
8	54.249028626	37.363555249	39.517453595
6	48.406507098	34.877203536	41.480771886
7	49.544771488	34.115022881	41.330569084
1	49.677348471	33.148246062	41.660170520
6	50.449774209	34.861676120	40.670129989
1	51.442109273	34.518272323	40.398916632
7	49.957510835	36.062572295	40.383130111
6	48.676168225	36.087559700	40.891019596
1	48.062335581	36.979633805	40.802492047
26	51.115947584	37.860234930	39.841710907
8	51.877344611	39.037461228	38.637967304
8	49.995364815	40.981667066	39.935399971
6	49.153839441	40.098401206	39.925935340
6	47.365305584	41.302580211	38.555896765
6	45.907172068	41.805972272	38.484148908
8	49.439329397	38.814240966	40.095389653
8	45.001524276	40.973472486	38.258419150
6	47.664705663	40.419862870	39.778799040
8	45.731390446	43.051591480	38.646571784
1	47.563930053	40.715087550	37.642707101
1	48.037536134	42.171041490	38.571690737
1	47.065806803	39.498545192	39.750570296
1	47.386587220	40.979501133	40.689659488
7	57.216571341	41.169847766	36.283571838
6	57.781694500	39.880416291	36.137102730
7	56.925468026	38.881163065	35.783416225
6	55.606109597	39.015804829	35.777962275
6	54.960409630	40.288139916	36.132539433
6	53.570264717	40.445525675	36.228235513

6	55.850556646	41.340743114	36.334858575
8	58.982458607	39.678954310	36.309179661
7	54.871328281	37.955029720	35.439044361
1	55.341454387	37.093829208	35.155165083
1	53.856887292	37.914646887	35.501665504
1	52.875113685	39.646364877	35.971185971
1	53.141112371	41.399445731	36.539848744
1	52.276832433	38.645940539	37.848951347
1	55.460026170	42.335500953	36.561561807
8	52.234636512	36.763677628	36.009294300
1	52.043180024	36.500948072	36.931544288
1	51.552989856	36.332480251	35.454213942
8	56.397723111	39.031178714	38.916772180
1	55.808126410	38.281444573	39.138003439
1	57.308154846	38.659476062	38.874672722
1	53.221592277	36.972347977	44.632347345
1	55.011333372	34.764224759	39.029113028
1	47.532965431	34.532931766	42.034368506
1	57.781164116	41.987640293	36.395029817

**TS<sub>Reb</sub>**

**QM/MM (B1) = -3185.631799 a.u.**

**QM/MM (B2+ZPE) = -3187.445453 a.u.**

6	52.753872161	37.391321343	43.785757036
7	51.633022396	38.179698970	43.919336529
1	51.203254871	38.469742460	44.806476173
6	51.198934292	38.501147007	42.685231059
1	50.306227535	39.084157664	42.478472347
7	51.978732702	37.962910471	41.756553313
6	52.946063585	37.253024399	42.430973159
1	53.701449117	36.679763526	41.900148682
6	54.550815723	35.043151928	38.245680361
1	53.783258046	34.332957970	37.911166107
1	55.204807221	35.307609872	37.407210430
6	53.936989778	36.320565000	38.789375916
8	52.756938023	36.268344895	39.260655311
8	54.615152262	37.373460384	38.729076227
6	48.531980591	34.964559274	41.401418996
7	49.653661984	34.171590903	41.295584244
1	49.753672267	33.207911940	41.641936532
6	50.595364147	34.886443198	40.645656097
1	51.589964693	34.520414374	40.416806411
7	50.145076124	36.091339269	40.319280097
6	48.853168950	36.157067053	40.792793551
1	48.260198172	37.059852711	40.665679519
26	51.424439055	37.841436559	39.684643432
8	52.481576450	38.828148188	38.145727839
8	50.261577628	41.046705665	39.115976859
6	49.462739770	40.161333081	39.408183546
6	47.456064468	41.375888400	38.370940553
6	45.979195558	41.821970485	38.459584225
8	49.805528235	38.934724904	39.711470808

8	45.082309184	40.970694883	38.269949785
6	47.953792289	40.451864451	39.490870455
8	45.776033220	43.055921653	38.680639448
1	47.572875397	40.839591161	37.413375599
1	48.088571385	42.272926754	38.351021390
1	47.388892242	39.508208127	39.505428968
1	47.786840852	40.943567775	40.468272957
7	57.004839914	41.165959160	36.418826288
6	57.654700077	39.899022401	36.167420379
7	56.854847877	38.896102183	35.746543572
6	55.524276178	38.948917772	35.787339249
6	54.828049144	40.120533516	36.346422008
6	53.422152772	40.174671507	36.515860134
6	55.659649915	41.214762834	36.601016009
8	58.863901779	39.786120720	36.310367241
7	54.845300095	37.916750742	35.314810456
1	55.365131052	37.114169813	34.952493631
1	53.831188678	37.785431185	35.423737428
1	52.778939906	39.511093720	35.945986789
1	52.951185746	41.070508809	36.924300222
1	53.349720144	38.376919505	38.287047761
1	55.215421601	42.160395725	36.927893944
8	52.290307387	37.140164238	35.963974672
1	52.123476782	37.682803322	36.779043925
1	51.445019123	36.846643032	35.592280387
8	56.655450312	39.129321921	38.881199314
1	56.060199347	38.352720626	38.823386794
1	57.566961722	38.753530513	38.835475658
1	53.278359444	36.946627443	44.631468419
1	55.152553381	34.560915135	39.016022352
1	47.637043531	34.636817965	41.930324105
1	57.539652297	42.006954712	36.500525090

**PD<sub>OH</sub>**

**QM/MM (B1) = -3185.701309 a.u.**

**QM/MM (B2+ZPE) = -3187.501137 a.u.**

6	52.709638457	37.351134348	43.900555171
7	51.571022005	38.102366420	44.069517731
1	51.180715106	38.409356837	44.968094519
6	51.060927131	38.374785185	42.854930413
1	50.138472140	38.924558499	42.688151821
7	51.809514454	37.838142679	41.901245058
6	52.839146275	37.186631123	42.540222210
1	53.595331938	36.636881886	41.985340160
6	54.352426564	35.224478142	38.199909376
1	53.619210543	34.476036692	37.869565240
1	55.009169318	35.482900180	37.360303735
6	53.661737380	36.506389258	38.654293930
8	52.463453447	36.408804782	39.084434567
8	54.283149441	37.585493775	38.554316335
6	48.310835778	34.739513388	41.589398111
7	49.434239035	33.955900553	41.460565232



1	49.554743643	32.991992626	41.800421890
6	50.357887035	34.675978976	40.795605773
1	51.348518429	34.311156010	40.546111015
7	49.890459072	35.876192861	40.486707222
6	48.608126932	35.935528188	40.980887752
1	48.006243746	36.834838961	40.868709986
26	51.063150464	37.574108468	39.932429694
8	52.943781762	39.504627407	37.287929555
8	50.275506589	40.860106797	39.292920021
6	49.376726274	40.062732167	39.537918583
6	47.464426077	41.363901916	38.423970078
6	45.995415677	41.843497919	38.473311877
8	49.581555821	38.789591715	39.780766087
8	45.089948207	41.003830046	38.270481036
6	47.904569253	40.495269099	39.612240522
8	45.807538846	43.080062005	38.687830163
1	47.580681831	40.768521471	37.502077448
1	48.120649919	42.242706468	38.363802508
1	47.261735548	39.607412198	39.698408999
1	47.789722090	41.080147529	40.543758287
7	57.165848908	41.182888604	36.279763571
6	57.792407995	39.911329693	36.143527666
7	56.990414643	38.892774029	35.744336480
6	55.663908406	38.999810007	35.670155704
6	54.980864675	40.211427715	36.079610881
6	53.478067620	40.262626428	36.204673664
6	55.792572467	41.276673958	36.328376169
8	58.994690788	39.766722887	36.350839394
7	54.978816817	37.959120631	35.197022580
1	55.481696655	37.120408109	34.903720269
1	53.960588036	37.906619035	35.154610198
1	53.017690017	39.900463049	35.268181685
1	53.157440569	41.308608275	36.337399774
1	53.553459381	38.791681081	37.592396368
1	55.356433701	42.246836326	36.586152155
8	52.286791248	37.105444405	35.437265712
1	51.894205574	37.616297193	36.163048158
1	51.578330869	36.557858138	35.039810459
8	56.552431149	39.128488520	38.884385791
1	55.935850504	38.382869516	38.749261905
1	57.459044526	38.745167084	38.832781241
1	53.251286085	36.910078647	44.737307843
1	54.964589437	34.766424634	38.976769026
1	47.434863272	34.418279123	42.152912116
1	57.704029383	42.017943728	36.393856573

## Snapshot 2

RC

QM/MM (B1) = -3192.804592 a.u.

QM/MM (B2+ZPE) = -3194.623459 a.u.

6	46.228883546	37.505377017	33.887379132
7	45.203198319	38.404453777	34.077465500

1	44.494259294	38.661615484	33.379136891
6	45.245346562	38.826704947	35.351004952
1	44.561490030	39.554341249	35.780867929
7	46.254974752	38.246376997	35.988506038
6	46.881261212	37.409714566	35.093339818
1	47.736523165	36.801492661	35.384305171
6	51.047914657	37.438665541	38.002705929
1	51.365584088	38.460199145	38.250329125
1	51.275234767	36.747696232	38.830929073
6	49.536901866	37.410189724	37.755189398
8	48.989695786	38.595295615	37.916981045
8	48.945418489	36.390674016	37.448479032
6	47.769999617	42.493926900	35.374925002
7	48.932914845	41.787429250	35.164868987
1	49.706681846	42.060283274	34.542020099
6	48.881698573	40.677659801	35.920329926
1	49.677215399	39.944022952	35.983448262
7	47.746708261	40.629669854	36.610091832
6	47.035534462	41.763905252	36.278915612
1	46.062727399	41.978280915	36.716751322
26	47.081705796	38.963431019	37.756721308
8	46.644170495	37.724695501	38.701979833
8	46.531946701	40.389387880	40.540627558
6	45.586055593	40.282804073	39.755358043
6	42.995314914	40.286514087	39.290047117
6	41.720400474	39.641325416	39.902345962
8	45.749660566	40.141806557	38.468136587
8	41.831552340	38.427500245	40.210106163
6	44.161145809	40.238049368	40.278401842
8	40.703986644	40.359458478	40.057534356
1	43.267022407	39.689706483	38.404219823
1	42.785965277	41.312739001	38.953017625
1	44.106633890	39.261834572	40.796448218
1	44.072386544	41.005875036	41.063385771
7	47.120353511	32.864758650	42.277500724
6	48.535469383	32.900667613	42.145908868
7	49.100767905	34.141642757	42.146438516
6	48.386475803	35.265596019	42.097105036
6	46.940897451	35.259068094	42.167454272
6	46.143011520	36.528125441	42.087368868
6	46.376028837	34.025756940	42.275200179
8	49.205624028	31.878890439	42.034028060
7	49.066455709	36.421235082	41.991391493
1	50.076963069	36.354584355	41.954091905
1	48.660727812	37.334651487	41.784869334
1	46.427024410	37.234684523	42.885950556
1	45.066067374	36.326223333	42.175396519
1	46.305795030	37.033198423	41.119547209
1	45.289762387	33.921413796	42.344440894
8	49.078796794	39.350429771	40.911115049
1	49.195871535	39.117798647	39.971759878
1	48.171032758	39.735202698	40.886972041

8	45.794983830	34.849630009	38.934740261
1	46.497099866	35.423421885	38.586291230
1	46.097973339	33.930901431	38.752528908
1	46.507284030	37.122742363	32.905467113
1	51.620419447	37.120303872	37.131527742
1	47.537358269	43.408165187	34.828927124
1	46.614115418	32.002397059	42.282789438

**T<sub>SHAT</sub>**

**QM/MM (B1) = -3192.777585 a.u.**

**QM/MM (B2+ZPE) = -3194.595030 a.u.**

6	46.232641715	37.391671045	33.919169116
7	45.196317681	38.270790753	34.151727658
1	44.500279214	38.574903679	33.458408448
6	45.209209360	38.596993014	35.453610087
1	44.516391804	39.291055052	35.922755601
7	46.210047016	37.975217944	36.071697459
6	46.861722041	37.211627180	35.126297025
1	47.725662670	36.603757951	35.390367140
6	51.091156217	37.404592146	37.992735594
1	51.396468719	38.430338646	38.239079050
1	51.325895578	36.727501040	38.831186179
6	49.579052093	37.370571494	37.758593596
8	48.981662220	38.464547140	38.158180062
8	49.006679725	36.410803008	37.264316713
6	47.766085679	42.328955268	35.443467712
7	48.939258289	41.638611056	35.239550788
1	49.714732336	41.931416305	34.628780794
6	48.879760546	40.511510781	35.976897545
1	49.687965349	39.790070087	36.033860788
7	47.736783097	40.434464267	36.646223886
6	47.025796336	41.569455596	36.320787297
1	46.042814369	41.768840603	36.743367827
26	47.006592092	38.626491174	37.875868154
8	46.592691502	37.346851547	38.987701400
8	46.448199803	40.254961836	40.569252751
6	45.501571852	40.123383373	39.784199923
6	42.923170952	40.261441024	39.299031256
6	41.610268920	39.675952002	39.886997081
8	45.659470294	39.873227074	38.518479753
8	41.645932884	38.448350972	40.158293863
6	44.072988684	40.163650661	40.303461502
8	40.637988054	40.447039180	40.061361392
1	43.183385307	39.652223070	38.418395841
1	42.768520118	41.296407782	38.958940547
1	43.959823192	39.200824954	40.837445765
1	44.021398680	40.949952463	41.072865764
7	47.136568359	32.942418947	42.089358675
6	48.565773088	32.965928376	42.113847654
7	49.140460549	34.200093458	42.153249943
6	48.464381394	35.330919183	41.948256694
6	47.021782013	35.329339340	41.752135260

6	46.275611887	36.544588510	41.405240629
6	46.425416034	34.094403601	41.860743641
8	49.226715467	31.935207911	42.085359142
7	49.162541131	36.474303866	41.928615259
1	50.158136954	36.397951415	42.107381944
1	48.816384432	37.402862959	41.647535519
1	46.598069848	37.459563814	41.923481562
1	45.185341862	36.425546633	41.444288094
1	46.488159681	36.884772068	40.214395388
1	45.343303600	34.000852710	41.741892114
8	48.993724492	39.234676836	40.939321556
1	49.137285856	39.012543927	39.995800019
1	48.092176093	39.636181093	40.896244290
8	45.490907094	34.642755318	38.820655150
1	46.152320271	35.316925186	38.581534821
1	45.907175974	33.772734849	38.615391904
1	46.514958106	37.045050993	32.925076914
1	51.668827613	37.087806864	37.124398005
1	47.539796379	43.257874091	34.920045990
1	46.620672935	32.087308544	42.140452791

### Snapshot 3

#### RC

**QM/MM (B1) = -3269.279573 a.u.**

**QM/MM (B2+ZPE) = -3271.165439 a.u.**

6	49.727924825	36.688694323	38.739333672
7	48.355428238	36.759764521	38.674225053
1	47.726051404	36.053555030	38.269665643
6	47.968614078	37.922229912	39.221682391
1	46.932006829	38.243518138	39.288007621
7	49.029204922	38.604233027	39.639510084
6	50.141648018	37.844854536	39.356137599
1	51.141600536	38.177439696	39.630881235
6	53.289467652	41.857086693	39.596319732
1	52.953878210	42.764779724	39.078366311
1	53.888086498	42.146216299	40.473634719
6	52.112908028	40.995336847	40.053588529
8	50.948151939	41.375326281	39.587413880
8	52.277897657	40.015135092	40.773357183
6	47.462232256	40.698608505	36.188275122
7	48.795416122	40.872140864	35.887463643
1	49.231335354	40.892931323	34.954686679
6	49.467639115	40.992805168	37.044798290
1	50.537923973	41.149993258	37.119475349
7	48.638686627	40.911986149	38.078063775
6	47.374752451	40.732775167	37.558116123
1	46.491085179	40.653846084	38.187627077
26	49.197649718	40.629323751	40.081939592
8	49.578335048	40.345873598	41.627825180
8	48.247276225	42.975475725	42.214696132
6	47.501011021	42.123461333	41.745951750
6	45.774547730	40.213293033	42.185766530

6	44.972243184	39.639063194	43.374177847
8	47.645371146	41.653603478	40.519893208
8	43.738009378	39.438099936	43.201299624
6	46.351040542	41.578289696	42.570146204
8	45.608311565	39.441974959	44.432095144
1	46.607442276	39.518047252	41.981566835
1	45.141686210	40.272862087	41.289140326
1	46.719661694	41.519134363	43.605116153
1	45.558053967	42.348094546	42.566340203
7	53.311657070	40.635927904	46.792764641
6	54.370000038	40.927416259	45.907227796
7	54.088030692	41.745081719	44.872715321
6	52.847178593	42.119344297	44.556016591
6	51.708285731	41.697495460	45.351224314
6	50.294339494	41.974592581	44.931169452
6	52.017284651	41.001712374	46.480462528
8	55.501883392	40.451059641	46.089422401
7	52.696665676	42.912443571	43.483568256
1	53.522922705	43.247137868	42.982261524
1	51.790845398	43.203839040	43.124769412
1	50.135832889	43.027182576	44.648602554
1	49.589827952	41.728952666	45.739183851
1	50.037831649	41.351265317	44.058945939
1	51.232014792	40.684329683	47.171449649
8	50.503553672	44.050893274	41.239889598
1	49.667757038	43.698092395	41.638447445
1	50.707483746	43.366585481	40.580033181
8	50.779695062	38.671588210	43.566558457
1	51.712798284	38.405255163	43.454993854
1	50.591692990	39.184865302	42.761497221
8	53.595825486	38.562454007	42.798915440
1	53.260476539	39.237458086	42.176992459
1	53.900470987	37.852200262	42.182442493
1	50.307912303	35.924454577	38.222014179
1	53.930244853	41.291765283	38.919648761
1	46.693884586	40.530953669	35.433555941
1	53.461096392	40.086917028	47.615095138

**T<sub>SHAT</sub>**

**QM/MM (B1) = -3269.251220 a.u.**

**QM/MM (B2+ZPE) = -3271.137762 a.u.**

6	49.837798590	36.695020712	38.880272063
7	48.463458784	36.792742784	38.875866546
1	47.807533042	36.124356326	38.448661800
6	48.123907217	37.913996385	39.532510677
1	47.098381172	38.251859427	39.662224726
7	49.212522631	38.546322176	39.963603431
6	50.297418554	37.791831663	39.568215700
1	51.313897314	38.091021643	39.819659456
6	53.455463835	41.848347087	39.631648145
1	53.107834922	42.764990003	39.138722332
1	54.088414510	42.124152645	40.489228138

6	52.286830565	40.997704709	40.120364761
8	51.107598273	41.442999426	39.783761886
8	52.465194742	39.964656731	40.765511156
6	47.585542869	40.683220184	36.353266503
7	48.913166019	40.867668877	36.037182259
1	49.329301726	40.911056522	35.096586876
6	49.599679253	40.949511801	37.194261223
1	50.669981192	41.114552766	37.252333823
7	48.792646054	40.833483868	38.238634149
6	47.523336760	40.670909616	37.726321001
1	46.647478895	40.570184219	38.363980359
26	49.404777743	40.595520146	40.400054480
8	49.836283477	40.523768908	42.087996821
8	48.189510638	43.100365414	42.228844098
6	47.513621225	42.152693905	41.826476647
6	45.748229686	40.282287697	42.260211879
6	44.963160714	39.674471137	43.441482626
8	47.743044391	41.558818138	40.683637863
8	43.729417899	39.465123532	43.277658038
6	46.366015279	41.621486615	42.666587112
8	45.615068217	39.449427219	44.485134309
1	46.562607861	39.578783756	42.014454074
1	45.100719731	40.380036006	41.377765117
1	46.754791776	41.525125830	43.693160595
1	45.598067535	42.413967271	42.704181224
7	53.207789334	40.503577345	46.543069287
6	54.316409199	40.912597973	45.753056577
7	54.061797751	41.765319875	44.743956405
6	52.832064894	42.054947844	44.316783696
6	51.662850662	41.438483639	44.941083339
6	50.313582061	41.581879767	44.388393633
6	51.930671326	40.711180973	46.082200031
8	55.451458642	40.488220346	46.004531083
7	52.710924072	42.914426975	43.301792506
1	53.553945181	43.339287413	42.901502149
1	51.822004292	43.175835451	42.865707647
1	50.030034836	42.593713690	44.063174981
1	49.528310134	41.126594559	45.005192146
1	50.179082541	41.008133263	43.267189785
1	51.115760895	40.266323086	46.658776306
8	50.584753794	43.941629745	41.360518267
1	49.683428041	43.670863368	41.680671593
1	50.789298131	43.245422487	40.708002512
8	50.822693147	38.393133972	43.649644302
1	51.756408147	38.155560693	43.485971393
1	50.615517841	38.999705775	42.914070209
8	53.624006069	38.463035143	42.808353152
1	53.297173087	39.137749233	42.179651786
1	53.946691307	37.759340122	42.192042027
1	50.386934177	35.937588778	38.320974029
1	54.069255298	41.286694029	38.927465492
1	46.804958097	40.548525343	35.604526199

1 53.347207208 40.001816489 47.396750254

**Snapshot 4**

**RC**

**QM/MM (B1) = -3268.123647 a.u.**

**QM/MM (B2+ZPE) = -3270.011227 a.u.**

6	37.877818802	38.377753875	42.158214557
7	38.016830056	39.441030277	41.294427738
1	37.367931476	39.708559851	40.543415529
6	39.139874430	40.104065752	41.620607641
1	39.510391227	40.977558592	41.086804341
7	39.727716470	39.517965335	42.658320162
6	38.951742001	38.437060647	43.011818682
1	39.211271797	37.800622012	43.855143318
6	42.755875449	36.268674344	45.509333528
1	43.694512749	36.146587253	44.953480083
1	42.994535208	36.401400195	46.577092744
6	41.961447956	37.487127429	45.029699578
8	42.546506359	38.174935084	44.078072860
8	40.862603254	37.770558103	45.495282120
6	42.218998650	38.232149469	39.224778861
7	42.209730634	37.058442670	39.940787885
1	42.239415133	36.108602238	39.544058568
6	42.133324038	37.377900514	41.245068391
1	42.121875537	36.658430629	42.053794513
7	42.103815067	38.694814757	41.406498542
6	42.148813448	39.246073858	40.144574361
1	42.125321010	40.319544320	39.983494616
26	41.722650277	39.744421754	43.207322571
8	41.443892100	40.553068425	44.582161069
8	44.473838217	41.340966580	43.059830405
6	43.642036628	41.653794606	42.208635391
6	44.210859058	44.006845481	41.296541118
6	42.886589453	44.775992822	41.434859997
8	42.401213993	41.260523368	42.217654894
8	42.287906788	45.093342969	40.371950109
6	44.028713259	42.506786812	40.999903826
8	42.490639921	45.059249820	42.595864441
1	44.759834601	44.451936089	40.451476951
1	44.811392489	44.127848944	42.206740412
1	44.988910484	42.097473227	40.646542538
1	43.289026962	42.380098318	40.196972471
7	41.590540832	40.928194753	50.515203229
6	42.043689217	39.607045060	50.744914887
7	42.930813118	39.109347697	49.855034894
6	43.310010179	39.757434556	48.756996833
6	42.828999103	41.096800017	48.460656383
6	43.246431897	41.824595083	47.215186640
6	41.982163107	41.625118650	49.387441425
8	41.654614037	38.958013365	51.720202352
7	44.159967130	39.131457527	47.928030390
1	44.481995230	38.189883600	48.170230250
1	44.465856303	39.524153762	47.037374279

1	44.320945336	42.073863058	47.234528503
1	42.679281773	42.751618705	47.058244162
1	43.080358053	41.208648206	46.316952880
1	41.571598033	42.630177379	49.256311895
8	41.850836057	43.464400689	44.783699077
1	42.164739122	44.010213122	44.031793918
1	41.967736439	42.545461721	44.493816759
8	39.297582453	40.341345502	46.834683253
1	38.527936727	39.818748853	46.496527063
1	40.035144046	39.996565723	46.301316772
8	45.108291485	39.364447745	44.958960618
1	44.360975208	38.813837971	44.654024568
1	44.937160818	40.190013192	44.453601759
1	37.119528008	37.601109081	42.058789941
1	42.162925150	35.360938964	45.397558121
1	42.247972115	38.287595142	38.136590625
1	40.922775263	41.359344679	51.121974505

**T<sub>SHAT</sub>**

**QM/MM (B1) = -3268.100598 a.u.**

**QM/MM (B2+ZPE) = -3269.982218 a.u.**

6	37.912714321	38.424511415	42.238338263
7	38.066930991	39.512168146	41.405031816
1	37.447304195	39.778693818	40.628880067
6	39.158481096	40.190704805	41.802169874
1	39.540016072	41.080448959	41.304238372
7	39.712367488	39.595738145	42.856661950
6	38.943524873	38.486875288	43.141478935
1	39.188873185	37.827112360	43.970010310
6	42.794695945	36.198988474	45.533107694
1	43.742060775	36.066865684	44.994336456
1	43.021063081	36.330319504	46.603921056
6	42.032798194	37.428266890	45.035299935
8	42.681118986	38.175844522	44.187427100
8	40.886538031	37.683828418	45.406641163
6	42.209844613	38.270481857	39.310673684
7	42.228740554	37.086268286	40.008836973
1	42.271070045	36.143101605	39.599123895
6	42.143976561	37.390188491	41.319416139
1	42.152250200	36.654718916	42.114226396
7	42.083091613	38.700960505	41.504053722
6	42.114858721	39.266777728	40.249129509
1	42.067766243	40.341414904	40.100683093
26	41.716814949	39.797544805	43.435626480
8	41.635234423	40.621833347	44.956333634
8	44.494911023	41.337912677	43.054033644
6	43.612286738	41.664547361	42.257489981
6	44.172656694	43.983866403	41.241947410
6	42.869339237	44.785022337	41.387035646
8	42.364709775	41.318097392	42.370014300
8	42.275320582	45.119774785	40.326860767
6	43.955545567	42.475979711	41.006980223
8	42.479889071	45.078349631	42.548129965



1	44.705057305	44.386627091	40.365721698
1	44.802134279	44.128007973	42.129228338
1	44.892521012	42.043571174	40.621407021
1	43.178652711	42.336680415	40.242084905
7	41.530391440	40.900585253	50.420563116
6	42.042431659	39.595839779	50.676062508
7	42.926965814	39.107378158	49.782022552
6	43.225257992	39.707794804	48.633216850
6	42.635020234	40.998134115	48.280987133
6	42.868095740	41.651939861	46.988289025
6	41.808005212	41.539051166	49.237331080
8	41.694260261	38.966318278	51.675390956
7	44.080351137	39.088367211	47.812604645
1	44.462626851	38.181877672	48.101266009
1	44.362151950	39.449918565	46.897067435
1	43.896992522	41.574594055	46.606167075
1	42.498079777	42.681383443	46.902414655
1	42.261164535	41.083993748	46.077327155
1	41.334305329	42.509972576	49.067083435
8	41.826771917	43.524623447	44.731891571
1	42.152241828	44.068015423	43.982553684
1	41.903129633	42.605832489	44.425989211
8	39.322665439	40.449978585	46.801826542
1	38.574864372	39.888390796	46.477576691
1	40.060061812	40.203006922	46.210863791
8	45.136747822	39.382683437	44.970177419
1	44.403696302	38.807764138	44.663219356
1	44.963434960	40.190010964	44.433997816
1	37.159954932	37.646038579	42.114238837
1	42.193280821	35.297655440	45.414930137
1	42.250810124	38.341214037	38.223757818
1	40.885121598	41.338328923	51.046646023

#### Snapshot 5

#### RC

**QM/MM (B1) = -3185.029625 a.u.**

**QM/MM (B2+ZPE) = -3186.848097 a.u.**

6	49.352346638	31.021773667	36.316750076
7	48.951780803	31.695247598	37.449749126
1	48.989636106	31.326403192	38.408924843
6	48.456253543	32.886734302	37.084748500
1	48.055572622	33.613639937	37.785345030
7	48.518579336	33.025214405	35.761535507
6	49.095233733	31.876506321	35.268721430
1	49.314046377	31.749816620	34.214978219
6	47.582599749	33.303318354	31.378904010
1	47.891884033	34.082211876	30.662553873
1	48.373281742	33.249994713	32.139918759
6	46.263864977	33.735595507	31.990951220
8	46.263605278	34.281264973	33.185801057
8	45.203330253	33.613814957	31.393671944
6	44.351311045	32.899767774	37.289018146

7	44.215884067	32.089061021	36.178775803
1	43.631439541	31.248891663	36.073525422
6	45.048461324	32.557734768	35.230733653
1	45.150873844	32.100792923	34.250025655
7	45.710402028	33.619898516	35.672310805
6	45.281728059	33.852292500	36.957029195
1	45.669055382	34.692340004	37.530255322
26	47.414163504	34.512184753	34.725439782
8	48.641446726	35.134032675	33.866085717
8	47.691389754	37.023855269	37.877086907
6	48.084076892	36.612839453	36.791854671
6	50.473355352	35.809083872	36.513883265
6	51.943727092	36.202857802	36.269256651
8	47.302537389	35.811666543	36.092469587
8	52.536478204	35.638602537	35.307683645
6	49.468184755	36.952487362	36.256009355
8	52.467149200	37.041163287	37.043347746
1	50.235250811	34.943770525	35.885712272
1	50.384377426	35.519629838	37.573862163
1	49.407114785	37.155149098	35.176228798
1	49.808864830	37.856580765	36.781380946
7	53.956649608	36.732890107	30.111666090
6	53.251658017	36.238544056	28.988807166
7	51.914142888	36.386795300	29.008145965
6	51.243628576	36.827362787	30.077030174
6	51.930308904	37.216582248	31.298339149
6	51.204040318	37.599605588	32.555659986
6	53.285799332	37.193997900	31.225927450
8	53.849638749	35.710486773	28.035289291
7	49.916857163	36.927192065	29.986010725
1	49.323588935	37.222386645	30.763086453
1	49.445768638	36.681902111	29.110190045
1	50.763749062	36.708894718	33.035056869
1	50.385018132	38.309455190	32.361452972
1	51.895484675	38.047175196	33.284045391
1	53.890741708	37.528356486	32.074006859
8	51.793189273	33.319894048	34.076829095
1	51.502067828	33.506837781	33.159069282
1	52.004704435	34.203705876	34.461928408
8	47.848522096	37.266500818	31.995620167
1	48.022528514	36.567955427	32.656046524
1	46.971697763	37.643812659	32.216008632
1	49.585181702	29.957019701	36.329165861
1	47.538095800	32.339715763	30.871403501
1	43.881841114	32.699632001	38.252143775
1	54.954752910	36.791220786	30.130635248

**T<sub>SHAT</sub>**

**QM/MM (B1) = -3185.000801 a.u.**

**QM/MM (B2+ZPE) = -3186.817594 a.u.**

6	49.460140171	31.023358997	36.257142027
7	49.042184322	31.734120784	37.361380114

1	49.010202712	31.376799329	38.325003132
6	48.645905134	32.950887153	36.958111913
1	48.247300260	33.705678149	37.630119668
7	48.790937552	33.074311661	35.638597234
6	49.314637992	31.880955024	35.190195172
1	49.568661635	31.721245732	34.148297071
6	47.665342227	33.303006039	31.277639424
1	47.974038510	34.056820068	30.533878424
1	48.494167892	33.242902500	31.998302143
6	46.410827083	33.818515582	31.964438858
8	46.584359776	34.594991954	33.000710085
8	45.283654830	33.569878228	31.547631075
6	44.516714269	32.966830057	37.099044985
7	44.366385659	32.148915587	35.996107733
1	43.766306364	31.319972460	35.903157008
6	45.227421365	32.589523324	35.051413184
1	45.311421824	32.122436193	34.072411466
7	45.918155465	33.635076648	35.481244157
6	45.477523789	33.889030736	36.758580524
1	45.872753692	34.727227453	37.330630306
26	47.831941433	34.641117202	34.534773028
8	49.142297789	35.312586419	33.594244612
8	47.737210037	37.010676634	37.833476024
6	48.224224385	36.688217937	36.754769961
6	50.624486057	35.937191418	36.626383358
6	52.094042001	36.320377232	36.388091181
8	47.561609330	35.923453204	35.920801979
8	52.633677105	35.877365173	35.330233893
6	49.637689764	37.090573244	36.354394211
8	52.664762490	37.041688490	37.238751584
1	50.385638492	35.078256668	35.989061806
1	50.508953640	35.646902539	37.681540239
1	49.649233432	37.341626774	35.284115360
1	49.929127276	37.970999708	36.945512626
7	53.802364668	36.503765862	30.251233504
6	53.144276978	36.128698389	29.043701183
7	51.809918164	36.284194864	29.016738888
6	51.085074314	36.581900703	30.096523509
6	51.702987201	36.716302162	31.414944155
6	50.931254151	36.910419167	32.649614242
6	53.077426329	36.723698134	31.398575041
8	53.790681292	35.697317636	28.078459581
7	49.776626500	36.758672929	29.948957273
1	49.155139222	37.030448707	30.715289317
1	49.347731832	36.672828028	29.021780687
1	50.172277660	35.948837202	33.010109131
1	50.143570604	37.674840580	32.573257918
1	51.559193454	37.020463185	33.544233499
1	53.630646492	36.911049560	32.323722825
8	52.039624916	33.511836151	34.061722567
1	51.652056441	33.651628085	33.174481115
1	52.171391512	34.410251832	34.443928577

8	47.797316429	37.363247697	31.938782255
1	47.932368834	36.606000472	32.541379582
1	46.892904800	37.701255330	32.121447081
1	49.654900688	29.951616585	36.295921665
1	47.572247418	32.328718883	30.797884049
1	44.019997419	32.801985412	38.055165233
1	54.794106540	36.627176764	30.285734231

**HAT cartesian coordinates for K1299E-S1303N Mutant  
RC**

**QM/MM (B1) = -3185.774486 a.u.**

**QM/MM (B2+ZPE) = -3187.588465 a.u.**

6	46.697073117	39.260654369	47.041496903
7	46.496677879	40.262453266	46.116182254
1	45.823294151	41.036172651	46.170589248
6	47.339127382	40.067918877	45.090974080
1	47.379031358	40.708395093	44.214800281
7	48.064610927	38.976819187	45.294797504
6	47.683984998	38.458756973	46.516469933
1	48.143925865	37.555627747	46.910252071
6	48.853240596	33.941916176	44.922099449
1	48.242995932	33.585982038	44.082053173
1	49.831243010	33.441899483	44.884222243
6	49.084873119	35.450842754	44.866980225
8	48.788039296	36.024784382	43.730912333
8	49.511934257	36.083229168	45.831583051
6	45.082875113	37.979030496	41.660485772
7	44.875230268	37.168269942	42.755254285
1	44.015110293	36.657464134	42.993780115
6	46.011883541	37.135562317	43.467787619
1	46.113841058	36.579313132	44.394263701
7	46.951190181	37.875452252	42.891487528
6	46.383001747	38.417681240	41.758992323
1	46.946941862	39.064926167	41.093351607
26	48.956635369	38.014408403	43.674039723
8	50.480900134	38.080148225	44.197207132
8	50.947927775	40.528628184	42.693427342
6	50.114727157	40.104244715	41.908755417
6	50.659399251	41.907815386	40.123773753
6	50.323686976	42.370355509	38.691878257
8	49.252597838	39.130230074	42.147019278
8	49.849192740	41.503203927	37.891125884
6	49.918041658	40.646101389	40.509319628
8	50.562405125	43.558129415	38.414177208
1	51.749730840	41.754775214	40.190928245
1	50.436886758	42.738073143	40.809692916
1	50.193894577	39.836477836	39.815437489
1	48.833464940	40.781061755	40.368434890
7	54.814846431	35.787402141	45.105578679
6	54.174411649	34.616699117	45.614767374

7	53.199610334	34.090703192	44.821256458
6	52.775124787	34.691921721	43.709856249
6	53.295199748	35.972370471	43.268487206
6	52.726980008	36.702356992	42.085413261
6	54.351821757	36.435660612	43.986571933
8	54.503134006	34.113977629	46.681560148
7	51.848488761	34.060161668	42.974163530
1	51.385015244	34.486870665	42.172862098
1	51.620147952	33.091942730	43.219357369
1	51.687190889	37.006692167	42.281374651
1	52.722387400	36.076016598	41.178551552
1	53.305337694	37.613969903	41.874936969
1	54.862390191	37.357647964	43.691782766
8	51.064290058	35.173718836	47.990796204
1	50.580836760	35.565605086	47.235015325
1	50.378354690	35.181518523	48.706521346
8	49.580983188	34.929878707	41.205087786
1	49.205966575	35.170976285	42.079034056
1	49.456636356	35.781184303	40.708602647
1	46.078386801	39.149389259	47.931954446
1	48.359672954	33.680303888	45.858057413
1	44.335919713	38.115384561	40.878480323
1	55.639601284	36.151955936	45.537843015

**T<sub>SHAT</sub>**

**QM/MM (B1) = -3185.732820 a.u.**

**QM/MM (B2+ZPE) = -3187.548591 a.u.**

6	46.770064853	39.251529305	46.980508516
7	46.571287923	40.250856939	46.052394070
1	45.896398776	41.023613534	46.102343364
6	47.422263228	40.052879607	45.031896706
1	47.458447046	40.690335591	44.153454667
7	48.152149693	38.965437638	45.238565277
6	47.763762834	38.453171835	46.460588197
1	48.221677392	37.551974481	46.859958563
6	48.827668555	33.891253630	44.879693105
1	48.202497944	33.532137729	44.051658306
1	49.799585146	33.379870389	44.832063708
6	49.075723730	35.398124095	44.804156339
8	48.818797099	35.959609346	43.652988427
8	49.492237481	36.037678130	45.768734236
6	45.110847972	37.976160535	41.662336516
7	44.906965387	37.177086665	42.765909972
1	44.045214451	36.673248666	43.013329023
6	46.051651883	37.139651486	43.467079331
1	46.158529441	36.592401215	44.398042910
7	46.992544806	37.862443906	42.872542771
6	46.417568552	38.400519313	41.741439038
1	46.981356592	39.035498298	41.064118623
26	48.994130339	37.960456703	43.587182199
8	50.610069104	38.029257228	44.141531616
8	50.940954531	40.534067570	42.641825379

6	50.126500065	40.089752698	41.845880407
6	50.649210218	41.925872570	40.087282441
6	50.318638800	42.394776859	38.657173718
8	49.314003280	39.071360851	42.055386691
8	49.847097944	41.530819402	37.850862158
6	49.913324736	40.657799969	40.459595519
8	50.558718919	43.583442741	38.384704099
1	51.739911157	41.776920520	40.158250296
1	50.421126664	42.750740784	40.778161207
1	50.181763972	39.861452801	39.748475030
1	48.826674760	40.793362094	40.332239478
7	54.792750037	35.798427597	45.138784462
6	54.185010228	34.595193592	45.627791384
7	53.211515552	34.073198442	44.833348375
6	52.704129520	34.723825585	43.790192277
6	53.103413599	36.091958465	43.463531701
6	52.337922486	36.964265313	42.581536819
6	54.217161149	36.529463476	44.137666717
8	54.550364816	34.070253809	46.668725118
7	51.815124569	34.079699834	43.026052915
1	51.342499022	34.505499900	42.228842251
1	51.657042799	33.084399192	43.215468244
1	51.427315948	37.523113250	43.360068854
1	51.722410239	36.484388121	41.810184311
1	52.879850975	37.843114267	42.208062276
1	54.660194560	37.500946904	43.897535220
8	51.063479332	35.182774948	47.930137230
1	50.570697946	35.562111135	47.173336033
1	50.383734618	35.200119696	48.652448755
8	49.622803447	34.945740700	41.165798624
1	49.221784270	35.179155931	42.033761720
1	49.466193461	35.782757378	40.653232656
1	46.158260392	39.144479256	47.876222149
1	48.348537101	33.640155665	45.825975397
1	44.358538067	38.112760461	40.885524058
1	55.627466244	36.158299014	45.555574464

**IM<sub>HAT</sub>**

**QM/MM (B1) = -3185.767923 a.u.**

**QM/MM (B2+ZPE) = -3187.583002 a.u.**

6	46.641227259	39.318510000	47.142598106
7	46.446125920	40.293521881	46.186888791
1	45.761048328	41.057199197	46.206400985
6	47.318681650	40.083129146	45.186614708
1	47.369184586	40.702049210	44.295442882
7	48.055068253	39.010998391	45.432385398
6	47.650681837	38.522993042	46.656361384
1	48.095690671	37.628683206	47.081034858
6	48.614987684	33.774235257	44.741103917
1	48.009610509	33.211969936	44.015222081
1	49.639896375	33.379814117	44.671141557
6	48.661522568	35.228387318	44.321349305

8	48.996801742	35.516581439	43.142697355
8	48.390186928	36.179358078	45.118730258
6	45.156808794	37.908556776	41.780121392
7	44.865198157	37.113021144	42.867499182
1	43.978628019	36.631520786	43.063732600
6	45.964161262	37.024386828	43.629459677
1	46.012030144	36.475926297	44.564126201
7	46.963991460	37.711227247	43.088734908
6	46.473531227	38.278854028	41.930465744
1	47.098354538	38.891461076	41.287150736
26	48.870517476	37.742252655	43.909408698
8	50.527331490	37.605790606	44.588754967
8	51.307904858	39.888625269	42.796682021
6	50.312339162	39.678536006	42.099565175
6	50.833927379	41.649702018	40.444800903
6	50.434311152	42.248414650	39.070343884
8	49.365595930	38.821150639	42.372021427
8	49.898473101	41.466839856	38.222383577
6	50.071076215	40.377141507	40.771285163
8	50.690725062	43.450746260	38.886066120
1	51.921923354	41.461406872	40.429603155
1	50.679320620	42.428288357	41.207534786
1	50.291414932	39.630850141	39.990733507
1	48.987377143	40.554963478	40.693209346
7	54.821608310	35.838838191	45.082551531
6	54.184505547	34.664144064	45.579843131
7	53.261347962	34.098839546	44.751091291
6	52.855040955	34.663260301	43.621027656
6	53.300617152	36.008905477	43.213472881
6	52.723688113	36.718349025	42.152338192
6	54.368109113	36.495016133	43.964771259
8	54.478310471	34.183772357	46.667452050
7	52.036793760	33.968696567	42.831702273
1	51.641444315	34.341560127	41.968281544
1	51.817690031	33.002093609	43.092356486
1	51.103136515	38.202744893	44.078943362
1	51.858865249	36.334146964	41.611767661
1	53.078588619	37.721932185	41.908838836
1	54.853683003	37.435552613	43.692202366
8	50.930362038	35.841183542	47.025039703
1	50.709377031	36.424648397	46.273482668
1	50.223268555	35.991068187	47.699880784
8	49.976354355	34.723448482	40.850043158
1	49.566832909	34.853711294	41.740978336
1	49.758445171	35.603517122	40.449048376
1	46.008559297	39.205325861	48.022932086
1	48.227512031	33.592167067	45.743491624
1	44.451240221	38.065900022	40.964349725
1	55.649940328	36.193648261	45.516081665

**HAT cartesian coordinates for N1387A Mutant**

**RC**

**QM/MM (B1) = -3183.972024 a.u.**

**QM/MM (B2+ZPE) = -3185.785848 a.u.**

6	48.560498006	43.516590308	30.609103917
7	47.772500794	42.385173318	30.602135764
1	47.143889679	42.110732546	29.837035137
6	47.925753378	41.753295608	31.784509423
1	47.453813395	40.805200757	32.042041834
7	48.766252873	42.437344797	32.554945305
6	49.183326488	43.532584045	31.834032068
1	49.895691640	44.244423380	32.248240887
6	51.243084836	45.655582175	36.204500982
1	50.554990918	45.633156654	37.059471507
1	52.253657110	45.400414726	36.557431584
6	50.825850467	44.615015849	35.170535158
8	49.721548678	43.993214314	35.461217211
8	51.490830585	44.399220536	34.152196149
6	44.950902619	43.459142006	34.660646446
7	45.492933330	44.697736487	34.936531946
1	44.985424868	45.584530583	35.062799872
6	46.828272054	44.538428253	35.030573401
1	47.520084157	45.339643767	35.271182713
7	47.168862236	43.271039513	34.822002040
6	46.001330974	42.582349688	34.592276439
1	45.993609060	41.511686649	34.406691321
26	49.079541516	42.345420550	34.640803670
8	50.548872936	41.678274568	34.481699624
8	49.599377606	39.329101557	36.263922714
6	48.470858264	39.747325874	36.030885902
6	47.269603112	37.562033723	36.821861884
6	47.193215053	36.626664262	35.597929291
8	48.184710217	40.884976164	35.450667824
8	47.694444906	37.032299626	34.519824813
6	47.198737478	39.054549938	36.517854322
8	46.680126523	35.490040755	35.788753464
1	46.463786660	37.279240607	37.516321900
1	48.221667173	37.339774733	37.335925783
1	46.938005598	39.606659771	37.441398561
1	46.400309034	39.282382996	35.798937618
7	55.968871190	41.460020232	36.469229532
6	55.308220970	42.373038310	37.342768426
7	54.004048379	42.101064567	37.627710462
6	53.346722270	41.093169793	37.066173765
6	53.986573491	40.150255020	36.177462962
6	53.241045082	38.997620240	35.569618975
6	55.308069732	40.380693445	35.937766407
8	55.895380631	43.342550118	37.817254333
7	52.041415223	40.935679415	37.376591028
1	51.421320015	40.309487217	36.865594219



1	51.599800140	41.627529809	37.973288563
1	52.395438264	39.341734918	34.949709878
1	52.823048608	38.324447226	36.338993095
1	53.899135978	38.407293930	34.920615771
1	55.884680381	39.697642776	35.307413944
8	54.280445625	44.319437763	34.939564926
1	54.393466133	45.182197549	35.400904012
1	53.373322725	44.373065930	34.595276561
8	50.068617869	39.538995040	32.776497172
1	50.322928173	40.222199604	33.424010741
1	50.128985833	38.703387635	33.287375244
1	48.506197435	44.299731049	29.852923154
1	51.255405612	46.670504551	35.807199974
1	43.899283860	43.273309837	34.442399535
1	56.919147437	41.576345340	36.180411215

**T<sub>SHAT</sub>**

**QM/MM (B1) = -3183.932205 a.u.**

**QM/MM (B2+ZPE) = -3185.746582 a.u.**

6	48.675822652	43.575775503	30.565841296
7	47.926799529	42.417704236	30.566643989
1	47.263911948	42.143995432	29.831380312
6	48.181402875	41.750584861	31.712355538
1	47.771058088	40.773471533	31.966227980
7	49.049221041	42.435222770	32.453702225
6	49.372100397	43.573572215	31.749908893
1	50.067220889	44.307262802	32.153991418
6	51.260211912	45.669683124	36.301917402
1	50.541078356	45.660240030	37.132154526
1	52.254535820	45.448659900	36.720757184
6	50.919632900	44.557978786	35.316722124
8	50.080133550	43.686434154	35.766280603
8	51.438474672	44.482113189	34.189625967
6	45.212266178	43.439837837	34.639939253
7	45.734440984	44.672356294	34.970412112
1	45.214582483	45.540068153	35.140777150
6	47.078749537	44.527656739	35.031958982
1	47.748366983	45.337064330	35.309693926
7	47.446069902	43.286835284	34.748789516
6	46.284891920	42.594203528	34.505067234
1	46.289674444	41.534311453	34.264053234
26	49.533696343	42.200740537	34.524646057
8	51.118402252	41.450760943	34.187236399
8	49.725607791	39.229991908	36.414359000
6	48.645943320	39.692662605	36.027132320
6	47.273426883	37.597533044	36.788355047
6	47.224781883	36.605700751	35.608443572
8	48.514707923	40.793827913	35.361379599
8	47.765756224	36.948863090	34.527421068
6	47.303074171	39.076077175	36.411941343
8	46.689751754	35.485117263	35.833676972
1	46.414984792	37.385331782	37.444933561

1	48.180211142	37.354650641	37.370207007
1	46.977909505	39.683409364	37.278744011
1	46.591006062	39.304071166	35.607785561
7	55.852543172	41.551513195	36.414818289
6	55.280094252	42.405455820	37.428313267
7	53.996626144	42.148735622	37.793339295
6	53.232496758	41.281519036	37.149083377
6	53.726019150	40.533372311	36.000323518
6	52.829810387	39.775353413	35.160535481
6	55.069850719	40.700008824	35.710763533
8	55.944766108	43.301161811	37.928203895
7	51.969760835	41.089833187	37.560819393
1	51.306539115	40.487923372	37.068001146
1	51.598727731	41.667987373	38.310141390
1	52.057907191	40.616065410	34.619909413
1	52.043800707	39.199422608	35.664164650
1	53.311073615	39.218228684	34.350288974
1	55.532151208	40.130585200	34.900755241
8	54.229369120	44.135904393	35.009318118
1	54.356074304	45.018642811	35.432979466
1	53.345091214	44.215249917	34.611963256
8	49.988123120	39.494451334	32.634880344
1	50.439527887	40.165988793	33.190633663
1	50.055712035	38.676896366	33.171810458
1	48.576011599	44.366125733	29.821898027
1	51.277286858	46.671324299	35.872393564
1	44.153893186	43.241922312	34.470400552
1	56.808709389	41.625843480	36.131633429

**IM<sub>HAT</sub>**

**QM/MM (B1) = -3183.966770 a.u.**

**QM/MM (B2+ZPE) = -3185.780193 a.u.**

6	48.638325289	43.591399101	30.566524305
7	47.899521194	42.426349013	30.547761315
1	47.264630682	42.143716973	29.790816558
6	48.115857764	41.768826998	31.705205576
1	47.700881395	40.791037090	31.949472312
7	48.947062277	42.468280351	32.475218561
6	49.288736030	43.604341131	31.775108081
1	49.964549798	44.344980292	32.199320376
6	51.221784103	45.726342651	36.296782303
1	50.532085740	45.714571743	37.151064717
1	52.227503742	45.482290014	36.673245909
6	50.828965739	44.643662462	35.302360667
8	49.947475640	43.800544201	35.750596837
8	51.328715309	44.562870770	34.171551283
6	45.091450425	43.471349696	34.641376155
7	45.605656138	44.710521282	34.959708640
1	45.079050029	45.579895356	35.115609533
6	46.947982261	44.576247815	35.031717715
1	47.613830880	45.390271277	35.303524089
7	47.321747968	43.331804005	34.764825174

6	46.166529384	42.627940509	34.522416988
1	46.178027083	41.565861683	34.290074774
26	49.351643023	42.312610507	34.554911588
8	51.071714499	41.608621829	34.243084368
8	49.719679524	39.231420379	36.334412637
6	48.630994375	39.723040141	36.033099207
6	47.277162197	37.611116368	36.776269962
6	47.225619211	36.627142431	35.588788362
8	48.479874365	40.881835349	35.460362981
8	47.747119490	36.987236082	34.504320337
6	47.295055029	39.092037738	36.410440972
8	46.706782101	35.499552472	35.814119898
1	46.423821057	37.390736169	37.436474593
1	48.187341541	37.366018654	37.351717289
1	46.957026318	39.694373191	37.275380201
1	46.586608425	39.316614006	35.601453458
7	55.989357134	41.414327682	36.489209286
6	55.315910853	42.336781710	37.335210558
7	53.998342287	42.072369656	37.597541320
6	53.351325869	41.058292747	37.062237861
6	54.013975098	40.046324064	36.234892008
6	53.348882790	38.929857966	35.702747985
6	55.365750115	40.297474073	35.999809153
8	55.888021130	43.311378102	37.812880313
7	52.014679416	40.980664915	37.266304912
1	51.432165043	40.193678406	36.979926223
1	51.578706558	41.668079471	37.875436282
1	51.521571386	41.354993006	35.067521138
1	52.288746727	38.749860558	35.874318774
1	53.877256838	38.239743929	35.045781844
1	55.957439644	39.599076830	35.402816061
8	54.182591777	44.257477156	34.937963990
1	54.320236913	45.130103378	35.377105561
1	53.300242537	44.353023950	34.544109699
8	50.043146462	39.588138694	32.723416899
1	50.532900070	40.220956477	33.293997013
1	50.106517390	38.742649512	33.216476256
1	48.551996186	44.384527570	29.823852210
1	51.239604591	46.730921903	35.874206541
1	44.037549424	43.269222863	34.450313984
1	56.936329457	41.544746966	36.195599470

**HAT cartesian coordinates for S1290A-Y1295A Mutant**

**RC**

**QM/MM (B1) = -3185.020421 a.u.**

**QM/MM (B2+ZPE) = -3186.832929 a.u.**

6	45.168468633	46.309897032	34.501275340
7	44.349974016	45.238199330	34.225592504
1	43.393231016	45.302917480	33.861846261

6	45.019023649	44.107193600	34.490430498
1	44.607266852	43.105367938	34.384711547
7	46.232888793	44.400129361	34.938290011
6	46.347979072	45.770421073	34.953835699
1	47.249634508	46.269870626	35.298649779
6	50.235242402	45.358219878	38.151173311
1	51.227505197	44.936331523	38.356372558
1	50.294204490	46.051496913	37.305794076
6	49.291395241	44.226723321	37.771263692
8	48.200556028	44.561314021	37.174485092
8	49.573189116	43.037280929	37.983532451
6	43.721254377	43.061208996	38.357194777
7	44.416725101	44.049771820	39.021268584
1	44.075931089	44.655090579	39.780695780
6	45.638158268	44.127978614	38.467442010
1	46.408990647	44.822503205	38.775706792
7	45.777705822	43.235265363	37.496668066
6	44.582043926	42.556510339	37.412060662
1	44.433212554	41.769766753	36.676052596
26	47.384736544	43.113231253	36.101727871
8	48.673779165	43.063282032	35.110520457
8	47.420150213	40.698202059	33.835352107
6	47.028409239	40.440416347	34.963281925
6	47.020995323	37.932985112	34.434893140
6	46.043179009	37.806615262	33.254782460
8	46.798100346	41.340469900	35.895369276
8	44.823190982	38.068206272	33.426047666
6	46.737975174	39.025799500	35.452445135
8	46.556408665	37.369670797	32.188141068
1	47.011665748	36.954521281	34.947131002
1	48.020326544	38.039575454	33.996688053
1	47.327335429	38.880502006	36.373844507
1	45.687144836	38.990772840	35.777269836
7	54.195985486	44.777707499	33.558260559
6	54.482130813	45.599558508	34.696353676
7	54.198735022	45.034790559	35.900255439
6	53.630065297	43.837314897	36.029341567
6	53.206412897	43.049328253	34.886597257
6	52.424358181	41.773813303	35.045737425
6	53.565570179	43.565514523	33.678092356
8	54.960300381	46.721862494	34.581788341
7	53.456329140	43.351849647	37.263461531
1	52.921866051	42.501020722	37.474328997
1	53.661238895	43.948837314	38.069109228
1	52.172589410	41.341528212	34.067858499
1	51.477672540	41.948211465	35.584107154
1	52.979835069	41.020360358	35.627145796
1	53.346855369	43.018829154	32.755805817
8	51.723302447	41.616276310	38.448145323
1	50.895196024	42.157504771	38.327316922
1	51.408485975	40.722807653	38.633631310
8	50.606646523	45.089558251	34.881882965

1	49.815038397	44.521503492	35.010924621
1	51.334432429	44.450569415	34.885604351
1	44.811484089	47.339671884	34.487378701
1	49.905122886	45.928048799	39.019725799
1	42.675627169	42.830937511	38.561415523
1	54.439417821	45.061751828	32.630881447

**T<sub>SHAT</sub>**

**QM/MM (B1) = -3184.981868 a.u.**

**QM/MM (B2+ZPE) = -3186.794332 a.u**

6	45.232027440	46.315664106	34.488342831
7	44.454541652	45.217489348	34.186905906
1	43.489616202	45.255915089	33.839975132
6	45.178707144	44.109098813	34.407270357
1	44.809768782	43.092678601	34.285117817
7	46.387011006	44.439451909	34.849374633
6	46.434403316	45.812700457	34.913954917
1	47.308868328	46.331748533	35.291015181
6	50.221271816	45.443172544	38.163864346
1	51.148514411	44.908099938	38.401944170
1	50.399438588	46.165006068	37.358218052
6	49.168347751	44.479188834	37.656954516
8	48.225982397	44.949083403	36.952413399
8	49.231688770	43.235005373	37.852894580
6	43.864043904	43.063296833	38.309719260
7	44.529714646	44.076670191	38.965652319
1	44.167943466	44.681178044	39.714816324
6	45.756598085	44.170594925	38.419817730
1	46.497090616	44.899590164	38.723262151
7	45.933546220	43.266125562	37.468233494
6	44.752319972	42.561749257	37.384893777
1	44.628118780	41.758462357	36.661087527
26	47.643294162	43.194503697	35.973199835
8	49.111266708	43.213412454	35.007917492
8	47.671546422	40.657240840	33.661946946
6	47.191266908	40.478205736	34.778244136
6	47.034469250	37.941318606	34.351392642
6	46.030705507	37.792029099	33.196007262
8	46.954216847	41.431705180	35.637781920
8	44.820874747	38.087236359	33.379335989
6	46.815155432	39.098525546	35.311933176
8	46.512186550	37.301276363	32.136848991
1	46.992384635	36.992355888	34.915213305
1	48.029585347	37.979202580	33.893060019
1	47.395089199	38.958085064	36.241021240
1	45.765687842	39.137540181	35.638135003
7	53.909449992	44.878439442	33.475070361
6	54.277881846	45.636559158	34.637556797
7	53.953975680	45.062565994	35.822019827
6	53.203028655	43.967204739	35.920828750
6	52.595921383	43.330951384	34.755309382
6	51.543529887	42.307968898	34.836052548

6	53.055696205	43.817647231	33.556086291
8	54.862186262	46.710175324	34.547055639
7	53.030768860	43.448217814	37.139066063
1	52.440936188	42.637508150	37.353386055
1	53.416926200	43.946217220	37.944470719
1	51.446032138	41.696503385	33.928801883
1	50.404781040	42.798364805	34.932761447
1	51.564248404	41.685572827	35.740557731
1	52.723560486	43.367436933	32.616128990
8	51.317055666	41.730387150	38.367307752
1	50.485747990	42.267822845	38.235861409
1	51.016914824	40.839190389	38.585731768
8	50.177376325	45.843958438	34.618352288
1	49.451140898	46.362858086	34.198750597
1	49.746523024	44.990780925	34.842215897
1	44.864064199	47.341652960	34.484189652
1	49.899810692	46.003927599	39.041522499
1	42.822931493	42.816097111	38.517191095
1	54.220940390	45.137657700	32.560875567

**IM<sub>HAT</sub>**

**QM/MM (B1) = -3185.011831 a.u.**

**QM/MM (B2+ZPE) = -3186.826631 a.u**

6	45.092540450	46.220145994	34.497641544
7	44.259205412	45.145673021	34.276160942
1	43.292013215	45.208025992	33.941373097
6	44.926903055	44.018132953	34.564591848
1	44.500185137	43.017667774	34.503167721
7	46.154464344	44.314858104	34.971404785
6	46.275187677	45.684589449	34.938468465
1	47.181884564	46.180376889	35.267565590
6	50.205252700	45.421105826	38.081305568
1	51.136485937	44.885208328	38.304196681
1	50.376734831	46.147168673	37.278647410
6	49.151477374	44.459142049	37.575738816
8	48.171097080	44.922305632	36.917517091
8	49.229468644	43.208974943	37.740753941
6	43.752120847	43.054505056	38.410370392
7	44.414599792	44.080961004	39.048677229
1	44.050995627	44.707619793	39.778418752
6	45.652021569	44.148846470	38.524698792
1	46.392846577	44.880883711	38.820470652
7	45.837896845	43.215683450	37.605195520
6	44.653799477	42.519075832	37.519292140
1	44.538062343	41.698999668	36.814025123
26	47.508390064	43.139712685	36.079887350
8	48.865724183	43.087666816	34.799571587
8	48.179411312	40.451807586	34.253309565
6	47.362751272	40.299521089	35.174391463
6	47.010774910	37.843834404	34.485094164
6	46.082902572	37.837130082	33.257860690
8	46.977978726	41.254703365	35.959607451

8	44.862701647	38.113795590	33.405750829
6	46.775864514	38.936623545	35.516226302
8	46.630367065	37.477527667	32.178726137
1	46.886395957	36.859265323	34.967723310
1	48.035527340	37.869029575	34.101314540
1	47.222174082	38.662574263	36.489134709
1	45.703364653	39.058620840	35.720342985
7	54.091026179	44.834255136	33.506135023
6	54.386749143	45.627200537	34.648938950
7	54.076530004	45.059135322	35.848346951
6	53.455412430	43.895172756	35.967616036
6	52.999099936	43.116672148	34.807508696
6	52.201128220	41.967385906	34.922714276
6	53.416626903	43.642753457	33.589265335
8	54.907564402	46.735798171	34.561203754
7	53.264744004	43.412826984	37.198791552
1	52.698694664	42.586797036	37.406311093
1	53.521117099	43.992920224	38.000791291
1	51.863788894	41.439686538	34.028677532
1	48.905835628	42.162047853	34.469855013
1	51.804300069	41.640832616	35.883602692
1	53.191472403	43.119651660	32.657253630
8	51.368300281	41.763946417	38.335474502
1	50.544333209	42.289699339	38.139854469
1	51.052001286	40.882464615	38.571041596
8	50.304666737	45.492677626	34.575922687
1	49.560967080	46.032354053	34.216912791
1	49.898586319	44.603296097	34.692316635
1	44.765141878	47.259323177	34.466204769
1	49.889233714	45.974050802	38.965868266
1	42.704000441	42.820423955	38.596695326
1	54.357551825	45.119989954	32.585650265

#### HAT cartesian coordinates for Y1902A Mutant

RC

QM/MM (B1) = -3186.463625 a.u.

QM/MM (B2+ZPE) = -3188.276703 a.u

6	44.267418327	35.744667258	44.983330998
7	45.441859100	35.359496141	44.379095095
1	46.211828666	34.859744338	44.837342621
6	45.414672571	35.790666085	43.104264302
1	46.217713440	35.634548774	42.388299846
7	44.288824886	36.445806813	42.863877991
6	43.556272411	36.425557560	44.024829146
1	42.593281114	36.923703178	44.100542176
6	41.245839493	40.785148448	41.962506908
1	41.621729058	41.810328665	41.831523669
1	40.498807416	40.632583869	41.166891338
6	42.379578999	39.800533170	41.702590474
8	42.625209468	38.837201512	42.503401062

8	43.064124281	39.903000158	40.657973984
6	47.495195114	39.508812326	43.109476650
7	46.504635435	40.232536066	43.739378031
1	46.607248740	40.931355439	44.486703749
6	45.329107240	39.867955638	43.201550163
1	44.373712447	40.273471752	43.512338856
7	45.503404271	38.963698147	42.248538800
6	46.856550788	38.727263335	42.176728775
1	47.256999438	38.018862562	41.456754039
26	43.982551900	37.853262659	41.261911691
8	42.748420463	37.074844778	40.558938028
8	44.302588251	35.837814196	38.709764015
6	45.287134446	36.471946518	39.053380446
6	47.111355830	34.886416548	38.383347627
6	48.156821026	34.508037988	37.329263336
8	45.363480022	37.257516796	40.110275928
8	49.027287062	35.367316417	37.021919502
6	46.592933696	36.329094834	38.279551330
8	48.066368970	33.355435238	36.839815085
1	46.277406099	34.175701996	38.298527796
1	47.575119188	34.726500057	39.374115395
1	46.360121007	36.562115866	37.226607844
1	47.348177355	37.050128788	38.619709567
7	37.247482167	35.441665868	38.573470821
6	37.002381918	35.936759001	39.889359296
7	37.949702816	36.757515629	40.401051725
6	39.107836028	36.990762361	39.792301796
6	39.416048528	36.472640630	38.474317652
6	40.739162770	36.737000830	37.800802165
6	38.428291953	35.717557703	37.915961538
8	35.987999165	35.641143630	40.517528802
7	39.991093686	37.779185073	40.431399310
1	40.984877590	37.736392271	40.195988016
1	39.748785440	38.015228654	41.391202012
1	40.745452857	36.329935734	36.779853143
1	41.580864916	36.283859033	38.351187446
1	40.973422336	37.814636678	37.747508592
1	38.553343887	35.291622713	36.917350569
8	41.445697870	40.402728671	37.308525239
1	42.331739757	39.978073804	37.362615631
1	41.650105754	41.354319336	37.371965072
8	43.869397289	39.304475632	38.032839472
1	44.815308659	39.581488984	37.922808356
1	43.623283285	39.625348740	38.916186963
1	44.066888529	35.630307863	46.048590143
1	40.774956161	40.690622707	42.940975660
1	48.541247003	39.548070880	43.413288310
1	36.627944474	34.808375858	38.109693609

**T<sub>SHAT</sub>**

**QM/MM (B1) = -3186.424819 a.u.**

**QM/MM (B2+ZPE) = -3188.241261 a.u**



6	44.193033347	35.738711611	44.937896300
7	45.345326739	35.338731273	44.298007646
1	46.133156239	34.855023531	44.743895624
6	45.259360631	35.722781074	43.010297996
1	46.031204712	35.553908861	42.263692743
7	44.117716824	36.363406666	42.793701229
6	43.437760896	36.381986693	43.988352609
1	42.476682490	36.878276063	44.088316927
6	41.210308262	40.783245638	41.966849559
1	41.641664853	41.786501819	41.839204137
1	40.454489525	40.670500392	41.173190516
6	42.280587378	39.725772606	41.718631525
8	42.418981950	38.726697406	42.491775721
8	43.010376177	39.804176423	40.695668941
6	47.407079593	39.465581164	43.075175503
7	46.418010601	40.191927549	43.703818352
1	46.525946985	40.892556581	44.448099146
6	45.240994619	39.818210992	43.167468301
1	44.287967439	40.229548739	43.480245293
7	45.409500890	38.907965549	42.221777158
6	46.762857072	38.675494633	42.150936517
1	47.164078739	37.962871180	41.434787855
26	43.792842661	37.721486274	41.161445067
8	42.419602267	36.975844944	40.373387497
8	44.276407599	35.670192370	38.609458060
6	45.240159371	36.318547109	39.001001016
6	47.119931878	34.803068142	38.340745207
6	48.173074451	34.462354322	37.284355000
8	45.260893519	37.058434489	40.082018874
8	49.036581764	35.336615665	37.001380006
6	46.561275054	36.231177162	38.246077774
8	48.094017000	33.321368723	36.764841406
1	46.304055434	34.072180644	38.248127441
1	47.587801387	34.650630412	39.330347833
1	46.342475422	36.469937407	37.191653978
1	47.287547518	36.969445831	38.612075121
7	37.368378488	35.443610298	38.704282040
6	36.949079651	35.955193505	39.979065387
7	37.792836444	36.821823942	40.583098647
6	39.009854082	37.080351555	40.123145889
6	39.503147568	36.542720890	38.862166168
6	40.854323196	36.891242175	38.369824847
6	38.616177589	35.727287405	38.199435932
8	35.886079860	35.618676685	40.488511955
7	39.802355296	37.875544985	40.857970958
1	40.821468862	37.759235445	40.769941534
1	39.427445185	38.130747968	41.771836360
1	41.202219010	36.297777696	37.514329209
1	41.721343002	36.745844540	39.269121835
1	41.036831376	37.969289132	38.225642816
1	38.880062493	35.285232257	37.233252638
8	41.488598026	40.405021956	37.361417929

1	42.372767028	39.975479412	37.416644200
1	41.695147638	41.356427743	37.427155322
8	43.890636405	39.312823541	38.105118274
1	44.843663183	39.560846065	37.979844170
1	43.650225042	39.676549083	38.973573521
1	44.018778226	35.628411546	46.008193630
1	40.741787468	40.704128262	42.947816446
1	48.456000956	39.518765293	43.366727804
1	36.793655234	34.815739508	38.179454501

**IM<sub>HAT</sub>**

**QM/MM (B1) = -3186.459331 a.u.**

**QM/MM (B2+ZPE) = -3188.273365 a.u**

6	44.294842636	35.745360993	44.954257407
7	45.475324518	35.372798778	44.352303110
1	46.246394101	34.875933732	44.812067872
6	45.449954003	35.809002220	43.080044478
1	46.256330271	35.662514405	42.365725557
7	44.318751283	36.457433748	42.837720039
6	43.581618053	36.424306897	43.997695942
1	42.614759826	36.914097907	44.071159138
6	41.191854878	40.706847651	41.967963805
1	41.587483839	41.718750002	41.799540112
1	40.441136705	40.532509339	41.179981738
6	42.303229803	39.688401146	41.769131275
8	42.440486041	38.678902546	42.524437186
8	43.106007518	39.818206044	40.799983630
6	47.553322478	39.533577657	43.139131558
7	46.567181021	40.276187172	43.752278251
1	46.668256384	40.972365860	44.501514446
6	45.392935012	39.929625245	43.195014136
1	44.444055629	40.366023678	43.489493819
7	45.563175799	39.018103569	42.251428547
6	46.911975221	38.757996023	42.202923758
1	47.312364692	38.038844629	41.492977614
26	43.967018564	37.834460859	41.232420627
8	42.615233381	36.928665882	40.336254574
8	44.290111834	36.037454150	38.506167375
6	45.337209875	36.544317180	38.935232137
6	47.106626806	34.873344235	38.364209287
6	48.152249167	34.435715084	37.334403001
8	45.425736662	37.208664338	40.047049322
8	49.046557157	35.269831781	37.020867164
6	46.624219618	36.320588977	38.167188363
8	48.034081792	33.279543653	36.863759090
1	46.260533727	34.173574471	38.306163453
1	47.557487050	34.762733516	39.367094176
1	46.401174938	36.487078802	37.100673126
1	47.400524347	37.035882675	38.470639246
7	37.154584048	35.445923443	38.624867765
6	36.912634092	35.925146635	39.945445343
7	37.875220668	36.712676763	40.486326733

6	39.042415274	36.945248720	39.904505233
6	39.326224717	36.515614326	38.524308085
6	40.500934026	36.861537377	37.833499344
6	38.312507368	35.751501132	37.947904455
8	35.890853018	35.636285793	40.564126859
7	39.969128147	37.617713234	40.594156610
1	40.976039044	37.473309918	40.381553564
1	39.723749985	37.809815233	41.563560746
1	40.663207081	36.477805326	36.823338849
1	43.027098342	36.523595319	39.527013986
1	41.288497783	37.465884090	38.284494438
1	38.420544539	35.376046926	36.928668670
8	41.426758262	40.583946108	37.505421230
1	42.287556081	40.113692709	37.531894168
1	41.688717865	41.525453555	37.473806434
8	43.832177517	39.384398431	38.169176905
1	44.780595484	39.636945014	38.023622882
1	43.602882380	39.760019751	39.036102015
1	44.086478640	35.625877253	46.017448548
1	40.729775494	40.648723420	42.953444166
1	48.597514542	39.558323806	43.450768993
1	36.545162303	34.806848949	38.155654135

## References

- (1) Waheed, S. O.; Ramanan, R.; Chaturvedi, S. S.; Lehnert, N.; Schofield, C. J.; Christov, C. Z.; Karabencheva-Christova, T. G. Role of Structural Dynamics in Selectivity and Mechanism of Non-Heme Fe(II) and 2-Oxoglutarate-Dependent Oxygenases Involved in DNA Repair. *ACS Cent. Sci.* **2020**, *6* (5), 795–814.
- (2) Chaturvedi, S. S.; Ramanan, R.; Lehnert, N.; Schofield, C. J.; Karabencheva-Christova, T. G.; Christov, C. Z. Catalysis by the Non-Heme Iron(II) Histone Demethylase PHF8 Involves Iron Center Rearrangement and Conformational Modulation of Substrate Orientation. *ACS Catal.* **2020**, *10* (2), 1195–1209.
- (3) Liu, H.; Llano, J.; Gault, J. W. A DFT Study of Nucleobase Dealkylation by the DNA Repair Enzyme AlkB. *J. Phys. Chem. B.* **2009**, *113* (14), 4887–4898.
- (4) Hu, L.; Li, Z.; Cheng, J.; Rao, Q.; Gong, W.; Liu, M.; Shi, Y. G.; Zhu, J.; Wang, P.; Xu, Y. Crystal Structure of TET2-DNA Complex: Insight into TET-Mediated 5mC Oxidation. *Cell.* **2013**, *155* (7), 1545–1555.
- (5) Yi, C.; Chen, B.; Qi, B.; Zhang, W.; Jia, G.; Zhang, L.; Li, C. J.; Dinner, A. R.; Yang, C. G.; He, C. Duplex interrogation by a direct DNA repair protein in search of base damage. *Nat. Struct. Mol. Biol.* **2012**, *19* (7), 671–676.
- (6) Zheng, G.; Fu, Y.; He, C. Nucleic Acid Oxidation in DNA Damage Repair and Epigenetics. *Chem. Rev.* **2014**, *114* (8), 4602–4620.
- (7) Álvarez-Barcia, S.; Kästner, J. Atom Tunneling in the Hydroxylation Process of Taurine/ $\alpha$ -Ketoglutarate Dioxygenase Identified by Quantum Mechanics/Molecular Mechanics Simulations. *J. Phys. Chem. B* **2017**, *121* (21), 5347–5354.
- (8) Koski, M. K.; Hieta, R.; Bollner, C.; Kivirikko, K. I.; Myllyharju, J.; Wierenga, R. K. The Active Site of an Algal Prolyl 4-Hydroxylase Has a Large Structural Plasticity. *J. Biol. Chem.* **2007**, *282*, 37112–37123.

## **D Appendix D: Supporting Information for Chapter 5**

### **D.1 Dynamics of Fe(IV)=O species of TET2 bound to N4 methylated 4mC and 4dmC dsDNA substrates**

The dynamics reveal that the protein-DNA of the two complexes are stable with average RMSD of 2.38 and 2.31 Å for TET2-dsDNA-4mC and TET2-dsDNA-4dmC, respectively [Figure D1 and Table D1]. The active site in the two complexes experiences some flexibilities when compared to TET2-dsDNA-5mC complex, possibly due to the steric effects in the active site pocket of the former two complexes, especially TET2-dsDNA-4dmC [Figure D29]. A series of hydrogen bonding interactions stabilize the Fe center. The backbones of the coordinating histidines are stabilized via hydrogen bonding interactions with each other in a similar manner as 5mC and unnatural 5eC substrate (Table D1). Furthermore, the non-coordinating oxygen of the coordinating aspartate is stabilized via hydrogen bonding interactions with Asn1387, which are found in 13.6% and 12.9% of the trajectories of 4mC and 4dmC, respectively, in comparison to 23% obtained in 5mC complex. The observed solvent-mediated hydrogen bonding interaction of 74.7% between the two residues observed in 5mC<sup>1</sup> significantly reduces in 4mC (10%) and disappears in 4dmC. The loss of the solvent-mediated hydrogen bonding interaction in 4dmC could be due to a more hydrophobic environment in the active site, arising from the two methyl groups at the exocyclic amine (N4) position of the 4dmC substrate. The backbones of Ala1876 and Glu1879 form hydrogen bonding interactions with Fe-coordinating Asp1384 and His1881 residues, respectively, in both complexes like in TET2 bound to 5mC dsDNA

substrate (Table D1). The succinate's non-coordinating “C-4” carboxylate group is stabilized by both Arg1896 and Ser1898 in both complexes, in a similar manner as in natural substrate.

The proper orientation of the substrates in the Fe center is enhanced via stacking interaction with Tyr1902, which is stable in both complexes and appears to be more rigid in 4dmC complex, possibly due to the extra hydrophobic environment created by the two methyl groups in the exocyclic amine (N4) of the cytosine ring [Figure D5]. In the TET2-dsDNA-4dmC complex, the two methyl groups of exocyclic amine (N4) occupy distinct regions, with one close to the ferryl oxygen atom and the other directed away from it. [Figure D2] The efficiency of substrate oxidation is determined by the distance between oxo atom (O) and methylated substrate carbon (C) distance and the Fe-O-C angle.<sup>2,3</sup> Figures D2 and D3 show these plots as a function of time with average O-C distance that varies between 3.64 and 4.40 Å, while the average Fe-O-C angle ranges between 112.89 and 118.74° when compared to 3.66 Å and 143.32°, respectively, for the TET2-dsDNA complex bound to 5mC.<sup>1</sup>

## **D.2 HAT in 4mC and 4dmC**

### **D.2.1 Hydrogen Atom Abstraction**

The QM/MM calculations were done using five (5) well-equilibrated snapshots from the ferryl complex production dynamics. The calculated energy barrier at B3LYP/def2-TZVP (BS) + ZPE level of theory in 4mC substrate varies from 10.4 to 11.3 kcal/mol with Boltzmann weighted average of 10.8 kcal/mol, whereas in 4dmC substrate, the barrier range between 13.4 and 19.4 kcal/mol with Boltzmann weighted average of 14.0 kcal/mol.

The higher barrier observed in 4dmC than 4mC, consistent in all the snapshots [Tables D12 and D13], might be due to the more hydrophobic nature of the substrate arising from extra methyl group on the N4 amine of 4dmC. This leads to the loss of the important hydrogen bonding interaction of the N4 amine with Asn1387. Studies have suggested the role of Asn1387 in the recognition of N4 amine group of the substrate and its mutation to Ala has been reported to lead to loss of activity of the enzyme.<sup>4</sup> Comparison of the results of N-demethylation of 4mC and 4dmC substrates with the previously reported HAT energy barrier for C-demethylation of 5mC,<sup>1</sup> 5eC, 5vC, and 5eyC by TET2 reveals that the HAT in the N-demethylation of 4mC and 4dmC substrates is faster than in the C5 alkylations, possibly due to the electronegativity difference in C—N bond when compared to C—C bond. Subsequent calculations were performed using the snapshots that give the lowest HAT barriers in both substrates. Based on the angle and the spin density of the methylene carbon radical at the HAT transition state, the HAT uses  $\sigma$ -channel for the electron transfer. In the 4mC and 4dmC substrates HAT transition states, i.e., **TS<sub>H4m</sub>** and **TS<sub>H4dm</sub>**, respectively, the cleavage of the C—H bond of the methylated substrates to react with the oxo group of the Fe(IV)=O result in the polarization and elongation of the Fe—O from 1.62 Å in the **RC** to 1.71 and 1.71 Å in **TS<sub>H4m</sub>** and **TS<sub>H4dm</sub>**, respectively, to form the Fe(III)-oxyl radical. The C—H/O—H distances are 1.24/1.31 Å in 4mC while in 4dmC, the corresponding distances are 1.21/1.39 Å. In **TS<sub>H4m</sub>**, the Fe—O—H angle in all the snapshots varies between 141.08 and 167.97°, whereas in **TS<sub>H4dm</sub>**, the angle varies from 137.26 to 150.29° in all the snapshots. The angle in the 4dmC appears to be less linear than in 4mC, possibly due to substrate orientation changes arising from more steric effects in

the active site of TET2 bound to 4dmC dsDNA substrate than the one bound to 4mC dsDNA substrate. The calculations reveal that the hydrogen atom abstraction in both substrates occurs through  $\sigma$ -channel, where an  $\alpha$ -electron is shifted from the substrates'  $\sigma_{\text{CH}}$  to the antibonding  $\sigma^*_z$  orbital that is located along the Fe—O axis to give the radical carbon **IM1<sub>4m</sub>** and **IM1<sub>4dm</sub>** intermediates for 4mC and 4dmC, respectively. The consistency in the electron transfer mechanism in all the snapshots and in the two different substrates indicates that both conformational flexibilities and change in the nature of the substrates (4mC vs 4dmC) do not alter the nature of the electron transfer during the oxidation of the substrates. Even though the Fe—O—H angle at the transition states deviate from 180° typical of  $\sigma$ -channel mechanism owing to the constraints in the geometry as the dsDNA substrates cannot move freely in the TET2 protein environment but still proceed via  $\sigma$ -channel hydrogen atom abstraction, in agreement with previous studies on other N<sub>H</sub>Fe<sub>2</sub>OGD enzymes.

The transition states are stabilized by a couple of second coordination sphere residues. In 4mC TS, the Fe(IV)=O oxo group and the non-coordinating oxygen of Asp1384 are stabilized via hydrogen bonding interaction with the guanidinium group of Arg1261. A network of hydrophobic interaction of second sphere residues, Thr1393, Val1395, Ala1876 and Val1900 in the vicinity of the Fe center and the substrate enhance the stability of the TS. For example, the C2-methylene group of the succinate co-product is stabilized by both Val1900 and Val1395 and C3-methylene group of the co-product is also stabilized by Thr1393, Val1395 and Val1900. Furthermore, the methylene group of the Fe-coordinating

Asp1384 sidechain also form stable hydrophobic interactions with the methyl group sidechain of Ala1876. The heteroaromatic cytosine base ring of the 4mC substrate is stabilized by cation- $\pi$  stacking interaction with the guanidinium group of Arg1261, by hydrogen bonding interaction between the O2 of the cytosine ring and the NH group in the imidazole ring of His1386 and by hydrophobic interaction of Val1900 with methylated exocyclic N4 amine group of the substrate. The stability and orientation of the substrate is further enhanced by couple of stacking interactions between His1386, and His1904 imidazole groups and phenolic group of Tyr1902, which are all in the substrate binding region. However, in 4dmC TS, some interactions observed in 4mC are lost, possibly due to conformational changes arising from the pressure in the active site caused by the second methyl group in 4dmC. The Arg1261 forms hydrogen bonding interaction with the non-coordinating oxygen of the succinate. Similar to the observation in 4mC, both the C2 and C3-methylene groups of the succinate are stabilized via hydrophobic interactions with Val1900. The methylene groups of both Asn1387 and Fe ligation Asp1384 sidechains form hydrophobic interactions with each other, enhancing the stability of the Fe center. The cytosine ring of the substrates is also stabilized via stacking interactions with Tyr1902 and His1904, in a similar manner as in 4mC and thereby contribute to the proper orientation and stability of the dimethylated-amine substrate. In contrast to 5mC<sup>1</sup> and 5eC substrates that show the absence of hydrophobic interactions between C2 and C3 methylene groups of the succinate with the Thr1393, Val1395 and Val1900 as well as the interaction between the methylene group of Asp1384 sidechain and the methyl group of Ala1876. These observed new interactions in 4mC and 4dmC could be due to the reorganization of the



second coordination sphere residues arising from the change in methylation status from the endo C5 to exocyclic N4 group of the cytosine base in the substrate.

The TS stabilizing residues are similar to that of 5mC; however, there are minor differences, for example, the C2 and C3 methylene groups of the succinate are stabilized via hydrophobic interactions with Val1900 while both methylene groups of Asn1387 and Fe coordinating Asp1384 sidechains form hydrophobic interactions with each other, enhancing the stability of the Fe center. The computationally predicted roles of TS stabilizing residues are in agreement with the experimentally reported results on the effects of substitution of some of the residues involved in the stabilization transition states, depicting their importance in TET2 catalysis.<sup>4,7</sup> For example, mutation of Arg1261, Asn1387, Tyr1902, and His1904 have been shown to significantly reduce TET2 activity.<sup>4</sup> Tyr1902 substitution to Ala results in active site misfolding and also affect the binding of both substrate and DNA.<sup>4,6</sup> The role of hydrophobic residues Thr1393, Val1395 and Val1900 as gatekeeper residues and the effects of mutating each of them to Ala on the rate of conversion of 5mC to 5hmC by TET2 has been reported in the experimental mutagenesis studies.<sup>6</sup>

The hydrophobic interactions observed in the succinate binding region in both systems further aid in the succinate stability as previous studies on other DNA demethylases, AlkB and AlkBH2, have shown that succinate experience more flexibilities in binding after the decarboxylation of 2OG.<sup>8</sup> The long-range interactions of the TS stabilizing residues are similar to those of TET2 bound to 5mC dsDNA substrate. The residues involved in the

stabilization of **TS<sub>H4dm</sub>** show positive correlated motions with iron, the ferryl oxo atom, Fe-ligating succinate, loop containing iron coordinating HxD motif and Zn3 finger region and its ligating residues and such correlated motions are crucial in catalysis. However, in **TS<sub>H4m</sub>**, in addition to the above correlated motion, we observed that the residues involve in the stabilization of this transition state also have positive correlation with GS-linker, DNA-interacting loops (loop1 and loop2), DNA, DSBH core  $\beta$ 17 directly opposite the Fe center. The results imply that residues involved in **TS<sub>H4m</sub>** stabilization does not only enhance the stability of the Fe center via long-range interaction but also involve in the interaction and binding of the dsDNA to TET2 in TET2 bound to 4mC dsDNA complex as observed during the HAT transition state of the oxidation of 5mC to 5hmC.<sup>33</sup> Overall, the analyses depict that more second sphere residues and stronger correlated motions participate in the overall stabilization of **TS<sub>H4m</sub>** than in **TS<sub>H4dm</sub>** and are important during catalysis.

After the HAT, the Fe(III)—OH complexes with methylene substrate radical intermediates, **IM1<sub>4m</sub>**, and **IM1<sub>4dm</sub>**, are formed for 4mC and 4dmC, respectively, similar to other substrates of TET2. The Fe—O/O—H distances are 1.85/0.97 Å and 1.86/0.97 Å in **IM1<sub>4m</sub>** and **IM1<sub>4dm</sub>**, respectively. The formation of **IM1<sub>4m</sub>** and **IM1<sub>4dm</sub>** intermediates are exergonic with energies of -5.7 and -7.7 kcal/mol, respectively, at BS + ZPE level of theory. However, the intermediate formed during demethylation of 5mC dsDNA substrate by the same protein is almost thermoneutral with energy of -0.4 kcal/mol at the same level of theory, implying that the Fe(III)—OH intermediate form during N-demethylation by

TET2 is more energetically favorable and stable over the one formed during C-demethylation by the same protein.

### **D.2.2 Mechanism of Rebound Hydroxylation**

The radical intermediates, **IM1<sub>4m</sub>** and **IM1<sub>4dm</sub>** formed from the first step of substrates oxidation undergo OH rebound reaction where the OH groups of the Fe(III)—OH intermediates are transferred to the methylene carbon radical, resulting in the formation of hydroxylated products and the Fe centers are reduced from Fe(III) to Fe(II).

The rebounding of the hydroxyl group passes through **TS<sub>RB4m</sub>** and **TS<sub>RB4dm</sub>**, with the former having barrier of 5.0 kcal/mol and the latter – 2.5 kcal/mol from their respective intermediate. The result implies that the rebound reaction occurs rapidly in TET2 bound to 4dmC dsDNA substrate. Recent QM/MM studies<sup>1</sup> of 5mC dsDNA substrate oxidation by TET2 reported a rebound barrier of 10.1 kcal/mol from the radical substrate intermediate. This suggests that the process of OH rebound from the Fe(III)—OH to the methylene carbon radical substrate is faster in N-methylated 4mC and 4dmC dsDNA substrates than the counterpart C-methylated 5mC dsDNA substrate, implying that the radical intermediates formed during N-demethylation of 4mC and 4dmC substrates have a shorter lifetime than the one formed during C-demethylation of 5mC and thereby easily collapse to the hydroxylated products. The rebound hydroxylation in 4mC/4dmC is also faster than the corresponding reactions in 5vC and 5eyC but proceeds with nearly the same barrier as the rebound reaction in 5eC. The rebound process is faster in all systems than HAT, confirming the rate-determining nature of the latter substrate oxidation of all dsDNA substrates with 5eC, 5vC, 5eyC, 4mC and 4dmC.

The formed **IM2<sub>OH4m</sub>** and **IM2<sub>OH4dm</sub>** for 4mC and 4dmC, respectively, are highly exothermic with overall energies of -37.6 and -42.8 kcal/mol, at BS + ZPE level of theory. **IM2<sub>OH4dm</sub>** is more stable than **IM2<sub>OH4m</sub>** by 5.2 kcal/mol as the OH group of the **IM2<sub>OH4dm</sub>** is locked in a strong hydrogen bonding interaction with the negatively charged oxygen atom of the C4 carboxylate of the succinate, unlike in **IM2<sub>OH4m</sub>** where the OH group forms weaker hydrogen bonding interaction with the non-coordinating carbonyl oxygen of the Fe-ligating Asp1382. The optimized stationary points and the QM/MM potential energy profiles are presented in Figures D26-D28.

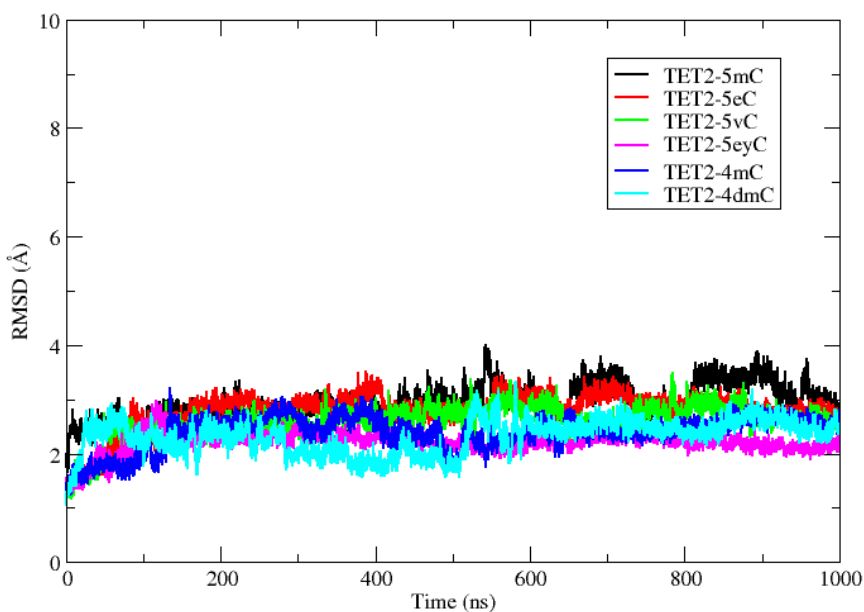


**Figure D1.** RMSD plots for TET2 bound to the five (5) dsDNA substrates.

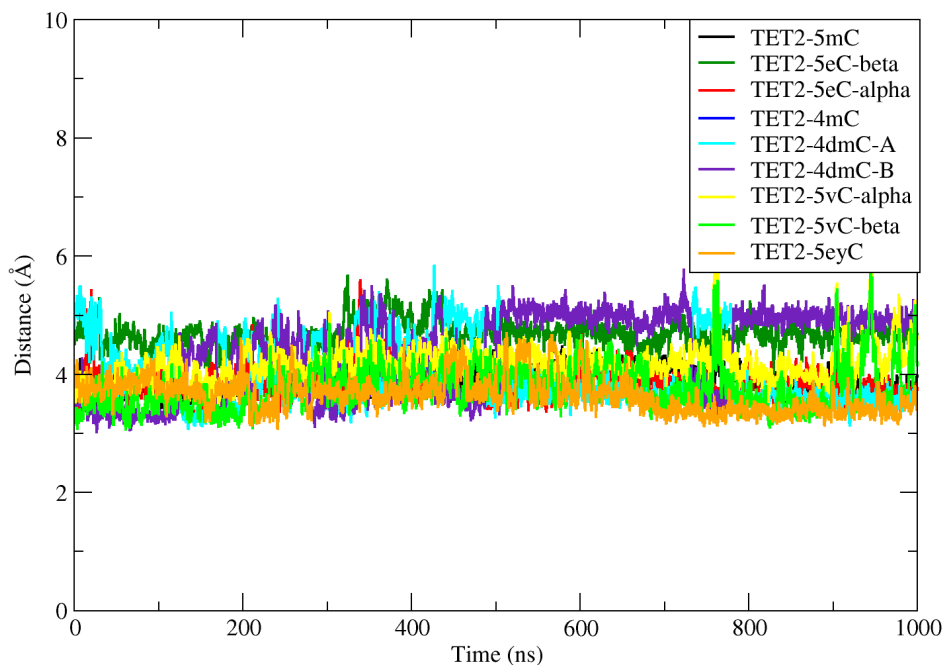


**Figure D2.** Plot of the distance between the oxygen atom (O) of the Fe(IV)=O and the carbon of the substituents of the substrates.

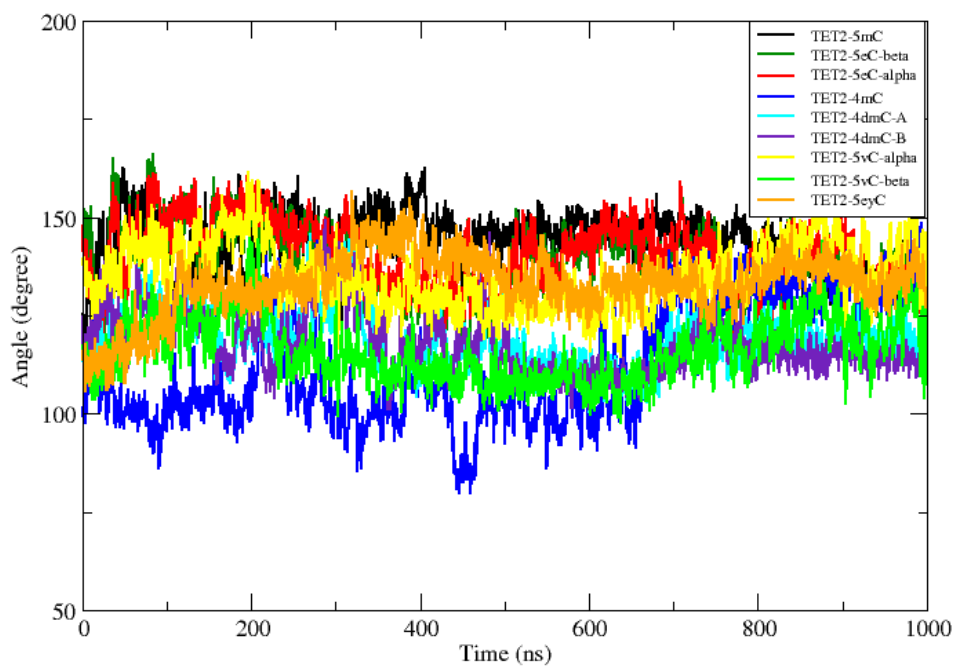


**Figure D3.** Plot of the angle between the Fe, oxygen atom (O) of the Fe(IV)=O and the carbon of the substituents of the substrates.

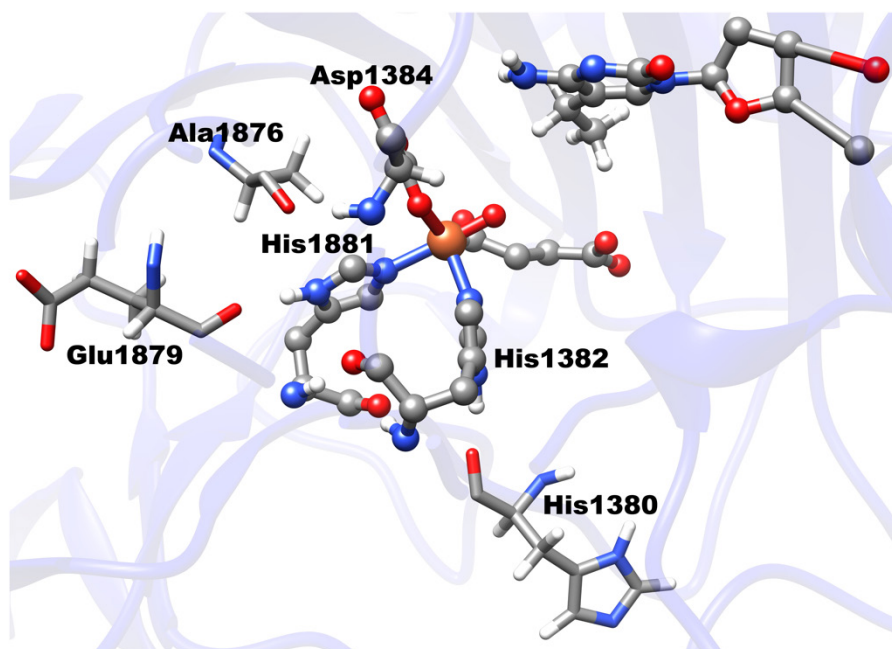


**Figure D4.** The network of hydrogen bonding interactions that stabilize the Fe center during the MD Simulation of TET2 bound to 5eC dsDNA substrates.

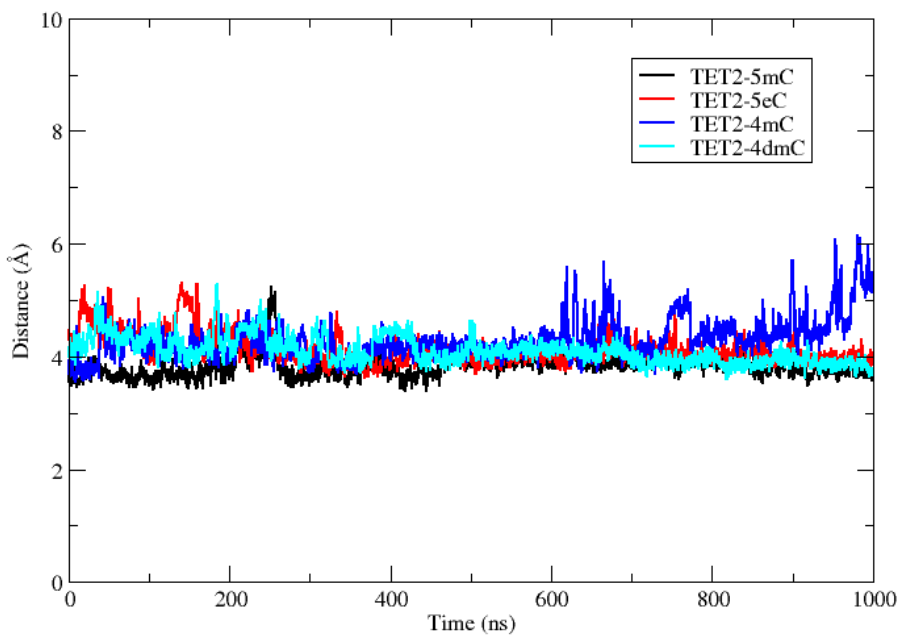


**Figure D5.** Stacking interaction of the Tyr1902 with the cytosine rings of the 5eC, 4mC and 4dmC dsDNA substrates in comparison to the 5mC substrate. Distances were measured between the center of mass of the Phenyl ring of Tyr1902 and the cytosine base.

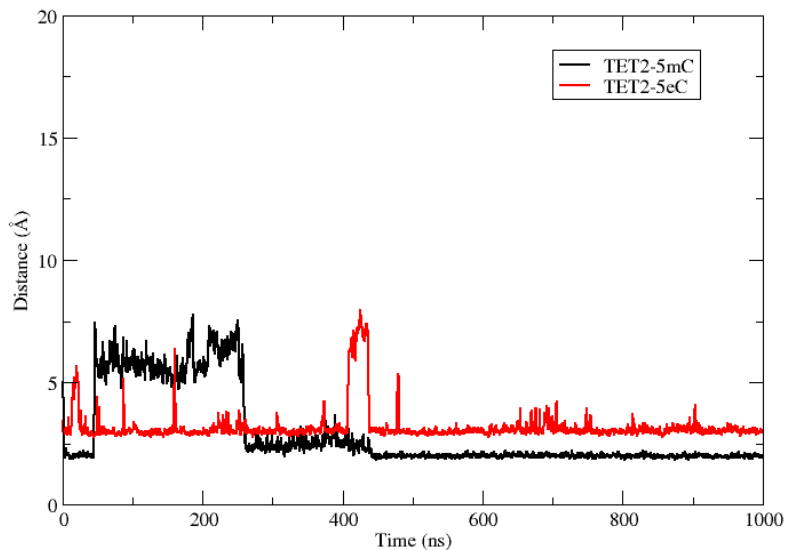


**Figure D6.** Hydrogen bonding interaction of Asn1387 sidechain with the exocyclic amine (N4) of the 5eC substrate in comparison to 5mC substrate. The distances were measured between the center of mass of atoms forming the carboxylate of the residue and the bases of the substrates.

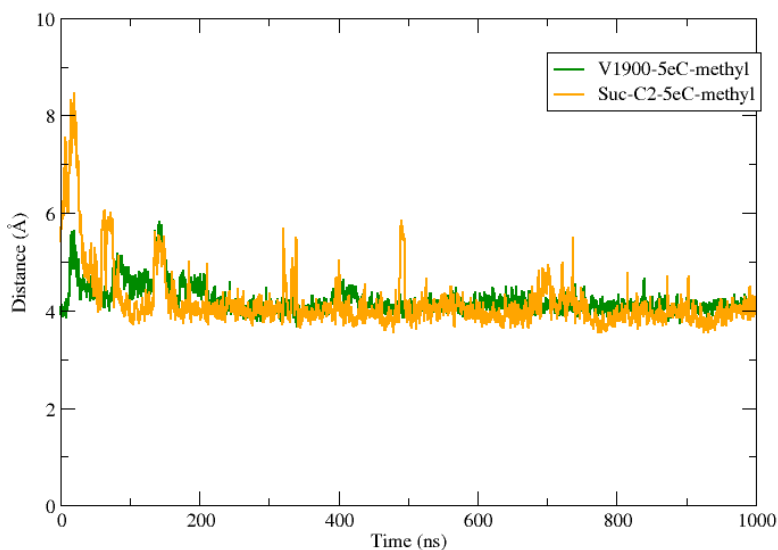


**Figure D7.** Hydrophobic interactions between the methyl component of the 5eC dsDNA substrate with the methylene group (C2) of the succinate and the isopropyl side chain of Val1900.

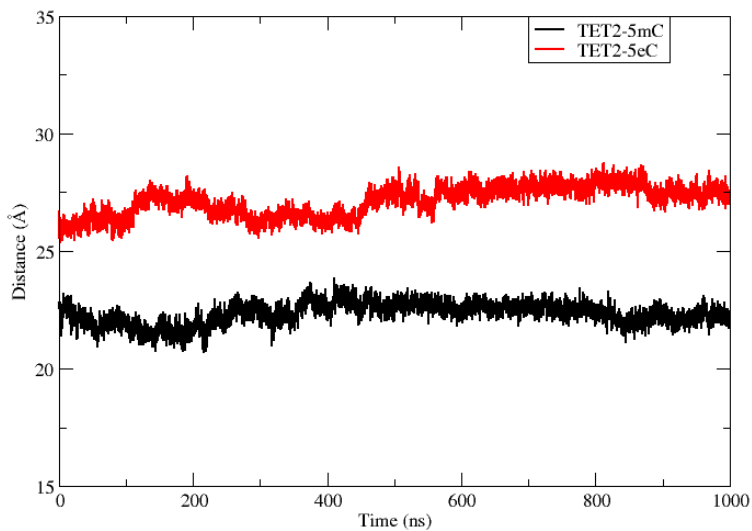


**Figure D8.** Measured distances between the center of mass of the protein and the dsDNA molecule in TET2 bound to 5eC and 5mC substrates.

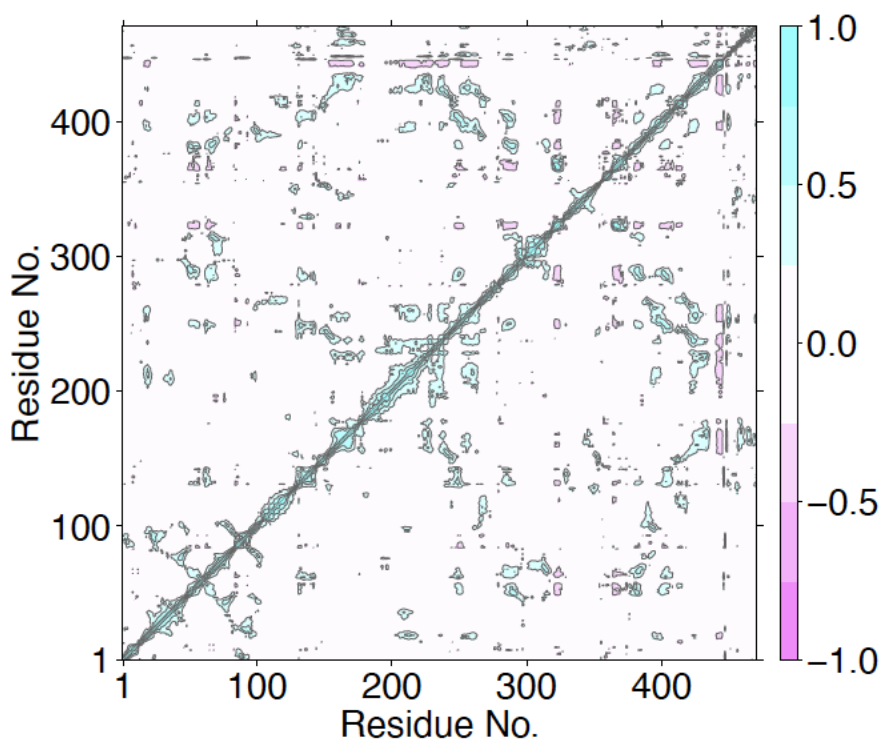


**Figure D9.** Dynamics cross-correlation for the TET2 bound to 4dmC dsDNA substrate. Residue numbers 1-445 (protein), 446-448 (Zn), 449 (Fe), 450 (O), 451 (succinate), 452-475 (DNA).



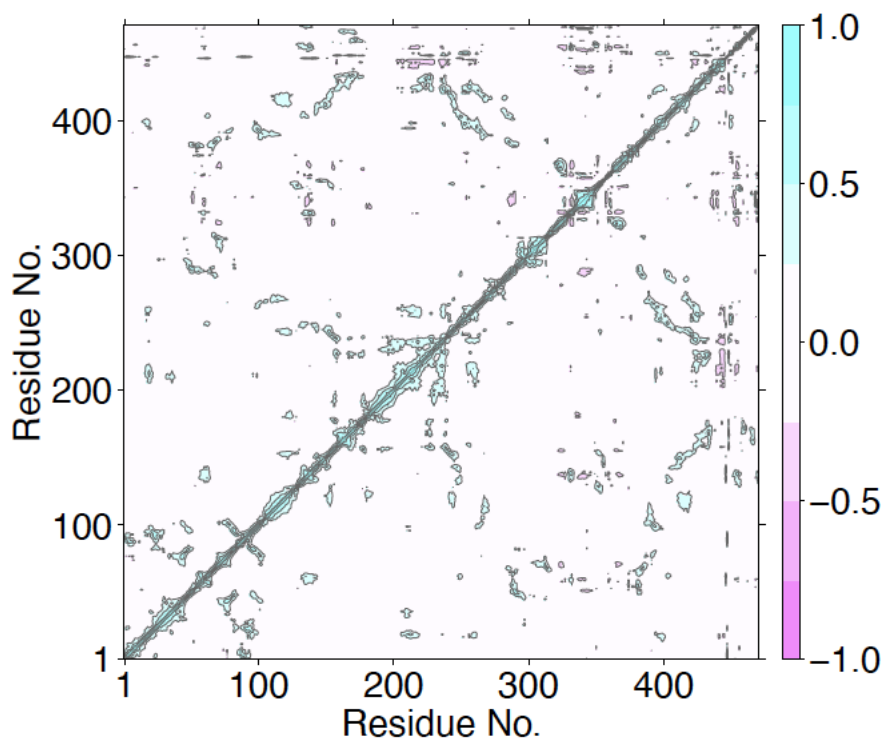


**Figure D10.** Dynamics cross-correlation for the TET2 bound to 4mC dsDNA substrate. Residue numbers 1-445 (protein), 446-448 (Zn), 449 (Fe), 450 (O), 451 (succinate), 452-475 (DNA).

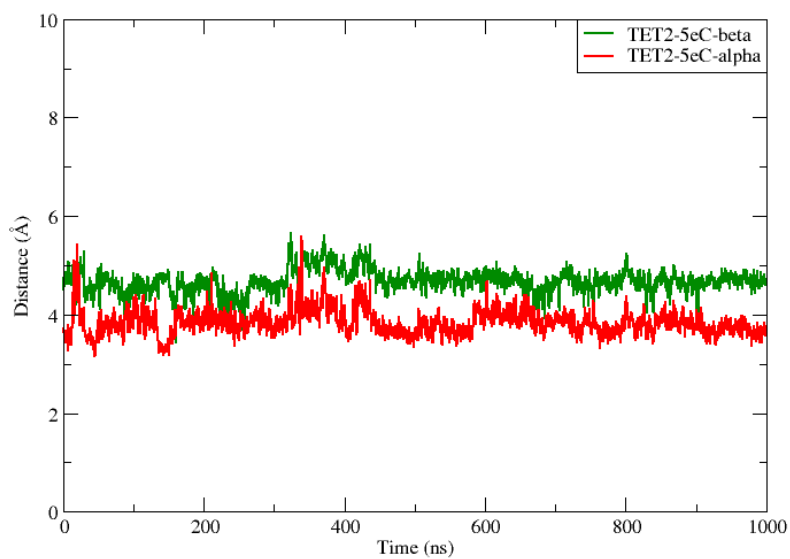


**Figure D11.** Distances plot between Fe(IV)=O oxo atom and the carbons ( $C\alpha$  and  $C\beta$ ) substituent of the 5c substrate during the MD simulation.

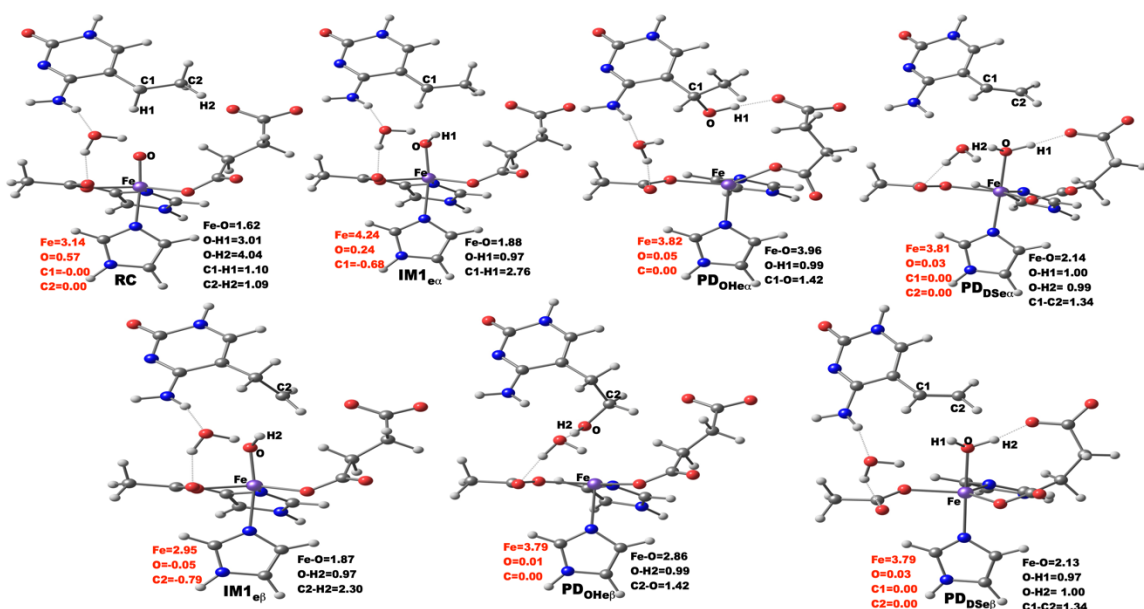


**Figure D12.** The stationary point geometries during the hydroxylation and desaturation reactions of 5eC dsDNA substrate by TET2. Distances (Å) and the spin densities are in black and red, respectively.

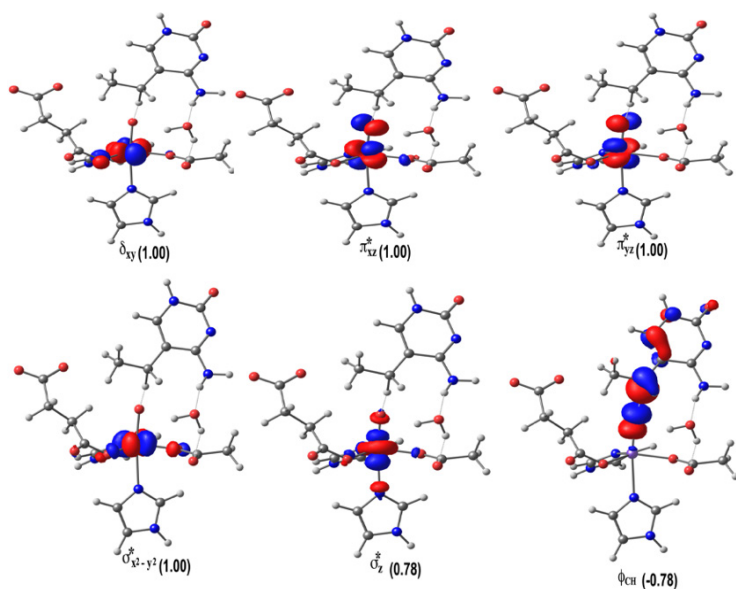


**Figure D13.** Spin natural orbitals (SNOs) for the HAT from C<sub>α</sub> of 5eC substrate with their respective population in parentheses, calculated from the TS<sub>H1eα</sub> structure.

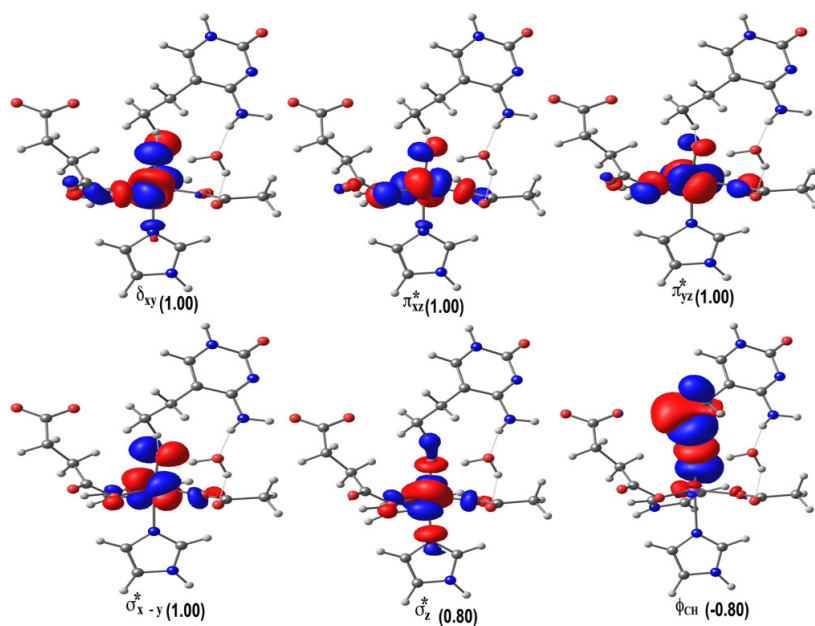


**Figure D14.** Spin natural orbitals (SNOs) with their respective populations (in parentheses) for the hydrogen atom abstraction from C $\beta$  transition state in TET2 bound to 5eC dsDNA.

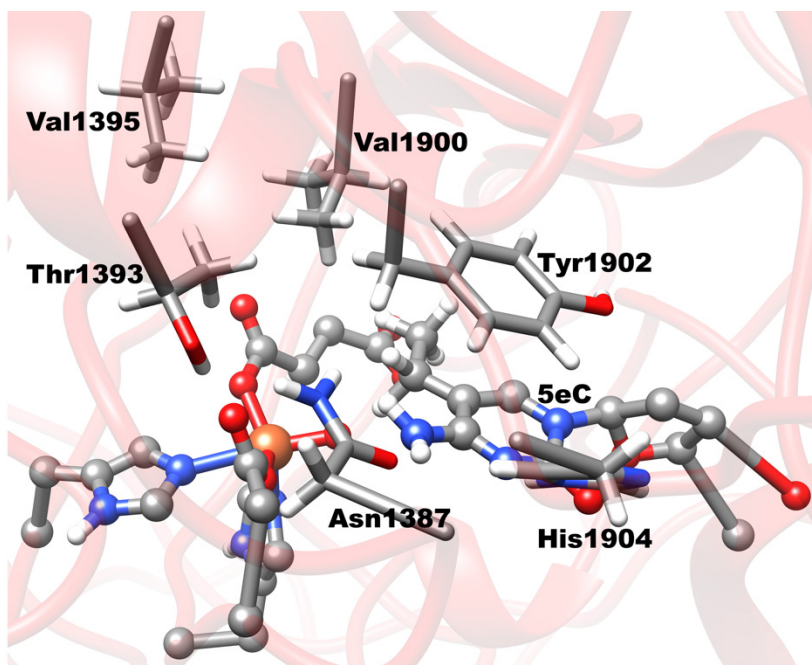


**Figure D15.** The residues that stabilize the TS<sub>H1e $\alpha$</sub>  during the HAT from C $\alpha$  of 5eC substrate.

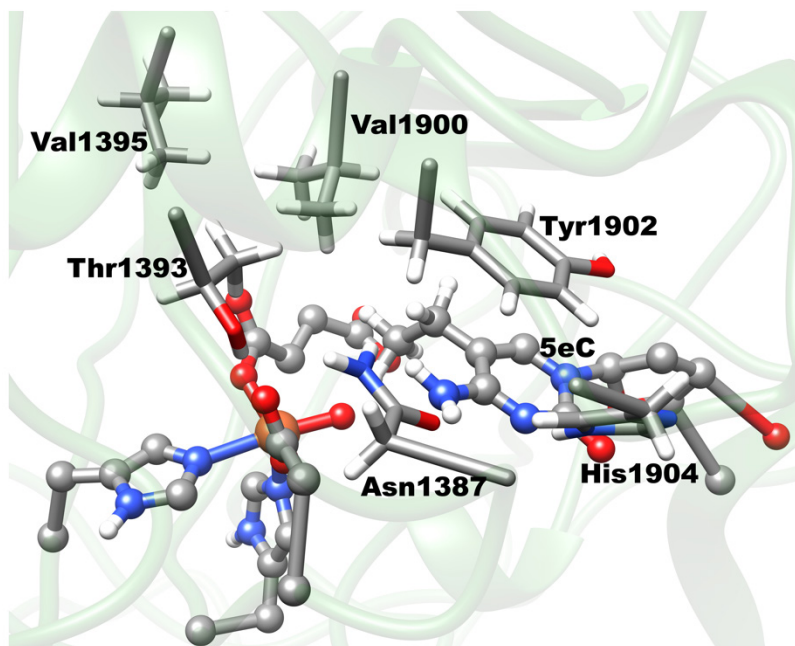


**Figure D16.** The residues that stabilize the  $TS_{H1\epsilon\beta}$  during the HAT from  $C_{\beta}$  of 5eC substrate.

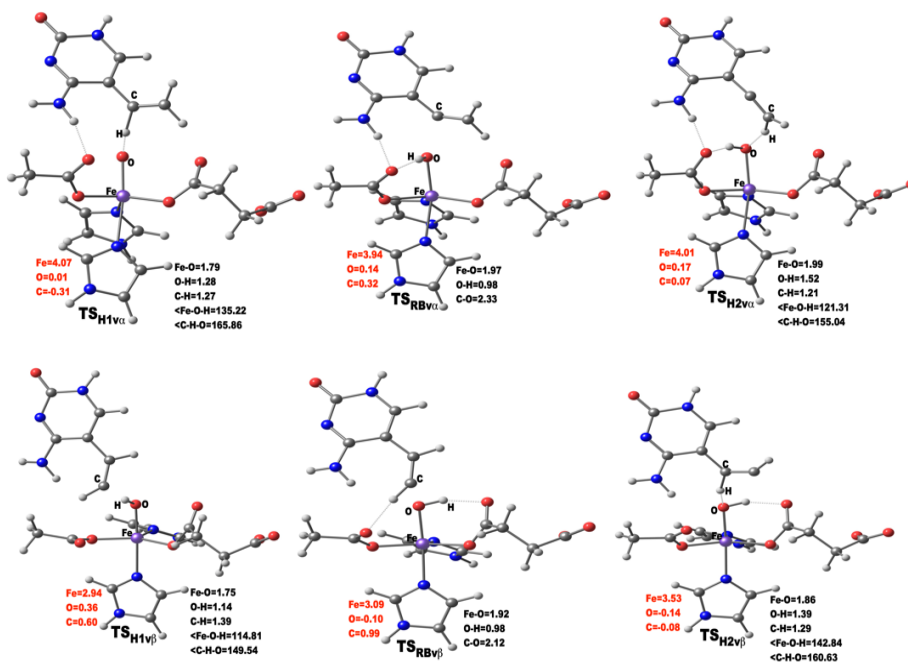


**Figure D17.** The transition states structures obtained during hydroxylation and desaturation processes of 5vC dsDNA by TET2. Distances (Å) and the spin densities are in black and red, respectively, while the Fe—O—H and C—H—O angles are in degrees.

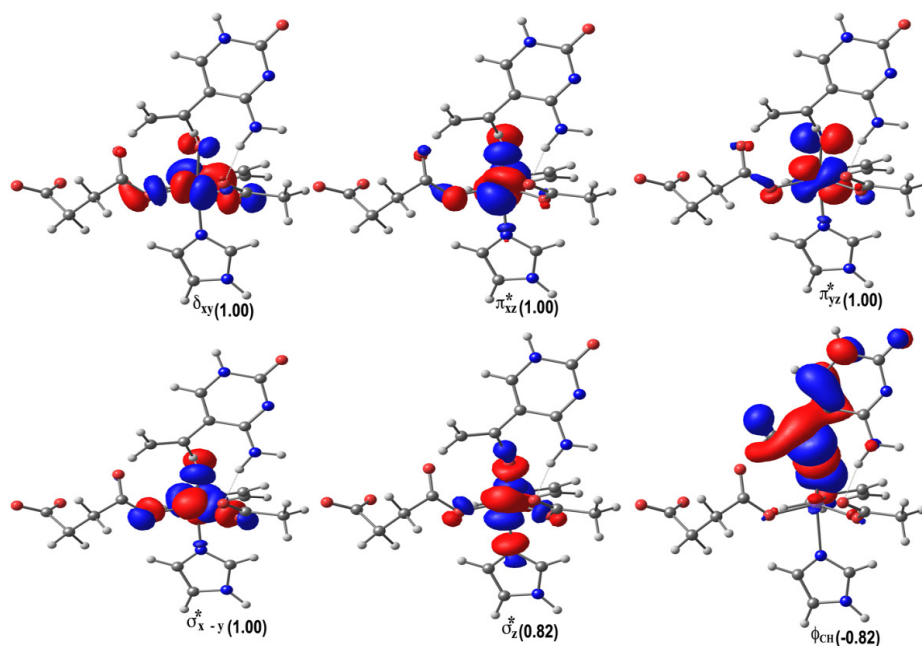


**Figure D18.** Spin natural orbitals (SNOs) with their respective populations (in parentheses) for the hydrogen atom abstraction from C $\alpha$  transition state in TET2 bound to 5vC dsDNA.

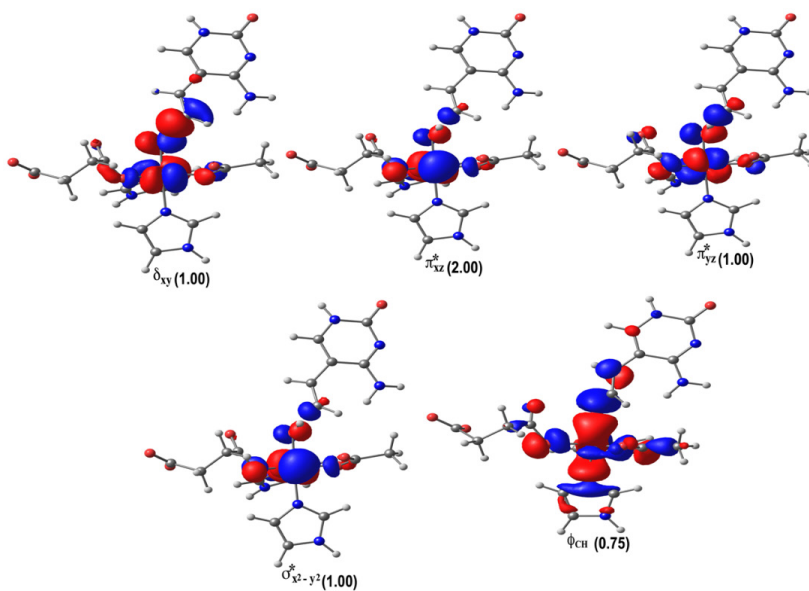


**Figure D19.** Spin natural orbitals (SNOs) with their respective populations (in parentheses) for the hydrogen atom abstraction from C $\beta$  transition state in TET2 bound to 5vC dsDNA.

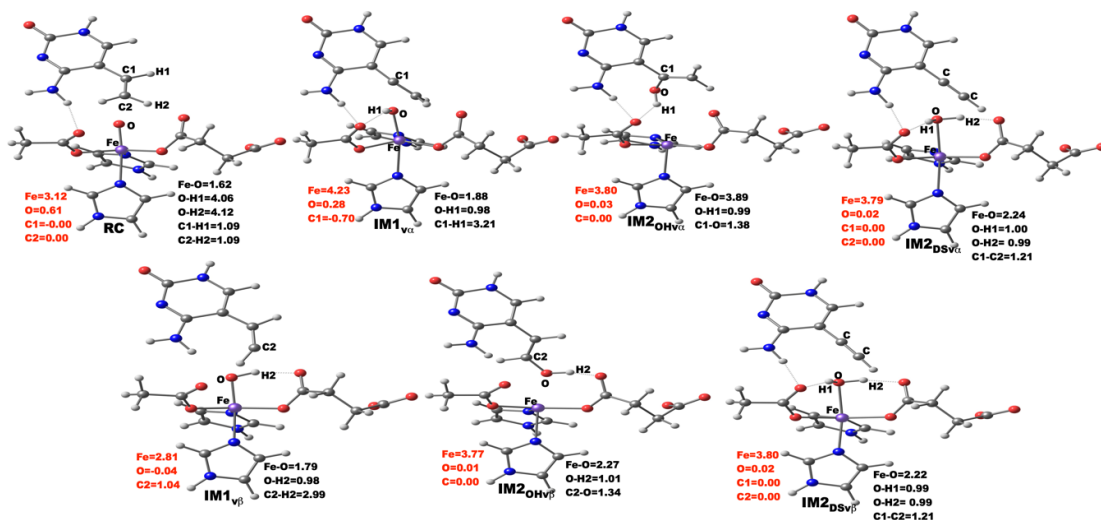


**Figure D20.** The stationary point geometries during the hydroxylation and desaturation reactions of 5vC dsDNA substrate by TET2. Distances (Å) and the spin densities are in black and red, respectively.

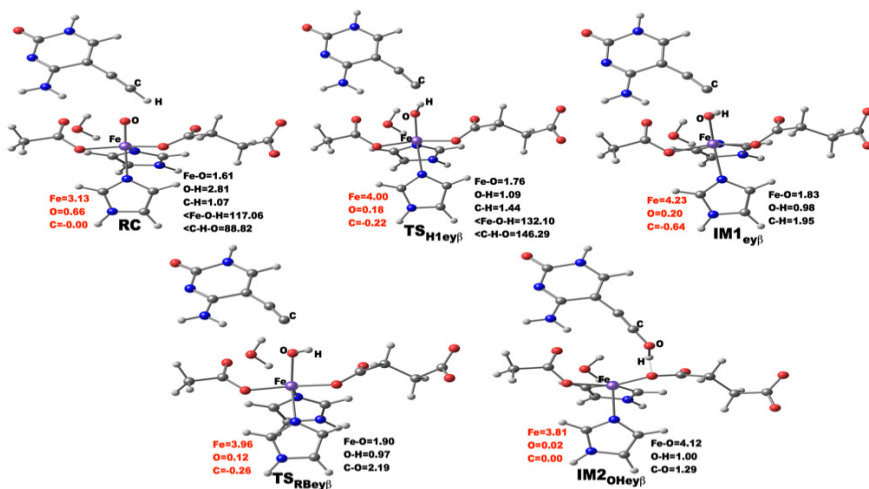


**Figure D21.** Stationary points geometries obtained during hydroxylation of 5eyC dsDNA by TET2. Distances (Å) and the spin densities are in black and red, respectively.

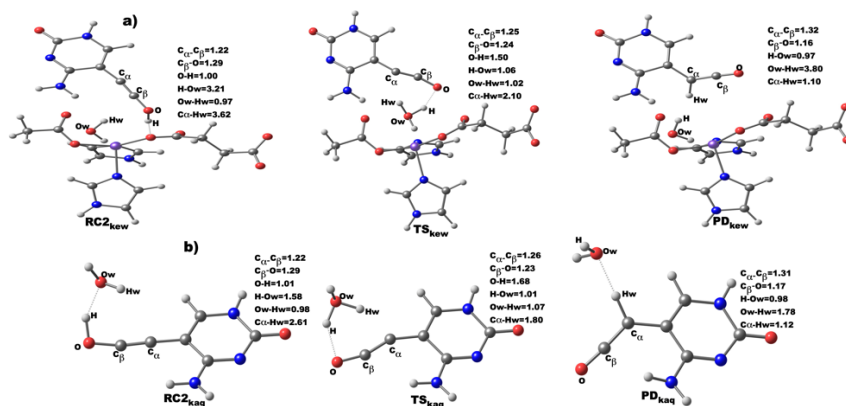


**Figure D22.** Stationary points geometries obtained along the formation of the ketene inside (a) and outside (b) the enzyme with the assistance of water molecules. Distances are in Å.

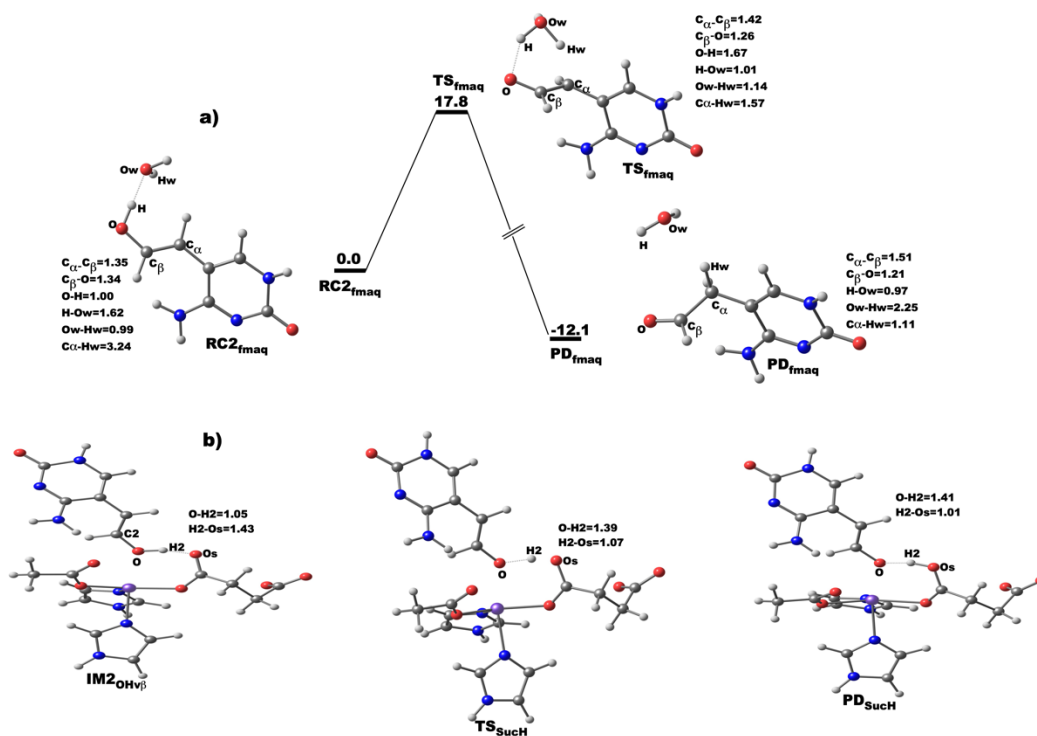


**Figure D23.** Stationary point geometries and potential energy profile for the formation of 5fC in aqueous solution outside of the enzyme (a) and via succinate (b). The distances are in Å.

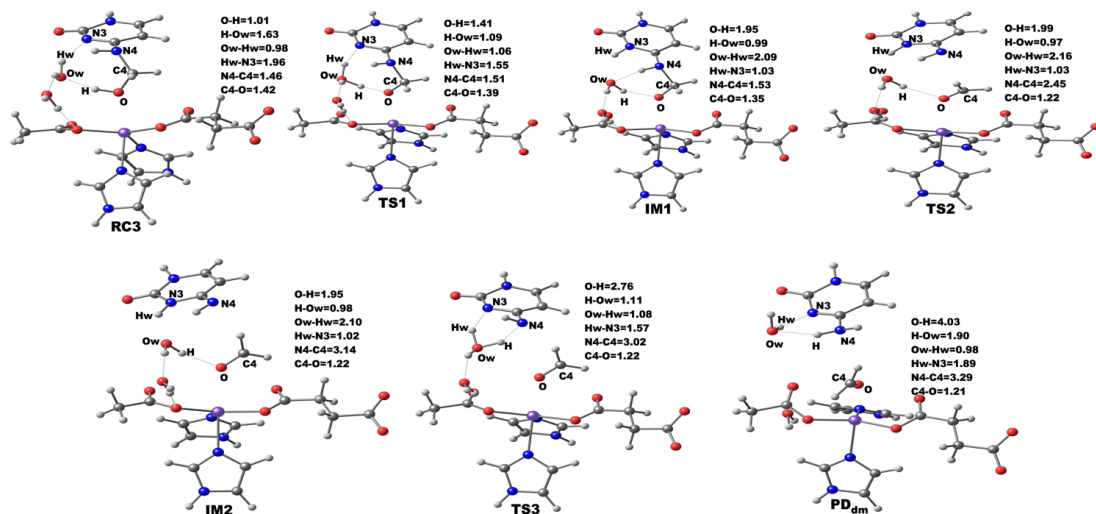


**Figure D24.** The stationary point geometries for the decomposition of hemiaminal intermediate of 4mC hydroxylation inside the enzyme. The distances are in Å.

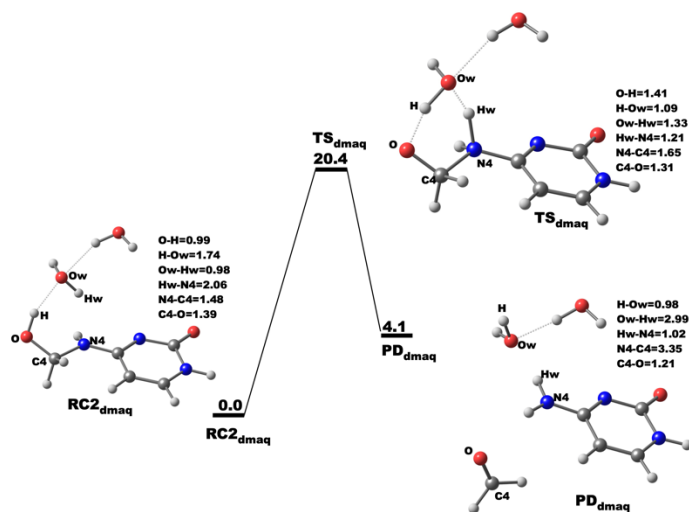


**Figure D25.** Stationary point geometries and potential energy profile for the decomposition of hemiaminal intermediate of 4mC in aqueous solution outside of the enzyme. The distances are in Å.



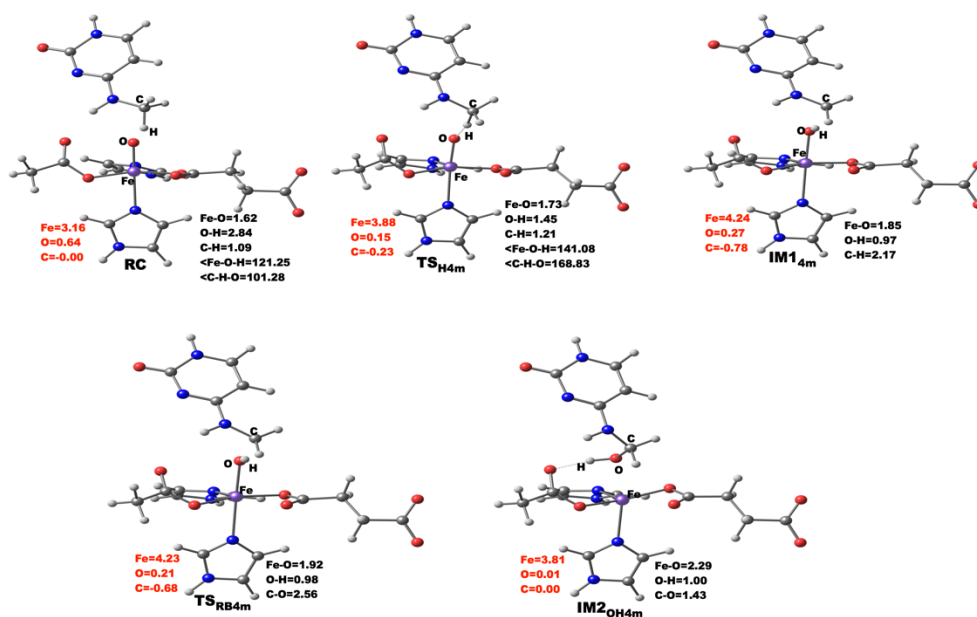


**Figure D26.** The stationary point geometries of the hydrogen atom abstraction and rebound hydroxylation steps of TET2 bound to 4mC dsDNA complex. Distances (Å) and the spin densities are in black and red, respectively.

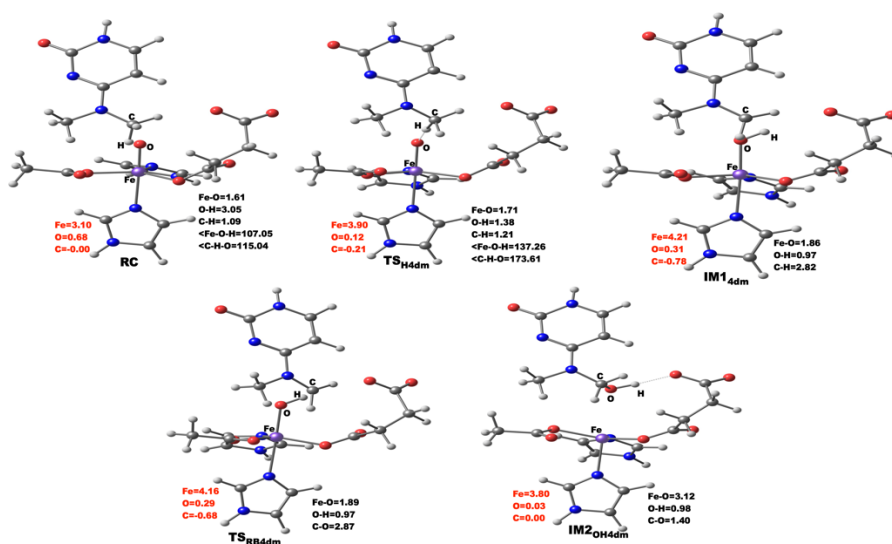


**Figure D27.** Stationary points geometries obtained during hydroxylation of 4dmC dsDNA by TET2. Distances (Å) and the spin densities are in black and red, respectively.

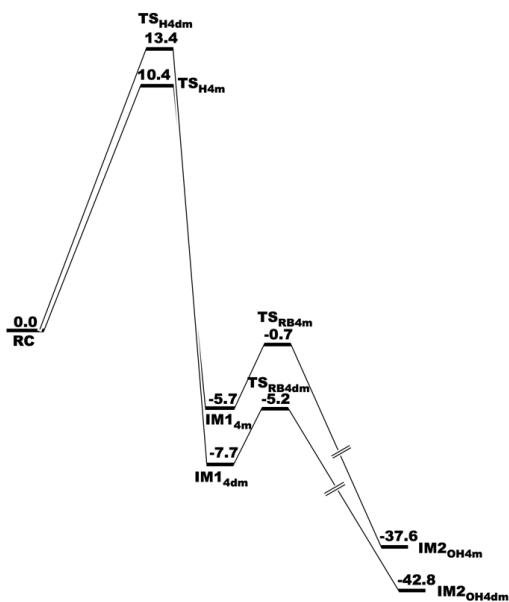


**Figure D28.** QM/MM potential energy profile for the hydroxylation of 4mC and 4dmC dsDNA substrates by TET2, calculated using UB3LYP/def2-TZVP with ZPE. The relative energies are in kcal/mol.

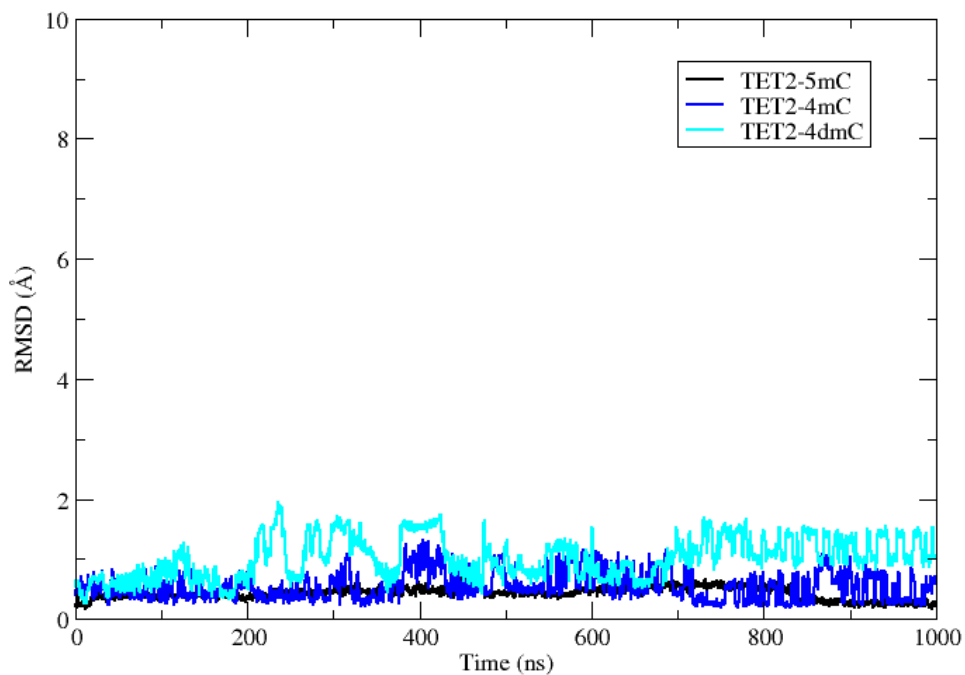


**Figure D29.** RMSD plots for the active site of TET2 bound to 4mC and 4dmC substrates in comparison to 5mC dsDNA substrate.

**Table D1.** Average RMSD, O-C $\alpha\beta$  distances, and Fe-O-C $\alpha\beta$  angles, and hydrogen bonding interactions percentages between Ala1876 and Asp1384, Glu1879 and His1881, His1380 and His1382, and the Fe coordinating histidines (His1382 and His1881) for the TET2 bound to 5eC, 4mC and 4dmC dsDNA substrates.

	Average RMSD (Å)	Average O-C $\alpha\beta$ distance (Å)	Average Fe-O-C $\alpha\beta$ Angle (deg)	Ala1876 – Asp1384 (%)	Glu1879 – His1881 (%)	His1380-His1382 (%)	His1382-His1881 (%)
5eC	2.78	3.84/4.67	140.48/139.34	76.1	61.2	63.2	67.4
4mC	2.38	3.64	112.89	90.8	70.8	16.4	70.6
4dmC	2.31	3.99/4.40	118.74/117.89	73.1	60.1	51.2	76.4

**Table D2.** Selected distances and angles for the different snapshots RC and TS for HAT step in the TET2 bound to 5eC dsDNA substrate, calculated at B3LYP/def2-TZVP. The data in black and red are for HAT from C $\alpha$  and C $\beta$ , respectively.

	d(Fe–O) (Å)	d(O–H) (Å)	d(C–H) (Å)	<(Fe–O–H) (deg)	Barrier with ZPE (kcal/mol)	C <sub>substrate</sub> spin density in TS
<b>Snapshot 1</b>						
RC	1.622	3.012/4.041	1.103/1.099	132.99/100.89	15.8/17.4	-0.306/0.601
TS	1.758/1.778	1.437/1.340	1.241/1.242	152.53/143.06		
<b>Snapshot 2</b>						
RC	1.616	3.533/4.187	1.102/1.102	154.22/167.49	21.9/23.4	-0.332/0.602
TS	1.767/1.738	1.360/1.234	1.271/1.310	161.40/169.79		
<b>Snapshot 3</b>						
RC	1.621	2.686/3.866	1.102/1.102	164.07/142.56	23.3/25.7	-0.247/0.598
TS	1.765/1.736	1.298/1.255	1.316/1.288	169.91/161.68		
<b>Snapshot 4</b>						
RC	1.623	2.723/3.561	1.112/1.099	146.85/165.41	19.2/22.5	-0.373/0.646
TS	1.755/1.766	1.309/1.226	1.299/1.320	161.97/158.48		
<b>Snapshot 5</b>						
RC	1.626	2.839/4.358	1.114/1.100	139.76/144.39	18.8/21.9	-0.311/0.557
TS	1.752/1.801	1.403/1.306	1.257/1.282	151.75/137.96		

**Table D3.** HAT step transition states and intermediates energies from C $\alpha$  carbon of TET2 bound to 5eC dsDNA substrate, calculated at B3LYP/def2-TZVP with ZPE contribution in kcal/mol

Reaction State	QM-only model	QM/MM <sup>a</sup>	QM/MM <sup>b</sup>	QM/MM <sup>c</sup>
TS <sub>H1e<math>\alpha</math></sub>	23.2	14.3	16.7	18.8
IM1 <sub>e<math>\alpha</math></sub>	5.9	-3.1	-2.52	3.2

<sup>a</sup>QM/MM performed with small QM size of 56 atoms, containing side chain of Asp1384, imidazole groups His1382 and His1881, Fe, oxo-atom, 5-ethylcytosine part of 5eC and succinate (excluding its C4 carboxylate group) in the QM region.

<sup>b</sup>QM/MM performed with large QM size of 83 atoms, containing side chains of Asp1384 and Asn1387, imidazole groups His1382 and His1881, Fe, oxo-atom, one water molecule, 5-ethylcytosine part of 5eC and succinate in the QM region.

<sup>c</sup>QM/MM performed in solution.

**Table D4.** Reaction State energies for the oxidation of 5eC dsDNA substrate by TET2 at quintet (M=5) and septet (M=7) ground states, calculated at B3LYP/def2-TZVP (BS) level of theory in kcal/mol.

Reaction State	BS+ZPE (M=5)	BS+D3+ZPE (M=5)	BS+ZPE (M=7)
TSH1e $\alpha$	15.76	14.30	18.11
TSH1e $\beta$	17.36	18.39	20.53
IM1e $\alpha$	-2.8	-5.05	-1.59
TSRBe $\alpha$	2.4	2.77	5.30
TSH2e $\alpha$	4.7	5.29	9.33
IM1e $\beta$	4.83	5.58	7.32
TSRBe $\beta$	9.3	8.74	15.04
TSH2e $\beta$	23.7	21.24	27.59
PD0He $\alpha$	-47.0	-46.27	-43.19
PD0Se $\alpha$	-44.3	-42.06	-31.33
PD0He $\beta$	-31.6	-34.88	-29.72
PD0Se $\beta$	-41.7	-43.41	-23.18

**Table D5.** Reaction State energies for the HAT from C $\alpha$  carbon of 5vC dsDNA substrate by TET2 at quintet (M=5) and septet (M=7) ground states, calculated at B3LYP/def2-TZVP (BS) level of theory in kcal/mol.

Reaction State	BS+ZPE (M=5)	BS+D3+ZPE (M=5)	BS+ZPE (M=7)
TSH1v $\alpha$	18.89	16.20	22.12
IM1v $\alpha$	3.4	4.09	4.90

**Table D6.** Reaction State energies for the HAT of 5eyC dsDNA substrate by TET2 at quintet (M=5) and septet (M=7) ground states, calculated at B3LYP/def2-TZVP (BS) level of theory in kcal/mol.

Reaction State	BS+ZPE (M=5)	BS+D3+ZPE (M=5)	BS+ZPE (M=7)
TSH1ey $\beta$	22.06	24.59	26.16
IM1ey $\beta$	7.9	11.44	12.75

**Table D7.** Reaction State energies for the HAT of 4mC dsDNA substrate by TET2 at quintet (M=5) and septet (M=7) ground states, calculated at B3LYP/def2-TZVP (BS) level of theory in kcal/mol.

Reaction State	BS+ZPE (M=5)	BS+D3+ZPE (M=5)	BS+ZPE (M=7)
TS <sub>H4m</sub>	10.4	9.45	16.87
IM1 <sub>4m</sub>	-5.72	-5.94	-3.24

**Table D8.** Energy Decomposition Analysis (EDA) of the residues that stabilizes the transition states and the products. All values are in kcal/mol.

Residue	TS <sub>H1</sub>	TS <sub>H1e</sub>	TS <sub>RBe</sub>	TS <sub>RBe</sub>	TS <sub>H2e</sub>	TS <sub>H2e</sub>	PD <sub>OHe</sub>	PD <sub>OHe</sub>	PD <sub>DSe</sub>	PD <sub>DSe</sub>
	$\alpha$	$\beta$	$\alpha$	$\beta$	$\alpha$	$\beta$	$\alpha$	$\beta$	$\alpha$	$\beta$
R1261				5.19			-4.79	-0.91	10.05	8.59
C1263	-0.65		-0.87		-0.75	-0.53				
R1269	-0.50						-1.34	-0.83		
K1299			-0.76		-0.98	-0.82	-2.69	-1.02		
K1310							-1.28			
R1359									-1.32	-0.76
V1371									-0.98	-0.95
T1372		-0.68								
D1376							-1.64	-1.10		
H1380	-0.62	-0.53	-0.73		-0.70	-0.54				
T1393		-0.57			-0.72	-0.67			-1.02	-1.09
K1826							-2.26	-0.82		
E1874	-1.46	-0.79	-2.20	1.00	-2.21	-1.58	-5.82	-3.69		
E1879			-0.84		-1.02	-0.73	-1.69	-1.94		
K1905							-1.39			

**Table D9.** Selected distances and angles for the different snapshots RC and TS for HAT step in the TET2 bound to 5vC dsDNA substrate, calculated at B3LYP/def2-TZVP. The data in black and red are for HAT from C $\alpha$  and C $\beta$ , respectively.

	d(Fe–O) (Å)	d(O–H) (Å)	d(C–H) (Å)	<(Fe–O–H) (deg)	Barrier with ZPE (kcal/mol)	C <sub>substrate</sub> spin density in TS
<b>Snapshot 1</b>						
RC	1.619	4.062/4.126	1.097/1.093	132.99/100.89	18.9/22.5	-0.306/0.601
TS	1.788/1.753	1.277/1.147	1.272/1.391	135.22/114.81		
<b>Snapshot 2</b>						
RC	1.622	4.381/3.991	1.095/1.093	139.07/108.23	21.1/26.1	-0.332/0.602
TS	1.781/1.727	1.253/1.190	1.274/1.357	140.24/116.19		
<b>Snapshot 3</b>						
RC	1.615	2.987/3.486	1.099/1.090	148.70/107.79	19.5/23.2	-0.247/0.598
TS	1.736/1.732	1.358/1.181	1.229/1.343	137.39/114.52		
<b>Snapshot 4</b>						
RC	1.619	4.716/3.590	1.092/1.092	140.39/111.01	24.4/26.9	-0.373/0.646
TS	1.767/1.778	1.233/1.095	1.317/1.459	150.88/116.06		
<b>Snapshot 5</b>						
RC	1.624	4.352/3.245	1.095/1.094	150.43/118.60	19.2/23.7	-0.311/0.557

TS	1.786/1.753	1.262/1.168	1.273/1.354	145.74/120.65		
----	-------------	-------------	-------------	---------------	--	--

**Table D10.** Selected distances and angles for the different snapshots RC and TS for HAT step in the TET2 bound to 5eyC dsDNA substrate, calculated at B3LYP/def2-TZVP.

	d(Fe–O) (Å)	d(O–H) (Å)	d(C–H) (Å)	<(Fe–O–H) (deg)	Barrier with ZPE (kcal/mol)	C <sub>substrate</sub> spin density in TS
<b>Snapshot 1</b>						
RC	1.614	2.815	1.075	117.06	22.1	-0.131
TS	1.757	1.096	1.444	132.10		
<b>Snapshot 2</b>						
RC	1.615	2.706	1.075	150.44	26.5	-0.214
TS	1.756	1.091	1.498	138.79		
<b>Snapshot 3</b>						
RC	1.611	3.174	1.075	130.49	24.6	-0.137
TS	1.775	1.148	1.348	127.16		
<b>Snapshot 4</b>						
RC	1.609	3.195	1.073	118.52	22.2	-0.135
TS	1.752	1.132	1.354	128.02		
<b>Snapshot 5</b>						
RC	1.610	2.982	1.074	117.57	26.7	-0.117
TS	1.770	1.152	1.342	131.82		

**Table D11.** Imaginary frequencies obtained for the transition states in cm<sup>-1</sup>.

Transition States	Imaginary Frequency (cm <sup>-1</sup> )
TS <sub>H1eα</sub>	i1171.41
TS <sub>H1eβ</sub>	i1026.61
TS <sub>H2eα</sub>	i576.34
TS <sub>H2eβ</sub>	i435.11
TS <sub>RBeα</sub>	i253.60
TS <sub>RBeβ</sub>	i255.44
TS <sub>H1vα</sub>	i970.94
TS <sub>H1vβ</sub>	i891.61
TS <sub>RBvα</sub>	i187.08
TS <sub>RBvβ</sub>	i117.22
TS <sub>H2vα</sub>	i509.25
TS <sub>H2vβ</sub>	i389.28
TS <sub>H1evβ</sub>	i976.91
TS <sub>RBevβ</sub>	i267.28
TS <sub>H4m</sub>	i1005.65
TS <sub>H4dm</sub>	i988.14
TS <sub>RB4m</sub>	i212.05
TS <sub>RB4dm</sub>	i197.23

**Table D12.** Selected distances and angles for the different snapshots RC and TS for HAT step in the TET2 bound to 4mC dsDNA substrate, calculated at B3LYP/def2-TZVP.

	d(Fe–O) (Å)	d(O–H) (Å)	d(C–H) (Å)	<(Fe–O–H) (deg)	Barrier with ZPE (kcal/mol)	C <sub>substrate</sub> spin density in TS
<b>Snapshot 1</b>						
RC	1.622	2.837	1.094	121.24	11.2	-0.249
TS	1.715	1.457	1.212	141.08		
<b>Snapshot 2</b>						
RC	1.618	2.514	1.102	143.92	10.4	-0.224
TS	1.724	1.359	1.224	144.37		
<b>Snapshot 3</b>						
RC	1.617	2.464	1.102	139.39	11.2	-0.230
TS	1.725	1.351	1.226	142.03		
<b>Snapshot 4</b>						
RC	1.616	2.442	1.099	158.23	10.9	-0.306
TS	1.711	1.255	1.282	167.97		
<b>Snapshot 5</b>						
RC	1.608	2.591	1.099	131.89	10.6	-0.259
TS	1.707	1.309	1.239	143.13		

**Table D13.** Selected distances and angles for the different snapshots RC and TS for HAT step in the TET2 bound to 4dmC dsDNA substrate, calculated at B3LYP/def2-TZVP.

	d(Fe–O) (Å)	d(O–H) (Å)	d(C–H) (Å)	<(Fe–O–H) (deg)	Barrier with ZPE (kcal/mol)	C <sub>substrate</sub> spin density in TS
<b>Snapshot 1</b>						
RC	1.615	3.050	1.099	107.08	13.4	-0.204
TS	1.714	1.388	1.209	137.26		
<b>Snapshot 2</b>						
RC	1.617	3.114	1.100	121.43	14.7	-0.219
TS	1.723	1.406	1.225	150.29		
<b>Snapshot 3</b>						
RC	1.616	3.173	1.099	105.09	19.4	-0.321
TS	1.732	1.272	1.308	148.27		
<b>Snapshot 4</b>						
RC	1.615	3.058	1.100	119.07	14.6	-0.259
TS	1.719	1.332	1.244	150.18		
<b>Snapshot 5</b>						
RC	1.621	3.099	1.100	119.21	13.8	-0.228
TS	1.735	1.373	1.230	147.21		

**The Cartesian coordinates of the QM/MM optimized QM region geometries of the stationary points.**

**5eC substrate**

**Snapshot 1**

**RC**

6	50.466120023	36.187226012	38.822099147
7	49.606655312	36.122120949	39.891960446
1	49.343653219	35.287494601	40.437632795
6	49.119954893	37.353792643	40.109117760
1	48.393106510	37.585826828	40.882747428
7	49.630699946	38.211930495	39.231295689
6	50.479886304	37.499332908	38.417668153
1	51.026479396	37.964925531	37.599363431
6	49.928913509	41.727428149	34.819499794
1	49.210644285	41.951420486	34.015991619
1	50.532959787	42.641132586	34.941877372
6	49.150587811	41.564751384	36.127649872
8	49.364328704	40.513441405	36.836981711
8	48.366760579	42.472196787	36.452643482
6	45.486287885	37.776771337	37.348046006
7	46.191097327	37.914317273	36.175042024
1	45.950662818	37.504840436	35.261117026
6	47.298966231	38.621417349	36.450316790
1	48.045044260	38.908495932	35.724832636
7	47.340887071	38.955110347	37.731307566
6	46.220405619	38.414844262	38.316552954
1	46.035708788	38.508373357	39.383638485
26	48.865786811	40.053689756	38.670411272
8	50.108839119	40.901772107	39.275907025
8	46.679180375	41.894040950	41.423815444
6	47.539356681	41.082038089	41.117242955
6	48.670703423	41.250514784	43.420650209
6	50.052560155	41.253167746	44.107804917
8	47.527085463	40.525682794	39.910175108
8	51.092391401	41.287662551	43.404721206
6	48.671168548	40.658861377	42.025647147
8	50.030414844	41.282336414	45.364799589
1	47.946732096	40.754479525	44.085664664
1	48.349392442	42.304822902	43.364209555
1	48.709785750	39.557056066	42.048281719
1	49.598715045	40.959930962	41.515901599
7	55.506011053	44.723298489	40.028242775
6	55.781432587	44.394120569	38.673763732
7	54.702711888	44.366743505	37.840461258
6	53.455686497	44.439550150	38.268114651
6	53.132658241	44.562347398	39.674421024
6	51.702579861	44.510695327	40.164115316
6	54.208183477	44.747343065	40.488406194
8	56.919461112	44.180039289	38.269500693
7	52.458232574	44.343050546	37.346724841



1	51.492913786	44.626684419	37.558202929
1	52.718826625	44.464332331	36.364294800
1	51.184001159	45.436452803	39.848848079
1	51.179865041	43.693523299	39.637832237
1	54.054530391	44.908554549	41.557282841
6	51.536154452	44.307300649	41.668142972
1	51.874228159	43.313425811	41.995931331
1	50.476532220	44.391053167	41.952898203
1	52.095509711	45.060858233	42.241043893
8	49.599768065	44.803366955	37.387558449
1	49.228732410	44.105020672	36.810964600
1	49.177544941	44.531401388	38.236087124
1	50.861895286	35.311630069	38.307549823
1	50.595797374	40.925257750	34.503499980
1	44.576178657	37.181107454	37.418423939
1	56.232595198	44.930574783	40.683288204

**TS<sub>IIIα</sub>**

6	50.611457136	36.363691284	38.772951937
7	49.755593360	36.328880586	39.848420287
1	49.448864515	35.495550030	40.373089750
6	49.368628449	37.587158942	40.108302764
1	48.665769871	37.846005909	40.894601269
7	49.934896758	38.437881168	39.253879228
6	50.718040753	37.683127665	38.406900010
1	51.291661948	38.129495406	37.595956837
6	49.972588497	41.833855701	34.715761886
1	49.254272430	42.039242769	33.908852134
1	50.588869846	42.742720430	34.806578984
6	49.206806009	41.730927995	36.035906772
8	49.558600139	40.839325853	36.882767259
8	48.313449819	42.577487904	36.237944598
6	45.672052859	37.954476312	37.414784983
7	46.368562352	38.088135690	36.236481349
1	46.116132263	37.678312401	35.327120870
6	47.480826296	38.800676274	36.509923215
1	48.217350479	39.078582951	35.770664842
7	47.538780089	39.144956892	37.783932894
6	46.418363699	38.606042840	38.372641726
1	46.238564124	38.706345752	39.441582918
26	49.246883375	40.361306703	38.793534334
8	50.617528932	41.301174520	39.367279150
8	46.807661108	41.753111672	41.740785514
6	47.751956398	41.116765245	41.307254322
6	48.959667343	41.159316155	43.574829572
6	50.345838780	41.021774436	44.232120347
8	47.834015374	40.792093524	40.022399087
8	51.371799651	41.072863928	43.506344500
6	48.910818356	40.636343456	42.154945892
8	50.351115799	40.928533897	45.484811888
1	48.202791230	40.686787383	44.218442502

1	48.717581060	42.237340743	43.575164197
1	48.898035762	39.533126941	42.148165571
1	49.838234283	40.911263616	41.633454123
7	55.356347382	44.441098396	39.993265175
6	55.688125123	44.220427202	38.615678813
7	54.636739958	44.206742933	37.752329291
6	53.380644601	44.112861681	38.141222995
6	53.023576940	43.993615430	39.552672722
6	51.641233115	43.683176629	39.983592313
6	54.069758181	44.241538538	40.419363200
8	56.845076212	44.092188287	38.244840996
7	52.416670040	44.070265649	37.188189163
1	51.436236469	44.307475796	37.400492488
1	52.695593748	44.329305448	36.236605446
1	50.910019295	44.225314122	39.364726532
1	51.286353252	42.542544547	39.644334815
1	53.879805313	44.284088522	41.494399725
6	51.307105224	43.798588076	41.459435359
1	51.840533793	43.067100708	42.085354200
1	50.234069370	43.618686152	41.614257615
1	51.535962594	44.813153553	41.828013224
8	49.617011861	44.801106807	37.284030635
1	49.210432895	44.201645781	36.624820804
1	49.152205109	44.456903132	38.086322925
1	50.977601389	35.469633749	38.268306684
1	50.634609752	41.017648039	34.426624851
1	44.751270862	37.374327806	37.475246013
1	56.057394644	44.701741475	40.657019962

**IM1<sub>ca</sub>**

6	50.539948547	36.225466244	38.788037124
7	49.691908487	36.165443262	39.868074380
1	49.415329711	35.328155396	40.402281189
6	49.240332589	37.403728518	40.110286257
1	48.531871999	37.639089905	40.899574095
7	49.757729585	38.265981844	39.237581881
6	50.577829118	37.541377310	38.400873613
1	51.126780498	38.003212621	37.581635253
6	49.951109293	41.800887577	34.763954847
1	49.243390779	42.011949245	33.947706529
1	50.564366177	42.710855398	34.863265097
6	49.161178404	41.695874537	36.068244858
8	49.348572414	40.694566305	36.840303875
8	48.383334236	42.637602577	36.329603305
6	45.522906596	37.803376363	37.357010062
7	46.208797486	37.964369540	36.176472670
1	45.959051098	37.563269346	35.261583490
6	47.318749232	38.674121747	36.452415951
1	48.049461620	38.978479079	35.717690754
7	47.382820632	38.986030650	37.735001323
6	46.272668513	38.430718315	38.323841175

1	46.103102268	38.500891685	39.396433351
26	49.013129988	40.145179665	38.732625340
8	50.505633884	41.117707371	39.344015021
8	46.681650262	41.750979976	41.628134156
6	47.592248751	41.046048707	41.231993041
6	48.835384817	41.191876775	43.479207608
6	50.247292710	41.106452141	44.093747286
8	47.644179100	40.642318206	39.964987531
8	51.243698899	41.243311137	43.337860153
6	48.741870529	40.572088479	42.097899601
8	50.300456614	40.964974699	45.340431374
1	48.105835004	40.757896746	44.178382196
1	48.589323090	42.266118322	43.408830998
1	48.674363212	39.472337678	42.163363467
1	49.677404331	40.762199803	41.551503046
7	55.529755697	44.699201821	40.019593400
6	55.808369408	44.365814264	38.671773110
7	54.731175395	44.349938381	37.827440672
6	53.484409301	44.409163163	38.233080858
6	53.138808942	44.464442066	39.661119989
6	51.822696360	44.277982176	40.128775329
6	54.235688078	44.695459390	40.491873950
8	56.943922262	44.147784962	38.265976717
7	52.501823656	44.360181903	37.298965356
1	51.546943884	44.679477734	37.501670813
1	52.778009073	44.491223499	36.322429884
1	51.041306117	44.102506032	39.386281699
1	50.322728033	41.999252516	39.703392054
1	54.079252091	44.849366296	41.560224903
6	51.435144120	44.207947218	41.568559132
1	51.403922863	43.167142545	41.951648027
1	50.428720384	44.627811370	41.731979851
1	52.139506995	44.748896899	42.217320951
8	49.656597696	44.910238417	37.332625490
1	49.255044156	44.153447936	36.852703197
1	49.213087502	44.822840339	38.196150027
1	50.919678266	35.344950153	38.269805446
1	50.613711616	40.984925994	34.475454978
1	44.613618598	37.206582602	37.428423379
1	56.254904866	44.914482853	40.673646346

**ТШпф**

6	50.540197831	36.317219631	38.793693982
7	49.697754922	36.276299619	39.879592875
1	49.407411061	35.442206529	40.412199071
6	49.285490051	37.527910453	40.130346229
1	48.592528242	37.784156238	40.926331435
7	49.821002325	38.378916371	39.256889829
6	50.612937308	37.633513208	38.410628117
1	51.168701915	38.084051934	37.589801267
6	49.936034864	41.809720826	34.749755630

1	49.233501377	42.021686864	33.930306895
1	50.551689836	42.717364278	34.856928125
6	49.141285409	41.703986999	36.051246626
8	49.431966044	40.772940472	36.881372591
8	48.276678562	42.577983801	36.256106528
6	45.579477231	37.859889927	37.384180054
7	46.272312895	38.014167490	36.206647542
1	46.026180502	37.607818430	35.293593226
6	47.379418181	38.730051125	36.486033317
1	48.113993346	39.026377753	35.751792613
7	47.435315756	39.055863747	37.765145588
6	46.322266661	38.500080318	38.350192900
1	46.147002130	38.579931361	39.421411120
26	49.079623051	40.265003942	38.771180580
8	50.471939269	41.190815780	39.375767503
8	46.711629773	41.849963914	41.642223383
6	47.596055504	41.104270381	41.256991654
6	48.853283353	41.251538292	43.495767792
6	50.258151247	41.080968574	44.109486674
8	47.661528700	40.706510026	39.993445762
8	51.260095022	41.138858104	43.351413509
6	48.687022757	40.555174498	42.156122904
8	50.301604420	40.955090716	45.358820701
1	48.094422890	40.930997736	44.223748689
1	48.702694669	42.336983453	43.357644868
1	48.470353191	39.482203151	42.300964401
1	49.636636675	40.598554475	41.605591940
7	55.427068905	44.701244408	40.056719317
6	55.715437188	44.354925702	38.702856230
7	54.644856865	44.308122985	37.862204458
6	53.390949899	44.371149694	38.272337168
6	53.054905074	44.542310625	39.672608152
6	51.632717161	44.568383622	40.189572398
6	54.124953781	44.754090218	40.493682720
8	56.858045997	44.150271999	38.312933874
7	52.415240521	44.242003584	37.332852724
1	51.437892413	44.500383118	37.520232795
1	52.697234076	44.371905650	36.357205772
1	51.598289233	45.280208934	41.037837866
1	50.965895946	45.010494582	39.433770716
1	53.951881535	44.972295642	41.552427540
6	51.034721104	43.274516710	40.732011146
1	50.825386151	42.369461591	39.908702138
1	50.009769586	43.422234512	41.102108903
1	51.634730575	42.757289178	41.494258487
8	49.571395385	44.796122550	37.374685508
1	49.186582082	44.232730049	36.674101996
1	49.120924055	44.377818761	38.151032809
1	50.915924002	35.427288128	38.288798861
1	50.601769012	40.994227824	34.467202046
1	44.664446401	37.270929466	37.446721894
1	56.154734407	44.914963864	40.708485693

**IM1<sub>eβ</sub>**

6	50.520080074	36.235723371	38.791256311
7	49.669071917	36.180500360	39.869507852
1	49.390990373	35.344848054	40.405479859
6	49.218222579	37.420870384	40.105507305
1	48.508299772	37.661155623	40.892073394
7	49.738122663	38.279061593	39.230603975
6	50.559652070	37.550371212	38.399335882
1	51.110646117	38.009212433	37.579862985
6	49.917191196	41.799358805	34.734616160
1	49.223806288	42.005851155	33.905418123
1	50.528816721	42.709508171	34.839752619
6	49.103650381	41.704495973	36.024923106
8	49.310174852	40.730478977	36.827153889
8	48.293850638	42.628261625	36.245400886
6	45.511138038	37.797524795	37.354829677
7	46.196352798	37.957371113	36.173647097
1	45.947733330	37.553860908	35.259742969
6	47.304128075	38.671812698	36.447571747
1	48.033705044	38.976594393	35.711826724
7	47.367591281	38.988371026	37.728585901
6	46.259536731	38.430571955	38.319519733
1	46.091021342	38.503288567	39.392240150
26	49.001211900	40.164821936	38.720361360
8	50.501014135	41.115870708	39.314341412
8	46.670985346	41.772102652	41.610653293
6	47.580154966	41.062993978	41.217826024
6	48.854142298	41.266039210	43.440181987
6	50.263152560	41.138873128	44.054646088
8	47.624650094	40.644533517	39.955377275
8	51.260448428	41.263358779	43.300112834
6	48.735390139	40.601237599	42.081719652
8	50.309679157	40.971878250	45.299466969
1	48.106597311	40.887985717	44.152497179
1	48.655408972	42.346668694	43.328767035
1	48.653354024	39.505032799	42.185701976
1	49.663925298	40.765213277	41.515744883
7	55.513949337	44.809801999	40.051129326
6	55.771489347	44.394144451	38.710745358
7	54.687226055	44.337293669	37.888483512
6	53.442891790	44.509545309	38.301227849
6	53.139312645	44.851724743	39.675590018
6	51.736257368	45.056918355	40.207869103
6	54.226036626	45.014951778	40.480517701
8	56.902439560	44.139509248	38.314832144
7	52.452400697	44.339762525	37.386536893
1	51.479275349	44.612083540	37.567770666
1	52.722905274	44.374446172	36.400408951
1	51.785610618	45.872578683	40.960337587
1	51.085501016	45.464967233	39.416795874
1	54.072914194	45.315483550	41.521885487

6	51.103795362	43.855650857	40.839182896
1	50.405244181	42.032985539	39.631218268
1	50.017107899	43.829164720	40.963890431
1	51.687141168	43.149817938	41.438785757
8	49.593137839	44.820752618	37.411924151
1	49.212652333	44.247520596	36.715658640
1	49.158788905	44.402295919	38.192842622
1	50.902651380	35.353064600	38.278791675
1	50.586661012	40.983281517	34.462779167
1	44.603189795	37.198733173	37.426564686
1	56.251744535	44.996811693	40.699710945

**TSRBeα**

6	50.574793715	36.331002365	38.795033006
7	49.747848624	36.289111667	39.891004186
1	49.445803257	35.453597715	40.411713138
6	49.371194561	37.551591849	40.165509661
1	48.696327534	37.806037897	40.978032317
7	49.906957866	38.408180280	39.302612447
6	50.667208356	37.654903907	38.436210265
1	51.219948778	38.105862604	37.613176137
6	49.991007072	41.849501429	34.723114143
1	49.262056400	42.039151168	33.920981744
1	50.607098721	42.761064116	34.782086957
6	49.245298902	41.771294160	36.058017042
8	49.542151109	40.858081318	36.888863386
8	48.408971456	42.681773785	36.272844637
6	45.609350123	37.884093605	37.401359995
7	46.300828643	38.049106444	36.224464051
1	46.055299401	37.646164550	35.310573487
6	47.411121698	38.761651458	36.513127155
1	48.145375726	39.065736396	35.780421166
7	47.470587340	39.073417022	37.794427378
6	46.356152368	38.514619670	38.372263216
1	46.179160311	38.581280440	39.444539431
26	49.104511718	40.325930744	38.785104080
8	50.723042361	41.498888613	39.619034581
8	46.648333464	41.823424178	41.754965544
6	47.575964803	41.170656249	41.300177132
6	48.854720673	41.281809967	43.525088366
6	50.263806131	41.120771593	44.120365865
8	47.710379216	40.936527696	40.014548113
8	51.259479975	41.304761612	43.365972583
6	48.665873119	40.575879627	42.186993824
8	50.340118470	40.873097114	45.347908833
1	48.103481891	40.964217367	44.261549466
1	48.699245582	42.365621235	43.379087786
1	48.398954009	39.516729394	42.350897460
1	49.616776896	40.564480720	41.634482362
7	55.418940176	44.539693801	40.014265236
6	55.741125511	44.273514290	38.621066430

7	54.690474902	44.290147040	37.765706521
6	53.429182982	44.268464548	38.147960935
6	53.076273722	44.146689935	39.574255205
6	51.773264119	43.841481247	40.011375510
6	54.148443424	44.394917489	40.447689618
8	56.893472408	44.100368891	38.270993095
7	52.466608746	44.331898390	37.216447705
1	51.480685601	44.559700639	37.432355478
1	52.739408318	44.531975630	36.249063417
1	51.009595292	43.709412740	39.249577155
1	50.192394052	42.033162374	40.220316030
1	53.956350972	44.471838091	41.520618356
6	51.346788871	43.841928809	41.431752367
1	51.378519673	42.827579929	41.891374982
1	50.300921549	44.176814086	41.516564038
1	51.974190297	44.485453414	42.067139967
8	49.703962002	44.867061538	37.312674021
1	49.302459570	44.188254898	36.721230951
1	49.219353114	44.632202129	38.136634081
1	50.938838960	35.440317636	38.282959676
1	50.646626447	41.025306112	34.442164622
1	44.690883769	37.299926548	37.458243390
1	56.130906031	44.786104515	40.671805259

**PD<sub>Offec</sub>**

6	50.460079179	36.375528138	38.842073181
7	49.634261029	36.319478826	39.939131004
1	49.348048174	35.477554511	40.457399709
6	49.215282524	37.573848727	40.198124654
1	48.531165081	37.829047487	41.004239873
7	49.718070746	38.436506980	39.321391931
6	50.501830809	37.698790296	38.465475550
1	51.042551467	38.159311824	37.640199553
6	50.049927313	41.901404695	35.016026509
1	49.351694078	42.166805321	34.208479791
1	50.707341249	42.777586242	35.144080328
6	49.247678416	41.792993321	36.315348921
8	49.527000203	40.902034436	37.184340436
8	48.361950432	42.675925493	36.467464064
6	45.381114177	37.744740397	37.455946062
7	46.105686066	37.937174412	36.303008560
1	45.917603226	37.509917612	35.385868784
6	47.157219003	38.721374645	36.615777916
1	47.908035687	39.046265880	35.905956715
7	47.137870537	39.057148283	37.893228914
6	46.041142507	38.440083885	38.445784997
1	45.842653693	38.531572122	39.516043692
26	48.575163174	40.263215709	38.952376770
8	51.350218384	42.872334391	40.059717704
8	46.407682553	40.236403669	41.563788044
6	47.542704759	40.704301155	41.711339071

6	49.146133943	42.359066745	42.864835373
6	50.435625321	41.617189717	43.244354004
8	48.524380330	40.541419943	40.890700423
8	51.470144025	41.816464095	42.534423078
6	47.871224689	41.519377129	42.963931343
8	50.424381527	40.915978289	44.284718576
1	49.081498964	43.196151513	43.585185338
1	49.255327223	42.782436569	41.858317173
1	46.985876199	42.135235881	43.188628771
1	47.965444566	40.814113346	43.806763700
7	55.534022882	44.627658084	39.968133241
6	55.847996253	44.313701646	38.612563621
7	54.797760663	44.286887562	37.752695571
6	53.531328998	44.364535852	38.136623762
6	53.176963574	44.409677195	39.545769335
6	51.737166156	44.239579566	40.015684547
6	54.225062765	44.602770565	40.391762246
8	57.002484355	44.124972797	38.242142833
7	52.585434121	44.434769060	37.188338555
1	51.600391046	44.601961310	37.391202903
1	52.855465741	44.503353628	36.207077795
1	51.091093880	44.698000742	39.250988735
1	51.432716371	42.504652154	40.985506146
1	54.041251222	44.734762045	41.460823957
6	51.455359691	44.960429440	41.327020749
1	52.000251573	44.503163071	42.167177581
1	50.384083293	44.904695232	41.569790903
1	51.751074760	46.016153308	41.235569819
8	49.684368087	44.942930919	37.245588284
1	49.143949584	44.134340182	37.088241038
1	49.259162092	45.397133208	37.983243234
1	50.853796286	35.489181149	38.344636576
1	50.674707274	41.068379828	34.693866776
1	44.515364412	37.083406983	37.490337498
1	56.240561389	44.859040640	40.636891747

#### TS<sub>H2α</sub>

6	50.523702609	36.299219551	38.847020221
7	49.679452459	36.238063896	39.928098960
1	49.373348048	35.395708925	40.435001938
6	49.279443238	37.491922220	40.205861124
1	48.582827635	37.728395276	41.006327636
7	49.818786744	38.363109132	39.360553128
6	50.602592348	37.627202822	38.500198224
1	51.159969776	38.091142274	37.687042370
6	49.932901659	41.869464207	34.723351410
1	49.211742629	42.032965874	33.908812371
1	50.534694885	42.792624173	34.764680312
6	49.167265779	41.796353989	36.052942893
8	49.478301434	40.913948407	36.904698708
8	48.311532218	42.701336304	36.229562415



6	45.564630190	37.852167744	37.399047564
7	46.259694436	38.027394794	36.225374109
1	46.021677892	37.625279945	35.308883454
6	47.359263746	38.754753225	36.522102938
1	48.091979906	39.075153576	35.794699363
7	47.410287058	39.059048887	37.805278682
6	46.299334681	38.486734611	38.375047577
1	46.116113604	38.550643792	39.446322086
26	48.985822346	40.270039694	38.865296992
8	50.545836273	41.482654371	39.450393698
8	46.632499401	41.905531367	41.824936323
6	47.522117298	41.232066390	41.321457694
6	48.882628094	41.311437892	43.506491379
6	50.292320974	41.112279420	44.094054219
8	47.546979326	40.933350685	40.044696060
8	51.291220683	41.276381587	43.342554389
6	48.691858114	40.684494591	42.135253334
8	50.354780246	40.856890860	45.323248380
1	48.133283254	40.952965175	44.226863236
1	48.722551850	42.402110229	43.423710530
1	48.544636225	39.593481617	42.230199284
1	49.607874304	40.814225219	41.542198850
7	55.460650705	44.667391320	40.082318970
6	55.758206532	44.450790664	38.661220469
7	54.712109779	44.571710110	37.820505101
6	53.451650044	44.686153797	38.206235722
6	53.109841166	44.526942228	39.630810055
6	51.787613972	44.326125611	40.064458084
6	54.192668370	44.587940008	40.513467954
8	56.894818053	44.200204821	38.310157958
7	52.507182967	44.891009947	37.296203680
1	51.499803108	44.921415678	37.494732701
1	52.761067220	44.988363437	36.309751009
1	51.005363615	44.630274198	39.361289038
1	50.290704882	42.312158648	39.024214921
1	53.990199487	44.631593104	41.587954039
6	51.327427985	43.572671587	41.188295811
1	51.039542962	42.562376649	40.613229142
1	50.351962917	43.877740223	41.591563139
1	52.038610034	43.268831081	41.964952702
8	49.639816173	44.801732400	37.386256540
1	49.276350679	44.158795484	36.732273832
1	49.069380043	44.543436836	38.149307442
1	50.900946233	35.417139519	38.329633141
1	50.602394515	41.049844278	34.462449489
1	44.649526217	37.262505805	37.453369254
1	56.186483989	44.883042707	40.735490476

**PD<sub>DSea</sub>**

6	50.332615112	36.400646250	38.833321552
7	49.470594798	36.286016996	39.896062152

1	49.200325313	35.426858002	40.393710226
6	48.990322803	37.513639278	40.167864473
1	48.264587920	37.698756418	40.954713550
7	49.494435688	38.422983670	39.340409165
6	50.338073115	37.734605991	38.494961433
1	50.880895220	38.233135225	37.693573582
6	50.012372244	41.819684752	34.761731757
1	49.290645984	42.015192255	33.953945195
1	50.637515581	42.723500861	34.821935687
6	49.245017856	41.765722563	36.087377833
8	49.470555020	40.831047070	36.931226877
8	48.471764443	42.728072243	36.277560305
6	45.374341015	37.765672559	37.264159267
7	46.083085985	37.957427782	36.102238310
1	45.890738802	37.524937419	35.189403724
6	47.135708239	38.746330358	36.404320434
1	47.884129237	39.074099418	35.695007053
7	47.133982973	39.078135019	37.681890655
6	46.049354973	38.452980643	38.240661480
1	45.837368049	38.517998292	39.304496228
26	48.547122252	40.320834412	38.754129563
8	49.908259991	41.618748742	39.774179841
8	46.096031243	42.104961752	41.567416226
6	46.815857021	41.209053874	41.133132639
6	47.929086358	40.794973682	43.423695973
6	49.418819127	41.171779745	43.484062513
8	47.003408746	41.010917746	39.859427925
8	50.014293925	41.450517093	42.400092502
6	47.473512643	40.209562254	42.085864560
8	49.959935404	41.182602706	44.613250032
1	47.726467919	40.103594928	44.254033635
1	47.336087354	41.701558811	43.637443242
1	46.704209427	39.435190351	42.258578367
1	48.319315203	39.728897599	41.579033778
7	55.417062211	44.858617753	40.181139614
6	55.595753779	44.542807703	38.800041965
7	54.479739821	44.583316110	38.024311342
6	53.257130800	44.718293393	38.515749183
6	53.027126295	44.860633892	39.945454630
6	51.677580930	44.910987303	40.529634864
6	54.153647385	44.974128018	40.706825934
8	56.701803832	44.272584018	38.342087645
7	52.215573314	44.731250991	37.663785046
1	51.258296370	44.672097833	38.004108010
1	52.395352362	44.652484932	36.663209174
1	50.925229288	45.488297536	39.980163763
1	49.707811041	42.545487661	39.475442827
1	54.048672520	45.165388186	41.778732471
6	51.304768208	44.269275025	41.645393684
1	49.878138095	41.590830827	40.774950075
1	50.286483080	44.343245765	42.033586843
1	51.980723694	43.604885601	42.189590233

8	49.197397528	43.912033153	38.558985197
1	48.964554406	43.484031387	37.692455880
1	48.276530064	44.010938862	38.906772741
1	50.770661106	35.538276917	38.330825626
1	50.657455683	40.988497003	34.477018570
1	44.492694612	37.129451473	37.341552234
1	56.187950450	45.036236208	40.792822132

**TSRBeß**

6	50.542121851	36.396986333	38.751656914
7	49.676832349	36.362456740	39.819416770
1	49.360750725	35.530450455	40.337532129
6	49.293805643	37.628197283	40.072537647
1	48.584673733	37.886748350	40.853532150
7	49.864953125	38.481797170	39.227505076
6	50.651084887	37.720098210	38.391288726
1	51.230503144	38.163935669	37.582474633
6	49.945578227	41.856632151	34.538983342
1	49.235824544	42.004645652	33.711094452
1	50.561934126	42.765963959	34.555234857
6	49.173799255	41.883312458	35.861493417
8	49.306854154	40.943352532	36.696633347
8	48.484869142	42.921431329	36.032079551
6	45.571558607	37.865211487	37.376826850
7	46.228020114	38.065837357	36.185322541
1	45.979947286	37.655515953	35.275313089
6	47.318332346	38.817000874	36.453408921
1	48.027573817	39.154243460	35.710112671
7	47.396397092	39.121372943	37.735063438
6	46.320457367	38.514104812	38.334899016
1	46.175853244	38.566820825	39.413075494
26	49.005638177	40.409590026	38.709201732
8	50.253378661	41.766383786	39.104461163
8	46.727599760	41.692642741	41.926868196
6	47.611351970	41.057825600	41.362434502
6	49.114392415	41.213450559	43.437781089
6	50.506285963	40.885400416	44.008506102
8	47.605363901	40.814158760	40.080795701
8	51.495712727	40.946534195	43.229521869
6	48.793290793	40.484007715	42.139876295
8	50.568058257	40.629969447	45.237242503
1	48.342509762	41.023747008	44.195315641
1	49.092047429	42.304038338	43.254810758
1	48.543364522	39.432101416	42.360794181
1	49.680277986	40.450586689	41.491540628
7	55.414645839	44.670105174	40.094087152
6	55.646123986	44.387815015	38.713432414
7	54.538518342	44.385791727	37.917706706
6	53.307652310	44.358384457	38.392206986
6	53.045508818	44.363508671	39.819154748
6	51.676010210	44.169653158	40.431844628
6	54.141270453	44.595901612	40.599628191

8	56.770256719	44.195179663	38.272020286
7	52.279531311	44.302985124	37.501776754
1	51.318847958	44.437371200	37.817125743
1	52.480539311	44.523350331	36.522308338
1	51.654065738	44.701162301	41.406957650
1	50.879789547	44.661444776	39.846449038
1	54.012987892	44.718878975	41.679860300
6	51.249509985	42.779937133	40.783945702
1	49.935951075	42.633169548	38.748341639
1	50.340046930	42.684104102	41.372972580
1	51.981910009	41.992381588	40.946060422
8	49.278235090	44.114257662	38.214774293
1	48.975234658	43.733081341	37.339068937
1	48.439568003	43.962790183	38.726167499
1	50.917202452	35.502345221	38.254666828
1	50.608166585	41.020099606	34.317043504
1	44.665947079	37.262483908	37.445051086
1	56.159865463	44.890560379	40.723388124

**PDонсб**

6	50.504073293	36.386829903	38.776041100
7	49.648260651	36.329122235	39.849123907
1	49.354777176	35.489652598	40.368950605
6	49.235061100	37.583869820	40.108194748
1	48.527828460	37.820946233	40.898300271
7	49.778006615	38.453857077	39.260886614
6	50.577863006	37.713103995	38.417752171
1	51.143942775	38.174013585	37.609275413
6	49.996928428	41.840104575	34.678767999
1	49.298324753	42.045111556	33.854266712
1	50.637530795	42.732924444	34.751034302
6	49.206145590	41.818519292	35.985737785
8	49.474694487	40.945288940	36.878477372
8	48.383128905	42.748776779	36.119020113
6	45.499330035	37.806546257	37.343052351
7	46.159720191	38.012431111	36.156060383
1	45.924202490	37.593266579	35.246034236
6	47.237292560	38.778985738	36.425631936
1	47.953089595	39.110335274	35.685563112
7	47.299453429	39.089694303	37.706360780
6	46.229543742	38.469866684	38.304401007
1	46.081304902	38.514801342	39.382805544
26	48.843731402	40.300855738	38.664587417
8	50.758253281	42.299724501	39.403695896
8	46.761875846	41.624769578	41.977632159
6	47.680627035	41.074491132	41.388202222
6	49.155051913	41.184430330	43.472900461
6	50.530788160	40.859039806	44.079234759
8	47.669414431	40.892461445	40.088751463
8	51.537417318	40.873447525	43.324810277
6	48.907257808	40.545845024	42.117436142

8	50.557221702	40.659636780	45.320782842
1	48.361186718	40.918568156	44.184165924
1	49.109371073	42.284031321	43.367511960
1	48.761911233	39.458488623	42.240882748
1	49.793906798	40.652613640	41.476873946
7	55.441244526	44.708947758	40.103317231
6	55.663161340	44.424421354	38.726211817
7	54.554090177	44.451652879	37.933028054
6	53.323684708	44.481645772	38.411647900
6	53.056688735	44.495998482	39.836350431
6	51.680113567	44.381846123	40.450230622
6	54.164273481	44.682825251	40.611508284
8	56.781759260	44.203895737	38.277998513
7	52.298561933	44.480578501	37.514986622
1	51.344377929	44.618563501	37.837051261
1	52.501939842	44.700990932	36.536954462
1	51.726516797	44.811036850	41.464727555
1	50.957447351	45.004627737	39.894530533
1	54.041929548	44.812074757	41.691542100
6	51.081924778	42.964826192	40.620156236
1	50.123894418	42.898538534	38.925676201
1	50.171998334	43.078381809	41.239126826
1	51.761590946	42.317897173	41.191994602
8	49.150921002	44.053422334	38.280207177
1	48.862521354	43.634690441	37.426021988
1	48.305376447	43.931116729	38.789902993
1	50.893384412	35.501340430	38.273634330
1	50.643186678	41.001646767	34.419141163
1	44.606766997	37.185106261	37.415238763
1	56.190670902	44.918864530	40.731224503

**TS<sub>H2eβ</sub>**

6	50.562877728	36.311404428	38.818174467
7	49.730720336	36.256287247	39.908928499
1	49.432981726	35.417531062	40.426603403
6	49.333147553	37.512440972	40.182551375
1	48.642697357	37.750444943	40.987411185
7	49.865895595	38.378941793	39.327980342
6	50.641700256	37.637666656	38.464635471
1	51.192906186	38.096346473	37.644838156
6	49.944212479	41.819092216	34.720353166
1	49.235374468	42.030556689	33.906095946
1	50.556419697	42.728733159	34.822156856
6	49.165504349	41.696875741	36.033252636
8	49.421174231	40.729351300	36.816818417
8	48.346110437	42.613540263	36.282656843
6	45.560310881	37.837563362	37.387165614
7	46.248829872	37.990179271	36.207122177
1	45.996347738	37.590093526	35.293368628
6	47.365844811	38.691720203	36.484643333
1	48.098595203	38.991311103	35.749511251

7	47.430239480	39.006100887	37.765952493
6	46.315480799	38.460566526	38.354715984
1	46.147054069	38.542006894	39.426982150
26	48.974931783	40.213298335	38.712840900
8	50.469039197	41.479724190	39.265419743
8	46.597307182	41.776246105	41.689745707
6	47.531190153	41.125397766	41.242882043
6	48.793332550	41.348044898	43.471045107
6	50.197646724	41.325146991	44.085446887
8	47.582731938	40.743558984	39.989734499
8	51.185490185	41.638105776	43.356721856
6	48.731660287	40.727015078	42.086313852
8	50.288101796	41.030572172	45.300072734
1	48.088311929	40.870029786	44.166790532
1	48.476772296	42.403449963	43.398058626
1	48.757233417	39.625922225	42.149492313
1	49.623697116	41.013048621	41.511027717
7	55.474767857	44.629972070	40.067057001
6	55.748287274	44.341724185	38.694212342
7	54.658958978	44.318415043	37.877256625
6	53.419413412	44.254746157	38.321699473
6	53.128499580	44.219814923	39.747261266
6	51.752888991	43.910312416	40.281242799
6	54.198700679	44.497894398	40.549498252
8	56.885483160	44.171022934	38.280612579
7	52.418323471	44.189474826	37.403594980
1	51.446220123	44.418744563	37.647619290
1	52.667541898	44.423859055	36.437521813
1	50.960799768	44.473010097	39.757050019
1	51.450990719	42.804620648	39.943162742
1	54.049456290	44.612915015	41.625680176
6	51.509545288	43.857391681	41.692148606
1	50.047969521	42.305560062	38.986853843
1	50.487852862	43.885737028	42.073119209
1	52.283289814	43.649271015	42.430026393
8	49.583916317	44.706838865	37.511662759
1	49.216552835	44.036041158	36.889029336
1	48.962807116	44.566079870	38.257668766
1	50.931883147	35.426596313	38.299506059
1	50.612544595	41.006718994	34.434960017
1	44.644598159	37.249991811	37.452718578
1	56.199267053	44.869331550	40.713416382

**PD<sub>DSeß</sub>**

6	50.374468370	36.316735619	38.878893784
7	49.505780000	36.196146126	39.934906630
1	49.224562393	35.335769796	40.423893047
6	49.029402501	37.421712411	40.217379403
1	48.297408620	37.603139444	40.999794070
7	49.544993013	38.334685482	39.402697714
6	50.390843871	37.653790026	38.555110429

1	50.941766569	38.161137083	37.764360120
6	49.991602990	41.847743169	34.879100165
1	49.272856611	42.061733236	34.074601021
1	50.623032920	42.747988866	34.962941024
6	49.220338802	41.753430173	36.203182241
8	49.602787900	40.937338523	37.107474906
8	48.286967556	42.578117281	36.341396814
6	45.432351557	37.818708152	37.303164303
7	46.167013693	37.980661251	36.152715660
1	45.971772736	37.554034008	35.237421130
6	47.232028040	38.748325759	36.467829445
1	47.989430250	39.059106609	35.761081733
7	47.216939524	39.094778564	37.741480183
6	46.104629579	38.502341154	38.285259036
1	45.869373530	38.591856354	39.342753637
26	48.678884884	40.255211094	38.875763166
8	50.169862474	41.278804494	40.001107582
8	46.323284111	42.209096754	41.618049127
6	46.969965983	41.252924583	41.201677434
6	47.984485750	40.761900850	43.524613546
6	49.481217042	41.096411125	43.635956535
8	47.162726326	41.021670347	39.933882635
8	50.138073161	41.318585002	42.573923069
6	47.532445880	40.209018106	42.172731291
8	49.971429679	41.142248606	44.785386697
1	47.740301041	40.067415629	44.341413579
1	47.416490349	41.684505302	43.737939114
1	46.709830977	39.486641350	42.322619011
1	48.354491959	39.666487836	41.687731336
7	55.474050928	44.791981092	40.065499987
6	55.745457202	44.442065679	38.707512027
7	54.672271527	44.422716197	37.871083407
6	53.422857383	44.555055410	38.278194509
6	53.102491280	44.759789557	39.680418009
6	51.716889280	44.821554660	40.177637361
6	54.180872200	44.909816451	40.507298557
8	56.881562269	44.204060972	38.316093633
7	52.437670365	44.439530587	37.354065514
1	51.459568105	44.693726959	37.545242071
1	52.705993336	44.520638118	36.369345172
1	51.009835893	45.406087781	39.576143701
1	50.320631935	42.215826348	39.807267506
1	54.011252402	45.137189082	41.563778196
6	51.274442726	44.212341379	41.289409831
1	50.063400679	41.253526792	41.002148940
1	50.238283176	44.312754127	41.620891735
1	51.914324835	43.562617992	41.893738959
8	49.590329892	44.868362288	37.358066157
1	49.195836440	44.265066372	36.694845353
1	49.137559160	44.502065050	38.158904389
1	50.800505454	35.457609233	38.360761009
1	50.636093830	41.021463375	34.579165861

1	44.538597775	37.197925120	37.365613675
1	56.210023719	44.986478058	40.713950046

**Snapshot 2  
RC**

6	52.500178756	41.007878803	36.542482962
7	52.356291467	41.394282575	37.853882278
1	53.098253660	41.424117096	38.563021444
6	51.076829923	41.740845343	38.057191876
1	50.682926307	42.071060397	39.015335575
7	50.378346223	41.590527815	36.937950736
6	51.251420203	41.135008467	35.977035687
1	50.932682157	40.938427263	34.957009656
6	46.841331614	39.367868617	33.479251041
1	46.277155047	38.422443327	33.528175425
1	46.279876574	40.013095066	32.790126920
6	46.754301964	40.051028597	34.853047970
8	47.848936558	40.151807584	35.549545906
8	45.658721212	40.444078857	35.237818225
6	49.110088267	38.340718108	39.824352390
7	49.056670692	37.622990116	38.647164828
1	49.202962716	36.613663012	38.519532636
6	48.749057338	38.482075671	37.660533797
1	48.618505590	38.203957868	36.621388460
7	48.586553926	39.709769344	38.134970062
6	48.820247781	39.640055004	39.489487519
1	48.765466743	40.520324964	40.122199635
26	48.263524602	41.438469219	36.919067210
8	47.988890246	42.697702734	35.944832362
8	46.558044400	43.929080984	39.453658340
6	47.521392002	43.570440041	38.788568614
6	47.921995182	45.631481755	37.356612761
6	48.931522463	46.748541542	37.047136671
8	47.727388915	42.291331173	38.535719491
8	49.258812766	47.495562083	38.003446528
6	48.539617661	44.585567632	38.295730946
8	49.379167712	46.837193638	35.873388115
1	47.048601632	46.078755558	37.859859013
1	47.587470715	45.143849111	36.431357994
1	48.921141181	45.111520361	39.187097065
1	49.385117411	44.091810735	37.799427500
7	48.226592316	47.191687636	30.073328797
6	49.158269554	46.218176052	29.586985726
7	48.987144205	44.954261805	30.039141544
6	48.027677636	44.611706120	30.890009431
6	47.147212045	45.591768003	31.504209975
6	46.249359187	45.233441984	32.675895211
6	47.297858981	46.864601305	31.034808350
8	50.049662931	46.535273903	28.804619754
7	47.897221209	43.307586473	31.185685298
1	48.557702659	42.633285252	30.789834612



1	47.164209578	42.972074148	31.794994027
1	45.215826594	45.035473050	32.337818943
1	46.602921520	44.283326792	33.106816469
1	46.691232302	47.677343591	31.444678445
6	46.248149905	46.271396001	33.802314582
1	45.608399430	45.930190686	34.631151921
1	45.857154246	47.238603316	33.460192585
1	47.261642772	46.434923370	34.202188328
1	53.420255847	40.555179028	36.172904301
1	47.818504654	39.167313551	33.039958622
1	49.411797252	37.899897579	40.774466211
1	48.317471005	48.147934028	29.795288529

**TS<sub>H1ca</sub>**

6	52.576287991	41.134495001	36.302228632
7	52.398087510	41.618561810	37.577191063
1	53.093892996	41.605388239	38.334152617
6	51.162495306	42.133992818	37.664340576
1	50.751003532	42.558802279	38.576023434
7	50.524410696	42.005138179	36.504438843
6	51.396162617	41.379297370	35.639056724
1	51.125146801	41.157037793	34.610565349
6	46.820024159	39.397237621	33.300352258
1	46.228406207	38.476144457	33.409013382
1	46.287015768	40.018006339	32.562529410
6	46.762575360	40.188702579	34.613493700
8	47.881435699	40.712665199	35.022836099
8	45.684098024	40.335966352	35.175206719
6	49.107109285	38.667175501	39.418485299
7	49.080144476	37.942091358	38.245826219
1	49.190268897	36.927674685	38.145364193
6	48.869579753	38.821826298	37.239823961
1	48.761127453	38.533457131	36.201281860
7	48.744139059	40.057812301	37.688665791
6	48.895798581	39.977490296	39.053756082
1	48.827362738	40.854976249	39.691830786
26	48.421687622	42.044999571	36.300572503
8	48.275273347	43.427922474	35.210559918
8	46.639034697	43.845452537	39.508637078
6	47.525932629	43.702106099	38.669236493
6	47.915274589	45.940661903	37.634640466
6	48.973675104	46.997106335	37.302546838
8	47.617185663	42.632771861	37.932598177
8	49.335209493	47.750866128	38.236603580
6	48.549957345	44.797124314	38.437103759
8	49.432058121	47.012384535	36.127232955
1	47.109140636	46.396950838	38.231595796
1	47.492391406	45.525427289	36.713906375
1	48.894667258	45.176486314	39.410624741
1	49.415667036	44.412355890	37.878604815
7	48.458048645	46.942156453	30.611739638

6	49.127474444	45.892732795	29.867167997
7	49.064382419	44.652354823	30.414266882
6	48.436530419	44.376180762	31.548194601
6	47.760354763	45.401584605	32.335177629
6	47.027856063	45.041863463	33.575346708
6	47.837386990	46.672324148	31.809630446
8	49.710230085	46.147594295	28.827772846
7	48.435385364	43.105315507	31.981751421
1	48.948558843	42.414105899	31.426054745
1	48.228361609	42.886803436	32.954312576
1	46.296941392	44.239549234	33.368983382
1	47.744206232	44.355675509	34.369893944
1	47.375731784	47.511520275	32.337205600
6	46.436125137	46.182883861	34.374363089
1	45.852078139	45.801588047	35.223635205
1	45.756978172	46.782691086	33.746008657
1	47.228908810	46.838752282	34.767422725
1	53.481375607	40.607164903	36.000887129
1	47.799533957	39.159506737	32.885488539
1	49.297021178	38.216385792	40.392543528
1	48.547137953	47.889584414	30.304468021

**ТШтеб**

6	52.433834068	41.072139712	36.504121961
7	52.280422827	41.496741826	37.803777993
1	53.013116158	41.515129174	38.524458990
6	51.009904559	41.897347858	37.969790263
1	50.608145402	42.264146698	38.911284427
7	50.324901803	41.746753962	36.840318253
6	51.201536024	41.229756357	35.911513680
1	50.895742346	41.011566877	34.891608984
6	46.809392962	39.396199491	33.406358335
1	46.239923983	38.453759031	33.444289469
1	46.265623444	40.039206159	32.700734145
6	46.689151318	40.084515177	34.775845761
8	47.771173094	40.262487562	35.467458761
8	45.569548744	40.421393383	35.150364969
6	49.104368576	38.391544599	39.775421926
7	49.035609035	37.679326146	38.596178520
1	49.178128650	36.670728174	38.465552238
6	48.728381002	38.552255258	37.616175461
1	48.587189468	38.277809755	36.576661377
7	48.581217555	39.778731697	38.092793074
6	48.826429349	39.695561835	39.443733314
1	48.792041289	40.571338355	40.085151179
26	48.186901630	41.630242091	36.797801147
8	47.744847198	42.969876067	35.783046716
8	46.509049355	44.075422058	39.446906441
6	47.444881428	43.682965953	38.761754838
6	47.906074318	45.910327838	37.606729621
6	49.037145523	46.852656308	37.175471600

8	47.614519260	42.410220548	38.480772016
8	49.581654979	47.535828656	38.080590300
6	48.502079198	44.662045773	38.267543314
8	49.381824425	46.853460965	35.963393953
1	47.251938022	46.423649931	38.328919699
1	47.298897073	45.608930793	36.742318018
1	49.083722212	44.975738389	39.152119147
1	49.191121724	44.172206582	37.568812161
7	48.257133389	47.168585583	30.190827017
6	49.101998946	46.198552932	29.551868402
7	48.921138614	44.911481169	29.929649273
6	48.077128096	44.556495819	30.887816415
6	47.360551779	45.530389697	31.698132968
6	46.737088204	45.106903543	33.019504440
6	47.480866402	46.824573840	31.277393388
8	49.931299014	46.539493028	28.714319281
7	47.911474704	43.244335784	31.121010763
1	48.524915736	42.571169601	30.653006558
1	47.292622248	42.908592029	31.845797816
1	46.140520407	45.934026639	33.433006437
1	46.025814989	44.275400543	32.859013918
1	46.981346553	47.631068490	31.824487536
6	47.857103573	44.717152969	33.990572220
1	47.578287293	43.837810323	34.921997008
1	48.258632675	45.547930361	34.592247477
1	48.663760262	44.147561871	33.508622410
1	53.353804811	40.608833457	36.147655312
1	47.794682624	39.191774573	32.987452544
1	49.394527431	37.942694932	40.725374099
1	48.334129923	48.130348548	29.928041876

**Snapshot 3  
RC**

6	53.106059443	42.388593285	37.935513150
7	52.773327442	43.034117370	39.104523712
1	53.424533271	43.389036297	39.815142489
6	51.436358000	43.125435197	39.174057306
1	50.900801672	43.566753999	40.011316988
7	50.884789171	42.572953823	38.101068756
6	51.912196987	42.105475683	37.313523731
1	51.723213853	41.594757708	36.372902043
6	48.413712492	39.039756608	34.841331462
1	48.002416445	38.037008341	35.036076987
1	47.825286442	39.444215013	34.003997700
6	48.100623725	39.931511095	36.039295073
8	49.077092986	40.470477308	36.681451734
8	46.910530916	40.111390756	36.346513174
6	49.979007714	39.482132378	41.296147622
7	50.287123125	38.656148585	40.237636477
1	50.708885256	37.719186586	40.280305923
6	49.961880204	39.300279680	39.107585373

1	50.084618485	38.895963507	38.111049419
7	49.442583017	40.491059240	39.380258477
6	49.461496833	40.627859290	40.749237734
1	49.114958174	41.533380773	41.236895498
26	48.884543838	41.924772776	37.956328089
8	48.436034803	42.988772114	36.817585947
8	46.043061537	43.917907343	39.613573482
6	47.233639649	43.847672880	39.359807871
6	47.457194827	45.964002842	37.999523182
6	48.414445016	47.093962976	37.595246464
8	47.858692909	42.676188076	39.349807199
8	48.461490869	48.105002323	38.335414863
6	48.075313775	45.082172079	39.091859776
8	49.101544970	46.924040854	36.547125862
1	46.515995039	46.393463666	38.373488547
1	47.247849556	45.337793615	37.122817114
1	48.143007563	45.651856392	40.035274901
1	49.092391654	44.788967497	38.799173845
7	47.686340218	46.348932083	30.679494832
6	47.884277978	45.150761563	29.931159598
7	47.545206645	44.000578800	30.567157365
6	47.221907117	43.938199851	31.852904619
6	47.260410128	45.118159535	32.700046347
6	47.051441028	45.077996797	34.195013553
6	47.434631461	46.291968756	32.034330959
8	48.304143903	45.180776132	28.778889526
7	46.874610592	42.739787085	32.361810765
1	46.625815368	41.980723644	31.718960422
1	46.474685336	42.632843040	33.300154086
1	47.452297641	44.133332062	34.596384442
1	47.653173891	45.869844593	34.669522283
1	47.384547935	47.236867958	32.585284116
6	45.585397709	45.226682004	34.616497522
1	45.497097590	45.246323264	35.713812250
1	44.966542808	44.408430745	34.220976465
1	45.173353389	46.166700166	34.225837963
8	45.544597640	41.914620119	34.819335786
1	45.238523795	42.634512229	35.386503194
1	46.056723179	41.330307458	35.421920418
1	54.120960472	42.053751502	37.721213843
1	49.449713220	38.951208442	34.514331408
1	50.241644907	39.245101622	42.327120680
1	47.856446023	47.247639869	30.275315631

**TS<sub>H1α</sub>**

6	53.107504583	42.443836389	37.687872189
7	52.734246040	43.156264428	38.806762575
1	53.356086834	43.493760660	39.553310613
6	51.403678754	43.340521486	38.762551011
1	50.836797732	43.844072929	39.541536128
7	50.894249410	42.785787881	37.668130036

6	51.947732779	42.216461282	36.985133190
1	51.796472077	41.677805045	36.053134884
6	48.430361805	38.887732938	34.669572962
1	48.013527923	37.892616846	34.878538951
1	47.863390125	39.280367068	33.810844184
6	48.098469381	39.824839641	35.821496455
8	49.014210065	40.617943228	36.239429565
8	46.934373680	39.831295603	36.261289083
6	49.940629240	39.634600134	40.954090957
7	50.271766348	38.794708330	39.914071461
1	50.663167940	37.847077800	39.985749197
6	50.012284485	39.453238761	38.767332641
1	50.159188984	39.029701447	37.782406127
7	49.514386210	40.657061566	39.003312335
6	49.476796083	40.790698030	40.371959046
1	49.123807018	41.700430029	40.849588690
26	48.876229659	42.192609258	37.380663682
8	48.403058201	43.302433456	36.092083197
8	45.984317449	44.004606622	39.457758178
6	47.121244597	43.884584014	39.023979210
6	47.344122508	46.298645660	38.209279137
6	48.388443871	47.319120296	37.739844317
8	47.638349784	42.708473555	38.754063120
8	48.533849735	48.358257161	38.423659816
6	48.038639866	45.079713183	38.817163897
8	49.047741699	47.032708365	36.695930754
1	46.658562804	46.757974047	38.932122781
1	46.755611678	45.979489712	37.336697969
1	48.452956870	45.343344907	39.808137902
1	48.875494404	44.797999229	38.164918663
7	47.851637209	46.177655055	30.933501912
6	47.977040432	44.969876354	30.171004079
7	47.604304092	43.832695936	30.808149537
6	47.330491426	43.762410836	32.106277676
6	47.479006561	44.929808752	32.973201685
6	47.253292408	44.936828854	34.450937275
6	47.679262271	46.108327772	32.297811878
8	48.370506736	44.995189654	29.011440003
7	46.942683794	42.578456081	32.604553863
1	46.670487697	41.830421182	31.956514561
1	46.591964640	42.450946706	33.560864550
1	47.863845794	43.993509208	35.134063770
1	47.760230364	45.789426479	34.930650200
1	47.677476917	47.048645755	32.857315857
6	45.800572423	44.839030247	34.893456146
1	45.735246873	44.663669775	35.976644943
1	45.245358616	44.060770351	34.355429492
1	45.300022923	45.799447175	34.680636328
8	45.516223654	41.671896797	34.929469780
1	45.255358294	42.338907119	35.577739184
1	46.008175050	41.006949906	35.466104787
1	54.121200157	42.076556903	37.527889752

1	49.473844131	38.812742362	34.363650800
1	50.127819844	39.380916577	41.997485249
1	47.963228784	47.073405678	30.503210570

**TS<sub>IIIeβ</sub>**

6	53.018777757	42.426279230	37.879102422
7	52.688003415	43.109969584	39.028604160
1	53.340786516	43.453553370	39.744810954
6	51.355171113	43.259407673	39.063800914
1	50.816818248	43.733956896	39.880768601
7	50.800081684	42.710230180	37.987202141
6	51.828616208	42.176044639	37.237840065
1	51.637140162	41.646240336	36.307882923
6	48.354161520	39.089731102	34.801315480
1	47.936121743	38.088758807	34.991680571
1	47.775375438	39.494949290	33.956507143
6	48.033454945	39.984780305	35.998080161
8	48.990620053	40.584302911	36.603001037
8	46.838598207	40.112993703	36.330396198
6	49.941613292	39.499736719	41.267428766
7	50.244011150	38.684345594	40.199046269
1	50.665488890	37.747469004	40.230924885
6	49.915865745	39.348437699	39.077580563
1	50.033327012	38.951019976	38.076908671
7	49.402576937	40.537020469	39.361692319
6	49.426995821	40.652941482	40.731739953
1	49.084715239	41.553999799	41.231243953
26	48.777197381	42.071174387	37.898191496
8	48.120189636	43.205748999	36.761446247
8	46.013799654	44.045025090	39.659409561
6	47.207915338	43.949961821	39.425300033
6	47.388927813	46.245874607	38.322018090
6	48.409215322	47.272779234	37.813542747
8	47.830297247	42.785064485	39.424656104
8	48.524470269	48.335814759	38.470957636
6	48.078412029	45.170322140	39.166311892
8	49.081962264	46.977829213	36.781709348
1	46.611318669	46.750883247	38.909638167
1	46.916838132	45.761906791	37.459145669
1	48.356735131	45.583789433	40.153070296
1	49.003364054	44.858677640	38.664074936
7	47.635583060	46.327783832	30.697631578
6	47.805573885	45.153177887	29.907949010
7	47.474342737	43.989524694	30.525195229
6	47.264778005	43.876893196	31.824659714
6	47.435438662	45.020558316	32.708600757
6	47.734839170	44.875893729	34.187611829
6	47.535460899	46.220844894	32.070676313
8	48.191998163	45.208518561	28.746564226
7	46.949903053	42.652138584	32.312443142
1	46.672169131	41.923778648	31.646688468

1	46.491917898	42.536499660	33.218797032
1	48.521700582	44.105230046	34.252446228
1	48.189016064	45.803258040	34.567604576
1	47.582535629	47.142390314	32.658320128
6	46.638876764	44.457789054	35.147614777
1	47.304259882	43.879562445	36.087445901
1	45.999851881	43.625138887	34.839679328
1	46.071954848	45.276130062	35.610559947
8	45.344964412	41.564963722	34.610129651
1	44.588913234	41.967343302	35.055283920
1	45.869662466	41.138370145	35.329626091
1	54.031441842	42.081134371	37.670646665
1	49.393355975	38.996186926	34.486051006
1	50.204863501	39.254571127	42.296341048
1	47.807855163	47.234264089	30.312159967

**Snapshot 4  
RC**

6	45.434680710	51.188634212	37.261231414
7	44.272778411	50.830070582	37.904838687
1	43.485216897	51.445638864	38.145184278
6	44.322605175	49.509623356	38.155016926
1	43.534926274	48.973049489	38.680539926
7	45.462099468	48.998536158	37.696525608
6	46.169986557	50.035435731	37.132155362
1	47.151113933	49.887702884	36.684673936
6	50.600765718	46.980762680	37.328565801
1	51.256027887	46.773686394	38.190555449
1	50.867635398	46.234132656	36.567188073
6	49.163520284	46.672672447	37.757427141
8	48.318885527	47.629949857	37.933358261
8	48.854152940	45.489750038	37.965081389
6	46.281805076	49.029819995	42.075919472
7	47.546582660	49.381025563	41.650776364
1	48.238027307	49.958482971	42.147759221
6	47.750807003	48.811821400	40.454492176
1	48.657135191	48.909674153	39.871437814
7	46.693261549	48.099372649	40.085783769
6	45.758234047	48.233439324	41.086638237
1	44.784455758	47.758321040	41.023488722
26	46.423435170	47.177097711	38.211728942
8	46.300712304	46.483517182	36.748981365
8	43.809103733	44.364110922	39.379646615
6	44.172071430	45.348889298	38.755021862
6	42.077934796	45.291684618	37.245958369
6	41.531082889	45.720500010	35.872371307
8	45.231880567	46.037105515	39.145808957
8	40.304004279	45.504302169	35.643745282
6	43.454829222	45.866947485	37.526820358
8	42.332838699	46.227609790	35.055200167
1	41.342293434	45.560915561	38.021252104

1	42.109708233	44.187749089	37.262725213
1	43.407901974	46.964502825	37.580085017
1	44.115483686	45.682440217	36.665045567
7	48.233062016	44.553763418	30.634497239
6	49.536829803	45.062012850	30.863513336
7	50.025473069	44.950492904	32.119630511
6	49.304841809	44.504596676	33.145288676
6	47.895979754	44.192507006	32.999337849
6	47.061860914	43.885240803	34.224974669
6	47.439491880	44.188203853	31.715893067
8	50.207553028	45.567297937	29.954166277
7	49.913137677	44.358716759	34.330509181
1	50.916698580	44.526042695	34.410903101
1	49.481838507	43.934659629	35.149789140
1	47.389477422	42.907277034	34.631638293
1	47.292116429	44.635980126	35.012159699
1	46.403150954	43.907276378	31.507603298
6	45.550646861	43.870103936	34.016476134
1	45.040213848	43.534819068	34.932038676
1	45.260544125	43.195133873	33.202425208
1	45.166608956	44.873106769	33.783145009
8	49.669782623	43.153564703	37.126179639
1	48.839875409	42.659874965	37.081352309
1	49.402409785	44.050798541	37.473619741
1	45.726067505	52.220888344	37.067292064
1	50.844667682	47.972268550	36.947127384
1	45.833177695	49.418559016	42.990076334
1	47.851485404	44.423406609	29.719413153

**TS<sub>IIIα</sub>**

6	53.018777757	42.426279230	37.879102422
7	52.688003415	43.109969584	39.028604160
1	53.340786516	43.453553370	39.744810954
6	51.355171113	43.259407673	39.063800914
1	50.816818248	43.733956896	39.880768601
7	50.800081684	42.710230180	37.987202141
6	51.828616208	42.176044639	37.237840065
1	51.637140162	41.646240336	36.307882923
6	48.354161520	39.089731102	34.801315480
1	47.936121743	38.088758807	34.991680571
1	47.775375438	39.494949290	33.956507143
6	48.033454945	39.984780305	35.998080161
8	48.990620053	40.584302911	36.603001037
8	46.838598207	40.112993703	36.330396198
6	49.941613292	39.499736719	41.267428766
7	50.244011150	38.684345594	40.199046269
1	50.665488890	37.747469004	40.230924885
6	49.915865745	39.348437699	39.077580563
1	50.033327012	38.951019976	38.076908671
7	49.402576937	40.537020469	39.361692319
6	49.426995821	40.652941482	40.731739953



1	49.084715239	41.553999799	41.231243953
26	48.777197381	42.071174387	37.898191496
8	48.120189636	43.205748999	36.761446247
8	46.013799654	44.045025090	39.659409561
6	47.207915338	43.949961821	39.425300033
6	47.388927813	46.245874607	38.322018090
6	48.409215322	47.272779234	37.813542747
8	47.830297247	42.785064485	39.424656104
8	48.524470269	48.335814759	38.470957636
6	48.078412029	45.170322140	39.166311892
8	49.081962264	46.977829213	36.781709348
1	46.611318669	46.750883247	38.909638167
1	46.916838132	45.761906791	37.459145669
1	48.356735131	45.583789433	40.153070296
1	49.003364054	44.858677640	38.664074936
7	47.635583060	46.327783832	30.697631578
6	47.805573885	45.153177887	29.907949010
7	47.474342737	43.989524694	30.525195229
6	47.264778005	43.876893196	31.824659714
6	47.435438662	45.020558316	32.708600757
6	47.734839170	44.875893729	34.187611829
6	47.535460899	46.220844894	32.070676313
8	48.191998163	45.208518561	28.746564226
7	46.949903053	42.652138584	32.312443142
1	46.672169131	41.923778648	31.646688468
1	46.491917898	42.536499660	33.218797032
1	48.521700582	44.105230046	34.252446228
1	48.189016064	45.803258040	34.567604576
1	47.582535629	47.142390314	32.658320128
6	46.638876764	44.457789054	35.147614777
1	47.304259882	43.879562445	36.087445901
1	45.999851881	43.625138887	34.839679328
1	46.071954848	45.276130062	35.610559947
8	45.344964412	41.564963722	34.610129651
1	44.588913234	41.967343302	35.055283920
1	45.869662466	41.138370145	35.329626091
1	54.031441842	42.081134371	37.670646665
1	49.393355975	38.996186926	34.486051006
1	50.204863501	39.254571127	42.296341048
1	47.807855163	47.234264089	30.312159967

**ТШпф**

6	45.465694010	51.132555367	37.197240767
7	44.302480664	50.758009780	37.831386583
1	43.524436795	51.372120681	38.104926204
6	44.336778483	49.426816435	38.014789808
1	43.547568059	48.880635382	38.527853885
7	45.465639193	48.919338496	37.520793342
6	46.184975567	49.978088517	37.006903441
1	47.163540883	49.840450266	36.550449297
6	50.657461949	46.989507588	37.291468724

1	51.302014597	46.774647729	38.159097804
1	50.930729985	46.247870267	36.527888539
6	49.212759147	46.688738231	37.696614128
8	48.341931493	47.628333612	37.746660770
8	48.919343020	45.515633261	37.993908722
6	46.307665777	48.977089355	41.988003462
7	47.567776261	49.340467911	41.559039884
1	48.255141545	49.919688759	42.058980424
6	47.764761497	48.777638365	40.354413381
1	48.668869569	48.888461014	39.769060041
7	46.714578586	48.059224908	39.983018722
6	45.788613615	48.181703771	40.992509066
1	44.816404453	47.701424585	40.935124615
26	46.428384348	47.076217244	37.969373297
8	46.410137189	46.258722518	36.403617834
8	43.830757089	44.252887363	39.284937292
6	44.178531901	45.263418446	38.689649109
6	42.042736672	45.245464589	37.215006527
6	41.500562226	45.717140042	35.853471291
8	45.279236787	45.909947503	39.003057637
8	40.272157286	45.517252321	35.616500348
6	43.380499742	45.875952204	37.553470804
8	42.309271711	46.232755816	35.047382774
1	41.282159705	45.424386461	37.991271509
1	42.141879575	44.146101194	37.166692115
1	43.250431091	46.946275818	37.774164763
1	44.022703674	45.870896614	36.659761483
7	48.189636651	44.504889973	30.652687712
6	49.465557697	45.081041963	30.906680436
7	49.927204584	45.005554289	32.174031139
6	49.232624149	44.494620806	33.190171585
6	47.873371932	44.021879126	33.003621037
6	47.021567723	43.490849079	34.141533111
6	47.440475726	44.013315895	31.709159869
8	50.130452824	45.599929472	30.002906894
7	49.843364673	44.412469319	34.379088007
1	50.832831125	44.652269059	34.444829501
1	49.467179308	43.936338666	35.199303953
1	46.477279680	42.606722772	33.759515827
1	47.669747225	43.089584322	34.937538061
1	46.451546563	43.601318470	31.481803722
6	45.960838373	44.403120006	34.748477106
1	45.276670532	43.856460890	35.414797550
1	45.393034868	44.996157874	34.019287441
1	46.346995151	45.335039613	35.599937497
8	49.620742254	43.179534326	37.096280150
1	48.811521135	42.656968183	37.176698762
1	49.381757982	44.076877581	37.474821682
1	45.753145399	52.169193484	37.021683283
1	50.901469854	47.983148969	36.915697160
1	45.861279452	49.357148350	42.906895037
1	47.820674186	44.391041112	29.730257429

**Snapshot 5  
RC**

6	53.580239650	40.344791251	39.964873874
7	52.855528454	40.030577670	41.088089077
1	53.122263977	39.362878856	41.826387332
6	51.709773534	40.730880929	41.059682107
1	50.935672479	40.654763661	41.821123410
7	51.666211700	41.486926387	39.965929895
6	52.831637001	41.259718203	39.268130162
1	53.044789528	41.752150823	38.321429471
6	50.804587247	43.647367438	35.003179143
1	50.109494737	43.198412142	34.274568679
1	50.793777844	44.726497604	34.806899909
6	50.197062512	43.463126335	36.390728384
8	50.675721797	42.535278647	37.167272729
8	49.239681548	44.158084957	36.723129506
6	48.786891744	38.333047165	38.578534216
7	49.476920429	38.532642833	37.397751069
1	49.698314358	37.830336865	36.678902719
6	49.880249237	39.811620899	37.372251812
1	50.463505660	40.263856210	36.582196989
7	49.472938762	40.459562985	38.453425517
6	48.792693273	39.547188842	39.230671102
1	48.369145470	39.828777952	40.195008350
26	50.081399527	42.435945187	38.999326678
8	50.600100394	43.928702210	39.382512544
8	48.059257691	41.450785301	42.076000505
6	48.473076750	42.400176716	41.415808299
6	49.559943392	43.536544344	43.423748668
6	49.915293334	44.910666458	44.008024741
8	48.527818427	42.321455319	40.101924299
8	50.851909674	45.527522794	43.437231231
6	48.902413751	43.705090526	42.051817248
8	49.233201508	45.334096408	44.975851131
1	50.492363584	42.961571143	43.298224353
1	48.903922928	42.978376315	44.107038880
1	49.570317102	44.243743974	41.369897161
1	47.985747599	44.318127499	42.143037864
7	51.819848503	50.397134704	39.568546986
6	52.348952747	50.170753423	38.266511419
7	51.660026094	49.315565322	37.477871484
6	50.622227375	48.609075715	37.906428701
6	50.216598175	48.626056188	39.303212460
6	49.231915406	47.597634617	39.809536105
6	50.806169741	49.591297493	40.062267163
8	53.368428973	50.757674134	37.900582223
7	49.946828488	47.862817539	37.021286828
1	50.200554934	47.904474488	36.034313811
1	49.073950234	47.381265449	37.234634325
1	48.284456361	47.694986879	39.247142124
1	49.622211245	46.590229945	39.537005778

1	50.511590319	49.738343648	41.104682673
6	48.955366434	47.636329359	41.308685011
1	48.194768035	46.890927846	41.583380847
1	48.580905626	48.621526679	41.617604211
1	49.849679133	47.402318935	41.905060193
8	47.453001029	46.207197053	36.857869289
1	47.974490830	45.380007513	36.916922364
1	46.611174579	45.941828606	36.448628958
1	54.471288939	39.804610666	39.645024820
1	51.805257345	43.266183227	34.799647149
1	48.455236581	37.349240052	38.910491650
1	52.210817344	51.113841300	40.145996133

**TS<sub>H1ca</sub>**

6	53.464989120	40.500022047	40.080120524
7	52.701301248	40.220772815	41.188507101
1	52.903880755	39.506494291	41.903752893
6	51.635230091	41.042637757	41.175303515
1	50.849000914	41.011108906	41.927096219
7	51.671885178	41.844948875	40.109721525
6	52.817626488	41.507368007	39.416488031
1	53.090515343	41.975469380	38.478762794
6	50.890828692	43.733474403	35.195418400
1	50.094921043	43.347993717	34.542377585
1	50.889277446	44.827528802	35.079472696
6	50.535946252	43.443437359	36.644196915
8	51.393022669	42.999167192	37.469120676
8	49.369189329	43.660868829	37.080657129
6	48.842397479	38.611800912	38.525988815
7	49.565301020	38.797852881	37.364181615
1	49.802266280	38.083382186	36.664564158
6	49.981733940	40.080268355	37.355726850
1	50.610552656	40.498811787	36.581142762
7	49.548776170	40.746652237	38.410760152
6	48.837620289	39.836533066	39.164166110
1	48.387829650	40.117161635	40.117094308
26	50.113833483	42.979389155	39.130342466
8	50.420321436	44.640575729	39.594472464
8	47.999966899	41.491513581	42.059335666
6	48.425013750	42.495186353	41.486603102
6	49.561185620	43.472891730	43.572899959
6	49.960597738	44.826270767	44.173320944
8	48.520553675	42.554580810	40.183420262
8	50.955762186	45.392387874	43.649121909
6	48.847479734	43.736586145	42.247089881
8	49.235740934	45.299677031	45.086155842
1	50.475833881	42.892417118	43.375920597
1	48.922484518	42.900190303	44.261671563
1	49.486661154	44.349083564	41.602362292
1	47.927330167	44.321480731	42.432653519
7	51.834606531	50.117632584	39.564324115

6	52.343020278	49.982883720	38.230710789
7	51.682785436	49.126654579	37.422354239
6	50.722979807	48.315634336	37.843371802
6	50.390613759	48.205370530	39.262635741
6	49.516567468	47.119842304	39.764884007
6	50.925895522	49.202805566	40.048271235
8	53.309899175	50.650633154	37.874902675
7	50.051261385	47.599057405	36.936773523
1	50.242129919	47.747592236	35.944748403
1	49.221001273	47.041710897	37.146078211
1	48.681639003	46.914286487	39.073383896
1	50.067307034	45.997761054	39.633468933
1	50.634310449	49.292356523	41.097585734
6	49.054002400	47.213597870	41.206936884
1	48.350870519	46.405103227	41.439691057
1	48.536760734	48.171519268	41.386382234
1	49.884726479	47.121399668	41.923957335
8	47.755268883	45.848182675	36.854539955
1	48.210259138	44.980188971	36.950391222
1	46.833041782	45.645197347	36.631808663
1	54.353174270	39.951432343	39.766681860
1	51.856443602	43.342625489	34.874650123
1	48.479023252	37.636124814	38.848607229
1	52.190453101	50.844097425	40.152197021

**TS<sub>нлсб</sub>**

6	53.539196382	40.451221427	39.980698406
7	52.806055567	40.147292887	41.104167784
1	53.051613592	39.455460025	41.828874344
6	51.700848748	40.908548534	41.102178839
1	50.926038448	40.847523888	41.864374369
7	51.686974641	41.697795948	40.026827517
6	52.835621134	41.420802637	39.312375243
1	53.063536712	41.925116995	38.375444598
6	50.802684733	43.702120603	35.027288258
1	50.096964513	43.276049080	34.295913694
1	50.805143846	44.785115420	34.850290538
6	50.208919618	43.502397335	36.417886586
8	50.754982791	42.663419944	37.233971452
8	49.192293487	44.133069378	36.729364114
6	48.769277820	38.401582319	38.584267201
7	49.466311018	38.612491991	37.410070369
1	49.696435085	37.914944486	36.690507258
6	49.863933448	39.897855232	37.403988894
1	50.455410798	40.352801094	36.620678447
7	49.448616220	40.538446417	38.484132519
6	48.767609461	39.613777861	39.243774753
1	48.339215369	39.880133811	40.211167253
26	50.104477058	42.687489952	39.092431562
8	50.579986891	44.389877039	39.436081988
8	48.091739924	41.387610375	42.098649434

6	48.496407174	42.379848287	41.495647906
6	49.618252015	43.425440665	43.582096128
6	49.995046997	44.811680726	44.125063726
8	48.502557108	42.442789550	40.184753117
8	50.952908973	45.393065957	43.550274425
6	48.995575676	43.621626118	42.204836284
8	49.287435815	45.287363156	45.050251928
1	50.535533822	42.826339421	43.470845957
1	48.937395357	42.899201149	44.266696095
1	49.718734297	44.123933985	41.555226527
1	48.122940913	44.297658240	42.282835354
7	51.826884952	50.336896537	39.548292050
6	52.392630661	50.097836174	38.258912804
7	51.723003378	49.242034809	37.456342522
6	50.641543170	48.573788991	37.837544222
6	50.150140186	48.648222915	39.202954977
6	49.022867760	47.762431879	39.679358358
6	50.750570315	49.590150274	39.985342439
8	53.422363824	50.680508417	37.922261885
7	49.997074206	47.836802286	36.924687141
1	50.306445069	47.861191282	35.953323239
1	49.106613330	47.367533527	37.088930318
1	48.449679426	48.318649758	40.448106504
1	48.307438005	47.577888294	38.862644205
1	50.395784609	49.768693154	41.004454285
6	49.385322403	46.437201166	40.339526127
1	48.485522998	45.865972836	40.602347136
1	50.045018183	46.531168985	41.213998506
1	49.993034234	45.534315472	39.661969986
8	47.510300479	46.221196574	36.848465471
1	48.021957685	45.381467386	36.883781618
1	46.652844536	45.976576035	36.459667236
1	54.423540498	39.898113396	39.664353167
1	51.798182711	43.313169081	34.813354136
1	48.440460428	37.414229845	38.908430013
1	52.206648020	51.057358936	40.128538925

**5vC substrate  
Snapshot 1**

**RC**

6	49.690167039	45.957750618	46.898954931
7	49.618728602	46.557685464	45.659492837
1	49.881414279	47.525069091	45.431054734
6	49.118487178	45.662765725	44.788212096
1	48.964961613	45.858902446	43.729534842
7	48.860997498	44.518542417	45.410178226
6	49.215459401	44.680090548	46.729550783
1	49.093657028	43.886887264	47.465256927
6	45.921826008	40.393619007	47.744279787

1	44.835719264	40.544617962	47.855595825
1	46.076028396	39.308243824	47.753099542
6	46.359723002	40.896184138	46.363389068
8	46.704179581	42.142659021	46.260721157
8	46.330303424	40.112182596	45.416011823
6	44.769358474	46.153632335	44.615894024
7	44.532383112	45.582028697	45.846996556
1	43.869354473	45.896844201	46.567510037
6	45.339174609	44.517891201	45.971406085
1	45.363120388	43.864145125	46.835008708
7	46.081722930	44.360926360	44.882307156
6	45.740455565	45.380960239	44.022050500
1	46.211477753	45.489124857	43.047837439
26	47.662745046	42.940612470	44.767564436
8	48.883966167	41.880666032	44.851805295
8	49.085228610	41.748113233	42.008627309
6	47.927576880	42.147092357	41.975780949
6	46.721814921	43.044924889	39.903627942
6	47.972856852	43.498385955	39.139530983
8	47.347218089	42.877529626	42.896853179
8	48.120509026	43.103305576	37.962174015
6	47.015118434	41.830036877	40.805395833
8	48.807465853	44.216323613	39.782610846
1	46.340033989	43.863335204	40.532247576
1	45.934910540	42.765882079	39.186718243
1	47.495523119	41.031772299	40.220314299
1	46.063900690	41.464020982	41.222748013
7	51.884224698	36.750975538	45.510480366
6	51.329746231	36.586734129	46.822767017
7	50.067586339	37.051940188	46.976871894
6	49.336763374	37.578460983	45.998298888
6	49.850847869	37.705570469	44.638987276
6	49.164023637	38.276354078	43.470612531
6	51.147312713	37.291949312	44.490141755
8	51.961933372	36.049410360	47.724228605
7	48.103568755	37.990107303	46.338910339
1	47.944000780	38.011419478	47.349038432
1	47.572088230	38.659352881	45.775230564
1	51.622117624	37.396593145	43.509592701
6	47.852838563	38.455425035	43.252854125
1	47.520706511	38.918842469	42.320658515
1	47.069894978	38.166208665	43.952427237
1	49.850108179	38.590512001	42.674710470
1	49.893611307	46.496030351	47.824661520
1	46.409031272	40.836383278	48.612990410
1	44.291678813	47.086161755	44.315430473
1	52.845889274	36.552646049	45.321168031

**TS<sub>H1vα</sub>**

6	49.714414533	45.823193306	46.909324048
7	49.646842414	46.398642771	45.656535922

1	49.870915196	47.373688768	45.418546979
6	49.217383061	45.464190681	44.789792585
1	49.067016282	45.642977644	43.727677028
7	49.003600231	44.312492153	45.422869114
6	49.308441882	44.520799687	46.752107916
1	49.209897018	43.735873661	47.500612397
6	45.890669692	40.334371798	47.782269004
1	44.813147717	40.545127750	47.875813047
1	45.988717319	39.245076836	47.829453977
6	46.373100650	40.770747005	46.393587589
8	46.699869390	42.008865185	46.229454803
8	46.401210922	39.926755427	45.492942543
6	44.797804143	46.102276085	44.644147659
7	44.563937618	45.526969180	45.873928212
1	43.898258436	45.837341463	46.593382698
6	45.387123598	44.470046191	45.993955502
1	45.410089197	43.811202095	46.854024274
7	46.135726130	44.321325762	44.910603989
6	45.780946292	45.339432768	44.055354492
1	46.251516573	45.457159043	43.081710672
26	47.787447866	42.737248076	44.748640232
8	49.013649508	41.437268193	44.806760468
8	49.039598714	41.822650933	41.767818063
6	47.865036601	42.187498157	41.848280104
6	46.690492544	43.171469601	39.814273892
6	47.969017417	43.559395202	39.060299835
8	47.347614623	42.810767296	42.864171964
8	48.131973323	43.101398617	37.907531115
6	46.907742755	41.930717119	40.701392480
8	48.805270355	44.291065464	39.683139108
1	46.349724473	44.002001805	40.449585322
1	45.892610153	42.939065997	39.093143597
1	47.336796134	41.119178579	40.096270765
1	45.939104095	41.614502798	41.116809844
7	51.926070591	36.892626725	45.677373059
6	51.416725783	36.644204514	47.009834816
7	50.173080104	37.115170064	47.254637947
6	49.441840550	37.780338066	46.365070528
6	49.977016848	38.149490876	45.060182436
6	49.318708180	39.024992383	44.109984370
6	51.232807637	37.664518475	44.790288275
8	52.073750731	36.016765870	47.826797661
7	48.188322889	38.087975995	46.693696982
1	47.930864944	37.912217339	47.665233703
1	47.561710567	38.640965548	46.093038386
1	51.699148697	37.921848354	43.833983948
6	49.114554682	38.835939344	42.807294898
1	48.812030928	39.648613504	42.144014805
1	49.268121819	37.841352626	42.375303178
1	49.028810240	40.192102648	44.523305759
1	49.910451780	46.382914719	47.823845047
1	46.391014835	40.782727430	48.640580881



1	44.312100747	47.028194774	44.336196177
1	52.861152497	36.653465671	45.415846170

**IM1<sub>vα</sub>**

6	49.710504331	45.956918736	46.859239533
7	49.622464927	46.576096440	45.629403644
1	49.856358593	47.554776228	45.417580183
6	49.164491467	45.680753100	44.739221702
1	48.999865716	45.896269943	43.685946406
7	48.949541504	44.511006939	45.334807405
6	49.288084544	44.665341812	46.662700356
1	49.201826192	43.853200105	47.383144673
6	45.934689788	40.357552333	47.657592574
1	44.866687600	40.617683963	47.717329510
1	46.014155748	39.267689924	47.723090641
6	46.521442967	40.787343237	46.313590398
8	46.555629330	42.047787510	46.048625656
8	46.930628555	39.917094169	45.530938184
6	44.744755288	46.240109581	44.632982586
7	44.501503196	45.633952865	45.845812913
1	43.835028422	45.927865365	46.571314647
6	45.321284545	44.574356880	45.947135174
1	45.330295285	43.888445262	46.786292126
7	46.080348075	44.457501600	44.866950104
6	45.734161509	45.496115722	44.033301464
1	46.214616954	45.642054219	43.068174085
26	47.717257663	42.939306905	44.676558745
8	49.038110382	41.621525885	44.872102550
8	48.930758109	41.742590316	41.807712048
6	47.770908611	42.150731324	41.833302017
6	46.613794244	43.141217702	39.789675267
6	47.891091977	43.545283706	39.042365510
8	47.240274764	42.827855414	42.814910389
8	48.061100064	43.101975071	37.885613037
6	46.838102193	41.895532553	40.668145268
8	48.721686639	44.275443491	39.675412056
1	46.266500603	43.965077557	40.429957566
1	45.820392503	42.908436408	39.063510401
1	47.288041108	41.090887948	40.069582711
1	45.867551393	41.566041042	41.069369517
7	51.913587024	36.640807804	45.618626950
6	51.474595459	36.516989932	46.968632445
7	50.184678595	36.900783580	47.205101390
6	49.343567683	37.278554074	46.264668194
6	49.745505728	37.373861558	44.851238847
6	48.878033772	37.750974369	43.840147138
6	51.074952545	37.037608327	44.604195370
8	52.196757851	36.071028521	47.848888191
7	48.071914759	37.558466163	46.626883248
1	47.973407451	37.678763054	47.640889089
1	47.537140471	38.230345583	46.055174812

1	51.465126525	37.102550774	43.586072350
6	48.350420692	38.527133140	42.928642571
1	48.644948742	39.583617917	42.827109141
1	47.576854133	38.180370565	42.229797162
1	48.538124741	40.778419573	44.866805940
1	49.907582052	46.489166446	47.789798540
1	46.428554092	40.806897453	48.519134411
1	44.266823384	47.176530507	44.345294792
1	52.871460134	36.484702495	45.377623358

**TS<sub>Ш1vβ</sub>**

6	49.602307169	45.853117417	46.797470800
7	49.578013768	46.459193143	45.558761307
1	49.877831103	47.417721454	45.341342511
6	49.057778339	45.580452590	44.677933727
1	48.924964121	45.792858972	43.618987027
7	48.743756321	44.443186678	45.285751753
6	49.078437382	44.595709573	46.612192547
1	48.907098425	43.807002417	47.342646982
6	45.744496944	40.466004538	47.674470719
1	44.668667844	40.443856274	47.905120487
1	46.018044524	39.408040732	47.542261917
6	45.926181290	41.135823151	46.302797072
8	46.633862112	42.227014828	46.247257813
8	45.422026103	40.593659061	45.324192019
6	44.638561363	46.253716062	44.603264648
7	44.452755578	45.706463091	45.853588856
1	43.826661590	46.032533100	46.600159395
6	45.239789994	44.628901809	45.958911501
1	45.301093877	43.995747057	46.834882721
7	45.916139003	44.438747965	44.833268443
6	45.559695046	45.452411757	43.971498896
1	45.984627578	45.525629483	42.973938603
26	47.331670835	42.980823776	44.607879232
8	48.556991164	41.732289468	44.500789918
8	49.098579064	42.443107644	41.888765847
6	47.883778917	42.583267683	41.836611793
6	46.628644551	43.016022244	39.639239722
6	47.835024933	43.559737701	38.864497300
8	47.162903934	43.209380282	42.738569744
8	48.054545759	43.114795400	37.713324752
6	47.077982579	41.992544210	40.697736584
8	48.565742861	44.390275282	39.482463564
1	46.098620925	43.837184227	40.144165275
1	45.929890939	42.522252261	38.946987756
1	47.728395336	41.239341233	40.235099665
1	46.189465805	41.502820136	41.125592678
7	51.949487811	36.549319371	45.791283616
6	51.577715912	36.311837179	47.163604866
7	50.413426955	36.882013345	47.559499389
6	49.623822261	37.577948459	46.755736336

6	49.955943947	37.805496179	45.356206036
6	49.319942851	38.812879488	44.496597612
6	51.154029428	37.284726778	44.960949632
8	52.270533753	35.620896911	47.895448889
7	48.509882186	38.107853924	47.295804926
1	48.472376331	38.089642702	48.318673925
1	48.083928199	38.897045860	46.823883687
1	51.506519420	37.494864387	43.945607332
6	48.093300960	39.327597604	44.539491402
1	48.157793029	40.686367762	44.250996888
1	47.176638406	39.041388358	45.057099111
1	50.029005904	39.301328838	43.813459973
1	49.832046249	46.374292029	47.726806206
1	46.276950134	40.873650872	48.533764257
1	44.183228179	47.202639980	44.319923151
1	52.883843480	36.402524761	45.466624844

**IM1<sub>vβ</sub>**

6	49.629293388	45.929016320	46.862466789
7	49.563178506	46.534729665	45.624755341
1	49.860263922	47.491530123	45.395196668
6	49.011702469	45.660809489	44.761781227
1	48.844307242	45.869911307	43.707156476
7	48.714352835	44.526999189	45.384299839
6	49.100430809	44.672356961	46.696533134
1	48.964298824	43.880813399	47.431813031
6	45.827115171	40.373224039	47.756316935
1	44.742750553	40.476862107	47.923253772
1	46.022801647	39.294651235	47.743434691
6	46.162433886	40.906331038	46.359188702
8	46.463449643	42.159211839	46.251488564
8	46.070043020	40.122877120	45.409707317
6	44.657633900	46.223568738	44.595742943
7	44.422128397	45.668238227	45.835549034
1	43.780410224	46.001017071	46.566264115
6	45.193419256	44.583358645	45.960996131
1	45.211782055	43.933802600	46.827628775
7	45.912579551	44.396434079	44.859900373
6	45.593302035	45.417861319	43.991622792
1	46.055436109	45.496651467	43.010713914
26	47.386628776	43.005332525	44.786916660
8	48.652696674	41.742745851	44.865579604
8	49.162166368	41.995322052	42.233298823
6	47.993005710	42.368724256	42.024223162
6	46.746567690	42.947174670	39.817054496
6	47.915373084	43.515971055	39.004730445
8	47.311034843	43.103092174	42.839132287
8	48.072923646	43.124969695	37.825687524
6	47.245579661	41.876487077	40.801591080
8	48.688759014	44.308317124	39.625840504
1	46.246891665	43.747919143	40.383077198

1	46.011637627	42.489786353	39.137334612
1	47.909924596	41.164416127	40.294158010
1	46.372980241	41.328266305	41.194657771
7	51.876443523	36.727308932	45.546870398
6	51.329273988	36.646585658	46.873807729
7	50.092732106	37.172715343	47.022858815
6	49.375830260	37.703111113	46.033908093
6	49.888641988	37.762000793	44.670112614
6	49.215996939	38.330024235	43.485206822
6	51.149834301	37.256151630	44.514176123
8	51.947146641	36.108473410	47.784372997
7	48.161069346	38.155315239	46.361345660
1	47.955879931	38.156159430	47.361800367
1	47.559774869	38.698853904	45.745609677
1	51.607312769	37.282801690	43.520225550
6	48.082187618	38.995680890	43.364833566
1	49.070369059	41.748847969	43.980842721
1	47.243140968	39.446598153	43.898394361
1	49.801942540	38.175606747	42.563260793
1	49.852813434	46.456003892	47.790038998
1	46.337874279	40.821488722	48.608520682
1	44.206943882	47.172386150	44.304725164
1	52.835381099	36.513495119	45.360604801

**TSRBva**

6	49.742087106	45.813903102	46.893430574
7	49.685773455	46.391964348	45.640956018
1	49.897983459	47.371364701	45.410262535
6	49.286784747	45.451999787	44.765524606
1	49.148826836	45.631446856	43.701606698
7	49.081121115	44.292675042	45.389463853
6	49.359413330	44.505989439	46.724918943
1	49.261064092	43.717334682	47.469735524
6	45.835043151	40.336467028	47.808361543
1	44.761257241	40.558807279	47.908273706
1	45.929184948	39.246941323	47.851527865
6	46.344244387	40.781676712	46.435882017
8	46.660715613	42.000014113	46.247855265
8	46.432029771	39.898353420	45.550545317
6	44.803972201	46.107981176	44.649219183
7	44.569567926	45.533561702	45.879640447
1	43.904583374	45.844953799	46.598865519
6	45.387420048	44.472740386	45.998651749
1	45.409438315	43.813130084	46.858054710
7	46.132836050	44.320045132	44.913625109
6	45.782507873	45.340916068	44.059267007
1	46.252069828	45.452969599	43.084592169
26	47.779009875	42.788893151	44.687339408
8	48.709309967	41.048011611	44.736557157
8	49.045538650	41.834183563	41.731079462
6	47.875827113	42.230065037	41.794823036

6	46.678036833	43.180316503	39.761582740
6	47.949849861	43.573086282	39.000145230
8	47.376806098	42.895591789	42.784914405
8	48.102586470	43.121898710	37.842970670
6	46.916448382	41.948708511	40.655186585
8	48.793610771	44.297284694	39.620946943
1	46.334495397	44.011188454	40.394960180
1	45.878114237	42.937973982	39.046014600
1	47.347122901	41.134422101	40.054696135
1	45.954245385	41.626256026	41.082051609
7	51.969312532	36.903663712	45.687642956
6	51.444878351	36.649535530	47.009851342
7	50.187020004	37.097136634	47.230858569
6	49.449210856	37.741173647	46.333590483
6	50.003455607	38.127821883	45.032472091
6	49.370674010	38.920244345	44.046117534
6	51.279903973	37.658402213	44.785442875
8	52.098561556	36.040448823	47.842548241
7	48.185426279	38.009515170	46.655578525
1	47.936559701	37.818736701	47.626751769
1	47.548972800	38.585032460	46.087040066
1	51.749825372	37.904174977	43.828180446
6	49.055731249	38.892546800	42.770776138
1	48.805263264	39.790031256	42.197852097
1	49.092575321	37.930534682	42.242124923
1	47.919090041	40.468857169	44.818375474
1	49.929098070	46.372088345	47.810776449
1	46.348593843	40.779033725	48.661864755
1	44.319579678	47.034373855	44.340629142
1	52.901588984	36.653398566	45.426490766

### IM2<sub>OH $\nu$</sub>

6	49.580121830	45.959458935	46.762853278
7	49.540740984	46.609087493	45.546994469
1	49.833175195	47.576007090	45.359185907
6	49.020369048	45.766039253	44.638361371
1	48.876113282	46.017959818	43.589545092
7	48.716267901	44.600530061	45.203468845
6	49.061095191	44.707372619	46.535352226
1	48.905637494	43.889482349	47.236647874
6	45.992341570	40.492525870	47.566943479
1	44.917275522	40.717499619	47.649651264
1	46.085260184	39.400368651	47.554198002
6	46.542834708	41.052325733	46.247238318
8	46.603998729	42.316222311	46.094778585
8	46.892551495	40.230311802	45.371501513
6	44.392179156	46.573826111	44.613060279
7	44.206002624	45.946343658	45.824410980
1	43.622196900	46.242984289	46.614064643
6	44.970013274	44.843134556	45.841558577
1	45.026653692	44.150391392	46.676092483

7	45.638800276	44.725080996	44.704800051
6	45.292800320	45.800050019	43.923779755
1	45.713224701	45.949506005	42.931671327
26	47.199636021	43.346688507	44.454367420
8	49.352325043	40.107664713	44.632618432
8	48.581140480	41.858079752	42.316155799
6	47.470573031	42.238524131	41.905395559
6	46.596086524	42.955962373	39.613683133
6	47.873014292	43.462742285	38.942755127
8	46.694638394	43.004365734	42.590935880
8	48.103918774	43.101790859	37.767707986
6	46.893017742	41.793824040	40.579611739
8	48.652924914	44.181796612	39.649566881
1	46.112036225	43.758756703	40.186926924
1	45.893808099	42.610268624	38.840583621
1	47.560138546	41.051133074	40.117436093
1	45.932510959	41.321504224	40.834178609
7	52.020512410	36.630546586	45.716868351
6	51.537709710	36.495522317	47.068560192
7	50.329138259	37.054956757	47.317426336
6	49.620072691	37.712080852	46.406003907
6	50.121888349	37.918429456	45.057128782
6	49.491747833	38.847566819	44.096464151
6	51.326453711	37.353717849	44.783200417
8	52.172654388	35.879214844	47.912407686
7	48.412413859	38.161436804	46.767275433
1	48.198612852	38.090058254	47.763614977
1	47.851296953	38.783220511	46.175383536
1	51.769546617	37.512488524	43.794455381
6	49.165764927	38.551429710	42.831512976
1	48.807867055	39.332559561	42.157478302
1	49.278181129	37.529585003	42.475313821
1	48.407565760	40.396931667	44.553564209
1	49.819960592	46.460897734	47.700458646
1	46.469786853	40.898081085	48.458929064
1	43.991735422	47.563212346	44.392091910
1	52.967764927	36.423761755	45.472072115

### TS<sub>H2 $\alpha$</sub>

6	49.690685098	45.870536741	46.829700525
7	49.632077077	46.470358730	45.588933814
1	49.867018853	47.446861340	45.370940135
6	49.193352709	45.553548266	44.704331639
1	49.051675703	45.750845780	43.643790808
7	48.962825795	44.393421203	45.310857261
6	49.269761575	44.576293790	46.642370382
1	49.162250152	43.779974663	47.377679717
6	45.796630190	40.329537034	47.775176214
1	44.736857402	40.612911646	47.852759430
1	45.855069753	39.240308779	47.850033014
6	46.381653192	40.728814921	46.422767719

8	46.479951274	41.963478552	46.125629058
8	46.766096447	39.807389206	45.667551815
6	44.716949643	46.193598430	44.634279774
7	44.486952478	45.612010451	45.861740969
1	43.835076144	45.923355124	46.592081927
6	45.290240578	44.538777087	45.963849582
1	45.305675123	43.868021820	46.815312386
7	46.022320784	44.386626239	44.870725022
6	45.678174948	45.417865859	44.027756089
1	46.141025306	45.531225416	43.050105233
26	47.627871000	42.867146030	44.647417938
8	48.839609979	41.285521087	44.730414108
8	49.010856690	41.836458554	41.740331115
6	47.846178021	42.250962257	41.758944544
6	46.682143127	43.173110241	39.698063361
6	47.962823128	43.575190286	38.959262033
8	47.315173888	42.956502631	42.701169105
8	48.128368795	43.134613046	37.798823243
6	46.921232743	41.945645326	40.595136794
8	48.800946554	44.290722155	39.596376693
1	46.321131216	43.998155295	40.328959585
1	45.897066302	42.926073722	38.967574476
1	47.379906458	41.134824445	40.010155068
1	45.953605462	41.614151785	41.003029052
7	51.945104477	36.649932005	45.614241520
6	51.478454923	36.468285924	46.973927044
7	50.193970874	36.841149225	47.206552886
6	49.369576475	37.305429515	46.282319066
6	49.828595362	37.523705409	44.899384018
6	49.096439701	38.181508444	43.931559719
6	51.146762120	37.152244926	44.641441516
8	52.201373097	35.983953939	47.826356486
7	48.107770645	37.578430645	46.642543058
1	47.979107467	37.606228098	47.660012427
1	47.532126252	38.252943219	46.106492172
1	51.548553626	37.302981144	43.635154783
6	48.567612810	39.103662201	43.222691466
1	48.803691941	40.205358644	43.660092600
1	47.886593235	39.044459089	42.369406651
1	48.232789590	40.644250925	45.163846741
1	49.892300683	46.407612151	47.756506057
1	46.322275176	40.777442929	48.618470342
1	44.248459568	47.132928678	44.340608086
1	52.901101792	36.484815670	45.371799313

#### IM2<sub>DSvβ</sub>

6	49.658748436	45.949419807	46.836767079
7	49.608934489	46.566362103	45.605825596
1	49.877736090	47.535271009	45.395921260
6	49.115397645	45.680166141	44.717288634
1	48.972818599	45.896981946	43.660293391

7	48.839721916	44.525527647	45.310979966
6	49.178782639	44.676876500	46.637171967
1	49.048029577	43.876355975	47.364121460
6	45.865055566	40.352101898	47.744759740
1	44.791986326	40.574492203	47.848278161
1	45.979965606	39.263794348	47.775489809
6	46.396508679	40.853569008	46.402204812
8	46.435865226	42.108525654	46.188142333
8	46.777814394	39.995042184	45.571028493
6	44.542293364	46.393968432	44.623508334
7	44.308570759	45.789274928	45.837205935
1	43.686528015	46.100062552	46.592131061
6	45.079347776	44.690553800	45.906094711
1	45.093885248	44.006542908	46.748540510
7	45.797150710	44.548815288	44.802227260
6	45.476833779	45.609445031	43.988908690
1	45.939494464	45.744346399	43.013596803
26	47.388798662	43.101102865	44.675681660
8	48.830893033	41.392365889	44.689527498
8	48.915827320	41.596218343	42.063698992
6	47.809957018	42.159306884	41.859151760
6	46.733269566	43.073000849	39.722328382
6	47.997103505	43.517340666	38.983508903
8	47.247235123	42.956924083	42.676530586
8	48.142516434	43.147551922	37.797699900
6	47.022275736	41.847949808	40.604083525
8	48.850762326	44.188392537	39.651536954
1	46.348314618	43.876692066	40.366063223
1	45.953336079	42.811322075	38.992461836
1	47.553812962	41.071066186	40.035119370
1	46.056774472	41.452182477	40.958990429
7	51.906197731	36.655795146	45.605620858
6	51.444472594	36.511452558	46.965086201
7	50.177206247	36.934688368	47.196397350
6	49.361779588	37.389646397	46.254339538
6	49.793671061	37.493630615	44.864039777
6	48.970887366	38.016201383	43.825872270
6	51.086495203	37.115029610	44.615826167
8	52.154684190	36.014664328	47.825191444
7	48.115587646	37.733387148	46.616445422
1	47.991886082	37.800681449	47.631379858
1	47.557541719	38.388304309	46.046604400
1	51.477613193	37.191300927	43.596831370
6	48.284072395	38.505593218	42.952655237
1	48.994566217	41.407853817	43.708895030
1	47.685154279	38.955422694	42.184398739
1	48.137042492	40.693956322	44.827866507
1	49.869645594	46.471404045	47.770106331
1	46.371789704	40.794288493	48.602523607
1	44.112637353	47.360797206	44.361391650
1	52.862165967	36.486933326	45.365656465



TSRBvβ

6	49.601883202	45.793400241	46.837977053
7	49.580280785	46.373443690	45.584825848
1	49.881879283	47.327551667	45.348947555
6	49.059950713	45.479132990	44.722904189
1	48.929404156	45.664343694	43.658443927
7	48.740250087	44.354712861	45.357696019
6	49.075698774	44.534528915	46.682232944
1	48.909369686	43.757997059	47.427046435
6	45.782748733	40.376446570	47.814719306
1	44.699416921	40.413468890	48.009387164
1	46.028062182	39.308229256	47.767435801
6	46.037669268	40.944277286	46.413650476
8	46.542513169	42.131035844	46.309782915
8	45.712528913	40.233428058	45.458717803
6	44.622071993	46.196030529	44.600347664
7	44.407815364	45.646924274	45.847103508
1	43.785528368	45.989036715	46.589812344
6	45.168561916	44.553126363	45.959020136
1	45.206320729	43.911324251	46.831278029
7	45.858115417	44.353707054	44.841314022
6	45.532960810	45.377513771	43.977905168
1	45.974711670	45.446897142	42.987443106
26	47.308677840	42.931836954	44.712047419
8	48.426448778	41.381107913	44.553938761
8	49.154528980	42.118967507	42.112155096
6	47.969876838	42.463069389	41.930109857
6	46.729664525	43.003438266	39.724326899
6	47.923241987	43.546612635	38.933168663
8	47.292818208	43.178408707	42.763589445
8	48.100917127	43.140154548	37.762424897
6	47.208488844	41.945236272	40.729870455
8	48.695550490	44.329849272	39.566262988
1	46.227309207	43.815534586	40.271121067
1	46.003506305	42.541042117	39.039150711
1	47.866930029	41.218181832	40.237255057
1	46.330483017	41.417260694	41.137420642
7	51.875006251	36.695952249	45.605903676
6	51.370666904	36.534728959	46.938087271
7	50.123982282	37.022925330	47.150329597
6	49.389760280	37.617207209	46.217223893
6	49.896748682	37.854758554	44.871780069
6	49.277577724	38.716014407	43.855255530
6	51.148483094	37.351974692	44.644298417
8	52.021978575	35.964746371	47.805268688
7	48.156617864	38.002658345	46.579934955
1	47.955589672	37.960953955	47.580402674
1	47.578773798	38.577846090	45.978391103
1	51.607184740	37.509748111	43.662883555
6	48.128705214	39.391988299	43.899341350
1	48.936764430	41.599926151	43.745916328

1	47.152445851	39.461356499	44.374286847
1	49.945694524	38.923734793	43.002695767
1	49.830406117	46.332341233	47.757426460
1	46.299443998	40.820787636	48.665398055
1	44.178821943	47.148845721	44.310969149
1	52.828865049	36.499532491	45.378868062

**IM2OHvβ**

6	49.526282877	45.901955661	46.718971604
7	49.472109642	46.550600665	45.505056781
1	49.758054447	47.518831610	45.314450041
6	48.933671966	45.702267520	44.605008869
1	48.767521475	45.966157250	43.562283679
7	48.641215444	44.536729250	45.170210653
6	49.003557992	44.649156994	46.495189414
1	48.835769454	43.841320261	47.205750331
6	45.894585799	40.374235900	47.687312967
1	44.810990880	40.539982459	47.802905678
1	46.034194770	39.287742995	47.699277273
6	46.334540880	40.877350815	46.303393020
8	46.641630264	42.124108533	46.171252355
8	46.354843289	40.058863088	45.376167888
6	44.463384003	46.340184809	44.568544810
7	44.301767328	45.757395920	45.804660127
1	43.736880786	46.092005194	46.593984447
6	45.025478934	44.624957951	45.825600004
1	45.094151139	43.959458261	46.680836811
7	45.640137989	44.436701499	44.667248802
6	45.301285238	45.503185213	43.868191278
1	45.677630266	45.597810334	42.852193259
26	47.260133432	43.007133765	44.489249075
8	48.900209850	41.507611614	44.039568934
8	48.074556560	41.163505884	41.733927621
6	47.248102428	42.088965999	41.594651979
6	46.404734623	43.470494858	39.598993697
6	47.737069393	43.693987694	38.874655598
8	47.068419473	43.023069261	42.463557555
8	47.908161721	43.146389933	37.765703002
6	46.387947697	42.135861454	40.351566995
8	48.612835250	44.400580358	39.476421794
1	46.196807187	44.285066880	40.304063669
1	45.593758768	43.430430600	38.857634373
1	46.716151613	41.341301798	39.680637861
1	45.358069693	41.907620474	40.667982403
7	51.981539791	36.709317149	45.843156729
6	51.396264716	36.537197640	47.138898861
7	50.157296329	37.065632612	47.294909998
6	49.548779281	37.794490652	46.365561711
6	50.228813348	38.201195775	45.145560111
6	49.729366076	39.264774924	44.253964329
6	51.423487494	37.583795534	44.929978337

8	51.962033656	35.911689652	48.027741201
7	48.276987522	38.146439720	46.598927904
1	47.891359285	37.864502231	47.495328398
1	47.704201638	38.698272401	45.954141539
1	51.989453611	37.815626944	44.020875086
6	49.316255401	40.445900200	44.752382600
1	48.657079389	41.272533162	43.040408097
1	49.313879188	40.636291073	45.831947337
1	49.760589243	39.111086399	43.169836793
1	49.774050719	46.399012169	47.656848593
1	46.383940090	40.815756303	48.555448575
1	44.053676307	47.320625784	44.325764204
1	52.913346477	36.419016342	45.625362720

**TS<sub>H2νβ</sub>**

6	49.620443274	45.853805273	46.850046634
7	49.565807988	46.433346300	45.598382914
1	49.853428592	47.390509683	45.356828036
6	49.039717747	45.533337865	44.746194115
1	48.889954739	45.715469344	43.683764138
7	48.745905442	44.406287571	45.387714361
6	49.107971627	44.588114705	46.704403646
1	48.971619769	43.810979026	47.454815863
6	45.829237039	40.364133610	47.824860809
1	44.746933127	40.507814494	47.969407156
1	45.987054105	39.280634139	47.825562032
6	46.213350194	40.870502061	46.431102853
8	46.521288701	42.128105975	46.317872231
8	46.168703514	40.081634061	45.489103108
6	44.671647466	46.166743558	44.612329549
7	44.436365869	45.618510880	45.856012556
1	43.799864488	45.961045948	46.587315056
6	45.196240188	44.526106578	45.982810394
1	45.217951749	43.881930725	46.853294089
7	45.907367494	44.327128280	44.877946825
6	45.595437910	45.349492925	44.006682282
1	46.052241593	45.417075443	43.022721057
26	47.361137933	42.919825557	44.779369137
8	48.623411730	41.549838392	44.744820572
8	49.185611317	42.075853352	42.213870261
6	47.997334337	42.382472159	42.013431513
6	46.748238085	42.899528471	39.800219532
6	47.918960657	43.483464315	39.001213560
8	47.288971571	43.081368856	42.841857369
8	48.092902992	43.097891299	37.822988641
6	47.258772690	41.851534137	40.803468284
8	48.677043072	44.280317012	39.634905755
1	46.223771313	43.696652684	40.348878002
1	46.032812892	42.419180196	39.115729517
1	47.935835247	41.141668919	40.309015921
1	46.395624350	41.296365432	41.206985076

7	51.845461269	36.844928773	45.630892601
6	51.348958741	36.640039116	46.964164173
7	50.121856128	37.156232827	47.217581861
6	49.406508554	37.828598290	46.321108880
6	49.919379122	38.140202778	44.997968723
6	49.216177616	39.060428356	44.070580192
6	51.142044690	37.601898561	44.718823878
8	51.991594567	36.006106627	47.793350685
7	48.172381837	38.208352040	46.668800230
1	47.921002149	38.068271710	47.646734942
1	47.556959101	38.743629199	46.052165243
1	51.601515145	37.800725048	43.745121091
6	49.134433188	38.924807773	42.770690216
1	49.120403837	41.778515741	43.925548054
1	49.391866828	38.228306816	41.975187953
1	48.770529710	40.180018716	44.532740931
1	49.848821977	46.396691224	47.767208201
1	46.340348733	40.807968576	48.679169121
1	44.222522538	47.113346701	44.311835603
1	52.786185232	36.616395704	45.380326131

**IM2<sub>DSvp</sub>**

6	49.669847273	45.939147186	46.870574689
7	49.622452862	46.558216425	45.640384009
1	49.905479625	47.522540730	45.428764736
6	49.112008625	45.681373666	44.753674486
1	48.960866183	45.905340867	43.699181569
7	48.823828824	44.530484435	45.347176817
6	49.172936210	44.673203136	46.671493832
1	49.037228529	43.872077307	47.396928349
6	45.821862055	40.367704530	47.769110609
1	44.751766627	40.593487238	47.885655734
1	45.934030169	39.279050200	47.791503803
6	46.340404804	40.871906613	46.423708083
8	46.345855092	42.123170069	46.192041713
8	46.753368871	40.013310198	45.607726951
6	44.522716658	46.407952597	44.610943158
7	44.283867347	45.813297660	45.828549225
1	43.664438045	46.130461758	46.582321629
6	45.046870723	44.711690335	45.907850421
1	45.055880088	44.034308049	46.755293187
7	45.763442209	44.557201112	44.804968700
6	45.452142723	45.613222034	43.982167083
1	45.918057837	45.735328975	43.006751646
26	47.353980789	43.134274928	44.717470586
8	48.811513684	41.460174424	44.830465979
8	49.130439414	41.754818268	42.239104840
6	48.025402179	42.280912181	41.941877182
6	46.816771275	42.938900597	39.734299784
6	47.982424604	43.500046243	38.915390583
8	47.395479758	43.089776630	42.694880939

8	48.112094160	43.121300195	37.728594305
6	47.316462678	41.835249940	40.677755772
8	48.783451472	44.265484645	39.534319627
1	46.345405122	43.729744735	40.336415528
1	46.059688260	42.517240153	39.056142386
1	47.985458393	41.139619844	40.152221649
1	46.434921629	41.276881438	41.040756294
7	51.928312577	36.685540279	45.641562889
6	51.515655761	36.552651002	47.022088730
7	50.274882292	37.013460641	47.307585259
6	49.441169246	37.505598668	46.396770029
6	49.816122305	37.576983499	44.985322853
6	48.948659985	38.117345438	43.997162743
6	51.082845615	37.159531162	44.681782428
8	52.250127551	36.033195797	47.847536985
7	48.243072816	37.930078997	46.800436791
1	48.118721979	37.963195825	47.815627872
1	47.638726452	38.525501522	46.214281964
1	51.432218876	37.219219292	43.646332282
6	48.178656879	38.630641670	43.212446727
1	49.071372437	41.501714102	43.872875322
1	47.485348269	39.114745189	42.555438898
1	48.137300677	40.736118975	44.910664193
1	49.878185525	46.460860289	47.804639962
1	46.341250948	40.806487563	48.621033110
1	44.101614940	47.378350063	44.348132521
1	52.875819782	36.515387182	45.370914571

**Snapshot 2  
RC**

6	50.538938003	46.484527239	46.102625336
7	50.512849538	46.768948987	44.752940046
1	50.841478686	47.632250921	44.299938904
6	49.920805006	45.738490179	44.118614357
1	49.775758501	45.685208306	43.041214510
7	49.558422198	44.810582953	44.995999449
6	49.933329657	45.259453358	46.241252260
1	49.726167173	44.689272699	47.144769897
6	46.012288504	41.975158287	48.262482128
1	44.944558298	42.184840290	48.417445351
1	46.120074083	40.889143012	48.399969060
6	46.371084374	42.273584913	46.797712025
8	47.427834459	42.981008094	46.567892727
8	45.672764603	41.804672364	45.889049880
6	45.628674697	46.694417785	44.020132285
7	45.386049506	46.493679206	45.363003318
1	44.817967495	47.067859736	45.998090980
6	46.083492065	45.410127351	45.743878484
1	46.088021997	45.024004064	46.755178769
7	46.753478168	44.893713212	44.719626364
6	46.479798215	45.691953570	43.630908115

1	46.893058806	45.488080425	42.646307273
26	48.131131921	43.287823888	44.777982618
8	49.187919101	42.068503498	44.933024149
8	49.162356030	41.583549459	42.142739303
6	48.007376164	41.986514875	42.152229081
6	46.984149589	42.626988996	39.942697357
6	48.297267430	42.600495170	39.137183595
8	47.518647467	42.847225269	43.021718800
8	49.063279433	43.597294882	39.233221768
6	47.023253295	41.579957488	41.073437911
8	48.508947103	41.561671329	38.461544276
1	46.804120584	43.629324324	40.357387897
1	46.147172234	42.379660006	39.269698961
1	47.365862575	40.621769486	40.657799345
1	46.021664392	41.463770623	41.509405932
7	52.064682253	36.905351322	46.483344517
6	51.736011073	37.397625522	47.776948296
7	50.709628305	38.274242910	47.835322759
6	50.040777362	38.682749717	46.774987588
6	50.195937296	38.041285776	45.479798685
6	49.351460341	38.270990761	44.298109761
6	51.275369273	37.198223195	45.399635407
8	52.367508717	37.065461159	48.778272494
7	49.200402006	39.741806010	46.956234801
1	49.412817940	40.256105165	47.823137665
1	48.997713552	40.335669145	46.146526146
1	51.530098140	36.734349842	44.443359798
6	48.077609970	38.693826048	44.255749810
1	47.579536453	38.805707035	43.289173306
1	47.466873648	38.911663005	45.134650074
1	49.844609017	38.035794943	43.348656856
8	44.889486435	39.277030373	46.566915919
1	43.931498017	39.132962359	46.465572575
1	45.027968380	40.182616453	46.220579480
1	50.848629511	47.191799170	46.871991900
1	46.599136548	42.514554325	49.005939326
1	45.231063290	47.535615578	43.452365807
1	52.940457995	36.448918894	46.326313349

### TS<sub>H1vα</sub>

6	50.561269072	46.424698337	46.105591735
7	50.525287881	46.693771697	44.752658169
1	50.813952690	47.568506605	44.293042746
6	49.998989558	45.623928395	44.126435596
1	49.855592768	45.557277981	43.049534097
7	49.687186892	44.680558981	45.010653785
6	50.023668554	45.169764842	46.254447935
1	49.843041493	44.603080769	47.165979745
6	46.029855162	41.913491913	48.274257057
1	44.961658179	42.119770084	48.426317240
1	46.145835432	40.832756472	48.445094354

6	46.382686585	42.170964315	46.800652885
8	47.526338137	42.722901531	46.538879759
8	45.600614724	41.801805477	45.918179754
6	45.691220040	46.623437124	44.069414615
7	45.444595719	46.407369105	45.408313125
1	44.870228087	46.973888498	46.043325046
6	46.160663513	45.326876826	45.777499089
1	46.154531968	44.926777392	46.783404935
7	46.847045103	44.830571751	44.758348804
6	46.562320475	45.637052579	43.679162693
1	46.977910468	45.452312546	42.691139238
26	48.319741889	43.090481462	44.776336358
8	49.489330742	41.752445289	44.898561878
8	49.054368231	41.522730620	41.921306803
6	47.907256580	41.947105839	42.055004826
6	46.893216623	42.689735611	39.879537079
6	48.213107890	42.619821602	39.086969315
8	47.514783922	42.719834234	43.032319739
8	48.990674976	43.610015578	39.162967826
6	46.866575797	41.633133918	41.000112312
8	48.416527302	41.564559029	38.435706557
1	46.753559063	43.695733397	40.300432026
1	46.053141003	42.485357478	39.195507855
1	47.139073886	40.661433861	40.565245741
1	45.863699882	41.580079935	41.443902276
7	52.093778397	37.123424594	46.557442387
6	51.824375127	37.464424916	47.931864507
7	50.970647582	38.491150638	48.144002040
6	50.370997973	39.151702621	47.161720667
6	50.433567790	38.667908041	45.785038949
6	49.628275796	39.236374399	44.729346699
6	51.376745982	37.693792053	45.543780834
8	52.356051035	36.853784845	48.848835359
7	49.698312204	40.269417206	47.443776924
1	49.752900578	40.618673080	48.405537709
1	49.395550299	40.907053476	46.701764903
1	51.570156641	37.367645519	44.516592500
6	48.994204382	38.664610309	43.706074938
1	48.591104718	39.260905734	42.883535269
1	48.860513618	37.577631937	43.674457328
1	49.548193239	40.507740039	44.758229252
8	44.592588624	39.387085096	46.762052490
1	43.623567395	39.342240293	46.659710261
1	44.823780285	40.238111551	46.338345728
1	50.863009267	47.145519789	46.865484237
1	46.617209406	42.469600929	49.004890391
1	45.272475378	47.455424449	43.503272118
1	52.932387428	36.631560178	46.323397979

**TS<sub>IIIvβ</sub>**

6	50.486646396	46.447602494	46.003096055
---	--------------	--------------	--------------

7	50.435414349	46.771362417	44.663451453
1	50.761538673	47.644337769	44.228352483
6	49.823105466	45.762914472	44.012367921
1	49.652380904	45.750664129	42.937723670
7	49.472111933	44.808492121	44.865723921
6	49.875225128	45.220870664	46.115791473
1	49.676570628	44.627824441	47.006567739
6	46.045478903	41.955914640	48.183601999
1	44.980932174	42.177694402	48.346733131
1	46.131685936	40.867668279	48.318267522
6	46.385151509	42.256155439	46.712277147
8	47.431763071	42.966101991	46.450515953
8	45.669049641	41.775892334	45.821039941
6	45.563032932	46.750024434	44.005429979
7	45.351714655	46.529606912	45.349946721
1	44.811924597	47.104557988	46.009131755
6	46.036828771	45.425427474	45.694638758
1	46.064749321	45.021769846	46.698893831
7	46.667102375	44.915741347	44.642701074
6	46.382279187	45.737739742	43.575058139
1	46.766222613	45.541980081	42.577156618
26	47.990860372	43.324657090	44.595789516
8	49.167710542	42.060344569	44.590393665
8	48.896455491	41.734774638	41.827335184
6	47.733141363	42.105276781	41.930047911
6	46.726715012	42.723379775	39.718765368
6	48.080298810	42.687340222	38.983297925
8	47.274407554	42.901047078	42.870741049
8	48.832037209	43.692827737	39.100668360
6	46.716579522	41.712742629	40.880317817
8	48.336009274	41.638682071	38.339505583
1	46.522112302	43.735098633	40.096843541
1	45.921859542	42.450254600	39.017088343
1	47.029351333	40.730352932	40.500765657
1	45.710498994	41.648144813	41.315360381
7	52.075209181	36.760928441	46.648224490
6	51.804578797	37.078684515	48.015684448
7	50.825700128	38.003401284	48.226460418
6	50.186507866	38.608068403	47.242430447
6	50.320287695	38.190682293	45.857472561
6	49.712091059	38.950506896	44.752698789
6	51.331416156	37.294335018	45.630541079
8	52.423549958	36.574327875	48.937004401
7	49.400193512	39.673363071	47.569817414
1	49.624050421	40.096906635	48.478875516
1	49.222827713	40.348315788	46.826931605
1	51.588964569	37.018649176	44.603228362
6	48.591686104	39.680445654	44.796554173
1	48.757995390	40.962078231	44.383382859
1	47.756493881	39.625433868	45.502202742
1	50.359191404	39.045604228	43.871941081
8	44.998243843	39.234527899	46.573002325



1	44.048049057	39.040990364	46.495106704
1	45.084014987	40.136186071	46.199932513
1	50.819641493	47.136049866	46.779769604
1	46.635855803	42.486653613	48.930487922
1	45.176445424	47.612623472	43.462714291
1	52.950059043	36.340701062	46.407352823

**Snapshot 3  
RC**

6	41.042599731	45.306432175	48.454551429
7	40.939489311	46.109104472	47.339842665
1	40.199280012	46.791987798	47.141659245
6	41.976888818	45.844245443	46.528396858
1	42.147553815	46.333572644	45.572610612
7	42.742890333	44.903616573	47.062967101
6	42.178031853	44.553432344	48.266667888
1	42.611495025	43.782627915	48.897411619
6	44.801318356	39.857780745	47.763715139
1	44.529756784	38.966839481	47.175436375
1	45.860069716	39.724077641	48.038481308
6	44.734628873	41.066973899	46.828586036
8	44.003270941	42.086302279	47.125483672
8	45.398889404	41.028542941	45.780126761
6	40.483974318	42.713927330	43.757636366
7	40.401354859	41.771679284	44.759986808
1	39.649614115	41.086094232	44.917788210
6	41.490468827	41.911615932	45.537675991
1	41.705520830	41.293665977	46.401293976
7	42.279529658	42.877779244	45.081355257
6	41.650427875	43.397099371	43.971176928
1	42.081270962	44.218853429	43.411365804
26	44.044023273	43.672386525	45.962058359
8	45.418174851	44.226142295	46.597702329
8	46.213107899	44.114550508	43.535667852
6	45.062138990	44.487991332	43.331989317
6	43.993086174	46.113614808	41.621075201
6	45.152697802	47.120672864	41.539031148
8	44.166415086	44.636535339	44.278791362
8	45.585450394	47.591331618	42.615976478
6	44.538788146	44.710826692	41.922130462
8	45.620326963	47.349262147	40.387166087
1	43.284221937	46.422725284	42.406063998
1	43.465877983	46.086842270	40.655673841
1	45.356459480	44.469074986	41.228501138
1	43.743547313	43.961738634	41.769516786
7	50.531442250	43.262060645	49.790201436
6	49.995644533	42.079351282	50.398869125
7	49.379432698	41.217581793	49.544178858
6	49.196865414	41.465969894	48.241798489
6	49.527003532	42.765977501	47.662379739
6	49.212242051	43.305449359	46.335672367

6	50.227758730	43.588063057	48.497774695
8	50.114749214	41.879883226	51.600956683
7	48.694349121	40.484023447	47.491098097
1	48.620856249	40.523497551	46.477642849
1	48.513925756	39.566905436	47.913306023
1	50.542708381	44.566256568	48.123848722
6	48.541452075	42.805301567	45.288190932
1	48.394987730	43.441642511	44.415904071
1	48.091018766	41.815574579	45.235467801
1	49.584170634	44.330098917	46.221849135
8	47.541820117	39.628561830	44.883548209
1	46.718702152	40.015886365	45.262481993
1	47.433372686	39.793196154	43.934659803
1	40.256363758	45.229861983	49.205575608
1	44.195901646	39.874834561	48.669941984
1	39.717419305	42.896097037	43.004459801
1	51.111060129	43.915092660	50.277607629

**TS<sub>H1 $\alpha$</sub>**

6	41.099120306	45.347621453	48.445063228
7	41.030565695	46.115919819	47.301483850
1	40.276557797	46.764239739	47.043868575
6	42.132389490	45.879226668	46.568861550
1	42.336731708	46.346726641	45.609220692
7	42.909275789	44.989920684	47.178223080
6	42.275118400	44.644756266	48.351786292
1	42.686800709	43.898081188	49.022390511
6	44.727467046	39.977559883	47.928226636
1	44.502957655	39.157720975	47.229997587
1	45.791909702	39.877973037	48.195345569
6	44.555122705	41.314220745	47.211608952
8	43.964077116	42.299896140	47.747517976
8	45.040466715	41.470660177	46.049385507
6	40.618015280	42.722982971	43.895296224
7	40.515221885	41.757669592	44.872458501
1	39.753435781	41.079122438	45.004797020
6	41.590873992	41.885815424	45.677323248
1	41.769972106	41.249082397	46.536455746
7	42.394060527	42.856500736	45.264219933
6	41.783096569	43.397584907	44.154276686
1	42.220242020	44.236430967	43.626072065
26	44.299377564	43.712170357	46.205069654
8	45.852889209	44.107634283	46.871716548
8	46.276161829	44.186142676	43.498858288
6	45.103757770	44.566145658	43.420268354
6	43.911182532	46.163565965	41.750960688
6	45.061284263	47.166041378	41.557306914
8	44.330943696	44.735831618	44.454044130
8	45.532902807	47.709997801	42.584758836
6	44.469223442	44.764067379	42.049373190
8	45.486908409	47.328905588	40.379535690

1	43.259678458	46.499267254	42.573853980
1	43.316613300	46.112145907	40.826439741
1	45.229466259	44.501363615	41.300951202
1	43.661196321	44.017466883	41.968742463
7	50.353868685	43.289133543	49.815456801
6	49.962280675	42.085800974	50.513148846
7	49.274765269	41.178615445	49.767476771
6	48.854957972	41.430690022	48.529177338
6	48.965367148	42.765344314	47.942251727
6	48.240887859	43.165225251	46.747806732
6	49.779227120	43.631267622	48.623732973
8	50.260987309	41.918382548	51.683940571
7	48.332344177	40.449236642	47.798308208
1	48.099945960	40.560045844	46.804070402
1	48.348210609	39.482746526	48.140593901
1	49.964530318	44.629717282	48.215637818
6	48.591701212	43.206112571	45.465349712
1	47.891378981	43.573807323	44.712430310
1	49.577853920	42.859051375	45.137258627
1	47.086640940	43.542905314	46.935245531
8	47.218738933	40.008777218	45.234202465
1	46.397133029	40.487716295	45.485499384
1	47.293581149	40.190543676	44.285185988
1	40.296501350	45.278544041	49.179296460
1	44.118158217	39.870890053	48.825685056
1	39.874299023	42.908576698	43.120371447
1	50.987798523	43.956946886	50.205496280

**TS<sub>III</sub>β**

6	41.062399257	45.275117846	48.390046220
7	40.940098039	46.084204719	47.282408037
1	40.201490660	46.774030766	47.104604381
6	41.957122916	45.810386428	46.446093487
1	42.103548404	46.300080715	45.486524792
7	42.728943158	44.861073363	46.954169248
6	42.186827488	44.512112496	48.168730329
1	42.626146212	43.733089426	48.786013839
6	44.756680350	39.792088951	47.635499027
1	44.479615398	38.872269014	47.096982969
1	45.824207268	39.680340379	47.888756771
6	44.659063758	40.953158404	46.643660850
8	43.999079831	42.018124850	46.930026372
8	45.266552419	40.822947023	45.563853400
6	40.382154630	42.692777174	43.686767145
7	40.297754341	41.783994107	44.717961588
1	39.548252467	41.101961437	44.898824731
6	41.396573510	41.933645369	45.480325782
1	41.617434324	41.337048510	46.356998104
7	42.190356476	42.874230280	44.983493037
6	41.557955796	43.368642277	43.865722534
1	41.994729818	44.166985973	43.277424793

26	43.967095908	43.612639927	45.760565591
8	45.435600721	44.279084315	46.392305122
8	46.146927400	44.115066467	43.405978616
6	44.993011894	44.461373193	43.170335156
6	43.937060781	46.079484913	41.454159690
6	45.075261914	47.110062246	41.426834167
8	44.065754593	44.587994196	44.091019631
8	45.429262046	47.615810617	42.517173096
6	44.501413934	44.682439909	41.750097198
8	45.613992040	47.324365406	40.304533351
1	43.195201994	46.358122595	42.219292703
1	43.445378571	46.057319451	40.470013786
1	45.336642851	44.460822060	41.070899093
1	43.718890172	43.924902601	41.577039203
7	50.641941275	43.229972972	49.847981861
6	50.188500208	42.025503597	50.481875445
7	49.548358384	41.149939848	49.659263310
6	49.208863625	41.436945347	48.401991703
6	49.341905770	42.796277026	47.887075617
6	48.506683881	43.426115974	46.861126711
6	50.127186085	43.617494482	48.641130151
8	50.392865191	41.819328446	51.669845909
7	48.709053342	40.463097127	47.640716588
1	48.558869294	40.537500629	46.632876069
1	48.637430128	39.512055860	48.018686422
1	50.291361639	44.647840338	48.310038017
6	47.479067871	42.913978683	46.189677751
1	46.418895348	43.723801662	46.038631180
1	47.154395668	41.891296129	46.017854131
1	48.665088614	44.510353606	46.802934333
8	47.670776533	39.741163885	44.991943104
1	46.731119640	39.952557062	45.202050946
1	47.760634084	40.050045174	44.078817603
1	40.292930668	45.210014714	49.159297153
1	44.179906761	39.846257238	48.558789525
1	39.606963471	42.880838423	42.943948890
1	51.206024035	43.915144128	50.308767734

**Snapshot 4  
RC**

6	43.469423878	40.484751230	48.241144251
7	42.534493528	41.210068201	47.534571617
1	41.554395402	41.362065719	47.803409609
6	43.120524903	41.662403711	46.407503352
1	42.605840533	42.257059877	45.652573797
7	44.385837072	41.257986111	46.355571887
6	44.621597263	40.524792363	47.493830763
1	45.587368031	40.064907446	47.692784967
6	48.767712429	38.214595045	44.609183532
1	48.668427622	37.328666514	43.962872137
1	49.792453461	38.581457910	44.474963274

6	47.839065212	39.312451323	44.055332537
8	46.790347476	39.603989934	44.753221219
8	48.140681517	39.833620718	42.982883630
6	42.295312555	39.151501153	43.135432117
7	43.104669456	38.088324278	43.482596216
1	42.902762961	37.082696440	43.416782134
6	44.275776052	38.586893502	43.913900577
1	45.108769152	37.981245172	44.252605846
7	44.269022517	39.911779901	43.852345796
6	43.037085615	40.282108771	43.368309398
1	42.780214422	41.327415933	43.232937745
26	45.693640264	41.210283057	44.678182991
8	46.845967238	42.111228004	45.371727630
8	45.640358079	44.477362468	44.291581883
6	45.414703597	43.753253032	43.340034801
6	44.075913589	44.402405173	41.240716242
6	43.323135759	45.591603407	41.840184893
8	45.100898487	42.468365422	43.423298730
8	42.339008340	45.343743780	42.588986243
6	45.457862187	44.245544526	41.898562632
8	43.753716576	46.745311338	41.572609344
1	43.486530601	43.482099213	41.350618556
1	44.225829313	44.588792417	40.166026503
1	45.952674734	45.221970913	41.900949592
1	46.059934914	43.530002697	41.315693266
7	52.673316333	43.881477702	48.263618266
6	52.539907193	42.785406630	49.185933041
7	52.091788262	41.619209984	48.669084045
6	51.806834621	41.454085594	47.382950873
6	51.776805495	42.581920308	46.452144941
6	51.153064939	42.604644904	45.123285871
6	52.250422414	43.763006891	46.968173104
8	52.859116001	42.928584657	50.359088373
7	51.529883718	40.204782677	46.977624622
1	51.546745252	39.493281307	47.712460629
1	51.641793297	39.897945303	46.008858964
1	52.250641901	44.659845972	46.341919505
6	50.398534716	41.678632461	44.512572451
1	49.931021434	41.885154006	43.548141539
1	50.159591752	40.716154477	44.958923698
1	51.268781366	43.565947073	44.617521651
1	43.237563818	39.894944842	49.127956895
1	48.633459928	37.878274249	45.637255470
1	41.253535810	39.045759780	42.832798183
1	52.959011251	44.779586861	48.597909827

**TS<sub>HIvα</sub>**

6	43.730003318	40.506662772	48.343991500
7	42.858584292	41.314113301	47.642629648
1	41.866845727	41.468032865	47.860993888
6	43.528560001	41.839440357	46.597393168

1	43.078095296	42.501197531	45.858826377
7	44.787780743	41.406443899	46.588663469
6	44.927759645	40.572064100	47.675377999
1	45.865681212	40.067357124	47.898261429
6	48.938990985	38.128380848	44.618980699
1	48.829809389	37.251059918	43.963331876
1	49.977402333	38.464433669	44.509406252
6	48.061960114	39.262456080	44.061613257
8	47.054541467	39.630732462	44.772664916
8	48.375785586	39.752377521	42.975579217
6	42.499036646	39.225431612	43.287905937
7	43.306526054	38.151644612	43.605550269
1	43.103041723	37.150177255	43.497608059
6	44.467646647	38.643894761	44.079674817
1	45.302296279	38.027113123	44.392838278
7	44.459055566	39.968565700	44.080066514
6	43.232022994	40.348454962	43.588201056
1	42.961914495	41.394463178	43.480476554
26	46.069765863	41.329233266	44.887463925
8	47.491446396	42.193008374	45.485280601
8	45.812117975	44.637487572	44.362980885
6	45.599543035	43.850352152	43.456815081
6	44.116247537	44.312508176	41.405961839
6	43.346216343	45.546622754	41.887363834
8	45.384471870	42.558661291	43.630612247
8	42.294605680	45.354314212	42.556660995
6	45.536966507	44.265251563	41.992980030
8	43.814927619	46.678193592	41.593452657
1	43.557157867	43.398502939	41.649236358
1	44.200959914	44.373613776	40.309106701
1	45.971336360	45.265776794	41.907261978
1	46.143719479	43.547693664	41.417955573
7	52.176031819	43.899762850	48.149668640
6	52.278745028	42.782818672	49.052795733
7	51.807845228	41.597837996	48.600677339
6	51.201835845	41.472050638	47.428300590
6	50.879491313	42.619106551	46.582201400
6	50.021115692	42.425614504	45.412810772
6	51.431087347	43.809580500	46.995177241
8	52.797435053	42.919609002	50.154787008
7	50.893742432	40.241068091	47.009015364
1	51.109487367	39.460408753	47.631870612
1	50.599356683	40.070239182	46.054679168
1	51.278833538	44.717098458	46.404352430
6	50.345723959	42.123553124	44.158405941
1	49.574022311	41.912959381	43.411743478
1	51.397792282	42.034467198	43.864350711
1	48.713943935	42.341408566	45.549164064
1	43.439264976	39.881427146	49.188159110
1	48.770569652	37.789059357	45.641019106
1	41.475238201	39.124083246	42.927860695
1	52.527883026	44.790408224	48.437633976

TS<sub>HIvβ</sub>

6	43.586758111	40.514542253	48.199532853
7	42.690381599	41.303921511	47.509987746
1	41.708673753	41.466270567	47.763097066
6	43.318569150	41.786760894	46.416374067
1	42.845036021	42.431868855	45.676594470
7	44.569883104	41.340530729	46.364870103
6	44.752279776	40.545259775	47.471724389
1	45.695570100	40.038512809	47.664350644
6	48.796631812	38.234551383	44.630542819
1	48.744991838	37.370368025	43.951220120
1	49.806400859	38.652236330	44.529823979
6	47.840356367	39.315854092	44.098837198
8	46.927086078	39.748153692	44.911160556
8	48.007589353	39.731506765	42.953675279
6	42.405068224	39.157735797	43.163601635
7	43.220235883	38.106991149	43.539330367
1	43.021124232	37.099324153	43.490986538
6	44.387363346	38.623296436	43.959854811
1	45.220713334	38.030466440	44.319531676
7	44.373044154	39.947473087	43.861642329
6	43.136788890	40.298616313	43.369073498
1	42.875969082	41.339882296	43.212293038
26	45.787192240	41.260879705	44.562638377
8	47.072463176	42.413286690	44.988508765
8	45.286178699	44.565115090	44.358068824
6	45.209903598	43.814556603	43.402821227
6	44.068535043	44.472812539	41.201411565
6	43.291676732	45.653823227	41.781978740
8	44.932318671	42.523264106	43.485205356
8	42.293723166	45.396388666	42.507473261
6	45.390244162	44.288387812	41.967034803
8	43.726162703	46.811004667	41.533960407
1	43.463249347	43.557206657	41.245448256
1	44.303787690	44.684199667	40.147095467
1	45.903345620	45.254816601	42.004687801
1	46.021779769	43.555057361	41.440827820
7	52.644824102	43.869805671	48.293797393
6	52.637992921	42.772825218	49.226315520
7	52.256751437	41.573561519	48.727816248
6	51.765464264	41.429457463	47.508464694
6	51.417932455	42.585886381	46.686038464
6	50.338872061	42.584119616	45.676921242
6	51.946891101	43.774127508	47.114441304
8	52.992872096	42.940563479	50.384773044
7	51.562652839	40.177259322	47.065902103
1	51.747181391	39.433679333	47.740241599
1	51.524252716	39.931443091	46.075482200
1	51.751328172	44.692361517	46.552877587
6	49.383390700	41.662113346	45.567039772
1	48.093710310	42.018141244	44.983981002

1	49.269519508	40.731016711	46.121567744
1	50.253844364	43.510504871	45.092129084
1	43.327000435	39.917643085	49.073778045
1	48.659898719	37.863603021	45.646302978
1	41.369557980	39.045237053	42.842463214
1	52.936875475	44.776819185	48.597120612

**Snapshot 5  
RC**

6	41.812132519	35.478303021	43.098375750
7	41.261531831	36.666323757	43.528427776
1	40.327397131	36.783815654	43.940612825
6	42.147239648	37.652765099	43.290891909
1	41.986471970	38.703417698	43.532901080
7	43.234952556	37.147563125	42.721216318
6	43.050532713	35.793018749	42.597700125
1	43.802687765	35.143868948	42.154970414
6	47.091338500	35.767728432	39.028467744
1	46.935936599	36.005255614	37.963073500
1	48.169955867	35.654105192	39.168812504
6	46.668742867	36.973667676	39.872429821
8	45.411908937	37.051578955	40.220650877
8	47.508193904	37.828976795	40.138560896
6	41.232991228	39.261479050	39.357999318
7	41.742170054	38.217892798	38.610293202
1	41.346615204	37.799032765	37.758928210
6	42.870508253	37.800336812	39.203914995
1	43.498787865	36.995477922	38.837160061
7	43.127974761	38.529693569	40.282994117
6	42.104579447	39.446057889	40.402419886
1	42.073080875	40.181475446	41.205059570
26	44.689557899	38.160257035	41.629636892
8	45.843757711	37.734408465	42.691315671
8	44.434981372	39.858641086	44.160837457
6	44.825931866	40.494588968	43.189555228
6	45.605219900	42.382829010	44.718439568
6	44.288427585	42.820914016	45.379856179
8	44.747387024	40.040231260	41.956936889
8	43.281898404	42.979486497	44.657305154
6	45.455530907	41.869318355	43.294386681
8	44.328240002	43.056365162	46.628687504
1	46.258947614	43.272935936	44.723624886
1	46.097204291	41.638329136	45.362403199
1	46.430422670	41.797109918	42.783626895
1	44.836602260	42.561491082	42.702250521
7	51.137692652	35.236333988	45.229114854
6	51.035831413	34.287743758	44.163908416
7	50.595559307	34.793805942	42.979027468
6	50.099173373	36.020318407	42.834801696
6	49.969480629	36.928624198	43.966507172
6	49.306031003	38.237098107	44.019404889



6	50.561602284	36.472535826	45.115925523
8	51.341200966	33.114473150	44.316264165
7	49.698268885	36.369400805	41.601786526
1	49.953436678	35.779190231	40.804436197
1	49.367490077	37.299202279	41.374157906
1	50.557154808	37.118596894	45.997909943
6	48.586705647	38.921684167	43.113665871
1	48.163845870	39.885961973	43.409699018
1	48.316860059	38.595068079	42.108731414
1	49.399838630	38.699591571	45.007265489
1	41.256728680	34.543467553	43.023032927
1	46.616795944	34.806697954	39.226702727
1	40.282578554	39.742820257	39.127578589
1	51.501371187	34.985143116	46.126117404

**TS<sub>H1vα</sub>**

6	41.930354474	35.415976308	43.138471605
7	41.425312894	36.610449842	43.608960854
1	40.483768188	36.756883590	43.996150322
6	42.368592142	37.558160225	43.444867518
1	42.254761448	38.606751958	43.719629528
7	43.451919213	37.025673660	42.885310151
6	43.197474170	35.688456230	42.688171284
1	43.928530163	35.019563259	42.238908229
6	47.124138133	35.704189633	38.970942383
1	46.922470838	35.958771314	37.917723852
1	48.206789233	35.584699420	39.056178042
6	46.737620572	36.894487127	39.854347622
8	45.509714456	36.961045878	40.275120753
8	47.589083234	37.748660367	40.102094266
6	41.308632559	39.211980429	39.434787403
7	41.818876926	38.167594046	38.689723093
1	41.431574817	37.761988289	37.828921665
6	42.927648178	37.729607372	39.312234270
1	43.552901403	36.921312609	38.947152579
7	43.174165971	38.441075108	40.404321537
6	42.160209756	39.370137279	40.501828579
1	42.110455659	40.100545337	41.308777141
26	44.909508872	38.063391499	41.780920354
8	46.234275190	37.515015737	42.845092823
8	44.515862870	39.816506104	44.036845983
6	44.994694841	40.478595581	43.112143275
6	45.648841785	42.356289723	44.729286214
6	44.325220771	42.794858397	45.379062519
8	45.099275062	40.002879813	41.900306345
8	43.331690983	42.979202933	44.646043765
6	45.532166584	41.883093802	43.287388116
8	44.351705118	43.007742276	46.632341611
1	46.308739626	43.241048694	44.770700298
1	46.123818483	41.593898949	45.365392807
1	46.505503878	41.901788248	42.771739013

1	44.863978409	42.557843463	42.727453725
7	50.853145060	35.304630340	45.186755030
6	50.949146973	34.315075922	44.143193857
7	50.539229294	34.719025746	42.911237201
6	49.881237904	35.855499808	42.701744559
6	49.514367202	36.742542607	43.802636695
6	48.612894872	37.865501095	43.609050412
6	50.082739382	36.424790047	45.014780833
8	51.383020103	33.198136211	44.371821172
7	49.550936282	36.182949869	41.452231071
1	49.918763445	35.637208800	40.666985444
1	49.030246395	37.029045763	41.203664987
1	49.908104519	37.073886163	45.878346799
6	48.767738311	39.162905917	43.859972616
1	47.942773052	39.869442155	43.741743866
1	49.742308725	39.553750005	44.160235618
1	47.458468800	37.627333724	43.128397092
1	41.345991113	34.500260135	43.048746047
1	46.652922457	34.743001682	39.176224716
1	40.371288187	39.709386643	39.185709308
1	51.223892953	35.122917619	46.097523380

**TS<sub>Ш1vβ</sub>**

6	41.840350912	35.491369207	43.122241485
7	41.291532355	36.661096507	43.601569581
1	40.355715374	36.765414150	44.012488584
6	42.179331264	37.655295202	43.399694387
1	42.023645105	38.697642024	43.678465735
7	43.266363655	37.175944510	42.808157187
6	43.076546135	35.827577246	42.628388257
1	43.825320750	35.199859171	42.150536089
6	47.082970631	35.755800777	39.188659212
1	47.068030570	35.965956753	38.106633123
1	48.141481776	35.662393615	39.469458340
6	46.560796106	37.000406171	39.908567875
8	45.375079466	36.967632457	40.444950227
8	47.290188329	37.992755259	39.921593769
6	41.245745744	39.268908746	39.388065931
7	41.757057556	38.204605047	38.672522419
1	41.368307476	37.771230020	37.825332219
6	42.878141450	37.797279903	39.288141836
1	43.500699391	36.973599333	38.955321171
7	43.130411638	38.558185912	40.346911299
6	42.108380813	39.479592730	40.435226431
1	42.072666180	40.233025745	41.220736351
26	44.660498453	38.282883422	41.685778910
8	45.846797019	37.934451959	42.928440494
8	44.250971451	40.008751860	44.193227841
6	44.722550815	40.611004809	43.236363073
6	45.589151015	42.434077731	44.788763859
6	44.278199456	42.881833858	45.450509946

8	44.683814823	40.151334870	42.001254674
8	43.276800464	43.066357843	44.725878842
6	45.431172413	41.943898956	43.359165294
8	44.314597522	43.098835531	46.702739822
1	46.259670533	43.311476079	44.807195875
1	46.067237762	41.671075561	45.421522119
1	46.408657260	41.817430669	42.864498948
1	44.859644442	42.673308875	42.763852828
7	51.165755747	35.232138354	45.205829446
6	51.179211248	34.308230977	44.110157316
7	50.876595110	34.852992988	42.897932970
6	50.428648167	36.091455921	42.752071437
6	49.987692968	36.866420646	43.906049100
6	48.902332512	37.859124186	43.864583406
6	50.459914980	36.404010368	45.105242339
8	51.463574909	33.131557585	44.262204751
7	50.332495258	36.605374572	41.520263712
1	50.614712121	36.089316389	40.680426376
1	50.179668213	37.597660264	41.400598115
1	50.224309955	36.946261364	46.026478873
6	48.234707715	38.314018026	42.800071010
1	46.892244429	38.454813470	42.916060170
1	48.370080992	38.194358212	41.722686933
1	48.508078681	38.109729503	44.860030932
1	41.289487773	34.554692937	43.037067036
1	46.605864952	34.787812200	39.341746121
1	40.296612022	39.745230062	39.142443247
1	51.510643399	34.985393311	46.111446298

**5eyC substrate  
Snapshot 1  
RC**

6	43.707330306	40.419644134	49.506685628
7	44.365391838	41.562583959	49.110885674
1	44.489779792	42.416249628	49.667801934
6	44.827511032	41.370467021	47.863352363
1	45.410265339	42.088887606	47.293654138
7	44.484908451	40.165726369	47.428868212
6	43.789688796	39.550531427	48.444651232
1	43.426877259	38.529510019	48.356498959
6	42.461213766	35.838036652	45.550168321
1	41.788762899	36.139633488	44.736486597
1	42.990015955	34.914679979	45.272592978
6	43.512449253	36.912292291	45.869572093
8	43.236242420	38.105293162	45.395142194
8	44.486349443	36.626444732	46.550554827
6	41.198736928	42.505362802	45.120029833
7	40.532770091	41.357728730	45.493156124
1	39.526417820	41.267534701	45.682983661
6	41.427977100	40.358209529	45.562989132
1	41.189526223	39.328297181	45.805933597

7	42.641614947	40.795870076	45.250293671
6	42.514437186	42.140861565	44.970954331
1	43.365958147	42.737817074	44.658714798
26	44.412646684	39.641634635	45.383732588
8	45.784460421	38.793374787	45.325109131
8	46.916264297	41.576854726	45.390505946
6	46.304626861	41.574291096	44.322902376
6	46.848140701	43.822391204	43.257481817
6	47.633588141	44.537389870	42.137354035
8	45.139126342	41.003284348	44.165631978
8	46.983757972	45.191421336	41.290302156
6	46.860847967	42.290835059	43.097786606
8	48.892648034	44.412328781	42.160234268
1	47.333171968	44.074814218	44.212304765
1	45.812677395	44.195732273	43.276038603
1	47.910666100	41.973262076	42.988707480
1	46.300801872	41.996397483	42.197473317
7	49.510355404	33.782301977	44.981111867
6	48.388800425	32.947430848	45.231324180
7	47.213859480	33.324791838	44.680304235
6	47.028735873	34.486158779	44.067900729
6	48.125643082	35.440965481	43.954230879
6	47.889337410	36.751238121	43.453639674
6	49.350463090	35.010993075	44.394851961
8	48.503998492	31.929568157	45.917598310
7	45.828338708	34.765320812	43.551388184
1	45.641917247	35.673497543	43.138970836
1	45.062415120	34.087849492	43.589993580
1	50.220447686	35.666409378	44.312051015
6	47.560035806	37.866254871	43.101983072
1	47.239135785	38.875990209	42.916979472
8	44.049727216	37.297822561	41.623286262
1	44.006772100	38.263859976	41.863443419
1	44.961122382	37.204769620	41.310192606
1	43.161277742	40.348218393	50.447319609
1	41.865066929	35.634156389	46.439611468
1	40.699249862	43.469754026	45.027674252
1	50.420888502	33.512686507	45.294495761

### TSИлеѢ

6	43.728378437	40.457306394	49.436621370
7	44.364979456	41.612599253	49.034502462
1	44.472671889	42.470580971	49.589726334
6	44.845800472	41.419562340	47.796658344
1	45.415725639	42.144941924	47.223196310
7	44.537529636	40.199738147	47.368001033
6	43.842941242	39.579152063	48.386058959
1	43.504489438	38.549606171	48.303337215
6	42.481516746	35.898814209	45.516335543
1	41.805387187	36.196823515	44.704748382
1	43.025598442	34.987190137	45.230244928

6	43.508995620	36.991528212	45.849000963
8	43.211489149	38.184334806	45.399856656
8	44.490398983	36.718581572	46.528804605
6	41.136814321	42.587301046	45.085638122
7	40.486013915	41.431810809	45.461981297
1	39.484693321	41.330289265	45.669742720
6	41.388672973	40.437806651	45.504177103
1	41.161042469	39.405086044	45.746545971
7	42.593316352	40.886817029	45.171813187
6	42.451397613	42.233232988	44.906052048
1	43.294840678	42.834879130	44.581809712
26	44.423826601	39.729345960	45.318999790
8	45.865614398	38.821915062	44.888598692
8	46.953866643	41.649869048	45.363391888
6	46.311387587	41.712931169	44.314983562
6	46.859900211	43.947342759	43.241691459
6	47.630369119	44.639403951	42.100106995
8	45.103041735	41.231529063	44.192095640
8	46.968588873	45.251598775	41.231369961
6	46.869030174	42.415861572	43.086555454
8	48.890898330	44.529482406	42.122284316
1	47.358180768	44.207563544	44.187548848
1	45.825037679	44.321659810	43.268842744
1	47.912833912	42.085547429	42.971977557
1	46.299165116	42.120309982	42.193365404
7	49.510673275	33.760160598	45.000751884
6	48.409391998	32.886620100	45.267419280
7	47.222087900	33.219640376	44.724815423
6	46.994703775	34.367703351	44.104126976
6	48.054495937	35.377620906	43.998583055
6	47.729757089	36.661120231	43.539174519
6	49.309467009	34.979969614	44.426913133
8	48.569217476	31.881593413	45.959720094
7	45.796820620	34.609345797	43.579362917
1	45.606844480	35.515147945	43.160072425
1	45.038343402	33.921795386	43.608502517
1	50.157374409	35.662732379	44.332912791
6	47.205887689	37.739894922	43.169629837
1	46.348686412	38.623879896	43.925016585
8	44.096739281	37.392393732	41.738642214
1	43.966802024	38.350681278	41.971733383
1	45.059570935	37.367896095	41.615296506
1	43.191287215	40.376770760	50.381668647
1	41.888142460	35.681546016	46.404462118
1	40.628969377	43.549613927	45.021491711
1	50.430501018	33.507648698	45.300963747

### IM1<sub>eyß</sub>

6	43.763465619	40.412390982	49.447760202
7	44.434998887	41.549311315	49.046783560
1	44.543667118	42.413412270	49.592370109

6	44.933296490	41.332992594	47.819071445
1	45.538167898	42.030400159	47.244260612
7	44.601634406	40.115981999	47.397395972
6	43.874337995	39.522260561	48.408330029
1	43.512314006	38.500517789	48.328067001
6	42.490979669	35.809794435	45.571602233
1	41.824994977	36.100240787	44.748656007
1	43.030607713	34.888789676	45.308317427
6	43.519342961	36.903776310	45.898456487
8	43.218819090	38.097473218	45.468446954
8	44.513926447	36.621855691	46.560456157
6	41.174126048	42.531114059	45.092014543
7	40.514828051	41.381202250	45.470635213
1	39.511989638	41.287858092	45.673793911
6	41.413197836	40.382608606	45.521405971
1	41.179666809	39.352011228	45.767947916
7	42.621661419	40.822298014	45.191692423
6	42.487305845	42.168064429	44.920053078
1	43.335625538	42.763788241	44.597721188
26	44.465345324	39.640463428	45.361716031
8	45.943136600	38.699821155	44.821505320
8	46.950297618	41.649036519	45.384330939
6	46.320177226	41.683777768	44.322164402
6	46.857718820	43.918811813	43.234489050
6	47.628147802	44.620524832	42.098587986
8	45.135159714	41.165164786	44.189509154
8	46.967033563	45.238515720	41.232822706
6	46.889960172	42.385588336	43.097230346
8	48.889655531	44.518214777	42.122526388
1	47.342737773	44.194254445	44.182834032
1	45.817693313	44.279151451	43.251066151
1	47.940715901	42.071093116	43.001190036
1	46.339774771	42.072105353	42.197702657
7	49.478550115	33.818975728	45.018154978
6	48.352861829	32.955838606	45.281404223
7	47.168694101	33.308296933	44.748090851
6	46.959131555	34.449213200	44.105326229
6	48.052730877	35.424665541	43.954918360
6	47.811829972	36.653680739	43.357838388
6	49.304640659	35.017105591	44.415788483
8	48.511394458	31.947499857	45.963310017
7	45.765869323	34.713660021	43.591314814
1	45.586674354	35.617299194	43.157192796
1	44.994396317	34.039577081	43.638165225
1	50.161816503	35.685087562	44.297412554
6	47.377340837	37.685713506	42.750899241
1	46.257293803	38.791851550	43.894651553
8	44.173234106	37.377119120	41.696693910
1	44.029784700	38.329534222	41.946546996
1	45.129750665	37.383480969	41.523933096
1	43.215810744	40.343562353	50.387655981
1	41.883395952	35.608101972	46.453775405

1	40.672396942	43.495577309	45.013618961
1	50.393804253	33.550864079	45.318818425

**TSR<sub>Beyß</sub>**

6	43.798121770	40.400306664	49.382112033
7	44.491397937	41.529036164	48.994240419
1	44.609744666	42.386169479	49.549711988
6	44.984202204	41.318873875	47.763257682
1	45.607627789	42.009404051	47.200163986
7	44.628272014	40.112686611	47.324802342
6	43.890264118	39.521642678	48.331784715
1	43.502880559	38.510718474	48.241763066
6	42.534096597	35.813025211	45.542435046
1	41.862888137	36.106882385	44.724996926
1	43.067451425	34.890743520	45.273446440
6	43.573794634	36.899268556	45.846324882
8	43.252947562	38.108884291	45.464712926
8	44.605952080	36.614760732	46.442800073
6	41.153334346	42.541690523	45.059159934
7	40.501880221	41.386900139	45.435949285
1	39.502154578	41.290533650	45.653260421
6	41.400501296	40.389744085	45.467699338
1	41.171098720	39.357347187	45.711912506
7	42.604411220	40.836977819	45.126306695
6	42.464906465	42.185570957	44.868388678
1	43.309530649	42.785942199	44.546178123
26	44.423697058	39.670951954	45.284495259
8	45.897700965	38.791409063	44.462251987
8	47.042718906	41.679531041	45.388414320
6	46.365159409	41.769226521	44.360699798
6	46.860256003	44.007588287	43.240601946
6	47.622710443	44.684931186	42.084371978
8	45.158172188	41.284176998	44.268806661
8	46.956311871	45.285958455	41.211654537
6	46.899495745	42.473084519	43.122209046
8	48.883451235	44.577416424	42.101619854
1	47.355074641	44.302347968	44.177637115
1	45.819736942	44.366052865	43.258874516
1	47.949483950	42.166041607	43.001755768
1	46.329798616	42.151698533	42.237414992
7	49.427845531	33.807031986	45.067008950
6	48.350069826	32.907859508	45.341080917
7	47.147486016	33.216251790	44.816651770
6	46.889885002	34.358798557	44.198901632
6	47.922678466	35.398217739	44.093095789
6	47.557143730	36.646913441	43.581462925
6	49.192393194	35.028758698	44.505200113
8	48.541361634	31.899883324	46.021802524
7	45.692767614	34.575012486	43.665968473
1	45.501759895	35.476272182	43.235536180
1	44.948641741	33.871453992	43.671532830

1	50.024457393	35.729368066	44.400273837
6	46.968252729	37.593638649	42.980322788
1	46.154318016	39.303044404	43.678003800
8	44.058704671	37.443406609	41.743601303
1	43.928325869	38.393329170	41.988282402
1	45.033381598	37.399748835	41.740634857
1	43.255594967	40.325254995	50.324502205
1	41.931120093	35.614332806	46.428441806
1	40.650042485	43.506441075	44.995748640
1	50.358799860	33.563081581	45.338642400

**IM20HevB**

6	43.733330213	40.366893122	49.544972227
7	44.397157597	41.507398895	49.154566885
1	44.503834888	42.368870537	49.703523589
6	44.897978264	41.300004531	47.924788042
1	45.484174166	42.024454386	47.366287669
7	44.580114884	40.086006145	47.488124883
6	43.855094268	39.485761815	48.496370656
1	43.491739081	38.464456757	48.410156326
6	42.584362117	35.741153097	45.547178406
1	41.903125384	35.977787087	44.719341212
1	43.128687525	34.812309164	45.325122884
6	43.599554908	36.869816455	45.762600119
8	43.231892335	38.040212774	45.337410264
8	44.676709856	36.643504248	46.314477823
6	41.171084168	42.680010900	45.066022664
7	40.525362160	41.505412469	45.375432871
1	39.520841276	41.388413385	45.560027756
6	41.441627926	40.522185927	45.411612212
1	41.217386743	39.477596737	45.610845044
7	42.653506935	40.998772520	45.145047343
6	42.498726744	42.351663180	44.930138413
1	43.336653507	42.995812801	44.673420729
26	44.312633999	39.682584614	45.422804692
8	46.910992777	38.728141462	42.370382624
8	46.869110556	41.582919749	45.458002535
6	46.514338593	41.321163810	44.310103283
6	46.874224367	43.619802711	43.258785514
6	47.659087563	44.424977429	42.195962051
8	45.669718436	40.337077106	44.054040767
8	47.008995578	45.143648505	41.404118196
6	47.037371655	42.097137887	43.110231384
8	48.918966135	44.311256254	42.218780787
1	47.269017429	43.911425625	44.243598064
1	45.809772699	43.896195671	43.217049087
1	48.114362315	41.873021008	43.023026678
1	46.544924059	41.740210352	42.194262645
7	49.503665016	33.743358495	45.045106552
6	48.403158549	32.896673500	45.323372869
7	47.215593535	33.244417153	44.781928180



6	47.016531834	34.379608595	44.125836801
6	48.088271416	35.359846260	43.984680690
6	47.817101557	36.630195652	43.404587589
6	49.319461749	34.960650628	44.431618307
8	48.543158952	31.887552145	46.021621169
7	45.820076828	34.617647286	43.582423006
1	45.650513313	35.498485238	43.110147314
1	45.057918246	33.937640667	43.626401054
1	50.180066895	35.624269067	44.325211447
6	47.363827931	37.658327133	42.935815150
1	46.397677759	39.305944533	43.013099963
8	44.015935211	37.316792030	41.611410673
1	43.905639051	38.273773334	41.857684759
1	44.937299997	37.303070020	41.312363439
1	43.162099290	40.307509110	50.471382558
1	41.979020763	35.580777920	46.439315705
1	40.644221069	43.632492159	45.008908309
1	50.423832993	33.487677892	45.341570417

**Snapshot 2  
RC**

6	40.890415286	38.286852934	47.141366303
7	41.188270421	39.612240284	47.356258929
1	40.855272641	40.184628877	48.140051447
6	42.028010876	40.016802784	46.390293672
1	42.412829174	41.028337134	46.288442504
7	42.287187356	39.017696785	45.559719690
6	41.588510893	37.922729598	46.013422975
1	41.658976061	36.958428779	45.515659111
6	41.728902246	35.585840332	41.849220172
1	41.336587893	36.164700837	41.002614627
1	42.504961542	34.896222684	41.495163465
6	42.396629000	36.492460461	42.888236617
8	42.061993993	37.750334446	42.798144175
8	43.166071570	36.021582648	43.718271897
6	39.218003937	41.586169633	43.376883234
7	38.784600817	40.319870368	43.051120465
1	37.816352806	40.018751373	42.872363200
6	39.860433029	39.512907798	43.047989381
1	39.836307330	38.455492865	42.816083633
7	40.963648348	40.189388112	43.345619362
6	40.572865121	41.488546977	43.568955001
1	41.283619393	42.261479576	43.846288335
26	42.914702894	39.330807752	43.550632979
8	44.404595532	38.720066217	43.678251677
8	43.486338594	40.737555834	41.984189607
6	43.823879399	41.603746419	42.854444845
6	45.382468219	43.535310562	43.454055739
6	45.813550109	45.003796420	43.234124129
8	43.622695718	41.332981391	44.076044190
8	45.148503209	45.745123861	42.483084016

6	44.416408658	42.936154660	42.437635882
8	46.834281348	45.346636675	43.900320846
1	46.310919254	42.945356798	43.507240461
1	44.927216582	43.491355766	44.459683800
1	44.885130581	42.803675167	41.451904066
1	43.584958114	43.644293727	42.280506075
7	48.833266679	32.489389341	42.784939562
6	47.888487821	31.654958339	42.113926125
7	47.057456990	32.275907702	41.246522518
6	46.892733801	33.597378643	41.221366960
6	47.637465095	34.455354286	42.144211511
6	47.363627399	35.845853510	42.291579278
6	48.636059104	33.841598468	42.848821368
8	47.844092639	30.446926167	42.343590507
7	46.038151645	34.129719599	40.355409578
1	45.582383833	33.541817752	39.650844886
1	45.857246455	35.134842380	40.302518683
1	49.280961263	34.436800390	43.499849670
6	47.075826505	37.019815726	42.420183288
1	46.774068343	38.042393677	42.560172489
8	44.451606279	36.499153463	40.497882398
1	44.657619412	36.592696845	41.441202218
1	44.293210140	37.440323601	40.208691323
1	40.165936352	37.747941734	47.751917133
1	40.921572962	34.991991495	42.277741235
1	38.554957391	42.437107409	43.532900842
1	49.583517085	32.106953662	43.324235193

**TS<sub>Шлеф</sub>**

6	40.921781511	38.271383945	47.137675768
7	41.230521330	39.595701198	47.347449774
1	40.891977984	40.179602111	48.120121435
6	42.083101095	39.987188374	46.387685252
1	42.479463893	40.995111719	46.280535267
7	42.339089208	38.978753240	45.566305994
6	41.627879447	37.891746847	46.020400913
1	41.697649636	36.922776165	45.528909710
6	41.756653651	35.532920384	41.834290277
1	41.384946602	36.125130920	40.987426912
1	42.527846506	34.834706671	41.483169753
6	42.425021355	36.421769778	42.890302689
8	42.180590393	37.692012953	42.747897213
8	43.112528400	35.924033304	43.776835668
6	39.290914952	41.541550063	43.355071410
7	38.852509784	40.276355742	43.031734967
1	37.881894858	39.980465267	42.859062663
6	39.930123222	39.467202177	43.027708690
1	39.899943418	38.409269639	42.796789767
7	41.035284972	40.139567947	43.318761664
6	40.647094512	41.438291548	43.541336229
1	41.360531570	42.211963444	43.811635518

26	43.080201274	39.230330280	43.587048851
8	44.672771497	38.513134412	43.766355911
8	43.615670562	40.638462785	41.962366464
6	43.922042551	41.517619922	42.827071157
6	45.423269251	43.487445109	43.448282394
6	45.828461948	44.963398696	43.238385588
8	43.721522437	41.249289189	44.053494529
8	45.160395441	45.695687873	42.481062929
6	44.487506865	42.870807889	42.413615500
8	46.835432668	45.323494955	43.917587836
1	46.361859788	42.916166391	43.519193680
1	44.951666164	43.430888428	44.445219322
1	44.973994671	42.754505890	41.433563629
1	43.640482847	43.560333761	42.250994235
7	48.719501349	32.615427063	42.813347368
6	47.837409591	31.725366816	42.102045054
7	47.006996822	32.307859361	41.213961199
6	46.735099625	33.610276370	41.226859471
6	47.333419427	34.487436091	42.250335193
6	46.828473051	35.767882380	42.529199490
6	48.402318136	33.931572835	42.936821677
8	47.855783292	30.520718580	42.334681501
7	45.909548127	34.119666396	40.328035202
1	45.537710340	33.533814502	39.572831830
1	45.695971734	35.120558584	40.268368335
1	48.980982391	34.548004232	43.629484755
6	46.330635245	36.908846918	42.664181293
1	45.380984861	37.947772028	43.177375542
8	44.415747250	36.578032195	40.277575574
1	44.779344631	36.766198100	41.160833962
1	44.259543577	37.492259369	39.918511316
1	40.193858061	37.738412416	47.749342442
1	40.937865954	34.950857410	42.257204840
1	38.633173990	42.397550848	43.505759167
1	49.493314282	32.261196268	43.338425065

**Snapshot 3**  
**RC**

6	52.466072192	45.117689890	44.899820748
7	51.555057521	45.961237039	44.309150843
1	51.538235918	46.982378237	44.404152828
6	50.727828516	45.231656842	43.549414998
1	49.892117900	45.636762140	42.985203422
7	51.053743306	43.948533519	43.622899467
6	52.144125278	43.851555390	44.459674904
1	52.622348987	42.894857969	44.661540853
6	51.189120505	38.999823782	45.102821782
1	50.178387371	38.744587968	45.447500981
1	51.607268720	38.148475734	44.543910127
6	51.207217324	40.242013032	44.203314023
8	50.049516904	40.862809014	44.126644288

8	52.231682814	40.608227338	43.647351102
6	47.292968854	44.499026048	45.972406838
7	48.028527638	43.623811758	46.737846134
1	47.995414514	43.546984778	47.765419688
6	48.767996189	42.871802949	45.901975490
1	49.440235814	42.080667764	46.210952412
7	48.543829653	43.205781126	44.637549507
6	47.624414436	44.233132473	44.665165961
1	47.278573619	44.713009230	43.753653265
26	49.699330071	42.451287438	43.004401835
8	50.568161362	41.992405153	41.727815946
8	47.835980362	41.679512446	42.103525221
6	47.675499577	42.792203996	41.530643350
6	46.033748885	44.435745271	40.438457650
6	45.651788318	44.861257602	39.006787278
8	48.503337031	43.732419763	41.771145387
8	46.559146512	44.780079705	38.126071603
6	46.577305346	43.004518285	40.517240982
8	44.488585492	45.278176909	38.836682928
1	46.827280545	45.128107893	40.764885907
1	45.169073588	44.576286212	41.103045690
1	47.040782234	42.766333145	39.544158900
1	45.788724785	42.255726403	40.683117211
7	54.226457692	37.253935648	38.718802679
6	54.329276874	36.529525639	39.942867080
7	53.258107540	36.585012233	40.770393420
6	52.220738100	37.389284207	40.580585642
6	52.176560409	38.273581327	39.420604749
6	51.159693196	39.248430338	39.210805571
6	53.201573931	38.134088982	38.520644993
8	55.342883165	35.887630551	40.203789554
7	51.226151000	37.372438817	41.476555503
1	50.420260618	37.989276379	41.404074529
1	51.272997893	36.720608389	42.264980036
1	53.219199116	38.764364819	37.629246928
6	50.333159074	40.119242699	39.026181502
1	49.648212374	40.933529632	38.880303729
8	48.396349356	38.958109967	42.595945172
1	48.835745615	39.473818020	43.300476738
1	48.168348962	39.683322801	41.986511663
1	53.161242480	45.476431990	45.658839658
1	51.816681975	39.179100355	45.975801643
1	46.657562352	45.269505107	46.409085111
1	54.948826532	37.218776614	38.028209023

### **TS<sub>H1eyß</sub>**

6	52.432822451	45.089447722	44.836524444
7	51.526270485	45.927599633	44.228106802
1	51.496125453	46.947987675	44.333844323
6	50.732396104	45.193958180	43.437413623
1	49.900618026	45.587479016	42.858908296

7	51.073974885	43.911875241	43.504511076
6	52.141242072	43.824335290	44.375443444
1	52.623346369	42.871697981	44.586520945
6	51.166556852	38.992594067	45.076675859
1	50.157117615	38.733544002	45.421081310
1	51.585195303	38.141820743	44.517164572
6	51.170592702	40.229828223	44.169839979
8	49.999218041	40.802515638	44.026630688
8	52.202934376	40.632152261	43.646780130
6	47.279572102	44.528938946	45.986906702
7	48.013777092	43.644187585	46.741904664
1	47.986618593	43.561461962	47.768577786
6	48.747032954	42.897557900	45.892439462
1	49.414761089	42.099515941	46.195330512
7	48.521701794	43.244297260	44.633267029
6	47.607134899	44.273482169	44.676276111
1	47.259211547	44.764378482	43.770885742
26	49.678960816	42.425664003	42.887577776
8	50.437202508	41.873077747	41.380966903
8	47.761381653	41.785096028	42.107628821
6	47.619585646	42.896117707	41.523182051
6	46.022090571	44.561976143	40.414911036
6	45.608590585	44.948197740	38.982945043
8	48.477455792	43.817782864	41.731246126
8	46.502070200	44.865690715	38.088735946
6	46.516182283	43.115164433	40.519837729
8	44.431619752	45.329655203	38.821799548
1	46.852102964	45.231258546	40.694491918
1	45.184865248	44.753095830	41.101886453
1	46.965256289	42.835749309	39.550204951
1	45.708691674	42.393448068	40.713279954
7	54.232168997	37.265393150	38.792734059
6	54.411005549	36.491687682	39.996884303
7	53.386611218	36.495429246	40.874218314
6	52.329910901	37.284105260	40.769541608
6	52.236739494	38.253775895	39.670510128
6	51.246429194	39.240009799	39.691569838
6	53.212696088	38.153889906	38.690437519
8	55.448384937	35.867294967	40.177504124
7	51.359544482	37.204754861	41.675741555
1	50.543169590	37.815437033	41.644853760
1	51.411272162	36.515223184	42.433957449
1	53.179116516	38.826101405	37.829374582
6	50.286515143	40.018732047	39.886513217
1	50.017749918	41.109194158	40.632721164
8	48.599601913	38.780994484	42.447147928
1	48.917735195	39.491651213	43.043043061
1	48.576405116	39.231368028	41.586291518
1	53.124929533	45.451435816	45.596800531
1	51.798536360	39.171107805	45.946619576
1	46.649790066	45.300349171	46.430041197
1	54.919259923	37.246049668	38.066439089

**Snapshot 4  
RC**

6	50.457963581	47.568439008	45.768691918
7	50.017373943	47.936872138	44.518257329
1	50.119550650	48.864110971	44.089403185
6	49.498923847	46.851036534	43.920938444
1	49.052816832	46.846801502	42.930151371
7	49.582167450	45.802125643	44.728222351
6	50.187153176	46.226205608	45.888908971
1	50.407223955	45.538122977	46.702986260
6	48.514328635	42.324275013	48.493350313
1	47.419028363	42.262550197	48.455362113
1	48.914932783	41.309267302	48.631245644
6	49.099690336	42.919746487	47.200892880
8	48.198478870	43.280379211	46.317676430
8	50.309962135	43.033737225	47.055866749
6	45.209910355	46.824033370	44.771618267
7	45.510020304	46.573602534	46.093344785
1	45.080194925	47.002618553	46.922966290
6	46.495594198	45.659986782	46.125867563
1	46.929654323	45.256628827	47.033062284
7	46.839284036	45.293557255	44.899151556
6	46.050676847	46.025000813	44.037501015
1	46.151524214	45.940611483	42.959469273
26	48.488709201	44.028439130	44.479246265
8	49.772077639	43.137498157	44.095069769
8	47.110189989	42.707559349	43.399718587
6	47.278159871	43.392493899	42.349909952
6	46.171634400	44.138257289	40.139597888
6	46.510957335	43.962860305	38.640512541
8	48.024561084	44.423841545	42.409935130
8	47.716273224	43.680644982	38.362936208
6	46.680893634	42.985509715	41.022991385
8	45.592543163	44.141975114	37.818422667
1	46.673637095	45.071110507	40.447816944
1	45.088113491	44.289726302	40.249783767
1	47.516164091	42.515268402	40.477035413
1	45.920748677	42.210178223	41.192761819
7	53.282256744	38.071361999	45.279849712
6	52.828173345	38.015117474	46.632674135
7	51.508237807	38.253702096	46.830115009
6	50.709218341	38.756564800	45.899312093
6	51.217083024	39.031285174	44.558844811
6	50.475020678	39.689239733	43.538688570
6	52.505952868	38.631091857	44.312171006
8	53.602861273	37.757441175	47.541736079
7	49.439758650	39.020913051	46.233338160
1	49.114881523	38.751132552	47.167388864
1	48.782338046	39.499194334	45.617973606
1	52.938097118	38.791532070	43.322083463
6	49.913822253	40.293367425	42.647038447

1	49.441610098	40.865426732	41.872101441
8	47.032275635	40.745147342	45.530970998
1	47.325394221	41.609555335	45.886636403
1	46.976148196	40.964498905	44.583740208
1	50.842638272	48.282581169	46.496767236
1	48.785937500	42.928814177	49.358698999
1	44.484304120	47.568998931	44.445138204
1	54.217709027	37.812446467	45.039299790

**TS<sub>H1eyß</sub>**

6	50.412780512	47.581150677	45.724435570
7	49.976377676	47.971070064	44.478877683
1	50.100243830	48.900052102	44.058764701
6	49.430395171	46.906698890	43.871475214
1	48.979990691	46.920676027	42.882645616
7	49.492901535	45.848282076	44.669788022
6	50.110730784	46.245135701	45.834421532
1	50.318754848	45.543893713	46.640402039
6	48.429984232	42.335236025	48.394336043
1	47.333795302	42.287148191	48.368707010
1	48.816510863	41.312318046	48.509820611
6	49.012240155	42.933638845	47.100456303
8	48.113330303	43.341179232	46.232683695
8	50.222945969	43.010477319	46.939486797
6	45.118348150	46.897989018	44.766896900
7	45.422381588	46.626189989	46.083621999
1	44.996877883	47.043037603	46.922148299
6	46.413140688	45.720783729	46.101437349
1	46.851082583	45.301953128	46.999626225
7	46.756441851	45.383120086	44.865937767
6	45.962562422	46.121809287	44.015695372
1	46.064556674	46.059235083	42.936642767
26	48.355341061	44.124471502	44.408134247
8	49.627334654	43.190500408	43.916827525
8	47.004673771	42.917510290	43.350631989
6	47.176457020	43.565283347	42.272399725
6	46.076839767	44.199981227	40.041658234
6	46.467825426	44.003213478	38.560353443
8	47.908715267	44.604591522	42.308128688
8	47.680487295	43.723881742	38.320121773
6	46.596255321	43.088631596	40.967536298
8	45.569674577	44.167521924	37.712958927
1	46.532160208	45.159628134	40.339726320
1	44.985658796	44.314423465	40.111184118
1	47.443067139	42.598976458	40.455644677
1	45.848053159	42.310560046	41.171736850
7	53.338387305	37.939130987	45.320323988
6	52.985916374	37.829229418	46.699450070
7	51.677104475	38.030485327	46.994378686
6	50.830275045	38.589132091	46.151879948
6	51.251429591	38.968753340	44.807075889

6	50.444200279	39.841992921	44.043334173
6	52.508781506	38.565889992	44.435230852
8	53.823964625	37.567762411	47.549765206
7	49.579952367	38.850128783	46.555560003
1	49.244926086	38.513068260	47.462646237
1	48.914217246	39.312766004	45.943388774
1	52.880926856	38.790901937	43.432879262
6	49.701211386	40.710528084	43.585741879
1	49.487962538	42.000589699	43.615870173
8	47.057976626	40.565751216	45.576134223
1	47.243120336	41.512381961	45.725966496
1	47.420187197	40.432427744	44.682468982
1	50.812766983	48.282349664	46.456827630
1	48.726254545	42.923919367	49.262519859
1	44.395032003	47.649559161	44.450632149
1	54.262539601	37.711014163	45.013929217

**Snapshot 5  
RC**

6	42.450860540	50.813590648	43.168849126
7	43.465874739	50.482004305	42.298344158
1	43.936104706	51.112398609	41.637811077
6	43.738166533	49.174347827	42.455629459
1	44.481221345	48.627928920	41.879880707
7	42.950336875	48.649198882	43.384212254
6	42.140604363	49.659647021	43.848607714
1	41.414360195	49.483726940	44.640248152
6	38.724904723	46.615987721	45.651637497
1	38.356549695	45.868806194	44.936545892
1	38.685118013	46.182899975	46.663347296
6	40.181894676	47.016216630	45.360805195
8	40.687572195	46.465508058	44.281607109
8	40.786975326	47.780339100	46.103463236
6	41.412265399	47.207035797	39.484124419
7	40.218653265	47.426102388	40.136526332
1	39.334361362	47.733174765	39.707509149
6	40.418901238	47.180318130	41.446298243
1	39.652423194	47.261711391	42.209750203
7	41.673559821	46.807128364	41.670859779
6	42.311509083	46.824243401	40.447220349
1	43.363401877	46.571110262	40.335910736
26	42.572495392	46.574700555	43.602180881
8	43.298838538	46.433022983	45.031663339
8	42.928872117	44.473833015	43.059836649
6	44.004590386	44.811792631	42.483785155
6	46.325458092	44.137391344	41.675160550
6	47.145406222	43.448598446	40.565390699
8	44.355936182	46.036071100	42.532451575
8	46.536633407	43.196752399	39.504025976
6	44.832751919	43.818628913	41.697433187
8	48.376894255	43.273785276	40.797502355



1	46.801019134	43.942751532	42.646516086
1	46.433725768	45.216597198	41.468433489
1	44.616961395	42.803670352	42.064050947
1	44.461567125	43.851406294	40.657571783
7	43.231028865	45.036696576	51.145386741
6	41.849839034	45.378992334	51.091192376
7	41.164698501	44.905497264	50.027390649
6	41.746815648	44.452012253	48.918978047
6	43.203469092	44.406369033	48.835413069
6	43.878654594	44.140746677	47.611298592
6	43.880617836	44.658372764	49.999794997
8	41.325555288	46.080473326	51.952362625
7	40.974464905	44.060626807	47.911360968
1	41.323654129	43.828749586	46.975383451
1	39.956768688	44.083279424	48.038578365
1	44.969366672	44.593541857	50.019396585
6	44.403825622	43.986491297	46.527549164
1	44.848380502	43.937856267	45.550909359
8	40.922717064	43.716071610	45.060828916
1	40.752007855	44.629364125	44.754232228
1	41.672485522	43.470106474	44.493542375
1	41.962015630	51.787773122	43.177002636
1	38.053252918	47.473952008	45.622509158
1	41.556130193	47.388164983	38.418965998
1	43.781849485	45.224469789	51.958596650

### TS<sub>Шлеф</sub>

6	42.463065542	50.731926252	43.176269022
7	43.486642321	50.408310647	42.311167049
1	43.951960867	51.043836457	41.651760221
6	43.773969888	49.105250047	42.474396926
1	44.523641310	48.563623406	41.902049275
7	42.988181531	48.571709557	43.402918114
6	42.162349357	49.576670383	43.857212358
1	41.432669500	49.394425009	44.644015328
6	38.740056438	46.531099234	45.618721630
1	38.354071346	45.790971941	44.905249593
1	38.689271991	46.096804053	46.629458796
6	40.210713320	46.891553784	45.333140682
8	40.734522865	46.297795304	44.291039757
8	40.817968989	47.669770107	46.065521317
6	41.391200953	47.207328348	39.411182394
7	40.204566815	47.424141215	40.076067566
1	39.318736668	47.742078008	39.658707973
6	40.416650595	47.156504905	41.380830312
1	39.654231012	47.233254027	42.149425510
7	41.669153589	46.772980948	41.589882938
6	42.295500572	46.804846451	40.361554379
1	43.345559369	46.548382417	40.238078271

26	42.642707126	46.472398592	43.573697022
8	43.569780882	46.126367847	45.041814239
8	42.962084287	44.430823123	42.911398044
6	44.041205303	44.770232489	42.336508215
6	46.369369273	44.091379440	41.589634754
6	47.205802058	43.417871864	40.487217979
8	44.392217738	45.993776392	42.385248361
8	46.619172215	43.188752133	39.408481023
6	44.877930326	43.770998452	41.573541532
8	48.431374021	43.230709179	40.739528591
1	46.820625998	43.879756685	42.568238933
1	46.483509313	45.172804330	41.398200010
1	44.654902287	42.762018445	41.951549653
1	44.532550655	43.794676361	40.524753950
7	43.208494096	45.062328938	51.146191053
6	41.819064667	45.427787208	51.149127352
7	41.078847743	44.953826186	50.128169149
6	41.604435101	44.480092817	49.004006978
6	43.061832071	44.461510937	48.837387117
6	43.620800459	44.300701523	47.567593441
6	43.805766259	44.702417054	49.980386676
8	41.356306418	46.154224087	52.021947195
7	40.802554358	44.064300615	48.035082260
1	41.152198054	43.775696418	47.119263580
1	39.785415914	44.081817271	48.179490736
1	44.895281656	44.641140303	49.941676709
6	43.929147232	44.191565372	46.359246123
1	43.870592954	45.052678311	45.331375039
8	40.869282307	43.481949651	44.965243725
1	40.732487877	44.392750852	44.627105728
1	41.818836417	43.352902217	44.801345619
1	41.977328814	51.707547671	43.193298205
1	38.083305715	47.400776055	45.598521749
1	41.529326211	47.405374436	38.348277654
1	43.787016589	45.229248656	51.944578195

**4mC substrate**  
**Snapshot 1**  
**RC**

6	53.229522861	43.405771930	39.707840170
7	52.545236876	42.279295428	40.109725864
1	52.894120340	41.314252882	40.096729303
6	51.337182775	42.663018759	40.558113379
1	50.570305800	41.983991859	40.922438627
7	51.209447817	43.979193768	40.458821206
6	52.383769641	44.463537210	39.935491053
1	52.544521412	45.526773956	39.777656356
6	50.174504798	48.718638208	38.607471465
1	49.356213532	48.538026499	37.900063677
1	49.954798982	49.638644400	39.161264298
6	50.357314709	47.562341225	39.600304670

8	49.638048456	46.504182618	39.332751012
8	51.155617790	47.646905940	40.527035133
6	48.527755857	42.408668661	37.088069383
7	49.152065469	43.479064069	36.476797513
1	49.454733292	43.556856453	35.496281501
6	49.387206116	44.408295413	37.421201808
1	49.869762531	45.361763763	37.231690539
7	48.943720465	44.002568432	38.605933400
6	48.407938343	42.747740121	38.413437397
1	47.988223006	42.175443377	39.236762355
26	49.340072118	44.980438827	40.462481874
8	49.516670081	45.760123749	41.873268642
8	46.561956173	44.782575877	41.402992509
6	47.163967760	43.744983415	41.678004185
6	45.170515147	42.185931390	42.048549906
6	44.642677282	40.898829998	42.705102156
8	48.384151873	43.506831946	41.278545314
8	43.985743490	40.120858700	41.964040294
6	46.564378413	42.614819395	42.509389676
8	44.869631847	40.684254561	43.925627192
1	45.149725053	42.030902226	40.959590686
1	44.453277601	42.996064065	42.264456954
1	47.256358864	41.760413132	42.484536581
1	46.515816283	42.959001252	43.556762826
7	51.948055535	49.075656222	46.302813074
6	51.919406254	49.660746842	44.992491104
7	50.840116827	49.365389175	44.228833119
6	49.861315439	48.575117893	44.655092918
6	49.856292049	48.016953314	45.981800571
6	50.922817330	48.296710376	46.767710337
8	52.846200472	50.366495934	44.600289788
7	48.863387024	48.282548487	43.799380651
1	48.929777459	48.705602921	42.876464773
1	50.996442232	47.902656802	47.786820420
1	49.057225603	47.389421779	46.349577192
6	47.773583570	47.369332592	44.070206942
1	48.131374263	46.457053769	44.571809098
1	47.325396677	47.056657212	43.121899033
1	46.994235528	47.823044572	44.707943633
1	54.176650831	43.372063921	39.169435404
1	51.101181686	48.858098692	38.050795583
1	48.284662116	41.474130760	36.582488868
1	52.687976380	49.262055971	46.949144858

**TS<sub>H4m</sub>**

6	53.190562112	43.435601286	39.743932985
7	52.509856836	42.311855784	40.161223637
1	52.854232520	41.345079230	40.139430335
6	51.313721315	42.701483896	40.635050883
1	50.548072222	42.029908754	41.014532191
7	51.187996061	44.019528653	40.537973374

6	52.354074076	44.497337370	39.987400955
1	52.516767071	45.559634307	39.825321573
6	50.146848396	48.713304091	38.632629070
1	49.332557119	48.525711068	37.922385834
1	49.920186805	49.636964548	39.177372184
6	50.325943298	47.562749279	39.635998030
8	49.612516686	46.502292640	39.379368205
8	51.120465461	47.660672999	40.567401392
6	48.506858351	42.398804644	37.103486428
7	49.130433328	43.475236493	36.502351958
1	49.439092379	43.558753691	35.524338796
6	49.357407446	44.398524017	37.455913380
1	49.838952424	45.354342068	37.275142823
7	48.909749561	43.983740697	38.635598008
6	48.380640978	42.728393311	38.430791881
1	47.963477519	42.144295036	39.247206483
26	49.286980728	44.973598640	40.534639510
8	49.353856392	45.786164017	41.975458378
8	46.660279598	44.688172248	41.310316528
6	47.216520712	43.644746153	41.669188912
6	45.154627864	42.161616066	42.045135517
6	44.624252595	40.873790961	42.697447904
8	48.451701280	43.381909237	41.355150319
8	43.972706626	40.094353080	41.953877260
6	46.550959563	42.567629437	42.516252671
8	44.851242250	40.657675792	43.917902273
1	45.136227001	42.011238904	40.955725284
1	44.441276877	42.974527784	42.263120819
1	47.215956228	41.692085724	42.532457693
1	46.497087584	42.943991214	43.552328389
7	51.930155109	49.108937788	46.313450436
6	51.905181732	49.788629092	45.050536392
7	50.814963249	49.564571867	44.275787043
6	49.879518570	48.680733797	44.599009433
6	49.936138208	47.927636704	45.823804723
6	50.964237017	48.203059465	46.662622165
8	52.840076542	50.501404763	44.696988580
7	48.851509070	48.520273089	43.736400949
1	48.906018941	49.107347965	42.902572706
1	51.050614763	47.705338417	47.634040006
1	49.195211439	47.186605857	46.095047121
6	48.007349885	47.362437724	43.637451841
1	47.856534591	46.878144009	44.610743441
1	48.516649792	46.568565703	42.875616391
1	47.030968414	47.632423480	43.212262044
1	54.136789396	43.397235380	39.204257807
1	51.075008553	48.854410839	38.078846682
1	48.269587983	41.465973482	36.592021747
1	52.655890352	49.271967408	46.981808276

**IM1<sub>4m</sub>**

6	53.227036966	43.489325234	39.701099071
---	--------------	--------------	--------------

7	52.595755374	42.350330002	40.153195007
1	52.971808799	41.395881351	40.150616470
6	51.390256337	42.700318685	40.626481339
1	50.661185510	42.009491217	41.037692051
7	51.203505341	44.010165105	40.496012085
6	52.347759531	44.521034334	39.922412575
1	52.461787058	45.585423586	39.735514267
6	50.070902608	48.674889331	38.640606141
1	49.253179065	48.531068189	37.922343479
1	49.853563373	49.589664404	39.207838744
6	50.204886784	47.489041799	39.621170457
8	49.287562394	46.571837712	39.516295903
8	51.134487780	47.452924324	40.428227839
6	48.496949390	42.320950965	37.093086116
7	49.123039261	43.410282049	36.520343408
1	49.442899470	43.511697266	35.548358173
6	49.323132509	44.319758508	37.496946170
1	49.802171150	45.280794024	37.333411741
7	48.858763216	43.886108950	38.660966686
6	48.345744845	42.631964331	38.423370631
1	47.921442525	42.025081170	39.219550712
26	49.247005096	44.876765167	40.663373724
8	49.425157306	45.762407001	42.280490835
8	47.169124999	44.387386963	41.232077164
6	47.573583056	43.307655001	41.753534505
6	45.368507100	41.992300725	41.952382779
6	44.667668752	40.816200373	42.655906865
8	48.791278036	42.976823561	41.595133043
8	43.896668317	40.122294035	41.943304770
6	46.697540153	42.399418230	42.587909415
8	44.884349378	40.603916813	43.878426026
1	45.500536824	41.706037736	40.897770887
1	44.671801425	42.848293773	41.950619539
1	47.296120533	41.504838169	42.810942311
1	46.511201429	42.903164951	43.551526696
7	51.864116746	49.082764221	46.283077773
6	51.836427499	49.789293066	45.033915062
7	50.716694240	49.619357948	44.283147533
6	49.781123294	48.742771617	44.607359252
6	49.867301487	47.910825250	45.770298944
6	50.913823312	48.149194994	46.602709262
8	52.780833699	50.483453054	44.676454370
7	48.701383606	48.678606076	43.769319430
1	48.729990076	49.366416636	43.009013969
1	51.026472046	47.599261233	47.542202009
1	49.146003453	47.135973622	46.000533144
6	47.657665897	47.795715043	43.786036161
1	47.534003360	47.116959468	44.627000628
1	48.706564145	46.374125497	42.524584318
1	46.866852123	47.942459149	43.053033758
1	54.171313412	43.459898227	39.157460064
1	51.002653264	48.821792423	38.094412478

1	48.278233739	41.393539557	36.563804656
1	52.592939961	49.238326907	46.949853199

**TSRB4m**

6	53.212107511	43.508396898	39.715606455
7	52.579420064	42.373841649	40.177467294
1	52.949977343	41.417116748	40.171567343
6	51.381609597	42.733196415	40.664292170
1	50.652876728	42.048258065	41.085861437
7	51.200310439	44.044095236	40.533128794
6	52.341678475	44.546099804	39.944962929
1	52.460891833	45.609462600	39.755268544
6	50.068742295	48.683283024	38.636069928
1	49.252406885	48.536754151	37.916732666
1	49.850210591	49.600622951	39.198603691
6	50.201974590	47.502631071	39.622644152
8	49.285207698	46.584328777	39.521938419
8	51.130137604	47.471885058	40.431212880
6	48.501753415	42.328552893	37.112730366
7	49.131055540	43.416795687	36.541471228
1	49.451101998	43.518116620	35.569650212
6	49.334992064	44.323774969	37.519726325
1	49.817107099	45.283798332	37.358502014
7	48.869324478	43.889750229	38.682858717
6	48.351762627	42.637841596	38.443750295
1	47.923149085	42.031260701	39.238292148
26	49.233914870	44.902175142	40.684371948
8	49.352748580	45.876914401	42.337394037
8	47.153195960	44.389293885	41.224963387
6	47.569576538	43.330499562	41.777570583
6	45.373857177	41.996551214	41.956308597
6	44.670921917	40.820671254	42.657904240
8	48.800165229	43.028811575	41.659740833
8	43.897092955	40.131093713	41.944265115
6	46.695011527	42.411507057	42.601341235
8	44.888726838	40.604063628	43.879570997
1	45.517025870	41.706002805	40.904161364
1	44.673322662	42.849383572	41.943464994
1	47.299251098	41.521240854	42.826969878
1	46.499858726	42.908742680	43.566713866
7	51.856862044	49.087440381	46.280476661
6	51.839353807	49.788852505	45.029334080
7	50.743007446	49.583646040	44.250687229
6	49.824717424	48.684698642	44.555660476
6	49.885069560	47.884574228	45.742203448
6	50.908409278	48.150379155	46.594925683
8	52.772404863	50.504964856	44.687842063
7	48.779122797	48.569622276	43.677727892
1	48.789754418	49.273134149	42.931548018
1	51.000570068	47.622636178	47.549258757
1	49.156087428	47.118539269	45.979479271

6	47.868371408	47.551874940	43.580330290
1	47.788255798	46.837274507	44.397536424
1	48.611192784	46.505263732	42.475915040
1	47.004598787	47.731976818	42.938504678
1	54.155758130	43.473868104	39.171181440
1	51.001796108	48.827806337	38.091468316
1	48.279123413	41.403741068	36.580540278
1	52.583786396	49.242055850	46.949541334

**IM2OH4m**

6	53.201869428	43.535190545	39.743944976
7	52.565016489	42.426719294	40.255043488
1	52.921148190	41.464354226	40.260269367
6	51.384536233	42.828354242	40.765574049
1	50.657769819	42.171281271	41.236001294
7	51.215569471	44.135388212	40.600703453
6	52.348414134	44.591103329	39.963868575
1	52.487372465	45.642523070	39.722239147
6	49.985865279	48.775340767	38.608111282
1	49.207656725	48.610034087	37.852100856
1	49.763561552	49.720523540	39.120360225
6	50.003716693	47.648745820	39.648910590
8	49.164722707	46.700727388	39.508518437
8	50.803768504	47.731442445	40.618613653
6	48.465716624	42.313040384	37.081338984
7	49.117410419	43.387180938	36.509824407
1	49.447182324	43.481151197	35.540606424
6	49.319649321	44.300314647	37.482717996
1	49.816973439	45.251735133	37.315347059
7	48.828601865	43.886615711	38.642249554
6	48.295608417	42.640438845	38.406375252
1	47.832212642	42.053329324	39.196982043
26	49.131036839	44.865215017	40.601912142
8	49.505710852	46.286841944	42.353395246
8	47.014387269	44.422807427	41.348436880
6	47.506173277	43.452318784	41.975179708
6	45.382369925	41.987353664	42.022131960
6	44.686150961	40.794655842	42.697199931
8	48.778486081	43.293198445	42.012307620
8	43.912333376	40.115105607	41.972893282
6	46.668501493	42.425068473	42.711618186
8	44.908765267	40.554683829	43.914673959
1	45.562475364	41.708780123	40.971986372
1	44.665843429	42.826152130	41.991340353
1	47.316597893	41.553689130	42.885122896
1	46.427610484	42.832667974	43.707819922
7	51.822209528	49.108637628	46.250993513
6	51.773570534	49.867164065	45.032919415
7	50.748300917	49.556526632	44.185374750
6	49.930407255	48.548974076	44.400409423
6	50.011320568	47.728991200	45.576985473

6	50.964193085	48.067184941	46.485417431
8	52.613901884	50.711076844	44.771377047
7	48.957243071	48.330572163	43.453252745
1	48.952199350	49.050700520	42.727458308
1	51.065958627	47.519286745	47.427251925
1	49.343526286	46.894035445	45.767537136
6	48.498450645	47.031521383	43.060570486
1	48.217617845	46.428119712	43.935510683
1	50.030020279	46.915514644	41.762980515
1	47.608081867	47.147696803	42.426185931
1	54.142664930	43.480755817	39.196215111
1	50.947927018	48.877224205	38.105991480
1	48.249388314	41.383018196	36.555669784
1	52.547357892	49.267713056	46.920939298

**Snapshot 2**  
**RC**

6	52.962211170	41.155749024	42.341641563
7	51.873358573	40.336776533	42.529829338
1	51.899052764	39.330278765	42.733853457
6	50.765284967	41.088836185	42.451182851
1	49.757166848	40.694643088	42.548240949
7	51.086735740	42.354283538	42.214515174
6	52.459618881	42.420407797	42.149892371
1	52.976069062	43.364448822	41.990640802
6	52.344072208	46.814307082	39.725048940
1	51.752737482	46.785368410	38.801992513
1	52.304814734	47.834468646	40.136419655
6	51.802064067	45.819331243	40.759696589
8	50.746800610	45.150787535	40.344384165
8	52.324918929	45.675836524	41.855537511
6	49.601301954	40.806819415	38.320793701
7	50.604410898	41.609601045	37.824185899
1	51.178576150	41.428362844	36.988829403
6	50.739336538	42.663110058	38.651095265
1	51.451879689	43.469422830	38.502061923
7	49.868918658	42.593759765	39.650151145
6	49.146412205	41.436261507	39.454907992
1	48.345012611	41.155634415	40.132140415
26	49.808900586	43.812465246	41.419971368
8	49.791113558	44.725133141	42.756449114
8	47.277924059	43.746267432	43.535889281
6	47.095992259	43.268243711	42.426064993
6	45.557222158	41.309790314	42.864657289
6	44.081490070	40.912090900	43.005270442
8	47.989898339	43.225572683	41.465000552
8	43.412586590	40.711219111	41.958266844
6	45.761139214	42.613596075	42.067426696
8	43.640530309	40.819364170	44.183706037
1	45.968255961	41.426561186	43.876324457
1	46.096248978	40.479963409	42.374212756



1	44.976620052	43.334114049	42.345522728
1	45.684938283	42.433678372	40.986633230
7	51.444708597	49.123987341	47.608370544
6	51.886517909	49.633807106	46.341514600
7	51.131072041	49.301888736	45.264938815
6	50.064058261	48.508267476	45.355843597
6	49.624956405	47.965939606	46.616473601
6	50.349360508	48.305017861	47.710454164
8	52.889038408	50.336303705	46.257780466
7	49.405244530	48.224687987	44.219170120
1	49.789457672	48.635971985	43.365797864
1	50.076702137	47.940267016	48.705960608
1	48.757689468	47.319525889	46.714633361
6	48.206140144	47.420596114	44.095020592
1	48.402956679	46.336090258	44.098040776
1	47.732049406	47.664754665	43.134144772
1	47.487485303	47.651918995	44.895165830
1	53.975739248	40.772520226	42.223472822
1	53.378612037	46.591902092	39.463647566
1	49.301966266	39.871701228	37.847486780
1	51.996810471	49.237920181	48.434309600

**TS<sub>H4m</sub>**

6	52.952126078	41.217616877	42.377445849
7	51.851258644	40.417436534	42.585694707
1	51.863241889	39.406057180	42.768874291
6	50.759484216	41.196821174	42.563418885
1	49.744890084	40.825373729	42.680073274
7	51.100969301	42.462479082	42.345631877
6	52.473882118	42.496744499	42.231143373
1	53.002255372	43.433117450	42.064298602
6	52.364123824	46.856038534	39.707657673
1	51.769077126	46.831782679	38.786704122
1	52.331239750	47.878569452	40.114901921
6	51.810971703	45.866912602	40.743177940
8	50.687723468	45.293705197	40.389258660
8	52.388896225	45.651400474	41.803807223
6	49.607923168	40.833147338	38.360272927
7	50.599942631	41.637276836	37.844837671
1	51.163403866	41.454174856	37.003472907
6	50.746300299	42.690163816	38.675868910
1	51.456426470	43.495868145	38.508269712
7	49.898659695	42.622034642	39.691301143
6	49.176394256	41.464097797	39.504690226
1	48.385574476	41.181038542	40.194220823
26	49.826466302	43.937447663	41.586868374
8	49.765016409	44.973615595	42.963104027
8	47.150727740	43.822210215	43.571589944
6	47.042836754	43.318052794	42.458952068
6	45.538847775	41.323370902	42.864226533
6	44.067343659	40.912803029	43.002772937

8	47.984274735	43.290521443	41.552795387
8	43.399822184	40.705022186	41.955999774
6	45.741715435	42.620491408	42.054474353
8	43.624974858	40.815495848	44.180990374
1	45.941249824	41.454232123	43.877515318
1	46.087594051	40.491734427	42.387787396
1	44.925490713	43.321741096	42.286858075
1	45.718235116	42.422702738	40.974283816
7	51.417853179	49.124246177	47.589091082
6	51.838659807	49.663592964	46.330064744
7	51.100609651	49.294325475	45.245750139
6	50.096558804	48.432237421	45.330289792
6	49.668970347	47.870755404	46.580165348
6	50.363517613	48.252902532	47.682357492
8	52.805086173	50.409154399	46.242032167
7	49.478960852	48.116385719	44.159180730
1	49.851264252	48.609029740	43.339165882
1	50.093476585	47.884815744	48.677320123
1	48.823057823	47.196049834	46.677059607
6	48.576348092	47.062797097	43.902829273
1	49.151691320	46.060301380	43.501011388
1	47.916197696	47.304682282	43.058094084
1	48.002638429	46.733760108	44.777517043
1	53.959402716	40.822787995	42.244889229
1	53.396499588	46.626699189	39.443704908
1	49.298823794	39.900613722	37.888143759
1	51.974032602	49.239373291	48.412123706

**Snapshot 3  
RC**

6	50.349835757	43.346856282	47.166448347
7	49.778195272	42.195540053	46.678181966
1	50.047243744	41.241726193	46.941309008
6	48.752598751	42.532391535	45.883013317
1	48.138319830	41.812914527	45.345376408
7	48.637638237	43.851471695	45.822596510
6	49.623720273	44.383969457	46.624103363
1	49.715353976	45.458119394	46.773541653
6	49.276257284	48.827457731	44.357941827
1	49.385090528	48.788153286	43.266638229
1	48.662407151	49.694708390	44.636492280
6	48.631849313	47.558115168	44.919924922
8	48.608502786	46.565491226	44.076031553
8	48.236117358	47.510324879	46.078261831
6	50.494416612	42.589801498	41.982937621
7	51.227194855	43.734199550	42.221085439
1	52.193917825	43.926403961	41.928586810
6	50.448364454	44.582254988	42.918348496
1	50.741814496	45.577339392	43.231305990
7	49.255654403	44.051165345	43.132146350
6	49.261817275	42.802823705	42.553351870

1	48.386164985	42.158056671	42.571236574
26	47.663238731	44.883107616	44.272146055
8	46.453443801	45.389985018	45.218352606
8	44.494133847	44.119314797	43.346154482
6	45.387967720	44.150247324	42.519837392
6	45.787883234	42.597575562	40.532539370
6	45.100539668	41.442298441	41.271678736
8	46.660299399	44.376589758	42.761329430
8	45.667145232	40.997475257	42.306229582
6	45.148599461	43.907337207	41.027613346
8	43.974281543	41.109082671	40.828916407
1	46.871069719	42.614139657	40.723312255
1	45.606166863	42.503929197	39.449267968
1	44.066658803	43.853318402	40.852610710
1	45.577043185	44.755979063	40.471046783
7	43.309736112	49.266259242	49.515854053
6	44.199636516	50.092883123	48.749444833
7	44.373635345	49.751098042	47.452801666
6	43.821119369	48.659311882	46.919191992
6	42.995292080	47.768937156	47.698722505
6	42.755011382	48.130089986	48.982947348
8	44.760655260	51.056623184	49.267664673
7	44.054697175	48.422622715	45.619990772
1	44.630868576	49.123163750	45.147785592
1	42.109820133	47.526050641	49.628894547
1	42.564370600	46.857747676	47.295103893
6	43.596426370	47.283411881	44.845202470
1	42.543868770	47.050863066	45.064615211
1	44.205692944	46.379538832	45.012205597
1	43.671356857	47.538217807	43.778829169
1	51.264710961	43.321810440	47.758430934
1	50.261400761	48.948738203	44.808331315
1	50.914407650	41.714449426	41.487525061
1	43.124691401	49.446956090	50.481814505

#### TS<sub>H4m</sub>

6	50.268378778	43.373127959	47.146684683
7	49.682598132	42.228871637	46.655275756
1	49.964830288	41.271006628	46.890850655
6	48.626438629	42.580716425	45.906113529
1	48.000337318	41.871129348	45.368493691
7	48.501265884	43.901412666	45.877942418
6	49.518712721	44.418121747	46.653713027
1	49.616054458	45.490367519	46.815201328
6	49.273368691	48.872423287	44.356486145
1	49.372210735	48.844811532	43.263895493
1	48.668027929	49.741430280	44.649333517
6	48.625142166	47.600534894	44.907955097
8	48.513541441	46.646221110	44.034740308
8	48.295048971	47.521059060	46.089111779
6	50.480569848	42.586325455	41.993013527

7	51.209318375	43.734675175	42.221921613
1	52.174301463	43.928459285	41.926841568
6	50.426091140	44.578162035	42.925224662
1	50.721597173	45.576569847	43.228299533
7	49.238730304	44.044690041	43.152608110
6	49.251977367	42.796349703	42.575524344
1	48.382425168	42.143066842	42.599538751
26	47.531751287	44.975191575	44.317644355
8	46.213016590	45.564187226	45.260166012
8	44.419346946	44.097180270	43.235001039
6	45.345955301	44.151911920	42.438808925
6	45.801954211	42.549400085	40.510025487
6	45.094961611	41.415788312	41.263518707
8	46.590552684	44.425957672	42.729256193
8	45.650718613	40.975322765	42.305429620
6	45.152008538	43.875039647	40.945283733
8	43.966342074	41.089623966	40.819096089
1	46.879207655	42.569991388	40.731444646
1	45.651254225	42.422317635	39.424887016
1	44.076491250	43.815724301	40.734543889
1	45.602236182	44.704751705	40.377007593
7	43.298154232	49.247589223	49.499171073
6	44.169620582	50.069372995	48.711123097
7	44.381913133	49.664789603	47.431705899
6	43.905011791	48.518840649	46.960263571
6	43.087787236	47.643696845	47.756888954
6	42.797542341	48.066135503	49.013699870
8	44.691203894	51.075424487	49.180634712
7	44.212906191	48.220146990	45.671458191
1	44.750189245	48.950904824	45.191787860
1	42.149968790	47.477450595	49.671710580
1	42.692676842	46.700378231	47.392022045
6	44.072854564	46.975716509	45.013656209
1	43.231229096	46.368880970	45.370579014
1	45.066258561	46.271738632	45.162498783
1	44.036909305	47.100887704	43.923471224
1	51.186514497	43.342527295	47.733334259
1	50.261488752	48.983562257	44.802954731
1	50.899961016	41.712538483	41.494340594
1	43.118286557	49.443429018	50.463155974

**Snapshot 4  
RC**

6	47.493908467	40.352873544	48.071439568
7	46.599187026	39.755890560	47.217629989
1	46.280393834	38.781896568	47.252942712
6	46.177719943	40.669114710	46.334572356
1	45.476751185	40.458395096	45.530794523
7	46.766547713	41.833812858	46.567937718
6	47.593378661	41.660754911	47.654642712
1	48.172834760	42.483066363	48.069155205

6	50.264030327	45.581138562	46.229770209
1	50.716006474	45.454764145	45.237418264
1	50.175596993	46.654575808	46.439857741
6	48.879709809	44.933868568	46.334998222
8	48.561087631	44.200961840	45.299105657
8	48.184712006	45.095985860	47.328129496
6	48.837395060	39.961174195	42.944918576
7	49.885814705	40.479828294	43.672507141
1	50.836651023	40.088695307	43.725350865
6	49.435670486	41.571934077	44.315695607
1	50.043144033	42.196071812	44.961366528
7	48.157756209	41.795691019	44.034661169
6	47.764712580	40.789853955	43.176094562
1	46.751386050	40.735542632	42.784368902
26	46.899071524	43.251920566	45.025466207
8	45.972032689	44.404046950	45.676482046
8	43.649769860	43.169750442	44.564548685
6	44.363903601	42.858226097	43.615166002
6	42.610857662	41.577405489	42.267376859
6	41.959630295	41.431493488	40.877707105
8	45.663593326	42.724529846	43.674879781
8	42.685089752	41.008573745	39.951092998
6	43.787757130	42.562721530	42.234784324
8	40.739454887	41.752443226	40.762049596
1	41.873364995	41.896669633	43.012455833
1	42.983020994	40.585615160	42.577680725
1	43.445328908	43.529166756	41.826802779
1	44.577876671	42.195086611	41.568687394
7	43.779334422	48.440575461	50.553044747
6	45.207741851	48.479057627	50.419668050
7	45.699020642	48.247429469	49.183002955
6	44.924220010	47.887420243	48.152738328
6	43.500418519	47.722331526	48.307337366
6	42.974637376	48.063627372	49.508540463
8	45.924978348	48.735897149	51.387794038
7	45.502229656	47.724651783	46.959723212
1	46.488965628	47.982395113	46.897290986
1	41.893234299	48.057243034	49.677064346
1	42.856242741	47.439810270	47.480775108
6	44.818258383	47.357186926	45.733870711
1	45.533970105	47.430212847	44.905555691
1	43.977015156	48.036216017	45.526198708
1	44.458026813	46.318080531	45.760979911
1	48.041579011	39.780568370	48.820165869
1	50.927443900	45.146143243	46.977251859
1	48.918127045	39.023607986	42.394901057
1	43.323331337	48.768440651	51.380412921

**TS<sub>H4m</sub>**

6	47.474033533	40.405939613	48.066758048
7	46.571769596	39.818328009	47.211772563

1	46.261644275	38.840615774	47.233796137
6	46.123011578	40.747840129	46.360977607
1	45.415778488	40.553286018	45.558912091
7	46.699955540	41.917209415	46.614609516
6	47.550203354	41.724012072	47.681638383
1	48.130812006	42.540950210	48.104267163
6	50.270748470	45.618328398	46.242722431
1	50.725212623	45.484221823	45.252147410
1	50.191337460	46.691595995	46.454919703
6	48.882511300	44.977703595	46.344878638
8	48.601012710	44.144491939	45.390125314
8	48.146693457	45.250588930	47.291141234
6	48.847391457	39.943259751	42.913713607
7	49.893393312	40.466516687	43.641449294
1	50.841896180	40.073367836	43.706327875
6	49.440649964	41.569090289	44.268209876
1	50.045310750	42.197395830	44.913040649
7	48.166247361	41.795632053	43.978492735
6	47.777033536	40.779803922	43.130715227
1	46.763202763	40.721512513	42.740806111
26	46.833158127	43.302404097	45.049607734
8	45.913927561	44.689416016	45.447500584
8	43.551723762	43.043072134	44.630240469
6	44.278653617	42.732737189	43.684583934
6	42.549166660	41.485828778	42.275197681
6	41.913962240	41.387509471	40.875704603
8	45.565101454	42.563646151	43.773379379
8	42.635178987	40.964609567	39.945576748
6	43.712674017	42.487137683	42.290034049
8	40.705654547	41.749867979	40.753268456
1	41.799392080	41.771837085	43.022258556
1	42.932403237	40.489066157	42.553218756
1	43.357533015	43.463235155	41.917722722
1	44.510962266	42.153653382	41.615438807
7	43.797357490	48.443684890	50.530419483
6	45.224026376	48.473984717	50.405336147
7	45.718834695	48.215765778	49.169499537
6	44.950013030	47.821580539	48.155239929
6	43.529513605	47.664585551	48.302257757
6	42.997895886	48.043009764	49.491931796
8	45.943655024	48.739769579	51.365519851
7	45.563502063	47.638995327	46.964069869
1	46.548016777	47.923046403	46.942037135
1	41.915349542	48.052164107	49.651011965
1	42.883056850	47.375952477	47.479919958
6	45.055628422	47.048346875	45.791087524
1	45.479110008	47.507742304	44.887337002
1	43.962222392	46.987465192	45.752335642
1	45.457969901	45.837007409	45.671741486
1	48.025410022	39.828044523	48.808437598
1	50.930709315	45.176584349	46.989302103
1	48.928608739	38.999068143	42.375221934

1 43.340112929 48.771010081 51.357316165

**Snapshot 5**  
**RC**

6 46.946185519 39.482527383 47.863676103  
7 46.138004661 38.974352856 46.875275757  
1 45.838528513 37.998315250 46.793334539  
6 45.743322372 39.991273215 46.092314318  
1 45.114612433 39.870912707 45.213271398  
7 46.264206524 41.129519158 46.525200691  
6 47.017534218 40.834086802 47.636463018  
1 47.569565780 41.601702916 48.170350141  
6 49.996825360 44.841961365 46.408101376  
1 50.673321100 44.837265711 45.538635405  
1 49.821960834 45.905015454 46.622440636  
6 48.677597454 44.211093579 45.979202009  
8 48.239178654 43.162170697 46.541130704  
8 48.027269699 44.711668496 45.026605515  
6 48.478813258 39.969688535 42.840164674  
7 49.494140069 40.294843840 43.715871417  
1 50.424913234 39.870797510 43.796778433  
6 49.043968062 41.265236299 44.525790960  
1 49.615152147 41.679058713 45.346977973  
7 47.807477680 41.618524805 44.202403700  
6 47.434293798 40.809381294 43.149363084  
1 46.448232231 40.879373775 42.696002123  
26 46.545909535 42.902581062 45.380317246  
8 45.639830637 43.861310852 46.299652203  
8 43.305544531 43.290326404 44.662720262  
6 44.064828501 42.943636379 43.758639517  
6 42.408515972 41.679815532 42.290541742  
6 41.822920311 41.566894081 40.870548898  
8 45.336800371 42.705926869 43.892859733  
8 42.577319858 41.106318598 39.984985287  
6 43.530850238 42.731678253 42.342932760  
8 40.633212627 41.959366082 40.680457111  
1 41.627490343 41.931563776 43.018191564  
1 42.826273666 40.697852749 42.570393664  
1 43.129331979 43.702817133 42.002225074  
1 44.345213574 42.445923168 41.664533719  
7 43.082966558 48.042977817 50.297943800  
6 44.508195060 48.225135136 50.202805334  
7 45.056576702 47.981976741 48.992786361  
6 44.357960666 47.518989548 47.958803238  
6 42.949202117 47.244500070 48.066163666  
6 42.355669030 47.550924935 49.242586429  
8 45.169074043 48.574699769 51.174444208  
7 45.008835669 47.339839834 46.802260325  
1 45.961070142 47.709305288 46.793180305  
1 41.276936625 47.422905115 49.377793328  
1 42.364751617 46.871873079 47.233764228

6	44.455097817	46.810335554	45.573143467
1	43.680121086	47.471389838	45.146909666
1	44.031634238	45.805633787	45.714075693
1	45.272199476	46.710798287	44.847062813
1	47.471060467	38.859098840	48.587492697
1	50.514987314	44.379145700	47.247968732
1	48.537430238	39.135427214	42.141137197
1	42.576324793	48.207395692	51.144261340

**TS<sub>H4m</sub>**

6	46.942918072	39.541732633	47.887393626
7	46.097544822	39.058334719	46.915570541
1	45.794956032	38.083962355	46.819381744
6	45.683575884	40.094518432	46.168480069
1	45.032140080	40.000850127	45.303106883
7	46.224681826	41.223367732	46.607529516
6	47.015462304	40.896834312	47.685818507
1	47.594724068	41.648613432	48.212711637
6	50.016828922	44.843969460	46.404417942
1	50.692353235	44.848840913	45.534619749
1	49.832997757	45.904626668	46.625631971
6	48.698589524	44.204113102	45.979449140
8	48.229190333	43.200065249	46.590676094
8	48.081419004	44.673274470	44.987319598
6	48.494598399	39.955060435	42.827935399
7	49.511336530	40.289585570	43.698841810
1	50.444064053	39.870548183	43.778998066
6	49.054018461	41.260702568	44.507125662
1	49.628493081	41.682237767	45.323076979
7	47.815389240	41.604765752	44.188320770
6	47.446093398	40.788427161	43.140489104
1	46.455103507	40.849212461	42.697035955
26	46.498938757	42.951901249	45.399155660
8	45.567234112	44.171374927	46.147304116
8	43.191231958	43.052087425	44.711782386
6	43.964958492	42.742355494	43.800687206
6	42.320415596	41.543101134	42.271404194
6	41.742057043	41.495021042	40.847883554
8	45.226299081	42.495108452	43.946374364
8	42.475074648	41.025881381	39.947724430
6	43.437688419	42.595266259	42.374157885
8	40.574129690	41.951199136	40.665685927
1	41.534262387	41.765565959	43.003940090
1	42.740535024	40.552433137	42.512395313
1	43.032499855	43.578623794	42.074172325
1	44.256856208	42.341480216	41.688419107
7	43.066077517	48.067283547	50.327236575
6	44.480896155	48.286494090	50.211844444
7	45.017877726	48.043238532	48.990504957
6	44.318632260	47.525446818	47.991156934
6	42.927201002	47.201652779	48.122542861



6	42.339206913	47.524135871	49.298120787
8	45.153996942	48.656006038	51.163774729
7	44.975475219	47.353520506	46.819921483
1	45.924795745	47.739881509	46.829151700
1	41.266133112	47.372827569	49.450772051
1	42.340377062	46.794752088	47.308525331
6	44.622944993	46.503024217	45.749330724
1	43.541574798	46.385888457	45.604267000
1	45.042568406	45.355647463	45.954488860
1	45.130295861	46.800866858	44.821609758
1	47.471563545	38.905054063	48.596788918
1	50.535816180	44.381423930	47.243924452
1	48.550948971	39.117180780	42.133061582
1	42.566122351	48.227474073	51.178327834

**4dmC substrate  
Snapshot 1  
RC**

6	40.592348961	39.730515638	47.896572713
7	41.131321271	40.995186142	47.909544726
1	40.805044983	41.784758249	48.480481029
6	42.124697724	41.044079501	47.004184674
1	42.739245768	41.918336552	46.794913630
7	42.242852833	39.868079989	46.399329733
6	41.296241795	39.030235677	46.946289778
1	41.182538448	37.998302137	46.620994474
6	41.969930286	35.927316389	42.529933321
1	41.434839952	35.949309313	41.566864929
1	42.812816656	35.233208128	42.385390979
6	42.580041988	37.320890408	42.756959521
8	42.210887109	37.978338904	43.812660545
8	43.378190651	37.760031466	41.926942768
6	39.802420020	42.140381770	43.283627121
7	39.268740325	40.892636899	43.045705341
1	38.329458841	40.672191532	42.688907645
6	40.195811911	39.980613595	43.375818825
1	40.062764643	38.910212250	43.281450160
7	41.309236462	40.568490407	43.798267495
6	41.072759998	41.923786040	43.759801680
1	41.828906645	42.641122405	44.062167348
26	43.050386078	39.575239041	44.504827736
8	44.366985868	38.780051983	44.995326817
8	45.068553248	42.180041610	45.442195291
6	45.083223925	41.656535877	44.328853636
6	47.580789063	42.233103996	44.028219960
6	48.209754954	41.378171122	45.151624926
8	44.022930945	41.096430445	43.794581617
8	48.610390070	42.000388702	46.181475250
6	46.308351252	41.646262160	43.426372266
8	48.300303897	40.147632005	44.962052797
1	47.409027606	43.254332143	44.394891062

1	48.350236210	42.281742328	43.235816168
1	46.475145434	40.596270144	43.142841302
1	46.022990759	42.171877479	42.497317117
7	49.218846426	34.453035066	45.760055427
6	48.063284497	33.841364175	45.177804193
7	47.367667297	34.589348776	44.274146377
6	47.708146808	35.851286382	43.962267684
6	48.825021547	36.501559018	44.601355376
6	49.540878570	35.760963737	45.481912171
8	47.729479589	32.699875259	45.482190677
7	46.967791969	36.485950549	43.029145342
1	50.404561384	36.192992690	45.995511458
1	49.095608835	37.539174329	44.422441014
6	46.025954729	35.729503858	42.209359559
1	46.523865805	34.867943484	41.739421163
1	45.614350234	36.394513821	41.441462849
1	45.181726047	35.350743089	42.803512990
6	47.100840777	37.906632841	42.733262652
1	47.733118804	38.073448936	41.841778759
1	47.517793650	38.475771858	43.574269570
1	46.098071332	38.308207167	42.528263534
1	39.715549642	39.450765048	48.480550357
1	41.304455906	35.516875270	43.289373414
1	39.238616571	43.061530567	43.136393002
1	49.690461838	34.060369667	46.549590280

**TS<sub>H4dm</sub>**

6	40.646296195	39.703073463	47.860839030
7	41.207891801	40.959574731	47.883196679
1	40.882361166	41.753442709	48.450180562
6	42.221032664	40.986848272	46.999187992
1	42.853499814	41.849282646	46.793239202
7	42.332862120	39.805518723	46.398988456
6	41.356083365	38.988273885	46.927203841
1	41.225816315	37.961188735	46.592990562
6	41.920778530	35.913655879	42.478781726
1	41.374370503	35.928323805	41.522341448
1	42.766835006	35.226167472	42.324228906
6	42.517205323	37.314872816	42.708267769
8	42.177065041	37.954194975	43.778826052
8	43.293345064	37.767001005	41.860012239
6	39.792315693	42.161537372	43.259556652
7	39.256131100	40.914415940	43.025599029
1	38.315591921	40.691483339	42.675972801
6	40.187155746	40.002781121	43.352064328
1	40.047732501	38.932413331	43.260987172
7	41.303743051	40.587462422	43.767304175
6	41.065698053	41.941128555	43.727997090
1	41.822830065	42.658964933	44.027773917
26	43.122631293	39.529842803	44.495277833
8	44.565861775	38.655914631	44.794770068

8	45.087270829	42.217785696	45.435523054
6	45.101471576	41.711807509	44.307927814
6	47.602794127	42.312939428	44.047069910
6	48.201363044	41.449879461	45.179475880
8	44.067084214	41.129477691	43.773726842
8	48.578378757	42.061318265	46.223438783
6	46.334880935	41.750177267	43.410323219
8	48.299372349	40.218063232	44.985179520
1	47.435790465	43.333346260	44.417849877
1	48.392151250	42.357833460	43.273342508
1	46.508786613	40.719603263	43.068403606
1	46.056522055	42.320628109	42.505648928
7	49.246283627	34.506230498	45.803567974
6	48.105086383	33.882241699	45.208985830
7	47.362626069	34.659862973	44.361687947
6	47.644673288	35.944474871	44.136454028
6	48.755961598	36.599194803	44.767406609
6	49.523485032	35.834270936	45.585198839
8	47.810594645	32.718917660	45.452697819
7	46.828365591	36.623784765	43.271128023
1	50.388873247	36.264723258	46.097320356
1	48.986345507	37.654534933	44.637863997
6	45.899991001	35.875327529	42.425633121
1	46.422929975	35.040657376	41.940888271
1	45.475678378	36.556598828	41.678710668
1	45.058763813	35.463343461	43.003392868
6	46.635475033	38.029626795	43.361445985
1	46.323445409	38.445945650	42.393659713
1	47.453622944	38.598888157	43.820473148
1	45.697123394	38.280244283	44.082479097
1	39.767112483	39.429738290	48.444269573
1	41.267297101	35.498494594	43.246030353
1	39.227944410	43.083671883	43.120919272
1	49.724388122	34.104226581	46.584453006

#### IM1<sub>4dm</sub>

6	40.581668217	39.660728472	47.921394158
7	41.132476761	40.921231987	47.929516410
1	40.801786474	41.721642956	48.483123418
6	42.154956793	40.942044226	47.056713565
1	42.779128386	41.809800197	46.848328549
7	42.284349341	39.753631444	46.475434868
6	41.308499593	38.937387539	47.006943703
1	41.193342554	37.900325149	46.697808107
6	41.951217462	35.871721308	42.482451983
1	41.410082940	35.885827924	41.522716137
1	42.784410395	35.164278267	42.344689666
6	42.576755999	37.258699343	42.688692756
8	42.278035172	37.907770668	43.771340528
8	43.328786779	37.699795299	41.817184173
6	39.825968355	42.128152421	43.300839426

7	39.294178716	40.882750323	43.049708668
1	38.358208035	40.665961999	42.683599166
6	40.221664347	39.970123434	43.390661109
1	40.087209166	38.900407696	43.284453415
7	41.328694616	40.550100297	43.833288826
6	41.090319813	41.903671918	43.794535679
1	41.837957385	42.624707586	44.113185146
26	43.165880166	39.416570291	44.598068534
8	44.662980347	38.416630246	45.075059763
8	45.075448967	42.186555338	45.404476495
6	45.125982500	41.644832413	44.294734716
6	47.594308277	42.290632728	44.043273429
6	48.058582212	41.409100892	45.218924567
8	44.160643498	40.922832864	43.807362369
8	48.524156002	42.008472223	46.230667519
6	46.324761139	41.790902648	43.363829050
8	47.950785271	40.164863318	45.097073499
1	47.474754108	43.324295350	44.394314846
1	48.422764318	42.283504039	43.310430980
1	46.488121823	40.808105670	42.899961132
1	46.020624093	42.468345657	42.545177420
7	49.246706508	34.512944244	45.791589094
6	48.114726251	33.878242431	45.179156600
7	47.410261383	34.625036606	44.281868644
6	47.708218469	35.904884100	44.025347856
6	48.797768278	36.574632670	44.676371289
6	49.536065284	35.834757568	45.542715230
8	47.810925666	32.722147827	45.457055816
7	46.923016626	36.565603218	43.107085526
1	50.388683600	36.277232384	46.065480697
1	49.038690699	37.622534648	44.517147919
6	45.990305597	35.778338721	42.290525051
1	46.519347472	34.942758680	41.814493513
1	45.538652048	36.435970641	41.541084207
1	45.182116670	35.371574236	42.911751921
6	46.927326822	37.923376237	42.938625674
1	46.217927053	38.320949523	42.216755536
1	47.467946143	38.579983432	43.620871766
1	45.522472946	38.850975392	45.201283856
1	39.691076512	39.395900003	48.491288554
1	41.288280074	35.482897121	43.255366658
1	39.264415793	43.049823473	43.148364801
1	49.719881738	34.119324479	46.579714192

**TSRB4dm**

6	40.603458583	39.660070308	47.907007041
7	41.156572456	40.919551653	47.916259038
1	40.822060048	41.720804332	48.465885935
6	42.187957991	40.934023249	47.052114533
1	42.815341382	41.800031003	46.845038717
7	42.321339900	39.744482890	46.475339346

6	41.338524782	38.932731002	47.001346664
1	41.224514840	37.894530161	46.694807572
6	41.950605489	35.864509458	42.473502505
1	41.406668799	35.881563078	41.515546738
1	42.778925410	35.151907902	42.332563977
6	42.582925105	37.249467539	42.682328252
8	42.300944054	37.888661903	43.770858992
8	43.329668547	37.691777279	41.803380266
6	39.825810813	42.123436949	43.301636711
7	39.294741004	40.877135086	43.052929987
1	38.358424861	40.659400503	42.688895976
6	40.223492490	39.965522301	43.396259524
1	40.089053428	38.895164095	43.292741178
7	41.330141884	40.546559381	43.837370296
6	41.090383283	41.899816190	43.795930003
1	41.837800389	42.621756586	44.113424705
26	43.190078235	39.418899296	44.576550325
8	44.714814518	38.410353728	45.032769721
8	45.106439661	42.209499574	45.400925414
6	45.143118730	41.667797091	44.289007499
6	47.619108010	42.287709775	44.035619964
6	48.071254922	41.401765760	45.212314133
8	44.171709880	40.956850611	43.805693058
8	48.526383293	41.996790503	46.230605552
6	46.342225052	41.806957970	43.355651711
8	47.965924260	40.156730880	45.086812070
1	47.512476948	43.322000176	44.388495976
1	48.447573449	42.270635893	43.302698992
1	46.495242538	40.827293172	42.881625421
1	46.044854617	42.494517404	42.543001301
7	49.249605166	34.518524169	45.786785599
6	48.121901233	33.878786912	45.173205182
7	47.406956099	34.629954166	44.285381873
6	47.689297403	35.913506874	44.047583884
6	48.780508152	36.585729115	44.687921799
6	49.531868120	35.842690072	45.542882603
8	47.825957804	32.719469026	45.441532491
7	46.870772723	36.581844965	43.151748456
1	50.387268411	36.284580508	46.061925319
1	49.013287397	37.636735050	44.531373997
6	45.970391260	35.787033887	42.304079254
1	46.526513712	34.966613017	41.833399677
1	45.525054013	36.446590107	41.552038817
1	45.156554181	35.363568355	42.905827205
6	46.773682727	37.934349394	43.085357984
1	46.061890870	38.336849674	42.368756398
1	47.345747580	38.587987354	43.745985471
1	45.535998251	38.870576482	45.269431207
1	39.713122089	39.397951105	48.478550363
1	41.289103506	35.477228008	43.248418969
1	39.264516008	43.045022152	43.147701102
1	49.722300306	34.123009262	46.574249728

**IM2OH4dm**

6	40.656980723	39.691280944	47.921625652
7	41.219060753	40.944579594	47.969140012
1	40.874193728	41.739855787	48.520402950
6	42.270278121	40.966324863	47.126286514
1	42.899262496	41.838375848	46.951084975
7	42.411404889	39.790192729	46.524356299
6	41.408060197	38.979295848	47.015511866
1	41.291002321	37.949490319	46.682995441
6	42.037935087	35.931327812	42.615824107
1	41.547589150	35.986368315	41.633064744
1	42.869987908	35.215953758	42.508360263
6	42.650814413	37.304898623	42.927111433
8	42.686236231	37.702446551	44.162033244
8	43.131851254	37.960295045	41.996024312
6	39.782334748	42.138042071	43.280911235
7	39.263790215	40.889363980	43.023584303
1	38.328658095	40.664554335	42.659926284
6	40.198389988	39.983853425	43.366440630
1	40.064268887	38.914034667	43.253275789
7	41.296581643	40.573632444	43.815357544
6	41.045041127	41.925323771	43.781246795
1	41.781848076	42.651790941	44.112121288
26	43.112624937	39.616611997	44.517552872
8	45.989329641	38.413634722	44.576880378
8	45.230624115	42.375401891	45.376630595
6	45.258151656	41.767240149	44.295033992
6	47.772779612	42.246570478	44.041303942
6	48.107466881	41.397952916	45.278998933
8	44.288045222	41.047845904	43.838147298
8	48.502541958	41.998738944	46.310369915
6	46.466725743	41.839226776	43.363080555
8	47.966435980	40.145560832	45.182730558
1	47.759273712	43.306444857	44.326740219
1	48.608603520	42.107875841	43.330764013
1	46.558845982	40.855863663	42.882328232
1	46.210936314	42.547726351	42.554522495
7	49.269040884	34.508012968	45.791166388
6	48.177876105	33.831858564	45.152013538
7	47.430368234	34.568376460	44.280092149
6	47.598388514	35.880057257	44.122554558
6	48.658330914	36.587450687	44.795704479
6	49.463910628	35.855550635	45.604607055
8	47.941120352	32.652458924	45.389505435
7	46.744373049	36.543334154	43.290694262
1	50.291036888	36.329341516	46.141429846
1	48.814895597	37.659986686	44.707886054
6	45.786839221	35.779443220	42.499389417
1	46.304039310	34.989158798	41.937279960
1	45.280338794	36.460320780	41.804350751
1	45.025335850	35.299766148	43.132914747

6	46.581266571	37.990310783	43.371381097
1	45.939831401	38.270794399	42.521579967
1	47.556306329	38.489002220	43.257127025
1	46.614629662	39.073604743	44.963290881
1	39.762005923	39.421159433	48.482091342
1	41.336655135	35.528424833	43.346538099
1	39.219021910	43.059113867	43.131336158
1	49.749364648	34.126171037	46.580760154

**Snapshot 2**  
**RC**

6	46.178727518	47.420707818	48.178489421
7	46.366799996	48.071420248	46.980597810
1	46.346069504	49.087966658	46.834179339
6	46.551542727	47.145412032	46.021411155
1	46.732977619	47.368013623	44.970884739
7	46.480187096	45.928260957	46.547690571
6	46.254696273	46.077949838	47.895170362
1	46.160690490	45.226404159	48.566175660
6	44.675419458	40.820993856	47.636612760
1	43.655143660	40.463221817	47.421318372
1	45.297002749	39.917464990	47.680289769
6	45.170017715	41.628927657	46.429740449
8	45.137183748	42.931579552	46.520777680
8	45.524237043	41.027368443	45.421887199
6	42.335301061	46.250244897	44.591938328
7	42.025361100	45.504937340	45.711849793
1	41.136141324	45.492920889	46.227814444
6	43.119646305	44.796302645	46.038012424
1	43.181988216	44.090975053	46.855739533
7	44.110018682	45.027946519	45.187350661
6	43.640711838	45.949187821	44.280469420
1	44.274862412	46.327006216	43.484148319
26	46.078623301	44.199103433	45.426785036
8	47.512166532	43.493330433	45.675019797
8	48.168900095	46.003850863	42.896166518
6	47.578116036	44.930668913	43.045485452
6	49.345837510	43.661863825	41.641600066
6	50.635747213	43.725219423	42.484881700
8	46.434203493	44.878463414	43.690019844
8	50.847802729	42.764113606	43.258107172
6	48.064117194	43.611926061	42.474295456
8	51.387678434	44.734802326	42.336317299
1	49.307909233	44.491693763	40.923513720
1	49.414428957	42.733709923	41.056906001
1	48.188146504	42.923822925	43.327269035
1	47.220945073	43.195986235	41.896619361
7	53.377223544	39.073590587	46.900661453
6	52.313355099	38.618965353	47.736053954
7	51.062686486	38.700715533	47.209350673
6	50.794942362	39.315870025	46.050477427

6	51.848976646	39.924242385	45.278143586
6	53.113459722	39.761539691	45.740680708
8	52.529929683	38.190934991	48.869618891
7	49.507162422	39.349825070	45.632729343
1	53.963444280	40.186624362	45.202639910
1	51.675977528	40.497352755	44.370110797
6	48.509655090	38.487383419	46.255454091
1	48.004225352	38.978043195	47.105536071
1	48.975153212	37.562149496	46.614578379
1	47.755596290	38.237666004	45.494336147
6	49.043026063	40.122923333	44.481925940
1	48.882533414	39.468866947	43.607848872
1	49.732563164	40.930049900	44.202389799
1	48.072215892	40.579333117	44.729368628
1	45.889490182	47.925286802	49.100340351
1	44.676098016	41.288564862	48.621216343
1	41.652421830	46.987542007	44.169876424
1	54.308709480	39.146998283	47.256916632

**TS<sub>H4m</sub>**

6	46.274937948	47.303818025	48.205624578
7	46.533177160	47.945508617	47.013403672
1	46.491534345	48.960081747	46.853202530
6	46.822155818	47.010530181	46.087596951
1	47.064066890	47.219815073	45.045852226
7	46.754947502	45.795641312	46.626130774
6	46.414682256	45.961135337	47.950764427
1	46.284163275	45.115937414	48.623914359
6	44.633857199	40.805723510	47.718872543
1	43.643503978	40.401716334	47.462116768
1	45.306110858	39.934813352	47.739563484
6	45.109896194	41.715751832	46.574008281
8	45.505717665	42.917195181	46.871925409
8	45.117861275	41.262275780	45.429192385
6	42.488433495	46.107123227	44.662624497
7	42.196464266	45.394250536	45.808176632
1	41.312984910	45.395097749	46.330518360
6	43.301945935	44.695209269	46.136360629
1	43.375707788	44.028894418	46.986166580
7	44.277946224	44.893976800	45.263324591
6	43.788221038	45.788255384	44.339505011
1	44.409299172	46.142646435	43.522304618
26	46.402009630	44.054611427	45.476266839
8	47.846739293	43.119043931	45.548309623
8	48.276869991	46.075108702	42.857952364
6	47.701396464	44.984320750	42.981076612
6	49.440006331	43.788402811	41.454723316
6	50.709112024	43.843049808	42.327059962
8	46.641941219	44.858448464	43.725412509
8	50.933294330	42.856157443	43.067865951
6	48.130104285	43.726179763	42.242287889



8	51.442860196	44.870541350	42.235609031
1	49.424112503	44.633144154	40.753781477
1	49.522674243	42.869306920	40.855225782
1	48.150479726	42.915953366	42.984374582
1	47.285994118	43.474098217	41.576531404
7	53.307819921	39.224014560	46.822250567
6	52.213171516	38.801125789	47.634326021
7	50.963512082	39.046346876	47.137426049
6	50.749674805	39.758940214	46.034994447
6	51.840363646	40.267879354	45.251397381
6	53.092763261	39.973220005	45.691091323
8	52.392249368	38.266338441	48.723410614
7	49.443329046	39.968445365	45.659368803
1	53.971246967	40.341332691	45.156595123
1	51.708987817	40.887652748	44.366559690
6	48.382729185	39.253624800	46.366251171
1	48.225806599	39.666333682	47.374275880
1	48.638841888	38.189526241	46.464508474
1	47.454253051	39.376007151	45.791848778
6	49.038286937	40.948393803	44.714863303
1	48.180466094	40.603853995	44.118923216
1	49.836100323	41.368290918	44.088462245
1	48.561690893	41.950392040	45.233021225
1	45.959953805	47.817233486	49.114061081
1	44.603056041	41.236710412	48.719556759
1	41.793777488	46.820170694	44.218683441
1	54.235886737	39.247453148	47.193888981

**Snapshot 3  
RC**

6	46.947114934	46.455326958	48.691245163
7	46.955401337	47.219303343	47.547543185
1	46.814749395	48.234767390	47.490516621
6	47.114550992	46.404404480	46.491443903
1	47.169771675	46.722264854	45.452391780
7	47.197056351	45.145373877	46.902626389
6	47.102403183	45.153766062	48.275362159
1	47.139432065	44.239302441	48.864105488
6	45.904639109	39.794505349	47.569636727
1	44.909107470	39.346965438	47.419345197
1	46.623342592	38.969861083	47.448869218
6	46.169239703	40.773415027	46.430298165
8	46.131091792	42.040361867	46.719312759
8	46.369618818	40.335772218	45.298275241
6	42.951612345	45.292800103	45.308170215
7	42.761843293	44.372320779	46.314442744
1	41.916529036	44.237794498	46.885815883
6	43.915199009	43.709555268	46.486989130
1	44.063297506	42.908314999	47.199408580
7	44.843086232	44.148831346	45.645189838
6	44.256420897	45.146607114	44.900854549

1	44.803450104	45.686247208	44.132526850
26	46.865647425	43.487387757	45.710296679
8	48.383089026	42.948046130	45.852854315
8	47.873709361	45.522724294	43.533344584
6	47.599666218	44.393795644	43.108367971
6	49.095372171	44.717107475	41.069771384
6	50.493821584	44.674741349	41.720693866
8	46.873749144	43.550358786	43.776174557
8	50.661545218	43.948016401	42.740634509
6	48.020653242	43.888549319	41.743843148
8	51.356208618	45.398984773	41.172102146
1	48.782384154	45.774364296	41.039851634
1	49.214858213	44.392187702	40.022944473
1	48.345475747	42.846081548	41.877892297
1	47.102442914	43.852495674	41.128346358
7	54.155436973	39.292155640	45.646714858
6	53.171591483	38.665785125	46.468146457
7	51.897203977	38.705971549	46.017690155
6	51.512193502	39.456505838	44.986349923
6	52.473143069	40.229902557	44.239719343
6	53.774857971	40.098631266	44.603290831
8	53.494559984	38.120135139	47.525394381
7	50.190290367	39.480900205	44.672788351
1	54.558891423	40.651825463	44.083954099
1	52.208349701	40.871018379	43.403334894
6	49.293373009	38.454497461	45.207042553
1	49.619651604	38.177222188	46.217835997
1	49.312252281	37.552807793	44.565800782
1	48.269253422	38.852107228	45.234642354
6	49.652579679	40.337103829	43.618782431
1	50.141409407	41.320923860	43.598200182
1	48.588599165	40.512574184	43.829100018
1	49.742517734	39.873202324	42.618733227
1	46.693385376	46.858016858	49.671821257
1	45.969072074	40.162713234	48.593520831
1	42.176413820	46.001427210	45.016653157
1	55.113150165	39.345297059	45.929440736

#### TS<sub>H4m</sub>

6	47.019238063	46.361749058	48.714323725
7	47.061445483	47.118988620	47.566621935
1	46.917614006	48.133779611	47.501201652
6	47.264992041	46.292780789	46.523955357
1	47.336627146	46.602882170	45.483883573
7	47.347161483	45.036136162	46.943042190
6	47.200766042	45.058034591	48.311965635
1	47.219319292	44.147445330	48.908354353
6	45.853842432	39.723907489	47.611941051
1	44.864563181	39.267158556	47.454022023
1	46.579872729	38.905464800	47.486594015
6	46.120197450	40.717575212	46.484663290

8	46.250123562	41.963418231	46.814202051
8	46.198193414	40.299363426	45.327629396
6	43.096984776	45.210821652	45.301785967
7	42.899354144	44.303368232	46.317657543
1	42.045715141	44.173723627	46.877834287
6	44.053278837	43.643907619	46.507901702
1	44.196539284	42.855692492	47.235291407
7	44.987837757	44.069292000	45.665503989
6	44.405699163	45.058952925	44.905035298
1	44.960955839	45.590702785	44.136871813
26	46.986061565	43.367305676	45.734368275
8	48.602407918	42.772642769	45.917110763
8	47.788538368	45.437638731	43.541333213
6	47.633534922	44.286385537	43.104748055
6	49.105001620	44.743930533	41.074249303
6	50.498020113	44.671090275	41.731553811
8	47.082774846	43.340047549	43.788400948
8	50.644728478	43.938074653	42.753890087
6	48.021218028	43.883673676	41.694977021
8	51.376492543	45.382991544	41.195743568
1	48.793267017	45.802088135	41.097161461
1	49.231480057	44.470204600	40.013932373
1	48.318955437	42.826306803	41.727684117
1	47.096705786	43.931355303	41.089591983
7	54.086231622	39.404676361	45.596326854
6	53.096922896	38.795192082	46.422751838
7	51.803862566	38.954565019	46.039579741
6	51.434732674	39.788277536	45.074503809
6	52.408251031	40.509068951	44.300997486
6	53.714484255	40.273105694	44.596826868
8	53.418467926	38.172155892	47.434221502
7	50.085655758	39.904714528	44.835706490
1	54.510941101	40.785062869	44.054582179
1	52.147786513	41.190188255	43.494292494
6	49.205621525	38.878038982	45.407852048
1	49.264623180	38.867939529	46.505809557
1	49.517697865	37.887769392	45.041936124
1	48.174479385	39.090568112	45.101477053
6	49.483447878	41.034837542	44.226446604
1	50.153621405	41.678408058	43.644276402
1	49.018703489	41.895827479	45.094296181
1	48.558634524	40.779026746	43.694002717
1	46.745020211	46.776277717	49.684394795
1	45.919179973	40.088775033	48.636963002
1	42.317068413	45.904974813	44.988817624
1	55.046306834	39.431280789	45.874751511

**Snapshot 4  
RC**

6	41.849401060	36.181402634	45.438485944
7	41.901870863	37.450601536	45.966489578

1	41.346025780	37.792503718	46.760489475
6	42.782753213	38.173182502	45.250215622
1	43.039582226	39.212348588	45.450078027
7	43.295656542	37.431523114	44.273138098
6	42.728675743	36.182060057	44.379583774
1	42.984129462	35.376065522	43.696171730
6	44.754445079	35.400696939	39.408067757
1	44.287659092	35.564011405	38.422822578
1	45.801411053	35.129858181	39.202072151
6	44.788164645	36.760737779	40.126215673
8	44.060138339	36.920205798	41.182208236
8	45.493564030	37.639788737	39.623575715
6	40.290207215	39.849022681	41.739074547
7	40.259546850	38.669192365	41.021903222
1	39.470536565	38.267306587	40.501177548
6	41.461632974	38.082487607	41.161253769
1	41.747603291	37.147701045	40.696224561
7	42.261210129	38.817870497	41.919718212
6	41.540661537	39.924084405	42.298681091
1	41.972373756	40.676814086	42.950084568
26	44.216991471	38.300060812	42.547925512
8	45.754059426	37.926621104	42.873914610
8	45.165747741	40.766071396	45.135633645
6	45.261444816	40.600429466	43.921503870
6	47.421210806	41.963596701	43.890084621
6	48.395817406	41.214084238	44.821217754
8	44.285103563	40.054480738	43.233490074
8	49.000994641	40.226493264	44.341843122
6	46.465088791	41.055587947	43.121770396
8	48.513881152	41.659608782	46.001889298
1	46.841701805	42.683092579	44.482647457
1	48.033353814	42.534930342	43.170938968
1	46.982080898	40.138074662	42.795725189
1	46.082432748	41.526576432	42.202606300
7	51.993970657	35.181037114	43.318391060
6	51.059580041	34.473941970	42.494271156
7	50.223483586	35.244748134	41.754257827
6	50.143138822	36.575687056	41.876214387
6	50.945816643	37.272221897	42.852226026
6	51.868291489	36.534131767	43.520947882
8	51.042069323	33.246195782	42.465102234
7	49.299185481	37.241144476	41.054208266
1	52.543600940	37.001856567	44.243071448
1	50.859930826	38.337838966	43.048054073
6	48.775104649	36.618310368	39.842993982
1	49.366331206	36.944218898	38.965883649
1	47.727605370	36.919153995	39.690546510
1	48.846064360	35.529229225	39.930641953
6	48.997931763	38.659231318	41.198192034
1	49.125232632	39.017522660	42.228875478
1	47.942243155	38.812261689	40.929656224
1	49.622201254	39.268398645	40.518701099

1	41.125857389	35.435248843	45.766824795
1	44.265118507	34.548093985	39.878912776
1	39.423413394	40.495318270	41.877052080
1	52.624739592	34.694019348	43.922474444

**TS<sub>H4m</sub>**

6	41.935828924	36.203231322	45.385203447
7	42.013788999	37.468174046	45.924086674
1	41.455075145	37.815728218	46.714370604
6	42.922341091	38.172339252	45.224072303
1	43.200828958	39.205321511	45.429191253
7	43.431896220	37.424035298	44.246524584
6	42.826795815	36.188487894	44.336819108
1	43.064051334	35.383777206	43.645015218
6	44.749475305	35.355742697	39.338804514
1	44.287168725	35.505860524	38.349696135
1	45.798581526	35.086648636	39.139463778
6	44.769647415	36.723466127	40.047721737
8	44.107569750	36.871083544	41.140288671
8	45.428171385	37.614608541	39.494895096
6	40.324296168	39.861671457	41.714870768
7	40.290135263	38.673487501	41.011726419
1	39.496252918	38.261935036	40.507232034
6	41.501750568	38.098972219	41.138098312
1	41.784448321	37.158080422	40.682325033
7	42.311164028	38.847941312	41.870517963
6	41.585921946	39.950863901	42.249499675
1	42.021161475	40.712362668	42.888879827
26	44.355069686	38.305078010	42.529008621
8	46.042405521	38.000935836	42.660365888
8	45.223455086	40.842625405	45.169265759
6	45.292931889	40.692516002	43.946586067
6	47.457371726	42.061560459	43.921448624
6	48.392127310	41.252843106	44.842418304
8	44.353533717	40.092793160	43.274796338
8	48.963474948	40.246238968	44.353963911
6	46.453602766	41.234007402	43.128730966
8	48.524418865	41.675164032	46.028635615
1	46.907285599	42.787261766	44.532306799
1	48.097593058	42.623491504	43.218518650
1	46.931061173	40.364116825	42.659770865
1	46.017317789	41.807296797	42.294410223
7	51.959100935	35.223742914	43.345654690
6	51.033236026	34.509880525	42.519155489
7	50.140738225	35.277559891	41.833501993
6	49.990313612	36.584160671	42.044128196
6	50.798194553	37.282978403	43.007247147
6	51.785355237	36.562976102	43.604534974
8	51.054437126	33.286990659	42.441292650
7	49.057718452	37.242111917	41.284587920
1	52.475703244	37.033678604	44.310404115

1	50.673841456	38.338751791	43.240081765
6	48.610279080	36.659785487	40.014906604
1	49.338938673	36.901238297	39.220232789
1	47.627368647	37.071968340	39.750311116
1	48.542764144	35.568839105	40.093824231
6	48.397957081	38.422708635	41.719593564
1	48.874854459	38.972000996	42.543207532
1	47.282852720	38.144750353	42.195010510
1	48.126827513	39.073966917	40.876514181
1	41.209877194	35.462805621	45.721106998
1	44.262095704	34.508320626	39.820887782
1	39.454672810	40.503050967	41.857891249
1	52.600423220	34.735594005	43.937591228

**Snapshot 5**  
**RC**

6	42.212472873	35.654340480	44.267608841
7	41.947204981	36.849880375	44.891408327
1	41.186806855	37.037011441	45.560798010
6	42.817220999	37.765963749	44.434404780
1	42.842615876	38.806507723	44.750752845
7	43.630310356	37.213710138	43.538202701
6	43.268880401	35.891314212	43.422556914
1	43.776159930	35.210344109	42.742559053
6	46.169916473	35.851714486	38.899000529
1	45.860059709	36.052990069	37.859914888
1	47.265374044	35.751411585	38.865792673
6	45.872138635	37.110821830	39.727008097
8	44.938743857	37.035493380	40.626480762
8	46.501539711	38.139602263	39.479920079
6	40.754558759	39.390381807	40.611931727
7	41.032543707	38.280150068	39.841227292
1	40.415603813	37.840412511	39.146273421
6	42.253432070	37.840869984	40.186859232
1	42.744774506	36.982070333	39.747533311
7	42.788541534	38.615727180	41.122790330
6	41.854957109	39.586069452	41.410048892
1	42.039657972	40.335779383	42.172183720
26	44.663871948	38.279100752	42.073560548
8	46.159890168	38.042836271	42.650949438
8	44.802188657	40.746804174	44.836250188
6	45.157892735	40.655494344	43.656052173
6	47.174181616	42.206251569	44.084756210
6	47.977756234	41.447205729	45.159402149
8	44.430427600	40.025098478	42.777372486
8	48.801683962	40.598384641	44.765644830
6	46.429345747	41.283554887	43.119738365
8	47.748169595	41.738346626	46.380064385
1	46.480012489	42.910994695	44.563421109
1	47.897036024	42.804514231	43.505629285
1	47.076340198	40.440274723	42.825734804

1	46.159393900	41.793166775	42.180045812
7	52.741908971	36.235157390	43.985965707
6	52.129675892	35.494236818	42.917975543
7	51.324976111	36.202022941	42.074807216
6	50.975452448	37.476125675	42.306408402
6	51.466156368	38.181897336	43.466483816
6	52.353969183	37.527619030	44.251902665
8	52.349761144	34.292459342	42.789283599
7	50.157194632	38.092902381	41.423840045
1	52.788466462	38.020472642	45.126128796
1	51.174480705	39.198582883	43.714591030
6	49.890634351	37.492115486	40.119293484
1	49.303513442	36.567272482	40.211534497
1	50.829695649	37.258842221	39.594047159
1	49.296236049	38.196080266	39.526242964
6	49.577732061	39.412650538	41.656604368
1	48.557985060	39.412794072	41.243443913
1	50.163868187	40.201184219	41.148515399
1	49.490686610	39.659462373	42.723078895
1	41.568215331	34.779193157	44.351969432
1	45.742832190	34.895953630	39.202624506
1	39.779377399	39.877264897	40.606144226
1	53.283077197	35.798486521	44.704594957

**TS<sub>H4m</sub>**

6	42.305650551	35.665391283	44.241924615
7	42.068069540	36.866104161	44.871262925
1	41.300797296	37.069193710	45.529257728
6	42.983748443	37.752284136	44.446309088
1	43.040870429	38.789326354	44.772840984
7	43.801612488	37.179328365	43.562592655
6	43.387870012	35.871339855	43.422446363
1	43.879614908	35.179291999	42.741312020
6	46.179387529	35.807857012	38.818323431
1	45.861818874	36.009355780	37.781914564
1	47.275423125	35.715213178	38.778277127
6	45.872939661	37.058900710	39.659213983
8	45.017103196	36.953384068	40.621353309
8	46.453524273	38.109255016	39.366949605
6	40.830898292	39.401076569	40.599988360
7	41.103013489	38.281059882	39.841980729
1	40.481401189	37.836794187	39.155347832
6	42.330330489	37.849713182	40.184795166
1	42.818161368	36.985361244	39.751211490
7	42.876526211	38.636926052	41.102270334
6	41.942226444	39.607504523	41.382688989
1	42.132536898	40.368875965	42.132050351
26	44.845496772	38.252320102	42.108081548
8	46.517914873	38.057152939	42.524778886
8	44.870197919	40.773244114	44.893571678
6	45.223432236	40.731112640	43.704707169

6	47.181033895	42.352606105	44.202297680
6	47.951866417	41.532069011	45.253938225
8	44.580089415	40.041943212	42.821923786
8	48.744245503	40.659008568	44.842983476
6	46.419650500	41.512570428	43.178888973
8	47.739794042	41.804850734	46.480933750
1	46.496357144	43.048270570	44.706082861
1	47.925784631	42.966483295	43.666566872
1	47.081216329	40.772103393	42.708298583
1	46.046044694	42.134538431	42.348053307
7	52.693903128	36.296048646	44.060636829
6	52.112052951	35.544732631	42.985770943
7	51.241145275	36.223950321	42.179244680
6	50.770957895	37.430043545	42.490895101
6	51.242501566	38.144808086	43.648966082
6	52.217297744	37.547831637	44.379002854
8	52.394105028	34.363221325	42.814169689
7	49.845597383	38.002080198	41.655101213
1	52.650799037	38.053020636	45.247220923
1	50.875553785	39.128870014	43.930890252
6	49.615561027	37.423416833	40.332987804
1	49.100236172	36.454818332	40.412917514
1	50.573979316	37.278543924	39.815251690
1	48.963804361	38.097790423	39.764621699
6	48.907609716	38.976324496	42.087719918
1	47.812543674	38.468460380	42.325754069
1	48.657811718	39.676090440	41.277167580
1	49.148551283	39.498857009	43.022150974
1	41.648775958	34.800267561	44.332168879
1	45.756618945	34.852550305	39.129326858
1	39.855367352	39.887240666	40.592834709
1	53.255042905	35.867243791	44.768606492

### Post hydroxylation Coordinates

#### Ketene Formation

#### In aqueous solution outside the enzyme

RC<sub>kaq</sub>

7	17.193297397	15.851140039	15.820912762
6	16.192934925	14.807546755	15.817872835
7	14.992987227	15.156755918	15.276820827
6	14.720198440	16.367421217	14.821701029
6	15.732360559	17.412418588	14.756310591
6	15.464370208	18.702911207	14.211742878
6	16.949861305	17.081316813	15.287594389
8	16.434024508	13.699901613	16.259820956
7	13.481425304	16.643407425	14.397487818
1	13.261798764	17.567325496	14.048855215
1	12.720147230	15.982815706	14.536000603
1	17.759230631	17.813636815	15.306599388
6	15.220381126	19.789767102	13.707912325



1	15.530211453	21.521718125	14.150252582
8	15.062847334	21.037487684	13.378919527
8	16.291209459	21.474003160	15.532567059
1	16.063881162	22.228118671	16.154845207
1	15.812787415	20.690880142	15.871033494
1	18.093394924	15.725458574	16.238047154

**TS<sub>kaq</sub>**

7	17.221946571	16.010827836	15.944383234
6	16.200302888	15.004028553	15.882455563
7	15.003306993	15.426454913	15.385003353
6	14.755123171	16.676088280	15.031799648
6	15.786752879	17.711601053	15.045263431
6	15.553433010	19.047798785	14.561770556
6	16.995384058	17.298403947	15.533068248
8	16.406446912	13.856547393	16.242849569
7	13.516281262	17.003915491	14.635798183
1	13.303867387	17.969145699	14.424169501
1	12.744586536	16.344271623	14.729293463
1	17.827312988	18.003614098	15.601076457
6	15.013571746	19.900879285	13.807617537
1	15.827517752	21.794159004	14.209963959
8	14.708481012	20.960263218	13.259667122
8	16.501921659	21.651787485	14.952910385
1	16.206796898	22.209925309	15.751679720
1	16.300927894	20.608149216	15.087646993
1	18.124439552	15.836034637	16.337989961

**PD<sub>kaq</sub>**

7	17.149213286	15.911803739	16.056445936
6	16.161548275	14.877692020	15.924722733
7	14.975109403	15.276130087	15.381144624
6	14.715227397	16.523951937	15.037494214
6	15.719407856	17.568550790	15.099487287
6	15.510871246	18.938660846	14.597381952
6	16.910376649	17.198092737	15.656205296
8	16.377772247	13.731797598	16.279351359
7	13.476161837	16.823029895	14.590963159
1	13.178618911	17.790511758	14.587770596
1	12.731439931	16.134440747	14.699604719
1	17.708820825	17.933735507	15.793210042
6	14.838206660	19.310711998	13.531820896
1	17.292767596	21.544674760	14.909128429
8	14.241175468	19.726490478	12.606545321
8	17.017801012	21.126647716	15.756930010
1	16.522384636	21.843059343	16.223325368
1	16.015384465	19.811095697	15.107464718
1	18.048840682	15.741015761	16.458284840

**Inside the enzyme without assistance of water molecule**

TS1<sub>ket</sub>

6	43.727640488	40.349631238	49.590490159
7	44.414713581	41.476082561	49.199158382
1	44.525828146	42.341226571	49.741152616
6	44.921663036	41.252478429	47.973766159
1	45.528186028	41.959065631	47.412256037
7	44.583679713	40.042313916	47.542048711
6	43.840539370	39.461835161	48.547211894
1	43.452240730	38.449739803	48.462130173
6	42.583363465	35.695055420	45.564033797
1	41.901229008	35.940188525	44.738734283
1	43.108809008	34.755367819	45.342802828
6	43.617300830	36.810696265	45.764275055
8	43.229354374	37.997097555	45.419216896
8	44.730408165	36.549852199	46.227450714
6	41.180404424	42.646175370	45.086933463
7	40.517537846	41.480764298	45.395475423
1	39.510579259	41.375206328	45.570509656
6	41.422999198	40.487736493	45.449312799
1	41.185392549	39.447047821	45.652166839
7	42.641559002	40.949544806	45.194932321
6	42.505684335	42.301760394	44.968629555
1	43.355577859	42.931953458	44.716854581
26	44.309768901	39.651924921	45.472714240
8	47.875287442	39.002095704	42.549755439
8	46.904675919	41.570719276	45.510236013
6	46.494960392	41.293510076	44.374857216
6	46.886350490	43.583696408	43.301559662
6	47.672506651	44.371137761	42.227751374
8	45.638147404	40.334047127	44.161400962
8	47.026235622	45.078360204	41.421077089
6	46.999974418	42.056901519	43.155998660
8	48.933582947	44.262110584	42.252628837
1	47.307171775	43.863263500	44.278892096
1	45.829850742	43.892511444	43.279909582
1	48.066208143	41.797378280	43.042578348
1	46.475866100	41.701196976	42.257773763
7	49.474577672	33.841568390	44.999997446
6	48.348962168	33.004618694	45.248456912
7	47.177394140	33.374225735	44.690045113
6	46.999979355	34.516329624	44.034192631
6	48.096037071	35.475304835	43.905929262
6	47.926714681	36.754653505	43.314315586
6	49.316568271	35.051306470	44.384276978
8	48.472097608	31.990000834	45.937483209
7	45.814275489	34.765083942	43.478821706
1	45.631840696	35.650521360	43.016471177
1	45.044558986	34.094125312	43.546555462
1	50.189080360	35.700927001	44.281160970
6	48.077654908	37.741509447	42.522464276
1	47.504972511	38.553873355	43.518258979

8	44.103369813	37.130156337	41.556764174
1	44.086496293	38.092698431	41.826014844
1	44.977036768	37.040443452	41.149386906
1	43.148899567	40.299214976	50.512761520
1	41.975692042	35.547416803	46.456785503
1	40.665093783	43.604324674	45.020059111
1	50.385580193	33.567195992	45.307839437

**IM1iKet**

6	43.710538924	40.369845507	49.548581517
7	44.431335097	41.482763540	49.179589428
1	44.560123732	42.336172040	49.735858822
6	44.928419095	41.269321548	47.947250235
1	45.556392662	41.966523310	47.397949820
7	44.551015184	40.080988274	47.490865301
6	43.791700178	39.503649593	48.484666409
1	43.361424215	38.511791106	48.371799204
6	42.594090231	35.735896558	45.501638237
1	41.899660860	35.994112586	44.690382050
1	43.103487375	34.792986585	45.259063794
6	43.646611397	36.842100755	45.658185045
8	43.215416528	38.046335307	45.464790223
8	44.814673260	36.556814860	45.942589521
6	41.112741609	42.693483292	45.077653218
7	40.458893486	41.530984320	45.415958186
1	39.455040276	41.420747517	45.603442119
6	41.368084015	40.542015511	45.469642011
1	41.137514587	39.503334452	45.689358093
7	42.579527004	41.003352183	45.186805085
6	42.436670488	42.350804812	44.940814347
1	43.280230962	42.977841778	44.661827953
26	44.259838466	39.721284738	45.413991044
8	46.431777141	37.140059884	41.869895137
8	46.913975018	41.530265289	45.451163898
6	46.461316466	41.337438677	44.313126790
6	46.854378701	43.623088992	43.247205375
6	47.660331500	44.422056106	42.198178869
8	45.504557687	40.492034868	44.074310674
8	47.028302864	45.142509864	41.392680739
6	47.019559458	42.098023317	43.116989644
8	48.920638251	44.307513590	42.240696155
1	47.228117065	43.923058211	44.238462531
1	45.791350827	43.900505815	43.179297011
1	48.098850198	41.878134835	43.065629071
1	46.545166321	41.732244869	42.194813313
7	49.587749428	33.785998492	44.983226126
6	48.411597302	32.974825095	45.298044694
7	47.261287081	33.320009801	44.708359503
6	47.108254751	34.412289926	43.962716458
6	48.211748042	35.394506264	43.853089147
6	48.131469329	36.685496368	43.362922294

6	49.459609935	34.937538129	44.318746827
8	48.544971945	32.019002996	46.052916505
7	45.987023264	34.593927286	43.287039610
1	45.907589351	35.375727870	42.633503517
1	45.197975202	33.943719718	43.360772591
1	50.329741372	35.584123834	44.169895045
6	46.991495294	37.395481465	42.957196668
1	46.661640647	38.247452539	43.597230624
8	43.712753663	37.390480698	41.673480301
1	43.638254450	38.362278139	41.862322897
1	44.682636393	37.313203981	41.569917303
1	43.139806667	40.310749114	50.475317526
1	41.997051588	35.587394959	46.401393456
1	40.596181014	43.651255356	45.015162031
1	50.490666359	33.500098037	45.304122438

**TS<sub>2iKet</sub>**

6	43.712816678	40.377284390	49.543151275
7	44.444597115	41.484621926	49.179025521
1	44.577488641	42.336101045	49.737277726
6	44.941214199	41.270813066	47.946425893
1	45.577869115	41.963026565	47.400564411
7	44.552561154	40.087983728	47.485251715
6	43.786823931	39.514522281	48.476094864
1	43.346026601	38.527886768	48.358869345
6	42.618780351	35.753920726	45.496791561
1	41.917541691	35.986327939	44.683109017
1	43.143723917	34.817025054	45.266058125
6	43.649321668	36.884792553	45.627255814
8	43.188428652	38.078129049	45.451179028
8	44.835674004	36.626037361	45.866658221
6	41.115584333	42.715449170	45.071632514
7	40.463344438	41.549841202	45.402253501
1	39.459362702	41.436662327	45.587259614
6	41.375078245	40.563148479	45.455414875
1	41.146348772	39.522991784	45.670181699
7	42.586757634	41.028890801	45.180125974
6	42.441120488	42.377060364	44.939547873
1	43.284275252	43.007248633	44.666464906
26	44.266983375	39.744053447	45.405152021
8	46.485503343	37.860257330	41.875824865
8	46.945288807	41.517790904	45.443789618
6	46.492858902	41.313789656	44.306607337
6	46.876768148	43.593846546	43.238389213
6	47.664720803	44.405246526	42.185355243
8	45.535603453	40.470072414	44.075354402
8	47.018332741	45.121681464	41.387157865
6	47.048790421	42.069341720	43.105456686
8	48.926878753	44.306387591	42.218442574
1	47.258668241	43.893037833	44.226749304
1	45.810950801	43.863284720	43.184487033

1	48.128360265	41.852088958	43.048017782
1	46.571563693	41.698059076	42.187442625
7	49.544759407	33.742571836	45.056436555
6	48.403653245	32.905203022	45.333117890
7	47.231881780	33.265394322	44.781242805
6	47.050687850	34.388216235	44.091490858
6	48.153819173	35.352598834	43.957993208
6	48.085171358	36.574044876	43.265727483
6	49.385029477	34.933176476	44.444615462
8	48.545108436	31.909359158	46.037208392
7	45.871890911	34.605934477	43.521512059
1	45.661281118	35.473509072	43.041897816
1	45.099183757	33.940029458	43.609967111
1	50.248024784	35.592752043	44.318338175
6	47.119836462	37.353900617	42.776071276
1	47.070342493	37.734256290	43.918535916
8	43.782952634	37.247913087	41.656252962
1	43.694013497	38.202186897	41.923014616
1	44.726457365	37.247407743	41.417842313
1	43.141848412	40.318273866	50.469747369
1	42.022749213	35.602263305	46.396688345
1	40.595340543	43.671268723	45.009804445
1	50.458154709	33.468719445	45.357578346

**IM2<sub>iKet</sub>**

6	43.703381701	40.371170562	49.574538026
7	44.427864689	41.481924133	49.207114181
1	44.560655301	42.333853201	49.764855089
6	44.920326705	41.271932471	47.973494722
1	45.549676922	41.968960071	47.425823200
7	44.536051543	40.086472551	47.513998851
6	43.777381769	39.508349259	48.507809065
1	43.342642058	38.518735923	48.394220629
6	42.630589221	35.765663228	45.514218913
1	41.917897314	35.966622209	44.701501996
1	43.183649705	34.843244612	45.290964609
6	43.621113965	36.932199621	45.620913435
8	43.127640982	38.110038410	45.444582632
8	44.823717545	36.718658673	45.834920636
6	41.128747453	42.726082637	45.067919664
7	40.475677745	41.557796043	45.386270326
1	39.471176277	41.443600455	45.568911366
6	41.386637927	40.570607682	45.435328693
1	41.157991915	39.529352976	45.644237419
7	42.600369983	41.039184717	45.169680338
6	42.455043480	42.389719358	44.939904872
1	43.299565871	43.023899005	44.680158044
26	44.270830748	39.748270794	45.441254822
8	48.832008914	38.713543806	42.740777180
8	46.896978300	41.502449495	45.463298271
6	46.479243446	41.278940265	44.318035830

6	46.887210223	43.563368297	43.261481048
6	47.676541829	44.368322649	42.203216070
8	45.551015751	40.401039691	44.074999954
8	47.030118899	45.075027096	41.396315859
6	47.043475841	42.037790558	43.123560158
8	48.937981897	44.271972649	42.240067323
1	47.276782528	43.856266581	44.248441491
1	45.823612663	43.843161109	43.213460863
1	48.120092204	41.805150756	43.069340995
1	46.566555814	41.677928322	42.200284587
7	49.461739339	33.829146419	45.022775071
6	48.384271070	32.939258562	45.236131321
7	47.199202286	33.288226759	44.687877576
6	46.963492489	34.480030022	44.156243960
6	47.971979614	35.528674679	44.210880019
6	47.572601559	36.915998849	43.909839681
6	49.218531603	35.121628210	44.596855761
8	48.536267689	31.899040032	45.884880530
7	45.786266783	34.699977064	43.560225984
1	45.542470311	35.621477832	43.217154521
1	45.055972646	33.983942687	43.536307929
1	50.052887970	35.827368576	44.622840745
6	48.267729037	37.852218487	43.284150324
1	46.628224056	37.279004774	44.345765109
8	44.018510934	37.171910142	41.593648140
1	44.007652079	38.147168995	41.812742650
1	44.910407394	37.044962599	41.239734174
1	43.130069435	40.314781958	50.499849162
1	42.038581170	35.608833300	46.415883017
1	40.606755574	43.681171974	45.009643151
1	50.385870843	33.575053660	45.308064977

#### Inside the enzyme with assistance of water molecule

RC<sub>kew</sub>

6	43.707330306	40.419644134	49.506685628
7	44.365391838	41.562583959	49.110885674
1	44.489779792	42.416249628	49.667801934
6	44.827511032	41.370467021	47.863352363
1	45.410265339	42.088887606	47.293654138
7	44.484908451	40.165726369	47.428868212
6	43.789688796	39.550531427	48.444651232
1	43.426877259	38.529510019	48.356498959
6	42.461213766	35.838036652	45.550168321
1	41.788762899	36.139633488	44.736486597
1	42.990015955	34.914679979	45.272592978
6	43.512449253	36.912292291	45.869572093
8	43.236242420	38.105293162	45.395142194
8	44.486349443	36.626444732	46.550554827
6	41.198736928	42.505362802	45.120029833
7	40.532770091	41.357728730	45.493156124
1	39.526417820	41.267534701	45.682983661

6	41.427977100	40.358209529	45.562989132
1	41.189526223	39.328297181	45.805933597
7	42.641614947	40.795870076	45.250293671
6	42.514437186	42.140861565	44.970954331
1	43.365958147	42.737817074	44.658714798
26	44.412646684	39.641634635	45.383732588
8	45.784460421	38.793374787	45.325109131
8	46.916264297	41.576854726	45.390505946
6	46.304626861	41.574291096	44.322902376
6	46.848140701	43.822391204	43.257481817
6	47.633588141	44.537389870	42.137354035
8	45.139126342	41.003284348	44.165631978
8	46.983757972	45.191421336	41.290302156
6	46.860847967	42.290835059	43.097786606
8	48.892648034	44.412328781	42.160234268
1	47.333171968	44.074814218	44.212304765
1	45.812677395	44.195732273	43.276038603
1	47.910666100	41.973262076	42.988707480
1	46.300801872	41.996397483	42.197473317
7	49.510355404	33.782301977	44.981111867
6	48.388800425	32.947430848	45.231324180
7	47.213859480	33.324791838	44.680304235
6	47.028735873	34.486158779	44.067900729
6	48.125643082	35.440965481	43.954230879
6	47.889337410	36.751238121	43.453639674
6	49.350463090	35.010993075	44.394851961
8	48.503998492	31.929568157	45.917598310
7	45.828338708	34.765320812	43.551388184
1	45.641917247	35.673497543	43.138970836
1	45.062415120	34.087849492	43.589993580
1	50.220447686	35.666409378	44.312051015
6	47.560035806	37.866254871	43.101983072
1	47.239135785	38.875990209	42.916979472
8	44.049727216	37.297822561	41.623286262
1	44.006772100	38.263859976	41.863443419
1	44.961122382	37.204769620	41.310192606
1	43.161277742	40.348218393	50.447319609
1	41.865066929	35.634156389	46.439611468
1	40.699249862	43.469754026	45.027674252
1	50.420888502	33.512686507	45.294495761

**TS<sub>kew</sub>**

6	43.697545617	40.379145612	49.567059508
7	44.424410474	41.489574104	49.203100191
1	44.564793731	42.337052215	49.765796501
6	44.910446908	41.286005575	47.965980591
1	45.542833977	41.981973820	47.420141842
7	44.518157552	40.105210040	47.500378167
6	43.763166046	39.522467221	48.494915402
1	43.332419560	38.531080173	48.381004396
6	42.539876610	35.794905054	45.516822529

1	41.816353840	36.030075985	44.722953974
1	43.068953664	34.863788146	45.270242885
6	43.570831087	36.925602988	45.670439811
8	43.151886344	38.115181246	45.374914627
8	44.720369117	36.663776340	46.032259193
6	41.054846649	42.735468570	45.071958704
7	40.400718010	41.578044740	45.425209522
1	39.399422477	41.468817831	45.625199029
6	41.305410478	40.585623807	45.477192153
1	41.072705032	39.550546927	45.711271191
7	42.514797270	41.040962642	45.177667559
6	42.375748132	42.387123257	44.923367395
1	43.221523276	43.008648117	44.638666320
26	44.216449710	39.801631096	45.434604307
8	48.062166700	39.133538660	43.267179630
8	46.875056297	41.598768142	45.460541205
6	46.390360798	41.491516370	44.330252342
6	46.873942405	43.768588674	43.275710126
6	47.652214000	44.514691468	42.169536484
8	45.351828719	40.735263724	44.083255495
8	46.996474619	45.177594141	41.332875312
6	46.976223255	42.239200086	43.141266614
8	48.912205880	44.406745072	42.192009435
1	47.310896913	44.061871702	44.241967060
1	45.820036250	44.087280999	43.257463222
1	48.038736059	41.957443486	43.079211755
1	46.482162975	41.907249124	42.215885569
7	49.601224170	33.689052717	44.987376701
6	48.487166978	32.876057431	45.254585330
7	47.306921173	33.281162491	44.728660087
6	47.145969658	34.446502098	44.124121748
6	48.247772836	35.374550286	43.926743592
6	48.038428428	36.671741051	43.350364638
6	49.464803075	34.912138278	44.358351225
8	48.580162508	31.851764417	45.942895629
7	45.914185191	34.758156620	43.669867642
1	45.691662559	35.741985186	43.597036919
1	45.144525363	34.120454658	43.868529047
1	50.356422399	35.529343601	44.238021970
6	48.221233057	37.911239022	43.357555490
1	46.578086962	38.961863887	43.165906583
8	45.759915825	38.344807982	42.873737849
1	45.182596411	38.887875043	42.254173924
1	46.311030334	37.557059959	42.535399468
1	43.131581294	40.318092819	50.496588562
1	41.964612102	35.622362235	46.426419719
1	40.542924071	43.696204523	45.017286731
1	50.508343726	33.420879202	45.311706114

**PD<sub>kew</sub>**

6	43.693554896	40.374623274	49.584833768
---	--------------	--------------	--------------



7	44.418772874	41.485565925	49.219730512
1	44.552761024	42.336166240	49.779116585
6	44.911392844	41.277894426	47.985961271
1	45.541167423	41.975725973	47.439846667
7	44.526666140	40.093503872	47.524085017
6	43.767405243	39.513802324	48.516522974
1	43.332165512	38.524674281	48.401040290
6	42.627174229	35.777313499	45.517055758
1	41.915078164	35.978441679	44.703894777
1	43.183272291	34.857086333	45.292558163
6	43.614010395	36.946352679	45.628771690
8	43.118328828	38.122796906	45.451275449
8	44.816454826	36.736259082	45.847843499
6	41.121793636	42.735980310	45.068758960
7	40.469220677	41.567354063	45.386842742
1	39.464668804	41.452208602	45.568472959
6	41.380796254	40.580892623	45.437709202
1	41.152555402	39.539575490	45.646819704
7	42.594594749	41.050339112	45.173782387
6	42.448541082	42.400635026	44.942966442
1	43.292885775	43.035468698	44.684268492
26	44.264115129	39.759727412	45.450814213
8	48.831592775	38.703355509	42.761191114
8	46.889177169	41.513598773	45.483091681
6	46.478485283	41.286871066	44.335797685
6	46.886647676	43.566508530	43.269939787
6	47.682722503	44.368755723	42.214806772
8	45.550495172	40.409878729	44.089451229
8	47.041204956	45.075506526	41.403906589
6	47.051327540	42.040952106	43.142683692
8	48.943719359	44.270732845	42.258262464
1	47.265239236	43.867647152	44.258729586
1	45.822317295	43.841092577	43.210034081
1	48.129443824	41.813233557	43.100122670
1	46.584691623	41.673639377	42.217122605
7	49.451639272	33.830981961	45.036475555
6	48.377174269	32.935850396	45.244035578
7	47.189309354	33.287233784	44.703378024
6	46.949489363	34.482295213	44.181218057
6	47.956656779	35.532075209	44.237952928
6	47.559331471	36.921079586	43.940418051
6	49.204467929	35.125511530	44.620039704
8	48.533883777	31.889148154	45.881023325
7	45.768896381	34.703500950	43.592317705
1	45.518925987	35.627802193	43.261429971
1	45.042297145	33.983696561	43.563123160
1	50.036781688	35.833555467	44.650564426
6	48.259592725	37.850291763	43.309681946
1	44.904465808	37.032318798	41.267327481
8	44.010558432	37.174066920	41.610204657
1	44.007598426	38.149869968	41.825673202
1	46.617745447	37.287290288	44.379219435

1	43.118859106	40.317811905	50.509260367
1	42.034709963	35.616626604	46.417740572
1	40.599139248	43.690684972	45.010118374
1	50.377737760	33.579300890	45.317492857

**5fmC formation**

**In aqueous solution outside of the enzyme**

**RC2<sub>fmaq</sub>**

7	17.242093476	14.755658264	16.420858573
6	16.906932287	15.149747198	17.758461382
7	15.653393788	15.666052596	17.926707287
6	14.847441634	15.941211605	16.914095749
6	15.149948603	15.569946277	15.539781771
6	14.260414130	15.714608700	14.382308141
6	16.374679730	14.982032830	15.379131205
8	17.699812990	15.013690239	18.674947825
7	13.685085503	16.550890906	17.232456974
1	13.569923431	16.868222479	18.189961723
1	12.991762223	16.839934997	16.553721274
1	16.696731743	14.676871778	14.378670545
6	13.396881931	16.717291285	14.103307718
1	12.839941609	16.003249192	12.398394292
1	13.247483546	17.584977495	14.756828010
1	14.375909108	14.947719511	13.613116650
8	12.651503252	16.792809821	12.991095893
8	12.836590827	14.546073767	11.693965931
1	12.472681840	13.915510566	12.362167548
1	13.721100380	14.167549106	11.469810386
1	18.198960764	14.627299443	16.160279408

**TS<sub>fmaq</sub>**

7	17.353210348	14.908748597	16.450201171
6	17.191046721	15.350597216	17.807857194
7	15.949206595	15.807352071	18.137048867
6	14.976872859	15.884230693	17.258154302
6	15.090174011	15.449722085	15.876832118
6	13.942913692	15.536422909	14.935520600
6	16.329908196	14.987363735	15.537897080
8	18.113303170	15.311206849	18.607537025
7	13.768392173	16.354838171	17.701980648
1	13.803760475	16.905304416	18.562346579
1	13.115625318	16.704638255	17.004850817
1	16.536801255	14.655441026	14.516923806
6	13.742321970	16.682287893	14.120483790
1	12.746694751	15.278837310	12.678758902
1	14.547235878	17.454009226	14.121240625
1	13.012649870	15.059217591	15.284830258
8	12.790636424	16.825840657	13.312390480
8	13.146632157	14.348469860	12.743004666
1	12.429426701	13.772335607	13.171027202

1	13.779982647	14.655636181	13.646070576
1	18.271070890	14.745787171	16.088333665

**PD<sub>fmaq</sub>**

7	17.185050058	14.873787015	16.402262263
6	17.019377203	15.305886808	17.766591677
7	15.805196320	15.843422285	18.073490266
6	14.854792308	16.006369877	17.176080308
6	14.968637052	15.546857623	15.807062135
6	13.842718626	15.665088531	14.818752062
6	16.180782846	15.010460951	15.482897630
8	17.919653174	15.185744586	18.580694800
7	13.706253804	16.596867212	17.608749057
1	13.758288454	17.109148371	18.491452354
1	12.976515044	16.902643702	16.973252373
1	16.378250390	14.666599855	14.464742563
6	13.484623239	17.078742080	14.421879264
1	12.192871225	14.930495924	12.094402680
1	14.326184888	17.816352346	14.430810676
1	12.920432464	15.166563122	15.164987116
8	12.372048345	17.419939176	14.081396811
8	12.846669701	14.227031005	12.243806753
1	12.396407946	13.684428825	12.934855629
1	14.097863093	15.169966780	13.859214652
1	18.103547814	14.714753926	16.040263865

**5fmC via succinate path**

**TS<sub>SucH</sub>**

6	49.558354918	45.914603432	46.741082974
7	49.504925765	46.564378932	45.527964599
1	49.783568813	47.535088475	45.339270015
6	48.982344668	45.711781926	44.623301066
1	48.818519292	45.978258073	43.580972007
7	48.699819639	44.542364316	45.184425470
6	49.052731915	44.656045157	46.511912707
1	48.889860228	43.844852111	47.219862810
6	45.874459061	40.361465694	47.715501467
1	44.788674888	40.498988072	47.846289127
1	46.035726505	39.277704741	47.715088206
6	46.278516414	40.879235940	46.325718860
8	46.683115459	42.101774120	46.219352439
8	46.183772466	40.096502053	45.374163327
6	44.521420491	46.297732369	44.584915120
7	44.355848306	45.716155068	45.821197223
1	43.774823091	46.045436934	46.601500817
6	45.099809176	44.596569788	45.853684869
1	45.167991019	43.931870346	46.709462231
7	45.730975407	44.413676161	44.703198284
6	45.382142019	45.472557000	43.897669298
1	45.769321109	45.572552481	42.886297913

26	47.358336415	42.958678661	44.550796840
8	48.833158631	41.531662894	44.007276300
8	48.009232973	41.167844931	41.726400677
6	47.182998963	42.142028660	41.579704531
6	46.371655769	43.463787113	39.551134583
6	47.717729113	43.683437868	38.850167190
8	47.036739050	43.049271916	42.434581286
8	47.901956340	43.138649049	37.742754754
6	46.361220282	42.140489744	40.321251287
8	48.586692518	44.375802538	39.475706950
1	46.143362983	44.285516057	40.240924118
1	45.572382483	43.399265182	38.799880879
1	46.722841647	41.340769928	39.673965672
1	45.330918936	41.894672110	40.623173012
7	51.986347187	36.748523357	45.860091915
6	51.387273608	36.560929123	47.142490699
7	50.149581047	37.097475006	47.290435375
6	49.563712970	37.851336105	46.367719442
6	50.267282936	38.293988064	45.172890740
6	49.781236581	39.357083498	44.280097403
6	51.454816321	37.659011994	44.961335449
8	51.933587363	35.914857159	48.030241637
7	48.283189442	38.191039974	46.582115705
1	47.866037032	37.861182559	47.446454413
1	47.721160552	38.727341706	45.920848628
1	52.036613204	37.900466392	44.065234676
6	49.237443948	40.509876560	44.746127153
1	48.465693917	41.244144464	42.694714793
1	49.122681151	40.650376851	45.832674342
1	49.949068119	39.240623211	43.203404374
1	49.795065400	46.413404742	47.680887597
1	46.368734335	40.803406169	48.580630295
1	44.094894050	47.268339288	44.331805006
1	52.912276078	36.443329052	45.637640526

**PD<sub>SuchH</sub>**

6	49.560578124	45.889687825	46.757112626
7	49.534691763	46.525726259	45.534014317
1	49.817275329	47.494457912	45.340856282
6	49.023309580	45.664760654	44.630882355
1	48.881208344	45.917351978	43.581915012
7	48.719773648	44.505408804	45.202542324
6	49.045735900	44.634217982	46.535327932
1	48.848975861	43.833775696	47.246486146
6	45.926887498	40.416724256	47.759677030
1	44.835049649	40.522463724	47.864666315
1	46.110846137	39.336652377	47.716891134
6	46.357090895	41.021019623	46.410859850
8	46.877933026	42.198526269	46.393177969
8	46.176801805	40.332613273	45.393957176
6	44.537332613	46.205343117	44.584716858

7	44.406340526	45.652872544	45.839975882
1	43.843172704	46.002011649	46.625244233
6	45.135536938	44.525732693	45.874992281
1	45.238512386	43.888234618	46.747696520
7	45.721733856	44.305826922	44.705008393
6	45.359483506	45.352188671	43.886018609
1	45.712306616	45.417042877	42.859919051
26	47.395534634	42.920393226	44.542423287
8	48.809457317	41.543657919	43.944520932
8	47.972696676	41.221820169	41.650696924
6	47.151178789	42.210578752	41.525758620
6	46.353819453	43.502491952	39.481168053
6	47.718582062	43.676959760	38.804901649
8	47.047159444	43.121002512	42.376153736
8	47.902885311	43.132648623	37.697405450
6	46.295929277	42.203879855	40.289632836
8	48.598281314	44.336700763	39.450404784
1	46.131783633	44.347889084	40.143528278
1	45.567787145	43.436143412	38.716438411
1	46.601998291	41.366509538	39.661355050
1	45.262016354	42.019704984	40.619444572
7	51.981991312	36.778158172	45.862491533
6	51.364195575	36.592428668	47.136990595
7	50.129794601	37.140742734	47.270619365
6	49.562260310	37.902369213	46.344061340
6	50.279328794	38.333067190	45.152524559
6	49.803601701	39.389562963	44.244976735
6	51.465048344	37.688169835	44.955061111
8	51.892704822	35.940387734	48.030476349
7	48.284344080	38.259529396	46.551730067
1	47.857640979	37.935342707	47.413446379
1	47.738027674	38.810984303	45.892003536
1	52.056346653	37.919341393	44.062399471
6	49.221625829	40.528313244	44.695540851
1	48.441059642	41.283567227	42.602989368
1	49.076418476	40.670202540	45.776933573
1	49.999980183	39.272855101	43.172950503
1	49.795485048	46.393426565	47.694733731
1	46.391857968	40.834822586	48.652461201
1	44.111599334	47.174443755	44.324596786
1	52.905789069	36.460294935	45.649106548

**Decomposition of hemiaminal intermediate of 4mC  
Inside the enzyme with assistance of water molecule  
RC**

6	53.037671877	43.455629618	39.761381626
7	52.386987044	42.355002690	40.273177598
1	52.739118662	41.391593449	40.291078204
6	51.203525455	42.774098609	40.769215646
1	50.486055569	42.118263982	41.255770081
7	51.047753782	44.080541297	40.591339990

6	52.194351978	44.519603921	39.962195676
1	52.332620268	45.567837951	39.714730434
6	50.075460433	48.794134344	38.514038861
1	49.257647999	48.706509693	37.786304290
1	49.869261554	49.682114459	39.124770716
6	50.104274377	47.595775019	39.469187010
8	48.988896284	46.944672077	39.576844242
8	51.107396630	47.305909995	40.131846267
6	48.470248514	42.453494504	37.064398105
7	49.144239668	43.484266500	36.442399367
1	49.485362738	43.524465122	35.473821398
6	49.347889468	44.448451065	37.365594497
1	49.869063943	45.375576061	37.141356014
7	48.832913945	44.112823888	38.537780451
6	48.281739285	42.863817326	38.364982256
1	47.782267649	42.351946660	39.184689620
26	49.127779060	45.124008378	40.533364458
8	49.287058718	46.531345825	42.430243583
8	47.641981337	43.950965316	41.296008565
6	47.883441206	43.285580235	42.363835749
6	45.642673801	41.902630481	42.069804760
6	44.803336199	40.779841255	42.711313824
8	48.935786643	43.413955201	43.025028158
8	43.993244757	40.176228320	41.960646294
6	46.872359202	42.271270112	42.884561778
8	44.957273935	40.520716751	43.936654812
1	45.904314749	41.578836543	41.050318617
1	44.979240347	42.776272596	41.940976083
1	47.459258079	41.363955786	43.103473087
1	46.556231529	42.638342800	43.874972547
7	51.652359162	48.980482271	46.350392676
6	51.296436820	49.700165324	45.161804820
7	50.128264930	49.287166099	44.555813107
6	49.522545250	48.165640008	44.904228212
6	49.994192709	47.331974202	45.962887543
6	51.032303743	47.809640263	46.698030489
8	52.000258108	50.590400798	44.725351025
7	48.362696953	47.817418042	44.226818758
1	48.030556673	48.595817433	43.667016477
1	51.387258522	47.284390594	47.590074865
1	49.510829658	46.393281444	46.213105682
6	48.313901403	46.568400171	43.475957867
1	48.492170978	45.705123940	44.129138729
1	49.342050447	47.475990547	42.065975057
1	47.301606111	46.485453029	43.051710122
8	49.244733783	49.089627169	41.865781144
1	49.526015404	49.520805315	42.705558667
1	48.332164225	49.339723639	41.617699960
8	47.161799678	49.046884231	40.209459757
1	47.645349270	48.253595977	39.891120620
1	46.267016106	48.970302303	39.811139115
1	53.996897792	43.421677447	39.244854555

1	51.019154223	48.924713143	37.984455505
1	48.236887158	41.504296567	36.582077602
1	52.455864035	49.239070729	46.886568415

**TS1**

6	53.085654241	43.463935452	39.749604527
7	52.436837504	42.374254688	40.288516404
1	52.778371115	41.407520150	40.306782708
6	51.266878122	42.810553381	40.803822743
1	50.552663670	42.173328737	41.318798493
7	51.118193486	44.114608506	40.610198316
6	52.253853340	44.535657984	39.951705415
1	52.389798869	45.576794604	39.677417426
6	50.082070994	48.820410439	38.423825766
1	49.269681204	48.741503772	37.688545943
1	49.875340382	49.710616824	39.032577049
6	50.088015227	47.614831115	39.372649781
8	48.946917568	47.042524941	39.556297671
8	51.109221270	47.263110652	39.980811359
6	48.518202858	42.522377041	37.118790800
7	49.198927634	43.542646118	36.485899679
1	49.531652994	43.573004418	35.514560987
6	49.426505184	44.505015732	37.407471484
1	49.961006167	45.422299153	37.174421733
7	48.919803468	44.181893896	38.585683454
6	48.349335069	42.940636140	38.420179248
1	47.849427471	42.440814655	39.246710665
26	49.222783495	45.222021794	40.636589196
8	49.336024182	46.527726073	42.353633264
8	47.694977491	43.961973753	41.297086854
6	47.930389023	43.274650391	42.346834167
6	45.663250551	41.921144361	42.064379233
6	44.808157803	40.814085061	42.713787738
8	48.994403173	43.358828939	43.002259810
8	43.988597015	40.216439912	41.967976918
6	46.899760640	42.278985156	42.874333692
8	44.958327998	40.558677667	43.940872260
1	45.918403702	41.586022130	41.046542641
1	45.011970457	42.803282946	41.930029300
1	47.471455609	41.364481095	43.101568747
1	46.587520753	42.661007023	43.860683354
7	51.573833905	48.984425297	46.273778282
6	51.253250331	49.692435288	45.073953279
7	50.098427323	49.266466415	44.439888861
6	49.434194536	48.169359373	44.805771203
6	49.873521653	47.365214592	45.896520101
6	50.917727671	47.834098926	46.630746903
8	51.962512832	50.576275014	44.638533168
7	48.316739052	47.819584435	44.084535003
1	47.922546394	48.591620814	43.558484964
1	51.254660996	47.311371204	47.531449704

1	49.371042746	46.439197466	46.154830027
6	48.333275862	46.524211061	43.312657896
1	48.454624667	45.700481531	44.036116613
1	49.575363315	47.881034524	42.031955014
1	47.325386824	46.443616789	42.868408145
8	49.557608302	48.965258201	41.955413091
1	49.814838230	49.318996655	42.919907923
1	48.605226099	49.136626517	41.732334612
8	47.363694240	49.060647766	40.488276974
1	47.777170577	48.281362129	40.035085979
1	46.420056617	49.011743634	40.240926346
1	54.039043812	43.424189240	39.222787773
1	51.030344612	48.953880843	37.903220230
1	48.262227784	41.577685461	36.639101430
1	52.379136683	49.228274883	46.814146037

**IM1**

6	53.091501703	43.507102896	39.749235791
7	52.457364252	42.405950780	40.282598165
1	52.809529463	41.443172181	40.294454582
6	51.284948398	42.824608620	40.806750072
1	50.580561112	42.177155742	41.322438651
7	51.119976914	44.127731647	40.624590302
6	52.246928251	44.568715358	39.964828090
1	52.372813126	45.617496220	39.710462852
6	50.090556214	48.811653095	38.494254447
1	49.280145345	48.697701051	37.762477905
1	49.870542576	49.718677516	39.070089678
6	50.129630874	47.637066381	39.486063737
8	49.037218766	46.959497931	39.584576384
8	51.129935554	47.413951050	40.182416096
6	48.510566825	42.502523072	37.126923011
7	49.191777476	43.533712822	36.512163354
1	49.530744206	43.576191865	35.543776508
6	49.406553037	44.485440349	37.449775141
1	49.934568297	45.410930748	37.234396899
7	48.894490698	44.143033066	38.619713488
6	48.332145587	42.902191879	38.432857170
1	47.830382493	42.388714800	39.249845363
26	49.185260822	45.176911222	40.714153383
8	49.267916842	46.343990250	42.461193255
8	47.699637834	43.851811782	41.319041354
6	47.947290754	43.150682656	42.355492269
6	45.670848415	41.834540721	42.067553736
6	44.789566769	40.755173430	42.721661764
8	49.025185085	43.205249699	42.991679186
8	43.962210464	40.165734862	41.977844147
6	46.900480253	42.180245200	42.890899744
8	44.928859826	40.510413702	43.952344722
1	45.935518919	41.479568521	41.058962288
1	45.039513090	42.726862703	41.908667362



1	47.451898186	41.260252932	43.142727323
1	46.579213252	42.589255070	43.863497735
7	51.680656079	48.962403999	46.404482782
6	51.335476268	49.676723169	45.238884212
7	50.168104404	49.198307951	44.648359164
6	49.525729241	48.020614723	44.936801930
6	50.041190237	47.260096490	46.028976574
6	51.066038464	47.777163856	46.751208161
8	51.965980832	50.593318025	44.769252585
7	48.483611854	47.675350111	44.198600318
1	48.276908775	48.394450186	43.486052511
1	51.435607383	47.267424473	47.646000772
1	49.595278509	46.307141178	46.292323331
6	48.401394436	46.316547838	43.496830068
1	48.594421919	45.543587986	44.266274188
1	49.190188060	48.201906737	41.876120405
1	47.335226626	46.229887200	43.206842348
8	48.906453633	49.142306129	41.996036124
1	49.901486205	49.649273338	43.762433533
1	48.154781857	49.239887535	41.361510220
8	47.204590893	48.982358828	39.952214584
1	47.676042381	48.160516816	39.680188103
1	46.287545707	48.902039940	39.605937677
1	54.044523030	43.467775713	39.221721772
1	51.036565752	48.939737692	37.968205393
1	48.261183267	41.561882656	36.635933425
1	52.490230684	49.226562439	46.928679103

**TS2**

6	53.115526678	43.468299122	39.714139920
7	52.494062361	42.359374440	40.242420816
1	52.869018098	41.404663900	40.273789555
6	51.301034370	42.749342544	40.732579588
1	50.604001193	42.085969845	41.236916045
7	51.108519846	44.048539938	40.533405151
6	52.242284668	44.511912165	39.898425436
1	52.361878737	45.562155789	39.647678189
6	50.116940637	48.735151459	38.639113359
1	49.300351783	48.629083949	37.913902906
1	49.911277778	49.641459189	39.219611075
6	50.162180598	47.547916398	39.612577031
8	49.128869805	46.766355987	39.565562882
8	51.101537055	47.388743739	40.400512959
6	48.485830011	42.336057695	36.935597828
7	49.144371206	43.384035180	36.325974303
1	49.482210323	43.445225486	35.357038684
6	49.344310320	44.336233918	37.260329802
1	49.851140689	45.274197813	37.049373514
7	48.843636013	43.972494209	38.430995752
6	48.304654125	42.719834721	38.243765608
1	47.822198856	42.188463371	39.060869579

26	49.133487072	44.917809356	40.400391216
8	48.695461372	46.212129260	42.391480079
8	47.743175019	43.672791219	41.170392237
6	47.997710201	43.036765034	42.258207784
6	45.726835939	41.723186069	42.001982483
6	44.817214269	40.685503303	42.686980296
8	49.059112369	43.179965393	42.897974151
8	43.981945812	40.094659876	41.954244398
6	46.951450854	42.088956410	42.824873796
8	44.944620624	40.479514889	43.924857763
1	46.000338057	41.325577265	41.012303206
1	45.110648816	42.616922108	41.798709880
1	47.496099198	41.178330234	43.121981199
1	46.621937594	42.538458864	43.777052536
7	51.898388815	48.920582306	46.517240643
6	51.545826595	49.518704249	45.296350745
7	50.280471790	49.177204008	44.879514730
6	49.325912896	48.371491609	45.532598562
6	49.822375672	47.748767697	46.747776606
6	51.048462414	48.053737827	47.202484137
8	52.275385578	50.258064732	44.658475536
7	48.138300849	48.219385911	45.074256530
1	48.020344165	48.771028169	44.216114296
1	51.425611780	47.630482284	48.136644561
1	49.198293394	47.059642688	47.302206108
6	47.855886883	46.036871714	43.255962046
1	47.865267942	45.128286453	43.891661443
1	48.897172542	48.182103040	42.191987829
1	47.053332011	46.774252031	43.439902275
8	48.700599529	49.132882778	42.277268833
1	49.975124235	49.554052882	43.976002099
1	47.981509996	49.251810809	41.619601601
8	47.187263444	48.921912456	40.029940101
1	47.649624699	48.099908621	39.771521561
1	46.289459545	48.855029077	39.629902760
1	54.070789986	43.435834807	39.190226375
1	51.055638253	48.860694369	38.099527331
1	48.270576264	41.385080193	36.448386441
1	52.716612484	49.217477958	47.009516473

**IM2**

6	53.115642023	43.479913367	39.712937777
7	52.502625751	42.373048365	40.254220712
1	52.878414598	41.418414359	40.284660131
6	51.315217336	42.762560646	40.756758967
1	50.625822891	42.102093283	41.274866712
7	51.116146957	44.061701174	40.554636563
6	52.241610629	44.522153677	39.899497380
1	52.355322882	45.570302330	39.638502954
6	50.098690367	48.709760926	38.649650151
1	49.286090710	48.586701048	37.922468280

1	49.874373517	49.621694360	39.214547573
6	50.147875979	47.534059400	39.638775136
8	49.088268432	46.784520118	39.647776827
8	51.113879887	47.351245393	40.387514402
6	48.493235979	42.354015124	36.949901685
7	49.157914159	43.401863390	36.347005087
1	49.499520478	43.464940550	35.379343690
6	49.356733608	44.349769690	37.286136136
1	49.868648396	45.286021840	37.079742737
7	48.849727536	43.983648160	38.453609502
6	48.307093897	42.733600066	38.258193789
1	47.818191672	42.200336505	39.069931787
26	49.110373896	44.915331558	40.439214019
8	48.687165561	46.142962232	42.508045862
8	47.751596816	43.613983243	41.176664940
6	48.022683616	42.937401200	42.231607599
6	45.763296119	41.610931461	41.973759619
6	44.844102469	40.590716275	42.672377851
8	49.105001403	43.041840273	42.849920062
8	44.002929849	40.000846470	41.946174630
6	46.971044509	42.003646730	42.807759632
8	44.969687486	40.396458244	43.912223291
1	46.056731270	41.185209136	41.001515811
1	45.149028116	42.496170310	41.732777602
1	47.508363521	41.106243767	43.152439318
1	46.616977722	42.491603913	43.732624364
7	51.954719871	48.863517033	46.515354428
6	51.624670661	49.409683851	45.265629031
7	50.329223811	49.149876485	44.881244007
6	49.318519829	48.524584667	45.631456355
6	49.791946901	47.901514435	46.855445305
6	51.055011749	48.105058971	47.261841389
8	52.399278461	50.045056342	44.568568543
7	48.087460594	48.492898338	45.263042482
1	47.950478936	48.991146409	44.375906976
1	51.422686573	47.685637042	48.201505954
1	49.112995858	47.304980632	47.455997849
6	48.096428408	45.864391390	43.539893957
1	48.005177004	44.811555555	43.871449385
1	48.844010263	48.082281934	42.329226271
1	47.682438785	46.661077306	44.193474258
8	48.723139586	49.049169345	42.385319440
1	50.055902333	49.490255024	43.954448424
1	48.021751512	49.212310299	41.718011133
8	47.201183859	48.963288804	40.104921691
1	47.654572967	48.137262534	39.841917461
1	46.299639624	48.896567692	39.715389423
1	54.070827918	43.447066864	39.188906925
1	51.037918647	48.840680690	38.112269866
1	48.276367770	41.404232308	36.461078498
1	52.767590837	49.173931878	47.008158562

TS3

6	53.109480584	43.474518807	39.711655940
7	52.492532965	42.363385620	40.240189763
1	52.866699846	41.408440204	40.265854473
6	51.304480542	42.751137280	40.742883664
1	50.613325137	42.089537791	41.256619135
7	51.108587337	44.052499898	40.553605588
6	52.236890669	44.516802806	39.906316241
1	52.352006538	45.566937593	39.654538723
6	50.079069051	48.699641163	38.632485218
1	49.274767841	48.560435341	37.898267253
1	49.832442248	49.614085977	39.184759308
6	50.128108934	47.524531902	39.630442039
8	49.049431225	46.808242250	39.677130946
8	51.114063046	47.323661415	40.347684786
6	48.503862710	42.367742976	36.950122574
7	49.176876776	43.412641090	36.350907229
1	49.523200811	43.474305442	35.385097302
6	49.373578526	44.359556802	37.292472774
1	49.891764748	45.293025125	37.088949151
7	48.857424954	43.996691199	38.456466233
6	48.310967014	42.748967617	38.256809218
1	47.816039302	42.219551613	39.066977877
26	49.091758562	44.916046307	40.472811419
8	48.626213470	45.957925035	42.453573838
8	47.772898534	43.515268773	41.141924459
6	48.040979877	42.833171676	42.192497564
6	45.749247331	41.563270408	41.958404694
6	44.823433218	40.559024882	42.667323685
8	49.127279606	42.913889003	42.807514972
8	43.979713150	39.963218047	41.948548408
6	46.975953914	41.922015810	42.777614722
8	44.946194323	40.381071643	43.910178979
1	46.017919431	41.140774742	40.977993623
1	45.151115493	42.464514758	41.736058347
1	47.494864886	41.011318233	43.115265849
1	46.643693309	42.418894535	43.705511444
7	51.660589371	49.083043214	46.318095311
6	51.294290186	49.875217883	45.181344891
7	50.026541087	49.653070168	44.708916161
6	49.246401622	48.625978891	45.140966910
6	49.803717612	47.640859545	46.026324904
6	50.961805639	47.950334984	46.656530975
8	52.081684130	50.668159944	44.692558863
7	47.997397966	48.473858921	44.658920293
1	47.606275742	49.409314162	44.499576832
1	51.360020022	47.324650442	47.460871286
1	49.263830964	46.730285985	46.261370441
6	48.073988811	45.682099501	43.506339653
1	48.045358803	44.637720066	43.877345933
1	48.452563299	48.593107718	43.254380986

1	47.629583566	46.492950957	44.123518946
8	49.000841921	49.167795612	42.476721321
1	49.502736696	49.749862963	43.232866576
1	48.309711890	49.519371478	41.860860579
8	47.352126277	49.136395653	40.396141505
1	47.764791253	48.280625282	40.148936178
1	46.433164649	49.071593665	40.061468915
1	54.066606771	43.442974921	39.191096851
1	51.020076319	48.843895934	38.101671499
1	48.284016932	41.418129535	36.462301438
1	52.473359974	49.293247038	46.861409953

**PD<sub>dm</sub>**

6	53.149192447	43.498276992	39.702764794
7	52.535959229	42.393467076	40.250071481
1	52.913202318	41.440603571	40.289871558
6	51.340983559	42.784858249	40.737779967
1	50.646249223	42.132486986	41.260241062
7	51.140327304	44.077525500	40.516093578
6	52.268165007	44.538903682	39.873297851
1	52.381245741	45.586755504	39.608405786
6	50.136513528	48.756322809	38.611091238
1	49.322580921	48.630574610	37.886099161
1	49.935327598	49.680538743	39.164519855
6	50.201037443	47.583008475	39.603610763
8	49.224783658	46.740050157	39.508065768
8	51.113004713	47.500133656	40.436329257
6	48.491148470	42.319239849	36.929520037
7	49.154795712	43.367019481	36.324298441
1	49.491920154	43.432174403	35.355755985
6	49.359133146	44.313821954	37.264073578
1	49.868885346	45.251700240	37.060275327
7	48.858456923	43.945828894	38.432516899
6	48.313312883	42.697884761	38.239911218
1	47.826980529	42.165559024	39.054294430
26	49.144141696	44.905067128	40.401436738
8	48.990943523	46.109114177	42.375124189
8	47.652104270	43.774145453	41.166254574
6	47.944786873	43.103233052	42.227700139
6	45.675433582	41.778180523	42.027702778
6	44.806731501	40.709989123	42.716006341
8	49.051633660	43.170230882	42.790338858
8	43.968068340	40.111976301	41.990735731
6	46.894665060	42.185257403	42.839201265
8	44.966637213	40.481515533	43.946426324
1	45.956589625	41.384099373	41.038055527
1	45.028460171	42.648821854	41.820927170
1	47.442846562	41.287195515	43.163583410
1	46.567772403	42.670760188	43.775018071
7	52.133512840	48.953795518	46.502721686
6	51.847099014	49.703810059	45.316731610

7	50.594826196	49.550525688	44.821003549
6	49.642108458	48.892391129	45.475992657
6	49.937200727	48.070216179	46.617798973
6	51.192796858	48.158208756	47.112501129
8	52.673015978	50.462161724	44.815513832
7	48.371645748	49.025492368	45.040927327
1	47.642887151	48.802471828	45.717227192
1	51.486854374	47.621934738	48.020343324
1	49.195797857	47.441534763	47.100688834
6	48.093081452	46.915295993	42.534942111
1	47.852408125	47.288929633	43.551159696
1	48.222179126	49.830801862	44.407266094
1	47.520729393	47.343808320	41.683693084
8	48.973821368	51.342525798	43.535574717
1	49.770397459	50.780303954	43.653624710
1	49.081135879	51.916643510	44.337568270
8	47.200128542	48.785495949	39.998200573
1	47.689303219	48.030939823	39.620450019
1	46.3111712555	48.734607709	39.577199727
1	54.102307651	43.459552161	39.175375831
1	51.074018590	48.868493289	38.066509407
1	48.275895400	41.369754892	36.439406012
1	52.925189395	49.185325995	47.068066152

#### Outside the enzyme in aqueous solution

##### RC2<sub>dmaq</sub>

7	17.960640223	16.279070233	16.599364098
6	18.251930522	16.169799915	15.197678819
7	17.388567167	15.421327968	14.467022190
6	16.328818864	14.818975433	14.988816279
6	15.999421018	14.947714188	16.382214187
6	16.857073694	15.682242430	17.144630849
8	19.234260543	16.716603937	14.705859970
7	15.565247532	14.086728621	14.125079277
1	16.071552333	13.772599439	13.293691600
1	16.691368373	15.802632519	18.219596861
1	15.142717258	14.461516704	16.844029527
6	14.387586430	13.269091382	14.486704515
1	14.693958192	12.295779410	14.907195985
1	13.408458069	13.900131563	12.936313935
1	13.829473806	13.817551221	15.265863037
8	13.621527896	13.021373865	13.354297757
8	13.804591379	15.477140578	12.312088758
1	14.090102116	15.307355127	11.367682151
1	14.637005866	15.395611843	12.819000520
8	14.390398875	18.277746620	12.195787997
1	13.887051921	17.441416147	12.157204488
1	14.387936317	18.510861226	13.145731598
1	18.550199189	16.816491656	17.202332532

##### TS<sub>dmaq</sub>

7	17.955334914	16.297936609	16.490438729
6	18.305509005	16.209709013	15.103664972
7	17.439986950	15.497407115	14.319831660
6	16.349541001	14.942149407	14.790077265
6	15.967025485	15.034128975	16.160924073
6	16.816871098	15.724046719	16.980564555
8	19.314717526	16.731866335	14.654335982
7	15.547266835	14.258926211	13.836768536
1	16.161422478	13.810661746	13.141455089
1	16.608700737	15.830951059	18.049800572
1	15.067570120	14.575939140	16.565089722
6	14.340004807	13.215038900	14.245462206
1	14.885013102	12.321963232	14.620463701
1	13.457620043	14.334913497	12.644827438
1	13.877848264	13.744277576	15.109909904
8	13.583424833	13.037164133	13.188664055
8	13.839875140	15.322540366	12.385989097
1	14.146966222	15.224191467	11.438201089
1	14.874527588	14.981645165	13.144903790
8	14.383396098	18.155055298	12.254003311
1	13.884323875	17.316556817	12.251635888
1	14.389150318	18.422007386	13.194788224
1	18.530184155	16.817649549	17.122435017

**PD<sub>dmaq</sub>**

7	18.061895299	16.518881996	16.372134572
6	18.479798093	16.495664201	14.997023077
7	17.610309882	15.954363094	14.116606937
6	16.447094874	15.420660829	14.477656653
6	16.027463777	15.397777125	15.857522747
6	16.864303440	15.973272788	16.761175833
8	19.576941262	16.938598328	14.663783791
7	15.683672008	14.896925909	13.510409030
1	16.030116807	14.953744982	12.556904569
1	16.607456610	16.013243800	17.824436576
1	15.079733481	14.960718951	16.171920858
6	14.951617775	11.792767224	14.543952957
1	14.952687311	10.696493106	14.748652841
1	12.584388644	16.540867644	11.483705141
1	15.835771160	12.357455505	14.916922252
8	14.048405219	12.328883008	13.947472379
8	13.325921632	16.052841027	11.902112812
1	13.797998820	15.647767443	11.128080911
1	14.774392366	14.474686121	13.673868204
8	14.668194520	18.391088565	12.239766696
1	14.213701675	17.517921921	12.160939681
1	14.659678841	18.575141508	13.198076018
1	18.610990674	16.996100929	17.058231397

## References

- (1) Waheed, S. O.; Chaturvedi, S. S.; Karabancheva-Christova, T. G.; Christov, C. Z. Catalytic Mechanism of Human Ten-Eleven Translocation-2 (TET2) Enzyme: Effects of Conformational Changes, Electric Field, and Mutations. *ACS Catal.* **2021**, *11* (7), 3877–3890.
- (2) Ma, G.; Zhu, W.; Su, H.; Cheng, N.; Liu, Y. Uncoupled Epimerization and Desaturation by Carbapenem Synthase: Mechanistic Insights from QM/MM Studies. *ACS Catal.* **2015**, *5* (9), 5556–5566. (b) Light, K. M.; Hangasky, J. A.; Knapp, M. J.; Solomon, E. I. Spectroscopic Studies of the Mononuclear Non-heme Fe<sup>II</sup> Enzyme FIH: Second-Sphere Contributions to Reactivity. *J. Am. Chem. Soc.* **2013**, *135*, 9665–9674.
- (3) Su, H.; Sheng, X.; Zhu, W.; Ma, G.; Liu, Y. Mechanistic Insights into the Decoupled Desaturation and Epoxidation Catalyzed by Dioxygenase AsqJ Involved in the Biosynthesis of Quinolone Alkaloids. *ACS Catal.* **2017**, *7* (8), 5534–5543.
- (4) Hu, L.; Li, Z.; Cheng, J.; Rao, Q.; Gong, W.; Liu, M.; Shi, Y. G.; Zhu, J.; Wang, P.; Xu, Y. Crystal Structure of TET2-DNA Complex: Insight into TET-Mediated 5mC Oxidation. *Cell* **2013**, *155* (7), 1545–1555.
- (5) Torabifard, H.; Cisneros, G. A. Insight into Wild-Type and T1372E TET2-Mediated 5hmC Oxidation Using *Ab Initio* QM/MM Calculations. *Chem. Sci.* **2018**, *9* (44), 8433–8445.
- (6) Sudhamalla, B.; Wang, S.; Snyder, V.; Kavooosi, S.; Arora, S.; Islam, K. Complementary Steric Engineering at the Protein–Ligand Interface for Analogue-Sensitive TET Oxygenases. *J. Am. Chem. Soc.* **2018**, *140* (32), 10263–10269.
- (7) Liu, M. Y.; Torabifard, H.; Crawford, D. J.; DeNizio, J. E.; Cao, X.-J.; Garcia, B. A.; Cisneros, G. A.; Kohli, R. M. Mutations along a TET2 Active Site Scaffold Stall Oxidation at 5-Hydroxymethylcytosine. *Nat. Chem. Biol.* **2017**, *13* (2), 181–187.
- (8) Waheed, S. O.; Ramanan, R.; Chaturvedi, S. S.; Lehnert, N.; Schofield, C. J.; Christov, C. Z.; Karabancheva-Christova, T. G. Role of Structural Dynamics in Selectivity and Mechanism of Non-Heme Fe(II) and 2-Oxoglutarate-Dependent Oxygenases Involved in DNA Repair. *ACS Cent. Sci.* **2020**, *6* (5), 795–814.



## E Appendix E: Supporting Information for Chapter 6

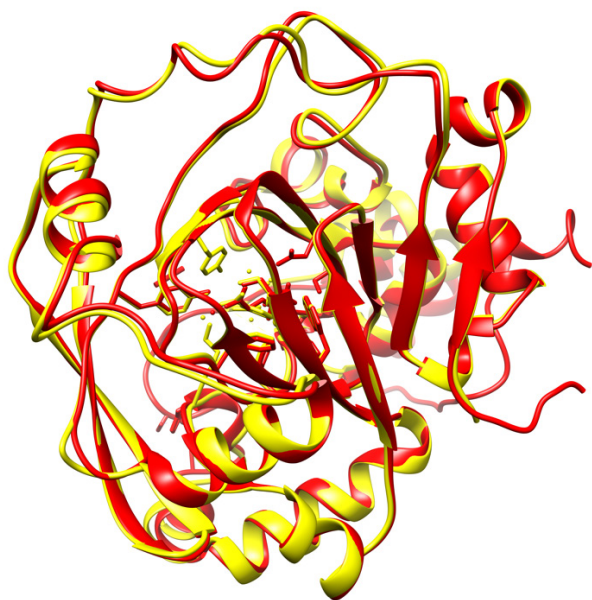


**Figure E1.** Overlay of views from crystal structures of KDM4A (red) and KDM4E (yellow). The superimposed structures have an RMSD of 0.651 Å

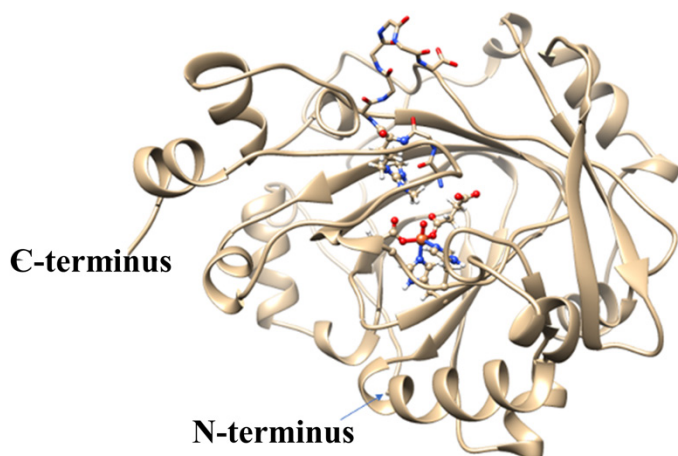


**Figure E2.** View of the catalytic domains of KDM4E (PDB ID: 2w2i) at the modeled ferryl.succinate intermediate state. Active site residues and the substrate residue R3 of H4(1-9)R3me2s are in ball and stick representation. The Fe is in orange.

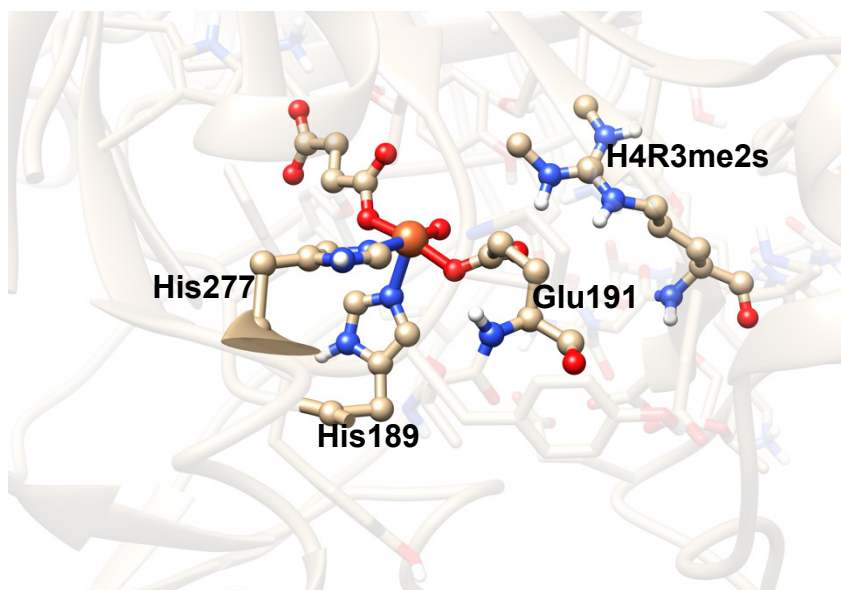


**Figure E3.** KDM4E showing the Fe and its coordinating residues.

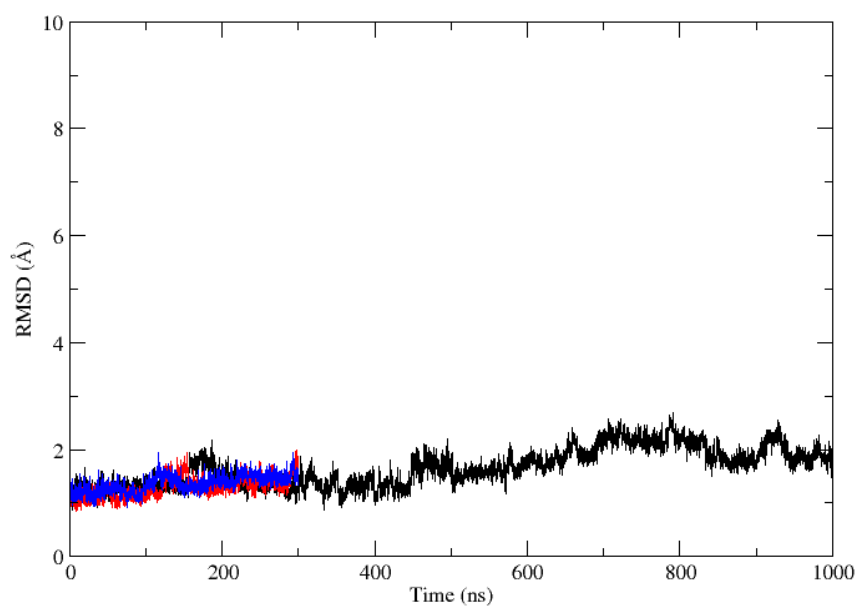


**Figure E4.** The RMSD plot for the KDM4E ferryl complex MD simulation, performed at different initial velocities.

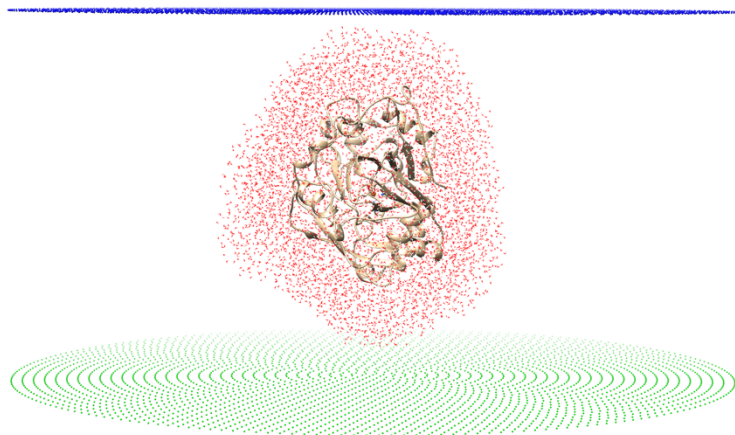


**Figure E5.** Two circular parallel charge plates generated by TITAN leading to a uniform electric field around KDM4E. In this sample figure, the field is oriented along the Fe-N<sup>ε</sup> (His189), perpendicular to Fe=O bond (Figure S5). Coloring: positive charge plate (blue) and negative charge plate (green).

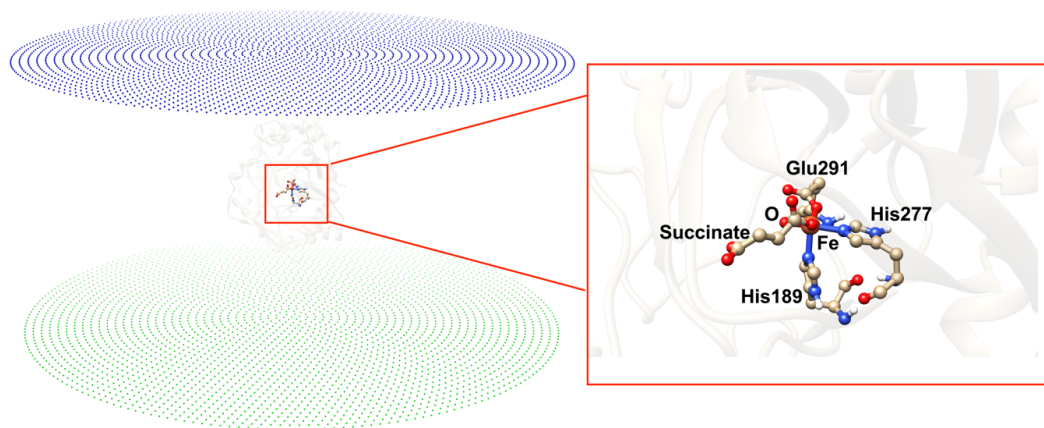


**Figure E6.** Sample figure showing the direction of the orientation of the external electric field (i.e., along the Fe-N<sup>ε</sup> (His189) bond).

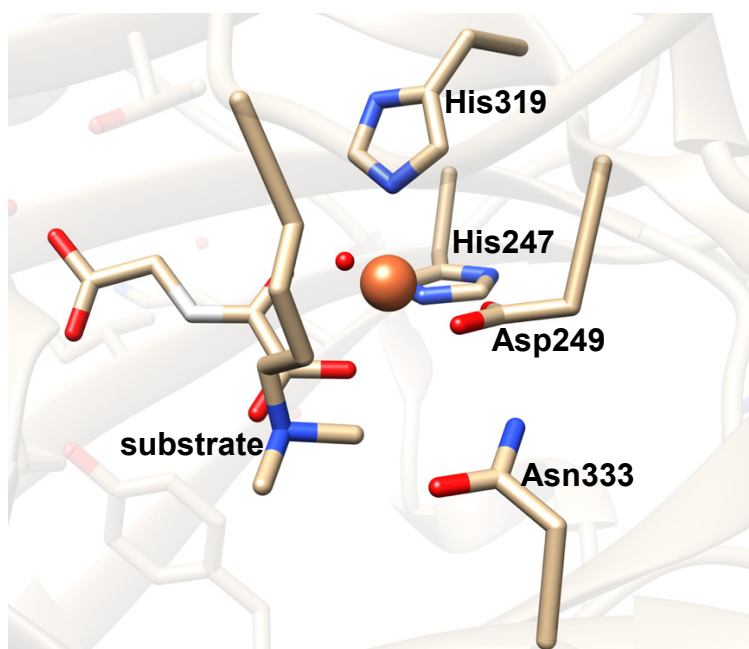


**Figure E7.** View of the active site of PHF8 and the residue (Asn333) stabilizing the non-coordinating oxygen of the ligating Asp249 carboxylate.

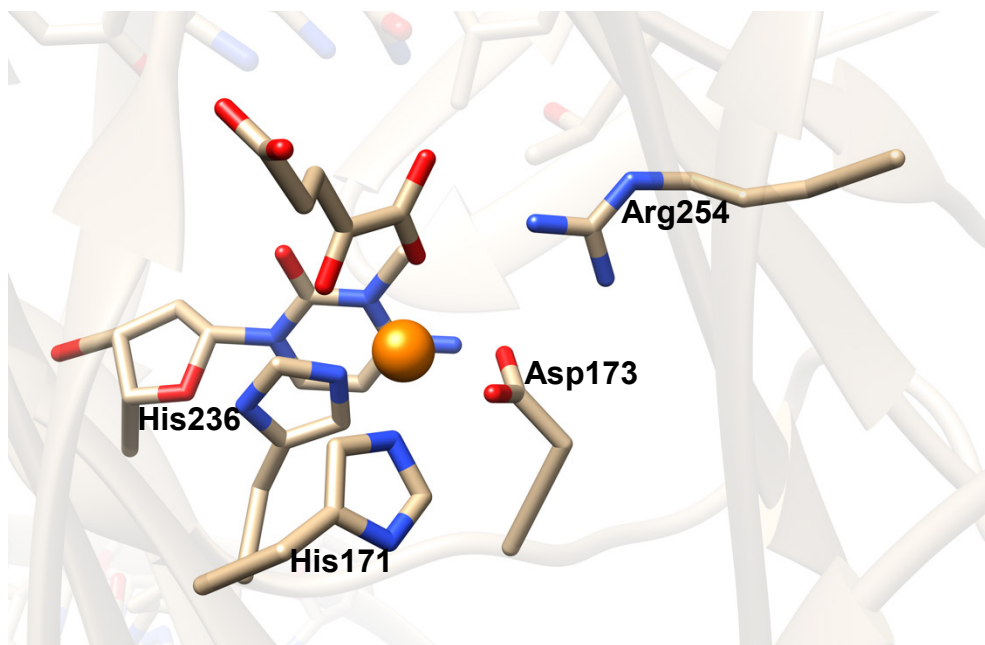


**Figure E8.** View of the active site of AlkBH2 and the residue (Arg254) stabilizing the non-coordinating oxygen of the ligating Asp173 carboxylate.

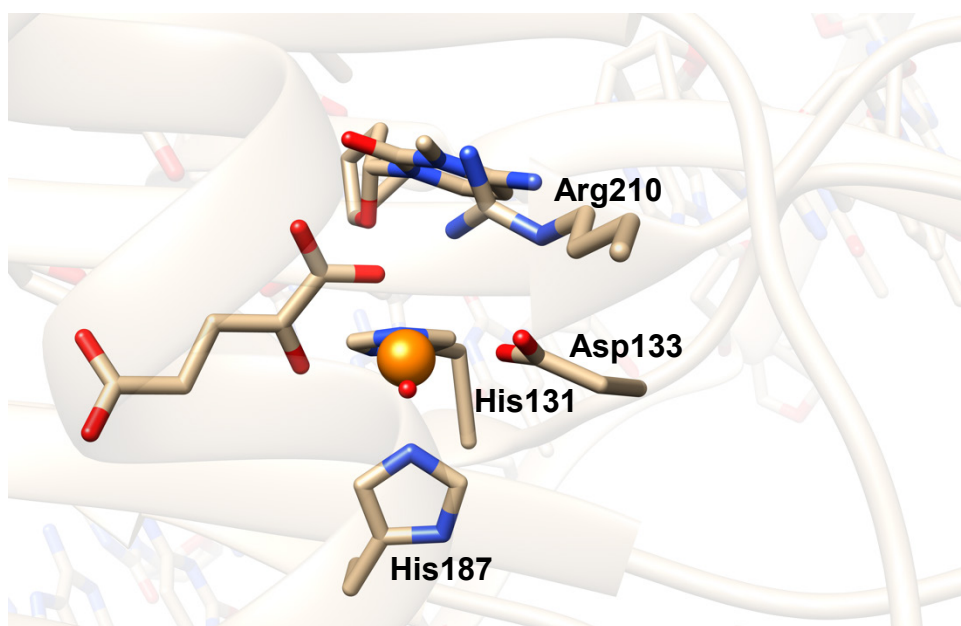


**Figure E9.** View of the active site of AlkB and the residue (Arg210) stabilizing the non-coordinating oxygen of the ligating Asp133 carboxylate.

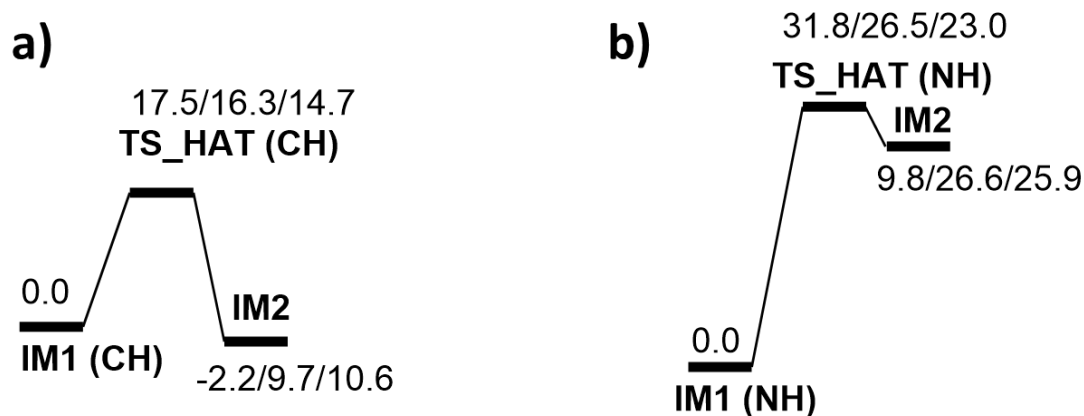


**Figure E10.** Potential energy profile for the RDM activity of KDM4E with dispersion correction. **(a)** C-H activation and **(b)** N-H activation pathways. Energies are given in kcal/mol at the QM(B1)/MM followed by QM(B2+ZPE)/MM and QM(B2+ZPE)/MM with DFT-D3 corrected level of theories.

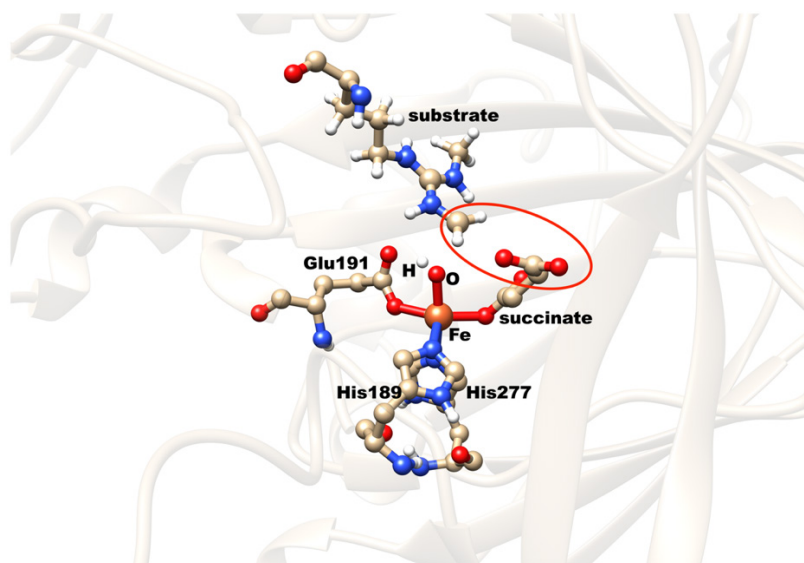


**Figure E11.** Stabilizing interaction between the non-coordinating carboxylate oxygens of the succinate and the methylene radical hydrogen at the rebound hydroxylation transition state in KDM4E.

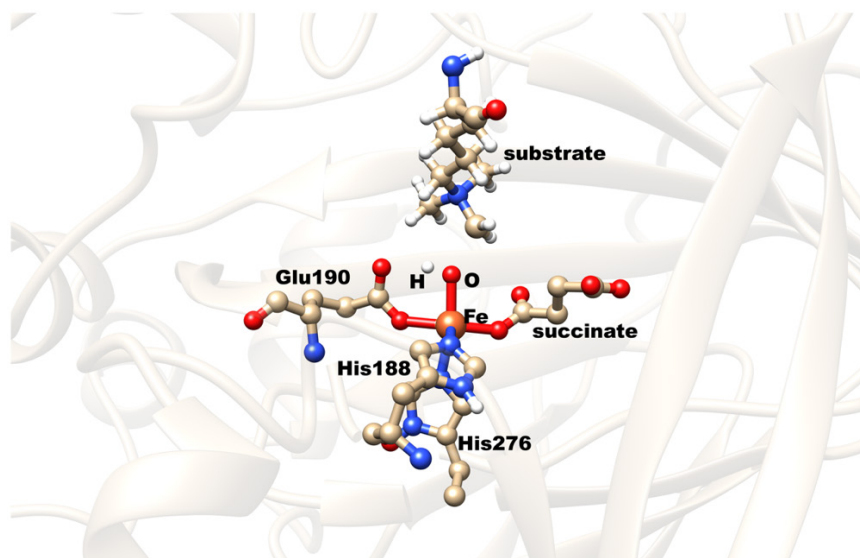


**Figure E12.** View depicting the absence of the observed stabilizing interaction in KDM4E between the non-coordinating carboxylate oxygens of the succinate and the methylene radical hydrogen in the rebound transition state of KDM4A.

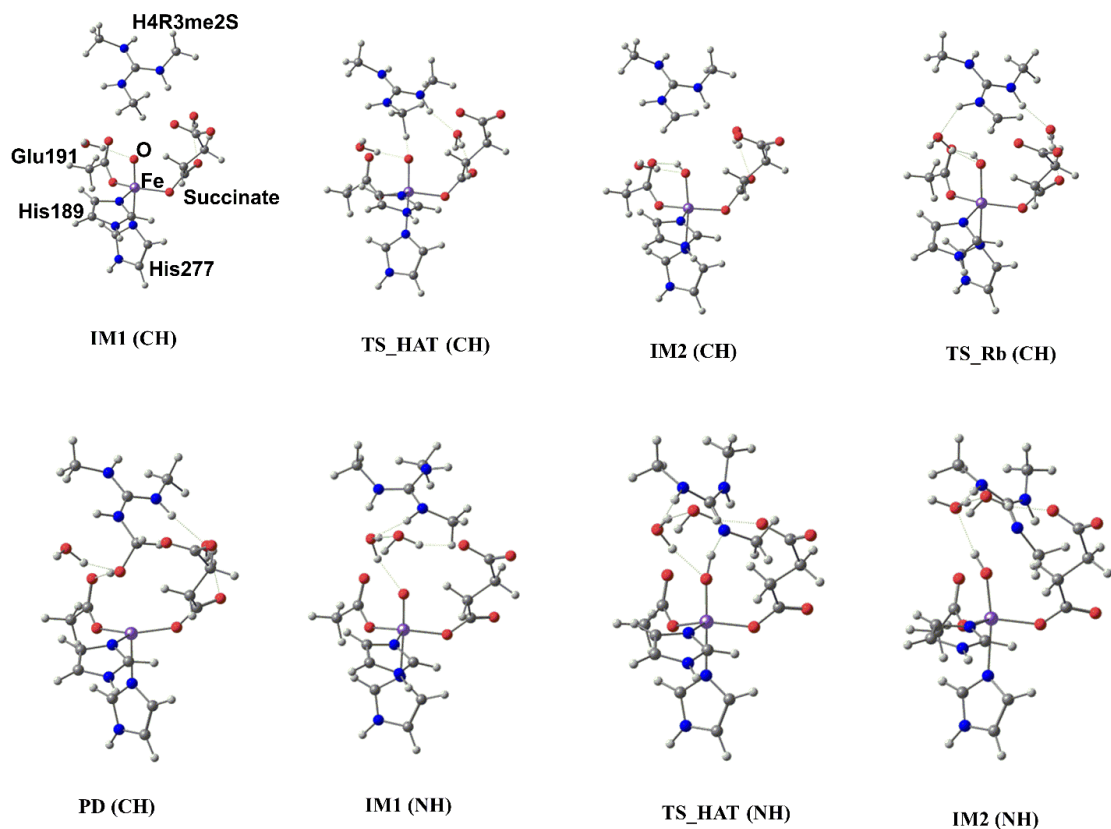


**Figure E13.** The optimized stationary point geometries along reaction of the N-methylated arginine demethylation catalyzed by KDM4E.

**The Cartesian Coordinates of the Optimized QM Region of QM/MM Geometry. QM/MM energies at the QM(B1)/MM level of theory are given in Hartree.**

IM1 (CH)				TS_HAT (CH)			
HF = -3041.501650				HF = -3041.473814			
6	37.788009691	44.216934823	45.165170224	6	37.822756226	44.136495605	45.157962782
7	36.809014820	44.234636066	44.198793611	7	36.834719282	44.109590017	44.199962341
1	36.000186615	44.866950411	44.155376533	1	36.030481901	44.746736416	44.133122619
6	37.102257287	43.287663182	43.293352287	6	37.116249850	43.112485531	43.344303939
1	36.505115052	43.074290544	42.412137000	1	36.515361384	42.860052960	42.475445813
7	38.224204169	42.667381005	43.628567818	7	38.238508904	42.500101023	43.701433530
6	38.670746707	43.228399490	44.800033926	6	38.698480876	43.128462657	44.835086363
1	39.568785497	42.867068538	45.298603219	1	39.605439589	42.797469394	45.337568085
6	43.484567925	40.884954415	42.699482543	6	43.580522350	40.882431282	42.713731804
1	43.499113727	41.751463004	42.035272918	1	43.566637776	41.745539600	42.044863578
1	44.035181065	40.062880422	42.219594334	1	44.148250521	40.070469315	42.236233169
6	42.036996274	40.447466004	42.931519062	6	42.145392190	40.419334852	42.975383622
8	41.763821002	39.367226624	43.425195915	8	41.917295618	39.356322313	43.539157390
8	41.186989140	41.350589753	42.505537515	8	41.263403573	41.264940214	42.528459510
6	39.397601991	45.013545193	40.002378830	6	39.428223097	44.978400252	40.029185838

7	40.674040059	44.986671811	40.530231808	7	40.703553110	44.954427850	40.559371207
1	41.469021590	45.582766137	40.260990958	1	41.496561435	45.552121419	40.291262532
6	40.796834983	43.857841677	41.255317348	6	40.822364896	43.824662655	41.288708417
1	41.713277436	43.553439640	41.753036052	1	41.739258240	43.521540285	41.786939121
7	39.667847007	43.158730294	41.230153853	7	39.696354759	43.123753842	41.266512040
6	38.783767119	43.869680420	40.450756587	6	38.816220041	43.834790510	40.483874208
1	37.778393408	43.504396038	40.257513190	1	37.808911616	43.473150995	40.290453489
26	39.281749650	41.392119203	42.346810338	26	39.307116560	41.223358736	42.398755811
8	39.001983460	40.109432097	43.302011569	8	39.116166167	39.759651761	43.328210071
8	37.591616805	38.867429365	40.334670894	8	37.463573194	38.835274661	40.219496472
8	33.314635096	37.853357456	43.284940380	8	33.325893707	37.795644475	43.338601170
6	34.538276234	38.111422384	43.268961582	6	34.552301622	38.040017354	43.299742632
8	35.308343989	38.084026010	44.274474689	8	35.336156974	38.012607841	44.296587212
6	35.193796207	38.510860606	41.927230730	6	35.188645318	38.421989097	41.946809087
6	36.154558403	39.689391178	42.084447026	6	36.134209892	39.615835408	42.072137659
6	37.277391297	39.788022546	41.073965257	6	37.229180487	39.726774698	41.028417182
8	37.957133306	40.937044179	41.049252981	8	37.959640373	40.829951610	41.060083477
1	35.624077055	40.654781785	42.119941839	1	35.584274110	40.571214342	42.100451209
1	36.657769036	39.577928939	43.062421728	1	36.661391947	39.534976818	43.038755198
1	35.762735401	37.635664001	41.572903582	1	35.765747541	37.548433524	41.602576323
1	34.405316555	38.712746685	41.186215250	1	34.392893215	38.596927275	41.207162541
6	42.497029493	34.564149948	46.110363855	6	42.334476302	34.894325060	46.120868616
7	41.907532308	34.469206432	44.769318151	7	41.757799166	34.855227937	44.766627782
6	40.975943739	35.283377142	44.237667130	6	40.855816709	35.679701617	44.209003165
7	40.715065785	36.474646317	44.797987418	7	40.570878187	36.876559475	44.793376972
6	39.593228395	37.307553511	44.387108516	6	39.377597207	37.610435095	44.602175717
7	40.267282966	34.890459574	43.174005773	7	40.194768199	35.316706186	43.113019010
6	40.302446614	33.537983376	42.662385498	6	40.272312399	33.983910137	42.546183127
1	41.268441674	33.296878357	42.195516319	1	41.256962994	33.787366113	42.091192067
1	40.098227181	32.806207982	43.459141868	1	40.059413924	33.215791162	43.305328992
1	39.524278769	33.441581310	41.901116140	1	39.511789879	33.921030005	41.763557472
1	39.722467513	37.721845210	43.377304088	1	39.410946497	38.565253122	43.767806058
1	38.653758302	36.735494585	44.431644613	1	38.523868037	36.991403887	44.296430083
1	39.542382722	38.157192173	45.074500258	1	39.169797715	38.227973339	45.482094520
1	39.807863068	35.591597013	42.576576660	1	39.755810681	36.022188583	42.493520085
1	42.234264265	33.686730465	44.203660613	1	42.077612162	34.080974977	44.187722736
1	42.653046266	35.610505484	46.412914946	1	42.300699690	35.912446312	46.531475564
1	43.492995374	34.107057224	46.048806280	1	43.395391705	34.618979543	46.033807470
1	41.462477885	36.922826945	45.320373672	1	41.317725132	37.340838501	45.313594652
8	40.224325796	40.417200002	45.788494741	8	40.277755717	40.465450352	45.806367830
1	39.474660660	40.546020864	46.406396753	1	39.529903056	40.616159779	46.421878304
1	39.811368868	40.244789737	44.917272072	1	39.864768811	40.265679146	44.938743751
8	38.907859994	36.448299154	40.904625008	8	38.892462523	36.559191421	40.861448616
1	39.525850923	36.734364130	40.187207796	1	39.527296265	36.817676611	40.145013483
1	38.369723271	37.258602239	40.997444438	1	38.302547204	37.342412750	40.854566824
1	44.060366690	41.134930334	43.590569039	1	44.155241640	41.149679223	43.600491975
1	38.996494436	45.856523091	39.439734787	1	39.030036416	45.815833609	39.456280911
1	37.854355363	44.985354688	45.935362722	1	37.881987723	44.916764379	45.916737842
1	41.909198201	34.037026224	46.861803994	1	41.835959032	34.203885834	46.801193191
<b>IM2</b> HF = -3041.505115				<b>TS_Rb</b> HF = -3041.503764			
6	37.773918341	44.194854553	45.139024957	6	37.754508866	44.119932617	45.181231938
7	36.790087346	44.200759234	44.175391419	7	36.748778389	44.077473424	44.243756786
1	35.982890578	44.835270522	44.127518208	1	35.959114713	44.729871236	44.164844721
6	37.077219699	43.239397142	43.284618656	6	36.995745707	43.039284453	43.423567113
1	36.478968362	43.012508830	42.406962049	1	36.374203940	42.768516721	42.573803084



7	38.200434564	42.618638372	43.623656254	7	38.109385358	42.415549463	43.781531857
6	38.653426328	43.201698862	44.784258549	6	38.600254614	43.080404001	44.878734617
1	39.552694074	42.846094100	45.284699817	1	39.525331536	42.778628652	45.365961541
6	43.584468123	40.894258224	42.655650929	6	43.559722503	40.780969265	42.810376340
1	43.622483835	41.769589569	42.005134617	1	43.554087565	41.623296317	42.112169236
1	44.155822592	40.078515350	42.189742101	1	44.116081148	39.946070248	42.338743106
6	42.125150821	40.474766020	42.804565608	6	42.108797117	40.363492332	43.068198110
8	41.830241759	39.355649141	43.238149432	8	41.860048181	39.188914815	43.403260063
8	41.286542029	41.367959790	42.395832001	8	41.244024409	41.280459549	42.866123036
6	39.422902294	45.124597214	39.962115469	6	39.404453730	44.886787970	40.057980023
7	40.706429998	45.097257182	40.472293180	7	40.674307690	44.857712945	40.600997692
1	41.500313810	45.692500951	40.199791916	1	41.469148212	45.452659618	40.336709280
6	40.837118289	43.964163367	41.191813454	6	40.778019589	43.729561137	41.338203058
1	41.763081212	43.656497745	41.670895112	1	41.682973508	43.424251207	41.857787842
7	39.708847856	43.265725028	41.182997821	7	39.648614346	43.035777600	41.308175800
6	38.816370116	43.980466180	40.418423455	6	38.781295703	43.749075278	40.513048057
1	37.805205433	43.621549494	40.240710918	1	37.774170754	43.390390224	40.310989800
26	39.280091473	41.401596175	42.290165518	26	39.194363896	41.159410968	42.445512934
8	39.195396363	39.853802877	43.318380646	8	39.205917026	39.421574588	43.321029125
8	37.554332834	38.875177605	40.274652182	8	37.208324506	38.769463633	40.045099045
8	33.314944262	37.848738914	43.290401648	8	33.358006532	37.732912502	43.459480547
6	34.545138530	38.078079698	43.275399372	6	34.583669122	37.963564566	43.383495361
8	35.311134563	38.039331329	44.283455282	8	35.381984745	37.962086230	44.377256082
6	35.212380955	38.458546138	41.935177946	6	35.198148463	38.285003338	42.011007612
6	36.163251896	39.645420983	42.085993472	6	36.101674969	39.518200258	42.046131519
6	37.247474123	39.782529745	41.036624372	6	37.127676300	39.635590045	40.926853527
8	37.903209086	40.939020603	41.020382197	8	37.914638611	40.667168169	40.971034789
1	35.618108714	40.600628929	42.161195100	1	35.503651368	40.444812360	42.051707782
1	36.708593325	39.519885693	43.039153719	1	36.675913015	39.520670643	42.986435695
1	35.792764231	37.583754554	41.599375150	1	35.797087307	37.410601350	41.704346369
1	34.432202014	38.645091929	41.181618542	1	34.394676161	38.386509276	41.266904801
6	42.537511537	34.506289464	46.098724311	6	41.567522035	35.172312802	46.138034962
7	41.931709697	34.483959587	44.761153099	7	41.197656026	35.060990149	44.717091960
6	41.006068868	35.337392052	44.286648851	6	40.276203757	35.683975665	43.977229621
7	40.773673424	36.499497719	44.947255191	7	39.456301718	36.651496772	44.544366410
6	39.656726273	37.296886975	44.793200798	6	38.317897874	37.094000492	44.010677750
7	40.276924962	35.049153851	43.207516271	7	40.085006751	35.375966793	42.701485563
6	40.305388956	33.758472707	42.553723617	6	40.695213907	34.246022853	42.023032826
1	41.248590532	33.598500367	42.009091995	1	41.715262560	34.038642390	42.373631693
1	40.157522042	32.942359896	43.277575365	1	40.087431330	33.333429847	42.136039225
1	39.483864878	33.738833802	41.833035386	1	40.778278473	34.503796981	40.961620821
1	40.039152955	39.344612700	43.250692351	1	40.141231352	39.109944943	43.249654037
1	38.758685462	36.884229000	44.336886404	1	37.932322809	36.640536119	43.097543386
1	39.680493190	38.258096130	45.294632369	1	37.690592758	37.791789498	44.559094625
1	39.850817814	35.810315500	42.656879541	1	39.524843137	35.996140245	42.075797867
1	42.251487926	33.734990430	44.147617435	1	41.810505506	34.452970475	44.179920081
1	42.791328208	35.530400114	46.414470722	1	40.964435076	35.941264808	46.635082828
1	43.488716495	33.968413753	46.012213747	1	42.621024612	35.489538095	46.191044796
1	41.541834559	36.883582885	45.495162859	1	39.777689318	37.214071699	45.354992225
8	40.154578938	40.462347537	45.779512047	8	39.684828331	39.007155961	45.925893492
1	39.435931162	40.577198326	46.437241420	1	39.152997237	39.543675343	46.549630635
1	39.689033571	40.283693409	44.924697259	1	39.466077739	39.338927066	45.002201094
8	38.906133749	36.495865304	40.928419627	8	38.715355354	36.586902560	40.573526815
1	39.518317466	36.758174910	40.197702719	1	39.416796541	36.851479416	39.918179057
1	38.378469454	37.315268767	41.008278993	1	38.113392394	37.369641809	40.504583904
1	44.127488019	41.138127559	43.568736059	1	44.146316982	41.088468063	43.676066080
1	39.002297775	45.967241190	39.413380294	1	39.024140963	45.721675043	39.469428336
1	37.839907448	44.961981353	45.910535964	1	37.833284096	44.915472821	45.922162141

1	41.925050890	34.016298637	46.855604926	1	41.437220556	34.222009122	46.655733489
<b>PD (CH)</b>				<b>IM1 (NH)</b>			
HF = -3041.582519				HF = -3041.257473			
6	37.734923063	44.068250992	45.139062290	6	36.818184515	47.028911608	40.960030675
7	36.719692818	44.033679355	44.212759561	7	36.161098330	46.387122001	39.935553099
1	35.930141063	44.688673908	44.148994195	1	35.537315005	46.822184166	39.243245395
6	36.958060582	43.001172864	43.381327068	6	36.502923380	45.089699917	39.975298015
1	36.320841802	42.740329184	42.539956896	1	36.160190458	44.347797266	39.264056746
7	38.075193031	42.369850726	43.719116506	7	37.343648188	44.859637854	40.974960083
6	38.574218612	43.026955739	44.820387401	6	37.554342031	46.062042241	41.604372457
1	39.498254155	42.718548153	45.305824187	1	38.222988722	46.159335749	42.456562372
6	43.518152625	40.830473183	42.769113712	6	42.368219580	42.834048518	42.744519178
1	43.494799403	41.701417124	42.109077697	1	42.606977862	43.034348150	41.694961701
1	44.077210455	40.021206464	42.280060127	1	42.862863759	41.903080822	43.057589731
6	42.086967201	40.378279497	43.028041749	6	40.851478990	42.677812274	42.878759047
8	41.866156315	39.206619556	43.388833056	8	40.328658256	42.074507394	43.799321436
8	41.177968452	41.254489202	42.826821359	8	40.221886109	43.227854765	41.863386236
6	39.410427078	45.022732271	40.005050926	6	39.821539914	44.348548317	37.283492038
7	40.688258269	44.986005994	40.525232527	7	40.813429019	44.817928224	38.119093152
1	41.484843302	45.578899883	40.256929915	1	41.666575782	45.311081700	37.844746652
6	40.800657961	43.853527686	41.253684350	6	40.528611414	44.407659971	39.368583747
1	41.718044651	43.549562395	41.752331066	1	41.156532952	44.589433981	40.232723135
7	39.668386948	43.163037521	41.238194009	7	39.401300564	43.707117841	39.386048189
6	38.790292398	43.885173539	40.463569593	6	38.946623100	43.660287321	38.087941847
1	37.773658605	43.542848560	40.281839346	1	38.038574510	43.124838560	37.823885300
26	39.248260175	41.295828772	42.292705484	26	38.454557787	43.069583221	41.179392849
8	39.337027002	39.029270919	43.706897343	8	37.765404149	42.657047322	42.587256907
8	37.093515099	38.793540642	39.931380494	8	36.295983441	39.976656360	39.742598855
8	33.343314783	37.769456028	43.435651606	8	31.895256240	41.157685559	42.163807537
6	34.576258180	37.965707385	43.373589962	6	33.120796834	41.286688161	42.402518775
8	35.362058777	37.985614202	44.373149090	8	33.590766827	41.795304260	43.468080577
6	35.224253523	38.223135659	42.002892314	6	34.095669494	40.773742339	41.334214951
6	36.105169735	39.474005227	42.015052161	6	35.303971286	41.676299165	41.125804534
6	37.120347169	39.574633207	40.886888870	6	36.404493665	41.080303594	40.263801503
8	38.015515479	40.515033387	40.991106964	8	37.484894058	41.815487011	40.070627164
1	35.484459983	40.386068304	41.970831618	1	35.005451123	42.639280042	40.673617368
1	36.649167461	39.532729497	42.971062604	1	35.748532236	41.950128934	42.094955650
1	35.849624707	37.345208965	41.768535368	1	34.441017673	39.774186059	41.653012509
1	34.447694773	38.280636138	41.226992284	1	33.533909616	40.620508795	40.401699872
6	41.557856692	35.093411098	46.100071659	6	39.379569900	40.131283550	48.321497472
7	41.025276235	34.901553187	44.743700860	7	38.789052520	40.201008463	46.978399089
6	40.246534836	35.672996385	43.961444962	6	37.948594073	39.358909910	46.363482378
7	39.646963069	36.786665263	44.432996565	7	37.164497062	39.878138648	45.405299312
6	38.813966826	37.712400724	43.666907577	6	36.592894371	39.182342391	44.261872534
7	40.059266892	35.297479102	42.689396758	7	37.844958609	38.045768918	46.699949180
6	40.700016587	34.156409882	42.067516392	6	38.997577070	37.142431863	46.803630047
1	41.734535217	34.029283081	42.417093248	1	38.663562438	36.185494502	47.227001110
1	40.144033960	33.215989625	42.228442066	1	39.451875320	36.941824276	45.819906052
1	40.761922578	34.359158350	40.992783117	1	39.777977032	37.559829335	47.449422568
1	40.338246947	39.002339130	43.535741312	1	35.548870210	39.498920109	44.118066362
1	38.750320207	37.368778536	42.626215159	1	37.156246839	39.419496684	43.344142296
1	37.794258311	37.746129418	44.086751203	1	36.611375616	38.094378468	44.397074982
1	39.426723298	35.825085176	42.077269731	1	36.988799626	37.613545678	46.358805938
1	41.409032343	34.091783623	44.270083295	1	38.813380931	41.124542807	46.538820295
1	41.032683182	35.906825048	46.616290321	1	40.017862207	41.021784893	48.408557507
1	42.624831175	35.367680867	46.046960959	1	40.041924251	39.258909026	48.430827921
1	39.775311714	37.042247597	45.410720934	1	37.270557195	40.898072132	45.307403172

8	39.744983894	39.001731085	46.355530844	8	37.971225651	42.618314161	45.399665115
1	39.231374389	39.577437069	46.968450207	1	37.049662170	42.975894373	45.378131966
1	39.512429998	39.292731808	45.446978641	1	38.256898221	42.598907745	44.462803130
8	38.636591977	36.583892838	40.438778866	8	35.284414340	43.400202815	45.173473872
1	39.371151442	36.884411984	39.840155628	1	35.487152278	44.333704011	44.920092682
1	37.987325583	37.313128526	40.310508921	1	34.862986829	42.964395235	44.403214507
1	44.108554189	41.097830251	43.645477513	1	42.844573012	43.617477295	43.333920640
1	39.007355635	45.863375888	39.440321751	1	39.764631303	44.610131140	36.226892229
1	37.817113434	44.854621364	45.889351368	1	36.853468456	48.115719871	41.035331137
1	41.435795969	34.169321717	46.665073711	1	38.651526243	40.149078749	49.132486430
<b>TS_HAT (NH)</b>				<b>IM2 (NH)</b>			
HF = -3041.206669				HF = -3041.241879			
6	36.882109026	46.917342009	41.128991065	6	36.813682232	47.155782721	41.015022050
7	36.194655100	46.222526270	40.159602349	7	36.094108507	46.496737416	40.047170911
1	35.586006213	46.631550845	39.437117519	1	35.474256858	46.925385048	39.347240182
6	36.486864300	44.919282358	40.304320775	6	36.356388273	45.183577781	40.161623483
1	36.109322676	44.136428342	39.656158741	1	35.935158976	44.423819372	39.512085811
7	37.327857005	44.733390249	41.318481056	7	37.208446735	44.961221899	41.150987085
6	37.588986503	45.979230373	41.844829567	6	37.508484906	46.185964990	41.698997572
1	38.258970653	46.123440079	42.690025711	1	38.218502855	46.298055463	42.517296791
6	42.471971601	42.902114322	42.839931704	6	42.359664287	42.879140648	42.860337509
1	42.646872259	43.108242064	41.779228088	1	42.525440702	43.053223918	41.791463671
1	42.997089208	41.977936542	43.123995036	1	42.884050518	41.959428827	43.161488106
6	40.973935448	42.714705602	43.075558802	6	40.852800357	42.728289984	43.111178447
8	40.511026907	42.116892296	44.018121846	8	40.418963893	42.195136852	44.135820634
8	40.260086219	43.248780291	42.087716182	8	40.138021771	43.181588867	42.135857739
6	39.768503182	44.215819571	37.547184628	6	39.752324223	44.308271541	37.479360991
7	40.756912603	44.720029497	38.366504715	7	40.748594191	44.773909689	38.310817990
1	41.605669026	45.210026161	38.077687461	1	41.618744255	45.228384759	38.031417763
6	40.483761848	44.350290728	39.627863591	6	40.437012287	44.406130951	39.571482443
1	41.113906434	44.575415684	40.479170505	1	41.067844258	44.596664595	40.432276066
7	39.364519766	43.635231128	39.671409455	7	39.291030318	43.743350491	39.603278260
6	38.901981581	43.544478060	38.375256936	6	38.850647053	43.674382370	38.301412939
1	38.001937489	42.987688152	38.130756054	1	37.928907595	43.160877055	38.036977744
26	38.508480801	42.937666540	41.497103609	26	38.251896263	43.135686514	41.542240592
8	37.965391265	42.314757469	42.967014599	8	37.503680374	42.926267157	43.169303562
8	36.343407576	39.934070747	39.976743018	8	36.195381808	39.931489785	39.952245493
8	31.798581394	41.140407482	42.128595136	8	31.727650814	41.119550813	42.176914056
6	33.003416594	41.262044403	42.447880029	6	32.926489304	41.183956764	42.536917694
8	33.409117968	41.784559379	43.530644917	8	33.303587806	41.659607777	43.655873322
6	34.051655615	40.724481192	41.463215817	6	33.988661456	40.644792432	41.573641800
6	35.320612985	41.565684424	41.422463285	6	35.199848503	41.559236109	41.422941555
6	36.424073239	41.011315560	40.544696661	6	36.321579999	40.987593042	40.564682993
8	37.507729712	41.768791919	40.377787331	8	37.431749348	41.691393168	40.502173920
1	35.102925483	42.596237278	41.093909365	1	34.903996923	42.526491701	40.973547423
1	35.727869965	41.683595270	42.439678787	1	35.621936951	41.825475343	42.405154797
1	34.301727050	39.694621079	41.773989524	1	34.323420889	39.667022141	41.962900854
1	33.583371596	40.643902065	40.471236376	1	33.507102565	40.449518524	40.605290700
6	39.024127448	40.961573550	47.937983743	6	39.049960606	40.801125553	48.272630170
7	38.302327505	40.906338261	46.650834736	7	38.342508521	40.695839140	46.995066177
6	38.504356023	39.999833678	45.674557990	6	38.540949672	39.824883081	46.004934141
7	38.210986660	40.264066791	44.394988325	7	38.062869265	40.236462027	44.798894518
6	38.198209601	39.188977686	43.423594863	6	38.458708527	39.607086425	43.580318130
7	38.969892955	38.751092022	45.983236287	7	39.073686797	38.597779091	46.140358664
6	38.651261649	37.953556623	47.151382718	6	39.198402677	37.791798219	47.340467724
1	38.708312423	36.890016850	46.872419359	1	39.207965836	36.732925493	47.043852557
1	39.337604557	38.117171519	47.998944306	1	40.123605554	37.998257051	47.898559869

1	37.618476070	38.160330527	47.470904905	1	38.327277048	37.963040358	47.986647910
1	37.693788232	38.291252736	43.813891152	1	37.812313834	38.718347471	43.415315589
1	37.649833949	39.513620430	42.527765303	1	38.256886293	40.300372641	42.754163645
1	39.210683378	38.893495345	43.093889189	1	39.512977120	39.283939549	43.539874949
1	39.691961281	38.386502460	45.362324929	1	39.586337428	38.256805837	45.327540552
1	37.896584025	41.794503900	46.330578443	1	37.804331994	41.536869998	46.683081025
1	39.507165759	41.946206069	48.012033093	1	39.490512646	41.809817618	48.323101514
1	39.829692286	40.216193644	47.936382575	1	39.877352820	40.084245942	48.315272104
1	38.151441318	41.433825440	43.744100293	1	37.710419209	42.885557546	44.124901993
8	37.474763245	43.510762236	45.540232304	8	37.237743617	43.072654587	46.048958974
1	36.499033181	43.485704989	45.658088279	1	37.463191795	43.767115513	46.701820604
1	37.593382210	43.257972602	44.607410952	1	36.266141348	43.162991213	45.869815531
8	34.603360225	43.502884787	45.318285337	8	34.572416676	43.377235316	45.362774825
1	34.865980734	44.387191925	44.963983627	1	34.793391908	44.255861789	44.962578931
1	34.348412237	42.942695788	44.552119010	1	34.298704924	42.784303179	44.623024867
1	42.959738936	43.693765233	43.408648844	1	42.869487656	43.680322115	43.395366210
1	39.740604518	44.423729074	36.477576001	1	39.732713422	44.514580134	36.409258430
1	36.910760926	48.006648857	41.154622596	1	36.893754153	48.242355649	41.046882405
1	38.393046891	40.824306268	48.816028354	1	38.394750947	40.672790338	49.134197175

The Cartesian Coordinates of the Optimized QM Region of QM/MM Geometry with External Electric Fields (EEFs). QM/MM energies at the QM(B1)/MM level of theory are given in Hartree.

Orthogonal EEF of field strength -0.0025 au				TS_HAT (CH)			
IM1 (CH)				HF = -2992.543403			
HF = -2992.577921							
6	45.220500854	44.247886506	37.862992636	6	45.269017062	44.182773532	37.887351692
7	44.263325866	44.240241567	36.873221976	7	44.311506084	44.139686443	36.897849499
1	44.220746386	44.858283488	36.055101899	1	44.237173789	44.768710369	36.089540411
6	43.364968173	43.287372521	37.174817563	6	43.468044011	43.133248589	37.184300049
1	42.489882160	43.047954694	36.577932768	1	42.600115417	42.863682777	36.589603153
7	43.694345719	42.690623856	38.310146830	7	43.833701907	42.533075332	38.309121691
6	44.853303401	43.271242256	38.758831488	6	44.959482932	43.172777801	38.766951575
1	45.343816822	42.926469330	39.667347744	1	45.465108089	42.839125206	39.671252051
6	42.703863220	40.911931204	43.518027638	6	42.794052550	40.856310072	43.587238329
1	42.036288102	41.775880555	43.533602605	1	42.101079861	41.700719160	43.578471052
1	42.224775355	40.086392979	44.064361115	1	42.333763336	40.024918066	44.140736871
6	42.946152977	40.482858929	42.070540624	6	43.076662808	40.416453645	42.151230317
8	43.455807025	39.411635856	41.793239299	8	43.623794396	39.356577567	41.895263863
8	42.519219218	41.389075090	41.220481478	8	42.651944137	41.298394572	41.279262836
6	39.996697530	45.032461465	39.441150781	6	40.094031086	44.926404046	39.475848557
7	40.514610940	45.005077992	40.722351862	7	40.604971246	44.906735613	40.759887161
1	40.225783632	45.585414574	41.523105209	1	40.297802687	45.482832553	41.556890118
6	41.249365342	43.882083514	40.844172349	6	41.368238725	43.801641423	40.880513015
1	41.737975858	43.574207678	41.764434832	1	41.856003441	43.502145108	41.803836687
7	41.242163954	43.191470633	39.710179155	7	41.388060948	43.115503699	39.744112540
6	40.462776007	43.898008823	38.823902314	6	40.594701885	43.806880262	38.857392756
1	40.281112368	43.530173495	37.817613512	1	40.422754686	43.439537497	37.849244521
26	42.337156140	41.417458813	39.322678520	26	42.496048271	41.279729475	39.368217360
8	43.242157955	40.095205272	39.046717511	8	43.362620531	39.864498449	39.167344995
8	40.327407841	39.107934223	37.589788493	8	40.240106925	39.110036157	37.520262752
8	43.283571943	37.964092405	33.282727210	8	43.299969384	37.916509305	33.297140750
6	43.270906806	38.129858003	34.524598505	6	43.293420758	38.059618196	34.540950283
8	44.282237613	38.042540244	35.282907709	8	44.312810654	37.979224408	35.290732790
				6	41.971020550	38.415273589	35.250651800

6	41.946063355	38.515908671	35.215191960	6	42.173002960	39.627605776	36.157283772
6	42.143360043	39.728909145	36.123315424	6	41.145360719	39.885030595	37.235818693
6	41.129441316	39.956302203	37.222209445	8	41.302715432	41.017830203	37.903299162
8	41.194431066	41.138962781	37.826311694	1	42.284268134	40.555028630	35.569510827
1	42.247315914	40.661802338	35.545288204	1	43.129512481	39.498291166	36.693651360
1	43.102103126	39.593876055	36.656635734	1	41.674229463	37.549312995	35.864598952
1	41.625912162	37.659038676	35.829309143	1	41.183052728	38.584282642	34.502082013
1	41.172505464	38.691228602	34.452655921	6	46.113110095	34.908642649	42.210948572
6	46.105039665	34.536511952	42.501935574	7	44.741235582	34.680401961	41.733614633
7	44.763956828	34.432636447	41.913552700	6	44.030567560	35.355593607	40.810130313
6	44.226966055	35.245523818	40.986835995	7	44.302858322	36.635408969	40.480091956
7	44.774133769	36.450859525	40.745536599	6	43.669632433	37.303418610	39.349167726
6	44.353243024	37.294734996	39.636550919	7	43.037334170	34.716906412	40.176412823
7	43.179450769	34.845019139	40.260150270	6	42.837111861	33.283131851	40.243208073
6	42.685916946	33.483627141	40.277813911	1	42.528183533	32.949347470	41.243303215
1	42.197912397	33.234917580	41.229824160	1	43.755045128	32.745546610	39.960268063
1	43.501456262	32.767325556	40.097019297	1	42.044928985	33.002440035	39.544133214
1	41.948580836	33.372312082	39.479427399	1	42.590953406	37.095808225	39.284471436
1	43.336029893	37.692510147	39.764367985	1	44.153931265	37.053903737	38.389769722
1	44.407213700	36.736028763	38.689371487	1	43.654649954	38.558824348	39.430927553
1	45.029212137	38.154615593	39.598154908	1	42.361390272	35.274141718	39.655155543
1	42.584645571	35.547202518	39.804455045	1	44.307187511	33.832389974	42.098920373
1	44.207408706	33.642091729	42.241614040	1	46.470011214	35.896848046	41.890593149
1	46.410593287	35.585178622	42.631810081	1	46.114765070	34.895302413	43.311749208
1	46.044822078	34.101249604	43.507317430	1	44.738029212	37.216704086	41.190373885
1	45.238230557	36.908144017	41.525165407	8	45.864612459	40.474876602	40.330409181
8	45.756275784	40.446157253	40.220314093	1	46.462176882	40.574557673	39.562127653
1	46.349017751	40.559301250	39.450305256	1	45.011905363	40.186218292	39.949884034
1	44.874072597	40.252259380	39.839447272	8	40.469642076	36.533676595	38.657030015
8	40.861413399	36.540527541	38.858210282	1	39.840763193	36.762780281	39.386955738
1	40.140383012	36.750132744	39.501726791	1	40.503438727	37.379404272	38.168237240
1	40.945321649	37.394599432	38.393790723	1	43.668941100	41.144732326	44.169861665
1	43.592954787	41.163913758	44.096031352	1	39.494094980	45.745468741	39.079266897
1	39.429181257	45.870369886	39.036302568	1	46.006519345	44.983237694	37.945788190
1	45.981413102	45.025886184	37.924607373	1	46.776189143	34.132651305	41.828547042
1	46.851970077	33.994303295	41.922132107				
Orthogonal EEF of field strength +0.0025 au				<b>TS_HAT (CH)</b>			
<b>IM1 (CH)</b>				HF = -2995.038648			
HF = -2995.067015				6	45.212607249	44.183046836	37.782877127
6	45.170147802	44.236016616	37.764207912	7	44.246447848	44.177910033	36.804070860
7	44.206789447	44.255210118	36.783625970	1	44.182992166	44.819327390	36.001389361
1	44.165446601	44.889559160	35.974659380	6	43.376780811	43.195459148	37.082157129
6	43.298580648	43.311492827	37.072127998	1	42.501853451	42.964026552	36.482349778
1	42.419318147	43.102741245	36.470740248	7	43.736748724	42.569948287	38.196697842
7	43.630358660	42.689282466	38.195522275	6	44.888408485	43.169103819	38.651694051
6	44.803052020	43.247342014	38.645345591	1	45.402361003	42.813038609	39.543410363
1	45.299840399	42.889276435	39.545618964	6	42.769081734	40.861144984	43.516642877
6	42.681266399	40.892485697	43.467661728	1	42.090452442	41.716837010	43.520376873
1	42.023844330	41.764128216	43.481507042	1	42.302210433	40.031860517	44.068133165
1	42.199066363	40.074569465	44.022677808	6	43.017917625	40.418054110	42.073269585
6	42.901455777	40.449608690	42.018829650	8	43.519234787	39.338976957	41.809790508
8	43.359476996	39.352369624	41.748358612	8	42.591207496	41.310399096	41.214757267
8	42.499632712	41.363107261	41.172349367	6	40.094910250	44.965240222	39.403522675
6	40.018719136	45.041461357	39.379139420	7	40.625173710	44.946609658	40.678609208
7	40.552662049	45.017261007	40.652672993	1	40.358813633	45.551355493	41.466853662
1	40.297923032	45.624541241	41.442644793	6	41.372412192	43.832343044	40.799525702
6	41.277959938	43.889167885	40.775768067	1	41.878790168	43.539281106	41.714390751

1	41.783355734	43.589581086	41.689383956	7	41.358226966	43.132032508	39.670474330
7	41.245162590	43.185434768	39.649342964	6	40.564469036	43.830447584	38.788018630
6	40.462656365	43.895219133	38.766504230	1	40.378767960	43.468353320	37.780144371
1	40.268587414	43.531954472	37.760535396	26	42.483643880	41.335271903	39.299794615
26	42.371836358	41.428257670	39.259839240	8	43.440648192	40.010768427	39.073916201
8	43.336242035	40.152665005	38.984138513	8	40.302530293	38.829668393	37.611841145
8	40.362982989	38.834264911	37.661241307	8	43.262511112	37.716482512	33.366601079
8	43.231095727	37.734112337	33.363411379	6	43.266507850	38.036537379	34.572593807
6	43.232567533	38.069988276	34.565929539	8	44.283769423	38.063472670	35.328177468
8	44.242750682	38.084908608	35.329473026	6	41.924540573	38.438546948	35.234309727
6	41.891508980	38.506210530	35.209593402	6	42.077448953	39.626937415	36.183207858
6	42.054250897	39.685028466	36.168786170	6	41.087499896	39.725208143	37.324524310
6	41.071594183	39.771272330	37.316959869	8	41.118522542	40.844753195	38.040682705
8	41.034148437	40.923773376	37.985735860	1	42.070187959	40.586000136	35.639643740
1	42.067717669	40.651679240	35.640630741	1	43.074619591	39.553647879	36.654170689
1	43.045539894	39.580796794	36.648275892	1	41.578888529	37.561500974	35.807064145
1	41.514946407	37.638587557	35.776547758	1	41.180184440	38.627894732	34.445734293
1	41.165409504	38.717546878	34.409128722	6	46.177942981	35.024815211	42.096332400
6	46.136228272	34.617411278	42.484249958	7	44.804394643	34.824275259	41.613694073
7	44.796049804	34.533315504	41.891376982	6	44.096385081	35.507935598	40.689988070
6	44.270289325	35.349726618	40.955694105	7	44.425737862	36.749384535	40.305952884
7	44.839655554	36.528419050	40.676764459	6	43.828896094	37.424946467	39.159671454
6	44.425288591	37.353774471	39.549096515	7	43.035022221	34.900007715	40.134102255
7	43.190823174	34.963380580	40.264319626	6	42.755264937	33.490628706	40.294977050
6	42.647180801	33.626466850	40.330090077	1	42.464742764	33.230156705	41.325614270
1	42.183343449	33.413956432	41.306125344	1	43.623041165	32.874940783	40.008870358
1	43.420763632	32.868874258	40.128496913	1	41.923032672	33.222450911	39.637430920
1	41.875394638	33.540083019	39.560368171	1	42.769462466	37.164096692	39.052034425
1	43.423220444	37.781769416	39.691808550	1	44.353243648	37.201997747	38.215306826
1	44.453205966	36.774334740	38.613576329	1	43.776395313	38.639115222	39.286612286
1	45.120293188	38.195747958	39.483609471	1	42.345973508	35.460257209	39.622755597
1	42.599944260	35.663845143	39.794905301	1	44.335486979	34.010345467	42.000154705
1	44.222009193	33.756586460	42.211412931	1	46.562457643	36.003656991	41.780039226
1	46.444295856	35.661446976	42.645374868	1	46.169125623	35.020860008	43.197663340
1	46.067935593	34.158177466	43.479491792	1	45.031447567	37.291704610	39.914653858
1	45.417792076	36.966781529	41.389682934	8	45.902588123	40.420358550	40.323903476
8	45.808758637	40.395752067	40.251020365	1	46.542428374	40.555851236	39.592471132
1	46.444465309	40.551561583	39.519687437	1	45.054566453	40.228498761	39.880914395
1	44.944556758	40.261501424	39.811633758	8	40.613097578	36.357362303	38.736110379
8	40.908292053	36.417283551	38.895922030	1	39.970730972	36.671651636	39.422076931
1	40.185377948	36.691923987	39.512150238	1	40.680865086	37.169135401	38.189834545
1	41.002618612	37.240383233	38.374056513	1	43.651312057	41.132514497	44.096380371
1	43.575393564	41.139406522	44.040054988	1	39.509099558	45.795685138	39.009499327
1	39.456968656	45.884866210	38.977677121	1	45.960341714	44.973070616	37.852324381
1	45.935975588	45.008314001	37.835844975	1	46.833476612	34.237802481	41.723567140
1	46.887932259	34.088519907	41.898346934				
Parallel EEF of field strength -0.0025 au <b>IM1 (CH)</b> HF = -2993.355685				<b>TS_HAT (CH)</b> HF = -2993.326225			
6	45.166136390	44.242146097	37.769839311	6	45.213021457	44.200728098	37.795270283
7	44.190259458	44.270981066	36.801338305	7	44.232912044	44.203721547	36.829914612
1	44.142013844	44.909035894	35.996790382	1	44.160406723	44.848806717	36.031963370
6	43.278604027	43.332875901	37.100157289	6	43.361391358	43.225084490	37.118733289
1	42.387339632	43.134670118	36.512958994	1	42.474432116	43.003067091	36.533210517
7	43.620719749	42.704656134	38.216040339	7	43.733735435	42.593752103	38.225125821
6	44.801498779	43.253576341	38.652647506	6	44.892954689	43.186590941	38.665994965
1	45.302584273	42.893902730	39.549802533	1	45.410811667	42.831062524	39.555433963
				6	42.776190521	40.858780710	43.531407509

6	42.696070260	40.889712602	43.474097470	1	42.087381436	41.705886941	43.528606532
1	42.029269058	41.753749939	43.486583873	1	42.315226733	40.029488861	44.087472583
1	42.219593979	40.069883950	44.030926538	6	43.043116257	40.415664139	42.094496684
6	42.929341524	40.448197269	42.029417408	8	43.583932691	39.352764586	41.833153800
8	43.434036530	39.369491529	41.759099566	8	42.603343869	41.295052834	41.229621612
8	42.499176693	41.344724601	41.178192394	6	40.072586305	44.923727537	39.420413139
6	39.989479669	45.002151600	39.391448326	7	40.584762327	44.897532903	40.702508065
7	40.505522426	44.967341865	40.671872681	1	40.292110698	45.484315101	41.498699369
1	40.226333299	45.555538957	41.471739005	6	41.336633227	43.788143752	40.826376864
6	41.234944860	43.843200105	40.794422967	1	41.827872854	43.493016811	41.748796342
1	41.725859631	43.538830554	41.714279671	7	41.344570531	43.095316042	39.690527009
7	41.223367748	43.149913306	39.659401809	6	40.556187867	43.796122073	38.802704119
6	40.447130495	43.864521725	38.773132789	1	40.376519094	43.438054901	37.792458156
1	40.260388199	43.508321522	37.763370209	26	42.490813618	41.324258343	39.324035558
26	42.365917368	41.415369621	39.272578119	8	43.485189258	40.019771404	39.101820897
8	43.368131139	40.163457151	38.998182030	8	40.378763467	38.809746124	37.591805272
8	40.399339625	38.825977905	37.606798985	8	43.358096145	37.711432832	33.367881006
8	43.339901930	37.722658968	33.364998783	6	43.352239857	37.990963279	34.586898923
6	43.324090897	38.018309990	34.581173728	8	44.371496871	37.978063409	35.343904637
8	44.333695989	37.998404691	35.349669827	6	42.021156961	38.394883734	35.253204873
6	41.988917912	38.449375729	35.223905806	6	42.176163297	39.594658285	36.188580039
6	42.140046066	39.649800650	36.160360064	6	41.165676648	39.704276844	37.312738490
6	41.126849644	39.755447474	37.283919667	8	41.185056278	40.829422803	38.016925197
8	41.084787392	40.908459791	37.944420214	1	42.180003292	40.548887211	35.635817995
1	42.158372723	40.605758837	35.612319170	1	43.161728638	39.523487538	36.682094938
1	43.118268306	39.563656198	36.667125218	1	41.683669837	37.527102203	35.843584657
1	41.626997716	37.590902374	35.812803358	1	41.264277928	38.571969582	34.474612284
1	41.248885691	38.632567881	34.430358556	6	46.141113186	34.990282157	42.205744622
6	46.114359302	34.630907579	42.495204546	7	44.776922597	34.795061627	41.696156219
7	44.776491185	34.552515992	41.896754470	6	44.086112518	35.492661479	40.767397123
6	44.258250141	35.376350579	40.962402262	7	44.417961968	36.744551935	40.411274201
7	44.859081884	36.540072877	40.672515367	6	43.802989328	37.426661769	39.273571856
6	44.431151880	37.375569970	39.557036587	7	43.049650807	34.889899715	40.164113585
7	43.171791711	35.011842616	40.274462684	6	42.763174814	33.479638335	40.302281294
6	42.572649784	33.701653618	40.383251054	1	42.455185717	33.209334940	41.324354632
1	42.068968486	33.562412595	41.351644377	1	43.635489567	32.865928137	40.024454676
1	43.322229998	32.906304880	40.247582845	1	41.939535488	33.222884376	39.629816260
1	41.823743245	33.608113919	39.592223387	1	42.726229045	37.222334399	39.220087599
1	43.437851708	37.816474035	39.719367752	1	44.271173115	37.138667603	38.317111564
1	44.431271876	36.798125083	38.619651474	1	43.806572286	38.657265192	39.350261942
1	45.134169523	38.209976397	39.479747392	1	42.352859395	35.464913895	39.675603952
1	42.581044922	35.725930420	39.819616698	1	44.295506547	33.986400578	42.080422342
1	44.180092069	33.806943983	42.249696000	1	46.487857108	36.014541813	42.014641996
1	46.412576183	35.671414241	42.695447000	1	46.120285944	34.860269832	43.298595000
1	46.044838112	34.138045902	43.473946761	1	44.920791238	37.311817325	41.088458242
1	45.398221175	36.992122526	41.408063250	8	45.922109038	40.441402601	40.342635060
8	45.823334226	40.394033083	40.243686952	1	46.525952234	40.565399425	39.583207043
1	46.422983295	40.547693509	39.486106298	1	45.052520654	40.252852731	39.937110002
1	44.936264926	40.270471444	39.842316730	8	40.637847537	36.366615168	38.811259666
8	40.919307946	36.455644705	38.947479473	1	39.983195054	36.686919188	39.484990999
1	40.194627263	36.730368249	39.564165996	1	40.712543345	37.170753937	38.255904034
1	40.990745070	37.265885782	38.402206023	1	43.655555709	41.143965300	44.108862218
1	43.588075344	41.147449128	44.045031916	1	39.487379753	45.754252496	39.025661438
1	39.429443438	45.846993201	38.990612441	1	45.963795108	44.988159915	37.861280716
1	45.935807463	45.010893142	37.838408591	1	46.831178957	34.273100784	41.761304045
1	46.872762668	34.125940390	41.896957278				

Parallel EEF of field strength +0.0025 au				TS_HAT (CH)			
IMI (CH)				HF = -2994.232869			
HF = -2994.259649							
6	45.162074050	44.203462240	37.809792098	6	45.190040358	44.108179325	37.813933682
7	44.203421472	44.211332868	36.822305562	7	44.231261868	44.078139065	36.825948254
1	44.165828794	44.835964723	36.007708139	1	44.165749201	44.710725762	36.018597999
6	43.300394028	43.260809379	37.114930182	6	43.378751917	43.078474970	37.108924010
1	42.427561739	43.034664688	36.510071533	1	42.516320919	42.815334895	36.503692057
7	43.628349194	42.650314409	38.243925747	7	43.739213267	42.471278463	38.231902052
6	44.794046328	43.219108222	38.695942339	6	44.874383949	43.097521965	38.689957429
1	45.290479137	42.857030246	39.595047961	1	45.387019980	42.748828824	39.585435890
6	42.701018236	40.906806229	43.511718718	6	42.780251877	40.833994350	43.562091662
1	42.041335575	41.777449766	43.525496340	1	42.095534681	41.685641419	43.559102683
1	42.215220356	40.085689152	44.058583960	1	42.313904409	40.003552545	44.111655300
6	42.931925719	40.469292565	42.062252507	6	43.046773062	40.390253408	42.121067436
8	43.419827502	39.389399770	41.788425966	8	43.584785412	39.329732141	41.863813600
8	42.504799487	41.374844360	41.212062643	8	42.599406346	41.267390755	41.252642310
6	40.008206188	45.037358619	39.412133463	6	40.088153906	44.921500489	39.437610601
7	40.547284285	45.021712875	40.684776192	7	40.621656988	44.906973806	40.712223674
1	40.291430091	45.630625631	41.471787282	1	40.352229842	45.511822910	41.498100478
6	41.267950122	43.888753270	40.811530246	6	41.365217562	43.787248696	40.832768246
1	41.772562216	43.587043316	41.725341339	1	41.868345394	43.489139948	41.748337080
7	41.230030423	43.181096145	39.690492147	7	41.349121339	43.086640160	39.706553994
6	40.447788437	43.885660292	38.806205848	6	40.555698828	43.783532740	38.825271200
1	40.248602178	43.507726171	37.806612938	1	40.365342738	43.411100353	37.821779820
26	42.328298226	41.387960796	39.306991913	26	42.453266593	41.228868646	39.340695095
8	43.245071325	40.081772002	39.026101242	8	43.346303869	39.853457017	39.136108260
8	40.270522425	38.919518022	37.597262090	8	40.129151273	38.936261572	37.439409273
8	43.210193120	38.025388625	33.263596447	8	43.272057332	37.954007387	33.285882680
6	43.199390316	38.228276505	34.496626238	6	43.263689452	38.137817962	34.521580549
8	44.202832530	38.179959823	35.264911047	8	44.275777909	38.106686649	35.281687326
6	41.855407746	38.592017192	35.174818731	6	41.920122213	38.457862187	35.216519560
6	42.026054095	39.741333201	36.166388086	6	42.074956089	39.622405472	36.192336542
6	41.020847572	39.831412520	37.291277389	6	41.017655125	39.757462518	37.264387671
8	41.014230417	40.974947002	37.990876362	8	41.099893360	40.835075004	38.045778867
1	42.081930423	40.718104643	35.658768455	1	42.146569186	40.586249691	35.658865183
1	43.004224327	39.597520610	36.662184686	1	43.040209915	39.499154079	36.714632348
1	41.511988280	37.697912655	35.720818086	1	41.618504442	37.555390194	35.774212176
1	41.108480991	38.819586693	34.398577716	1	41.148798561	38.650225134	34.455864312
6	46.134943943	34.515825545	42.495417196	6	46.135239107	34.884204614	42.141072034
7	44.786853068	34.400473975	41.924828281	7	44.760717041	34.656234420	41.672603365
6	44.230633333	35.202570585	41.000379573	6	44.044392633	35.330849522	40.754393857
7	44.745488040	36.418998599	40.758138172	7	44.344604623	36.593638415	40.397151874
6	44.336140200	37.248146470	39.634687512	6	43.779367358	37.269328186	39.238623805
7	43.181537214	34.780582549	40.285632049	7	43.009564027	34.707642730	40.171126877
6	42.747652823	33.398727705	40.265073767	6	42.802453175	33.274724680	40.244008994
1	42.323228734	33.079499106	41.227056071	1	42.518494277	32.942128931	41.252305943
1	43.580091912	32.727424708	40.005781027	1	43.707529287	32.729954297	39.934056184
1	41.972089837	33.292178390	39.502753373	1	41.990007488	33.000332607	39.565808721
1	43.311881529	37.633700129	39.743139097	1	42.730803354	36.988344296	39.075496144
1	44.414382502	36.682954438	38.693236571	1	44.353855631	37.086526493	38.314588823
1	45.004458278	38.114236442	39.600899311	1	43.692196387	38.481748433	39.378645227
1	42.579171354	35.467479621	39.818630619	1	42.344450012	35.262346611	39.633557813
1	44.252423143	33.589026109	42.237654508	1	44.323981845	33.814382411	42.045604188
1	46.449247119	35.566429909	42.577605767	1	46.508633009	35.853146641	41.782797457
1	46.085860858	34.121030038	43.518205664	1	46.138002995	34.912614278	43.241812085
1	45.263752220	36.865093146	41.508010073	1	44.941284564	37.128764622	41.019111071
8	45.759707726	40.457932585	40.230813112	8	45.849992668	40.462651793	40.316526682
				1	46.484211278	40.577441028	39.576002967



1	46.391989770	40.572198765	39.488591516	1	45.024473243	40.155195059	39.897425630
1	44.905582753	40.236800128	39.809610692	8	40.521050990	36.451525754	38.661388668
8	40.869515753	36.451723983	38.878566350	1	39.914412209	36.765504438	39.376428117
1	40.159149119	36.749780365	39.496423630	1	40.544406328	37.246569950	38.093650913
1	40.988638781	37.262727271	38.350236224	1	43.656891660	41.109209224	44.148459112
1	43.591393413	41.148771076	44.092022411	1	39.493873668	45.747684682	39.047331209
1	39.443926204	45.877806716	39.008026521	1	45.942200507	44.895146203	37.868756721
1	45.933465881	44.970912028	37.873375041	1	46.791617131	34.089569112	41.786403699
1	46.873153037	33.949459878	41.927663206				

Parallel EEF of field strength -0.005 au IMI (CH) HF = -2973.587480				TS_HAT (CH) HF = -2973.550834			
6	45.172174631	44.274549250	37.758466022	6	45.214458406	44.222308231	37.781812539
7	44.185786228	44.315546887	36.801755043	7	44.226934304	44.234560812	36.824645303
1	44.131537347	44.960246794	36.002371371	1	44.147831418	44.887417897	36.033153553
6	43.268532504	43.386025972	37.106170785	6	43.350401384	43.262690027	37.116370301
1	42.366473390	43.204915672	36.530189216	1	42.454981889	43.052398984	36.539522739
7	43.618908063	42.748011706	38.214357900	7	43.728184509	42.624037869	38.217252198
6	44.809270006	43.284362127	38.640162998	6	44.894909486	43.207145069	38.651507955
1	45.313474730	42.926130593	39.535953843	1	45.414649832	42.852484222	39.540056951
6	42.702294755	40.903688449	43.471058035	6	42.782248770	40.876918890	43.520605938
1	42.032625592	41.765214104	43.481468047	1	42.098700129	41.727785317	43.514491676
1	42.231985390	40.087317584	44.038598116	1	42.317913456	40.057439299	44.088901726
6	42.930271013	40.454970801	42.028899470	6	43.041351980	40.421987432	42.086192528
8	43.436697794	39.373870408	41.760488932	8	43.582801257	39.355674055	41.829170969
8	42.500615023	41.347896998	41.176392435	8	42.601786241	41.295450823	41.217511063
6	39.983301477	44.998361357	39.383593150	6	40.059659034	44.929406217	39.409714609
7	40.491740169	44.961565806	40.666445768	7	40.564219862	44.897768863	40.694335028
1	40.204833515	45.546341576	41.468229264	1	40.264827271	45.480046366	41.493794589
6	41.225391438	43.842224228	40.791862390	6	41.317581359	43.791502763	40.819256456
1	41.711839609	43.541109255	41.714890797	1	41.804040304	43.496315057	41.744087432
7	41.223262637	43.149412985	39.654200140	7	41.333118040	43.101833394	39.679200986
6	40.447611528	43.863798228	38.764783975	6	40.547553991	43.805622561	38.789234917
1	40.263212095	43.511401244	37.753340109	1	40.371730775	43.454231760	37.776051391
26	42.391861410	41.445679984	39.271380887	26	42.489933993	41.356717282	39.308570596
8	43.438734158	40.224442612	39.004516965	8	43.520512845	40.061386607	39.078252110
8	40.483239275	38.785246826	37.642515809	8	40.448169254	38.774089896	37.610380796
8	43.382558009	37.600711457	33.416016392	8	43.400934832	37.583502804	33.410714443
6	43.363822938	37.930217525	34.624048981	6	43.387169026	37.904735752	34.620040019
8	44.373175787	37.907905497	35.396785351	8	44.405878269	37.901166493	35.381879751
6	42.036681217	38.403327450	35.248714868	6	42.058743294	38.344690404	35.264235552
6	42.190288768	39.621121815	36.164689073	6	42.203683011	39.574395464	36.165062011
6	41.186795795	39.728512802	37.300607694	6	41.205171496	39.687432915	37.304078240
8	41.127647982	40.886036318	37.939552297	8	41.205750818	40.823405989	37.981291247
1	42.186232709	40.569481974	35.603730528	1	42.172626244	40.513899540	35.589398678
1	43.172958812	39.557135496	36.665559049	1	43.195046416	39.541898250	36.650028543
1	41.656459871	37.564003485	35.853410494	1	41.712581145	37.499204868	35.881273909
1	41.302972432	38.578780818	34.447765551	1	41.306105124	38.496236534	34.476268382
6	46.117999618	34.673286215	42.477677671	6	46.166148943	35.096878453	42.163504313
7	44.781753631	34.596654110	41.876499301	7	44.798372791	34.909345730	41.659314195
6	44.259499327	35.428785953	40.947493196	6	44.102322884	35.603930441	40.728506993
7	44.879300016	36.572763955	40.629047044	7	44.454505080	36.836504869	40.332699408
6	44.425455144	37.410337180	39.523435218	6	43.822389987	37.506483082	39.200166250
7	43.150866053	35.078258123	40.288710194	7	43.043917511	35.006023984	40.159922951
6	42.512144213	33.793757130	40.450827751	6	42.720156577	33.613294601	40.361393419
				1	42.410989691	33.398157384	41.397033392

1	42.033223970	33.699937221	41.437647714	1	43.573581751	32.962899540	40.106048310
1	43.228662036	32.967788080	40.314086397	1	41.885000491	33.353477394	39.703587443
1	41.735115904	33.711489393	39.685785047	1	42.748677956	37.290882105	39.152682530
1	43.445353028	37.866047180	39.720365542	1	44.293410154	37.243572515	38.238105867
1	44.387035547	36.831646424	38.587436687	1	43.793884383	38.775875869	39.283090834
1	45.134409780	38.236558833	39.421511150	1	42.333595994	35.580112787	39.682859877
1	42.554531168	35.795741393	39.839412981	1	44.289346893	34.142018991	42.087972437
1	44.160721789	33.893088695	42.268247779	1	46.518459359	36.119181750	41.973914599
1	46.406983616	35.710082603	42.707249378	1	46.145778720	34.973699965	43.257005870
1	46.048709562	34.156812268	43.444816458	1	44.969340726	37.415301413	40.992065124
1	45.451056269	37.025441055	41.342742076	8	45.937465545	40.407955038	40.333502296
8	45.862005182	40.338874546	40.277412270	1	46.525794322	40.558484544	39.568478415
1	46.438887289	40.532062449	39.513307269	1	45.051991111	40.271064361	39.937716831
1	44.958563645	40.273664711	39.893881973	8	40.655245070	36.364270558	38.849830591
8	40.920591820	36.447381618	38.992097233	1	39.989226262	36.682599546	39.515887727
1	40.189469325	36.722798601	39.603509933	1	40.730131593	37.169031761	38.292128810
1	40.992664274	37.258398400	38.444417195	1	43.666718090	41.164428256	44.089042128
1	43.597120232	41.172498563	44.032391989	1	39.478887972	45.762014405	39.012806680
1	39.425256656	45.843785022	38.981210083	1	45.963988623	45.010697696	37.850469889
1	45.940690616	45.044215603	37.829629265	1	46.854369144	34.377672823	41.719473292
1	46.884900946	34.190855876	41.871715100				
<b>Parallel EEF of field strength +0.005 au</b>				<b>TS_HAT (CH)</b>			
<b>IMI (CH)</b>				<b>HF = -2975.368623</b>			
<b>HF = -2975.391690</b>							
6	45.156600701	44.187634660	37.823163523	6	45.135972191	44.080461751	37.840173947
7	44.209321449	44.189621900	36.823883706	7	44.192499333	44.038830345	36.836781714
1	44.181099178	44.808284191	36.004919756	1	44.137150785	44.666385582	36.025507947
6	43.306003259	43.236376334	37.110226119	6	43.345351583	43.030134126	37.111611061
1	42.443897573	43.000158669	36.493809937	1	42.496914873	42.752680806	36.492446459
7	43.621306924	42.632424318	38.245979008	7	43.690726877	42.429830735	38.242896334
6	44.780649867	43.205959458	38.708856015	6	44.811859493	43.072078334	38.715071604
1	45.270886042	42.840669118	39.610288323	1	45.313869766	42.734758816	39.620301024
6	42.661010510	40.945584835	43.517463297	6	42.682131784	40.913197420	43.601284873
1	42.025563457	41.835421526	43.528544745	1	42.042117799	41.799771542	43.582810269
1	42.151523417	40.138401349	44.063407866	1	42.171856529	40.117066965	44.162603930
6	42.887657507	40.496962005	42.068774817	6	42.939855614	40.438409834	42.164898335
8	43.360557671	39.411113971	41.802189692	8	43.488941189	39.371089809	41.946527025
8	42.471515836	41.404793331	41.212853298	8	42.496277310	41.284381763	41.277239415
6	40.008770032	45.067806309	39.378539841	6	40.034234406	44.996931563	39.393798127
7	40.561399787	45.066747192	40.645033970	7	40.593532392	44.999076175	40.656981078
1	40.324373989	45.701110601	41.414288946	1	40.360248153	45.637090970	41.422909386
6	41.270454294	43.926724801	40.782682641	6	41.308126126	43.857814901	40.788042651
1	41.781793375	43.629504266	41.694307321	1	41.823272944	43.563656111	41.698872178
7	41.213870853	43.205006347	39.673591618	7	41.251098869	43.133531979	39.682953477
6	40.431522047	43.902711923	38.785875726	6	40.462118795	43.831259945	38.801980643
1	40.222740884	43.507561899	37.794732851	1	40.248983138	43.439244513	37.809741699
26	42.294966129	41.384750521	39.306666770	26	42.374892775	41.153529760	39.319269423
8	43.176365337	40.054974879	39.039241089	8	43.218148972	39.662188673	39.154521278
8	40.188760248	38.973871781	37.570493584	8	40.118854886	38.846941458	37.477977827
8	43.162706203	38.161260397	33.222473543	8	43.226670869	38.088071744	33.233076737
6	43.152041239	38.320692861	34.461104808	6	43.191434310	38.216272225	34.475411030
8	44.151499897	38.263828786	35.230743569	8	44.181974469	38.151389480	35.258466478
6	41.801310554	38.646145987	35.151732532	6	41.828706679	38.512252554	35.148106779
6	41.973192923	39.776604648	36.162812171	6	41.960106560	39.656213797	36.149519016
6	40.961121892	39.869530189	37.278132272	6	40.930785192	39.734181661	37.255433367
8	40.973238394	41.008881123	37.993725860	8	40.980235742	40.825200604	38.018700602
1	42.051048300	40.758744615	35.668027723	1	42.001302030	40.633582839	35.639859703
				1	42.933425359	39.535185483	36.658222705

1	42.947229779	39.610271062	36.660841820	1	41.518537896	37.599349651	35.682198037
1	41.472651646	37.736487846	35.681207777	1	41.076276402	38.720094359	34.371805946
1	41.048995954	38.885566635	34.383968063	6	46.144579657	34.763281019	42.300600702
6	46.156141079	34.470587616	42.505388382	7	44.783111738	34.678957582	41.744606365
7	44.803410516	34.341251156	41.947888482	6	44.183330469	35.491045588	40.865418726
6	44.234007827	35.131142452	41.024172250	7	44.692687691	36.739762039	40.629598410
7	44.719388213	36.362363324	40.790187776	6	44.531159845	37.488192070	39.442089044
6	44.311156097	37.187795551	39.665247545	7	43.112269023	35.090401455	40.185990513
7	43.194713976	34.689413447	40.306144611	6	42.648331862	33.713487228	40.199328823
6	42.800981285	33.294305847	40.261181854	1	42.218785947	33.433133540	41.173788978
1	42.372168719	32.949049834	41.211485904	1	43.466772472	33.021202506	39.951823919
1	43.658472482	32.653739417	40.008985687	1	41.872424885	33.613810364	39.437075084
1	42.042616083	33.170783526	39.484091223	1	44.269327535	36.868758551	38.573993394
1	43.277701140	37.554704338	39.759713596	1	45.417542463	38.109454797	39.266454311
1	44.411092120	36.628086325	38.722392951	1	43.694384476	38.398436519	39.464854090
1	44.966557042	38.064647258	39.641066283	1	42.478511533	35.781296753	39.751469199
1	42.597884654	35.366246638	39.824785972	1	44.264550144	33.846890674	42.030584064
1	44.288594746	33.513110225	42.253657473	1	46.569851710	35.761013183	42.127944486
1	46.479118836	35.521178936	42.532560369	1	46.078559773	34.608570849	43.387442929
1	46.115379392	34.122829431	43.545310567	1	45.206347294	37.183245044	41.389418732
1	45.252771654	36.801518093	41.532307215	8	45.748191718	40.448289049	40.257555275
8	45.717489320	40.483546330	40.226971677	1	46.381655362	40.584630218	39.518154273
1	46.366452512	40.586407015	39.495287661	1	44.905820099	40.179803886	39.838565737
1	44.881939044	40.221219298	39.795228173	8	40.866613592	36.508075741	38.875916685
8	40.825680097	36.472798102	38.834249660	1	40.154464467	36.792807497	39.498849601
1	40.124130614	36.783400271	39.453271168	1	40.895811195	37.283707620	38.283026427
1	40.969302083	37.282074759	38.312604895	1	43.572622786	41.146647419	44.184889357
1	43.556532305	41.161309624	44.100190384	1	39.459565101	45.835718931	39.001040868
1	39.446501784	45.910621415	38.976564182	1	45.899733990	44.856138426	37.895499635
1	45.931685876	44.951274012	37.887702150	1	46.803523386	34.011063540	41.866977190
1	46.884716285	33.875434294	41.954899493				
<b>Parallel EEF of field strength -0.0075 au</b>				<b>TS_HAT (CH)</b>			
<b>IM1 (CH)</b>				HF = -2940.896361			
	HF = -2940.934238			6	45.180498038	44.271997785	37.727052584
6	45.151109121	44.317684006	37.710580503	7	44.179833830	44.303555857	36.784952205
7	44.153030791	44.361970750	36.766630591	1	44.102076134	44.958944452	35.995054268
1	44.089309547	45.011670853	35.971451195	6	43.282121331	43.358061187	37.093479549
6	43.233721542	43.439637009	37.083658580	1	42.371007550	43.173794001	36.532664639
1	42.321139437	43.268838934	36.521457612	7	43.661631680	42.713675601	38.190802919
7	43.596301870	42.798857955	38.187316138	6	44.849039391	43.267928247	38.605011283
6	44.795013622	43.329773589	38.597433184	1	45.369464509	42.918373267	39.494833199
1	45.304446241	42.982431999	39.494287649	6	42.839430859	40.930559826	43.481168586
6	42.759391710	40.975986290	43.462554411	1	42.165172560	41.788066612	43.490710736
1	42.096728844	41.842404813	43.470351245	1	42.382691953	40.121391640	44.070532349
1	42.293816163	40.176698621	44.058472939	6	43.044837623	40.461808745	42.043570740
6	42.953458703	40.496616908	42.026050163	8	43.555921704	39.379473416	41.778935521
8	43.450451894	39.404832103	41.770573113	8	42.594740765	41.335916504	41.183066873
8	42.510532191	41.371437755	41.165592631	6	40.008706377	44.958062758	39.393383459
6	39.966621000	45.003298533	39.365101819	7	40.510221203	44.921107506	40.679088648
7	40.469133421	44.965881299	40.650046755	1	40.212069612	45.500565463	41.482928204
1	40.178195812	45.548865508	41.453468960	6	41.259481259	43.814266042	40.805338465
6	41.206639317	43.851426890	40.779373208	1	41.747084565	43.520637244	41.729904720
1	41.692208620	43.556546683	41.704753015	7	41.272998975	43.124439121	39.662572856
7	41.211305407	43.156824933	39.640252488	6	40.490058401	43.832832062	38.771666857
6	40.435528829	43.870249836	38.747484240	1	40.310044441	43.485610579	37.757824579
1	40.251711862	43.519724689	37.735342394	26	42.452124019	41.430107922	39.276450818
26	42.404997007	41.486039243	39.259123406	8	43.531856802	40.174130635	39.019742616

8	43.488169177	40.291091984	38.996657788	8	40.451174505	38.780318344	37.610355311
8	40.569284829	38.734569182	37.685375859	8	43.410400167	37.513230563	33.446021848
8	43.430246552	37.505508586	33.463079358	6	43.388821837	37.851394013	34.651336964
6	43.406832613	37.856908886	34.665722748	8	44.407186855	37.841388737	35.417579329
8	44.415873670	37.832238722	35.442332880	6	42.062966293	38.313441641	35.281889884
6	42.084619226	38.355270308	35.276822954	6	42.193548341	39.573802865	36.145294505
6	42.230958040	39.592560690	36.170395953	6	41.197501421	39.699690063	37.289307167
6	41.238585303	39.696440602	37.320591073	8	41.186961999	40.843169309	37.944255449
8	41.152727517	40.859188680	37.934924261	1	42.132813991	40.495432487	35.544815961
1	42.196050656	40.531344794	35.595264497	1	43.187102338	39.582905592	36.624670856
1	43.218907881	39.559533690	36.663239120	1	41.719543122	37.487642858	35.926628496
1	41.699440298	37.531609788	35.899740629	1	41.307780457	38.434528407	34.491472776
1	41.352086521	38.514086725	34.471569515	6	46.200344890	35.277290910	41.967444322
6	46.103023489	34.715148840	42.472398409	7	44.808963237	35.082765803	41.542764075
7	44.768922135	34.627028757	41.869366325	6	44.072650079	35.752986183	40.622772425
6	44.231350542	35.464126506	40.949155284	7	44.425965356	36.962536226	40.164720028
7	44.837236447	36.615229366	40.633223247	6	43.732792076	37.610197753	39.054496719
6	44.358378467	37.455511512	39.537791961	7	42.986432123	35.145237718	40.123573141
7	43.124924038	35.103289387	40.294824059	6	42.640687135	33.777502768	40.428298913
6	42.505372411	33.810780720	40.456994973	1	42.342216043	33.646112132	41.481988983
1	42.050983174	33.700397102	41.453595973	1	43.479122924	33.094028985	40.210087346
1	43.226783059	32.992989448	40.294366406	1	41.791214101	33.489024781	39.800853428
1	41.709300410	33.731838936	39.711462193	1	42.656615614	37.406936750	39.074874705
1	43.384929723	37.912756766	39.759895982	1	44.145355996	37.329656551	38.071047149
1	44.296512011	36.875548694	38.603918971	1	43.727897039	38.899531363	39.131318036
1	45.065834721	38.280674678	39.421751656	1	42.253639127	35.707284674	39.657997277
1	42.501500056	35.816261331	39.863700296	1	44.298387658	34.368044591	42.050827824
1	44.142601337	33.939778729	42.280097931	1	46.638176017	36.123847744	41.423195248
1	46.383382067	35.752886979	42.706964342	1	46.240274097	35.523137262	43.040671495
1	46.038018160	34.194717436	43.438197080	1	44.928825313	37.576012840	40.803233715
1	45.387324902	37.082115002	41.355980456	8	45.934377357	40.180522176	40.281738146
8	45.871410556	40.301349508	40.272052170	1	46.483038907	40.420634125	39.510733525
1	46.435664954	40.534070031	39.511335607	1	45.014879165	40.210072439	39.941621730
1	44.957770160	40.294744339	39.901287639	8	40.598999778	36.393074745	38.857627674
8	40.922702454	36.433512798	39.058676817	1	39.929568951	36.708024322	39.525336124
1	40.181294261	36.712144432	39.658624945	1	40.673574579	37.201763369	38.302181299
1	41.002522889	37.242823481	38.506131608	1	43.743186054	41.215848240	44.019596292
1	43.668242427	41.252948963	43.996735443	1	39.441431176	45.797455670	38.991281839
1	39.411177351	45.848841019	38.959383231	1	45.935703247	45.055065292	37.794414953
1	45.917752036	45.089450542	37.779154360	1	46.775702982	34.376145533	41.755389145
1	46.875323626	34.243477912	41.864824259				
Parallel EEF of field strength +0.0075 au <b>IM1 (CH)</b> HF = -2943.639391				<b>TS_HAT (CH)</b> HF = -2943.619692			
6	45.115672434	44.161966340	37.815828470	6	45.107269617	44.061707450	37.847780552
7	44.152789428	44.176345478	36.830762381	7	44.158268672	44.021886688	36.848502461
1	44.128546289	44.787033957	36.005850854	1	44.108236836	44.641041691	36.030920859
6	43.236488318	43.241252972	37.138409311	6	43.304499041	43.020733975	37.135189035
1	42.363408417	43.012201378	36.534935799	1	42.453701867	42.742195222	36.519814564
7	43.556647529	42.639444553	38.274019523	7	43.649192649	42.425801711	38.269046379
6	44.734879798	43.193345503	38.713919125	6	44.778887189	43.061401024	38.730588007
1	45.236765646	42.814439532	39.603836467	1	45.287288537	42.716205835	39.629688025
6	42.630191820	41.102790198	43.585311182	6	42.640089038	41.068065502	43.659257579
1	42.079061282	42.051688568	43.600689437	1	42.082261953	42.013140736	43.637999418
1	42.052884789	40.355185223	44.149506444	1	42.060589393	40.332839677	44.237480516
6	42.810380764	40.605084570	42.141063340	6	42.856548134	40.532822051	42.231494646
8	43.243287061	39.499909379	41.899859005	8	43.359704886	39.439331729	42.049627862
				8	42.432076843	41.359567933	41.316787572

8	42.403955666	41.500749195	41.265892892	6	40.027573054	45.051767333	39.357612431
6	40.007998989	45.152008670	39.361961311	7	40.614289116	45.071774646	40.607432281
7	40.596348769	45.173457536	40.611201959	1	40.438025413	45.753196444	41.347217704
1	40.436169451	45.861740207	41.349261989	6	41.291009459	43.909326771	40.756847551
6	41.257726158	44.008484168	40.772373866	1	41.819562274	43.617834172	41.659906815
1	41.784883140	43.716105303	41.675162619	7	41.189493932	43.158856238	39.675971460
7	41.143429550	43.253695559	39.692719195	6	40.405992912	43.855404287	38.791406221
6	40.366326246	43.949439941	38.801161630	1	40.163450690	43.439640078	37.815335997
1	40.118753464	43.524149822	37.831432823	26	42.337861798	41.136723853	39.353829978
26	42.213254685	41.410703797	39.355981592	8	43.176357108	39.643637238	39.222796923
8	43.064548729	40.058804058	39.120406846	8	40.070813768	38.837985202	37.524869007
8	40.096739341	39.037630231	37.594955591	8	43.147915255	38.200351054	33.214153501
8	43.069292232	38.274561157	33.216027985	6	43.123049978	38.313424929	34.457241327
6	43.072208840	38.437553386	34.453288166	8	44.116377054	38.262349048	35.234742244
8	44.076342853	38.408165395	35.215333748	6	41.756604633	38.572160001	35.147195716
6	41.718098913	38.731073199	35.160881118	6	41.889729426	39.682411013	36.184857542
6	41.893182397	39.836644955	36.197509191	6	40.870992613	39.733298364	37.300759240
6	40.879381115	39.924144863	37.308933547	8	40.920879893	40.818981496	38.078234239
8	40.898607458	41.061348930	38.037560236	1	41.931918960	40.673941352	35.703083726
1	41.988540746	40.826703832	35.721784152	1	42.868934327	39.541655066	36.679632417
1	42.866643878	39.647502343	36.690399264	1	41.456675610	37.637958820	35.649933327
1	41.400307707	37.804860478	35.668538273	1	41.001012760	38.804320787	34.380057851
1	40.959339475	38.988078841	34.404970606	6	46.134356926	34.680236498	42.311048783
6	46.178094161	34.409809715	42.503394437	7	44.772810271	34.586862199	41.755531224
7	44.820677983	34.262240971	41.962195646	6	44.159505253	35.404961235	40.895864896
6	44.227791360	35.043905117	41.050214374	7	44.644205694	36.676031747	40.698363691
7	44.676327494	36.293849174	40.832751900	6	44.500764724	37.446622160	39.526504552
6	44.250235328	37.129183572	39.723888148	7	43.097977062	35.004926778	40.203899353
7	43.195748528	34.582745009	40.333842282	6	42.666569554	33.616040650	40.175384023
6	42.853241131	33.173442440	40.251111330	1	42.255179456	33.291896185	41.143389158
1	42.440237672	32.785193835	41.191111315	1	43.500874850	32.955491715	39.898230858
1	43.734528429	32.575000149	39.980919142	1	41.887159683	33.520323234	39.416873547
1	42.098267554	33.041147546	39.472142766	1	44.256605505	36.842634986	38.641984220
1	43.205982525	37.468528553	39.820293796	1	45.388725439	38.073343826	39.377245399
1	44.364921267	36.590883365	38.769933002	1	43.665048213	38.343676484	39.553833858
1	44.886508781	38.021231990	39.714036222	1	42.460545833	35.696492215	39.779399238
1	42.602346735	35.248715783	39.840176748	1	44.272577334	33.735472849	42.024043184
1	44.327524898	33.417975295	42.263111135	1	46.549285733	35.685140601	42.152509809
1	46.499760553	35.461129891	42.493352986	1	46.070855413	34.503213103	43.394500470
1	46.151217450	34.090724020	43.552770750	1	45.167820348	37.089987651	41.467478605
1	45.227476558	36.720184296	41.568108559	8	45.717716712	40.469629334	40.263598310
8	45.664530742	40.522448161	40.231470160	1	46.362047201	40.588319435	39.528270120
1	46.326691774	40.605541477	39.506673370	1	44.885576249	40.175624751	39.841664477
1	44.843373104	40.223972311	39.798326516	8	40.853423992	36.487523211	38.904804307
8	40.730233772	36.501972813	38.797189922	1	40.136341622	36.784497176	39.512849059
1	40.031213820	36.812713626	39.415306605	1	40.894154849	37.251425945	38.299552188
1	40.893361010	37.315674471	38.290825245	1	43.554220060	41.224574854	44.231915079
1	43.551023470	41.237188810	44.152826290	1	39.462241135	45.897361403	38.965901038
1	39.458854369	46.000920147	38.954706098	1	45.884328778	44.824969976	37.888728029
1	45.909538052	44.907545873	37.860053639	1	46.802465534	33.943551350	41.864962248
1	46.901893897	33.802168005	41.960298847				

Orthogonal EEF of field strength -0.0025 au IM1 (NH)				TS_HAT (NH)			
HF = -2991.889036				HF = -2991.825025			
6	41.868429745	46.585128173	38.842424941	6	41.961243974	46.362791172	38.957976932
				7	41.365353391	45.866934484	37.816610118

7	41.207885630	46.154817475	37.710657725	1	41.005042233	46.413688948	37.027124336
1	40.901295334	46.727816881	36.916884205	6	41.273635115	44.530048228	37.953629914
6	40.983282771	44.834998382	37.843821656	1	40.821189663	43.873586457	37.217052925
1	40.466776677	44.221585190	37.110980028	7	41.776974708	44.141464712	39.121819119
7	41.462137809	44.402835881	39.001938750	6	42.203705374	45.278723411	39.766798972
6	42.022980755	45.478220049	39.641002671	1	42.681420707	45.249662357	40.744191965
1	42.505919533	45.395483286	40.613130747	6	41.069275429	41.526807259	44.129587789
6	40.944222722	41.600440739	43.969622714	1	40.020193635	41.810051033	43.995982207
1	39.904234786	41.933680078	43.904357341	1	41.129732522	40.541600334	44.615693375
1	40.975180919	40.593446226	44.411951160	6	41.772814184	41.495059429	42.782896784
6	41.566853160	41.582665183	42.578872655	8	42.819330188	40.904726742	42.590558899
8	42.588322443	40.948074831	42.341167991	8	41.139362421	42.207223932	41.874765886
8	40.902979875	42.309075376	41.722292156	6	37.249244280	43.949171743	39.882617605
6	36.978770717	44.094472963	39.798385435	7	37.536289377	44.049692550	41.228587002
7	37.285025292	44.185421079	41.139626909	1	36.873130518	44.254338230	41.991041341
1	36.642590444	44.365030902	41.925725263	6	38.779312071	43.569545801	41.424369879
6	38.531366404	43.708664150	41.312744515	1	39.245171103	43.481155314	42.400419381
1	39.012844939	43.603974205	42.280434456	7	39.318655323	43.181722130	40.274458271
7	39.053108015	43.340084782	40.150022145	6	38.372112813	43.415470230	39.301215731
6	38.093763321	43.573622116	39.193704467	1	38.552255713	43.162318100	38.261886124
1	38.265674975	43.330578002	38.149877461	26	41.265721920	42.231238059	40.009520188
26	40.973006006	42.536131056	39.829777007	8	42.668973612	41.311889063	39.900598534
8	42.461350638	41.927794193	39.599749198	8	40.170232393	39.647735758	37.539808771
8	40.223405414	39.682784718	37.637667540	8	43.739256421	40.410824909	33.798024722
8	43.729227232	40.407327089	33.818271954	6	43.691015671	40.574830856	35.035971527
6	43.658846091	40.573203445	35.056569482	8	44.567166054	41.202727031	35.715573325
8	44.557478009	41.155660556	35.751479155	6	42.486474502	40.032933154	35.806591304
6	42.410405839	40.091324900	35.800355331	6	41.859294934	41.137479777	36.642350515
6	41.761794274	41.226406744	36.583824485	6	40.755055265	40.714925823	37.581032033
6	40.658332401	40.818530340	37.540073491	8	40.403162803	41.635650383	38.456744125
8	40.167530017	41.801601167	38.268170003	1	41.421713504	41.909053338	35.979583115
1	41.328178700	41.974633534	35.894463679	1	42.626629668	41.650601312	37.237593654
1	42.516358020	41.761522828	37.178815857	1	42.835046176	39.224176970	36.468171421
1	42.707077734	39.290843555	36.497298892	1	41.745216141	39.605642258	35.120573862
1	41.690654553	39.656930752	35.095198791	6	46.706126329	38.306468270	42.659833646
6	47.134769140	38.019082689	42.949991883	7	45.588960643	38.901215993	41.875257761
7	45.991236129	38.552030205	42.187528457	6	44.982854982	38.466939974	40.762662516
6	45.573571952	38.274748242	40.944722884	7	43.972307944	39.135661343	40.143166231
7	44.906710223	39.235464945	40.276816634	6	43.099521821	38.363581979	39.265119715
6	43.984432183	39.019930808	39.175882164	7	45.350997355	37.282441611	40.198249058
7	45.789823960	37.095033816	40.336851189	6	45.653685032	36.014684172	40.858441174
6	45.815353836	35.784647715	40.977507728	1	45.286674411	35.195372801	40.223078975
1	45.243419431	35.075309029	40.363112192	1	45.138968806	35.944101198	41.824814914
1	45.343611755	35.842045143	41.965299106	1	46.731593201	35.860231753	41.023544301
1	46.836253560	35.393608859	41.086819988	1	42.179640187	38.936724618	39.103588667
1	43.066711477	39.594940347	39.363181747	1	42.815199399	37.399269067	39.713125148
1	43.717746006	37.957575291	39.099173000	1	43.538439540	38.158818472	38.270478295
1	44.408369069	39.353810970	38.213102982	1	45.238800809	37.234055146	39.190568097
1	45.759135532	37.110665051	39.319022112	1	45.206832512	39.750923919	42.276301074
1	45.568756968	39.378753406	42.603991619	1	46.599902701	38.715369235	43.671841303
1	47.061612492	38.487446778	43.940479615	1	46.578909520	37.223886079	42.760793506
1	47.052118644	36.936524958	43.101174833	1	43.489354196	40.270841752	40.211695780
1	45.006926742	40.194855481	40.623149019	8	45.061016107	42.521015198	38.175013645
8	45.061016107	42.521015198	38.175013645	1	44.340015847	42.310015120	38.795013866
1	44.340015847	42.310015120	38.795013866	1	44.811016016	42.052015028	37.347013348
1	44.811016016	42.052015028	37.347013348	8	45.221388046	41.845409376	41.525930492
8	45.062362895	41.782561746	41.590321822	1	45.243939929	42.832388769	41.704062444
1	45.132127121	42.774237016	41.684076457	1	44.282482850	41.625295485	41.664344310

1	44.112646211	41.591494108	41.757242916	1	41.519947376	42.232462178	44.827451134
1	41.459201706	42.248842590	44.678452035	1	36.307662531	44.283696629	39.447204886
1	36.058398266	44.478952826	39.358889003	1	42.084723976	47.427619550	39.155361173
1	42.013099513	47.637154346	39.088146147	1	47.720333633	38.515033285	42.319317125
1	48.103921378	38.269272983	42.518464288				
Orthogonal EEF of field strength +0.0025 au <b>IM1 (NH)</b> HF = -2994.579546				<b>TS_HAT (NH)</b> HF = -2994.506092			
6	41.857248193	46.601947199	38.802773483	6	41.951646783	46.396143499	38.909655709
7	41.194457181	46.179398102	37.671680752	7	41.338594379	45.917105091	37.771853365
1	40.885044619	46.757787004	36.878888189	1	40.983349548	46.473830519	36.981753076
6	40.967351700	44.861914633	37.792755982	6	41.224519624	44.584962915	37.898179695
1	40.444220825	44.262290229	37.053440231	1	40.754350962	43.946530503	37.157364858
7	41.452088590	44.419765891	38.948498637	7	41.734930702	44.179683957	39.062032721
6	42.015854478	45.491721757	39.594294597	6	42.185843790	45.306755417	39.711758738
1	42.499572179	45.407338084	40.565700283	1	42.669264680	45.268729491	40.686122737
6	40.918142766	41.625960512	43.954330004	6	41.033629457	41.567851405	44.091185370
1	39.885238747	41.978684036	43.882753649	1	39.993264138	41.882737941	43.960831841
1	40.928869486	40.617020851	44.392782740	1	41.065308954	40.576504733	44.566637269
6	41.546136686	41.600797240	42.563255708	6	41.732436928	41.521679717	42.73864189
8	42.560247028	40.939571037	42.339971881	8	42.738242448	40.864015379	42.536996875
8	40.901430047	42.331381588	41.712139795	8	41.135965219	42.276168562	41.848573697
6	36.985830921	44.144992022	39.791404672	6	37.243635604	44.003097482	39.873627852
7	37.298613945	44.243296751	41.130379642	7	37.541559903	44.113466901	41.216142753
1	36.662192576	44.445470247	41.915143920	1	36.887584905	44.344214096	41.978899676
6	38.545755448	43.770044657	41.300839964	6	38.784831924	43.637921656	41.408519157
1	39.033888948	43.682186221	42.266199106	1	39.261931819	43.569363933	42.380084422
7	39.062005458	43.390360182	40.137727040	7	39.313386311	43.235807220	40.256199491
6	38.097171942	43.619042797	39.184386095	6	38.359805251	43.462415200	39.286698563
1	38.262723520	43.381266509	38.138401507	1	38.531352741	43.211339217	38.245770295
26	40.977362474	42.597277297	39.802232913	26	41.247430935	42.321773957	39.968026887
8	42.467351010	41.983432640	39.589341927	8	42.685870225	41.417890722	39.846191578
8	40.241402579	39.654664810	37.663788391	8	40.184093265	39.649759654	37.543276914
8	43.769237191	40.334842501	33.849876599	8	43.816243837	40.335936967	33.805134769
6	43.670822870	40.551507008	35.075463353	6	43.663832147	40.595479516	35.014692786
8	44.563251275	41.142495150	35.773273537	8	44.531984768	41.174239657	35.746574185
6	42.398958798	40.095773683	35.804138880	6	42.336244860	40.176119945	35.660894012
6	41.747482025	41.223806177	36.595820382	6	41.810561567	41.209085571	36.639102848
6	40.658322320	40.800297094	37.563291064	6	40.729387178	40.739702706	37.581388629
8	40.155325941	41.765555703	38.300006899	8	40.353426047	41.629938782	38.480027369
1	41.298303887	41.967633493	35.912851604	1	41.398380137	42.076516014	36.092190144
1	42.502127073	41.768187900	37.182574688	1	42.630999307	41.611545470	37.251040789
1	42.674121115	39.280329698	36.493622090	1	42.510895371	39.220665021	36.181051069
1	41.684763667	39.677540142	35.083543805	1	41.594214603	39.975774645	34.877067013
6	47.104169450	38.082775775	42.907873872	6	46.613345185	38.334386767	42.613278415
7	45.960091048	38.622872348	42.155490331	7	45.510401852	38.936320347	41.827181638
6	45.557178496	38.362291088	40.900449397	6	45.010571133	38.573563681	40.632850156
7	44.909486192	39.324472711	40.231602460	7	44.078077956	39.287483746	39.974853712
6	44.030111007	39.133372694	39.088930065	6	43.474869715	38.701222565	38.787912979
7	45.776260523	37.174616497	40.297695163	7	45.460360787	37.403339663	40.066071255
6	45.773486830	35.871026487	40.943676034	6	45.582752436	36.108298760	40.723238530
1	45.197359340	35.163409585	40.329273593	1	45.204603110	35.324990471	40.047478765
1	45.292815550	35.938823650	41.927202514	1	44.978359865	36.076327924	41.639545990
1	46.786963165	35.461101009	41.070639320	1	46.621493853	35.847563456	40.990166018
1	43.103693177	39.697613730	39.264250663	1	42.483547909	39.145014292	38.640938486
1	43.776768897	38.071879645	38.968264312	1	43.326030348	37.614958989	38.883193317
1	44.483455966	39.507662233	38.156491590	1	44.064072386	38.896083948	37.871969551
				1	45.484658088	37.380673927	39.050485455

1	45.765071885	37.186163891	39.279008385	1	45.156046610	39.812781781	42.197028787
1	45.573087453	39.476674735	42.553993916	1	46.493755429	38.725544837	43.630773746
1	47.026736160	38.529166858	43.908421285	1	46.491757636	37.247417115	42.696050897
1	47.027142727	36.994974654	43.035103407	1	43.426033634	40.464934886	40.108593404
1	44.996027955	40.284020175	40.596362570	8	45.061016107	42.521015198	38.175013645
8	45.061016107	42.521015198	38.175013645	1	44.340015847	42.310015120	38.795013866
1	44.340015847	42.310015120	38.795013866	1	44.811016016	42.052015028	37.347013348
1	44.811016016	42.052015028	37.347013348	8	45.186727142	41.848776049	41.570346899
8	45.030330214	41.776990684	41.625853169	1	45.225362823	42.842101738	41.725196635
1	45.115129122	42.771875065	41.689944588	1	44.237608571	41.653380096	41.658090546
1	44.073853206	41.602776400	41.783897664	1	41.500873552	42.252788046	44.798724821
1	41.439083223	42.263238323	44.668868566	1	36.304019575	44.345654368	39.440218323
1	36.065340860	44.530221169	39.352811619	1	42.073020576	47.457764307	39.124823047
1	41.997771470	47.651841433	39.059761080	1	47.630983811	38.552890377	42.289650353
1	48.075542930	38.345823642	42.489177450				
<b>Parallel EEF of field strength -0.0025 au</b>				<b>TS_HAT (NH)</b>			
<b>IM1 (NH)</b>				HF = -2992.211113			
HF = -2992.282485							
6	41.850793035	46.604004386	38.824594689	6	41.943332943	46.375817944	38.939503968
7	41.169635619	46.181983905	37.703156786	7	41.312783542	45.891521688	37.812713384
1	40.846098120	46.761039872	36.918659420	1	40.936842689	46.445358846	37.032959282
6	40.938004064	44.865051331	37.831631957	6	41.198425105	44.559124978	37.948731855
1	40.396952538	44.265107177	37.105748142	1	40.709315491	43.916946167	37.223582744
7	41.437815204	44.422897588	38.979285841	7	41.725338947	44.158515295	39.105404549
6	42.014165620	45.493010214	39.615317005	6	42.186534234	45.287999100	39.742532353
1	42.504370689	45.407454551	40.583336327	1	42.677124894	45.253804179	40.713331163
6	40.929099524	41.621500406	43.962909264	6	41.057509829	41.555006977	44.119736191
1	39.892822211	41.964129704	43.891242588	1	40.010635974	41.846371785	43.988006046
1	40.946604512	40.615106949	44.407118565	1	41.108836313	40.567826576	44.602840221
6	41.558407248	41.597143377	42.575134081	6	41.759807759	41.519762433	42.771798128
8	42.580796246	40.949903413	42.347601988	8	42.799980986	40.916917875	42.574625499
8	40.908293825	42.320956611	41.717007781	8	41.127249268	42.236949845	41.868856082
6	36.981333311	44.115047644	39.803446682	6	37.235033103	43.961570964	39.891728142
7	37.291561039	44.206953630	41.142628762	7	37.531413532	44.071349192	41.234010735
1	36.651117024	44.402468764	41.928703092	1	36.873204799	44.298617993	41.997071173
6	38.536112690	43.730735503	41.315309734	6	38.769241124	43.587098467	41.431074925
1	39.018499537	43.637120000	42.283156544	1	39.239701120	43.514847204	42.405798547
7	39.055441295	43.354510868	40.150598440	7	39.298726587	43.179687962	40.278821655
6	38.091889912	43.588260921	39.196025756	6	38.347259575	43.411655190	39.306812807
1	38.255485518	43.347062693	38.150713826	1	38.514959158	43.152433910	38.267482475
26	40.970143649	42.576248232	39.818556158	26	41.222642696	42.274269208	40.002074045
8	42.468756500	41.978962897	39.588965555	8	42.658088383	41.365297870	39.878140929
8	40.261040918	39.668306544	37.653632849	8	40.197396458	39.650945445	37.542642255
8	43.771436049	40.353588828	33.834449215	8	43.797233192	40.358801927	33.802321022
6	43.676080749	40.548061758	35.067196075	6	43.688146678	40.572444203	35.028824623
8	44.577441671	41.122719791	35.767414868	8	44.566890628	41.166690520	35.735487525
6	42.406763549	40.098914651	35.795355395	6	42.413815079	40.105649622	35.734997099
6	41.761305579	41.235190150	36.581640088	6	41.849877431	41.181254595	36.646959289
6	40.669611607	40.815470638	37.550555630	6	40.750309460	40.735555602	37.581355339
8	40.168198061	41.786985440	38.276891474	8	40.373790248	41.643686754	38.458726249
1	41.316419006	41.979652828	35.896657261	1	41.437129575	42.014114628	36.047788649
1	42.516447043	41.774741210	37.171956736	1	42.645670614	41.622896306	37.262738389
1	42.679251271	39.288531178	36.491526071	1	42.666928453	39.213976327	36.330667158
1	41.688573849	39.678567836	35.079990279	1	41.662708274	39.798291702	34.996615091
6	47.120423526	38.065323870	42.957530468	6	46.651647351	38.325618750	42.654741321
7	45.971420584	38.605126151	42.212188546	7	45.535948556	38.920038722	41.877757192
6	45.543361641	38.333322666	40.970070422	6	44.973909759	38.519998566	40.724793190
				7	44.002044668	39.207427652	40.090726252



7	44.876891413	39.288410552	40.305507994	6	43.235043252	38.491193527	39.080281404
6	43.953621193	39.074826095	39.202290781	7	45.397905272	37.343131288	40.157580569
7	45.763675301	37.148382170	40.363303448	6	45.583049130	36.057297980	40.821984291
6	45.755248043	35.841228516	41.006712623	1	45.183451070	35.260379025	40.176123972
1	45.153234864	35.145736679	40.404104411	1	45.032920278	36.020434471	41.770899520
1	45.297703211	35.913749750	42.000493288	1	46.641045497	35.824065875	41.029442421
1	46.765680990	35.417477827	41.107252638	1	42.296185237	39.028887651	38.908961259
1	43.055285878	39.682245825	39.378039382	1	42.967997292	37.472286061	39.400573750
1	43.655780059	38.019346352	39.144478785	1	43.750158594	38.417510332	38.102862375
1	44.390034644	39.383163040	38.236749194	1	45.314607132	37.298180178	39.147523031
1	45.706707995	37.160442252	39.347359199	1	45.139813584	39.761035147	42.284132442
1	45.560240188	39.436652658	42.633169849	1	46.541832261	38.721047190	43.671678200
1	47.054810088	38.520039609	43.955052998	1	46.534158350	37.239382130	41.029442421
1	47.040489837	36.979438962	43.095413315	1	43.390604212	40.404798564	40.168075323
1	44.966228429	40.250229869	40.658773412	8	45.061016107	42.521015198	38.175013645
8	45.061016107	42.521015198	38.175013645	1	44.340015847	42.310015120	38.795013866
1	44.340015847	42.310015120	38.795013866	1	44.811016016	42.052015028	37.347013348
1	44.811016016	42.052015028	37.347013348	8	45.228180433	41.855509607	41.528897086
8	45.034632896	41.783791030	41.624023602	1	45.240527223	42.844397828	41.709124580
1	45.107108642	42.778387681	41.700460784	1	44.285495842	41.635775581	41.639926585
1	44.081276637	41.598731321	41.799159993	1	41.511827987	42.254670160	44.821258649
1	41.444154223	42.266369263	44.674899525	1	36.297539614	44.308367359	39.457095495
1	36.061816868	44.503585889	39.365731175	1	42.067195551	47.438758075	39.146587652
1	41.992954693	47.654182979	39.079510959	1	47.664422866	38.546892888	42.318005776
1	48.086819798	38.322516067	42.523943400				
<b>Parallel EEF of field strength +0.0025 au</b>				<b>TS_HAT (NH)</b>			
<b>IM1 (NH)</b>				HF = -2994.092270			
HF = -2994.162372							
6	41.873461850	46.581086926	38.818214701	6	41.965682199	46.449466299	38.911194112
7	41.230710305	46.150152587	37.677693242	7	41.385067106	45.962404833	37.758633437
1	40.937398188	46.722175291	36.876162190	1	41.032135700	46.512183370	36.965781374
6	41.010032581	44.830013246	37.804167859	6	41.311322039	44.623906545	37.875411098
1	40.510928046	44.217375506	37.058730262	1	40.875554947	43.971368628	37.125063943
7	41.473952247	44.398040180	38.970064673	7	41.812413280	44.227396816	39.041934072
6	42.022872718	45.475214745	39.617992112	6	42.216809412	45.360411461	39.707271754
1	42.499297700	45.394018349	40.593457932	1	42.688288766	45.323912878	40.687537714
6	40.932745884	41.606964055	43.960473207	6	41.042131356	41.535480866	44.075073346
1	39.896206644	41.951083612	43.895868497	1	40.002861704	41.851557431	43.933338353
1	40.956300108	40.597423586	44.396939190	1	41.070329285	40.546418604	44.555205220
6	41.553524450	41.587964581	42.566196542	6	41.755024266	41.495861741	42.726022364
8	42.565980172	40.938111831	42.332228949	8	42.765343065	40.822465350	42.553095796
8	40.895518989	42.321776434	41.716920843	8	41.201490095	42.256200165	41.834085067
6	36.981095435	44.122881970	39.786970600	6	37.206205537	44.014164986	39.860082539
7	37.291130543	44.222052284	41.127768650	7	37.495995461	44.118384710	41.205411944
1	36.653001466	44.408176713	41.913175661	1	36.836418666	44.305245848	41.971014819
6	38.540123706	43.748126009	41.298105996	6	38.758816063	43.669323081	41.385930644
1	39.028264408	43.650148301	42.262956716	1	39.234942964	43.588209342	42.358463716
7	39.057722668	43.374472683	40.136916145	7	39.303654196	43.306655401	40.237240817
6	38.096305160	43.601830714	39.182261856	6	38.345915417	43.517691008	39.274907780
1	38.269340125	43.360409417	38.138109925	1	38.531792736	43.282791296	38.231163125
26	40.978710632	42.556454399	39.812652562	26	41.413310741	42.329584360	39.901555811
8	42.458119132	41.930970854	39.598108886	8	42.898258525	41.366178627	39.751884646
8	40.205558790	39.667901570	37.647413630	8	40.174982044	39.628185659	37.558697477
8	43.726097111	40.389752250	33.832089576	8	43.764235000	40.387698937	33.786911719
6	43.652571197	40.577532681	35.063785840	6	43.655915513	40.567835392	35.016303491
8	44.542081111	41.176350714	35.756508456	8	44.538211079	41.125073630	35.747557703
				6	42.360363870	40.102116226	35.692305672

6	42.401970013	40.088813181	35.808226467	6	41.792176520	41.170347516	36.607199217
6	41.746195193	41.215767556	36.595998683	6	40.711511391	40.729746257	37.572550179
6	40.646347457	40.802782571	37.551534973	8	40.367447350	41.636923763	38.444771109
8	40.151841737	41.779025376	38.289604031	1	41.365883770	41.993923886	36.004483344
1	41.306543865	41.961842537	35.908084363	1	42.595413751	41.620790763	37.207476716
1	42.499866211	41.757236418	37.186682389	1	42.585605678	39.191457109	36.269781658
1	42.701344691	39.284222209	36.499458131	1	41.620929815	39.821137173	34.932548671
1	41.686614507	39.655431752	35.097946433	6	46.672782109	38.323205315	42.645878142
6	47.119691886	38.035488089	42.899821207	7	45.600922240	38.906781821	41.804980366
7	45.980812274	38.569854699	42.131650298	6	45.053584041	38.445080186	40.677680936
6	45.585894104	38.303151127	40.877027673	7	44.057501285	39.178603389	40.059160803
7	44.938898122	39.271740458	40.205004550	6	43.413668879	38.605168464	38.896503712
6	44.063798251	39.079736632	39.061977285	7	45.370806550	37.245804405	40.139120702
7	45.796509755	37.119689783	40.273652403	6	45.743889338	36.003690779	40.813324184
6	45.830326462	35.813232204	40.917569609	1	45.447675297	35.166103616	40.166432614
1	45.278546216	35.093243174	40.296474283	1	45.203755929	35.904467288	41.762947928
1	45.343893177	35.866162491	41.898743277	1	46.824241395	35.922749595	41.005866601
1	46.854144709	35.434688899	41.044803077	1	42.479676802	39.147084481	38.726909918
1	43.127830184	39.629530219	39.235461145	1	43.191408058	37.537169250	39.037803531
1	43.823536201	38.016051668	38.935320515	1	44.041704148	38.714120561	37.990749571
1	44.514657357	39.458943345	38.130013788	1	45.314958363	37.190258352	39.123495897
1	45.806474443	37.134325560	39.254194941	1	45.270402025	39.830935657	42.100223483
1	45.587997684	39.422743403	42.523538130	1	46.539449582	38.754208622	43.644170800
1	47.034586182	38.493288572	43.894447407	1	46.542765836	37.240761674	42.746935285
1	47.040696062	36.950512959	43.037713399	1	43.564962173	40.343033080	40.128382315
1	45.040248668	40.229279403	40.560366161	8	45.061016107	42.521015198	38.175013645
8	45.061016107	42.521015198	38.175013645	1	44.340015847	42.310015120	38.795013866
1	44.340015847	42.310015120	38.795013866	1	44.811016016	42.052015028	37.347013348
1	44.811016016	42.052015028	37.347013348	8	45.172824423	41.808402338	41.591198330
8	45.058162636	41.775011656	41.594337589	1	45.231981349	42.800185010	41.723449202
1	45.140830928	42.767228365	41.673743324	1	44.213078534	41.636848170	41.652162719
1	44.104678453	41.596044995	41.742560581	1	41.502724154	42.222224017	44.785218001
1	41.454364513	42.247142375	44.671917548	1	36.264710749	44.345384006	39.421962877
1	36.059919211	44.504702967	39.346840605	1	42.079271276	47.511431087	39.128899505
1	42.016888845	47.632810664	39.065950840	1	47.690065610	38.532394633	42.315058825
1	48.093283227	38.293543274	42.483174183				

Parallel EEF of field strength -0.005 au IM1 (NH)				TS_HAT (NH)			
HF = -2972.029066				HF = -2971.958750			
6	41.839104245	46.616412042	38.827788956	6	41.929904689	46.384780815	38.941916645
7	41.138260817	46.199002743	37.716719228	7	41.276769585	45.906542406	37.825373362
1	40.798754886	46.781579834	36.941867526	1	40.888241251	46.464243986	37.054342467
6	40.901165511	44.883782566	37.846367512	6	41.144674641	44.577132706	37.965149807
1	40.339024309	44.290621871	37.131091621	1	40.629367191	43.942401227	37.251701461
7	41.419503342	44.436345067	38.983974764	7	41.685451926	44.170625622	39.114432255
6	42.009990575	45.502736862	39.613480575	6	42.170296726	45.295062770	39.743458197
1	42.507740474	45.414739014	40.577349829	1	42.665582718	45.258174707	40.711712018
6	40.927266883	41.629177519	43.963572000	6	41.055530150	41.568450249	44.118435791
1	39.890935694	41.970826532	43.888443066	1	40.007833171	41.856997982	43.988709031
1	40.941999003	40.624454854	44.411855474	1	41.107329009	40.580596850	44.600766714
6	41.560834224	41.602206058	42.579035964	6	41.758399015	41.535052804	42.771396186
8	42.588086885	40.955978188	42.354455039	8	42.814821418	40.959694928	42.575621236
8	40.914938074	42.321221793	41.716476281	8	41.101964766	42.226330988	41.862360659
6	36.981610499	44.111535182	39.811944819	6	37.216354728	43.953638941	39.900841744
7	37.292422338	44.200543732	41.150334636	7	37.516494110	44.064214285	41.241592268
				1	36.858802134	44.298542072	42.006356239

1	36.650657703	44.400440348	41.936882590	6	38.749407296	43.574199629	41.439652967
6	38.534851412	43.723245724	41.323971413	1	39.218666774	43.504508742	42.415076564
1	39.014890167	43.631965067	42.293079660	7	39.274414486	43.158696183	40.284568080
7	39.054685677	43.345336125	40.157232217	6	38.321539428	43.394226891	39.312883740
6	38.089645851	43.581816458	39.202887470	1	38.481714174	43.131105929	38.273657534
1	38.248169236	43.339738293	38.157137408	26	41.185677067	42.283432542	40.001940237
26	40.966685074	42.587791054	39.820965862	8	42.640015059	41.376373465	39.869046500
8	42.475183580	42.004711662	39.582768365	8	40.221729139	39.653487364	37.559893021
8	40.291793424	39.668665194	37.659050360	8	43.803369700	40.338551372	33.811079361
8	43.793652614	40.334850137	33.835186814	6	43.702672286	40.549035984	35.040733778
6	43.686770748	40.532112493	35.068318465	8	44.587761527	41.148002901	35.736415273
8	44.593606380	41.093213809	35.773588059	6	42.442496110	40.082491736	35.768499321
6	42.407331404	40.104194226	35.786938836	6	41.853021844	41.185438027	36.634431991
6	41.768370974	41.245252037	36.573358808	6	40.754693726	40.748512845	37.577008539
6	40.682027953	40.822144859	37.550593424	8	40.365714157	41.672053200	38.430555408
8	40.176633215	41.791509466	38.270228222	1	41.429426426	41.988008875	36.002966452
1	41.319940733	41.989157946	35.890698927	1	42.634240010	41.660684287	37.243632635
1	42.525199111	41.783360586	37.162816120	1	42.719355461	39.229367108	36.409085447
1	42.664212752	39.290304086	36.485209738	1	41.695514872	39.721366269	35.050583931
1	41.687642699	39.692276496	35.068126194	6	46.667028290	38.321480155	42.668043096
6	47.122444163	38.078164451	42.987504533	7	45.540235611	38.920015248	41.912446280
7	45.967710909	38.621763018	42.256028743	6	44.931449979	38.507718368	40.783371778
6	45.517256041	38.344914854	41.023129262	7	43.937491150	39.183562505	40.183301764
7	44.839856504	39.292764998	40.363161708	6	43.120490856	38.431565306	39.238632409
6	43.888089163	39.065889497	39.285667593	7	45.352520137	37.327040214	40.211403753
7	45.736553586	37.157751978	40.415439535	6	45.533050553	36.040236342	40.874858544
6	45.711295506	35.851148124	41.059671634	1	45.098012603	35.247015802	40.247380255
1	45.076492161	35.170387576	40.473968841	1	45.014940925	36.013955802	41.841946006
1	45.280259459	35.933550679	42.064316758	1	46.594087043	35.788688037	41.047020282
1	46.714161087	35.402996241	41.134949437	1	42.184350325	38.975990977	39.070256601
1	43.022750791	39.722584027	39.448324297	1	42.848223038	37.433964229	39.619465183
1	43.540708435	38.023692977	39.285423246	1	43.595800517	38.295756362	38.245924386
1	44.319576048	39.308525458	38.298650914	1	45.189750269	37.269286159	39.213195690
1	45.635469280	37.167683831	39.403904360	1	45.135495472	39.742786655	42.346530261
1	45.552674975	39.445509444	42.690099600	1	46.566496578	38.701366548	43.692584353
1	47.067216479	38.529005988	43.987482192	1	46.559541427	37.232664849	42.743463168
1	47.042860927	36.991464737	43.122975623	1	43.306562472	40.440028550	40.196628643
1	44.928542552	40.257751245	40.710644636	8	45.061016107	42.521015198	38.175013645
8	45.061016107	42.521015198	38.175013645	1	44.340015847	42.310015120	38.795013866
1	44.340015847	42.310015120	38.795013866	1	44.811016016	42.052015028	37.347013348
1	44.811016016	42.052015028	37.347013348	8	45.278014510	41.861121934	41.507322032
8	45.024554700	41.788495198	41.638987401	1	45.259077960	42.846562374	41.706479927
1	45.091779123	42.784278318	41.713615602	1	44.338854800	41.617730351	41.600229824
1	44.070745581	41.600943933	41.826070334	1	41.508672926	42.268325775	44.820506445
1	41.438948553	42.276607176	44.675670325	1	36.282256393	44.309227780	39.466003601
1	36.062841879	44.503487245	39.375705060	1	42.054683891	47.446855476	39.152854740
1	41.980773191	47.665752910	39.086402508	1	47.676417160	38.552865283	42.327951419
1	48.084572625	38.336311914	42.545083883				
<b>Parallel EEF of field strength +0.005 au</b>				<b>TS_HAT (NH)</b>			
<b>IM1 (NH)</b>				HF = -2975.716452			
HF = -2975.781162							
6	41.887928567	46.568661357	38.811784372	6	41.967874946	46.504019642	38.880753365
7	41.266739740	46.133141565	37.661137255	7	41.413092884	46.017002478	37.715650047
1	40.991119071	46.701341281	36.850434587	1	41.079707444	46.565888691	36.914149417
6	41.050654152	44.811651743	37.786887306	6	41.352662848	44.675613994	37.826611838
1	40.574088510	44.193215908	37.031447868	1	40.944180764	44.021437570	37.061835485
				7	41.834730912	44.279992706	38.999571930

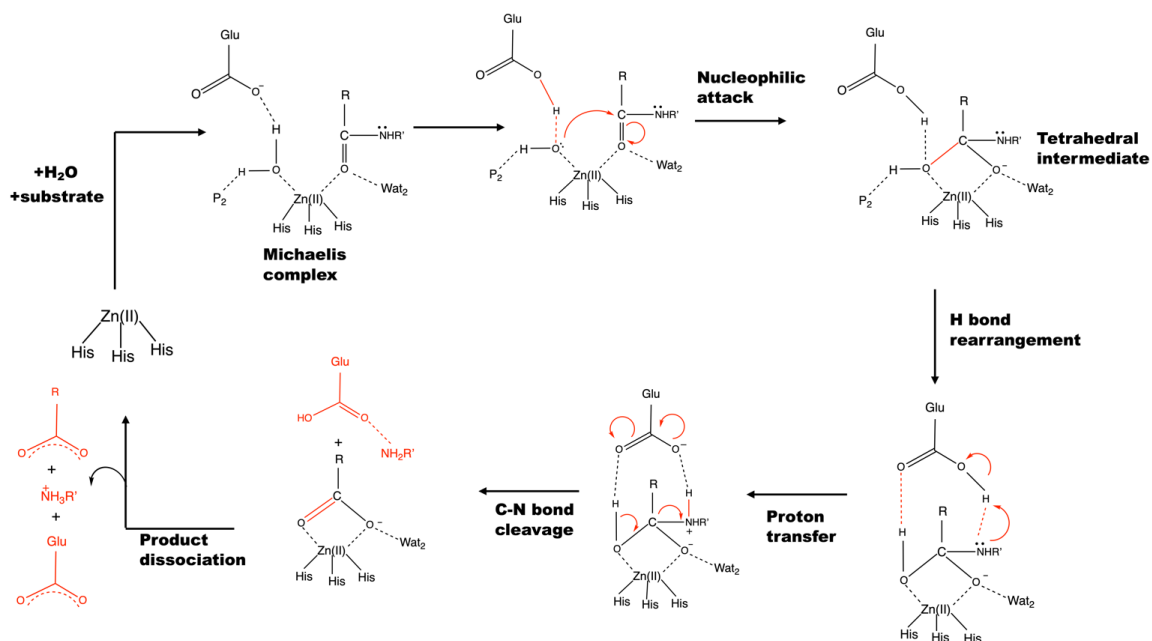
7	41.494089108	44.384979842	38.962563570	6	42.215905640	45.413579497	39.675176895
6	42.028250286	45.465707938	39.616714784	1	42.674520633	45.375664804	40.661568743
1	42.495933313	45.386949901	40.596707027	6	41.011276967	41.547169677	44.050595458
6	40.934722107	41.599593304	43.959007275	1	39.976093575	41.879034542	43.913665802
1	39.897894894	41.944197899	43.897244892	1	41.027044931	40.555526988	44.526025545
1	40.961240131	40.588989765	44.392773575	6	41.717619283	41.505503356	42.635199287
6	41.551823902	41.581963070	42.561701096	8	42.716593844	40.809548160	42.526886345
8	42.558010440	40.928586376	42.324738355	8	41.179163117	42.277066148	41.811715655
8	40.891876202	42.322260573	41.716577359	6	37.181242865	44.090620944	39.830502435
6	36.983953072	44.127841033	39.779662207	7	37.454868975	44.163679853	41.182161663
7	37.293779853	44.229516896	41.121509039	1	36.789415995	44.314682275	41.947972055
1	36.656327403	44.410189042	41.906630543	6	38.728754598	43.735003439	41.358907642
6	38.545122610	43.757011450	41.290328996	1	39.197900985	43.628456886	42.333084079
1	39.036277575	43.655817478	42.253565576	7	39.293046108	43.422168138	40.209289489
7	39.062216721	43.386024464	40.130420452	6	38.341563665	43.639590718	39.245855022
6	38.101786071	43.610688374	39.175773994	1	38.546726970	43.443197176	38.197031610
1	38.279714645	43.370121835	38.131990339	26	41.483875955	42.366631482	39.865902864
26	40.986613111	42.548167050	39.809443610	8	42.985211682	41.423760605	39.715997866
8	42.456762200	41.908605395	39.601781789	8	40.183215709	39.629076211	37.595963547
8	40.180771471	39.666636392	37.644727442	8	43.756683196	40.417420309	33.792757583
8	43.704190136	40.409382689	33.828976627	6	43.625299238	40.556631281	35.022890779
6	43.640084514	40.592003488	35.060562151	8	44.522932297	41.041163380	35.792569986
8	44.523342097	41.199995222	35.751767001	6	42.290413998	40.135528563	35.650946252
6	42.397465402	40.084713068	35.810489695	6	41.749128994	41.192324813	36.596496893
6	41.741069651	41.205567315	36.604732341	6	40.692501826	40.746679765	37.590617745
6	40.636934796	40.795536742	37.553242776	8	40.353371754	41.657548859	38.453793031
8	40.145821356	41.773354030	38.297593914	1	41.312472931	42.027506009	36.019046704
1	41.306065976	41.957294629	35.919446862	1	42.570040750	41.628338265	37.184297710
1	42.496397248	41.742658273	37.197460010	1	42.447763752	39.188957139	36.192195177
1	42.707283483	39.278881858	36.495445126	1	41.561892346	39.921212041	34.858938655
1	41.681825352	39.651034972	35.100707420	6	46.696282891	38.334785306	42.588184206
6	47.117329490	38.009508121	42.879056953	7	45.670109228	38.933121503	41.700563011
7	45.983596212	38.542447429	42.100508693	6	45.181566558	38.474530641	40.550802769
6	45.602102549	38.277559031	40.841150302	7	44.313358712	39.300294476	39.835745915
7	44.963526349	39.252895937	40.166732155	6	43.816895894	38.931194932	38.538440340
6	44.109966135	39.071616889	39.007016152	7	45.431389021	37.246853790	40.056404451
7	45.805831546	37.094580581	40.239049142	6	45.725436985	36.009948909	40.781794914
6	45.872538264	35.789313217	40.883372006	1	45.417316086	35.169146083	40.145650564
1	45.339423513	35.056692717	40.261124496	1	45.149688804	35.966305671	41.714557527
1	45.385838396	35.830337869	41.864856629	1	46.794665060	35.891938905	41.011662346
1	46.905250404	35.436589281	41.008649534	1	42.754161163	39.213329545	38.508802101
1	43.165421899	39.610357460	39.171204713	1	43.922341568	37.871967847	38.287053571
1	43.881098996	38.007968888	38.861282934	1	44.311027882	39.563445511	37.767168712
1	44.572154703	39.465640173	38.087154050	1	45.468814643	37.174866274	39.038310012
1	45.841037274	37.110727996	39.219256023	1	45.388666488	39.895270688	41.939899980
1	45.601771479	39.406090343	42.478243563	1	46.532753231	38.769317236	43.579794249
1	47.025984623	38.472800850	43.870645359	1	46.556637466	37.253360395	42.680893848
1	47.036520314	36.925472583	43.021419281	1	43.774210642	40.377092574	40.028523589
1	45.076089309	40.208863681	40.519728301	8	45.061016107	42.521015198	38.175013645
8	45.061016107	42.521015198	38.175013645	1	44.340015847	42.310015120	38.795013866
1	44.340015847	42.310015120	38.795013866	1	44.811016016	42.052015028	37.347013348
1	44.811016016	42.052015028	37.347013348	8	45.137676285	41.779931592	41.616562150
8	45.070485988	41.769859788	41.579247216	1	45.224780432	42.770648024	41.719458555
1	45.158070972	42.760783525	41.659556463	1	44.173137748	41.626555758	41.686889341
1	44.116562276	41.594385332	41.712386445	1	41.485293394	42.223883167	44.761534694
1	41.459088695	42.238336046	44.669721499	1	36.237555706	44.414540948	39.391642905
1	36.062017622	44.506867392	39.338707140	1	42.075718776	47.565301315	39.104624393
1	42.031852210	47.621006259	39.056577168	1	47.722355027	38.538311258	42.281882920

1	48.093997928	38.264296547	42.467633892				
Parallel EEF of field strength -0.0075 au				<b>TS_HAT (NH)</b>			
<b>IM1 (NH)</b>				HF = -2938.828335			
HF = -2938.895654				6	41.909993517	46.402912486	38.944169940
6	41.826436456	46.629352696	38.830276264	7	41.230407075	45.929285613	37.841184125
7	41.105975564	46.216417554	37.730092659	1	40.825098742	46.489149110	37.079922774
1	40.750255738	46.802419824	36.965314481	6	41.086645561	44.602980553	37.983725309
6	40.863410614	44.902984736	37.861162704	1	40.549015383	43.973093720	37.282613366
1	40.280558398	44.316809022	37.157003859	7	41.647266607	44.191786907	39.123233245
7	41.400261981	44.450348123	38.988441179	6	42.156101790	45.311757629	39.742000631
6	42.004867467	45.513072186	39.610968877	1	42.664779707	45.271671193	40.703064415
1	42.510250304	45.422716822	40.570540265	6	41.088242057	41.579662779	44.111552867
6	40.924077357	41.638363379	43.964442423	1	40.034124189	41.844807019	41.982378029
1	39.887855592	41.979590591	43.885953298	1	41.155545195	40.591156916	44.591632691
1	40.935475041	40.635231528	44.416661435	6	41.799442907	41.568015667	42.766972825
6	41.561992492	41.608637684	42.583193525	8	42.889456911	41.061917357	42.571940978
8	42.594815511	40.964102244	42.362329800	8	41.093063105	42.210511107	41.851681084
8	40.919900492	42.321658777	41.715623088	6	37.199638029	43.948078844	39.912904710
6	36.980700034	44.108314313	39.819749485	7	37.503844101	44.057826422	41.252714272
7	37.292312746	44.194956896	41.157420870	1	36.845606088	44.299527104	42.018673961
1	36.648954747	44.399005780	41.944463408	6	38.732310770	43.564077844	41.451813646
6	38.532691475	43.716833292	41.332008451	1	39.201314300	43.495110935	42.427611106
1	39.010517041	43.628062305	42.302377346	7	39.253077414	43.142752363	40.292441253
7	39.052956157	43.336860055	40.163162071	6	38.298434354	43.380744873	39.320935553
6	38.086291931	43.575640674	39.208990747	1	38.450845032	43.111274244	38.282430060
1	38.239645751	43.332195818	38.162944901	26	41.156495693	42.310098021	40.002890687
26	40.962364913	42.600465754	39.822931369	8	42.656396746	41.421840993	39.848556677
8	42.480746344	42.030766037	39.575968210	8	40.261657309	39.654064998	37.598712543
8	40.326389847	39.669211215	37.667776487	8	43.809899853	40.317317484	33.818777932
8	43.815726979	40.314514305	33.835745101	6	43.715158546	40.524584333	35.051078490
6	43.697294136	40.515240227	35.069450550	8	44.606218584	41.122231329	35.740585057
8	44.608974957	41.062774529	35.779704157	6	42.464067418	40.063308478	35.794332807
6	42.407702870	40.109413782	35.778111138	6	41.848773657	41.191902726	36.612533636
6	41.775540722	41.255626986	36.564414141	6	40.768779604	40.760462282	37.581313746
6	40.695583928	40.829345819	37.551260119	8	40.370994155	41.700484042	38.412059218
8	40.184720689	41.797062033	38.262417333	1	41.395431450	41.950879418	35.948808325
1	41.322688830	41.998427597	35.884058932	1	42.619417723	41.713919381	37.196680490
1	42.534333912	41.792854730	37.152230971	1	42.759990977	39.248227753	36.474880886
1	42.648015997	39.292434813	36.478944406	1	41.724772320	39.653216764	35.095490521
1	41.686545259	39.706179850	35.055761756	6	46.718037109	38.312767029	42.725275314
6	47.126973238	38.088462203	43.018031504	7	45.569475845	38.905183071	42.001514431
7	45.966185566	38.638126740	42.303385302	6	44.940941937	38.502374328	40.871556737
6	45.483957378	38.353167172	41.084609710	7	43.940031339	39.183935675	40.310129569
7	44.792105560	39.292798998	40.431550162	6	43.111887513	38.435866405	39.369908457
6	43.799626486	39.046189218	39.394059223	7	45.387703730	37.333155127	40.280480609
7	45.693665855	37.162354947	40.476189989	6	45.513090421	36.035198453	40.937884660
6	45.660467995	35.857071411	41.122457277	1	45.007167660	35.267172353	40.332222084
1	44.987661764	35.191691823	40.562063989	1	45.035219828	36.039642526	41.925416848
1	45.268223836	35.947974162	42.141811671	1	46.563974958	35.720921857	41.068178815
1	46.655596374	35.385667660	41.160628451	1	42.167742764	38.971084753	39.212564228
1	42.990012754	39.777594754	39.521667724	1	42.846729282	37.433599536	39.745852560
1	43.375227607	38.036778763	39.489571568	1	43.571902417	38.310221549	38.367124640
1	44.220837632	39.175263936	38.380809143	1	45.161986159	37.271715585	39.295415361
1	45.533804096	37.169534813	39.473255097	1	45.105739554	39.656565874	42.501676288
1	45.553741839	39.457861542	42.749376385	1	46.633281265	38.682283427	43.755327444
1	47.083330466	38.532699159	44.021667026	1	46.629136268	37.220674339	42.792031749
1	47.047606959	37.000644926	43.148147114	1	43.216854620	40.536695401	40.243483489

1	44.884978422	40.261989500	40.767771442	8	45.061016107	42.521015198	38.175013645
8	45.061016107	42.521015198	38.175013645	1	44.340015847	42.310015120	38.795013866
1	44.340015847	42.310015120	38.795013866	1	44.811016016	42.052015028	37.347013348
1	44.811016016	42.052015028	37.347013348	8	45.496291118	41.905571236	41.407895024
8	45.015309502	41.793710193	41.654816220	1	45.361231765	42.870233864	41.667172577
1	45.077315793	42.790706017	41.727216865	1	44.581282392	41.576821071	41.385545356
1	44.060710544	41.604596278	41.853846017	1	41.524352935	42.285954129	44.817971416
1	41.432905047	42.287933660	44.676636322	1	36.268290257	44.313535167	39.480353755
1	36.062649978	44.503626472	39.385031512	1	42.035377716	47.464120905	39.159071811
1	41.967763548	47.677820041	39.092593258	1	47.718726040	38.560992350	42.371618443
1	48.084438315	38.348342166	42.566600061				
Parallel EEF of field strength +0.0075 au				<b>TS_HAT (NH)</b>			
<b>IMI (NH)</b>				HF = -2944.445337			
HF = -2944.518056							
6	41.897010354	46.558204217	38.807607501	6	41.967697290	46.500978513	38.873856249
7	41.292728936	46.118502432	37.649637381	7	41.423844633	46.012244566	37.704371788
1	41.030120355	46.683351339	36.832216644	1	41.101334765	46.559016790	36.897422929
6	41.082404274	44.795595410	37.774543591	6	41.372860268	44.669507103	37.814098410
1	40.625449046	44.171836777	37.011301740	1	40.979635369	44.012310744	37.043908351
7	41.510587706	44.373563478	38.957418771	7	41.847336586	44.276187487	38.989696959
6	42.032317093	45.457554804	39.616138870	6	42.217255312	45.410966245	39.668579473
1	42.495322050	45.380631604	40.598627258	1	42.676103444	45.374192882	40.654974438
6	40.936484346	41.592611101	43.957521689	6	40.989739601	41.554442006	44.037475313
1	39.899181080	41.937408719	43.899306879	1	39.959081854	41.901379686	43.902836846
1	40.966608518	40.580634300	44.387792186	1	40.994113834	40.559502379	44.506492649
6	41.549355189	41.577642386	42.556947783	6	41.694917499	41.512137354	42.679199565
8	42.550380069	40.922348418	42.316534012	8	42.694522189	40.813764353	42.521693254
8	40.886085209	42.323315345	41.716217455	8	41.157551963	42.279862590	41.794974921
6	36.983754075	44.131521678	39.771636785	6	37.142926929	44.103928069	39.810806103
7	37.294137074	44.238636699	41.114273318	7	37.415756759	44.183560116	41.163452114
1	36.657464293	44.414087729	41.899225278	1	36.750903718	44.319362604	41.930658338
6	38.547854520	43.767434686	41.281864673	6	38.697288772	43.768015511	41.337078472
1	39.042488406	43.664518464	42.243419195	1	39.168746473	43.662597344	42.310785994
7	39.063700921	43.396609972	40.123694646	7	39.263866904	43.464789095	40.189365221
6	38.103754044	43.616725239	39.169067678	6	38.311071842	43.669084925	39.227498446
1	38.285993137	43.374098200	38.126222439	1	38.523491199	43.476853717	38.178709287
26	40.992757812	42.540543151	39.806118736	26	41.528084428	42.346907061	39.843200916
8	42.454008896	41.887735629	39.604340308	8	43.021133975	41.409352278	39.694968648
8	40.157145929	39.666090710	37.643603009	8	40.147376762	39.625034006	37.596081897
8	43.681510287	40.427681490	33.826344357	8	43.734399844	40.452054616	33.807103223
6	43.625748272	40.607421353	35.057196419	6	43.607626877	40.526521926	35.041749233
8	44.501877483	41.225390904	35.747145019	8	44.518626573	40.958968188	35.829758499
6	42.390282699	40.082608848	35.811786317	6	42.269152461	40.106994913	35.661316406
6	41.731160860	41.198083754	36.609728462	6	41.729219531	41.173143752	36.599494328
6	40.625811464	40.789906460	37.554362198	6	40.665287319	40.740390504	37.593413309
8	40.137745085	41.768948327	38.305079164	8	40.335499866	41.653128578	38.455879386
1	41.296629316	41.951650874	35.925385627	1	41.302367905	42.007634726	36.013492025
1	42.487664902	41.735005666	37.201444466	1	42.549334256	41.605969191	37.190925290
1	42.709845617	39.277125106	36.492351096	1	42.417995325	39.162547532	36.207852003
1	41.675739692	39.646703672	35.102313706	1	41.543248193	39.895350715	34.866150504
6	47.116011093	37.992182064	42.847850021	6	46.721874644	38.328387299	42.552139149
7	45.986779165	38.524876882	42.061177536	7	45.722534115	38.930236957	41.639328657
6	45.615841186	38.260537902	40.798244548	6	45.248119509	38.460293868	40.487533554
7	44.985246133	39.242369385	40.121729678	7	44.447572488	39.324232714	39.733576420
6	44.154108032	39.070451624	38.945718128	6	43.919754193	38.969953641	38.454684621
7	45.809729010	37.077235919	40.197925921	7	45.456382851	37.222493232	40.012089455
6	45.897461846	35.772553089	40.841715845	6	45.759584888	35.989775143	40.744325048
				1	45.459489603	35.146342994	40.108160224

1	45.377803617	35.032654311	40.217014980	1	45.183632048	35.944005893	41.676847520
1	45.409665956	35.805094151	41.822821006	1	46.829710543	35.880911111	40.970804433
1	46.935358828	35.436703884	40.965916163	1	42.855347495	39.255088589	38.462226587
1	43.207876937	39.611817169	39.093516778	1	44.024687300	37.917633278	38.178804343
1	43.923832689	38.008209235	38.792088421	1	44.370091228	39.634615432	37.673758778
1	44.633429968	39.463748935	38.034561558	1	45.506180552	37.140327558	38.994131432
1	45.868058440	37.094522779	39.178226921	1	45.464749979	39.908557471	41.849878907
1	45.619752959	39.400905449	42.423718631	1	46.543476314	38.768935900	43.538734270
1	47.015443184	38.452845010	43.839849391	1	46.579753389	37.247048914	42.640563503
1	47.036441689	36.907993429	42.985828285	1	43.938417761	40.360260192	39.967893344
1	45.112719048	40.197204483	40.469761898	8	45.061016107	42.521015198	38.175013645
8	45.061016107	42.521015198	38.175013645	1	44.340015847	42.310015120	38.795013866
1	44.340015847	42.310015120	38.795013866	1	44.811016016	42.052015028	37.347013348
1	44.811016016	42.052015028	37.347013348	8	45.124833534	41.759254927	41.623932245
8	45.084354316	41.765916835	41.564848388	1	45.221102475	42.749477796	41.702993279
1	45.177070610	42.755643907	41.645737200	1	44.160346502	41.605690473	41.702273396
1	44.129709680	41.594551922	41.681561198	1	41.475379671	42.219576072	44.751490524
1	41.463731511	42.229555154	44.667718860	1	36.201071295	44.430053657	39.369651505
1	36.061158444	44.507417556	39.329384693	1	42.078871154	47.562797682	39.093509946
1	42.042168140	47.611171839	39.048969732	1	47.752060122	38.530428274	42.258941869
1	48.095592212	38.249332526	42.444908603				

## F Appendix F: Supporting Information for Chapter 7



**Scheme F1.** Proposed catalytic mechanism of collagen hydrolysis by MMP-1.

Hydrolysis of THP substrates in MMPs has been proposed to happen in a four-step mechanism involving an initial nucleophilic attack followed by hydrogen bond rearrangement, proton transfer, and C—N bond cleavage [Scheme F1].<sup>1-5</sup> In the first step of the mechanism, the catalytic water molecule, polarized by the conserved negatively charged glutamate residue nucleophilically attacks the carbonyl carbon of the scissile bond in the THP substrate. The accepted proton from the catalytic water by the glutamate side chain is then transferred to the scissile bond nitrogen atom and finally, the peptide C—N bond in the substrate is cleaved.



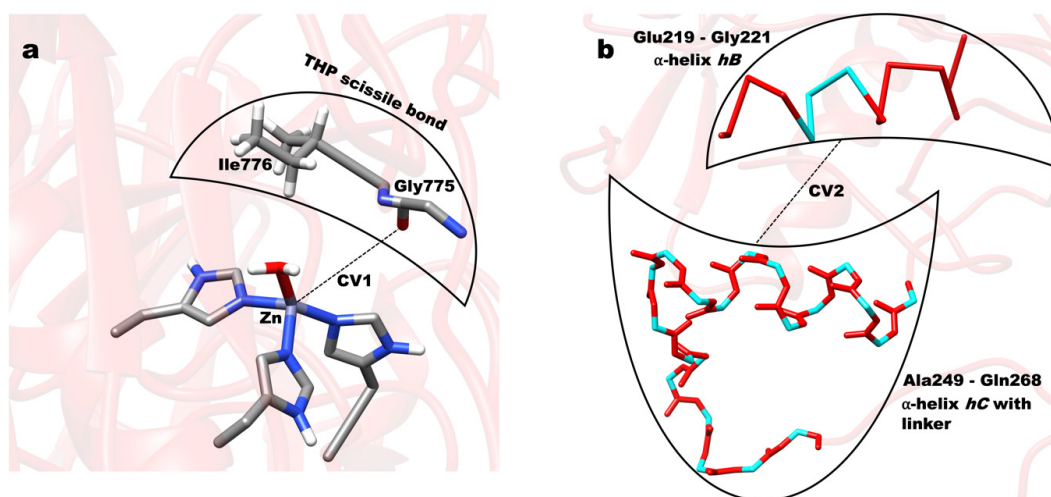


**Figure F1.** (a) CV1 – distance between the catalytic zinc(II) and the scissile bond Gly775 carbonyl oxygen. (b) CV2 – distance between the center of masses of the alpha carbons of residues Glu219-Gly221 (in cyan) and the alpha carbons of residues Ala249-Gln268 (in cyan).

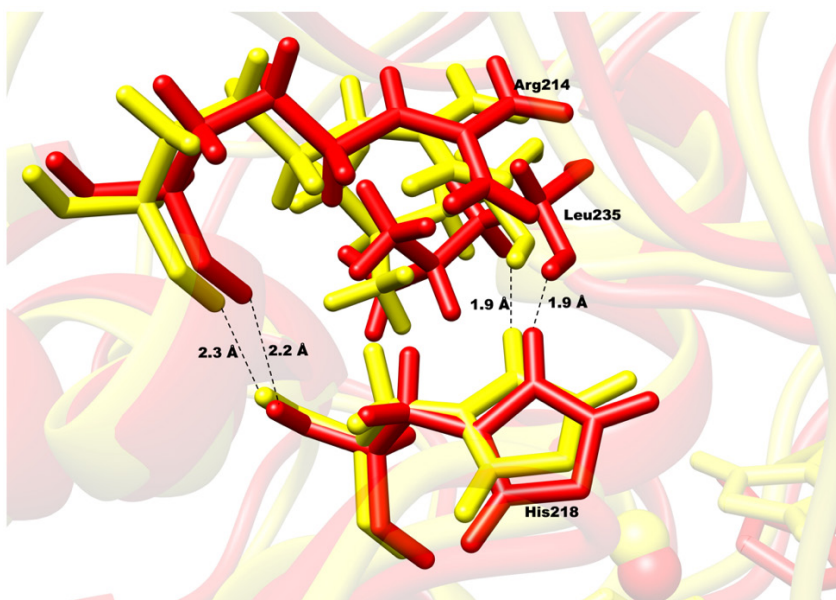


**Figure F2.** Hydrogen bonding interactions of Arg214 and Leu235 backbone with catalytic zinc(II) coordinated His218 in both open-4C (in red) and open-5C (in yellow) forms.

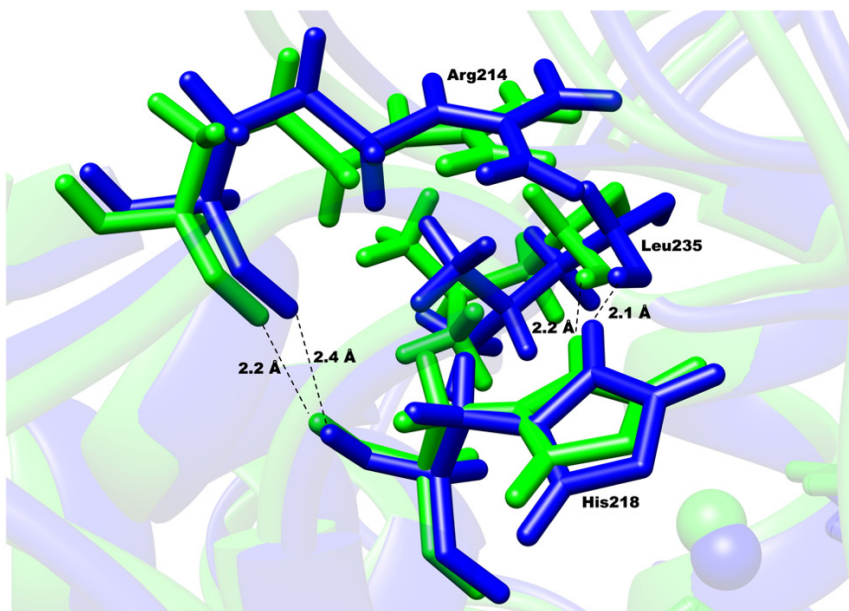


**Figure F3.** Hydrogen bonding interactions of Arg214 and Leu235 backbone with catalytic zinc(II) coordinated His218 in both closed-4C (in blue) and closed-5C (in green).

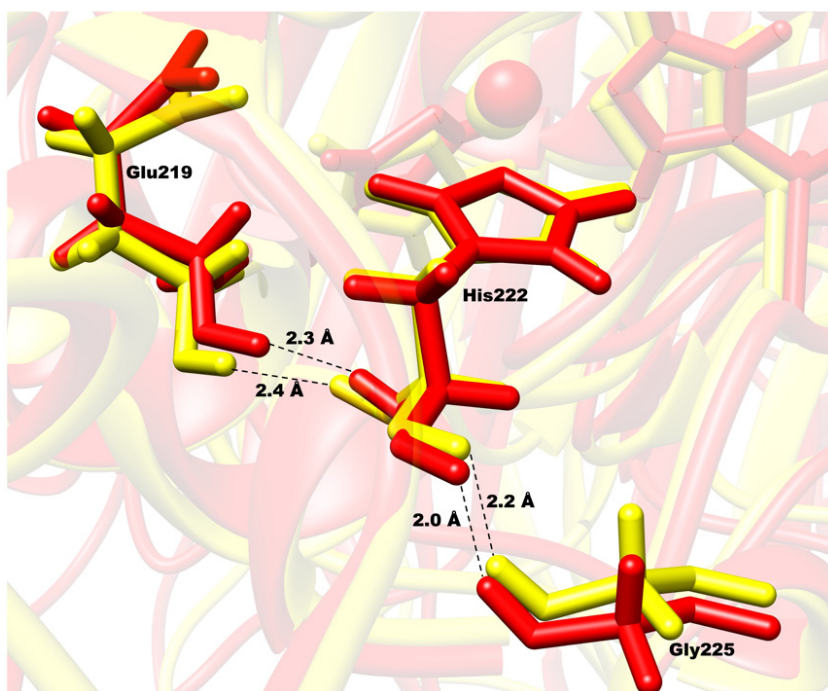


**Figure F4.** Hydrogen bonding interactions of Glu219 and Gly225 backbone with catalytic zinc(II) coordinated His222 in both open-4C (in red) and open-5C (in yellow).

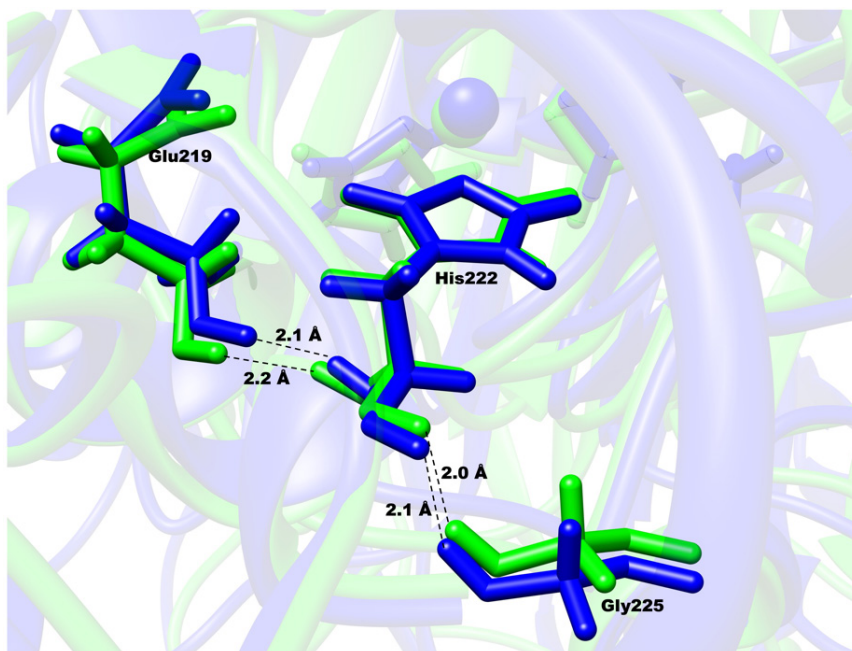


**Figure F5.** Hydrogen bonding interactions of Glu219 and Gly225 backbone with catalytic zinc(II) coordinated His222 in both closed-4C (in blue) and closed-5C (in green).

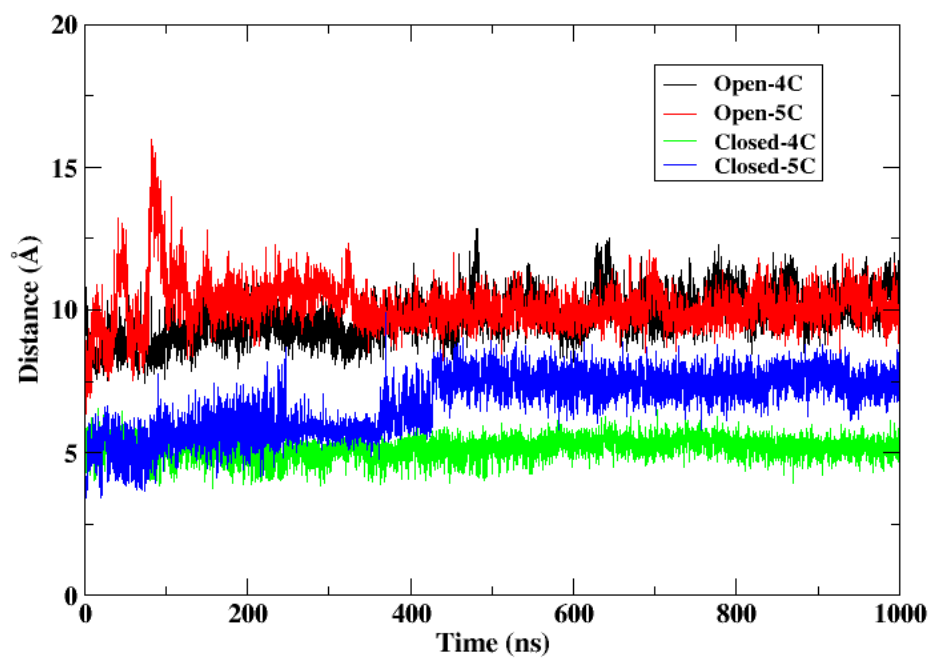


**Figure F6.** Distance between catalytic zinc(II) and the carbonyl oxygen of scissile bond Gly.

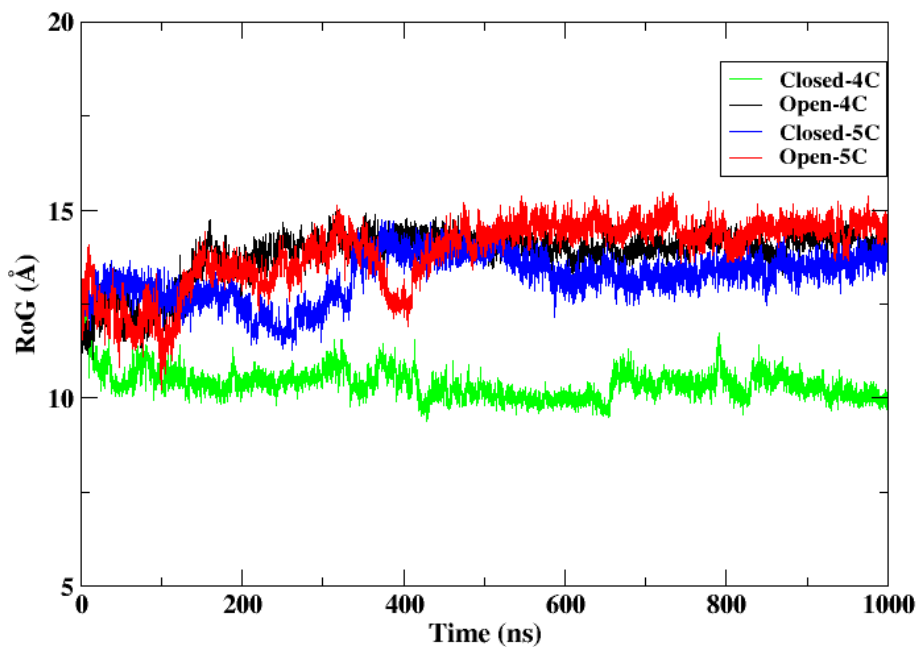


**Figure F7.** Radius of gyration (ROG) of the linker region during the classical MD.

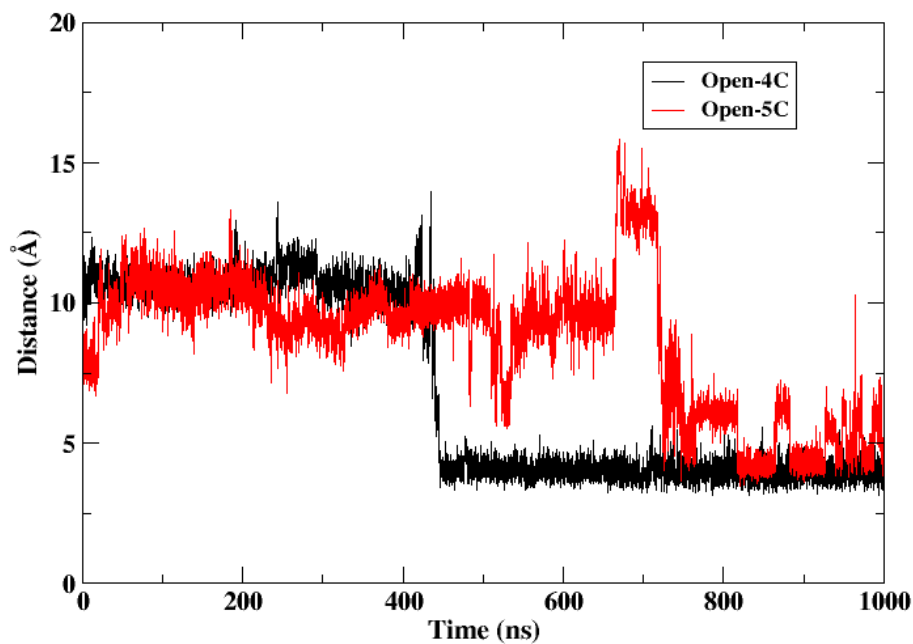


**Figure F8.** Stacking interactions between catalytic zinc(II) coordinated His218 and Tyr240.

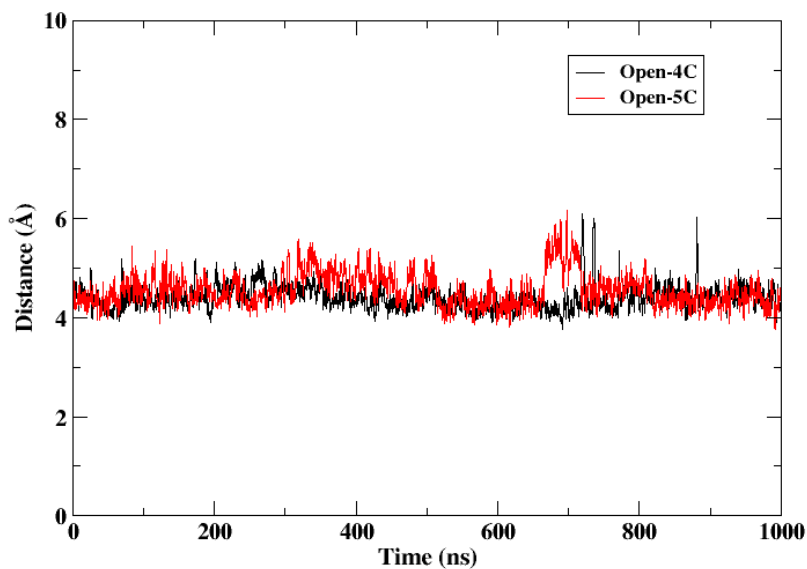


**Figure F9.** Hydrophobic interactions between the side chains of the third catalytic zinc(II)-coordinating His228 and Pro238. Distances were measured between the center of masses of the atoms of the imidazole group of His228 and the pyrrolidine group of Pro238.

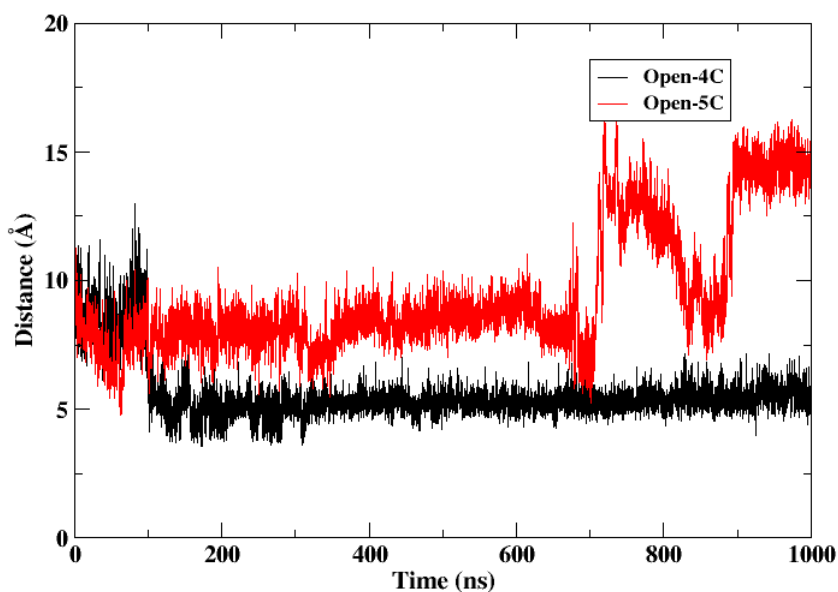


**Figure F10.** Hydrophobic interactions between the side chains of the third catalytic zinc(II)-coordinating His228 and scissile bond Ile776. Distances were measured between the center of masses of the atoms of the imidazole group of His228 and the sec-butyl group of Ile776.

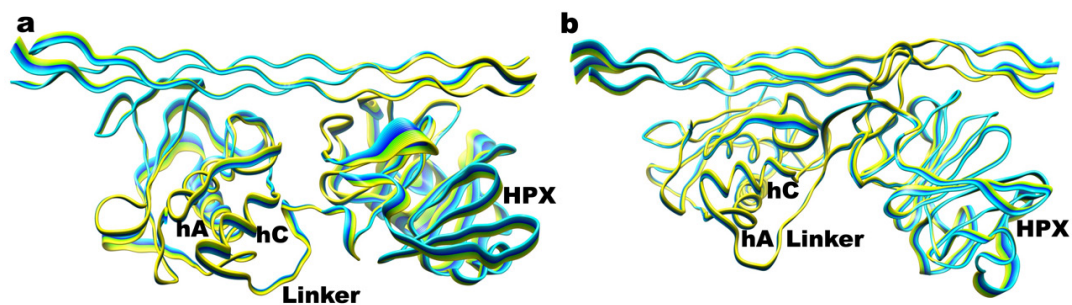


**Figure F11.** PCA of open-4C (a) and open-5C (b) forms. Yellow to blue represents the direction of motion.

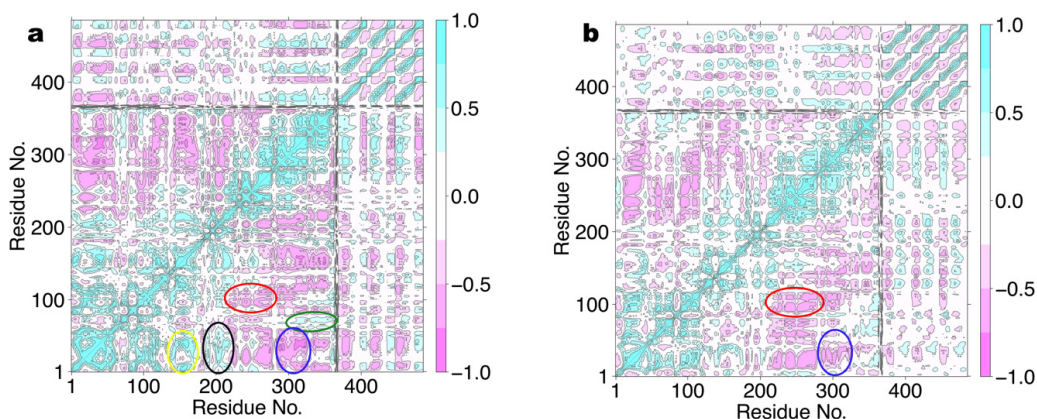


**Figure F12.** Dynamic cross correlation analysis (DCCA) of (a) open-4C and (b) open-5C forms of MMP-1•THP. The oval shapes indicate a correlated motion between S-loop and blade IV of HPX (green); a correlated motion between blade I of the HPX and residues from  $\alpha$ -helix *hA* and  $\beta$ 1- $\beta$ 2 (black); a correlated motion between the linker residues and the residues that constitute  $\alpha$ -helix *hA* and  $\beta$ 1- $\beta$ 2 (yellow); an anti-correlated motion between V-B loop residues and blade II of HPX (red); and an anti-correlated motion between blade IV of the HPX and residues that constitute  $\alpha$ -helix *hA* and  $\beta$ 1- $\beta$ 3 (blue).

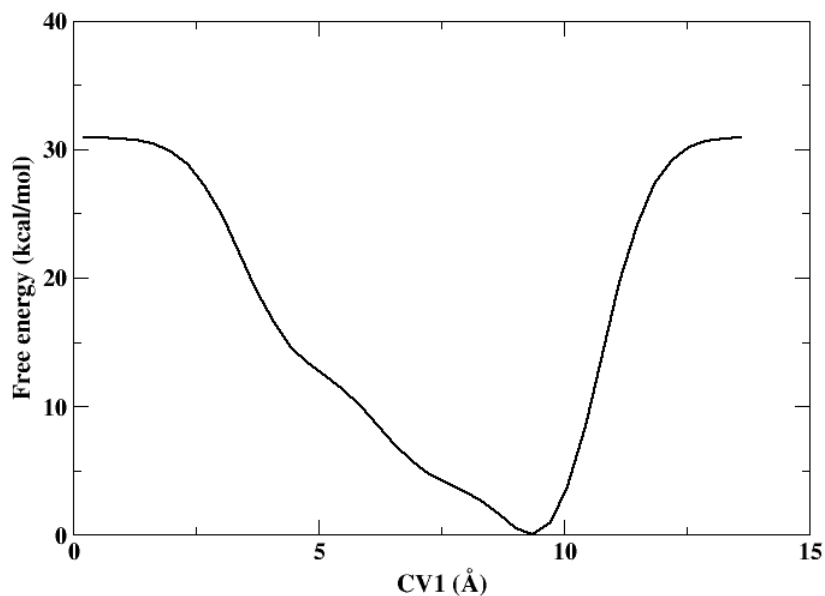


**Figure F13.** Free energy surface (FES) for the transition from open-4C to closed-4C with just one collective variable (CV), involving the distance between the catalytic zinc(II) and scissile bond Gly 775 carbonyl oxygen.

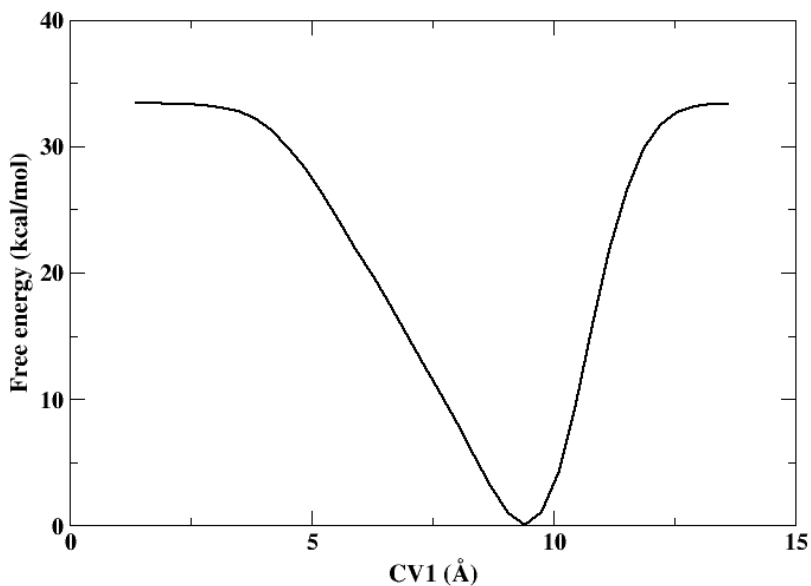


**Figure F14.** FES for the transition from open-5C to closed-5C with just one collective variable (CV), involving the distance between the catalytic zinc(II) and scissile bond Gly 775 carbonyl oxygen.

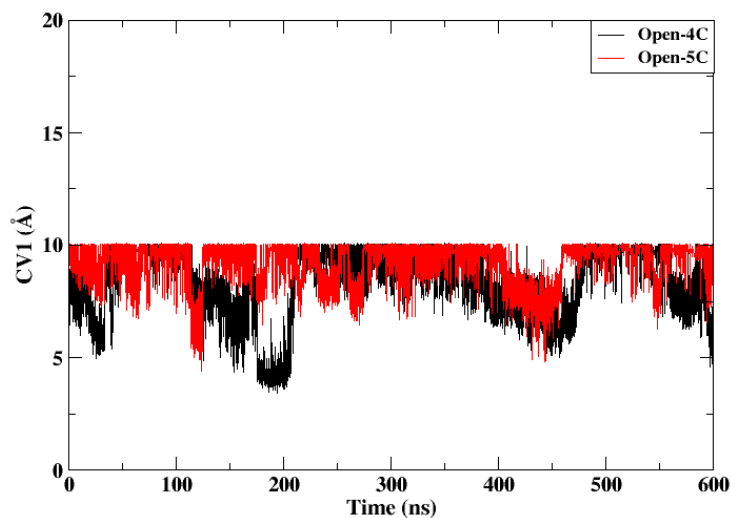


**Figure F15.** Collective variable (CV1) as a function of time for the transition from both open-4C and open-5C to their respective closed forms for MetD with just one CV, involving the distance between the catalytic zinc(II) and scissile bond Gly 775 carbonyl oxygen (CV1).

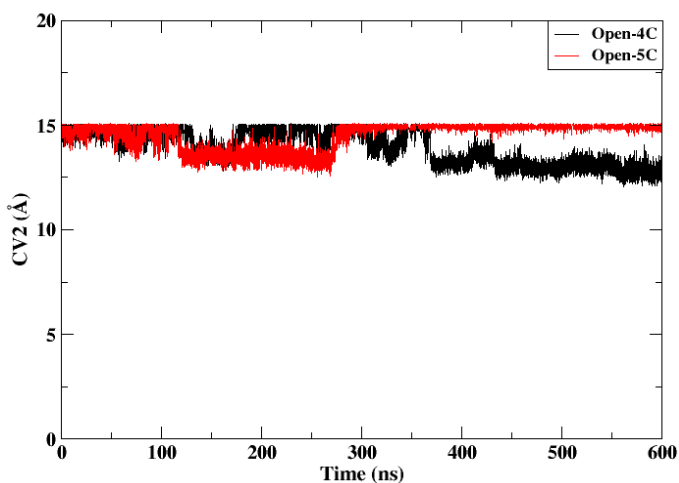


**Figure F16.** Collective variable (CV2) as a function of time for the transition from both open-4C and open-5C to their respective closed forms for MetD with two CVs. CV2 includes the distance between the center of masses of residues that make up  $\alpha$ -helix *hB* (Glu219-Gly221) and residues containing  $\alpha$ -helix *hC* with the linker region (Ala249-Gln268).



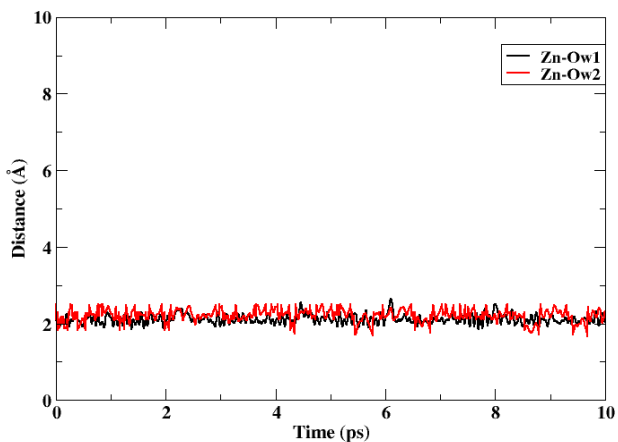


**Figure F17.** Distance between catalytic zinc(II) and oxygen atoms (Ow1 and Ow2) of the two coordinated water molecules in the open-5C form during the QM/MM MD, shows that the transformation from open-5C to open-4C state requires energy barrier.

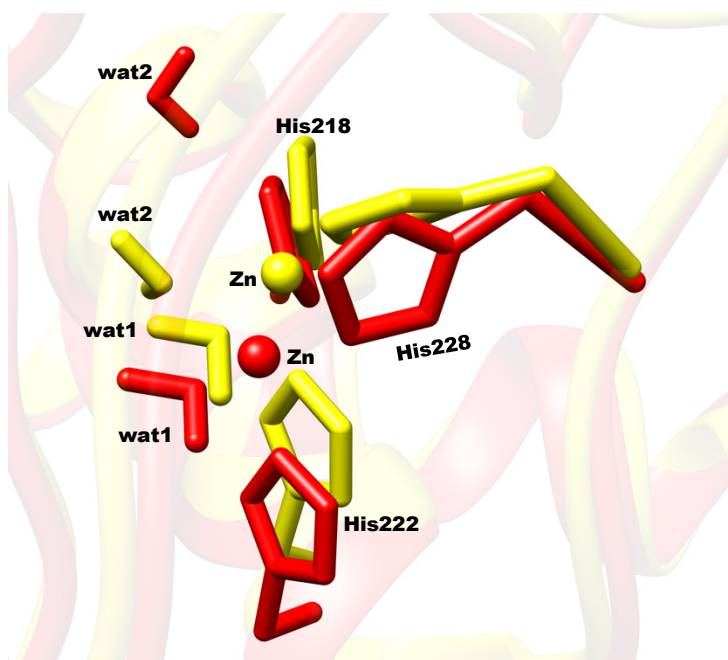


**Figure F18.** Overlaid structures of RC1 (yellow) and PC1 (red), depicting the structures of the catalytic zinc(II) site before (RC1) and after (PC1) the removal of one water molecule from open-5C to open-4C.

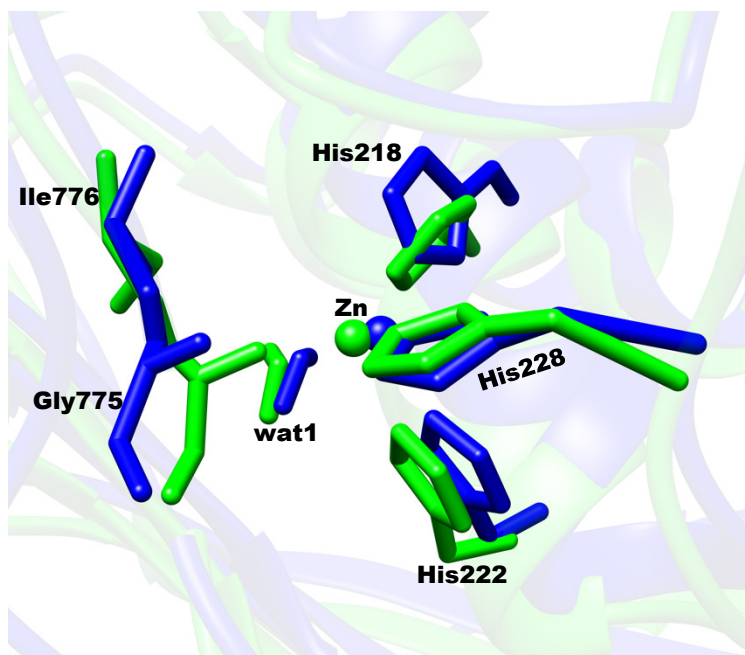


**Figure F19.** Overlaid structures of RC2 (blue) and PC2 (green), depicting the structures of the catalytic zinc(II) site before (RC2) and after (PC2) the coordination of scissile bond Gly775 carbonyl oxygen to the catalytic zinc(II) site to form closed-5C that initiates catalysis.

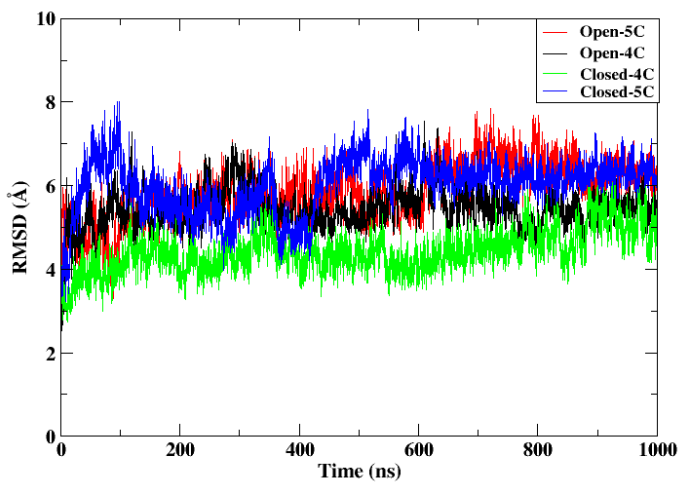
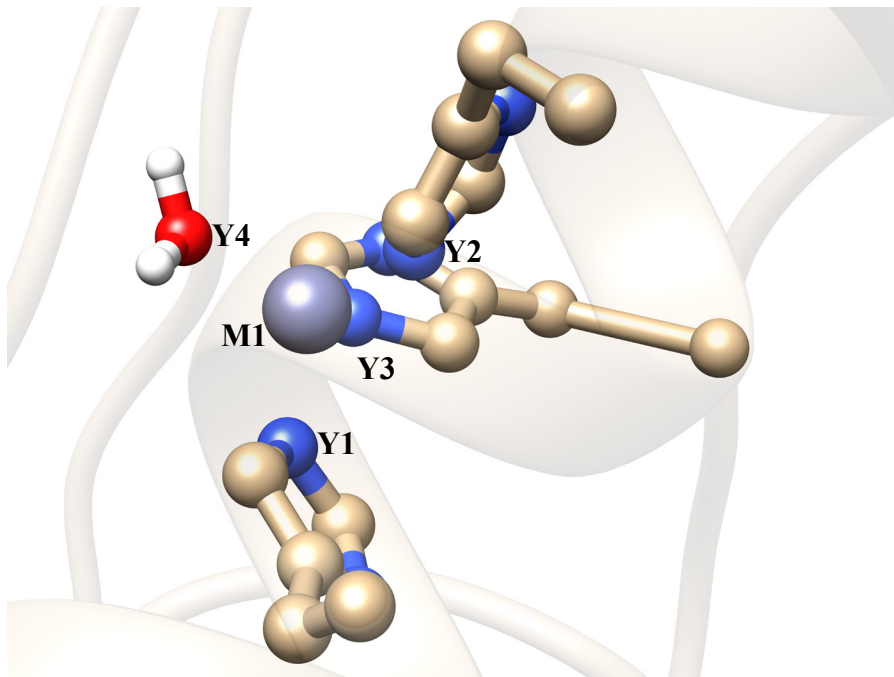


**Figure F20.** Root mean square deviation (RMSD) for the four studied systems with classical MD. RMSD shows average values of 5.43, 5.86, 4.41, and 6.01 Å respectively for the open-4C, open-5C, closed-4C, and closed-5C.

## Zinc(II) Parameters for the 4C state (3-Histidine residues and 1-water molecule)



### MASS

M1	65.4		Zn ion
Y1	14.01	0.530	sp2 N in 5 memb.ring w/LP (HIS,ADE,GUA)
Y2	14.01	0.530	sp2 N in 5 memb.ring w/LP (HIS,ADE,GUA)
Y3	14.01	0.530	sp2 N in 5 memb.ring w/LP (HIS,ADE,GUA)
Y4	16.000	0.465	same as ow

### BOND

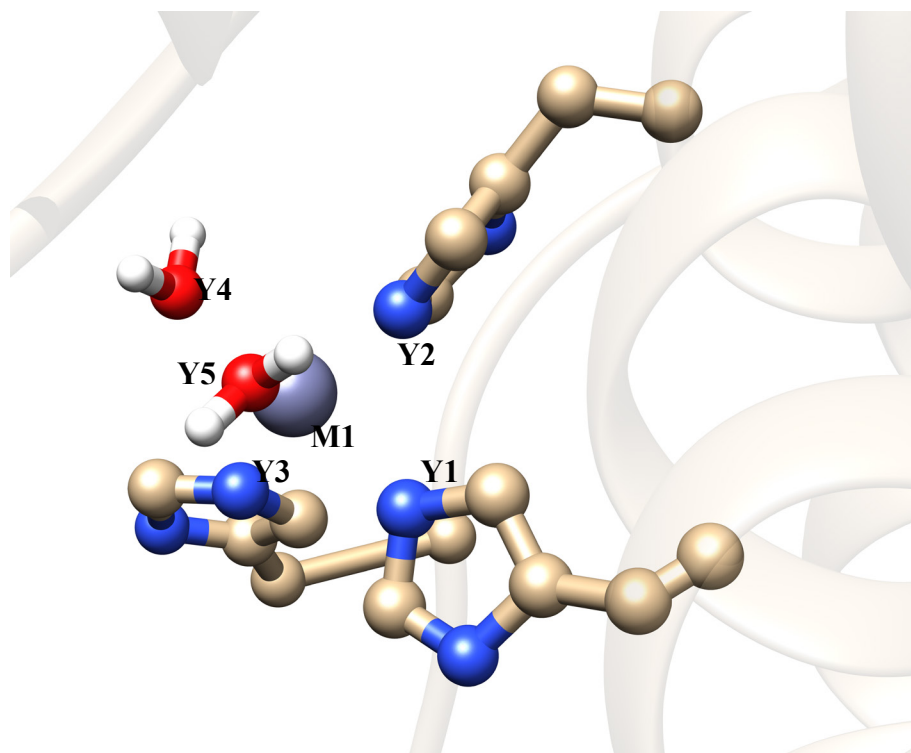
M1-Y4	55.5	2.0569	Created by Seminario method using MCPB.py
Y1-M1	92.3	1.9814	Created by Seminario method using MCPB.py
Y2-M1	93.9	1.9769	Created by Seminario method using MCPB.py
Y3-M1	91.8	1.9834	Created by Seminario method using MCPB.py
CR-Y1	488.0	1.335	JCC,7,(1986),230; HIS
CR-Y2	488.0	1.335	JCC,7,(1986),230; HIS
CR-Y3	488.0	1.335	JCC,7,(1986),230; HIS
Y1-CV	410.0	1.394	JCC,7,(1986),230; HIS
Y2-CV	410.0	1.394	JCC,7,(1986),230; HIS
Y3-CV	410.0	1.394	JCC,7,(1986),230; HIS
Y4-HW	553.0	0.9572	! TIP3P water

### ANGLE

CR-Y1-M1	45.59	125.81	Created by Seminario method using MCPB.py
CR-Y2-M1	50.01	127.69	Created by Seminario method using MCPB.py
CR-Y3-M1	55.64	127.66	Created by Seminario method using MCPB.py
M1-Y1-CV	46.69	127.90	Created by Seminario method using MCPB.py
M1-Y2-CV	50.91	125.97	Created by Seminario method using MCPB.py
M1-Y3-CV	56.74	125.92	Created by Seminario method using MCPB.py
M1-Y4-HW	43.22	123.34	Created by Seminario method using MCPB.py
Y1-M1-Y2	39.62	115.09	Created by Seminario method using MCPB.py

Y1-M1-Y3	38.02	115.99	Created by Seminario method using MCPB.py
Y1-M1-Y4	33.06	100.29	Created by Seminario method using MCPB.py
Y2-M1-Y3	34.76	111.61	Created by Seminario method using MCPB.py
Y2-M1-Y4	33.67	109.27	Created by Seminario method using MCPB.py
Y3-M1-Y4	27.44	102.96	Created by Seminario method using MCPB.py
CC-CV-Y1	70.0	120.00	AA his
CC-CV-Y2	70.0	120.00	AA his
CC-CV-Y3	70.0	120.00	AA his
CR-Y1-CV	70.0	117.00	AA his
CR-Y2-CV	70.0	117.00	AA his
CR-Y3-CV	70.0	117.00	AA his
HW-Y4-HW	100.0	104.52	same as hw-ow-hw
NA-CR-Y1	70.0	120.00	AA his
NA-CR-Y2	70.0	120.00	AA his
NA-CR-Y3	70.0	120.00	AA his
Y1-CR-H5	50.0	120.00	AA his
Y1-CV-H4	50.0	120.00	AA his
Y2-CR-H5	50.0	120.00	AA his
Y2-CV-H4	50.0	120.00	AA his
Y3-CR-H5	50.0	120.00	AA his
Y3-CV-H4	50.0	120.00	AA his

### Zinc(II) Parameters for the 5C state (3-Histidine residues and 2-water molecules)



MASS

M1	65.4		Zn ion
Y1	14.01	0.530	sp2 N in 5 memb.ring w/LP (HIS,ADE,GUA)
Y2	14.01	0.530	sp2 N in 5 memb.ring w/LP (HIS,ADE,GUA)
Y3	14.01	0.530	sp2 N in 5 memb.ring w/LP (HIS,ADE,GUA)
Y4	16.000	0.465	same as ow
Y5	16.000	0.465	same as ow

BOND

M1-Y4	57.7	2.0569	Created by Seminario method using MCPB.py
M1-Y5	52.8	2.0751	Created by Seminario method using MCPB.py
Y1-M1	53.0	2.0822	Created by Seminario method using MCPB.py
Y2-M1	65.3	2.0461	Created by Seminario method using MCPB.py
Y3-M1	61.8	2.0523	Created by Seminario method using MCPB.py
CR-Y1	488.0	1.335	JCC,7,(1986),230; HIS
CR-Y2	488.0	1.335	JCC,7,(1986),230; HIS
CR-Y3	488.0	1.335	JCC,7,(1986),230; HIS
Y1-CV	410.0	1.394	JCC,7,(1986),230; HIS
Y2-CV	410.0	1.394	JCC,7,(1986),230; HIS
Y3-CV	410.0	1.394	JCC,7,(1986),230; HIS
Y4-HW	553.0	0.9572	! TIP3P water
Y5-HW	553.0	0.9572	! TIP3P water

ANGLE

CR-Y1-M1	44.03	128.01	Created by Seminario method using MCPB.py
CR-Y2-M1	62.59	129.70	Created by Seminario method using MCPB.py
CR-Y3-M1	58.35	128.46	Created by Seminario method using MCPB.py
M1-Y1-CV	44.67	125.98	Created by Seminario method using MCPB.py
M1-Y2-CV	64.80	124.23	Created by Seminario method using MCPB.py
M1-Y3-CV	59.35	125.47	Created by Seminario method using MCPB.py
M1-Y4-HW	35.19	117.00	Created by Seminario method using MCPB.py
M1-Y5-HW	41.89	123.69	Created by Seminario method using MCPB.py
Y1-M1-Y2	21.91	99.22	Created by Seminario method using MCPB.py
Y1-M1-Y3	35.46	97.43	Created by Seminario method using MCPB.py
Y1-M1-Y4	23.60	163.41	Created by Seminario method using MCPB.py
Y1-M1-Y5	32.92	85.22	Created by Seminario method using MCPB.py
Y2-M1-Y3	37.50	124.97	Created by Seminario method using MCPB.py
Y2-M1-Y4	29.16	90.12	Created by Seminario method using MCPB.py
Y2-M1-Y5	27.62	111.17	Created by Seminario method using MCPB.py
Y3-M1-Y4	32.35	88.21	Created by Seminario method using MCPB.py
Y3-M1-Y5	33.03	122.24	Created by Seminario method using MCPB.py
Y5-M1-Y4	30.14	78.61	Created by Seminario method using MCPB.py
CC-CV-Y1	70.0	120.00	AA his
CC-CV-Y2	70.0	120.00	AA his
CC-CV-Y3	70.0	120.00	AA his
CR-Y1-CV	70.0	117.00	AA his
CR-Y2-CV	70.0	117.00	AA his
CR-Y3-CV	70.0	117.00	AA his
HW-Y4-HW	100.0	104.52	same as hw-ow-hw
HW-Y5-HW	100.0	104.52	same as hw-ow-hw
NA-CR-Y1	70.0	120.00	AA his
NA-CR-Y2	70.0	120.00	AA his
NA-CR-Y3	70.0	120.00	AA his
Y1-CR-H5	50.0	120.00	AA his

Y1-CV-H4	50.0	120.00	AA his
Y2-CR-H5	50.0	120.00	AA his
Y2-CV-H4	50.0	120.00	AA his
Y3-CR-H5	50.0	120.00	AA his
Y3-CV-H4	50.0	120.00	AA his

### References

- (1) H. Laronha, J. Caldeira, *Cells* **2020**, *9* (5), E1076.
- (2) I. Bertini, V. Calderone, M. Fragai, C. Luchinat, M. Maletta, K. J. Yeo, *Angew. Chem. Int. Ed Engl.* **2006**, *45* (47), 7952–7955.
- (3) V. Pelmeshnikov, P. E. M. Siegbahn, *Inorg. Chem.* **2002**, *41* (22), 5659–5666.
- (4) B. Chen, Z. Kang, E. Zheng, Y. Liu, J. W. Gauld, Q. J. Wang, *Chem. Inf. Model.* **2021**, *61* (10), 5203–5211.
- (5) H. Yang, K. Makaroff, N. Paz, M. Aitha, M. W. Crowder, D. L. Tierney, *Biochemistry* **2015**, *54* (23), 3631–3639.

## G Copyright documentation

### G.1 Copyright Permission for Chapter 2

#### Conformational flexibility influences structure–function relationships in nucleic acid *N*-methyl demethylases

S. O. Waheed, R. Ramanan, S. S. Chaturvedi, J. Ainsley, M. Evison, J. M. Ames, C. J. Schofield, C. Z. Christov and T. G. Karabancheva-Christova, *Org. Biomol. Chem.*, 2019, **17**, 2223  
**DOI:** 10.1039/C9OB00162J

To request permission to reproduce material from this article, please go to the [Copyright Clearance Center request page](#).

If you are **an author contributing to an RSC publication**, **you do not need to request permission** provided correct acknowledgement is given.

If you are **the author of this article**, **you do not need to request permission to reproduce figures and diagrams** provided correct acknowledgement is given. If you want to reproduce the whole article in a third-party publication (excluding your thesis/dissertation for which permission is not required) please go to the [Copyright Clearance Center request page](#).

Read more about [how to correctly acknowledge RSC content](#).

×

## G.2 Copyright Permission for Chapter 3

10/17/22, 9:42 AM

Creative Commons — Attribution 4.0 International — CC BY 4.0

This page is available in the following languages:



**Creative Commons License De**  
**Attribution 4.0 International (CC BY 4.0)**



This is a human-readable summary of (and not a substitute for) the [license](#).

### You are free to:

**Share** — copy and redistribute the material in any medium or format

**Adapt** — remix, transform, and build upon the material

for any purpose, even commercially.

The licensor cannot revoke these freedoms as long as you follow the license terms.

### Under the following terms:

**Attribution** — You must give appropriate credit, provide a link to the license, and indicate if changes were made. You may do so in any reasonable manner, but not in any way that suggests the licensor endorses you or your use.

**No additional restrictions** — You may not apply legal terms or technological measures that legally restrict others from doing anything the license permits.

### Notices:

You do not have to comply with the license for elements of the material in the public domain or where your use is permitted by an applicable exception or limitation.

No warranties are given. The license may not give you all of the permissions necessary for your intended use. For example, other rights such as publicity, privacy, or moral rights may limit how you use the material.

<https://creativecommons.org/licenses/by/4.0/>

1/1



## G.3 Copyright Permission for Chapter 4

10/13/22, 5:25 PM

Rightslink® by Copyright Clearance Center



Home Help Live Chat Sodiq Waheed

### Catalytic Mechanism of Human Ten-Eleven Translocation-2 (TET2) Enzyme: Effects of Conformational Changes, Electric Field, and Mutations



**Author:**  
Sodiq O. Waheed, Shobhit S. Chaturvedi, Tatyana G. Karabencheva-Christova, et al  
**Publication:** ACS Catalysis  
**Publisher:** American Chemical Society  
**Date:** Apr 1, 2021

Copyright © 2021, American Chemical Society

#### PERMISSION/LICENSE IS GRANTED FOR YOUR ORDER AT NO CHARGE

This type of permission/license, instead of the standard Terms and Conditions, is sent to you because no fee is being charged for your order. Please note the following:

- Permission is granted for your request in both print and electronic formats, and translations.
- If figures and/or tables were requested, they may be adapted or used in part.
- Please print this page for your records and send a copy of it to your publisher/graduate school.
- Appropriate credit for the requested material should be given as follows: "Reprinted (adapted) with permission from (COMPLETE REFERENCE CITATION). Copyright (YEAR) American Chemical Society." Insert appropriate information in place of the capitalized words.
- One-time permission is granted only for the use specified in your RightsLink request. No additional uses are granted (such as derivative works or other editions). For any uses, please submit a new request.

If credit is given to another source for the material you requested from RightsLink, permission must be obtained from that source.

[BACK](#)

[CLOSE WINDOW](#)

© 2022 Copyright - All Rights Reserved | Copyright Clearance Center, Inc. | [Privacy statement](#) | [Data Security and Privacy](#)  
| [For California Residents](#) | [Terms and Conditions](#) Comments? We would like to hear from you. E-mail us at [customer-care@copyright.com](mailto:customer-care@copyright.com)

## G.4 Copyright Permission for Chapter 5

10/13/22, 5:23 PM

Rightslink® by Copyright Clearance Center



### How Human TET2 Enzyme Catalyzes the Oxidation of Unnatural Cytosine Modifications in Double-Stranded DNA



Author: Sodiq O. Waheed, Ann Varghese, Shobhit S. Chaturvedi, et al

Publication: ACS Catalysis

Publisher: American Chemical Society

Date: May 1, 2022

Copyright © 2022, American Chemical Society

#### PERMISSION/LICENSE IS GRANTED FOR YOUR ORDER AT NO CHARGE

This type of permission/license, instead of the standard Terms and Conditions, is sent to you because no fee is being charged for your order. Please note the following:

- Permission is granted for your request in both print and electronic formats, and translations.
- If figures and/or tables were requested, they may be adapted or used in part.
- Please print this page for your records and send a copy of it to your publisher/graduate school.
- Appropriate credit for the requested material should be given as follows: "Reprinted (adapted) with permission from {COMPLETE REFERENCE CITATION}. Copyright {YEAR} American Chemical Society." Insert appropriate information in place of the capitalized words.
- One-time permission is granted only for the use specified in your RightsLink request. No additional uses are granted (such as derivative works or other editions). For any uses, please submit a new request.

If credit is given to another source for the material you requested from RightsLink, permission must be obtained from that source.

[BACK](#)

[CLOSE WINDOW](#)

© 2022 Copyright - All Rights Reserved | [Copyright Clearance Center, Inc.](#) | [Privacy statement](#) | [Data Security and Privacy](#)  
| [For California Residents](#) | [Terms and Conditions](#) Comments? We would like to hear from you. E-mail us at [customercare@copyright.com](mailto:customercare@copyright.com)

## G.5 Copyright Permission for Chapter 6

10/13/22, 5:20 PM

RightsLink Printable License

### JOHN WILEY AND SONS LICENSE TERMS AND CONDITIONS

Oct 13, 2022

---

This Agreement between Mr. Sodiq Waheed ("You") and John Wiley and Sons ("John Wiley and Sons") consists of your license details and the terms and conditions provided by John Wiley and Sons and Copyright Clearance Center.

License Number 5407261407259

License date Oct 13, 2022

Licensed Content Publisher John Wiley and Sons

Licensed Content Publication Chemistry - A European Journal

Licensed Content Title What Is the Catalytic Mechanism of Enzymatic Histone N Methyl Arginine Demethylation and Can It Be Influenced by an External Electric Field?

Licensed Content Author Christo Z. Christov, Christopher J. Schofield, Sodiq O. Waheed, et al

Licensed Content Date Jun 4, 2021

Licensed Content Volume 27

Licensed Content Issue 46

<https://s100.copyright.com/AppDispatchServlet>

1/6

Licensed 10  
Content Pages

Type of use Dissertation/Thesis

Requestor type Author of this Wiley article

Format Print and electronic


Portion Full article

Will you be translating? No

Title What Is the Catalytic Mechanism of Enzymatic Histone N Methyl Arginine Demethylation and Can It Be Influenced by an External Electric Field?

Institution name Michigan Technological University

Expected presentation date Jan 2023

Requestor Location Mr. Sodiq Waheed  
  
HOUGHTON, MI 49931  
United States  
Attn: Mr. Sodiq Waheed

Publisher Tax ID EU826007151

Total 0.00 USD

Terms and Conditions

**TERMS AND CONDITIONS**

This copyrighted material is owned by or exclusively licensed to John Wiley & Sons, Inc. or one of its group companies (each a "Wiley Company") or handled on behalf of a society with which a Wiley Company has exclusive publishing rights in relation to a particular work (collectively "WILEY"). By clicking "accept" in connection with completing this licensing transaction, you agree that the following terms and conditions apply to this transaction (along with the billing and payment terms and conditions established by the Copyright Clearance Center Inc., ("CCC's Billing and Payment terms and conditions"), at the time that you opened your RightsLink account (these are available at any time at <http://myaccount.copyright.com>).

### Terms and Conditions

- The materials you have requested permission to reproduce or reuse (the "Wiley Materials") are protected by copyright.
- You are hereby granted a personal, non-exclusive, non-sub licensable (on a stand-alone basis), non-transferable, worldwide, limited license to reproduce the Wiley Materials for the purpose specified in the licensing process. This license, **and any CONTENT (PDF or image file) purchased as part of your order**, is for a one-time use only and limited to any maximum distribution number specified in the license. The first instance of republication or reuse granted by this license must be completed within two years of the date of the grant of this license (although copies prepared before the end date may be distributed thereafter). The Wiley Materials shall not be used in any other manner or for any other purpose, beyond what is granted in the license. Permission is granted subject to an appropriate acknowledgement given to the author, title of the material/book/journal and the publisher. You shall also duplicate the copyright notice that appears in the Wiley publication in your use of the Wiley Material. Permission is also granted on the understanding that nowhere in the text is a previously published source acknowledged for all or part of this Wiley Material. Any third party content is expressly excluded from this permission.
- With respect to the Wiley Materials, all rights are reserved. Except as expressly granted by the terms of the license, no part of the Wiley Materials may be copied, modified, adapted (except for minor reformatting required by the new Publication), translated, reproduced, transferred or distributed, in any form or by any means, and no derivative works may be made based on the Wiley Materials without the prior permission of the respective copyright owner. **For STM Signatory Publishers clearing permission under the terms of the [STM Permissions Guidelines](#) only, the terms of the license are extended to include subsequent editions and for editions in other languages, provided such editions are for the work as a whole in situ and does not involve the separate exploitation of the permitted figures or extracts**, You may not alter, remove or suppress in any manner any copyright, trademark or other notices displayed by the Wiley Materials. You may not license, rent, sell, loan, lease, pledge, offer as security, transfer or assign the Wiley Materials on a stand-alone basis, or any of the rights granted to you hereunder to any other person.
- The Wiley Materials and all of the intellectual property rights therein shall at all times remain the exclusive property of John Wiley & Sons Inc, the Wiley Companies, or their respective licensors, and your interest therein is only that of having possession of and the right to reproduce the Wiley Materials pursuant to Section 2 herein during the continuance of this Agreement. You agree that you own no right, title or interest in or to the Wiley Materials or any of the intellectual property rights therein. You shall have no rights hereunder other than the license as provided for above in Section 2. No right,

license or interest to any trademark, trade name, service mark or other branding ("Marks") of WILEY or its licensors is granted hereunder, and you agree that you shall not assert any such right, license or interest with respect thereto

- NEITHER WILEY NOR ITS LICENSORS MAKES ANY WARRANTY OR REPRESENTATION OF ANY KIND TO YOU OR ANY THIRD PARTY, EXPRESS, IMPLIED OR STATUTORY, WITH RESPECT TO THE MATERIALS OR THE ACCURACY OF ANY INFORMATION CONTAINED IN THE MATERIALS, INCLUDING, WITHOUT LIMITATION, ANY IMPLIED WARRANTY OF MERCHANTABILITY, ACCURACY, SATISFACTORY QUALITY, FITNESS FOR A PARTICULAR PURPOSE, USABILITY, INTEGRATION OR NON-INFRINGEMENT AND ALL SUCH WARRANTIES ARE HEREBY EXCLUDED BY WILEY AND ITS LICENSORS AND WAIVED BY YOU.
- WILEY shall have the right to terminate this Agreement immediately upon breach of this Agreement by you.
- You shall indemnify, defend and hold harmless WILEY, its Licensors and their respective directors, officers, agents and employees, from and against any actual or threatened claims, demands, causes of action or proceedings arising from any breach of this Agreement by you.
- IN NO EVENT SHALL WILEY OR ITS LICENSORS BE LIABLE TO YOU OR ANY OTHER PARTY OR ANY OTHER PERSON OR ENTITY FOR ANY SPECIAL, CONSEQUENTIAL, INCIDENTAL, INDIRECT, EXEMPLARY OR PUNITIVE DAMAGES, HOWEVER CAUSED, ARISING OUT OF OR IN CONNECTION WITH THE DOWNLOADING, PROVISIONING, VIEWING OR USE OF THE MATERIALS REGARDLESS OF THE FORM OF ACTION, WHETHER FOR BREACH OF CONTRACT, BREACH OF WARRANTY, TORT, NEGLIGENCE, INFRINGEMENT OR OTHERWISE (INCLUDING, WITHOUT LIMITATION, DAMAGES BASED ON LOSS OF PROFITS, DATA, FILES, USE, BUSINESS OPPORTUNITY OR CLAIMS OF THIRD PARTIES), AND WHETHER OR NOT THE PARTY HAS BEEN ADVISED OF THE POSSIBILITY OF SUCH DAMAGES. THIS LIMITATION SHALL APPLY NOTWITHSTANDING ANY FAILURE OF ESSENTIAL PURPOSE OF ANY LIMITED REMEDY PROVIDED HEREIN.
- Should any provision of this Agreement be held by a court of competent jurisdiction to be illegal, invalid, or unenforceable, that provision shall be deemed amended to achieve as nearly as possible the same economic effect as the original provision, and the legality, validity and enforceability of the remaining provisions of this Agreement shall not be affected or impaired thereby.
- The failure of either party to enforce any term or condition of this Agreement shall not constitute a waiver of either party's right to enforce each and every term and condition of this Agreement. No breach under this agreement shall be deemed waived or excused by either party unless such waiver or consent is in writing signed by the party granting such waiver or consent. The waiver by or consent of a party to a breach of any provision of this Agreement shall not operate or be construed as a waiver of or consent to any other or subsequent breach by such other party.
- This Agreement may not be assigned (including by operation of law or otherwise) by you without WILEY's prior written consent.

- Any fee required for this permission shall be non-refundable after thirty (30) days from receipt by the CCC.
- These terms and conditions together with CCC's Billing and Payment terms and conditions (which are incorporated herein) form the entire agreement between you and WILEY concerning this licensing transaction and (in the absence of fraud) supersedes all prior agreements and representations of the parties, oral or written. This Agreement may not be amended except in writing signed by both parties. This Agreement shall be binding upon and inure to the benefit of the parties' successors, legal representatives, and authorized assigns.
- In the event of any conflict between your obligations established by these terms and conditions and those established by CCC's Billing and Payment terms and conditions, these terms and conditions shall prevail.
- WILEY expressly reserves all rights not specifically granted in the combination of (i) the license details provided by you and accepted in the course of this licensing transaction, (ii) these terms and conditions and (iii) CCC's Billing and Payment terms and conditions.
- This Agreement will be void if the Type of Use, Format, Circulation, or Requestor Type was misrepresented during the licensing process.
- This Agreement shall be governed by and construed in accordance with the laws of the State of New York, USA, without regards to such state's conflict of law rules. Any legal action, suit or proceeding arising out of or relating to these Terms and Conditions or the breach thereof shall be instituted in a court of competent jurisdiction in New York County in the State of New York in the United States of America and each party hereby consents and submits to the personal jurisdiction of such court, waives any objection to venue in such court and consents to service of process by registered or certified mail, return receipt requested, at the last known address of such party.

## WILEY OPEN ACCESS TERMS AND CONDITIONS

Wiley Publishes Open Access Articles in fully Open Access Journals and in Subscription journals offering Online Open. Although most of the fully Open Access journals publish open access articles under the terms of the Creative Commons Attribution (CC BY) License only, the subscription journals and a few of the Open Access Journals offer a choice of Creative Commons Licenses. The license type is clearly identified on the article.

### The Creative Commons Attribution License

The [Creative Commons Attribution License \(CC-BY\)](#) allows users to copy, distribute and transmit an article, adapt the article and make commercial use of the article. The CC-BY license permits commercial and non-

### Creative Commons Attribution Non-Commercial License

The [Creative Commons Attribution Non-Commercial \(CC-BY-NC\) License](#) permits use, distribution and reproduction in any medium, provided the original work is properly cited and is not used for commercial purposes.(see below)

**Creative Commons Attribution-Non-Commercial-NoDerivs License**

The [Creative Commons Attribution Non-Commercial-NoDerivs License](#) (CC-BY-NC-ND) permits use, distribution and reproduction in any medium, provided the original work is properly cited, is not used for commercial purposes and no modifications or adaptations are made. (see below)

**Use by commercial "for-profit" organizations**

Use of Wiley Open Access articles for commercial, promotional, or marketing purposes requires further explicit permission from Wiley and will be subject to a fee.

Further details can be found on Wiley Online Library  
<http://olabout.wiley.com/WileyCDA/Section/id-410895.html>

**Other Terms and Conditions:**

**v1.10 Last updated September 2015**

**Questions? [customercare@copyright.com](mailto:customercare@copyright.com) or +1-855-239-3415 (toll free in the US) or +1-978-646-2777.**





## G.6 Copyright Permission for Chapter 7


12/7/22, 5:50 PM

RightsLink - Your Account

### JOHN WILEY AND SONS LICENSE TERMS AND CONDITIONS

Dec 07, 2022

This Agreement between Mr. Sodiq Waheed ("You") and John Wiley and Sons ("John Wiley and Sons") consists of your license details and the terms and conditions provided by John Wiley and Sons and Copyright Clearance Center.

License Number	5418320044992
License date	Oct 29, 2022
Licensed Content Publisher	John Wiley and Sons
Licensed Content Publication	ChemPhysChem
Licensed Content Title	Mechanism of the Early Catalytic Events in the Collagenolysis by Matrix Metalloproteinase-1
Licensed Content Author	Sodiq O. Waheed, Ann Varghese, Isabella DiCastrì, et al
Licensed Content Date	Oct 25, 2022
Licensed Content Volume	0
Licensed Content Issue	0
Licensed Content Pages	1
Type of Use	Dissertation/Thesis
Requestor type	Author of this Wiley article
Format	Print and electronic
Portion	Full article
Will you be translating?	No
Title	Mechanism of the Early Catalytic Events in the Collagenolysis by Matrix Metalloproteinase-1
Institution name	Michigan Technological University
Expected presentation date	Jan 2023
Requestor Location	Mr. Sodiq Waheed  HOUGHTON, MI 49931 United States Attn: Mr. Sodiq Waheed
Publisher Tax ID	EU826007151
Total	<b>0.00 USD</b>
Terms and Conditions	

#### TERMS AND CONDITIONS

This copyrighted material is owned by or exclusively licensed to John Wiley & Sons, Inc. or one of its group companies (each a "Wiley Company") or handled on behalf of a society with which a Wiley Company has exclusive publishing rights in relation to a particular work (collectively "WILEY"). By clicking "accept" in connection with completing this licensing transaction, you agree that the following terms and conditions apply to this transaction (along with the billing and payment terms and conditions established by the Copyright Clearance Center Inc., ("CCC's Billing and Payment terms and conditions"), at the time that you opened your RightsLink account (these are available at any time at <http://myaccount.copyright.com>).

#### Terms and Conditions

- The materials you have requested permission to reproduce or reuse (the "Wiley Materials") are protected by copyright.
- You are hereby granted a personal, non-exclusive, non-sub licensable (on a stand-alone basis), non-transferable, worldwide, limited license to **reproduce the Wiley Materials for the purpose specified in the licensing process**. This license, **and any CONTENT (PDF or image file) purchased as part of your order**, is for a one-time use only and limited to any maximum

<https://s100.copyright.com/MyAccount/web/jsp/viewprintablelicensefrommyorders.jsp?ref=477018dd-172a-4743-adf6-591350c50509>

1/3

distribution number specified in the license. The first instance of republication or reuse granted by this license must be completed within two years of the date of the grant of this license (although copies prepared before the end date may be distributed thereafter). The Wiley Materials shall not be used in any other manner or for any other purpose, beyond what is granted in the license. Permission is granted subject to an appropriate acknowledgement given to the author, title of the material/book/journal and the publisher. You shall also duplicate the copyright notice that appears in the Wiley publication in your use of the Wiley Material. Permission is also granted on the understanding that nowhere in the text is a previously published source acknowledged for all or part of this Wiley Material. Any third party content is expressly excluded from this permission.

- With respect to the Wiley Materials, all rights are reserved. Except as expressly granted by the terms of the license, no part of the Wiley Materials may be copied, modified, adapted (except for minor reformatting required by the new Publication), translated, reproduced, transferred or distributed, in any form or by any means, and no derivative works may be made based on the Wiley Materials without the prior permission of the respective copyright owner. **For STM Signatory Publishers clearing permission under the terms of the [STM Permissions Guidelines](#) only, the terms of the license are extended to include subsequent editions and for editions in other languages, provided such editions are for the work as a whole in situ and does not involve the separate exploitation of the permitted figures or extracts.** You may not alter, remove or suppress in any manner any copyright, trademark or other notices displayed by the Wiley Materials. You may not license, rent, sell, loan, lease, pledge, offer as security, transfer or assign the Wiley Materials on a stand-alone basis, or any of the rights granted to you hereunder to any other person.
- The Wiley Materials and all of the intellectual property rights therein shall at all times remain the exclusive property of John Wiley & Sons Inc, the Wiley Companies, or their respective licensors, and your interest therein is only that of having possession of and the right to reproduce the Wiley Materials pursuant to Section 2 herein during the continuance of this Agreement. You agree that you own no right, title or interest in or to the Wiley Materials or any of the intellectual property rights therein. You shall have no rights hereunder other than the license as provided for above in Section 2. No right, license or interest to any trademark, trade name, service mark or other branding ("Marks") of WILEY or its licensors is granted hereunder, and you agree that you shall not assert any such right, license or interest with respect thereto
- NEITHER WILEY NOR ITS LICENSORS MAKES ANY WARRANTY OR REPRESENTATION OF ANY KIND TO YOU OR ANY THIRD PARTY, EXPRESS, IMPLIED OR STATUTORY, WITH RESPECT TO THE MATERIALS OR THE ACCURACY OF ANY INFORMATION CONTAINED IN THE MATERIALS, INCLUDING, WITHOUT LIMITATION, ANY IMPLIED WARRANTY OF MERCHANTABILITY, ACCURACY, SATISFACTORY QUALITY, FITNESS FOR A PARTICULAR PURPOSE, USABILITY, INTEGRATION OR NON-INFRINGEMENT AND ALL SUCH WARRANTIES ARE HEREBY EXCLUDED BY WILEY AND ITS LICENSORS AND WAIVED BY YOU.
- WILEY shall have the right to terminate this Agreement immediately upon breach of this Agreement by you.
- You shall indemnify, defend and hold harmless WILEY, its Licensors and their respective directors, officers, agents and employees, from and against any actual or threatened claims, demands, causes of action or proceedings arising from any breach of this Agreement by you.
- IN NO EVENT SHALL WILEY OR ITS LICENSORS BE LIABLE TO YOU OR ANY OTHER PARTY OR ANY OTHER PERSON OR ENTITY FOR ANY SPECIAL, CONSEQUENTIAL, INCIDENTAL, INDIRECT, EXEMPLARY OR PUNITIVE DAMAGES, HOWEVER CAUSED, ARISING OUT OF OR IN CONNECTION WITH THE DOWNLOADING, PROVISIONING, VIEWING OR USE OF THE MATERIALS REGARDLESS OF THE FORM OF ACTION, WHETHER FOR BREACH OF CONTRACT, BREACH OF WARRANTY, TORT, NEGLIGENCE, INFRINGEMENT OR OTHERWISE (INCLUDING, WITHOUT LIMITATION, DAMAGES BASED ON LOSS OF PROFITS, DATA, FILES, USE, BUSINESS OPPORTUNITY OR CLAIMS OF THIRD PARTIES), AND WHETHER OR NOT THE PARTY HAS BEEN ADVISED OF THE POSSIBILITY OF SUCH DAMAGES. THIS LIMITATION SHALL APPLY NOTWITHSTANDING ANY FAILURE OF ESSENTIAL PURPOSE OF ANY LIMITED REMEDY PROVIDED HEREIN.
- Should any provision of this Agreement be held by a court of competent jurisdiction to be illegal, invalid, or unenforceable, that provision shall be deemed amended to achieve as nearly as possible the same economic effect as the original provision, and the legality, validity and enforceability of the remaining provisions of this Agreement shall not be affected or impaired thereby.
- The failure of either party to enforce any term or condition of this Agreement shall not constitute a waiver of either party's right to enforce each and every term and condition of this Agreement. No breach under this agreement shall be deemed waived or excused by either party unless such waiver or consent is in writing signed by the party granting such waiver or consent. The waiver by or consent of a party to a breach of any provision of this Agreement shall not operate or be construed as a waiver of or consent to any other or subsequent breach by such other party.

- This Agreement may not be assigned (including by operation of law or otherwise) by you without WILEY's prior written consent.
- Any fee required for this permission shall be non-refundable after thirty (30) days from receipt by the CCC.
- These terms and conditions together with CCC's Billing and Payment terms and conditions (which are incorporated herein) form the entire agreement between you and WILEY concerning this licensing transaction and (in the absence of fraud) supersedes all prior agreements and representations of the parties, oral or written. This Agreement may not be amended except in writing signed by both parties. This Agreement shall be binding upon and inure to the benefit of the parties' successors, legal representatives, and authorized assigns.
- In the event of any conflict between your obligations established by these terms and conditions and those established by CCC's Billing and Payment terms and conditions, these terms and conditions shall prevail.
- WILEY expressly reserves all rights not specifically granted in the combination of (i) the license details provided by you and accepted in the course of this licensing transaction, (ii) these terms and conditions and (iii) CCC's Billing and Payment terms and conditions.
- This Agreement will be void if the Type of Use, Format, Circulation, or Requestor Type was misrepresented during the licensing process.
- This Agreement shall be governed by and construed in accordance with the laws of the State of New York, USA, without regards to such state's conflict of law rules. Any legal action, suit or proceeding arising out of or relating to these Terms and Conditions or the breach thereof shall be instituted in a court of competent jurisdiction in New York County in the State of New York in the United States of America and each party hereby consents and submits to the personal jurisdiction of such court, waives any objection to venue in such court and consents to service of process by registered or certified mail, return receipt requested, at the last known address of such party.

**WILEY OPEN ACCESS TERMS AND CONDITIONS**

Wiley Publishes Open Access Articles in fully Open Access Journals and in Subscription journals offering Online Open. Although most of the fully Open Access journals publish open access articles under the terms of the Creative Commons Attribution (CC BY) License only, the subscription journals and a few of the Open Access Journals offer a choice of Creative Commons Licenses. The license type is clearly identified on the article.

**The Creative Commons Attribution License**

The [Creative Commons Attribution License \(CC-BY\)](#) allows users to copy, distribute and transmit an article, adapt the article and make commercial use of the article. The CC-BY license permits commercial and non-

**Creative Commons Attribution Non-Commercial License**

The [Creative Commons Attribution Non-Commercial \(CC-BY-NC\) License](#) permits use, distribution and reproduction in any medium, provided the original work is properly cited and is not used for commercial purposes.(see below)

**Creative Commons Attribution-Non-Commercial-NoDerivs License**

The [Creative Commons Attribution Non-Commercial-NoDerivs License](#) (CC-BY-NC-ND) permits use, distribution and reproduction in any medium, provided the original work is properly cited, is not used for commercial purposes and no modifications or adaptations are made. (see below)

**Use by commercial "for-profit" organizations**

Use of Wiley Open Access articles for commercial, promotional, or marketing purposes requires further explicit permission from Wiley and will be subject to a fee.

Further details can be found on Wiley Online Library <http://olabout.wiley.com/WileyCDA/Section/id-410895.html>

**Other Terms and Conditions:**

v1.10 Last updated September 2015

Questions? [customer care@copyright.com](mailto:customer care@copyright.com) or +1-855-239-3415 (toll free in the US) or +1-978-646-2777.

## G.7 Copyright Permission for Chapter 3 Cover Image

2/15/23, 11:29 AM

Michigan Technological University Mail - Supplementary Cover Image



Michigan Tech

Sodiq Waheed <sowaheed@mtu.edu>

---

### Supplementary Cover Image

ACSPubsMultimedia <ACSPubsMultimedia@acs.org>  
To: Sodiq Waheed <sowaheed@mtu.edu>

Wed, Jan 18, 2023 at 2:07 PM

Yes you may use the cover. Here is some information for you:

Beginning with the January 2010 covers, viewers to the ACS Web site can now download high resolution covers two days before they are published in print. **No permission is necessary to use the covers and they may be used for any purpose. The entire cover must be used.** You should not use the RightsLink permission system to obtain permission to use entire ACS journal covers. Please follow these instructions:

- Go to [pubs.acs.org](https://pubs.acs.org)
- Select the journal you are interested in among the ACS journal titles listed
- Select the requested cover
- Click on the image of the desired cover
- When it appears on the screen, click on "Download High-Resolution Cover"

If you have any problems, please contact the Journal Help Desk at [support@services.acs.org](mailto:support@services.acs.org).

**NOTE:** The above instructions do not apply to ACS journal covers published prior to 2010. If you want to request ACS journal covers published prior to 2010, you should send your request to [copyright@acs.org](mailto:copyright@acs.org). You need to include a **complete** reference citation (name of the ACS journal, the month, day, year of publication, and the volume and issue numbers), how you plan to use the cover, your complete mailing address, your 24-hour fax number, and the specific date that you need to receive our reply.

### Christine Filippetti

Publications Division

American Chemical Society

[C\\_Filippetti@acs.org](mailto:C_Filippetti@acs.org)

Office hours: 7:30AM to 4:00PM EST

2/15/23, 11:31 AM

Michigan Technological University Mail - Supplementary Cover Image



Michigan Tech

Sodiq Waheed <sowaheed@mtu.edu>

---

### Supplementary Cover Image

Sodiq Waheed <sowaheed@mtu.edu>  
To: [acspubsmultimedia@acs.org](mailto:acspubsmultimedia@acs.org)

Mon, Jan 16, 2023 at 2:31 PM

Hello,

I am Sodiq Waheed, a 5th-year Ph.D. candidate in Chemistry at Michigan Technological University. One of my studies published in *ACS Central Science* ([Link](#)) in 2020 had its designed cover image selected as a supplementary front cover of the May 2020 issue of the Journal ([Link](#)). I am currently writing my Ph.D. Dissertation, and I want to reuse this cover in its entirety in my dissertation. Hence, I would like to know how I can request permission to reuse it for the stated purpose.

Thank you, and looking forward to hearing from you.  
Sodiq

--

Sodiq O. Waheed  
Ph.D. Candidate  
Department of Chemistry  
Michigan Technological University  
1400 Townsend Drive  
Houghton, MI 49931, USA

## G.8 Copyright Permission for Chapter 6 Cover Image

1/16/23, 12:45 PM

RightsLink Printable License

### JOHN WILEY AND SONS LICENSE TERMS AND CONDITIONS

Jan 16, 2023

---

This Agreement between Mr. Sodiq Waheed ("You") and John Wiley and Sons ("John Wiley and Sons") consists of your license details and the terms and conditions provided by John Wiley and Sons and Copyright Clearance Center.

License Number 5470870757673

License date Jan 16, 2023

Licensed Content  
Publisher John Wiley and Sons

Licensed Content  
Publication Chemistry - A European Journal

Licensed Content  
Title Front Cover: What Is the Catalytic Mechanism of Enzymatic Histone N Methyl Arginine Demethylation and Can It Be Influenced by an External Electric Field? (Chem. Eur. J. 46/2021)

Licensed Content  
Author Rajeev Ramanan, Sodiq O. Waheed, Christopher J. Schofield, et al

Licensed Content  
Date Jun 30, 2021

Licensed Content  
Volume 27

Licensed Content  
Issue 46

Licensed Content  
Pages 1

<https://s100.copyright.com/AppDispatchServlet>

1/6



(along with the billing and payment terms and conditions established by the Copyright Clearance Center Inc., ("CCC's Billing and Payment terms and conditions"), at the time that you opened your RightsLink account (these are available at any time at <http://myaccount.copyright.com>).

### Terms and Conditions

- The materials you have requested permission to reproduce or reuse (the "Wiley Materials") are protected by copyright.
- You are hereby granted a personal, non-exclusive, non-sub licensable (on a stand-alone basis), non-transferable, worldwide, limited license to reproduce the Wiley Materials for the purpose specified in the licensing process. This license, **and any CONTENT (PDF or image file) purchased as part of your order**, is for a one-time use only and limited to any maximum distribution number specified in the license. The first instance of republication or reuse granted by this license must be completed within two years of the date of the grant of this license (although copies prepared before the end date may be distributed thereafter). The Wiley Materials shall not be used in any other manner or for any other purpose, beyond what is granted in the license. Permission is granted subject to an appropriate acknowledgement given to the author, title of the material/book/journal and the publisher. You shall also duplicate the copyright notice that appears in the Wiley publication in your use of the Wiley Material. Permission is also granted on the understanding that nowhere in the text is a previously published source acknowledged for all or part of this Wiley Material. Any third party content is expressly excluded from this permission.
- With respect to the Wiley Materials, all rights are reserved. Except as expressly granted by the terms of the license, no part of the Wiley Materials may be copied, modified, adapted (except for minor reformatting required by the new Publication), translated, reproduced, transferred or distributed, in any form or by any means, and no derivative works may be made based on the Wiley Materials without the prior permission of the respective copyright owner. **For STM Signatory Publishers clearing permission under the terms of the [STM Permissions Guidelines](#) only, the terms of the license are extended to include subsequent editions and for editions in other languages, provided such editions are for the work as a whole in situ and does not involve the separate exploitation of the permitted figures or extracts**, You may not alter, remove or suppress in any manner any copyright, trademark or other notices displayed by the Wiley Materials. You may not license, rent, sell, loan, lease, pledge, offer as security, transfer or assign the Wiley Materials on a stand-alone basis, or any of the rights granted to you hereunder to any other person.
- The Wiley Materials and all of the intellectual property rights therein shall at all times remain the exclusive property of John Wiley & Sons Inc, the Wiley Companies, or their respective licensors, and your interest therein is only that of having possession of and the right to reproduce the Wiley Materials pursuant to Section 2 herein during the continuance of this Agreement. You agree that you own no right, title or interest in or to the Wiley Materials or any of the intellectual property rights therein. You shall have no rights hereunder other than the license as provided for above in Section 2. No right, license or interest to any trademark, trade name, service mark or other branding ("Marks") of WILEY or its licensors is granted hereunder, and you agree that you shall not assert any such right, license or interest with respect thereto

- NEITHER WILEY NOR ITS LICENSORS MAKES ANY WARRANTY OR REPRESENTATION OF ANY KIND TO YOU OR ANY THIRD PARTY, EXPRESS, IMPLIED OR STATUTORY, WITH RESPECT TO THE MATERIALS OR THE ACCURACY OF ANY INFORMATION CONTAINED IN THE MATERIALS, INCLUDING, WITHOUT LIMITATION, ANY IMPLIED WARRANTY OF MERCHANTABILITY, ACCURACY, SATISFACTORY QUALITY, FITNESS FOR A PARTICULAR PURPOSE, USABILITY, INTEGRATION OR NON-INFRINGEMENT AND ALL SUCH WARRANTIES ARE HEREBY EXCLUDED BY WILEY AND ITS LICENSORS AND WAIVED BY YOU.
- WILEY shall have the right to terminate this Agreement immediately upon breach of this Agreement by you.
- You shall indemnify, defend and hold harmless WILEY, its Licensors and their respective directors, officers, agents and employees, from and against any actual or threatened claims, demands, causes of action or proceedings arising from any breach of this Agreement by you.
- IN NO EVENT SHALL WILEY OR ITS LICENSORS BE LIABLE TO YOU OR ANY OTHER PARTY OR ANY OTHER PERSON OR ENTITY FOR ANY SPECIAL, CONSEQUENTIAL, INCIDENTAL, INDIRECT, EXEMPLARY OR PUNITIVE DAMAGES, HOWEVER CAUSED, ARISING OUT OF OR IN CONNECTION WITH THE DOWNLOADING, PROVISIONING, VIEWING OR USE OF THE MATERIALS REGARDLESS OF THE FORM OF ACTION, WHETHER FOR BREACH OF CONTRACT, BREACH OF WARRANTY, TORT, NEGLIGENCE, INFRINGEMENT OR OTHERWISE (INCLUDING, WITHOUT LIMITATION, DAMAGES BASED ON LOSS OF PROFITS, DATA, FILES, USE, BUSINESS OPPORTUNITY OR CLAIMS OF THIRD PARTIES), AND WHETHER OR NOT THE PARTY HAS BEEN ADVISED OF THE POSSIBILITY OF SUCH DAMAGES. THIS LIMITATION SHALL APPLY NOTWITHSTANDING ANY FAILURE OF ESSENTIAL PURPOSE OF ANY LIMITED REMEDY PROVIDED HEREIN.
- Should any provision of this Agreement be held by a court of competent jurisdiction to be illegal, invalid, or unenforceable, that provision shall be deemed amended to achieve as nearly as possible the same economic effect as the original provision, and the legality, validity and enforceability of the remaining provisions of this Agreement shall not be affected or impaired thereby.
- The failure of either party to enforce any term or condition of this Agreement shall not constitute a waiver of either party's right to enforce each and every term and condition of this Agreement. No breach under this agreement shall be deemed waived or excused by either party unless such waiver or consent is in writing signed by the party granting such waiver or consent. The waiver by or consent of a party to a breach of any provision of this Agreement shall not operate or be construed as a waiver of or consent to any other or subsequent breach by such other party.
- This Agreement may not be assigned (including by operation of law or otherwise) by you without WILEY's prior written consent.
- Any fee required for this permission shall be non-refundable after thirty (30) days from receipt by the CCC.



- These terms and conditions together with CCC's Billing and Payment terms and conditions (which are incorporated herein) form the entire agreement between you and WILEY concerning this licensing transaction and (in the absence of fraud) supersedes all prior agreements and representations of the parties, oral or written. This Agreement may not be amended except in writing signed by both parties. This Agreement shall be binding upon and inure to the benefit of the parties' successors, legal representatives, and authorized assigns.
- In the event of any conflict between your obligations established by these terms and conditions and those established by CCC's Billing and Payment terms and conditions, these terms and conditions shall prevail.
- WILEY expressly reserves all rights not specifically granted in the combination of (i) the license details provided by you and accepted in the course of this licensing transaction, (ii) these terms and conditions and (iii) CCC's Billing and Payment terms and conditions.
- This Agreement will be void if the Type of Use, Format, Circulation, or Requestor Type was misrepresented during the licensing process.
- This Agreement shall be governed by and construed in accordance with the laws of the State of New York, USA, without regards to such state's conflict of law rules. Any legal action, suit or proceeding arising out of or relating to these Terms and Conditions or the breach thereof shall be instituted in a court of competent jurisdiction in New York County in the State of New York in the United States of America and each party hereby consents and submits to the personal jurisdiction of such court, waives any objection to venue in such court and consents to service of process by registered or certified mail, return receipt requested, at the last known address of such party.

#### **WILEY OPEN ACCESS TERMS AND CONDITIONS**

Wiley Publishes Open Access Articles in fully Open Access Journals and in Subscription journals offering Online Open. Although most of the fully Open Access journals publish open access articles under the terms of the Creative Commons Attribution (CC BY) License only, the subscription journals and a few of the Open Access Journals offer a choice of Creative Commons Licenses. The license type is clearly identified on the article.

#### **The Creative Commons Attribution License**

The [Creative Commons Attribution License \(CC-BY\)](#) allows users to copy, distribute and transmit an article, adapt the article and make commercial use of the article. The CC-BY license permits commercial and non-

#### **Creative Commons Attribution Non-Commercial License**

The [Creative Commons Attribution Non-Commercial \(CC-BY-NC\) License](#) permits use, distribution and reproduction in any medium, provided the original work is properly cited and is not used for commercial purposes.(see below)

#### **Creative Commons Attribution-Non-Commercial-NoDerivs License**

The [Creative Commons Attribution Non-Commercial-NoDerivs License \(CC-BY-NC-ND\)](#) permits use, distribution and reproduction in any medium, provided the original work is

properly cited, is not used for commercial purposes and no modifications or adaptations are made. (see below)

**Use by commercial "for-profit" organizations**

Use of Wiley Open Access articles for commercial, promotional, or marketing purposes requires further explicit permission from Wiley and will be subject to a fee.

Further details can be found on Wiley Online Library  
<http://olabout.wiley.com/WileyCDA/Section/id-410895.html>

**Other Terms and Conditions:**

**v1.10 Last updated September 2015**

**Questions? [customercare@copyright.com](mailto:customercare@copyright.com) or +1-855-239-3415 (toll free in the US) or +1-978-646-2777.**

## G.9 Copyright Permission for Chapter 7 Cover Image

2/1/23, 3:37 PM

RightsLink Printable License

### JOHN WILEY AND SONS LICENSE TERMS AND CONDITIONS

Feb 01, 2023

---

This Agreement between Mr. Sodiq Waheed ("You") and John Wiley and Sons ("John Wiley and Sons") consists of your license details and the terms and conditions provided by John Wiley and Sons and Copyright Clearance Center.

License Number	5480370232830
License date	Feb 01, 2023
Licensed Content Publisher	John Wiley and Sons
Licensed Content Publication	ChemPhysChem
Licensed Content Title	Front Cover: Mechanism of the Early Catalytic Events in the Collagenolysis by Matrix Metalloproteinase 1 (ChemPhysChem 3/2023)
Licensed Content Author	Sodiq O. Waheed, Ann Varghese, Isabella DiCastrì, et al
Licensed Content Date	Feb 1, 2023
Licensed Content Volume	24
Licensed Content Issue	3
Licensed Content Pages	1

<https://s100.copyright.com/AppDispatchServlet>

1/6

Type of use           Dissertation/Thesis

Requestor type        Author of this Wiley article

Format                Print and electronic

Portion                Full article

Will you be  
translating?         No

Title                   Mechanism of the Early Catalytic Events in the Collagenolysis by  
Matrix Metalloproteinase 1

Institution name     Michigan Technological University

Expected presentation  
date                   Feb 2023

Mr. Sodiq Waheed

Requestor Location  
HOUGHTON, MI 49931  
United States  
Attn: Mr. Sodiq Waheed

Publisher Tax ID    EU826007151

Total                0.00 USD

Terms and Conditions

#### TERMS AND CONDITIONS

This copyrighted material is owned by or exclusively licensed to John Wiley & Sons, Inc. or one of its group companies (each a "Wiley Company") or handled on behalf of a society with which a Wiley Company has exclusive publishing rights in relation to a particular work (collectively "WILEY"). By clicking "accept" in connection with completing this licensing transaction, you agree that the following terms and conditions apply to this transaction (along with the billing and payment terms and conditions established by the Copyright

Clearance Center Inc., ("CCC's Billing and Payment terms and conditions"), at the time that you opened your RightsLink account (these are available at any time at <http://myaccount.copyright.com>).

### Terms and Conditions

- The materials you have requested permission to reproduce or reuse (the "Wiley Materials") are protected by copyright.
- You are hereby granted a personal, non-exclusive, non-sub licensable (on a stand-alone basis), non-transferable, worldwide, limited license to reproduce the Wiley Materials for the purpose specified in the licensing process. This license, **and any CONTENT (PDF or image file) purchased as part of your order**, is for a one-time use only and limited to any maximum distribution number specified in the license. The first instance of republication or reuse granted by this license must be completed within two years of the date of the grant of this license (although copies prepared before the end date may be distributed thereafter). The Wiley Materials shall not be used in any other manner or for any other purpose, beyond what is granted in the license. Permission is granted subject to an appropriate acknowledgement given to the author, title of the material/book/journal and the publisher. You shall also duplicate the copyright notice that appears in the Wiley publication in your use of the Wiley Material. Permission is also granted on the understanding that nowhere in the text is a previously published source acknowledged for all or part of this Wiley Material. Any third party content is expressly excluded from this permission.
- With respect to the Wiley Materials, all rights are reserved. Except as expressly granted by the terms of the license, no part of the Wiley Materials may be copied, modified, adapted (except for minor reformatting required by the new Publication), translated, reproduced, transferred or distributed, in any form or by any means, and no derivative works may be made based on the Wiley Materials without the prior permission of the respective copyright owner. **For STM Signatory Publishers clearing permission under the terms of the STM Permissions Guidelines only, the terms of the license are extended to include subsequent editions and for editions in other languages, provided such editions are for the work as a whole in situ and does not involve the separate exploitation of the permitted figures or extracts**. You may not alter, remove or suppress in any manner any copyright, trademark or other notices displayed by the Wiley Materials. You may not license, rent, sell, loan, lease, pledge, offer as security, transfer or assign the Wiley Materials on a stand-alone basis, or any of the rights granted to you hereunder to any other person.
- The Wiley Materials and all of the intellectual property rights therein shall at all times remain the exclusive property of John Wiley & Sons Inc, the Wiley Companies, or their respective licensors, and your interest therein is only that of having possession of and the right to reproduce the Wiley Materials pursuant to Section 2 herein during the continuance of this Agreement. You agree that you own no right, title or interest in or to the Wiley Materials or any of the intellectual property rights therein. You shall have no rights hereunder other than the license as provided for above in Section 2. No right, license or interest to any trademark, trade name, service mark or other branding ("Marks") of WILEY or its licensors is granted hereunder, and you agree that you shall not assert any such right, license or interest with respect thereto
- NEITHER WILEY NOR ITS LICENSORS MAKES ANY WARRANTY OR REPRESENTATION OF ANY KIND TO YOU OR ANY THIRD PARTY, EXPRESS,

IMPLIED OR STATUTORY, WITH RESPECT TO THE MATERIALS OR THE ACCURACY OF ANY INFORMATION CONTAINED IN THE MATERIALS, INCLUDING, WITHOUT LIMITATION, ANY IMPLIED WARRANTY OF MERCHANTABILITY, ACCURACY, SATISFACTORY QUALITY, FITNESS FOR A PARTICULAR PURPOSE, USABILITY, INTEGRATION OR NON-INFRINGEMENT AND ALL SUCH WARRANTIES ARE HEREBY EXCLUDED BY WILEY AND ITS LICENSORS AND WAIVED BY YOU.

- WILEY shall have the right to terminate this Agreement immediately upon breach of this Agreement by you.
- You shall indemnify, defend and hold harmless WILEY, its Licensors and their respective directors, officers, agents and employees, from and against any actual or threatened claims, demands, causes of action or proceedings arising from any breach of this Agreement by you.
- IN NO EVENT SHALL WILEY OR ITS LICENSORS BE LIABLE TO YOU OR ANY OTHER PARTY OR ANY OTHER PERSON OR ENTITY FOR ANY SPECIAL, CONSEQUENTIAL, INCIDENTAL, INDIRECT, EXEMPLARY OR PUNITIVE DAMAGES, HOWEVER CAUSED, ARISING OUT OF OR IN CONNECTION WITH THE DOWNLOADING, PROVISIONING, VIEWING OR USE OF THE MATERIALS REGARDLESS OF THE FORM OF ACTION, WHETHER FOR BREACH OF CONTRACT, BREACH OF WARRANTY, TORT, NEGLIGENCE, INFRINGEMENT OR OTHERWISE (INCLUDING, WITHOUT LIMITATION, DAMAGES BASED ON LOSS OF PROFITS, DATA, FILES, USE, BUSINESS OPPORTUNITY OR CLAIMS OF THIRD PARTIES), AND WHETHER OR NOT THE PARTY HAS BEEN ADVISED OF THE POSSIBILITY OF SUCH DAMAGES. THIS LIMITATION SHALL APPLY NOTWITHSTANDING ANY FAILURE OF ESSENTIAL PURPOSE OF ANY LIMITED REMEDY PROVIDED HEREIN.
- Should any provision of this Agreement be held by a court of competent jurisdiction to be illegal, invalid, or unenforceable, that provision shall be deemed amended to achieve as nearly as possible the same economic effect as the original provision, and the legality, validity and enforceability of the remaining provisions of this Agreement shall not be affected or impaired thereby.
- The failure of either party to enforce any term or condition of this Agreement shall not constitute a waiver of either party's right to enforce each and every term and condition of this Agreement. No breach under this agreement shall be deemed waived or excused by either party unless such waiver or consent is in writing signed by the party granting such waiver or consent. The waiver by or consent of a party to a breach of any provision of this Agreement shall not operate or be construed as a waiver of or consent to any other or subsequent breach by such other party.
- This Agreement may not be assigned (including by operation of law or otherwise) by you without WILEY's prior written consent.
- Any fee required for this permission shall be non-refundable after thirty (30) days from receipt by the CCC.
- These terms and conditions together with CCC's Billing and Payment terms and conditions (which are incorporated herein) form the entire agreement between you and WILEY concerning this licensing transaction and (in the absence of fraud) supersedes

all prior agreements and representations of the parties, oral or written. This Agreement may not be amended except in writing signed by both parties. This Agreement shall be binding upon and inure to the benefit of the parties' successors, legal representatives, and authorized assigns.

- In the event of any conflict between your obligations established by these terms and conditions and those established by CCC's Billing and Payment terms and conditions, these terms and conditions shall prevail.
- WILEY expressly reserves all rights not specifically granted in the combination of (i) the license details provided by you and accepted in the course of this licensing transaction, (ii) these terms and conditions and (iii) CCC's Billing and Payment terms and conditions.
- This Agreement will be void if the Type of Use, Format, Circulation, or Requestor Type was misrepresented during the licensing process.
- This Agreement shall be governed by and construed in accordance with the laws of the State of New York, USA, without regards to such state's conflict of law rules. Any legal action, suit or proceeding arising out of or relating to these Terms and Conditions or the breach thereof shall be instituted in a court of competent jurisdiction in New York County in the State of New York in the United States of America and each party hereby consents and submits to the personal jurisdiction of such court, waives any objection to venue in such court and consents to service of process by registered or certified mail, return receipt requested, at the last known address of such party.

#### **WILEY OPEN ACCESS TERMS AND CONDITIONS**

Wiley Publishes Open Access Articles in fully Open Access Journals and in Subscription journals offering Online Open. Although most of the fully Open Access journals publish open access articles under the terms of the Creative Commons Attribution (CC BY) License only, the subscription journals and a few of the Open Access Journals offer a choice of Creative Commons Licenses. The license type is clearly identified on the article.

##### **The Creative Commons Attribution License**

The [Creative Commons Attribution License \(CC-BY\)](#) allows users to copy, distribute and transmit an article, adapt the article and make commercial use of the article. The CC-BY license permits commercial and non-

##### **Creative Commons Attribution Non-Commercial License**

The [Creative Commons Attribution Non-Commercial \(CC-BY-NC\) License](#) permits use, distribution and reproduction in any medium, provided the original work is properly cited and is not used for commercial purposes.(see below)

##### **Creative Commons Attribution-Non-Commercial-NoDerivs License**

The [Creative Commons Attribution Non-Commercial-NoDerivs License \(CC-BY-NC-ND\)](#) permits use, distribution and reproduction in any medium, provided the original work is properly cited, is not used for commercial purposes and no modifications or adaptations are made. (see below)

**Use by commercial "for-profit" organizations**

Use of Wiley Open Access articles for commercial, promotional, or marketing purposes requires further explicit permission from Wiley and will be subject to a fee.

Further details can be found on Wiley Online Library  
<http://olabout.wiley.com/WileyCDA/Section/id-410895.html>

**Other Terms and Conditions:**

**v1.10 Last updated September 2015**

**Questions? [customercare@copyright.com](mailto:customercare@copyright.com) or +1-855-239-3415 (toll free in the US) or +1-978-646-2777.**

